IN TWO SECTIONS—SECTION TWO

TRANSACTIONS

of The American Society of Mechanical Engineers

SOCIETY RECORDS—PART 1

FEBRUARY, 1935

VOL. 57, NO. 2

Published by The American Society of Mechanical Engineers

TRANSACTIONS

of The American Society of Mechanical Engineers

Published on the tenth of every month, except March, June, September, and December

Publication Office, 20th and Northampton Streets, Easton, Pa.
Editorial Department at the Headquarters of the Society, 29 West Thirty-Ninth Street, New York, N. Y.

Includes Aeronautical Engineering

BY-LAW: The Society shall not be responsible for statements or opinions advanced in papers or. . .printed in its publications (B2, Par. 3).

Entered as second-class matter March 2, 1928, at the Post Office at Easton, Pa., under the act of August 24, 1912. Price $1.50 a copy, $12.00 a year; to members and affiliates, $1.00 a copy, $7.50 a year. Changes of address must be received two weeks before they are to be effective on our mailing list. Please send old, as well as new, address.

Foreword

THE Transactions of The American Society of Mechanical Engineers include selected technical papers and reports delivered at meetings of the Society, its Professional Divisions, and its Local Sections, the *Journal of Applied Mechanics* (contributions of the Applied Mechanics Division), and certain Records of the Society of permanent value.

In order to secure the advantages of timeliness and greater usefulness in issuing these Society Records, the material comprising them is divided into a number of parts, each one of which is mailed as a supplement to one of the regular monthly sections of the Transactions. For 1935, the first of these, the present issue, contains the personnel of the Council and committees for the year. The second, to be issued sometime later in the year, will contain the memorial notices of deceased members. Following the plan adopted in 1934, it is expected that the reports of Council and the Society's committees will appear as a supplement to the November issue. The presidential address and the indexes to miscellaneous publications, *Mechanical Engineering,* and to the Transactions themselves, must, necessarily, be delayed until 1936, and will probably be mailed as a supplement to the January issue of that year.

In binding the 1935 Transactions, all of these parts of the Society Records will be assembled at the back of the volume as has been customary for several years. To aid in locating references in the bound volumes, the page numbers of the sections containing the Society Records are preceded by the letter RI.

THE COMMITTEE ON PUBLICATIONS

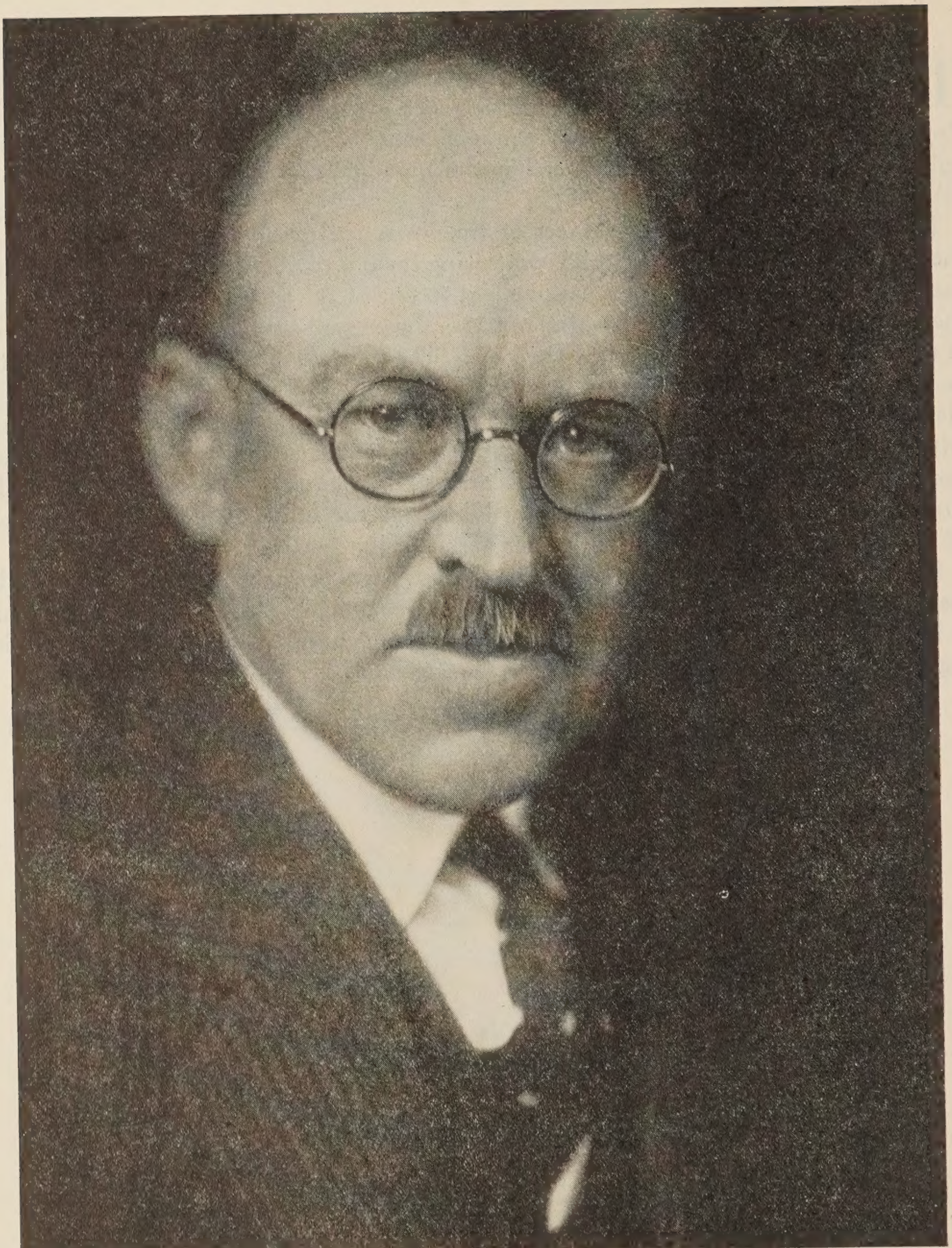

Harris and Ewing

RALPH E. FLANDERS

President of The American Society of Mechanical Engineers
1934–1935

Ralph E. Flanders

RALPH E. FLANDERS, president of The American Society of Mechanical Engineers for the term 1934–1935, is president of the Jones & Lamson Machine Company and of the Bryant Chucking Grinder Company, both of Springfield, Vt. He was born at Barnet, Vt., on September 28, 1880, and was educated at the Central Falls (R. I.) High School. His early experience in machine design and construction was received at Brown & Sharpe Manufacturing Company, Taft-Pierce Manufacturing Company, International Paper Box Machine Company, and General Electric Company. After four years as associate editor of *Machinery* and two years as sales engineer with the Fellows Gear Shaper Company, he joined the Jones & Lamson Machine Company in 1912 as manager of the Fay Lathe Department. In 1914 he was made general manager and in 1933 president of the company.

Mr. Flanders is regarded as a national authority on machine design and construction, especially on the engineering problems of screw threads and thread grinding. His 1924 A.S.M.E. paper on "The Design, Manufacture, and Production Control of a Standard Machine" brought a successful solution to the problem of building machinery economically at widely varying rates of demand.

Mr. Flanders has devoted a large amount of time and effort to the welfare of his profession, serving on many committees of The American Society of Mechanical Engineers. Since 1921 he has been a member and since 1930 chairman of the Sectional Committee on Standardization and Unification of Screw Threads. He represented the A.S.M.E. on the National Screw Thread Commission from 1919 to 1924. He has been a member since 1926 and chairman since 1930 of the Special Research Committee on Strength of Gear Teeth. He served on the Publications Committee from 1918 to 1924 and acted as chairman in 1925 through 1928. He was a manager of the Society from 1926 to 1929 and vice-president in 1930 and 1931.

He was a delegate of the A.S.M.E. to the American Engineering Council in 1924–1925. Since 1932 he has been active in the Public Works program of the Council, and was a member of its Committee on Government Reorganization. As chairman of its Committee on the Relation of Consumption, Production, and Distribution he has been in a position of strong leadership.

Serving as president of the National Machine Tool Builders Association in 1924, Mr. Flanders presented a presidential address that dealt with current economic problems. In this address he pointed out the importance of the transition from the economy of need to the economy of plenty, a contribution of great importance to economic thinking of the times. His address before The American Society of Mechanical Engineers in December, 1930, on "Engineering, Economics, and Social Well-Being" marks his entry into a course of economic study, discussion, and writing that has brought him to the forefront of leadership in his field and led to his selection as a member of the American Engineering Council's Committee on the Relation of Consumption, Production, and Distribution, already mentioned. He is also a director of the Social Science Research Council.

Upon the passage of the National Industrial Recovery Act in 1933 and the organization of the National Recovery Administration, Mr. Flanders was called into service as a member of the Industrial Advisory Board. He is also a member of the Business Advisory and Planning Council appointed by Secretary of Commerce, Daniel C.

Roper. At the conference of the industrial leaders engaged in the administration of various codes for industries held in Washington the first week in March, 1934, his grasp of the basic industrial and economic problems at the present time enabled him to step into a position of leadership in the discussion, which had a profound effect on the deliberations of that important occasion.

Mr. Flanders has written on a wide range of subjects. In his early career his papers and books on gears and gear machinery were highly regarded. Later his discussions of industrial and economic problems have appeared in a wide range of magazines and and his book, "Taming Our Machines," published in 1931, was very well received.

Mr. Flanders was granted the degree of Mechanical Engineer by Stevens Institute of Technology in June, 1932, and the degree of Master of Arts by Dartmouth College the same year. In June, 1934, he was honored with the degree of Doctor of Science, by Middlebury College, and Doctor of Engineering by Brooklyn Polytechnic Institute. He is lecturer at the Tuck School of Business Administration at Dartmouth College and has spoken before many groups of economists, engineers, and industrialists on subjects dealing with economics, engineering, and related problems.

The American Society of Mechanical Engineers

THE members of the Council and of its standing and special committees given on the following pages are those in office on February 1, 1935, serving for the official year 1934–1935. The terms of office of members of other committees are not fixed by the official calendar.

Officers and Council

PRESIDENT

Ralph E. Flanders

PAST-PRESIDENTS

Terms expire December

Charles M. Schwab (1935)
Roy V. Wright (1936)
Conrad N. Lauer (1937)
A. A. Potter (1938)
Paul Doty (1939)

VICE-PRESIDENTS

Terms expire December, 1935

William L. Batt
Harold L. Doolittle
Ely C. Hutchinson
Elliott H. Whitlock

Terms expire December, 1936

Eugene W. O'Brien
James H. Herron
Harry R. Westcott

MANAGERS

Terms expire December, 1935

Robert L. Sackett
Alex D. Bailey
John A. Hunter

Terms expire December, 1936

James A. Hall
Ernest L. Ohle
James M. Todd

Terms expire December, 1937

Bennett M. Brigman
Jiles W. Haney
Alfred Iddles

TREASURER

Erik Oberg

SECRETARY

C. E. Davies

Executive Committee of Council

Ralph E. Flanders, *Chairman*
William L. Batt
James A. Hall
Alfred Iddles
Harry R. Westcott

Advisory Members: Chairmen of the Finance Committee, the Local Sections Committee, and the Professional Divisions Committee

Chairmen of Standing Committees

Representatives on Council but without vote

Finance, Walter Rautenstrauch
Meetings and Program, R. I. Rees
Publications, S. W. Dudley
Membership, H. A. Lardner
Professional Divisions, W. A. Shoudy
Local Sections, W. L. Dudley
Constitution and By-Laws, H. H. Snelling
Awards, W. L. Batt
Relations With Colleges, W. L. Abbott
Education and Training for Industries, G. A. Seyler
Library, E. P. Worden
Research, G. M. Eaton
Standardization, C. W. Spicer
Power Test Codes, F. R. Low
Safety, W. M. Graff
Professional Conduct, C. G. Spencer

ASSISTANT SECRETARIES

Ernest Hartford
C. B. LePage

EDITOR

G. A. Stetson

Standing Committees

FINANCE

Walter Rautenstrauch, *Chairman and Representative on Council* (1936)

W. T. Conlon (1935)
W. D. Ennis (1937)
T. R. Weymouth (1938)
K. M. Irwin (1939)

Council Representatives E. C. Hutchinson (1935), J. H. Herron (1936)

MEETINGS AND PROGRAM

R. I. Rees, *Chairman and Representative on Council* (1935)

E. C. Hutchinson (1936)
H. N. Davis (1937)
Clarke Freeman (1938)
R. F. Gagg (1939)

Junior Adviser: To be appointed

PUBLICATIONS

S. W. Dudley, *Chairman and Representative on Council* (1936)

W. F. Ryan, *Vice-Chairman* (1937)
S. F. Voorhees (1935)
M. H. Roberts (1938)
G. F. Bateman (1939)

O. B. Schier, 2nd, *Junior Adviser* (1935)

Advisory Members: A. J. Dickie, E. B. Norris, E. L. Ohle

(Personnel of Special Committee, p. 8)

MEMBERSHIP

H. A. Lardner, *Chairman and Representative on Council* (1935)

R. H. McLain (1936)
C. L. Davidson (1937)
L. R. Ford (1938)
F. C. Spencer (1939)

Advisory Member: O. E. Goldschmidt (1935)

PROFESSIONAL DIVISIONS

W. A. Shoudy, *Chairman and Representative on Council* (1935)

K. H. Condit (1936)
G. B. Pegram (1937)
Crosby Field (1938)
L. K. Sillcox (1939)

(Personnel of Professional Divisions' Executive Committees, p. 9)

LOCAL SECTIONS

W. L. Dudley, *Chairman and Representative on Council* (1935)

To be appointed (1936)
R. E. W. Harrison (1937)
W. R. Woolrich (1938)
D. B. Prentice (1939)

Junior Advisers

Jensen Clausen
F. X. Krogmann
S. E. Oren
J. M. Tucker

(Personnel of Local Sections' Executive Committees, p. 12)

CONSTITUTION AND BY-LAWS

H. H. Snelling, *Chairman and Representative on Council* (1935)

Richard Kutzleb, Jr. (1936)
H. B. Lewis (1937)
W. H. Kavanaugh (1938)
R. D. Brizzolara (1939)

Junior Adviser: G. N. Cole (1935)

AWARDS

The members of this Committee serve as members also of the Special Council Committee on Honors

W. L. Batt, *Chairman and Representative on Council* (1935)

Herman Diederichs (1936)
R. C. H. Heck (1937)
L. P. Alford (1938)
Harte Cooke (1939)

Junior Adviser: C. B. Arnold (1935)

RELATIONS WITH COLLEGES

W. L. Abbott, *Chairman and Representative on Council* (1935)

E. W. Burbank (1936)
R. V. Wright (1937)
W. A. Hanley (1938)
F. V. Larkin (1939)

Junior Advisers R. F. Warner, Jr. (1935), G. D. Wilkinson, Jr. (1935)

(Student Branches and Officers, p. 18)

EDUCATION AND TRAINING FOR THE INDUSTRIES

G. A. Seyler, *Chairman and Representative on Council* (1935)
C. J. Freund (1936) J. A. Randall (1938)
John Younger (1937) P. E. Bliss (1939)

LIBRARY

E. P. Worden, *Chairman and Representative on Council* (1935)
G. F. Felker (1936) J. S. Kerins (1938)
L. K. Sillcox (1937) The Secretary, C. E. Davies. *Ex-Officio*

RESEARCH

Organized in 1909 to supervise all research activities of the Society, to cooperate with similar committees of kindred societies, to encourage research, and to disseminate knowledge of researches conducted in the United States and in other countries

G. M. Eaton, *Chairman and Representative on Council* (1935)
D. B. Bullard (1936) H. A. Johnson (1938)
C. R. Richards (1937) N. E. Funk (1939)

(*Personnel of Special Committees, p. 20*)

STANDARDIZATION

Organized in April, 1911, to supervise all standardization activities of the Society and to advise concerning the Society's participation in the activities of the American Standards Association

C. W. Spicer, *Chairman and Representative on Council* (1935)
Alfred Iddles (1936) Walter Samans (1938)
L. A. Cornelius (1937) O. A. Leutwiler (1939)

(*Personnel of Special Committees, p. 22*)

POWER TEST CODES

Organized December, 1918, to revise and extend the Power Test Codes of the Society. These codes had been formulated by various technical committees appointed to develop particular codes. This work began in 1886

F. R. Low, *Chairman and Representative on Council* (1935)
R. H. Fernald, *Acting Chairman*

Term expires 1935
A. T. Brown
R. H. Fernald
C. F. Hirshfeld
F. R. Low
R. J. S. Pigott

Term expires 1936
A. G. Christie
Paul Diserens
E. C. Hutchinson
G. A. Orrok
W. M. White

Term expires 1937
Harte Cooke
E. R. Fish
O. P. Hood
H. B. Oatley
W. J. Wohlenberg

Term expires 1938
Hans Dahlstrand
Louis Elliott
G. A. Horne
H. B. Reynolds
E. N. Trump

Term expires 1939
C. H. Berry
Francis Hodgkinson
E. B. Ricketts
D. S. Jacobus
L. F. Moody

(*Personnel of Technical Committees, p. 26*)

SAFETY

Appointed in October, 1921, to extend the knowledge of accident prevention, to promote cooperation in this field, and to supervise all safety code activities of the Society with the exception of those of the Boiler Code group of committees

W. M. Graff, *Chairman and Representative on Council* (1936)
M. H. Christopherson (1935) H. L. Miner (1938)
H. H. Judson (1937) To be appointed (1939)

(*Personnel of Special Committees, p. 27*)

PROFESSIONAL CONDUCT

C. G. Spencer, *Chairman and Representative on Council* (1935)
E. R. Fish (1936) E. F. Scott (1938)
J. H. Herron (1937) Hugo Diemer (1939)

Special Technical Committees

BOILER CODE

F. R. Low, *Chairman*
D. S. Jacobus, *Vice-Chairman*
C. W. Obert, *Honorary Secretary*
M. Jurist, *Acting Secretary*
C. A. Adams
H. E. Aldrich
W. H. Boehm
R. E. Cecil
F. S. Clark
W. F. Durand
A. J. Ely
E. R. Fish
V. M. Frost
C. E. Gorton
A. M. Greene, Jr.
F. B. Howell
J. O. Leech
M. F. Moore
I. E. Moultrop
C. O. Myers
H. B. Oatley
James Partington
Walter Samans
C. L. Warwick
A. C. Weigel
H. LeRoy Whitney

Honorary Members

F. W. Dean
T. E. Durban
C. L. Huston
W. F. Kiesel
H. H. Vaughan

Conference Committee to the Boiler Code Committee

T. R. Archer, Delaware
L. M. Barringer, Seattle, Wash.
H. D. Bombeck, St. Joseph, Mo.
B. M. Book, Pennsylvania
J. C. Bryan, St. Louis, Mo.
John Campbell, Pennsylvania
T. C. Cannon, Tulsa, Okla.
A. L. Daniels, Parkersburg, W. Va.
James Donohue, Indiana
L. F. Duge, Maryland
M. A. Edgar, Wisconsin
E. W. Farmer, Rhode Island
M. J. Flyzik, Washington
C. W. Foster, Omaha, Nebraska
W. H. Furman, New York
Gerald Gearon, Chicago, Ill.
E. M. Goodman, Evanston, Ill.
C. H. Gram, Oregon
P. M. Greenlaw, District of Columbia
F. A. Heckinger, Memphis, Tenn.
J. M. Lukens, Philadelphia, Pa.
J. M. Lynch, Erie, Pa.
C. E. McGinnis, Los Angeles, Calif.
H. H. Mills, Detroit, Mich.
A. C. Mitchell, Scranton, Pa.
C. O. Myers, Ohio
J. D. Newcomb, Arkansas
W. L. Newton, Oklahoma
Daniel O'Connor, Michigan
F. A. Page, California
L. C. Peal, Nashville, Tenn.
J. J. Ryan, Kansas City, Mo.
E. K. Sawyer, Maine
A. H. Schleman, Tampa, Florida
J. F. Scott, New Jersey
C. I. Smith, Utah
Wm. E. Smith, Hawaii
George Wilcox, Minnesota

Executive Committee

D. S. Jacobus, *Chairman*
H. E. Aldrich
W. H. Boehm
E. R. Fish
V. M. Frost
C. E. Gorton
F. R. Low
C. W. Obert
James Partington

Subcommittee on Boilers of Locomotives

James Partington, *Chairman*
F. H. Clark
H. B. Oatley
A. G. Pack, *Conference Member*

Subcommittee on Care of Steam Boilers and Other Pressure Vessels in Service

F. M. Gibson, *Chairman*
V. M. Frost
J. R. Gill
J. A. Hunter
H. J. Kerr
W. H. Larkin, Jr.
S. T. Powell
C. W. Rice
H. F. Scott
Nicholas Stahl
F. G. Straub

Subcommittee on Heating Boilers

F. B. Howell, *Chairman*
W. H. Boehm
C. E. Bronson
J. A. Darts
C. E. Gorton
F. W. Herendeen
W. E. Stark
J. W. Turner

Subcommittee on Material Specifications

Members of A.S.M.E. Boiler Code Committee

P. R. Cassidy, *Chairman*
A. M. Greene, Jr.
J. O. Leech
C. L. Warwick

Members of Conference Committee of American Society for Testing Materials

C. L. Warwick, *Chairman*
E. J. Edwards
C. F. W. Rys

Members of Conference Committee of Association of American Steel Manufacturers, Technical Committees

J. O. Leech, *Chairman*
E. F. Kenney
A. D. Peace

Subcommittee on Miniature Boilers

C. E. Gorton, *Chairman*
James Partington, *Vice-Chairman*
E. R. Fish
W. H. Furman
C. O. Myers
C. W. Obert
J. H. Plunkett

Subcommittee on Rules for Inspection

J. A. Collins, *Chairman*
S. H. Barnum
L. E. Connelly
William Ferguson
C. E. Gorton
F. W. Herendeen
James Partington

Subcommittee on Special Design

D. B. Wesstrom, *Chairman*
W. L. Bowler
R. E. Cecil
Paul Diserens
H. E. Rockefeller
D. B. Rossheim
W. H. Rowand
E. O. Waters
F. S. G. Williams

Subcommittee on Unfired Pressure Vessels

E. R. Fish, *Chairman*
C. A. Adams
W. H. Boehm
C. E. Bronson
R. E. Cecil
Paul Diserens
A. W. Limont, Jr.
H. S. Smith
D. B. Wesstrom

Subcommittee on Welding

Members of A.S.M.E. Boiler Code Committee

James Partington, *Chairman*
C. A. Adams
A. M. Candy
R. E. Cecil
J. H. Deppeler
E. R. Fish
R. K. Hopkins
T. McLean Jasper
L. A. Sheldon
Henry Torrance, Jr.

Members of Conference Committee of American Welding Society

C. W. Obert, *Chairman*
L. H. Burkhart
J. J. Crowe
E. H. Ewertz
F. C. Fyke
J. W. Owens
A. Kidd
H. E. Rockefeller
L. H. Roller

API-ASME COMMITTEE ON UNFIRED PRESSURE VESSELS

A.S.M.E. Representatives

R. E. Cecil
E. R. Fish
D. S. Jacobus
T. McLean Jasper
James Partington

A.P.I. Representatives

Walter Samans, *Chairman*
A. J. Ely
R. C. Powell
K. V. King
(P. D. McElfish, *Alternate*)
T. D. Tifft

SHAFT COUPLINGS

Appointed in December, 1928

A.S.M.E. Members (Total personnel, 6)

D. J. McCormack
H. G. Reist
R. E. B. Sharp

DEVELOPMENT OF APPLICATIONS OF STATISTICS IN ENGINEERING AND MANUFACTURING

Joint sponsorship with the American Society for Testing Materials. Appointed in December, 1929

A.S.M.E. Members (Total personnel, 4)

W. H. Fulweiler
†L. K. Sillcox

STANDARD HEIGHT FOR LOADING PLATFORMS AT FREIGHT TERMINALS AND WAREHOUSES

Joint sponsorship with the Society of Terminal Engineers. Appointed in December, 1931

A.S.M.E. Members (Total personnel, 13)

†C. B. Crockett

Special Council Committees

ADVERTISING REVENUE

S. W. Dudley, Chairman of Committee on Publications
Walter Rautenstrauch, Chairman of Finance Committee
H. R. Westcott, Chairman of Committee on Policies and Budget

ADVISORY BOARD ON TECHNOLOGY

A. A. Potter, *Chairman*

D. B. Bullard, Research
K. H. Condit, Professional Divisions
S. W. Dudley, Publications
R. I. Rees, Meetings and Program

ADVISORY BOARD ON STANDARDS AND CODES

Alex D. Bailey, *Chairman*

V. M. Frost, Boiler Code
W. M. Graff, Safety
Francis Hodgkinson, Power Test Codes
L. A. Cornelius, Standardization

BOARD OF REVIEW (DELINQUENT MEMBERS)

A. D. Blake
J. P. Neff
H. B. Oatley

BOND ISSUE (CERTIFICATES OF INDEBTEDNESS)

Dexter S. Kimball, *Chairman*
Paul Doty
W. A. Hanley
C. F. Hirshfeld
J. H. Lawrence
W. R. Webster
W. H. Winterrowd
Erik Oberg, *Ex-Officio*

Trustees for Issue of Certificates of Indebtedness:

D. S. Kimball
Erik Oberg
R. V. Wright

CAPITAL GOODS INDUSTRIES

L. P. Alford, *Chairman*
R. E. Flanders
L. W. W. Morrow
Erik Oberg

CITIZENSHIP (MANUAL ON)

A. R. Cullimore, *Chairman*
Lillian M. Gilbreth
J. W. Roe
W. H. Winterrowd
R. V. Wright

COOPERATIVE RELATIONS

H. V. Coes, *Chairman*
R. I. Rees
D. Robert Yarnall

ECONOMIC STATUS OF THE ENGINEER

C. F. Hirshfeld, *Chairman*
D. S. Kimball
C. N. Lauer
H. B. Oatley
H. L. Whittemore
W. E. Wickenden
W. L. Abbott } *Ex-Officio*
W. L. Dudley } *Ex-Officio*

EMPLOYMENT (MEMBER RELATIONS)

Crosby Field
J. N. Landis
W. A. Shoudy

ENGINEERING HISTORY

(To be appointed)

FREEMAN SCHOLARSHIP

Charles T. Main, *Chairman*
Clarke Freeman
E. C. Hutchinson

† Official A.S.M.E. representatives serving on this committee.

HONORS

The members of the Standing Committee on Awards (see page 5) also serve as a Special Committee on Honors

JUNIOR PARTICIPATION

W. A. Hanley
A. A. Potter
D. B. Prentice
W. H. Winterrowd
(Junior Member to be appointed)

MANUAL OF PRACTICE

W. A. Shoudy, *Chairman*
Alfred Iddles
Wynn Meredith
J. M. Todd
B. F. Wood
C. G. Spencer, *Ex-Officio*
Theodore Baumeister, Jr., *Acting Secretary*

Junior Adviser, Philip Werner

POLICIES AND BUDGET

H. R. Westcott, *Chairman*
L. P. Alford
B. M. Brigman
H. M. Burke
W. H. Carrier
Alfred Iddles
A. C. Jewett
J. N. Landis
J. H. Lawrence
R. G. Macy
A. L. Maillard
M. C. Maxwell
Erik Oberg
L. K. Sillcox
W. H. Winterrowd

PUBLIC AFFAIRS

R. V. Wright, *Chairman*
L. P. Alford
Paul Doty
R. E. Flanders
A. A. Potter
J. W. Roe
D. Robert Yarnall

REGISTRATION OF ENGINEERS

J. H. Lawrence, *Chairman*
Paul Doty
C. F. Hirshfeld
D. S. Kimball
V. M. Palmer
J. M. Todd

CALVIN W. RICE MEMORIAL

H. N. Davis, *Chairman*
J. D. Cunningham
W. F. Durand
C. E. Fuller
C. N. Lauer
E. W. O'Brien
J. W. Parker
R. L. Sackett

SPIRIT OF ST. LOUIS MEDAL BOARD OF AWARD

(Dates in parentheses denote expiration of terms)

V. J. Azbe, *Chairman* (1943)
J. H. Doolittle, *Secretary* (1940)
H. I. Cone (1937)
W. B. Mayo (1937)
Orville Wright (1940)
C. B. Millikan (1943)

GEORGE WESTINGHOUSE BUST

Ambrose Swasey, *Honorary Chairman*
D. S. Kimball, *Chairman*
L. B. Stillwell, *Vice-Chairman*
W. W. Atterbury
K. T. Compton
S. W. Dudley
C. H. Lauer
L. A. Osborne
C. F. Scott

GEORGE WESTINGHOUSE MEMORIAL

(Ninetieth Birthday in 1936)

R. V. Wright, *Chairman*
S. W. Dudley
J. H. McGraw
C. F. Scott
R. I. Rees, *Ex-Officio*

Special Publications Committee

BIOGRAPHY ADVISORY COMMITTEE

R. V. Wright, *Chairman*
L. P. Alford
R. E. Flanders
F. R. Low
G. A. Orrok
J. W. Roe
W. H. Winterrowd

Special Administrative Committee

REGULAR NOMINATING COMMITTEE (FOR 1935)

GROUP

I W. K. Simpson, Waterbury, Conn.
Prof. C. H. Berry, Cambridge, Mass., *Alternate*

II A. D. Blake, New York, N. Y.
E. A. Kerbey, New York, N. Y., *Alternate*

III Prof. A. G. Christie, Baltimore, Md.
A. R. Stevenson, Jr., Schenectady, N. Y., *1st Alternate*
Prof. F. V. Larkin, Bethlehem, Pa., *2nd Alternate*

IV Dean B. R. Van Leer, Gainesville, Fla.
R. P. Kolb, Raleigh, N. C., *Alternate*

V A. N. Goddard, Detroit, Mich.
Prof. F. W. Marquis, Columbus, Ohio, *Alternate*

VI F. H. Dorner, Milwaukee, Wis.
A. A. Luebs, Lincoln, Neb., *Alternate*

VII Prof. R. L. Daugherty, Pasadena, Calif.
H. P. Vail, Los Angeles, Calif., *1st Alternate*
R. R. Robertson, Los Angeles, Calif., *2nd Alternate*

LOCAL SECTIONS IN NOMINATING COMMITTEE GROUPS

GROUP I

Boston
Bridgeport
Green Mountain
Hartford
Meriden
New Britain
New Haven
Norwich
Providence
Waterbury
Western Massachusetts
Worcester

GROUP II

Metropolitan (N. Y.) and Foreign Members

GROUP III

Anthracite-Lehigh Valley
Baltimore
Central Pennsylvania
Ontario
Philadelphia
Plainfield
Rochester
Schenectady
Susquehanna
Syracuse
Utica
Washington, D. C.

GROUP IV

Atlanta
Birmingham
Charlotte
Chattanooga
Florida
Greenville
Houston
Knoxville
Memphis
New Orleans
North Texas
Raleigh
Savannah
Virginia

GROUP V

Akron-Canton
Buffalo
Cincinnati
Cleveland
Columbus
Dayton
Detroit
Erie
Indianapolis
Louisville
Peninsula
Pittsburgh
Toledo
West Virginia
Youngstown

GROUP VI

Chicago
Kansas City
Mid-Continent
Milwaukee
Minnesota
Nebraska
Rock River Valley
St. Joseph Valley
St. Louis
Tri-Cities

GROUP VII

Colorado
Inland Empire
Los Angeles
Oregon
San Francisco
Utah
Western Washington

Professional Divisions

(*Personnel of Standing Committee, page 5*)

Aeronautic Division

Organized, 1920

EXECUTIVE COMMITTEE

J. H. Doolittle, *Chairman*
Alexander Klemin, *1st Vice-Chairman*
Jerome Lederer, *Secretary*
R. M. Mock
E. A. Sperry
B. M. Woods

COMMITTEE ON INDUSTRIAL AERODYNAMICS

Alexander Klemin, *Secretary*
Oliver Allen
W. H. Carrier
H. E. Davison
H. P. Frear
W. G. Grove
O. E. Hovey
A. L. Kimball
R. J. S. Pigott
L. K. Sillcox

REPRESENTATIVES ON OTHER ACTIVITIES

Aircraft Safety and Inspection, Jerome Lederer
Marking of Obstructions to Air Navigation, J. E. Whitbeck
Spirit of St. Louis Medal Board of Award, V. J. Azbe
Daniel Guggenheim Medal Fund, E. E. Aldrin

Applied Mechanics Division

Organized, 1927

EXECUTIVE COMMITTEE

J. A. Goff, *Chairman*
E. O. Waters, *Secretary*
Rupen Eksergian
J. C. Hunsaker
C. R. Soderberg

Associates

A. L. Kimball
J. M. Lessells
G. B. Pegram

JOURNAL OF APPLIED MECHANICS

J. M. Lessells, *Technical Editor*

SUBCOMMITTEE CHAIRMEN

Elasticity, Stephen Timoshenko
Hydromechanics, Theodor von Karman
Materials, R. E. Peterson
Plasticity, A. Nadai
Thermodynamics, J. A. Goff
Vibration, F. M. Lewis

Fuels Division

Organized, 1920

EXECUTIVE COMMITTEE

K. M. Irwin, *Chairman*
W. G. Christy, *Secretary*
L. C. Bosler
M. D. Engle
T. A. Marsh
R. A. Sherman

Associates

A. D. Blake
A. C. Stern
John Van Brunt
F. M. Van Deventer

SUBCOMMITTEE ON PROGRAMS, MEETINGS, AND AIMS

M. D. Engle, *Chairman*
Ollison Craig
R. M. Hardgrove
J. N. Landis
J. F. Muir
H. G. Thielscher

SUBCOMMITTEE ON FUELS ENGINEERING PROGRESS REPORT

K. M. Irwin, *Chairman*

SUBCOMMITTEE ON CINDERS AND FLY ASH

A. C. Stern, *Chairman*

COMMITTEE ON SAMPLING PULVERIZED FUEL IN A MOVING GAS STREAM

(Research Committee; see page 21)

K. M. Irwin, *Chairman and Representative of Fuels Division*

COMMITTEE ON REMOVAL OF ASH AS MOLTEN SLAG FROM POWDERED-COAL FURNACES

(Research Committee; see page 21)

K. M. Irwin, *Chairman and Representative of Fuels Division*

PURE AIR COMMITTEE

Organized, 1932

E. C. Hutchinson, *Chairman*
E. H. Whitlock, *Secretary*
J. W. Armour
M. D. Engle
O. P. Hood
W. F. Keenan

Representatives

Philip Drinker, American Society of Heating and Ventilating Engineers
H. C. Murphy, *Alternate*
K. M. Irwin, A.S.M.E. Fuels Division
H. B. Meller, Mellon Institute of Industrial Research
E. B. Ricketts, Edison Electric Institute

Hydraulic Division

Organized, 1926

EXECUTIVE COMMITTEE

C. F. Merriam, *Chairman*
S. Logan Kerr, *Secretary*
Paul Diserens
D. J. McCormack
B. R. Van Leer

MEETINGS AND PAPERS COMMITTEE

S. Logan Kerr, *Chairman*
R. W. Angus

COMMITTEE ON WATER HAMMER

Honorary Member, Lorenzo Allievi, Rome, Italy

S. Logan Kerr, *Chairman*
Eugene Halmos (A.S.C.E.)
N. R. Gibson
L. F. Moody
R. S. Quick
E. B. Strowger

COMMITTEE ON TRANSLATIONS AND TERMINOLOGY

B. R. Van Leer, *Chairman*

Iron and Steel Division

Organized, 1927

EXECUTIVE COMMITTEE

T. H. Wickenden, *Chairman*
J. H. Hitchcock, *Secretary*
W. A. James
S. M. Marshall
Willis McKee
W. R. Webster

Associates

F. C. Biggert, Jr.
A. J. Boynton
A. G. McKee
C. S. Robinson
G. T. Snyder
W. Trinks
S. M. Weckstein

Machine Shop Practice Division

Organized, 1921

EXECUTIVE COMMITTEE

R. E. W. Harrison, *Chairman*
G. F. Nordenholt, *Secretary*
B. P. Graves
E. R. Norris
B. G. Tang
Carlos de Zafra

SUBCOMMITTEE ON FOUNDRY PRACTICE

James Thomson, *Chairman*
R. E. Kennedy, *Secretary*

Machine Shop Practice Division (continued)

SUBCOMMITTEE ON MACHINE DESIGN

J. A. Hall, *Chairman*
J. B. Armitage
G. H. Ashman
G. F. Cosgrove
Frederick Franz
G. B. Karelitz
G. F. Nordenholt
Albert Palmer

SUBCOMMITTEE ON LUBRICATION ENGINEERING

W. F. Parish, *Chairman*
C. H. Bromley
G. B. Karelitz
C. M. Larson
H. J. Masson

SUBCOMMITTEE ON CUTTING METALS

Coleman Sellers, 3rd, *Chairman*

SUBCOMMITTEE ON WELDING

Everett Chapman, *Chairman*

Management Division

Organized, 1920

EXECUTIVE COMMITTEE

J. A. Piacitelli, *Chairman*
G. W. Kelsey, *Vice-Chairman*
W. H. Kushnick, *Secretary*
C. I. Day
Walter Rautenstrauch
J. R. Shea

Associates

C. W. Lytle
F. E. Raymond

Student Associates

F. Weaver, Stevens Institute of Technology
R. Brugger, Polytechnic Institute of Brooklyn
M. J. Massimo, New York University
V. S. Myers, Columbia University
R. H. Curtiss, Columbia University

SUBCOMMITTEE CHAIRMEN

Economics, Kerr Atkinson
Finance and Accounting, K. W. Jappe
Human Relations, R. Likert
Job Shop Management, A. J. Graf
Management Research, W. E. Freeland
Marketing, G. W. Kelsey
Metropolitan Section, A. F. Ernst
Quality Control, M. F. Skinker
Time and Motion Study, D. B. Porter
Waste Elimination, C. B. Auel

NATIONAL MANAGEMENT COUNCIL

(*See page 30*)

Materials Handling Division

Organized, 1920

EXECUTIVE COMMITTEE

J. B. Webb, *Chairman*
M. W Potts, *Secretary*
N. W. Elmer
G. E. Hagemann
F. E. Moore
G. L. Morehead

Associates

F. D. Campbell
J. A. Jackson
R. H. McLain
R. B. Renner
F. J. Shepard, Jr.
E. D. Smith

National Defense Division

Organized, 1920

EXECUTIVE COMMITTEE

H. I. Cone, *Chairman*
W. C. Dickerman
Ralph Earle
T. A. Morgan
J. L. Walsh

Oil and Gas Power Division

Organized, 1921

EXECUTIVE COMMITTEE

Ralph Miller, *Chairman*
M. J. Reed, *Secretary*
L. B. Jackson
E. J. Kates
Ernest Nibbs
Lee Schneitter

Associates

Harte Cooke
L. R. Ford
L. M. Goldsmith
H. C. Major
H. T. Moore
L. H. Morrison

SUBCOMMITTEE ON 1934 OIL ENGINE POWER COST REPORT

H. C. Major, *Chairman*
M. J. Reed, *Secretary*
L. R. Ford
W. G. G. Godron
K. M. Irwin
E. J. Kates
H. C. Lenfest
Howard McCurdy
A. B. Morgan
L. H. Morrison
H. A. Person
Lee Schneitter
P. H. Schweitzer
H. C. Thuerk
C. A. Trimmer

Petroleum Division

Organized, 1925

EXECUTIVE COMMITTEE

H. F. Brindel, *Chairman*
Harold Adkison, *Midwestern Secretary*
H. J. Masson, *Secretary*
W. H. Carson
F. H. Eberle
W. G. Heltzel
T. D. Tifft

Associates

E. H. Barlow
H. P. Porter
Walter Samans

SUBCOMMITTEE ON PRODUCTION

W. H. Carson, *Chairman*
R. M. Carr
H. W. Manley
R. R. Hawkins
H. Decker
J. R. Johnston

SUBCOMMITTEE ON OIL TRANSPORTATION

W. G. Heltzel, *Chairman*
A. N. Horne
H. N. Hunter
B. P. Sibole
H. M. Stevenson
F. A. Stivers
F. E. Warterfield
Oscar Wolfe

SUBCOMMITTEE ON GAS TRANSPORTATION

R. W. Hendee, *Chairman*

SUBCOMMITTEE ON PETROLEUM REFINING

T. D. Tifft, *Chairman*
T. H. Hamilton, *Vice-Chairman*

SUBCOMMITTEE ON LUBRICATION ENGINEERING

(Machine Shop Practice Division; see preceding column)

H. J. Masson, *Representative of Petroleum Division*

SURVEY COMMITTEES ON PETROLEUM PROBLEMS

(Now at work or in the process of formation in the Mid-Continent Section)

Unfired Pressure Vessels
Diesel Engine Driven Reciprocating Pumping Stations
Uniform Code of Economic Analysis of Different Types of Oil Pipe Line Pumping Stations

Power Division

Organized, 1920

EXECUTIVE COMMITTEE

J. M. Brentlinger, *Chairman*
W. A. Carter, *Secretary*
J. C. Hobbs
W. E. Caldwell
A. E. Grunert

Printing Industries Division

Organized, 1922

EXECUTIVE COMMITTEE

Edward Epstean, *Chairman*
Edward P. Hulse, *Secretary*
J. M. Farrell
R. G. Macdonald
John Clyde Oswald
Burt D. Stevens

Associates

V. Winfield Challenger
Summerfield Eney, Jr.
F. M. Flynn
Harry L. Gage
A. E. Giegengack
Wm. C. Glass
Harry Groesbeck, Jr.
Wells F. Harvey
T. R. Jones
Hadar Ortman
H. M. Tillinghast

CHAIRMEN OF DIVISIONAL COMMITTEES

Meetings and Programs, G. D. Bearce
Paper and Pulp, W. R. Maull
Progress Report, W. S. Huson
Research and Survey, Arthur C. Jewett

The Division sponsors the Conference of the Technical Experts in the Printing Industry, a forum for the discussion of the mechanical and process problems of the entire graphic arts field; also the Graphic Arts Research Bureau, formed to act as a clearing house for graphic arts research and for the collection, correlation, and distribution of research information pertaining to the industry and for the sponsorship of research work.

Process Industries Division

Organized, 1934

EXECUTIVE COMMITTEE

Victor Wichum, *Chairman*
W. K. McAfee, *Vice-Chairman*
T. R. Olive, *Secretary*
C. E. Harrington
H. D. Munson
C. W. Thomas

SUBCOMMITTEE CHAIRMEN

Air Conditioning, G. B. Bailey
Brewing, C. F. Kayan
Ceramics, W. K. McAfee
Cottonseed Processing, W. R. Woolrich
Drying, C. W. Thomas
Food Processing, G. L. Montgomery
Pulp and Paper, H. D. Fisher
Pulverizing and Grinding, J. C. Hardigg
Sanitation, William Raisch
Sugar, F. M. Gibson
Unit Operation Costs, H. J. Masson

HEAT TRANSFER COMMITTEE

J. H. Sengstaken, *Chairman*
R. E. Birch
T. H. Chilton
M. S. Van Dusen
F. H. Eberle
H. C. Hottel
C. E. Lucke

Railroad Division

Organized, 1920

EXECUTIVE COMMITTEE (RR1)

C. E. Barba, *Chairman*
G. W. Rink, *1st Vice-Chairman*
W. H. Winterrowd, *2nd Vice-Chairman*
C. T. Ripley, *3rd Vice-Chairman*
E. C. Schmidt, *4th Vice-Chairman*
M. B. Richardson, *Secretary*

GENERAL COMMITTEE (RR2)

C. E. Barba, *Chairman*
O. C. Cromwell (1935)
J. R. Jackson (1935)
M. H. Roberts (1935)
A. I. Lipetz (1936)
F. E. Lyford (1936)
Eliot Sumner (1936)
T. C. McBride (1937)
P. C. Morales (1937)
K. F. Nystrom (1937)
W. G. Black (1938)
W. H. Clegg (1938)
G. A. Young (1938)
L. H. Fry (1939)
F. E. Russell (1939)
R. W. Salisbury (1939)

PAST-CHAIRMEN (RR3)

E. B. Katte* (1920–1922)
James Partington (1923–1924)
C. E. Chambers (1925)
H. B. Oatley (1926–1927)
Wm. Elmer (1928)
R. S. McConnell (1929)
A. F. Steubing (1930)
Eliot Sumner (1931)
T. C. McBride (1932)
L. K. Sillcox (1933)
C. B. Peck (1934)

CHICAGO GROUP (RR4)

W. O. Moody, *Chairman*
E. L. Woodward, *Secretary*
Walter Dunham
Peter Parke
C. T. Ripley
W. H. Winterrowd

COMMITTEE ON MEETINGS AND PAPERS (RR5)

W. H. Winterrowd, *Chairman*
W. G. Black, L. H. Fry } Spring Meeting, 1935

COMMITTEE ON SURVEY (RR6)

A. I. Lipetz, *Chairman* (Locomotive and Foreign Developments)
W. H. Clegg (Canadian and Automotive Equipment)
P. C. Morales (Mexican and South American Developments)
K. F. Nystrom (Cars)

COMMITTEE ON TECHNICAL CONTACTS (RR7)

E. C. Schmidt, *Chairman*
O. C. Cromwell
J. R. Jackson
F. E. Lyford
F. E. Russell
R. W. Salisbury

COMMITTEE ON PROFESSIONAL SERVICE (RR8)

L. K. Sillcox, *Chairman* (Membership)
H. B. Oatley (Professional Survey)
M. B. Richardson

COMMITTEE ON RESEARCH (RR9)

L. H. Fry, *Chairman*
T. C. McBride
James Partington
G. A. Young
G. W. Rink
A. F. Steubing
Eliot Sumner

Textile Division

Organized, 1921

EXECUTIVE COMMITTEE

H. D. Learnard, *Chairman*
M. A. Golrick, Jr., *Secretary*
A. W. Benoit
Wendell Brown
W. L. Conrad
C. H. Ramsey

Associates

H. M. Burke
Paul Merriam
Albert Palmer
Earle Stall

Wood Industries Division

Organized, 1921

EXECUTIVE COMMITTEE

G. Rollo Petrie, *Chairman*
H. B. Carpenter, *Secretary*
A. W. Keuffel
L. M. Nichols
A. D. Smith, Jr.

Associates

C. L. Babcock
P. H. Bilhuber
F. P. Cartwright
A. S. Kurkjian
Sern Madsen
J. H. Mansfield
J. S. Mathewson
R. H. McCarthy
P. T. Norton, Jr.
T. D. Perry

SAWS AND KNIVES COMMITTEE

C. L. Babcock, *Chairman*
G. E. French, *Secretary*

RESEARCH SURVEY COMMITTEE

G. R. Petrie, *Chairman*
A. Koehler, *Secretary*

---

* Deceased.

Local Sections

(*Personnel of Standing Committee, p. 5*)

Midwest Office

R. R. Leonard, Midwest Representative,
Room 1617, 205 West Wacker Drive, Chicago, Ill.

Mid-Continent Office

J. Harold Adkison, Mid-Continent Petroleum Secretary,
213 Midco Bldg., Tulsa, Okla.

AKRON–CANTON

Organized: 1920
Territory: Counties of Richland, Ashland, Medina, Summit, Portage, Wayne, Stark, Holmes, Tuscarawas, Carroll, and Coshocton in Ohio
Number of Members: 108

Executive Committee

U. A. Whitaker, *Chairman*
H. E. Waner, *Vice-Chairman*
H. A. Trishman, *Secretary-Treasurer*
R. F. Bache
F. P. Brown
C. H. Bruggemeir
Jas. Forrest
A. J. Keller
A. D. MacLachlan
C. W. Traut

ANTHRACITE–LEHIGH VALLEY

Organized: 1920, as Lehigh Valley; reorganized, 1928, as Anthracite–Lehigh Valley
Territory: Counties of Bradford, Susquehanna, Wayne, Sullivan, Wyoming, Lackawanna, Columbia, Luzerne, Monroe, Pike, Schuylkill, Carbon, Berks, Lehigh, Northampton in Pennsylvania, and Warren in New Jersey
Place of Meeting: One meeting annually at Allentown, Bethlehem, Easton, Hazleton, Pottsville, Reading, Scranton, and Wilkes-Barre
Local Organization: The Engineers' Club of Lehigh Valley
Number of Members: 205

Executive Committee

F. H. Dechant, *Chairman*
H. C. Pickel, *Vice-Chairman*
M. C. Stuart, *Vice-Chairman*
P. B. Eaton, *Vice-Chairman*
C. W. Bell, *Secretary*
R. J. Prince, *Treasurer*
W. W. Hagerty
A. W. Luce
C. M. Merrick
J. A. Powell
Christian Schillinger
E. E. Smith
P. A. Weaver
D. G. Williams

ATLANTA

Organized: 1913
Territory: Radius of sixty miles from Atlanta, Ga.
Place of Meeting: Atlanta Athletic Club
Number of Members: 70

Executive Committee

E. W. Klein, *Chairman*
W. C. Wroe, *Vice-Chairman*
R. M. Matson, *Secretary-Treasurer*
George Braungart, Jr.
J. W. Parker, Jr.
P. R. Yopp

BALTIMORE

Organized: 1916
Territory: Radius of thirty miles from Baltimore, Md.
Place of Meeting: Engineers' Club of Baltimore
Luncheon meeting every Wednesday at 12:00 noon at Engineers' Club
Number of Members: 158

Executive Committee

J. C. Strott, *Chairman*
F. W. Kouwenhoven, *Secretary-Treasurer*
J. R. Baker
O. C. Cromwell
K. A. Hawley
N. B. Higgins
J. E. Howard
A. L. Penniman, Jr.
A. W. Taylor

BIRMINGHAM

Organized: 1915
Territory: Radius of sixty miles from Birmingham, Ala.
Place of Meeting: Auditorium of the Alabama Power Company Building
Number of Members: 51

Executive Committee

J. A. Sirnit, *Chairman*
J. W. Eshelman, *Vice-Chairman*
R. A. Polglaze, *Secretary-Treasurer*
J. M. Gilfillan
J. W. Orcutt

BOSTON

Organized: 1909
Territory: Radius of thirty miles from Boston, Mass.
Place of Meeting: Rooms of the Engineering Societies of Boston
Local Organization: Engineering Societies of Boston
Number of Members: 501

Executive Committee

A. W. Benoit, *Chairman*
J. T. Croghan, *Vice-Chairman*
G. C. Eaton, *Secretary-Treasurer*
E. L. Root
W. E. Farnham
W. F. Ryan

BRIDGEPORT

Organized: 1917, as a Branch of Connecticut Section; reorganized as a Section, 1923
Territory: Fairfield County, Conn.
Place of Meeting: University Club
Number of Members: 107

Executive Committee

H. E. Wells, *Chairman*
H. P. Harris, *Vice-Chairman*
W. H. Sniffen, *Secretary*
C. N. Hoagland, *Treasurer*
T. H. Beard
Julius Brenzinger
Arthur Brewer
W. R. Clark
A. H. Emery, Jr.
A. W. Hagan
I. C. Jennings
R. C. Moody

BUFFALO

Organized: 1915
Territory: Radius of thirty miles from Buffalo, N. Y.
Place of Meeting: Hotel Statler
Local Organization: Engineering Society of Buffalo
Number of Members: 162

Executive Committee

J. L. Yates, *Chairman*
Paul Dubosclard, *Acting Vice-Chairman*
W. A. Miller, *Secretary*
C. E. Harrington, *Treasurer*
C. Gale Kiplinger
J. Arthur Fish
H. D. Munson

CENTRAL PENNSYLVANIA

Organized: 1921
Territory: Radius of approximately sixty miles from State College, Pa.
Place of Meeting: Pennsylvania State College, State College, Pa.
Number of Members: 51

Executive Committee

F. E. Burpee, *Chairman*
C. E. Bullinger, *Secretary-Treasurer*
G. F. Elliott
H. A. Everett
S. K. Hoffman
C. H. Kent

CHARLOTTE

Organized: As a Branch, 1923; as a Section, 1927
Territory: Radius of sixty miles from Charlotte, N. C.
Number of Members: 23

Executive Committee

W. S. Lee, Jr., *Chairman*
H. M. McKelvie, *Vice-Chairman*
V. E. Fuller, *Secretary-Treasurer*
J. H. Sadler
Asa Hosmer, *Ex-Officio*

CHATTANOOGA

Organized: 1922
Territory: Radius of sixty miles from Chattanooga, Tenn.
Number of Members: 14

Executive Committee

Newell Sanders, *Chairman*
H. H. Bailey, *Vice-Chairman*
F. Ward Reilly, *Secretary-Treasurer*
T. C. Ervin
M. P. Wall

CHICAGO

Organized: 1913
Territory: Radius of fifty miles from Chicago, Ill.
Headquarters: Mid-West A.S.M.E. Office, 205 West Wacker Drive, Chicago, Ill.
Local Organization: Western Society of Engineers
Number of Members: 639

Executive Committee

R. D. Brizzolari, *Chairman*
A. E. Grunert, *Vice-Chairman*
F. B. Orr, *Secretary*
Hugo Diemer, *Treasurer*
C. C. Austin
C. B. Cole
L. D. Gayton
W. W. Winterrowd

CINCINNATI

Organized: 1912
Territory: Radius of thirty miles from Cincinnati, Ohio
Place of Meeting: Engineers' Club Rooms, Ninth & Race Sts.
Local Organization: Engineers' Club of Cincinnati
Number of Members: 199

Executive Committee

. T. Faig, *Chairman*
. A. Seyler, *Vice-Chairman*
. A. Joerger, *Secretary-Treasurer*
. H. Anderson
. W. Bunting
. E. Cardullo
. S. Dewey
W. E. M. Fielman
O. C. Hilmer
C. L. Koehler
E. A. Muller
R. S. Parker
W. W. Tangeman
H. C. Uihlein

CLEVELAND

Organized: 1918
Territory: Counties of Lorain, Cuyahoga Lake, Geauga, and Ashtabula in Ohio
Place of Meeting: Statler Hotel
Local Organization: Cleveland Engineering Society
Number of Members: 238

Executive Committee

. E. Jermy, *Chairman*
. J. Stock, *Vice-Chairman*
. M. Hammond, *Secretary*
erdinand Jehl, *Treasurer*
David Gaehr
H. A. MacKenzie
McRea Parker
G. L. Tuve
E. H. Whitlock

COLORADO

Organized: 1919
Territory: Entire State of Colorado
Place of Meeting: Parisienne Rotisserie Inn, Denver, Colo.
Local Organization: Colorado Engineering Council (Colorado Society of Engineers)
Number of Members: 84

Executive Committee

. A. Lockwood, *Chairman*
. A. Richter, *Secretary-Treasurer*
. D. Crain
Arthur Halliwell
J. A. Hunter
D. J. Nevill
F. H. Prouty

COLUMBUS

Organized: 1920
Territory: Counties of Union, Delaware, Licking, Madison, Franklin, Fayette, Pickaway, and Ross in Ohio
Place of Meeting: Batelle Memorial Institute and Ohio State University
Local Organization: Engineers' Club of Columbus
Number of Members: 79

Executive Committee

F. W. Marquis, *Chairman*
H. S. Dickerson, *Vice-Chairman*
E. M. Sampson, *Secretary-Treasurer*
S. R. Beitler
T. H. Kerr

DAYTON

Organized: 1926
Territory: Counties of Drake, Miami, Champaign, Preble, Montgomery, Greene, and northern part of Butler and Warren in Ohio
Place of Meeting: Engineers' Club of Dayton
Local Organization: Engineers' Club of Dayton
Number of Members: 73

Executive Committee

J. Q. Salisbury, *Chairman*
R. W. Martin, *Vice-Chairman*
W. E. Blank, *Secretary*
B. E. Tate, *Treasurer*
G. A. Buvinger
T. F. Rataiczak
C. M. Ripsch
H. C. Weinland

DETROIT

Organized: 1916
Territory: Radius of thirty miles from Detroit, Mich.
Place of Meeting: Place varies
Local Organization: Associated Technical Societies of Detroit
Number of Members: 356

Executive Committee

L. J. Schrenk, *Chairman*
Sabin Crocker, *Secretary-Treasurer*
B. W. Beyer, Jr.
J. A. Clauss
C. L. Eksergian
L. T. Knocke
F. J. Linsenmeyer
R. W. Smith
Stephen Timoshenko
P. H. Smith, *Ex-Officio*

ERIE

Organized: 1917
Territory: Radius of thirty miles from Erie, Pa.
Place of Meeting: Auditorium of Pennsylvania Telephone Company
Number of Members: 51

Executive Committee

A. J. Woodward, *Chairman*
G. S. Brewer, *Vice-Chairman*
H. C. Mitchell, *Vice-Chairman*
H. O. Davidson, *Vice-Chairman*
H. L. Kauffman, *Vice-Chairman*
N. A. Newton, *Vice-Chairman*
W. J. Brenner, *Secretary*
Frank Derby, *Treasurer*
George Bach
H. E. Goetz
W. L. Hunter
Herman Mueller
M. E. Smith

FLORIDA

Organized: 1925
Territory: State of Florida
Place of Meeting: Place varies
Local Organization: Florida Engineering Society, Gainesville, Fla.
Number of Members: 55

Executive Committee

H. S. Riddle, *Chairman*
Burdett Loomis, Jr., *1st Vice-Chairman*
Robert Peyinghaus, *2nd Vice-Chairman*
B. R. Van Leer, *Secretary-Treasurer*
F. J. Howe, *Student Chairman*
Charles Beensen
C. M. Lowry
H. J. B. Scharnberg
G. H. Smith
J. P. Warren

GREEN MOUNTAIN

Organized: 1923
Territory: Entire State of Vermont and neighboring and closely related communities of Claremont and Hanover, N. H.
Place of Meeting: Springfield, Windsor, Vt., and Claremont, N. H.
Local Organization: Vermont Engineering Society
Number of Members: 37

Executive Committee

J. B. Johnson, *Chairman*
M. H. Arms, *Secretary-Treasurer*
C. H. Adams
O. F. Anderson
C. S. Beach
F. E. Cheever
C. J. Dewell
H. R. Finn
R. H. Hackel
F. A. Joy
H. J. Lockwood
E. L. Susdorff

GREENVILLE

Organized: As a Branch, 1923; as a Section, 1927
Territory: Radius of sixty miles from Greenville, S. C.
Place of Meeting: Meetings held at Greenville, Clemson College, S. C., Canton, Asheville, and Enka, N. C.
Number of Members: 26

Executive Committee

J. R. Gill, *Chairman*
R. H. Chapman, *Vice-Chairman*
J. B. Mayo, *Secretary-Treasurer*
C. D. Blackwelder
W. R. Crute
B. E. Fernow
R. B. Fuller
W. H. Taylor
R. C. Trammell

HARTFORD

Organized: 1917, as a Branch of Connecticut Section; reorganized as a Section, 1923
Territory: Hartford County except that portion served by Meriden and New Britain Sections
Place of Meeting: Connecticut State Trade School
Number of Members: 101

Executive Committee

E. R. Fish, *Chairman*
H. B. Van Zelm, *Vice-Chairman*
E. S. Wolston, *Secretary-Treasurer*
W. C. Beekley
E. P. Herrick
L. W. Stevens

HOUSTON

Organized: 1919
Territory: South Texas and the northern part of the State not included in the North Texas Section territory
Place of Meeting: Electric Bldg., Houston, Tex.
Number of Members: 112

Executive Committee

J. H. Dubendorf, *Chairman*
J. M. Robertson, *Vice-Chairman*
J. E. Montgomery, *Secretary*
W. T. Alliger
V. M. Faires
G. G. Harrington
J. H. Pound
C. M. Rosebrugh
B. E. Short
J. K. Swinford
E. R. Breaker

INDIANAPOLIS

Organized: 1916
Territory: Radius of eighty miles from Indianapolis, within Indiana
Place of Meeting: Place varies
Local Organization: Indiana Engineering Society
Number of Members: 115

Executive Committee

D. B. Prentice, *Chairman*
J. H. Maguire, *Vice-Chairman*
J. C. Siegesmund, *Secretary-Treasurer*
F. C. Hockema
Homer Rupard

INLAND EMPIRE

Organized: 1921
Territory: East of Columbia River in State of Washington, and Counties of Okanogan and Benton, and portion of Northern Idaho
Place of Meeting: Davenport Hotel, Spokane
Luncheon Meetings every Wednesday at 12:00 noon, Davenport Hotel, Spokane
Local Organization: Associated Engineers of Spokane
Number of Members: 21

Executive Committee

D. R. Gray, *Chairman*
U. B. Hough, *Vice-Chairman*
C. I. Carpenter, *Secretary-Treasurer*
H. F. Gause
H. J. MacCamy
L. J. Pospisil

KANSAS CITY

Organized: 1921
Territory: Radius of sixty miles from Kansas City, Mo.
Place of Meeting: Hotel President
Local Organization: Engineers' Club of Kansas City
Number of Members: 89

Executive Committee

E. L. McDonald, *Chairman*
E. D. Hay, *Vice-Chairman*
H. A. Smith, *Secretary*
P. A. White, *Treasurer*
H. A. Atwater
W. G. Cramer
E. L. Hendrickson
F. J. Holzbaur
A. C. Kirkwood
J. A. Walter

KNOXVILLE

Organized: 1923
Territory: All the counties east of the west boundaries of the following, Morgan, Roane, Loudon, McMinn, Scott, and Polk, Tenn., and Bell County, Ky.
Place of Meeting: Andrew Johnson Hotel
Number of Members: 39

Executive Committee

E. W. Palmer, *Chairman*
J. P. Ferris, *Vice-Chairman*
E. L. Carpenter, *Secretary-Treasurer*
Walter Carson, Jr.
Wendell Kennedy
W. F. Searle, Jr.

LOS ANGELES

Organized: 1915
Territory: South of southern boundaries of following counties, Monterey, Kings, Tulares, and Inyo, Calif.
Place of Meeting: Place varies
Local Organization: Technical Societies of Los Angeles
Number of Members: 318

Executive Committee

D. P. Vail, *Chairman*
J. R. Hoffman, *Vice-Chairman*
S. M. Dunn, *Secretary-Treasurer*
E. C. Barkstrom
D. E. Dickey
L. G. Metcalf
W. Roy Shettel

LOUISVILLE

Organized: 1922
Territory: Radius of thirty miles from Louisville, Ky.
Place of Meeting: Engineers' and Architects Club of Louisville
Local Organization: Engineers' and Architects Club
Number of Members: 34

Executive Committee

J. F. Hurst, *Chairman*
L. S. Vance, *Vice-Chairman*
H. H. Fenwick, *Secretary-Treasurer*
B. M. Brigman
J. H. Romann

MEMPHIS

Organized: 1923
Territory: Radius of sixty miles from Memphis, Tenn.
Number of Members: 28

Executive Committee

L. H. Hungate, Jr., *Chairman*
R. V. Downs, *Vice-Chairman*
J. J. Ryan, *Secretary-Treasurer*
T. H. Allen
M. W. Rice
W. H. Roberts
J. S. Robinson

MERIDEN

Organized: 1917, as a Branch of Connecticut Section; reorganized as a Section, 1923
Territory: Meriden, Middletown, Southington, Portland, Plantsville, and Wallingford, Conn.
Place of Meeting: State Trade School Auditorium
Number of Members: 25

Executive Committee

C. A. Newton, *Chairman*
R. W. Stetson, *Secretary-Treasurer*
H. C. Cashen
J. A. Hutchinson
L. B. Marcy
E. A. Robinson

METROPOLITAN

Organized: 1910
Territory: Metropolitan District, New York and New Jersey
Place of Meeting: Engineering Societies Building, New York, N. Y.
Number of Members: 3459

Executive Committee

J. N. Landis, *Chairman*
R. B. Purdy, *Secretary*
W. H. Armacost, *Treasurer*
W. W. Clinedinst
E. S. Crosby
W. C. Glass
John Hoffhine
T. E. Keating
W. L. Tann
G. B. Pegram, *Ex-Officio*

MID-CONTINENT

Organized: 1919
Territory: Entire States of Oklahoma and Arkansas, and a part of Louisiana. In Texas north of the southern boundaries of the counties of Gaines, Dawson, Bordon, Scurry, Fisher, Jones, and Shackelford
Place of Meeting: 213 Midco Building, Tulsa, Okla.
Number of Members: 148

Executive Committee

Hollis P. Porter, *Chairman*
J. M. McGregor, *Vice-Chairman*
J. F. Eaton, *Secretary*
H. W. Manley, *Treasurer*
F. S. Kelly, Jr.
V. L. Maleev
R. G. Paddock

MILWAUKEE

Organized: 1904
Territory: Radius of fifty miles from Milwaukee, Wis.
Place of Meeting: Milwaukee Athletic Club
Local Organization: Engineers' Society of Milwaukee
Number of Members: 196

Executive Committee

W. D. Bliss, *Chairman*
A. H. Luedicke, *Secretary-Treasurer*
C. A. Cahill
Hans Dahlstrand
F. H. Dorner
Arthur Simon

MINNESOTA

Organized: Minneapolis, 1913; St. Paul, 1913; merged the two Sections, 1934
Territory: Entire State of Minnesota
Place of Meeting: Minnesota Union
Local Organization: Minneapolis Engineers' Club, Minnesota Federation of Architectural and Engineering Societies
Number of Members: 92

Executive Committee

G. F. Endicott, *Chairman*
Melvin Ovestrud, *Vice-Chairman*
L. A. Cobb, *Secretary-Treasurer*
P. J. Frawley
R. E. Gibbs
C. A. Herrick
H. O. Washburn

NEBRASKA

Organized: 1922
Territory: State of Nebraska, and Council Bluffs, Iowa
Place of Meeting: Lincoln and Omaha
Local Organization: Engineers' Club of Lincoln and Omaha
Number of Members: 32

Executive Committee

W. L. DeBaufre, *Chairman*
R. B. Boals, *Vice-Chairman*
L. A. Luebs, *Secretary-Treasurer*
A. E. Bunting
C. F. Moulton
R. H. Park
R. J. Prohaska

NEW BRITAIN

Organized: 1921, as a Branch of Connecticut Section; reorganized as a Section, 1923
Territory: New Britain, Plainville, Forestville, Bristol, Kensington, and Berlin, Conn.
Place of Meeting: Auditorium of the State Trade School
Number of Members: 35

Executive Committee

R. A. Grise, *Chairman*
P. W. Bauer, *Vice-Chairman*
C. W. Lund, *Secretary-Treasurer*
R. H. Barlow
B. S. Lewis
H. L. Spaunburg
C. C. Stevens
W. Clements Zinck

NEW HAVEN

Organized: 1912; reorganized, 1923
Territory: Portions of New Haven and Middlesex Counties, Conn.
Place of Meeting: Mason Laboratory, Yale University
Number of Members: 88

Executive Committee

C. W. Taylor, *Chairman*
H. R. Polleys, *Secretary-Treasurer*
A. L. Breckenridge
P. H. English
G. E. Hulse
J. C. Menzies
M. J. Radecki

NEW ORLEANS

Organized: 1916
Territory: All of Louisiana except the northern part allotted to Mid-Continent Section
Place of Meeting: Room 422, St. Charles Hotel
Local Organization: Louisiana Engineering Society
Number of Members: 83

Executive Committee

R. F. Muller, *Chairman*
C. A. Bender, Jr., *Secretary-Treasurer*
J. S. Netherwood
A. D. Stancliff
D. W. Stewart

NORTH TEXAS

Organized: 1922
Territory: Radius of one hundred and twenty-five miles from Dallas, in Texas
Place of Meeting: University Club, Dallas, Texas
Local Organization: Technical Club of Dallas
Number of Members: 50

Executive Committee

E. W. Burbank, *Chairman*
R. R. Crowdus, *Secretary-Treasurer*
P. M. Cordell
W. B. Gregory
R. W. Howe

NORWICH

Organized: 1930
Territory: Counties of Tolland, Windham, and New London in Connecticut, and Westerly District in Rhode Island
Place of Meeting: Arcanum Club, 150 Main St., Norwich
Number of Members: 30

Executive Committee

Lovelock Holm, *Chairman*
W. E. Beaney, *Secretary-Treasurer*
C. E. Barber
W. L. Edel
F. S. English
C. W. Phelps
L. E. Whiton

ONTARIO

Organized: 1917
Territory: Province of Ontario, Canada
Place of Meeting: Mining Building, University of Toronto
Number of Members: 86

Executive Committee

O. W. Ellis, *Chairman*
F. G. East, *Secretary-Treasurer*
E. A. Allcut
W. S. Ball
C. H. McL. Burns
F. H. Eland
S. L. Fear
W. G. McIntosh
W. A. Osbourne
W. A. Richards
P. G. Welford

OREGON

Organized: 1919
Territory: State of Oregon and that territory in Washington within a radius of thirty miles from Portland, Ore.

Place of Meeting: University Club, Portland, Ore.
Local Organization: Oregon Society of Engineers
Number of Members: 52

EXECUTIVE COMMITTEE

W. H. MARTIN, *Chairman* S. M. LISTER
J. E. DYER, *Secretary-Treasurer* G. F. McDOUGALL
A. A. OSIPOVICH

PENINSULA

Organized: 1923
Territory: West of the east boundaries of the following counties: Emmet, Charlevoix, Antrim, Kalkaska, Missaukee, Clare, Isabella, Gratiot, Clinton, Eaton, Calhoun, and Branch, Mich.
Place of Meeting: Grand Rapids, Mich.
Local Organization: Engineers' Club of Grand Rapids
Number of Members: 50

EXECUTIVE COMMITTEE

LEROY L. BENEDICT, *Chairman* S. H. DOWNS
B. A. PARKS, *Vice-Chairman* C. H. GRINNELL
F. H. MEYER, *Secretary-Treasurer* E. E. NORMAN

PHILADELPHIA

Organized: 1912
Territory: Counties of Bucks, Montgomery, Chester, Philadelphia, Delaware, Pa., and the State of Delaware
Place of Meeting: Philadelphia Engineers' Club
Local Organization: Philadelphia Engineers' Club
Number of Members: 771

EXECUTIVE COMMITTEE

G. E. CROFOOT, *Chairman* E. R. GLENN
W. F. OBERHUBER, *Vice-Chairman* C. C. JONES
J. P. HARBESON, *Secretary-Treasurer* COLEMAN SELLERS, 3RD

PITTSBURGH

Organized: 1920
Territory: Counties bounded by and including Beaver, Butler, Venango, Forest, Jefferson, Indiana, Somerset, Fayette, Greene, and Washington, Pa.
Place of Meeting: Engineers' Society of Western Pennsylvania, William Penn Hotel
Local Organization: Engineers' Society of Western Pennsylvania
Number of Members: 365

EXECUTIVE COMMITTEE

L. E. HANKISON, *Chairman* LOUIS ELLMAN
K. F. TRESCHOW, *Secretary-Treasurer* W. N. FLANAGAN
R. B. AMBROSE R. J. S. PIGOTT

PLAINFIELD

Organized: 1921
Territory: Plainfield and territory included between Elizabeth, Bound Brook, Metuchen, and Watchung, N. J.
Place of Meeting: Elks Club, Elizabeth, Park Hotel, Plainfield
Local Organization: Plainfield Engineers Club, Singer Engineering Society
Number of Members: 217

EXECUTIVE COMMITTEE

F. C. SPENCER, *Chairman* D. V. WATERS, *Secretary*
RICHARD KAIER, *Vice-Chairman* J. P. FABER, *Treasurer*
W. B. UPDEGRAFF

PROVIDENCE

Organized: 1920
Territory: Radius of thirty miles from Providence, R. I.
Place of Meeting: Providence Engineering Society Building, 195 Angell St., Providence, R. I.
Local Organization: Providence Engineering Society
Number of Members: 134

EXECUTIVE COMMITTEE

A. C. CHICK, *Chairman* F. A. CHIFFELLE
Z. R. BLISS, *Vice-Chairman* C. F. MILLER
A. WILLIAM MEYER, *Secretary-Treasurer* S. A. VAULE

RALEIGH

Organized: As a Branch, 1923; as a Section, 1927
Territory: Radius of sixty miles from Raleigh, N. C.
Place of Meeting: N. C. State College, Raleigh, N. C.
Local Organization: N. C. Engineering Council, Raleigh Engineers Club
Number of Members: 31

EXECUTIVE COMMITTEE

R. P. KOLB, *Chairman* R. D. ANTHONY
R. S. WILBUR, *Vice-Chairman* B. B. GUY
J. M. FOSTER, *Acting Secretary-Treasurer*

ROCHESTER

Organized: 1919
Territory: Radius of thirty miles from Rochester, N. Y.
Place of Meeting: Rochester Engineering Society Rooms, Sagamore Hotel
Local Organization: Rochester Engineering Society, Sagamore Hotel
Number of Members: 99

EXECUTIVE COMMITTEE

A. E. SCHELL, *Chairman* J. F. ANCONA
W. D. SEELEY, *Vice-Chairman* K. C. CASTLE, JR.
I. G. McCHESNEY, *Secretary-Treasurer* C. C. ROSS
O. V. SPRAGUE

ROCK RIVER VALLEY

Organized: 1926
Territory: Radius of thirty miles from Rockford, Ill.
Local Organization: Rockford Engineering Society
Number of Members: 43

EXECUTIVE COMMITTEE

F. P. GRUTZNER, *Chairman* A. C. MATTISON
M. B. MACNEILLE, *Vice-Chairman* ROBERT VON ROTZ
HERMAN HUGLE, *Secretary-Treasurer*

ST. JOSEPH VALLEY

Organized: 1929
Territory: Counties of La Porte, Starke, Pulaski, St. Joseph, Marshall, Fulton, Elkhart, and Kosciusko in Indiana, and Cass and Berrien Counties in Michigan
Place of Meeting: Morningside Hotel, South Bend, Ind.
Local Organization: St. Joseph Valley Engineers' Club
Number of Members: 35

EXECUTIVE COMMITTEE

C. R. ADAMS, *Chairman* C. C. WILCOX, *Vice-Chairman*
K. W. KNORR, *Secretary-Treasurer*

ST. LOUIS

Organized: 1909
Territory: Radius of thirty miles from St. Louis, Mo.
Place of Meeting: Place varies
Local Organization: Engineers' Club of St. Louis
Number of Members: 213

EXECUTIVE COMMITTEE

R. M. BOYLES, *Chairman* E. W. DAVIS
G. L. SHANKS, *Vice-Chairman* J. R. JACKSON
E. H. SAGER, *Secretary-Treasurer* F. W. RABE

SAN FRANCISCO

Organized: 1910
Territory: All territory north of the northern boundaries of the counties of San Luis Obispo, Kern, and San Bernardino
Place of Meeting: Engineers' Club, 206 Sansome St.
Luncheon Meetings every Thursday at 12:15 Noon at the Engineers Club
Local Organization: San Francisco Engineers' Club
Number of Members: 337

Executive Committee

H. B. Langille, *Chairman*
F. W. Collins, *Vice-Chairman*
R. L. Grutzmacher, *Secretary-Treasurer*
S. R. Dows
W. M. Moody
M. P. O'Brien
H. J. Smith
Lawrence Washington

SAVANNAH

Organized: 1923
Territory: Radius of 125 miles from Savannah in Georgia
Place of Meeting: Savannah Hotel
Local Organization: Engineers' Council of Savannah Chamber of Commerce
Number of Members: 15

Executive Committee

A. P. Keisker, *Chairman*
Bruce Sams, *Vice-Chairman*
T. R. Jones, *Secretary*
Frank Exley, *Treasurer*
W. H. Artley
D. E. Kehoe
A. M. Ormond

SCHENECTADY

Organized: As a Branch, 1919; as a Section, 1927
Territory: Radius of thirty miles from Schenectady, N. Y.
Place of Meeting: Edison Club Hall
Number of Members: 173

Executive Committee

W. E. Johnson, *Chairman*
J. E. Anderson, *Secretary*
B. O. Buckland, *Treasurer*
A. I. Lipetz
A. J. Nerad
E. L. Robinson

SUSQUEHANNA

Organized: 1927
Territory: Counties of Cumberland, Dauphine, Lebanon, Adams, York, and Lancaster
Place of Meeting: Engineering Society of York
Local Organization: Engineering Society of York
Number of Members: 67

Executive Committee

William Noyes, *Chairman*
Jacob Fisch, *Vice-Chairman*
H. B. Martin, *Secretary-Treasurer*
Walter Knapp
R. M. Spengler

SYRACUSE

Organized: 1920
Territory: Radius of thirty miles from Syracuse, N. Y.
Place of Meeting: Ball Room of the Onondaga Hotel
Local Organization: The Technology Club of Syracuse
Number of Members: 115

Executive Committee

H. B. Craig, *Chairman*
S. T. Hart, *Vice-Chairman*
E. K. Rhodes, *Secretary-Treasurer*
K. H. Caskey
D. W. Diefendorf
A. G. Forssell
E. W. Zimmerman

TOLEDO

Organized: 1920
Territory: Radius of thirty miles from Toledo, Ohio
Place of Meeting: University Club, Toledo, Ohio
Local Organization: Affiliated Technical Societies of Toledo
Number of Members: 58

Executive Committee

E. P. Raymond, *Chairman*
Henry Kerr, *Vice-Chairman*
C. W. Kirsch, *Secretary-Treasurer*
R. M. Batch
D. M. Palmer, *Ex-Officio*
D. L. Feltham
J. R. Moser
C. B. Schafer
I. F. Zarobsky

TRI-CITIES

Organized: 1920
Territory: Radius of thirty miles from Moline, Ill.
Place of Meeting: Rock Island, Ill., Moline, Ill., and Davenport, Iowa
Luncheon Meeting every Wednesday, Davenport Hotel, 12:00 Noon
Number of Members: 62

Executive Committee

R. M. Barnes, *Chairman*
G. T. Schoemaker, *Vice-Chairman*
C. A. Carlson, *Secretary-Treasurer*
J. M. Hartman
W. P. Hunt
J. H. Ploehn

UTAH

Organized: 1923
Territory: State of Utah
Place of Meeting: University Club, Salt Lake City
Local Organization: Utah Society of Engineers
Number of Members: 26

Executive Committee

E. W. Pace, *Chairman*
W. J. Cope, *Vice-Chairman*
M. B. Hogan, *Secretary-Treasurer*
Julius Billeter
H. D. Landes
F. W. McEntire

UTICA

Organized: 1920
Territory: Radius of thirty miles from Utica, N. Y.
Local Organization: Mohawk Valley Technical Club
Number of Members: 26

Executive Committee

E. G. Munson, *Chairman*
Rex Witherbee, *Secretary-Treasurer*
W. J. Clement

VIRGINIA

Organized: 1919
Territory: State of Virginia
Place of Meeting: Richmond, Norfolk, Charlottesville, Roanoke, University, Petersburg
Number of Members: 126

Executive Committee

A. F. Macconochie, *Chairman*
F. T. Morse, *Secretary*
H. C. Hesse, *Treasurer*
F. F. Groseclose
J. B. Woodward
A. F. Keane
E. F. Kroner
E. W. Miller
E. J. F. Wilson

WASHINGTON, D. C.

Organized: 1919
Territory: District of Columbia
Place of Meeting: Auditorium, Potomac Electric Power Co., 10th & E Sts., Washington, D. C.
Number of Members: 162

Executive Committee

H. N. Eaton, *Chairman*
M. E. Weschler, *Vice-Chairman*
J. F. Fox, *Secretary-Treasurer*
J. G. Adair
Tawson Price
A. J. Schwartz
M. X. Wilberding

WATERBURY

Organized: 1917, as a Branch of Connecticut Section; reorganized as a Section, 1923
Territory: Litchfield County and a portion of New Haven County
Place of Meeting: Waterbury Club
Number of Members: 72

Executive Committee

M. J. Dempsey, *Chairman*
A. L. Davis, *Vice-Chairman*
R. L. Palatine, *Secretary-Treasurer*
S. G. Bean
E. J. Daly
J. H. Roberts

WEST VIRGINIA

Organized: 1925
Territory: State of West Virginia
Place of Meeting: Charleston, W. Va.
Number of Members: 61

Executive Committee

E. L. Hudson, *Chairman*
J. F. Malloy, *Secretary-Treasurer*
E. R. Habicht
Andrew Hill

WESTERN MASSACHUSETTS

Organized: 1922
Territory: Includes counties of Berkshire, Franklin, Hampden, and Hampshire
Place of Meeting: Highland Hotel, Springfield, Mass.
Local Organization: Engineering Society of Western Massachusetts
Number of Members: 95

Executive Committee

P. W. Bidwell, *Chairman*
R. L. Bosworth, *Vice-Chairman*
L. G. Carlton, *Secretary-Treasurer*
C. E. Maynard
E. Lovell Smith
G. R. Wholean

WESTERN WASHINGTON

Organized: 1919
Territory: State of Washington west of the Columbia River with the exception of the territory included in the thirty-mile radius of Portland, Ore.
Place of Meeting: Engineers' Club, Arctic Bldg., Seattle, Wash.
Local Organization: Seattle Engineers' Club
Number of Members: 77

Executive Committee

F. B. Lee, *Chairman*
R. E. Johnson, *Vice-Chairman*
R. L. Dyer, *Secretary-Treasurer*
C. P. Mann
W. A. McKenzie
R. E. Walter
G. S. Wilson

WORCESTER

Organized: 1915
Territory: Radius of thirty miles from Worcester, Mass.
Place of Meeting: Rooms of the Worcester Engineering Society
Local Organization: Worcester Engineering Society
Number of Members: 138

Executive Committee

H. C. Kendall, *Chairman*
S. N. McCaslin, *Secretary-Treasurer*
H. W. H. Beth
A. W. Blackburn
E. H. Carroll
Robert Erickson
V. C. King
T. L. F. Larsson
K. C. Monroe
F. W. Roys

YOUNGSTOWN

Organized: 1928
Territory: Counties of Trumbull, Mahoning, and Columbiana in Ohio, and Mercer and Lawrence in Pennsylvania
Place of Meeting: Central Y. M. C. A., Youngstown, Ohio
Number of Members: 67

Executive Committee

E. M. Richards, *Chairman*
S. M. Adams, *Secretary-Treasurer*
Gordon Armstrong
E. E. Kendall
Cornel Kmentt
M. H. Mawhinney
H. Ovesen
F. R. Schaefer
R. M. Smith

Student Branches

(*Personnel of Standing Committee on Relations With Colleges, page 5. Communicate with Student Branch through Honorary Chairman*)

Name and Location	Year Authorized	Chairman	Secretary	Honorary Chairman
Akron, Univ. of, Akron, Ohio	1924	William Leavenworth	Paul Wagner	F. S. Griffin
Alabama Polytechnic Inst., Auburn, Ala.	1920	F. R. Ball, Jr.	D. O. Nichols, Jr.	C. R. Hixon
Alabama, Univ. of, University, Ala.[1]	1931	L. E. Morrison	Herman Schwabe	J. M. Gallalee
Arkansas, Univ. of, Fayetteville, Ark.	1910	J. W. Cartinhour	R. H. Blood	R. G. Paddock
Armour Inst. of Technology, Chicago, Ill.	1909	J. H. DeBoo	F. J. Meyer	Daniel Roesch
Brooklyn, Polytechnic Inst. of, Brooklyn, N. Y.	1909	Donald McCormick	J. R. Blizard	Gerado Immediato
Brown Univ., Providence, R. I.	1923	R. S. Shaw	R. F. Hopkins	J. A. Hall
Bucknell Univ., Lewisburg, Pa.	1916	J. D. Morris	G. F. Zimmerman	G. M. Kunkel
California Inst. of Technology, Pasadena, Calif.	1914	Allen Ray	Robert Hallanger	Howard Clapp
California, Univ. of, Berkeley, Calif.	1912	Charles Harband	W. L. Rodman[2]	N. F. Ward
Carnegie Inst. of Technology, Pittsburgh, Pa.	1913	W. H. Stafford	Walter Applegate	S. B. Ely
Case School of Applied Science, Cleveland, Ohio	1913	R. A. Taborsky	R. M. Skidmore	E. S. Ault
Catholic Univ of America, Washington, D. C.	1922	C. J. Dvorak	R. J. Green	M. E. Weschler
Cincinnati, Univ. of, Cincinnati, Ohio[3]	1909	George Gentry	A. P. McArthur	C. A. Joerger
Clarkson College of Technology, Potsdam, N. Y.	1930	S. O. Carpenter	E. I. Bricker	J. H. Davis
Clemson Agricultural College, Clemson College, S. C.	1921	H. A. Plowden	J. B. Cox, Jr.	B. E Fernow
Colorado Agricultural College, Fort Collins, Colo.	1914	Carl Ritter	John Sudduth	Joseph Pinsky
Colorado, Univ. of, Boulder, Colo.	1914	W. T. Lucking	W. B. Swan	G. S. Dobbins
Columbia Univ., New York, N. Y.	1909	William Geoghegan	M. A. Shriro	J. R. Hicks
Cooper Union, New York, N. Y.	1920	N. M. Stefano	M. Yesowitz	H. F. Roemmele
Cornell Univ., Ithaca, N. Y.	1908	H. A. Mason	J. S. Leslie	F. O. Ellenwood
Delaware, Univ. of, Newark, Del.	1929	Eugene Madey	D. W. Selby	W. Francis Lindell
Detroit, Univ. of, Detroit, Mich.	1930	W. B. Oakley	Karl Santti	H. E. Mayrose
Drexel Inst., Philadelphia, Pa.	1920	J. W. Reid	A. E. Juram[4]	Dawson Dowell
Florida, Univ. of, Gainesville, Fla.	1926	Fred Howe	E. W. McKnight	B. R. Van Leer
George Washington Univ., Washington, D. C.	1924	E. J. Thomas	C. H. Swanson	B. C. Cruickshanks
Georgia School of Technology, Atlanta, Ga.	1915	M. G. Keiser	L. J. Drum	N. C. Ebaugh
Idaho, Univ. of, Moscow, Idaho	1925			H. E. Gauss
Illinois, Univ. of, Urbana, Ill.	1909	W. A. Johnson	C. W. Brissenden	C. H. Casberg
Iowa State College, Ames, Iowa	1919	D. E. Pfitzenmaier	W. J. Schlagel	N. P. Bailey
Iowa, State Univ. of, Iowa City, Iowa	1913	William Busby	D. E. Nelson	R. M. Barnes
Johns Hopkins Univ., Baltimore, Md.	1917	T. H. Marshall	J. R. Curtis, Jr.	A. G. Christie
Kansas State Agricultural College, Manhattan, Kan.	1914	T. G. Beckwith	R. E. Torkelson	A. J. Mack
Kansas, Univ. of, Lawrence, Kan.	1909	D. C. Williams	R. G. Warren	J. A. King
Kentucky, Univ. of, Lexington, Ky.	1911	Stanford Neal	Elizabeth Warren	C. C. Jett
Lafayette College, Easton, Pa.	1919	G. L. Williams	M. E. Ackerly	C. M. Merrick, 3rd
Lehigh Univ., Bethlehem, Pa.	1911	G. A. Dornin, Jr.	R. M. Eichnor	A. W. Luce
Lewis Inst., Chicago, Ill.	1933	Charles Mackie	David Redman	J. S. Kozacka
Louisiana State Univ., Baton Rouge, La.	1916	I. J. Kirkman	Luke Hadnot	Hamilton Johnson
Louisville, Univ. of, Louisville, Ky.	1928	V. E. Furnas, Jr.	K. W. Scott	R. S. Trosper
Lowell Textile Inst., Lowell, Mass.	1921	E. H. Fairbanks	J. Raymond Kaiser	H. J. Ball

[1] Aeronautic Division, E. Boniface, *Chairman*, J. Smole, *Secretary*
[2] Frederick Woodward, *Corresponding Secretary*
[3] Section 2, Harry Paine, *Chairman*, R. J. Thompson, *Secretary*
[4] Bayard Quinn, *Corresponding Secretary*

Student Branches (continued)

Name and Location	Year Authorized	Chairman	Secretary	Honorary Chairman
Maine, Univ. of, Orono, Maine	1910	S. T. Favor	R. L. Perkins, Jr.	I. H. Prageman
Marquette Univ., Milwaukee, Wis.	1923	J. W. Krueger	Joseph Kropka	J. E. Schoen
Massachusetts Inst. of Technology, Cambridge, Mass.	1909	P. P. Johnston	H. B. Kimball	James Holt
Michigan College of Mining and Technology, Houghton, Mich.	1930	H. C. Cuskie	R. J. Cosgrove	H. W. Risteen
Michigan State College, East Lansing, Mich.	1917	Paul DeKoning	H. G. English	W. E. Reuling
Michigan, Univ. of, Ann Arbor, Mich.	1914	J. F. Schmidt	L. V. Colwell	O. W. Boston
Minnesota, Univ. of, Minneapolis, Minn.	1913	E. S. Howard	M. L. Olson	J. J. Ryan
Mississippi State College, State College, Miss.	[illegible]	W. W. Denton, Jr.	S. L. Foster, Jr.	O. D. M. Varnado
Missouri School of Mines and Metallurgy, Rolla, Mo.	1930	George Nolde	Rudolph Knoll	R. O. Jackson
Missouri, Univ. of, Columbia, Mo.	1909	B. Morris Baker	K. W. Miller	J. R. Wharton
Montana State College, Bozeman, Mont.	1920	Wayne Linthacum	G. B. Hill	Eric Therkelsen
Nebraska, Univ. of, Lincoln, Neb.	1909	H. E. Simonson	E. R. Dexter	W. F. Weiland
Nevada, Univ. of, Reno, Nev.	1923	Lawrence Kearney	James Crawford	F. H. Sibley
Newark College of Engineering, Newark, N. J.	1924	B. B. Reilly	A. B. Sweet	R. B. Rice
New Hampshire, Univ. of, Durham, N. H.	1926	Joseph VanderHoeff	H. H. Wilkins	T. J. Laton
New York, College of the City of, New York, N. Y.	1922	Bernard Maslow	Milton Dormont	Frederick Kuhle
New York Univ., New York, N. Y.[5]	1917	Bartholomew Antonucci	M. E. Mundel	A. C. Coonradt
New York Univ., Evening Division, New York, N. Y.	1933	E. A. Horner	H. W. Koster	A. C. Coonradt
North Carolina State College, Raleigh, N. C.	1920	J. L. Summers	W. F. Moody, Jr.	L. L. Vaughan
North Carolina, Univ. of, Chapel Hill, N. C.	1929	Calder Atkinson	J. D. Maynard	Colin Carmichael
North Dakota Agricultural College, Fargo, N. D.	1929	Ernest Hall	Charles Martin	R. M. Dolve
North Dakota, Univ. of, Grand Forks, N. D.	1923	C. F. MacKean	J. H. Reinertson	A. J. Diakoff
Northeastern Univ., Boston, Mass.	1922	M. C. Bennett (Div. A) C. [illegible] (Div. B)	A. W. Dudley (Div. A) R. L. Allen (Div. B)	J. W. Zeller (Divs. A and B)
Notre Dame, Univ. of, Notre Dame, Ind.	1929	Paul Dougher	Louis Crystal	C. C. Wilcox
Ohio Northern Univ., Ada, Ohio	1922	Stanley Schear	Charles Bailey	J. A. Needy
Ohio State Univ., Columbus, Ohio	1911	H. E. Allspach	J. A. Lucas	F. W. Marquis
Oklahoma A. & M. College, Stillwater, Okla.	1921	Louis Sumpter	Sanford Kroehler	R. E. Venn
Oklahoma, Univ. of, Norman, Okla.	1917	A. C. Frampton	James Mills	H. V. Beck
Oregon State Agricultural College, Corvallis, Ore.	1909	Ross Roberts	R. H. Edson	J. C. Othus
Pennsylvania State College, State College, Pa.	1909	R. Lee Homsher	F. H. Light	C. L. Allen
Pennsylvania, Univ. of, Philadelphia, Pa.	1925	O. E. Jansson	C. M. Hoffner	W. A. Sloan
Pittsburgh, Univ. of, Pittsburgh, Pa.	1917	Joseph Schmueler	R. P. Haase	J. A. Dent
Porto Rico, Univ. of, Mayaguez, P. R.	1923	Rafael Pumarada	E. H. Ruiz	Luis Stefani
Pratt Inst., Brooklyn, N. Y.	1923	John Hanby	E. C. Smith	J. W. Hunter
Princeton Univ., Princeton, N. J.	1926	Irving Warner, Jr.	Robert Cheesman	L. F. Rahm
Purdue Univ., Lafayette, Ind.	1909	J. E. Pearson	P. F. Lilly	F. C. Hockema
Rensselaer Polytechnic Inst., Troy, N. Y.	1910	D. M. Rickey	W. W. Manville	T. F. Fitzgerald
Rhode Island State College, Kingston, R. I.	1930	Raymond Pearson	Fritz Sattler	C. D. Billmyer
Rice Inst., Houston, Tex.	1925	R. H. Nollet	B. R. Ramey	A. H. Burr
Rose Polytechnic Inst., Terre Haute, Ind.	1926			H. C. Gray
Rutgers Univ., New Brunswick, N. J.	1920	L. A. Benton	Jack Spachner	U. C. Holland
Santa Clara, Univ. of, Santa Clara, Calif.	1925	J. W. Conley	E. E. Polomik	G. L. Sullivan
Southern California, Univ. of, Los Angeles, Calif.	1929	Orrin Broberg	C. H. Collins	S. F. Duncan
Southern Methodist Univ., Dallas, Tex.	1933	N. Blankenship	J. F. Schenewerk	R. R. Slaymaker
Stanford Univ., Stanford University, Calif.	1909	J. W. Clyne	K. C. Burch	Lawrence Washington
Stevens Inst. of Technology, Hoboken, N. J.	1908	W. H. Molinari	A. E. Blirer	R. F. Deimel
Swarthmore College, Swarthmore, Pa.	1921			G. A. Bourdelais
Syracuse Univ., Syracuse, N. Y.	1912	H. Carlyle Dugan	H. F. Howe	A. R. Acheson
Tennessee, Univ. of, Knoxville, Tenn.	1923	R. S. Robinson	Virgil Condron	F. L. Wilkinson
Texas, A. & M. College of, College Station, Tex.	1921	Karl White	H. M. Long	J. A. Trail
Texas Technological College, Lubbock, Tex.	1930	Truman Green	Lyle Hardgrave	J. C. Hardgrave
Texas, Univ. of, Austin, Tex.	1921	Marvin Williams	E. H. Moss	M. L. Begeman
Toronto, Univ. of, Toronto, Ont., Can.	1933	L. P. Baker	M. Willer	R. W. Angus
Tufts College, Tufts College, Mass.	1917	Mark Goedecke	F. Robt. Hartin	E. E. Leavitt
Tulane Univ. of Louisiana, New Orleans, La.	1933	J. T. Barrow	D. W. B. Murphy	W. B. Gregory
U. S. Naval Academy, Post Graduate School, Annapolis, Md.	1925			P. J. Kiefer
Utah, Univ. of, Salt Lake City, Utah	1923	F. C. Allen	T. R. Mackay	M. B. Hogan
Vanderbilt Univ., Nashville, Tenn.	1928	B. M. Bayer	Frank Pittman	J. E. Boynton
Vermont, Univ. of, Burlington, Vt.	1922	J. M. Libby	W. H. Connor	E. L. Sussdorff
Villanova College, Villanova, Pa.	1925	M. A. Donnelly	G. O. Hazzard	J. S. Morehouse
Virginia Polytechnic Inst., Blacksburg, Va.	1915	A. N. Bodine	B. W. Bishop	F. P. Grosclose
Virginia, Univ. of, University, Va.	1923	C. T. Montgomery	R. C. Carrick	F. T. Morse
Washington, State College of, Pullman, Wash.	1920	Don Appel	Louis Ellis	H. H. Langdon
Washington Univ., St. Louis, Mo.	1911	Arnold Schainker	L. Gross	E. H. Sager
Washington, Univ. of, Seattle, Wash.	1917	Clarence Gerber	Sholto Salmon	R. H. G. Edmonds
West Virginia, Univ. of, Morgantown, W. Va.	1922	J. F. Millan	R. B. Creel	L. D. Hayes
Wisconsin, Univ. of, Madison, Wis.	1909	Harold Mittelstaedt	William Meade	B. G. Elliott
Worcester Polytechnic Inst., Worcester, Mass.	1914	E. J. Abendschein	F. M. Angevine	H. W. Dows
Wyoming, Univ. of, Laramie, Wyo.	1925	Gale Baker	Eldon Messersmith	R. S. Sink
Yale Univ., New Haven, Conn.	1910	J. F. G. Miller	Neil Macneale, Jr.	S. W. Dudley

[5] Aeronautic Division, Sidney Freedman, *Chairman*, Irving Berler, *Secretary*

Special Research Committees

(*Personnel of Standing Committees, p. 6*)

LUBRICATION

Appointed October, 1915, to investigate the fundamental problems of lubrication, to formulate results of investigations previously made, and to keep in touch with contemporary research in this field

(The Committee is now being reorganized. In December, 1934, the Standing Committee on Research appointed a special committee to formulate a statement of the lubrication problem in its broad, present-day aspects and to recommend a program of research under the auspices of the A.S.M.E. The personnel of this special committee is as follows: N. E. Funk, *Chairman*, D. B. Bullard, M. D. Hersey, G. B. Karelitz, A. L. Kingsbury, and W. F. Parish.)

FLUID METERS

Appointed 1916, to develop the theory of fluid meters of all kinds and to report on the best methods for their installation and use

(Reorganized July, 1929)

R. J. S. Pigott, *Chairman*
J. R. Carlton, *Secretary*
H. S. Bean
S. R. Beitler
R. K. Blanchard
G. D. Conlee
W. W. Frymoyer
Louis Gess
T. H. Kerr
W. S. Pardoe
E. S. Smith, Jr.
R. E. Sprenkle
E. C. M. Stahl
T. R. Weymouth

THERMAL PROPERTIES OF STEAM

Appointed in December, 1921, to direct research on the thermal properties of water-vapor and steam from 0 C to the upper limits of temperature and pressure

(Reorganized April, 1929)

W. L. Abbott, *Vice-Chairman*
G. L. Bourne
H. N. Davis
H. C. Dickinson
Alex Dow
A. M. Greene, Jr.
R. C. H. Heck
D. S. Jacobus
J. H. Keenan
F. G. Keyes
L. S. Marks
G. A. Orrok
R. J. S. Pigott
H. V. Rasmussen
E. L. Robinson

STRENGTH OF GEAR TEETH

Appointed in December, 1921. Is investigating factors affecting the strength and life of gear teeth

R. E. Flanders, *Chairman*
C. H. Logue, *Secretary*
C. G. Barth
Earle Buckingham
A. M. Greene, Jr.
C. W. Ham
F. E. McMullen
E. W. Miller
Ernest Wildhaber

CUTTING OF METALS

Appointed in September, 1923. Is studying the problems of metal cutting, including tool materials, tool design, lubrication, cooling, and speeds and feeds

Coleman Sellers, 3rd, *Chairman*
L. N. Gulick, *Secretary*
A. L. DeLeeuw
King Hathaway
L. P. Alford
C. J. Oxford
R. D. Prosser

ELEVATOR SAFETIES

Appointed June, 1924, as a subcommittee of the Sectional Committee on Safety Code for Elevators, to study the function and operation of elevator safeties and buffers and their associated mechanisms and to develop methods of test for the approval of elevator safety devices

M. H. Christopherson, *Chairman*
O. P. Cummings, *Vice-Chairman*
J. A. Dickinson, *Secretary*
Bassett Jones
D. L. Lindquist
M. G. Lloyd
J. J. Matson
M. B. McLauthlin
W. S. Paine
S. F. Voorhees
S. W. Jones

MECHANICAL SPRINGS

Appointed December, 1923, to determine the status of the mechanical-spring art, to promote and conduct necessary and adequate research, and to develop the art to the point of standardization

J. R. Townsend, *Chairman*
C. T. Edgerton, *Secretary*
C. E. Barba
W. G. Brombacher
R. W. Cook
W. T. Donkin
Rupen Eksergian
G. E. Hansen
Benjamin Liebovitz
David Lofts
(R. D. Brizzolara, *Alternate*)
A. N. Lukens
D. J. McAdam, Jr.
R. E. Peterson
J. B. Reynolds
J. W. Rockefeller, Jr.
B. W. St. Clair
M. F. Sayre
Keith Williams
J. Kaye Wood
F. P. Zimmerli
O. B. Zimmerman

EFFECT OF TEMPERATURE ON THE PROPERTIES OF METALS

Appointed December, 1924, as a joint research committee of the A.S.T.M. and the A.S.M.E. to encourage the investigation and accumulation of data on the properties of metals used in the mechanic arts at extremely high and low temperatures

H. J. French, *Chairman*
N. L. Mochel, *Secretary*
A. D. Bailey
R. A. Bull
E. S. Dixon
H. W. Gillett
Louis Jordan
H. J. Kerr
C. L. Kinney, Jr.
H. W. Maack
C. E. MacQuigg
J. A. Mathews
P. E. McKinney
E. L. Robinson
A. E. White

BOILER FEEDWATER STUDIES

Appointed March, 1925, as a Joint Research Committee of the American Boiler Manufacturers Association, American Railway Engineering Association, American Water Works Association, Edison Electric Institute, the American Society for Testing Materials, and the A.S.M.E., to study methods of analysis and treatment of boiler feedwater for stationary and railroad practice

W. L. Abbott
S. B. Applebaum
A. D. Bailey
A. G. Christie
H. C. Dinger
D. K. French
R. E. Hall
J. A. Holmes
C. F. Hirshfeld
C. R. Knowles
A. L. Penniman, Jr.
E. B. Powell
T. E. Purcell
C. W. Rice
F. N. Speller
Kurt Toensfeldt
A. E. White
J. D. Yoder

CONDENSER TUBES

Appointed May, 1925, to investigate and report on the causes of failure of tubes used in steam condensers and similar heat interchange apparatus

A. E. White, *Chairman*
Bert Houghton, *Vice-Chairman*
P. A. Bancel
R. H. Barber
D. K. Crampton
H. M. Cushing
H. F. Eddy
V. M. Frost
W. L. Green, Jr.
C. F. Harwood
C. F. Hirshfeld
H. W. Leitch
E. F. Miller
W. B. Price
H. A. Staples
W. R. Webster
Robert Worthington
Representative of Bureau of Engineering, U. S. Navy Department

WORM GEARS

Appointed May, 1927, to investigate certain problems in connection with the action of worm gear drives and to recommend improvements in their design, manufacture, and use

Earle Buckingham, *Chairman*
G. H. Acker
L. R. Buckendale
W. H. Himes
D. L. Lindquist
A. A. Ross
B. F. Waterman
Representative of Bureau of Engineering, U. S. Navy Department

BOILER FURNACE REFRACTORIES

Appointed June, 1925, to determine the principal factors governing the failure of refractories in various types of installations, to subject these factors to detailed experimental analysis, to undertake the formulation of suitability tests and, if necessary, to attempt to develop a suitable refractory to meet the needs of severe service

W. A. Carter, *Chairman*
S. H. Barnum
G. A. Bole
M. C. Booze
W. H. Fulweiler
C. B. Grady
R. A. Heindl
C. F. Hirshfeld
D. P. Hood
R. K. Hursh
N. E. Lewis
J. S. McDowell
(F. A. Harvey, *Alternate*)
S. J. McDowell
Percy Nicholls
S. M. Phelps
E. B. Powell
R. A. Sherman
R. B. Sosman
L. J. Trostel
G. B. Wilkes

VELOCITY MEASUREMENT OF FLUID FLOW

Appointed November, 1927, to sponsor the development of an absolute method for determining the velocity of the flow of fluids by means of the location of nodal points in wave systems

W. F. Durand, *Chairman*
T. R. Weymouth

MEASURES OF MANAGEMENT

Appointed March, 1928, to attempt the reconciliation of certain economic laws affecting production, to develop formulas for management, and to collect and report information on management research

W. E. Freeland, *Chairman*
F. E. Raymond, *Secretary*
J. H. Barber
T. H. Brown
R. C. Davis
G. E. Hagemann

ABSORPTION OF RADIANT HEAT IN BOILER FURNACES

Appointed April, 1928, to make a study of the absorption of radiant heat in boiler furnaces with the purpose of developing recommendations on improved furnace design

W. J. Wohlenberg, *Chairman*
E. G. Bailey
R. M. Gates
C. W. Gordon
E. L. Lindseth
G. A. Orrok
R. J. S. Pigott
John Van Brunt

STRENGTH OF VESSELS UNDER EXTERNAL PRESSURE

Appointed June, 1929, to develop reliable design data on the strength of cylindrical and spherical surfaces under external pressure, particularly with reference to jacketed vessels

W. D. Halsey, *Chairman*
A. J. Ely
F. V. Hartman
T. McL. Jasper
A. W. Limont, Jr.
Carl Rigdon
H. E. Saunders
E. E. Shanor
J. H. Taylor
(F. S. G. Williams, *Alternate*)
D. B. Wesstrom
D. F. Windenburg

WIRE ROPE

Authorized in October, 1928, to study the factors affecting the life of wire rope so that it may be better understood and more effectively used

W. H. Fulweiler, *Chairman*
W. M. Bager
H. LeR. Brink
D. L. Lindquist
G. W. Martin
C. A. McCune
A. H. McDougall
B. V. E. Nordberg, Jr.
W. S. Paine
W. J. Ryan
George Simpson
L. E. Young

HEAVY DUTY ANTI-FRICTION BEARINGS

Appointed March, 1929, to investigate the possibilities and limitations of anti-friction bearings when applied to roll necks of rolling mills

W. Trinks, *Chairman*
H. E. Brunner
W. R. Clark
G. C. Farkell
H. H. Talbot
S. M. Weckstein
H. A. Winne

REMOVAL OF ASH AS MOLTEN SLAG FROM POWDERED-COAL FURNACES

Appointed March, 1929, to investigate the adding of fluxes as a means of increasing the fluidity of slag in boiler furnaces and thus permit its removal at operating furnace temperatures

K. M. Irwin, *Chairman*
Andrew Carnegie
T. G. Coghlan
H. M. Cushing
C. F. Hirshfeld
Percy Nicholls
E. B. Powell
P. B. Rice

AUTOMATIC OIL PIPE LINE PUMPING STATIONS

Authorized March, 1930, to develop methods of automatic control for oil pipe line pumping stations

W. G. Heltzel, *Chairman*
J. N. Hunter, *Vice-Chairman*
T. D. Williamson, *Secretary*
W. S. Baugh
W. C. Dreyer
W. H. Elliot
J. B. Ford
L. T. Gibbs
F. A. Graham
C. F. Guinn
A. N. Horne
J. K. McGoldrick
J. M. McGregor
J. B. McMahon
R. L. Middleton
O. L. Olsen
William Parkerson
W. R. Reed
F. A. Stivers
W. H. Stueve
Fred Thilenius
J. B. Thomas
F. E. Warterfield
Oscar Wolf

PRIME MOVERS FOR ROTARY DRILLING OF OIL WELLS

Appointed June, 1930, to investigate existing types of prime movers used for rotary drilling of oil wells as to their relative efficiencies, costs of operation, and general satisfaction

D. L. Trax, *Chairman*
Raymond Carr
W. H. Carson
R. R. Hawkins
H. W. Manley

CRITICAL PRESSURE STEAM BOILERS

Appointed June, 1931, to study the characteristics of high-pressure forced-circulation steam-generating units

A. A. Potter, *Chairman*
A. D. Bailey
E. G. Bailey
A. G. Christie
F. S. Clark
A. M. Houser
H. J. Kerr
G. A. Orrok
H. L. Solberg
P. W. Thompson

SAMPLING PULVERIZED FUEL IN A MOVING GAS STREAM

Appointed November, 1932, to investigate the present methods of sampling pulverized fuel and to evolve a generally satisfactory method that may be adopted as a standard

K. M. Irwin, *Chairman*
F. M. Gibson, *Secretary*
John Blizard
Ollison Craig
M. D. Engle
C. S. Gladden
A. E. Grunert
R. M. Hardgrove
J. C. Hardigg
H. J. Klotz
Henry Kreisinger
J. W. McKenzie
W. S. Morrison
G. B. Randall
R. C. Roe
E. H. Tenney

COTTON SEED PROCESSING

Appointed December, 1932, to study the mechanical problems involved in storing, conditioning, and cooking cotton seed meats

W. R. Woolrich, *Chairman*
Homer Barnes
E. L. Carpenter
W. D. Edwards
C. E. Garner
B. J. Sams

A.S.M.E. Representatives on Other Research Committees

See also A.S.M.E. Representatives on Other Activities, page 29

CORROSION COMMITTEE

American Society of Refrigerating Engineers
A. D. Little

HIGHWAY RESEARCH

Advisory Board of National Research Council
J. G. Bergquist

NON-FERROUS METALS AND ALLOYS

Advisory to the National Bureau of Standards' Committee
C. H. Bierbaum

PROPERTIES OF REFRACTORY MATERIALS

Advisory to the National Bureau of Standards' Committees
E. B. Powell

NATIONAL COMMITTEE ON WOOD UTILIZATION

Department of Commerce, National Bureau of Standards
A. E. Hall

FATIGUE PHENOMENA OF METALS

American Society for Testing Materials
W. R. Webster

Standardization Technical Committees

(*Personnel of Standing Committee, p. 6*)

SHAFTING

**Sole sponsorship. Organized October, 1918*

A.S.M.E Members (Total personnel, 17)

†C. M. Chapman, *Chairman*
†A. A. Adler
†A. H. Beyer
†J. E. Bushnell
E. E. Greve
H. C. E. Meyer
L. C. Morrow
C. W. Spicer
†G. N. VanDerhoef
†L. W. Williams

BALL AND ROLLER BEARINGS

**Joint sponsorship with the Society of Automotive Engineers. Sectional Committee organized December, 1920*

A.S.M.E. Members (Total personnel, 18)

†W. P. Kennedy, *Vice-Chairman*
†G. R. Bott
H. E. Brunner
F. H. Buhlmann
L. A. Cummings
F. G. Hughes
†G. E. Hulse
†W. L. Iliff
L. F. Nenninger
†A. E. Norton

GEARS

**Joint sponsorship with the American Gear Manufacturers Association. Sectional Committee organized June, 1921*

A.S.M.E. Members (Total personnel, 33)

B. F. Waterman, *Chairman*
†Earle Buckingham, *Vice-Chairman*
G. H. Acker
L. H. Fry
C. B. Hamilton
D. T. Hamilton
†August Hoffman
O. A. Leutwiler
G. L. Markland, Jr.
H. E. Vehslage

BOLT, NUT, AND RIVET PROPORTIONS

**Joint sponsorship with the Society of Automotive Engineers. Sectional Committee organized March, 1922*

A.S.M.E. Members (Total personnel, 52)

†A. E. Norton, *Chairman*
F. C. Billings
B. G. Braine
(D. L. Braine, *Alternate*)
†J. H. Buckley
Ellwood Burdsall
G S. Case
T. G. Crawford
M H. Flynn
H. P. Frear
Herman Koester
S. F. Newman
E. W. Reed
†F. O. Wells
R. J. Whelan
E. M. Whiting
V. R. Willoughby
(J. J. McBride, *Alternate*)
O. B. Zimmerman

* *Note:* All of the Standards Committees for which the Society is Sponsor, Joint Sponsor, or on which it has representation are organized under the procedure of the American Standards Association.

† Official A.S.M.E. representatives serving on this committee.

PIPE FLANGES AND FITTINGS

**Joint sponsorship with the Heating, Piping, and Air Conditioning Contractors National Association and the Manufacturers Standardization Society of the Valve and Fittings Industry. Sectional Committee organized October, 1921*

A.S.M.E. Members (Total personnel, 53)

†C. P. Bliss, *Chairman*
J. J. Harman, *Secretary*
W. R. Conard
Sabin Crocker
Ferdinand Fink
H. E. Haller
J. S. Hess
†N. S. Hill, Jr.
Francis Hodgkinson
†H. A. Hoffer
A. M. Houser
D. S. Jacobus
L. H. Jenks
W. R. Kremer
John Knickerbacker
C. R. Knowles
M. B. MacNeille
F. H. Morehead
†E. L. Moreland
†W. S. Morrison
L. S. Morse
C. W. Mowry
(A. L. Brown, *Alternate*)
A. L. Penniman, Jr.
Walter Samans
†C. W. Stephen
†J. R. Tanner
J. H. Taylor
H. L. Underhill
G. W. Watts
J. H. Williams
J. H. Zink

SCHEME FOR IDENTIFICATION OF PIPING SYSTEMS

**Joint sponsorship with the National Safety Council. Sectional Committee organized June, 1922*

A.S.M.E. Members (Total personnel, 30)

W. L. Bunker
Crosby Field
Willis Lawrence
†W. S. Morrison
A. K. Ohmes
†R. S. Peck
A. L. Penniman, Jr.
G. E. Sanford
H. S. Smith
F. N. Speller

SMALL TOOLS AND MACHINE TOOL ELEMENTS

**Joint sponsorship with the National Machine Tool Builders Association and the Society of Automotive Engineers. Sectional Committee organized September, 1922*

A.S.M.E. Members (Total personnel, 26)

C. W. Spicer, *Chairman*
F. O. Hoagland, *Vice-Chairman*
F. S. Blackall, Jr.
E. J. Bryant
Earle Buckingham
†F. H. Colvin
K. H. Condit
S. A. Einstein
†H. E. Harris
J. E. Lovely
†Simon MacKay
†W. C. Mueller
†E. R. Norris
Erik Oberg
C. J. Oxford
D. M. Palmer

Technical Committee No. 1 on T-Slots

A.S.M.E. Members (Total personnel, 11)

Erik Oberg, *Chairman*
E. P. Burrell
Harry Cadwallader, Jr.
Herman Casler
S. A. Einstein
R. T. Hazelton
F. O. Hoagland
E. R. Norris

Technical Committee No. 2 on Tool Holders and Tool Post Openings

A.S.M.E. Members (Total personnel, 13)

E. P. Burrell
J. D. Karle
P. M. Mueller
R. R. Weddell

Technical Committee No. 3 on Machine Tapers

A.S.M.E. Members (Total personnel, 21)

F. S. Blackall, Jr., *Chairman*
E. J. Bryant
Earle Buckingham
B. P. Graves
F. H. Colvin
J. B. Dillard
H. E. Harris
F. O. Hoagland
J. H. Horigan
A. H. Lyon
L. F. Nenninger
C. W. Spicer
F. W. Stein

Technical Committee No. 4 on Spindle Noses and Collets for Machine Tools

A.S.M.E. Members (Total personnel, 26)

J. E. Lovely, *Chairman*
B. P. Graves
F. O. Hoagland
A. M. Johnson
M. E. Lange
A. H. Lyon
J. H. Mansfield
L. F. Nenninger
H. W. Ruppel
L. D. Spence

Technical Committee No. 5 on Milling Cutters

A.S.M.E. Members (Total personnel, 21)

A. N. Goddard
J. H. Horigan
G. L. Markland, Jr.
E. K. Morgan
Erik Oberg
C. J. Oxford
E. D. Vancil

Technical Committee No. 6 on Designations and Working Ranges of Machine Tools

A.S.M.E. Members (Total personnel, 22)

K. H. Condit, *Chairman*
Earle Buckingham
T. H. Doan
B. P. Graves
J. J. McBride
Charles Schenck
E. R. Smith
W. E. Whipp

Technical Committee No. 7 on Twist Drill Sizes

A.S.M.E. Members (Total personnel, 9)

C. R. Alden, *Secretary*
J. H. Horigan
W. C. Mueller
C. J. Oxford

Technical Committee No. 8 on Drill Bushings

A.S.M.E. Members (Total personnel, 9)

C. R. Alden, *Secretary*
J. H. Horigan
W. C. Mueller
C. J. Oxford
H. E. Wells

Technical Committee No. 9 on Punch Press Tools

A.S.M.E. Members (Total personnel, 17)

D. M. Palmer, *Chairman*
D. H. Chason
A. J. Cummings
N. W. Dorman
H. E. Harris
W. C. Mueller
H. E. Wells

Technical Committee No. 10 on Circular Forming Tools and Holders

A.S.M.E. Members (Total personnel, 9)

W. C. Mueller
D. H. Montgomery
L. D. Spence
H. E. Wells

Technical Committee No. 11 on Chucks and Chuck Jaws

A.S.M.E. Member (Total personnel, 9)

J. E. Lovely, *Chairman*

Technical Committee No. 12 on Cut and Ground Thread Taps

A.S.M.E. Member (Total personnel, 7)

W. C. Mueller

Technical Committee No. 13 on Splines and Splined Shafts

A.S.M.E. Members (Total personnel, 11)

C. W. Spicer, *Chairman*
W. F. Groene
R. E. W. Harrison
F. O. Hoagland
B. F. Waterman

Technical Committee No. 14 on Electric Welding Dies and Electrode Holders

A.S.M.E. Members (Total personnel, 12)

Lewis Fine
N. McD. Loney

Technical Committee No. 15 on Milling Machine Tables

A.S.M.E. Members (Total personnel, 6)

B. P. Graves
L. F. Nenninger

Technical Committee No. 16 on Rotating Tool Shanks

A.S.M.E. Members (Total personnel, 19)

E. J. Bryant, *Chairman*
J. H. Horigan, *Secretary*
J. B. Dillard
E. W. Howe
W. C. Mueller
C. J. Oxford
H. E. Wells

Technical Committee No. 17 on Nomenclature

A.S.M.E. Members (Total personnel, 15)

H. E. Harris, *Chairman*
O. W. Boston, *Secretary*
F. S. Blackall, Jr.
F. H. Colvin
F. O. Hoagland

Ex-Officio Members

C. R. Alden
B. P. Graves
A. N. Goddard
C. J. Oxford
C. W. Spicer
H. E. Wells

Technical Committee No. 18 on Multiple Spindle Drilling Heads

A.S.M.E. Member (Total personnel, 10)

H. E. Wells

Technical Committee No. 19 on Single Point Cutting Tools

A.S.M.E. Members (Total personnel, 2)

F. H. Colvin, *Chairman*
O. W. Boston

SCIENTIFIC AND ENGINEERING SYMBOLS AND ABBREVIATIONS

**Joint sponsorship with the A.S.C.E., A.I.E.E., A.A.A.S., and S.P.E.E. Sectional Committee organized January, 1926*

A.S.M.E. Members (Total personnel, 33)

S. A. Moss, *Vice-Chairman*
R. M. Anderson
(E. P. Warner, *Alternate*)
K. H. Condit
†H. N. Davis
†(R. J. S. Pigott, *Alternate*)
G. W. Lewis

PLAIN AND LOCK WASHERS

**Joint sponsorship with the Society of Automotive Engineers. Sectional Committee organized March, 1926*

A.S.M.E. Members (Total personnel, 37)

†S. G. Baits
Eugene Caldwell
T. G. Crawford
†B. S. Lewis
C. H. Loutrel
J. J. McBride
H. C. E. Meyer
E. H. Waring
E. M. Whiting
O. B. Zimmerman

MACHINE PINS

**Joint sponsorship with the Society of Automotive Engineers. Sectional Committee organized March, 1926*

A.S.M.E. Members (Total personnel, 18)

†M. E. Steczynski, *Chairman*
†E. J. Bryant
J. J. McBride
H. C. E. Meyer
O. B. Zimmerman

DRAWINGS AND DRAFTING ROOM PRACTICE

**Joint sponsorship with the Society for Promotion of Engineering Education. Sectional Committee organized July, 1926*

A.S.M.E. Members (Total personnel, 52)

F. DeR. Furman, *Chairman*
C. W. Keuffel, *Secretary*
Douglas Baker
C. E. Coolidge
T. G. Crawford
H. C. Fletcher
T. E. French
A. C. Harper
A. M. Houser
Alfred Iddles
†Samuel Ketchum
F. R. Laney
H. B. Langille
W. L. McIntosh
F. W. Ming
E. B. Neil
†J. K. Olsen
J. W. Owens
F. C. Panuska
Carl Rossmassler
†E. S. Smith, Jr.

CODE FOR PRESSURE PIPING

**Sole sponsorship. Sectional Committee organized March, 1926*

A.S.M.E. Members (Total personnel, 72)

E. B. Ricketts, *Chairman*
G. S. Coffin
H. C. Cooper
Sabin Crocker
(J. A. Walker, *Alternate*)
H. D. Edwards
C. A. Ellis
Charles Fitzgerald
O. S. Hagerman
H. E. Haller
(G. J. Stuart, *Alternate*)
J. J. Harman
J. S. Haugh
(E. B. Severs, *Alternate*)
J. S. Hess
H. A. Hoffer
G. G. Hollins
†A. M. Houser
†Alfred Iddles
J. H. Lawrence
M. B. MacNeille
G. W. Martin
H. C. E. Meyer
J. W. Moore
F. H. Morehead
H. H. Morgan
W. S. Morrison
A. W. Moulder
Fred Nolde
E. W. Norris
G. A. Orrok
A. L. Penniman, Jr.
†C. S. Robinson
G. W. Saathoff
G. K. Saurwein
H. S. Smith
(H. H. Moss, *Alternate*)
F. N. Speller
C. G. Spencer
J. R. Tanner
J. H. Vance
F. H. Wagner
H. L. Whittemore
J. H. Williams
T. F. Wolfe
G. H. Woodroffe

GRAPHIC PRESENTATION

**Sole sponsorship. Sectional Committee organized November, 1926*

A.S.M.E. Members (Total personnel, 38)

†G. E. Hagemann, *Secretary*
M. F. Behar
C. N. Bigelow
Wallace Clark
H. G. Crockett
E. F. DuBrul
T. E. French
†D. B. Porter

TRANSMISSION CHAINS AND SPROCKETS

**Joint sponsorship with the Society of Automotive Engineers and the American Gear Manufacturers Association. Sectional Committee organized December, 1926*

A.S.M.E. Members (Total personnel, 16)

†F. V. Hetzel, *Chairman*
†G. M. Bartlett, *Secretary*
W. J. Belcher
Joseph Joy
†L. V. Ludy
†E. B. Nichols
F. L. Morse
G. A. Young
O. B. Zimmerman

WIRE AND SHEET METAL GAGES

**Joint sponsorship with the Society of Automotive Engineers. Sectional Committee organized November, 1927*

A.S.M.E. Members (Total personnel, 28)

J. F. Howe
†E. E. Rose

PIPE THREADS

**Joint sponsorship with the American Gas Association. Sectional Committee reorganized December, 1927. In August, 1908, the A.G.A. and the A.S.M.E. appointed a Joint Committee on this subject which was reorganized as a Sectional Committee under the procedure of the A.S.A. in the spring of 1919*

A.S.M.E. Members (Total personnel, 43)

B. H. Blood
A. F Breitenstein
E. J. Bryant
L. A. Cornelius
E. S. Cornell, Jr.
J. J. Crotty
J. J. Harman
†A. M. Houser
F. B. Howell
A. H. Jarecki
J. O. Johnson
W. R. Kremer
A. S. Miller
P. V. Miller
F. H. Morehead
W. C. Morris
S. F. Newman
E. S. Sanderson
L. N. Shannon
W. D. Sizer
J. H. Williams

ELECTRIC MOTOR FRAME DIMENSIONS

**Joint sponsorship with the National Electrical Manufacturers Association. Sectional Committee organized November, 1927*

A.S.M.E. Members (Total personnel, 31)

†W. F. Dixon, *Chairman*
C. A. Adams
S. A. Einstein
E. W. Ely
F. S. English
W. F. Jones
A. L. McHugh
P. G. Rhoads
†A. G. Trumbull
†E. H. Waring

WROUGHT IRON AND WROUGHT STEEL PIPE AND TUBING

**Joint sponsorship with the American Society for Testing Materials. Sectional Committee organized April, 1928*

A.S.M.E. Members (Total personnel, 39)

H. H. Morgan, *Chairman*
Sabin Crocker, *Secretary*
J. B. Aston
†A. M. Houser
†D. S. Jacobus
(F. S. Clark, *Alternate*)
W. R. Kremer
H. C. E. Meyer
F. H. Morehead
C. W. Mowry
†H. B. Oatley
A. L. Penniman, Jr.
(A. B. Morgan, *Alternate*)
F. N. Speller
J. R. Tanner
A. E. White
H. LeR. Whitney
G. H. Woodroffe

SPEEDS OF MACHINERY

**Sole sponsorship. Sectional Committee organized May, 1928*

A.S.M.E. Members (Total personnel, 29)

†C. M. Bigelow
R. C. Deale
Paul Diserens
F. S. English
A. E. Hall
D. C. Jackson
W. F. Jones
H. C. E. Meyer
John Reid
P. G. Rhoads
F. C. Spencer
O. B. Zimmerman

SCREW THREADS FOR HOSE COUPLINGS

**Sole sponsorship. Sectional Committee organized August, 1928*

A.S.M.E. Members (Total personnel, 24)

A. L. Brown, *Secretary*
†A. F. Breitenstein
W. L. Curtiss
†W. E. Dunham
J. J. Harman
(F. C. Ernst, *Alternate*)
A. M. Houser
H. C. E. Meyer
J. H. Williams

PLUMBING EQUIPMENT

**Joint sponsorship with the American Society of Sanitary Engineering. Sectional Committee organized August, 1928*

A.S.M.E. Members (Total personnel, 30)

†L. A. Cornelius
J. J. Crotty
O. E. Goldschmidt
G. W. Martin
(A. H. Morgan, *Alternate*)
†W. R. Webster

ROLLED THREADS FOR SCREW SHELLS OF ELECTRIC SOCKETS AND LAMP BASES

**Joint sponsorship with the National Electrical Manufacturers Association. Sectional Committee organized March, 1929*

A.S.M.E. Members (Total personnel, 18)

†E. J. Bryant
†Earle Buckingham
†E. S. Sanderson

STOCK SIZES, SHAPES, AND LENGTHS FOR HOT AND COLD FINISHED IRON AND STEEL BARS

**Sole sponsorship. Sectional Committee organized April, 1929*

A.S.M.E. Members (Total personnel, 24)

J. B. Aston
F. H. Dechant
†L. W. Williams
G. H. Woodroffe
O. B. Zimmerman

STANDARDIZATION AND UNIFICATION OF SCREW THREADS

Joint sponsorship with the Society of Automotive Engineers. Sectional Committee originally organized in June, 1921. Reorganized in February, 1928

A.S.M.E. Members (Total personnel, 37)

R. E. Flanders, *Chairman*
F. O. Wells, *Vice-Chairman*
Earle Buckingham, *Secretary*
H. E. Bilger
E. J. Bryant
G. S. Case
T. G. Crawford
†A. M. Houser
(R. E. Perry, *Alternate*)
H. C. E. Meyer
†P. V. Miller
O. B. Zimmerman

PRESSURE AND VACUUM GAGES

Sole sponsorship. Sectional Committee organized July, 1930

A.S.M.E. Members (Total personnel, 45)

M. D. Engle, *Chairman*
(A. B. Morgan, *Alternate*)
A. W. Lenderoth, *Secretary*
E. J. Bryant
J. P. Cavanaugh
Paul Diserens
W. F. Jones
R. J. Kehl
†J. C. McCune
A. H. Morgan
†S. A. Moss
H. B. Reynolds
C. Z. Rosencrans
W. C. Schoenfeldt

ALLOWANCES AND TOLERANCES FOR CYLINDRICAL PARTS AND LIMIT GAGES

Sole sponsorship. Sectional Committee originally organized in June, 1920. Reorganized in September, 1930

A.S.M.E. Members (Total personnel, 44)

F. E. Banfield
(E. E. Blake, *Alternate*)
F. S. Blackall, Jr.
H. E. Brunner
(William Jetter, *Alternate*)
E. J. Bryant
Earle Buckingham
F. H. Colvin
R. E. W. Harrison
F. O. Hoagland
N. E. Jacobi
H. C. E. Meyer
P. V. Miller
W. C. Mueller
†E. C. Peck
W. C. Schoenfeldt
F. W. Stein
C. C. Stevens
O. B. Zimmerman

FOUNDRY EQUIPMENT AND SUPPLIES

Joint sponsorship with the American Foundrymen's Association. Sectional Committee organized February, 1931

A.S.M.E. Members (Total personnel, 23)

. S. Carman, *Chairman*
. W. Ely
., W. Herendeen
(F. B. Howell, *Alternate*)
G. F. Jenks
A. S. Phelps
†H. P. Van Cleve
O. B. Zimmerman

SPECIFICATIONS FOR LEATHER BELTING

Sole sponsorship. Sectional Committee organized February, 1931

A.S.M.E. Members (Total personnel, 24)

R. W. Chandler
H. T. Coates
R. W. Drake
King Hathaway
Fred Nolde
J. E. Rhoads
C. A. Schieren
†C. O. Streeter
O. B. Zimmerman

NIFICATION OF RULES FOR THE DIMENSIONING OF FURNACES FOR BURNING SOLID FUEL

Sole sponsorship. Sectional Committee organized June, 1933

A.S.M.E. Members (Total personnel, 22)

. E. Bronson, *Temporary Chairman*
. G. Christy
hn Hunter
. G. Leach
T. A. Marsh
W. L. Martwick
J. F. McIntire
†John Van Brunt

CLASSIFICATION AND DESIGNATION OF SURFACE QUALITIES

Joint sponsorship with the Society of Automotive Engineers. Sectional Committee organized May, 1932

A.S.M.E. Members (Total personnel, 56)

C. G. Mettler, *Temporary Chairman*
John Cetrule
J. S. Chafee
T. G. Crawford
†R. C. Deale
U. S. Eberhardt
S. A. Einstein
R. F. Gagg
J. J. Harman
†R. E. W. Harrison
F. V. Hartman
F. O. Hoagland
H. J. Holtzclaw
R. T. Kent
A. H. Lyon
M. J. Reed
F. C. Spencer
C. C. Stevens
J. S. Tawresey
C. H. Whitaker

A.S.M.E. Representatives on Miscellaneous Standardization Committees

See also A.S.M.E. Representaitves on Other Activities, page 29

SPECIFICATIONS FOR CAST IRON PIPE

Sponsor bodies: American Gas Association, American Society for Testing Materials, American Water Works Association, and New England Water Works Association

G. W. Biggs
J. E. Gibson

CLASSIFICATION OF COAL

Sponsor body: American Society for Testing Materials

F. R. Wadleigh

DRAINAGE OF COAL MINES

Sponsor body: American Mining Congress

M. J. Lide
O. M. Pruitt
W. M. White

FIRE TESTS OF BUILDING CONSTRUCTION AND MATERIALS

Sponsor bodies: A.S.A. Fire Protection Group, National Bureau of Standards, and the American Society for Testing Materials

E. C. Rack

MANHOLE FRAMES AND COVERS

Sponsor bodies: A.S.A. Telephone Group and American Society of Civil Engineers

Anton Hansen
Homer Rupard

SPECIFICATIONS FOR AND RECOMMENDED PRACTICE IN THE USE OF WIRE ROPE FOR MINES

Sponsor body: American Mining Congress

J. L. Harrington

ROTATING ELECTRICAL MACHINERY

Sponsor bodies: American Institute of Electrical Engineers and the National Electrical Manufacturers Association

H. R. Sewell (C. A. Booth, *Alternate*)

SPECIFICATIONS FOR FUEL OILS

Sponsor body: The American Society for Testing Material

W. H. Butler
Harte Cooke
H. W. Dow
L. H. Morrison
Lee Schneitter
Denistoun Wood

ELECTRIC WELDING

Sponsor bodies: American Institute of Electrical Engineers and the National Electrical Manufacturers Association

N. McD. Loney

SPECIFICATIONS FOR SIEVES FOR TESTING PURPOSES

Sponsor bodies: American Society for Testing Materials and National Bureau of Standards

D. McM. Blackburn

METHODS OF RATING RIVERS

Sponsor body: U. S. Geological Survey

D. W. Mead

METHODS OF TESTING WOOD

Sponsor body: U. S. Forest Service and the American Society for Testing Materials

C. M. Bigelow

METHODS OF TESTING PETROLEUM PRODUCTS AND LUBRICANTS

Sponsor body: American Society for Testing Materials

A. E. Flowers

MISCELLANEOUS OUTSIDE COAL-HANDLING EQUIPMENT

Sponsor body: American Mining Congress

J. H. Stratton

SPECIFICATIONS FOR MATERIALS FOR USE IN MANUFACTURE OF SPECIAL TRACKWORK

Sponsor body: American Transit Association

W. R. Hulbert

ELECTRICAL DEFINITIONS

Sponsor body: American Institute of Electrical Engineers

C. H. Berry J. V. B. Duer

ACOUSTICAL MEASUREMENTS AND TERMINOLOGY

Sponsor body: Acoustical Society of America

E. E. Free
(P. H. Bilhuber, *Alternate*)
R. V. Parsons
(J. S. Parkinson, *Alternate*)
W. B. White
(H. S. Read, *Alternate*)

SPECIFICATIONS FOR CLEAN BITUMINOUS COAL

Sponsor body: American Institute of Mining and Metallurgical Engineers

R. A. Sherman (E. L. Lindseth, *Alternate*)

PREFERRED NUMBERS

Special Committee of A.S.A.

K. H. Condit

FOREST FIRE PROTECTION

Committee of National Fire Protection Association

E. H. Davis

BUILDING CODE COMMITTEE

Advisory Committee of Department of Commerce

Thornton Lewis

SPECIFICATIONS FOR TOOL STEEL

Subcommittee No. XIV of A.S.T.M. Committee A1 on Steel

O. W. Boston C. M. Inman

PETROLEUM SPECIFICATIONS

Advisory Board of U. S. Bureau of Mines

H. A. S. Howarth

Power Test Codes Technical Committees

(*Personnel of Standing Committee, p. 6*)

(1) GENERAL INSTRUCTIONS

Appointed December, 1918

W. H. Kavanaugh, *Chairman*
A. M. Greene, Jr.
C. F. Hirshfeld
M. C. Stuart

(2) DEFINITIONS AND VALUES

Appointed December, 1918

F. R. Low
L. S. Marks
A. C. Wood

(3) FUELS

Appointed December, 1918

W. J. Wohlenberg, *Chairman*
E. G. Bailey
B. L. Boye
L. P. Breckenridge
H. W. Brooks
S. B. Flagg
D. M. Myers
F. G. Philo
G. S. Pope
C. R. Richards
E. B. Ricketts
F. M. Rogers
E. X. Schmidt
Nicholas Stahl
E. N. Trump

(4) STATIONARY STEAM-GENERATING UNITS

Appointed December, 1918

E. R. Fish, *Chairman*
A. D. Bailey
Alfred Iddles
E. B. Powell
E. B. Ricketts
C. U. Savoye

(5) RECIPROCATING STEAM ENGINES

Appointed December, 1918

A. G. Christie, *Chairman*
Harte Cooke
K. S. M. Davidson
Herman Diederichs
Henrik Greger
Thomas Hall
J. A. Hunter
H. G. Mueller
B. V. E. Nordberg
J. F. M. Patitz
A. V. Saharoff
A. G. Witting
J. C. Workman

(6) STEAM TURBINES

Appointed December, 1918

C. H. Berry, *Chairman*
I. E. Moultrop, *Secretary*
O. D. H. Bentley
W. E. Caldwell
A. G. Christie
Hans Dahlstrand
V. M. Frost
A. E. Grunert
Francis Hodgkinson
S. A. Moss
R. O. Muller
T. E. Purcell
C. C. Thomas

(7) RECIPROCATING STEAM-DRIVEN DISPLACEMENT PUMPS

Appointed December, 1918

R. D. Hall, *Chairman*
C. H. Anderson
E. H. Brown
J. N. Chester
J. E. Gibson
G. L. Kollberg
M. B. MacNeille
D. W. Mead
L. A. Quayle

(8) CENTRIFUGAL AND ROTARY PUMPS

Appointed December, 1918

W. B. Gregroy, *Chairman*
Max Spillman, *Secretary*
W. C. Brown
M. B. MacNeille
L. F. Moody
F. H. Rogers
W. M. White

(9) DISPLACEMENT COMPRESSORS AND BLOWERS

Appointed December, 1918

Paul Diserens, *Chairman*
T. Felbeck
J. F. Huvane
R. M. Johnson
S. B. Redfield

(10) CENTRIFUGAL AND TURBO-COMPRESSORS AND BLOWERS

Appointed December, 1918

. T. Brown, *Chairman*
. L. Anderson
. A. Booth
. H. Carrier
. E. Day
. S. Dean
. G. Deutsch
. H. Downs
. E. Good
J. J. Grob
H. F. Hagen
Paul Hoffman
H. D. Kelsey
A. L. Kimball
L. S. Marks
Arvid Peterson
H. F. Schmidt
M. C. Stuart

(11) COMPLETE STEAM POWER PLANTS

Appointed December, 1918

. M. Van Deventer, *Chairman*
. F. Davidson
. H. Fellows
. A. Foresman
. M. Frost
W. W. Johnson
E. W. Norris
C. U. Savoye
D. S. Wegg
H. S. Whiton

(12) CONDENSERS, WATER HEATING, AND COOLING EQUIPMENT

Appointed December, 1918

. A. Orrok, *Chairman*
H. Hardie, *Secretary*
H. Baker, Jr.
N. Ehrhart
J. F. Grace
D. W. R. Morgan
J. J. Mullan
H. B. Reynolds
P. E. Reynolds

(13) REFRIGERATING SYSTEMS

Appointed December, 1918

M. Anderson, *Chairman*
B. Bright
N. H. Hiller
G. A. Horne
G. T. Voorhees

(14) EVAPORATING APPARATUS

Appointed December, 1918

N. Trump, *Chairman*
N. Bump
E. A. Newhall
H. L. Parr
L. C. Rogers

(15) STEAM LOCOMOTIVES

Appointed December, 1918

C. Schmidt, *Chairman*
F. Kiesel, Jr.
B. Oatley
G. E. Rhoads
L. K. Sillcox
W. E. Woodard

(16) GAS PRODUCERS

Appointed December, 1918

T. Magruder, *Chairman*
H. Fernald
C. D. Smith
H. F. Smith

(17) INTERNAL-COMBUSTION ENGINES

Appointed December, 1918

ax Rotter, *Chairman*
rte Cooke
L. B. Jackson
B. V. E. Nordberg
J. H. Suter

(18) HYDRAULIC PRIME MOVERS

Appointed December, 1918

E. C. Hutchinson, *Chairman*
C. M. Allen
H. L. Doolittle
W. F. Durand
N. R. Gibson
J. P. Growdon
T. H. Hogg
D. J. McCormack
L. F. Moody
R. V. Terry
W. M. White

(19) INSTRUMENTS AND APPARATUS

Appointed December, 1918

C. F. Hirshfeld, *Chairman*
W. A. Carter, *Secretary*
C. M. Allen
E. G. Bailey
H. S. Bean
L. J. Briggs
C. R. Cary
J. D. Davis
R. E. Dillon
F. M. Farmer
J. B. Grumbein
W. H. Kenerson
E. S. Lee
E. L. Lindseth
Osborn Monnett
S. A. Moss
R. J. S. Pigott
E. B. Ricketts
W. A. Sloan
R. B. Smith

(20) SPEED-RESPONSIVE GOVERNORS

Appointed December, 1921

Francis Hodgkinson, *Chairman*
Harte Cooke
J. F. M. Patitz
F. H. Rogers

(21) DUST SEPARATING APPARATUS

Appointed October, 1934

M. D. Engle, *Chairman*
J. W. Armour, *Secretary*
E. L. Anderson
A. D. Bailey
H. M. Bubar
W. G. Christy
H. O. Croft
J. M. DallaValle
Philip Drinker
H. F. Hagen
P. H. Hardie
C. W. Hedberg
J. H. Leech
H. E. Macomber
B. F. Tillson

A.S.M.E. Representatives on Other Committees

See also A.S.M.E. Representatives on Other Activities, page 29

DEVELOPMENT OF DEFINITIONS FOR THE NET CALORIFIC VALUE AND GROSS CALORIFIC VALUE OF FUELS

Sponsor Body: American Society for Testing Materials

W. J. Wohlenberg

COMMITTEE ON REDEFINING SO-CALLED STANDARD TON OF REFRIGERATION

Sponsor Body: American Society of Refrigerating Engineers

G. B. Bright

Safety Technical Committees

(*Personnel of Standing Committee, p. 6*)

SAFETY CODE FOR MECHANICAL POWER-TRANSMISSION APPARATUS

**Joint sponsorship with the International Association of Industrial Accident Boards and Commissions, National Bureau of Casualty and Surety Underwriters. Sectional Committee organized February, 1921*

A.S.M.E. Members (Total personnel, 27)

†C. B. Auel, *Chairman*
†L. A. DeBlois
W. J. Hamilton
R. McA. Keown
†G. M. Naylor
W. W. Nichols
W. S. Paine
P. G. Rhoads
†D. C. Wright
(G. N. VanDerhoef, *Alternate*)

SAFETY CODE FOR ELEVATORS

**Joint sponsorship with the American Institute of Architects and the National Bureau of Standards. Sectional Committee organized November, 1922*

A.S.M.E. Members (Total personnel, 35)

O. P. Cummings, *Vice-Chairman*
C. R. Callaway
M. H. Christopherson
I. N. Haughton
†D. L. Holbrook
S. V. James
Bassett Jones
D. L. Lindquist
N. O. Lindstrom
J. J. Matson
J. C. McCabe
M. B. McLauthlin
W. S. Paine
S. F. Voorhees

SAFETY CODE ON MACHINERY FOR COMPRESSING AIR

**Joint sponsorship with the American Society of Safety Engineers—Engineering Section, National Safety Council. Sectional Committee organized May, 1923*

A.S.M.E. Members (Total personnel, 23)

Paul Diserens
H. D. Edwards
W. M. Graff
W. J. Graves
O. P. Hood
†H. H. Judson
C. E. Pettibone
D. L. Royer

SAFETY CODE FOR CONVEYORS AND CONVEYING MACHINERY

**Joint sponsorship with the National Bureau of Casualty and Surety Underwriters. Sectional Committee organized November, 1925*

A.S.M.E. Members (Total personnel, 45)

M. H. Christopherson
E. L. Gifford
W. J. Graves
F. V. Hetzel
†M. A. Kendall
R. McA. Keown
W. S. Paine
C. G. Pfeiffer
D. L. Royer
(W. M. Graff, *Alternate*)
†William Staniar
G. R. Wadleigh
J. G. Wheatley

SAFETY CODE FOR CRANES, DERRICKS, AND HOISTS

**Sole sponsorship. Sectional Committee organized November, 1925*

A.S.M.E. Members (Total personnel, 58)

B. F. Tillson, *Secretary*
H. LeR. Brink
J. F. Howe
W. D. Keller
Franklin Moeller
†Lewis Price
F. H. Schwerin
†R. H. White
H. L. Whittemore

A.S.M.E. Representatives on Other Safety Committees

See also A.S.M.E. Representatives on Other Activities, page 29

SAFETY CODE CORRELATING COMMITTEE

M. H. Christopherson (T. A. Walsh, Jr., *Alternate*)

SAFETY CODE FOR AMUSEMENT PARKS

**Sponsor bodies: National Association of Amusement Parks, and National Bureau of Casualty and Surety Underwriters*

G. P. Smith

SAFETY CODE FOR FLOOR OPENINGS, RAILINGS, AND TOE BOARDS

**Sponsor body: National Safety Council*

William Collins

SAFETY CODE FOR FORGING AND HOT METAL STAMPING

**Sponsor bodies: American Drop Forging Institute and the National Safety Council*

O. F. Luckenbach
C. F. Park

SAFETY CODE FOR LADDERS

**Sponsor body: National Safety Council*

W. T. Hatch

SAFETY CODE FOR LAUNDRY MACHINERY AND OPERATION

**Sponsor bodies: Laundry Owners National Association, Association of Governmental Officials in Industry of U. S. and Canada, and National Association of Mutual Casualty Companies*

E. J. Carroll

SAFETY CODE FOR LIGHTING FACTORIES, MILLS, AND OTHER WORKS PLACES

**Sponsor body: Illuminating Engineering Society*

L. A. Blackburn

SAFETY CODE FOR LOGGING AND SAWMILL MACHINERY

**Sponsor body: National Bureau of Standards*

J. H. Dickinson

SAFETY CODE FOR PAPER AND PULP MILLS

**Sponsor body: National Safety Council*

R. L. Weldon

SAFETY CODE FOR POWER PRESSES, AND FOOT AND HAND PRESSES

**Sponsor body: National Safety Council*

E. E. Barney

SAFETY CODE FOR TEXTILES

**Sponsor body: National Safety Council*

G. L. Warfield

SAFETY CODE FOR VENTILATION

**Sponsor body: American Society of Heating and Ventilating Engineers*

P. A. McKittrick (L. H. Eggert, *Alternate*)

SAFETY CODE FOR WALKWAY SURFACES

**Sponsor bodies: American Institute of Architects and National Safety Council*

W. M. Graff

SAFETY CODE FOR WINDOW WASHING

**Sponsor body: National Safety Council*

W. G. Boyle

SAFETY CODE ON COLORS FOR IDENTIFICATION OF GAS MASK CANISTERS

**Sponsor body: National Safety Council*

L. C. Lichty

SAFETY CODE FOR PROTECTION OF INDUSTRIAL WORKERS IN FOUNDRIES

*Sponsor bodies: *American Foundrymen's Association and National Founders Association*

H. M. Lane

SAFETY CODE FOR PREVENTION OF DUST EXPLOSIONS

*Sponsor bodies: *National Fire Protection Association and U. S. Department of Agriculture*

J. H. Morrow

SAFETY CODE FOR WORK IN COMPRESSED AIR

*Sponsor body: *International Association of Industrial Accident Boards and Commissions*

L. J. Eibsen

SAFETY CODE FOR EXHAUST SYSTEMS

*Sponsor body: *International Association of Industrial Accident Boards and Commissions*

A.S.M.E. Representative

J. C. Hardigg (E. H. deConingh, *Alternate*)

SPECIFICATIONS AND METHODS OF TEST FOR SAFETY GLASS

*Sponsor bodies: *National Bureau of Casualty and Surety Underwriters and National Bureau of Standards*

T. A. Walsh, Jr. (G. E. Sanford, *Alternate*)

LOW VOLTAGE ELECTRICAL HAZARD

Special Committee of the American Society of Safety Engineers—Engineering Section, National Safety Council

J. P. Jackson

A.S.M.E. Representatives on Other Activities

See also A.S.M.E. Representatives on Other Research Committees, etc., pages 21, 25, 27, and 28

(Dates in parentheses denote expiration of terms)

AMERICAN ASSOCIATION FOR THE ADVANCEMENT OF SCIENCE

SECTION M, ENGINEERING

(To be appointed)

AMERICAN BUREAU OF WELDING

James Partington

COMMITTEE ON STRUCTURAL STEEL WELDING

G. A. Orrok

AMERICAN ENGINEERING COUNCIL

(One year term)

.. E. Flanders, *Chairman* — Paul Doty
. P. Alford — A. A. Potter
D. Robert Yarnall
Alternates: H. V. Coes, J. W. Roe

AMERICAN STANDARDS ASSOCIATION

. W. Spicer (1937) — *Alternates:* V. R. Willoughby, C. B. LePage

AMERICAN YEAR BOOK CORPORATION

C. E. Davies

THE ENGINEERING FOUNDATION

E. White (1936) — W. H. Fulweiler (1937)
D. Robert Yarnall (1937)

EDUCATIONAL RESEARCH COMMITTEE

H. N. Davis

RESEARCH PROCEDURE COMMITTEE

W. H. Fulweiler

ENGINEERING SOCIETIES EMPLOYMENT SERVICE

NATIONAL BOARD

C. E. Davies

METROPOLITAN BOARD

Ernest Hartford, *Chairman*

ENGINEERS' COUNCIL FOR PROFESSIONAL DEVELOPMENT

. E. Wickenden (1935) — C. F. Hirshfeld (1936)
To be appointed (1937)

ENGINEERS NATIONAL RELIEF FUND

W. A. Shoudy

JOHN FRITZ MEDAL BOARD OF AWARD

R. V. Wright (1935) — A. A. Potter (1937)
C. N. Lauer (1936) — Paul Doty (1938)

GANTT MEDAL BOARD OF AWARD

J. W. Roe (1935) — D. B. Porter (1936)
F. E. Raymond (1937)

DANIEL GUGGENHEIM MEDAL FUND, INC.

H. I. Cone (1935) — E. E. Aldrin (1937)
P. H. Adams (1936) — B. M. Woods (1938)

JOSEPH A. HOLMES SAFETY ASSOCIATION

O. P. Hood

HOOVER MEDAL BOARD OF AWARD

Ambrose Swasey (1935) — To be appointed (1937)
C. N. Lauer (1939)

INTERNATIONAL CONGRESSES OF PHOTOGRAPHY, JULY, 1935

AMERICAN NATIONAL COMMITTEE

Edward Epstean

INTERNATIONAL ELECTROTECHNICAL COMMISSION

U. S. NATIONAL COMMITTEE

H. N. Davis — Francis Hodgkinson
E. C. Hutchinson
Alternates: C. Harold Berry, Paul Diserens

MECHANICAL STANDARDS ADVISORY COUNCIL

W. S. Monroe

NATIONAL BUREAU OF ENGINEERING REGISTRATION

J. H. Lawrence

NATIONAL FIRE WASTE COUNCIL

H. O. Lacount — J. A. Neale

NATIONAL MANAGEMENT COUNCIL

J. A. Piacitelli (1936)—G. W. Kelsey, *Alternate*
C. W. Lytle (1937)
H. V. Coes (1938)—J. W. Roe, *Alternate*

NATIONAL RESEARCH COUNCIL

DIVISION OF ENGINEERING AND INDUSTRIAL RESEARCH

W. R. Webster (1935) F. M. Farmer (1936)
W. D. Ennis (1935) D. S. Jacobus (1936)

C. E. Davies, *Secretary, Ex-Officio*

NEW YORK STATE JOINT LEGISLATION COMMITTEE

Sigmund Firestone J. H. Lawrence

ALFRED NOBEL PRIZE

A. M. Greene, Jr.

PROFESSIONAL ENGINEERS COMMITTEE ON UNEMPLOYMENT

W. T. Conlon J. N. Landis G. B. Pegram
H. N. Davis A. H. Meyer Walter Rautenstrauch

STUDY OF COAL

JOINT COMMITTEE WITH THE A.I.M.E.

A. D. Bailey H. Drake Harkins A. L. Penniman, Jr.
E. H. Barry J. C. Hobbs E. B. Ricketts
F. M. Gibson E. H. Tenney

UNITED ENGINEERING TRUSTEES, INC.

H. V. Coes (1936) D. Robert Yarnall (1937)
W. L. Batt (1938)

ENGINEERING SOCIETIES MONOGRAPHS COMMITTEE

S. W. Dudley W. A. Shoudy

WESTERN SOCIETY OF ENGINEERS

WASHINGTON AWARD

G. F. Gebhardt (1935) C. B. Nolte (1936)

Awards

The following paragraphs deal with the awards, scholarships, and loan funds which come within the jurisdiction of the A.S.M.E. The Society also participates with other engineering societies in a number of joint awards.

Honorary Membership, to which persons of acknowledged professional eminence are elected by unanimous vote of Council under the provisions of the By-Laws and Rules. A list of honorary members is given on page RI-32.

Life Membership, which may be conferred by the Council for distinguished service to the Society; or secured by a member by payment for an annuity in accordance with the provisions of the By-Laws.

A.S.M.E. Medal, established by the Society in 1920 to be presented for distinguished service in engineering and science. May be awarded for general service in science having possible application in engineering.

Holley Medal, instituted and endowed in 1924 by George I. Rockwood, Past Vice-President of the Society, to be bestowed for some great and unique act of genius of engineering nature that has accomplished a great and timely public benefit.

Worcester Reed Warner Medal, provision for which was made in the will of Worcester Reed Warner, Honorary Member of the Society, is a gold medal to be bestowed on the author of the most worthy paper received, dealing with progressive ideas in mechanical engineering or efficiency in management.

Melville Medal, established in 1914 by the bequest of Rear-Admiral George W. Melville, Honorary Member and Past-President of the Society, to be presented for an original paper or thesis of exceptional merit, presented to the Society for discussion and publication, to encourage excellence in papers. The medal may be presented annually.

Spirit of Saint Louis Medal, endowed by members of the Society and citizens residing in St. Louis, Mo., to be awarded for meritorious service in the field of aeronautical engineering. This medal will be awarded at the discretion of the Council of the Society at approximately three-year periods upon the recommendation of a Spirit of Saint Louis Medal Board of Award made up of six members, each appointed for a term of nine years and the terms of two members expiring at each three-year period. The St. Louis Section and the Aeronautic Division will each be responsible for the nomination of three members.

Junior Award, annual cash award of $50, established in 1914, from a fund created by Henry Hess, Past Vice-President of the Society, to be presented, together with an engraved certificate, for the best paper or thesis submitted by a Junior Member.

Student Awards, two annual cash awards of $25 each, established in 1914, from a fund created by Henry Hess, Past Vice-President of the Society, to be presented, together with engraved certificates, for the best papers or theses submitted by members of Student Branches.

Charles T. Main Award, annual cash award of $150, established in 1919 from a fund created by Charles T. Main, Past-President of the Society, to be awarded to a student of engineering, preferably a member of a Student Branch of the Society, for the best paper within the general subject of the "Influence of the Profession Upon Public Life." The exact subject is assigned by the Committee on Awards, subject to the approval of the Council, and is announced each year through the Honorary Chairmen of the Student Branches.

SCHOLARSHIPS AND LOAN FUNDS

Max Toltz: Loan Fund of $15,000 established by Major Max Toltz, former member of the Council of the Society, the income to be used for assistance to students.

John R. Freeman: Fund of $25,000 established in 1926 by John R. Freeman, Past-President of the Society, the income to be used for travel scholarships and research.

Woman's Auxiliary: Scholarship or Fellowship offered by the Woman's Auxiliary to the Society to assist sons and daughters of members or worthy students of mechanical engineering.

RECIPIENTS OF AWARDS

The names of the recipients of the different awards to date are given in the following lists, together with the dates of presentation, and the services or papers for which the awards were made. There were no awards for the years not listed.

A.S.M.E. Medal

1921 Hjalmar Gotfried Carlson, in recognition of the services rendered the Government because of his invention and part in the production of 20,000,000 Mark III drawn steel booster casings used principally as a component of 75-mm high-explosive shells, but also used extensively in gas shells and bombs

1923 Frederick Arthur Halsey, for his paper describing the premium system of wage payments presented before the Society at the Providence Meeting in 1891, as the adoption of the methods there proposed has had a profound effect toward harmonizing the relations of worker and employer

1923 John Ripley Freeman, for his eminent service in engineering and manufacturing by his meritorious work in fire prevention and the preservation of property

1926 R. A. Millikan, in recognition of his contributions to science and engineering

1927 Wilfred Lewis, for his contributions to the design and construction of gear teeth

1928 Julian Kennedy, for his services and contributions to the iron and steel industry

1929 William LeRoy Emmet, for his contributions in the development of the steam turbine, electric propulsion of ships, and other power-generating apparatus

1931 Albert Kingsbury, for his research and development work in the field of lubrication

1933 Ambrose Swasey, for his contributions to the advancement of the engineering profession and for his part in the development of the turret lathe and the astronomical telescope

1934 Willis H. Carrier, in recognition of his research and development work in air-conditioning.

Holley Medal

1924 Hjalmar Gotfried Carlson, for his inventions and processes which made possible the timely production of drawn steel booster casings for artillery ammunition, thereby aiding victory in the World War
1928 Elmer Ambrose Sperry, for achievements and inventions that have advanced the naval arts, including the gyroscope that has freed navigation from the dangers of the fluctuating magnetic compass
1929 Baron Chuzaburo Shiba, for his contributions to knowledge through fundamental research, including the field of aerodynamics, by the development of ultra-rapid kinematographic methods.

Worcester Reed Warner Medal

1933 Dexter S. Kimball, for his contributions to efficiency in management as exemplified by his recently revised "Principles of Industrial Organization" and by his many articles, engineering society papers, and public addresses
1934 Ralph E. Flanders, for his contributions to a better understanding of the relationship of the engineer to economic problems and social trends as exemplified by the many papers which he has presented.

Melville Medal

1927 Leon P. Alford, "Laws of Manufacturing Management"
1929 Joseph Wickham Roe, "Principles of Jig and Fixture Practice"
1930 Herman Diederichs and William D. Pomeroy, "The Occurrence and Elimination of Surge or Oscillating Pressure in Discharge Lines From Reciprocating Pumps"
1931 Arthur E. Grunert, "Comparative Performance of a Pulverized-Coal-Fired Boiler Using Bin System and Unit System of Firing"
1932 Alexey J. Stepanoff, "Leakage Loss and Axial Thrust in Centrifugal Pumps"
1933 William E. Caldwell, "Characteristics of Large Hell Gate Direct-Fired Boiler Units."

Spirit of Saint Louis Medal

1929 Daniel Guggenheim, founder of the Guggenheim Fund for the Promotion of Aeronautics
1932 Paul Litchfield, for his work in encouraging and sponsoring airship design and construction in this country.

Junior Award

1915 Ernest O. Hickstein, "Flow of Air Through Thin Plate Orifices"
1916 L. B. McMillan, "The Heat Insulating Properties of Commercial Steam-Pipe Coverings"
1919 E. D. Whalen, "Properties of Airplane Fabrics"
1921 S. Logan Kerr, "Moody Ejector Turbine"
1922 R. H. Heilman, "Heat Losses From Bare and Covered Wrought-Iron Pipe at Temperatures Up to 800 Degrees Fahrenheit"
F. L. Kallam, "Preliminary Report on the Investigation of the Thermal Conductivity of Liquids"
1923 S. S. Sanford and S. Crocker, "The Elasticity of Pipe Bends"
1924 R. H. Heilman, "Heat Losses Through Insulating Material"
1925 Gilbert S. Schaller, "An Investigation of Seattle as a Location for a Synthetic Foundry Industry"
1927 Wm. M. Frame, "Stresses Occurring in the Walls of an Elliptical Tank Subjected to Low Internal Pressure"
1928 M. D. Aisenstein, "A New Method of Separating the Hydraulic Losses in a Centrifugal Pump"
1929 Arthur M. Wahl, "Stresses in Heavy, Closely Coiled Helical Springs"
1930 Ed Sinclair Smith, Jr., "Quantity-Rate Fluid Meters"
1931 M. K. Drewry, "Radiant-Superheater Developments"
1932 Edmond M. Wagner, "Frictional Resistance of a Cylinder Rotating in a Viscous Fluid Within a Coaxial Cylinder"
1933 Townsend Tinker, "Surface Condenser Design and Operating Characteristics"
1934 John I. Yellott, Jr., "Supersaturated Steam."

Student Award

1916 Boynton M. Green, Stanford University, "Bearing Lubrication"
Howard Stevens, Rensselaer Polytechnic Institute, "An Investigation of the Dynamic Pressure on Submerged Flat Plates"
M. Adam, Louisiana State University, "The Adaptability of the Internal Combustion Engine to Sugar Factories and Estates"
1917 H. R. Hammond and C. W. Holmberg, Pennsylvania State College, "Study of Surface Resistance With Glass as the Transmission Medium"
1919 C. F. Leh and F. G. Hampton, Stanford University, "An Experimental Investigation of Steel Belting"
W. E. Helmick, Stanford University, "An Experimental Investigation of Steel Belting"
1920 Howard G. Allen, Cornell University, "Wire Stitching Through Paper"
1921 Karl H. White, University of Kansas, "Forces in Rotary Motors"
Richard H. Morris and Albert J. R. Houston, University of California, "A Report Upon an Investigation of the Herschel Type of Improved Weir"
1923 Charles F. Olmstead, University of Minnesota, "Oil Burning for Domestic Heating"
H. E. Doolittle, University of California, "The Integrating Gate: A Device for Gaging in Open Channels"
1924 George Stuart Clark, Stanford University, "Two Methods Used for the Determination of the Gasoline Content of Absorption Oils in Absorption Plants"
L. J. Franklin and Charles H. Smith, Stanford University, "The Effect of Inaccuracy of Spacing on the Strength of Gear Teeth"
1925 Harry Pease Cox, Jr., Rensselaer Polytechnic Institute, "A Study of the Effect of End Shape on the Towing Resistance of a Barge Model"
W. S. Montgomery, Jr., and E. Ray Enders, Jr., Pennsylvania State College, "Some Attempts to Measure the Drawing Properties of Metals"
1926 R. E. Peterson, University of Illinois, "An Investigation of Stress Concentration by Means of Plaster of Paris Specimens"
Cecil G. Heard, University of Toronto, "Pressure Distribution Over U. S. A. 27 Aerofoil With Square Wing Tips Model Tests"
1927 Alfred H. Marshall, Princeton, "Evaporative Cooling"
Roger Irwin Eby, University of Washington, "Measurement of the Angular Displacement of Flywheels"
1928 Clarence C. Franck, Johns Hopkins University, "Condition Curves and Reheat Factors for Steam Turbines"
1929 Frank Vernon Bistrom, University of Washington, "An Investigation of a Rotary Pump"
William Wallace White, University of Washington, "An Investigation of a Rotary Pump"
1930 Gerard Eden Claussen, Polytechnic Institute of Brooklyn, "High-Temperature Oxidation of Steel"
Harold L. Adams and Richard L. Stith, University of Washington, "A Wind Tunnel for Undergraduate Laboratory Experiments"
1931 Jules Podnossoff, Polytechnic Institute of Brooklyn, "Pressure and Energy Distribution in Multi-Stage Steam Turbines Operating Under Varying Conditions"
1932 H. E. Foster, Jr., University of Tennessee, "Factors Affecting Spray Pond Design"
William A. Mason, Stanford University, "An Experimental Investigation of the Flame Propagation in Internal-Combustion Engines"
1933 Hugo V. Cordiano, Polytechnic Institute of Brooklyn, "Thermal Analysis of Lithium-Magnesium System of Alloys"
James A. Ostrand, Jr., Princeton University, "Sudden Enlargement in the Open Channel"
1934 H. Reynolds Hudson, Georgia School of Technology, "Dynamic Balance and Functional Utility Applied to Automotive Design."

Charles T. Main Award

1925 Clement R. Brown, Catholic University of America. Subject: "The Influence of the Locomotive on the Unity of the United States"
1926 W. C. Saylor, Johns Hopkins University. Subject: "The Effect of the Cotton Gin Upon the History of the United States During Its First Seventy Years"
1927 No award. Subject: "Scientific Management and Its Effect Upon the Industries"
1928 Robert M. Meyer, Newark College of Engineering. Subject: "Scientific Management and Its Effect Upon Manufacturing"
1930 Jules Podnossoff, Polytechnic Institute of Brooklyn. Subject: "The Value of the Safety Movement in the Industries"

1931 Robert E. Klise, University of Michigan. Subject: "Interchangeability—Its Development and Significance in Industry"
1932 Marshall Anderson, University of Michigan. Subject: "Apprenticeship and Vocational Training"
1933 George D. Wilkinson, Jr., Newark College of Engineering. Subject: "Progress in the Prevention of Smoke and Atmospheric Pollution"
1934 Philip P. Self, Colorado State College, "Air Conditioning—Its Practicability and Relation to Public Welfare."

Freeman Travel Scholarship

1927 Herbert N. Eaton
1928 Blake R. Van Leer
1929 Robert T. Knapp
1931 Reginald Whitaker
1932 G. Ross Lord
1933, 1934 H. J. Casey.

Honorary Members

HONORARY MEMBERS IN PERPETUITY

Alexander Lyman Holley, Founder of the Society. Died 1882.

John Edson Sweet, Founder of the Society. Died 1916.

Henry Rossiter Worthington, Founder of the Society. Died 1880.

DECEASED HONORARY MEMBERS

	Elected	Died
Horatio Allen	1880	1889
Sir William Arrol	1905	1913
Sir Benjamin Baker	1886	1907
Johann Bauschinger	1884	1893
Sir Henry Bessemer	1891	1898
Sir Frederick Joseph Bramwell	1884	1903
John Alfred Brashear	1908	1920
Gustave Canet	1900	1908
Andrew Carnegie	1907	1919
Daniel Kinnear Clark	1882	1896
Rudolph Julius Emmanuel Clausius	1882	1888
Sir John Coode	1889	1892
Peter Cooper	1882	1883
Carl Gustaf Patrick de Laval	1912	1913
Rudolph Diesel	1912	1913
James Dredge	1886	1906
Victor Dwelshauvers-Dery	1886	1913
Thomas Alva Edison	1904	1931
Alexandre Gustave Eiffel	1889	1923
Marshal Ferdinand Foch	1921	1929
Sir Charles Douglas Fox	1900	1921
John Ripley Freeman	1932	1932
John Fritz	1900	1913
Major-General George Washington Goethals	1917	1928
Franz Grashof	1884	1893
Rear-Admiral Robert Stanislaus Griffin	1920	1933
Otto Hallauer	1882	1883
Charles Haynes Haswell	1905	1907
Friedrich Gustav Herrmann	1884	1907
Gustav Adolph Hirn	1882	1890
Joseph Hirsch	1889	1901
Ira N. Hollis	1928	1930
Robert Woolston Hunt	1920	1923
Benjamin Franklin Isherwood	1894	1915
Henri Léauté	1891	1916
Erasmus Darwin Leavitt	1915	1916
Anatole Mallet	1912	1919
Charles H. Manning	1913	1919
Rear-Admiral George Wallace Melville	1910	1912
The Honorable Sir Charles Algernon Parsons	1920	1931
Charles Talbot Porter	1890	1910
Auguste C. E. Rateau	1919	1930
Sir Edward J. Reed	1882	1906
Franz Reuleaux	1882	1905
Calvin Winsor Rice	1931	1934
Palmer C. Ricketts	1931	1934
Henri Adolphe-Eugene Schneider	1882	1898
C. William Siemans	1882	1883
Viscount Ei-ichi Shibusawa	1929	1931
Henry Robinson Towne	1921	1924
Henri Tresca	1882	1885
William Cawthorne Unwin	1898	1933
Oskar von Miller	1912	1934
Francis A. Walker	1886	1897
Worcester Reed Warner	1925	1929
George Westinghouse	1897	1914
Sir William Henry White	1900	1913
Sir Alfred Fernandez Yarrow	1914	1932

LIVING HONORARY MEMBERS

	Elected
Sir John Audley Frederick Aspinall	1911
William Wallace Atterbury	1925
Mortimer Elwyn Cooley	1928
William Frederick Durand	1934
Charles de Fréminville	1919
Nathanael Greene Herreshoff	1921
Herbert Clark Hoover	1925
David Schenck Jacobus	1934
Masawo Kamo	1929
Henri Le Chatelier	1927
Grande Ufficiale Ing. Pio Perrone	1920
Charles M. Schwab	1918
Ambrose Swasey	1916
Elihu Thomson	1930
Samuel Matthews Vauclain	1920
Right Honorable Lord Weir	1920
Orville Wright	1918

Past-Presidents

A list of past vice-presidents, managers, treasurers, and secretaries will be found in the 1930 Record and Index, pages 10–12. Dates in parentheses denote year of death.

Alexander Lyman Holley, *Chairman of the Preliminary Meeting for Organization of The American Society of Mechanical Engineers* (1882)

1880–1882	Robert Henry Thurston (1903)
1883	Erasmus Darwin Leavitt (1916)
1884	John Edson Sweet (1916)
1885	Josephus Flavius Holloway (1896)
1886	Coleman Sellers (1907)
1887	George H. Babcock (1893)
1888	Horace See (1909)
1889	Henry Robinson Towne (1924)
1890	Oberlin Smith (1926)
1891	Robert Woolston Hunt (1923)
1892	Charles Harding Loring (1907)
1893–1894	Eckley Brixton Coxe (1895)
1895	Edward F. C. Davis (1895)
1895	Charles Ethan Billings (1920)
1896	John Fritz (1913)
1897	Worcester Reed Warner (1929)
1898	Charles Wallace Hunt (1911)
1899	George Wallace Melville (1912)
1900	Charles Hill Morgan (1911)
1901	Samuel T. Wellman (1919)
1902	Edwin Reynolds (1909)
1903	James Mapes Dodge (1915)
1904	Ambrose Swasey
1905	John Ripley Freeman (1932)
1906	Frederick Winslow Taylor (1915)
1907	Frederick Remsen Hutton (1918)
1908	Minard Lafever Holman (1925)
1909	Jesse Merrick Smith (1927)
1910	George Westinghouse (1914)
1911	Edward Daniel Meier (1914)
1912	Alexander Crombie Humphreys (1927)
1913	William Freeman Myrick Goss (1928)
1914	James Hartness (1934)
1915	John Alfred Brashear (1920)
1916	David Schenck Jacobus
1917	Ira Nelson Hollis (1930)
1918	Charles Thomas Main
1919	Mortimer Elwyn Cooley
1920	Fred J. Miller
1921	Edwin S. Carman
1922	Dexter Simpson Kimball
1923	John Lyle Harrington
1924	Frederick Rollins Low
1925	William Frederick Durand
1926	William Lamont Abbott
1927	Charles M. Schwab
1928	Alex Dow
1929	Elmer Ambrose Sperry (1930)
1930	Charles Piez (1933)
1931	Roy V. Wright
1932	Conrad N. Lauer
1933	A. A. Potter
1934	Paul Doty

Index to Committees

A New Basis for the Rating of Roller-Chain Drives

By G. M. BARTLETT,[1] WEST LAFAYETTE, IND.

Reference tables giving horsepower ratings for roller transmission chains are commonly based upon certain allowable working pressures per square inch of projected bearing area at the chain joints. The allowable working load is assumed to increase in proportion to the projected area of the pins and to decrease with an increase in chain velocity and an increase in the "centrifugal pull" of the chain.

An analysis of the bending action of the links at both driving and driven wheels and the work of friction between pins and bushings yields an algebraic expression for the heat generated per minute, or for the rate of wear in the chain. This is proportional to the rate of elongation of the chain; and this rate of elongation is found to be directly proportional to the horsepower transmitted and inversely proportional to the pitch, the length of the bushing, the number of links in the chain, and the product of the number of teeth in the two sprockets (very nearly). A set of tables is developed based upon chain velocity and the number of teeth in both sprockets. The horsepowers taken from these tables are such as will produce approximately the same rate of elongation in all drives whose design and operation conform to average conditions. Similar tables are computed on the basis of the rpm of the smaller sprocket instead of the chain velocity.

These tables also allow for the extra pull on the chain due to centrifugal force, and for the chain lengths and center distances necessary to keep the rate of elongation within the limits allowed.

An examination of these tables shows that, with certain combinations of sprocket teeth and chain lengths, loads twice as great as those usually given in tables can be transmitted. And these figures seem to be supported by actual practice.

The subject of limiting speeds for sprockets is treated and three sets of limiting conditions are investigated, namely: (*a*) the effect of a single impact between chain rollers and sprocket teeth, (*b*) the energy of impact per tooth per minute, and (*c*) the effect of centrifugal action. A table is compiled giving maximum chain velocities and sprocket speeds, based upon these investigations, for various chains and various numbers of teeth in the sprockets. This table shows the conditions under which certain chains can be operated at velocities above 3000 fpm and other conditions under which the same chains should not be operated at more than 240 fpm.

In DESIGNING a chain drive it is customary to refer to tables and charts to determine the allowable load carried by a given chain at a given speed, and, after making due allowances for special conditions as dictated by one's judgment, a selection of a suitable chain model is made.

By means of one chart frequently used, the chain is selected on the basis of the horsepower to be transmitted and the revolutions per minute of the smaller sprocket. By means of certain tables in common use, the chain is selected on the basis of chain velocity and either chain pull or horsepower. In another table, the revolutions per minute of the smaller sprocket and its number of teeth are the given data.

While such tables are easy to use and economical to print, it has long been realized that unless all other conditions are satisfactory the tabulated ratings are likely to be erroneous. It is the purpose of this paper to present the results of a mathematical investigation of the conditions that cause chain and sprocket wear, and also to present evidence of the possibility as well as the desirability of compiling a set of tables for the proper rating of roller chains on the basis of all factors that affect the satisfactory performance of the drive.

The number of teeth in the smaller sprocket affects the rapidity of wear of the chain, the uniformity of chain velocity, the efficiency of the drive, and the endurance limit of the chain.

The rapidity of chain elongation is affected by the chain pull, the horsepower, the sprocket speed, the length of the chain bushing, the chain length, the product of the number of teeth in the two sprockets, and the character of the lubrication; but it is independent of the pin diameter unless the unit pressure on the pin is excessive.

The rapidity of sprocket-tooth wear due to roller impact is affected by the pitch, the weight of the chain, the size of the rollers, the revolutions per minute, the material and heat-treatment of the sprockets, the design of the tooth form, and the character of the lubrication.

The centrifugal force of the chain is affected by the weight of the chain and its velocity.

The efficiency of a chain drive is affected by the number of teeth, the chain pull, the pin diameter, the chain weight, the revolutions per minute, the character of the lubrication, and the tangential distance along the tight strand of the chain.

The principal consideration in the design of a chain drive is long service for both chain and sprockets. But such considerations as compactness, quiet action, light weight, or low initial cost may sometimes become paramount. In the present investigation it is assumed that the end to be attained is a certain

[1] Professor of Machine Design, Purdue University, and Consulting Engineer, Diamond Chain & Manufacturing Co., Indianapolis, Ind. Mem. A.S.M.E. Mr. Bartlett was graduated from Amherst College with the degree of B.S. in 1901 and received the M.A. degree in 1905. He was instructor in mathematics and drawing at Case School of Applied Science from 1901 to 1903, and instructor in mechanism and drawing, University of Michigan, from 1903 to 1910. From 1910 until 1920 was chief engineer of the Diamond Chain & Manufacturing Co., for which concern he has been consulting engineer since 1920. He has been professor of machine design at Purdue University since 1927. He is the author of several textbooks and articles in the technical press, and the inventor of many machines and tools.

Contributed by the Machine Shop Practice Division for presentation at the Semi-Annual Meeting, Cincinnati, Ohio, June 19 to 21, 1935, of The American Society of Mechanical Engineers.

Discussion of this paper should be addressed to the Secretary, A.S.M.E., 29 West 39th Street, New York, N. Y., and will be accepted until July 10, 1935, for publication in a later issue of the Transactions.

number of hours of service under average conditions before the chain has elongated to such an extent that it is no longer satisfactory.

The first procedure will be the development of formulas from which maximum chain velocities and maximum sprocket speeds may be calculated for various standard chains and for various numbers of sprocket teeth. Having tabulated the results obtained from these formulas, other formulas will be developed to express the rate of chain wear and the allowable horsepower of a chain based upon pitch, pin diameter, bushing length, chain length, number of sprocket teeth, and sprocket speed. From these it will be possible to construct a set of tables for use in the selection of a chain expected to operate for a reasonable number of hours before being worn out.

Cause of Sprocket Wear[2]

The wear of sprocket teeth is mainly due to roller impact. While engagement between a chain and sprocket is taking place, each link, AB, as shown in Fig. 1, turns about the pin A with an

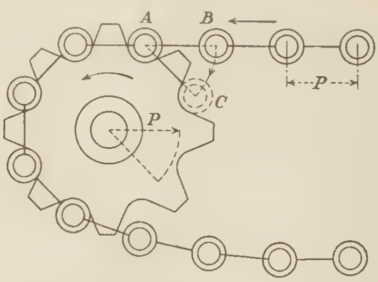

Fig. 1 Engagement Between a Chain and Sprocket; Analysis of Impact Conditions

angular speed equal to that of the sprocket. Hence the linear speed of the roller B along the arc BC, relative to the sprocket, is equal to the linear speed of a point on the sprocket at a distance P from the center. That is, the roller strikes the sprocket with a speed equal to $2\pi Pn/12$ fpm, or $\pi Pn/360$ fps, where P is the pitch and n is the revolutions per minute of the sprocket. The energy of one impact is $wv^2/2g$ ft-lb, in which w is the weight of the impinging body in pounds, v the speed of the roller along the arc BC in feet per second, and g the acceleration of gravity.

It is uncertain how much of the mass of the chain plays a part in the impact, but we may reasonably assume that it is proportional to the weight of a link and nearly equal to it.

Substituting $\pi Pn/360$ for v, and 32.2 for g, the energy of impact in foot-pounds is

$$\frac{wv^2}{2g} = \frac{wP^2n^2}{845617} \qquad [1]$$

where w is the mean weight of one chain link.

Examination of this expression shows that, in the case of any given chain, the destructive action due to impact between the chain and the sprocket is proportional to the square of the revolutions per minute, and is independent of both the chain velocity and the number of teeth in the sprocket.

The destructive action is also proportional to the weight of the chain link and to the square of the pitch. Hence, if sprocket wear is to be reduced, the revolutions per minute, the pitch, and the chain weight should be as low as is consistent with strength and pin bearing area.

The question might arise as to whether the chain tension F does not affect the amount of the impact. Undoubtedly it does, but to only a slight extent as is deduced from the fact that under conditions of high sprocket speed the wear on the sprocket teeth seems to be as rapid under a light load as under a heavy load. Such as it is, this effect is proportional to F and, very nearly, inversely proportional to the distance from the point of impact to the nearest seated roller. This distance is the pitch P. The expression for the energy in foot-pounds of one impact would then be

$$\frac{P^2n^2}{845617}\left(w + \frac{KF}{P}\right) \qquad [2]$$

in which K is a very small constant, undetermined.

Effects of Roller Impact

There are four detrimental tendencies which result from excessive roller impact, namely, the breaking of rollers, noise, heating, and the wear of sprocket teeth. Roller breakage has been nearly eliminated by the use of better materials and proper heat treatment. Noise caused by impact has been reduced by the introduction of new designs of sprocket teeth,[3] and can be further reduced by better lubrication and the use of short-pitch multiple-width chains. Heating is caused by wear and is always accompanied by a loss of power. Sprocket-tooth wear is the result of a continuous succession of blows administered by the rollers. This wear may be reduced in the case of the smaller sprockets by case-hardening. But assuming that reasonable attention is given to all other matters the most important consideration is that of keeping the impact per square inch of roller area within practical limits determined by experience. And this means the determination of the maximum sprocket speed to be used with a chain of a given pitch, weight, and roller size.

Maximum Allowable Sprocket Speed

The allowable amount of impact between a roller and a sprocket is proportional to the projected area A of the roller, which is the product of its length by its diameter.

The impact in foot-pounds per square inch of projected roller area is

$$\frac{P^2n^2}{845617A}\left(w + \frac{KF}{P}\right) \qquad [3]$$

Experience shows that for satisfactory service the energy of impact should not exceed, say, 0.362 ft-lb per sq in. of projected roller area. Hence, putting [3] equal to 0.362 and solving for n, the maximum value of the sprocket speed in revolutions per minute is

$$n_{\max} = \sqrt{\frac{845617 \times 0.362 \times A}{P^2\left(w + \dfrac{KF}{P}\right)}} = \frac{554}{P}\sqrt{\frac{A}{w + \dfrac{KF}{P}}}$$

where w is the mean weight of one link.

If we disregard the effect of the chain pull F, the constant K being very small, and substitute $W_FP/12$ for w, where W_F is the weight per foot of chain, the maximum value of n will be

$$n_{\max} = \frac{1920}{P}\sqrt{\frac{A}{W_FP}} \qquad [4]$$

By means of this formula a table of sprocket speeds may be made, showing the maximum number of revolutions per minute at which the smaller sprocket should run for each standard

[2] "Roller Chain Drives in Theory and Practice," by G. M. Bartlett, *Product Engineering*, July, 1931, p. 299.

[3] The British tooth form introduced by Hans Renold; the Diamond tooth form designed by the author; and the American tooth form adopted by the A.S.A.

chain when the pitch, the roller diameter, the width, and the weight per foot are known. Substituting $12V/NP$ for n in formula [4] and solving for the maximum value of V, the velocity of the chain in feet per minute, we have

$$V_{\max} = 160\ N \sqrt{\frac{A}{W_F P}} \quad \text{[5]}$$

Maximum Revolutions per Minute Based Upon Energy of Impact per Tooth per Minute. Multiplying the energy of one roller impact in Equation [1] by the number of impacts per tooth per minute, and dividing by A, the total energy of impact in foot-pounds per minute per tooth per square inch of projected roller area is

$$\frac{wP^2n^3}{845617\,A}$$

Substituting $W_FP/12$ for w, this becomes

$$\frac{W_FP^3n^3}{12 \times 845617 \times A}$$

Let K_1 be the maximum value of $W_FP^3n^3/A$. Then the maximum value of n will be

$$n_{\max} = \sqrt[3]{\frac{AK_1}{W_FP^3}} = \frac{K}{P}\sqrt[3]{\frac{A}{W_F}}$$

in which K is $\sqrt[3]{K_1}$.

If K is taken as 2000, the maximum value of n will be

$$n_{\max} = \frac{2000}{P}\sqrt{\frac{A}{W_F}} \quad \text{[6]}$$

This is based upon an assumed maximum impact in foot-pounds per tooth per minute, with only moderate lubrication.

Maximum Chain Velocity. To find the maximum chain velocity based upon the rate of sprocket wear per tooth per minute due to roller impact, substitute $12\ V/NP$ for n in formula [6] and solve for V. Then

$$V = 166\ N \sqrt[3]{\frac{A}{W_F}} \quad \text{[7]}$$

This means that, in so far as the rate of tooth wear is concerned, the permissible chain velocity is proportional to the number of teeth in the smaller sprocket for any given chain.

Allowable Chain Velocity as Affected by Centrifugal Force. The formula here developed will be based upon the theory that the maximum allowable centrifugal force for one chain link is proportional to the projected area of the roller.

A body, such as a chain link, rotating about an axis at a speed of n revolutions per minute will exert a centrifugal pull directed radially and equal in pounds to

$$F_R = 0.0000284\ W_L r n^2$$

where F_R = centrifugal force of one chain link, lb
r = virtual radius of sprocket = $PN/2\pi$ in.
W_L = weight of one link = $W_FP/12$, lb
W_F = weight per ft of chain, lb
P = pitch of chain, in.
N = number of teeth in sprocket
n = rpm of sprocket = $6V/\pi r$
V = chain velocity, fpm

Substituting

$PN/2\pi$ for r, $W_FP/12$ for W_L, and $6V/\pi r$ for n

$$F_R = \frac{W_FV^2}{18454\ N}$$

According to this theory the maximum permissible value of this quantity bears a constant ratio to the value of the projected roller area A.

Max $W_FV^2/18454\ N = K_1A$ where K_1 is a constant, and A is the product of the roller diameter times the chain width. Then

$$\max V = K\sqrt{\frac{NA}{W_F}}$$

This applies to multiple-width chains as well as to single chains.

Assuming 1634 fpm as the maximum velocity of a standard $^1/_2$-in.-pitch chain over a 17-tooth sprocket, the value of the constant K will be 793, and

$$\max V = 793\sqrt{\frac{AN}{W_F}} \quad \text{[8]}$$

where N is the number of teeth in the smaller sprocket.

Maximum Sprocket Speed Based Upon the Effect of Centrifugal Force. Substituting $nNP/12$ in place of V in the centrifugal formula, and solving for n, we have a formula for the maximum revolutions per minute based upon maximum centrifugal action,

$$\max \text{rpm} = \frac{9516}{P}\sqrt{\frac{A}{NW_F}} \quad \text{[9]}$$

Table 1 gives the maximum chain velocities and maximum sprocket speeds for standard roller chains and for various numbers of teeth in the sprockets. They are the minimum calculated results from formulas [4] to [9], inclusive.

Chain Elongation or Stretch

This is caused by wear between the pins and bushings which increases the size of the holes and reduces the size of the pins. This causes an increase in the pitch distance between the roller centers of each pin link, but does not affect the pitch of the roller links.

In Fig. 3*a*, the forward roller B of a pin link BC has just seated itself between the teeth of the driving sprocket. The pin link now begins to turn about the center of the forward pin B until the next roller C has seated itself. The angle of bend is $360/N_1$. During this turn, the pressure between the pin and bushing is equal to the whole load on the chain; but there is no wear between the bushing and the roller, nor between the roller and the sprocket. At this instant, the next link, CD, in Fig. 4*a*, which is a roller link, begins to turn about the rear pin C. During this turn the average pressure between the rear pin and its bushing is less than the load on the chain, and there is definite wear between the bushing and the roller.

As the same links leave the driven sprocket, Figs. 3*b* and 4*b*, the reverse conditions hold. It is evident that if the driving sprocket is smaller than the driven sprocket the forward pin of the pin link will wear more rapidly than the rear pin, and if the driving sprocket is the larger of the two, the rear pin will wear more rapidly.

Maximum Elongation. The stretching that can take place in a chain, before it becomes unfit for further use, varies according to the number of teeth on the larger sprocket, and the character of the drive. In some cases, chains are not discarded until they have stretched to the extent of 3 per cent or more of their original length, and in others they are considered unfit for use before they have stretched half that amount. As the number of teeth increases, a chain with 3 per cent elongation acts at higher points on the teeth, until when the number of teeth has reached

TABLE 1 MAXIMUM REVOLUTIONS PER MINUTE AND MAXIMUM CHAIN VELOCITIES FOR AMERICAN STANDARD ROLLER-CHAINS

Chain No.	Pitch	Roll diam	No. of teeth in smaller sprocket 7	9	11	13	14	15	16	17	20	24	28	32	37	48	54	62
35N	3/8	0.200	3043[a]	3043	3043	3043	2935	2835	2744	2662	2455	2240	2073	1940	1805	1585	1495	1395
			667[b]	857	1048	1238	1284	1330	1373	1414	1524	1680	1817	1940	2088	2377	2520	2700
41	1/2	0.306	2654	2654	2654	2654	2654	2654	2580	2500	2306	2106	1950	1823	1695	1488	1407	1310
			772	993	1213	1434	1545	1655	1718	1770	1920	2100	2275	2428	2612	2973	3195	3380
40	1/2	5/16	2517	2517	2517	2517	2517	2460	2381	2310	2130	1945	1800	1685	1567	1375	1298	1210
			732	942	1150	1360	1465	1534	1585	1634	1770	1940	2100	2240	2411	2748	2910	3120
50	5/8	0.400	1900	1900	1900	1900	1900	1900	1885	1830	1688	1542	1426	1335	1241	1089	1028	958
			692	890	1089	1287	1384	1480	1570	1620	1760	1925	2080	2222	2390	2722	2885	3095
60	3/4	15/32	1500	1500	1500	1500	1500	1500	1500	1500	1392	1270	1176	1100	1023	898	848	791
			657	844	1032	1220	1313	1407	1500	1584	1740	1905	2060	2200	2368	2697	2860	3061
80	1	5/8	940	940	940	940	940	940	940	940	940	940	885	828	771	677	638	594
			549	705	862	1019	1097	1173	1254	1330	1567	1880	2032	2195	2360	2690	2850	3055
100	1 1/4	3/4	645	645	645	645	645	645	645	645	645	645	645	639	593	522	492	459
			470	604	738	872	940	1010	1075	1145	1347	1612	1880	2131	2292	2611	2768	2968
120	1 1/2	7/8	520	520	520	520	520	520	520	520	520	520	520	520	515	453	427	398
			455	585	715	845	910	975	1040	1104	1300	1560	1820	2080	2385	2715	2878	3085
140	1 3/4	1	370	370	370	370	370	370	370	370	370	370	370	370	370	370	364	339
			378	486	594	702	756	810	864	917	1080	1296	1510	1728	1996	2590	2851	3060
160	2	1 1/8	325	325	325	325	325	325	325	325	325	325	325	325	325	325	301	281
			379	487	595	704	758	813	867	922	1083	1300	1516	1734	2003	2600	2708	2905
200	2 1/2	1 9/16	240	240	240	240	240	240	240	240	240	240	240	240	240	240	240	229
			350	450	550	650	700	750	800	850	1000	1200	1400	1600	1850	2400	2700	2955

NOTE: [a] Upper figures are maximum revolutions per minute. [b] Lower figures are maximum chain velocities.

about 60 the roller centers are acting as far out as the addendum circle of the sprocket.

Forces Acting on the Links

In Fig. 2, the sprocket is driving counter-clockwise and the tight strand of the chain is moving in the direction XBA. The roller B has just seated itself, and at this instant, its pressure upon the tooth is zero. The first active roller on the sprocket is A, upon which there are three forces acting, namely, AX which is equal to the tension F in the chain, ZA which is normal to the tooth curve at the point of contact with the roller, and YA which acts along the center line of the link AD. By drawing XZ through X parallel to AD, we have the force diagram AXZ in which XZ is the tension in the link AD, and ZA is the pressure between the roller and the tooth. The angle XAZ is the pressure angle. During the time that the link AB has been turning about the pin A the tension in the link has not changed.

If AB is a pin link, the forward pin A supports a bearing pressure equal to AX during the entire bending motion of AB about A.

If AB is a roller link, the pin is attached to the pin link AD and hence, during the bending, the pin pressure has decreased from AX to XZ, and the average pressure can be taken as about one half the sum of AX and XZ.

If N_1 is the number of teeth; ϕ_1 the pressure angle; and F the tension AX in the straight portion of the chain, then the pressure in pounds on the first tooth at A is, from the law of sines,

$$AZ = \frac{F \sin \dfrac{360}{N_1}}{\sin\left(\dfrac{360}{N_1} + \phi_1\right)} \quad \text{[10]}$$

The tension in pounds in the link AD is

$$F' = XZ = \frac{F \sin \phi_1}{\sin\left(\dfrac{360}{N_1} + \phi_1\right)} \quad \text{[11]}$$

The average pin pressure on the *rear* pin of a pin link during the flexing of a link at the driver is, in pounds, very nearly

$$\frac{F}{4}\left[1 + \frac{\sin \phi_1 + 2 \sin\left(\dfrac{180}{N_1} + \phi_1\right)}{\sin\left(\dfrac{360}{N_1} + \phi_1\right)}\right] \quad \text{[12]}$$

By laying out the force triangle successively for each link, the tooth pressures and link tensions can be determined for any link.

No significant rolling action takes place between the chain rollers and the sprocket teeth. Each bushing, however, turns within its roller an amount equal to $360/N_1$ every time it passes around a sprocket with N_1 teeth. The forward bushing on a roller link turns in the roller during approach and the rear bushing turns during departure. Thus the hole in the roller

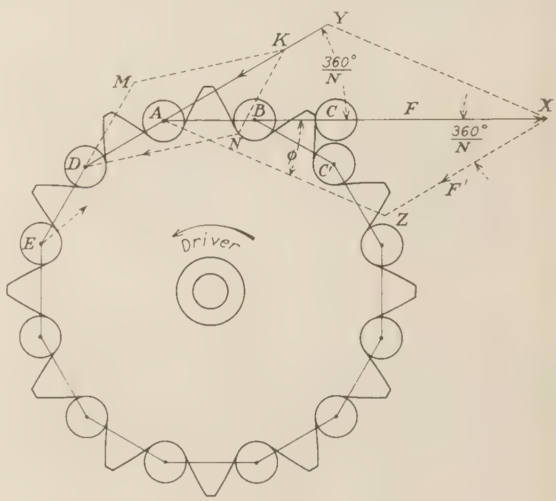

Fig. 2 Forces Acting on the Links

receives uniform wear in all parts throughout the life of the chain. The rate at which the rollers turn over their bushings in turns per minute is theoretically equal to $n_1/N_1 + n_2/N_2$, where n_1 and n_2 are the sprocket speeds, and N_1 and N_2 the numbers of teeth on the sprockets.

Rate of Wear Between Pins and Bushings. As chain elongation or "stretch" is caused by wear between the pins and the bushings in which they turn, and since a reduction of this elongation means a longer period of service for the chain, a careful study of what takes place when a chain approaches and leaves each sprocket is important.

In Fig. 3 are shown a driving sprocket at a, and a driven sprocket at b, and a chain in which a link on each sprocket is about to flex. Fig. 4 represents the same sprockets and chain as in Fig. 3, but advanced one pitch.

In Fig. 3a, the link AB is a roller link and BC is a pin link.

B will be called the forward pin and C the rear pin of the pin link. While the driving sprocket is turning through $1/N_1$ revolutions, C moves to the position B and seats itself between the next pair of teeth. In doing so, the link BC turns through an angle of $360/N_1$ with respect to AB, and the pin B turns within its bushing the same amount. During this rotation, the bearing pressure between pin and bushing has been equal to the working load F of the chain.

If d is the pin diameter, F the chain pull in pounds, and f the coefficient of friction, one bend of a pin link at the driver produces a frictional loss, in foot-pounds, of

$$\frac{\pi d f F}{12\,N_1} \qquad [13]$$

During this action, the roller has not turned between the teeth of the sprocket, nor has the bushing turned within its roller. This pin comes into action on the driving sprocket $n_1N_1/2L$ times per minute, where L is the total number of links in the chain, and n_1 is the revolutions per minute of the driving sprocket. Hence, the frictional loss in foot-pounds per minute on each forward pin over the driver is

$$\frac{\pi d f F n_1}{24\,L} \qquad [14]$$

Now this same pin B which plays a part in the bending of a pin link over the driver, plays its part in the bending of a roller link when leaving the driven sprocket, Fig. 3*b*. In this case the pressure between pin and bushing at B is F lb at the end of the motion; but at the beginning of the turn it is less than F lb as given in formula [11]. The average pressure in pounds during the turn is very nearly as in formula [12], as follows:

$$\text{Av. pressure} = \frac{F}{4}\left[1 + \frac{\sin\phi_2 + 2\sin\left(\dfrac{180}{N_2} + \phi_2\right)}{\sin\left(\dfrac{360}{N_2} + \phi_2\right)}\right] \qquad [12]$$

where ϕ_2 is the pressure angle corresponding to N_2 teeth. Multiplying by $\dfrac{\pi d f n_2}{24\,L}$ as in [14], the frictional loss in foot-pounds per minute on each forward pin over the driven sprocket is

$$\frac{\pi d f F n_2}{96\,L}\left[1 + \frac{\sin\phi_2 + 2\sin\left(\dfrac{180}{N_2} + \phi_2\right)}{\sin\left(\dfrac{360}{N_2} + \phi_2\right)}\right] \qquad [15]$$

Assuming the average pressure angle during the life of the chain to be (26 deg — 92 deg/N_2),[4] substituting this for ϕ_2, and adding formulas [14] and [15], we have for the frictional loss of each forward pin over both sprockets, in foot-pounds per minute

$$\frac{\pi d f F n_1}{96\,L}\left[4 + \frac{N_1}{N_2}\left(1 + \frac{\sin\left(26 - \dfrac{92}{N_2}\right) + 2\sin\left(26 + \dfrac{88}{N_2}\right)}{\sin\left(26 + \dfrac{268}{N_2}\right)}\right)\right] \qquad [16]$$

By a similar process each rear pin of a pin link can be shown to undergo a rate of wear, in foot-pounds per minute over both sprockets, equal to

$$\frac{\pi d f F n_2}{96\,L}\left[4 + \frac{N_2}{N_1}\left(1 + \frac{\sin\left(26 - \dfrac{92}{N_1}\right) + 2\sin\left(26 + \dfrac{88}{N_1}\right)}{\sin\left(26 + \dfrac{268}{N_1}\right)}\right)\right] \qquad [17]$$

in which n_2 can be replaced by N_1n_1/N_2, since $n_2/n_1 = N_1/N_2$.

The projected area of the pin is dB, where B is the effective length of the bushing. If the sum of Equations [16] and [17] is divided by 2, we shall have the average foot-pounds per minute per pin lost in friction. If this is then divided by dB the result

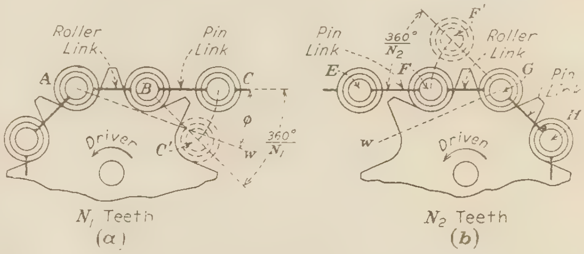

FIG. 3 ANALYSIS OF WEARING CONDITIONS BETWEEN ROLLERS, BUSHINGS, AND PINS

(*a*, Driving sprocket, *b* driven sprocket, and a chain in which a link on each sprocket is about to flex.)

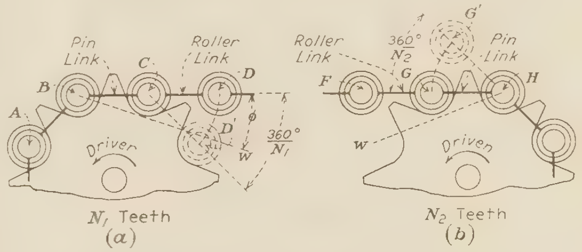

FIG. 4 THIS REPRESENTS THE SAME SPROCKET AND CHAIN AS IN FIG. 3 BUT ADVANCED ONE PITCH

will be the number of foot-pounds per minute per square inch of pin area lost in friction, namely,

$$\frac{\pi f F n_1}{192\,LB}\Big([16] + N_1/N_2\,[17]\Big) \qquad [18]$$

where [16] and [17] represent the parenthetic portion of formulas [16] and [17], respectively.

For purposes of study, we must assume that the chain length bears a constant relationship to the size of the sprockets. As the minimum number of pitches in a practical drive is about equal to the sum of the teeth in the two wheels, we may put $N_1 + N_2$ in place of L in formula [18]. Also, since the expression for the horsepower of a chain drive is $H = \dfrac{N_1PFn_1}{396000}$, we can substitute $\dfrac{396000\,H}{N_1P}$ for Fn_1. Then the work of friction in foot-pounds per minute per square inch of projected pin area is

$$\frac{6480\,fH}{BP}(M) \qquad [19]$$

where (M) is equal to the expression

[4] See A.S.A. Standard, B29a—1930.

$$\left[\frac{5+\sin\left(26-\frac{92}{N_1}\right)+2\sin\left(26+\frac{88}{N_1}\right)}{N_1(N_1+N_2)\sin\left(26+\frac{268}{N_1}\right)} + \frac{5+\sin\left(26-\frac{92}{N_2}\right)+2\sin\left(26+\frac{88}{N_2}\right)}{N_2(N_1+N_2)\sin\left(26+\frac{268}{N_2}\right)}\right]$$

TABLE 2 VALUES OF M AND $7.35/N_1N_2$

Teeth on larger sprocket	Teeth on smaller sprocket: 12	16	20	30	60
20	0.02915[a]	0.02220	0.01792	.....	.....
	0.03062[b]	0.02293	0.01836	.....	.....
30	0.01953	0.01492	0.01209	0.00819	.....
	0.02043	0.01533	0.01224	0.00817	.....
40	0.01465	0.01121	0.00910	0.00619	.....
	0.01533	0.01147	0.00918	0.00612	.....
60	0.00974	0.00747	0.00607	0.00414	0.00212
	0.01021	0.00767	0.00612	0.00408	0.00204
100	0.00582	0.00447	0.00363	0.00248	0.00128
	0.00612	0.00459	0.00367	0.00245	0.00122

[a] Upper figures are values of M. [b] Lower figures are values of $7.35/N_1N_2$.

Values of this quantity, M, for various combinations of N_1 and N_2 are found to be very close to those obtained from the simple expression $7.35/N_1N_2$. In the body of Table 2, the upper figures are values of M and the lower figures are values of $7.35/N_1N_2$. It is evident that without serious error we can put this shorter expression in place of M and simplify formula [19] thus:

Work of friction in foot-pounds per minute per square inch of pin area is

$$\frac{47628fH}{BPN_1N_2}\text{ (nearly)} \qquad [20]$$

where the chain length $= N_1 + N_2$ pitches. But for any other chain length, L_p, the work lost in friction between pins and bushings is

$$\frac{47628fH}{BPN_1N_2} \times \frac{N_1+N_2}{L_p} \qquad [21]$$

where L_p is the actual chain length in pitches.

Assuming that chain elongation is proportional to the unit wear between pins and bushings, and that unit wear is proportional to the work of friction per square inch of projected pin area, the value of the expression in any one of formulas [18], [19], [20], or [21] is proportional to the rate of elongation of the chain due to wear between pins and bushings.

An inspection of formulas [18], [20], and [21] shows that the rapidity of chain elongation varies directly as the chain tension, the sprocket speed, the coefficient of friction, and the horsepower. It varies inversely as the chain length, the bushing length, the pitch, and, very nearly, the product of the numbers of teeth in the two sprockets, assuming that $L = N_1 + N_2$. It is independent of the pin diameter providing that the diameter is sufficient for strength and for proper bearing area. It also appears that if N_1 and N_2 are interchanged in the formula, the value of the expression is not changed, and so we can consider N_1 as the number of teeth on the smaller sprocket regardless of whether it is the driving or the driven wheel.

Maximum Horsepower. In order to derive a formula for use in the selection of a chain for a given horsepower, sprocket speed, and number of teeth on driving and driven wheels, let it be assumed tentatively that the chain length L will be equal to the minimum of $N_1 + N_2$ links. In the average drive this will be somewhat greater, but the difference will be on the side of safety.

Let it be further assumed that the maximum rate of wear (expressed in terms of the work of friction) should not exceed, say, 44 ft-lb per min per sq in. of projected pin area, and that the coefficient of friction f is 0.04. Then, 44 will be the maximum value of

$$\frac{47628 \times 0.04 \times H}{BPN_1N_2}$$

Whence, max hp $= 0.023\ BPN_1N_2$ ....[22]

It should be noted that the constant 0.023 is arbitrary and can be increased or decreased depending upon what may be considered a reasonable rate of wear.

For a chain whose length is other than $N_1 + N_2$ links, the horsepower determined from [22] should be multiplied by $L_p/N_1 + N_2$, where L_p is the number of links or pitches in the chain.

Maximum Unit Bearing Pressure on Pins. From formula [22] it might appear that the amount of power that a given chain drive can transmit satisfactorily depends only upon the pitch, the bushing length, the number of links in the chain, and the product of the number of teeth in the two sprockets. This would mean that the horsepower is independent of the pin diameter and of the chain velocity. If, however, the chain velocity is too low, the working pull on the chain may become very high and produce an excessive bearing pressure on the pins. The pressure per square inch of projected pin area should not exceed 5000 to 6000 lb for standard roller transmission chains.

The unit pressure on a pin is equal to $\frac{33000H}{VBd}$ where Bd is the projected pin area, and if this is put equal to 5000 lb as a maximum, we have

$$\text{max hp} = 0.152VBd \qquad [23]$$

It now appears that the maximum horsepower of a drive whose chain contains $N_1 + N_2$ links is the lesser of the two values obtained from formulas [22] and [23].

Centrifugal Pull in Chain. The extra pull in the chain in pounds due to centrifugal force is

$$F_c = \frac{W_FV^2}{115920} \qquad [24]$$

Where W_F is the weight in pounds per foot of chain, and V is the chain velocity in feet per minute. This formula is derived in the following way. The well-known expression for the tension induced in a belt by centrifugal force is Wv^2/g lb; where W is the weight of a strip of belt 1-ft long and 1 sq in. cross-section, v is the belt velocity in feet per second, and g is the force of gravity. If V is the velocity in feet per minute,

$$v^2 = \left(\frac{V}{60}\right)^2 \text{ and } F_c = \frac{W_FV^2}{3600 \times 32.2} = \frac{W_FV^2}{115920}$$

This extra chain pull imposes an added horsepower load equivalent to:

$$\frac{VF_c}{33000} = \frac{V}{33000} \times \frac{W_FV^2}{115920}$$

Hence,
$$\text{centrifugal hp} = \frac{W_FV^3}{3,825,360,000} \qquad [25]$$

This amount of power is not actually added to that required by the chain; but its effect on the rate of wear of the chain is the same as if that amount of extra power actually were being transmitted. The only additional demand upon the source of power

is that required to overcome the extra friction due to such an increase in the load; and this is comparatively small.

If formulas [22] and [23] are to express the maximum power that can be transmitted by a given drive without producing excessive wear or excessive pin pressure, this centrifugal horsepower must be deducted from that given by these formulas. We now have, for a drive using a chain containing $N_1 + N_2$ links, the lesser of the values found from the two formulas:

$$\text{max hp} = 0.023BPN_1N_2 - \frac{W_FV^3}{3{,}825{,}360{,}000} \quad \ldots\ldots [26]$$

$$\text{max hp} = 0.152VBd - \frac{W_FV^3}{3{,}825{,}360{,}000} \quad \ldots\ldots [27]$$

Horsepower Tables Based on Chain Velocity and the Product $N_1 \times N_2$

The horsepower values yielded by the two formulas, [26] and [27], are equal when $V = \dfrac{0.1513PN_1N_2}{d}$.

Table 3 shows horsepower values for various values of N_1N_2 and various chain velocities for 1-in.-pitch standard roller chain No. 80. Where the chain length is other than $N_1 + N_2$ pitches, the tabulated horsepowers *above* the heavy line should be multiplied by the actual chain length in pitches and divided by $N_1 + N_2$, but they should not be multiplied by more than 1.5 nor should they in any case exceed those shown in the same column below the heavy line. For chain velocities below 100 fpm, the horsepower is proportional to the velocity.

TABLE 3 HORSEPOWERS FOR STANDARD ROLLER CHAIN NUMBER 80[a]

$N_1 \times N_2$	Chain velocity in fpm 48	60	78	97	121	155	194	242	310	388	485	620	775	1200	1600
100	2.01	2.01	2.01	2.01	2.01	2.01	2.01	2.01	2.00	1.99	1.96	1.91	1.81	1.27	..
125	2.01	2.51	2.51	2.51	2.51	2.51	2.51	2.51	2.50	2.49	2.46	2.41	2.31	1.77	..
160	2.01	2.51	3.22	3.22	3.22	3.22	3.22	3.22	3.21	3.20	3.17	3.12	3.02	2.48	1.48
200	2.01	2.51	3.22	4.02	4.02	4.02	4.02	4.02	4.01	4.00	3.97	3.92	3.82	3.28	2.20
250	2.01	2.51	3.22	4.02	5.03	5.03	5.03	5.03	5.02	5.01	4.98	4.93	4.83	4.29	3.29
320	2.01	2.51	3.22	4.02	5.03	6.44	6.44	6.44	6.43	6.42	6.39	6.34	6.24	5.70	4.70
400	2.01	2.51	3.22	4.02	5.03	6.44	8.04	8.04	8.03	8.02	7.99	7.94	7.84	7.30	6.30
500	2.01	2.51	3.22	4.02	5.03	6.44	8.04	10.0	10.0	10.0	10.0	9.95	9.85	9.31	8.31
640	2.01	2.51	3.22	4.02	5.03	6.44	8.04	10.0	12.8	12.8	12.8	12.8	12.7	12.1	11.1
800	2.01	2.51	3.22	4.02	5.03	6.44	8.04	10.0	12.8	16.0	16.0	16.0	15.9	15.3	14.3
1000	2.01	2.51	3.22	4.02	5.03	6.44	8.04	10.0	12.8	16.0	20.0	20.0	19.9	19.4	18.4
1280	2.01	2.51	3.22	4.02	5.03	6.44	8.04	10.0	12.8	16.0	20.0	25.6	25.5	25.0	24.0
1600	2.01	2.51	3.22	4.02	5.03	6.44	8.04	10.0	12.8	16.0	20.0	25.6	31.9	31.4	30.4

[a] P = 1 in., B = 0.875 in., d = 0.312 in., roller diameter = 0.625 in., and W_F = 1.63 lb.

Values of N_1N_2 lying between 400 and 1000 will probably comprise 80 per cent or more of all chain drives in use. Any value of N_1N_2, such as 720, may stand for a number of combinations, such as 8×90; 15×48; 18×40; etc.

Not all of these possible combinations will make satisfactory drives. For example, 10 teeth combined with a chain velocity of 1000 fpm or 16 teeth combined with a velocity of 1500 fpm would not be good practice because these velocities are beyond those given as the maximum in Table 1.

Elastic Stretch in the Chain. Due to the polygon effect in sprocket action, the angular speed ratio between the two wheels tends to vary between a maximum and a minimum during the passage of each tooth. But due to the inertia of the wheels and their attached masses this variation is resisted, and the result is that in order to compensate for the polygon action there must be a rapid succession of changes in the length of that portion of the chain which spans the distance between the two sprockets. This elastic stretch is greatest when the tangential distance between the sprockets is an odd multiple of half the pitch; in which case it is very nearly equal, in inches, to

$$\delta = 0.6P\left(\frac{1}{N_1^2} + \frac{1}{N_2^2}\right)$$

And if the tangential distance is an exact multiple of the pitch, the elastic stretch is a minimum and equal, in inches, to

$$\delta = D_1 \sin\theta - D_2 \sin\frac{N_1\theta}{N_2}$$

where $\sin\theta = \sqrt{1 - \dfrac{N_1}{\pi D_1}}$, and D_1 and D_2 are the pitch diameters of the smaller and larger sprockets, respectively.

A part of this stretch may be absorbed by the films of lubricant between the pins and bushings if the working load is not too great, and a part is taken up by an elastic stretch in the chain itself. This induces stresses in the chain over and above those due to the working load, and these stresses are inversely proportional to the length of the chain span and directly proportional to the elastic stretch. Hence, a short center distance should not be combined with a low number of teeth on the sprockets. A safe rule for the minimum center distance is 20 pitches. This insures that the minimum span of the chain from the driving to the driven sprocket will generally be between 17 and 20 pitches.

Horsepower Tables Based on Sprocket Speed

In most cases of chain drive calculations, the known quantity is the revolutions per minute of the smaller sprocket rather than the chain velocity; and so a more convenient and informative table for reference would be one in which the sprocket speeds are read at the top of the table and various combinations of teeth are listed in the left-hand column, as shown in Table 4 which is calculated for the same chain (No. 80) as in Table 3.

Tables of this sort should be much more extensive than Table 4, but their greater usefulness offsets the disadvantage of cumbersomeness.

For the computation of such tables, the necessary data are the pitch P, the bushing length B, the pin diameter d, and the weight per foot W_F. Then, putting V equal to $PN_1n_1/12$ in formulas [26] and [27], we have for the horsepower the lesser of the two values,

$$\text{hp} = 0.023PBN_1N_2 - \frac{W_FP^3N_1^3n_1^3}{6{,}609{,}081{,}600{,}000} \quad \ldots\ldots [28]$$

$$\text{hp} = 0.0127PBdN_1n_1 - \frac{W_FP^3N_1^3n_1^3}{6{,}609{,}081{,}600{,}000} \quad \ldots\ldots [29]$$

This assumes a chain length of $N_1 + N_2$. But a more reasonable chain length is one that will make the center distance be-

TABLE 4 HORSEPOWERS FOR STANDARD ROLLER-CHAIN NUMBER 80[a]

N_1	N_2	L_P	Cent. dist. (pitches)	Speed of the smaller sprocket, rpm 162	183	202	225	252	281	313	348	386	433	487	547	940
15	15	56	20.50	8.42	8.42	8.41	8.41	8.41	8.40	8.39	8.38	8.37	8.32	8.32	8.28	7.72
15	18	58	20.74	8.42	9.52	9.51	9.51	9.51	9.50	9.39	9.38	9.37	9.32	9.32	9.28	8.72
15	21	60	20.97	8.42	9.52	10.5	10.5	10.5	10.5	10.5	10.5	10.5	10.4	10.4	10.4	9.81
15	25	62	20.93	8.42	9.52	10.5	11.7	11.7	11.7	11.7	11.7	11.7	11.6	11.6	11.6	11.0
15	30	66	21.61	8.42	9.52	10.5	11.7	13.1	13.1	13.1	13.1	13.1	13.0	13.0	13.0	12.4
15	36	68	20.97	8.42	9.52	10.5	11.7	13.1	14.6	14.6	14.6	14.6	14.5	14.5	14.5	13.9
15	43	72	21.01	8.42	9.52	10.5	11.7	13.1	14.6	16.2	16.2	16.2	16.2	16.2	16.1	15.6
15	51	78	21.73	8.42	9.52	10.5	11.7	13.1	14.6	16.2	18.1	18.1	18.0	18.0	18.0	17.4
15	60	84	22.06	8.42	9.52	10.5	11.7	13.1	14.6	16.2	18.1	20.8	20.8	20.8	20.7	20.2
15	72	90	21.28	8.42	9.52	10.5	11.7	13.1	14.6	16.2	18.1	20.8	22.4	22.4	22.3	21.8
15	86	102	22.91	8.42	9.52	10.5	11.7	13.1	14.6	16.2	18.1	20.8	22.4	25.2	25.2	24.6
15	102	116	24.82	8.42	9.52	10.5	11.7	13.1	14.6	16.2	18.1	20.8	22.4	25.2	28.3	30.1
19	19	60	20.50	10.8	11.6	11.6	11.6	11.6	11.6	11.6	11.5	11.5	11.4	11.4	11.3	10.2
19	21	62	20.99	10.8	12.1	12.4	12.4	12.4	12.4	12.4	12.4	12.3	12.3	12.2	12.1	11.0
19	25	64	20.97	10.8	12.1	13.3	13.9	13.9	13.9	13.9	13.9	13.8	13.8	13.7	13.7	12.5
19	30	68	21.67	10.8	12.1	13.3	14.8	15.7	15.7	15.7	15.7	15.7	15.6	15.6	15.5	14.4
19	36	70	21.07	10.8	12.1	13.3	14.8	16.6	17.7	17.7	17.7	17.7	17.6	17.6	17.5	16.4
19	43	74	21.15	10.8	12.1	13.3	14.8	16.6	18.5	19.9	19.9	19.8	19.8	19.7	19.7	18.5
19	51	80	21.89	10.8	12.1	13.3	14.8	16.6	18.5	20.6	22.2	22.1	22.1	22.0	22.0	20.8
19	60	86	22.27	10.8	12.1	13.3	14.8	16.6	18.5	20.6	22.9	24.9	24.8	24.8	24.7	23.6
19	72	92	21.57	10.8	12.1	13.3	14.8	16.6	18.5	20.6	22.9	25.3	27.8	27.8	27.7	26.6
19	86	104	23.26	10.8	12.1	13.3	14.8	16.6	18.5	20.6	22.9	25.3	28.4	31.4	31.3	30.2
19	102	120	26.38	10.8	12.1	13.3	14.8	16.6	18.5	20.6	22.9	25.3	28.4	31.4	35.7	37.6

[a] P = 1 in., B = 0.875, d = 0.312, W_P = 1.63 lb., and maximum speed = 940 rpm.

tween the sprockets approximately 20 pitches. This will be accomplished if the chain length is made equal to 38 + 0.6 $(N_1 + N_2)$ pitches for all values of $N_1 + N_2$ less than 95, but equal to $N_1 + N_2$ when the sum exceeds 95.

Formula [28], then, can be used when $N_1 + N_2$ is over 95, but for values of 95 and less, the first term of [28] must be multiplied by the quotient of 38 + $0.6(N_1 + N_2)$ divided by $N_1 + N_2$ and the formula will then be

$$\text{hp} = 0.0138\, PBN_1N_2\left(\frac{63.33}{N_1 + N_2} + 1\right) - \frac{W_P P^3 N_1^3 n_1^3}{6{,}609{,}081{,}600{,}000} \quad [30]$$

Table 4 gives horsepower values for drives using 15 teeth on the smaller wheel, and also for drives using 19 teeth. Values of N_2 are chosen for convenience in an approximate geometric series. Values for the revolutions per minute may be arbitrarily chosen, but in the first half of this table they were computed from the formula

$$n_1 = \frac{1.0866\, N_2}{d}\left(\frac{63.33}{N_1 + N_2} + 1\right)$$

for the several values of N_2, so that the horsepower found from formula [30], for any given value of N_2, would be equal to that found from formula [29] using the corresponding value of n_1. This determines the location of the heavy lines, below which are the horsepower values based upon a maximum unit pin pressure of 5000 lb and calculated from [29]. All values *above* the heavy line are calculated from formula [30], except where $N_1 + N_2$ is greater than 95, in which case, formula [28] is used. For convenience in this case the same values of revolutions per minute have been tabulated for 19 teeth as for 17 teeth.

In tables previously published it has been customary to reduce the allowable pin pressure as the speeds increase. It can be shown that the actual rubbing distance in feet per minute between any pin and bushing acting over both sprockets is

$$\frac{\pi d n_1 (N_1 + N_2)}{12\, N_2 L_P}$$

This is the expression for the average rubbing velocity. It gives 3.06 fpm for No. 80 chain with 10 and 10 teeth at 940 rpm; and it gives 0.96 fpm for the same chain with 16 and 100 teeth at 940 rpm. As we have numerous examples of punch-press pressures ranging from 5000 to 7000 lb at more than 100 fpm rubbing speed, it would seem that there is no theory supporting a gradual reduction of unit bearing pressures in chains where the maximum rubbing speed is as low as 3 or 4 fpm, and where the periods of rest are relatively much greater than in punch presses.

Radiation Intensities and Heat Transfer by Radiation in Boiler Furnaces

By HUBER O. CROFT[1] and C. F. SCHMARJE,[2] IOWA CITY, IOWA

This paper describes the development of an absorption calorimeter with a fused-quartz window and discusses its use in connection with a series of boiler tests. The results of these tests are compared with the Hudson-Orrok formula and the Wohlenberg method of computing radiation heat transfer.

A tentative empirical equation is given for computing radiation intensities, taking into account the dirtiness of the cold surfaces. Tentative formulas are also given for computing the average heat transfer by radiation in boiler furnaces.

THERE have been several methods suggested for the computation of the radiant-heat exchange occurring in boiler furnaces. Of these, probably the best known are the Hudson-Orrok formula, and the Wohlenberg method.

The purpose of this investigation is, first, to secure experimental data which will serve as a basis for comparing the results obtained by the two methods of computation mentioned above, and, second, to arrive at a simple empirical equation to fit these data.

The method consisted of determining, experimentally, the intensities of radiation at various locations inside a boiler furnace during a series of boiler tests.[3] For this purpose there has been developed a quartz-window radiation calorimeter.

Description of the Radiation Calorimeter and Its Calibration

Description of the Calorimeter. The principle of operation of the radiation calorimeter developed for this investigation is to absorb in a stream of water, the radiant energy passing through a fused-quartz window. The energy absorbed by the water is indicated by the increase in the temperature of a measured quantity of flow.

The calorimeter is shown in Fig. 1. The pyralin-walled, water chamber, A, is surrounded by an air chamber, except at the front end, which is closed by means of the fused-quartz window W, held in place by an aluminum tube T against a bakelite partition D. This partition in addition to being the support for the inner assembly, consisting of the absorption chamber and its surrounding air chamber (shown in detail in Fig. 1-A), is also the boundary between the front cooling chamber F and the rear cooling chamber R. Into the rear of the outer copper shell S is screwed an iron water-cooled pipe P, through which are led the water tubes to the absorption and cooling chambers, A, F, and R, together with the thermocouple leads.

The thermocouples for the main chamber are made of No. 22 copper and constantan wires with the junctions formed by soldering the two wires together. These couples are insulated with a thin layer of pyralin and sealed into the inlet and outlet pyralin water tubes of the absorption-chamber A. These couples were calibrated in air, and in flowing water before installation, and the calibration was checked after assembly in the tubes.

The thermocouple leads, insulated with silk and two coats of varnish, are carried out through a glass tube to the rear of the supporting pipe, P.

Operation of the Calorimeter. In operation, the three chambers, A, F, and R were supplied with water from a constant level tank. The flow through the absorption chamber was regulated to about 30 to 35 lb per hr, which should give turbulent flow about the outlet thermocouple.

The electromotive forces of the couples were determined against a third copper-constantan junction placed in a thermos jar of ice water, by means of a Leeds and Northrup precision potentiometer; the electromotive forces were determined for both the inlet and the outlet thermocouple about 15 separate times in the course of observations of approximately six minutes duration, readings being made to 0.005 millivolt, corresponding to a temperature interval of 0.2 F.

The water discharged from the absorption chamber was collected in a calibrated glass flask, the time of collection being noted with a stopwatch. The probable error in the water-rate determinations is less than one-half of 1 per cent.

Calibration of the Calorimeter. The calibration of the calorimeter consisted in comparing the radiation received by the calorimeter from an electrically heated carbofrax plate, with that received by a special "black-body" absorber in the same location.

The black-body absorber was similar to those which have been used by H. C. Hottel and J. D. Keller,[4] and by E. Schmidt.[5] It consists of a cylindrical cavity C, Fig. 2, with blackened walls which are surrounded by a water chamber W. Pyralin-insulated, copper-constantan thermocouples are sealed in the inlet and outlet tubes of the water chamber. The outer walls of the water chamber, W, are thermally insulated with 85 per cent magnesia. Water-cooled shields F, and O, protect the absorption chamber

[1] Professor and Head of Department of Mechanical Engineering, University of Iowa, Iowa City, Iowa. Mem. A.S.M.E. Professor Croft received the B.S. degree from the University of Colorado in 1918, and M.S. from the University of Illinois in 1925. He served on the faculties of the University of Illinois and Stanford before assuming his present responsibilities. Professor Croft represented the Society at a joint meeting with the Mexican Society of Engineers in Mexico during the summer of 1934.

[2] Graduate Student in Mechanical Engineering, University of Iowa. Jun. Mem. A.S.M.E. Mr. Schmarje received the degree of B.S. in M.E. from the University of Iowa in 1932. Following his graduation he was research assistant in mechanical engineering, engaged in work relating to the utilization of Iowa coals. He received the M.S. degree in 1934. At present he is pursuing post-graduate work in an experimental investigation of heat transfer by radiation in boiler furnaces.

[3] These tests were conducted in cooperation with the Committee on Utilization of Iowa Coal. A report of these investigations will be made in the near future.

Contributed by the Fuels Division for presentation at the Semi-Annual Meeting, Cincinnati, Ohio, June 19 to 21, 1935, of The American Society of Mechanical Engineers.

Discussion of this paper should be addressed to the Secretary, A.S.M.E., 29 West 39th Street, New York, N. Y., and will be accepted until July 10, 1935, for publication in a later issue of Transactions.

[4] "Effects of Reradiation on Heat Transmission in Furnaces and Through Openings," by H. C. Hottel and J. D. Keller, Trans. A.S.M.E., vol. 55, 1933, paper IS-55-6-39.

[5] "Die Wärmestrahlung von Wasser und Eis, von bereiften und benetzten Oberflächen," by E. Schmidt, *Forschung auf dem Gebiete des Ingenieurwesens*, vol. 5, 1934, p. 1.

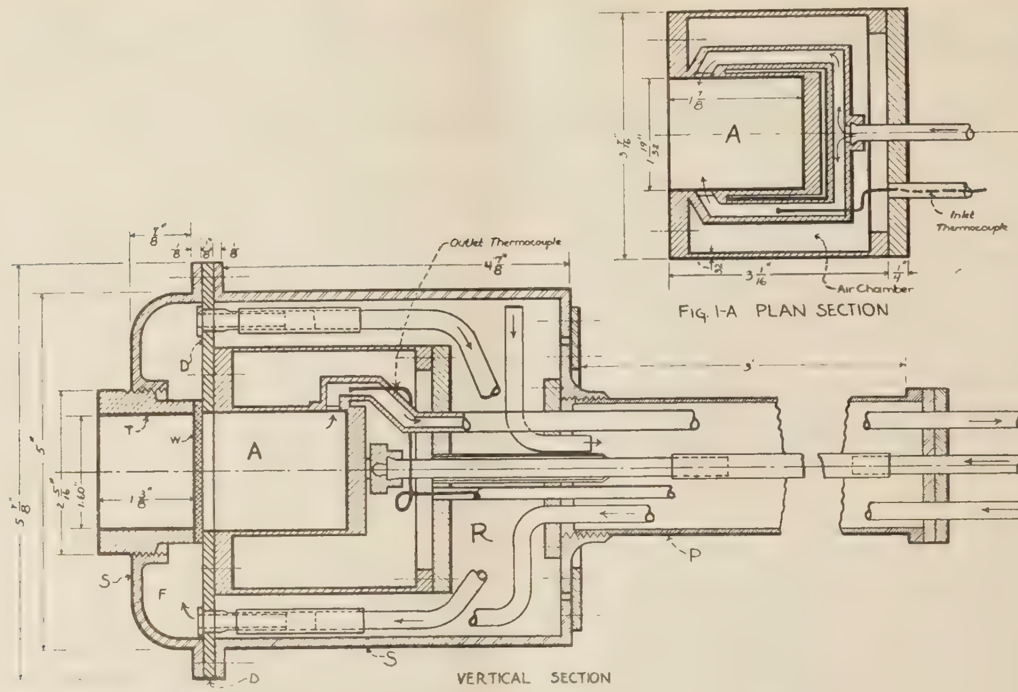

Fig. 1 Details of the Quartz-Window Radiation Calorimeter

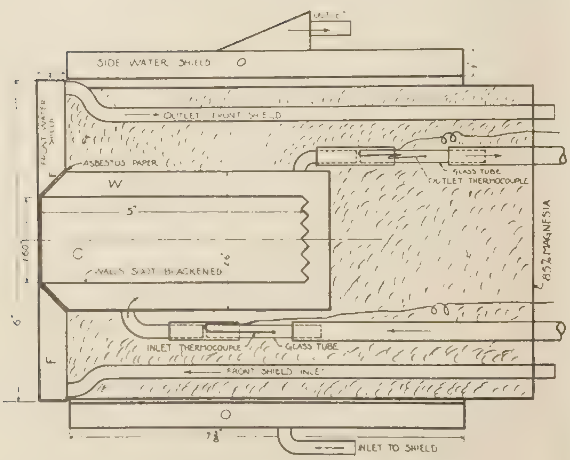

Fig. 2 Details of the Black-Body Absorber

from radiation at the front and sides, and define the opening of C, which is of the same size as the opening of the quartz-window calorimeter.

The calibration arrangements are shown in Figs. 3 and 4. In Fig. 3, the absorption of the black body was determined for a series of different temperatures of the heated plate, as indicated by the chromel-alumel thermocouple imbedded in the front surface of the hot-plate. Then in another series of tests (Fig. 4), the absorption of the radiation calorimeter with the quartz-window was determined for the corresponding hot-plate temperatures. A special water-cooled shield was used with the quartz-window instrument in order to duplicate the shape of the black-body absorber.

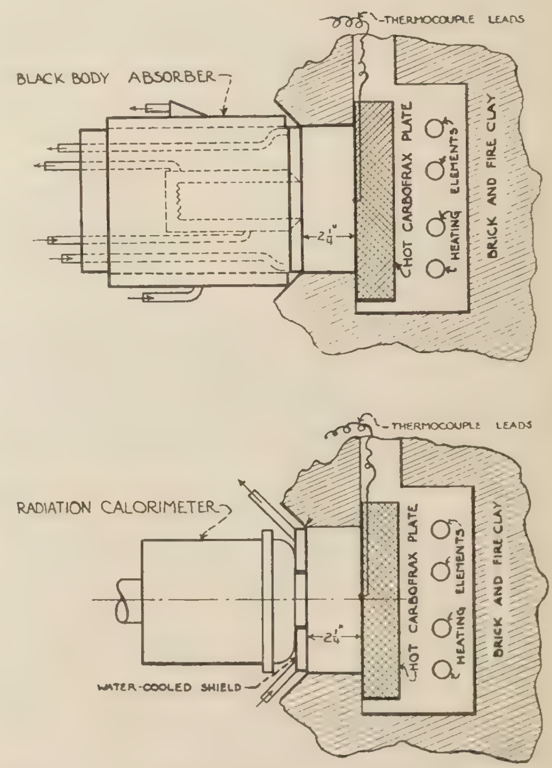

Figs. 3 and 4 Vertical Sections Through Calibration Arrangements

The calibration data are shown in Fig. 5. In these graphs the energy absorbed by the quartz-window calorimeter, and by the special black-body absorber, have been plotted against the radiation intensity at the surface of the hot plate. The radiation

intensity has been computed by means of the Stefan-Boltzmann law, which may be expressed as

$$I = 0.172 \times 0.92[(T_f/100)^4 - (T_e/100)^4] \ldots\ldots [1]$$

in which I is the radiation intensity in Btu per sq ft per hr; 0.172 is the radiation constant; 0.92 is the emissivity of the hot plate as determined experimentally in an earlier investigation;[6] T_f is the absolute temperature of the surface of the hot plate as measured by the chromel-alumel thermocouple; and T_e is the absolute temperature of the receiver.

It will be noted in Fig. 5 that the energy absorbed by the black-body absorber is directly proportional to the radiation intensity I. Also, the energy absorbed by the quartz-window instrument is apparently proportional to the radiation intensity I.

The ratio between the energy absorbed by the quartz-window instrument and the energy which would be absorbed by the special black-body absorber is 0.464 from Fig. 5. The calibration equation for the quartz-window instrument is

[6] "The Construction and Calibration of an Instrument for the Measurement of Radiant Energy in Boiler Furnaces," by L. P. Meade, Thesis, State University of Iowa, 1934.

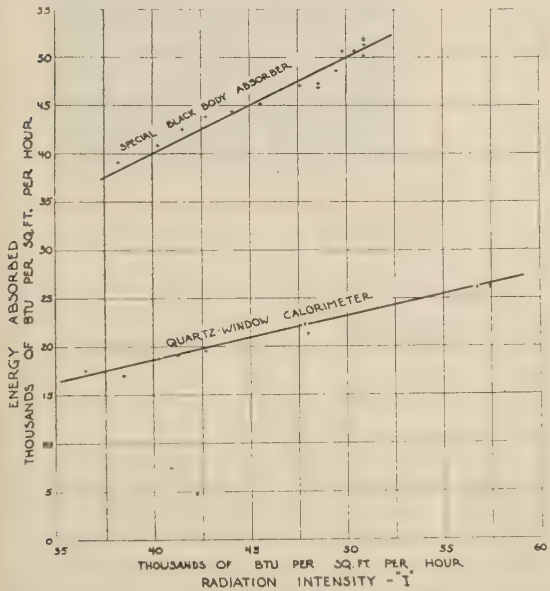

FIG. 5 CALIBRATION CURVES OF THE QUARTZ-WINDOW CALORIMETER AND THE BLACK-BODY ABSORBER

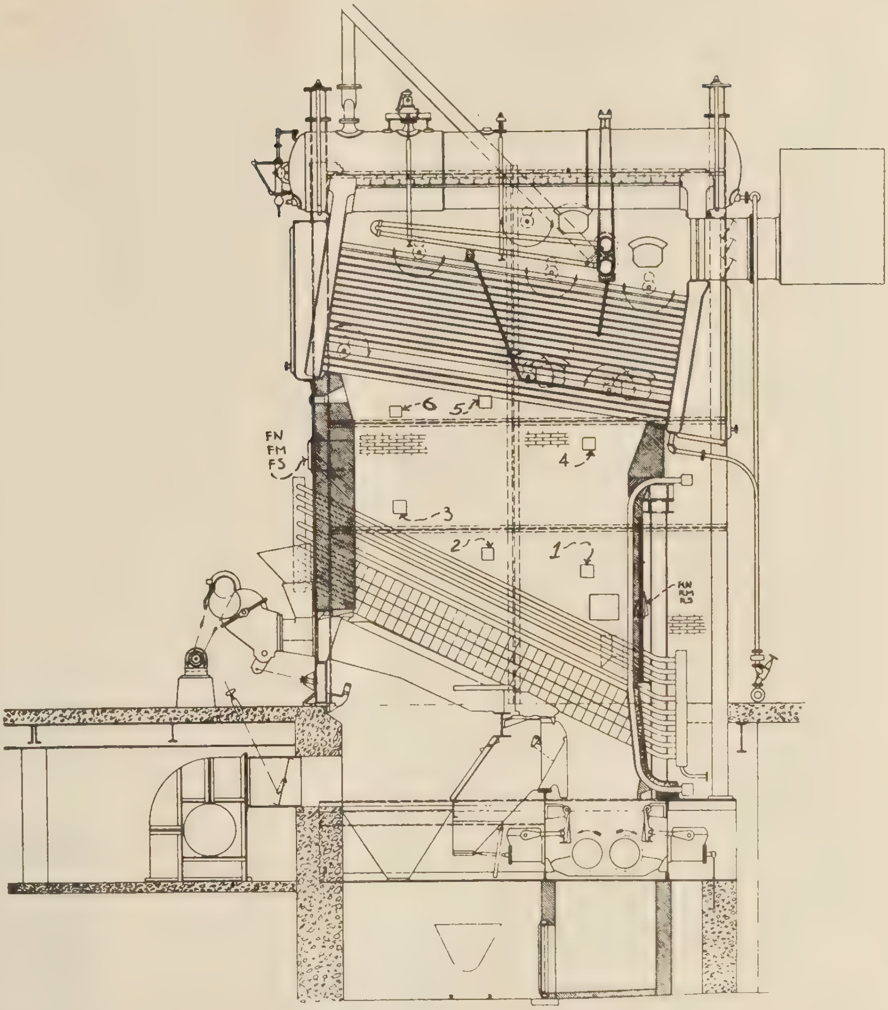

FIG. 6 CROSS-SECTION OF BOILER, STOKER, AND SETTING, SHOWING THE LOCATION OF THE OBSERVATION DOORS

$$I = M/0.464 = 2.155M \ldots\ldots\ldots\ldots\ldots [2]$$

in which I is the radiation intensity in Btu per sq ft per hr; and M is the measured energy-absorption rate of the calorimeter in Btu per sq ft per hr. The radiation intensity, I, which has been studied in this investigation, is the rate of radiant-energy absorption in Btu per sq ft per hr, which would be experienced by a perfectly black surface at 90 F.

It was the object of the calibration tests to have the two arrangements of Figs. 3 and 4 such that it would not be necessary to determine the exact temperature of the front surface of the hot plate, but to use the temperature as indicated by the chromel-alumel thermocouple as a guide to show when the true surface temperatures were identical in the two separate arrangements.

Then, for a given hot-plate temperature, the energy absorbed by the quartz-window calorimeter could be compared directly with that received by a black-body absorber of similar size for the same radiation intensity. Thus the calibration does not depend upon the accurate determination of the temperature at the exact boundary of the hot-plate, nor upon geometrical "form factors." It depends, rather, almost wholly upon how nearly the so-called black-body absorber approximates a true black body (which absorbs all incident radiation, reflecting none)

TABLE 1 ACTUAL RADIATION INTENSITIES,[a] I[b]

Door No.[c] / Test No.	1	2	3	4	6	RS	RM	RN	FM	FN	Average
53	30.5	49.6	34.0	28.5	..	..	..	..	..	..	36.1
	34.8	..	..	..	..	..	..	..	..	..	
54	36.9	49.9	46.9	30.6	..	..	..	..	..	..	41.0
	37.1	55.2	..	41.2	..	..	..	..	..	..	
	19.5	..	..	..	..	..	..	..	..	..	
	18.5	..	..	..	..	..	..	..	..	..	
55	36.6	49.2	50.0	44.4	..	41.4	42.5	51.9	..	..	44.1
						..	46.8	33.2	..	..	
S2	33.8	45.8	48.8	23.3	..	34.0	38.8	37.2	27.4	..	37.1
						..	41.2	..	..	..	
						..	50.6	..	..	..	
S3	41.6	70.1	52.1	43.6	50.1	40.0	57.5	47.5	70.5	..	49.5
						..	60.0	33.2	..	..	
						..	..	30.4	..	..	
56	57.8	79.0	65.9	62.4	..	35.7	48.1	32.6	75.9	..	62.0
	58.9	78.3	..	..	..	51.6	62.6	..	76.0	..	
						..	66.0	..	77.5	..	
57	33.5	89.0	76.1	49.3	..	51.5	65.9	47.5	74.0	..	64.9
	72.0	88.0	77.6	63.5	..	..	..	..	70.1	..	
	48.0	..	..	..	..						
58	48.4	77.6	84.6	55.2	..	69.7	78.1	57.8	81.0	67.8	64.9
						52.2	72.6	43.0	56.5	79.0	
59	86.9	62.5	72.9	88.8	..	71.6	70.1	80.6	..	..	75.6
						70.5	97.0	68.9	..	..	
60	52.0	75.0	60.6	40.2	..	76.0	53.0	64.0	65.4	67.6	65.9
	69.7	79.7	76.2	66.4	..	61.7	73.3	61.0	72.8	72.7	
S5	87.6	107.0	77.6	71.5	..	40.6	60.0	43.6	..	..	62.6
						..	61.1	67.5	..	..	
						..	60.4	..	..	..	
S6	57.7	79.1	65.9	52.4	..	54.3	51.6	40.3	80.3	47.3	63.4
	..	86.1	84.5	33.7	..	46.5	55.5	39.3	48.1	80.3	
	..	83.3	..	..	..	..	..	..	97.0	83.0	
S7	67.0	105.3	71.2	72.0	..	62.1	89.1	83.1	..	..	81.9
	..	103.5	76.0	..	..	88.4	90.2	75.4	..	..	
69	46.5	77.8	79.6	58.3	..	52.1	62.8	49.4	..	..	61.2
	41.4	75.9	90.7	59.1	..	54.6	59.1	44.6	..	..	
						57.7	63.3	53.5	..	..	
70	76.6	89.4	81.8	79.7	..	63.1	84.4	73.2	..	..	65.2
	49.4	86.0	72.1	58.8	..	57.1	62.5	71.0	..	..	
						48.9	..	52.2	..	..	
						..	..	32.1	..	..	
S8	66.0	80.6	77.3	70.5	..	51.3	56.0	44.1	..	..	68.9
	73.0	65.4	79.4	78.9	..	52.9	54.1	38.2	..	..	
						..	64.9	..	..	..	
S9	23.9	64.3	48.1	31.2	..	38.5	49.6	55.8	..	..	45.5
	31.2	55.2	59.3	38.8	..	46.6	51.0	35.6	..	..	
	25.8	55.8	64.2	42.7	..	37.6	47.2	..	..	..	
S10	29.3	78.6	60.4	45.3	..	52.1	56.5	43.1	..	..	51.0
	29.3	62.6	74.0	63.9	..	44.5	53.0	44.2	..	..	
	40.8	50.9	..	54.9	..	44.1	47.6	46.2	..	..	
S11	16.4	42.0	38.6	19.3	..	36.3	50.1	38.9	..	..	34.6
	27.0	39.0	36.6	29.0	..	32.1	31.8	30.4	..	..	
	20.5	53.2	47.1	23.6	..	36.2	49.2	28.1	..	..	
S12	24.3	41.0	48.1	21.9	30.9	43.4	42.9	35.2	..	..	40.3
	24.0	55.7	50.6	26.5	35.8	44.4	50.6	44.9	..	..	
	21.9	58.6	49.2	26.2	32.0	38.4	64.4	59.8	..	..	
S13	36.6	53.6	37.7	45.5	33.7	31.5	50.6	37.4	..	..	42.7
	40.5	59.0	43.1	39.1	31.3	39.4	52.7	33.6	..	..	
						34.3	54.3	47.5	..	..	
S17	20.8	39.4	39.4	29.0	29.9	30.4	38.6	22.5	37.8	25.0	32.3
	19.4	43.9	51.5	23.9	23.4	20.2	41.7	..	42.8	34.4	
S18	25.3	51.1	56.6	24.1	34.3	28.9	39.4	23.9	42.3	35.4	35.8
	30.7	43.1	39.1	24.1	31.2	32.1	41.3	33.2	43.1	37.6	
71	24.5	38.6	34.1	25.4	20.9	25.0	28.1	26.1	30.3	24.2	27.9
	24.8	33.3	24.0	19.7	17.9	38.3	32.6	24.7	34.6	30.7	
72	27.3	48.0	31.3	26.8	22.6	22.6	29.5	26.2	32.7	28.7	34.1
	29.6	86.8	40.3	40.5	31.0	25.3	41.6	25.6	34.3	32.3	
78	27.6	42.4	29.9	34.3	21.9	27.3	40.5	26.5	31.0	34.2	35.4
	37.6	63.2	32.6	30.8	31.6	31.6	41.9	28.2	45.2	37.2	
						..	..	..	56.5	..	
79	30.2	45.6	33.5	40.8	22.3	46.0	54.4	39.1	46.2	39.4	38.2
	19.9	57.4	35.7	24.5	29.3	33.4	45.3	37.0	44.4	34.1	
80	12.6	54.0	30.6	20.1	41.9	49.2	61.5	46.4	61.1	24.2	44 2
	44.5	67.0	44.8	43.8	45.1	57.1	53.2	43.4	44.4	34.1	

[a] All intensities expressed in thousands of Btu per sq ft per hr.
[b] $I = 2.155\ M$, see Equation [2].
[c] For location of various doors see Figs. 6 and 13.

It has been assumed in the foregoing discussion, that the emissivity of the black-body absorber (Fig. 2) is 1.00, i.e., that the absorber is a true black body. Actually, the emissivity might be slightly less than unity. The emissivity of the inner, acetylene-soot-covered surfaces is about 0.945.[7] But the net emissivity of the cavity is considerably greater than the individual emissivities of the surfaces which form its walls, because the absorbing surfaces form an inclosure, and since the amount of incident radiation which is not completely absorbed at the blackened surface which it strikes inside the cavity will be more likely to be absorbed at another part of the blackened surface than to escape through the front opening. It is reasonable to suppose that the resultant emissivity is about 0.98.

If it were assumed that the emissivity of the special absorber is 0.98, the calibration equation for the quartz-window instrument would be changed by 2 per cent. Since the resulting correction for emissivity is only 2 per cent or less, it will not be used at this time.

[7] "Surface Heat Transmission," by R. H. Heilman, Trans. A.S.M.E., vol. 51, 1929, p. 289, paper FSP-51-41.

Application of Radiation Calorimeter to Boiler Tests

Description of Boiler and Furnace. The tests herein described were conducted on a steam-generation unit equipped with an underfeed stoker, located in the heating plant of the State University of Iowa. The unit tested (Fig. 6) has a 6000-sq-ft, straight-tube boiler, equipped with an extended-tube superheater. The rear water wall, consisting of twenty-one $3^1/_4$-in. bare tubes, spaced 6 in. on centers, provides 91 sq ft of cold surface. The side walls, with four $3^1/_4$-in. bare slag-drip tubes, and five $3^1/_4$-in. armored side-wall tubes on each side, have a total of 95 sq ft of cold surface; the top of the furnace has 150 sq ft of cold surface. All the surfaces have been computed as projected areas. The total cold surface in the furnace is 336 sq ft. The total wall area of the furnace is 835 sq ft, so the "fraction cold" of the furnace is 336/835, or 0.402.

Fig. 7 View of Radiation Calorimeter in Door No. 1, With Accessory Equipment

Radiation Observations. Radiation observations were made through ten special observation doors, during a series of 8-hr boiler tests. The locations of these doors are shown in Figs. 6 and 13.

During an observation, the radiation calorimeter was placed in the observation door as shown in Fig. 7. The water rate in the absorption chamber of the calorimeter was determined by noting the time required to fill a calibrated glass flask B (Fig. 7) to a mark on its narrow neck, while the electromotive forces of the inlet and outlet thermocouples were determined continuously by means of the potentiometer shown. During a single observation, lasting about six minutes, about 15 sets of

temperature determinations were made, of which, the average values were used in determining the temperature increase of the water.

The actual radiation intensities as measured and corrected by Equation [2], are shown in Table 1. The average value of the radiation intensity for each boiler test, shown in Table 1, is the arithmetic average of all the observations made in all the doors. For this paper, no attempt has been made to determine a weighted average; the authors believe that the system of averaging here used is best for the purposes of this paper, because the radiation intensity was not constant at the various observation points throughout an entire test.

Methods of Computing Heat Absorption

Computations of Radiation by the Hudson-Orrok Formula. There are shown in Table 2 the average heat-transfer rates by radiation, as computed by means of the Hudson-Orrok formula.[8] These heat-transfer rates are plotted in Fig. 9. The quantity U in this table is the heat released in the furnace per lb of fuel burned. U also enters into the calculation of radiation by the Wohlenberg method, and is computed in Table 3, in which it is shown as the calorific heating value of the fuel, in Btu per lb, minus the losses due to (*a*) incomplete combustion of carbon to carbon-dioxide, (*b*) combustible in the refuse, and (*c*) evaporation of moisture.

Computations of Radiation by the Wohlenberg Method. In the computations of furnace heat balances by the Wohlenberg method,[9,10,11] as shown in Table 3, some shortcuts have been taken, the most important one being in evaluating the solid angles which enter into the computations of the radiation coefficients. The "fraction cold" for the furnace used in these tests was found to be 0.402. This corresponds to the Type *B* cubical furnace mentioned by Wohlenberg and Lindseth, which has one wall and the top cold. It has been assumed that the furnace in question is approximately represented, in so far as our purposes are concerned, by the Type *B* furnace, even though its shape differs from that of a cube. Hence the values for the various solid angles have been taken for those quoted for the Type *B* cubical furnace.

The radiation from the carbon dioxide and water vapor present in the burning gases is a function of the temperature, and of the product of the percentage concentration and the thickness of the radiating gas; this product may be expressed as $c = ps/328$, where p is the percentage by volume of the carbon dioxide or water vapor, and s is the thickness of the gas column in feet.[10] For a given temperature, the radiation from these gases increases with the factor c, until $c = 0.15$. Any further increase of c above 0.15 produces no increase in the radiation intensity from the gases at constant temperature.

In all the boiler tests of this investigation, the factor c was greater than 0.15 for both the carbon dioxide and water vapor; hence, the radiation from these gases could be plotted as a function of the temperature alone.

The radiation term in the heat balance for this furnace, then, may be plotted as a function of the "mean flame temperature" as shown in Fig. 8. From this graph, the total value of the radiation term may be determined for any assumed mean flame temperature.

The solution of the heat-balance equation consists of finding the mean flame temperature, T_u; for this temperature, the energy released in the furnace per hr (called GU in Table 3) is equal to the sum of the three quantities, (*a*) the radiation term, Q_r, (*b*) the heat transferred by convection to the surfaces exposed to radiation (except for that radiant surface in the aperture through which the gases leave the furnace), and (*c*) the sensible heat of the products of combustion leaving the furnace at the mean flame temperature (represented in Table 3 by $\Sigma G_b \Delta h_b$). It was usually possible to select the correct mean flame temperature after a choice of three or four values.

The radiation-heat-absorption rates as computed by the Wohlenberg method are shown in Fig. 8. It is interesting to compare the results calculated from the same data using the two different methods.

TABLE 2 VARIOUS FACTORS USED IN COMPUTING RADIATION BY THE HUDSON-ORROK FORMULA

Test No.	A	C_r	μ	U	X_h
53	8.83	16.88	0.427	9209	67100
54	9.32	13.05	0.447	9639	56300
55	8.65	12.83	0.466	9383	56100
S2	10.24	11.69	0.430	10185	51200
S3	10.22	15.61	0.400	9209	57500
56	8.85	12.32	0.474	8375	49000
57	8.42	14.45	0.456	8475	55900
58	9.51	16.80	0.409	8874	61000
59	8.35	17.36	0.437	8790	66600
60	9.06	13.33	0.449	8514	51000
S5	8.92	14.62	0.416	9888	60100
S6	10.45	10.59	0.443	10385	48700
S7	9.50	13.90	0.433	9894	59600
S8	9.70	14.38	0.424	9821	59900
S9	9.77	12.35	0.430	9997	53000
S10	9.49	14.75	0.426	9708	60900
S11	10.82	10.13	0.440	10408	46300
S12	10.48	12.40	0.422	10316	54000
S13	8.75	15.03	0.452	9296	63200
S17	9.94	14.88	0.443	9674	63700
S18	10.16	15.83	0.448	10203	72400
69	9.11	13.55	0.446	9965	60100
70	7.65	15.83	0.469	10572	78500
71	9.55	11.98	0.394	8704	41100
72	9.92	12.86	0.431	8772	48600
78	8.65	14.42	0.452	8995	58600
79	9.40	12.30	0.450	9539	52900
80	8.99	15.90	0.447	9364	66500

$\mu = \dfrac{1}{1 + \dfrac{A\sqrt{C_r}}{27}}$ = fraction of energy released which is transferred to the cold surfaces in the furnace by radiation.

A = lb of air per lb of fuel.

U = heat release per lb of coal.

$X_h = C_r U \left[\dfrac{1}{1 + \dfrac{A\sqrt{C_r}}{27}}\right]$ = heat transfer rate by radiation, Btu per sq ft per hr.

C_r = fuel burned, lb per hr per sq ft of water-cooled surface exposed to radiation.

Discussion of Test Results

Effect of Dirty Surfaces. In Fig. 10, the measured average radiation intensities are plotted against the energy release rate in the furnace. The measured radiation intensity, according to Fig. 10, varies considerably with constant energy release rate. This effect was noticed early in the tests, when it was found that the variation was due to the difference in dirtiness of the water-cooled surfaces in the furnace.

Attempts were made to estimate, in each of the tests, the fraction of the radiant surface which was covered with slag or ash. The covering on the tubes was found to consist mostly of patches of powdery ash, between 1/8 in. and 1 1/8 in. in thickness. At times, after the boiler had been operated at high ratings, the slag-drip tubes of the side walls were covered with slag. In Table 4 are listed the values of the furnace dirtiness D, which is the estimated fraction of the total water-cooled surface in the furnace that is covered with slag or ash. Fig. 11 shows a portion of the rear water wall, which the authors estimate to be about 0.4 covered with ash, i.e., $D = 0.4$.

---

[8] "Radiation in Boiler Furnaces," by Geo. A. Orrok, Trans. A.S.M.E., vol. 47, 1925, pp. 1148–1155.

[9] "Radiation in the Pulverized-Fuel Furnace," by W. J. Wohlenberg and D. G. Morrow, Trans. A.S.M.E., vol. 47, 1925, p. 127.

[10] "The Influence of Radiation in Coal-Fired Furnaces on Boiler Surface Requirements and a Simplified Method for Its Calculation," by W. J. Wohlenberg and E. L. Lindseth, Trans. A.S.M.E., vol. 48, 1926, p. 848.

[11] Complete details of the computations and boiler test data are given in a thesis, "Radiation in Steam Boiler Furnaces," by C. F. Schmarje, which is on file in the library of the State University of Iowa.

TABLE 3 SUMMARY OF CALCULATIONS BY THE WOHLENBERG METHOD

Boiler Test No.	53			54			55			S-2			S-3		
T_u °F	2450			2350			2375			2315			2405		
	A	B	C	A	B	C	A	B	C	A	B	C	A	B	C
Product of Combustion															
CO_2	1.993	616	1229	2.08	585	1217	2.02	593	1199	2.207	575	1270	2.263	602	1364
O_2	0.299	531	159	0.368	499	184	0.22	506	111	0.468	468	227	0.414	515	213
N_2+CO	7.032	577	4060	7.38	546	4030	6.87	554	3805	8.05	535	4310	8.045	562	4520
Refuse	0.147	565	83	0.112	531	62	0.154	539	83	0.190	521	57	0.124	547	68
H_2O	0.498	1167	581	0.501	1105	576	0.485	1120	544	0.527	1083	572	0.525	1139	598
$\Sigma G_b \Delta h_b \div G$			6112			6069			5742			6436			6763

Boiler Test No.	56			57			58			59			60		
T_u °F	2155			2343			2330			2423			2195		
	A	B	C	A	B	C	A	B	C	A	B	C	A	B	C
Product of Combustion															
CO_2	1.922	524	1010	1.916	552	1059	1.99	579	1152	1.935	607	1175	1.958	538	1053
O_2	0.644	483	279	0.436	462	201	0.486	491	238	0.246	521	128	0.543	446	242
N_2+CO	7.15	486	3478	6.86	513	3520	7.486	540	4040	6.746	567	3823	7.36	498	3665
Refuse	0.172	474	81	0.180	500	90	0.093	525	49	0.095	552	52	0.164	486	80
H_2O	0.711	985	700	0.646	1039	671	0.696	1093	761	0.636	1151	731	0.720	1009	726
$\Sigma G_b \Delta h_b \div G$			5548			5541			6240			5909			5766

Boiler Test No.	S-5			S6			S-7			S-8		
T_u °F	2438			2268			2380			2365		
	A	B	C	A	B	C	A	B	C	A	B	C
Product of Combustion												
CO_2	2.155	612	1319	2.285	559	1280	2.190	595	1305	2.186	590	1290
O_2	0.174	526	91	0.492	470	231	0.319	506	161	0.38	502	191
N_2+CO	7.16	572	4100	8.27	520	4300	7.57	554	4200	7.757	550	4265
Refuse	0.102	557	52	0.094	507	48	0.125	540	67	0.187	535	100
H_2O	0.717	1160	831	0.655	1054	690	0.675	1123	758	0.692	1114	770
$\Sigma G_b \Delta h_b \div G$			6398			6549			6471			6616

Boiler Test No.	53	54	55	S-2	S-3	56	57	58	59	60	S-5	S6	S-7	S-8
G Pounds of Fuel per Hour	5666	4384	4309	3901	5209	4114	4486	5650	5831	4481	4918	5560	4674	4827
Heating Value of Fuel – Btu/lb.	9930	10360	9960	10975	10870	9260	9390	9847	9920	9405	11010	11223	10853	10710
Losses (from H) Btu/lb														
(a) Due to Unconsumed Carbon (CO)	80	82	10	25	4	0	0	154	366	0	246	43	47	28
(b) Due to Combustible in Refuse	95	68	36	187	380	106	206	56	66	101	90	76	172	101
(c) Due to Evaporation of Moisture	546	571	531	578	576	780	709	763	698	790	786	719	740	760
L Total Losses Btu/lb	721	721	577	790	960	886	915	973	1130	891	1122	838	959	889
U Heat Released (H–L) Btu/lb.	9209	9639	9383	10185	9910	8374	8475	8874	8790	8514	9888	10385	9894	9821
$\Sigma G_b \Delta h_b$ Btu/hr.	34,650,000	26,600,000	24,730,000	25,100,000	35,210,000	22,850,000	24,860,000	35,250,000	34,450,000	25,840,000	31,450,000	25,315,000	30,360,000	31,900,000
Z_c Btu/hr.	685,000	576,000	583,000	564,000	664,000	436,000	516,000	615,000	660,000	502,000	660,000	490,000	610,000	595,000
Q_R Btu/hr	16,780,000	14,680,000	15,600,000	14,010,000	15,770,000	11,130,000	12,660,000	14,280,000	16,160,000	11,800,000	16,500,000	13,120,000	15,260,000	14,960,000
$\Sigma G_b \Delta h_b + Z_c + Q_R$ Btu/hr	52,115,000	41,856,000	40,473,000	39,674,000	51,644,000	34,416,000	38,036,000	50,145,000	51,270,000	38,140,000	48,610,000	36,925,000	46,230,000	47,455,000
G·U Heat Released per Hour Btu/hr	52,130,000	41,800,000	40,500,000	39,670,000	51,600,000	34,455,000	38,019,000	50,138,000	51,250,000	38,150,000	48,630,000	36,950,000	46,220,000	47,406,000
ERR GU ÷ Volume = GU/2160 Btu/ft³/hr	24,100	19,320	18,720	18,350	23,800	16,720	18,500	24,300	24,900	18,530	22,450	17,200	21,460	21,900
Heat-Transfer Rate by Radiation: X_R = Q_R/area = Q_R/336 Btu/ft²/hr	49,900	43,600	45,100	41,700	46,900	33,100	37,700	42,700	48,100	35,100	49,100	39,000	45,400	44,500

Col. "B" = Heat Capacity of Product above 80°F [for water, above 212°F] per pound.

Note: Col. C = (Col. B) × (Col. A)
Col. A = Lbs. of Product per Pound of Fuel.

Boiler Test No.	S-9			S-10			S-11			S-12			S-13		
T_u °F	2330			2378			2230			2325			2393		
	A	B	C	A	B	C	A	B	C	A	B	C	A	B	C
Product of Combustion															
CO_2	2.200	580	1273	2.147	595	1278	2.317	549	1272	2.300	577	1325	2.065	598	1238
O_2	0.450	490	199	0.366	506	185	0.586	457	268	0.526	489	257	0.318	511	162
N_2+CO	7.775	540	4200	7.575	553	4190	8.545	509	4350	8.277	537	4442	0.935	558	3870
Refuse	0.116	525	61	0.119	539	64	0.066	496	33	0.078	523	41	0.154	544	84
H_2O	0.628	1093	686	0.706	1123	791	0.660	1031	680	0.660	1090	719	0.675	1132	766
$\Sigma G_b \Delta h_b \div G$			6419			6508			6603			6784			6119

Boiler Test No.	S-17			S-18			69			71		
T_u °F	2360			2413			2395			2155		
	A	B	C	A	B	C	A	B	C	A	B	C
Product of Combustion												
CO_2	2.114	588	1243	2.240	605	1356	2.045	600	1223	1.961	525	1030
O_2	0.426	500	213	0.460	518	239	0.420	512	215	0.688	432	297
N_2+CO	7.88	548	4320	8.20	564	4628	7.297	559	4085	7.697	485	3738
Refuse	0.092	534	49	0.132	550	73	0.117	544	63	0.170	471	80
H_2O	0.68	1111	755	0.68	1140	779	0.731	1133	827	0.68	984	669
$\Sigma G_b \Delta h_b \div G$			6580			7075			6413			5824

Boiler Test No.	72			78			79			80		
T_u °F	2170			2322			2280			2390		
	A	B	C	A	B	C	A	B	C	A	B	C
Product of Combustion												
CO_2	1.970	562	1108	2.000	576	1152	2.135	563	1203	2.08	597	1242
O_2	0.736	472	348	0.397	487	194	0.434	474	206	0.436	510	222
N_2+CO	7.986	522	4165	7.09	536	3800	7.628	524	4010	7.26	557	4045
Refuse	0.185	509	80	0.13	522	68	0.121	510	62	0.113	543	61
H_2O	0.68	1059	720	0.68	1087	738	0.68	1061	722	0.68	1130	769
$\Sigma G_b \Delta h_b \div G$			6421			5952			6203			6339

Boiler Test No.	S-9	S-10	S-11	S-12	S-13	S-17	S-18	69	71	72	78	79	80
G Pounds of Fuel per Hour	4151	4959	3405	4165	5054	4998	5312	4558	4032	4322	4851	4132	5340
H Heating Value of Fuel – Btu/lb.	10890	10670	11210	11180	10250	10700	11130	10853	9600	9580	9840	10340	10230
Losses (from H) Btu/lb.													
(a) Due to Unconsumed Carbon (CO)	81	62	0	9	0	208	0	7	0	0	36	12	19
(b) Due to Combustible in Refuse	123	125	78	131	214	73	182	75	151	63	73	44	102
(c) Due to Evaporation of Moisture	689	775	724	724	740	745	745	801	745	745	745	745	745
L Total Losses Btu/lb.	893	962	802	864	954	1026	927	883	896	808	854	801	866
U Heat Released (H–L) Btu/lb.	9997	9708	10408	10316	9296	9674	10203	9965	8704	8772	8995	9539	9364
$\Sigma G_b \Delta h_b$ Btu/hr.	26,630,000	32,370,000	22,480,000	28,260,000	30,900,000	32,900,000	37,600,000	29,240,000	23,460,000	26,150,000	28,860,000	25,620,000	33,900,000
Z_c Btu/hr.	570,000	615,000	470,000	550,000	600,000	610,000	620,000	600,000	460,000	470,000	570,000	520,000	620,000
Q_R Btu/hr.	14,290,000	15,220,000	12,420,000	14,190,000	15,500,000	14,850,000	15,950,000	15,550,000	11,250,000	11,360,000	14,130,000	13,350,000	15,460,000
$\Sigma G_b \Delta h_b + Z_c + Q_R$ Btu/hr	41,490,000	48,105,000	35,370,000	43,000,000	47,000,000	48,360,000	54,170,000	45,390,000	35,045,000	37,980,000	43,560,000	39,490,000	49,980,000
G·U Heat Released per Hour Btu/hr	41,500,000	48,100,000	35,400,000	43,000,000	47,000,000	48,400,000	54,200,000	45,420,000	35,095,000	37,913,000	43,610,000	39,420,000	50,000,000
ERR GU ÷ Volume = GU/2160 Btu/ft³/hr	19,200	22,200	16,400	19,900	21,800	22,400	25,100	21,000	16,200	17,600	20,200	18,250	23,100
Heat-Transfer Rate by Radiation: X_R = Q_R/area = Q_R/336 Btu/ft²/hr	42,500	45,300	37,000	42,200	46,100	44,200	47,500	46,300	33,500	33,800	42,000	39,700	46,000

In Fig. 10 curves of equal dirtiness, D, have been drawn for the furnace clean ($D = 0$), slightly dirty ($D = 0.1$), moderately dirty ($D = 0.2$), and very dirty ($D = 0.4$). Since there was a similarity between the constant dirtiness curves and the Orrok curve of Fig. 9, and also an increase in intensity with D, at a given energy-release rate, a tentative formula (based upon the Hudson-Orrok formula) for calculating the average radiation intensity has been derived.

The proposed formula is as follows:

$$I = C_r U \left[\frac{0.5 + 1.7\,D}{1 + \frac{A\sqrt{C_r}}{27}} \right] \qquad [3]$$

in which I is the average radiation intensity at the furnace walls in Btu per sq ft per hr; U is the energy release per lb of fuel burned as found by subtracting from the heating value of the fuel the losses due to unconsumed carbon, evaporation of moisture, and combustible in the refuse; A is the lb of air entering the furnace per lb of fuel burned; C_r is the fuel burned, lb per hr per sq ft of projected cold surface exposed to radiation; and D is the fraction of the cold surface in the furnace which is covered with slag or ash.

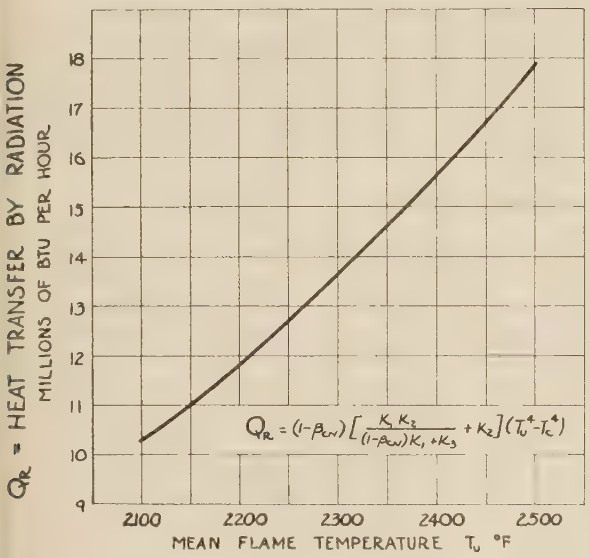

Fig. 8 Heat Transferred by Radiation as Computed by the Wohlenberg Method

TABLE 4 DIRTINESS FACTORS, D

Test No.	D	Test No.	D
53	0.1	70	0.4
54	0.1	S8	0.4
55	0.1	S9	0.2
S2	0.1	S10	0.2
S3	0.1	S11	0.1
56	0.4	S12	0.1
57	0.4	S13	0.1
58	0.4	S17	0.0
59	0.4	S18	0.0
60	0.4	71	0.1
S5	0.4	72	0.1
S6	0.4	78	0.1
S7	0.4	79	0.1
69	0.4	80	0.15

It is to be noted that Equation [3], here tentatively proposed, gives "radiation intensity," as contrasted to "heat-transfer rate" by radiation. The two quantities may be very nearly equal for a clean furnace, but for a dirty furnace the average radiation intensity is probably much greater than the average heat-transfer rate by radiation.

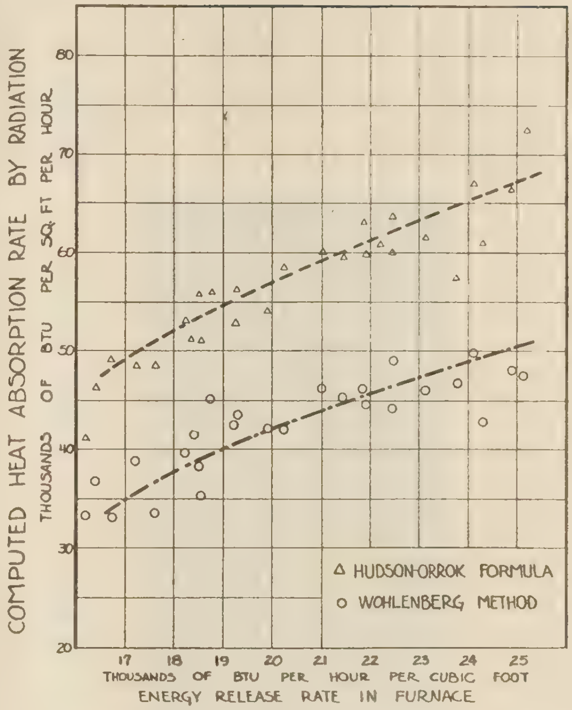

Fig. 9 Radiant-Heat-Absorption Rates Computed by the Hudson-Orrok Formula and the Wohlenberg Method

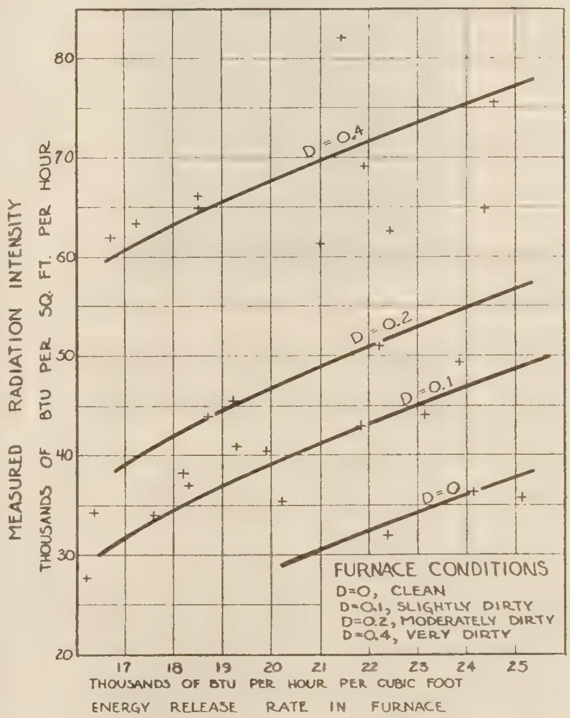

Fig. 10 Radiation Intensities, I, Determined During the Boiler Tests

Heat-Transfer Rates by Radiation. Having found an equation

for radiation intensities, it is possible to predict an approximate equation for the average heat-transfer rates by radiation. A perfectly black, cold surface placed in the furnace would absorb heat by radiation at a rate equal to the radiation intensity I, given by Equation [3]. But the cold surfaces employed in the furnace probably absorb only about 95 per cent of the radiation which a perfectly black surface would at the same temperature.[9]

Fig. 11 A Portion of the Rear Water Wall (D = 0.4)

Hence, for a clean furnace, the average heat absorption by radiation would be 95 per cent of the radiation intensity. For a clean furnace (D = 0), the equation for the average heat-transfer rate by radiation would be

$$X = 0.95\, C_r U \left[\frac{0.5}{1 + \dfrac{A\sqrt{C_r}}{27}} \right] \qquad [4]$$

Those parts of the water-cooled surfaces which are covered with ash or slag would absorb only about one-half as much radiant energy as a clean surface.[12] Taking this into account, the average heat-transfer rate by radiation for a partially dirty furnace would then be

$$X = 0.95(1 - 0.5D) C_r U \left[\frac{0.5 + 1.7D}{1 + \dfrac{A\sqrt{C_r}}{27}} \right] \qquad [5]$$

[12] This conclusion is based upon a study of data given in the paper, "Heat Absorption in Water-Cooled Furnaces," by W. L. DeBaufre, Trans. A.S.M.E., vol. 53, 1931, paper FSP-53-19a. Figs. 3 and 4 of this paper especially would indicate that 0.5 is about the correct value.

where X is the average heat-transfer rate by radiation to the water-cooled surfaces in the furnace in Btu per sq ft per hr, and the other symbols are the same as in Equation [3]. This may be closely represented, when the value of D is between 0 and 0.5, by the formula,

$$X = C_r U \left[\frac{0.48 + 1.1D}{1 + \dfrac{A\sqrt{C_r}}{27}} \right] \qquad [6]$$

which the authors propose (tentatively) to replace the Hudson-Orrok formula. For values of D greater than 0.5, Equation [5] should be used.

The constants in the numerator of this new equation depend upon the relationship between heat absorption and radiation intensity, with varying degrees of furnace dirtiness. An experimental investigation is now under way to study this relationship.

Hudson-Orrok Formula and Wohlenberg Method Compared to Results Based Upon Measured Radiation Intensities. In Fig. 12, the heat-transfer rates by radiation, as computed by the new formula, Equation [6], are shown in comparison to those corresponding to the Hudson-Orrok formula and the Wohlenberg method. The single curves for the Hudson-Orrok formula

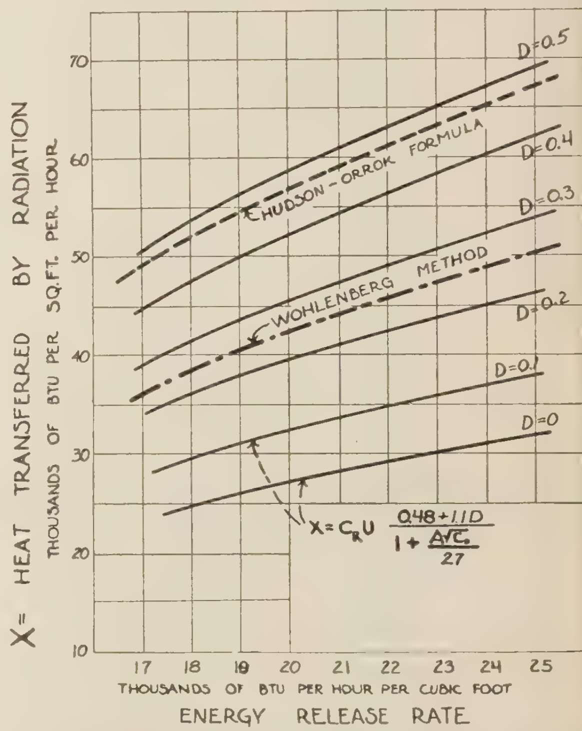

Fig. 12 Comparison of Heat Transfer by Radiation From the Hudson-Orrok Formula and the Wohlenberg Method With the Heat Transfer Based Upon Measured Radiation Intensities

and the Wohlenberg method are justified, because the computed data, for these boiler tests, all cluster closely about these two curves, as shown in Fig. 9.

It is found, for the boiler tests represented here, that for a given energy release rate, the Hudson-Orrok formula results in higher heat-transfer rates than does the Wohlenberg method. The proposed formula, which represents actual heat-transfer

rates by radiation, gives values at constant energy release depending upon the dirtiness of the furnace. The Hudson-Orrok formula is in agreement with the proposed formula, Equation [6], for these tests, when the furnace is fairly dirty. The Wohlenberg method gives results which are apparently correct for a comparatively clean furnace.

Distribution of Radiation. The typical distribution of radiation intensities about the furnace is shown in Fig. 13 for three different tests of approximately equal energy-release rates.

During one of these tests, the furnace was clean, having been in operation only two days following a thorough cleaning; in the other tests the fractions of the radiant surface dirty were approximately 0.2 and 0.4.

Summary

Conclusions. The development of a fused-quartz-window absorption calorimeter for determining radiation intensities in boiler furnaces is described. This instrument has been used during 28 boiler tests and the results compared with the Hudson-Orrok formula and the Wohlenberg method of computation of radiation heat transfer.

The results show that, for these tests, the Hudson-Orrok formula gives results which are correct for a furnace with a considerable part of the water-cooled surfaces covered with ash or slag. The Wohlenberg method of computation shows correct results, for these tests, when the water-cooled surfaces are comparatively clean.

A tentative empirical equation, Equation [3], is given for computing radiation intensities, taking into account the dirtiness of the cold surfaces; tentative formulas, Equations [5] and [6], are given for computing the average heat transfer by radiation in boiler furnaces.

There is a variation in radiation intensity from point to point at the walls of the furnace, as indicated by Fig. 13.

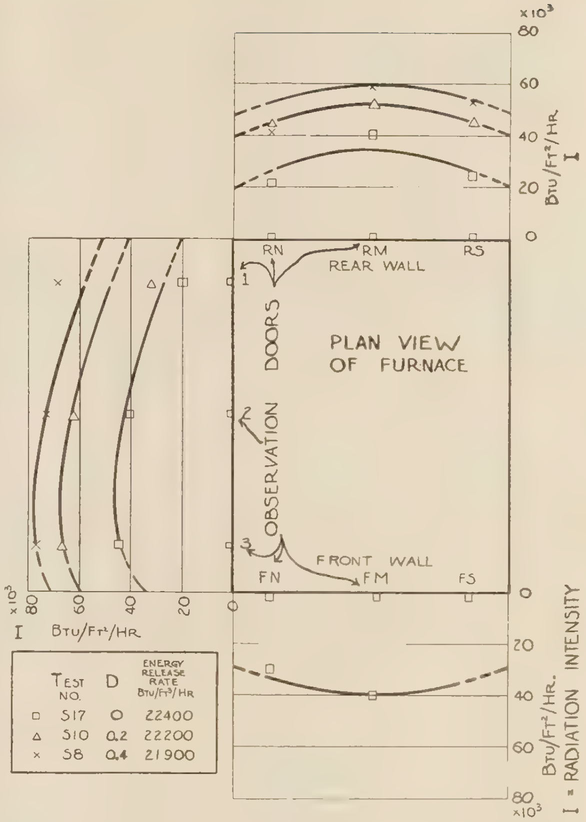

Fig. 13 Distribution of Radiation Intensities About the Boiler Furnace

The Leakage of Steam Through Labyrinth Seals

By ADOLF EGLI,[1] PHILADELPHIA, PA.

This paper gives a rational theoretical treatment of the labyrinth problem, based on the actual flow characteristics typical for a sharp-edged orifice. The general relations between leakage, number of throttlings, and pressure distribution are given in graphical form on a chart intended for use in practical turbine design.

It is also shown how the effect of kinetic energy being carried from one throttling into the next can be considered rationally. The numerical constants left open by the theory are derived experimentally with the aid of a static labyrinth leakage-testing device.

INTRODUCTION

With ever-increasing operating pressures, leakage loss of steam through unavoidable seals (shaft packings, dummy pistons, etc.) becomes more and more detrimental to the efficiency of modern steam turbines. Also, it has become common practice to improve the efficiency of turbine stages by introducing leakage seals which reduce the amount of steam uselessly by-passing each row of blades. Inasmuch as the labyrinth-type seal is still the most common, an accurate method for predicting the leakage through it is desirable. It is also important to know accurately the pressure distribution in the labyrinth when calculating the thrust of certain types of dummy pistons. In this paper a refined, yet sufficiently simple method, is developed for predicting the performance of labyrinths.

DEVELOPMENT OF A RATIONAL THEORY FOR THE EXPANSION OF COMPRESSIBLE FLUIDS THROUGH LABYRINTHS

1 Expansion Through a Single Sharp-Edged Throttling

A schematic illustration of two-dimensional flow through a single sharp-edged throttling is given in Fig. 1. The steam (or gas) expands from the pressure p_0 to p_1 when passing through the slot, forming at the same time some kind of a jet with a minimum area A_m. We are not particularly interested in knowing this minimum area. In some other section, A_1, which may be located somewhere near (before or after) the minimum section, the pressure in the steam jet will be equal to the chamber pressure, p_1. If A_1 is known and adiabatic change of state of the steam, for instance, is assumed, it is possible to calculate the weight of the theoretical flow passing through the throttling by applying Saint Venant's equation. This equation, neglecting the approach velocity w_0 of the steam, is given as

$$G_{th} = A_1 \sqrt{\left(2g \frac{k}{k-1}\left[\beta^{2/k} - \beta^{1+1/k}\right]\frac{p_0}{v_0}\right)} \quad \ldots\ldots [1]$$

where G_{th} = theoretical flow, lb per sec; g = acceleration of gravity, 32.17 ft per sec per sec; k = exponent of adiabatic expansion (1.3 for superheated steam); β = the pressure ratio p_1/p_0; p_0 = abs pressure before throttling, lb per sq ft; p_1 = abs pressure after throttling, lb per sq ft; v_0 = specific volume before throttling, cu ft per lb; and A_1 = jet area, sq ft.

Introducing the flow coefficient

$$\alpha = A_1/A \quad \ldots\ldots [2]$$

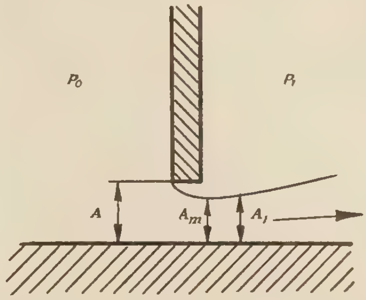

Fig. 1 Expansion Through a Single Sharp-Edged Throttling

and abbreviating the dimensionless expression

$$\psi_{th} = \sqrt{\left(\frac{2k}{k-1}\left[\beta^{2/k} - \beta^{1+1/k}\right]\right)} \quad \ldots\ldots [3]$$

we finally write for the theoretical flow

$$G_{th} = A\alpha\psi_{th}\sqrt{\left(g\frac{p_0}{v_0}\right)} \quad \ldots\ldots [4]$$

where A is the area of the throttling opening (Fig. 1). For superheated steam (k = 1.3), ψ_{th} was calculated and is plotted in Fig. 2 as a function of the pressure ratio β. It has the well-known nozzle characteristics, reaching a maximum value of 0.667 at the critical pressure ratio $\beta_c = p_c/p_0 = 0.546$.

The flow coefficient, α, of a sharp-edged opening, when plotted against Reynolds' number, gives a curve such as shown in Fig. 3. For Reynolds' numbers higher than the critical value R_c, the coefficient α is constant, i.e., independent of the velocity of the steam. For sharp-edged round orifices, the critical value of $R = wd/\nu$ is about 10^3, where w = velocity of the jet discharging from the orifice, ft per sec; d = diameter of the orifice opening, (clearance of throttling); and ν = kinematic viscosity of the fluid in ft² per sec. Although results of tests on the flow coefficient

[1] Research Engineer, Westinghouse Electric & Manufacturing Co. Mr. Egli received his technical education at the Federal Technical University in Zurich, Switzerland, where he was graduated as Diplom Mechanical Engineer under Professor Stodola in 1929. After graduation he was engaged as assistant to Professor Stodola and Professor Eichelberg and as instructor of thermodynamics and heat-engine design. From 1930 to 1931 he was employed as experimenting engineer with the Terry Steam Turbine Company, Hartford, Conn. Since 1931, Mr. Egli has been connected with the Westinghouse Company at South Philadelphia as research engineer on turbine efficiency and design.

Contributed by the Power Division for presentation at the semi-annual meeting, Cincinnati, Ohio, June 19 to 21, 1935, of The American Society of Mechanical Engineers.

Discussion of this paper should be addressed to the Secretary, A.S.M.E., 29 West 39th Street, New York, N. Y., and will be accepted until July 10, 1935, for publication at a later date.

of a narrow slot as a function of Reynolds' number are not available, we may assume that R_c is in the order of 10^3. In a steam labyrinth, R is as high as 10^4 and above. We can assume that for velocities far enough below the acoustic velocity (about 500 ft per sec or less for superheated steam) α is independent of the velocity. In this range (that is, for throttling pressure ratios β = 0.8 to 1.0) we should expect Equation [4] to give the correct flow.

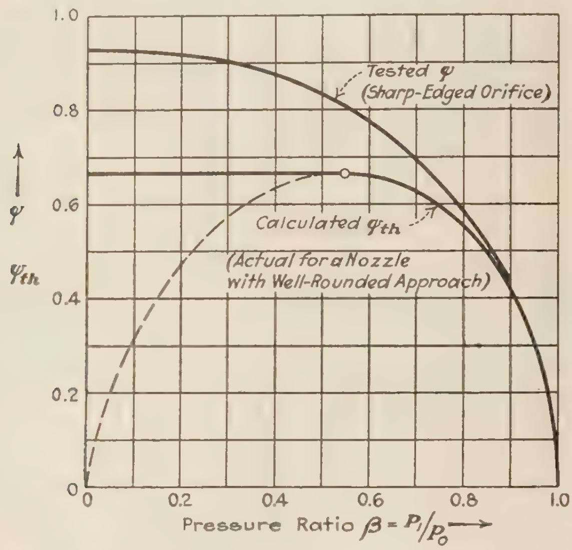

Fig. 2 Expansion Function ψ of a Sharp-Edged Orifice Operating With Superheated Steam

The last throttlings in a labyrinth very often work with velocities comparable with, or as high as, the acoustic velocity (β less than 0.8). Under these conditions, adiabatic change of state and the constance of α can no longer be assumed. The actual flow G through the throttling will differ from the theoretical value G_{th}, calculated from Equation [4].

There is complete information available on the flow through sharp-edged round orifices which can be applied to this problem. Assuming, for simplicity, a constant-flow coefficient, Schiller[2] calculated from flow tests made with VDI orifices, the function ψ as defined by the equation

$$G = A\alpha\psi\sqrt{\left(g\,\frac{p_0}{v_0}\right)} \qquad [5]$$

where G = the actual measured flow (see Table 1). The values in Table 1 are used in plotting the curve ψ versus β shown in Fig. 2. A comparison of the (theoretical) ψ_{th} curve with the (tested) ψ curve reveals the fact that for pressure ratios of β = 0.8 and above, the theoretical flow checks rather closely with the actual. As the pressure ratio decreases below 0.8, ψ rises increasingly above ψ_{th}. It is remarkable that no critical pressure ratio exists for the actual flow through a sharp-edged opening.

TABLE 1 EXPANSION FUNCTION ψ OF A SHARP-EDGED ORIFICE AND OF A WELL-ROUNDED OPENING

Pressure ratio β	Sharp-edged orifice ψ	Theoretical ψ_{th}	Well-rounded opening ψ
1.00	0.000	0.000	0.000
0.95	...	0.307	0.307
0.90	0.432	0.421	0.421
0.85	...	0.499	0.499
0.80	0.588	0.555	0.555
0.70	0.698	0.629	0.629
0.60	0.778	0.663	0.663
0.546	...	0.667	0.667
0.50	0.835	0.664	0.667
0.40	0.877	0.635	0.667
0.30	0.905	0.575	0.667
0.20	0.921	0.475	0.667
0.10	0.928	0.322	0.667
0.00	0.929	0.00	0.667

[2] "Überkritische Entspannung kompressibler Flüssigkeiten," by W. Schiller, *Forschung auf dem Gebiete des Ingenieurwesens*, 1933, p. 128.

2 Expansion Through a Series of Throttlings

General Thermodynamic Relations. A group of throttlings as used in steam-turbine labyrinths is shown diagrammatically in Fig. 4.[3] The arrangement shall be isolated perfectly so that no heat can be exchanged with the surroundings. As the steam flows through the labyrinth, a pressure drop occurs across each throttling. After each throttling, a small part of the kinetic energy of the steam jet will be reconverted into pressure energy, a second part will be destroyed and transferred into heat, and the remaining kinetic energy will enter the following throttling. The velocity w_ν of the steam jet issuing from the ν^{th} throttling is obtained from the energy equation

$$(w_\nu/223.7)^2 = i_0 - i_\nu \qquad [6]$$

where w_ν = velocity of steam jet issuing from the ν^{th} throttling, ft per sec; i_0 = total heat of steam before entering the labyrinth, Btu per lb; and i_ν = total heat of steam issuing from ν^{th} throttling, Btu per lb.

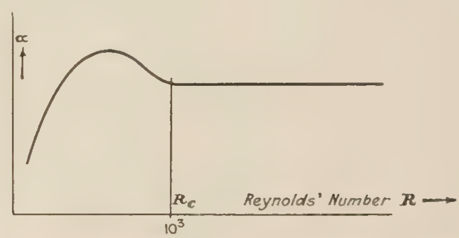

Fig. 3 Flow Coefficient α of a Sharp-Edged Orifice as a Function of Reynolds' Number

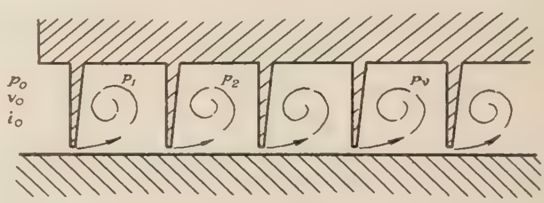

Fig. 4 Expansion Through a Series of Labyrinth Throttlings

Inasmuch as Equation [6] is general, nothing has to be said about the nature of the flow preceding the ν^{th} labyrinth. The condition of continuity for the ν^{th} throttling, however, may be written as

$$Gv_\nu = \alpha A_\nu w_\nu \qquad [7]$$

where G = the flow, lb per sec; A_ν = the leakage area of the ν^{th} throttling, sq ft; v_ν = the specific volume of steam leaving the ν^{th} throttling, cu ft per lb; and α = the flow coefficient.

For the great majority of the throttlings of the labyrinth, the pressure ratio β is higher than 0.8 and α is practically constant. Then, in a labyrinth with a constant leakage area A, the expression

$$W_\nu/v_\nu = G/\alpha A \qquad [7a]$$

is a constant. Combining Equation [7a] with Equation [6]

[3] A series of instructive illustrations of flow through labyrinths produced with water is published in *Escher Wyss News*, January-February, 1934.

$$\text{Constant} = G/\alpha A = (223.7/v_\nu)\sqrt{(i_0 - i_\nu)} \ldots\ldots\ldots [8]$$

which represents a definite relation between v_ν and i_ν. For a given initial total heat i_0, Equation [8] determines a series of Fanno curves[4] $G/\alpha A$ = a constant on the total-heat-entropy diagram as shown in Fig. 5. In a labyrinth of constant-leakage area A, all points of the condition in the steam jet issuing

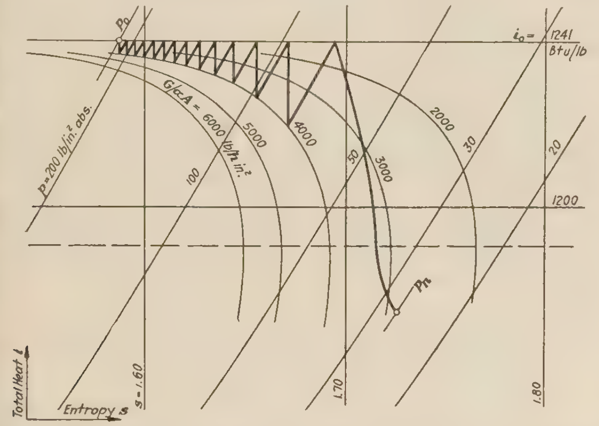

FIG. 5 TOTAL HEAT-ENTROPY DIAGRAM WITH FANNO CURVES
(The heavy zig-zag line is the condition curve for an ideal labyrinth.)

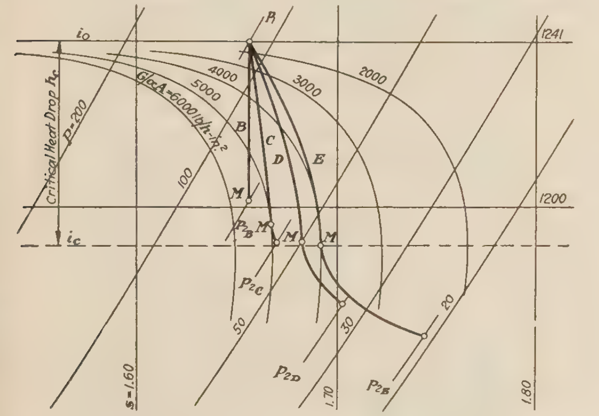

FIG. 6 CONDITION CURVES FOR THE EXPANSION OF STEAM THROUGH A SHARP-EDGED THROTTLING

from each throttling lie on a Fanno curve,[5] as long as α is constant. In an ideal labyrinth with completely destroyed kinetic energy after adiabatic expansion in each throttling, the condition of the steam will follow the zig-zag line of Fig. 5. In the last throttling the pressure ratio β often is considerably smaller than 0.8, and the conditions appear as observed previously.

[4] "Steam and Gas Turbines," by A. Stodola, McGraw-Hill, 1927, sixth edition, p. 61. The curves are named in honor of Fanno, who first used this relationship.

[5] A total-heat-entropy diagram with drawn-in Fanno curves, such as shown in Fig. 6, is helpful when studying the expansion through all kinds of channels. It shows at once that the flow in a passage with constant cross-section never exceeds the critical velocity $w_c = 223.7\sqrt{(h_c)}$, because a flow with decreasing entropy is impossible. The condition of the steam when expanding through a sharp-edged opening may be reproduced by curves like B, C, D, or E, Fig. 6, for decreasing pressure ratios, β. The velocity in the minimum section of the jet (points M, Fig. 6) cannot exceed the critical. This, however, does not mean that when the acoustic velocity in the narrowest section is reached, the flow has to be independent of the back pressure. Because of the change of contraction of the jet, the flow can still increase when the back pressure is lowered.

The curve for the conditions in the last throttling will be similar to the one in Fig. 5.

Derivation of a Practical Method of Calculating the Performance of Ideal Labyrinths With Constant-Leakage Area. In view of the complicated relation between pressure ratio and flow in each throttling, a graphical method is the most practical for computing the conditions in the whole labyrinth.

The equation for leakage through an ideal labyrinth (a labyrinth in which the kinetic energy of the steam jet is completely destroyed and reconverted into heat after each throttling) is similar to the equation for the single throttling

$$G = A\alpha\varphi\sqrt{\left(g\,\frac{p_0}{v_0}\right)} \ldots\ldots\ldots [9]$$

where G = the leakage, lb per sec; A = leakage area of the single throttling, sq ft; α = flow coefficient, assumed to be constant for all throttlings; p_0 = abs pressure before the labyrinth, lb per sq ft; v_0 = specific volume before the labyrinth, cu ft per lb; p_n = pressure after the labyrinth, lb per sq ft; φ is a function of the labyrinth pressure ratio p_n/p_0 and the number n of throttlings.

For the labyrinth with one throttling, ($n = 1$) φ is identical with ψ in Fig. 2. The calculation of φ is a matter of mathematical analysis, the result of which is represented graphically in Figs. 7 and 7*a*.

The φ curves were obtained as follows:

In a labyrinth with two throttlings, the relation for the first is

$$G_1 = A\alpha\varphi_1\sqrt{\left(g\,\frac{p_0}{v_0}\right)} \ldots\ldots\ldots [10]$$

and for the second throttling

$$G_2 = A\alpha\psi\sqrt{\left(g\,\frac{p_1}{v_1}\right)} \ldots\ldots\ldots [11]$$

Since $G_1 = G_2$

$$\varphi_1\sqrt{\left(\frac{p_0}{v_0}\right)} = \psi\sqrt{\left(\frac{p_1}{v_1}\right)} \ldots\ldots\ldots [12]$$

The pressure and volume of the steam on a constant total-heat line are, with sufficiently close approximation, related in the form

$$p_0v_0 = p_1v_1 \ldots\ldots\ldots [13]$$

Thus, we can write Equation [12] as

$$\psi = \left(\frac{1}{p_1/p_0}\right)\varphi_{n=1} \ldots\ldots\ldots [14]$$

Inasmuch as ψ versus $\beta = p_2/p_1$, and φ_1 versus p_1/p_0 (in this case identical with ψ versus β) are given graphically in Fig. 2, Equation [14] must also be solved graphically. The result is the curve $\varphi_{n=2}$ of Fig. 7*a*.

For the labyrinth with three throttlings, the following equation is obtained similar to Equation [14]:

$$\psi = \left(\frac{1}{p_2/p_0}\right)\varphi_{n=2} \ldots\ldots\ldots [15]$$

from which $\varphi_{n=3}$ of Fig. 7*a* is calculated. In this manner we can proceed up to any number of throttlings. For a large number of throttlings, however, this method would be too cumbersome and inaccurate since errors are cumulative. For a labyrinth with $n + 1$ throttlings, Equation [14] can be generalized as

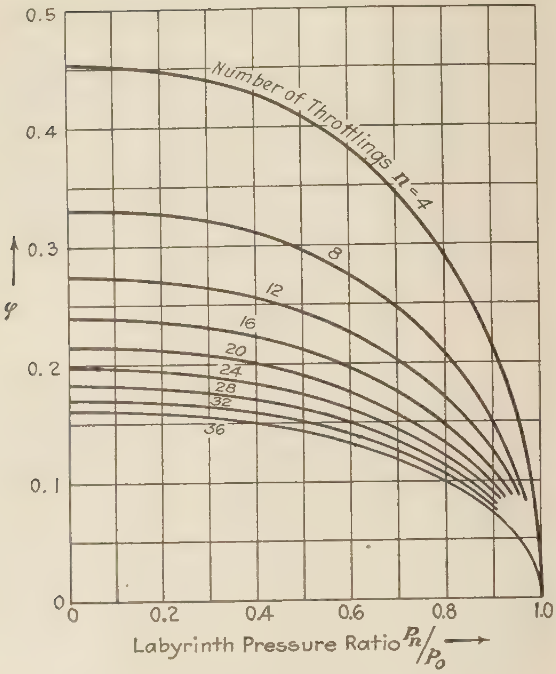

FIG. 7 LEAKAGE FUNCTION φ FOR LABYRINTHS WITH FOUR AND MORE THROTTLINGS

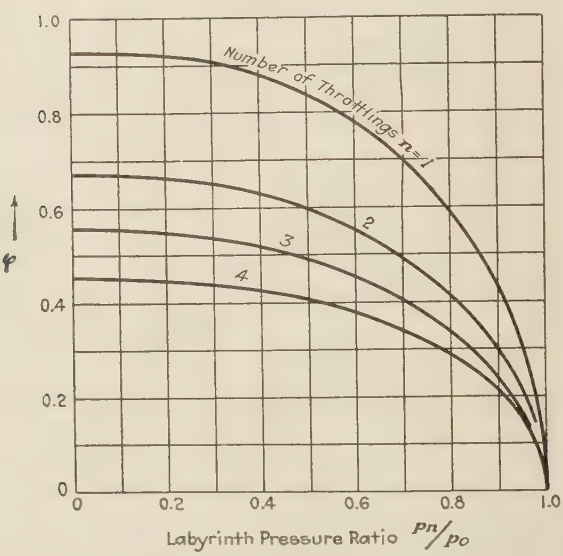

FIG. 7a LEAKAGE FUNCTION φ FOR LABYRINTHS WITH ONE TO FOUR THROTTLINGS

$$\psi\beta = p_{n+1}/p_0 = \left(\frac{1}{p_n/p_0}\right) \varphi_{n, p_n/p_0} \quad \text{.........[16]}$$

which, when φ_n for p_n/p_0 is known, can again be solved graphically for φ_{n+1}

$$\varphi_{n+1, p_{n+1}/p_0} = \varphi_{n, p_n/p_0} \quad \text{............[17]}$$

If the number of $n + 1$ throttlings is sufficiently large, the throttling pressure ratio β in the first n throttlings is greater than 0.8 and it is only in the last ($n + 1^{th}$) throttling that β is smaller than 0.8. For the first n throttlings, therefore, an explicit formula, based on the theoretical Equation [4], can be developed. The formula, as derived in the appendix, takes the form

$$\varphi_n = \sqrt{\left[\frac{1 - (p_n/p_0)^2}{n + \log_e (p_0/p_n)}\right]} \quad \text{..........[18]}$$

and is identical with the expansion term in Martin's[6] labyrinth formula.

The solution with Equations [16], [17], and [18] was used in calculating the φ curves for $n = 8$ to 36 of Fig. 7.

It is now possible to predict the leakage through any ideal labyrinth by applying Equation [9] and utilizing Figs. 7 and 7*a*, once the flow coefficient α has been determined by actual leakage measurement.

The pressure distribution in the labyrinth is obtained from Fig. 7 by simply intersecting the curves n = constant with the horizontal line φ = constant corresponding to the operating conditions.

APPLICATION OF THE THEORY ON THE TYPES OF LABYRINTHS USED IN PRACTICE

From the point of view of flow, there are two types of labyrinths used in practical turbine design; (*a*) a so-called "straight-through" type as shown in Fig. 8, and (*b*) the staggered type schematically shown in Fig. 9.

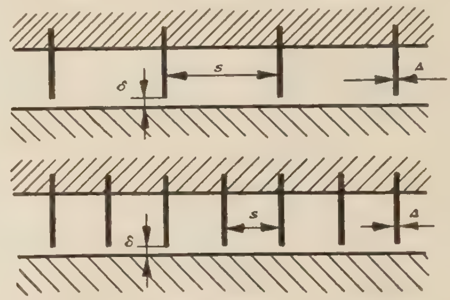

FIG. 8 STRAIGHT-THROUGH LABYRINTHS

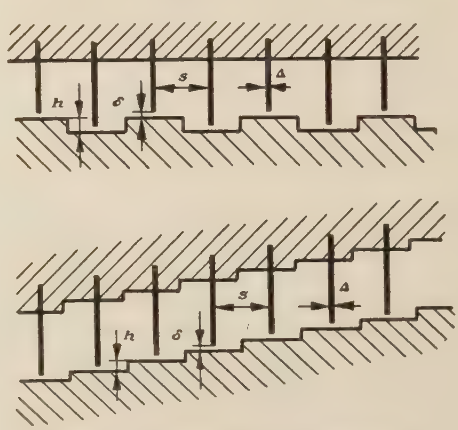

FIG. 9 STAGGERED-TYPE LABYRINTHS

The staggered-type labyrinth obviously gives a better seal than the straight-through type, but it is more costly and involves a more difficult machine assembly. By making the steps h (Fig. 9) sufficiently high, it is possible to have practically all

[6] "Steam Leakage in Dummies of the Ljungstrom Type," by H. M. Martin, *Engineering*, Jan. 3, 1919, pp. 1, 2, and 3.

of the kinetic energy of the steam jet destroyed before the steam enters the following throttling. The theory of the ideal labyrinth can, therefore, be applied directly to this case. Leakage and pressure distribution are obtained with Equation [9] and Figs. 7 and 7*a* as already described.

The straight-through-type labyrinth is frequently used in turbine design since it is easy and cheap to manufacture and has many advantages from an assembly standpoint. It is not as tight, however, as the staggered-type labyrinth because it permits a considerable percentage of kinetic energy to be carried from one throttling into the next. This results in conditions represented by the heavy zig-zag line in Fig. 10. The zig-zag dashed line in Fig. 10 represents the conditions in an ideal labyrinth (with the same leakage area A and the same flow coefficient α) through which the same amount of steam is leaking. The Fanno curve is the same for both labyrinths. These two curves, representing the two conditions, demonstrate clearly that the straight-through-type labyrinth needs more strips for the same leakage than is required in the ideal labyrinth. Apparently, we

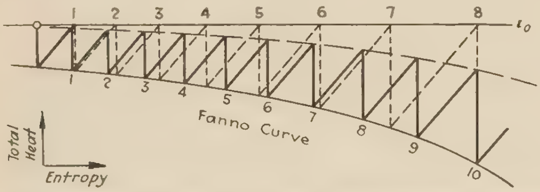

Fig. 10 Condition Curve of a Straight-Through Labyrinth

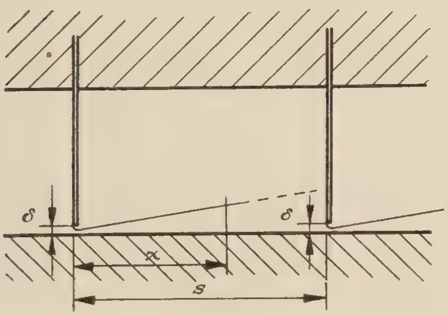

Fig. 11 Broadening of a Steam Jet Issuing From a Throttling

can calculate the leakage through such a straight-through labyrinth by again utilizing Figs. 7 and 7*a* and applying Equation [9], but, instead of taking n as the number of strips, a smaller number of strips n' has to be used which will be equivalent to the number used in the ideal labyrinth. Neglecting the term $\log_e(p_0/p_n)$, it is seen that the flow through a labyrinth is approximately proportional to $\sqrt{(1/n)}$. Therefore, for the leakage through a straight-through labyrinth

$$G = A\alpha\varphi\gamma\sqrt{\left(g\frac{p_0}{v_0}\right)} \qquad [9a]$$

where $\gamma = \sqrt{(n/n')}$, and n' = the number of strips in the equivalent ideal labyrinth. It is assumed that α is constant and of the same magnitude as determined from tests with staggered labyrinths. (Strictly, α depends on the percentage of kinetic energy carried through each throttling, i.e., on γ itself. For practical reasons of simplicity it is assumed, nevertheless, that α is constant and we take account of the change in leakage by varying only γ.) Values of γ are obtained by comparing Equation [9*a*] with the leakage determined from tests. As the jet issuing from the throttling broadens out proportionally with the distance x (Fig. 11), the percentage of kinetic energy available for expansion through the following throttling must be expected to be primarily a function of the ratio δ/s, where δ is the strip clearance and s is the pitch of the strips (see Fig. 8).

TEST RESULTS

Experiments have been conducted with various types of labyrinths in a static-testing device built especially for this purpose. A schematic drawing of the test arrangement and test

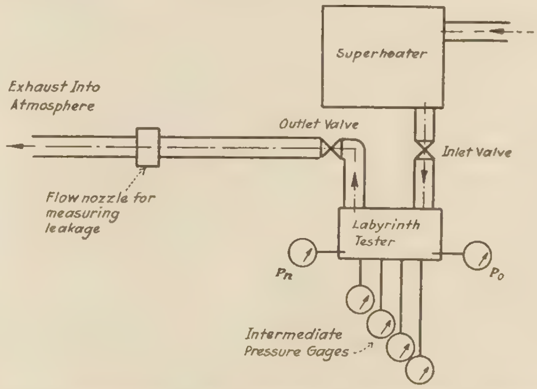

Fig. 12 Arrangement for the Static Testing of Labyrinths

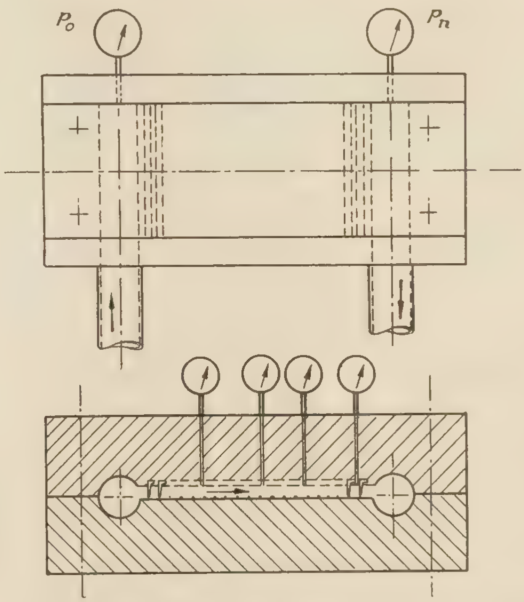

Fig. 13 Test Block Used in the Static Testing of Labyrinths

block is shown in Figs. 12 and 13. When testing, both the inlet and the back pressure were varied over a wide range, and the temperature was adjusted so that the whole labyrinth always operated with superheated steam.

Staggered-Type Labyrinth. In Fig. 14, test curves $\alpha\varphi$ are shown as a function of p_n/p_0 for a well-staggered labyrinth. Fig. 15 demonstrates the agreement between theoretical and actual pressure distribution. By dividing the values of $\alpha\varphi$ obtained from the test curves in Fig. 14 with φ from Fig. 7, the flow coefficient α is determined, which in turn is plotted in Fig. 18 as a function of the ratio δ/Δ = clearance/strip thickness (Friedrich's tests, compared on the basis of the same theory, give for

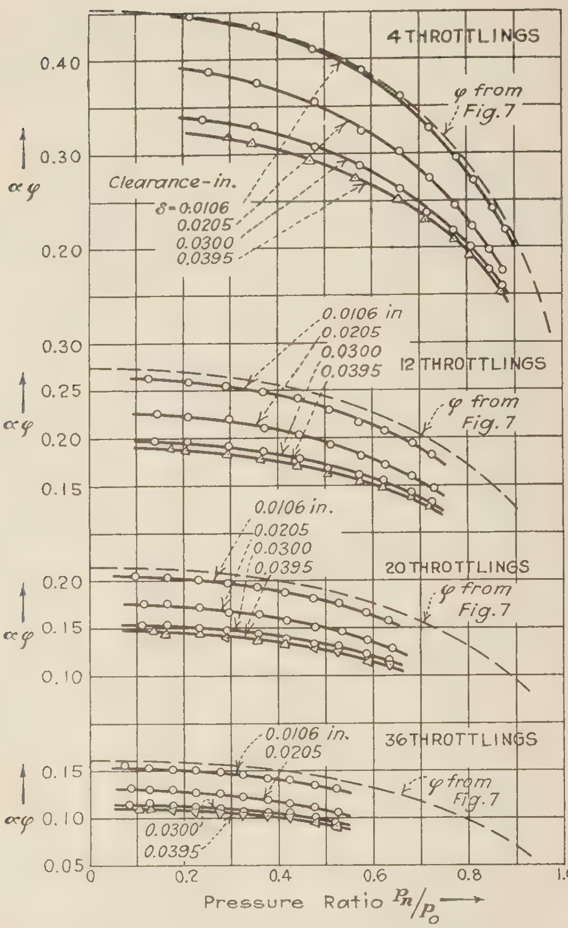

Fig. 14 Results of Static Tests of Staggered-Type Labyrinth
(Thickness of strips Δ = 0.010 in.)

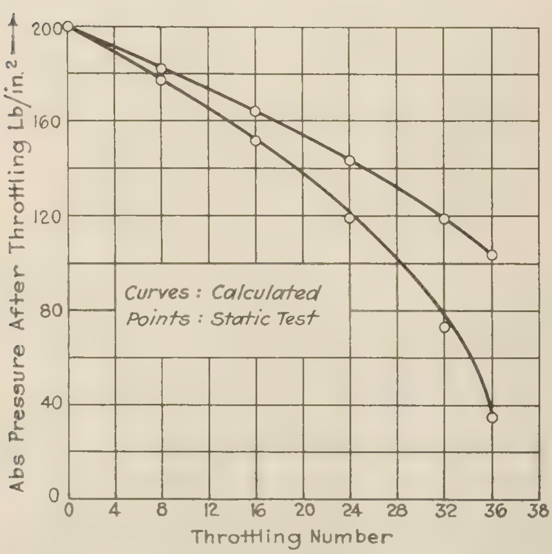

Fig. 15 Pressure Distribution in a Staggered-Type Labyrinth

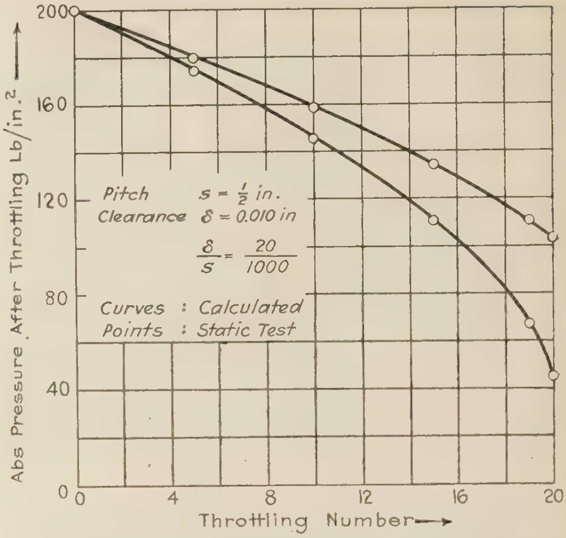

Fig. 16 Pressure Distribution in a Straight-Through Labyrinth With 0.5-In. Pitch and 0.010-In. Clearance

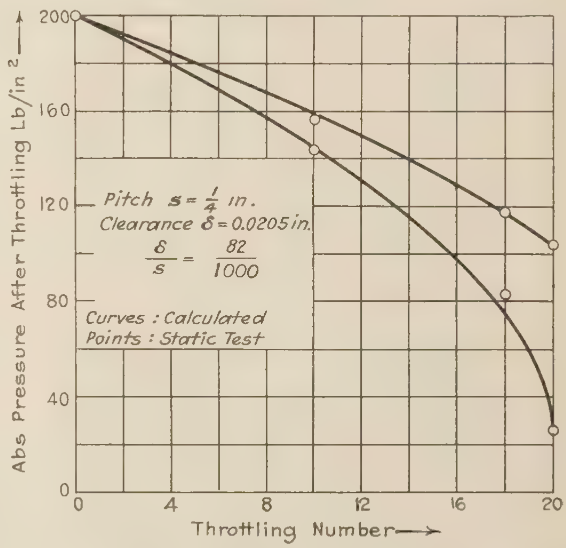

Fig. 17 Pressure Distribution in a Straight-Through Labyrinth With 0.25-In. Pitch and 0.0205-In. Clearance

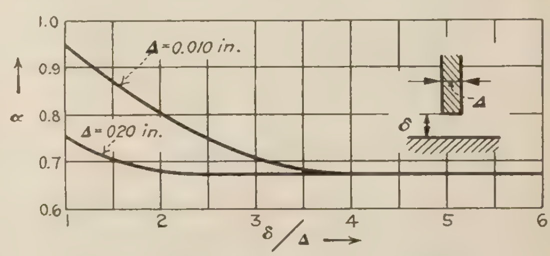

Fig. 18 Flow Coefficient α for Labyrinths With Sharp-Edged Strips Determined From Tests

the range of δ/Δ = 1.3 to 2.3, an average value of α = 0.71 which checks the average in the same range of δ/Δ in Fig. 18).[7]

[7] "Untersuchungen ueber das Verhalten der Schaufelspaltdichtungen in Gegenlauf-Dampfturbinen," by H. Friedrich, *Mitt. Forsch. Anst. G. H. H.*, Oct., 1933.

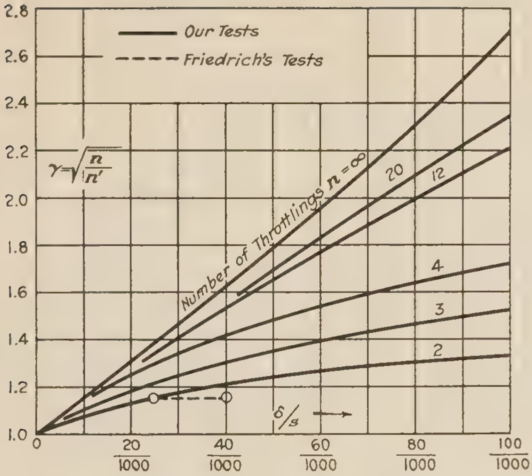

FIG. 19 CARRY-OVER CORRECTION FACTOR γ FOR STRAIGHT-THROUGH LABYRINTHS
(Refer to footnote 7 for Friedrich's tests.)

TABLE 2- LABYRINTHS WITH CONSTANT LEAKAGES

These Labyrinths (with 0.010-in. Thick Sharp-edged Strips) have the Same Leakage						
Type of Labyrinth	Clearance - Inches					
	0.010		0.020		0.030	
	Number of Strips n	Total Length Inches	Number of Strips n	Total Length Inches	Number of Strips n	Total Length Inches
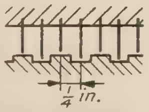 $\frac{1}{4}$ in.	4	1.0	10	2.5	18	4.5
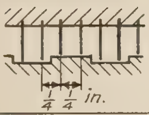 $\frac{1}{4}$ $\frac{1}{4}$ in.	5	1.25	18	4.5	34	85
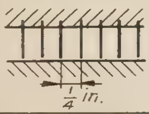 $\frac{1}{4}$ in.	8	2.0	54	13.5	183	45 7
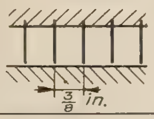 $\frac{3}{8}$ in.	5	1.9	35	13.1	97	36.4
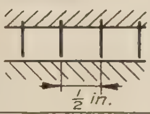 $\frac{1}{2}$ in.	5	2.5	25	12.5	64	32.0

Straight-Through Type Labyrinths. During tests of this type labyrinth, the pitch s and the clearance δ were both varied. The pressure distribution obtained with Fig. 7 checks the test results very closely as can be seen from a study of Figs. 16 and 17. The carry-over correction factor γ was calculated upon the assumption that α is the same as found in the tests of the staggered-type labyrinths. It is found that γ is a function of the ratio δ/s = clearance/pitch, only, and is given in Fig. 19. When evaluating these tests it was considered that a factor $\gamma = 1$ always applies to the first throttling of a group, and it was necessary to solve graphically the equation

$$\varphi_{n-1,\, p_n/p_1} = \frac{1}{\gamma_\infty} \frac{1}{p_1/p_0} \varphi_{1\, p_1/p_0}$$

Friedrich's findings[7] with straight-through-type labyrinths of two and three throttlings are somewhat contradictory to our test results. The discrepancy can be explained probably when we consider that Friedrich tested clearances of as little as 0.006 to 0.010 in. It seems possible that for such narrow clearances, the boundary layer which develops along the smooth surface across the strip prevents kinetic energy from being carried over from one throttling to the other. Our tests were made with clearances of 0.015 to 0.040 in., which is about what occurs in axial-flow turbines built in this country.

CONCLUSION

The leakage through labyrinth seals with constant-leakage area is calculated by applying Equation [9a], in which α depends on the type of sealing strip used. For sharp-edged strips, α is given in Fig. 18.

TABLE 3-COMPARISON OF SINGLE-STRIP AND DOUBLE-STRIP SEALS
(Thickness of Sharp-Edged Strip Δ = 0.010 In.)

Clearances of One Column Give the Same Leakage						
Type of Seal	Clearance - Inches					
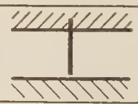	0.010	0.015	0.020	0.030	0.040	0.050
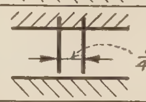 $\frac{1}{4}$ in.	0.012	0.017	0.022	0.031	0.041	0.050
 $\frac{1}{2}$ in.	0.013	0.018	0.023	0.033	0.043	0.053
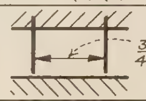 $\frac{3}{4}$ in.	0.014	0.020	0.025	0.035	0.045	0.055

The value of γ is equal to unity in well-staggered labyrinths. In straight-through labyrinths, γ depends on the ratio δ/s (clearance/pitch) and the number of throttlings in the labyrinth group (Fig. 19).

The expansion function φ is given graphically in Figs. 7 and 7*a*.

The pressure distribution in any labyrinth with constant leakage area is obtained from Figs. 7 and 7*a* by intersecting with a line φ = constant.

In Tables 2 and 3, examples are calculated to demonstrate the effectiveness of various types of labyrinths. Particular attention should be given to the double-strip seals in Table 3 which are often used in sealing shrouded reaction stages. For clearances greater than 0.020 in. the single-strip seal is practically as tight as the double strip. The second strip is only effective if a step is provided to prevent the steam jet from shooting directly into the second throttling.

Appendix

The derivation of an explicit formula for the leakage through an ideal labyrinth when the throttling-pressure ratio is greater than 0.8 is as follows:

The velocity of the steam jet after having expanded adiabatically from p_1 to p_2 (Fig. 20) is obtained by integrating the energy equation

$$d\left(\frac{w^2}{2g}\right) = -vdp \quad [19]$$

with

$$p^{1/k}v = \text{constant} \quad [20]$$

as the condition for the adiabatic change of state we get

$$\frac{w^2}{2g} = p_1v_1\frac{k}{k-1}\left[1-\left(\frac{p_2}{p_1}\right)^{1-1/k}\right] \quad [21]$$

We write

$$\Delta p = p_2 - p_1$$

and develop the series

$$\left(\frac{p_2}{p_1}\right)^{1-1/k} = \left(1+\frac{\Delta p}{p_1}\right)^{1-1/k}$$
$$= 1 + \frac{k-1}{k}\left(\frac{\Delta p}{p_1}\right) - \frac{k-1}{2k^2}\left(\frac{\Delta p}{p_1}\right)^2 + \ldots\ldots$$

which when introduced in Equation [21] gives

$$\frac{w^2}{2g} = -p_1v_1\left[\frac{\Delta p}{p_1} - \frac{1}{2k}\left(\frac{\Delta p}{p_1}\right)^2 + \ldots\ldots\right]$$

Since this formula is used only as long as p_2/p_1 is larger than 0.8 or $\Delta p/p_1$ is less than 0.2, the term with $(\Delta p/p_1)^2$ can be neglected so that

$$\frac{w^2}{2g} = -vdp \quad [22]$$

The equation of continuity for the jet is

$$\frac{G}{\alpha A} = \frac{w}{v'_2} \quad [23]$$

where v'_2 is the specific volume at the end of the adiabatic expansion and is obtained from

$$v'_2 = \left(\frac{p_1}{p_2}\right)^{1/k} v_1$$

or in a series of $(\Delta p/p_1)$,

$$v'_2 = v_1\left[1 - \frac{1}{k}\left(\frac{\Delta p}{p_1}\right) + \frac{k+1}{2k^2}\left(\frac{\Delta p}{p_1}\right)^2 + \ldots\ldots\right]$$

We can neglect again the term with $(\Delta p/p_1)^2$ so that

$$v'_2 = v_1\left[1 - \frac{1}{k}\left(\frac{\Delta p}{p_1}\right)\right] \quad [24]$$

Combining Equations [22], [23], and [24] we obtain

$$\left(\frac{G}{\alpha A}\right)^2 = \frac{-2g\,\Delta p}{v_1\left[1-\frac{2}{k}\left(\frac{\Delta p}{p_1}\right)+\ldots\right]} \quad [25]$$

All initial-state points to the various throttlings lie on a curve of constant total heat, along which the relation

$$p_1v_1 = p_0v_0 = \text{constant} \quad [26]$$

holds sufficiently well for gases and steam. Thus we have

$$\frac{1}{v} = \frac{p_1}{p_0v_0}$$

and combined with Equation [25]

$$\left(\frac{G}{\alpha A}\right)^2 = -\frac{2gp_1\,\Delta p}{p_0v_0\left(1-\frac{2}{k}\frac{\Delta p}{p_1}\right)} \quad [27]$$

We now write this equation in the form

$$\left(\frac{G}{\alpha A}\right)^2\frac{1}{\Delta x} - \left(\frac{G}{\alpha A}\right)^2\frac{2}{k}\frac{1}{p_1}\left(\frac{\Delta p}{\Delta x}\right) = -\frac{2g}{p_0v_0}p_1\left(\frac{\Delta p}{\Delta x}\right)$$

which can be integrated if the number of throttlings is large enough so that $\Delta p/\Delta x$ can be replaced by dp/dx.

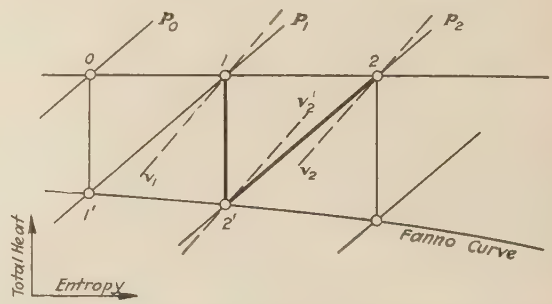

Fig. 20 Condition Curve for an Ideal Labyrinth Throttling

We write

$$\frac{1}{\Delta x}\left(\frac{G}{\alpha A}\right)^2\int_{x_0}^{x_n}dx - \left(\frac{G}{\alpha A}\right)^2\frac{2}{k}\int_{p_0}^{p_n}\frac{dp}{p_1} = -\frac{2g}{p_0v_0}\int_{p_0}^{p_n}p_1dp$$

and, noting that $(x_n - x_0)/\Delta x = n$ = the number of throttlings, we obtain as the leakage formula

$$G = A\alpha\varphi\sqrt{\left(g\frac{p_0}{v_0}\right)} \quad [28]$$

in which

$$\varphi = \sqrt{\left(\frac{1-(p_n/p_0)^2}{n+\frac{2}{k}\log_e(p_0/p_n)}\right)}$$

where p_n = pressure after n^{th} throttling, and $k = 1.3$ for superheated steam.

It has been found by comparing φ from Equation [28] with the thermodynamically strict graphical solution, using the Fanno curve, that for small numbers of strips, a more correct numerical result is obtained if for steam $k = 2$. For large numbers of throttlings n, the logarithmic term is of little importance. We, therefore, write for any number of throttlings, the final formula for the leakage as

$$G = A\alpha\varphi\sqrt{\left(g\frac{p_0}{v_0}\right)} \quad [28a]$$

in which

$$\varphi = \sqrt{\left(\frac{1-(p_n/p_0)^2}{n+\log_e(p_0/p_n)}\right)}$$

This formula can with sufficient accuracy also be used for air and other gases.

The Division of Load Among Generating Units for Minimum Cost

By JAMES E. MULLIGAN,[1] CAMBRIDGE, MASS.

The criteria for minimum-input division of load among several generating units which are to be operated together depend upon the forms of the input-output curves of the units. When the curves are continuous and uninflected the greatest input-curve slope at which any unit operates should be kept a minimum. When the curves are discontinuous or inflected a comparison of two curves of total input against total output will determine the load at which a change should be made from one loading definitely prescribed by the slopes of the input curves, to another definite distribution. When a varying load is to be supplied with part of the units operating at constant load, minimum-input loading may be determined by means of curves of average input against average output.

DURING the whole history of power generation an enormous amount of effort has been applied to the problem of increasing the efficiencies of individual generating units. The fruitfulness of this endeavor is well known. The margin of possible improvement in present types of apparatus has, however, become so small that it is at least exceedingly unlikely that the striking improvements of recent years can be duplicated.

In view of the limitations on further increase of unit efficiencies and of a current hesitancy to increase capital expenditures in order to decrease future operating costs, it is not surprising that attention has recently been turned to the increasing of system efficiency by a better distribution of the load among existing units. The improvement obtainable may be large, a case having been reported where an effort to operate a hydro plant with optimum load distribution resulted in an increase in output of approximately eight per cent.[2]

Although the development of methods for the optimum distribution of load has been altogether from the viewpoint of the operation of power-generating apparatus, the principles involved have no such limited application. It should be recognized that the same principles may be used to obtain a given output with minimum input to several productive agencies of any kind, whether the agencies are turbo-generators, generating stations, machines, or factories.

[1] Instructor in Electrical Engineering, Massachusetts Institute of Technology. Jun. A.S.M.E. Mr. Mulligan was graduated from the University of Maine with the degree of B.S. in 1925. Since that time he has been assistant and instructor in the department of electrical engineering at the Massachusetts Institute of Technology. He received the degree of S.M. from the Massachusetts Institute of Technology in 1933. This paper is taken from a part of a thesis submitted for that degree and prepared under the direction of Dr. V. Bush. He is also the author of a paper on power-system switching.

[2] "Automatic Operator for Economy Control," by S. Logan Kerr, A.I.E.E. Trans., vol. 50, March, 1931, p. 133.

Contributed by the Power Division for presentation at the Semi-Annual Meeting, Cincinnati, Ohio, June 19 to 21, 1935, of The American Society of Mechanical Engineers.

Discussion of this paper should be addressed to the Secretary, A.S.M.E., 29 West 39th Street, New York, N. Y., and will be accepted until July 10, 1935, for publication in a later issue of Transactions.

The first publication of the basic principles affecting optimum distribution of a constant load between two generating units, except for the simplest case where the input curves are all straight lines, was by F. H. Rogers in 1924.[3] The treatment was extended by Rogers and Moody during the following year.[4] Since that time there have been published many papers dealing principally with the practical application of the methods of Rogers and Moody.

It is the purpose here to expand the theory underlying load division by a demonstration of the criteria for distribution where more than two units are involved, where the curves of input plotted against output are discontinuous or inflected, and where part of the units operate at constant load as the total load changes.

Any method for distributing load for maximum economy will require a knowledge of the relationship between input and output for the units concerned, with each of the inputs and each of the outputs expressed in common units. Thus hydroelectric generating units in the same station, taking water from the same forebay and delivering energy to the same bus, can be represented by their turbine discharge curves. The input of a distant generating station might be plotted against the output at the receiving end of its transmission line. In some cases dollars of cost will be the only common measure of input. Much study has been given to the problem of determining such input curves.[4,5]

When the amount of generating capacity which shall be operated to supply an expected load has been decided upon there still remain two questions: (1) Which of a number of available generating units shall be operated to supply the required capacity? (2) How shall the system load be divided among the units which are to be operated?

In general the first question will be answered by giving preference to the generating units of higher efficiency. With increasing load the units will be started in order of decreasing efficiency. In some simpler cases a comparison of individual input-output curves will indicate the order in which the units should be started. When the comparison of individual curves becomes inadequate, curves of total input versus total output for various combinations of units, with most efficient distribution of load among the units in each case, may be plotted together to give an envelope curve of minimum input. The envelope curve will determine the particular units which will give least input at each load. Such curves have been published. We are here directing attention to the second question of the preceding paragraph; that is, to the division of load among a number of units all of which are to be operated together. The no-load inputs to all of them must then be supplied and load division among them depends only on the relative increments of input above the no-load values.

[3] "Acceptance Tests of Hydroelectric Plants," by F. H. Rogers, A.I.E.E. Trans., vol. 43, 1924, p. 568.

[4] "Interrelation of Design and Operation of Hydraulic Turbines," F. H. Rogers and L. F. Moody. *Engineers and Engineering*, vol. 42, 1925, p. 174.

[5] "Incremental Loading of Generating Stations," by M. J. Steinberg and T. H. Smith, *Electrical Engineering*, vol. 53, 1933, no. 3, p. 432 and no. 4, p. 571.

Input Curves Continuous and Uninflected

The great majority of input-output curves are either made up of straight lines or have an upward concavity which increases with the load. In Fig. 1, I_1, I_2, etc. are curves of this kind, representing input plotted against output for any number of generating units which are to be operated together. The curves are continuous, although the slopes of some of them are discontinuous. I'_1, I'_2, etc. are the first derivatives of the input curves, that is, they simply indicate the slope at all values of output of I_1, I_2, etc., respectively.

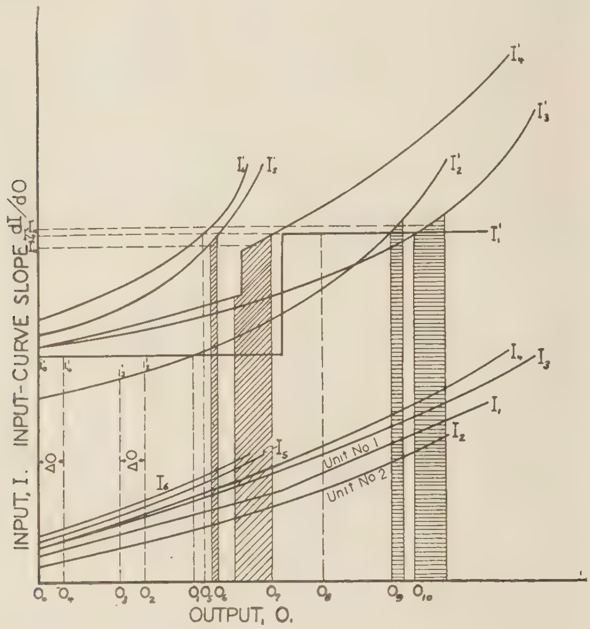

Fig. 1

It will be proved that for units with this type of input-output curve the load should always be so apportioned that the greatest value of input-curve slope at which any unit operates is kept a minimum. This criterion will be examined for three cases; for low values of slope which apply to only one unit, for intermediate values where there may be any number of units, and for the highest values applying only to the unit with greatest slope.

Any loads in the range from no load to O_1 should be applied to Unit No. 2 because the slope of I_2 is less than that of any other in this range. Suppose a load of O_2, which is all being supplied by No. 2, is redistributed by applying any fraction of it to any of the other units. For instance, suppose the load on No. 2 is reduced by the amount ΔO from O_2 to O_3 and the load on No. 1 is increased by the same amount from O_0 to O_4. The decrease in input to No. 2, $\frac{dI_2}{dO}\,\Delta O = \Delta I_2$, is shown by the area $O_3i'_3i'_2O_2$, with a width equal to the change in output and a height equal to the slope of the input curve. The increase in input to No. 1, $\frac{dI_1}{dO}\,\Delta O$, is shown by the area $O_0i'_0i'_4O_4$, of the same width but of greater height than $O_3i'_3i'_2O_2$. Since

$$\frac{dI_2}{dO} < \frac{dI_1}{dO}, \text{ then } \frac{dI_2}{dO}\,\Delta O < \frac{dI_1}{dO}\,\Delta O, \text{ and } \Delta I_2 < \Delta I_1.$$

That is, the decrease in input to No. 2 is less than the increase in input to No. 1, and the redistribution of load has resulted in a net increase in input at constant output. For best efficiency all the load should be supplied by the unit whose slope is least at the given load.

Total loads greater than O_1 cannot be applied to a single unit so that it will be loaded to a point where its slope is less than that of any other, but the load should still be so distributed that the greatest slope at which any unit operates is as small as possible. This will lead to operation with load so divided that all units operate at equal values of slope. Any load in the range of equal slopes,

$$O = O_5 + O_6 + O_7 + O_8 + O_9 + O_{10}$$

should be so distributed that the operating points on all the input curves have the same slope, I', as is now to be proved. Suppose any other distribution of load whatever be used. Then in order that the total output still be O, some of the outputs will be less with smaller values of slope and some greater with larger values of slope than with the equal-derivatives distribution. Let the load of N of the units be less by a total of Δ_1O and that of M of the units be greater, with the loads of any number of the units remaining unchanged. With O constant the load on the M units must be greater by a total of Δ_1O.

The decrease in input to the N units is shown in Fig. 1 by the diagonally cross-hatched areas of average height I'_N and the increase to the M units by the horizontally cross-hatched areas of average height I'_M. Since the derivatives either remain constant or increase with increased load, $I' < I'_M$ and $I'_N < I'$ and therefore $I'_N < I'_M$. The sum of the widths of the N areas representing load decrease is equal to the sum of the widths of the M areas representing load increase, each sum being Δ_1O. The total decrease in input is then $I'_N \; \Delta_1O$ and the total increase $I'_M \; \Delta_1O$. Since $I'_N < I'_M$, $I'_N\Delta_1O < I_M\Delta_1O$ and the net input has again been increased by any change from operation at minimum slope.

When increase in load at equal slopes results in any unit reaching its maximum output, equal-slopes operation of all units will have to be abandoned and minimum input for higher loads will result from leaving the output of that unit constant at its maximum value and continuing to load the others at equal slopes. The load on the fully loaded unit will either have to be left constant or be reduced. If it is reduced, some of its load will have to be transferred to other units with greater input-curve slope, and the change will result in a net increase in input. This will hold until the unit of highest input-curve slope reaches full load.

To summarize: For input-output (input as ordinates against output as abscissas) curves which are continuous and which have no decrease of slope with increasing load, a given output will be supplied with minimum input if it is so divided among the units chosen to operate that the greatest slope at which any one of them operates is kept a minimum. At points of discontinuity in the slopes of their input curves, units should operate at constant load until load change on other units gives equality of slopes beyond the discontinuity.

Discontinuous Input Curves

Although the great majority of input-output curves are of the kind just discussed, some of them, notably those of some turbines whose valves open successively as load increases, are discontinuous or show a decreasing slope at the valve points. The criterion of equal slopes alone is inadequate with curves of these kinds.

In Fig. 2, are shown the input-output curves of two identical turbines which have an abrupt increase in input at load at O_1 where a by-pass valve is opened. The criterion of equal slopes, which means equal loads on the identical units used in this example, still holds with both units operating above, or both below, the

discontinuity. The derivative curve, however, gives no indication of the amount of increase in input at the valve point. For the range of loads between twice O_1 and the maximum load of one unit, curves of total input for each of the two conditions may be used to determine whether one unit should be operated at O_1 with the other taking the remainder of the load, or whether both units should be operated above O_1 at equal loads. The load above which it becomes economical to supply the increased input caused by opening the second by-pass valve rather than to go further up the increasing slope toward full load can be determined by the intersection of the two curves of Fig. 3. Curve BB' gives total input with one unit operating at load O_1 (Fig. 2) with its by-pass valve closed, and is AA' (Fig. 2) with O_1 added to its abscissas and I_1 to its ordinates. CC' is a curve of total input with equal loading obtained by multiplying by two the abscissas and ordinates of AA'. Evidently best operation will be that along the envelope curve of minimum input BDC', so for total loads less than O_2 one unit should operate at a load of O_1 with its by-pass valve closed, and for greater total loads the unit loads should be equal.

Although the discussion of discontinuous curves was simplified by the use of only two similar curves with a single discontinuity, the procedure is the same for any number of units, similar or not.

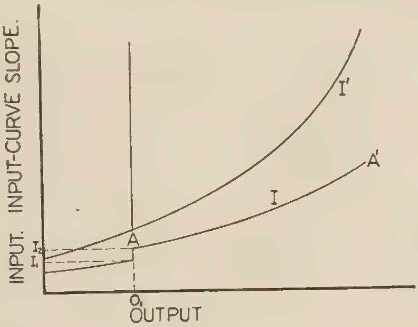

Fig. 2

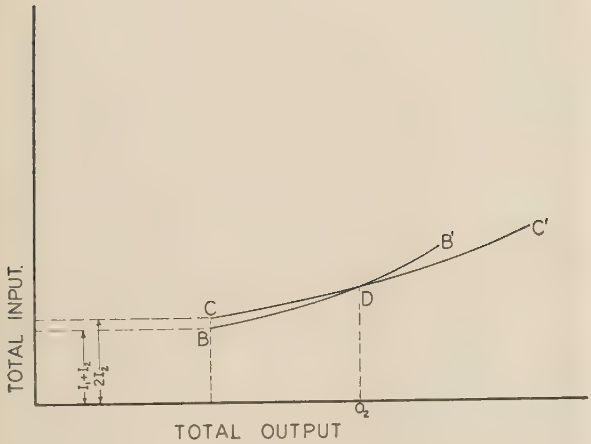

Fig. 3

The region in which equal-slopes operation must be abandoned will be determined by the comparison of curves of total input for the two methods of operation.

The use of curves of total input versus total output, as thus described, to determine the load at which operation should be changed from one distribution definitely prescribed by the derivative curves to another definite distribution, should not be confused with the use of input curves alone for minimum-input-load division. It is possible to determine optimum distribution between two units as the locus of the minima of curves of total input versus output of one of the two units, with total output as a parameter. This latter method requires the drawing of many curves even when only two units are involved, and would rapidly become unwieldy with an increase in the number of generators.

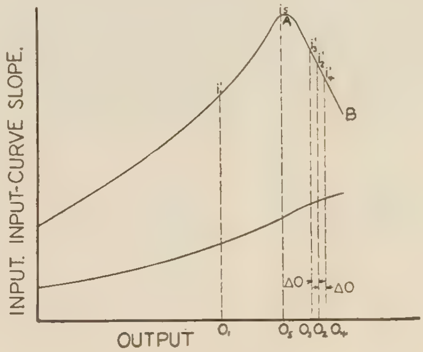

Fig. 4

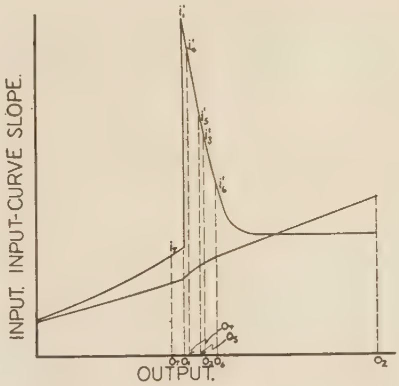

Fig. 5

The method used here requires the determination of only one intersection at each critical point in the loading schedule, regardless of the number of units in operation.

Inflected Input Curves

Another type of input curve is continuous but exhibits points of inflection. Here again, as in the case of discontinuous input curves, there will be loads at which it will be incorrect to operate at equal slopes, or to operate similar units at equal loads. The methods which have been discussed may again be used to determine most economical operation.

Fig. 4 shows an input curve whose first derivative curve has a region AB whose negative slope is greater than that of the positive slope of the curve at lighter loads. Light loads should be divided equally between two similar units of this kind. For instance, for a load of twice O_1 distributed equally the argument is the same as for single curvature; any redistribution by moving the operating point of one unit from i'_1 toward A will sweep off a larger area representing load increase than will be swept off by the moving of the operating point of the other to the left from i'_1, where the derivative curve is lower. On the other hand, a heavier load such as twice O_2 is not supplied at minimum input by operating both units at O_2. Remove ΔO from one unit and apply it to the other so that operation is at O_3 and O_4. The decrease in in-

put, $O_3i'_3i'_2O_2$, is greater than the increase in input, $O_2i'_2i'_4O_4$, and the change has resulted in a net decrease in input. Improvement will continue with further change until one unit is operated at full load. The division between the regions where the units should be operated at equal slopes and that where one should operate at full load is at a load of twice O_5, the load where the area under the derivative curve from i'_5 to full load is equal to the area under the curve from i'_5 an equal distance to the left. For any greater load a change to full load on one unit will result in decreased total input, because the area under the derivative curve from any such point to full load is less than the area from the same point an equal distance toward no load. For a practical determination of O_5 the measurement of areas under the derivative curve may be avoided by comparing two curves of total input, as was done in the case of discontinuous input curves. A curve of total input with equal loads and one of total input with one unit at full load will intersect at a total output of twice O_5.

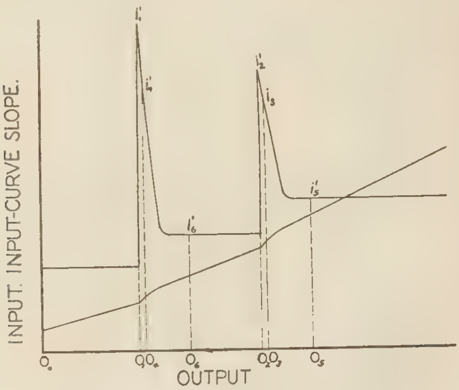

Fig. 6

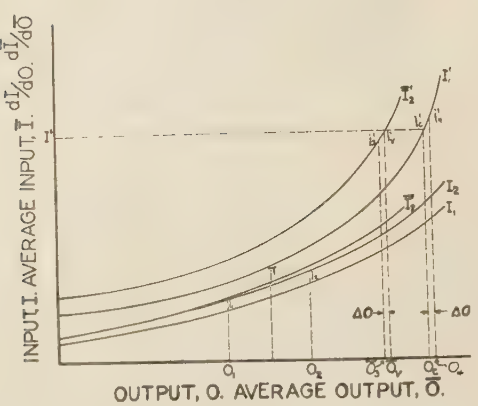

Fig. 7

In Fig. 5 the input curve again has points of inflection, but here the change in curvature is abrupt at a valve point, giving a derivative curve with positive slope greater than negative, and making unnecessary the use of curves of total input in prescribing load division. For loads below twice O_1, two equal units should divide output equally. For loads greater than twice O_1 and less than $O_1 + O_2$, one unit should carry O_1 and the other should carry the remainder. For greater loads one unit should operate at full load. For loads between twice O_1 and $O_1 + O_2$ the reasoning is as follows: Let the units operate at O_1 and O_3. A change of distribution by increasing load on one unit above O_1 will result in an input increase $O_1i'_1i'_4O_4$, which is greater than the decrease in input $O_5i'_5i'_3O_3$ caused by an equal decrease in output of the other unit. In the same way a decrease in output below O_1, with an equal increase above O_3, is shown to result in a net increase in input by the greater height of area $O_3i'_3i'_6O_6$ over $O_1i'_1i'_7O_7$. Therefore, for any load in this range one unit should operate at O_1. For the other two ranges of load the reasoning is similar to that in cases which have been treated previously and need not be repeated.

For curves with more than one point of inflection, curves of total input may again be used to determine critical points in the operating program. In Fig. 6 loads from O_0 to twice O_1 should be distributed equally, and for loads from twice O_1 to $O_1 + O_2$ one unit should operate at O_1 as in the previous case. For a range of loads beyond $O_1 + O_2$ it will be better to supply a smaller increment of input, $O_2i'_2i'_3O_3$, than the larger one, $O_1i'_1i'_4O_4$, so with increasing load one unit should remain for a time at O_1. Because of the increasing trend of curvature, the more heavily loaded unit may reach a load such as O_5, where a decrease in its load to O_2 will result in a decrease in input which is greater than the increase produced by an equal increase in input to the other unit beyond O_1. In the figure this point would be reached when $O_2i'_2i'_5O_5 = O_1i'_1i'_6O_6$, $O_6 - O_1$ being equal to $O_5 - O_2$. This load may be determined practically by the comparison of curves of total input for one unit at O_1 and for one unit at O_2.

Distribution of a Varying System Load—Constant-Load Operation of Some Generators

The criteria for least input which have been discussed can be followed exactly only if the loads of all units can be adjusted continuously as the total load changes. The ordinary method of power-system operation, where part of the generating units operate at fixed throttle, and the remainder control frequency by sharing the load changes, is not covered.

Although an assumption that good operation will be obtained by keeping the loads near those which the previous theory would dictate (by, for instance, keeping the load on constant-load units equal to the average load on similar frequency-controlling units) may in some cases give nearly optimum operation, a definite criterion is desirable. Approximations may be far wrong when the load swing on the frequency-controlling units is large. Such a definite criterion may be used in comparing the relative efficiency of different methods of operation, to show the improvement which would result from a more frequent readjustment of the load on constant-load units, or in determining the advantage to be derived by having more units share in frequency control.

A criterion for this case is easily established if it is assumed that a curve of load against time will be a straight line within the range of load change absorbed by the frequency-controlling units. The effect of this assumption with a typical load curve and a typical range of load swing on the frequency-controlling units was investigated and the assumption was found to be justified. In Fig. 7, I_1 is the input curve of the unit or units which are to be operated at constant load while the system load changes by O_2—O_1. The load change is to be absorbed by a frequency-controlling unit or units represented by input curve I_2. If there are several constant-load units their share of the load is distributed in accordance with the principles previously discussed, and I_1 represents total input to them. If there are several frequency-controlling units their controls are so interlocked that they always operate with optimum distribution of load among themselves, so that I_2 may be treated in the same way as the input curve of a single frequency-controlling unit.

Curve $\bar{I}_2$ shows average input plotted against average output for the varying-load units as the load is changed uniformly over an interval, $O_2 - O_1$. The method of determining a point on this curve, $\bar{i}$ for instance, is as follows: Area $O_1i_1i_2O_2$ is measured and

divided by the length of its base, $O_2 - O_1$, to give the ordinate of $\bar{i}$. Then $\bar{i}$ is plotted against average output in the interval and under the assumption of linear load change with time, the average is at the middle of the interval, at $\frac{O_1 + O_2}{2}$. For other points the position of the constant interval, $O_2 - O_1$, on the output scale is changed. $\bar{I}'_2$ is $\frac{d\bar{I}_2}{d\bar{O}}$, the derivative of $\bar{I}_2$, and I'_1 is $\frac{dI_1}{dO}$ the derivative of I_1.

It can be proved by a method similar to those already used that the average input will be minimum when the constant-load units are operated so that the slope of their input curve is equal to the slope of the curve of average input to the frequency-controlling units. A load which is to vary over the range $O_2 - O_1$, for which $\bar{I}_2$ was drawn, is distributed so that

$$\frac{dI_1}{dO} = \frac{d\bar{I}_2}{d\bar{O}} = I'$$

with the constant-load units carrying a steady load of O_c and the frequency-controlling units supplying a varying load whose average is $\bar{O}_v$. It may be shown that the total average load $\bar{O} = O_c + \bar{O}_v$ is being supplied with minimum average input by decreasing the average load on the frequency-controlling units by any amount, ΔO, and increasing the load on the constant-load units by ΔO. The average output is unchanged at $\bar{O}$. From the geometry of the figure, the total average input has been increased because the increase in constant input, $O_c i'_c i'_4 O_4$, is greater than the decrease in average input, $\bar{O}_3 i'_3 i'_v \bar{O}_v$.

An increase in the average load on the frequency-controlling units with an equal decrease in load on the constant-load units would evidently give the same result of increased average input at the same average output. The equal-slopes distribution gives best operation.

All other methods of load distribution, equal fractions of rating, equal efficiencies, all units but one at maximum efficiency, etc., will lead to larger inputs except when they accidentally coincide with the methods which have been discussed.

Discussion

The Design of Light-Weight Trains[1]

E. L. Larson.[2] I regret that I cannot agree with Dr. Eksergian's statement, "On the other hand, without any partition whatsoever, the torsional effect is manifested by a couple exerted on the main side frames, ..." in the section entitled, "Torsional Strength Through Step Wells and Openings." His plain meaning is that the roof and underframe-floor lateral construction do not exert a couple "without any partition whatsoever." Actually, they exert a couple under this condition. Equilibrium in the doorway region can be established in two ways: (1) Without rigid bulkheads ("without any partition whatsoever"), by means of (*a*) a couple exerted by the roof and the underframe-floor construction acting as lateral members, and (*b*) a couple exerted by the side frames acting as vertical members; (2) with rigid bulkheads fore and aft of the door openings, by means of either couple (*a*), or (*b*), or both couples. In other words, with rigid bulkheads, one couple is sufficient for equilibrium but without rigid bulkheads, one couple is not enough; both couples are required. The actions in portions of the framing depend upon how these portions function with respect to the couples mentioned. Local torque, in the individual framing members across the door opening, is of minor importance compared with the action of the couples discussed, and, therefore, the local torque will not be referred to after this. For the sake of brevity, an intermediate condition, which might be termed "partially rigid bulkheads," will not be discussed. Theoretically, what we are here calling a rigid bulkhead is at best but a partially rigid bulkhead. For the same reason, the action of the bulkheads in attempting to retain the original form of cross-section (such as trying to keep a rectangular section from becoming that of a parallelogram) will not be referred to.

The accompanying diagram, Fig. 1, and equations show why the two couples, instead of only one couple, are required in the case of the door region when "without any partition whatsoever." The diagram and the equation set forth an approach to a first approximation. For the sake of simplicity, a car with rectangular cross-section is considered. Some tacit assumptions are made as to end conditions. The diagram is essentially that of a box unfolded, with sides separated. Only one source of torsion is considered, namely, uneven jacking at diagonally opposite corners of an articulated unit of a train. In order to avoid complication of force arrows, the total torsional moment transmitted to the unit by the external forces is indicated by T and the semi-circular arrows in the end views. The deflections are not shown.

From the diagram, it is evident that "without any partition whatsoever," equilibrium of moments is established in the various planes as follows:

In the end views: $fW\,H + fH\,W = T$ or $2fHW = T$
In plan and bottom view: $fW\,L = fL\,W$
In side elevations: $fH\,L = fL\,H$

From equilibrium in the end views, it follows that the portion of the total torsional moment resisted by (*a*), the couple exerted by the roof and the underframe-floor construction acting as lateral members, is equal to the portion of the total torsional moment resisted by (*b*), the couple exerted by the side frames acting as vertical members.

Obviously, the approach indicated in the diagram does not apply to open top cars, nor does it apply to certain types of closed-top freight cars, those with so-called flexible roofs. The action of torque perhaps explains some of the creaking of wood-framed passenger cars.

The five equations, at the end of the section referred to in Dr. Eksergian's paper, can be made of service under the conditions for which he evidently intended them ("without any partition whatsoever") by substituting $T/2$ for his T, where T still has the value assigned by him, namely, the total torsional moment transmitted across the door opening.

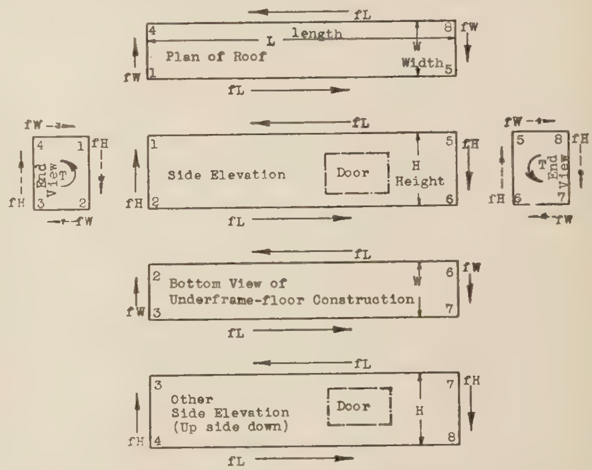

Fig. 1 General Torsional Action in a Car With Hollow Rectangular Cross-Section, Without Rigid Bulkheads Fore and Aft of the Side Door Openings

[All views are *outside* views.
The arrows with long heads refer to external forces or moments, in the plane considered, with reference to the member of the car shown.
The forces shown in the end views by dotted arrows show how equilibrium is established in the end views with reference to the applied torque.
The numerals, 1 to 8 inclusive, refer to the corners in order to assist in comparing the views.
The thicknesses of the members are neglected for simplicity in discussing the general overall actions and because secondary actions are neglected. (Among the secondary actions are restraints, at edges, other than those of direct shear.)]

Dr. Eksergian also states, ". . . ., if the bulkheads are very rigid, a pure torque is applied by the truss to the openings." In this case, probably in most instances, there will be considerable beam action on the part of the members extending across the door openings, whereas the pure torque in these members will be of less importance, and then this will be merely as secondary action.

As a matter of possible interest, reference might be made to "The Torsional Stress of Wings," by C. P. Burgess in the fifteenth annual report of the National Advisory Committee for Aeronautics, 1929, as well as to "The Torsion of Members Having Sections in Common in Aircraft Construction," by G. W. Trayer and H. W. Marsh in the same report.

[1] Published as paper RR-56-4, by R. Eksergian, in the September, 1934, issue of the A.S.M.E. Transactions.
[2] Chicago, Ill. Mem. A.S.M.E.

J. C. Fitterer.[3] In recent years, the automobile and the airplane have seriously challenged the economic existence of the locomotive as a result of the design of internal-combustion engines with a marked reduction of weight per horsepower developed, and the introduction of cheaper and better fuels for these engines. The young science of metallurgy is swinging into a vigorous stride and places at our disposal alloys such as duraluminum and stainless steel, in which desirable properties have been obtained by controlling composition. Very often, substances of three ingredients offer useful compounds whose properties can be plotted on a tri-linear diagram in which each element occupies one of the vertices. Any point, at a vertex, on a side, or within the triangle, locates a substance containing one, two, or all three ingredients. The memorable researches of Prof. Thurston clearly brought this means of graphical analysis into general prominence. Any property under investigation can be noted for a given composition, and after the field has been thoroughly covered, a characteristic topography may be developed, and the compound best suited for a given purpose easily selected.

Stainless steel possesses a triangular array of its own in which steel, chromium, and nickel compose the leading triumvirate. Compounds of these furnish interesting avenues of investigation of stainless steels and enhance our knowledge of their properties such as tensile strength, compressive strength, torsion, flexure, corrosion, weight, etc. (with or without previous heat treatment). Suitable alloys, thus attained, have contributed much to the design of engines of low unit weight, such as found in the *Zephyr*.

Regarding mathematical calculations developed in the paper, the unhesitating use of the process of resolving indeterminateness by setting up an inclusive energy function and differentiating, may be an augury of greater future usefulness in the application of modern methods on the part of the progressive engineer thoroughly grounded in the use of mathematical analysis.

As an addendum or extension to Dr. Eksergian's paper, it might be interesting and practical for some one to investigate the effect that varying widths of track gage would have on the economics of design in equipment of the *Zephyr* type. We have railroad-track gages, varying from the monorail to gages wider than the so-called standard gage. We might include among them the negative gage as a limiting case, clearly indicating the airplane which is not fettered to any ground track whatsoever. If a suitable function could be set up, the orthodox process of differentiation and equating the derivative to zero might lead to some suggestive results applicable to future designs. Any reduction in costly trackage must surely reflect its helpfulness in diminishing capital charges and, perchance, in a further reduction in the cost of operation, all of which may prolong the economic life of the railroads in competition with newer developments arising on all sides. Adaptation to the changing order of events is surely a healthful sign of continued progress.

A. M. Wright.[4] Dr. Eksergian states that train resistance may be divided into two primary components which are (1) that due to rolling and bearing friction, and (2) that due to wind resistance. This is true, but from tests on the actual performance of trains, it is impossible to determine what portion of the total resistance is due to friction, and what portion is due to the air. All tests hitherto made indicate merely that the total resistance can be approximately represented by the equation

$$R = A + BV + CV^2 \qquad [1]$$

where V is the velocity of the train, and A, B, and C, are constants depending on the dimensions and weight of the train. It is usual to assume that the term CV^2 is due to air resistance alone, and in designing a train of a radically new type, such as the *Zephyr*, it was logical to resort to wind-tunnel tests to determine the value of the constant C. Such tests, however, must be accepted with caution, for several reasons. An important one is the scale effect. It is well known that for the flow around similar bodies to be similar in any two cases, the Reynolds number $\left(\frac{\rho vl}{\mu}\right)$ must be the same in both cases. When testing a small scale model in a wind tunnel, this equality requires the velocity used to be much higher than the velocity of the full-size train. It is found, however, that the drag coefficient changes very little over a wide range of Reynolds' numbers above the critical region, so that the tunnel tests may usually be carried out with reasonably low wind velocities. On the other hand, it seems very necessary to know just how much this small variation in the drag coefficient amounts to, in order that the results obtained with one value of vl may be applied to another. An error in the coefficient C in the train resistance equation may lead to very incorrect results at high speeds. To the writer, it is not obvious that the same scale effect applies to both the conventional and the streamlined train, for the air flow is by no means the same in both cases. Another point which would seem to require careful attention in testing such an elongated body as a train model is that the velocity of the undisturbed air stream should be uniform over the whole length occupied by the train. It would appear that very different results would be obtained with different types of wind tunnels due to variations in velocity along the length of the model. Dr. Eksergian makes no mention of this effect, and it would be interesting to know how this was allowed for in predicting the train resistance of the *Zephyr*.

For the above reasons, Dr. Eksergian's train-resistance formula can be considered only as contingent. The most satisfactory way of determining the train resistance, of course, is by road tests. In a train of the Zephyr type, which will always operate as a unit, resistance values can be obtained very simply from a coasting test. The only apparatus needed is an accurate speedometer. Suppose the power is shut off from the motors at some point on the run, and that the train is allowed to coast down to a low speed or even to a stop, under the retarding influence of the train resistance and the grades encountered. At the instant of shutting off power, the total energy in the train is composed of potential energy due to its elevation H above some datum level, and kinetic energy due to its velocity v. The total energy in the train is then

$$E = WH + \frac{Wv^2}{2g}$$

where g should be taken at about 30 instead of 32.2, to allow for rotational inertia.

Dividing through by W, $\frac{E}{W} = H + \frac{v^2}{2g}$ [2]

In Fig. 2, let the distance traversed from the point of shutting off power be denoted by the abscissas, and the quantity $\left(\frac{H + v^2}{2g}\right)$ feet be denoted by the ordinates. Then if OM is the total value of $\frac{E}{W}$ at the beginning of the test, it is clear that if there were no train resistance, this value would remain constant ever after, as shown by the line MN. Now plotting the profile of the railway on the same diagram, as shown by the line $OABCD$, the distance of the points on this line above the axis OX give the values of H in the above equation, and the vertical distances between $OABCD$

[3] Professor of mathematics, Colorado School of Mines, Golden, Colo.

[4] Electrical engineer, The Reading Company, Philadelphia, Pa.

and the line OM are then equal to $\frac{v^2}{2g}$. From this the velocity may be obtained at any point. The quantity $\frac{E}{W}$ in Equation [2] has the dimension of a length, and may be referred to as the "total head," from analogy with hydraulics. Now actually there is a dissipation of energy due to the train resistance, so that the

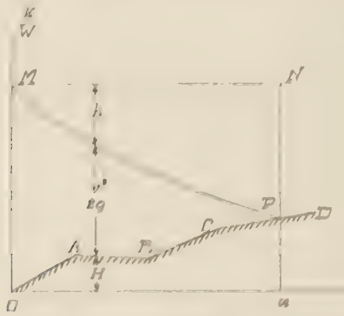

Fig. 2

line MN is lowered to some such position as MP. This line may be obtained by observing the speed at marked points on the route of the test, and plotting the value $\frac{v^2}{2g}$ above the line of the profile $OABCD$ on the diagram. It is then obvious that length NP gives a measure of the work done in overcoming train resistance while the train travels from O to P. Symbolically, if we denote the ordinates of the curve MP by h, and the elevation of the track above the datum line OX by H, we have for the work done against the train resistance

$$\frac{1}{W}\int R dx = OM - h = OM - \left[\frac{v^2}{2g} + H\right] \ldots\ldots [3]$$

We can thus, by differentiating the curve MP, get a value of the total resistance R at each point, and to this corresponds an observed value of the speed. The train resistance at each speed is therefore completely determined.

Since the performance curves shown in Figs. 1 to 3 in Dr. Eksergian's paper are based on the wind-tunnel tests of train resistance, they also must be regarded as contingent on revision of the train-resistance values.

The author's remarks on the low power requirements of light-weight trains are more significant than appears from the horsepower requirements alone when oil-electric motive power is involved. The limitations of the Diesel engine are the piston speed and the mean effective pressure in the cylinder. The latter of course is a function of the cylinder volume, to the extent that the engine cannot burn more fuel than the air in the cylinder requires for complete combustion. Leaving supercharging out of consideration, we may assume that each pound of fuel requires about 14.6 pounds of free air for its complete combustion, and in that case the horsepower developed by the engine is proportional to the piston area and to the piston speed of the engine. If H is the Btu content of the fuel per pound, and if 1 lb of free air weighs 0.0727 lb, we get for the output of the engine

$$\text{bhp} = \frac{Av}{n}\,\frac{0.0727 \times 778\,H}{14.6 \times 33000}\,K \qquad [4]$$

where A is the piston area in sq ft, v is the piston speed in ft per min, and n is the number of strokes per cycle. The constant K for modern engines is usually between 0.13 and 0.16, and it may be increased to 0.20 by supercharging. The piston speed v is usually between 1000 and 1800 ft per min. To see the variation in the size and weight of oil-electric sets for railway service, we may use Equation [4] in a hypothetical line of engines, as shown in the writer's Table 1. It is seen that as the engine size increases

TABLE 1

(Output of Diesel Generating Sets—2-Stroke Cycle)

Diam × stroke	Piston speed, ft/min	No. cylinders	Bhp (K = 0.16)	Rpm	Relative generator weight per kw%
4 × 4	1500	6	190	2250	100
5 × 5	1500	6	300	1800	125
6 × 6	1500	6	430	1500	150
8 × 8	1500	6	760	1125	200
10 × 10	1500	6	1200	900	250

the speed of revolution decreases. This has a very adverse effect on the size of the electric generator. It may easily be shown that the output of an electrical machine is proportional to D^2L, where D is the diameter of the frame and L the length. The output is also proportional to the angular velocity of the machine. Assuming the same proportional constant in all cases in the table, the last column shows how the weight of the electric generator per kilowatt increases as the size of the engine increases. The weight per brake horsepower of a large Diesel engine is also greater than that of a small engine, so that the net weight per horsepower of large-cylinder-capacity oil-electric sets is considerably greater than that of small sets. It is therefore desirable to use generating equipment of as small a capacity as possible. The implication of this is that if a service requires a given horsepower per ton of total train weight, as shown in Dr. Eksergian's Fig. 4, the total horsepower required by the train must be as small as we can make it, if a reasonable overall-weight efficiency is to result. The economical use of Diesel-electric power in important passenger service, therefore, compels the railway engineer to use equipment of as low a weight as possible, and it seems that the best field for the Diesel-electric drive in main line service is in light-weight trains of the *Zephyr* type.

An attempt to duplicate the performance of the *Zephyr* with heavy conventional equipment, using oil-electric drive, leads to extravagant sizes and weights of motive power.

Author's Closure

Mr. Larson's criticism is constructive and well received because his analysis really points out that in discussing torsional conditions through an opening, it is necessary to differentiate the loading conditions due to centrifugal inertia rolling moments which result in augmented torsional loadings under operating conditions, and extreme jacking loadings with a light car body. In the former, the end couples act as balancing moments for a distributed inertia moment along the car, while in the latter under extreme jacking conditions, with supports at the ends diagonally opposite, we have the condition of equal and opposite balancing couples at the ends of the cars. (Along with the distributed inertia rolling moment we also have distributed lateral forces, equal to the centrifugal loadings, reduced to the floor plane and balanced by lateral reactions at the center pins.) The author's discussion was primarily postulated on the former condition because it represented augmented torsional loadings which would superimpose on the loadings previously discussed in the paper, and based on maximum operating loading conditions. Mr. Larson's analysis pertains strictly only to extreme jacking conditions, and should be classified in a separate analysis since much higher stresses would be permissible. On the basis of the author's postulation of augmented operating loadings, the distributed inertia rolling moments increase the loadings on one main side frame and decrease the loadings on the other main side frame over and above the normal vertical loadings. From the point of view of equilibrium conditions alone, such augmented loadings

can be balanced entirely by vertical supports at the ends of the main side frames and no resultant longitudinal-shear forces at top and bottom of main side frames are needed since no balancing couple is then required for equilibrium of a side frame. If, therefore, reacting longitudinal-shear forces do not act on the roof, transverse-shear forces would likewise not necessarily exist in the roof or floor system. However, the ability to transmit lateral-shear forces to the roof and floor across an opening is very much dependent on the relative rigidity of the bulkheads adjacent to the opening. As an extreme case, without any partitions whatsoever, only the augmented vertical loadings and the corresponding total bending moment are maintained across the openings, such up and down reactions on either side of opening being the resisting torsional moment for the particular section at which the step well is located.

Obviously under the dynamic torsional loading postulated by the author, the torsional shear varies for different sections of the car body in a manner similar to a beam with distributed gravity loadings and balancing supporting reactions at the ends. Now in a car body, openings near the ends are subjected to drastic vertical-shear loadings resulting in high secondary bending stress. For this reason augmented torsional-shear loadings which may induce additional bending stresses become of considerable importance. With a uniform lateral centrifugal loading inducing a corresponding distributed rolling moment, it is seen that the torsional shear would coincide with the vertical-shear loading at any section of the car. For this reason the dynamic roll loading may assume considerable importance for openings toward the ends subjected to heavy vertical-shear loading and therefore to correspondingly large torsional-shear loadings, augmenting the vertical-shear loadings.

On the other hand for openings near the center of the car, though vertical-shear loadings and corresponding dynamic torsional-shear loadings are greatly decreased, ample reinforcement of the roof structure is still of major importance due to secondary bending under operating conditions, and to the extreme jacking conditions, resulting in transverse-shear forces through the roof under light load static conditions.

For the case of extreme jacking, with equal and opposite end couples, Mr. Larson presents an analysis as a proof that lateral-shear forces equal to the vertical-shear forces in side frames, are induced in the roof and floor. His analysis, however, actually postulates rigid bulkheads at the ends of the car, which may only partly exist, and also a uniform distribution of longitudinal shear which may far from exist in an actual car construction. It is, of course, true that with equal and opposite couples applied at the ends, as under the extreme jacking conditions assumed, transverse-shear forces are induced in both roof and floor system in any actual car construction. However, the magnitude and distribution of such forces at different sections of the car body depend upon the distribution and the yield of the bulkheads as well as the cross-framing of the car.

In the *Zephyr* construction, the end cross frames are relatively rigid, so that the assumption of rigid end bulkheads is permissible. For a first approximation, the author is in agreement with Mr. Larson's recommendation that without any adjacent bulkheads at the opening, and with a symmetrical car, the moment resulting from extreme eccentric jacking conditions is resisted equally by a transverse couple for roof-and-floor system and a couple with up-and-down reactions exerted on the side frames.

In the analysis of a highly redundant structure as a car body, the criterion of the equilibrium of a system of reactions acting on several portions of the structure is not sufficient to determine their distribution. The distribution is effected by the relative yields of the various elastic members. It is always possible for non-statical systems to have various combinations of equilibrating systems, where the transfer between parts is effected by the action and reaction between any two portions of the structure. In fact the condition equations of a redundant system are necessarily supplied by the equilibrium conditions for each and every portion of the structure, together with the mutual reactions between the parts. The particular distribution of the equilibrating system, however, is dependent on the relative deformation of the various members due to their elastic properties. On the basis of equal and opposite torsional moments applied at the ends of the car, it is evident that every cross-section of the car must sustain a mutual torsional-shear moment between the parts. However, the distribution of the shearing forces which make up the resultant resisting couple at the section is dependent on the elastic yield of the structure on either side of the opening. Mr. Larson does not specify the elastic properties of his system; only the balancing system of reactions, he assumes, postulates the elastic system considered and, therefore, the effectiveness of end bulkheads in transferring a lateral-shear couple to the roof and floor equal to the vertical-shear couple in the side frames.

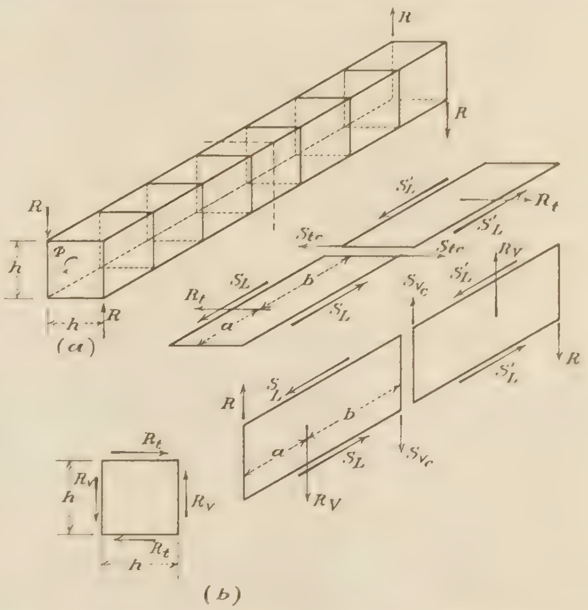

FIG. 3 SYMMETRICAL CAR WITHOUT END BULKHEADS SUBJECTED TO EQUAL AND OPPOSITE END BALANCING COUPLES

There arises the important question as to the effectiveness of partial end bulkheads as compared with rigid bulkheads in transferring transverse shear to a roof-and-floor system in extreme jacking conditions. Without end bulkheads, the following approximate analysis is of interest in showing that the maximum lateral-shear force in a roof-and-floor system may exceed values postulated on the rigidity of end bulkheads.

Case 1. Symmetrical Car Without End Bulkheads Subjected to Equal and Opposite Couples at Ends as in Extreme Jacking Conditions. Referring to Fig. 3*a*, we assume a symmetrical car with end balancing couples $\Phi = Rh$. For simplicity the car cross-section is assumed square with the common dimension, h. Let mn be the mid-section, which sustains a vertical shear S_{vc} in the side walls, and a transverse shear S_{tc} in the roof. We will assume the torque transferred to the roof by light bulkheads consisting simply of frame bents at panel points, i.e., posts, carlines, and cross-floor beam. Let the resultant reactions of these cross frames on the side frame be R_v on either side of the mid-section at distance b from the mid-section "a" and a distance a from ends as shown in

Fig. 3b. Evidently $S_{vc} = R - R_v$ for the vertical shear at the mid-section.

To obtain the longitudinal shear S_L or S'_L, observing that due to symmetry no bending noment exists at center section, we have

$$S_L h = R_v a + S_v(a + b) = R(a + b) - R_v b$$

now for the equilibrium conditions of the cross-frame bents, we have $R_v h = R_t h$, so that the resultant transverse reaction on the roof equals the vertical reaction on the side frame, and this

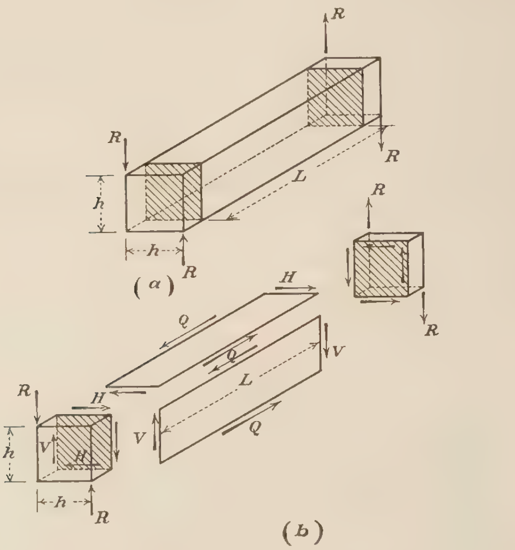

Fig. 4 Rigid Bulkhead With a Couple That Is Balanced by a Couple Caused by Side-Frame and Roof Reaction

equals the transverse shear in the roof $S_{t_c} = R_t = R_v$. But for equilibrium of the roof, $R_t b = S_L h$, so that since $R_t = R_v$, then, $R_v b = R(a + b) - R_v b$, and since $S_{t_c} = R_t = R_v, S_{t_c} = R\left(\frac{a+b}{2b}\right)$ and $S_{v_c} = R\left(\frac{b-a}{2b}\right)$.

It is evident that the values of the transverse- and vertical-shear forces depend upon the relative values of a and b which in turn depend upon the relative flexibilities and distribution of the bulkhead systems in general. Thus with rigid heavy end bulkheads, $a = 0$, and $b = L/2$ so that $S_{tc} = S_{vc} = R/2$.

If, on the other hand, the bulkheads were so distributed elastically that $a = b$, then $S_{tc} = R$ and $S_{vc} = 0$.

It is to be noted that the structure itself is assumed to be a symmetrical plated walled structure with symmetrical distribution of bulkheads. The action of a trussed system is different and is considered later.

Case 2. With Rigid End Bulkheads. As another extreme we will consider the case postulated by Mr. Larson's analysis for rigid end bulkheads. In this case, Fig. 4, the rigid bulkhead has a couple $Rh = \Phi$, which is balanced by a couple $Vh + Hh$, due to side frame and roof reaction. For equilibrium of side frame $VL = Qh$ and for the roof $Qh = HL$, so that $H = V$. This is based on the premise that the rigidity of cross frames is small compared with end bulkhead and the frame and roof are reasonably symmetrical. Since $Hh = Vh$, evidently H which also is the transverse shear for any section of the roof, is $\Phi/2h = R/2$.

Thus, on the premise of rigid end bulkheads, the transverse shear in the roof is reduced to one-half the end reaction R and the transverse shear in the roof equals the vertical shear in the side frame.

Distribution of Torsional Shear in Truss Space Framework. In order to show more clearly the effect of the elasticity of the system on the distribution of the lateral-shear forces, the simple frame structure shown in Fig. 5 has been analyzed. Three cases have been considered: (a) with rigid end bulkheads, (b) with the forward end bulkhead having a diagonal with the same rigidity as the diagonals in subsequent cross-panel frames, and (c) with light diagonals in both forward and intermediate cross frames with a rigid bulkhead at the back end. Evidently the transverse and vertical shear for top and bottom and the side frames correspond to the components of the diagonal tensions in these directions.

(a) Truss space framework with rigid end bulkheads. If Φ is the total torque transmitted, Vb is the reacting couple on the rigid bulkhead due to the vertical force V, and Hh is the reacting couple on the rigid bulkhead due to the lateral forces H, then the total torque requires the condition:

$$Hh + Vb = \Phi \text{ (equilibrium of rigid bulkhead)}$$

We may therefore choose either H or V as redundant. In addition we select the tensions in the diagonals of the truss bulkheads

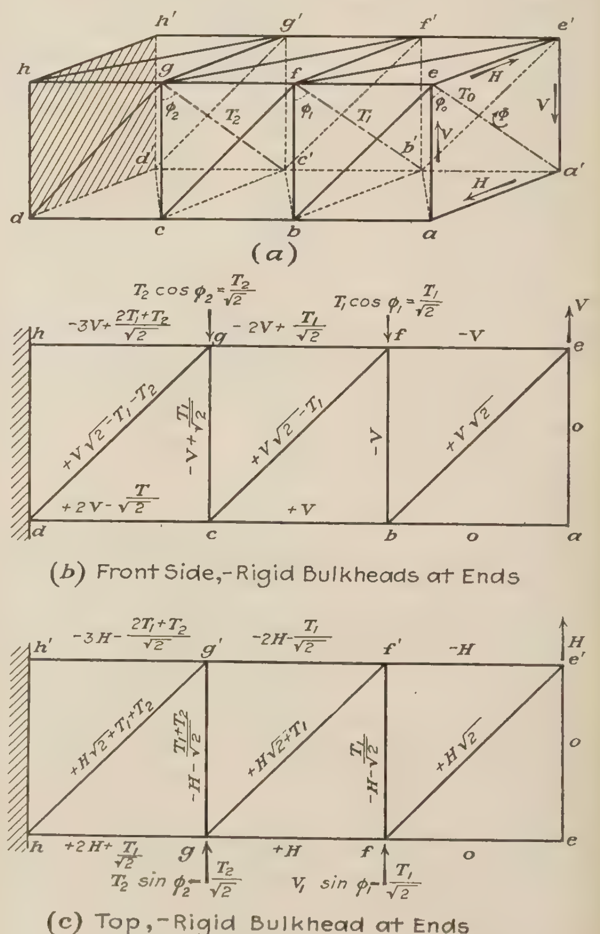

Fig. 5 Distribution of Torsional Shear in Truss Space Framework

as tension redundant reactions. The system is indeterminate to the third degree. The redundants are H, T_1, and T_2. Evidently $V = \frac{\Phi - Hh}{L}$ (lb). Assume the diagonals in the bulkheads make angles ϕ_1 and ϕ_2 with respect to the vertical. Then the loadings

on the left vertical side frame are V, $T_1 \cos \phi_1$ and $T_2 \cos \phi_2$. For the top horizontal side frame, the loadings are H, $T_1 \sin \phi_1$ and $T_2 \sin \phi_2$. In like manner we have a similar loading system for the right and bottom side frames.

Considering now the rear end bulkhead, the reactions of the vertical side frames are

$$V' = V - T_1 \cos \phi_1 - T_2 \cos \phi_2$$

and for top and bottom frame

$$H' = H + T_1 \sin \phi_1 + T_2 \sin \phi_2$$

The couple on the rear bulkhead is

$$\Phi' = V'b + H'h = Vb + Hh = \Phi$$

since $h \sin \phi - b \cos \phi = 0$ at any intermediate bulkhead, thus giving an equilibrium check.

It is to be noted that the distribution for the component couples due to vertical- and horizontal-shear forces are definitely different. In other words they are affected by the relative rigidity of the intermediate truss bulkheads.

For a solution of this system, we have the loading conditions for each side truss. Evidently the total stress in any member has the form

$$T = \alpha\Phi + \beta H + \gamma T_1 + \mu T_2$$

where H, T_1, and T_2 are the redundant forces. Therefore, equating the differential coefficients of the elastic energy $\Sigma \frac{T^2 l}{2EA}$ with respect to each of the redundants to zero, we have

$$\Sigma\,(\alpha\Phi + \beta H + \gamma T_1 + \mu T_2)\,\beta\,\frac{l}{A} = 0$$

$$\Sigma\,(\alpha\Phi + \beta H + \gamma T_1 + \mu T_2)\,\gamma\,\frac{l}{A} = 0$$

$$\Sigma\,(\alpha\Phi + \beta H + \gamma T_1 + \mu T_2)\,\mu\,\frac{l}{A} = 0$$

from which we can solve for H, T_1, and T_2 in terms of the applied moment, and V from the relation $Vb = \Phi - Hh$. On the basis of equal cross-sectional areas for truss members and diagonals in intermediate cross frames, and assuming square panels, i.e., $h = b$, we have

$$\begin{aligned} 187.94H + 74.69T_1 + 25.68T_2 &= 93.97\,\Phi/h \\ 74.69H + 38.23T_1 + 14.16T_2 &= 36.99\,\Phi/h \\ 25.68H + 14.16T_1 + 11.57T_2 &= 12.49\,\Phi/h \end{aligned}$$

hence $H = 0.5149\,\Phi/h \quad T_1 = -0.027\,\Phi/h$
$V = 0.4851\,\Phi/h \quad T_2 = -0.0305\,\Phi/h$

(*b*) With tension diagonal bulkheads of same rigidity as truss frames, considering rigid bulkhead only at rear end. In this case we have no rigid forward bulkhead, the forward bulkhead being replaced by a diagonal brace. The tension T_0 in this diagonal replaces the redundant reaction H in the previous analysis. The redundants are now T_0, T_1, and T_2, the redundant tensions in the diagonals of the cross-frames.

On the basis of equal cross-sections for all members, we have

$$\begin{aligned} 96.88T_0 + 52.81T_1 + 18.16T_2 &= 66.45\,\Phi/h \\ 52.81T_0 + 38.23T_1 + 14.16T_2 &= 36.99\,\Phi/h \\ 18.16T_0 + 14.16T_1 + 11.57T_2 &= 12.49\,\Phi/h \end{aligned}$$

so that

$$T_0 = 0.638\,\Phi/h,\ T_1 = 0.104\,\Phi/h,\ T_2 = -0.050\,\Phi/h$$

(*c*) Assuming flexible bulkheads, with tension members in cross-frames having one quarter the cross-sectional area of main members in truss frames. In this case we arrive at the equations:

$$\begin{aligned} 101.13T_0 + 52.81T_1 + 18.16T_2 &= 66.45\,\Phi/h \\ 52.81T_0 + 42.47T_1 + 14.16T_2 &= 36.99\,\Phi/h \\ 18.16T_0 + 14.16T_1 + 15.81T_2 &= 12.49\,\Phi/h \end{aligned}$$

so that

$$T_0 = 0.577\,\Phi/h,\ T_1 = 0.158\,\Phi/h,\ T_2 = -0.015\,\Phi/h$$

For the conditions in (*a*), the stresses in the side-frame diagonals and stresses in the top- and bottom-frame diagonals are listed in Table 2. The vertical- and transverse-shear components were similarly estimated for conditions (*b*) and (*c*).

TABLE 2 STRESSES IN MEMBERS AND DISTRIBUTION OF SHEAR IN PANELS FOR CONDITION (*a*)

Stresses in side-frame diagonals:

Member	Tension	Vertical Shear Comp.
be	$V\sqrt{2} = 0.686\,\Phi/h$	$V\frac{\sqrt{2}}{\sqrt{2}} = 0.4851\,\Phi/h$
cf	$(V\sqrt{2} - T_1) = 0.713\Phi/h$	$(V\sqrt{2} - T_1)\,\frac{1}{\sqrt{2}} = 0.5043\,\Phi/h$
dg	$(V\sqrt{2} - T_1 - T_2) = 0.744\,\Phi/h$	$(V\sqrt{2} - T_1 - T_2)\,\frac{1}{\sqrt{2}} = 0.5258\,\Phi/h$

Stresses in Top- and Bottom-Frame Diagonals:

Member	Tension	Transverse Shear Comp.
fe'	$H\sqrt{2} = 0.728\,\Phi/h$	$H\frac{\sqrt{2}}{\sqrt{2}} = 0.5149\,\Phi/h$
gf'	$(H\sqrt{2} + T_1) = 0.701\,\Phi/h$	$(H\sqrt{2} + T_1)\,\frac{1}{\sqrt{2}} = 0.4957\,\Phi/h$
hg'	$(H\sqrt{2} + T_1 + T_2) = 0.670\,\Phi/h$	$(H\sqrt{2} + T_1 + T_2)\,\frac{1}{\sqrt{2}} = 0.4742\Phi/h$

The values of the transverse- and vertical-shear components in bays I, II, and III are given in Table 3.

TABLE 3 VALUES OF TRANSVERSE- AND VERTICAL-SHEAR COMPONENTS IN BAYS I, II, AND III

Bay	Rigid end bulkhead	Bulkhead with diagonal	Bulkheads with light diagonals (A/A)
Transverse shear in the roof:			
I	0.5149 R[a]	0.4514 R	0.4080 R
II	0.4957 R	0.5252 R	0.5200 R
III	0.4742 R	0.4896 R	0.5095 R
Vertical shear in side frame:			
I	0.4851 R	0.5486 R	0.5920 R
II	0.5043 R	0.4748 R	0.4800 R
III	0.5258 R	0.5104 R	0.4905 R

[a] $R = \Phi/h$.

From this we note that as the end bulkheads become more flexible the transverse shear is reduced in the end bay but, even with relative flexible end bulkheads due to the greater distortion at the ends, they are very effective in equalizing the torsional-shear distribution in roof and floor system and side frames.

It is also of interest to note that intermediate bulkheads are not subjected to heavy loadings as indicated by the relative small values of the cross-frame tension diagonals T_1 and T_2 for all three cases.

On the other hand to transmit torsional-shear stresses through openings under operating conditions with heavy inertia rolling moments, relative rigid bulkheads adjacent to the openings are effective in inducing lateral-shear forces in the roof and floor system and thereby providing a better torsional-shear distribution. The relative magnitudes of this distribution are obviously greatly dependent on the relative flexibilities in the transverse and vertical directions through the opening.

Mr. Wright's discussion is also most interesting and valuable. He raises the question of the validity of premising the train-resistance component due to air resistance on the basis of wind-tunnel experiments on models mentioned in the paper. On similarity tests with models and full-scaled trains let P' and P be the total resistance of model and the air-resistance component for a full-size train.

From dimensional analysis,

$P' = k\rho' v'^2 A' f'(R')$ for model

$P = k\rho v^2 A f(R)$ for large-size train

where k is numeric, consistent for units used, ρ is the mass density, v is the velocity, A is the cross-section of train, and

$R = \frac{\rho v L}{\mu}$ the Reynolds number, a non-dimensional parameter.

If we write the drag coefficient in the form $P = D_e A v^2$ then

$D_e' = k\rho' f'(R')$ for the model

$D_e = k\rho f(R)$ for the large-size train.

Since $\rho' = \rho$, approximately, evidently the condition for no scaling up from the model to full-size train, requires equality of the drag coefficients, so that

$$f'(R') = f(R)$$

Let us first assume that $\frac{P}{k\rho v^2 A} = f(R)$ has the same function for both the model in the wind tunnel and for the full-size train. Then the condition for equal drags reduces to $f(R') = f(R)$. Now for the full-size train, even assuming considerable speeding up of the velocity v' in the wind tunnel, $R = \frac{\rho v L}{\mu}$ is still greater than $R' = \frac{\rho v' L'}{\mu'}$ for the model. But in the range of turbulent motion considered which in both cases is considerably above the critical velocity, the function $f(R)$ is practically constant so that $f(R)$ can be assumed practically equal to $f(R')$ of the model, even though $R > R'$.

Actually it would be anticipated that the function of the Reynolds number, $\frac{P}{k\rho v^2 A} = f(R)$ to decrease somewhat with increasing Reynolds numbers. Therefore since R is inherently greater than R', the drag coefficient for the full-size train should be somewhat less than for the model. Actually it has been found that a positive scaling up is necessary.

This would indicate that in scaling up the drag coefficient, the $f'(R)$ is not the same as $f(R)$ for the full-size train, $f(R)$ in general being greater than $f'(R)$ for the model. This would be anticipated inasmuch as the boundary disturbing effect at the rail is different from that in a wind tunnel even with a dividing plane in an image duplication of the model.

Mr. Wright also raises the question that the scale effect in a wind-tunnel experiment may be different for conventional and streamlined trains due to the fact that the air flow is different; also that the scaling may be seriously affected by non-uniformity and disturbances of air flow in a long model in a wind tunnel. This conclusion seems reasonable and further points to the fact that the Reynolds function may be appreciably different for these cases as well.

On the other hand from a practical point of view, on the basis of the Davis formula modified for drag coefficients for air resistance obtained from the Massachusetts Institute of Technology wind-tunnel tests, test results for balance speeds of the *Zephyr* indicate a remarkable consistency. In the author's paper, the drag coefficient was scaled up by 20 per cent in the correction for the air-resistance component in the Davis formula. At 4.3 hp per ton computed balance speeds indicated a top speed of 96 mph. Actual top speeds of the *Zephyr* were somewhat over 100 mph and test results indicated that actually very little scaling up of the drag coefficient was necessary. For these reasons the author is convinced that reasonably satisfactory drag coefficients can be obtained from wind-tunnel tests, particularly for short trains with small modification in drag coefficients.

Mr. Wright suggests simple coasting retardation tests for obtaining train resistance on the basis of accurate speedometer data and a profile of the road. He introduces an ingenious graphical method which has the advantage of materially aiding in the faring of the plotting data by resolving the energy components in terms of heads. The gradient of the curve MP corresponds to the resistance at any point.

From the energy equation

$$d\left[\frac{kW}{2g}v^2 + WH\right] = -R dx, \text{ where } dH = dx \sin \alpha$$

we have, between any two points,

$$\left[H_2 + \frac{kv_2^2}{2g}\right] - \left[H_1 + \frac{kv_1^2}{2g}\right] = -\frac{1}{W}\int_1^2 R dx \ldots [5]$$

Instead of plotting the curve,

$$\frac{kv_0^2}{2g} - \left[H + \frac{kv^2}{2g}\right] = \frac{1}{W}\int_0^x R dx \ldots\ldots\ldots [6]$$

and differentiating with respect to x for the train resistance, perhaps a closer approximation would be obtained by directly plotting the velocity curve and below it the profile curve. Then for any two adjacent points 1 and 2 along the curves, we can write either Equation [5] or [6] in the form

$$k\left(\frac{v_1^2 - v_2^2}{2g}\right) - (H_2 - H_1) = \frac{R}{W}(x_2 - x_1)$$

or

$$\frac{k}{g}\left(\frac{v_2 + v_1}{2}\right)(v_1 - v_2) - (H_2 - H_1) = \frac{R}{W}(x_2 - x_1)$$

where the interval $x_2 - x_1$ is taken sufficiently small to assume R constant.

Allowable Working Stresses Under Impact[1]

Author's Closure

In a criticism of the author's paper, E. Dillon Smith states that the "raising factor" of the yield point or ultimate strength under impact cannot always be the same and that it depends on the velocity of impact, the inertia of the beams, and its natural period. The illustration of the idea given by the author at the end of this article will show that in some cases the dynamic force may produce a greater deflection and consequently a greater stress than the static one.

The author fears that Mr. Smith does not make enough distinction between two different things namely, (1) the relation between the dynamical and statical yield point and tensile strength and (2) the relation between the statical and dynamical external

[1]By N. N. Davidenkoff, Head of the Mechanical Department of the Physico-Technical Institute in Leningrad, U.S.S.R. Published with discussion in A.S.M.E. Trans., March, 1934, vol. 56, no. 3, paper APM-56-1.

forces, revealing the same stresses in the specimen. The data given by the author in Tables 1 and 2 do not relate to the method of calculation of dynamical stresses, but only assume that this method of calculation is correct. In cases similar to those cited by Mr. Smith, as when an elastic impact is being produced by a light hammer against a heavy beam, the inertia of the beam cannot be neglected when calculating the stress. If we take into account this inertia and observe that the beam is deflected, not only by the pressure of the hammer, but also by its own inertia forces, then there will be no discrepancy between the deflection and the actual force. The author however, wishes to assure Mr. Smith that the values given in Tables 1 and 2 have been obtained from tests of small specimens in longitudinal tension or compression using sufficiently large hammers. In this case the inertia forces of the specimen can be completely neglected, especially due to the long duration of non-elastic impact and the high natural frequency of the longitudinal oscillations of the specimen. In this manner the measurement of the impact stresses was reduced to the simple measurement of the impact pressure of the hammer.

The question of the influence of the impact rate or rather the rate of increase of the impact stresses on the value of the "raising factors" will now be considered. There is no doubt that this influence exists. Up to now, however, all attempts which have been made to investigate this influence have led either to doubtful results[2] which could be explained by the conditions of the experiment or a negative[3] answer. R. Plank[4] gives some data stating the following dependence of dynamic tensile strength σ on the velocity v.

$$\sigma = \frac{a\ v}{v + b}$$

where a and b are constants. Owing to the peculiarity of these data the author did not dwell on them in his paper.

Mr. Smith objects to the connection of the upper and lower branches of the curve Fig. 8. In admitting this operation for Fig. 7, he must accept it for Fig. 8, which represents a picture of the same physical phenomenon, but only more definitely pronounced. Moreover, some of the values in Fig. 8 tend to approach the connecting curve.

Mr. Smith does not seem to agree with the author as to the difficulty of accurately double differentiating curves. With small-scale diagrams this difficulty will undoubtedly exist and the best proof of this is the discrepancy which exists between diagrams obtained by different investigators[5,6] under similar conditions. In the proper choice of equations for the curves to be differentiated, apart from the tediousness of the process, there is the risk of smoothing out imperceptible deviations which under double differentiation will grow into considerable waves. See for instance Mr. Smith's diagram, Fig. 11.

As to the use of piezo quartz, the author does not understand why Mr. Smith neglects the possibility of safeguarding the quartz crystal from rupture during the experiment by keeping the proper relation between the size of the crystal and specimen.

The author is greatly obliged to Mr. Smith for the detailed account of the principles of the piezo-quartz method on which the author did not dwell in his paper. Mr. Smith, however, suspects that the photographs given in the paper are not those given by a cathode-ray oscillograph. From the explanation given of Fig. 3, Mr. Smith might have seen that the cathode rays get two mutually normal deviations, the latter of which is created by the magnetic field for the special purpose of developing a picture without using a moving film.

Finally it might have been better if the author had given a description of the calibration of the piezo quartz which was done by a simple static loading. This omission may have given rise to the suspicion that a more complicated method was used.

The author is greatly interested in the work of Prof. R. V. Southwell, which shows how careful one must be in respect to the value of the so-called "mean impact force" computed as the quotient of the energy of fracture and the deformation of the specimen. It is obvious that under ordinary test conditions we will always obtain an exaggerated meaning of the impact force.

In connection with Figs. 7 and 8, Messrs. Mason and Stone mention the phenomenon of "blue-heat brittleness" whereas the phenomenon is displayed under impact at higher temperatures namely, above 500 C and the phenomenon shown in Figs. 7 and 8 should be called "cold brittleness," and is of quite a different physical nature.

[2] Proc. Intern. Assoc. of Testing Materials, 1912, no. 9.
[3] Charpy a Cornu Thenard., *Jour. of Iron & Steel Inst.*, vol. 96, 1917, p. 61.
[4] *Zeit. V.D.I.*, vol. 56, 1912, p. 17.
[5] Mitt. K-W. Instit. f. Eisenfor., vol. 7, 1925, p. 81.
[6] *Deutsch. Ver. f. Materialpr.*, 1927, no. 78.

Effects of Side Leakage in 120-Degree Centrally Supported Journal Bearings[1]

Mayo D. Hersey.[2] The author brings out the point that the side-leakage effect depends not only on the bearing design, but also upon the load carried. Since, however, the side-leakage effect is expressed as a simple ratio, it would seem probable that the situation might be more completely and exactly described by saying that the side-leakage ratio depends also on the dimensionless generalized variable G, more commonly known as ZN/P, and which, in the author's notation, is written as $\mu N/p_0$.

The author has presented two side-leakage factors or ratios, one being the ratio of the frictional resistance of the actual bearing to that of an ideal bearing without side leakage; the other the corresponding ratio of load capacities. The writer's previous statement regarding G has reference only to the friction ratio. It is not clear to him what is meant by saying that the other ratio, the ratio of load capacities, depends on the load. It is suggested, however, that the side-leakage factor for load capacity depends not only on the bearing design, but also on the product of the viscosity μ by the speed N, and might be so represented on a diagram.

Another point which is not yet clear to the writer is how it comes to pass that the Sommerfeld variable $G\left(\frac{a}{\eta}\right)^2$ remains intact in the side-leakage problem, as shown by Fig. 13 in the article under discussion. When this variable was introduced by Sommerfeld in 1904, it resulted from a detailed integration, valid only for the ideal bearing free from side leakage.

If the paper presented by Mr. Needs contains a mathematical proof that this simple result may be derived from Reynolds' equations, as I believe it probably does, it would seem well worth while to segregate this proposition from the rest of the paper. Otherwise, it might be construed that the proposition has been tacitly assumed in the very beginning.

Some remarks might be offered concerning the methods of graphical representation selected by Mr. Needs. It is natural that he should lean toward the viewpoint of the machine de-

[1] Published as paper APM-56-16, by S. J. Needs, in the October, 1934, issue of the A.S.M.E. Transactions.
[2] Division of Engineering, Brown University, Providence, R. I. Mem. A.S.M.E.

signer as contrasted with that of the operating or lubrication engineer. Consequently, most of his results are presented in terms of the more intangible factors such as the eccentricity ratio c. A welcome exception is found in Figs. 13 and 13a of the author's paper. Here the Sommerfeld variable has been selected for the independent variable, or abscissa, in the coefficient of friction diagram. Would it be possible to give a similar diagram for the eccentricity ratio, or better still, for the relative film thickness, h_0/η?

Referring to Fig. 10 in the author's paper, it seems paradoxical that the friction ratio decreases as the bearing becomes narrower and side leakage worse. The explanation lies in the fact that the curves shown are for equal eccentricities. But in actual practice, if we compare a collection of bearings, all having the same clearance-diameter ratio, and all being tested under the same operating conditions, that is, at the same value of G, the eccentricities will not be equal. A curve of this type plotted against the length-width ratio would show an increasing frictional resistance ratio as the bearing is made narrower. Such a curve might be constructed by cross-plotting from the author's Figs. 13 and 13a.

In conclusion it might be asked if the author has compared his results with the approximate solutions of Gümbel, Stodola, Boswall, Karelitz, or Duffing?

R. Baudry.[3] The bearing characteristics given by Mr. Needs have been compared with those obtained by a method of analysis[4] based on data previously presented.

In Fig. 1 are plotted curves from data given by Mr. Howarth and Mr. Needs, which show the characteristics of a 120-deg. bearing of infinite width. The characteristics of the bearing have been given in functions of the characteristic number ZN/P, where Z is the viscosity in centipoises, N is the revolutions per minute, and P is the unit pressure in lb per sq in. The curve for n/r gives the relation between the clearance ratio n/r and ZN/P given eccentricity C.

Similar curves are plotted for the coefficient of friction, oil-film thickness, location of the minimum oil-film thickness, with respect to the time of action of the load (ϕ), and the ratio of the maximum to the minimum oil-film thickness, h_m/h_o. These curves reveal the condition of minimum friction and maximum oil-film thickness as shown by Mr. Kingsbury. It is also clearly seen that for a rather large variation of the clearance ratio, there is only a small change in the coefficient of friction and minimum oil-film thickness.

Boswall, in his book, "The Theory of Film Lubrication," has given some data for the leakage factors of a plane bearing having an $\frac{\text{inlet}}{\text{outlet}}$ oil-film ratio of 2 and 3. These data have been plotted as solid curves in Fig. 2.

In his paper Mr. Needs presented data for the location of the point of negative pressure, which for large eccentricities is located between the point of maximum pressure and the outlet edge. This shows that it is not permissible to assume that the negative pressure begins at the point of nearest approach as many authors have done. In the absence of complete data for the location of this point, we have assumed, in finite bearings, that it is located half way between the outlet edge and the point of nearest approach for the infinitely wide bearing. We obtain in this manner the oil-film ratio of $\frac{\text{length}}{\text{width}}$, from which the broken-

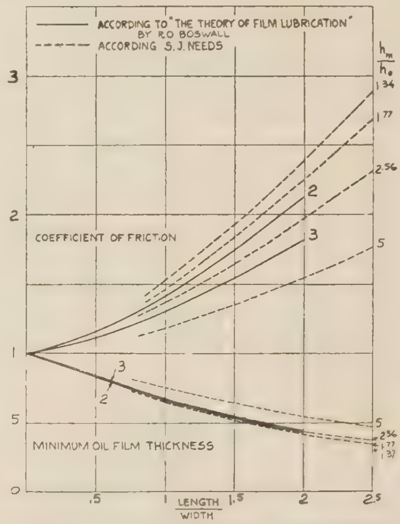

LEAKAGE FACTORS FOR PLANE AND 120° JOURNAL BEARINGS

Fig. 2

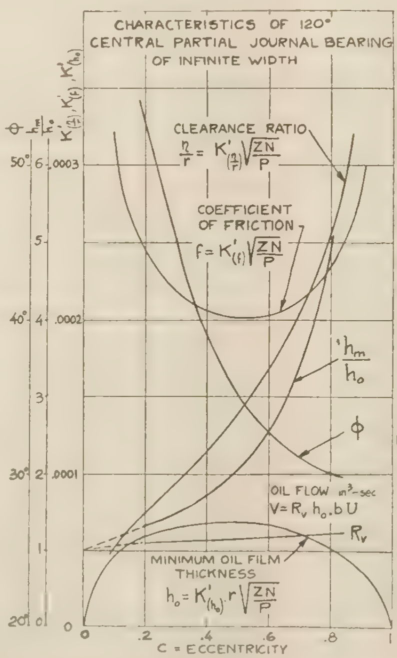

Fig. 1

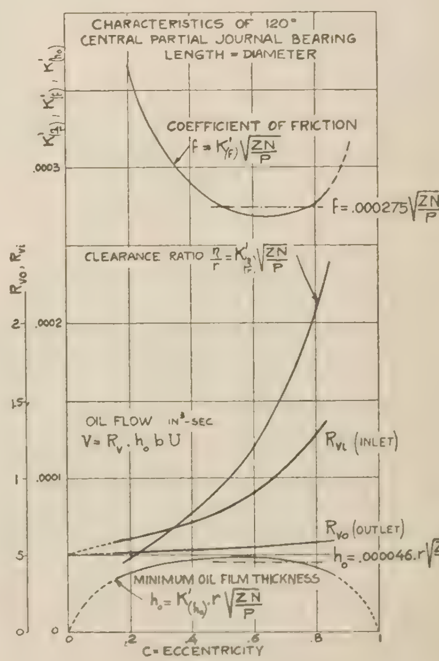

Fig. 3

[3] Westinghouse Electric and Manufacturing Company, East Pittsburgh, Pa.

[4] "Performance of Large Journal Bearings," by R. Baudry and L. M. Tichvinsky, presented at the Annual Meeting, New York, N. Y., December 3 to 7, 1934, of The American Society of Mechanical Engineers.

line curves in Fig. 2 were plotted. These correspond to the different bearing eccentricities calculated by Mr. Needs. It is interesting to note that these curves agree closely with data published by Boswall and interpolated for different values of h_m/h_o.

In Fig. 3 are shown the characteristics of a 120-deg bearing in which the length of the bearing is equal to the diameter of the shaft. It is seen that for a variation of the clearance ratio from less than 0.001 per in. to more than 0.002 per in., the coefficient of friction will vary only plus or minus two per cent of the mean

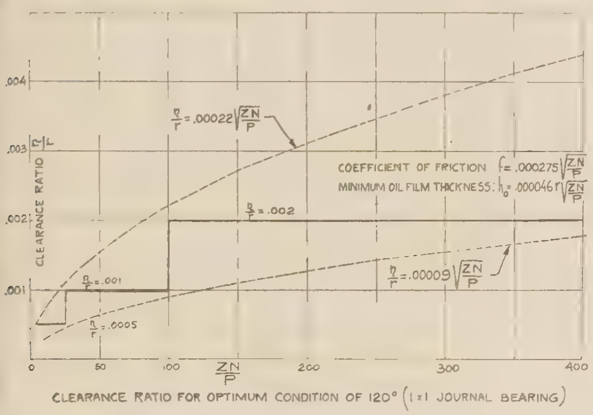

Fig. 4

value shown on the curve. There is also a variation of the same order for the oil-film thickness.

In Fig. 4 is shown the permissible clearance ratio necessary to operate at the optimum condition. It is interesting to note that this corresponds with the clearance used on Westinghouse bearings. For high-speed turbo-generators which operate under values of ZN/P from 100 to 400, a clearance ratio of 0.002 is used. For formerly used slow-speed power bearings, with a 120-deg angle and having a value of ZN/P below 100, a clearance ratio of 0.001 was used. This shows a rather close agreement between theory and practice.

The leakage factors for oil flow published by Boswall also show close agreement with those of Mr. Needs. From this comparison it is seen that the different leakage factors are mainly a function of the $\frac{\text{length}}{\text{width}}$ ratio and h_m/h_o. It seems, as suggested by Mr. Needs, that a single set of curves for leakage factors can be used with a reasonable degree of accuracy for many different types of bearings.

Albert Kingsbury.[5] The paper on "Optimum Conditions in Journal Bearings," to which Mr. Needs refers, contains several assumptions which are known to be not strictly true, but were taken as near enough to the truth to provide for the development of a theory that would be serviceable for practical work.

Among these assumptions are: (1) That the viscosity of the oil during its passage through the film may be taken as a constant value represented by its average value; (2) that the form of the surfaces is definitely known; (3) that the friction per unit width, with given clearance ratio and eccentricity, is the same for narrow bearings as for wide bearings; and (4) that the optimum conditions are obtained with the same eccentricity for both wide and narrow bearings.

The theory is open to improvement in respect to these assumptions. Mr. Needs has investigated the degree of inaccuracy involved in the third and fourth of these assumptions, while still retaining the first two. The results of his work are interesting, and form a valuable extension of the theory.

[5] President, Kingsbury Machine Works, Philadelphia, Pa. Mem. A.S.M.E.

J. R. Connelly.[6] In that part of the paper by Mr. Needs dealing with the selection of dimensions of a proposed bearing, it is implied that wear at starting and stopping in the absence of an oil film is directly proportional to p_0 (the ratio of total load to projected area).

Experimental evidence obtained in the laboratory at Lehigh University using the same journal, lubricant, and bearing metal seems to indicate that variation of the length to diameter ratio results in a variation in the unit pressure at which wear ceases. Also, for certain values of the length to diameter ratio, there seems to be an inverse relation with the unit pressure at which wear ceases.

Should the above condition be found to exist for other metals, journals, and lubricants, then the selection of the dimensions of a bearing must include a consideration of the maximum value of p_0 at which wear ceases.

Author's Closure

The statement referred to by Mr. Hersey, that side-leakage factors depend on bearings loads as well as $\frac{\text{length}}{\text{width}}$ ratios, assumes that the speed, viscosity, and clearance ratio remained constant while the load was varied. Fig. 9 of the paper shows the side-leakage factors to vary with the eccentricity for a given $\frac{\text{length}}{\text{width}}$ ratio. Any change in eccentricity causes a change in the side-leakage factor. Hence, Mr. Hersey's suggestion that the side-leakage factors depend on the speed and viscosity as well as the load, gives a much clearer picture of the situation. Another factor affecting eccentricity is the clearance ratio, which must also be included in the group determining the side-leakage factors.

It may be shown mathematically that the Sommerfeld variable remains intact in the side-leakage problem. If in Reynolds' equation,

$$\frac{\partial}{\partial x}\left(h^3\frac{\partial p}{\partial x}\right)+\frac{\partial}{\partial z}\left(h^3\frac{\partial p}{\partial z}\right)=6\mu U\frac{\partial h}{\partial x} \qquad [1]$$

we write $h = \eta(1 + c\cos\theta)$, $x = a\theta$, $z = a\phi$, and $p = \left[\frac{6\mu Ua}{\eta^2}\right]q$, Equation [1] becomes $\frac{\partial}{\partial\theta}\left[(1 + c\cos\theta)^3\frac{\partial q}{\partial\theta}\right] + \frac{\partial}{\partial\phi}\left[(1 + c\cos\theta)^3\frac{\partial q}{\partial\phi}\right] = -c\sin\theta$. Any solution of this equation is of the form, $q = f'(\theta, \phi, c)$. Hence, any solution of Equation [1] is of the form,

$$p=\left[\frac{6\mu Ua}{\eta^2}\right]f'\left(\frac{x}{a}\ \frac{z}{a}\ c\right)$$

When, for infinite width Equation [1] reduces to

$$\frac{d}{dx}\left(h^3\frac{dp}{dx}\right)=6\mu U\frac{dh}{dx}\ldots\ldots\ldots\ldots\ldots[2]$$

the solution is of the form,

$$p=\left[\frac{6\mu Ua}{\eta^2}\right]f''\left(\frac{x}{a}\ c\right)$$

[6] Instructor, Department of Mechanical Engineering, Lehigh University, Bethlehem, Pa. Jun. A.S.M.E.

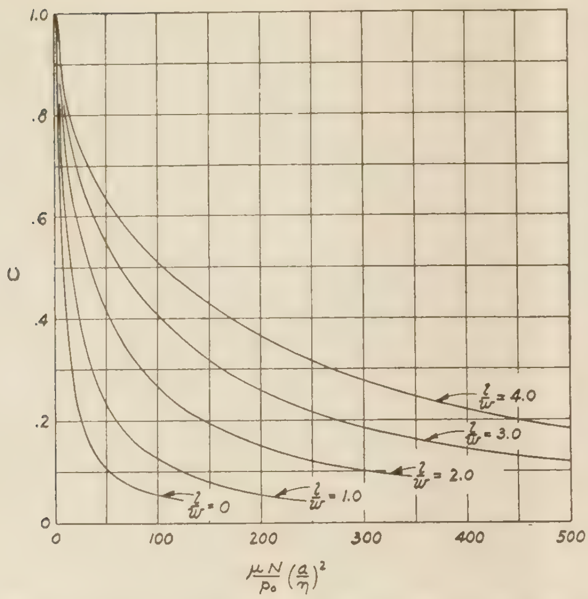

Fig. 5 Variation of Eccentricity With Values of the Sommerfeld Variable From 0 to 500

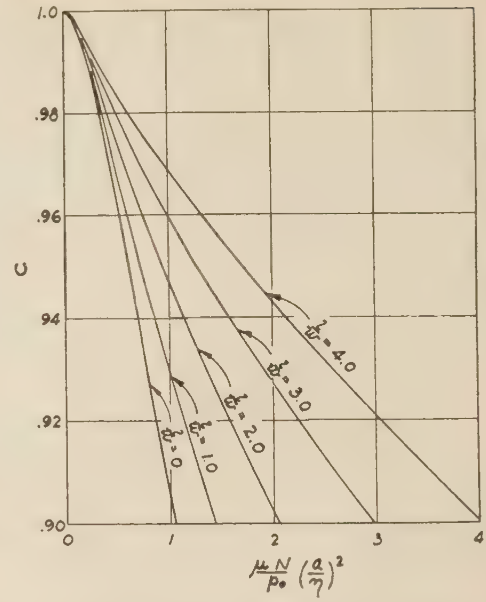

Fig. 6 Variation of Eccentricity With Values of the Sommerfeld Variable From 0 to 4

As far as the absence of η is concerned f, and f are of the desired form. The group coefficients of f, and f_n are identical in the cases of finite and infinite widths, hence, when the Sommerfeld variable is taken as the abscissa, the curve for each $\frac{\text{length}}{\text{width}}$ ratio will be independent of the clearance ratio.

Variation of eccentricity with the Sommerfeld variable is given in Figs. 5 and 6 of this discussion. Since $h_0/\eta = (1 - c)$, the relative film thickness may also be found from these charts.

No comparison of the results of the present paper with the approximate solutions mentioned by Mr. Hersey has been made by the author. Mr. Baudry has made some comparisons of side-leakage factors with data published by Boswall. Comparison with other formulas should prove equally interesting.

Mr. Baudry's curves are of special interest in that they express the thought that the data as presented are not in suitable form for all designers who might care to use them. The results of future research, together with the information now available, will no doubt indicate a more logical and useful method of presentation. Attention should be called to the fact that Mr. Baudry has plotted the values of K' and not the absolute value of the quantities referred to by the curves. This accounts for the peculiar appearance of the h_0 curve, which at first glance appears to indicate that $h_0 = 0$ when $c = 0$; when in fact, when $c = 0$, h_0 = the radial clearance η and the film is of uniform thickness.

It should be pointed out that assumptions (1) and (2) mentioned by Dr. Kingsbury may be included in solutions by the electrical method. He has made investigations of (1), particularly with reference to plane surfaces; and has pointed out that the electrical method may be used for any form of bearing surfaces.

From Mr. Connelly's comments it may be inferred that there is some value of the unit pressure, other than zero, at which there will be no wear at starting and stopping; but he does not state that the experimental evidence on which his remarks are based was obtained with a journal bearing under actual starting and stopping conditions. Experimental results, showing the relationship between wear, unit loading, and length-width ratio in a practical bearing, as the speed is varied from zero to the point where a film is formed, would be of great interest and value.

Attention is called to one or two typographical errors in the paper itself. In Tables 1 and 2, the third column from the left should be headed c and not c, deg. In Fig. 17, the left-hand vertical scale should read 0, 0.2, 0.4, 0.6, 0.8, 1.0.

Exact Construction of the $(\sigma_1 + \sigma_2)$-Network From Photoelastic Observations[1]

E. E. Weibel.[2] In its practical application, Dr. Neuber's proposed method of determining the values of principal normal stresses from photoelastic observations does not appear to the writer to permit a saving in time over the existing methods.

It may be compared with Filon's integration method which also makes use of quantities determined graphically and obtains its results by means of a step-by-step process. In Filon's methods, in one of its forms, either principal stress is found directly by numerically adding quantities of the type $(\sigma_1 - \sigma_2)\,\frac{ds}{dx}$, where dx is the intercept between isoclinics, drawn in the direction of one of the principal stresses, and ds is the increment of length along the stress trajectory which is the path of integration.

In the method proposed by Dr. Neuber, the graphical construction which must be made at each point considered requires the taking into account of six quantities: the directions 1, 5, and 7; the spacings b and c; and the value of $(\sigma_1 - \sigma_2)$.

In a simple curved-beam problem studied recently, about 400 points would have had to be considered for either the Filon or the Neuber method in order to cover satisfactorily that portion of the member which was of interest. It is the large amount of detailed measurement which has caused Filon's method to be described by a number of workers as tedious. The Neuber method does not reduce the amount of measurement and

[1] Published as paper APM-56-17, by H. P. Neuber, in the October, 1934, issue of the A.S.M.E. Transactions.

[2] University of Michigan, Ann Arbor, Mich.

requires in addition a graphical construction at each point considered.

It is the writer's opinion that problems for which principal stresses can be obtained by either of these graphical methods can be solved in a shorter time by means of the membrane-analogy method, using either a soap film or a stretched rubber membrane.

Thomas H. Evans.[3] Although it appears to the writer that two other methods for constructing a $(\sigma_1 + \sigma_2)$-network have decided advantages over any yet developed, that proposed by the author seems somewhat simpler than the graphical integration used by Filon and others.

Any such method, no matter how exact theoretically, that requires the plotting of lines obtained with the polariscope, and the construction of others at given gradients to these, is susceptible to graphical error. Although the method under discussion does not require a plot of the stress trajectories, as does that of Filon, it is necessary to trace out isoclinics, which in some parts of a stressed model are extremely difficult to resolve accurately. Assuming, however, that the basic systems upon which the network is constructed are accurate, a great deal of tedious plotting and checking is necessary unless further inaccuracy is to be introduced by sketching in lines from only a small number of calculated points.

The two methods mentioned above, which appeal to the writer as being simpler to apply once the necessary equipment has been assembled, are the membrane analogy, and an optical method. The former was described in an excellent paper by McGivern and Supper[4] while the latter was successfully used by Tesar and Cornu in France. The membrane analogy relies only on the accuracy of boundary stress determinations, photoelastically, to plot accurately a $(\sigma_1 + \sigma_2)$-surface. The optical method of measuring thickness variation in a stressed model (and hence $\sigma_1 + \sigma_2$) by the method of interference-fringes is entirely independent of the previous photoelastic work to determine $(\sigma_1 - \sigma_2)$, and is extremely simple and accurate.

M. S. Noyes.[5] This is the first paper that the writer has seen, on the photoelastic examination of material under stress, which sets up mathematical descriptions of the observed lines of stress. The writer feels that the author has bridged the gap between the photographic record of the stressed model and the older approximate formulas for the apparent stresses.

The usefulness of the theory and method given, however, is exactly in proportion to the ease with which they can be applied to all of the ordinary problems met in design work. The writer wishes, therefore, that the author had lengthened his short paper sufficiently to include in some detail the application of his graphical method to the symmetrical angle plate analyzed in Figs. 8 and 9. It is not readily apparent, for instance, whether the formula, $-100 = \frac{P}{dh}\left(\frac{6l}{h} + 1\right)$, in these figures, is supposed to represent the true stress for $(\sigma_1 + \sigma_2)$ or an apparent one.

A. M. Wahl.[6] In connection with the problem of determining the principal stresses from photoelastic observations, a recently developed lateral extensometer described elsewhere[7] has proved very useful.

This lateral extensometer differs from that used by Coker in that the points are pressed against the specimen with a small but definite pressure and are held in one location while the specimen is being loaded. There is thus no possibility of sidewise motion of the points during the loading of the specimen, and hence no errors are introduced due to slight variations in thickness from point to point. The whole apparatus is balanced and supported by springs so that the specimen may deform slightly without causing slippage of the points (which carry practically no load). The results obtained by using this extensometer were very consistent, successive readings obtained by removing and reclamping the extensometer at the same point seldom differing by more than 50 lb per sq in. for a 0.33 in. thick specimen (bakelite may easily carry values of $\sigma_1 + \sigma_2$ equal to 5000 lb per sq in. within the elastic limit).

The instrument was checked against a theoretical solution (obtained by Howland[8]) for a plate having a hole with a diameter half the width. It was also checked against photoelastic values of σ_1 (σ_2 being zero) near the free edges of some specimens designed to simulate the conditions in press fits. In all these cases the results obtained by the lateral extensometer agreed closely with those obtained by other means.

In most practical cases, we are interested only in the stresses in a comparatively localized region, such as, for example, the minimum section in the case of a tension bar with a hole or along the line of contact between hub and shaft in the case of a press fit. In such cases the instrument has proved particularly useful, since a few measurements made near such points will give a good idea of the stress distribution in a relatively short time.

Dr. Neuber has presented a very ingenious method of determining $\sigma_1 + \sigma_2$, and one which appears to represent a definite improvement over previously used graphical methods. The writer feels, however, that the use of an accurate lateral extensometer will result in a considerable saving of labor as compared to the graphical method, while, at the same time, giving sufficiently accurate results for most practical work.

Author's Closure

In the discussion of the paper, the author's graphical method for determining the construction of the $(\sigma_1 + \sigma_2)$-network is compared with other methods used for this purpose. In order to understand both the usefulness of the author's method and its practical application, one must realize that it has two important advantages:

(*a*) It eliminates the necessity of drawing the principal stress lines.

(*b*) In most practical problems it will be sufficient to make use of the particular cases (constructions 1 *a,b,c;* 2 *a,b,c;* 3 *a,b*) in which the application of the method becomes extraordinarily simple. These particular cases will furnish a sufficient number of points for obtaining an excellent conception of the $(\sigma_1 + \sigma_2)$-network, inasmuch as the boundary values are already known.

Further details of the method and its application are outlined in, "Einfuhrung in die Photoelastizitat," by Dr. L. Foppel and the author, a treatise which has not yet been published.

It would be very useful for investigators to compare results

---

[3] Instructor in Engineering Mechanics, Sheffield Scientific School, Yale University, New Haven, Conn.

[4] "A Membrane Analogy Supplementing Photoelasticity," by J. G. McGivern and H. L. Supper, A.S.M.E. Trans., August, 1934, paper APM-56-9.

[5] Bureau of Engineering, Washington, D. C. Assoc-Mem. A.S.M.E.

[6] Westinghouse Research Laboratories, East Pittsburgh, Pa. Assoc-Mem. A.S.M.E.

[7] "Fatigue of Shafts at Fitted Members (With a Related Photoelastic Analysis)," by R. E. Peterson and A. M. Wahl, presented at the Annual Meeting, New York, N. Y., December 3 to 7, 1934, of The American Society of Mechanical Engineers.

[8] "On the Stresses in the Neighborhood of a Circular Hole in a Strip Under Tension," by R. C. J. Howland, Proceedings Royal Society of London, January, 1930.

of experimental methods (membrane-analogy or optical methods) with the exact theory of the $(\sigma_1 + \sigma_2)$-network given by the author.

Dynamic Balancing of Rotating Machinery in the Field[1]

T. C. Rathbone.[2] In referring to the writer's paper[3] on the same subject, the author may leave the impression that heretofore the problem had been carried only to the point of solving for the effect of unbalance at one bearing at a time, using the crude shaft marking for phase-angle determination. This paper[3] not only describes an accurate stroboscopic phase-determining apparatus[4] developed and used in the field some ten years ago for the study of vibration phenomena, but also points out the necessity for taking into account the inter-action of influences from one bearing to the other. It also describes a method of determining at all bearings, "unit vectors," which are produced by a unit of unbalance at each bearing, and then describes a rapid practical method for determining the necessary corrections at both ends of the rotor simultaneously, from the results of two trial runs.

The experiments leading up to this solution were carried out on large turbine rotors at speeds up to 2000 rpm. At first, the complete vibratory motion was recorded. Starting with the rotor in practically perfect balance, known unbalances were inserted, first at one end and then the other, and observations made with stroboscopic vibrometers at both ends simultaneously.

It was found that the resulting vibration for a variety of combinations responded with great fidelity—both in shape, size, and inclination of the ellipse, and in phase. The angles could be read to within 2 or 3 deg. From these data the "unit ellipses" were determined for a unit of unbalance and it was found that the resultant figure for any combination of unbalance weights at both ends could be predicted with almost uncanny accuracy, by superimposing the adjusted unit ellipses. Reversing the procedure, unknown unbalance corrections were determined by building up the unit ellipses to produce synthetically the same figures resulting from the unknown unbalance.

Professor Den Hartog solved the problem analytically for this general case, using the complete data observed. As two independent solutions were possible with the ellipse information, which should check, the observations were then confined to either the vertical or lateral component, and this made possible the graphical solution by unit vectors described in the writer's paper. The method involves reproducing synthetically the initial unbalance vectors by adjusting the unit vectors, and the solution is rapidly determined. Mr. Thearle's vector-operator method applied to these unit vectors gives a more direct and mathematically satisfactory solution, and for this contribution, as well as for his improvements in stroboscopic vibrometers, he is to be congratulated.

There are two important by-products of these developments which may be overlooked. First, the analysis of vibration by unit vectors, which affords a measure of the sensitivity or response of any installation due to a given unit of unbalance. Many futile attempts have been made to determine by analysis the resonance characteristics of foundation structures. It is almost impossible to predict these with any accuracy on complicated structures. There has been a great deal of controversy concerning the relative merits of concrete and steel structures. From the standpoint of smoothness of operation, these unit vectors afford a very potent means for direct comparisons of existing structures, which may well guide future design.

Second, the balancing processes under discussion are based on assumptions which do not always apply. Experience has shown that a fairly satisfactory linear relation holds between force and amplitude, and a fairly constant phase relation between cause and effect, so long as the condition of the rotor remains unchanged, or no impactive effects or changes occur in the bearings or structure. In such ideal cases where the rotor responds normally, it has been the writer's experience that operators in the field have little difficulty in arriving sooner or later at a satisfactory balance, each by his own individual and sometimes crude methods.

Rotors which exhibit erratic behavior, however, are difficult to balance by even the refined methods developed. There are many causes for such erratic tendencies, and under these changing conditions it is sometimes impossible to evaluate the unit vectors. In such cases, the stroboscopic vibrometer has proved itself to be a most useful tool in diagnosing the difficulty by continued observations over extended periods, covering all phases of operation of the unit.

James J. Ryan.[5] The solution of the problem of field balancing of rotating machinery proposed by the author and the equipment he has developed to obtain the required data, are ideal. There appears, however, to be a need for more adaptable instruments to measure vibration from a scientific standpoint that may be placed in the hands of less expert operators. A universal oscillo-vibrograph has been developed in the machine design research laboratory of the mechanical engineering department at the University of Minnesota by means of which the data required in the solution of the dynamic-balancing problem presented by Mr. Thearle may be conveniently obtained. This instrument either displays visually or records photographically vibration movements indicating the amplitude of the vibration, the wave form, the frequency and the phase position to large scale. Such instruments promote the methods of scientific analysis in vibration problems, and permit engineers in general to solve problems in the field with little difficulty.

Author's Closure

The author appreciates the interest shown in this paper. Much of the discussion calls for no further comment.

Under certain conditions where the rotor exhibits erratic behavior, Mr. Rathbone questions the validity of the assumptions upon which the balancing process is based. It has been the experience of the author, also, that ". . . a fairly satisfactory linear relation holds between force and amplitude, and a fairly constant phase relation between cause and effect, so long as the condition of the rotor remains unchanged, and no impactive effects or changes occur in the bearings or structure."

Regarding rotors which exhibit erratic behavior, such as changes in vibration amplitude and phase caused by changes in load or temperatures, it is obvious that no single combination of balance weights can give smooth operation under all conditions. Observations of both amplitude and phase of the vibration are necessary in order to establish the nature of the variations in vibration. It is clearly an advantage to know the extent and nature of the variations in vibration before attempting to correct for them by balancing. This knowledge may save much time and effort.

[1] Published as paper APM-56-19, by E. L. Thearle, in the October, 1934, issue of the A.S.M.E. Transactions.

[2] Chief Engineer Turbine Division, Fidelity & Casualty Company of New York, New York, N. Y. Mem. A.S.M.E.

[3] "Turbine Vibration and Balancing," by T. C. Rathbone, Trans. A.S.M.E., APM-51-23, vol. 51, 1929.

[4] "Unusual Vibration of a 25,000-Kw Turbine Generator," by T. C. Rathbone, *Electric Journal*, vol. 25, no. 2, Feb., 1928.

[5] Assistant Professor of Machine Design, Mechanical Engineering Department, University of Minnesota, Minneapolis, Minn., Jun. A.S.M.E.

If, with a knowledge of the nature of the variations in vibration, their cause cannot be eliminated, then a compromise balance must be sought. When this is to be done, observations of the amplitudes and phase angles of the vibration are made over the normal range of operating conditions of the machine. From a plot of these vectors (N and F), the best compromise balance obtainable is readily seen. The balancing process is then completed in the usual way, taking care in the calculations to compare each subsequent vector observed (N_2, F_2, N_3, and F_3) with a value of the original vectors (N and F) corresponding to the same conditions of operation.

It is also obvious that the addition of balance weights to a machine cannot correct effects not caused by unbalance, such as disturbances caused by journals which are not round. However the first observations to be made usually reveal these defects, if they exist, and give information leading to their correction, thus saving much time which might otherwise be spent in attempting to correct, by balancing, for vibrations which are not at all due to unbalance.

High-Pressure Steam and Binary Cycles as a Means of Improving Power-Station Efficiency[1]

LUCIAN A. SHELDON.[2] The essence of Mr. Gaffert's paper is given in Fig. 12 which shows plant performance for steam cycles at various pressures up to the critical pressure, for the diphenyloxide-steam cycle, and for the mercury-vapor-steam cycle. These can be divided roughly into four groups: (1) Steam pressures ranging from 400 lb to 600 lb; (2) high-pressure steam ranging from 1200 lb per sq in. to the critical pressure; (3) the diphenyloxide-steam cycle; and (4) the mercury-vapor-steam cycle. Here we find the poorest economies with the normal steam pressures, the economies of the diphenyloxide-steam cycle about the same as those effected with 1200 lb per sq in. steam pressure, the economies from the use of 2500-lb and critical-pressure steam slightly better, and the mercury-vapor-steam cycle the most economical of all. I believe a brief explanation of the reason for this would be of interest.

The efficiency of any cycle depends upon the temperature range through which we work. In general, the greater this temperature range, the better the efficiency. However, it makes quite a difference whether the higher temperature is obtained by pressure, using saturated vapor, or by superheating. With steam we cannot get the high temperature by means of pressure and hence must resort to superheat. But the energy carried in superheat is only a fraction of that which can be carried in mercury at the same temperature where the temperature is obtained by pressure using saturated mercury vapor. A glance at the temperature entropy diagrams shows this quite clearly. With mercury we approach much more nearly the Carnot cycle and hence get considerably better efficiencies. With the diphenyloxide-steam cycle, as Mr. Gaffert points out, we cannot go much above 800 F as this substance breaks down above this temperature, thus limiting future gains in economy. Mercury, however, is an element and does not break down at high temperatures. Therefore, the upper temperature limit of the mercury-vapor-steam cycle is not limited by the heat-carrying medium but only by the ability of the materials which are available to withstand these temperature conditions. When better materials are produced the temperature range of this cycle can be increased still more and still better economies can be obtained.

In regard to the amount of mercury required, the Kearny boiler contains 300,000 lb of mercury, or approximately 7 lb per kw for mercury and steam. I have not included the kilowatts made from the steam in the water walls as this heat does not pass through the mercury boiler. Estimates made on more recent studies of mercury boilers show that we shall require from 5 to 7 lb of mercury per kilowatt and there is some possibility that in future this may be reduced to as low as 4 lb per kw.

According to conclusion No. 3, Mr. Gaffert feels that the annual rate of production of mercury is so small that there is slight possibility that the mercury-steam cycle will become universal. We all realize that prophecies of this nature are always more or less uncertain. There is apparently plenty of mercury in the world, the yearly production being the amount that is required rather than the amount which is available.

The General Electric Company in the past twenty years has produced an average of about 1,000,000 kw of turbo-generators per year. If we assume that 50 per cent of this turbine capacity would at some future time be mercury, it would require, at the most liberal estimate, 7 lb per kw, 3,500,000 lb of mercury per year, or about 1600 metric tons. From the curve of yearly production of mercury which is published in Minerals Yearbook, we find the variation in yearly output from 2150 metric tons to 5600 metric tons, so that this 1600 metric tons necessary, if half of the General Electric turbines were mercury, would come well within the normal variation of the production curve. Therefore, it would seem that it would not be necessary or advisable for us to slacken our efforts in the mercury process for many years to come because of lack of mercury.

Regarding the operation of mercury-vapor-steam equipment, the record of the Hartford, Kearny and Schenectady plants up to July 1, 1934, is listed in Table 1.

TABLE 1 RECORD OF OPERATION OF MERCURY-STEAM PLANTS

	Hartford	Kearny	Schenectady
Dates	October, 1928, to July 1, 1934	March 27, 1933, to July 1, 1934	Jan. 1, 1934, to July 1, 1934
Hours elapsed	50016	11063	4344
Hours in service	24905	6259	2946
Per cent available	49.8	56	68
Kilowatt-hours	202732000	82245000	29923000
Capacity factor, per cent	40.5	37.2	34.4

The figures in this table cover outages for the entire equipment. That is, they include the furnace and the steam part of the unit as well as the mercury portion. If the mercury portion alone were considered, the availability factor would be very much better. The capacity factor for the Schenectady equipment is rather low because the demand for steam was low and, therefore, the equipment was not called on to carry anywhere near the load it was capable of carrying. The availability factor of the Schenectady unit would have been higher but for the fact that the plant was shut down over week-ends.

The experience and knowledge which we have gained to date lead us to believe that we may expect future mercury-steam equipments to operate at higher availability factors than these first installations and, in fact, to be just as reliable and to operate just as large a percentage of the time as steam equipments.

A. G. CHRISTIE.[3] Mr. Gaffert's conclusion, that the thermal advantages of high steam-pressure and temperature cycles provide a considerable margin for increased capital costs, will stimulate renewed study in their possible application to many systems. The mercury-steam plants offer enticing possibilities from a

[1] Published as paper FSP-56-11, by G. A. Gaffert, in the October, 1934, issue of the A.S.M.E. Transactions.

[2] Engineer in Charge of Design, General Electric Company, Schenectady, N. Y. Mem. A.S.M.E.

[3] Prof. of Mechanical Engineering, Johns Hopkins University, Baltimore, Md., Mem. A.S.M.E.

purely thermodynamic point of view. Certainly a station performance of 8600 Btu per kwhr, or 0.67 lb of coal per kwhr, will be attractive in regions where coal costs are high. More data on the commercial performance of stations that are now in operation, together with cost figures for mercury make-up, for repairs and for supervision, are desired before a final appraisal of such systems can be made.

In considering Dr. Gaffert's results, it must be borne in mind that his values apply to base load stations, for he has assumed 70 per cent station average load factor and 8000 hours' operation per year. This raises the question: "Should the new equipment be designed for base-load service?" It is obvious from Dr. Gaffert's results that the possibilities of further improvements in the steam cycle, or in fact in any of the other cycles, are limited until metals can be developed for temperatures well above 1000 F. This temperature, though at present regarded as the safe upper limit for metals, may soon be exceeded, as much study and research are devoted to this subject and new alloys suitable for still higher temperatures may appear at any time. The justification for a new station for base-load service over any considerable period is, therefore, dependent to a large degree upon such developments in metals.

The late Peter Junkersfeld repeatedly called attention to the fact that many new turbine units were installed on the assumption of high capacity factors over a long period of use. Junkersfeld found from analyzing actual station records that few of these units developed the expected capacity factors over their useful life. In other words, expenditures have been made in many new stations that were in excess of the costs warranted by actual performance. The difficulty of financing new utility plants at present should cause any additional expenditures for securing high thermal efficiency to be subjected to the most conservative analysis of actual operating performance.

Dr. Gaffert could advantageously supplement this valuable paper by additional contributory data that he must already have at hand. For instance, he might indicate in the various cases, the heat to the condenser. Such data would clearly show the advantage of high pressure and temperature cycles where cooling water is limited or where cooling towers have to be used. He might also indicate the percentage of the main generator output required in the various cases to supply power to auxiliaries. It would be interesting to learn how this varies with the increased thermal efficiency of the plant.

A. B. Clark.[4] The calculations in Dr. Gaffert's paper are all based on a unit of about 50,000-kw capacity. It would therefore appear doubtful if such small units could be economically constructed for operating at steam pressures of 2500 lb or 3000 lb as shown in Figs. 1 and 2, because the blade height, nozzles, etc., of the turbine unit would be very small, and the gland-packing leakage and other leakages would be correspondingly high.

In practice the heater system would be changed somewhat. Those who have had experience with feedwater under high pressure would not want to put so many heaters under the full feedwater pressure, but would reduce the number to an absolute minimum.

Then again, small heater drain pumps for high temperatures and pressures are not practical. Their use leads to a very unbalanced design that results in low efficiencies and high maintenance costs. If the drains are flashed down, the lower-pressure heaters are not able to extract as much steam from the turbine and would modify the efficiency of the cycle. The application of drain coolers would help in this respect.

Increasing the number of heaters does not necessarily increase the economy. It has been found that the omission of an intermediate heater in one particular case did not change the economy of the unit; in fact, there was a slight gain. The machine in question was a reheating unit, and in such cases it is necessary that sufficient heat be taken out of the steam and converted into work before the steam is extracted. This may not be done easily when a large number of heaters are employed.

It is for such reasons as given above that it is sometimes difficult, except in a general way, to benefit from such a system of curves as presented in Fig. 12, which is probably the reason why they are given.

Some years ago, when determining the heat balance of units operating at 2400-lb and 3200-lb pressure, it was found that when the work of the boiler feed pump was taken into account, there was but 0.5 per cent difference in efficiency and only about 1 per cent gain in the heat charged to the turbine cycle. Owing to the dense steam, it would be expected that a turbine operating on a pressure of 3200 lb would not be quite as efficient as one operating at a lower pressure. These figures are somewhat less than those given by the author.

Binary cycles are very interesting and that of the mercury-steam cycle has been commercially worked out. It is, of course, an evaporation-and-condensation cycle. If, however, a system is used by which concentration by evaporation and dilution by absorption of vapor is considered, there are more materials available. However, they effect more of a solution cycle than a binary cycle. For instance, it is well known that caustic soda when mixed with water generates considerable heat. A small turbine has been run experimentally on steam generated with concentrated caustic soda by diluting it with the turbine exhaust steam, and then reconcentrating the caustic soda. As most chemicals boil at higher temperatures than water, steam generated in such a cycle is in a superheated condition. Thus it would appear possible to generate steam by concentrating a suitable compound and use it in a steam turbine, and then dilute the compound by exhaust or bled steam from the turbine to generate steam for a second steam turbine.

Dr. Koenemann's cycle is something of this order in that it uses ammoniacate. The cycle uses ammonia vapor instead of steam and then by a heat-exchanger device generates steam for a turbine from the heat given up from an ammonia condenser.

It has taken years of careful work to give us the steam tables and there still seems to be some doubt as to their accuracy at the higher pressures and temperatures. Before any new fluid can be accepted, its heat properties, as well as any corrosive properties it may have, must be determined. This is apt to be quite an expensive and lengthy undertaking.

G. A. Hendrickson.[5] For those interested in comparing the cycles considered in Dr. Gaffert's paper with actual plant results, it should be noted that an important item, which amounts to some 10 per cent of the total heat consumption of actual plants, has been omitted. This item may be designated as the plant operating efficiency ratio, or the ratio of the thermal efficiency of routine operation to the thermal efficiency that would be obtained if each apparatus in the plant operated continuously under test conditions at its most favorable load. Among the items that contribute to the reduction of the operating efficiency ratio below unity are: operation of turbines at loads other than maximum efficiency load; redistribution of heat quantities in the turbine due to changes in load; pressure drop; temperature loss; leaks in steam lines; banking loss in the boiler room; loss due to burning out fires; and numerous unaccounted-for losses. Some of these have been considered in Dr. Gaffert's paper and some have not. In consequence, the results given are probably 1000 Btu

[4] Engineer, Sargent & Lundy, Inc., Chicago, Ill., Mem. A.S.M.E.

[5] Engineer, The Detroit Edison Company, Detroit, Mich., Assoc-Mem. A.S.M.E.

per kwhr lower than those obtainable from actual plants operating on similar cycles. This difference should be borne in mind when comparing the paper with actual plant results.

In a paper, "A Thermal Study of Available Steam-Power-Plant Heat Cycles," presented by S. T. Vesselowsky and the writer at the A.S.M.E. meeting held in Chicago, June, 1933, an attempt was made to present steam-plant results comparable with actual operating data. It was pointed out in that paper that for steam plants the regenerative feed-heating cycle without reheat is probably best suited to ordinary conditions where a relatively low-capacity use factor is encountered. In base load plants and other situations where a high-capacity use factor is found, reheating or a binary cycle might be justified. From a comparison of Dr. Gaffert's results with those of Mr. Vesselowsky and the writer it appears that at a given limiting temperature the reduction in heat rate available from the use of reheating is about 1500 Btu per kwhr. A binary cycle using mercury and steam makes possible a further reduction of about 1000 Btu per kwhr. This improvement is not immediately available, however, but must follow out a slow and costly process of development, and in the end the net economic gain is much reduced. In the meantime the type of plant which converts chemical energy in coal into heat and then into mechanical power is slowly approaching a minimum limit in heat rate in the neighborhood of 9000 Btu per kwhr. This limit, which is now in sight, is imposed by the properties of commercial materials available for construction.

In this situation it is pertinent to mention that no decreases in heat rate comparable to those in the past need be expected unless radical changes are made in the basic cycle. In the period 1910 to 1930 the minimum heat rate attainable was reduced by one-half. With plants now operating at around 12,000 Btu per kwhr, the margin for further reduction is small. Only the magnitude of the coal bill makes further development practicable. Papers such as the present point out the most promising possibilities in this development. The same magnitude that makes such work possible, however, also makes imperative the highest accuracy attainable in theoretical comparisons, and this with the least possible confusion. Heat rates chargeable to the operation of the turbine alone are probably the easiest means of comparing different cycles. Such comparisons, however, are not final since they do not give overall performance. For those who wish to make quick comparisons with actual plant data, a plant heat rate estimated from the computed turbine results may be added with little difficulty. The writer believes such a presentation to be much more convenient for the general reader.

J. J. Grebe.[6] On the basis of the same boiler efficiencies, the performance figures given in Dr. Gaffert's paper check closely the values which were published by Dr. H. H. Dow in 1926.

Regarding the diphenyloxide or Dowtherm boilers, these units do not have to have forced circulation. In fact, the first boiler built in 1926 was operated at a heat input of 10,000 Btu per sq ft without any circulation difficulties as long as the boiler pressure was maintained above 35 lb. It is merely necessary to proportion the circulation path so that, first, the vapor volume produced can be discharged at a reasonable velocity, and, second, this vapor has the chance to use its air-lift effect as much as possible. For boilers operating at the maximum allowable temperature and high capacity, and using a small inventory of Dowtherm, it is naturally most economical and practical to use forced-circulation boilers such as illustrated in Fig. 2 of Dr. Gaffert's paper.

It might be suggested to Dr. Gaffert that his study be continued to include a cycle in which mercury and a second fluid other than water be used. A mercury condenser boiler used to vaporize a lower-boiling fluid, such as benzol or alcohol, would give a high-pressure vapor requiring little or no superheat for efficient expansion in a turbine, and would permit condensation at a lower temperature, particularly in the winter when very cold condenser water is available, and still not reach enormous vapor volumes. Such a fluid would also have the advantage of a higher vapor density so that the turbines could operate at a lower speed. It would, however, require a larger condenser surface on account of the decreased heat-transfer rates.

[6] Director, Physical Research, The Dow Chemical Company, Midland, Mich. Mem. A.S.M.E.

Frank O. Ellenwood.[7] Regarding the high-pressure cycle, the statement is made that for a throttle pressure of 1200 lb, the reheating pressure would lie near 200 lb per sq in., depending on the initial temperature of the steam. As a matter of interest to engineers who have not investigated the question of the optimum reheating pressure, it seems appropriate to mention that the 200-lb reheating pressure, as given, would be close to the best one, provided the throttle temperature is about 800 F. On the other hand, the writer believes that if the throttle temperature were 1000 F and the throttle pressure were 1200 lb, the reheat pressure would then be closer to 100 lb per sq in., for the best thermal results. For the 2500 lb (800 F) throttle steam, the writer agrees with the author in selecting a reheat pressure of 500 lb, as specified in Fig. 1. The heat rate of this 2500-lb station is given as 10,520 Btu per kwhr, which has been checked roughly by the writer. This performance, according to the author, is equaled by the 1200-lb (1000 F) plant without reheating. Such a result implies about $2^1/_2$ per cent better performance of the 1000-F turbine than that estimated by Carter and Ellenwood.[8]

It is particularly interesting to note that the curves in the author's Fig. 12 that are below the value of 9300 Btu per kwhr, represent a region that has seldom, if ever, been entered by the performances of the very best of our internal-combustion engines.

Authors' Closure

We are indebted to Mr. Sheldon of the General Electric Company for presenting the operating records of the three mercury-steam plants now in operation. It seems certain that when this binary cycle is used for a base-load station, the availability will be as great as in the case of ordinary steam plants.

Regarding the availability of mercury as a fluid, it is significant to note, according to Minerals Yearbook, that a high rate of production over a sixteen-year period caused by an increase in demand has resulted in an increase in the price per pound. Admittedly, the present method of recovery is crude and all mercury-bearing ore deposits have not been tapped. Mr. Sheldon's figures showing variation in yearly output from 2150 metric tons to 5600 metric tons are for world production. If, as indicated in the author's paper, an average world-production rate were taken at 3000 metric tons per year, allowing no more mercury than 4 lb per kw installed, approximately 1,650,000 kw could be installed per year. However, since a considerable percentage of this production is absorbed in the chemical industry, the amount available for power is at present entirely inadequate to supply the annual increase in generating capacity required throughout the world. It seems evident, therefore, that the mercury-steam cycle must share the increase in load with other methods of generation.

In answer to Prof. A. G. Christie's remarks relative to the per cent of main generator output required for plant auxiliaries, the author has listed in Table 2 of this discussion figures based upon a study of the various cycles. These figures include power

[7] Prof. of Heat-Power Engineering, Cornell University, Ithaca, N. Y. Mem. A.S.M.E.

[8] "The Thermal Performance of the Detroit Turbine Using Steam at 1000 F," Trans. A.S.M.E., FSP-56-8, July, 1934.

for preparation of fuel, for driving the boiler feed pumps, hotwell pumps, heater drain pumps, mercury or diphenyloxide boiler feed pumps in the case of binary cycles, and forced and induced draft fans.

TABLE 2 PER CENT OF MAIN GENERATOR OUTPUT REQUIRED FOR AUXILIARIES

Type of cycle	Auxiliary power, per cent
Steam cycle:	
400 lb (800 F)—5 pt. extr.	3.97
1200 lb (800 F) -5 pt. extr.	4.74
[a]2500 lb (800 F) -6 pt. extr.	5.39
[a]3200 lb (800 F)—6 pt. extr.	5.88
Mercury-vapor-steam cycle:	
200 lb (1020-F) hg	
500 lb (800-F) steam, 4 pt. extr.	2.67
Diphenyloxide-steam cycle:	
210 lb (800 F) diphenyloxide	
730 lb (1000 F) steam, 4 pt. extr.	4.33

[a] Using multicylinder reciprocating boiler feed pumps.

The author agrees with A. B. Clark's comments regarding the arrangement of extraction heaters in the feedwater cycle. It is undoubtedly true, as mentioned in the author's paper, that it would be more expedient to drain all of the heaters in the high-pressure steam cycles back to the deaerating heater to eliminate the complicated problem of handling small quantities of drainage at high discharge pressures. The balance of increase in fixed charges versus the increase in efficiency due to additional extraction heaters will determine the optimum number of heaters to install in any given cycle. The author's paper dealt only with the thermodynamics of the question inasmuch as available costs on high-pressure heaters for extremely high-pressure steam cycles are not available.

Referring to the use of a caustic solution such as potassium hydroxide or sodium hydroxide, this cycle has the advantage that it can store energy in a chemical form until required. However, there appears to date to be no authentic data as to the purity of steam leaving such a caustic solution, and in case there were even slight traces of caustic the resulting corrosion on the turbine plant would become a serious factor in a short time. Dr. Koenemann's cycle, to the author's knowledge at least, has never been put into actual practice. The main difficulty is that ammonia at temperatures approaching 800 to 1000 F is entirely unstable and a considerable percentage breaks up into the constituent gases which are very corrosive.

G. A. Hendrickson of the Detroit Edison Company points out several losses which are ordinarily summed up into the figure "operating ratio" for a given plant. The author prefers to consider auxiliary power, that is power required by all pumps and draft equipment as auxiliary power, and then, depending upon the type of plant as well as operating staff, to allow a certain operating ratio to account for these various losses. This method is in constant practice among various capable designing engineers. In short, it enables comparisons between cycles to be made more readily, but, as pointed out by Mr. Hendrickson, necessitates correction for any particular plant to obtain actual day-to-day performance. Mr. Hendrickson also states that heat rates chargeable to the turbine alone are probably more interesting for comparison. In the author's original paper, heat rates chargeable to the turbine for each cycle are stated on each cycle diagram. A comparison of turbine heat rates for a binary cycle is likely to be quite misleading as the per cent of auxiliary power varies considerably for various "top" fluids, being almost twice as much in the case of the diphenyloxide-steam cycle as in the case of the mercury-steam cycle.

If it were possible to obtain a high capacity as well as maximum allowable temperature without a circulating pump, the efficiency of the diphenyloxide-steam cycle could be slightly improved, as brought out by the remarks of J. J. Grebe of the Dow Chemical Company. It is also quite true that were it possible to find a fluid with temperature entropy characteristics not unlike mercury for use as the "bottom" fluid in a binary cycle, the overall cycle efficiency could be improved somewhat with considerable less capital expenditure for extraction equipment.

Prof. F. O. Ellenwood points out that the best reheat pressure is a function of throttle temperature. For lack of space the author did not include curves showing this effect, but the author's results are exactly in accord with the statements made by Professor Ellenwood regarding the location of the best reheat pressure as a function of the throttle pressure.

A New Theory for the Buckling of Thin Cylinders Under Axial Compression and Bending[1]

STEWART WAY.[2] This paper is interesting in that it provides an explanation of the difference between the buckling loads obtained in practice for thin cylinders and the values arrived at by old theories.

If there were no initial eccentricities in the cylinder, failure would take place with the reaching of the point of elastic instability. To determine this point, it is not necessary to consider large deflections. It appears that in the problem at hand it is necessary to consider large deflection phenomena only because of the assumed presence of initial eccentricities.

The principle that the final buckling shape will be the same as that of one of the components of initial deflection is probably quite sound. However, in certain very improbable cases, it is conceivable that the final buckling shape would be totally different from the initial shape. I have in mind the case of a strut with initial deflection in the form of a full sine wave, which, with axial loading, becomes unstable and buckles to the side.

[1] Published as paper AER-56-12, by L. H. Donnell, in the November, 1934, issue of the A.S.M.E. Transactions.

[2] Westinghouse Research Laboratories, East Pittsburgh, Pa.

Rolling-in of Boiler Tubes

By F. F. Fisher[1] and E. T. Cope,[2] Detroit, Mich.

This paper presents an introductory study of boiler-tube rolling and reviews the methods now in common use. It points out their limitations and explains and proposes specifications for a new method which approximates the ideal. Test results are given which show the superiority of this new method. A few pertinent details of tube rolling are also mentioned, including the over-rolling of tubes as a source of high stress concentration in the sheet metal around the tubes. This high stress concentration may be a source of corrosion fatigue.

Introduction

Although much has been written about boiler shells and tubes, and riveted and welded joints, apparently nothing has been published in English about the method of fastening tubes into boiler shells and tube sheets. It is true that test methods have been applied for determining the water-tightness of these joints, but such tests do not disclose the condition of the joint. Manufacturers of rolling tools furnish instruction booklets briefly explaining the use of the tools, yet engineering publications printed in English contain no information regarding this very important item of boiler design and construction. Although all other parts of the boiler are designed with great care by engineers after careful study of strength of metals, effects of temperature, the permissible oxygen and carbon-dioxide content of boiler feedwater, etc., the production of the joints between the tube ends and the tube sheets or drums has been left largely to the ingenuity of the mechanics who assembled the structure. It appears, therefore, that the expanded tube joint, if its use is to be continued, should be subjected to scientific study, its limitations recognized, and an effort made along scientific lines to standardize field practice so that all the joints in a given boiler may be of maximum strength as determined by such investigation.

The knowledge of what constitutes a satisfactory rolled joint is now lacking. Once this knowledge is available and the correct procedure for rolling the joint has been established, the production of joints of maximum strength and tightness could be controlled. If the tubes could be machined to fit into carefully tooled tube holes, or if the tube ends could be shrink-fitted into the holes, the problem would be relatively easy. But liberal clearances must be allowed to permit easy introduction of the tubes into the holes, particularly in tight places, of which there are many in a modern large-capacity boiler. Commercial practice and the demand for low-cost production puts precise machining out of the question. On the other hand, if the differences in diameters between the tubes and tube holes were constant to a micrometer tolerance and the tube-wall thickness did not vary, the problem of securing uniform joints would be relatively simple. Also, if the surfaces of tube and tube hole which are to produce the joint were of uniform and standard finish, the production of uniformly tight and strong joints would not be so difficult. But when joints are to be made between the surfaces of tube ends and tube holes in which the clearance may have any value from ten-thousandths to sixty-thousandths of an inch in a bank of tubes, where the tube holes are reamed to commercial finish yet the tubes are covered with mill scale or are indifferently cleaned, one should not be surprised if a considerable percentage of the joints shows leaks when the assembled structure is subjected to a hydrostatic-pressure test. Neither should one be surprised if the rerolling operation causes leaks in joints accepted on the first hydrostatic test, nor that such joints fail after a comparatively short period of service.

The production of a joint by expanding a tube into a tube hole entails the execution of two distinct phases of the rolling-in operation. The first consists of stretching the tube wall until there is contact between the outside surface of the tube and the inside surface of the tube hole. A joint does not begin to exist until this contact has occurred. As already noted, the difference in diameter of the tube and the tube hole is by no means constant in any group of prospective joints. Therefore, the amount of expanding of the tube necessary to produce contact between tube wall and tube hole may vary widely from tube to tube. Consequently, this fact must be taken into account when producing a joint. The second phase of the rolling-in operation consists of giving the tube wall further permanent stretch, thus pressing the outside surface of the tube against the inside surface of the tube hole. This pressure alone is the source of fluid tightness in the joint. Also this pressure, coupled with the friction between the two metal surfaces, is the source of the strength of the joint which holds the tube in the tube hole when pressure is applied within the boiler. Since the pressure between the two surfaces is the only variable in any given case entirely within the control of the mechanic doing the assembling, it might be at once concluded that the greater the expansion the better the joint. That this is not true has been demonstrated by tests which show that both the tube wall and the metal surrounding the tube hole are subjected to severe cold working when excessive expansion is practiced. When a tube must be replaced in a tube hole which has been heavily over-expanded, the hole is badly distorted and should be rereamed to true it up and to remove the metal which was overstressed at the previous rolling.

The formation of an ideal joint by rolling-in requires:

1 A device for expanding the tube so that it is cylindrical at all times during the rolling-in operation.

2 A means by which the completion of the first phase of the rolling-in will be indicated definitely. This anticipates a mechanical, a magnetic, or an electrical device for positively indicat-

[1] General Foreman of Mechanical Erection, The Detroit Edison Company, Detroit, Mich. Mr. Fisher was born near Hempstead, N. Y., educated in public and technical schools in England, Germany, and the United States. He served as shop superintendent, erecting engineer, and master mechanic in shops in the Far East, South America, and the United States. For the past fifteen and a half years he has been connected with the Construction Bureau of The Detroit Edison Company.

[2] Research Department of The Detroit Edison Company. Mem. A.S.M.E. Mr. Cope was graduated in 1907 with the degree of B.S. in M.E. from the Towne Scientific School, University of Pennsylvania, and was granted the degree of M.E. in 1910 by the same university. After graduation he spent three years with the Westinghouse Machine Company of Pittsburgh, Pa., and three years as instructor in the Engineering College at the University of Michigan. Since 1913 he has been connected with The Detroit Edison Company, and since 1919 in the Research Department.

Contributed by the Power Division for presentation at the Semi-Annual Meeting, Cincinnati, Ohio, June 19 to 21, 1935, of The American Society of Mechanical Engineers.

Discussion of this paper should be addressed to the Secretary, A.S.M.E., 29 West 39th Street, New York, N. Y., and will be accepted until July 10, 1935, for publication at a later date.

ing the establishment of a firm contact between the outside surface of the tube and the inside surface of the tube hole.

3 A means for indicating the amount of deformation of the metal surrounding the tube hole. This metal should not be stressed beyond its elastic limit.

A method of tube expanding based on these requirements should produce fluid-tight joints which show the optimum strength to resist destruction when subjected to fluid pressure. Furthermore, it has been well established that corrosion fatigue occurs at points of high stress concentration. The metal of tubes and tube sheet surrounding the holes in boilers in which the tubes have been heavily over-rolled should be an ideal point for the beginning of this form of failure.

This paper presents the results of a study of the expanding of boiler tubes and proposes a method which, over a five-year period, has produced uniform joints of optimum strength. In this method the severe cold working of the tube and drum metal, because of excessive expanding of the tubes, has been either avoided entirely or reduced to a minimum.

Conventional Methods of Tube Expanding

Three methods of tube expanding are generally accepted. These are the tube-bulge method, the uniform-expander-entrance method, and the measured-energy-input method. These will be reviewed briefly and their limitations pointed out. In the tube-bulge method, a few tubes in a bank, used as samples, are expanded until their outside diameters are increased a definite amount ($^1/_{32}$ in. usually) over the nominal tube-hole diameter. This measurement is made immediately next to the tube sheet or drum on the gas side in a water-tube boiler and the water side in a fire-tube boiler. The amount of tube bulge is measured by a gage of fixed opening. The expanding or rolling operation is carried out until this outside gage fits the bulge of the tube. After the operator gets the "feel" of rolling-in these samples, he proceeds to roll-in the remainder without measurement.

In the second method of tube expanding, the tool is entered a fixed distance into all the tubes in a given bank. This distance is determined by trial on a few tubes and the stop is set. In the uniform-energy-input method all joints are rolled-in with a consumption of a given amount of energy expressed in watthours or horsepower-hours.

In these methods of tube expansion there is no way of knowing definitely when the tube surface contacts the tube hole. Also, there is no way of knowing how much the tube is expanded after contact occurs.

TABLE 1 MEASUREMENTS OF FIVE GROUPS OF TUBES AND TUBE HOLES

Nominal tube size, in.	2	2	$3^1/_4$	4	4
Minimum outside tube diam, in.	1.981	1.994	3.236	4.002	3.987
Maximum outside tube diam, in.	1.991	2.004	3.285	4.013	4.008
Minimum wall thickness, in.	0.186	0.138	0.189	0.204	0.211
Maximum wall thickness, in.	0.213	0.143	0.211	0.256	0.262
Nominal tube-hole diam, in.	2.031	2.031	3.281	4.031	4.031
Minimum tube-hole diam, in.	2.025	2.030	3.267	4.020	4.025
Maximum tube-hole diam, in.	2.040	2.038	3.320	4.041	4.039

Measurements made on five groups of tubes and tube holes revealed the values given in Table 1. The customary allowance of $^1/_{32}$ in. for tube bulge would result in a wide variation in the actual amount of expansion in the cases of the minimum and maximum sizes of the tube holes shown. The holes of minimum diameter might be over-expanded. The tube-bulge method of expansion, therefore, does not meet the second and third requirements of the ideal expansion method. If, on the other hand, these joints had been assembled by the uniform-expander-entrance method, in which no exact account is taken of the variation in clearance between tube and hole, and no allowance is made for the variation in tube-wall thickness, it is obvious that

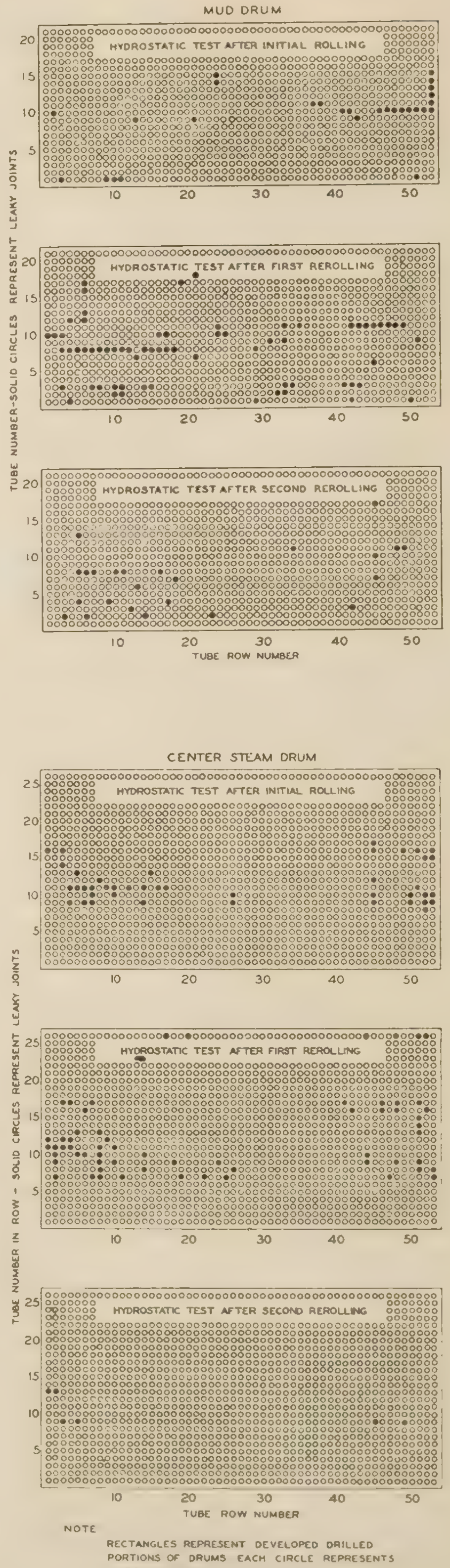

Fig. 1 Record of Rolling-in Joints in Two Drums of a Boiler Using One Conventional Method

the resulting joints would not have been expanded uniformly. If by chance, resulting from random choice of tubes, the smallest tube having the thinnest wall had been expanded into the largest hole, the resulting joint would have been very different from the one resulting from expanding the largest tube having the thickest wall into the smallest hole. In the first case the tube might have been expanded only enough to contact the tube hole, whereas in the second case the joint would have been heavily over-expanded, resulting in severe cold working of the metal of tubes and tube sheet and the setting up of points of very high stress concentration. This second method also falls short of meeting the requirements of the ideal method of tube expanding.

In the uniform-energy-input method no account is taken of the influence of differences in tensile strength of the metal of the tubes and sheets, differences in clearance between tube and tube hole, nor the condition of the rolling tool. When the self-feeding expander is used, the power required to flare the tube is at maximum at the same instant as that required for completing the rolling-in operation of the joint itself. The flare does not constitute an essential portion of the joint, as will be shown later, and the energy required to complete the flare cannot be separated from the total. This method also falls far short of meeting the requirements of the ideal joint.

The consequence of using an uncontrolled method of expansion is shown by the results obtained in the erection of a boiler under the authors' observation. The tubes in this boiler were expanded by one conventional method. The mechanics who did the work were experienced and careful. Fig. 1 shows graphically the results of the rolling-in and testing of the joints. It is to be noted particularly that the second rolling-in both drums produced a greater number of leaks than it was sought to remedy. These leaks were not necessarily in the same joints. The third rolling left the mud-drum joints in scarcely better condition than did the first rolling. The results on both drums indicate that the use of one conventional method of tube rolling with the lack of knowledge of the separate operations involved leads only to imperfectly rolled and probably badly over-rolled tubes and consequently permanently deformed tube and tube-sheet metal in which there are points of high stress concentration with consequent predisposition to corrosion fatigue.

The shape of the entering ends of the expanding-tool rollers is a matter of considerable importance. Since the metal on the inside of the tube wall is cold worked, it is of the highest importance that this cold working should take place with the least possible disturbance of the metal surface. If the entering ends of the rolls are not sufficiently rounded they leave a sharp shoulder at the inner end of the rolled portion. This produces an ideal starting point for cracks or corrosion, as shown by numerous tube failures which have been investigated. With self-feeding expanders, especially when used for rolling-in tubes into thick sheets (such as $1^1/_4$ in. and upward), the metal on the inside of the tube is plowed up by one roller and then rolled down by the succeeding ones. This leaves a spiral mark on the inside of the tube. It is usually not noticeable upon casual inspection, yet constitutes an excellent starting point for corrosion. To correct this condition the boiler erectors in the authors' company have ground the entering ends of the rollers of their expanders to a five-inch radius. A certain amount of cold working takes place, but instead of the metal being plowed into a sharp crest it is moved ahead of the rollers in the form of a gentle undulation. No roller scars are visible on the inside surface of the tubes.

The Elongation Method of Tube Rolling

The elongation method of tube rolling, as developed by the company with which the authors are associated, more nearly fills the specifications for an ideal method than does any one of the other methods noted. In this method advantage is taken of the fact that the tube is loose in the tube hole until the first phase of the rolling-in is completed. It further takes advantage of the fact that during the expanding operation the wall of the tube within the tube sheet is thinned. The metal is squeezed between the expanding tool and the surface of the tube hole and is forced to flow axially. This moves the tube axially a measurable amount, which is a function of the degree of the expansion. The only extra tool required by this method is a dial indicator fitted with the proper-size clamp, so that the indicator may be readily attached to the tubes. The tube is inserted into its tube hole and manually held in place. The dial indicator is attached as shown in Fig. 2. The clamp extends half way around the tube and

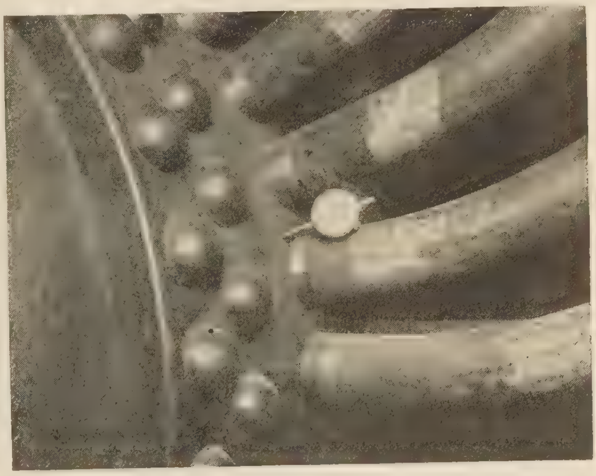

Fig. 2 Dial Indicator Attached to a Tube

bears at three points to prevent rocking. The end of the shaft of the dial indicator rests on the tube sheet or drum. The expanding operation proceeds, using a "parallel" expanding tool. During the first phase the needle of the dial indicator vibrates until the tube has been stretched into circumferential contact with the tube hole. At the instant of this contact the needle comes to rest, indicating that the first phase has been completed, and item two of the ideal method of expanding has been met. Continued expansion further stretches the tube wall into firmer contact with the hole and squeezes it so that axial flow occurs. This axial flow causes movement of the dial-indicator needle. The amount of movement of the needle necessary to produce the best joint has been established by tests which will be described later.

TABLE 2 DIMENSIONS AND CHANGE IN DIMENSIONS OF FOUR TUBES SUBJECTED TO DIFFERENT DEGREES OF ROLLING[a]

Before expanding			After expanding			
Outside diam	Inside diam	Wall thickness	Outside diam	Inside diam	Wall thickness	Elongation
3.996	3.580	0.208	4.010	3.608	0.201	0.010
3.990	3.578	0.206	4.031	3.630	0.196	0.020
4.008	3.586	0.211	4.036	3.642	0.197	0.030
3.995	3.575	0.210	4.031	3.645	0.193	0.040

[a] All dimensions in inches.

The dimensions and change in dimensions of four tubes of a given size, with different degrees of rolling, are given in Table 2. The tube dimensions were taken during a test conducted in connection with the elongation method of tube expanding. These tubes were cleaned, using a mechanical tube-end cleaner having carborundum cutters of 120-grit grade *H*. In place of a regular tube sheet, blocks of boiler plate 10 in. square, $2^1/_4$ in.

thick, and with one reamed tube hole each, were used. Three tubes were expanded to each of several elongations (axial movement caused by the rolling-in operation), all without flare. Each tube assembly was then subjected to hydrostatic pressure until the joint broke and the tube was forced out of the hole. Measurements of the tube diameters and wall thickness were made before expanding and after the assembled tube and block had been separated.

TABLE 3 CHANGES IN DIMENSIONS DURING EXPANDING OPERATION OF THE FOUR TUBES LISTED IN TABLE 2

Elongation, in.	Outside diam increase, in.	Inside diam increase, in.	Wall thickness decrease, in.
0.010	0.014	0.028	0.007
0.020	0.041	0.052	0.010
0.030	0.028	0.056	0.014
0.040	0.036	0.070	0.017

TABLE 4 ASSEMBLIES OF TUBES AND TUBE SHEETS FOR WHICH HOLDING STRENGTH HAS BEEN DETERMINED

Nominal outside diam, in.	Nominal wall thickness, gage	Plate thickness, in.
2	8	1.25
2	11	1.25
$3^1/_4$	7	2.25
$3^1/_4$	7	1.00
$3^1/_4$	11	1.00
4	5	1.25
4	7	2.25
4	7	1.00

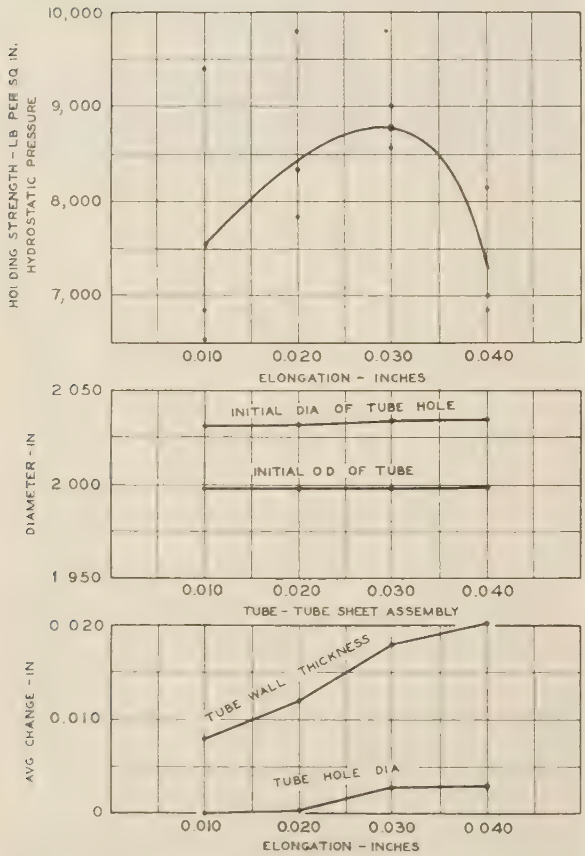

FIG. 3 TEST RESULTS FOR 2-IN., 8-GAGE TUBES ROLLED INTO $1^1/_4$-IN. PLATES

During the expanding operation, the changes given in Table 3 occurred. Even though the changes in outside and inside diameter of the tube rolled to 0.020-in. elongation were not consistent with the others in the schedule, the decrease in wall thickness and the axial movement were consistent.

It is evident from Table 3 that the elongation of the tube and the decrease in wall thickness are related. It remained only to establish experimentally the values of the relationship in terms of strength and water-tightness of the joints produced. The experimental determination of the relationship between elongation and the strength of the joint to resist destruction by hydrostatic pressure, called "holding strength," has been found for the assemblies of tubes and tube sheets listed in Table 4.

Test Procedure and Results

Sample joints were produced by expanding short lengths (usually 15-in. long) of boiler tube into blocks of boiler plate of the

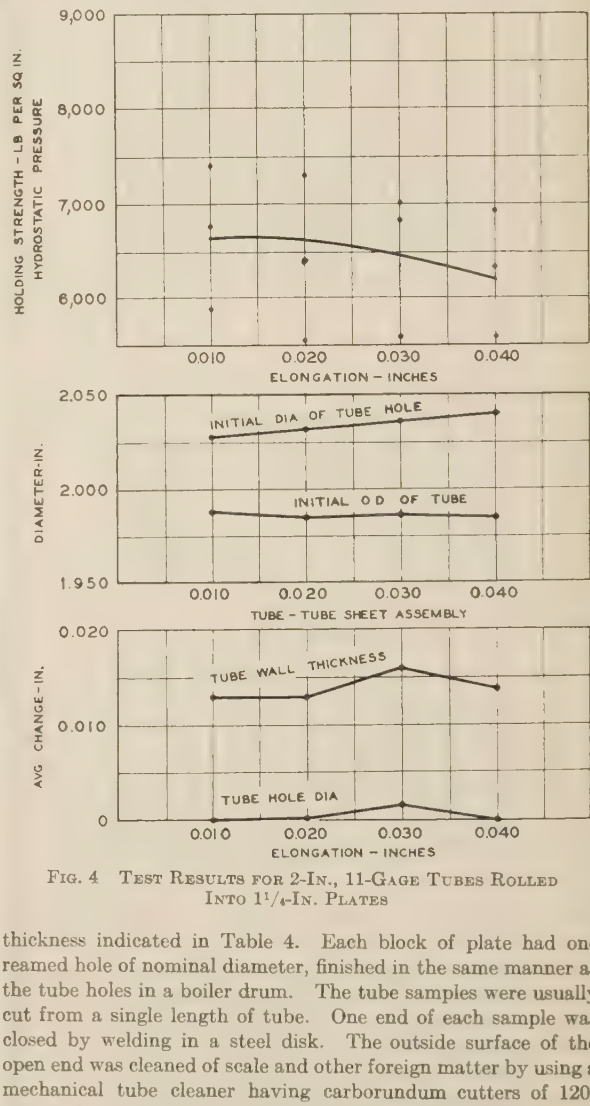

FIG. 4 TEST RESULTS FOR 2-IN., 11-GAGE TUBES ROLLED INTO $1^1/_4$-IN. PLATES

thickness indicated in Table 4. Each block of plate had one reamed hole of nominal diameter, finished in the same manner as the tube holes in a boiler drum. The tube samples were usually cut from a single length of tube. One end of each sample was closed by welding in a steel disk. The outside surface of the open end was cleaned of scale and other foreign matter by using a mechanical tube cleaner having carborundum cutters of 120-grit grade *H*. The $3^1/_4$-in. and one group of 4-in. tubes were given a supplementary rubbing with No. 1 carborundum cloth. Expanding was done by the use of an air-driven "parallel" expander without flaring rolls. The taper of the rolls was $^1/_4$ in. per ft, and that of the mandrel $^1/_2$ in. per ft, and the feed angle of the rolls was $1^1/_2$ deg. Dimensions of tubes and tube holes were measured, using appropriate micrometers, both before

expanding and after the tubes had been forced from the tube holes. Three joints were made for each of the combinations for each of several elongations (usually 0.010 in., 0.020 in., 0.030 in., and 0.040 in.). For instance, there were 12 joints made using 2-in., 8-gage tubes in $1^1/_4$-in. plate, 12 joints using 2-in., 11-gage tubes in $1^1/_4$-in. plate, etc. Each tube-hole plate was drilled so that a blank flange could be bolted to it. This blank flange carried the necessary connections for the introduction of hydrostatic pressure within the tube. Elongation during expanding was indicated by the dial indicator shown in Fig. 2.

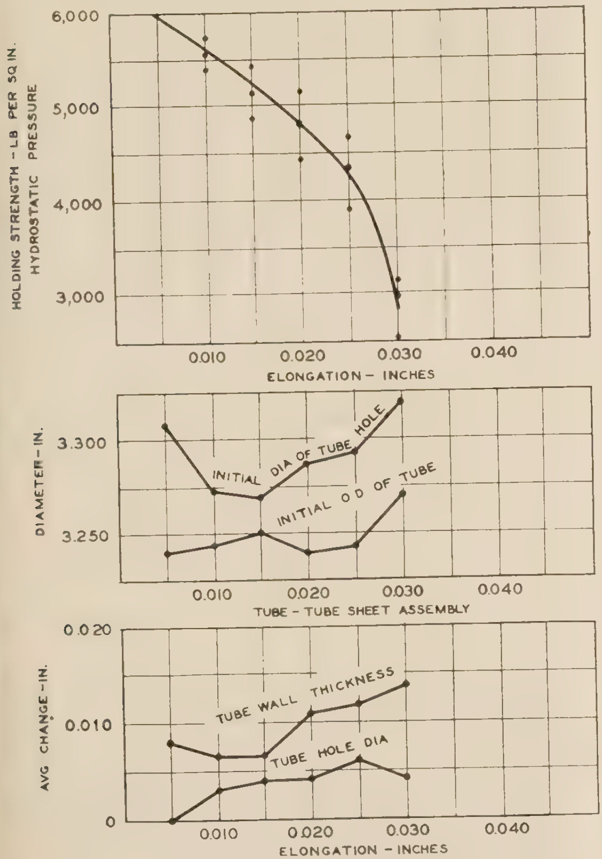

Fig. 5 Test Results for $3^1/_4$-In., 7-Gage Tubes Rolled Into $2^1/_4$-In. Plates

The results of these tests are shown on Figs. 3 to 10, inclusive. In these figures the holding strength is expressed in pounds per square inch hydrostatic pressure necessary to cause failure of the joint at room temperature. Failure occurs when the tube slips in the tube hole. The values of holding strength shown on Figs. 3, 4, 8, and 9 are somewhat scattered for each elongation owing doubtless to the fact that the tube surfaces were finished exactly as are those in a boiler. The values are probably such as would be obtained in actual practice. The values shown in Figs. 5, 6, 7, and 10 are not so scattered, doubtless because of the fact that the ends of these tubes were somewhat smoothed with No. 1 carborundum cloth after mechanical cleaning. The clearance (difference in diameters) between the tube and the tube hole is shown by the width of the band between the two curves, "Initial Diameter of Hole" and "Initial OD of Tube." In some cases this band is of almost uniform width, whereas in others, notably Figs. 5 and 6, the width varies considerably. The tube-wall thickness decreases at a relatively uniform rate with increase in elongation, as would be expected, whereas the increase in tube-hole diameter does not follow the increase in elongation. This condition might be expected if the tubes were made from much softer steel than were the tube sheets. In the cases of the tubes and tube sheets represented by Figs. 3, 4, 8, and 9, in which the Rockwell hardness numbers of tubes and tube sheets were obtained, in all instances the tubes were harder, consequently of higher tensile strength than the plates.

The tubes in several boilers have been expanded using the elongation method and the results have been highly satisfactory. Among these are the following:

1 Boiler No. 14, Trenton Channel power plant, operating at 400 lb per sq in. There were no leaks, but only small beads of water appeared on some joints. A light reexpanding of the joints on one drum was carried out and the boiler was passed.

2 Two boilers at the Ford Motor Company, Dearborn, Mich., operating at 1425 lb per sq in. The erector expanded the tubes in the same manner as were those at the Trenton Channel power plant. The tubes on the first boiler were expanded to 0.020-in. elongation. It was found necessary to reexpand a small portion of the tubes in order to pass the hydrostatic test. In the second

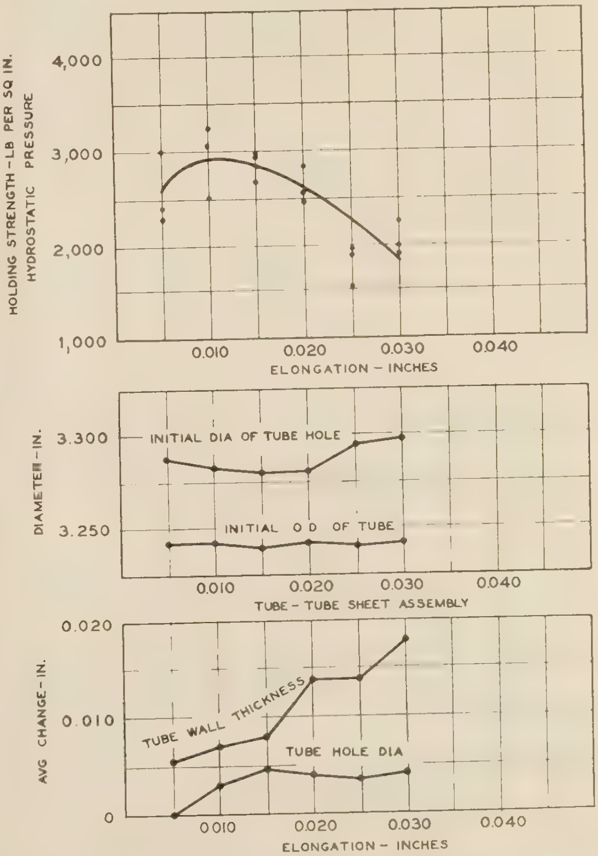

Fig. 6 Test Results for $3^1/_4$-In., 7-Gage Tubes Rolled Into 1-In. Plates

boiler, the tubes were all expanded to 0.025-in. elongation, and were passed on the first inspection without exception.

3 Two boilers at the Springwells Plant of the Detroit Board of Water Commissioners operating at 400 lb per sq in. Elongation failed to show on the first few tubes expanded. An investigation disclosed the fact that some of the tube holes were tapered. This condition was corrected and the tubes were then expanded to

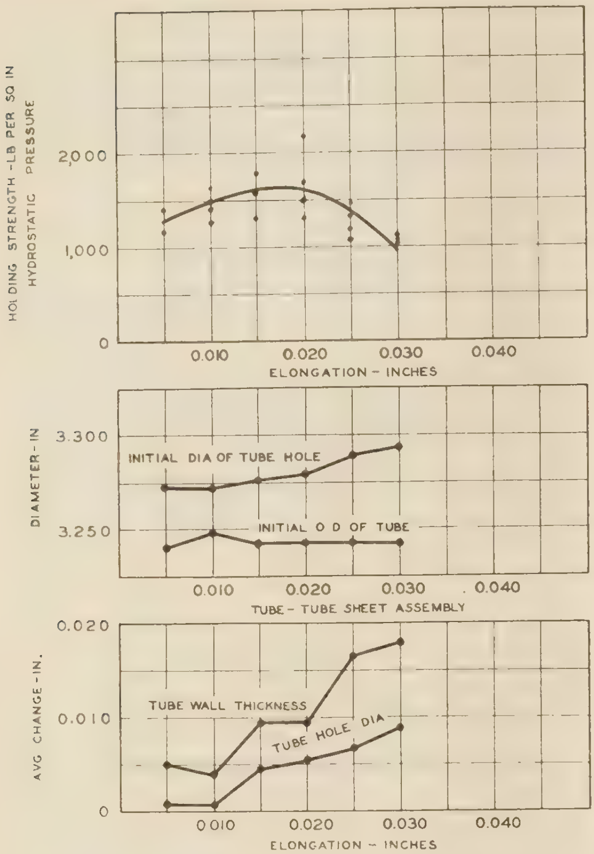

Fig. 7 Test Results for $3^1/_4$-In., 11-Gage Tubes Rolled Into 1-In. Plates

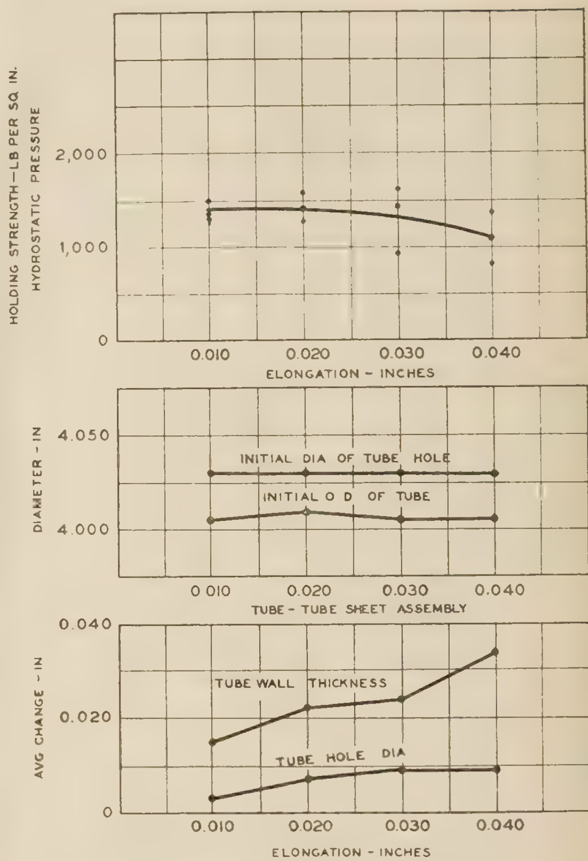

Fig. 8 Test Results for 4-In., 5-Gage Tubes Rolled Into $1^1/_4$-In. Plates

0.016-in. elongation. The hydrostatic test showed 25 slight leaks among 532 tubes (1064 joints). These were corrected by light reexpanding. By either of the conventional methods this condition of tapered holes would probably not have been discovered and serious trouble might have developed.

Other Considerations

There are several other related matters in the expansion of boiler tubes which should be given consideration. These are discussed briefly as follows:

1 *Effect of the Condition of Finish of Surfaces of Tube and Tube Hole on Tightness and Holding Strength.* When joints of any group are rolled-in to uniform elongation, the tightness and holding strength will depend largely on the finish of the surfaces which are forced into contact. It is obvious that a threaded joint between tube and sheet would produce a holding strength equal to the tensile strength of the net area at the root of the thread. This may be regarded as the strongest type of mechanically assembled joint. The minimum value of holding strength might be developed if the surfaces were polished. Logically, the holding strength of a joint in which the tube surfaces had been cleaned, using a mechanical tube cleaner equipped with carborundum cutters of 120-grit grade *H*, would fall between the maximum and minimum values suggested above. The strength of the threaded joint can be calculated if the form of the thread is known. The holding strengths of the joints in which the surface of the tubes had been polished and those in which the tube surface had been cleaned using a mechanical tube cleaner, were determined by hydrostatic test. In both cases the tube holes were smooth bored. The outside diameter of the tube was 3.996 in., the inside diameter was 3.580 in., it had a hardness of 70 Rockwell *B* (124 Brinell), and an approximate tensile strength of 60,000 lb per sq in. Tests on joints showed an average holding strength to be 2033 lb per sq in. for the one having polished tube ends and a holding strength of 3700 lb per sq in. for those joints in which the tube ends were cleaned by a mechanical tube cleaner. The calculated strength of a threaded joint (25 threads per in.) between this size tube and a tube sheet $2^1/_4$ in. thick is 118,800 lb. The total strength of the polished-tube joint was 27,600 lb, and that of the tube of standard finish used in the authors' company was 46,500 lb. It is probable that a machined tube rolled into a roughened hole would show the same holding strength as the roughened tube rolled into a machine-finished tube hole. It is evident from these figures that the condition of the two surfaces is a factor of first importance in the production of joints of high holding strength. It must be concluded that attention to the cleaning of tube ends is an important factor in the production of joints of uniform strength.

2 *The Effect of Hardness of Tube and Sheet Metal on Strength and Tightness of Joints.* Enough data have not been collected to warrant any conclusions in this matter. It merits some study and research.

3 *The Effect of Grooves in the Tube Hole.* Grooved tube holes have been used in an effort to improve the tightness and holding strength of rolled-tube joints. There are, however, few test data available to show the amount of improvement resulting

from this expedient. A. Thum and W. Ruttmann in their "Mitteilungen Nr. 45 der Vereinigung der Grosskesselbesitzer" (Dec., 1933) note in their summary under item 6: "The yield limit (due to a repeated bending movement) can be improved 50 per cent by a groove." Experimental results to establish this statement were not shown. Further investigation of this matter should be made, taking into account the depth, width, and shape of the groove or grooves and their location in the tube hole.

4 *The Function of the Bulge and Flare.* The opinion is held by boiler men that the tightness and strength of the joint depends in part on the bulge and the flare made during the expanding operation. It is true that the flare will prevent the tube from slipping out of the tube hole. When the tube is rolled-in, the backing out of the expander pushes the flare a few thousandths of an inch away from the tube sheet so that the flare does not contribute to the tightness or holding strength of the joint. Also, in many cases the flare is not correctly rolled and its effect on holding strength is therefore doubtful. In the case of flat tube sheets, the initial expanding of both bulge and flare will produce contact completely around the tube. On the other hand, in joints expanded into curved tube sheets excessive work on the flare is necessary to produce contact all around the tube. This produces a rounded edge in the tube hole which makes very difficult the refitting of a new tube in case of replacement. The flare does perform an important function in providing a smooth entrance to the tube which reduces the resistance to flow.

5 *Effect of Lengthening the Tubes Caused by Rolling-in.* The tests which established the elongation method of rolling-in tubes, showed that the tube is lengthened a measurable amount by the rolling operation. The more heavily the tube joint is rolled-in, the greater the lengthening of the tube. If adjacent tubes in a drum or tube sheet are rolled-in to different elongations, the difference in lengthening sets up considerable thrust on the tube which has been rolled the least, or compression on the tube which has been rolled the most. This compression may lead to the bowing of the more heavily rolled-in tube with the possibility of failure because of interference. If it were possible to roll-in all the tubes of a given bank or bundle simultaneously and equally, there would be no difference in lengthening of adjacent tubes. But at present tubes are rolled-in one at a time. The elongation given each tube except the first, imposes a thrust on all tubes that have been previously rolled-in. The presence of accumulation of thrust is especially evident in straight "tack tubes." That this is true is shown by the failure of tack-tube joints during assembling of the boiler, and perhaps more frequent failure after the boiler has been in service for some time. The actual value of this axial loading is a difficult matter to calculate, because of the shapes and arrangements of the tubes in any given boiler. An approximation has been made, however, by actually weighing the axial thrust during the rolling-in operation. This was carried out by having the free end of a short tube, which was being rolled into a 10-in. square plate, exert its axial thrust against the ram on a hydraulic jack. The base of the jack and the plate were rigidly joined together. The hydrostatic pressure shown by the gage on the jack was multiplied by the area of the jack plunger to give the value of the thrust. While this test is not presumed to reproduce the conditions occurring during the erection of a

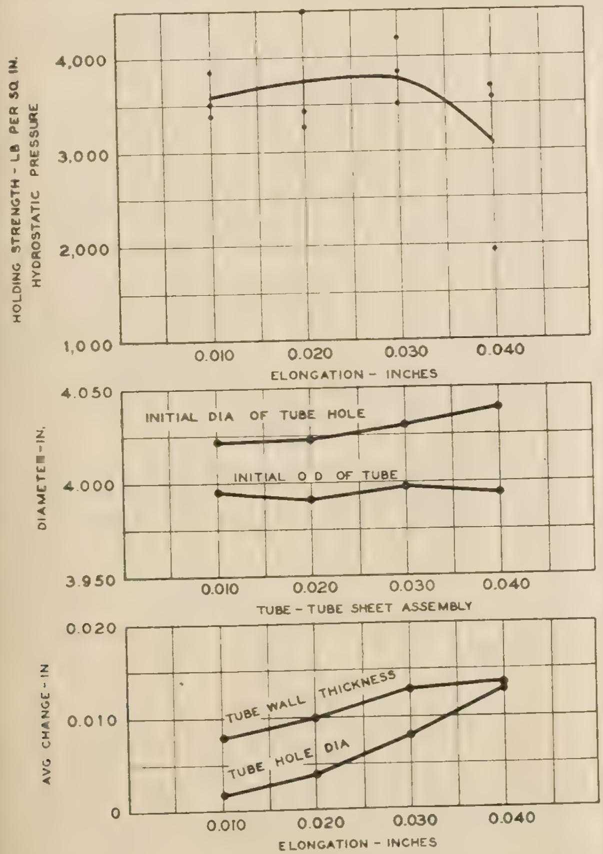

Fig. 9 Test Results for 4-In., 7-Gage Tubes Rolled Into $2^1/_4$-In. Plates

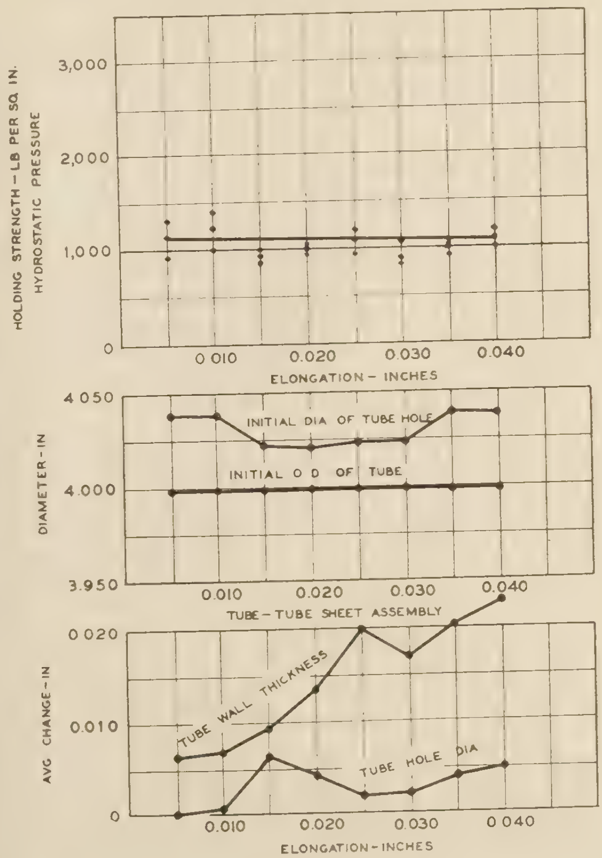

Fig. 10 Test Results for 4-In., 7-Gage Tubes Rolled Into 1-In. Plates

boiler, yet it does indicate the possible magnitude of the thrust. Fig. 11 shows the results obtained in one of the tests described.

The accumulation of thrust, if not controlled, often results in the bulging of the tube sheets, the raising of steam drums off their supports during erection or even the rupture of tubes. Control of cumulative thrust applied to boilers having drums may be effected by either of two procedures. In both cases tack tubes are installed first. They are fully rolled-in at one end and partly rolled-in at the other. Next, the remaining tubes are fully rolled-in at one (usually the upper) end and partly rolled in (usually to 0.005-in. elongation) at the other end. In the first procedure, the partly rolled-in ends are then fully rolled-in proceeding along

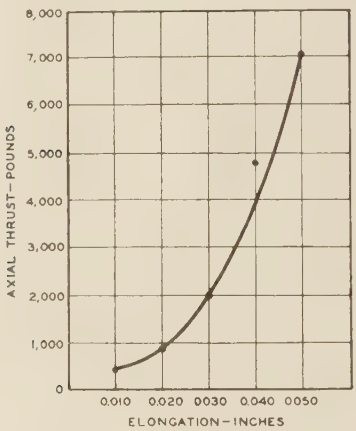

Fig. 11 Axial Thrust Produced by Rolling-in Several $3^1/_4$-In., 7-Gage Tubes 1 Ft Long, Into $1\ ^7/_8$-In. Plates. The Degree of Expansion Is Expressed as Elongation

the length of the drum. In the second procedure, tack tubes are rolled-in as in the first procedure. All remaining tubes are fully rolled-in at one end (usually the upper end), the remaining joints are then rolled-in, starting at the middle of the length of the bank and rolling tubes to full elongation toward the ends of the bank. This divides the amount of accumulated elongation and the consequent thrust in half. In long banks, the rolling-in of the remaining tubes is carried out by dividing the length of the bank into four parts and rolling the tubes in each fourth of the length separately. Any of these methods reduces the amount of accumulated thrust and makes less likely the failure of the joints from this cause.

A few tests were made to determine the characteristics of the expanding tool. These tests were conducted by rolling-in $3^1/_4$-in., 7-gage tubes into $2^3/_{16}$-in. plate. The feed angle was changed for the different tests and a record made of the revolutions of the head of the tool and the time in seconds to complete the joint. The results are given in Table 5.

TABLE 5 CHARACTERISTICS OF THE EXPANDING TOOL

Feed angle of expander, deg.	No. of revolutions of expander head	Time to roll—joint, sec.
1	$18^3/_4$	150
$1^1/_4$	$17^3/_4$	110
$1^1/_2$	$17^1/_2$	90
2	12	60

Conclusions

This paper presents the results of an elementary study of the fundamentals of rolling-in boiler tubes. From these results the following conclusions have been drawn:

1 The rolling-in of boiler tubes may be broken down into two separate phases; in the first the tube is enlarged until it fits the tube hole; in the second the tube is further expanded into tight contact with the wall of the tube hole. Definite control of these two phases of the operation is necessary if the rolling-in is to produce joints of maximum strength and tightness.

2 In the usual methods of rolling-in tubes the two phases are not controlled with the result that uniformity of strength and tightness of joints cannot be assured. Records of such rolled-in joints show that some are under-rolled and others are over-rolled. Over-rolling of joints results in heavy cold-working of the metal of the tube and of that surrounding the tube hole, thus setting up points of high-stress concentration with predisposition to corrosion fatigue.

3 In the "Elongation" method of tube rolling, the two phases of the rolling-in operation are definitely controlled by the use of a dial indicator clamped to the tube being rolled-in. The relationship between elongation and holding strength has been investigated experimentally, using several tube sizes and sheet thicknesses. It appears that the most satisfactory joint is produced when the elongation is about 0.020 in.

4 There are several other matters in the tube-rolling problem which merit investigation. Some of these are: (*a*) The effect of the condition of finish of the surfaces to be forced together in rolling-in a joint. (*b*) The effect of the relative hardness of tube and tube sheet on the tightness and holding strength of the joint. (*c*) The effect of grooves in the tube hole on holding strength and rigidity of the joint.

In this paper little has been said about the tool used for rolling-in the joint. This tool, like most others, has been the result of growth over a period of years. There does seem to be a need for some further development in the tools ordinarily used. In the work done in Germany for the Association of Owners of Large Boilers, A. Thum and W. Ruttmann, the investigators, lay great stress on the effect of rate at which the joint is formed. This rate is a function of rate of feed of the tool and the number of revolutions of the tool to form the joint. They have merely touched on this matter and state that it should be studied further.

Steam-Turbine Leaving Losses and Vacuum Corrections

By LINN HELANDER,[1] MANHATTAN, KAN.

Based upon the discussion of steam flow through non-divergent nozzles with oblique exit faces in "Die Dampfturbinen," by Gustav Flügel,[2] this paper presents a procedure wherewith steam-turbine vacuum corrections may be calculated with a fair degree of accuracy when the design characteristics of the last row of blades and one set of water rates for specified steam conditions and loads are known. The procedure outlined is designed primarily for consulting engineers and power engineers, not for the turbine engineer. On that account certain simplifying assumptions have been introduced. These simplifying assumptions, although perhaps not acceptable where precise results are required, will be found satisfactory for the purposes for which the formulas presented herein have been developed. A comprehensive sample calculation is used to exemplify the procedure outlined.

In addition to a procedure for evaluating vacuum corrections, the paper presents simple formulas for evaluating small increments of isentropic heat drop when the expanding steam is saturated. These formulas give evaluations of small increments of heat drop more accurately than they can be read from ordinary steam charts and may be solved with little if any more labor than is used in reading charts.

Certain formulas are also presented which evaluate the mass rate of steam flow through a blade or nozzle when the critical velocity is reached therein, the mass rate of steam flow through a nozzle or blade when the terminal nozzle or blade pressure is the minimum attainable (that is, when the exhaust-chamber pressure is at or below that corresponding to the limiting vacuum), the rate of change of internal shaft work with a change in the exhaust-chamber vacuum temperature for expansions beyond the critical pressure, and the approximate rate of change of internal shaft work with vacuum temperature when the terminal blade pressure is above the critical pressure. Approximate formulas are given which express the specific volume and latent heat of dry saturated steam in terms of the temperature of the steam. These formulas have been developed for use where the exhaust steam is saturated and where, in addition, the temperature of the exhaust steam does not exceed approximately 140 F.

THE procedure herein proposed for calculating leaving losses and vacuum corrections is based on Flügel's discussion of the flow of steam in nozzles with exit faces not at right angles to the nozzle axis.[2] According to Flügel's analysis, where steam flows through a non-divergent nozzle with an oblique exit face, the velocity of the steam relative to the nozzle at the exit will be directed along the axis of the nozzle so long as the critical velocity is not exceeded; but when the critical velocity is exceeded, the steam leaving the nozzle will be directed, relative to the nozzle, along a line that makes an angle δ with the nozzle axis. Where the pressure in the exhaust chamber does not fall below a certain value P_{vd}, defined as the minimum pressure attainable at the exit boundary of the nozzle, the magnitude of δ can be determined from the continuity equation wherein $M = F_b \sin(\alpha + \delta) V_{ro}/v \sin \alpha$. In this equation, M is the mass velocity of the steam in the nozzle, lb per sec; F_b is the cross-sectional area of the nozzle at the exit face measured at right angles to the axis of the nozzle, sq ft; α is the angle that the nozzle axis makes with the plane of the exit face; V_{ro} is the velocity of the steam measured relative to the nozzle at the exit face, ft per sec; and v is the specific volume of the steam at the exit face; see Fig. 1.

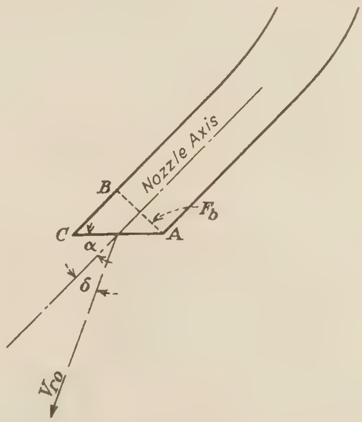

Fig. 1 Expansion of Steam Beyond Critical Pressure in a Non-Divergent Nozzle. When Expansion Proceeds Beyond the Critical Pressure the Relative Leaving Velocity V_{ro} Is Deflected From the Nozzle Axis an Amount δ

The last row of blades of a turbine may be treated as non-divergent nozzles. Then $F_b/\sin \alpha$ becomes the free area of the annulus of the last row of blades, V_{ro} becomes the exit steam velocity relative to the blades, v becomes the specific volume of the steam leaving the blades, M becomes the total mass rate of steam flow through the last row of blades, α becomes the blade angle of the last row of blades, sin α becomes the gaging of the last row of blades, and $(\alpha + \delta)$ becomes the efflux angle of the last row of blades, i.e., the angle that the relative leaving velocity makes with

[1] Head of the Department of Mechanical Engineering, Kansas State College of Agriculture and Applied Science, Manhattan, Kan. Professor Helander was graduated from the University of Illinois in 1915 with the degree of B.S. in mechanical engineering. Since that time he has worked as steam engineer for the Pittsburgh Crucible Steel Company, Midland, Pa.; as general engineer on steam apparatus for the Westinghouse Company, East Pittsburgh and South Philadelphia, Pa.; as a senior engineer for the U.G.I. Contracting Company and the United Engineers and Constructors, Philadelphia, Pa.; and as a consultant. Since 1931 he has been engaged in research and teaching.

[2] "Die Dampfturbinen," by Gustav Flügel, J. A. Barth, Leipzig, 1931.

Contributed by the Power Division for presentation at the Semi-Annual Meeting, Cincinnati, Ohio, June 19 to 21, 1935, of The American Society of Mechanical Engineers.

Discussion of this paper should be addressed to the Secretary, A.S.M.E., 29 West 39th Street, New York, N. Y., and will be accepted until July 10, 1935, for publication at a later date.

the plane of the exit face. Herein, the efflux angle will be denoted by β. When the exhaust-chamber pressure falls below the value P_{vd}, defined above, the circumferential component of the relative exit velocity, in accordance with Flügel's discussion, remains constant as the exhaust-chamber pressure is reduced, and, since the magnitude of this component determines the magnitude of the turning torque on the blades, the turning torque on the blades likewise remains constant under this condition. Consequently, reducing the exhaust-chamber pressure, when it is already at or below the value P_{vd}, has no effect upon the economy of the turbine. The pressure P_{vd} therefore constitutes the true limiting pressure and the corresponding vacuum constitutes the true limiting vacuum.

In accordance with the interpretations of Flügel's discussion given in the preceding paragraph, the following procedure is suggested for evaluating leaving losses:

(*a*) Where the critical velocity is not exceeded in the last row of blades, assume the efflux angle and the blade angle to be identical.

(*b*) Where the critical velocity is exceeded in the last row of blades, calculate the magnitude of the efflux angle by means of the continuity equation.

In order to employ the continuity equation for evaluating the efflux angle when the critical velocity is exceeded, the relative leaving velocity must be known. To obtain this, the following procedure is suggested:

(*a*) From known exhaust conditions, employing curves and formulas presented herein, determine the critical pressure, the quality of the steam at the critical pressure and the relative velocity at the critical pressure, the latter being directed along the blade axis.

(*b*) Having determined the critical pressure and the quality at the critical pressure, determine the isentropic heat drop from the critical pressure to the blade-terminal pressure, i.e., to the exhaust-chamber pressure if the latter is not below P_{vd}, otherwise to P_{vd}, and therefrom, knowing the efficiency of incremental energy conversion in the last row of blades, the actual heat drop from the critical pressure to the terminal-blade pressure.

(*c*) Having determined the relative velocity at the critical pressure and the actual heat drop from the critical pressure to the blade terminal pressure, calculate the relative exit velocity using the formula

$$V_{ro} = \sqrt{(2gJH' + V^2_{rc})}$$

where H' is the actual heat drop from the critical pressure to the blade terminal pressure, V_{rc} is the relative velocity at the critical pressure, and V_{ro} is the relative exit velocity.

The following procedure is suggested for evaluating vacuum corrections: Assuming that the steam rate of the turbine is known for a specified vacuum, calculate the leaving losses implicit in this steam rate. Add these losses, expressed in Btu, to the internal work done per pound of steam as evaluated from the known steam rate, the mechanical efficiency of the turbine, and the generator efficiency. The result will be the gross internal conversion of heat energy into mechanical energy, including in the latter the kinetic energy of the steam. For convenience, designate this quantity by H'_1. Deduct H'_1 from the heat content of the steam as it enters the turbine in order to find the heat content of the steam as it leaves the last row of blades. From the heat content so evaluated, determine the quality of the steam leaving the last row of blades. Therefrom, knowing the nozzle efficiency of incremental energy conversion in the last row of blades and making use of formulas given herein, determine the actual increase in heat drop that will occur when the vacuum is increased to its new value. Add this increase of actual heat drop o H'_1 and deduct from the result the leaving losses evaluated for the new vacuum. From the result so obtained, knowing the efficiency of the generator and the mechanical efficiency of the turbine, the new steam rate can be determined and therefrom the vacuum correction evaluated. When the exhaust pressure is below the critical pressure, determining the critical pressure and the state of the steam at the critical pressure is one part of the above procedure. That the entire procedure is not difficult, will be seen from the following example which illustrates the manner in which vacuum corrections may be evaluated.

Calculation of Vacuum Corrections

The itemized steps of the following example illustrate the method of calculating for vacuum corrections when, as in Case 1, the critical velocity is not exceeded in the last row of blades, and when, as in Case 2, the critical velocity is exceeded in the last row of blades. In both cases, the problem is to determine the steam rate at a vacuum of 29 in. hg when the steam rate is given for a vacuum of $28^1/_2$ in. hg. The symbols used in the problem are those tabulated in the nomenclature while the formulas referred to are found in Appendix A.

		Case 1	Case 2
1	Steam flow through last row of blades, lb per hr.	53,000	123,000
2	Dry steam nozzle efficiency, E'_n, of incremental energy conversion in last row of blades, per cent. Assumed for this problem but should be obtained from manufacturer....................	90	90
3	Gaging = sin α of last row of blades. Should be obtained from manufacturer..................	0.45	0.45
4	F_b = spouting area of last row of blades = free area of annulus of last row of blades multiplied by sin α, sq ft. To be obtained from manufacturer..	9.35	9.35
5	Steam rate, lb per kwhr, with vacuum $28^1/_2$ in. hg. To be obtained from manufacturer........	10.59	9.83
6	Generator and mechanical losses, per cent of gross load. To be obtained from manufacturer or may be estimated from published data......	8.7	4.1
7	Internal steam rate, lb per kwhr. Item 5 × (1 — Item 6/100)...........................	9.67	9.43
8	Internal work per lb steam, Btu per lb = 3415/Item 7...............................	353.5	362.5
9	Heat content of steam entering turbine, Btu per lb, from steam tables.........................	1332.4	1332.4
10	Approximate heat content of steam leaving last row of blades, vacuum $28^1/_2$ in. (Item 9 — Item 8), Btu per lb............................	979	970
11	Heat content of liquid at a vacuum of $28^1/_2$ in., Btu per lb, from steam tables................	59.7	59.7
12	Latent heat of dry saturated steam at a vacuum of $28^1/_2$ in., Btu per lb, from steam tables......	1040.8	1040.8
13	Approximate quality of steam leaving last row of blades, vacuum $28^1/_2$ in. (Item 10 — Item 11)/ Item 12..	0.88	0.87
14	Value of M/F_b, Item 1/Item 4...............	5670	13,150
15	Critical temperature, deg F, i.e., temperature corresponding to critical pressure, from Fig. 3 using curve for which $E_n/X_c = 0.90$. This assumes E_n = (Item 2) X_c..................	74.5	101
16	Value of (M/F_b) sin α. Item 14 × Item 3....	2550	5920
17	Limiting temperature, deg F, i.e., temperature corresponding to limiting vacuum, from Fig. 3..	50	76
18	Temperature corresponding to exhaust-chamber vacuum of $28^1/_2$ in. hg, deg F, from steam tables..	91.8	91.8
19	Estimated quality at critical pressure..........	....	0.87
20	Specific volume of dry saturated steam at critical pressure from steam tables, cu ft per lb........	....	341
21	Approximate relative velocity at critical pressure, ft per sec., Item 14 × Item 19 × Item 20/ 3600..	....	1083
22	Latent heat of dry saturated steam at critical pressure, from steam tables, Btu per lb.........	....	1036
23	Approximate isentropic heat drop from critical pressure to $28^1/_2$ in. vac. from formula 4*a*. $(\text{Item 15} - \text{Item 18})\left[1 + \left(\frac{\text{Item 19} \times \text{Item 22}}{\text{Item 15} + 460}\right)\right] - (\text{Item 18} + 460)\log_e\left[1 + \left(\frac{\text{Item 15} - \text{Item 18}}{\text{Item 18} + 460}\right)\right]$....		14.9
24	Approximate actual heat drop from critical pressure to $28^1/_2$ in. vac. Btu per lb. Item 23 × Item 2 × (Item 19 + Item 13)/2..........	....	11.65
25	Approximate velocity of steam relative to blade at exit boundary face. Vac. $28^1/_2$ in. Ft per sec = $\sqrt{[2g \times 778 \times \text{Item 24} + (\text{Item 21})^2]}$.......	....	1325
26	Specific volume of dry saturated steam at $28^1/_2$ in. vac. from steam tables, cu ft per lb	445.3	445.3
27	Estimated sin β = sin efflux angle, at $28^1/_2$ in. vac. In Case 1, gaging, i.e., Item 3. In Case 2, $\frac{\text{Item 14} \times \text{Item 3} \times \text{Item 26} \times \text{Item 13}}{\text{Item 25} \times 3600}$......	0.45	0.48
28	V_b = mean blade speed of last row of blades, ft per sec. From manufacturer.................	878	878
29	Approximate leaving loss at $28^1/_2$ in., Btu per lb, from formula 1*b*. See calculation *A* in Appendix B[4].	3.7	9.8

30	Approximate total heat converted into mechanical energy, including therein the kinetic energy of the leaving steam, at $28^1/_2$ in., vac., Btu per lb (Item 8 + Item 29)........	357.2	372.3
31	Revised estimate of heat content of steam leaving last row of blades at $28^1/_2$ in. vac., Btu per lb (Item 9 — Item 30)........	975.2	960.1
32	Revised estimate of quality of steam leaving last row of blades, $28^1/_2$ in. vac. (Item 31 — Item 11) /Item 12........	0.88	0.865
33	Heat content at critical pressure, Btu per lb, Item 31 + Item 24........	....	971.75
34	Heat content of liquid at critical pressure from steam tables, Btu per lb........	....	68.9
35	Revised estimate of quality at critical pressure. (Item 33 — Item 34)/Item 22........	....	0.872
36	Revised estimate of isentropic heat drop from critical pressure to $28^1/_2$ in. vac. (Item 15 — Item 18) $\left[1 + \left(\frac{\text{Item 35} \times \text{Item 22}}{\text{Item 15} + 460}\right)\right]$—(Item 18 + 460) $\log_e \left[1 + \left(\frac{\text{Item 15} - \text{Item 18}}{\text{Item 18} + 460}\right)\right]$	....	14.9
37	Revised estimate of actual heat drop from critical pressure to $28^1/_2$ in. vac., Btu per lb. Item 36 × Item 2 × (Item 35 + Item 32)/2........	....	11.65
38	Revised estimate of velocity of steam relative to blade at exit boundary face at $28^1/_2$ in. vac., ft per sec = $\sqrt{[2g \times 778 \times \text{Item 37} + (\text{Item 21} \times \text{Item 35/Item 19})^2]}$........	....	1325
39	Revised estimate of sin β = sin efflux angle, $28^1/_2$ in. vac. For Case 1, Item 3 and for Case 2 $\frac{\text{Item 14} \times \text{Item 3} \times \text{Item 26} \times \text{Item 32}}{\text{Item 38} \times 3600}$......	0.45	0.479
40	Revised estimate of leaving losses at $28^1/_2$ in. vac., Btu per lb, from formula 1*b*. See calculation *B* in Appendix B[4]........	3.7	9.8
41	Temperature corresponding to exhaust-chamber vacuum of 29 in. hg, deg F........	79.1	79.1
42	Isentropic heat drop from $28^1/_2$ in. vac. in Case 1, from critical pressure in Case 2, to vacuum of 29 in., Btu per lb, for Case 1, (Item 18 — Item 41) $\left[1 + \left(\frac{\text{Item 32} \times \text{Item 12}}{\text{Item 18} + 460}\right)\right]$ — (460 + Item 41) $\log_e \left[1 + \left(\frac{\text{Item 18} - \text{Item 41}}{\text{Item 41} + 460}\right)\right]$ For Case 2, substitute Item 15 for Item 18, Item 35 for Item 32, and Item 22 for Item 12........	21.2	35.6
43	Estimated actual heat drop from $28^1/_2$ in. vac. to 29 in. vac. in Case 1, and from critical pressure to 29 in. vac. in Case 2. Item 42 × average quality × Item 2 = Item 42 × Item 32 × Item 2, approximately........	16.75	27.70
44	Approximate heat content of steam leaving last row of blades at 29 in. vac., Btu per lb. Case 1, Item 31 — Item 43. Case 2, Item 33 — Item 43........	958.45	944.05
45	Heat content of liquid at 29 in. vac., from steam tables, Btu per lb........	47	47
46	Latent heat of dry steam at 29 in. vac., Btu per lb........	1048	1048
47	Quality of steam leaving last row of blades at 29 in. vac. (Item 44 — Item 45)/Item 46......	0.87	0.856
48	Revised estimate of actual heat drop from $28^1/_2$ in. vac. to 29 in. vac. in Case 1, and from critical pressure to 29 in. vac. in Case 2. Case 1, Item 42 × Item 2 × (Item 47 + Item 32)/2. Case 2, Item 42 × Item 2 × (Item 35 + Item 47)/2	16.7	27.70
49	Velocity of steam relative to blade at exit from last row in Case 2 at 29 in. vac., ft per sec = $\sqrt{\left[2g \times 778 \times \text{Item 48} + \left(\frac{\text{Item 21} \times \text{Item 35}}{\text{Item 19}}\right)^2\right]}$....		1600
50	Specific volume of dry saturated steam at 29 in. vac., from steam tables, cu ft per lb........	652.7	652.7
51	Sin β = sin efflux angle at 29 in. vac. Case 1, Same as Item 3. Case 2, $\frac{\text{Item 14} \times \text{Item 3} \times \text{Item 50} \times \text{Item 47}}{\text{Item 49} \times 3600}$......	0.45	0.574
52	Cos β = cos $\sin^{-1}$ Item 51........	0.893	0.819
53	Leaving losses at 29 in. vac., Btu per lb, from formula 1*b*. See calculation *C* in Appendix B[4].	3.4	20.9
54	Total gross conversion of heat into mechanical energy at 29 in. vac. Case 1, Item 8 + Item 40 + Item 48. Case 2, Item 8 + Item 40 — Item 37 + Item 48........	373.9	388.3
55	Net conversion of heat into internal shaft work at 29 in. vac., Btu per lb. Item 54 — Item 53..	370.5	367.4
56	Internal steam rate at 29 in. vac., lb per kwhr. 3415/Item 55........	9.22	9.30
57	External steam rate at 29 in. vac., lb per kwhr. $\frac{\text{Item 56}}{(1 - \text{Item 6}/100)}$........	10.10	9.70
58	Per cent reduction in internal steam rate due to change of vacuum. (Item 55 — Item 8)/ Item 55	4.6	1.33

The foregoing procedure assumes that the actual increment of heat drop due to a change of vacuum is equal to the incremental isentropic heat drop multiplied by the nozzle efficiency of incremental energy conversion in the last row of blades. This is correct when the critical pressure has been attained in the last row of blades; otherwise it is an approximation. The procedure assumes also that the influence of leakage losses in the last row of blades can be ignored; likewise variations in E'_n, the dry-steam nozzle efficiency of incremental energy conversion. Although these assumptions are satisfactory for general purposes, the turbine designer very likely will want to take cognizance of the fact that leakage losses influence the result and may increase when the exhaust-chamber pressure is reduced below the critical pressure, also of the fact that E'_n may vary with a change in the exhaust pressure and the rate of steam flow.[3] In evaluating E_n, the nozzle efficiency applicable for the

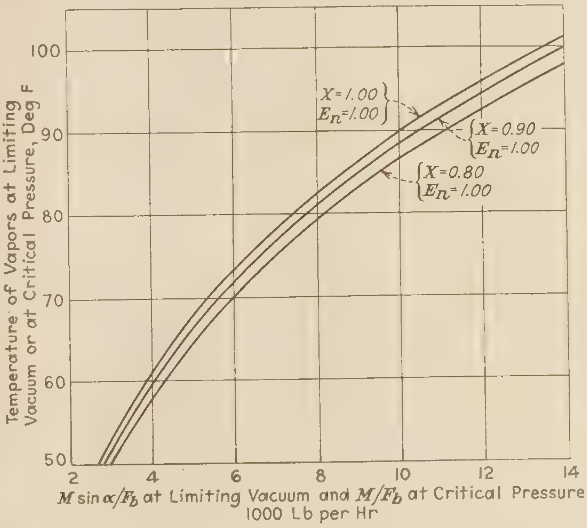

Fig. 2 Values of M Sin α/F_b at Limiting Vacuum and of M/F_b at Critical Pressure Assuming Nozzle Efficiency of Incremental Energy Conversion in Last Row of Blades to Be Unity

$(M_d \sin \alpha/F_b = 3600\sqrt{[(k_d g P'_{vd})/(v_{vd} X_d)]}$
$M_c/F_b = 3600\sqrt{[(k_c g P'_{vc})/(v_{vc} X_c)]}$
$k = 1.035 + 0.1\ X)$

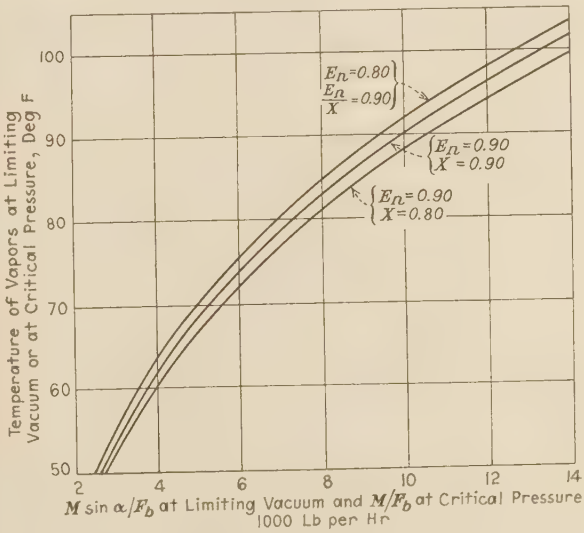

Fig. 3 Values of M Sin α/F_b at Limiting Vacuum and of M/F_b at Critical Pressure Assuming Nozzle Efficiency of Incremental Energy Conversion in Last Row of Blades to Be as Indicated. Curves Obtained by Use of Formulas [2*b*] and [8*b*]

[3] "Die Düsencharakteristik," by Gustav Flügel. *Forschungsarbeiten auf dem Gebiete des Ingenieurwesens*, No. 217, Berlin, 1919.

incremental heat drop, E'_n was multiplied by the average quality of the steam during its incremental expansion. This is consistent with the practice of reducing the efficiency of a stage 1 per

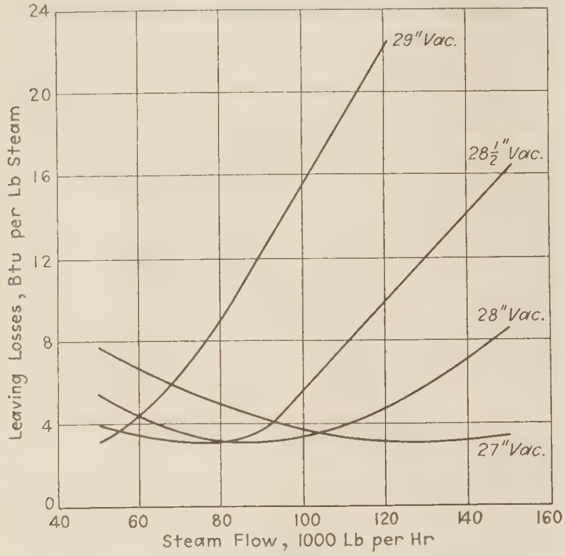

Fig. 4 Leaving Losses Assuming X = 0.88 and E_n = 0.90 Calculated by Use of Formula [1b]

(Blade speed V_b = 878 ft per sec, sin α = gaging = 0.45, and F_b = 9.35 sq ft.)

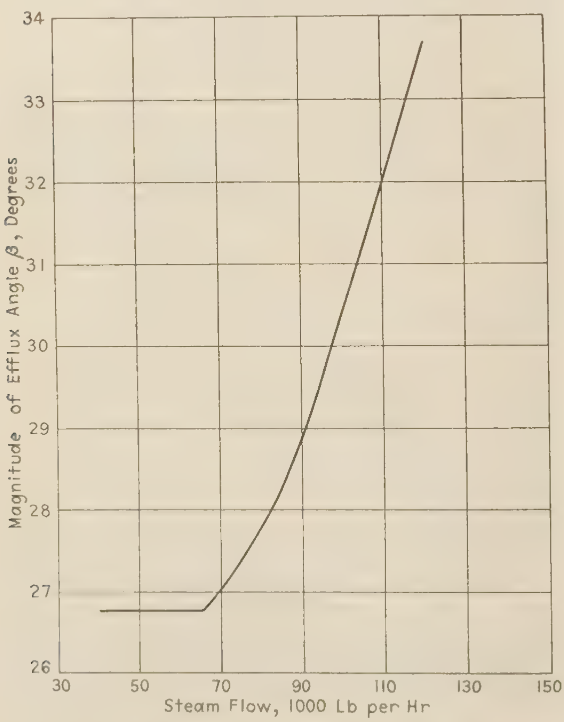

Fig. 5 Magnitude of Efflux Angle β Corresponding to Leaving-Loss Curve for a Vacuum of 29 In. Hg Given in Fig. 4

cent for each average per cent of moisture in the steam in the stage. Actually, however, the effect of a unit percentage of moisture on the efficiency of incremental energy conversion within a blade may be less than its effect on the over-all stage efficiency, and further it may differ appreciably in the nozzle proper and in the triangular section following section F_b of Fig. 1. Time did not permit of a more comprehensive investigation of the influence of moisture, but a discussion of this will be welcomed.

Fig. 2 shows values of the saturation temperature corresponding to the limiting pressure P_{vd} when the abscissas represent $M \sin \alpha/F_b$ and of the saturation temperature corresponding to the critical pressure when the abscissas represent M/F_b, the nozzle efficiency of incremental energy conversion in both cases being unity. Fig. 3 is the same as Fig. 2 except that the nozzle efficiency of incremental energy conversion is no longer assumed to be unity; also the data plotted in Fig. 3 were obtained from a formula developed by the writer while those plotted in Fig. 2 were obtained from formula [45] in Flügel's "Die Dampfturbinen."[2] The curves of these two figures should agree approximately where the ratios of E_n/X are identical. Fig. 4 shows curves of charac-

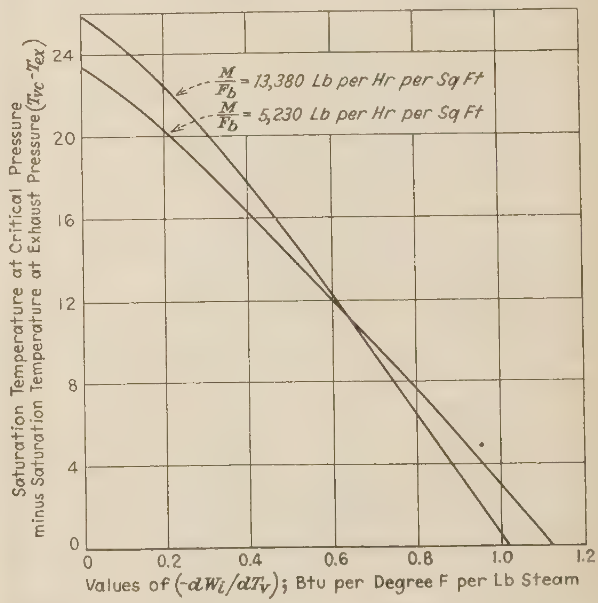

Fig. 6 Rate of Change of Internal Shaft Work With a Change of Vacuum Temperature, i.e., Increment of Internal Shaft Work Per Pound of Steam Per Degree Decrease in Vacuum Temperature When Exhaust Pressure Is Below Critical Pressure

(E_n = 0.90, X = 0.90, and sin α = gaging = 0.45.)

teristic leaving losses calculated by assuming the quality of the exhaust steam to be 88 per cent and the nozzle efficiency of incremental energy conversion in the last row of blades to be 90 per cent. The spouting area of the last row of blades, F_b, was assumed to be 9.35 sq ft and the gaging was assumed to be 45 per cent in developing Fig. 4 as was assumed in the illustrative example previously presented. Fig. 5 shows values of β, the efflux angle of the last row of blades, corresponding to the data presented in Fig. 4.

From Figs. 2 and 3 it will be seen that the depression of the temperature corresponding to the limiting vacuum below that corresponding to the critical pressure is approximately 25 F when the gaging, i.e., sin α, is 0.45, and 33 F when the gaging is 0.35. The value of 25 F for 45 per cent gaging is verified also by the curves of Fig. 6 which show values of $(-dW_i/dT_v)$, the rate of change of internal work with a change of vacuum temperature, plotted as abscissas and the difference between the satura-

tion temperature at the critical pressure and that at the exhaust-chamber pressure as ordinates. Here the difference between the saturation temperature at the critical pressure and that at the limiting vacuum is the ordinate where $(-dW_i/dT_v) = 0$.

The author is grateful for the many helpful suggestions offered to him during the preparation of this manuscript; to W. E. Caldwell and his associates on the Power Division Executive Committee of the A.S.M.E. for their interest in the paper; and to various members of the engineering staff of Kansas State College who assisted with translations and with the correction of the manuscript.

Nomenclature

a = free fraction of area of annulus of last row of blades
β = efflux angle of last row of blades
α = blade angle of last row of blades
C = specific heat, Btu per lb per deg F
C_w = specific heat of water = 1, approximately
D'_m = mean diam of last row of blades, ft
E_n = nozzle efficiency of incremental energy conversion in last row of blades. E_n is the efficiency with which the next increment of isentropic heat drop selected is converted into relative kinetic energy, i.e., into kinetic energy of the expanding steam measured relative to the blade. Thus

$$E_n(dH) = \frac{d(V^2_r)}{2 \times 778g} \quad \text{or} \quad E_n(\Delta H) = \frac{V^2_{r2} - V^2_{r1}}{2 \times 778g}$$

where V_r = velocity of steam relative to blade, ft per sec
E'_n = dry-state value of E_n
F_b = spouting area, last row of blades = $a\pi D'_m L_b \sin\alpha$, sq ft
g = acceleration of gravity, ft per sec per sec
H = isentropic heat drop, Btu per lb
H_{12} = isentropic heat drop, state 1 to state 2, Btu per lb
h_{ex} = heat content of steam leaving the last row of blades, the quality of this steam being X; Btu per lb
h_f = heat content of saturated liquid at pressure of steam leaving last row of blades, Btu per lb
j = leaving losses = kinetic energy of steam leaving last row of blades, Btu per lb
k = $1.035 + 0.1X$; $k_c = k$ when $X = X_c$, and $k_d = k$ when $X = X_d$
L_b = blade height, ft
M = steam leaving last row of blades, lb per hr
M_c = steam leaving last row of blades when critical pressure exists at exit section F_b (see Fig. 1), lb per hr
M_d = steam leaving last row of blades when pressure at blade exit section CA of Fig. 1 is that corresponding to the limiting vacuum, lb per hr
P_v = pressure of steam leaving last row of blades, lb per sq in.
P_{vc} = critical pressure of steam in last row of blades, lb per sq in.
P'_{vc} = critical pressure of steam in last row of blades, lb per sq ft
P_{ex} = pressure existing in the exhaust chamber, lb per sq in.
P_{vd} = limiting pressure, lb per sq in.
P'_{vd} = limiting pressure, lb per sq ft
r_v = latent heat of vapors leaving last row of blades, Btu per lb
r_{vd} = latent heat of vapors at limiting pressure, P_{vd}, Btu per lb
r_{vc} = latent heat of vapors at critical pressure, Btu per lb
r_s = Latent heat of steam leaving last row of blades = Xr_v, where X is quality of steam, Btu per lb
s = entropy, Btu per deg F
T_v = absolute temperature of steam leaving last row of blades, deg F
T_{vc} = absolute temperature of steam at critical pressure, P_{vc}, deg F
T_{vd} = absolute temperature of steam at limiting pressure, P_{vd}, deg F
T_{ex} = absolute temperature of steam in exhaust chamber, deg F
V = velocity, ft per sec
V_{ro} = velocity of steam leaving last row of blades measured relative to blade, ft per sec
V_b = mean velocity of blade, ft per sec
V_o = absolute velocity of steam leaving last row of blades, ft per sec
V_{rc} = critical relative velocity of steam in last row of blades, ft per sec
v_v = specific volume of dry saturated vapors leaving last row of blades, cu ft per lb
v_{vd} = specific volume of dry saturated vapors at limiting pressure, P_{vd}, cu ft per lb
v_{vc} = specific volume of dry saturated vapors at critical pressure, P_{vc}, cu ft per lb
W_i = internal shaft work, Btu per lb steam
X = dry fraction of steam leaving last row of blades
X_d = dry fraction of steam leaving last row of blades when terminal pressure in blades is the limiting pressure, P_{vd}
X_c = dry fraction of steam at section F_b of last row of blades when critical pressure P_{vc} exists at that section
z = $5.99 \log_e (T_v/550) + 12{,}200\,(550 - T_v)/550\,T_v$
z_c = value of z at critical pressure, P_{vc}, i.e., when $T_v = T_{vc}$
z_d = value of z at limiting pressure, P_{vd}, i.e., when $T_v = T_{vd}$

Appendix A

The following formulas will be helpful in evaluating leaving losses and vacuum corrections. Their derivation will be given in Appendix B.[4] Definitions of symbols are given in the nomenclature.

I Formulas for evaluating leaving losses.

$$j = \frac{V^2_{ro} + V^2_b - 2V_bV_{ro}\cos\beta}{2g \times 778} \qquad [1a]$$

$$= \frac{[X(M/F_b)(\sin\alpha/\sin\beta)v_v]^2}{64.9 \times 10^{10}} + \frac{V_b^2}{5.01 \times 10^4} - \frac{XV_b(M/F_b)(\sin\alpha/\sin\beta)v_v\cos\beta}{9.02 \times 10^7} \qquad [1b]$$

$$= \frac{[X(M/F_b)(\sin\alpha/\sin\beta)e^z]^2}{29.56 \times 10^6} + \frac{V_b^2}{5.01 \times 10^4} - \frac{XV_b(M/F_b)(\sin\alpha/\sin\beta)e^z\cos\beta}{1.925 \times 10^5} \qquad [1c]$$

Note: Formula [1c] expresses j as a function of the terminal temperature of the steam and, therefore, is in such form that the derivative dj/dT_v can be evaluated.

II Mass velocity of steam leaving last row of blades when critical pressure exists at blade exit section F_b.

$$M_c/F_b = \frac{10^3}{X_ce^{z_c}} \sqrt{\left(\frac{X_cr_{vc}E_n}{0.678\left[\dfrac{9.07r_{vc}}{T_{vc}} - 1 - E_n + \dfrac{T_{vc}(1 - 0.55X_c)}{X_cr_{vc}}\right]}\right)} \qquad [2a]$$

[4] Appendix B has been filed in the Archives of the Society and may be obtained upon request.

$$M_c/F_b = \frac{10^3 \times 569}{X_c v_{vc}} \sqrt{\left(\frac{X_c r_{vc} E_n}{\left[\frac{9.07\, r_{vc}}{T_{vc}} - 1 - E_n + \frac{T_{vc}(1 - 0.55X_c)}{X_c r_{vc}}\right]}\right)} \quad [2b]$$

$$M_c/F_b = 3600 \sqrt{[(E_n/X_c)\ (k_c g P'_{vc}/v_{vc})]}, \text{ approximately} \ldots [2c]$$

In formula [2c] $k_c = (1.035 + 0.1\, X_c)$, see Flügel's Die Dampfturbinen, page 69.[2] Formula [2c] is derived by recognizing from formula [2a] that $M_c/F_b = (\sqrt{E_n}) \times [(M_c/F_b)$ evaluated for $E_n = 1]$, approximately; also by employing the equation for the velocity of sound.

III Critical velocity of steam in last row of blades.

$$V_{rc} = 130.2 \sqrt{\left[\frac{X_c r_{vc} E_n}{0.678\left(\frac{9.07 r_{vc}}{T_{vc}} - 1 - E_n + \frac{T_{vc}(1 - 0.55X_c)}{X_c r_{vc}}\right)}\right]} \ldots [3a]$$

$$V_{rc} = \frac{(M_c/F_b)\ X_c v_{vc}}{3600} \ldots [3b]$$

$$V_{rc} = \sqrt{(E_n k_c g P'_{vc} X_c v_{vc})} = 52.5\sqrt{(E_n k_c X_c T_{vc})}, \text{ approximately} \ldots [3c]$$

IV Small increments of isentropic adiabatic heat drop when low-pressure saturated steam is the expanding medium.

$$H_{12} = (T_{v1} - T_{v2})(C_{w12} + X_1 r_{v1}/T_{v1}) - C_{w12} T_{v2} \log_e(T_{v1}/T_{v2}) \ldots [4a]$$

$$H_{12} \text{ (approximate)} = X_1 r_{v1} \log_e(T_{v1}/T_{v2}) \ldots [4b]$$

$$dH = -dT_v X r_v / T_v \ldots [4c]$$

where T_{v1}, X_1, r_{v1} = initial absolute temperature, quality, and latent heat, respectively, of the expanding steam; T_{v2} = terminal absolute temperature of the expanding steam, deg F; and C_{w12} = average specific heat of water between states 1 and 2, = unity approximately for temperature range herein considered, Btu per lb per deg.

V Specific volume of dry saturated water vapors between 40 F and 140 F.

$$v_v = 468.5 e^z \ldots [5]$$

VI Latent heat of water vapors between 40 F and 140 F.

$$r_v = 1344.3 - 0.55\, T_v \ldots [6]$$

Error = +0.7 Btu when $T_v = (140 + 460)$ F, and +0.2 Btu when $T_v = (\ 40 + 460)$ F.

VII Rate of change of internal shaft work with change of vacuum temperature.

$$-\frac{dW_i}{dT_v}\text{ (where critical pressure is attained)} = \frac{V_b \sin\beta}{\cos\beta}\left\{\frac{3600\, E_n r_v F_b}{T_v M\ (\sin\alpha) v_v} + \frac{M(\sin\alpha) v_v X}{90{,}200{,}000\, F_b}\left[\frac{(1 + E_n)}{T_v} - \frac{9.07 r_v}{T_v^2} - \frac{(1 - 0.55X)}{X r_v}\right]\right\} . [7a]$$

$$-\frac{dW_i}{dT_v}\text{ (Where critical pressure is not attained)} = \frac{E_n X r_v}{T_v} + \left[\frac{(1 + E_n)}{T_v} - \frac{9.07 r_v}{T_v^2} - \frac{(1 - 0.55X)}{X r_v}\right]\left[\frac{\left(\frac{M}{F_b}\frac{v_v X}{468.5}\right)^2}{14.78 \times 10^5} - X\left(\frac{M}{F_b}\right)\left(\frac{v_v V_b \cos\alpha}{468.5 \times 1.925 \times 10^5}\right)\right] \ldots [7b]$$

(Formula [7b] is approximate.)

VIII Mass velocity of steam leaving last row of blades when limiting pressure P_{vd} exists at exit face of blade; i.e., when exhaust-chamber vacuum is greater than or equal to the limiting vacuum.

$$M_d/F_b \text{ (when } E_n = \text{unity)} = 3600\, \frac{\sqrt{(k_d g P'_{vd}/v_{vd} X_d)}}{\sin\alpha}$$

(see formula 45 in Die Dampfturbinen[2] by Flügel) ..... [8a]

$$M_d/F_b = \left(\frac{10^3 \times 569}{(\sin\alpha) X_d v_{vd}}\right) \sqrt{\left(\frac{X_d r_{vd} E_n}{\frac{9.07 r_{vd}}{T_{vd}} - 1 - E_n + \frac{T_{vd}(1 - 0.55X_d)}{X_d r_{vd}}}\right)} \ldots [8b]$$

$$M_d/F_b = 3600\, \frac{\sqrt{[(E_n/X_d)(k_d g\, P'_{vd}/v_{vd})]}}{\sin\alpha} \text{ approximately. } [8c]$$

Principles Underlying the Rational Solution of Automatic-Control Problems

By SERGEI D. MITEREFF,[1] PETERSBURG, VA.

The author presents twelve fundamental equations covering the characteristics of automatic regulators. It is the author's belief that six of these equations completely cover all present forms of commercial regulators. The additional six equations cover modifications and improvements which will permit greatly increased accuracy and flexibility of automatic control and will permit a satisfactory solution of those control problems which could not be handled with complete success by previous types of regulators.

IN SPITE of the widespread use of automatic regulators and governors in all branches of industry, little has been published relative to the fundamental principles of the subject. In the absence of data necessary for rational solutions the majority of automatic-control problems are solved at present by purely empirical methods.

Because of the variety of automatic-control apparatus on the market, it is a difficult task to select the regulator suited exactly to the requirements of a given installation. The adjustment of a regulator after its selection and installation is a problem in itself, inasmuch as the usual cut-and-try method of adjustment is very tedious and unreliable. Therefore, the development of a solid basis for a rational approach to the problem of automatic control is a matter of considerable practical importance.

Principal Factors of an Automatic-Control Installation

Any automatic-control installation can be considered as consisting of two major parts which are, (*a*) the system to be controlled, and (*b*) the automatic-control apparatus added to this system in order to produce the desired result.

The system external to the regulator can be divided into four factors common to any control installation, practically without exception, these are: (*a*) storage of a fluid or energy, (*b*) inflow of a fluid or energy to the storage, (*c*) outflow of a fluid or energy from the storage, and (*d*) a function (temperature, pressure, speed, level, etc.) which is indicative of the amount of fluid or energy in storage and which it is desired to maintain constant.

It should be pointed out that either the inflow or the outflow of fluid or energy is capable of being varied at will, while the other flow varies under the influence of factors which cannot be controlled.

It is evident, therefore, that an automatic-control problem consists essentially of equalizing automatically the rate of flow to the storage with the rate of flow from the storage, this being the necessary condition for maintaining constant both the amount of fluid or energy in the storage and the function indicative of the amount of fluid or energy in the storage.

Taking as an example the speed control of a turbine-generator unit, the energy-storing capacity of the rotating parts will be identified as the storage. The flow of steam to the turbine is the inflow of energy which can be controlled, while the electrical output of the generator is the outflow of energy varying under the influence of the demand which is not under our control. The speed of the turbine is, of course, the function which we desire to maintain constant and which is indicative of the amount of energy stored in the rotating mass.

Analyzing the example of the temperature control of a gas-fired oven, the storage is represented by the heat-storing capacity of the oven. The flow of energy under our control is the inflow of gas to the oven. The uncontrollable flow of energy is the heat loss from the oven by radiation and heat absorption of the product. The temperature in the oven is the function indicative of the amount of heat stored in the oven and which it is desired to maintain constant. These examples are typical and could be extended considerably.

Principal Parts of an Automatic-Control Apparatus

An automatic-control apparatus consists of (*a*) the impulse-receiving element, (*b*) the final operating element, and (*c*) the operative connection between the impulse-receiving element and the final operating element.

The function of the impulse-receiving element is to produce a force or motion proportional to the function to be maintained constant. In a pressure regulator, for instance, the impulse-receiving element is represented by a diaphragm acted upon by the pressure transmitted from the tank through a pilot line. In a thermocouple type of temperature regulator, the impulse-receiving element consists of the thermocouple and the galvanometer. In a speed governor, the flyball pendulum constitutes the impulse-receiving element.

The function of the final operating element is to modify the rate of the controllable flow of fluid or energy. In most cases the final operating element is simply a valve or an electrical contactor.

The function of the operative connection is, first, to provide the desired characteristic of the automatic-control apparatus and, second, to generate a sufficient force for actuating the final operating element.

Characteristic of an Automatic-Control Apparatus

In spite of the fact that the concept of the characteristic of a regulator or governor is one of the most important factors entering into the general problem of automatic control, it has received little attention in literature on the subject. This oversight is very surprising, especially in view of many elaborate attempts to cover such comparatively insignificant factors as "lack of sensi-

[1] Jun. A.S.M.E. Mr. Mitereff was born at Pskov, Russia, in 1902. He was a member of Pskov Cadet Corps and was educated at the Russian Naval Academy, Engineering Division, Vladivostok. In 1927 he was graduated with honor from Johns Hopkins University, receiving a B.S. in mechanical engineering. From the time of his graduation from Johns Hopkins until 1933, he was assistant engineer in the power and development sections of the Atmospheric Nitrogen Corporation, Hopewell, Va. He now resides in Petersburg, Va., and is engaged in the preparation of a book on the subject of automatic regulation.

Contributed by the Power Division for presentation at the Semi-Annual Meeting, Cincinnati, Ohio, June 19 to 21, 1935, of The American Society of Mechanical Engineers.

Discussion of this paper should be addressed to the Secretary, American Society of Mechanical Engineers, 29 West 39th Street, New York, N. Y., and will be accepted until July 10, 1935, for publication at a later date.

tiveness" and "sticking," factors which hardly deserve more than a passing remark to the effect that they could and should be kept down to a required minimum in any properly designed automatic-control apparatus.

By the characteristic of an automatic-control apparatus is meant the relationship between the primary impulse actuating the apparatus and its final effect. The best, since the most definite, way of expressing this relationship is by means of a mathematical equation. By the primary impulse is meant the extent of change of a form of energy derived from the variation of the function to be controlled from its value corresponding to the normal value of the controlled function. By the final effect is meant the extent of actuation of the final operating element of the regulator. It should be pointed out that the mathematical equation expressing the characteristic of a control apparatus gives the relationship between the primary impulse and the final effect both measured at the same moment under consideration.

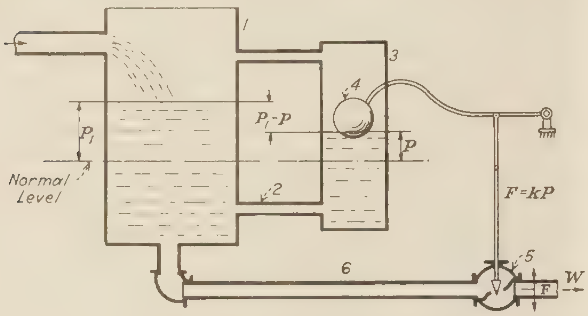

Fig. 1 An Automatic Level-Control Installation With One Pilot Line

(The following equations express the relationship between the level in the float chamber and the level in the tank.)

(a) $P_1 - P = k_1 \frac{dP}{dT}$; $P_1 = P + k_1 \frac{dP}{dT}$ —Pilot line 2 has fluid friction but no inertia

(b) $P_1 - P = k_2 \frac{d^2P}{dT^2}$; $P_1 = P + k_2 \frac{d^2P}{dT^2}$ —Pilot line 2 has inertia but no fluid friction

(c) $P_1 - P = k_1 \frac{dP}{dT} + k_2 \frac{d^2P}{dT^2}$; $P_1 = P + k_1 \frac{dP}{dT} + k_2 \frac{d^2P}{dT^2}$—Pilot line has both fluid friction and inertia

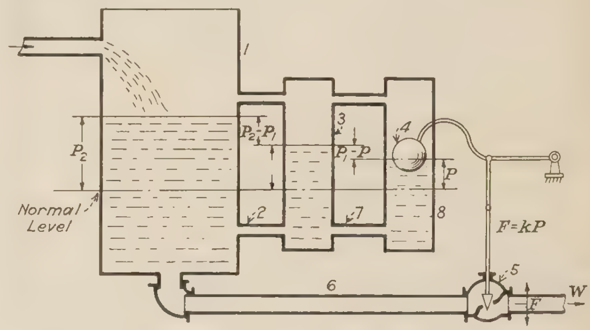

Fig. 2 An Automatic Level-Control Installation With Two Pilot Lines

(The following equations express the relationship between the level in the float chamber and the level in the tank.)

(d) $P_2 = P + k_1 \frac{dP}{dT} + k_2 \frac{d^2P}{dT^2}$—Plot lines 2 and 7 have only fluid friction

(e) $P_2 = P + k_1 \frac{dP}{dT} + k_2 \frac{d^2P}{dT^2} + k_3 \frac{d^3P}{dT^3}$—Of the pilot lines 2 and 7 one has only friction while the other has both friction and inertia

(f) $P_2 = P + k_1 \frac{dP}{dT} + k_2 \frac{d^2P}{dT^2} + k_3 \frac{d^3P}{dT^3} + k_4 \frac{d^4P}{dT^4}$—Both pilot lines have friction and inertia

k_1, k_2, k_3, and k_4 Constants of proportionality depending upon the physical dimensions of the system

In the above example of the temperature control in a gas-fired oven, the primary impulse takes the form of the value of the thermoelectric current (or potential) generated by the thermocouple by which it deviates from its normal value corresponding to the normal temperature in the oven. The final effect is represented in this case by the distance between the position of the valve admitting gas to the oven at the moment under consideration and the position of the valve at the beginning of operation of the regulator when the temperature was held constant at its normal value.

Time Lag in a Control Installation

One of the greatest practical difficulties encountered in an automatic-control installation is the phase displacement between different factors commonly known as the time lag. The time lag is caused by fluid friction, resistance to heat flow, and inertia forces inherent in any physical layout, and the most frequent factor contributing to the time lag is the fluid friction and inertia of the impulse-transmitting means. For instance, in the case of a pressure regulator, the friction and inertia of the liquid in the pilot line connecting the tank with the regulator distort considerably a perfect correspondence between the pressure in the tank and the pressure as reaching the regulator.

Another source of time lag is the inertia and friction of the fluid in the pipe in which the regulating valve is located. For instance, in the case of the speed control of a hydraulic turbine there exists a phase displacement between the opening of the gate and the rate of water flow through it because of inertia of water in the penstock.

It should be pointed out that the aforementioned types of time lag are very often unavoidable features of the control installation in contradistinction to the time lag frequently encountered in the regulator itself which, as a rule, can be eliminated by correct design. It will be clear, therefore, that since some of the principal causes of the time lag cannot be eliminated, means should be found in such cases to counteract the time lag by selecting a regulator which has a characteristic suitable for just this particular purpose.

In order to pave the way for a rational solution of the problem of the time lag, a typical control installation will be analyzed. In Figs. 1 and 2 is shown an automatic level-control installation where the float (4) is placed in a float chamber connected by a pilot line to the tank (1). Equations (a), (b), and (c) in Fig. 1 express the relationship between the level in the float chamber (3) and the level in the tank (1) if only one pilot line is used. Equations (d), (e), and (f) in Fig. 2 give the relationship between these levels when two pilot lines in series are used. In both of these cases the conditions when the pilot line has only fluid friction, only inertia, and both friction and inertia are covered by these equations.

The time lag arising from the use of a pilot line is typical of any other source of time lag in any other part of controlled system. Therefore, the equations in Figs. 1 and 2 have the virtue of universality and they are applicable to any type of automatic-control installation, whatsoever, including automatic piloting of ships and aircraft.

It will be clear also that in order to obtain the level in the tank from the indication of the level in the float chamber, it is only necessary to design an automatic-control apparatus which would solve automatically the given equations. It is rather surprising that there are at present no commercial automatic controls which have the characteristics capable of performing this task.

The exact mathematical solution of the time lag, caused by inertia of fluid in the pipe (6) as affected by the extent of opening of the regulating valve (5) and the corresponding rate of flow

through it, is rather complex. It could be shown, however, that if we increase the opening of the valve (5) by the amount equal to $k_2 \frac{dP}{dT}$, the rate of flow through the valve (5) will closely correspond to the change of level in the float box.

In other words, by designing a regulator which has the characteristic $F = k_1P + k_2 \frac{dP}{dT}$ we can obtain the relationship $W = kP$, where W = the rate of flow through pipe (6), P = the extent of change of the level in the float box, F = the distance traversed by the valve (5), k_1, k_2, and k = constants of adjustment, and T = time.

In this way the retarding effect of inertia of the fluid in the pipe (6) could be almost completely counteracted. This method of counteracting the inertia of fluid in the pipe in which the regulating valve is located is applicable equally well in the case of the speed governing of a hydraulic turbine, and many other automatic-control installations.

Classification of the Automatic-Control Apparatus

All automatic-control apparatus now in commercial use, practically without exception, can be grouped according to their characteristics (expressed by the equations) under only six classes:

I $\quad F = k_1\int PdT + (C)$ ....[1]

II $\quad F = k_1P$ ....[2]

III $\quad F = k_1\int PdT + k_2P + (C)$ ....[3]

IV $\quad F + k_2\frac{dF}{dT} = k_1P$ ....[4]

V $\quad k_3\int FdT + F = k_1\int PdT + k_2P$ ....[5]

VI $\quad F + k_3\frac{dF}{dT} = k_1 \int PdT + k_2P + (C)$ ....[6]

The following classes of automatic-control apparatus are more or less new to the art:

VII $\quad F = k_1P + k_2 \frac{dP}{dT}$ ....[7]

VIII $\quad F = k_1\int PdT + k_2P + k_3 \frac{dP}{dT} + (C)$ ....[8]

IX $\quad F = k_1P + k_2 \frac{dP}{dT} + k_3 \frac{d^2P}{dT^2}$ ....[9]

X $\quad F = k_1\int PdT + k_2P + k_3 \frac{dP}{dT} + k_4\frac{d^2P}{dT^2} + (C)$ ....[10]

XI $\quad k_5\int FdT + F + k_4 \frac{dF}{dT} = k_1\int PdT + k_2P + k_3 \frac{dP}{dT}$. [11]

XII $\quad k_7\int FdT + F + k_6 \frac{dF}{dT} + k_5 \frac{d^2F}{dT^2} =$

$\quad k_1\int PdT + k_2P + k_3 \frac{dP}{dT} + k_4 \frac{d^2P}{dT^2}$ ....[12]

where P = the deviation from its normal value of the primary impulse actuating the regulator as measured at the moment under consideration; F = the final regulating effect of the automatic-control apparatus as measured at the same moment under consideration; T = time; and k_1, k_2, k_3, k_4, k_5, k_6, and k_7 = arbitrary constants of adjustment.

Only six of the above characteristics may be found in existing commercial regulators. The reader can prove this statement by analyzing, in the light of this article, a number of controls with which he may be familiar. The statement applies to all regulators and governors irrespective of either the field of application (control of temperature, pressure, speed, combustion, level, etc.) or the motive power actuating them (electrical, hydraulic, or pneumatic operation). The only limitation in this connection is that the controls selected for analysis should be of a continuous type, because it is obvious that the characteristic of regulators of mere on-and-off type cannot be expressed by a mathematical equation.

The on-and-off type does not include, however, the majority of the electric regulators of the contact-making type, since, even though their operation may be intermittent, there still exists in practically all of these regulators a definite mathematical relationship between the variation of the controlled function and the actuation of the regulating valve.

Elementary examples of the automatic-control apparatus of the first and twelfth classes only will be given in this paper. Space limitations forbid demonstration of all twelve characteristics. The author, however, has placed on file in the archives of the Society, a complete demonstration of all twelve cases where they are available to the more serious students of control problems.

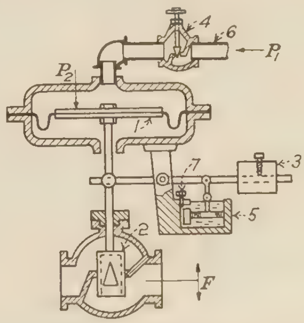

Fig. 3 A Common-Type Pressure-Regulating Valve

Example of Class I

Consider a pressure regulator of the most common type, such as illustrated in Fig. 3. This regulator consists of the diaphragm (1) moving the regulating valve (2). The pressure to be kept constant is transmitted to the regulator through the pilot line (6), in which is inserted the needle valve (4). When the pressure is held steady at its desired normal value the weight (3) is in balance with the force produced by the pressure acting upon the diaphragm (1) and, therefore, the valve (2) is at a standstill.

Let P_2 = the normal value of the pressure. It is evident that the pressure on the top of the diaphragm (1) is always equal to P_2, provided the valve (2) is in its normal operating position and is neither wide open nor closed tight. Let P_1 = the pressure existing in the line (6) in front of the needle valve (4). By definition, the primary impulse actuating the regulator will be equal to the difference between the pressure before the needle valve (4) and the normal desired pressure always existing in the space above the diaphragm (1).

We may write, therefore,

$$P = P_1 - P_2 \quad\text{....[13]}$$

It follows from the law of viscous flow through an orifice such as the needle valve (4), that the speed of fluid flow through the valve (4) is proportional to the pressure difference existing across it. It is evident, on the other hand, that the speed of movement

of the valve (2) is proportional to the speed of fluid flow through the valve (4).

Therefore, the following relationship holds:

$$\frac{dF}{dT} = k_1 (P_1 - P_2) = k_1 P \quad [14]$$

where $\frac{dF}{dT}$ is the mathematical expression of the speed of movement of the valve (2) existing at the moment under consideration, while k_1 is the arbitrary constant of adjustment depending upon the opening of the valve (4).

By multiplying both sides of Equation [14] by dT and integrating it we obtain Equation [1] given previously as expressing the characteristic of the regulator of Class I

$$F = k_1 \int P dT + (C) \quad [1]$$

In this equation the constant of integration depends upon the position of the regulating valve at the beginning of operation of the regulator.

The operation of the dashpot (5) is equivalent to the operation of the needle valve (4) and either one of them could be omitted without changing the characteristic of the regulator. If the dashpot is used, the constant of adjustment k_1 will depend on the opening of the bypass valve (7).

It will be seen from the above explanation that the Class I regulator is characterized by the fact that the regulator moves the regulating valve with a speed proportional at any given moment to the extent of deviation of the controlled function from its normal desired value as existing at the same moment. This means also that the regulating valve continues to move as long as this deviation exists.

In this as well as in all other examples it is assumed that the parts of the regulator are so designed and so proportioned that the effect of friction and inertia of the regulator on its operation is so small that it can be neglected.

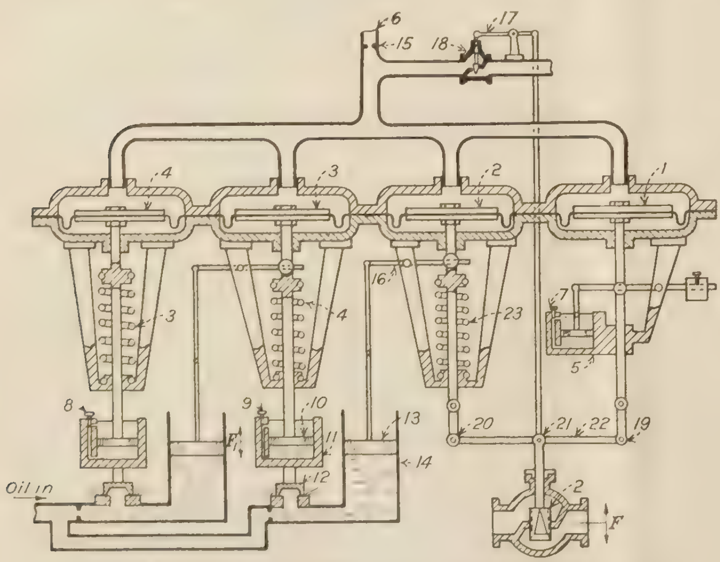

Fig. 11 Regulator Provided With Automatic Adjustment of the Primary Impulse

Example of Class XII[2]

This class of regulator, represented by Fig. 11, is provided with automatic adjustment of the primary impulse by means of the valve (18).

Without this adjustment the characteristic of this regulator is

$$F = k_8 \int P dT + k_9 P + k_{10} \frac{dP}{dT} + k_{11} \frac{d^2P}{dT^2} + (C). \quad [48]$$

This equation is modified by the operation of the valve (18) into

$$F = k_8 \int (P - k_{12}F)dT + k_9(P - k_{12}F) + k_{10} \frac{d(P - k_{12}F)}{dT} + k_{11} \frac{d^2(P - k_{12}F)}{dT^2} \quad [49]$$

By combining the like terms and the groups of constants, we get Equation [12], expressing the characteristic of Class XII.

Remarks Concerning Classes VII, VIII, IX, X, XI, and XII

To the best of the author's knowledge and belief the regulator characteristics of Classes VII to XII, inclusive, are new to the art. The principal difference between the automatic-control apparatus of these new classes and those of the classes widely used at present is the existence of the terms $\frac{dP}{dT}$ and $\frac{d^2P}{dT^2}$ in the characteristic equations. These terms are obtained by the use of a single dashpot or the series combination of two dashpots.

The alternate means available for obtaining these terms are:

1 *The Electric Condenser.* The use of a condenser for this purpose is based on the fact that if we impress a variable potential across a condenser connected in series with a very small resistance, the potential drop across the resistance will be proportional to the rate of change of the variable potential.

2 *Electrical Coil Moving Across a Uniform Magnetic Field.* The use of a coil for the purpose of obtaining the rate of change of a function is based on the law that the potential induced in the coil is proportional to the speed of movement of the coil in respect to the magnetic field.

3 *Orifice.* The use of an orifice is a general case of the use of the dashpot since the purpose of the dashpot is to force the fluid through a resistance (bypass valve) in a volume proportional to the extent of change of the function, thus obtaining pressure drop across the resistance which is proportional to the rate of change of the function. Strictly speaking the use of a condenser is a particular case of the use of an orifice.

4 *Induction Coil.* The fact that the drop of potential across an induction coil is proportional to the rate of change of current passing through it is the basis of the use of such a coil for the purpose of obtaining the rate of change of a function.

5 *Inertia.* The use of inertia is based on the principle that the reaction of a mass is proportional to its acceleration. The precession of a gyroscope should also be classed under this heading.

6 *Step-by-Step Differentiation.*

7 *Differentiating Calculating Machine.* Several of these are available, based on the principle of finding the tangent of a curve.

Theoretically there is no reason why the derivatives of higher orders than the second of the controlled function could not be added to any of the characteristics covered. In actual practice, however, the usefulness of such complicated characteristics is limited to very special cases. Therefore, the twelve characteristics shown are the practical limit of the development in this respect.

[2] A complete demonstration of all twelve classes of regulators has been filed by the author in the archives of the Society. This demonstration includes Figs. 4 to 10, inclusive, Equations [16] to [47], inclusive, and Equations [50] to [55], inclusive.

Solution of the Problem of Automatic Control as a Whole

It is beyond the scope of this article to present a detailed solution of the problem of automatic control in all its various ramifications but there are two basic principles which should be particularly emphasized in this connection.

First, it could be definitely shown that the characteristic of the Class II regulator, Equation [2], would be entirely adequate in all cases of automatic control, provided there were no time lag in any part of the controlled system and provided the regulator performs in perfect accordance with this characteristic. More generally this means that an automatic-control problem is completely solved when the controllable flow of fluid or energy to or from the storage is made to vary strictly in phase with and in proportion to the change of the amount of fluid or energy in storage, or mathematically when $W = kP_2$ (Fig. 2). Under these ideal conditions the variation of the controlled function could be made as small as desired by the simple expedient of increasing the value of the constant of adjustment k_1.

For instance, in the example of the level control shown in Fig. 1, the level in the tower (1) could be held as steady as desired by simply increasing the ratio of the leverage between the float (4) and the valve (5), provided the float is located in the tower to eliminate the time lag in transmission of the impulses and provided the float and the valve are entirely devoid of inertia and friction and also that there is no inertia of the fluid flowing through the pipe (6). In actual practice, however, the above conditions can be only approximated. Therefore, there exists just one optimum value of k_1 in Equation [2] with the result that the attempt to minimize the variation of the controlled function by increasing k_1 beyond its optimum value for this particular installation is invariably followed by a rapid periodic oscillation of the system known as "hunting."

Second, the current methods for eliminating hunting are based on the misconception that a regulator could be stabilized by means of a dash pot or a similar retarding device.

In the discussion of Class IV in the complete paper, filed in the archives of the Society, it is shown that the effect of stabilizers is equivalent to an artificially created time lag. Since hunting is the result of the time lag inherent in the system, the addition of an artificial time lag cannot possibly correct the situation. The only result attained by the stabilizers is to increase the magnitude of fluctuation of the controlled function for a given change in the rate of flow of fluid or power to or from the system. It is admitted, however, that by retarding the response of the regulator, the system may be made apparently more stable from the standpoint of hunting.

The only rational method of combating hunting is by counteracting the time lag. It could be stated without going into a detailed mathematical proof that the addition of the terms $\frac{dP}{dT}$ and $\frac{d^2P}{dT^2}$ to the characteristic of a regulator will counteract the time lag. Whether these terms should be used singly or together depends entirely upon the type of time lag. It is interesting to note that the elimination of hunting by the rational method involves advancing the response of the regulator.

Of course, if hunting is the result of the imperfect operation of the regulator, due either to its excessive inertia or friction, the regulator should be redesigned to make it perform strictly in accordance with its characteristic equation.

There are certain types of regulators, however, in which the inertia effect of some essential part cannot be entirely eliminated even by a most careful design. For instance, in the spring-loaded flyball speed governor the ever-present inertia of the flyballs introduces a phase displacement between the change of the turbine speed and the corresponding change of the angle of inclination of the flyballs.

From the elementary law of the reaction of a mass to its acceleration, and for normal small changes in turbine speed

$$k_3P_1 + k_4\frac{d^2P_1}{dT^2} = P \qquad [56]$$

where P_1 = the angle of inclination of the flyballs, P = the extent of change of the turbine speed, k_4 = constant of proportionality depending on the inertia of flyballs, k_3 = constant of proportionality depending on the design of the governor in respect to the rotative speed of the flyballs. By using an operative connection between the flyballs and the throttle valve having the characteristic

$$F = k_5P_1 + k_6\frac{d^2P_1}{dT^2} \qquad [57]$$

Since k_5 and k_6 are two perfectly arbitrary constants of adjustment we can make $k_5 = k_1k_3$ and $k_6 = k_1k_4$.

Substituting these values of k_5 and k_6 into Equation [57]

$$F = k_1\left(k_3P_1 + k_4\frac{d^2P_1}{dT^2}\right) = k_1P \qquad [2]$$

It will be seen, therefore, that by using characteristic Equation [57], the unavoidable retarding effect of the inertia of the flyballs can be completely counteracted. Of course, this case is just a particular example of the use of new characteristics for counteracting the time lag in the impulse-transmitting (or rather impulse-generating) means.

It could be shown in a similar manner that if a regulator has an unavoidable series combination of inertia and a fluid friction, as is the case when the flyballs are dampened with a dashpot, the retarding effect of such combination can be counteracted by using characteristic Equation [9]. If in addition to this retarding effect existing in the regulator itself there is also a time lag in the system external to the regulator, an introduction of the derivatives of the higher order than the second in the characteristic of the regulator will be necessary if a precise and stable regulation is to be achieved under all conditions of operation.

Bibliography

"Regelung der Kraftmaschinen," by Dr. Ing. Max Tolle, Julius Springer, Berlin, 1921.

"Regler für Druck und Menge," by Guido Wünsch, R. Oldenbourg, Berlin, 1930.

"The Manual of Instrumentation," by M. F. Behar, Instrument Publishing Company, Pittsburgh, 1932.

Application of the Elastic-Point Theory to Piping Stress Calculations

By S. W. SPIELVOGEL[1] and S. KAMEROS,[2] NEW YORK, N. Y.

The application of the neutral-point theory to piping expansion problems leads to a simplification in their solution. A simple transfer formula introduced by the authors eliminates what would have been a laborious step in the computations and resolves the procedure into the determination of two moments of inertia and the product of inertia of the pipe line with respect to two rectilinear axes through its center of gravity.

THEORETICAL and experimental research of recent years has led to the development of a well-defined technique in the design and mathematical analysis of pipe lines subjected to expansion. Various authors have simplified the tedious labor of calculating the unknown quantities by grapho-analytical procedures or through graphs and tables which furnish either solutions for the most frequently occurring integrals entering into the calculation or direct results for a great variety of pipe-line shapes. A further simplification of the procedure for calculating the three redundant end reactions in fully restrained pipe lines can be obtained by making use of the well-known principle of the elastic-point, or so-called "rigid-bracket," theory. The inherent advantage of this method is particularly apparent when applied to irregular, unsymmetrical pipe lines, the solutions for which lead to unwieldy equations not suitable for graphical representation and consequent utilization for pipe lines of similar form. Where the shape of the pipe line is of such character as to call for individual solution, the elastic-point method has the advantage of simplicity, time saving, and elimination of sources of error.

Mention of the possibilities of the application of the elastic-point theory to pipe-line stresses has been made before in the discussion of technical papers presented to the A.S.M.E., but to the author's knowledge the advantages of the theory have never been fully demonstrated. The application of the method in its original form offers but little advantage over prevalent procedures. The authors have discovered, however, that in conjunction with a transfer formula derived herein, it permits interpretations which remove some of the obstacles which make this subject a specialty for experts. This paper is presented, therefore, in the belief that it will contribute toward opening this field to those not fully equipped with the complex knowledge of statically indeterminate systems.

The authors have purposely not repeated in this paper a discussion of such subjects as flexibility constant, the effect of flattening of curved pipe, and stress-multiplication factor. These subjects have already been covered in papers of the Society. Those who are not conversant with them may have recourse to the bibliography at the end of this paper.

The following discussion leading to the neutral-point theory is along the line of reasoning applied to statically indeterminate problems and is presented for completeness only.

A pipe line situated wholly in one plane with its ends fully restrained and subjected to temperature changes constitutes a statically indeterminate system with three unknown quantities at each of the two terminal points. These unknown quantities are the horizontal and vertical components of the end reactions and two restraining moments, one for each end. To solve this problem, there are available

1 The three fundamental equations of equilibrium; namely,

The sum of all horizontal forces equals zero.....$\Sigma X = 0$
The sum of all vertical forces equals zero.......$\Sigma Y = 0$
The sum of all moments equals zero..........$\Sigma M = 0$

2 Three more equations, which are obtained by considering the distortion in the system caused by the restrictions which prevent the free expansion of the pipe.

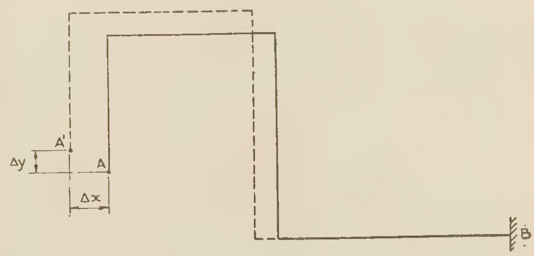

Fig. 1

The pipe line shown in Fig. 1 is subjected to temperature changes. If the end A were made free and end B were securely fixed, the pipe line would become a cantilever which, when heated, would lengthen horizontally the amount Δx and vertically the amount Δy. There would be no angular distortion at the free end and the ultimate shape of the line would be similar to the original shape, the point A merely being translated to A'.

If two unit forces are now applied at the free end and in directions opposite to the expansions Δx and Δy, part of the translatory displacements will be restored and the free end will undergo a rotary motion resulting in an angular displacement. Inasmuch as no angular displacement exists in the original, i.e., the fully restrained system, a counteracting moment must be applied at the free end to hold the pipe element at point A in its position, which in the case illustrated by Fig. 1 is a vertical position.

Let all translatory motions produced by the unit forces be

[1] Assistant Engineer, The Brooklyn Edison Company, Inc. Mr. Spielvogel was graduated in 1919 from the Technische Hochschule in Vienna, Austria, with the degree of C.E. afterward engaging successively in the design of bridges and steel and concrete structures in connection with steam-generating stations and high-pressure steam piping at the "Gutehoffnungshutte," Germany, Electric Bond and Share Company, and Erie Railroad, New York. Since 1925, Mr. Spielvogel has been connected with the mechanical engineering department of the Brooklyn Edison Company, Inc.

[2] Mechanical Engineering Department of the New York Edison Company, Inc. Mr. Kameros was graduated from Columbia College in 1924 with a B.A. degree, and from the Columbia School of Mines, Engineering, and Chemistry in 1926 with an M.E. degree.

Contributed by the Power Division for presentation at the Semi-Annual Meeting, Cincinnati, Ohio, June 19 to 21, 1935, of The American Society of Mechanical Engineers.

Discussion of this paper should be addressed to the Secretary, A.S.M.E., 29 West 39th Street, New York, N. Y., and will be accepted until July 10, 1935, for publication at a later date.

denoted by δ and all rotary motions by ζ. Give these symbols subscripts such that the first indicates the direction in which the displacement takes place and the second the direction of the unit action (force or moment) causing that displacement. Thus δ_{xy} shall denote the horizontal displacement caused by a vertical unit force, δ_{ym} the vertical displacement caused by a unit moment at the free end, ζ_{my} the angular displacement at the free end caused by a unit vertical force, etc.

If we apply at the free end forces X and Y and a moment M which have such intensities as to move point A', Fig. 1, back to A and restore the original position of the tangent at A, it is evident that these forces and the moment are identical with the actual end reactions. This statement is expressed mathematically by Equations [1], in which the sum of all horizontal movements produced by X, Y, and M is made equal to the expansion Δx, the sum of all vertical movements made equal to Δy, and the sum of all rotations made equal to zero.

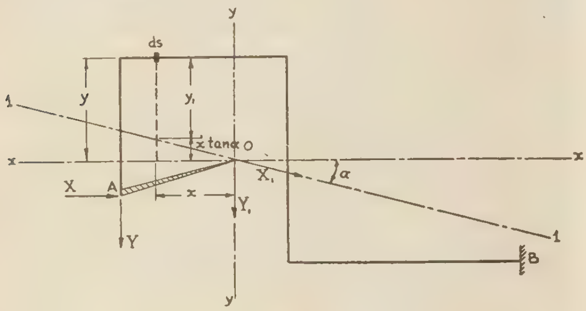

FIG. 2

$$\left.\begin{aligned} X\delta_{xx} + Y\delta_{xy} + M\delta_{xm} &= \Delta x \\ X\delta_{yx} + Y\delta_{yy} + M\delta_{ym} &= \Delta y \\ X\zeta_{mx} + Y\zeta_{my} + M\zeta_{mm} &= 0 \end{aligned}\right\} \ldots\ldots\ldots\ldots\ldots [1]$$

In Equations [1], Δx and Δy are known. The nine coefficients for X, Y, and M represent deflections or rotations of the free end of the cantilever due to unit loads or a unit moment and can be calculated. Actually only six of these coefficients need be computed because, owing to Maxwell's law of reciprocity, $\delta_{xy} = \delta_{yx}$, $\delta_{xm} = \zeta_{mx}$, and $\delta_{ym} = \zeta_{my}$.

In solving Equations [1], slide-rule accuracy is insufficient. It is no infrequent occurrence that one set of solutions fails to satisfy the equations for the only reason that insufficient significant figures had been developed in solving for X, Y, and M. Furthermore, the moments at points between the two supports are materially affected by slight changes in the values of the end reaction. In applying the principle of the elastic center we gain the advantage that only two of the six coefficients in Equations [1] need be calculated and that X and Y can be found directly from equations which contain one unknown only. In the following discussion, statements will be made, the proof of which will be found in the latter part of this paper.

Release one of the two supports, say support A, Fig. 2, and connect end A rigidly to a bracket leading to the center of gravity O of the line. Let point O be temporarily the support of the pipe line. Loads upon the system or expansions within the system will cause point O, if it were free, to move in the same direction and with the same magnitude as point A if it were free to move. The translatory forces required to nullify the displacements at O have the same intensity as the reacting forces at A. The final result, therefore, is obtained by transferring to point A the reactions found for point O and adding at A the moment caused by the offset of O against A.

A rectangular-coordinate system is now passed through O, for example y-axis vertical, x-axis horizontal. The reactions Y_1 and X_1 at O are then assumed to act along y and axis 1–1, respectively, where axis 1–1 is inclined to the x-axis at an angle α. The angle is so selected as to make axis 1–1 conjugated to axis y–y. This means that the product of inertia or moment of deviation of the pipe line about axes 1–1 and y–y is zero; or, in other words, that the sum of each small element of pipe multiplied by its coordinates with reference to these axes is zero. These axes are not necessarily principal axes.

Angle α is obtained from

$$\tan \alpha = I_{xy}/I_{yy} \ldots\ldots\ldots\ldots\ldots\ldots\ldots [2]$$

where I_{xy} and I_{yy} denote, respectively, the product of inertia and the moment of inertia of the pipe line for the rectangular system of coordinates, that is, with reference to axes x–x and y–y.

As a result of these assumptions, the displacements δ and ζ which carry dissimilar subscripts become zero. Thus,

$$\delta_{xy} = \delta_{yx} = 0; \; \delta_{xm} = \zeta_{mx} = 0; \; \delta_{ym} = \zeta_{my} = 0$$

and Equations [1] change to

$$X_1 = \frac{\Delta x_1}{\delta_{11}}; \; Y_1 = \frac{\Delta y}{\delta_{yy}}; \; M = 0 \ldots\ldots\ldots [3]$$

Note that a uniform temperature change causes no moment at point O.

The terms Δx_1 and Δy now denote, respectively, the expansion movements of point O in direction of the inclined axis 1–1 and in the direction of the vertical axis y–y if O were the end of a free cantilever and the terms δ_{11} and δ_{yy} the movements due to unit loads acting at O in the direction of these respective axes.

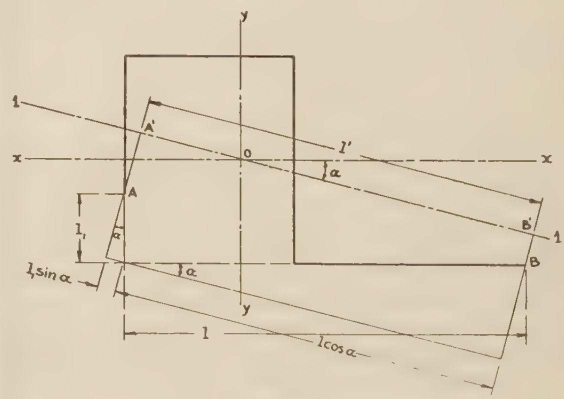

FIG. 3

Referring to Fig. 3 and denoting the coefficient of expansion by c and the temperature change by Δt, the movements are then calculated as follows:

$$A'B' = l' = l \cos \alpha + l_1 \sin \alpha$$

$$\Delta x_1 = l' \cdot c \cdot \Delta t \ldots\ldots [4] \qquad \Delta y = l_1 \cdot c \cdot \Delta t \ldots\ldots [5]$$

When both ends of the pipe line are at the same level $l_1 = 0$ and $\Delta x_1 = l \cos \alpha \cdot c \cdot \Delta t$; and $\Delta y = 0$

The divisor δ_{11} is obtained by summing the products of each length of pipe element ds and the square of the distance y_1 from the inclined axis 1–1 measured as shown in Fig. 2 and dividing the result by EI, the product of the modulus of elasticity of the material and the moment of inertia of the cross-sectional area of the pipe. The divisor δ_{yy} is obtained by summing the products of each length of pipe element ds and the square of the horizontal distance x from y–y and dividing the result by EI.

It is evident, therefore, that δ_{yy} is proportional to the moment of inertia of the pipe line about a vertical axis through the center of gravity of the line and that a similar interpretation may be given to δ_{11} with the modification, however, that the multipliers are the squares of the distances y_1 from the inclined axis 1–1. In both cases the factor of proportionality is $1/EI$. Accordingly

$$\delta_{yy} = \frac{I_{yy}}{EI} = \frac{1}{EI}\int x^2 ds$$

$$\delta_{11} = \frac{I_{11}\cos^2\alpha}{EI} = \frac{\cos^2\alpha}{EI}\int y_1^2\, ds$$

I_{11} denoting what may be called the modified moment of inertia about axis 1–1.

An attempt to calculate I_{11} in accordance with the foregoing definition would soon reveal that the apparent simplification demonstrated by a comparison of Equations [1] and [3] is offset by the necessity of establishing analytical equations for each branch of pipe line and the tedious labor of integrating in this special case, of non-rectangular coordinate axes. The following derivation, however, will show that I_{11} is obtainable directly from a simple transfer formula which contains I_{xx}, I_{yy}, and I_{xy}, all referring to the original, that is, rectangular system of coordinates.

Referring to Fig. 2

$$\begin{aligned} y_1 &= y - x\tan\alpha \\ I_{11} &= \int y_1^2\, ds = \int (y - x\tan\alpha)^2\, ds \\ &= \int y^2\, ds - 2\tan\alpha \int xy\,ds + \tan^2\alpha \int x^2\, ds \end{aligned}$$

The first integral represents the moment of inertia of the line about axis x–x, the second the product of inertia about axes x–x and y–y, and the third the moment of inertia about axis y–y, so that

$$I_{11} = I_{xx} - 2\tan\alpha I_{xy} + \tan^2\alpha I_{yy} \qquad [6]$$

I_{xx}, I_{xy}, and I_{yy} are all introduced in Equation [6] with positive sign.

Equations [3] can now be written as

$$X_1 = \frac{EI\,\Delta x_1}{I_{11}\cos^2\alpha};\quad Y_1 = \frac{EI\,\Delta y}{I_{yy}} \qquad [7]$$

Summary of Procedure

As a result of the foregoing analysis the procedure for calculating the end reactions may be summarized as follows:

1 Determine the center of gravity of the pipe line
2 Calculate moments of inertia I_{xx}, I_{yy}, and product of inertia I_{xy} of the pipe line about horizontal and vertical axes through the center of gravity of the line
3 Calculate angle of the conjugated axis from Equation [2]
4 Calculate modified moment of inertia I_{11} from Equation [6]
5 Calculate the expansions

(a) For pipe supports at same level

$$\Delta x_1 = l\cos\alpha \cdot c \cdot \Delta t;\quad \Delta y = 0$$

(b) For pipe supports at different levels

$$\begin{aligned} \Delta x_1 &= (l\cos\alpha + l_1\sin\alpha)\cdot c\cdot \Delta t \\ \Delta y &= l_1 \cdot c \cdot \Delta t \end{aligned}$$

6 Calculate reactions at center of gravity from Equations [7]
7 Calculate horizontal and vertical components of X_1

Horizontal component of $X_1 = X_1\cos\alpha = X$
Vertical component of $X_1 = X_1 \sin\alpha$

8 Add vertical component of X_1 to Y_1 obtaining

$$Y = Y_1 + X_1\sin\alpha$$

9 Transfer X and Y to left support.
10 Calculate moment at left support due to the offsets of center of gravity to left support A
11 Calculate moments along pipe line and determine the maximum.

Illustration of Procedure

The method of procedure is illustrated by the solution of an example involving a 6-in., 600-lb standard seamless pipe with

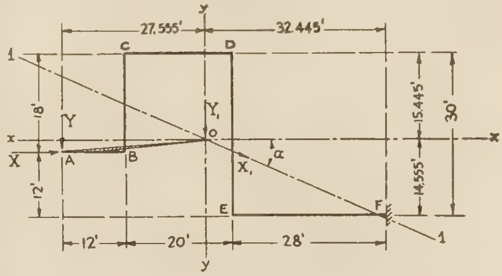

Fig. 4

a coefficient of expansion, $c = 6.14$ in. per 100 ft; a moment of inertia of cross-section, $I = 37$ in.^{4}; and a modulus of elasticity, $E = 25.5 \times 10^6$ lb per sq in. The steam temperature is given as 750 F, and the room temperature as 60 F. The pipe supports are on different levels as shown in Fig. 4.

1 Center of gravity of pipe line

27.555 ft from left end; 14.555 ft from bottom

2 Moment of inertia about axis $x-x$

$$I_{xx} = (12\times 2.555^2) + \left[\frac{18^3}{12} + (18\times 6.445^2)\right] + (20\times 15.445^2) + \left[\frac{30^3}{12} + (30\times 0.445^2)\right] + (28\times 14.555^2) = 14{,}270.667$$

Moment of inertia about axis $y-y$

$$I_{yy} = \left[\frac{12^3}{12} + (12\times 21.555^2)\right] + (18\times 15.555^2) + \left[\frac{20^3}{12} + (20\times 5.555^2)\right] + (30\times 4.445^2) + \left[\frac{28^3}{12} + (28\times 18.445^2)\right] = 23{,}306.667$$

Product of inertia

$$I_{xy} = (12\times -2.555\times -21.555) + (18\times 6.445\times -15.555) + (20\times 15.445\times -5.555) + (30\times 0.445\times 4.445) + (28\times -14.555\times 18.445) = -10{,}317.333$$

3 Angle of conjugated axis

$$\tan\alpha = \frac{I_{xy}}{I_{yy}} = \frac{-10{,}317.333}{23{,}306.667} = -0.4426$$

$$\alpha = -23 \text{ deg, } 52 \text{ min, } 30 \text{ sec.}$$

4 Moment of inertia about conjugated axis

$$\begin{aligned} I_{11} &= I_{xx} - 2\tan\alpha I_{xy} + \tan^2\alpha I_{yy} \\ &= 14{,}270.667 - 9123.903 + 4565.776 = 9703.54 \end{aligned}$$

5 Projected length of pipe line and expansions

$$l' = l \cos \alpha + l_1 \sin \alpha = 54.87 + 4.856 = 59.726 \text{ ft}$$

$$EI\,\Delta x_1 = \frac{25.5 \times 10^6 \times 37}{144} \times \frac{6.14}{12} \times \frac{59.726}{100} = 2{,}002{,}390$$

$$EI\,\Delta y = \frac{25.5 \times 10^6 \times 37}{144} \times \frac{6.14}{12} \times \frac{12}{100} = 402{,}315$$

6 $$X_1 = \frac{EI\,\Delta x_1}{\cos^2 \alpha\, I_{11}} = \frac{2{,}002{,}390}{0.8363 \times 9703.54} = 246.75 \text{ lb}$$

$$Y_1 = \frac{EI\,\Delta y}{I_{yy}} = \frac{402{,}315}{23{,}306.667} = 17.26 \text{ lb}$$

7 $$X = X_1 \cos \alpha = 246.75 \times 0.9145 = 225.65 \text{ lb}$$

8 $$Y = Y_1 + X_1 \sin \alpha = 17.26 + (246.75 \times 0.4047) = 117.12 \text{ lb}$$

9, 10, and 11 Bending moments

at A	$(225.65 \times 2.555) + (117.12 \times 27.555)$	$= +3804$ ft-lb
B	$(225.65 \times 2.555) + (117.12 \times 15.555)$	$= +2397$ ft lb
C	$(-225.65 \times 15.445) + (117.12 \times 15.555)$	$= -1663$ ft-lb
D	$(-225.65 \times 15.445) + (-117.12 \times 4.445)$	$= -4006$ ft-lb
E	$(225.65 \times 14.555) + (-117.12 \times 4.445)$	$= +2764$ ft-lb
F	$(225.65 \times 14.555) + (-117.12 \times 32.445)$	$= -516$ ft-lb

Derivation of Equations

It has been stated that Fquations [1] change into Equations [3] if the support is transferred to the center of gravity O of the pipe line and the reactions assumed to act along a vertical axis y–y and its conjugated axis 1–1. This means that all coefficients carrying dissimilar subscripts in Equations [1] become zero. The proof of this follows:

If m_1 and m_y denote the moments produced by loads of 1 pound acting, respectively, along axes 1–1 and y–y, and δ_{xm} is the horizontal movement and δ_{ym} the vertical movement of point O produced by a unit moment at O, then from the theory of elasticity

$$\delta_{xm} = \frac{1}{EI} \int m_1\, m\, ds \quad \text{[8]}$$

and

$$\delta_{ym} = \frac{1}{EI} \int m_y\, m\, ds \quad \text{[9]}$$

From Fig. 5 it is evident that $m_1 = 1$ lb $y_1 \cos \alpha$, and $m_y = 1$ lb x also $m = 1$ ft-lb (if x and y are in feet).

Hence, substituting these values in Equations [8] and [9] the following are obtained:

$$\delta_{xm} = \frac{\cos \alpha}{EI} \int y_1\, ds; \qquad \delta_{ym} = \frac{1}{EI} \int x ds$$

The products under the integral represent the statical moments of the pipe line about the two axes. Inasmuch as these axes have been selected to pass through the center of gravity, the statical moments are zero. Therefore, the expressions δ_{xm} and δ_{ym} are both zero for these conditions. Since, by the law of reciprocity of deflections and angular changes $\delta_{xm} = \zeta_{mx}$ and $\delta_{ym} = \zeta_{my}$, the terms ζ_{mx} and ζ_{my} are both also zero for the conditions selected.

Taking now the terms δ_{xy} and δ_{yx} and referring to Fig. 5, from the theory of elasticity,

$$\delta_{xy} = \delta_{yx} = \frac{1}{EI} \int m_1\, m_y\, ds = \frac{\cos \alpha}{EI} \cdot \int x y_1\, ds \quad \text{[10]}$$

The term under the integral represents the product of inertia of the pipe line with respect to the two selected axes. By choosing axis 1–1 to be a conjugated axis of y–y the product of inertia may be made zero and therefore both δ_{xy} and δ_{yx} made zero. Referring to Fig. 5 it is seen that $y_1 = y \mp x \tan \alpha$. Therefore, from Equation [10],

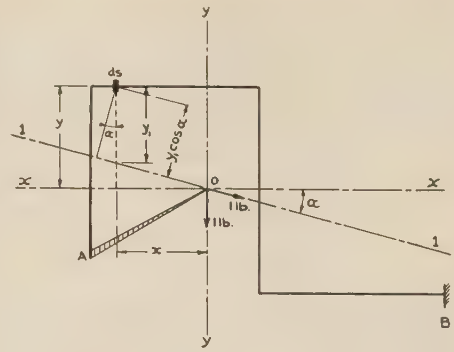

Fig. 5

$$\delta_{xy} = \frac{\cos \alpha}{EI} \int (xy \mp x^2 \tan \alpha) ds = 0$$

$$\text{From which } \tan \alpha = \pm \frac{\int xy\, ds}{\int x^2\, ds} = \pm \frac{I_{xy}}{I_{yy}}$$

The last derived equation is Equation [2]. From the above it will be seen therefore that by selecting the two axes as indicated Equations [1] are transformed into Equations [3].

Returning again to Fig. 5 it is seen that

$$\delta_{yy} = \frac{1}{EI} \int m_y\, m_y\, ds = \frac{1}{EI} \int x^2\, ds$$

The term under the integral is the moment of inertia of the pipe line with respect to the y–y axis. Therefore,

$$Y_1 = \frac{\Delta y}{\delta_{yy}} = \frac{EI\,\Delta y}{\int x^2 ds} = \frac{EI\,\Delta y}{I_{yy}} \text{ as given in Equations [7]}$$

also

$$\delta_{11} = \frac{1}{EI} \int m_1 m_1 ds = \frac{1}{EI} \int y_1 \cos \alpha \cdot y_1 \cos \alpha\, ds = \frac{\cos^2 \alpha}{EI} \int y_1^2\, ds$$

The term under the integral is the moment of inertia of the pipe line with respect to axis 1–1. Therefore,

$$X_1 = \frac{\Delta x_1}{\delta_{11}} = \frac{EI\,\Delta x_1}{\cos^2 \alpha \int y_1^2\, ds} = \frac{EI\,\Delta x_1}{\cos^2 \alpha\, I_{11}} \text{ as given in Equations [7]}$$

The authors have prepared a number of additional problems of typical pipe lines containing quarter bends or sloping branches. Their solutions as well as the appendix are available upon request either to the authors or to the society headquarters.

Bibliography

1 "Discussion of Neutral-Point Theory as Applied to Arches," by C. B. McCullough in "Reinforced Concrete and Masonry Structures," compiled by C. B. Hool and W. S. Kinne, McGraw-Hill Book Company, 1924, page 468.

2 "Stresses and Reactions in Expansion Pipe Bends," by A. M. Wahl, Trans. A.S.M.E., vol. 50, 1928, paper FSP-50-49, p. 241.

3 "The Elastic Deformation of Pipe Bends," by W. Hovgaard, Publication of the Massachusetts Institute of Technology, vol. 62, no. 64, November, 1926.

4 "Deformation of Plane Pipes and Further Research on Pipe Bends," by W. Hovgaard, Publication of the Massachusetts Institute of Technology, vol. 64, no. 59, December, 1928.

5 "Design of Steam Piping to Care for Expansion," by W. H. Shipman, Trans. A.S.M.E., vol. 51, 1929, paper FSP-51-52, p. 415.

6 "Piping Handbook," by Walker and Crocker, Second Edition, McGraw-Hill Book Company, 1931, Chapter 7.

The Loading and Friction of Thrust and Journal Bearings With Perfect Lubrication

By H. A. S. HOWARTH,[1] PHILADELPHIA, PA.

The author brings together here for the first time important formulas and charts that have been offered by bearing analysts in this field during the past fifteen or twenty years. Some new material is added for completeness, and some references made to earlier fundamental work. Descriptive matter that accompanied the original publication of the charts and formulas has been eliminated as far as practicable. Improved charts derivable from earlier ones, and the rearrangement of others will, it is hoped, prove more useful to the designing engineer than the original publications. The net result is a concise summary of valuable information.

In order that the reader at the beginning may have a fair idea of what is to be found and where in this paper, an explanation of the contents follows:

The first section dealing with journal bearings begins with a concise illustrated description of their several kinds. The side-leakage chart is then explained because from its curves are obtained the correction factors that are necessary for the proper application of the subsequent material to the solving of journal-bearing problems.

Optimum conditions for journal bearings of three classes are shown by charts, tables, and formulas. The titles, captions, and notes on these pages are intended to be sufficient explanation.

General conditions for journal bearings of several classes are next shown by a series of charts which are accompanied by the necessary textual explanation.

Thrust-bearing loading and friction data follow the charts for general conditions for journal bearings. They refer only to Kingsbury thrust bearings, which are made with freely pivoted shoes supporting a thrust collar having an unbroken flat surface. Data are given only for a single set of such surfaces having six pivoted shoes.

The appendixes, of which there are five, contain descriptive matter, the reading of which will help the reader in understanding the first section of the paper. Appendix A contains the symbols and their explanation. Appendix B gives a number of examples together with their solutions, which explain applications of the charts. These are by no means exhaustive. Appendix C discusses viscous flow in general, the viscosity coefficient, the relation between viscosity and friction, and gives useful formulas for several kinds of viscous flow useful to those dealing with bearing problems. Conversion factors are given for several units of absolute viscosity. The symbols for these formulas differ in some respects from those in Appendix A. Appendix D contains an explanation of perfect lubrication as it occurs in bearings, and covers such headings as tapered oil film, side leakage, film thickness, viscosity change within film, the flat-wedge film, the curved-wedge film, optimum conditions, deviations from optimum. This is a valuable introduction to the charts in the body of this paper. Appendix E is a bibliography of the technical literature referred to in or forming parts of the paper.

Journal Bearings

For the purpose of analytical study, journal bearings may be separated into several groups that approximate the forms that are used or should be used. The broadest divisions are (*a*) clearance bearings, and (*b*) fitted bearings.

Clearance bearings are those in which the bearing has a larger radius of curvature than the journal. The angular extent β to which the useful bearing surface surrounds the journal determines whether the bearing is full or partial. The full bearing completely surrounds the journal and β = 360 deg. Partial bearings are usually less than 180 deg and probably average about 120 deg. Characteristics of partial bearings are given in the charts for a wide range of useful angles β.

Fitted bearings are those in which the journal and bearing have the same radius of curvature. Such a bearing must have an angular extent β less than 180 deg and preferably much less. The characteristics of such bearings are given only up to β = 150 deg.

The direction in which the load of the journal is applied to the bearing, with relation to the angular limits of the bearing surface, is of considerable importance to the analytical study. This leads to a division of partial bearings into (*a*), centrally loaded and, (*b*) eccentrically loaded. That there may be different degrees of load eccentricity of the latter is seen by comparing Classes *A* with *D*, and *B* with *E*, given in the journal-bearing classification which follows.

Centrally loaded bearings have their angular extent β divided into two equal parts by the line of action of the applied load. In such bearings the leading angle α equals $\beta/2$.

[1] Vice-President and General Manager, Kingsbury Machine Works, Philadelphia, Pa. Mem. A.S.M.E. H. A. Stevens Howarth was graduated from Yale University in 1899 with honors in mechanical engineering. Several years of practical experience with steel mills and manufacturing were followed by teaching of mechanical engineering subjects at Lehigh University and Carnegie Institute of Technology. In 1914 Mr. Howarth became associated with Albert Kingsbury, in his thrust-bearing business, and in 1917 became general manager and chief engineer. He continued in the same position and business with the Kingsbury Machine Works, formed by Dr. Kingsbury in 1921 and incorporated in 1925. In 1928 he became vice-president and general manager. The present paper is the second of a group planned to simplify for designers the various analytical studies of bearings published by Albert Kingsbury, and other members of his organization, including the author. The first paper of this group was published in the A.S.M.E. Trans., vol. 56, 1934, paper MSP-56-2, p. 891.

Contributed by the Machine Shop Practice Division for presentation at the Semi-Annual Meeting, Cincinnati, Ohio, June 19 to 21, 1935, of The American Society of Mechanical Engineers.

Discussion of this paper should be addressed to the Secretary, A.S.M.E., 29 West 39th Street, New York, N. Y. and will be accepted until July 10, 1935, for publication at a later date.

OPTIMUM CONDITIONS CLASS-A ECCENTRICALLY LOADED JOURNAL BEARINGS WITH RUNNING CLEARANCE SIDE LEAKAGE NEGLECTED EXCEPT IN CHART A

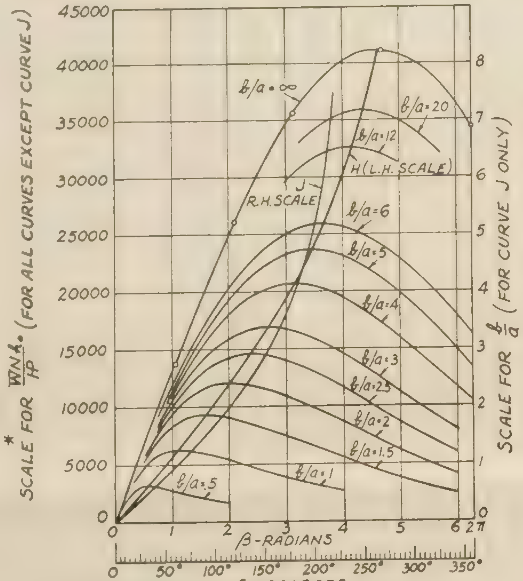

CHART- A

THIS SHOWS FOR CLASS "A" BEARINGS THE VALUES OF THE NON-DIMENSIONAL GROUP WNh_o/HP AS AFFECTED BY SIDE LEAKAGE, WITH FILM FORMS FOR THE MINIMUM COEFFICIENT OF FRICTION. CURVE J GIVES THE VALUE OF ℓ/a AT WHICH GROUP WNh_o/HP IS GREATEST FOR EACH VALUE OF β.

* WHEN THE CURVE FOR A GIVEN RATIO OF ℓ/a IS CHOSEN, EACH ORDINATE OF IT WILL BE CORRECT FOR THE OPTIMUM RELATION OF THE SYMBOLS IN THIS GROUP. HENCE THE CORRECTION FACTORS FOR SIDE LEAKAGE ARE ALREADY ALLOWED FOR IN THE HEIGHTS OF THOSE ORDINATES.

	β	60°	120°	180°	270°	360°
1	A	122.3°	66.33°	12.17°	-62.48°	-118.6°
2	α	32.94°	66.49°	101.3°	156.6°	208.6°
3	α/β	.5490	.5541	.5627	.5799	.5796
4	C	.7481	.4821	.3655	.3310	.3379
5	h_m/h_o	2.382	2.305	2.139	1.990	2.021
6	h_1/h_m	1.200	1.209	1.226	1.257	1.266
7	η/h_m	3.970	1.931	1.576	1.495	1.510
8	θ	158.8°	140.8°	127.4°	118.8°	118.6°
9	ϕ	155.3°	132.8°	113.5°	94.09°	90.00°

TABLE A-1, GEOMETRICAL OPTIMA FOR MAXIMUM LOAD W

	β	60°	120°	180°	270°	360°
10	$W\frac{h_o^2}{\mu N a^3}$	.0201	.0759	.1543	.2635	.2939
11	$F\frac{h_o}{\mu N a^2}$	.0936	.1863	.2768	.4080	.5379
12	$\lambda\frac{a}{h_o}$	4.660	2.453	1.794	1.549	1.830
13	$\lambda\frac{\ell}{h_o}$	4.880	5.138	5.637	7.297	11.50
14	$HP\frac{h_o(10)^6}{\mu N^2 a^3}$	1.485	2.956	4.392	6.473	8.534
15	$HP\frac{(10)^5}{WNh_o}$	7.394	3.893	2.847	2.457	2.904
16	$\frac{WNh_o}{HP(10)^5}$	.1352	.2569	.3513	.4070	.3444
17	$\lambda/\sqrt{\frac{\mu N}{p_o}}$	.4671	.4780	.4983	.5620	.7016

TABLE A-2, DYNAMICAL OPTIMA FOR MAXIMUM LOAD W

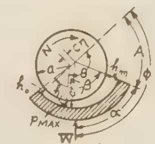

FIG. "A"
ECCENTRICALLY LOADED CLEARANCE BEARING.

	β	60°	120°	180°	270°	360°
1	A	117.9°	58.04°	1.119°	-72.15°	-121.0°
2	α	33.89°	68.54°	104.7°	161.4°	211.0°
3	α/β	.5649	.5711	.5815	.5977	.5860
4	C	.7496	.4911	.3844	.3520	.3660
5	h_m/h_o	2.586	2.476	2.249	2.086	2.155
6	h_1/h_o	1.248	1.263	1.283	1.292	1.280
7	η/h_o	3.986	1.965	1.624	1.543	1.577
8	θ_1	156.4°	136.7°	123.1°	117.5°	121.0°
9	ϕ	151.8°	126.6°	105.8°	89.24°	90.0°

TABLE A-3, GEOMETRICAL OPTIMA FOR MINIMUM FRICTION COEFFICIENT
SEE CHART A-3 FOR OTHER VALUES OF β.

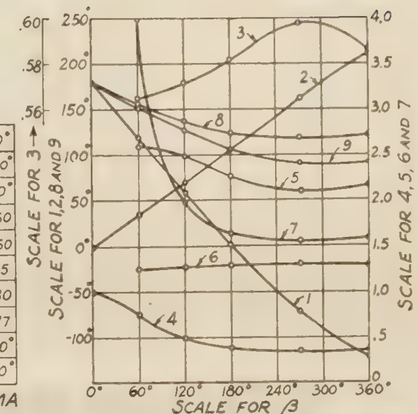

CHART A-3, GEOMETRICAL OPTIMA FOR MINIMUM FRICTION COEFFICIENT

	β	60°	120°	180°	270°	360°
10	$W\frac{h_o^2}{\mu N a^3}$	.0197	.0742	.1507	.2602	.2925
11	$F\frac{h_o}{\mu N a^2}$	.0902	.1790	.2658	.3985	.5327
12	$\lambda\frac{a}{h_o}$	4.584	2.413	1.763	1.531	1.821
13	$\lambda\frac{\ell}{h_o}$	4.801	5.054	5.540	7.217	11.44
14	$HP\frac{h_o(10)^6}{\mu N^2 a^3}$	1.432	2.840	4.217	6.323	8.452
15	$HP\frac{(10)^5}{WNh_o}$	7.274	3.829	2.798	2.430	2.890
16	$\frac{WNh_o}{HP(10)^5}$	.1375	.2612	.3574	.4115	.3460
17	$\lambda/\sqrt{\frac{\mu N}{p_o}}$	.4548	.4647	.4841	.5524	.6965

TABLE A-4, DYNAMICAL OPTIMA FOR MINIMUM FRICTION COEFFICIENT.
SEE CHART A-4 FOR OTHER VALUES OF β.

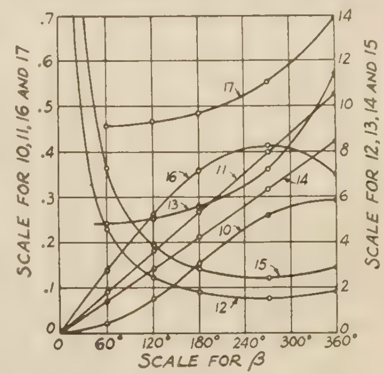

CHART A-4, DYNAMICAL OPTIMA FOR MINIMUM FRICTION COEFFICIENT.

[OPTIMUM CONDITIONS CLASS-B ECCENTRICALLY LOADED FITTED BEARINGS WITHOUT RUNNING CLEARANCE—SIDE LEAKAGE NEGLECTED EXCEPT IN CHART B

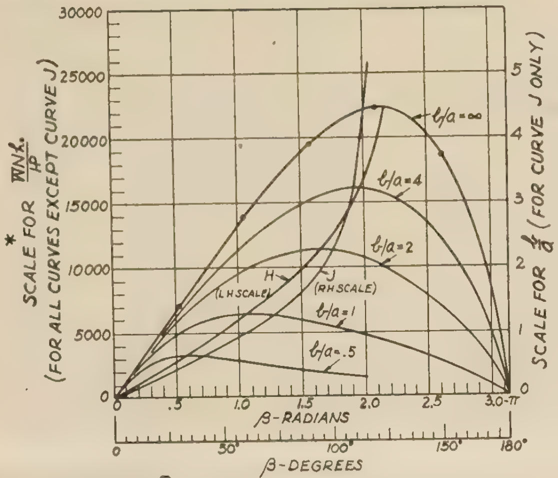

*WHEN THE CURVE FOR A GIVEN RATIO OF l/a IS CHOSEN, EACH ORDINATE OF IT WILL BE CORRECT FOR THE OPTIMUM RELATION OF THE SYMBOLS IN THIS GROUP. HENCE THE CORRECTION FACTORS FOR SIDE LEAKAGE ARE ALREADY ALLOWED FOR IN THE HEIGHTS OF THOSE ORDINATES.

CHART- B

THIS SHOWS FOR CLASS "B" BEARINGS THE VALUES OF THE NON-DIMENTIONAL GROUP WNh_0/HP AS AFFECTED BY SIDE LEAKAGE, WITH FILM FORMS FOR THE MINIMUM COEFFICIENT OF FRICTION. CURVE J GIVES THE VALUE OF l/a AT WHICH GROUP WNh_0/HP IS GREATEST FOR EACH VALUE OF β.

	β	0°	30°	60°	90°	120°	150°
1	A	180°	129.1°	92.21°	64.30°	40.67°	19.39°
2	α	0°	17.47°	35.79°	55.72°	77.76°	101.1°
3	α/β	.5774	.5822	.5964	.6191	.6480	.6739
4	h_A/h_0	2.189	2.176	2.143	2.078	1.969	1.804
5	h_m/h_0	2.189	2.176	2.143	2.306	3.021	5.433
6	h_1/h_0	1.373	1.398	1.480	1.624	1.843	2.131
7	θ_1	180°	150.1°	136.4°	135.2°	142.4°	156.9°
8	ϕ	180°	146.6°	128.0°	120.0°	118.4°	120.5°

TABLE B-1, GEOMETRICAL OPTIMA FOR MAXIMUM LOAD W

	β	0°	30°	60°	90°	120°	150°
9	$W\frac{10h_0^2}{\mu Na^3}$	0	.0451	.1685	.3309	.4534	.3924
10	$F\frac{h_0}{\mu Na^2}$	0	.0407	.0774	.1073	.1284	.1339
11	$\lambda\frac{a}{h_0}$	∞	9.027	4.597	3.242	2.831	3.413
12	$\lambda\frac{l}{h_0}$	4.706	4.727	4.814	5.093	5.930	8.935
13	$HP\frac{h_0(10)^6}{\mu Na^3}$	0	.6455	1.229	1.702	2.037	2.125
14	$HP\frac{(10)^3}{WNh_0}$	∞	14.32	7.293	5.144	4.492	5.415
15	$\frac{WNh_0}{HP(10)^3}$	0	.0698	.1371	.1944	.2226	.1847
16	$\lambda/\sqrt{\frac{\mu N}{P_0}}$	.4311	.4285	.4219	.4171	.4263	.4781

TABLE B-2, DYNAMICAL OPTIMA FOR MAXIMUM LOAD W

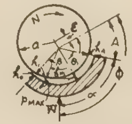

FIG "B"
FITTED PARTIAL BEARING

	β	0°	30°	60°	90°	120°	150°
1	A	180°	133.0°	95.59°	66.29°	41.73°	20.08°
2	α	0°	17.84°	36.26°	55.95°	77.45°	99.41°
3	α/β	.5914	.5946	.6043	.6217	.6455	.6627
4	h_A/h_0	2.533	2.501	2.408	2.276	2.122	1.993
5	h_m/h_0	2.533	2.501	2.408	2.486	3.189	5.804
6	h_1/h_0	1.434	1.457	1.528	1.662	1.873	2.165
7	θ_1	180°	154.8°	140.8°	138.1°	144.0°	158.1°
8	ϕ	180°	150.8°	131.9°	122.2°	119.2°	119.5°

TABLE B-3, GEOMETRICAL OPTIMA FOR MINIMUM FRICTION COEFFICENT SEE CHART B-3 FOR OTHER VALUES OF β.

	β	0°	30°	60°	90°	120°	150°
9	$W\frac{10h_0^2}{\mu Na^3}$	0	.0443	.1663	.3281	.4504	.3876
10	$F\frac{h_0}{\mu Na^2}$	0	.0393	.0755	.1054	.1267	.1307
11	$\lambda\frac{a}{h_0}$	∞	8.877	4.538	3.214	2.813	3.372
12	$\lambda\frac{l}{h_0}$	4.622	4.648	4.752	5.049	5.892	8.829
13	$HP\frac{h_0(10)^6}{\mu Na^3}$	0	.6238	1.197	1.673	2.010	2.074
14	$HP\frac{(10)^3}{WNh_0}$	∞	14.08	7.201	5.100	4.463	5.351
15	$\frac{WNh_0}{HP(10)^3}$	0	.0710	.1389	.1961	.2240	.1869
16	$\lambda/\sqrt{\frac{\mu N}{P_0}}$	.4194	.4177	.4138	.4117	.4221	.4695

TABLE B-4, DYNAMICAL OPTIMA FOR MINIMUM FRICTION COEFFICENT SEE CHART B-4 FOR OTHER VALUES OF β.

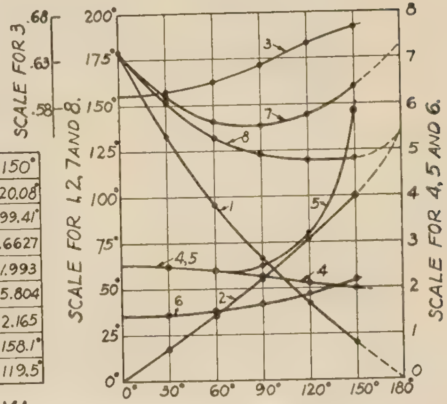

CHART B-3, GEOMETRICAL OPTIMA FOR MINIMUM FRICTION COEFFICENT

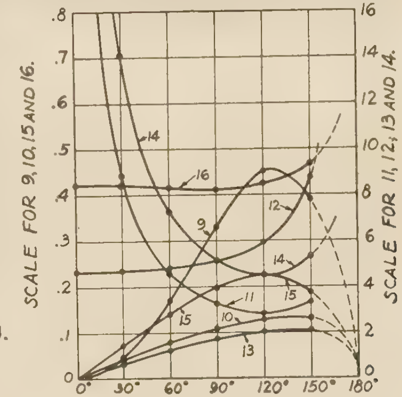

CHART B-4, DYNAMICAL OPTIMA FOR MINIMUM FRICTION COEFFICENT

OPTIMUM CONDITIONS CLASS-C CENTRALLY LOADED JOURNAL BEARINGS WITH RUNNING CLEARANCE—SIDE LEAKAGE NEGLECTED EXCEPT IN CHART C

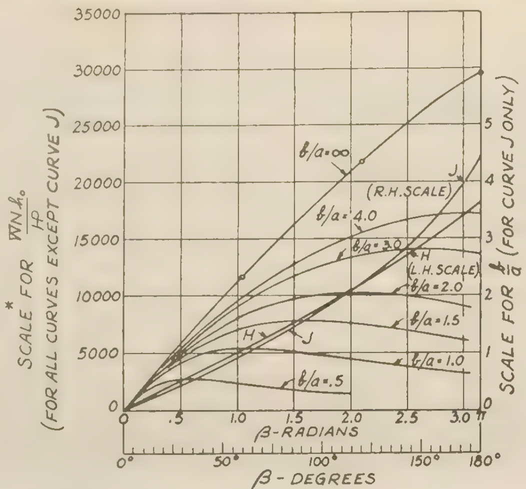

*WHEN THE CURVE FOR A GIVEN RATIO OF b/a IS CHOSEN, EACH ORDINATE OF IT WILL BE CORRECT FOR THE OPTIMUM RELATION OF THE SYMBOLS IN THIS GROUP. HENCE THE CORRECTION FACTORS FOR SIDE LEAKAGE ARE ALREADY ALLOWED FOR IN THE HEIGHTS OF THOSE ORDINATES.

CHART- C

THIS SHOWS FOR CLASS "C" BEARINGS THE VALUES OF THE NON-DIMENSIONAL GROUP $W N h_o/HP$ AS AFFECTED BY SIDE LEAKAGE, WITH FILM FORMS FOR THE MINIMUM COEFFICIENT OF FRICTION. CURVE J GIVES THE VALUE OF b/a AT WHICH GROUP $W N h_o/HP$ IS GREATEST FOR EACH VALUE OF β.

	β	60°	120°	180°
1	A	131.2°	83.66°	37.83°
2	α	30°	60°	90°
3	α/β	.50	.50	.50
4	C	.7466	.4688	.3437
5	h_m/h_o	2.004	1.980	1.937
6	h_1/h_o	1.137	1.144	1.158
7	η/h_o	3.946	1.883	1.524
8	θ_1	162.5°	146.8°	134.3°
9	ϕ	161.2°	143.7°	127.8°

TABLE C-1, GEOMETRICAL OPTIMA FOR MAXIMUM LOAD W

	β	60°	120°	180°
10	$W \frac{h_o^2}{\mu N a^3}$	.0180	.0673	.1352
11	$F \frac{h_o}{\mu N a^2}$	.0982	.1954	2902
12	$\lambda \frac{a}{h_o}$	5.464	2.906	2.147
13	$\lambda \frac{l}{h_o}$	5.722	6.087	6.744
14	$HP \frac{h_o (10)^6}{\mu N^2 a^3}$	1.559	3.101	4.605
15	$HP \frac{(10)^5}{W N h_o}$	8.670	4.611	3.406
16	$\frac{W N h_o}{HP (10)^5}$	.1153	.2169	.2936
17	$\lambda / \sqrt{\frac{\mu N}{p_o}}$	.5181	.5329	.5581

TABLE C-2, DYNAMICAL OPTIMA FOR MAXIMUM LOAD W

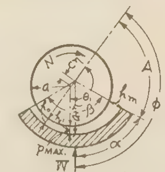

FIG "C"

CENTRALLY LOADED CLEARANCE BEARING

	β	60°	120°	180°
1	A	131.6°	84.39°	38.71°
2	α	30°	60°	90°
3	α/β	.50	.50	.50
4	C	.7615	.4904	.3645
5	h_m/h_o	2.072	2.056	2.021
6	h_1/h_o	1.140	1.148	1.163
7	η/h_o	4.193	1.962	1.574
8	θ_1	163.0°	147.8°	135.7°
9	ϕ	161.6°	144.4°	128.7°

TABLE C-3, GEOMETRICAL OPTIMA FOR MINIMUM FRICTION COEF. SEE CHART C-3 FOR OTHER VALUES OF β.

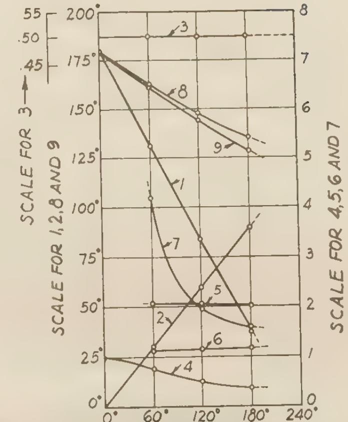

CHART C-3, GEOMETRICAL OPTIMA FOR MINIMUM FRICTION COEF.

	β	60°	120°	180°
10	$W \frac{h_o^2}{\mu N a^3}$	.0180	.0671	.1349
11	$F \frac{h_o}{\mu N a^2}$	.0980	.1948	.2890
12	$\lambda \frac{a}{h_o}$	5.458	2.902	2.142
13	$\lambda \frac{l}{h_o}$	5.716	6.078	6.731
14	$HP \frac{h_o (10)^6}{\mu N^2 a^3}$	1.555	3.091	4.586
15	$HP \frac{(10)^5}{W N h_o}$	8.660	4.604	3.399
16	$\frac{W N h_o}{HP (10)^5}$	.1155	.2172	.2942
17	$\lambda / \sqrt{\frac{\mu N}{p_o}}$	.5171	.5317	.5564

TABLE C-4, DYNAMICAL OPTIMA FOR MINIMUM FRICTION COEF. SEE CHART C-4 FOR OTHER-VALUES OF β.

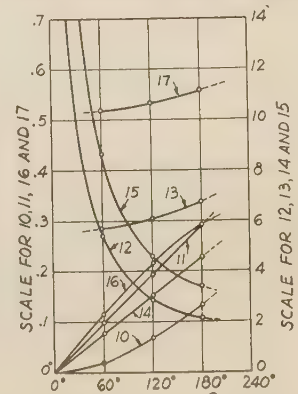

CHART C-4, DYNAMICAL OPTIMA FOR MINIMUM FRICTION COEF.

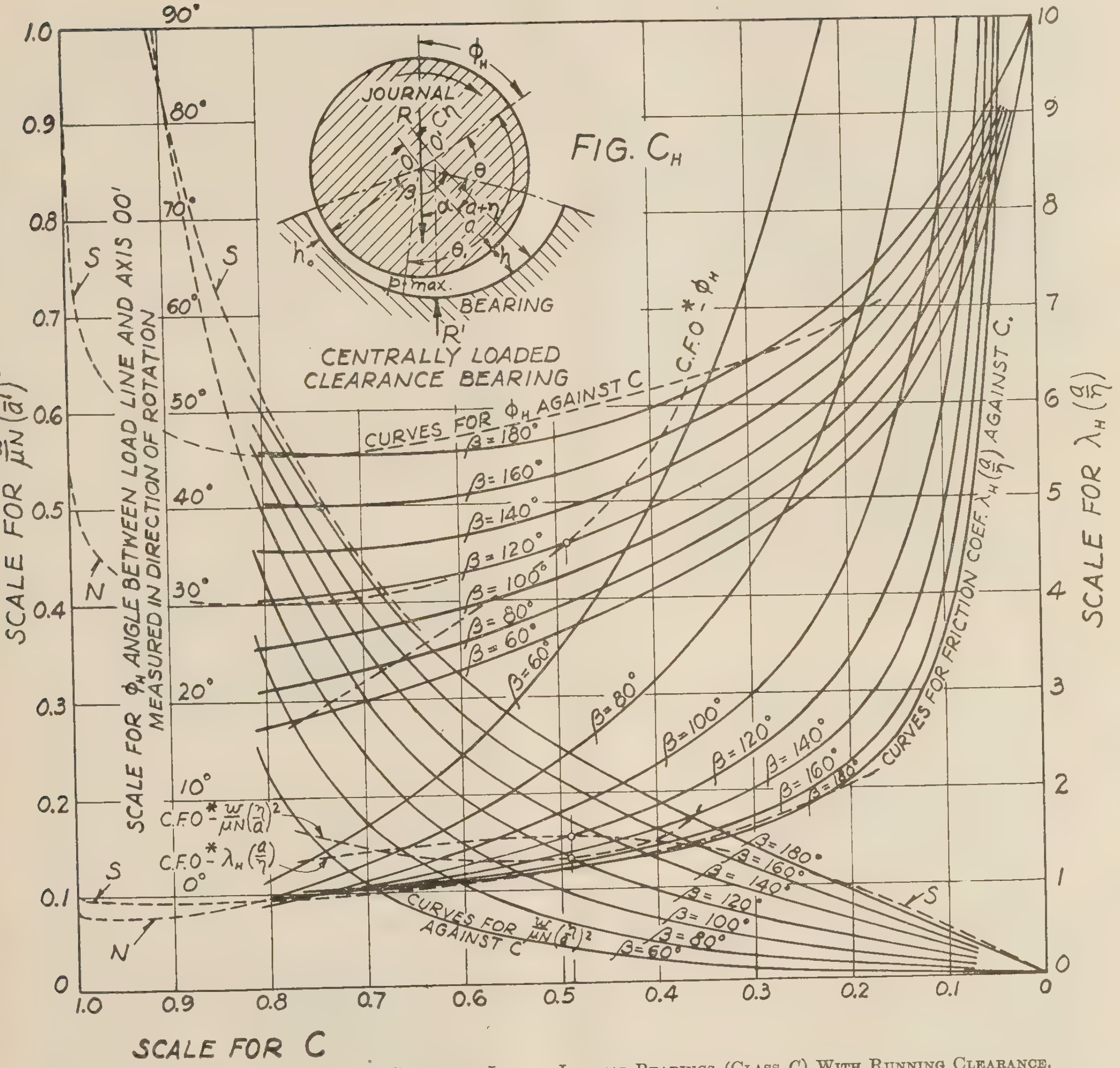

CHART C-5 GENERAL CONDITIONS OF CENTRALLY LOADED JOURNAL BEARINGS (CLASS C) WITH RUNNING CLEARANCE. SIDE LEAKAGE NEGLECTED

Eccentrically loaded bearings have their angular extent β divided into two unequal parts by the line of action of the applied load. The leading angle α is that portion of the angular extent β passed over by a point on the journal as it rotates from the edge of the bearing to a position directly under the load. The ratio of α/β may vary considerably when bearings are in service, because designers do not always need to trouble themselves to analyze individual bearings. There are, however, some ratios that are better than others.

Journal-Bearing Classification

The bearings whose optimum and general characteristics are given in the accompanying charts and tables may be divided into Classes A to F. The sources of data available for each class are given.

Class A. In Class A are found the special series of eccentrically loaded partial bearings with running clearance that Dr. Kingsbury found to be best. In this class the values of α/β vary not only for various values of β but they are different for the two optimum conditions studied by him. In all cases, however, the α/β ratio is appreciably greater than $\beta/2$.

Optimum conditions for this class are given for bearing angles β varying from 0 to 360 deg, in the figures, charts, and Tables A, A-1, A-2, A-3, and A-4. The letter A is used in every case to identify the class. This must not be confused with the symbol A. The data are reproduced from the work of Dr. Kingsbury (5).[2]

Class B. In Class B are found the special series of eccentrically loaded fitted partial bearings that Dr. Kingsbury found to be best. The values of the ratio α/β vary not only for various values of β but they are also different for the two sets of optimum conditions studied by him. In all cases the α/β ratio is appreciably greater than $\beta/2$.

Optimum conditions for this class are given for bearing angles

[2] Numbers in parentheses refer to Bibliography at the end of the paper.

β varying from 0 to 150 deg in figures, charts, and Tables *B*, *B*-1, *B*-2, *B*-3, and *B*-4. The data are reproduced from the work of Dr. Kingsbury (5).

Class C. In Class *C* are found partial bearings of the centrally loaded clearance series whose characteristics were studied by Dr. Kingsbury and by the author. The nominal values of α/β always equal $\beta/2$.

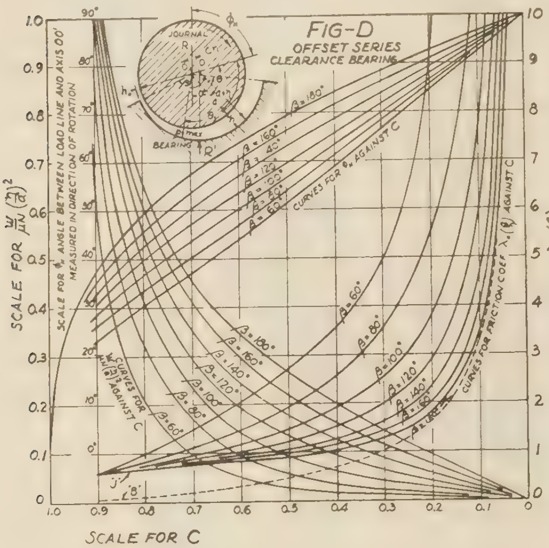

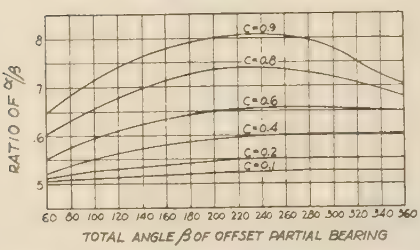

Charts *D*-1 (Below) and *D*-2 (Above) General Conditions for Offset (Eccentrically Loaded) Journal Bearings (Class *D*) With Running Clearance. Side Leakage Neglected

Optimum conditions for this class are given for bearing angles β varying from 0 to 180 deg, in figures, charts, and Tables *C*, *C*-1, *C*-2, *C*-3, and *C*-4. The data are reproduced from the work of Dr. Kingsbury (5).

General conditions for this class are given in Chart *C*-5, which has been prepared by the author from his earlier work (7) and made more usable.

Class D. In Class *D* are found the special series of offset (eccentrically loaded) partial bearings with running clearance whose characteristics were presented by the author in his graphical analysis (7). This series differs a little from Class *A*.

General conditions for this class are given in Charts *D*-1 and *D*-2 for bearing angles β varying from 60 to 180 deg. Chart *D*-2 is more usable than the original previously published (7).

Class E. In Class *E* are found the special series of eccentrically loaded fitted partial bearings that the author described in his earlier work (7). The values of α/β vary for different bearing angles β. This series differs a little from Class *B*.

General conditions for this class are given for bearing angles β varying from 60 to 120 deg, in Chart *E*-1. This chart is reproduced in improved form from earlier work of the author (7). On this chart are also shown by dotted lines some of the optimum conditions determined by Dr. Kingsbury. It should be noted here that for a fitted bearing the general conditions and the optimum conditions are the same for a given bearing or series when considered from the same point of view. This is true because there is no running clearance to introduce the question of eccentricity.

Classes ACD. The designation, Class *ACD*, has been used for a study made by the author of all classes for a single bearing of angular extent β = 120 deg and having running clearance (8).

General conditions as to capacity only (no friction data are given) are shown in Chart *ACD*-120. An immense amount of data on the 120-deg-clearance bearing are given on this chart, which is presented in improved form.

Class F. The designation, Class *F*, has been applied to full bearings, which must of course have running clearance. Such a bearing is a limit for the angle β to approach as will be seen by examining the optimum charts and tables given by Dr. Kingsbury for Class *A*. Hence, those charts and tables for values of β = 360 deg should be looked upon as optimum for the full bearing, especially if there be one common groove for oil supply and discharge located at the limits of the film.

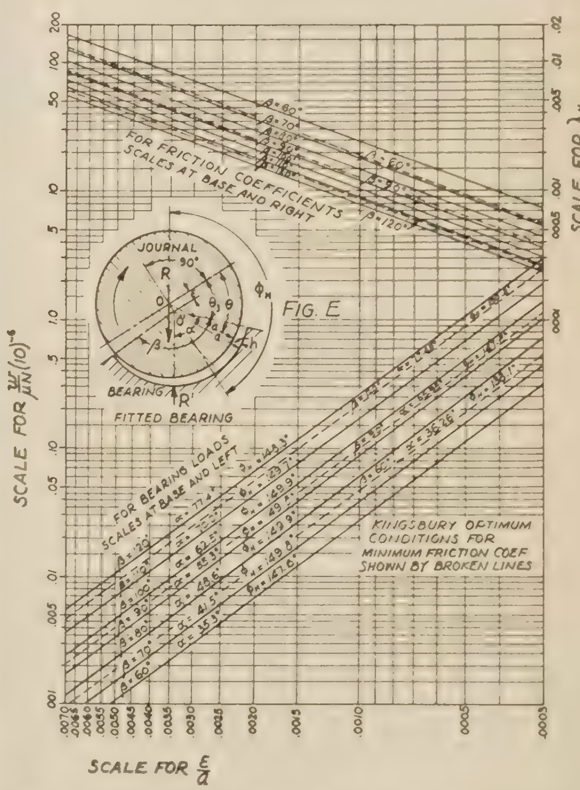

Chart *E*-1 General Conditions for Eccentrically Loaded Fitted Journal Bearings (Class *E*) Without Running Clearance. Side Leakage Neglected

General conditions for the full bearing are given in Chart *F*-1 in an approximate manner only because no one has yet been able to produce a continuous film in such a bearing, with all pressures positive. In Chart *F*-1, therefore, the load-carrying portion of the film is assumed to be 180-deg long and to have the load-carrying characteristics of a 180-deg offset partial bearing of Class *D*. For friction, however, the film is assumed to be that of a perfect full bearing. This is an approximation and is

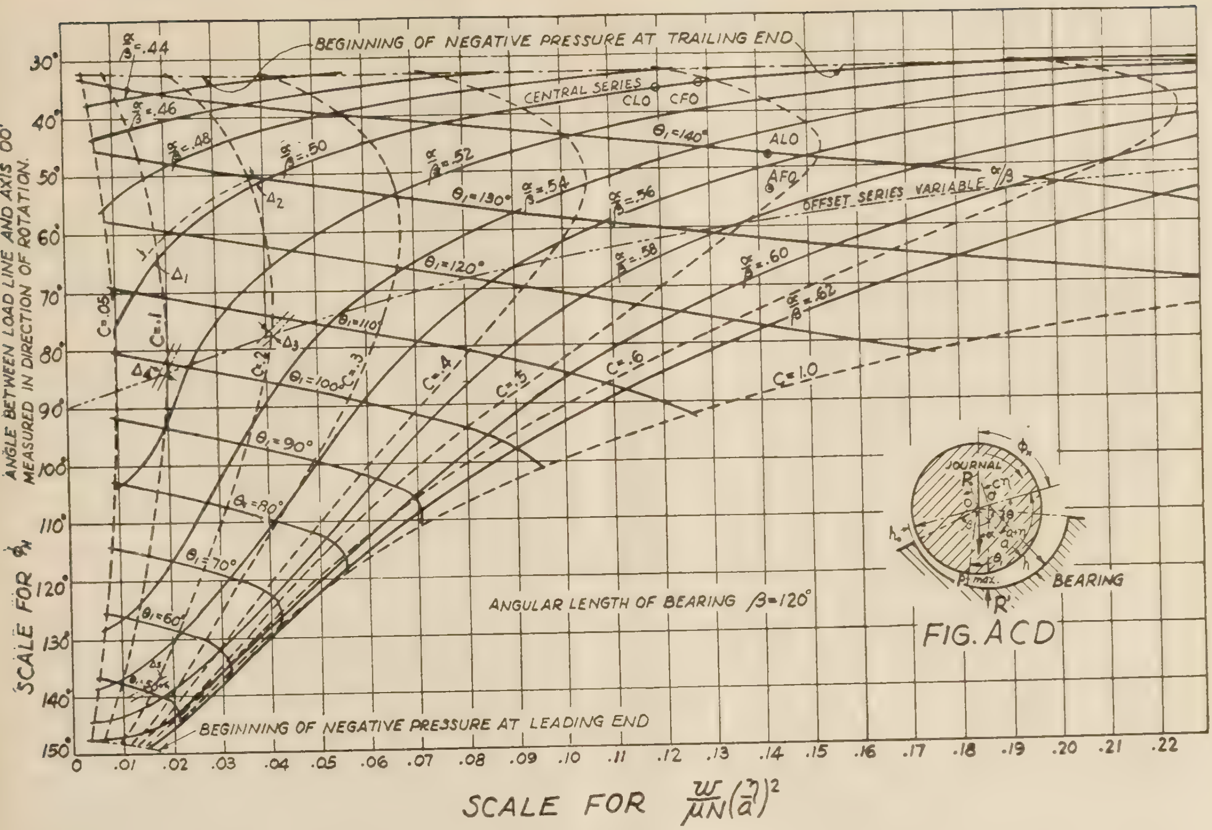

Chart *ACD*-120 General Conditions for 120-Deg Journal Bearings, With Running Clearance, for Capacities Only. Side Leakage Neglected

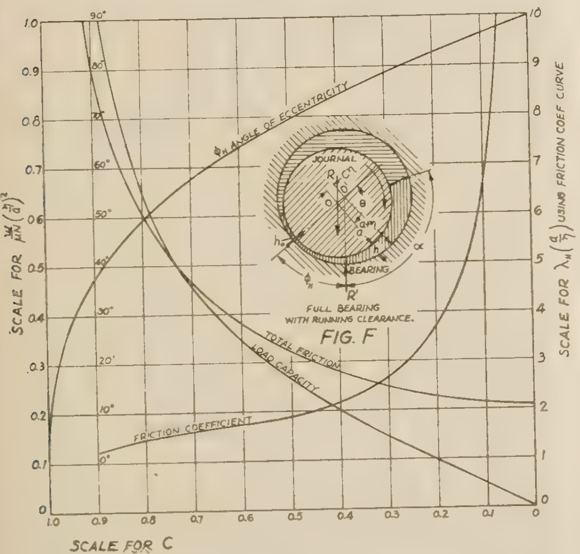

Chart *F*-1 Approximate General Conditions for Full Journal Bearings (Class *F*) With Running Clearance. Side Leakage Neglected

(For horsepower equivalents of total friction for the journal, multiply $\frac{\mu b}{2l}(a/\eta)a^2N^2(10)^{-5}$ by the scale reading obtained from the use of the total-friction curve and the right-hand vertical scale. To allow for side leakage multiply by F_1 taken from Chart *KX* for β = 180 deg.)

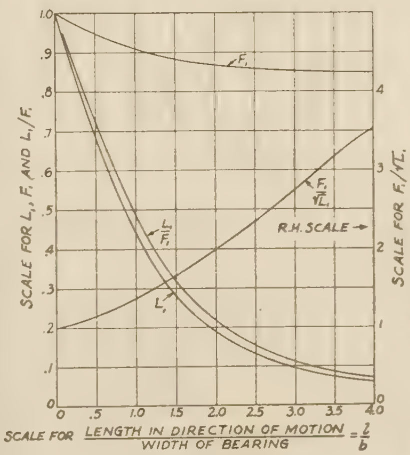

TABULAR QUANTITY	CORRECTION FACTOR
$\overline{W}$	L_1
F	F_1
$\lambda\left(\text{OR } \frac{F}{\overline{W}}\right)$	$\frac{F_1}{L_1}$
HP	F_1
$\frac{HP}{\overline{W}}$	$\frac{F_1}{L_1}$
$\frac{\overline{W}}{HP}$	$\frac{L_1}{F_1}$
$\lambda/\sqrt{\frac{\mu N}{p_0}}$	$\frac{F_1}{\sqrt{L_1}}$

TABLE-K.

MULTIPLY THE NUMERICAL VALUE OF THE DYNAMICAL SYMBOL GROUP BY THE CORRECTION FACTOR AS INDICATED IN ABOVE TABLE.

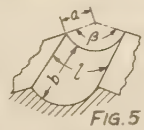

FIG. 5

$l = \frac{\pi a \beta}{180°}$

Chart *KX* Correction Factors for the Influence of Side Leakage Upon the Load-Carrying Capacity and Upon Friction, for Optimum Journal Bearings

(Apply these factors as shown in Table *K*.)

probably near enough to the correct value, for estimating purposes.

Correction Factors for Side Leakage

Correction factors for the influence of side leakage upon load capacity and upon friction are obtainable from Chart *KX*. These are reproduced from Plate *X* in Dr. Kingsbury's paper (5).

These factors apply to optimum film proportions as determined by Dr. Kingsbury but they will be reasonably dependable when applied to film forms not far different from optimum. Even when applied to abnormal conditions they tend to bring the results toward the correct values, and are usually on the safe side.

If the influence of side leakage upon capacity and upon friction were neglected in the solving of bearing problems, the information obtainable from Dr. Kingsbury's optimum-loading and friction charts and from the author's general charts would not agree well with actual conditions determined by reliable tests.

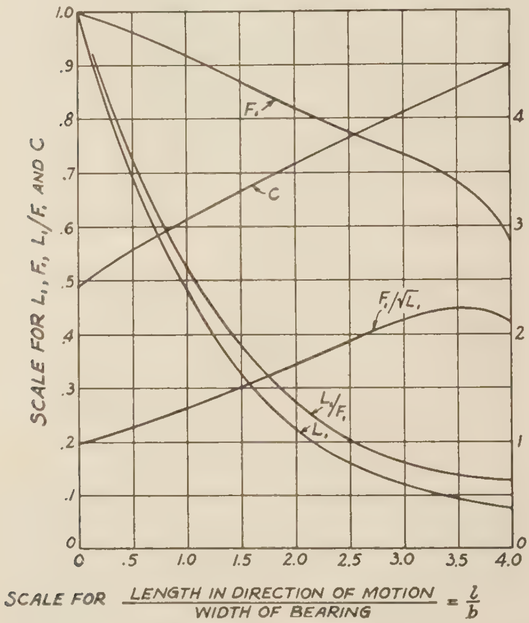

Fig. 1 Optimum 120-Deg Central Bearings for Minimum Coefficient of Friction

(Side-leakage factors obtained by comparing the actual capacities for various values of l/b with the capacity at infinite width when $c = 0.4904$.)

The use of the correction factors is explained by Dr. Kingsbury (5) as follows. "In the dynamical tables and curves" (see charts and tables for Classes *A*, *B*, and *C*) "the numerical coefficients are for the infinitely wide conditions (under which the side-leakage influence is negligible). Thus, for correction for bearings of finite width and given length/width ratio, these (numerical) coefficients are to be multiplied by the proper correction factor (from Chart *KX*) as below." If the symbol group in the dynamical table or chart contains the symbol or set of symbols tabulated in Table *K*, the corresponding numerical value of the group, in the dynamical table or chart, must be multiplied by the corresponding correction factor in Table *K*. The numerical value of the correction factor must be found from Chart *KX* by applying thereto the actual developed proportions of the useful film of the bearing being studied. See examples in Appendix B.

The side-leakage effect upon a 120-deg bearing of Class *C* was given special study by S. J. Needs (15) following a suggestion by Dr. Kingsbury (5) that the optimum film form of a narrow bearing would be different from that of a wide one. Needs found this to be true for the 120-deg Class-*C* bearing. He also found that negative pressures occur near the trailing end of a narrow 120-deg bearing earlier than would be expected if side leakage were negligible, thereby making them equivalent to eccentrically loaded bearings of angular extent less than 120 deg.

A study of these results since made by Needs has yielded a special chart, Fig. 1 herein, that may be used for obtaining correction factors and also optimum eccentricities for this 120-deg Class-*C* bearing, that may be used with the charts and tables of optimum and general conditions herein for the solution of bearing problems, particularly those with length/width ratios greater than 1.5.

Thus we now have two charts from which the correction factors of Table *K* may be obtained. Those in Chart *KX* are on the safe side and applicable to all optimum bearings. Those in Fig. 1 all apply directly to the 120-deg centrally loaded clearance bearing, and they also indicate that the capacities of narrow clearance bearings in general do not fall off as rapidly by becoming narrower, as Chart *KX* would indicate, if the eccentricities are allowed to increase in the manner indicated by Fig. 1.

The Loading and Friction of Journal Bearings

The charts here presented give the optimum and general characteristics of several useful forms of journal bearings that are described under "Journal-Bearing Classification." The headings and captions and notes on each set of charts are as complete as believed necessary to facilitate their use after the reading of the introductory pages of this paper.

The viscosity coefficient μ is assumed to have a constant mean value throughout the film. Although this is not in accordance with the facts, it is found to be satisfactory for the solution of bearing problems and has been so stated by several investigators, including Boswall and Kingsbury.

The charts and tables of bearing characteristics were all prepared under the assumption that the bearings were finite parts of infinitely wide ones and that, therefore, the flow of oil in the film was only in the planes of the direction of rotation. Therefore, the charted and tabulated data represent upper limits of load that a bearing film may carry, and the corresponding friction. Therefore, the correction factors must be applied to the ideal values to bring them in line with the actual capacities of bearings of finite width for which side leakage becomes more and more important as the length-width ratio increases.

Although Dr. Kingsbury's optimum conditions for Classes *A*, *B*, and *C* show ideal relations of viscosities, clearances, eccentricities, loads, and load directions, the designer may want to know how far wrong he is in some particular design that deviates from those optima. In one important case, Class *C*, the journal bearings examined by the author for general conditions are identical with those whose optima were found by Dr. Kingsbury. It was therefore possible to add a series of points to the general conditions, Chart *C*-5, to show the relation thereto of Dr. Kingsbury's optima. Three dotted curves are drawn marked by symbol groups preceded by the letters *C*, *F*, *O*. These letters mean Class-*C* friction optima. For a complete discussion of this comparison see Appendix D on perfect lubrication in the sections on optima and deviations from optima.

Chart *ACD*-120 yields so much loading information about all classes of 120-deg clearance bearings that it may be used for studying the influences upon running position, of various changes in design proportions such as the α/β ratio and the clearance ratio η/a. Side-leakage-correction factors may be applied to this chart as in Example 4, Appendix B, but only for L_1 as in

$p_0 = wL_1$. The farther one departs from good film proportions the less reliable will be the L_1 factor taken from Chart *KX*. In such cases Fig. 1 should be kept in mind.

Chart *ACD*-120 also gives the angular location θ_1 of the maximum oil pressure in the film.

The optima of Dr. Kingsbury for this bearing appear only as four points. Those for the Class-*A* bearing are marked *ALO* and *AFO*, for maximum-load and minimum-friction coefficient, respectively. For Class-*C* bearings they are marked *CLO* and, *CFO*. These afford the user a way to tell how nearly optimum are his actual conditions.

When operating conditions are such that the Chart *ACD*-120 shows negative pressure is likely to appear at the trailing end of the bearing it is best to study such bearings as if they were of the eccentrically loaded Class *A*, or of the offset Class *D*, in either case with a leading angle of $\alpha = 60$ deg, letting the trailing angle $(\beta - \alpha)$ be determined by the class used. See Example 5 in Appendix B.

In Chart F-1 for full bearings they are treated as half bearings so far as carrying capacity is concerned, but as full bearings so far as friction is concerned, the running position of the journal for the latter being established by applying the first assumption. The load-capacity curve of Chart *F*-1 was taken from Chart *D*-2 for the $\beta = 180$-deg offset series because the pressure film is not apt to be greater than 180 deg in extent. Experiments by Stanton (16), Bradford (17), and McKee (18) might lead one to expect shorter films than 180 deg for some conditions. Hence, if a β value of 100 deg is to be expected, the charts and tables for Class *D* may be used to estimate the capacity and the eccentricity. Then Chart *F*-1 can be entered with that eccentricity, and the approximate total friction and horsepower loss estimated. Care must be exercised not to use the friction-coefficient curve on Chart *F*-1 with any other line than the load-capacity line on Chart *F*-1. See Example 7 in Appendix B for application of side-leakage-correction factors to full-bearing problems.

The data available from the charts and tables of this paper, and the problems solved in examples of Appendix B depend entirely upon absolute-viscosity coefficients. No ready means are offered herein for converting absolute into commercial viscosities or vice versa. For such conversions the reader is referred to a recent paper by the author (20) entitled "Current Practice in Pressures, Speeds, Clearances, and Lubrication of Oil-Film Bearings," Trans. A.S.M.E., Vol. 56, 1934, paper MSP-56-2, p. 891.

TABLE 1 THRUST-BEARING CAPACITY FOR FREELY PIVOTED SHOES

(Viscosity coefficient = 3.4×10^{-6} Reyn, lb-sec per sq in.)

	SURFACE SPEED, FEET PER SECOND, = U/12								
	5	10	20	40	60	80	100	120	140
FACE AREA (SQ IN)	CAPACITY, POUNDS PER SQUARE FACE AND MINIMUM FILM THICKNESS, INCH								
4	855 00036	1015 .00047	1210 .00061	1440 .00079	1590 .00092	1710 .00102	1810 .00112	1890 .00119	1960 .00126
16	4060 00047	4830 .00061	5750 .00079	6850 .00103	7550 .00119	8150 .00132	8600 .00145	9000 .00155	9350 .00163
36	10 100 .00055	12,000 .00071	14,300 .00092	17,000 .00119	18,750 .00138	20,200 .00154	21,400 .00168	22,400 .00180	23,200 .00192
64	19,300 00061	23,000 .00079	27,400 .00102	32,500 .00133	36,000 .00155	38,600 .00172	40,900 .00188	42,800 .0020	44,500 .00215
100	31,900 00066	38,000 .00086	45,200 .00112	53,500 .00145	59,500 .00168	64,000 .00186	67,500 .00205	70,700 .0022	73,500 .00235
144	48 000 .00071	57,200 .00092	68,000 .00119	81,000 .00155	89,500 .00180	96,500 .0020	102,000 .0022	106,500 .00235	111,000 .0025
196	68,000 .00075	81,000 .00098	96,000 .00127	114,500 .00163	126,500 .00190	136,000 .0021	144,000 .0023	150,000 .0025	156,000 .00265
256	92,000 00079	109,000 .00103	130,000 .00133	155,000 .00172	171,000 .0020	184,000 .0022	194,000 .00245	203,000 .0026	211,000 .0028
324	119,000 .00083	142,000 .00108	168,000 .00138	201,000 .00180	222,000 .0021	239,000 .0023	252,000 .00255	264,000 .0027	274,000 .0029
400	152,000 .00086	181,000 .00112	215,000 .00145	256,000 .00188	283,000 .0022	304,000 .0024	321,000 .00265	336,000 .0028	350,000 .0030

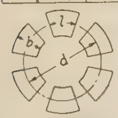

FOR AVERAGE PROPORTIONS OF THRUST BEARINGS, $d = 3b$.
FOR ANY RATIO OF b TO d, IF $l = b$ THE BEARING AREA WILL TOTAL $6 \times l^2$ FOR SIX SHOES, AND THE TOTAL CAPACITY WILL BE THAT IN THE TABLE TIMES THE NUMBER OF SHOES

TO FIND THE FEET PER SECOND FROM THE R.P.M

$$\frac{U}{12} = \frac{\pi dN}{12 \times 60}$$

TABLE IS BASED ON ASSUMPTION THAT $l = b$.
FOR OTHER PROPORTIONS MULTIPLY THE TABULAR LOAD BY THE CORRECTION FACTOR IN TABLE AT LEFT

$l \div b$	LOAD CORRECTION FACTOR*
0.50	1.557
0.67	1.357
1.00	1.000
1.33	0.732
1.50	0.630
2.00	0.423

* TABLE IS BASED ON DATA GIVEN IN BULLETINS ON KINGSBURY BEARINGS PUBLISHED BY KINGSBURY MACHINE WORKS INC, PHILA. PA
THE UPPER VALUE IS THE CAPACITY AND THE LOWER ONE IS THE MINIMUM FILM THICKNESS - h_0

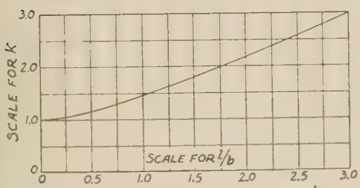

FRICTION CORRECTION FACTOR K FOR FLAT BEARING FACES.

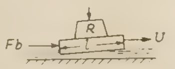

LOADED PLATE RIDING ON A FILM OF OIL. THE LENGTH OF THE PLATE IS "l" AND THE WIDTH IS "b"

TABLE 2 CAPACITY, POWER LOSS, AND COEFFICIENT OF FRICTION—KINGSBURY THRUST BEARINGS

(6 shoes, 51-deg subtended angle, viscosity = 3.4×10^{-6} Reyn)

OUTER DIA. OF BEARING INCHES	350 LB./SQ.IN. PRESSURE, SHOE BORE = 1/2 OF OUTSIDE DIA.	
	CAPACITY POUNDS	POWER LOSS HORSEPOWER AT 100 R.P.M.
5	4,380	.0128
6	6,300	.0220
7	8,600	.0350
8	11,200	.0522
9	14,200	.0744
10½	19,300	.118
12	25,200	.176
15	39,500	.344
17	50,800	.501
21	77,300	.944
25	109,500	1.59
29	147,500	2.49
33	191,000	3.66
37	240,000	5.17
45	355,000	9.30
53	493,000	15.2
61	652,000	23.2
73	935,000	39.7

SPEED (R.P.M.)	SPEED FACTOR FOR POWER LOSS	COEF. OF FRICTION AT 350 LB./SQ IN. PRESSURE
50	.354	.00069
60	.465	.00076
80	.716	.00088
100	1.00	.00098
120	1.32	.0011
160	2.02	.0012
200	2.83	.0014
250	3.95	.0016
300	5.20	.0017
400	8.00	.0020
500	11.2	.0022
600	14.7	.0024
800	22.6	.0028
1000	31.6	.0031
1250	44.2	.0035
1500	58.1	.0038
2000	89.4	.0044
3000	164	.0054

PRESSURE LB. PER SQ. IN.	CORRECTION FACTOR FOR COEF OF FRICTION
100	.53
175	.71
250	.85
300	.93
350	1.00
400	1.07
500	1.19

The Loading and Friction of Kingsbury Thrust Bearings

Although loading tables for thrust bearings have been published in bulletins issued by Dr. Kingsbury describing their design and construction, this paper will deal more with their theoretical aspects, and will include the data on their friction losses. See Appendixes C and D for a discussion of the fundamental ideas involved.

Loading of Thrust Bearings. It is found from the study of film forms that a certain one may be looked upon as productive of the least friction, and that the minimum film thickness is a proper criterion for bearing safety. Because of the difficulty involved in measuring film thicknesses, very little of this has been done. That little, however, has indicated that the mathematical theory is practically correct. It is reasonable, therefore, to build up a basic loading table and to mark upon it the minimum film thicknesses that are to be expected under the conditions set forth. Table 1 is based on the experience and practice of Dr. Albert Kingsbury, inventor of the pivoted-shoe thrust bearing, and is supplemented by data derived by means of the mathematical theory of lubrication.

Table 1 is for average thrust bearings used for steam turbines,

centrifugal pumps, ordinary industrial machinery, marine propulsion, and hydroelectric units, where the oil is not heavy. At operating temperature the viscosity coefficient of the lubricant is assumed to be about 0.23 poise. This is equivalent to 23 centipoises or 3.4×10^{-6} Reyn. The commercial viscosity equivalents (when the basic specific gravity = 0.875) are 125 sec Saybolt universal, 110 sec Redwood No. 1, and number 3.7 Engler.

The decimal values, below the capacity figures, are the corresponding approximate estimated minimum film thicknesses, on the median line of the shoe at the trailing edge, when the previously described oil is used. The viscosity given is assumed to be the mean value within the film. The bath viscosity or supply viscosity must be higher by an amount which may be estimated approximately.

The load-correction factors for various shoe-face proportions, are based on a study of side leakage which is discussed in Appendix D.

Friction in Thrust Bearings. In a letter to the editor of *Mechanical Engineering*, April, 1927, the author presented a formula for the friction coefficient for a perfectly lubricated surface moving upon tiltable rectangular shoes, with straight-line motion. This is approximately the condition under which the Kingsbury thrust bearing operates, and is deducible from the equations of Osborne Reynolds. The symbols for this formula which follows are defined in Appendix A, the notations differing somewhat from the original.

$$\lambda = \frac{Fb}{R} = 1.81\, k \sqrt{\left(\frac{\mu U}{lp_0}\right)}$$

The factor k is so applied as to yield a coefficient of friction that takes side leakage of oil into account. The relation of this factor to the length/width ratio of the bearing shoe faces is given in the curve in Table 1. This curve is based upon data published by Michell (9). When there is no side leakage $k = 1$. See also the discussion "Side Leakage Reduces Capacity" in Appendix D, and the Kingsbury Chart *KX* in the text of this paper and compare curve for F_1/L_1.

Power Losses in Thrust Bearings. Table 2 gives the relations between capacity, speed, and friction, for Kingsbury thrust bearings of various sizes, when the mean viscosity of the oil in the bearing films is 3.4×10^{-6} Reyn. The l/b ratio of the shoes for these tables is 4/3 and the outer diameter of the bearing is 4/3 times the mean diameter. For such a bearing the net area of the segments in square inches, there being six, is one-half the square of the outer diameter in inches. The friction coefficients and power losses are calculated upon the assumption that the correction factor for side leakage is $k = 1.6$. By a study of the formula for λ one may readily make corrections for other conditions than for those assumed.

Appendix A

An effort has been made to standardize the symbols used in the text of this paper so that a given character will have the same meaning throughout for journal bearings and a corresponding meaning for other bearings. The symbols used are in most cases those appearing in Dr. Kingsbury's paper (5). When comparing the present work with original source material care must be used to avoid confusion of symbols.

Nomenclature

a = radius of the journal[3]

A = least angle from line of centers to leading edge of partial bearing, measured in direction of rotation. See exception in study of fitted bearings, Fig. *B*

b = width of bearing surface; measured along the shaft axis in a journal bearing, or in general at right angles to direction of motion

c = eccentricity factor. When multiplied by the radial clearance η the product $c\eta$ equals the distance from the center of the bearing to the center of the journal

F = the total tangential friction force per unit width of the moving surface, at the surface of the journal, or at mean diameter of a thrust bearing[1]

F_1 = correction factor for friction, with side leakage

h = film thickness at any angular position θ in journal bearings, or any distance x for flat tapered films. For fitted journal bearings $h = \epsilon \sin \theta$. For clearance journal bearings $h = \eta(1 + c \cos \theta)$

h_0 = minimum thickness of the oil film in a bearing. Exception: When the line of centers for a clearance bearing does not intersect the partial bearing surface, h_0 is measured where the bearing surface if extended would cross that line

h_1 = thickness of the oil film at region of maximum pressure

h_A = thickness of oil film at entering edge of the bearing film if less than h_m

h_E = film thickness at trailing edge of partial clearance bearing, when greater or less than h_0

h_m = maximum thickness of the oil film

HP = horsepower friction developed by a journal bearing or a thrust bearing per unit of bearing width

hp = horsepower

l = the length of a bearing face in the direction of motion. In a partial journal bearing, whose angular extent β is expressed in degrees, $l = \pi\beta a/180$. This is useful for determining the length over width ratio l/b used for selecting side-leakage-correction factors

L_1 = correction factor for load-carrying capacity, with side leakage

N = rpm

n = number of pivoted segments in a thrust bearing

O = center of curvature of journal when running on oil film

O' = center of curvature of bearing surface supporting the journal

p = pressure within the oil film where the thickness is h

p_0 = nominal mean pressure acting upon the bearing. In journal bearings this is obtained by dividing the total applied load by the product of the journal diameter and bearing width (axial). This is also expressed by dividing the load $\overline{W}$ (per unit of width) by the journal diameter $2a$. In thrust bearings $p_0 = R/nlb$. See Table 1

P_m or P_{max} = maximum pressure within the oil film of a bearing

R = total load applied by the journal to the bearing, or by a collar to a thrust bearing

R' = total reaction of the bearing against the journal

s = a film-form dimension in Fig. 9

t = time, sec

T = distance apart of plane surfaces. See Appendix C and Figs. 2 to 4

u = velocity of any element of viscous flow, within the film

U = relative velocity of the bearing surfaces. In thrust bearings it is measured on the mean diameter

w = nominal mean unit load a bearing would carry if side leakage could be neglected. See p_0. Their relation is $p_0 = L_1 w$

[3] Exceptions occur in Appendix *C* on "Viscous Flow" for which the symbols are described by the figures and at end of that section.

$\overline{W}$ = actual load applied by a journal to its bearing, per unit of width (axial) = R/b

Z = character expressing the viscosity coefficient in centipoises. See Appendix C

α = leading angle for partial bearing, measured in direction of motion of journal from leading edge of bearing to line of action of the load

β = angular extent of the bearing surface over which perfect film lubrication is assumed to be maintained. Usually expressed in deg

ϵ = eccentricity of journal axis when running in a fitted bearing

η = radial clearance provided in a clearance bearing. When a = the journal radius, $(a + \eta)$ = radius of curvature of a bearing surface, and $c\eta$ = eccentricity with which the journal axis runs in such a clearance bearing

θ = angle from diameter through line of centers, to point within oil film of a journal bearing where thickness is h. See exception in study of fitted bearing, Fig. B.

θ_1 = angle θ corresponding with location of maximum unit pressure within the oil film

λ = coefficient of friction for the journal surface. In thrust bearings this is the coefficient for the mean diameter of the thrust-collar face

λ' = coefficient of friction for the bearing surface

λ_H = uncorrected coefficient of journal friction in charts of general conditions for journal bearings. $\lambda = \frac{F_1}{L_1}\lambda_H$

μ = coefficient of viscosity. See Appendix C

ϕ = angle relating load line to line of centers of journal and bearing in charts of optimum conditions. See bearing cross-sections, Figs. A, B, and C

ϕ_H = angle relating load line to line of centers of journal and bearing in charts of general conditions. See bearing cross-sections, Figs. C_H, D, E, ACD, and F

Appendix B—Examples

Example 1. Required, a bearing of Class A, of minimum friction, to support a load of 25,000 lb at 1500 rpm, with h_0 = 0.003 in., and with 200 lb per sq in. on the projected area of the journal.

This requires a projected area of 125 sq in. Assume for this example that $b/a = 3$, i.e., that the width of the bearing (b) will be 1.5 times the journal diameter ($2a$). The projected area being $2a^2(b/a) = 125$, it follows that $a = \sqrt{(125/6)} = 4.564$ in. This radius may or may not be sufficient for strength in bending or in torsion, or both; but it will be assumed that it is sufficient.

Referring to Chart A, the least horsepower loss (per unit of width b) when $b/a = 3$, is incurred when $\beta = 153.6$ deg (2.68 radians), for which the value of group $\overline{W}Nh_0$/HP is 16,900. As the ratio of load to power loss is the same for the whole width as for unit width

$$\text{total power loss (HP} \times b) = \frac{25{,}000 \times 1500 \times 0.003}{16{,}900} = 6.66 \text{ hp}$$

This does not include losses in any clearance spaces outside of the film arc β.

The clearance η (see Chart A-3, curve 7) for $\beta = 153.6$ deg is found from the height to the curve, which is 1.72. This is the value of group 7 in Table A-3. Hence $\eta = 1.72\, h_0 = 0.00516$ in. The bore diameter of the bearing is therefore larger than the 9.128-in. diameter of the journal by $2 \times 0.00516 = 0.01032$ in., which makes it 9.138. The clearance ratio η/a is therefore 0.00113.

In order to determine the required oil-viscosity coefficient it is necessary to determine the correction factors. This may be done as follows:

The arc length of the bearing surface, $l = 2.68 \times 4.564 = 12.23$ in.

$$\text{The width } b = 3.00 \times 4.564 = 13.69 \text{ in.}$$

The ratio l/b is therefore 0.893. By reference to Chart KX, several correction factors which may now be determined are: $L_1 = 0.487$; $F_1 = 0.916$; and $L_1/F_1 = 0.532$. The required mean viscosity in the oil film may now be determined from group 10, Table A-4 and curve 10, Chart A-4. For the infinitely wide bearing and $\beta = 153.6$ deg, the height of curve 10 measures 0.117. To this is to be applied the correction factor $L_1 = 0.487$. Hence group 10 = 0.117 L_1. The actual mean load per unit of bearing width is

$$25{,}000/13.69 = 1826 \text{ lb} = \overline{W}$$

Substituting this and other known values in group 10 and solving for μ, we obtain

$$\mu = \frac{1826 \times (0.003)^2}{0.117 \times 0.487 \times 1500 \times (4.564)^3} = 2.022 \times 10^{-6} \text{ in.-lb-sec (Reyn)}$$

With the conversion factor 69,000, this viscosity coefficient is 0.1395 poise, which is that of a light machinery oil at about 130 to 140 F. For determination of corresponding commercial viscosities see the viscosity-temperature-conversion charts in the author's recent paper (20).

The coefficient of friction may be found from group 12, Table A-4 and Chart A-4, curve 12.

$$\lambda = \frac{F_1}{L_1} \times 2.00 \times \frac{h_0}{a} = \frac{2.00 \times 0.003}{0.532 \times 4.564} = 0.00247$$

Inspection of Chart A-1 indicates that by increasing the ratio b/a, other things being equal, the relative power loss will be reduced; this is shown more specifically in Example 2. The extent to which b/a may be increased must be limited eventually by considerations of space, cost, and the strength or elasticity of the journal.

In the present example, the angle β might be increased, following curve for $b/a = 3$, on Chart A-1, securing, thereby, a somewhat greater bearing area; but this would involve a relatively greater friction loss, as is obvious on inspection.

Other data for this bearing can be found from the charts and tables, e.g., the leading angle α from group 3 and curve 3.

Example 2. In Example 1, suppose that b/a is taken as 4 instead of 3, the other data remaining unchanged. We then have, referring to the same tables and charts

$$a = \sqrt{(125/8)} = 3.953 \text{ in.}$$

$$\beta = 180.8 \text{ deg} = 3.155 \text{ radians, for the least power loss.}$$

$$\text{Total power loss} = \frac{25{,}000 \times 1500 \times 0.003}{20{,}700} = 5.435 \text{ hp.}$$

Clearance $\eta = 1.622\, h_0 = 0.004866$ in.
= 0.00123 in. per in. of diam.

Length $l = 3.155 \times 3.953 = 12.47$ in.
Width $b = 4 \times 3.953 = 15.81$ in.
Ratio $l/b = 0.789$. This determines the correction factors:

$$L_1 = 0.533, F_1 = 0.924, \text{ and } L_1/F_1 = 0.577$$

$$25{,}000/15.8 = 1581 \text{ lb} = \overline{W}$$

$$\mu = \frac{1581 \times 0.003^2}{0.1517 \times 0.533 \times 1500 \times (3.953)^3} = 1.90 \times 10^{-6} \text{ in.-lb-sec (Reyn)}$$

This corresponds to 0.131 poise.
The coefficient of friction is found to be

$$\lambda = \frac{F_1}{L_1} \times 1.762 \times \frac{h_0}{a} = \frac{1.762 \times 0.003}{0.577 \times 3.953} = 0.002318$$

These optimum charts and tables may also be used for determining the proper radial clearance or the oil viscosity for a known set of other conditions.

Example 3. What radial clearance η is best for following conditions? Total load $R = 25{,}000$ lb, $N = 1500$ rpm, $\beta = 120$ deg, $p_0 = 125$ lb per sq in., $b/a = 4$, oil viscosity $= \mu = 3.4 \times 10^{-6}$ in.-lb-sec (Reyn). Bearing is centrally loaded which means Class C. Proceed as follows:

From above data it is found that $2a = 10$ in., $b = 20$ in., $\overline{W} = 1250$.

$$l = 10.47 \text{ in.} \qquad l/b = 0.524$$

Correction factors from Chart KX will then be $L_1 = 0.672$, $F_1 = 0.947$, $L_1/F_1 = 0.710$.

Then from group 10 in Table C-4 and by introducing correction-factor L_1, we obtain

$$\frac{\overline{W}h_0^2}{\mu N a^3} = 0.0671\ L_1 = 0.0451$$

This may be solved for h_0, the only unknown. (Hence $h_0 = 0.0048$.) Thereafter the desired value of η may be found from group 7, Table C-3. It will be $1.962\ h_0 = 0.0094$. The clearance ratio will therefore be $\eta/a = 0.00188$. The friction coefficient λ is to be found from group 12, Table C-4, which group equals $2.902\ F_1/L_1$. Hence

$$\lambda = 2.902/0.710 \times 0.0048/5 = 0.00392$$

The procedure for examples under Class-B journals would be similar to that already described, but having reference to the approximate Class-B tables and charts, corresponding to those referred to in Examples 1, 2, and 3.

As explained under "Deviations from Optimum," in Appendix D, it is practicable to explore other than optimum conditions by the use of the charts of general conditions which follow those on optimum conditions. To these, with fair approximation, may be applied the side-leakage-correction factors given on Chart KX. Kingsbury's optimum points have been marked on the charts of general conditions when the bearing class is the same or the chart suitable for showing both conditions. This is practicable for the Chart C-5 of centrally loaded bearings and of Chart ACD-120 which gives loading characteristics of a wide variety of 120-deg bearings.

Example 4. Find the running positions of the journal in the following centrally loaded 120-deg bearing using two different oils whose viscosity coefficients are 3.4×10^{-6} Reyn and 10.2×10^{-6} Reyn, respectively. The total load $R = 10{,}000$ lb, the actual nominal pressure $p_0 = 125$ lb per sq in., the journal diameter = 8 in., the bearing width = 10 in.; the clearance ratio $\eta/a = 0.001$, and the speed $N = 400$ rpm.

The first step in solving this problem is to set down the known values of the symbols as far as practicable. The scale at the left of Chart C-5 represents a symbol group for which all values are known except w. This w is the ideal nominal pressure the bearing would sustain if side leakage could be neglected. It is reduced to the actual nominal pressure p_0 by side leakage. Hence $p_0 = L_1 w$ and the correction factor L_1 must be found from Chart KX. From the problem data the l/b ratio is found to be $8\pi \times 120/10 \times 360 = 0.839$.

This yields the following correction factors: $L_1 = 0.51$, $L_1/F_1 = 0.555$, $F_1 = 0.92$. Hence,

$$\frac{w}{\mu N}\left(\frac{\eta}{a}\right)^2 = \frac{245 \times 1 \times 10^{-6}}{\mu \times 400} = \frac{0.613 \times 10^{-6}}{\mu}$$

First, substituting $\mu = 3.4 \times 10^{-6}$, the group is found to equal 0.180. With this we may enter the Chart C-5 at left. This reaches the loading curve for $\beta = 120$ deg, where $c = 0.581$. Reading down to friction, coefficient curve for $\beta = 120$ deg, we find that $\lambda_H \frac{a}{\eta} = 1.29$. Then reading upward on $c = 0.581$ to the ϕ_H-curve for $\beta = 120$ deg, we find that $\phi_H = 33.2$ deg. The actual friction coefficient will be $\lambda = \frac{F_1}{L_1}\lambda_H$. Hence, $\lambda = 1.29 \times 10^{-3}/0.555 = 0.00233$. The journal running position will be on the line $\phi_H = 33.2$ deg. Its distance from the center of the bearing will be $c\eta = 0.581 \times 0.001 \times 8/2 = 0.002324$. The minimum film thickness will be $h_0 = (1 - c)\eta = 0.001676$.

Dr. Kingsbury's optimum eccentricity factor is seen from the C, F, O, dotted loading curve $\frac{w}{\mu N}\left(\frac{\eta}{a}\right)^2$ on Chart C-5 to be 0.49 for a 120-deg bearing. For this, $h_0 = 0.00204$. Hence, for $\mu = 3.4 \times 10^{-6}$, our assumed bearing is not quite as safe as the optimum would be.

Solving this same problem with $\mu = 10.2 \times 10^{-6}$ leads to the following results, the group value for entering the chart being 0.060. Proceeding as before we find $c = 0.28$, $\phi_H = 46$ deg, $\lambda_H(a/\eta) = 2.54$, $\lambda = 0.00458$, and $h_0 = 0.00288$. Hence, with this heavier oil the friction is greater, as would be expected. The minimum film thickness is also greater than for the lighter oil. An intermediate oil would cause the journal to run with optimum eccentricity, but as the clearance is fixed it is necessary to decide which is the more important, a least film thickness of $h_0 = 0.00168$, or $h_0 = 0.00204$ or $h_0 = 0.00288$. The degree of perfection of the shaft alignment may be the deciding factor. Heavier oil is better when conditions of alignment are not ideal. See film thicknesses noted in loading Table 1 for Kingsbury thrust bearings.

Example 5. In a 120-deg bearing, would negative pressures in the oil film be expected with a 6-in.-diam journal 10 in. wide, carrying 600 lb at 1000 rpm with a clearance ratio of $\eta/a = 0.002$, and an oil viscosity of 4.0×10^{-6} Reyn, (*a*) when $\alpha/\beta = 0.44$? (*b*) when $\alpha/\beta = 0.52$? (*c*) when $\alpha/\beta = 0.62$?

First find correction factor L_1 from Chart KX. It will be the one corresponding to $l/b = (6\pi \times 120)/(10 \times 360) = 0.628$. Therefore, $L_1 = 0.613$ and $w = 600/(6 \times 10 \times 0.613) = 16.30$. Then since $\mu = 4.0 \times 10^{-6}$ the group $\frac{w}{\mu N}\left(\frac{\eta}{a}\right)^2 = \frac{16.3 \times 4 \times 10^{-6}}{4 \times 10^{-6} \times 1000} = 0.0163$. Referring to Chart ACD-120 the answer to (*a*) is that the bearing is close to the region there indicated for negative pressure at the trailing edge. The answer to (*b*) is that the bearing is not likely to have negative pressure. The answer to (*c*) is that negative pressure is likely at the leading edge.[4]

Abnormal conditions were assumed for this bearing in order

[4] An investigation by S. J. Needs shows that negative pressure is to be expected in a finite bearing for conditions where the infinite-width bearing would show all positive pressures. Hence, when the data of a problem show that the running position approaches the upper-limit line of Chart ACD-120, some negative pressure is probable. Such a condition would place the bearing in some other class for which $\alpha = 60$ deg and $\beta - \alpha < 60$ deg.

to bring out the negative-pressure feature. Note the locations of the optimum points for the Class-A bearings near the center of the Chart ACD-120. These points are marked AFO and ALO. For a Class-C bearing the optimum points are marked CFO and CLO. By comparing these points with those located by the problem data some idea of the divergences may be gained.

Example 6. Find the minimum film thickness in a 100-deg fitted bearing running under the following conditions: $N = 300$, $\mu = 3 \times 10^{-6}$ Reyn, total load $= 3000$ lb, journal diameter $=$ 5 in., and its width $= 6$ in. The procedure is as follows:

$$l/b = (\pi 5 \times 100)/(6 \times 360) = 0.727$$

Therefore, $L_1 = 0.565$ and $w = 3000/(30 \times 0.565) = 177$. Then $\frac{w}{\mu N} \times (10^{-6}) = \frac{177 \times 10^{-6}}{3 \times 10^{-6} \times 300} = 0.197$, the value with which Chart E-1 is entered at the left. Reading across to lower diagonal for $\beta = 100$ deg and then down to ϵ/a the latter is found to be 0.0008. As $h = \epsilon \sin \theta$ (see symbols in Appendix A) it is necessary that θ be known for the h_0 location, which is at the trailing end of the bearing. This value of θ is seen from Fig. E of Chart E-1 to be equal to 270 deg $+ \beta - (\phi_H + \alpha)$. For this problem it is found to be 157.6 deg. Hence $h_0 = 0.0008 \times 2.5 \times 0.381 = 0.00076$.

Other data can of course be obtained. $\lambda_H = 0.00082$. Applying the correction factor $L_1/F_1 = 0.61$ we have $\lambda = \frac{\lambda_H}{L_1/F_1} = \frac{0.00082}{0.61} = 0.00134$ which is the actual coefficient of friction. (NOTE: This problem could have been solved by means of optimum charts of class-B journals, because for fitted bearings all conditions are optimum for a given series. Kingsbury's Class B differs a little from the author's Class E.)

Example 7. What total friction-power loss and what friction coefficient are to be expected in a full bearing operating under conditions where $2a = 4$ in., $b = 8$ in., $N = 3600$, $\mu = 2 \times 10^{-6}$, total journal load $= 3600$ lb, and $\eta/a = 0.003$. Proceed as follows: Assume $\beta = 180$ deg for purpose of finding L_1. Then $l/b = (4\pi \times 180)/(8 \times 360) = 0.79$ and $L_1 = 0.53$ and $F_1 = 0.925$ and $L_1/F_1 = 0.575$. $w = 3600/(32 \times 0.53) = 212$ lb per sq in. because $w = p_0/L_1$. Now,

$$\frac{w}{\mu N}\left(\frac{\eta}{a}\right)^2 = \frac{212 \times 9 \times 10^{-6}}{2 \times 3600 \times 10^{-6}} = 0.265$$

Entering Chart F-1 at the left with this value and reading across to the load-capacity curve we find the value of $c = 0.5$. Holding this value of c for the other curves, the right-hand scale readings therefore lead to $\lambda_H \frac{a}{\eta} = 1.88$. The total power loss $= 3.2 \times \frac{\mu b}{2}\left(\frac{a}{\eta}\right) a^2 N^2 10^{-6} F_1$ hp. The actual coefficient of friction λ may be found from $\lambda = \frac{\lambda_H}{L_1/F_1} = \frac{\lambda_H}{0.575}$. Solving, these give the desired answers to the problem. The total power loss will be 4.1 hp and the friction coefficient $\lambda = 0.0098$. Checking back from λ_H to the total power loss, it is found that the latter is the same if the correction factor is properly introduced as in $\lambda = \frac{F_1}{L_1} \lambda_H$.

Appendix C—Viscous Flow

Fundamentals

Laminar or viscous flow in a film is that kind in which particles of liquid or other matter move as if they were parts of a laminar structure. Hersey (19) has illustrated it by means of a thick book, with a stiff binding, one of the covers of which is shifted relative to the other as from position A to position B in Fig. 2. All the leaves will be shifted a little, if held to the binding. The sum of their relative shifting will, if integrated, equal the relative shift of the covers. This represents the viscous flow of oil between parallel plates when one plate moves relative to and parallel with the other in the absence of pressure.

If the book binding be elastic as in Fig. 3, and a pressure P be applied to the leaf edges as in D while the covers are held, the leaves will shift to the right from position C to position D, the greatest shift being at center in D. This represents the viscous flow of oil between two fixed parallel plates when subjected to a greater pressure at one end than at the other. In the case of the books, the extent of movement is limited. In the case of a liquid, continuous laminar motion is possible.

The force that opposes the viscous flow of a liquid is called the resistance to distortion. The velocity with which the upper surface of an oil film or the upper cover in B of Fig. 2, moves relative to the lower, when compared with the film thickness or the book-thickness T, establishes what is called the rate of distortion. The resistance which such a medium offers to such a rate of change of shape or such a rate of distortion is an indication of its viscosity. The ratio of the unit resistance to the rate of distortion it produces is a measure of the viscosity of the liquid and is called the coefficient of viscosity. The viscosity coefficient enables us to connect the internal forces in the liquid with the external forces that cause it to become distorted. The force acting on a unit area of the upper face of the film, as upon the book cover in Fig. 2, is designated as f. This will cause the upper face to move with a velocity U with respect to the stationary one. The rate of distortion produced will be U/T. The coefficient of viscosity μ equals the ratio of the force f to the rate of distortion U/T which it produces. Thus, we have our first relation of the force, distance, and velocity concerned with viscous flow

$$\mu = \frac{f}{U/T} \quad [1]$$

from which

$$f = \mu\, U/T \quad [2]$$

We have here the fundamental formula for the study of the viscous flow of liquids. This equation is so important that it can be used very directly to find the approximate frictional resistance to the rotation of a journal in a bearing, if the surface speed, the film thickness, and the viscosity are known.

Friction and Viscosity

This relation was expressed by Petroff (1) in 1883, when he assumed that a shaft ran concentric within its sleeve bearing. Fig. 4 may be thought of as illustrative of the viscous flow of oil in absence of pressure, between fixed and moving parallel plates, their distance apart being T. This is still a useful assumption for high-speed bearings, moderately loaded, whose journals run nearly concentric within their bearings, and the latter use practically complete sleeves.

The tangential friction force at the journal surface, resisting rotation, is

$$2\pi abf = F \quad [3]$$

The surface speed of the journal is

$$U = 2\pi aN/60 \quad [4]$$

In this formula N is revolutions per minute. Combining Equations [3] and [4] with Equation [2] a useful formula [5] is found.

This is independent of unit system employed, so long as but one is used and $N/60$ represents revolutions per second. It is similar to the one proposed by Petroff. The viscosity coefficient μ must be expressed in the system of units employed for rest of equation.

$$F = \frac{\mu\pi^2 a^2 bN}{15T} \qquad [5]$$

This friction force F can be again combined with speed and expressed as power loss.

Poises, Centipoises, and Reyns

The relation between the viscosity coefficient in English units

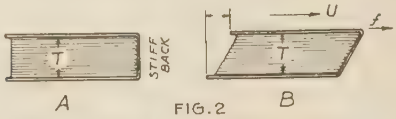

FIG. 2

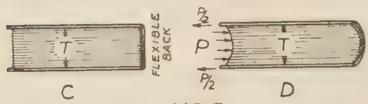

FIG. 3

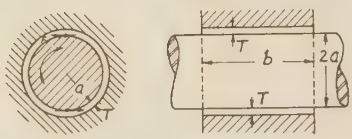

FIG. 4, A JOURNAL CENTRAL WITHIN ITS BEARING

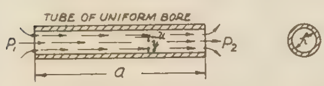

FIG. 5, VISCOUS FLOW THROUGH TUBE

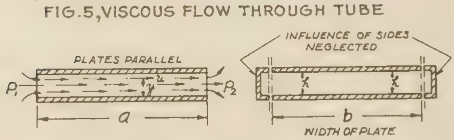

FIG. 6, VISCOUS FLOW BETWEEN PARALLEL PLATES

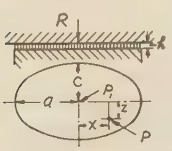

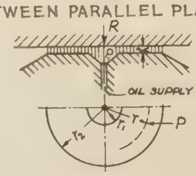

FIG. 7, APPROACHING FACES WITH OIL FILM BETWEEN THEM

FIG. 8, SEPARATION OF FACES BY PRESSURE OIL

(pound-seconds per square inch) Reyn, and metric units (dyne-seconds per square centimeter), poise, may be expressed as follows when μ_E is the former and μ_M the latter.

$$\mu_M/\mu_E = 69{,}000 \qquad [6]$$

There appears in literature another unit for viscosity coefficient called the centipoise, designated as Z and having a magnitude of one hundredth part of a poise. The relation between it and the poise is expressed in Equation [7] and that between it and the Reyn in Equation [8].

$$Z/\mu_M = 100 \qquad [7]$$

$$Z/\mu_E = 6{,}900{,}000 \qquad [8]$$

Viscous Flow Through Tubes

By applying the laws of viscous flow to the flow through tubes, and assuming that there is no molecular slippage of liquid at the tube surface, the law of volume of flow per second is

$$\frac{V_r}{t} = \frac{\pi(P_1 - P_2)h^4}{128\mu a} \qquad [9]$$

Referring to Fig. 5, the linear velocity of flow u at any distance y from the side of the tube is

$$u = \frac{(P_1 - P_2)(hy - y^2)}{4\mu a} \qquad [10]$$

The variation in this velocity is seen to be parabolic and the velocity of flow, therefore, greatest at the tube axis.

Viscous Flow Between Parallel Plates

Viscous flow between plates that are parallel, Fig. 6, is simply expressed by Equations [11] and [12]. In this case, also, the velocity distribution, transversely, is parabolic. There is assumed to be no slippage at the plate surface.

Volume rate of flow is

$$\frac{V_p}{t} = \frac{bh^3(P_1 - P_2)}{12\mu a} \qquad [11]$$

$$u = \frac{(P_1 - P_2)(hy - y^2)}{2\mu a} \qquad [12]$$

In the Equations [9], [10], [11], and [12], one system of units only is to be applied and the viscosity coefficient must be in that system also. P_1 and P_2 are the pressures acting upon the liquid at two ends of the tube or plates. The pressure drop from P_1 to P_2 is assumed to be uniform with distance throughout the length a.

Viscous Flow From Approaching Faces

Osborne Reynolds in 1886 (2) investigated the time rate at which such surfaces, if parallel, will approach when the space between them is filled with a viscous liquid, and a constant normal force R is maintained. See Fig. 7. With elliptical plates, no central cavity, no oil supply, and the plate moving downward, the formulas which are applicable are

$$t = \frac{3\mu\pi a^3 c^3}{2R(a^2 + c^2)}\left(\frac{1}{h_1^2} - \frac{1}{h_2^2}\right) \qquad [13]$$

$$P_1 = \frac{2R}{\pi ac} \qquad [14]$$

$$P = -\frac{2R}{\pi ac}\left(\frac{x^2}{a^2} + \frac{z^2}{c^2} - 1\right) \qquad [15]$$

where P_1 = oil pressure at the center, and P = oil pressure at any point with coordinates x and z.

Separation of Parallel Circular Plates by High-Pressure Oil

This condition of viscous flow, illustrated by Fig. 8, may be accomplished by forcing oil into the small recess at the center with sufficient pressure to cause separation and outward radial flow.

Case 1. Circular Plates, Load Carried by Continuous Flow of Pressure Oil. Pressure at Outer Edge of Plate Assumed to be Zero. The formulas applicable to this case are

$$G = \frac{0.0867\, h^3 R}{\mu(r_2^2 - r_1^2)} \qquad [19]$$

$$P_1 = \frac{2R \log_e(r_2/r_1)}{\pi(r_2^2 - r_1^2)} \quad [20]$$

$$P = \frac{2R \log_e(r_2/r)}{\pi(r_2^2 - r_1^2)} \quad [21]$$

$$P_1 = \frac{7.35\mu G \log_e(r_2/r_1)}{h^3} \quad [22]$$

$$\frac{P_1}{P_0} = \frac{2r_2^2 \log_e(r_2/r_1)}{r_2^2 - r_1^2} \quad [23]$$

where P_1 = oil pressure supplied to central cavity, P = oil pressure at any radius r, P_0 = specific pressure on the plate produced by the load = $R/\pi r_2^2$. In Equations [19] and [22], G represents U. S. gallons per minute, provided all other units are inches, pounds, and seconds, in which case μ must be introduced as Reyns.

Case 2. Circular Plates, Oil Supply Stopped, Plates Moving Together. The formulas applicable to this case are

$$t = \frac{3\mu\pi(r_2^4 - r_1^4)}{4R}\left(\frac{1}{h_1^2} - \frac{1}{h_2^2}\right) \quad [24]$$

$$P_1 = \frac{2R}{\pi(r_2^2 - r_1^2)} \quad [25]$$

$$P = \frac{2R(r_2^2 - r^2)}{\pi(r_2^4 - r_1^4)} \quad [26]$$

where P_1 = oil pressure in the central cavity, and P = oil pressure at any radius r.

The symbols used in Equations [1] to [26] are as follows, and must not be confused with the symbols that appear in Appendix A

- R = total load on plate
- G = flow of pressure oil, U. S. gpm where other units in the equations are inches, pounds, and seconds, and μ is introduced as Reyns
- μ = absolute viscosity of oil
- h = thickness of oil film
- t = time for moving plate from height h_2 to height h_1, sec

Appendix D—Perfect Lubrication

Tapered Oil Film

The tapered oil film is the secret of the success of the sliding-surface bearing, by virtue of which it attains its great capacity, its very low friction coefficient, and its remarkable durability. The existence of an oil film completely separating the bearing surface from its journal was discovered in 1883 by Beauchamp Tower (3). When this fact came to the attention of Osborne Reynolds (2) he was so intrigued with the idea that he developed the hydrodynamical theory which explains it. He showed that the film of oil must have the shape of a wedge in order to keep the surfaces apart, whether the bearing be flat or cylindrical. In 1896 Albert Kingsbury (4), by actual measurement, discovered that the lubricating film was wedge shaped below the air-borne journal of his test bearing. Further evidence of the necessity for a wedge-shaped film has been since deduced from other analyses and tests, as well as from the observation of wear in bearings not adequately lubricated. A good review of Reynolds' work, including a few needed corrections in the formulas, appears in Kingsbury's paper (4).

Side Leakage. Reynolds, in his bearing analysis, neglected the influence of side leakage upon the pressures and friction that are developed within the oil film. Therefore, he determined the maximum pressures that a bearing could develop with a given film under ideal conditions. His work is most valuable as an upper limit or standard with which actual conditions may be compared. It is generally recognized however that, if all other conditions are held the same, the narrower the bearing surface (perpendicular to the direction of motion) the less will be the pressures developed within a film of given form and thickness. This is true because a larger percentage of the oil drawn in at the front edge, will leak away at the sides of the narrower bearing, before reaching the far end of the film. See fuller discussion following under heading "Side Leakage Reduces Capacity."

Film Thickness

The chief importance in the consideration of film thickness and shape lies in the fact that upon them largely depends the factor of safety of a bearing. If the relative shapes of the two co-operating bearing faces are such as to permit safe starting and stopping under load, then the safe running of the bearing may well depend upon the minimum thickness of the oil film and its shape. This point was discussed by Dr. Kingsbury (5) and led him to propose the minimum film thickness as an important criterion of bearing safety. The reason for this seems obvious when one remembers that a bearing, first, has to maintain its film under changes of load and temperature, second, has to support deflected shafts or misaligned ones and, third, has to pass particles of foreign matter through its film to a reasonable extent, without serious injury to the bearing surfaces.

Film thicknesses are difficult to measure and few reliable tests of heavily loaded bearings are available. Therefore, reliance is usually placed upon calculations, when the bearings so investigated have proved themselves in service. Calculated minimum film thicknesses together with capacities for flat surfaces, based on Kingsbury's thrust-bearing practice, are given in Table 8 in the body of this paper.

Viscosity Change Within Oil Film. The friction generated in a bearing, the surfaces of which are completely separated by an oil film, is produced within the oil itself. This friction is dependent upon the viscosity of the oil, upon the film thickness, upon the speed, and upon the extent and shape of the bearing surfaces covered by the film. See Appendix C. As the oil passes through a bearing film, the heat generated must be disposed of in one way or another. Some passes into the bearing faces while the rest remains in the oil itself and passes out with the oil discharged from the sides and the far end of the bearing film. Oil thus discharged is therefore hotter than when it entered. This rise in temperature reduces the oil viscosity, i.e., makes the oil thinner. A fair idea of the maximum possible rise of temperature within a perfect film may be had by simple calculation involving the mean film thickness, the speed, and the specific heat of oil. It is customary to assume the mean viscosity within the film to be that of the whole film, when making bearing calculations.

The Flat-Wedge Film

This film is shown in three views in Fig. 9, giving the plan view, longitudinal section A-A, and a front view looking into the film in the direction of the entering oil. Dotted lines in the plan view show the oil flow and how side leakage takes place.

A study of this film by means of Reynolds' equations in Kingsbury (5), assumes the oil flow to be all parallel to A-A, in the plan view. This is the direction of motion. This analysis discloses a number of important characteristics of an oil film. The lower or stationary bearing surface of 9-*a* may be assumed to be placeable at will in any desired relation to the upper or moving face of the bearing. The proportions of s to l may therefore be varied at will, as may also be the thicknesses h_0 and h_m. In order to study these variations quantitatively, the load $\overline{W}$, per unit of width b, may be assumed fixed. The length l of

the bearing face may also be assumed fixed, and likewise the speed U and the mean viscosity μ. It is assumed that the position of support of the inclined face, if pivoted, may be altered at will to satisfy these imposed conditions. Three different sets of conditions, or cases, will now present themselves, and the results are given below. These are limited here to the conditions in which the influence of side leakage upon the pressure is negligible, as with infinitely wide bearings.

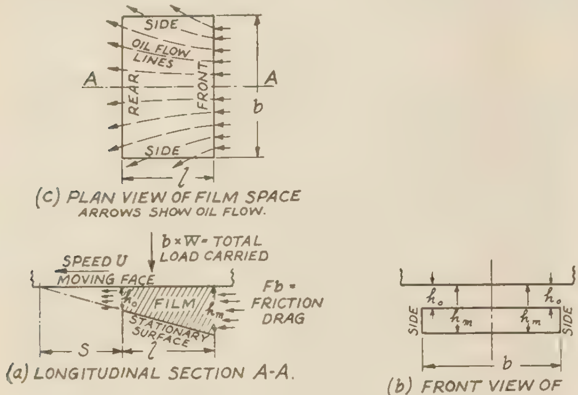

FIG. 9, THE FLAT-WEDGE FILM.

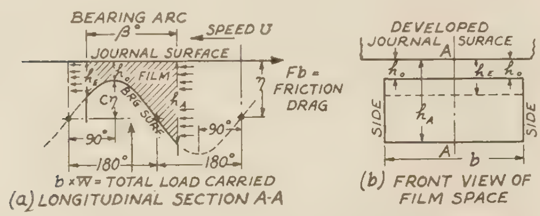

FIG. 10, CURVED-WEDGE FILM OF CLEARANCE BEARING

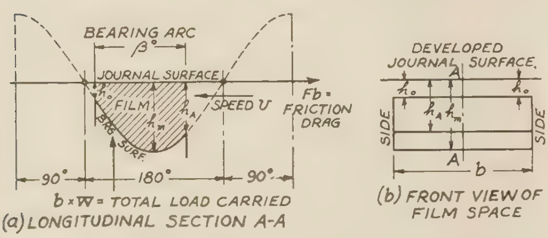

FIG. 11, CURVED-WEDGE FILM OF FITTED BEARING

Case I. *Minimum Friction Condition.* The frictional resistance to motion will be a minimum when $s/l = 0.484$. The film proportions in this case will be $h_m/h_0 = (s + l)/s = 3.065$.

Case II. *Optimum Load Condition.* The film thickness at h_0 will be greatest when $s/l = 0.841$. This condition was determined by Reynolds. The film proportions in this case will be $h_m/h_0 = (s + l)/s = 2.190$.

Case III. *Optimum Friction Condition.* The friction, per unit of least film thickness h_0, will be at minimum when $s/l = 0.652$. The film proportions for this case will be $h_m/h_0 = (s + l)/s = 2.533$. Kingsbury (5) has selected this as the optimum friction condition for flat-surfaced bearings.

The curves for which the preceding-case data are critical points, and upon which the following discussion is based, are given in Fig. 12. They are plotted from Reynolds' equations as given by Kingsbury (5). The case conditions are marked on curves having the same numbers. The symbol groups and the film picture in this chart carries the slope-angle C which does not appear in Fig. 9.

Examination of the curves of Fig. 12 show their critical points to be grouped in such a way that the range of variations of least film thickness and of friction does not exceed 4 per cent. Although any one of the case criteria would be a reasonable choice, Case III is the best from the combined viewpoint of bearing efficiency and factor of safety.

Deviations From Optimum. Side-Leakage Effect Negligible. (*Fig. 12.*) If a bearing be constructed with the ratio $M = s/l$ appreciably less than 0.484(see curve No. 1) the friction will be considerably increased. The minimum film thickness h_0 would be reduced at the same time. Therefore, a change of proportion in this direction leads more quickly toward higher friction and toward metallic contact. In this direction also the angularity of the bearing faces increases. From a study of curve No. 1, it appears safer to deviate from the minimum friction condition ($M = 0.484$) toward the right, in the direction of nearer parallelism of the bearing surfaces, which follows an increase of s/l.

Thus we are led toward Case III and Case II. In this direction beyond $M = 0.841$ the least film thickness h_0 decreases

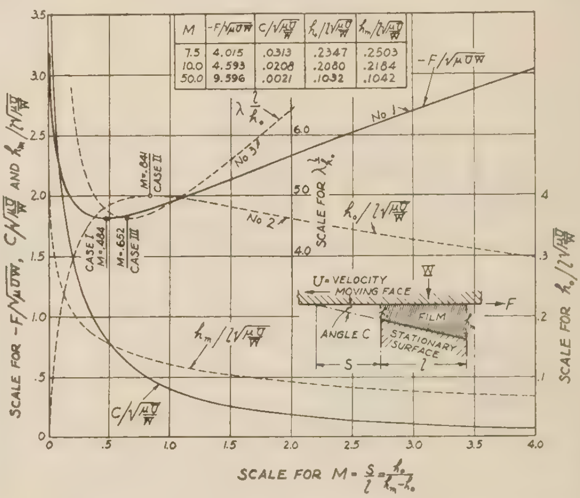

FIG. 12 EFFECT OF DEVIATIONS FROM OPTIMUM CONDITIONS FOR A BEARING WITH FLAT-WEDGE FILMS

slowly, as is seen from curve No. 2, and the friction increases but slowly, as is seen from curve No. 1.

A further study of the curves of Fig. 12, if they were extended beyond the chart limits, would give an idea of how high pure film-friction coefficients could be expected to rise in bearings that have nearly parallel faces, far removed from the best. The values tabulated at the top of the chart show that when the least film thickness h_0 reaches one-quarter of the best value assumed in Case II, the friction will be more than five times the least obtainable. In spite of this high friction, the bearing surfaces might run with perfect lubrication and without wear, if great care is used in producing and maintaining the surfaces.

It seems reasonable to expect that correction factors for side leakage set up for optimum conditions may be used with a fair degree of accuracy for proportions differing materially therefrom, if the deviation is in the direction of nearer parallelism of bearing surfaces.

The Curved-Wedge Film

Oil-film shapes in journal bearings, when geometrically accurate and simple, are of two forms. Both may be expressed

by a sine-curve equation and are, therefore, easily shown in developed section when the journal surface is represented by a straight line. For convenience of comparison, the angular extent of the bearing $\beta°$ in Figs. 10 and 11 is drawn equal to the length l of the flat wedge film in Fig. 9.

Clearance-Bearing Films. For bearings with running clearance the sine-curve axis is spaced from the sine-curve median line by an amount equal to the radial clearance η as in Fig. 10-*a*. Half of the total height of the sine curve, the half equaling $c\eta$, when deducted from the radial clearance η, equals the minimum film thickness, $h_0 = \eta(1 - c)$. As the minimum thickness h_0 is apt to lie within the film the thickness at the far end has been lettered h_B. The thickness h_A may obviously be less than the maximum film thickness for some film proportions.

Fitted-Bearing Films. When the running clearance is zero the bearing is said to be fitted to the journal. The film-formation limitations in this case are illustrated by Fig. 11. The fitted bearing cannot have an arc β much greater than 90 deg, and an angle of 180 deg is geometrically impossible. In a fitted bearing the maximum film thickness h_m is apt to be within the film limits and not at the entering end. The minimum film thickness h_0 will be at the far end of the film. For this reason the thickness at the beginning of the film has been lettered h_A.

Optimum Conditions for Journal Bearings. For these conditions reference must be made to tables and curves mentioned in "The Loading and Friction of Journal Bearings." See Classes *A*, *B*, and *C*, taken from Kingsbury's paper (5). As curved-wedge films cannot be so well and simply examined mathematically as was done for the flat-wedge film, recourse was had by Kingsbury to electrical methods described in Section V of (6), for checking his analytical study of them. In general the meaning of the results obtained by Kingsbury will be understood by keeping in mind the explanations of optimum conditions previously offered for the flat-wedge film.

General and Special Conditions. For a study of general bearing conditions one is referred to the charts for Classes *C*, *D*, *E*, and *F*, mentioned under the heading "The Loading and Friction of Journal Bearings," adapted from Howarth (7) and (8). Also upon some of these charts there are marked such optimum conditions as determined by Kingsbury (5), for the particular class of bearings studied by Howarth. This discussion is continued and amplified with examples in Appendix B that illustrate the use of the loading and friction charts.

Deviations From Optimum. In view of the many possible series of journal-bearing films, the study of deviations from optimum is here limited to a centrally loaded bearing with 120 deg clearance. In order to study the curved-wedge film of this bearing as fully as done for the flat-wedge film in Fig. 12, the film in the 120 deg bearing was assumed to be a curved wedge extending, as in Fig. 13, from h_{max} at the entering edge to h_0 where the film thickness is least, for which the wedge length is l_0. This length l_0 will usually be a little less than the full arc 120 deg, depending upon operating conditions.

Kingsbury's study of the 120-deg centrally loaded bearing, (see the charts and tables of Class *C*), gives values of dimensionless groups for optimum conditions. On Fig. 13 certain of these groups are used as ordinates, and are also marked along the corresponding curves. The base scale shows the curved-film wedge proportion M for a considerable range, including the optima for minimum friction and for maximum load, as well as the minimum frictional drag for carrying a given load under specified conditions. Curves No. 1, No. 2, and No. 3 on Fig. 13 correspond with those of the same numbers in Fig. 12. There appear in Fig. 13, however, two additional curves. Curve No. 4 shows the clearance-ratio variation and curve No. 5 shows the eccentricity change. The optimum points were obtained from Kingsbury (5) and the curves were plotted from data taken from Howarth (7).

Let it now be assumed that the 120-deg bearing is running under the optimum friction condition, at which $M = 0.943$. The optimum clearance ratio corresponding with this is assumed to be unity when plotting curve No. 4. If, the clearance ratio for this optimum friction condition is increased 20 per cent, the value of M will change, and be no longer that for this optimum condition. Referring to curve No. 4, the point X will be reached for which $M = 0.7$. Following vertically through this point we find from curve No. 1 that the frictional-drag group has changed but little, from curve No. 2 that the capacity group has reduced but little, and from curve No. 3 that the friction-coefficient group has increased a small amount. If next we assume the clearance ratio for minimum friction to have been decreased 20 per cent, we find from curve No. 4 a point Y for which the value of M is about 1.4. For this condition the frictional-drag group as shown by curve No. 1 has increased a little in value, the capacity group as shown by curve No. 2 has decreased but little, and the friction coefficient group shown by curve No. 3 has increased but little. These facts will be found useful when arranging tolerances for the bearing and journal diameters.

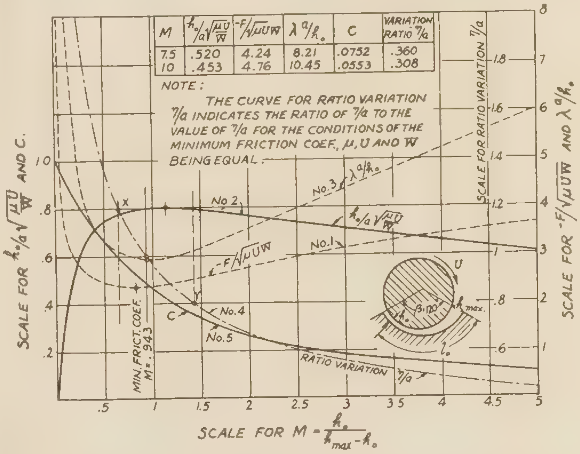

FIG. 13 EFFECT OF DEVIATION FROM OPTIMUM FRICTION-COEFFICIENT CONDITIONS IN A 120-DEG-CLEARANCE BEARING. THIS CHART IS COMPARABLE WITH FIG. 12 FOR FLAT BEARING FACES

In the same way as in Fig. 12, a table was prepared to show increases in friction that would accompany wide deviations from optimum conditions for flat-wedge films. For the same purpose similar figures have been tabulated on Fig. 13 for the curved-wedge film, for values of M beyond the limits of the chart curves. When $M = 10$ the frictional-drag group of curve No. 1 will reach a value of 4.76, which may be compared with its minimum of 2.4. It is not practicable to extend this comparison farther for this group with the data available. For $M = 10$, however, we find that the clearance-ratio reduction from optimum has reached nearly 70 per cent. The friction-coefficient group has increased from the optimum of 2.95 to the larger value of 10.45. The capacity group has decreased from 0.8 to 0.453. It is quite probable that with the value of M equal to 10 or even 20, the bearing would still function properly with pure film lubrication if accurately and carefully made.

From the curves of Fig. 13, another set shown in Fig. 14 has been drawn for more convenient use. The characteristic groups for capacity, frictional drag, and the friction coefficient as well as for the eccentricity are plotted directly over the variation

of the clearance ratio. As before, the clearance-variation figure has been made unity for the optimum condition of minimum-friction coefficient. This chart shows in a more direct way the influence of deviation of the clearance ratio from this optimum. It is clearly seen that small deviations have little influence, as demonstrated already by means of Fig. 13. If, however, the clearance-ratio variation is large, the efficiency of the bearing is sensibly affected, especially if the clearance ratio is reduced. If, for example, the clearance ratio is increased 40 per cent, the group factor for the frictional drag as shown by curve No. 1 increases from 2.4 to 2.5, the group factor for the capacity (as shown by curve 2) decreases from 0.8 to 0.74 and the friction-coefficient factor, as shown by curve No. 3, increases from 2.9 to 3.3. A reduction of the clearance ratio by 40 per cent on the other hand yields more undesirable results. The frictional-drag factor rises from 2.4 to 2.9; the capacity-group factor falls from 0.8 to 0.74; and the friction-coefficient factor increases from 2.9 to 4.

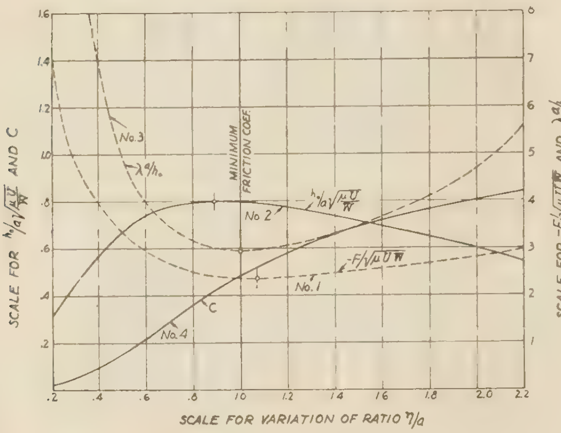

Fig. 14 Effect of Deviations From Optimum Friction-Coefficient Conditions in a 120-Deg-Clearance Bearing

The increase of the friction-coefficient factor is far more noticeable with a reduction of the clearance ratio than with an increase. If, therefore, it is not feasible to design the bearing with the clearance ratio corresponding to the optimum conditions, a larger rather than a smaller clearance ratio should be provided. This conclusion has also been corroborated by practical experience. The relation of curvatures to safety of starting and stopping under heavy loads should not be overlooked, as it leads in the other direction, the choice of a smaller clearance.

Side Leakage Reduces Capacity

The influence of side leakage upon the capacity of a perfectly lubricated thrust bearing, and other bearings with wedge-shaped films, is considerable. It has been determined by several investigators, notably by Michell (9), Martin (10), Boswall (11), Kingsbury (6), and Duffing (12). In Fig. 15, the coordinates of which are capacity factor and length/width ratio, the results of several investigators are shown as plotted by Kingsbury who drew this curve to compare them all. The capacity factor shows what percentage of the ideal load can be carried on a film with finite dimensions of length and width. The ideal, with which the bearing of finite width and length is compared, is a bearing having the same finite length (in direction of motion), but which is understood to be a part of one whose width is so great (infinite) that there is no side leakage to reduce the capacity.

The points determined by Michell, by Martin, and by Duffing, apply to a flat-wedge film whose proportions are two to one, i.e., $h_m/h_0 = 2.0$. Kingsbury also found points for such a film. These are all included under the heading (plane surfaces) marked on the curve of Fig. 15. Kingsbury extended the investigation to cover curved-wedge films such as occur in journal bearings of the fitted and the clearance types. By taking a variety of such points for his optimum bearings and comparing their capacities for various values of l/b, with the ideal capacities he found his points to lie fairly well along a line through the points determined only for plane surfaces. By this means Kingsbury found a set of correction factors that could be used with ideal capacity and friction charts and tables for the solving of practical

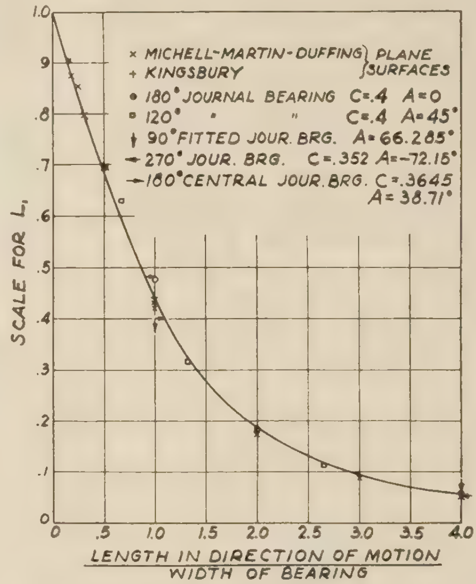

Fig. 15 Influence of Side Leakage Upon Carrying Capacity of Oil Film as Determined by Analyses of Michell (9), Martin (10), Duffing (12), and Kingsbury (6)

bearing problems. See Chart *KX*, and also the examples in Appendix B.

BIBLIOGRAPHY

*1 "New Theory of Friction," by N. P. Petroff, *Engineering Journal* (Russian), St. Petersburg, 1883, pp. 71–140, 228–279, 377–436, 535–564. Abs., *Fortschritte der Physik*, pp. 250–252; German trans., L. Voss, Hamburg, 1887; French trans., *Revue de Mecanique*, vol. 7, 1900, pp. 571–602.

*2 "On the Theory of Lubrication and Its Application to Mr. Beauchamp Tower's Experiments, Including an Experimental Determination of the Viscosity of Olive Oil," by O. Reynolds, Philosophical Transactions of the Royal Society of London, vol. 177, 1886, part 1, pp. 157–234; Papers on mechanical and physical subjects, by O. Reynolds, University Press, Cambridge, London, vol. 2, 1901, pp. 228–310.

3 "First Report on Friction Experiments," by B. Tower, Proceedings, Institution of Mechanical Engineers, 1883, pp. 632–659.

4 "Experiments With an Air Lubricated Journal," by A. Kingsbury, *Journal American Society of Naval Engineers*, 1897, vol. 9, pp. 267–292.

5 "Optimum Conditions in Journal Bearings," by A. Kingsbury, Trans. A.S.M.E., vol. 54, 1932, paper RP-54-7, p. 123.

6 "On Problems in the Theory of Fluid-Film Lubrication, With an Experimental Method of Solution," by A. Kingsbury, Trans. A.S.M.E., vol. 53, 1931, paper APM-53-5, p. 59.

7 "A Graphical Analysis of Journal Bearing Lubrication," by H. A. S. Howarth, Trans. A.S.M.E., vol. 45, 1923, p. 421; vol. 46, 1924, p. 881; vol. 47, 1925, p. 1120.

8 "Journal Running Positions," by H. A. S. Howarth, Trans. A.S.M.E., vol. 51, part 1, 1929, paper APM-51-3, p. 21.

*9 "The Lubrication of Plane Surfaces," by A. G. M. Michell, *Zeitschrift für Mathematik und Physik*, vol. 52, 1905.

10 "The Theory of the Michell Thrust Bearing," by H. M. Martin, *Engineering*, London, Feb. 20, 1920.
11 "The Theory of Film Lubrication" by R. O. Boswall, Longmans, London and New York, 1928, 280 pp.
12 "Die Schmiermittelreibung bei Gleitflächen von endlicher Breite," by G. Duffing, vol. 5, 1930, pp. 839–850; Handbuch der physikalishen u. techn. Mechanik, F. Auerbach and W. Hort, J. A. Barth, Leipzig, vol. 1, 1930, p. 195.
13 "A Graphical Study of Journal Lubrication," by H. A. S. Howarth, Mechanical Engineering, vol. 49, no. 4, 1927, p. 375.
*14 "Zur hydrodynamischen Theorie der Schmiermittelreibung," by A. Sommerfeld, *Zeitschrift für Mathematik und Physik*, 1904, vol. 50, pp. 97–155.
15 "Effects of Side Leakage in 120-Degree Centrally Supported Journal Bearings," by S. J. Needs, Trans. A.S.M.E., vol. 56, 1934, paper APM-56-16, p. 721.
16 "Friction," by T. E. Stanton, Longmans, London, 1923, 183 pp.
17 "Oil Film Pressures in a Complete Bearing," by L. J. Bradford and L. J. Grunder, Pennsylvania State College Bulletin No. 39, 1930.
18 "Pressure Distribution in Oil Films of Journal Bearings," by S. A. McKee and T. R. McKee, Trans. A.S.M.E., vol. 54, 1932, paper RP-54-8, p. 149.
19 "Fundamental Action of Lubricants," by M. D. Hersey, *American Machinist*, June 13 and 20, 1929.
20 "Current Practice in Pressures, Speeds, Clearances, and Lubrication of Oil-Film Bearings," by H. A. S. Howarth, Trans. A.S.M.E., vol. 56, no. 12, 1934, paper MSP-56-2, p. 891.
* The four papers of Petroff (1), Reynolds (2), Sommerfeld (14), and Michell (9), are collected in German translations in "Hydrodynamische Theorie der Schmiermittelreibung." Ostwald's Klassiker No. 218, Leipzig, 1927.

Discussion

Pulsating Air Flow[1]

Sanford A. Moss.[2] Professor Bailey is to be congratulated on his distinctly novel and ingenious contribution to the measurement of pulsating flow. Inquiry might be made as to the technique of operating the apparatus. Is it difficult to regulate the valves 6 and 9, shown in Fig. 1, so as to secure constancy of head? Does the rpm of the blower have to be regulated with more than ordinary care in order to preserve constancy once it is established? In order to avoid surface-tension changes, the orifice 8, Fig. 1, was finally made an orifice in a thin plate. Such an orifice has a coefficient of discharge subject to some variation, so that the actual flow may not be at all times proportionate to the square root of the head. It would seem the author's original orifice with rounded approach was more nearly theoretically correct. Could not the orifice be made of stainless steel or bronze, or even of brass artificially seasoned so that it would remain constant with respect to surface tension?

At first thought it would seem that the use of the apparatus is limited to the case where pressure difference, in the air flow being measured, is such as to cause negligible density change. However, it was shown in a paper read at the December, 1927, meeting of The American Society of Mechanical Engineers, that air flow by weight with a differential pressure up to 10 per cent of the initial absolute pressure, varies exactly with the square root of the differential pressure, which would make the instrument usable up to this differential-pressure ratio. It is to be assumed that the instrument could be used with measurements made with an impact tube in the pipe and a static hole in the pipe wall, as well as with the pitot tube with static and impact openings discussed by the author. No doubt the instrument could also be used when air flow is measured by means of a nozzle at the end of a pipe line, with initial pressure measured with a static hole preceding the nozzle, or an impact tube preceding the nozzle, or an impact tube in the nozzle jet.

The author speaks of possible sources of error due to a particular type of connecting pipe used. It would seem that error from this source is always possible, because air in the tubing between the pressure-measuring instrument and the author's apparatus has a period, inertia, and compressibility of its own, which may at times give oscillations other than those of the original jet, or give friction which may dampen some of the original pulsations, as the author mentions. Possibly this effect might be eliminated by filling all of the tubing with water, which is practically incompressible. With this arrangement, the tubes 11 and 12, Fig. 1, would be connected as closely as possible to the pitot tube or other flow-measuring apparatus with as short column of air between as possible. Then there could be tubing of any convenient length between the lower ends of the glass tubes and connections 13, Fig. 1, to the water box, all filled with water. By this means the air column between the original source of pulsation and the water box would be made a minimum, and this presumably would increase the accuracy of the instrument.

One further item, the effect of the inertia of the water flowing through the orifice, may be mentioned. When the pulsation is at a given point in the cycle and the velocity through the orifice is a given amount, and the next phase of the pulsation changes the head on the water orifice, the water itself does not instantly assume the velocity corresponding to the new head but, on account of its mass, must be accelerated, which requires a certain time. For this reason, the pulsation of the water cannot be in phase with the pulsation of the air. Perhaps for low velocities through the water nozzle, and comparatively low frequencies of pulsation, this error is negligible, and perhaps the author has some definite mathematical treatment of it.

P. H. Hardie.[3] The author, apparently because of the brevity of his paper, has not fully explained many important points regarding the operation of the fluid-velocity meter and pulsating air flow. The writer would like to ask the author to clarify the following points:

(1) The fluid-velocity meter actually consists of three orifices in series, since valves 6 and 9, Fig. 1, are restrictions. They are also subject to pulsating differential pressures. Will the author show mathematically, from the equation of the flow through three resistances in series, how the flow is affected by intermediate pressure pulsations?

(2) Does the water flow change when the area through the gage lines is restricted to such an extent that it effectively eliminates pulsations, the two valves 6 and 9 remaining fixed? If it does, how much change occurs, and do the two water legs become unbalanced?

(3) Was the fluid-velocity meter checked for accuracy by any method other than the cut-out disk? For example, it would be interesting to make a check in a duct having a rotating butterfly valve some distance back from the pitot station, the gas having been previously metered accurately.

(4) How does the author account for such excessive pulsation from the blower on which he made his experiments? Referring to Fig. 5*b*, with the blower alone, V_0/V_{av} is almost 1 at the lowest speed reported, 800 rpm. The values of V_0/V_{av} plot a straight line on semi-log paper. Extrapolation values for lower speeds indicate that at 600 rpm the air reverses and reaches a speed in the reverse direction of 25 per cent of the average forward velocity. This is astounding and should certainly be checked with a vibrograph, phonodyke, or some similar type of recording device which has been successfully used for such records in the past. Has the author made similar measurements on commercial-type fans of larger sizes, and if so, what was the magnitude of pulsation found?

(5) Did the tests on this blower at different speeds indicate that the fan laws apply when the flow pulsated? If they do not, the present practice of checking performance at reduced speeds will have to be discontinued.

In conclusion, it might be well to point out that it is not an established fact that pulsations in the discharge of air blowers assume serious proportions. H. F. Hagen's paper,[4] to which the author makes frequent reference, attributed large errors in pitot-tube velocity measurements to pulsating flow, but it was pointed

[1] Published as paper PTC-56-1, by N. P. Bailey, in the October, 1934, issue of the A.S.M.E. Transactions.

[2] Research Engineer, General Electric Company, West Lynn, Mass. Mem. A.S.M.E.

[3] Test Engineer, Research Bureau, Brooklyn Edison Company, Inc., Brooklyn, N. Y. Assoc-Mem. A.S.M.E.

[4] "Pulsation of Air Flow From Fans and Its Effects of Test Procedure," by H. F. Hagen, Trans. A.S.M.E., vol. 55, 1933, paper FSP-55-7.

out in the discussion of Mr. Hagen's paper (fourth paragraph, page 111) that the vibrograph records showed pulsations, the magnitude of which would account for only a very small fraction of the total error. The experiments of Lionel S. Marks, recently reported in A.S.M.E. Transactions for November, 1934, paper PTC-56-2, indicated that the errors attributed to pulsating flow were due to other causes.

Lionel S. Marks.[5] The theory of the instrument developed by Mr. Bailey demands that the instantaneous static and impact pressures be exerted at the instrument or that the difference between the two be maintained at the instrument. This does not seem possible of achievement with rapid pulsation, primarily on account of the small size of the static-pressure orifices. The author speaks of increasing the static-orifice area but, even if carried to the limit at which the static pressure will be registered accurately, this would not give an opening adequate for the purpose.

It would seem desirable to verify the indications of this instrument by determining independently the true average air velocity by a nozzle or other means. A possible method of verification would be to measure the same air quantity at two stations, for example, in a duct and, later, in a nozzle of not more than half the duct diameter. With pulsating flow, the volumes determined from the effective velocities at these two stations are different; the volumes determined from the average velocities should be the same.

H. F. Hagen.[6] The curves of Fig. 5 in the author's paper indicate a possible explanation of the not infrequent reports of tests of fans, particularly propeller fans, that do not follow the accepted fan laws with change of speed. The author's results show an increasing pulsation effect with reducing speed and his explanation of increased damping at higher frequencies is entirely reasonable. The relations between the fan performances wide open, and at the reduced orifices, showing decreased pulsation with increased resistance, agree with the writer's findings in many tests comparing pitot-tube traverse and nozzle volumes.

The nature of air flow from fans is apparently an extremely complicated phenomenon. The author has found indications of severe pulsation in a fan discharge. In Professor Marks' paper[7] are described peculiar spins indicated by a direction tube. A fan test seemingly must guard against both these actions. The new instruments developed by the author, therefore, seem a necessity.

The writer built an arrangement described in the third paragraph of the author's conclusions for the purpose of decreasing noise. There was no difference either in noise or performance between the rotors with blades staggered or in line.

Author's Closure

The questions on the theory of the instrument, asked by Messrs. Moss and Hardie, can best be answered by considering what would take place if a cyclic air velocity of amplitude V_a and frequency ω were applied at the open end of the air tube leading to the instrument. The amplitude of the cyclic-pressure wave of the same frequency which would reach the water surface can be shown mathematically to be $V_a\sqrt{P_aE_a}$ where P_a is the mass density of air and E_a is the bulk modulus of elasticity of air. Any damping due to fluid friction would reduce this amplitude; but for simplicity, damping is being ignored.

[5] Professor of Mechanical Engineering, Harvard University, Cambridge, Mass. Mem. A.S.M.E.

[6] Vice-President and Director of Research, B. F. Sturtevant Company, Hyde Park, Boston, Mass.

[7] "Air Flow in Fan Discharge Ducts," by Lionel S. Marks, Trans. A.S.M.E., November, 1934, paper PTC-56-2.

If the openings from which water can escape or enter the water chamber are small compared with the tube diameter, as they are in the instrument, it can be demonstrated mathematically that the amplitude of the pressure wave of the same frequency which is transmitted to the water, approaches very closely to $V_w\sqrt{P_wE_w}$ where V_w is the amplitude of the cyclic water-velocity wave which results, P_w is the mass density of water, and E_w is its bulk modulus of elasticity. Since the instantaneous pressures of the surface of contact of the air and water must balance, it follows that,

$$V_w = V_a\sqrt{\frac{P_aE_a}{P_wE_w}} = \frac{V_a}{3450}$$

This indicates that for ordinary frequencies of pulsation, the cyclic air motion does not appreciably penetrate the more dense and less elastic water. At very low frequencies, the amount of water that would be discharged or taken in through even the very small orifice used during any half cycle, becomes large enough to cause a rapid and appreciable motion of the water surface. This lower frequency limit is approximately 5 cycles a second for the instrument described.

On the other hand, if a steady air velocity V_a impinges on the open end of the air tube, the resulting water velocity through the orifice would be given by

$$V_w = V_a\sqrt{\frac{P_a}{P_w}} = \frac{V_a}{28.8}$$

From this it is apparent that any cyclic air velocity is scaled down by the action of the water 120 times as much as is a steady air velocity. It is the conviction of the author that the real explanation of the instrument is that the cyclic air velocity does not penetrate the water and that the flow through the orifice is practically steady and is affected very little by the cyclic component.

At low frequencies, this cyclic component of air velocity does penetrate to the orifice, with the result that the water surface in the gage glasses oscillates and the instrument becomes useless. The instrument can probably be designed for slightly lower frequencies by decreasing the orifice size and increasing the size of the gage glasses.

In reply to the question by Dr. Moss on the technique of operating the instrument, it may be said that considerable practice is required to adjust the two valves, watch the two water columns, keep an eye on a stop watch, and handle the graduate for collecting the water; but once the skill is acquired, more consistent results are obtainable than are possible with a manometer because the instrument effectively averages the small variations of speed that usually occur in most testing.

The points involved in questions 4 and 5, asked by Mr. Hardie, can best be cleared up by a brief résumé of experimental work that has been carried on since the paper was published. A series of careful tests at low air velocities showed a consistent discrepancy which caused the method of calibration to be restudied. As explained in paragraph 2, column 2, page 782 of the paper, the head for calibrating the instrument was obtained by holding the two column heights at different levels. When the head for calibration was created by an air pressure which was also connected to a manometer for measurement, and the water levels in the two columns were made equal as they are in actual operation, a different calibration curve was found. It was raised 15 per cent above the one shown in Fig. 2, page 782, at a discharge of 20 cc per minute, and 4 per cent above at a discharge of 100 cc per minute.

A very careful study of the technique previously used in calibrating the instrument revealed that the method followed indi-

cated a head that was smaller than the actual head by an amount equal to twice the capillary head of the glass tubing used in the instrument. Later, it was found that by properly manipulating the water columns during calibration to eliminate this effect, the same calibration was obtained by the two methods.

When the data used in the calculation of Fig. 5 in the paper were referred to this corrected calibration curve, it was found that for the blower there was no detectable pulsation under any of the conditions of operation. All values of V_{av} were equal to the corresponding values of V_{eff} within a variation of 2 per cent, which may be attributed to lack of refinement of the work.

When the data for the square wave form given in column 1, page 783, were corrected from the new calibration curve, it was found that for the undisturbed jet, $V_{av} = 122.2$, as compared with the value $V_{eff} = 121.5$. With the disk rotating, $V_{av} = 61.0$ and $V_{eff} = 82.5$. This gave a value of $V_{av}/V_{eff} = 0.73$ for the square wave, as compared with the theoretical value of 0.707.

In a like manner, the ratio of V_{av}/V_{eff} for the single-cylinder engine in Fig. 6 of the paper, had an average value of 0.98 when the receiver tank was used, and 0.77 for the direct-intake measurement.

The propeller tests shown in Figs. 7 and 8 of the paper showed no appreciable pulsation when this connection was made.

This experimental blunder in the calibration of the instrument caused the author to draw misleading conclusions about air blowers that he is very happy to correct. It is believed that the field of application of the instrument is primarily the measurement of air to internal-combustion engines and the intake and discharge of reciprocating machines. A comprehensive experimental program is under way, that is designed to improve and simplify the instrument and study in detail the action of pitot tubes, nozzles, and orifices, both on intake and exhaust, when the air is pulsating. It is felt that the work will result in a very useful contribution to the art of air measurement.

The Relative Grindability of Coal[1]

R. M. HARDGROVE.[2] The authors' contribution on the grindability of coal has developed some points which may assist toward the standardization of a uniform method for making this determination.

The authors' experience with an Abbé Mill confirms our own experience of seven years ago and also the experience of Yancey, of the Bureau of Mines, in that the results are spotty unless lifting ribs are used.

The development of the 3000 factor for the fraction less than 300 mesh is very interesting. The 1000 factor used in our method was chosen arbitrarily to give results that generally agreed with pulverizing practice. As we learned more about the subject we found that this factor was still too large. In the writer's paper, presented before The American Society of Mechanical Engineers in Chicago, 1933, this question was discussed thoroughly and it was shown that pulverizer capacities at 100 grindability are only about 60 per cent more than those at 50 grindability for air-swept pulverizers, i.e., the range is greater than practical results warrant. The most thoroughly scavenged pulverizers, as used in closed circuit systems, however, do approach capacities proportional to the grindability scale. The use of the 3000 factor instead of 1000 naturally increases the range of the grindability scale and, therefore, makes the agreement between it and actual pulverizer capacity still more of an arbitrary relation than it is now. There does not seem to be any good reason for changing the 1000 factor now in use.

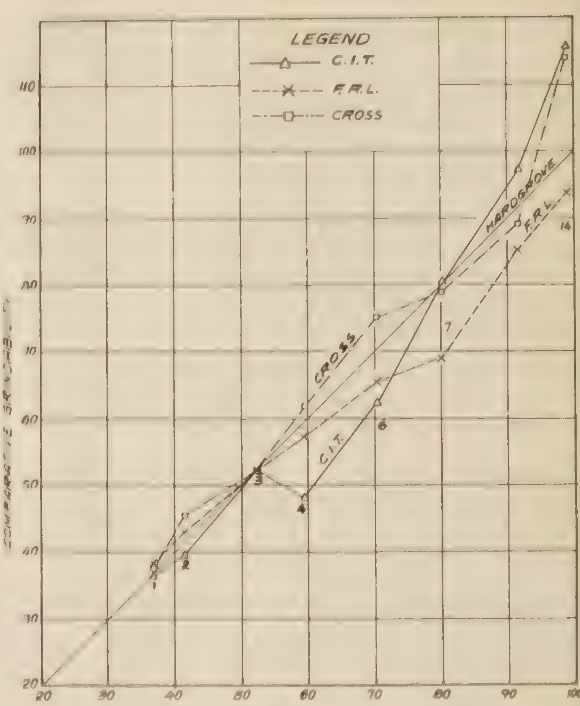

FIG. 1 COMPARISON OF THE RESULTS OBTAINED BY THE C.I.T., F.R.L., CROSS, AND HARDGROVE METHODS OF DETERMINING GRINDABILITY

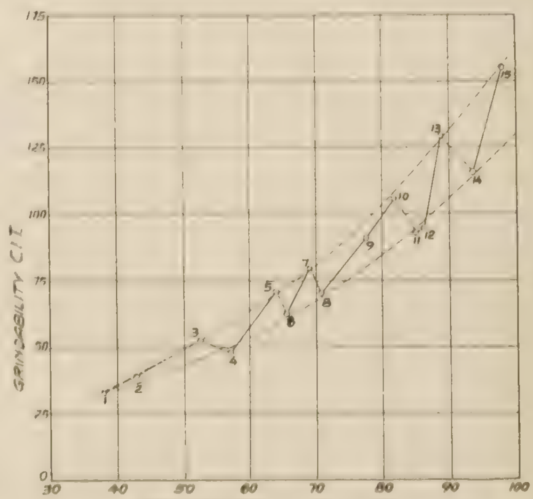

FIG. 2 COMPARISON OF THE C.I.T. AND F.R.L. METHODS OF DETERMINING GRINDABILITY

The particle-size distribution differs widely in Figs. 4 and 5. Fig. 4 is that obtained with the roll and would represent a factor of 1300–1500. Fig. 5 is based on an Abbé Mill and represents a factor of 2500–3000. This difference would be expected with these types of machines but the writer cannot understand why the authors use the 3000-factor with the roll machine.

The comparative results in Table 11 are plotted in Fig. 1, using a multiplier of 0.25 for the F.R.L. method and 0.17 for the

[1] Published as paper FSP-56-13, by H. J. Sloman and A. C. Barnhart, in the October, 1934, issue of the A.S.M.E. Transactions.

[2] Engineer in Charge of Design, Babcock & Wilcox Company, New York, N. Y. Mem. A.S.M.E.

Cross method which brings all results together at 52 grindability. From this graph it is evident that samples four and six are too low on the C.I.T. curve.

The general trend of the C.I.T. line shows the wider range, as compared to the writer's, due largely to the 3000-factor used in the C.I.T. method. The high values at 100 grindability are especially noticeable.

In Fig. 2, the C.I.T. values of all 15 samples in Table 11 are plotted against the F.R.L. values as a base.

Assuming the F.R.L. values to be consistent, it would look as though the C.I.T. values fall on two distinct lines. We have obtained similar results in working with an Abbé Mill and it was attributed to either slippage or coated balls, and we rather suspect that the low points in this series are low because the roll, or the plate became coated and thereby cushioned the grinding.

The results are not equal in consistency to the F.R.L., the Cross, the Bureau of Mines, or the Hardgrove methods, and the scale is not nearly as close to the commercial results as the Bureau of Mines or the Hardgrove methods. The Bureau of Mines method has many desirable features and checks very well with the Hardgrove method, but has the one disadvantage of being tedious and costly to run. The time required to make a test by the C.I.T. method as proposed by the authors of the paper being discussed, is even longer than is required for our method. The C.I.T. method would seem to be open to more variation in results depending upon details in manipulating the roller.

G. B. Gould.[3] Although the work of Messrs. Sloman and Barnhart is interesting and valuable, there are two serious objections to the method they propose. It appears that their index is based upon a method of grinding which reduces only a small part of the sample to minus 200-mesh.

While it may be possible to demonstrate by a series of experiments that such a method yields reliable results, it is, in my opinion a dangerous one to rely on in dealing with a material like coal, which is not uniform in structure or hardness. On the contrary, coal, as it is mined and shipped, is a mixture of portions of a seam which often differ materially in these respects.

To take an extreme and impossible condition for purpose of illustration, if a sample composed of 75 per cent diamond chips and 25 per cent fusain were subjected to test by this method, a high grinding index would result, reflecting not at all the great amount of work required to reduce the major portion to the desired size of minus 200-mesh. Coal is a material similar to this hypothetical mixture, only differing from it in the range of hardness of its various portions.

For this reason, we have believed from the beginning of our experimental work on pulverizing-test methods several years ago that one important requirement of a satisfactory and reliable method is that at least 80 per cent of the entire sample of the most easily pulverized coal should be reduced to minus 200-mesh.

The disadvantage of assuming that the reduction in size resulting from a very slight grinding effect can be reliably projected for the whole sample is also present in the method proposed by Hardgrove, but the error, if any, is magnified in the method here proposed by the high value given to the superfines.

Assuming that the values assigned to the sizes below 200-mesh are theoretically correct, the accuracy of the final index depends to a high degree upon the separation and measurement of sizes as small as 300-mesh. From the standpoint of practical commercial laboratory practice, the accurate screening of coal through a 300-mesh screen is out of the question. By striving to simplify and minimize the grinding work, the difficulties of accurately measuring the result are greatly accentuated.

The adoption of a fixed screening period would be found unsatisfactory if the experiments had been extended over a wider range of coals. We tried that but found that some coals, when pulverized, are of a very gummy nature and are screened through even a 200-mesh screen with great difficulty

The unsatisfactory results reported with the pebble mill by Messrs. Sloman and Barnhart, as well as by Hardgrove, do not indicate any inherent unfitness of this type of mill for the purpose.

The method proposed by Yancey employs the pebble mill with very successful results, and has the advantages of reducing every sample to 80 per cent through a 200-mesh screen, and requires screening only through that one screen. From a practical commercial standpoint, the primary requirement is to reduce the major part of the whole quantity to minus 200 mesh, and Yancey's method measures the work necessary to do that in a simple and direct manner

Ollison Craig.[4] Manufacturers of pulverized coal equipment realize keenly the necessity of knowledge concerning the grindability of the various coals to be used in plants in which coal is fired in powdered form.

R. M. Hardgrove in his paper, "Grindability of Coal,"[5] gave the industry definite information which was of very great value The main value of Mr. Hardgrove's paper lay in the fact that he gave figures of relative grindability for a large number of coals. This was of more practical value than the statement of the method by which the figures were arrived at.

So far as the manufacturers are concerned it is of more importance that the order of coals as to grindability be known than the absolute values be known. Any system which will place coals in their proper order of grindability and give reasonably accurate values and which at the same time makes the values easy to determine, is the most desirable from the manufacturers' viewpoint. Mr. Sloman and Mr. Barnhart have proposed a method which can be used by any manufacturer or user of coal pulverizing equipment.

It is our opinion that some method should be standardized and adopted by the Society as the recognized method for determining relative grindability of coal and it is certainly desirable that such a method be reduced to the simplest possible form

Authors' Closure

Mr. Hardgrove's discussion of the development of our 3000 factor for minus 300-mesh coal should be amplified by the following explanation. In our Fig. 4 where minus 300-mesh coal was obtained with the roll and plate, it is true that the factor was low Because of limited crushing action in the roll test we found that there was not a sufficient quantity of minus 300 mesh coal produced to perform a satisfactory determination of particle-size distribution in that size of coal. In order to obtain a sufficient range of size in minus-300-mesh coal, it was necessary to use the product from a pebble mill. This determination was by the sedimentation-velocity method and was described in the latter half of our paper.

Mr. Hardgrove's discussion of our 3000 factor does not suggest the retention of his 1000-factor, but rather the improvement of performance of commercial pulverizing systems to a point where they may make full use of the properties of the coals which may be fed to the mills. We do not agree that any grindability scale should be brought into line of agreement with existing machine

[3] President, Fuel Engineering Company of New York, New York, N. Y. Mem. A.S.M.E.

[4] Engineer, Riley Stoker Corp., Worcester, Mass. Mem. A.S.M.E.

[5] "Grindability of Coal," by R. M. Hardgrove, Trans. A.S.M.E., vol. 54, 1932, paper FSP 54-5.

performance because the expected future improvement in pulverizers would render such a scale worthless. Mr. Hardgrove has stated that with the use of closed circuits and thoroughly scavenged machines capacities are realized proportional to his grindability scale. Our factor of 3000 was determined by experimentation as the proper one to use for minus-300-mesh coal. While this factor does increase the range of the grindability scales that have been proposed previously, this increase of range is desirable inasmuch as a greater differentiation may be obtained with coals of nearly the same grindability.

In Mr. Hardgrove's Fig. 1, all results are brought together at 52-grindability by the arbitrary choice of factors. In this case it would be expected to find a wider range of grindability with the C.I.T. method because of the use of the 3000-factor. Mr. Hardgrove has plotted his values as a straight line, but should any other set of values from the remaining methods be so plotted, the variation would be quite as apparent as in his graph. This plot has no inherent value and the fact that samples 4 and 6 are too low on the C.I.T. curve, as plotted on his Fig. 1, has no significance.

Mr. Hardgrove's Fig. 2 is plotted with the assumption that the F.R.L. values are consistent and the C.I.T. values are shown as falling on two distinct lines. We have plotted Mr. Hardgrove's eight values from our Table 11 and, in comparison with the F.R.L. method, his values also fall on two distinct lines with greater divergence than the C.I.T. method. Nothing is proved but the arbitrary assumption of the accuracy of the F.R.L. method.

We agree that there is some cushioning between the plate and roll of the C.I.T. method, but we also assert that there is less cushioning and attrition in this method than in any of the other proposed methods. The best that can be hoped for is to reduce cushioning to a minimum inasmuch as it cannot be eliminated entirely.

Contrary to the opinion expressed by Mr. Hardgrove, the variation in the results of the C.I.T. method depends very little upon details in manipulating the roller. This is evident from the results quoted in the paper where three different operators checked very closely when using the same coal.

The time taken to actually perform a test is less than any other proposed method. We stated in the paper that 90 minutes were required to make complete duplicate tests; this included screen analysis, weighing, and calculations. The actual grinding with the roll can be accomplished in less than one minute.

The data obtained by H. F. Yancey et al do not substantiate the opinion expressed by Mr. Gould that it is necessary for 80 per cent of a material to pass through 200-mesh. Doctor Yancey of the U. S. Bureau of Mines, in his paper presented before the A.I.M.E. in February, 1934, showed that plotting cumulative per cent passing 200 mesh against the number of revolutions of the mill gave a straight line up to 50 per cent or more through 200 mesh, depending upon the grinding characteristics of the particular coal, and stated that the slope falls off at higher percentages, probably due to increased weight of unfinished material and accumulation of material harder to grind. The data from Doctor Yancey's paper indicate that the hypothetical case of Mr. Gould's mixture of 75 per cent diamond chips and 25 per cent fusain has no application in coal grindability testing. Coals which are shipped today do not have large percentages of hard extraneous material as in Mr. Gould's assumption.

Mr. Gould thinks it is impractical to screen coal through 300 mesh and adopt a definite screening period. This might be true if 500 gram samples were used as in the Bureau of Mines method. However, when 20 gram samples were used as discussed in the paper, no difficulty was experienced. The data given in Table 6 show that by simplifying and minimizing the grinding work, the difficulties of accurately measuring the results have not been greatly accentuated.

In regard to the Bureau of Mines method, we agree with Mr. Hardgrove when he mentions the disadvantages of its being tedious and costly to operate. The Bureau of Mines method requires the handling of the sample too many times, resulting in the loss of fine coal and difficulty of cleaning mill and balls. We feel that this method would require more rigid technique than the average consumer would care to provide.

In closing, we again wish to stress the simplicity and ease of duplication of the C.I.T. method, and one which does not call for expensive special apparatus nor a high degree of skill to operate.

Further Experiments on the Variation of the Maximum-Lift Coefficient With Turbulence and Reynolds' Number[1]

E. A. Stalker.[2] The investigations conducted by Dr. Millikan on the value of the maximum-lift coefficient have been very important. As to the behavior of the three airfoils, U.S.N. P6, Clark Y-18, and N.A.C.A. 2412, it is pertinent to consider the stagnation point on the lower surface of the section. A high arching of the mean-camber line will shift the stagnation point rearward so that in the case of the highly cambered section, the flow going over the upper surface will travel a greater distance than in the case of the low mean-camber section. There will consequently be time or distance in which the boundary layer may become turbulent. On a flat plate the turbulence would just be forming at the trailing edge for a Reynolds number of 500,000, the value at which Dr. Millikan's curves begin; but for a flow about a wing nose the turbulence would occur much earlier. It would appear that the highly cambered wing, already having the mechanics for generating its turbulence, would benefit little from additional turbulence introduced into the airstream. It would also appear that a wing section of low mean-camber height would be benefited by a flap to a greater extent that a highly cambered wing. The above observations appear to be borne out by Dr. Millikan's experiments since wing U.S.N. P6 has a value of the mean camber line of 9.2 per cent, while Clark Y-18 and N.A.C.A. 2412 have only 4 and 2 per cent, respectively. The presence of a depressed flap may also be considered as converting a given wing section into a more highly cambered one.

It thus appears that certain assumptions should be made about the behavior of both the upper- and lower-surface stagnation points. It may be that the assumption that the upper-surface stagnation remains at the trailing edge will prove sufficient, but it is, of course, possible to have an orderly travel of this point forward and yet preserve a straight-line lift curve. In fact, this is what experiment actually shows. It seems to be more desirable, however, to use the simpler assumption, at least until the effect of the lower stagnation point is investigated. It might also be that a connection with the location of the most forward center of pressure position could be established.

[1] Published as paper AER-56-14, by Clark B. Millikan, in the November, 1934, issue of the A.S.M.E. Transactions.

[2] Professor of Aeronautical Engineering, University of Michigan, Ann Arbor, Mich. Mem. A.S.M.E.

Some Physical Properties of Water and Other Fluids

By ROBERT L. DAUGHERTY,[1] PASADENA, CALIF.

Absolute and kinematic viscosities of various liquids and gases as functions of temperature are shown by curves plotted on the same diagrams to the same scales so that these properties for different fluids can be readily compared.

Pressure, volume, and temperature relations for water are shown graphically, as are values of the volume modulus of elasticity for a wide range of pressures and temperatures. From recent data presented by Smith and Keyes it was possible to compute values of the specific heat of water for all temperatures up to the critical and for all pressures from saturation up to 350 atmospheres. These values are here shown.

ONE of the important physical properties of all fluids is viscosity but, although much has been published on the subject, the material as presented is tabulated in different units or shown on charts with different scales. Furthermore, different classes of fluids, such as gases and liquids, have been shown separately, so that it is not at all obvious as to how they compare, one with the other.

The writer, therefore, thought it would be of interest to engineers to gather together data on fluids which differed widely and to plot all of it on one chart to the same scale so that their relationships could be seen at a glance. In Fig. 1 are shown the viscosities of such dissimilar fluids as mercury, hydrogen, air, residuum or fuel oil, ammonia, and brine. These are all fluids that are of interest to the engineer. Furthermore the viscosity curves for saturated water and saturated steam have been joined at the critical temperature to illustrate the way in which the viscosities of all liquids and their vapors must coincide at the critical point.

It may be noted that the viscosity of either a liquid or a gas is practically independent of pressure for a moderate pressure range such as is ordinarily encountered in engineering work, but for very high pressures of the order of several thousand pounds per square inch there is an appreciable variation, especially in the case of liquids. But even then the change in viscosity is only a small fraction of the viscosity values shown in Fig. 1.

In most engineering problems one is concerned with the ratio of viscosity to density, and this ratio is called kinematic viscosity. Since the density of all gases varies in a marked manner with the pressure, it is obvious that the kinematic viscosity of a gas is affected greatly by the pressure. Values of kinematic viscosities are shown in Fig. 2, and it is very interesting to compare these values with those in Fig. 1. Thus hydrogen which gives the lowest curve in Fig. 1 appears near the top in Fig. 2, while the lowest curve in Fig. 2 is for mercury. Of course for a gas one

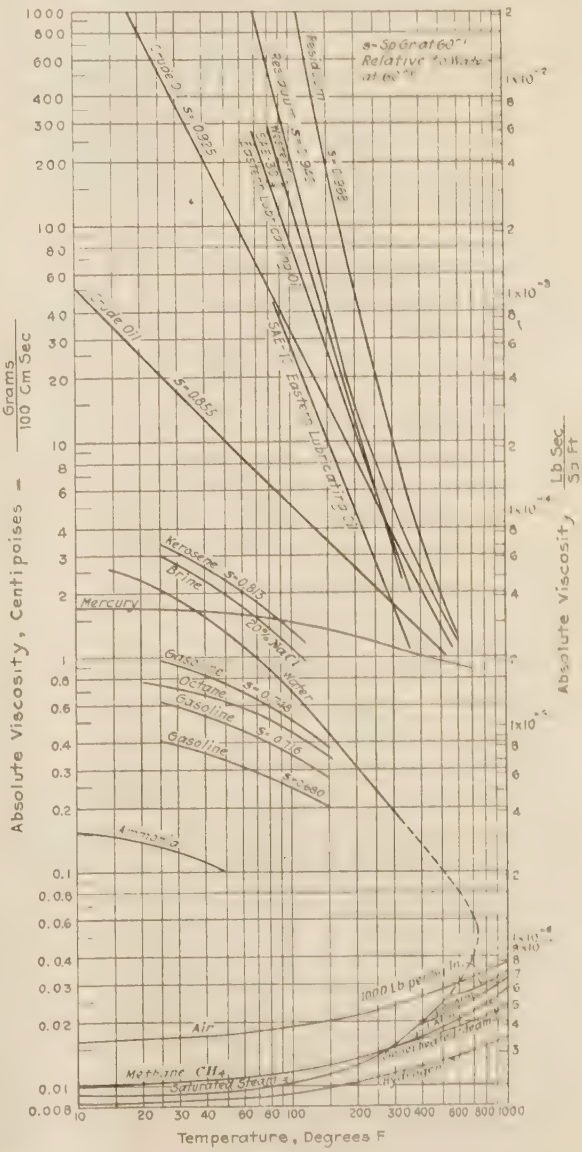

FIG. 1

[1] Professor of Mechanical and Hydraulic Engineering, California Institute of Technology. Vice-President, A.S.M.E., 1928–30. Professor Daugherty was graduated in mechanical engineering from Stanford University in 1909 and received his master's degree in 1914. He was assistant in mechanics at the University during 1907–1908; assistant in hydraulics, 1908–1909; and instructor in mechanical engineering, 1909–1910. From 1910 to 1916 he was assistant professor of hydraulics at Cornell University, resigning to become professor of hydraulics at Rensselaer Polytechnic Institute. Three years later he joined the faculty of the California Institute of Technology as head of the mechanical engineering department. In addition to teaching Professor Daugherty has been actively engaged in consulting work.

Contributed by the Hydraulics Division and presented at the National Aeronautic-Hydraulic Meeting, Berkeley, Calif., June 19, 20, and 21, 1934, of THE AMERICAN SOCIETY OF MECHANICAL ENGINEERS.

Discussion of this paper should be addressed to the Secretary, A.S.M.E., 29 West 39th Street, New York, N. Y., and will be accepted until September 10, 1935, for publication at a later date.

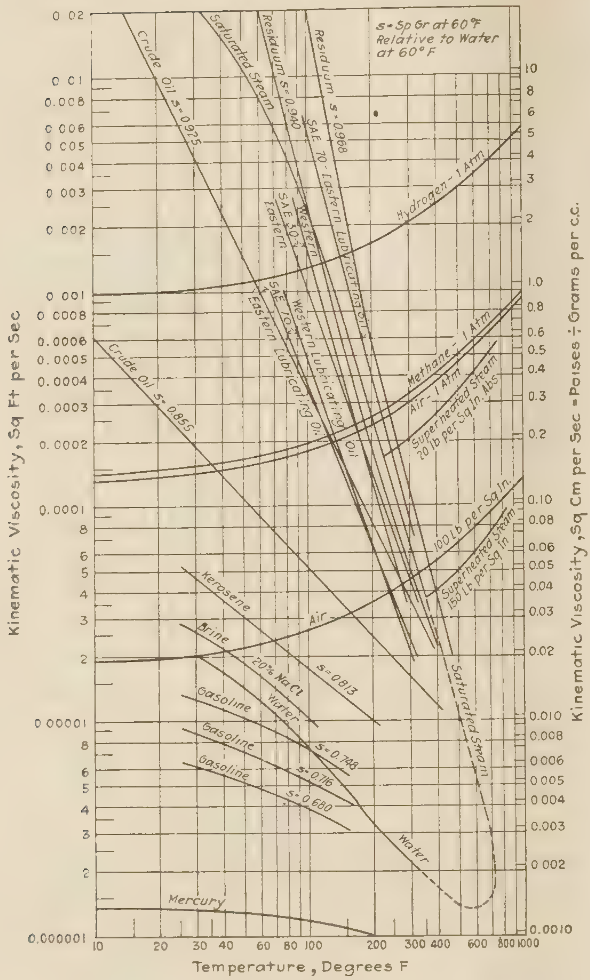

FIG. 2

may draw any number of curves for kinematic viscosity, depending upon the pressure chosen, such as is illustrated in Fig. 2 by air at atmospheric pressure and at 100 lb per sq in.

It is also interesting to note in Fig. 2 that at a temperature of about 200 F the kinematic viscosities of residuum, lubricating oils, heavy crude oils, saturated steam, and air at atmospheric pressure, as well as methane and therefore natural gas, are all approximately the same. Thus in the case of flow in a pipe line they would all have about the same Reynolds number for the same pipe size and velocity of flow and, therefore, would have about the same friction factor.

Another important property of fluids is the relation between pressure, volume, and temperature. This relationship is very simple in the case of the ideal or perfect gas and in so far as actual gases may be assumed to follow the perfect gas laws, the problem offers no difficulties. But vapors, which depart widely from perfect gases, cannot be treated so simply and neither can liquids. So far as our present knowledge goes these relationships are complex and are also purely empirical. In the upper right-hand corner of Fig. 3 is shown the field covered by the known data for water. P. W. Bridgman has thoroughly covered the range from 0 to 95 C from 500 atmospheres up to 12,000 atmospheres, while L. B. Smith and F. G. Keyes have measured these properties from 30 to 360 C and for pressures up to 350 atmospheres. Apparently Bridgman extrapolates back to saturation pressure, while Smith and Keyes extrapolate down to 0 deg temperature. Thus values as given by these two sources do not agree precisely in the field of low temperatures combined with low pressures, and the accuracy of values given by either may be questioned in this range. A limited amount of data has been determined in this low-temperature low-pressure field by several investigators such as Amagat and Tyrer. On the other hand no data at all have been determined for very high pressures combined with very high temperatures. While such a combination might be of great theoretical interest, it is fortunately of small practical value.

The lower portion of Fig. 3 shows Bridgman's values in more detail and to the same scale is shown a small portion of the Smith and Keyes data.

The compressibility of gases is important because of the magnitude of the volume changes. The compressibility of solids is very small, but in many cases of engineering structures even small changes in dimensions may result in stresses so great that they cannot be neglected, small though they be.

In the case of liquids their compressibility is often of small practical importance and hence this property is frequently ignored. However, it is of interest to note, for instance, that water is about 100 times as compressible as mild steel. But air at atmospheric pressure is 20,000 times as compressible as water, and at 300 lb per sq in. it is still 1000 times as compressible.

A practical case where compressibility of water is important is in the study of water-hammer phenomena. The volume modulus of elasticity, which enters into formulas dealing with water hammer, is the reciprocal of the coefficient of compressibility. For a perfect gas it may be shown that its isothermal volume modulus of elasticity is equal to the absolute pressure of the gas, but for other fluids calculation of the values is more involved.

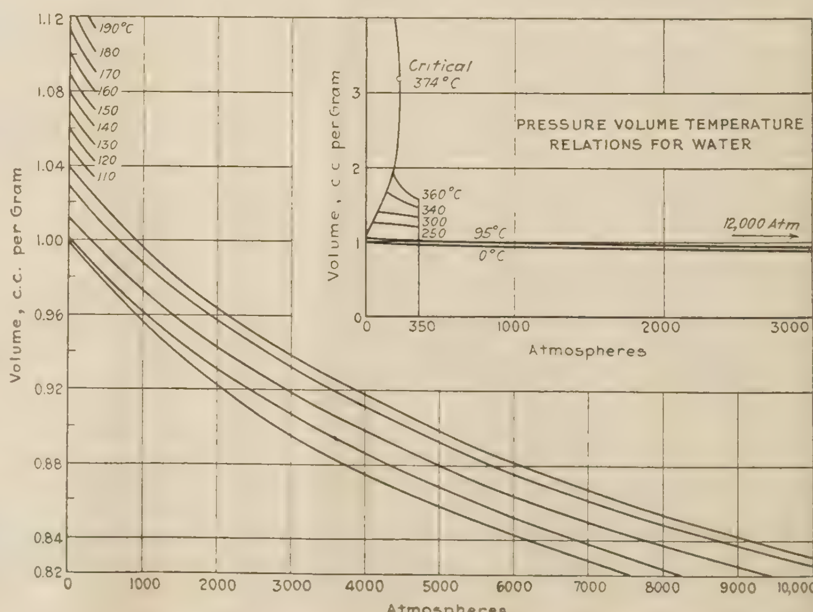

FIG. 3

In Fig. 4 are shown values of the isothermal modulus of elasticity for water at various temperatures and pressures. In the case of water hammer the action is practically adiabatic. The value of the adiabatic modulus may be obtained by multiplying the isothermal value by c_p/c_v, the ratio of the specific heat at constant pressure to that at constant volume. Values of this ratio are given in Fig. 7, which shows that for the temperatures usually encountered in such problems the difference between the two moduli is less than 2 per cent. This is really less than the uncertainty as to the correct value of the isothermal modulus itself, as may be seen in Fig. 5. Also any uncertainty as to the proper value of the modulus for water is less than the uncertainty as to the value to be used for the pipe line in connection therewith. The construction of a pipe line with joints, saddles which restrict movement, and other similar features makes the pipe as a whole behave differently from what it would if it were a homogeneous structure.

According to the Bridgman data, the value of the isothermal modulus at any one temperature increases with the pressure almost as a straight line, even up to 12,000 atmospheres. Hence the lines in Fig. 4 could readily be extended, if desired. From the Bridgman and Tyrer data the value of K at any given pressure is found to increase from 0 deg up to a maximum value at about 50 C and then to diminish again, while the Smith-Keyes data show that it continually decreases at an increasing rate as higher temperatures are reached.

Values of K as a function of temperature according to various observers are shown in Fig. 5. An approximate arithmetical determination of the modulus from the pressure-volume data direct involves very small differences between large quantities. Hence any slight error in the volumes is much magnified when differences are taken. Therefore the derivative of the pressure-volume curve is very much less accurate than the curve itself. This accounts for the discrepancies observed in Fig. 5.

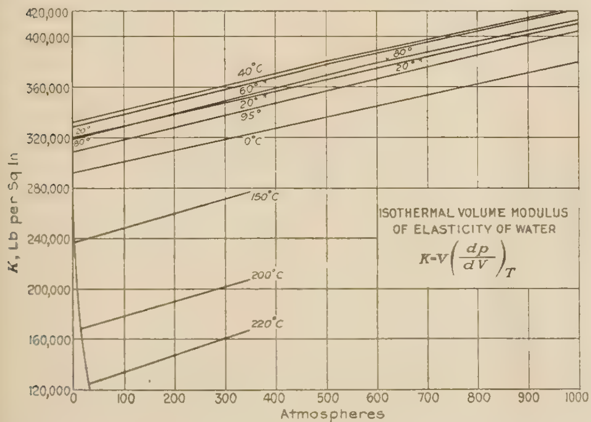

Fig. 4

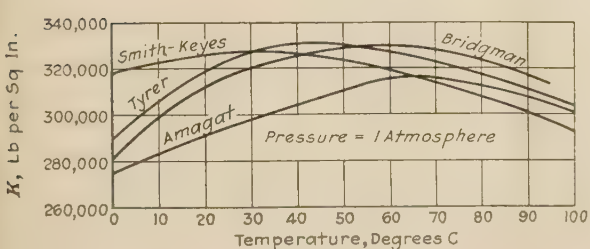

Fig. 5

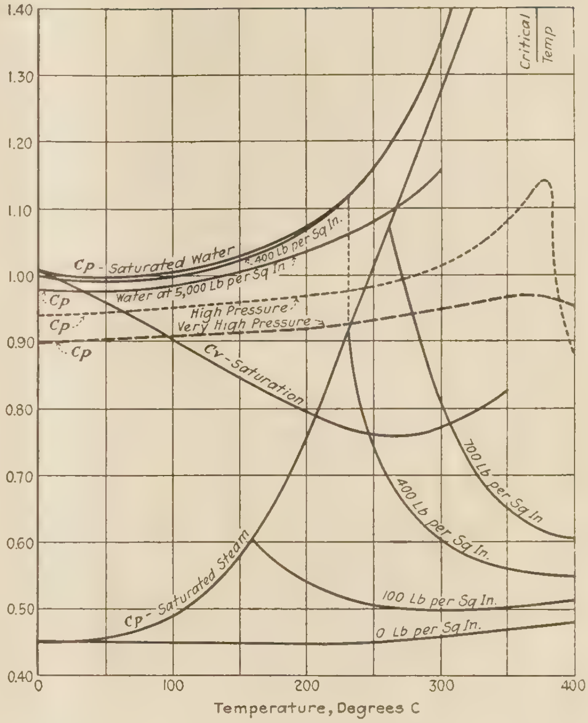

Fig. 6

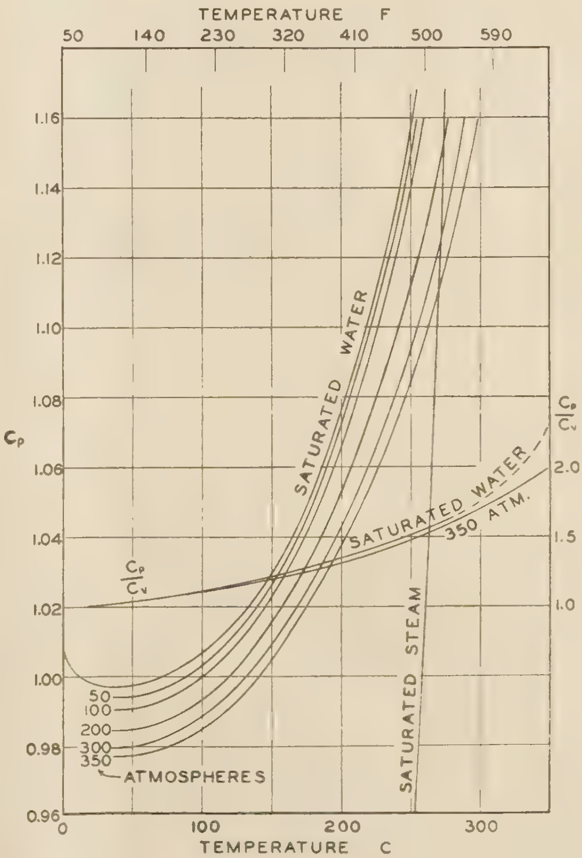

Fig. 7

The values of K so far shown are so-called "instantaneous" values, that is, they apply to an infinitesimal change of volume only. From the definition of $K = V\ (dp/dV)$ may be obtained $dV/V = dp/K$. The integral of dV/V is $\log_e V_2/V_1$, but to evaluate the integral of dp/K it is necessary to resort to graphical methods. Values of $1/K$ may be plotted against simultaneous values of p as obtained from Fig. 4. The area under this curve between the limits of p_1 and p_2 will then be the value of $\log_e V_2/V_1$, from which V_2 may be obtained for any pressure change from p_1 to p_2, assuming V_1 to be known.

If curves of $(1/K_m)$ were constructed as functions of pressure for various temperatures, where K_m is a mean value from some fixed initial pressure p_1, it is obvious that the value of $\log_e V_2/V_1$ could then be obtained by multiplying $(p_2 - p_1)$ by the value of $(1/K_m)$ corresponding to p_2.

There is often given the expression $K_m = V_1 \dfrac{p_1 - p_2}{V_1 - V_2}$ where K_m is a mean value for the pressure range concerned. This equation is not correct theoretically, but it may be shown that if $(V_1 - V_2)$ is 1/10 of V_1 the value of $(V_1 - V_2)$ computed by it will be 4.8 per cent too high. As the change in volume becomes smaller the error in this formula rapidly diminishes, so that it may often be used as an approximation.

Some thermal properties of water and steam are shown in Figs. 6 and 7. The values are for the various specific heats and are given in this paper because they are derived in large part from the pressure-volume-temperature relations such as those in Fig. 3. Since the specific heats involve second derivatives there may be some question as to the absolute accuracy of the values shown, but at least they show the way in which these quantities vary.

The values given in both Figs. 6 and 7 are instantaneous values. Mean values for any given range could be obtained by graphical integration. The saturation curves are of course merely the loci of the terminal points of a series of constant-pressure curves. The saturation curves for both water and steam for the specific heats at constant pressure approach infinity at the critical temperature. On the other hand the specific heat at constant volume may have a large value at the critical temperature, but it is still finite.

For pressures above the critical the specific heat of water at constant pressure is finite at the critical temperature, and the higher the pressure the less the maximum value attained by a given curve. However there is a complete absence of actual data in this region and the dotted curves are merely hypothetical. The critical pressure is about 220 atmospheres or about 3224 lb per sq in. The highest pressure for which data now exist is 350 atmospheres and does not go beyond 300 C, but the dotted curves correspond to very much higher pressures and temperatures than these.

For moderate temperatures the ratio of c_p/c_v is apparently very nearly independent of the pressure. But at the critical temperature the saturation value would be infinite, while that for a pressure above the critical would be finite. Hence the values of this ratio for different pressures must diverge very greatly as the critical temperature is approached.

It is surprising that for a substance as common as water, and of so much importance to us, there is still so much uncertainty about exact values of many of its properties.

Propeller Pumps

By M. P. O'BRIEN[1] and R. G. FOLSOM,[2] BERKELEY, CALIF.

This paper presents a simplified method of design with performance prediction throughout a reasonable portion of the operating range near the design point of propeller or axial-flow pumps. The results obtained by this method are compared with test characteristics for a known pump and very good agreement obtained. Cavitation phenomena are not considered.

The system of computations is based essentially on the propeller-blade element theory as used by Pfleiderer. The assumptions involved are clearly stated and the validity of each discussed. A theoretical proof for the desirability of constant total head being developed over the propeller disk is given. A sample computation is included which clearly illustrates the application to an actual pump.

Equally good agreement was found in computing the characteristics of a propeller fan.

THE theory of propeller pumps may be developed from two essentially different points of view. One treatment starts from a theory applicable to an infinite number of blades and applies a correction for real conditions. The other starts from the lift and drag exerted by streamlined sections and corrects for the interference of adjacent blades. The latter conception forms the basis for the computations included in this paper.

The method of computations is essentially that used by Pfleiderer[3] with, however, modifications which result in a better agreement between the computed and measured head-capacity characteristics. Many of the basic principles involved have been discussed in a recent paper by Spannhake[4] and will not be repeated here. The original aim was to compare measured results with those computed from a very simplified theory and give an indication of the direction and magnitude of the corrections that must be applied. The discrepancies between theory and measurement were found to be so small as to indicate that the simplified theory provides a practical method of design.

Data on a 20-in. pump of the Pfleiderer type were furnished by the Byron-Jackson Company for making the comparison. The method outlined is applicable to any similar type of axial-flow pump, provided the aerodynamic characteristics of the blade sections are known.

Cavitation is an important factor in the operation of propeller pumps. In the computations which follow it is assumed that the pressures are everywhere sufficient to prevent the formation of cavities.

Basic Equations

The fundamental equation for the operation of centrifugal pumps (radial, mixed, and axial flow) is obtained from the principle of torque and angular momentum. As applied to fluid problems, the equation is

$$\Delta T = \frac{\gamma}{g}\left(V_{u3}r_3 - V_{u0}r_0\right)\Delta Q \qquad [1]$$

If the discharge is imagined to be divided into small elements ΔQ, the quantities $V_{u3}r_3$ and $V_{uo}r_o$ for the elements may vary both radially and with position between the blades at a constant radius. Equation [1] is often stated to be valid only for an infinite number of blades but this view is not correct; it has the same validity as Newton's equations of motion and the reason for assuming an infinite number of blades is that the velocity component V_u can then be specified. This distinction is unimportant perhaps but it places the application of the equation on a somewhat different basis, in that the problem is to find methods for predicting the component V_u rather than to devise corrections which will make Equation [1] valid.

Integrating Equation [1] so as to take into account the variations mentioned, the actual torque is

$$T = \frac{\gamma Q}{g}\left(V_{u3}r_3 - V_{u0}r_0\right) \qquad [2]$$

Multiplying by the angular velocity and equating the result to the power output, gives as the equation for the head developed

$$H_d = \frac{1}{g}\left(V_{u3}u_3 - V_{u0}u_0\right) \qquad [3]$$

The simplified theory presented here is based upon the characteristics of airfoils and it is convenient to rewrite the preceding equations in terms of the circulation about the blades so as to obtain the forms commonly used in aerodynamics. The circulation is the line integral of the velocity around a closed path and its value at a constant radius for axially symmetrical flow is

$$\Gamma = 2\pi r V_u \qquad [4]$$

The equation for the torque becomes

$$T = \frac{\gamma Q}{2\pi g}\left(\Gamma_3 - \Gamma_0\right) \qquad [5]$$

[1] Associate Professor of Mechanical Engineering, University of California. Assoc-Mem. A.S.M.E. Professor O'Brien received his B.S. in Civil Engineering from the Massachusetts Institute of Technology in 1925, and served as assistant in civil engineering at Purdue University from 1925 to 1926, and research assistant, Engineering Experiment Station, from 1926 to 1927. During 1927 and 1928 he held the Freeman Traveling Scholarship of the American Society of Civil Engineers, and was assistant research engineer at the Royal College of Engineering, Stockholm, Sweden, during the same period. Since 1928 Professor O'Brien has been on the faculty of the University of California.

[2] Instructor, Department of Mechanical Engineering, University of California. Jun. A.S.M.E. Mr. Folsom received the degrees of B.S., M.S., and Ph.D. from the California Institute of Technology in 1928, 1929, and 1932, respectively. Since his graduation in 1928 he has worked for one year as part-time research assistant at Riverside Cement Company, Riverside, California; four years as teaching fellow at the California Institute of Technology; and one year as engineer for the Water Department of the City of Pasadena, California. He has been at the University of California since 1933.

[3] "Die Kreiselpumpen," by C. Pfleiderer, second edition, J. Springer, Berlin, 1932.

[4] "Problems of Modern Pump and Turbine Design," by W. Spannhake, Trans. A.S.M.E., 1934, pp. 225–248, paper HYD-56-1.

Contributed by the Hydraulics Division and presented at the National Aeronautic-Hydraulic Meeting, Berkeley, Calif., June 19, 20, and 21, 1934, of The American Society of Mechanical Engineers.

Discussion of this paper should be addressed to the Secretary, A.S.M.E., 29 West 39th Street, New York, N. Y., and will be accepted until September 10, 1935, for publication at a later date.

The circulation about each of the blades is

$$\Gamma_s = (\Gamma_3 - \Gamma_0)/z \qquad [6]$$

and

$$T = \frac{\gamma Q z \Gamma_s}{2\pi g} \qquad [7]$$

Including the drag of the blades, Equation [7] becomes

$$T_a = \frac{\gamma Q z \Gamma_s}{2\pi g} + zrL \tan\lambda \cos\beta_\infty \qquad [8]$$

The lift on a unit length of one blade in an infinite row is

$$L = \rho\, v_\infty\, \Gamma_s \qquad [9]$$

where the numerical value of $V_{u\infty}$ is $V_{u3}/2$. Substituting for Γ_s

$$T_a = \frac{QzL}{2\pi v_\infty} + zrL \tan\lambda \cos\beta_\infty \qquad [10]$$

Multiplying Equation [10] by the angular velocity and equating the result to the power input gives

$$H_d = \frac{zL\omega}{2\pi\gamma v_\infty} + \frac{\omega zrL \tan\lambda \cos\beta_\infty}{\gamma Q} \qquad [11]$$

Since L is referred to unit length of blade, the discharge at any radius can be expressed as

$$Q = 2\pi r V_f \qquad [12]$$

The number of blades is $2\pi r/t$ and the equation for the lift is

$$L = C_L\, \rho(v_\infty^2/2)c \qquad [13]$$

Substituting these quantities in Equation [11] and simplifying

$$H_d = C_L \frac{c}{t} \frac{u}{V_f} \frac{v_\infty^2}{2g} \frac{1}{\cos\lambda} \left(\frac{V_f}{v_\infty} \cos\lambda + \sin\lambda \cos\beta_\infty\right) \qquad [14]$$

But $V_f/v_\infty = \sin\beta_\infty$ and

$$H_d = C_L \frac{c}{t} \frac{u}{V_f} \frac{v_\infty^2}{2g} \frac{\sin(\beta_\infty + \lambda)}{\cos\lambda} \qquad [15]$$

Equation [15] gives the head developed at a certain radius on the assumption that the flow is two-dimensional or, in other words, that radial flow does not occur. Equation [15] provides a method of estimating the velocity terms entering Equation [3], which may be rewritten as

$$H_d = \frac{u}{g}(V_{u3} - V_{u0}) \qquad [16]$$

for an axial-flow pump. Here, H_d is the head developed at the radius corresponding to u and the velocity terms are average values.

Equations [15] and [16] apply to the conditions at a given radius and the next problem is to determine how H_d should vary radially to give optimum results. The most desirable condition is that H_d be a constant. The stability of the pressure distribution at discharge resulting from a constant developed head will be investigated. Solving Equation [16] for the tangential component at discharge

$$V_{u3} = \frac{gH_d}{u} + V_{u0} \qquad [17]$$

Assuming that the flow is originally axial, $V_{u0} = 0$. The pressure change between inlet and discharge at any radius is then

$$\frac{\Delta p}{\gamma} = H_d - h + \frac{V_{f0}^2}{2g} - \frac{V_{f3}^2}{2g} - \frac{V_{u3}^2}{2g} \qquad [18]$$

For pure axial flow, $V_{f0} = V_{f3}$ and the pressure change as a function of radius is

$$\frac{\Delta p}{\gamma} = H_d - h - \frac{gH_d^2}{2\omega^2 r^2} \qquad [19]$$

Since all of the flow had the same pressure originally, Equation [19] represents the variation in pressure in the plane of discharge.

It has been assumed here that each element of flow remains at a constant radius and it is now necessary to determine whether such a condition is possible with the pressure distribution given by Equation [19]. For motion in circular or spiral paths, the radial-pressure gradient is

$$\frac{dp}{dr} = \rho \frac{V_u^2}{r} \qquad [20]$$

Substituting $V_u = \frac{gH_d}{\omega r}$ and integrating gives

$$\frac{p}{\gamma} = \text{constant} - \frac{gH_d^2}{2\omega^2 r^2} \qquad [21]$$

The pressure variation of Equation [19] is seen to be consistent with that necessary for flow at constant radius and it is evident

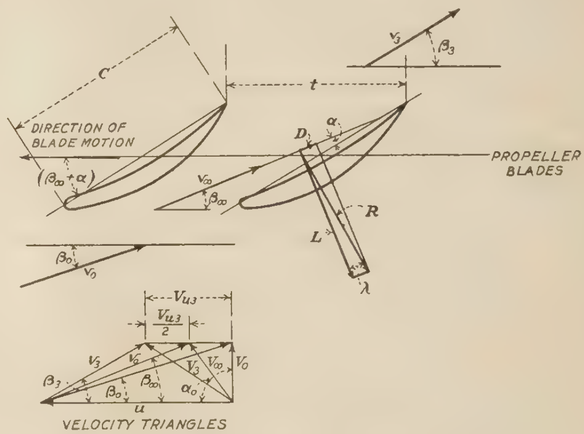

Fig. 1 Velocity Diagrams for Propeller Pumps

that an axial-flow pump should be designed so as to make H_d a constant. This requirement has not been generally adopted for the design of propeller pumps and fans and, in fact, some methods[5] aim at a constant pressure over the section at discharge, a condition which would result in radial flow.

An interesting feature of Equation [19] is that it shows the necessity for a hub on both fans and pumps. For a constant developed head, the pressure drops rapidly from the tip of the blade inward and will reach very low values if the inner radius is small.

Prediction of Head-Capacity Characteristic

The theoretical treatment of propeller pumps and fans has been carried to such a point as to make application difficult and very few experimental checks on the validity of this theoretical work have been published. Having this in mind, the authors have used a simplified theory to predict the head-capacity curve of a pump which had been tested and for which complete design drawings were available. Certain corrections were omitted deliberately because the primary aim was to find the simplest

[5] "The Propeller-Type Fan," by O. G. Tietjens, Trans. A.S.M.E., vol. 54, 1932, paper APM-54-13, pp. 143–152.

method of design which is also reliable. The good agreement between theory and measurement may have been fortuitous and comparisons for other pumps may show that certain modifications of this simplified treatment are necessary. Recent applications of this method to propeller fans showed good agreement between computed and measured head-capacity curves.

The assumptions upon which the simplified theory is based are as follows:

1 No radial component of velocity in the pump.

2 No rotational component and uniform axial velocity at entrance.

3 Lift and drag coefficients of blade sections are the same as for a single airfoil with an infinite aspect ratio. The angle of attack is corrected for mutual interference.

4 The shock loss on entering the guide vanes depends upon change in the rotational component of velocity.

TABLE 1 GENERAL CHARACTERISTICS OF PROPELLER PUMP OF FIG. 2

Section radius, ft.	0.354	0.474	0.594	0.714	0.833
Blade velocity, ft per sec	32.8	44.0	55.1	66.2	77.3
		thick		thin	thin
Blade sections, Gött.	No. 387	No. 490	No. 490	No. 490	No. 490
Section multiplication factor	...	1.287	...	0.800	0.655
Approx. N.A.C.A. equivalent	6415	5311	4309	3307	2306
Normal($\beta_\infty + \alpha$)N.A.C.A.	38° 48′	25° 55′	19° 24′	15° 21′	12° 47′
c/t	0.736	0.625	0.602	0.581	0.562
Guide-vane entrance angle	54°	60° 40′	66° 25′	69° 13′	71° 48′
Number of impeller blades	3	...	...	...	...
Number of guide vanes	8	...	...	...	...
Pump speed, rpm	885	...	...	...	...
Blade radial clearance	0.03 in.	...	...	...	...

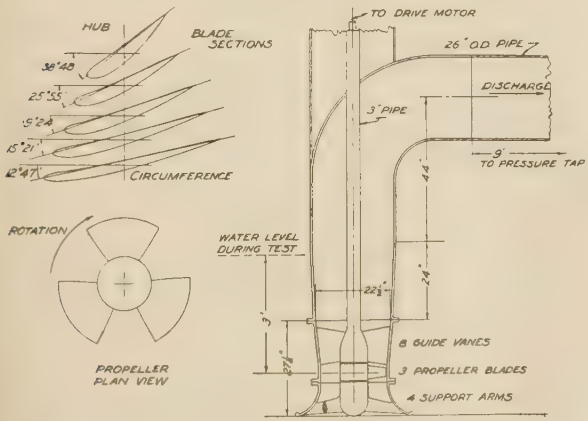

FIG. 2 20-IN. PROPELLER PUMP OF THE PFLEIDERER TYPE

5 The friction losses may be broken into two distinct portions, namely, that caused by the drag of the propeller blades and that resulting from frictional resistance in the stationary water passages.

6 The head developed by the pump as a whole is the weighted average of the heads developed at each radius.

Before discussing the errors introduced by making these assumptions, the method of computation will be illustrated by a numerical example based upon the pump shown in Fig. 2. The general characteristics of this pump appear in Table 1. Application of the method requires the assumption of a discharge and computation of the corresponding head by successive approximation. A direct computation of the head does not appear possible.

EXAMPLE

For a discharge of 12,000 gpm, the axial velocity just previous to entrance to the pump is $V_{f0} = 15.0$ ft per sec. At a radius

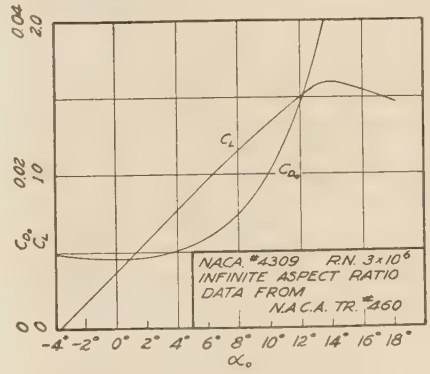

FIG. 3 INFINITE-ASPECT-RATIO DATA FOR N.A.C.A. AIRFOIL SECTION NO. 4309 FROM N.A.C.A. TECHNICAL REPORT NO. 460

of 0.594 ft, the blade profile is a Göttingen No. 490 airfoil section, the characteristics of which may be closely approximated from the N.A.C.A. test results given in Technical Report No. 460. Fig. 3 presents the characteristic curves for the N.A.C.A. airfoil section No. 4309 which is very nearly identical with the No. 490 Göttingen section. Five radii were used in computing the head characteristics, and curves similar to those in Fig. 3 must be known for each section if the blade shape changes. This example will be carried through for one radius only since the method is exactly the same for the other radii.

The operating speed of the pump is 885 rpm, and the peripheral velocity of the blade section is 55.1 ft per sec. The next step is to assume a value of H_d and compute the corresponding head given by Equation [15]:

Assume H_d = 18 ft

From Equation [16] with $V_{u0} = 0$

$$V_{u3} = 18 \times 32.2/55.1 = 10.5 \text{ ft per sec}$$

$$v_\infty{}^2 = V_f{}^2 + (u - V_{u3}/2)^2 = 15.0^2 + (55.1 - 10.5/2)^2 = 2704 \text{ (ft per sec)}^2$$

TABLE 2 COMPLETE COMPUTATIONS FOR THE 20-IN. PFLEIDERER-TYPE PROPELLER PUMP SHOWN IN FIG. 2

Blade angle at tip		12° 47′			12° 47′			12° 47′			12° 47′			9° 47			15° 17′	
Capacity, gpm		6,000			10,000			12,000			14,000			9,700			14,300	
Axial velocity, ft per sec		7.49			12.47			14.98			17.43			12.11			17.85	
Heads, ft	H_d	h_s	h_p	H_d	h_s	h_p	H_d	h_s	h_p	H_d	h_s	h_p	H_d	h_s	h_p	H_d	h_s	h_p
Section r = 0.354 ft	18.5	2.5	2.8	16.6	0.8	0.9	14.7	0.2	0.4	13.0		0.4	15.5	0.7	0.6	14.0	...	0.4
Section r = 0.474 ft	27.6	3.9	2.7	20.4	1.0	0.8	16.3	0.2	0.5	13.0	Less	0.5	17.4	0.6	0.7	15.5	...	0.5
Section r = 0.594 ft	34.3	4.4	2.3	23.5	1.1	1.0	18.0	0.3	0.8	12.9	than	0.8	18.2	0.4	1.1	17.3	0.1	0.7
Section r = 0.714 ft	41.6	4.7	4.7	25.7	0.9	1.6	18.8	0.2	1.3	12.2	0.05	1.2	17.4	0.2	1.6	19.0	0.1	1.2
Section r = 0.833 ft	47.2	4.6	5.2	28.5	1.0	2.3	20.0	0.2	1.8	12.1		1.7	16.7	0.1	2.3	21.7	0.1	1.6
$(H_d)_{avg}$, ft	35.8	..	..	23.7	..	..	18.1	..	..	12.6		..	17.3	..	..	17.7	..	..
$(H_d - h_s - h_p)_{avg}$, ft		28.0			21.5			16.6			11.6			15.6			16.8	
h_f, ft		0.4			1.0			1.4			2.0			0.9			2.0	
H, ft		27.6			20.5			15.2			9.6			14.7			14.8	
e_h, per cent		77.1			86.4			84.0			76.2			85.0			83.7	
e (Test overall effi.), per cent		53			77			81			77			76			82	
Test, bhp		81			67			58			48			...			...	

$$\tan \beta_\infty = V_f/(u - V_{u3}/2) = 15.0/(55.1 - 10.5/2) = 0.3005$$
$$\beta_\infty = 16 \text{ deg } 44 \text{ min}$$
$$\text{Blade angle } (\beta_\infty + \alpha) = 19 \text{ deg } 24 \text{ min}$$
$$\text{Angle of attack, } \alpha = (19 \text{ deg } 24 \text{ min}) - (16 \text{ deg } 44 \text{ min}) = 2 \text{ deg } 40 \text{ min}$$

From Fig. 3, $C_L = 0.64$ and $C_{D0} = 0.0098$

$$\operatorname{Tan} \lambda = C_{D0}/C_L = 0.0098/0.64 = 0.0153$$
$$\lambda = 0 \text{ deg } 53 \text{ min}$$
$$\operatorname{Cos} \lambda = 0.9999$$
$$(\beta_\infty + \lambda) = 16 \text{ deg } 44 \text{ min} + 0 \text{ deg } 53 \text{ min} = 17 \text{ deg } 37 \text{ min}$$
$$\operatorname{Sin} (\beta_\infty + \lambda) = 0.3026$$
$$c/t = 0.602$$

From Equation [15] $H_d = 0.64 \times 0.602 \times (55.1/15.0) \times (2704/64.4) \times (0.3026/0.9999)$

$$H_d = 18.04 \text{ ft}$$

This head agrees with the assumed value within the accuracy of the computation. If the assumed and computed values do not agree, another assumption is made and the computation repeated.

The shock loss on entering the guide vanes is assumed to be

$$h_s = [V_{u3} - (V_{f4}/\tan \alpha_4)]^2/2g$$
$$\alpha_4 = 66 \text{ deg } 25 \text{ min and } \tan \alpha_4 = 2.291$$
$$h_s = [10.5 - (15.0/2.291)]^2/64.4 = 0.25 \text{ ft}$$

The friction loss through the propeller resulting from the section drag is

$$h_p = C_L \frac{c}{t} \frac{v_\infty^2}{2g} \frac{\tan \lambda}{\sin \beta_\infty}$$
$$\sin \beta_\infty = 0.2879$$

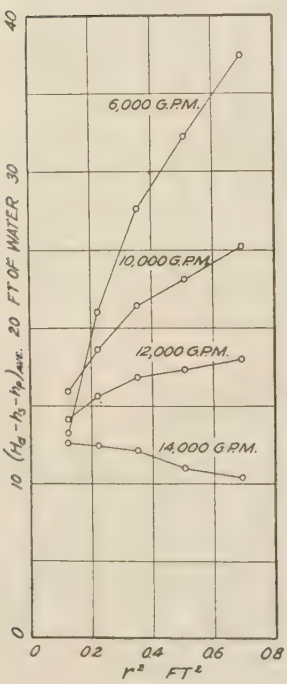

Fig. 4

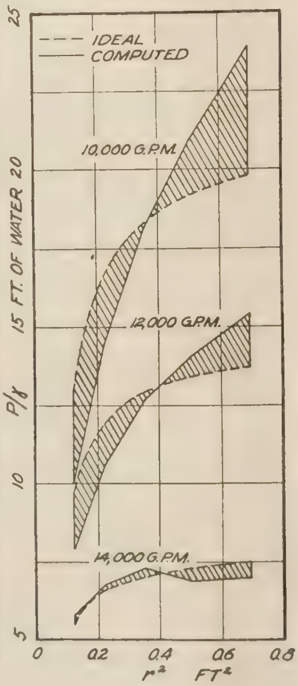

Fig. 5

Fig. 4 Curves Used for Averaging Net Heads at the Various Radii Given in the Example

Fig. 5 Pressure Distribution at Each Radius of the 20-In. Pfleiderer-Type Pump

$$h_p = 0.64 \times 0.602 \times (2704/64.4) \times (0.0153/0.2879) = 0.86 \text{ ft}$$

The net head at the radius $r = 0.594$ ft uncorrected for friction in fixed passages is

$$H_d - h_s - h_p = 18.04 - 0.25 - 0.86 = 16.93 \text{ ft}$$

A similar computation is carried through for all five radii. The resulting heads are averaged on the basis of area by plotting head versus r^2 as shown in Fig. 4. The average ordinate is obtained by planimetering the area. For this problem the average head uncorrected for friction in the fixed passages is 16.6 ft.

All other losses in the pump test section can be represented by an equation of the type

$$h_f = K(V_f^2/2g)$$

where K is a characteristic of the water passages and should not vary with either capacity or speed, within the usual range of

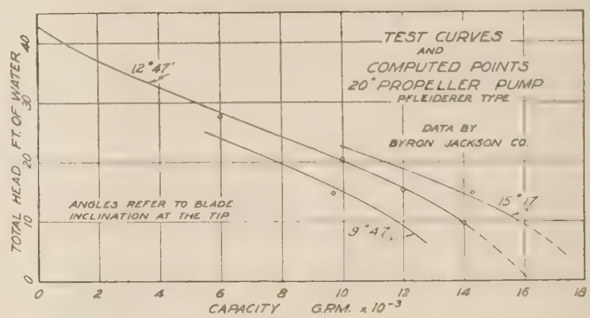

Fig. 6 Test Curves and Computed Points for the 20-In. Pfleiderer-Type Propeller Pump

conditions. The magnitude of K can be approximated from tables of hydraulic friction losses. For the pump under consideration, K has been estimated at 0.4. Therefore, at 12,000 gpm

$$h_f = 0.0062 \times 15.0^2 = 1.4 \text{ ft}$$

The estimated net head is then

$$H = (H_d - h_s - h_p)_{\text{avg}} - h_f = 16.6 - 1.4 = 15.2 \text{ ft}$$

The hydraulic efficiency is

$$e_h = 15.2/18.1 = 84 \text{ per cent}$$

The results of all computations appear in Table 2 and a comparison of the computed and measured results is shown in Fig. 6. In addition to the normal angles shown in Fig. 2, and listed in Table 1, the comparison includes two points with the blades rotated about their own radial axes.

Equation [21] gives the pressure distribution which will tend to prevent radial flow and this was also found to be the pressure distribution resulting from the condition, H_d = constant. In this example, the computations indicate that H_d varied materially along the radius producing a radial flow and a corresponding additional energy loss. In Fig. 5, the pressure distribution has been computed at each radius from

$$\frac{p}{\gamma} = H_d - (V_f^2 + V_{u3}^2)/2g$$

and compared with the ideal pressure distribution, assuming $(H_d)_{\text{avg}}$ to be the head developed at each radius. The difference between the two curves is a measure of the head available to cause cross-flow.

Limitations of the Simplified Theory

The surprisingly good agreement between the computed and measured head-capacity characteristics should not obscure the fact that the theory, on which the method of computation is based, neglects a number of important factors. The computed results themselves show an inconsistency in the case of the point for 14,000 gpm on the curve for 12 deg 47 min, in that the hydraulic efficiency computed is 76.2 per cent while the measured overall efficiency is 77 per cent.

To emphasize the degree of approximation involved in this simplified theory, the neglected factors are enumerated and discussed.

(*a*) *Leakage Around the Blade Tips.* The leakage expressed as a percentage of the net discharge will decrease with increasing pump size. Assuming that the average pressure difference between the two sides of the blades is equal to the average developed head, the backflow around the blade tips from the upper to the lower side is approximately

$$Q_L = 0.6\, a \sqrt{(2g\, H_d)}$$

For the pump considered in the example the radial clearance was 0.03 in. and the length of each blade was 0.83 ft. Using

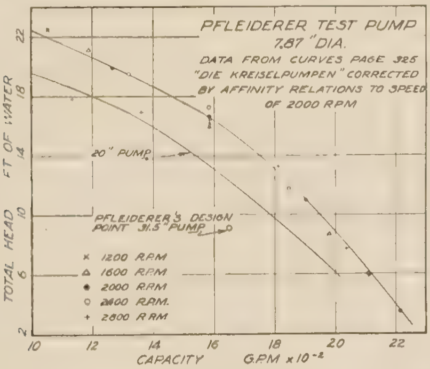

Fig. 7 Head-Capacity Characteristics for 7.87-In. Pfleiderer Test Pump

these values, the total backflow for the three blades is 0.135 cu ft per sec or 0.5 per cent of the net discharge.

In computing the head produced by a 32-in. pump of the same type as considered here, Pfleiderer assumes arbitrarily that the leakage and obstruction of the blades together account for an increase in the axial component amounting to 10 per cent.

A correction for the obstruction of the blades is unnecessary if the head is based upon airfoil characteristics with corrected angles of attack and Pfleiderer's correction really represents leakage only. In Fig. 7, his point for a 32-in. pump is compared with measured values for a geometrically similar 20-in. pump. The difference is believed to result from his excessive correction of the axial velocity.

In the theory of airplane propellers, where the tip of the blade is free, the circulation decreases from the center outward and an induced drag develops. In addition to the added resistance in the direction of motion, there is a change in the effective angle of attack. Because of the small leakage around the blade tips, conditions in a propeller pump with small clearance are believed to correspond closely to an infinite length of airfoil and no correction has been made for induced drag and the accompanying change in the angle of attack.

(*b*) *Interference of Adjacent Blades.* Numachi and Weinig find that in an ideal fluid adjacent blades at certain angles cause an increase in the lift coefficient, while experiments on airplane-propeller sections show a decrease for the same arrangement.[6,7] The magnitude of the effect depends upon the value of c/t and the propeller experiments do not apply to the pump studied so that a correction could not be made on the basis of experimental data. In the example, the method of computing the angle of attack includes a correction for blade interference.

(*c*) *Variation in Blade Section.* The lift and drag coefficients have been selected from data which are applicable to an infinite length of constant section and have been applied to a blade having a section which changes with radius. The method of handling this problem in the design of airplane propellers does not appear to be applicable to pumps with small clearance at the blade tips and no correction has been made.

(*d*) *Uniform Axial Velocity and No Tangential Velocity at Entrance.* This assumption is believed to correspond very closely with the actual conditions because the bell-mouthed inlet section is short and contracts rapidly. Such an inlet is known to give an almost uniform velocity distribution for some distance beyond the end of the converging section. The arms supporting the lower bearings are streamlined and tend to prevent prerotation although they probably do not eliminate it entirely.

(*e*) *Frictional Drag at Walls.* The relative velocity decreases to zero at both the hub and the housing. The combined effect is a rotation of the fluid in planes perpendicular to the shaft and in a direction opposite to that of the impeller. The water moves in a spiral path between the blades and even in a pump developing the same head at every radius, radial flow occurs.

(*f*) *Average Head.* The method of computing the head as the weighted average of the heads developed at each radius seemed at first to be based upon a very unsound assumption but closer study gave it a better appearance without fully justifying it. The axial component of velocity is probably uniform in the discharge plane and loss of head will not result from mixing with elements at different radii. Variations in pressure from the ideal curve result in cross-flow without, however, bringing about a substantial loss of mechanical energy. The remaining factor is the tangential component of velocity. Taking an average of the heads developed at each radius is equivalent to assuming that the dragging effect of concentric layers brings about a radial distribution of rotational velocities which corresponds approximately to the distribution which would result from a constant developed head at all radii. This situation is not the same as for the mixing streams of different axial velocities with the consequent Borda-Carnot shock loss and a rational method has not been found for estimating the loss resulting from the variation in developed head.

The tangential component of velocity also varies between the blades. This effect has been treated extensively by Spannhake[4] and will not be discussed here except to state that the method of computing the tangential velocity gives a properly averaged value.

(*g*) *Limits of Applicability.* As the rate of discharge is increased, negative lifts and heads appear first at the blade tips and develop inward. The method for computing the average head probably will not apply when the heads are partly negative but this limitation is of little practical importance.

At low rates of discharge, the angle of attack of the blades is above the "burble-point" and computation of the head is limited

[6] "Airfoil Theory of Propeller Turbines and Propeller Pumps With Special References to the Effects of Blade Interference Upon the Lift and Cavitation," by F. Numachi, The Technical Reports of the Tohoku Imperial University, vol. 8, no. 3, 1929, pp. 136–191.

[7] "Über die Winkelübertreibung von Turbinenschaufeln," by F. Weinig, *Wasserkraft und Wasserwirtschaft*, part 3, Feb. 2, 1934, pp. 25–31.

by the available experimental data on the lift and drag coefficients of the blade sections used. In the extreme case of zero net discharge from the pump as a whole, the outer sections of each blade are developing positive head and delivering a positive discharge which equals in total amount the downward flow through the sections near the hub. In these extreme cases, radial flow is important and the methods of computation suggested here are believed to be inapplicable to them.

(*h*) *Friction and Shock Losses.* Omitting frictional losses on the blade surfaces, which are represented by the drag coefficient, and the shock loss on entering the guide vanes, all other shock and surface-friction losses are represented by a single coefficient which is a characteristic of the water passages between the suction sump level and the point of discharge pressure measurement. Use of such a coefficient is basically correct but determination of its proper value for a given installation is difficult. Direct measurement of the friction loss with the impeller removed would give a value slightly too great because of the curvature of the guide vanes.

The shock loss on entering the guide vanes has been assumed to be proportional to the square of the difference in the tangential components at discharge from the runner and after entrance to the guide vanes. A coefficient of unity for the entering loss alone is probably excessive but there is an additional loss in the recovery of tangential velocity as pressure within the guide vanes.

Affinity Laws

The affinity laws are important aids in the design of centrifugal pumps and it is interesting to investigate their validity for the same pump at different speeds and for geometrically similar pumps of different sizes. Pfleiderer[3] gives data on the head-capacity characteristics of a 7.87-in. pump at five different speeds. The results have been corrected to a speed of 2000 rpm and plotted in Fig. 7. The agreement is very good except for the highest speed at low capacities. The same figure shows the corresponding test data for the 20-in. pump. Apparently these pumps are not strictly geometrically similar. The affinity laws used in making the corrections are exactly the same as for radial- and mixed-flow pumps.

One interesting feature of Fig. 7 is the comparison of the design point computed by Pfleiderer and the test data on a 20-in. geometrically similar pump. The discrepancy is believed to result from his excessive correction of the axial-flow component.

Conclusion

In conclusion it should be pointed out that no theory can be considered satisfactory until it has been found to apply to a wide variety of conditions. Subsequent comparisons of theory and experiment may indicate that the theory should be modified to take into account certain secondary phenomena which have combined in such a way as to neutralize each other in the pump used for comparison here. On the basis of these results, it appears that the modified method of Pfleiderer may be used to predict a portion of the head-capacity curve in the region of the design point.

Appendix

Nomenclature

a = area, sq ft
c = chord length of airfoil, ft
C_L = lift coefficient of airfoil
D = drag per unit of blade length, lb per ft
g = acceleration of gravity, ft per sec per sec
h = elevation head, ft
h_p = head lost in friction in the propeller, ft
h_s = head lost in shock at guide vanes, ft
h_f = all other friction and shock losses, ft
H = measured head developed by the pump, ft
H_d = developed head of the impeller, ft
K = coefficient of friction and shock losses
L = lift per unit of blade length, lb per ft
p = pressure, lb per sq in.
Q = capacity, cu ft per sec
Q_L = leakage, cu ft per sec
r = radius, ft
s = distance, ft
t = blade separation measured along the arc, ft
T = torque, ft-lb
T_a = net torque, ft-lb
u = velocity of a point on the blade, ft per sec
v = velocity of the fluid relative to the impeller, ft per sec
v_∞ = geometric mean value of the relative velocities in front and in rear of the impeller, ft per sec
V = absolute velocity of the fluid, ft per sec
V_u = tangential component of absolute velocity of fluid, ft per sec
V_f = axial component of absolute velocity of fluid, ft per sec
z = number of blades
α_4 = angle between the guide vanes at entrance and the pump axis, deg
β_∞ = angle between v_∞ and the direction of blade motion, deg
γ = weight per unit volume of fluid, lb per cu ft
Γ = $\int_0 V \cos (V, s)\, ds$ = circulation, ft sq per sec
Γ_s = circulation about a single airfoil section, ft sq per sec
$\tan \lambda = D/L$
ρ = γ/g = density, lb sec[2] per ft[4]
ω = angular velocity, radians per sec

Subscripts:
0 — conditions before entrance into impeller
3 — conditions after leaving impeller
4 — conditions just after entrance into guide vanes.

Concerning the Degree of Accuracy of the Gibson Method of Measuring the Flow of Water[1]

By D. THOMA,[2] MÜNCHEN, GERMANY

The paper first discusses the limitations of various methods of measuring water which were in use when the Gibson method was first announced. These limitations of the current-meter method of flow measurement include: The effect of turbulent accessory motions which cause periodic velocity changes in the direction and magnitude of flow; the difficulty in obtaining readings close to the wall of the canal or closed conduit; and the necessity of determining the velocity at several points simultaneously due to temporary changes in distribution; and the expense involved in taking a number of such simultaneous readings. Reference is also made to the use of the pitot tube for taking readings close to the wall of the passage.

The greater part of the paper, devoted to a discussion of the Gibson method of water measurement, includes the derivation of formulas involved in this method of water measurement, its limits of accuracy, and the errors which may arise in its use. These errors, due to (*a*) accessory motions, (*b*) to false valuation of friction, (*c*) to friction of the mercury column, and (*d*) to inertia of the mercury column, are presented with derived formulas and approximate values together with suggestions for minimizing them.

IN ORDER to make the peculiarity of the Gibson method stand out clearly, a short criticism of other methods for measuring large quantities of water will first be given.

When the velocities of water are measured at a sufficient number of points in a cross-section to determine the flow per second through a canal or a closed conduit, the measurement will always be affected by the turbulent accessory motions which cause periodic changes in the velocities both in magnitude and direction. The problem in such measurements is to determine for a given interval of time the average value of the components of velocities vertical to the measuring cross-section.

When measuring with Woltman's current meter, the changes in magnitude of the water velocity are not serious because the revolutions of the meter are sufficiently proportional to the water velocity and, therefore, the average speed of the meter, which is obtained from the test, exactly corresponds to the average value of the water velocity. The changes in the direction caused by the accessory motions, however, are disturbing since the speed of the meter is affected by an additional side component of the flow so that the meter in general no longer indicates exactly the component of the velocity in the shaft direction, upon which it is exclusively dependent when the flow quantity is being determined. Lately, some meters have been invented which are practically independent of these errors within a sufficiently wide angle. However, these meters (blades separately fixed on spokes) are subject to errors through the collection of water plants and other thread-like debris. We hope soon to have current meters which are independent of accessory motions of flow and which will repel the debris like a pointed screw.

One more deficiency in the current-meter measurement is the impossibility of determining the water velocity close to the walls. To obviate this deficiency, special small meters, called wall meters, can be used near the edge of the measuring cross-section. These have been made by L. A. Ott[3] according to the author's directions, and make it possible to determine the velocity of the water one inch from the walls. However, wall meters are still being developed and are not yet commonly available. By using wall meters, and by interpolation of the water velocity in accordance with the new experiments on the distribution of the velocities close to a wall, the limit of the errors is reduced to a fraction of previous values.

Considerable difficulty arises with current measurements because of the need for determining the water velocities at a number of measuring points at the same time, this being necessary because the flow may temporarily undergo slow changes which cause errors, if the measurements are made at many points, one after the other. To repeat the measurements several times in order to decrease the errors takes a very long time and in most cases, therefore, is not done. To fill the requirements for simultaneous measurements is very expensive. For instance, 27 meters were used to determine the discharge of the water at the powerhouse at Aufkirchen on the Mitlere Isar.

If, on the other hand, one uses the pitot tube to determine the water velocity, it is possible by a suitable shaping of the tube (Prandtl's tube) to minimize the errors caused by fluctuations in the direction of flow. It is also possible to make dependable measurements at very short distances from the wall. Pitot tubes, however, give errors caused by fluctuations in the magni-

[1] Translated from "Mitteilungen des Hydraulischen Instituts der Technischen Hochschule München," Bull. 1, 1926, pp. 59–74, by E. B. Strowger, assistant hydraulic engineer, The Niagara Falls Power Company, Mem. A.S.M.E., and P. Olsen, engineering assistant, The Niagara Falls Power Company.

[2] Professor of hydraulic engineering, Technische Hochschule, München, Germany. Mem. A.S.M.E. Dr. Thoma was graduated from the Technical University at Munich, as a mechanical engineer, in 1906. From 1906 to 1908 he was employed as designer by the firm of Briegleb, Hansen & Co., of Gotha, manufacturers of water turbines, governors, etc. For the following two years he was associated with Prof. A. Föppl as assistant in technical mechanics. During this time he remained in touch with Briegleb, Hansen & Co., Gotha, and in 1910 became head of its governor department, remaining with the company for ten years. He became chief engineer of its turbine testing stations, as well as head of the governor department, in 1913. In 1915 he became superintendent of all work on designing water-power machinery and water-power plants. In 1920 Dr. Thoma was appointed professor of technical mechanics of the Technical University of Munich. He resigned in 1921 to become professor of hydraulics, and director of the Hydraulic Institute of the Technical University at München.

Contributed by the Hydraulics Division and presented at the Annual Meeting of The American Society of Mechanical Engineers, New York, N. Y., December 4 to 8, 1933.

[3] L. A. Ott, Mathematik Institut, Kempten, Germany.

tude of the water velocity. Because the velocity head is proportional to the square of the water velocity, meters do not indicate, with quickly changing velocities, the average water velocity but the square root of the average square of the velocities, which is always larger than the average velocity. Furthermore, instruments are not yet developed which register the necessary readings when measuring at many points. The pitot tube is, therefore, in general not so applicable as the Woltman current meter for measurements where great accuracy is required.

The accuracy of the total flow, obtained from measurements with current meters, may be assumed to be about 1 per cent when the test is carefully prepared and performed under favorable conditions, and values accurately computed. The most favorable condition exists when the turbulence of the flow does not exceed the turbulence unavoidable even in a straight conduit at velocities above the critical velocity. If the water flow, however, contains strong eddies which are produced, for instance, by bends or by contractions in an improperly made intake, larger errors are possible because even with current meters of suitable shape the disturbing influence of the side components will be too large.

In many cases it is quite impossible to find or to arrange a cross-section in which the flow is steady. Also, the required number of meters and the necessary care to obtain the desired accuracy are often obstacles. However, as the weir, the traveling screen, and other methods for measuring large quantities of water are generally very expensive, one has either to be contented with the lesser accuracy of the current-meter measurement or give up the measurement altogether.

For that reason, a sensation was caused about five years ago (the "salt-velocity method" by Allen was not known at that time) when the American engineer, Norman R. Gibson, presented a new water-measuring method which promised to fill all desires and required only a comparatively simple apparatus.

The Gibson Method of Flow Measurement

The Gibson method is applicable for measurements in closed conduits and is founded on the pressure rise which takes place in such conduits when the water flow is brought to rest. For example, in conducting a test, a steady continuous flow is maintained after which the turbine gates are gradually closed, the increased pressure in the conduit being continuously registered by a pressure-time recorder, designed by Gibson. The difference between the initial water flow and the leakage flow, which goes through the gates when they are closed, is obtained from the pressure diagram. The dimensions of the conduit must, of course, be known. Since the small leakage water loss can be determined with great accuracy by a special test, it is, therefore, possible to determine the water flow per second at the open steady position of the gates.

The rise in the pressure when closing the gates is a result of the retardation which is forced on the water column in the pipe. This depends fundamentally upon the magnitude of the momentum (the impulse) which this water column had at the start and at the end of the closing of the turbine gates. For a pipe with known dimensions, the sum of all momentum quantities of the water particles contained in the pipe, or, expressed in a shorter way, the magnitude of momentum contained in the pipe, is dependent only upon the flow of water per second through the pipe and absolutely independent of the accessory motions. A short calculation leads, therefore, to the presumption that the result from the pressure diagram must be absolutely independent of the accessory velocities, which for other methods might be very disturbing. The sensibility of the pressure-recording apparatus can be increased almost as one desires when requisite care is used in the design and construction of this single instrument. We might hope that we could obtain the water quantity from this very exact pressure diagram without any errors in accordance with the exact physical nature of the method. Then it would be possible to make water measurements for water-power plants with the same general precision as for tank measurements.

The purpose of this paper is to discuss these considerations in detail, to determine the limits of eventual errors, and to find out how to arrange for the measurement in order to minimize the errors.

With the expression "errors" I will, of course, not censure or in any way try to diminish the splendid merits of the man who invented and developed this important method. Neither will I express any doubts about the high efficiencies on the turbines which Gibson has found by using his method in several large American water-power plants. The results which have been obtained in Germany, in both water-power plants and in laboratories, show that Gibson's results are possible of attainment considering the immense size of the American turbines and the hydraulic demands for which careful consideration has been given in the design of all constructional parts in these power houses.

When deducing the general formulas we will neglect the action of gravity and the differences in the pressure that are added to the static-pressure difference corresponding to differences in heights. The introduction of these pressures in general formulas would only lead to unnecessary complexities. We neglect, also, the elasticity of water and of the walls of the pipe.

The water pipe which the water enters from a large reservoir may be supposed to be straight and of uniform cross-section. We use the following symbols: c_0 is the average velocity of the water for steady continuous flow in a cross-section of the pipe at the beginning of the test $= \dfrac{\text{the quantity of water per second}}{\text{area of the pipe}}$; c is the average velocity (in a cross-section) of the flow during the test; and c_1 is the average velocity of the water after the test, i.e., the average velocity of the water corresponding to the leakage. During the test, the pressure p_C in the measuring cross-section C, and the pressure p_A at point A sufficiently distant in the reservoir are registered. (In practical tests the pressure measurement at A is registered by recording the changes in the water level in the reservoir with a water-level gage.)

To understand the fundamental laws for the method, we at first neglect the friction. The velocity of the water is then the same everywhere in the pipe. Accessory velocities do not arise.

If B, Fig. 1, is a cross-section of the pipe close to the inlet where the water velocity is already uniform all over the section, the difference in pressure $p_A - p_B$ is almost completely determined by the instantaneous value of the water velocity in the pipe. As the distance is very short in which the water velocity rises from zero (in the reservoir) to the value c, the acceleration for each water particle, caused by the change in position, is great compared with the change in the water velocity for a fixed point due to the decrease in the water quantity per second in the pipe. The pressure difference $p_A - p_B$ may, therefore, be calculated without any noticeable errors as there should be a steady flow. Therefore, the following holds true

$$p_A - p_B = \gamma \frac{c^2}{2g} \qquad [1]$$

The mass between the cross-sections B and C is $\dfrac{\gamma f l}{g}$, where f is the cross-sectional area of the pipe; l is the distance $(B - C)$; and γ is the weight of a unit volume of water. For the acceleration the force, $f(p_B - p_C)$, is available. Using the fundamental dynamic law we get

$$f(p_B - p_C) = \frac{\gamma f l}{g}\frac{dc}{dt} \quad \text{[2]}$$

If we cancel f in Equation [2] and add Equation [1] we get the expression

$$p_A - p_C = \frac{\gamma}{g}\, l\, \frac{dc}{dt} + \gamma\, \frac{c^2}{2g}$$

We have now to take into consideration that the change in the water quantity on the way to the cross-section B also has some effect, and we do that by increasing the actual length l. If this corrected length is called L, we get

$$p_A - p_C = \frac{\gamma}{g} L \frac{dc}{dt} + \gamma \frac{c^2}{2g} \quad \text{[3]}$$

This is a differential equation of the first order with respect to c, which it is possible to integrate graphically or analytically when we have to take the changes in $p_A - p_C$ from the diagram obtained by the pressure recorder. One can, for instance, starting from the known water velocity c_1 corresponding to the leakage, reconstruct backward the changes in the water velocity and from that find the water velocity c_0 which was present at the start of the test.

In another method given by Gibson, the change in c is assumed and afterward corrected. This proceeding converges very fast and is very suitable for graphic integration which, of course, in this case is still more to be recommended because the change in $p_A - p_C$ is given graphically.

The chain of reasoning used to derive Equation [3] and on which also Gibson's deduction (1)[4] is founded, is not quite uninterrupted; when deducing Equation [1] it was assumed that the difference in pressure between the points A and B was as big as it should be at steady flow, but in reality there exists a non-stationary flow. There may be some doubt whether it is admissible to use the fundamental dynamic law without any correction on "the mass (existing) between the cross-sections B and C." The "mass" in that way defined does not contain the same individual parts at the end of the test as at the beginning. During the test, outgoing water, by passing the cross-section C, has left the "mass," and new water, by passing the cross-section B, has entered into the "mass." The dynamic fundamental equation refers, however, to a fixed system of mass always consisting of the same particles.

To remove all doubts we shall start from the general equation for the pressure conditions at unsteady flow without friction and eddies. Referring to Fig. 2, the following symbols will be used: x is the distance from one general point on the pipe axis to point A, v is the water velocity on the axis and on the expanded axis from the pipe, p is the pressure, and ϕ the velocity potential, which is defined so that at every instant and in every place $\frac{\delta\phi}{\delta x} = v$. The point A is supposed to lie on the expanded axis from the pipe and so far from the inlet that at this point the square of the velocity is negligible ($v_A^2 = 0$). The cross-section B is as close to the inlet as possible, but at such distance, that at every point of this section, the water velocity is equal to the pipe velocity c. The cross-section C is the measuring section. The values of v, p, and ϕ in A, B, and C will be designated by v_A, p_A, ϕ_A, v_B, p_B, etc., respectively.

The relation between v, p, and ϕ is given by the well-known general equation

$$\frac{\gamma}{g}\frac{\delta\phi}{\delta t} + \gamma\frac{v^2}{2g} = -p + \psi(t)$$

in which $\psi(t)$ is a function of the time alone (not of x) and depends on the way in which ϕ is chosen. To wit, ϕ being defined by $\frac{\delta\phi}{\delta x} = v$, only $\frac{\delta\phi}{\delta x}$ is prescribed for a given flow and any function of the time may be added. Therefore, we are at liberty to stipulate that during the whole test $\phi_A = 0$. In applying the general equation to the point A, we get

$$\frac{\gamma}{g}\frac{\delta\phi_A}{\delta t} + \gamma\frac{v_A^2}{2g} = -p_A + \psi(t)$$

Considering that $\phi_A = 0 =$ constant and therefore $\frac{\delta\phi_A}{\delta t} = 0$, and that $v_A^2 = 0$, we get from this $\psi(t) = p_A$. By introducing this, the general equation is transformed to

$$\frac{\gamma}{g}\frac{\delta\phi}{\delta t} + \gamma\frac{v^2}{2g} = p_A - p \quad \text{[4]}$$

First of all we now have to determine ϕ for the cross-section B. Considering that $\phi_A = 0$ and $\frac{\delta\phi}{\delta x} = v$ we get

$$\phi_B = \int_A^B v\, dx$$

In order to make the integration we express the velocity at any point of the axis between A and B as a fraction of the present pipe velocity c by the equation $v = \alpha c$. Then

$$\phi_B = c\int_A^B \alpha\, dx$$

The value of α for the point in the section B is 1. In order to compute $\int_A^B \alpha\, dx$, the values of α for a sufficient number of other points between A and B must be found. This is easily effected by drawing the streamlines, either by estimating or by one of the several well-known graphical methods. The values of α will be found by considering that α varies inversely as the areas of the cross-sections of the fluid tube confined by the streamlines adjacent to the axis. The integral $\int_A^B \alpha\, dx$ can then be computed. It has a length the dimension of which we will designate by l' and which may be considered as the reduced length of the inlet; which may be longer or shorter than the distance between the cross-section B and the reservoir wall, depending on the shape of the inlet. Therefore

$$\phi_B = l'c \quad \text{[5]}$$

The velocity potential in the measuring cross-section C results in

$$\phi_C = \phi_B + \int_B^C v\, dx = \phi + lc$$

and when considering Equation [5] we get

$$\phi_C = l'c + lc = Lc \quad \text{[6]}$$

By differentiating with respect to time from Equations [5] and [6]

$$\frac{\delta\phi_B}{\delta t} = l'\frac{dc}{dt} \quad \text{and} \quad \frac{\delta\phi_C}{\delta t} = L\frac{dc}{dt}$$

---

[4] Numbers in parentheses refer to similarly numbered references at the end of the report.

If we now at last combine these values with Equation [4] we get[5]

$$p_A - p_B = \frac{\gamma}{g} l' \frac{dc}{dt} + \gamma \frac{c^2}{2g} \ldots\ldots\ldots\ldots [7]$$

and

$$p_A - p_C = \frac{\gamma}{g} L \frac{dc}{dt} + \gamma \frac{c^2}{2g} \ldots\ldots\ldots\ldots [8]$$

The last equation is identical with Equation [3]. The considerations made at first, which theoretically were not quite indisputable, have given a correct result. This also shows that the suggestion given in the literature (2) to substitute the last term in Equation [3] by the expression $\frac{c_1^2}{2g} - \frac{(c_1 - c)^2}{2g}$ is entirely out of order.

We shall now study the method, considering friction. For the water-way from the reservoir to the section B, it is possible to use the considerations above for flow without friction, because the friction on the short distance to B, without doubt, may be neglected. In order to follow the conditions between B and C it is convenient to use the law of impulse and momentum. As we know, it is permitted to deal with the momentum which is contained in any space, and also with the momentum which enters or goes out from this space, in the same way as if the momentum were a material substance, which is carried along with the water and is produced or consumed by outside forces.

The momentum which is contained in the space between B and C is indicated by J. If i_B is the momentum which the inflowing water has supplied through the section B during any length of time, $\frac{di_B}{dt}$ is the impulse current through the section B. In the same way the impulse current through section C is signified by $\frac{di_C}{dt}$. From the law of impulse and momentum, it follows that the increase per second in momentum in the space between B and C is equal to the momentum supplied per second through B with the outgoing momentum through C deducted and with all external forces acting in the direction of flow added, i.e.,

$$\frac{dJ}{dt} = \frac{di_B}{dt} - \frac{di_C}{dt} + \Sigma P \ldots\ldots\ldots\ldots [9]$$

The next step is to determine J. Suppose dm is the mass of one small water particle, which has the length dx, the cross-section df, and the velocity v. The momentum for this small particle is $dm\, v$ and, because $dm = \frac{\gamma}{g}\, dx\, df$, it is also equal to $\frac{\gamma}{g}\, dx\, df\, v$. The momentum for all the water between the cross-sections on the distance dx from each other, therefore, is

$$dJ = \int \frac{\gamma}{g}\, dx\, df\, v = \frac{\gamma}{g}\, dx \int v\, df$$

[5] The method chosen here for the demonstrations has the advantage that it is also applicable to bent pipes. At the same time it shows that the length in a bend is not to be measured along the pipe axis but along the line in which the water velocity has the average speed. This line lies about $\frac{r^2}{4R}$ closer to the center of the bend than the pipe center line does (r = the radius of the pipe, R = the radius of the bend to the center line of the pipe) and is for that reason shorter. If one does not consider these things the length of the pipe will be used with too high a value and the water flow will be too little. The difference is, however, very small and it will cause (e.g., for the power plant at Queenston, where the pipe has two bends) an error in the water flow of only about —0.1 per cent.

Since $\int v\, df = cf$ it is possible also to write $dJ = \frac{\gamma}{g}\, cf\, dx$, from which the momentum of the water between B and C is

$$J = \frac{\gamma}{g} cf\, l \ldots\ldots\ldots\ldots [10]$$

which is dependent only on the average velocity and, therefore, also on the quantity of water per second. It is absolutely independent of the distribution and all accessory velocities.

Differentiating with respect to time we get from Equation [10]

$$\frac{dJ}{dt} = \frac{\gamma}{g} fl \frac{dc}{dt} \ldots\ldots\ldots\ldots [11]$$

It is also easy to express the impulse current through the cross-section B, because the friction has not yet been acting and the velocity is the same at all points. The inflowing mass per second is $\frac{\gamma}{g}\, cf$ and therefore the impulse current is

$$\frac{di_B}{dt} = \frac{\gamma}{g} fc^2 \ldots\ldots\ldots\ldots [12]$$

The impulse current through the cross-section C should, of course, be just as big if the distribution were uniform both in place and time. However, the flow is not uniform at that point on account of the friction. We can divide the instantaneous velocity v at any point in the cross-section into one component v_m which is the average value for the place in question and one component of oscillating velocity v'. This division is shown in Fig. 3, where the full line refers to the instantaneous value of the velocities and the broken line to the average value with respect to time. Accordingly, if we write

$$v = v_m + v' \ldots\ldots\ldots\ldots [13]$$

the value of momentum, which during the time dt is discharged through the element df in section C (mass per second times velocity) is equal to

$$\frac{\gamma}{g} (v_m + v')^2\, df$$

Further, if Δt is a short time interval which is large compared with the period for the fluctuations in v', but still short compared with the time during which the turbine gates are closing, we will obtain the value of momentum which during the time Δt is discharged through the cross-section element df as

$$\frac{\gamma}{g} \int_{(\Delta t)} (v_m + v')^2\, df$$

or as

$$\frac{\gamma}{g}\, df \int_{(\Delta t)} v_m^2\, dt + \frac{2\gamma}{g}\, df \int_{(\Delta t)} v_m v'\, dt + \frac{\gamma}{g}\, df \int v'^2\, dt$$

Because v is constant in the element of the cross-section considered, the first integral is equal to $v_m^2 \Delta t$. The second integral is zero, because v_m is constant and v' is the variation in the actual instantaneous velocity from the average value with respect to time so that $\int v' dt = 0$. The outgoing impulse during the time Δt through an element in the section is, therefore

$$\frac{\gamma}{g}\, \Delta t\, v_m^2\, df + \frac{\gamma}{g}\, df \int_{(\Delta t)} v'^2\, dt$$

Taking the sum for the whole cross-section, the outgoing impulse during the time t is

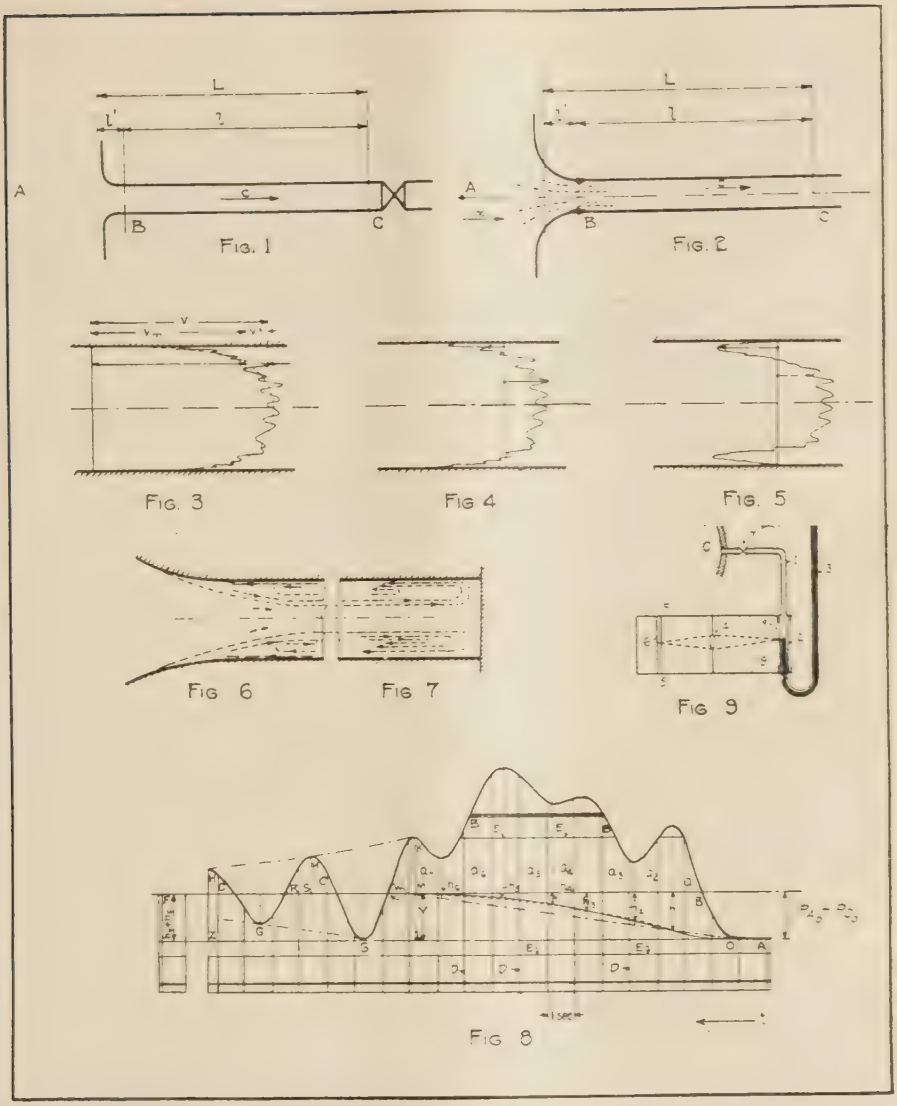

Fig. 1 Fig. 2 Fig. 3 Fig. 4 Fig. 5 Fig. 6 Fig. 7 Fig. 8 Fig. 9

$$\Delta i_c = \frac{\gamma}{g}\Delta t \int_{(f)} v_m^2\, df + \frac{\gamma}{g}\int_{(f)} df \int_{(\Delta t)} v'^2\, dt \ \ldots\ldots [14]$$

The second term on the right side we may consider as the product of $f\,\Delta t$ and one average value of the square of the variable velocity v' for the whole section, the average taken with respect both to time and place. If we use the symbol v_I^2 for this average value, Equation [14] takes the form

$$\Delta i_c = \frac{\gamma}{g}\,\Delta t \int_{(f)} v_m^2\, df + \frac{\gamma}{g}\,\Delta t\, f\, v_I^2 \ \ldots\ldots\ldots [15]$$

As the distinction between Δt and dt was necessary only for the definition of the average value v_I^2, it is now possible again to write dt instead of Δt and di_c instead of Δi_c. Equation [15] then takes the form

$$\frac{di_c}{dt} = \frac{\gamma}{g}\int_{(f)} v_m^2\, df + \frac{\gamma}{g} f v_I^2 \ \ldots\ldots\ldots\ldots [16]$$

For further simplification we presume

$$v_m = c - v'' \ \ldots\ldots\ldots\ldots\ldots\ldots\ldots [17]$$

where v'' is then the deviation of the average velocity with respect to time in the considered element of the cross-section from the average velocity in the whole cross-section. By substituting $v_m^2 = c^2 + 2cv'' + v''^2$ in Equation [16] we get

$$\frac{di_c}{dt} = \frac{\gamma}{g}\int_{(f)} c^2 df + \frac{2\gamma}{g}\int_{(f)} cv''\, df + \frac{\gamma}{g}\int_{(f)} v''^2\, df + \frac{\gamma}{g} f v_I^2 \ \ldots\ldots [18]$$

As c is constant, the first integral is simplified to $c^2 f$. The second integral is equal to zero because v'' is the variation from the average value c and, therefore, $\int_{(f)} v''\, df$ is zero. Finally, if we now use v_{II}^2 instead of the average value of the square of v'', i.e., $\int_{(f)} v''^2\, df = v_{II}^2 \cdot f$, Equation [18] takes the form

$$\frac{di_c}{dt} = \frac{\gamma}{g} f c^2 + \frac{\gamma}{g} f v_{II}^2 + \frac{\gamma}{g} f v_I^2 \ \ldots\ldots\ldots\ldots [19]$$

Substituting Equations [11], [12], and [19] in Equation [9] the first term of $\frac{di_c}{dt}$ is eliminated by $\frac{di_B}{dt}$ and

$$\frac{\gamma}{g} fl \frac{dc}{dt} = -\frac{\gamma}{g} fv_{II}^2 - \frac{\gamma}{g} fv_I^2 + \Sigma P$$

The forces acting on the water volume consist of (*a*), the force corresponding to the pressure difference between B and C, and (*b*), the force R caused by the friction on the pipe wall acting on the water opposite to the direction of flow. By substituting $\Sigma P = f(p_B - p_C) - R$, the equation above takes the form

$$\frac{\gamma}{g} fl \frac{dc}{dt} = -\frac{\gamma}{g} fv_{II}^2 - \frac{\gamma}{g} fv_I^2 + f(p_B - p_C) - R \quad \ldots . [20]$$

In order to make it possible to express $p_B - p_C$ by the observed pressure difference $p_A - p_C$ we have to eliminate $p_A - p_B$ in Equation [7]. Though when deducing Equation [7] we had assumed no friction acting, it is possible to use the equation for actual flow, as it is shown before, because the friction on the way from A to B hardly ever comes to action.

If we substitute

$$p_B - p_C = p_A - p_C - (p_A - p_B) = p_A - p_C - \frac{\gamma}{g} l' \frac{dc}{dt} - \gamma \frac{c^2}{2g}$$

in Equation [20] and again set $l + l' = L$, then it follows that

$$\frac{\gamma}{g} fL \frac{dc}{dt} = f(p_A - p_C) - \gamma f \frac{c^2}{2g} - \frac{\gamma}{g} f(v_{II}^2 + v_I^2) - R \quad . . [21]$$

In this expression R, besides v_{II}^2 and v_I^2, is not yet known. The simplest assumption which one can make for the action of the friction during the closing of the gates is that it is of the same magnitude as it should be at a continuous flow with the same quantity of water per second. This premise is also a fundamental point in Gibson's deduction. Because it is possible in this case to assume, with very sufficient accuracy, that the magnitude of the friction at constant flow is proportional to the square of the average water velocity, we therefore get

$$R = \frac{c^2}{c_0^2} R_0 \quad \ldots\ldots\ldots\ldots\ldots\ldots . [22]$$

where R_0 is the value at constant flow before the test. R_0 we can determine, considering Equation [21] $\left(\frac{dc}{dt} = 0\right)$ for the steady continuous conditions before the test, to be

$$R_0 = f(p_{A_0} - p_{C_0}) - \gamma f \frac{c_0^2}{2g} - \frac{\gamma}{g} f(v_{II_0}^2 + v_{I_0}^2) \quad \ldots . [23]$$

If we substitute the value of R, which is obtained from Equations [22] and [23] in Equation [21] and arrange in order, we get after a few calculations

$$-\frac{dc}{dt} = \frac{g}{\gamma L} \left[(p_C - p_A) + \frac{\gamma}{g}(v_{II}^2 + v_I^2) + \frac{c^2}{c_0^2} \left\{ (p_{A_0} - p_{C_0}) - \frac{\gamma}{g}(v_{II_0}^2 + v_{I_0}^2) \right\} \right] \quad \ldots\ldots [24]$$

The second term within the brackets indicates, for every instant of time, the influence of the accessory motions (existing at that instant). The last term, $\frac{\gamma}{g}(v_{II_0}^2 + v_{I_0}^2)$, takes care of the fact that the friction force, which at continuous steady flow is transmitted from the walls of the pipe to the water, would be judged too high, if the accessory motions were neglected.

If we neglect the accessory velocities, Equation [24] takes the form

$$-\frac{dc}{dt} = \frac{g}{\gamma L} \left[(p_C - p_A) + \frac{c^2}{c_0^2} (p_{A_0} - p_{C_0}) \right]$$

The valuation used by Gibson corresponds to this equation.

We could also get this equation if we supposed that v_{II}^2 and v_I^2 during the test decrease proportionally with c^2. The two last terms in Equation [24] should then balance each other. This assumption, however, would not be correct. We notice this very readily if we consider the case when the quantity of water per second is decreased rapidly from the value at the start to zero. All water particles are then for the same short time under the action of the same strong pressure gradient so that the velocity of each particle is subjected to a change by the same amount but not in the same proportion (Fig. 4). The values of v_{II} and v_I have then not changed during the sudden decrease in the water quantity to zero. If the closing time is longer, the action of the wall friction, which tries to keep hold of the back-flowing water, becomes active up to a marked distance from the wall so that the distribution of the water indicated in Fig. 5 exists after the closure. In any case the valuation $v_{II}^2 + v_I^2 = v_{II_0}^2 + v_{I_0}^2$ will come closer to the truth than the presumption given above. If we apply Equation [24] on a complete closure considering the time, we get with $\frac{dc}{dt} = 0$ and $c = 0$

$$p_C - p_A = -\frac{\gamma}{g}(v_{II}^2 + v_I^2)$$

In the measuring cross-section, therefore, a pressure below the normal will exist until the accessory motions have died out. (This does not appear in the diagrams published by Gibson on account of the strong natural period of oscillation in the mercury column.) One understands this action if one considers that the water in the pipe in spite of the decrease of the water-flow to zero has not come to rest. The core of the water column flows forward while an edge current runs backward. Although it is true that the impulse *contained* has become *zero* and remains at zero, that is not the case with the impulse *current* through the section; the measuring cross-section C sends water upward and receives returning water. Because the impulse contained in the pipe above the cross-section does not change any more, it is necessary that this impulse current be counter-balanced by a pressure below the normal in the measuring section.

Of course, these circumstances assist during the closure in keeping the pressure in the measuring section from increasing as much as it would without accessory motions. The blockade of the pressure takes place near the inlet, where the back-flowing water again turns; the back-flowing water at the walls cannot press itself into the reservoir with higher pressures. Therefore, it turns and forces a reduction in the cross-section of the fresh water entering from the reservoir with a corresponding increase in the velocity which affects the additional pressure drop. Fig. 6 indicates this action but it gives, of course, only an imperfect picture because it refers in reality to non-stationary conditions, which cannot be represented completely by drawing current lines, and also because our present means of description of hydraulic actions are not well suited to show the non-stationary conditions.

Also, there is at the lower end of the pipe, an alternation in the direction of flow. If we could measure the average pressure immediately in front of a slide, which shuts off the pipe, Fig. 7, the pressure would not be below normal.

Therefore, the hope that the Gibson method of water measurement (contrary to the methods mentioned above) is independent of accessory motions, is unfortunately unfulfilled. It, therefore, remains for us to determine the order of magnitude of the possible errors.

Because no information is published about the magnitude of v_1^2, one has to resort to an indirect estimation. It is known that in turbulent flow, measurements of the velocity with the pitot tube give, according to the foregoing reasons, a water velocity about 1 to 2 per cent too large. A simple calculation shows that the relative error in the velocity measurement is $\frac{v_1^2}{2v_m^2}$, where v_m is the average velocity at the point of measuring and v_1^2 is the average value of the square of the variable additional velocity varying with respect to time. Within the possible limits for the degree of accuracy required, it is permitted to use the average values in the measuring section (v_I and c) instead of v_1 and v_m. To avoid too large errors, we obtain for the beginning of a test run

$$v_{I0}^2 = 0.02\, c_0^2$$

if we cautiously state that the pitot-tube measurements give an error of 1 per cent.

Two methods can be used for the valuation of v_{II0}^2. On one hand, the known formulas for the water distribution in long, straight, smooth pipes, can be used, from which $v_{II0}^2 = 0.02\, c_0^2$. The conditions are then, however, judged too favorably because the turbine conduits hardly ever are as straight and smooth as the pipes with which the formulas for the water distribution were obtained in the laboratory and also because in most cases the flow is affected by dissymmetries, which are caused by an unsymmetrical inlet, and result in an increase in v_{II0}^2. For these reasons it is perhaps better to base our calculations on the known value α, which gives the proportion between the actual velocity energy flowing through a cross-section and the energy corresponding to the average water velocity. From present information, α ranges between 1.085 and 1.15. The impulse transported, on account of the irregularity in the distribution in the water velocity, is affected in the proportion of about 3 to 1 less than the energy transported. One can, therefore, presume $v_{II0}^2 = 0.028$ to $0.05\, c_0^2$ or, as an average, about $v_{II0}^2 = 0.04\, c_0^2$. Therefore

$$v_{II0}^2 + v_{I0}^2 = 0.06\, c_0^2$$

for the beginning of the experiment.

If we choose the afore-mentioned valuation

$$v_{II}^2 + v_I^2 = v_{II0}^2 + v_{I0}^2$$

and further suppose that c, during the observed time, decreases uniformly from c_0 to the end value zero, then in Equation [24], the expression

$$\frac{\gamma}{g}\,(v_{II}^2 + v_I^2) - \frac{c^2}{c_0^2}\,\frac{\gamma}{g}\,(v_{II0}^2 + v_{I0}^2)$$

(which may be considered as the term for the average error for the whole observed time) is equal to $\frac{2}{3}\frac{\gamma}{g}\, 0.06\, c_0^2$.

The circumstance that $v_{II}^2 + v_I^2$ does not stay quite invariable but instead lies between $v_{II0}^2 + v_{I0}^2$ and $\frac{c^2}{c_0^2}\,(v_{II0}^2 + v_{I0}^2)$ we take into account by decreasing the factor $\frac{2}{3}$ to $\frac{1}{3}$. By that we get the average value of the error as

$$0.02\,\frac{\gamma}{g}\,c_0^2 = 0.04\gamma\,\frac{c_0^2}{2g}$$

From the pressure diagram published by Gibson, it is not possible to get $\frac{c_0^2}{2g}$, because from the diagrams the resulting value of $\frac{p_{A0} - p_{C0}}{\gamma}$ is composed of the velocity head and the friction-loss head. In one numerical example given by Gibson, which refers to a pressure diagram not reproduced here, there is a note from which it appears that two thirds of $\frac{p_{A0} - p_{C0}}{\gamma}$ belongs to the velocity head and one-third to the friction-loss head. If we suppose that this proportion exists also for Gibson's pressure diagram (3) reproduced in Fig. 8, it follows that the error in the result for this pressure diagram, caused by the term for the error, is —1.5 per cent, while the error for the diagram in the numerical example is —0.9 per cent. The true water quantities should for that reason have been about 1.5 per cent and 0.9 per cent greater, respectively, than given by Gibson.

However, Gibson reports errors averaging +0.1 per cent from tests made on his method in the hydraulic laboratory at Cornell University. During the tests, the actual quantity of water was determined by the only indisputable method, measuring by means of a calibrated tank.

Therefore, there must be other sources of errors, which act in the opposite direction. In reality, the assumption made when deducing Equation [24], that the friction during the closing is just as great as at continuous steady flow with the same amount of water, Equation [22], is not quite true. If, for instance, the condition after complete stoppage of the water flow is considered, the friction according to this supposition should be zero. In reality, however, a downward directed friction force is carried over on the water from the pipe wall which touches the backflowing edge current. This condition is also active during the flow, and decreases the value of friction below the amount which should be present for equal quantities of water at steady flow.

If the errors which are made by this valuation of the friction are estimated to be between $\frac{1}{20}$ and $\frac{1}{10}$ of the friction at continuous flow at the beginning of the measurement, the result obtained from the pressure diagram, Fig. 8, would then be affected with an error from +0.9 to +1.8 per cent for this reason, and the pressure diagram in the numerical example with an error from +0.6 to +1.1 per cent.

It must be taken into consideration that the statements for the errors are founded on very rough estimates. Thus it is possible as a final outcome to say only that, when calculating the results from the diagrams given by Gibson, two opposite acting errors arise, of which the first has an order of magnitude of —1 per cent, and the second +1 per cent.

One more objection, which, however, does not refer to Gibson's method, itself, but to the calculation of the results from the measurements, is connected with the apparatus used by Gibson for recording the pressure diagram. This objection, therefore, has to be taken into closer consideration. The main parts of the pressure-recording apparatus are shown in Fig. 9. The glass tube 2 is connected through the water-filled tube 1 to the conduit at the measuring cross-section C; the lower end of the glass tube is connected by a U-tube to the smaller riser pipe 3. The riser pipe and the glass tube are filled with mercury as illustrated in the figure. The pressure fluctuations in the measuring section cause oscillations in the mercury column which are recorded photographically by illuminating the glass tube from the right. The lens 4 casts through the narrow vertical slot 5–5, an image of the mercury column on the photographic film 6 which is moved in a horizontal direction by a clock-work mechanism. A cord pendulum, not shown in the figure, covers the slot for a short time during each second and in that way marks the seconds on the film.

This arrangement has considerable experimental advantages

because, on one hand, only friction from fluid exists and because, on the other hand, the instrument can be calibrated easily before each test. Calibration is accomplished by adjusting different pressures in the tube, 1, by means of the valve 7, the pressures being measured by determining the difference in height between the levels of the mercury columns, which are photographically recorded. The pictures of two fine wires, 8 and 9, which are stretched across the glass tube, serve as marks for the measurements and consequently one is independent of accidental displacements of the film in a vertical direction.

Although this arrangement has great experimental advantages it also has the disadvantage of having a long natural period of oscillation. Consequently, the instrument does not show the instantaneous value of the pressure in the measuring section. It also oscillates a long time after the turbine gates are completely closed. To separate the influence of the oscillations which occur after closure, Gibson first determines the point at which the recorded pressure line runs into the line for the damped oscillations which remain after entirely closing the gates. The point k in Fig. 8, indicates the time when the gates reached the closed position. Gibson now considers, as the end of the authoritative pressure diagram for the calculations, the time at which the line for the damped oscillations first reaches a maximum or minimum; the position of this maximum or minimum is thereby exactly determined by a small additional calculation. One might now ask if this determination of the end position of the diagram causes errors. Of the terms standing on the right side in the equation for $\frac{dc}{dt}$, Equation [24], the first one predominates. For that reason, it is of great importance to take correctly from the diagram the time integral of the pressure difference or the time integral of the pressure in the measuring section, because the pressure in the inlet changes very little and furthermore is recorded by an independent apparatus. If the motion of the mercury column should take place without friction, the stipulations selected by Gibson for the limits of the diagram should correspond to the real facts; the impulse in the mercury column is zero at the end as well as at the start of the observation, because at both times it is at rest and, therefore, the content of the diagram surface corresponds to the time integral of the pressure in the measuring section. When, however, in reality the fluid friction of the motion of the mercury column has to be overcome, there is also impulse absorbed by the friction force during the observation. When, as in this case, it is permitted to consider the friction proportional to the velocity of the mercury column, it is easily shown that the total impulse absorbed by the friction is dependent only on the difference in the pressure at the beginning and at the end of the observation.

In order to prove this specifically, we simply indicate with p the pressure in the measuring section and with p', the pressure recorded by the apparatus. The error in the result, which is obtained if one takes into consideration only the predominating first term in Equation [24], is

$$\Delta c = \frac{g}{\gamma L}\left(\int p\, dt - \int p'\, dt\right)$$

It is possible to write the equation for the motion of the mercury column in the following form

$$a\frac{d^2p'}{dt^2} + k\frac{dp'}{dt} + p' = p \qquad [25]$$

where a is a coefficient depending on the mass of the mercury column, its cross-section, etc., and k is a friction coefficient which we might consider constant at deflections which are not too large. By integrating Equation [25] once for the time between the beginning (index 0) and the end (index 1) of the observation:

$$a\left[\left(\frac{dp'}{dt}\right)_1 - \left(\frac{dp'}{dt}\right)_0\right] + k\,(p_1' - p_0') + \int_{t_0}^{t_1} p'\, dt = \int_{t_0}^{t_1} p dt$$

In this expression the first term is zero because the mercury column is at rest at the beginning and at the end of the observation. The third term on the left side is the time integral for the pressure diagram which, therefore, is too small by the amount $k(p_1' - p_0')$. It is possible to calculate the heretofore unknown constant k from two quantities which we can take from the diagrams, namely the time T for the natural period of the apparatus and the proportion ψ, in which each deflection of the damped oscillation stands to the following deflection on the same side. If one indicates the (almost) constant pressure, which appears after complete closing of the gates by p_2, the general solution of Equation [25] results in

$$p' = p_2 + e^{-\frac{k}{2a}t}\left[A \sin\sqrt{\frac{1}{a} - \frac{k^2}{4a^2}}\; t + B\cos\sqrt{\frac{1}{a} - \frac{k^2}{4a^2}}\; t\right]$$

and, after some calculations the expression

$$k = \frac{T \log_e \psi}{2\pi^2 + \frac{(\log_e \psi)^2}{2}}$$

The second term in the denominator one can neglect for the values of ψ here occurring. The time integral of the pressure difference according to this is too small by an amount of

$$\frac{T \log_e \psi}{2\pi^2}(p_1' - p_0')$$

$p_1' - p_0'$ we can read from the diagrams, but no unit for measuring is given. One can, nevertheless, give the proportional error in the quantity of water.

From the first diagram (Fig. 8) $\psi = 1.54$, $T = 3.8$ sec, and the error in the water quantity = —0.83 per cent.

For the second diagram (numerical example, Gibson's Fig. 10) $\psi = 1.57$, $T = 4.0$ sec, and the error in the water quantity = —0.62 per cent.

The true quantity of water has in both cases been greater than it was calculated to be according to these values. In both diagrams the first extreme value of the recorded pressure which appears after the complete closing of the gates is a maximum. If the first recorded extreme value should have been a minimum the error should have been positive and, concerning the amount, much smaller. From Gibson's publications in which the calculations of the test on the method at Cornell University appear, it is not possible to see in which direction the error has been acting.

In the deductions above it was presumed that only the time integral of the recorded pressure was of any importance, corresponding to the excluding of the three last terms in Equation [24]. Of these, the two last ones are very small correction terms, but the term $\frac{c^2}{c_0^2}(p_{A0} - p_{e0})$ is worthy of consideration.

It is now easy to understand that an error is added by the inertia of the mercury column which tends to increase apparently the quantity of water; at the beginning of the observation the recorded pressure stays below the real pressure and this causes the water velocity at the beginning and, therefore, also the abovementioned term to be judged too great. It is not possible to determine the value of this latter error as exactly as the errors covered before. To get some idea of the valuation, the condition for the recording apparatus was calculated, presuming the simple case that $\frac{dc}{dt}$ is constant during the observation. By this it was

shown that the relative error in the quantity of water calculated according to Gibson's direction, is

$$+\frac{1}{2\pi^2}\left(\frac{T}{T_s}\right)^2\frac{p_{A_0}-p_{C_0}}{p_m}$$

where T is the time for the natural period of the apparatus, T_s is the time for closing the gates and p_m is the average value of

$$p_C - p_A + \frac{c^2}{c_0^2}(p_{A_0} - p_{C_0})$$

during the observation. Of course, the retardation of the water velocity during the observation is in reality not uniform, but nevertheless it is possible to use the above formula to determine the magnitude of the errors.

By the formula, it follows, for the first diagram Fig. 8, that the error in the water quantity = +0.3 per cent. For the second diagram (numerical example, Gibson's Fig. 10) the error in water quantity = +0.09 per cent. These are, therefore, unimportant and disappear compared with the other errors.

To sum up, it can be said the four sources of errors have been ascertained to be:

		Order of magnitude, per cent
1	Error due to accessory motions	—1
2	Error through false valuation of friction	+1
3	Error through friction of the mercury column	—0.5 to —1
4	Error through inertia of the mercury column	+0.1 to +0.3

Besides these sources of error (as in every method) there are still others such as those caused by lack of precision of instruments, errors in measurement of the pipe line, inaccuracies in evaluation, etc. These errors, however, may with sufficient care be reduced to insignificant magnitude and need not be separately treated here since they affect every water measurement in a similar manner.

Of the above four errors it is possible to eliminate the third one in the calculations of the result. The fourth is so insignificant that a rough valuation is sufficient. The errors Nos. 1 and 2 are determinative in fixing the accuracy of the measurement. But these errors, also, are small so that one might well say in drawing a conclusion regarding the Gibson measurement in its existing form, that the accuracy under favorable circumstances is approximately equal to the aforementioned current-meter measurements taken with great care under favorable circumstances.

For the review of the specified magnitude of errors it should be noted that they are drawn only from the diagrams published by Gibson and furthermore that in the evaluation of error No. 1 it has been assumed that the stream is as smooth as can be practically attained in a straight pipe. In case, however, the measurement section lies behind a bend as occasionally appears to have been the case (e.g., at the Queenston Plant, denoted by Gibson as a typical plant) greater amounts of error No. 1 have to be reckoned with. When, for example, one-tenth of the measured cross-section is taken up by the dead water area adjoining a bend, v_{II}^2 increases $\frac{1}{9}$, i.e., from about 0.04 to 0.15. A measurement section with smooth current is desired for the Gibson water measurement method even as for the current-meter measurement. For the test at Cornell University, the measuring section lay in a long straight stretch; the conditions in this respect were also particularly favorable.

On the other hand it must not be forgotten that the Gibson method looks back on only a brief period of development and that improvements are possible which must be founded on experiments. Through tests in a single experimental laboratory certainly no judgment can be attained of the expected accuracy under other conditions, because it remains indeterminate in what way the opposing errors have neutralized one another. One should seek to separate the individual errors. This can be done in various ways. If, for example, under otherwise permanent conditions, the length L be increased, error No. 1 is increased to a lesser degree than error No. 2 (the magnitude of the accessory motions will not increase after L has exceeded a definite value depending upon the pipe diameter). On the other hand, one may isolate error No. 2 if the pressure difference between two points on the pipe is used instead of the pressure difference between the measured section and the reservoir. (This method of water measurement has already been applied by Mr. Gibson.) If we have for the first measuring section a sufficiently long straight "runway" and, back of the second measuring section, a sufficiently long outlet stretch (because of the back current) then the accessory motions are of the same magnitude in both sections and their influence on the pressure disappears. In present plants these conditions can only seldom be attained. We can, however, attain them in a special experimental installation. Also the influence of a bend in front of the measuring cross-section, the disturbance due to too close proximity to the outlet, and other conditions can only be determined in an experimental installation. In contrast to the present conditions where only a rough valuation of the magnitude of the errors is possible, one will then be able to give the corrections which must be applied to cancel the error in the final results. Since the errors are not large in themselves, no very great relative accuracy in such corrections is necessary.

One must not be startled by the considerable work which will be necessary for the attainment of this perfection. Even for such simple measuring apparatus as, for example, the scale, or the compass being affected by the ship's movements, it was necessary to do an exceedingly great amount of work in the theoretical and also in the practical field in order to attain present-day perfection. One must not expect that it will be different with the new water-measuring method. Furthermore, sufficient incentive for work is not lacking here. The Gibson method has in many cases great practical advantages over other methods; it also makes possible a measurement under conditions where the other methods could not be applied. Therefore, we should strive for a further step in accuracy since the most exact measurements are of the highest importance to the technical advancement of water-turbine construction as a supplement to, and check of, experiments in experimental laboratories.

References

(1) "The Gibson Method and Apparatus for Measuring the Flow of Water in Closed Conduits," by N. R. Gibson, Trans. A.S.M.E., 1923, vol. 45, p. 343.

(2) *Zeit. V.D.I.*, 1924, p. 366.

(3) "The Gibson Method and Apparatus for Measuring the Flow of Water in Closed Conduits," by N. R. Gibson, Trans. A.S.M.E., 1923, vol. 45, Fig. 8, p. 362.

Experimental and Practical Experience With the Gibson Method of Water Measurement

A Discussion of Prof. D. Thoma's Paper on "The Degree of Accuracy of the Gibson Method of Water Measurement (1)

By N. R. GIBSON[1] and E. B. STROWGER[2], NIAGARA FALLS, N. Y.

The Gibson method is based on the equation of impulse and momentum applied to an enclosed column of water in motion. It is applicable in testing hydraulic power plants where the turbine is supplied with water through a closed conduit and means, such as turbine gates, are available for interrupting the flow of the water. To apply the method, it is necessary to obtain pressure-time diagrams, which show the changes with respect to time that occur in the conduit during and after the closure of the turbine gates. There are two kinds of diagrams: (*a*) simple diagrams, in which the changes of pressure at one point in the conduit are recorded, and (*b*) differential diagrams, in which the difference between the changes of pressure at two points in the conduit are recorded.

Professor Thoma (1)[3] has discussed quite thoroughly, in an accompanying paper (Trans. A.S.M.E., 1935, HYD-57-4), the conditions of water flow which may affect the degree of accuracy of the Gibson method of water measurement, when using the simple application method. In general, he has considered four errors due to (No. 1) accessory motions, or extra currents due to turbulence, (No. 2) false valuation of the friction in the conduit during closure, (No. 3) friction of the mercury column, and (No. 4) the inertia of the mercury column.

In discussing the Thoma article, the authors have first given a somewhat more detailed proof of the fundamental equation applying to the method and have supplemented the derivation with a graphical representation of the terms of the equation on the diagram itself. Test results on a long pipe are shown where both kinds of diagrams were taken and where the agreement between the two sets of diagrams is within 0.2 per cent. The test results are discussed and a detailed study is made of the effects of the four errors.

The authors conclude that the residual error is probably within the limits of precision possible when large quantities of water are being measured.

THE Gibson method is based on the equation of impulse and momentum applied to an enclosed column of water in motion. It is applicable in testing hydraulic power plants where the turbine is supplied with water through a closed conduit and means, such as turbine gates, are available for interrupting the flow of the water. To apply the method, it is necessary to obtain pressure-time diagrams, which show the changes of pressure with respect to time that occur in the conduit during and after the closure of the turbine gates. There are two kinds of diagrams:

Simple diagrams—in which the changes of pressure at one point in the conduit are recorded

Differential diagrams—in which the difference between the changes of pressure at two points in the conduit are recorded.

Prof. Thoma's Conclusions

Prof. Thoma has discussed quite thoroughly the conditions of water flow which may affect the degree of accuracy of the Gibson method of water measurement when using the "simple" application of the method. In general, he has considered and enumerated four errors due to (No. 1) accessory motions or extra currents due to turbulence, (No. 2) false valuation of friction in the conduit during the closure, (No. 3) friction of the mercury column, and (No. 4) the inertia of the mercury column. The first two are regarded as about 1 per cent in magnitude and are negative and positive, respectively. The last two are of opposite sign also, but are of the order of 0.5 of 1 per cent. Under favorable conditions, Prof. Thoma regards the accuracy of current-

[1] Vice-President and Chief Engineer, The Niagara Falls Power Company, Niagara Falls, N. Y. Mem. A.S.M.E. Mr. Gibson was graduated from the University of Toronto with the degree of B.A.Sc. in 1904. His professional career includes engagements with the Ontario Power Company of Niagara Falls, the firm of Smith, Kerry & Chace, Consulting Engineers, and The Niagara Falls Power Company. He became vice-president and chief engineer of the latter company in 1926. After the merger of this company with others, he was appointed vice-president and chief engineer of the Buffalo, Niagara, and Eastern Power Corporation in 1929 and vice-president of Niagara Hudson Power Corporation in 1931. In 1930, Mr. Gibson was awarded the Elliott Cresson Gold Medal by the Franklin Institute, Philadelphia, for his invention of the Gibson Method and Apparatus for measuring the flow of fluids in closed conduits. In 1931, he received an honorary degree, D.Eng., from the University of Toronto.

[2] Hydraulic Engineer, The Niagara Falls Power Company, Niagara Falls, N. Y. Mem. A.S.M.E. Mr. Strowger was graduated from the University of Rochester in 1918 with the degree of B.S. in Mechanical engineering. He was employed from 1918 to 1919 by the Interlake Engineering Company of Cleveland, Ohio, and in 1919 became connected with the Niagara Falls Power as draftsman and designer. In 1928, he became assistant hydraulic engineer of The Niagara Falls Power Company and in 1929 became associated with the engineering staff of the Buffalo, Niagara, and Eastern Power Corporation.

[3] Numbers in parentheses refer to similarly numbered references at the end of this paper.

Contributed by the Hydraulics Division and presented at the Annual Meeting of The American Society of Mechanical Engineers, December 4 to 8, 1933, New York, N. Y.

meter measurements as about 1 per cent, so that he concludes as follows:

> Of the above four errors, it is possible to eliminate the third one in the calculations of the result. The fourth is so insignificant that a rough valuation is sufficient. Errors Nos. 1 and 2 are determinative in fixing the accuracy of the measurement. But these errors also are small so that one might truly say in forming a conclusion regarding the Gibson measurement in its existing form that the accuracy under favorable circumstances is approximately equal to the aforementioned current-meter measurements taken with great care under favorable circumstances.

Friction Neglected

In the following discussion the equations given, when identical with those of Prof. Thoma, will have the same number assigned to them as those in the Thoma article. First neglecting friction, the velocity of the water in the pipe is uniform and no accessory motions arise.

Considering Fig. 1, if A is a point sufficiently distant in the reservoir, then it can be readily shown that the supernormal pressure existing at any point C in the conduit caused by a retardation forced on the water column is given by

$$p_A - p_C = \frac{\gamma}{g} L \frac{dc}{dt} + \gamma \frac{c^2}{2g} \quad \ldots\ldots [3]$$

where c is the velocity in the conduit, γ the weight of a unit volume of water, and L is the "equivalent length" of the water conduit. If B is a point near the inlet where the pipe section is typical and if we draw the stream line going through A and designate by u the velocity at any point of the stream line, then the equivalent length to point B is l' and may be found from

$$\frac{1}{c}\int_A^B u\, dx = l' \quad \ldots\ldots [3a]$$

where dx is a small length.

Prof. Thoma points out that Equation [3] is the fundamental equation for pressure at section C neglecting friction and accessory motions. He then shows that this is the pressure recorded by the Gibson apparatus if no friction or accessory motions exist and concludes therefrom that with no accessory motions and with no friction the Gibson method is rigidly correct. The inertia of the mercury and the friction of the mercury in the U-tube in the Gibson apparatus will be considered later on and it will be shown that they have only a small influence upon the measurement. The following is a demonstration of Prof. Thoma's rigorous proof of the Gibson method. Let us designate A as a point on the extended axis of the pipe as shown in Fig. 2, ϕ as a measure of velocity potential expressed as $\frac{\delta\phi}{\delta x} = v$ or $\phi = \int v\, \delta x$, p, as before, the pressure at any point, and dt any small interval of time during the closure, then

$$\frac{\gamma}{g}\frac{\delta\phi}{\delta t} + \gamma \frac{v^2}{2g} = p_A - p \quad \ldots\ldots [4]$$

The velocity potential at B may be written

$$\phi_B = \int_A^B V\, dx = l'c \quad \ldots\ldots [5]$$

and that at C is

$$\phi_C = \phi_B + \int_B^C V\, dx = \phi_B + lc = l'c + lc = Lc \ldots [6]$$

Then

$$\frac{\delta\phi_B}{\delta t} = l'\frac{dc}{dt} \quad \text{and} \quad \frac{\delta\phi_C}{\delta t} = L\frac{dc}{dt}$$

Substituting in [4], we get

$$p_A - p_B = \frac{\gamma}{g} l' \frac{dc}{dt} + \gamma \frac{c^2}{2g} \quad \ldots\ldots [7]$$

and

$$p_A - p_C = \frac{\gamma}{g} L \frac{dc}{dt} + \gamma \frac{c^2}{2g} \quad \ldots\ldots [8]$$

This equation is identical with Equation [3], whence the foregoing conclusion.

Graphical Explanation of Equations [3] and [4]

Fig. 3 shows graphically the equality expressed in Equations [3] and [4] neglecting accessory motions and friction and using a diagram made by a gage having zero inertia and zero friction.

Accessory Components of Velocity and Friction Considered

Now considering friction and the accompanying accessory components of velocity or "accessory motions," Prof. Thoma shows that the Gibson method, as applied by the use of the simple diagram, is not entirely independent of these motions. We may designate the value of momentum contained in the space between B and C as J, and we may define i_B as the value of momentum supplied from $t = 0$ to $t = t$ through section B by the inflowing water, and i_C similarly as the value of momentum which has gone out through section C from $t = 0$ to $t = t$. If we coin a new term for the first derivative of i_B with respect to time and call this derivative the "impulse current" through section B, then the impulse current is the momentum gained or lost per second and has, therefore, the dimension of a force. The increase per second in the value of momentum contained in the space between B and C is equal to the value of momentum supplied per second through B with the value of momentum through C deducted and with all external forces acting in the direction of flow added. This is expressed as follows

$$\frac{dJ}{dt} = \frac{di_B}{dt} - \frac{di_C}{dt} + \Sigma p \quad \ldots\ldots [9]$$

To determine J, we must integrate the expression for the momentum of a small particle of mass. This may be expressed as

$$dm\, V = \frac{\gamma}{g} dx\, df\, V$$

Then

$$dJ = \int \frac{\gamma}{g} dx\, df\, V = \frac{\gamma}{g} dx \int V\, df$$

But

$$\int V\, df = cf$$

so that

$$dJ = \frac{\gamma}{g} cf\, dx$$

and

$$J = \frac{\gamma}{g} cfl \quad \ldots\ldots [10]$$

where f is the cross-sectional area of the conduit. The momentum contained between B and C depends only upon the quantity of water flowing per second and is independent of the distribution and side components of flow. By taking the first derivative of

Equation [10], we get an expression for the left-hand side of Equation [9]

$$\frac{dJ}{dt} = \frac{\gamma}{g} fl \frac{dc}{dt} \ldots\ldots\ldots\ldots\ldots\ldots [11]$$

The impulse current through section B is $\frac{di_B}{dt}$ which equals the product of mass per second by velocity because in this section all particles have the same velocity c

$$\frac{di_B}{dt} = \frac{\gamma}{g} cf\, c = \frac{\gamma}{g} fc^2 \ldots\ldots\ldots\ldots\ldots [12]$$

To get an expression for $\frac{di_C}{dt}$ in Equation [9], consider Fig. 4. The flow is not uniform with respect to both time and cross-section. The instantaneous velocity at any point in the section is v. Prof. Thoma divided this instantaneous velocity into two components, v_m the average value of velocity for the point in question, and v' the component of oscillating velocity. The full line in Fig. 4 refers to the instantaneous values of velocity and the broken line to the average value with respect to time.

$$v = v_m + v' \ldots\ldots\ldots\ldots\ldots\ldots [13]$$

The value of momentum discharged through the element df in section C in the time dt is

$$\frac{\gamma}{g} (v_m + v')^2 \, df \, dt$$

Taking a short interval of time Δt, then this expression for the element becomes

$$\frac{\gamma}{g} \int_{\Delta t} (v_m + v')^2 \, df \, dt$$

or

$$df \frac{\gamma}{g} \int_{\Delta t} v_m^2 \, dt + \frac{2\gamma}{g} df \int_{\Delta t} v_m v' \, dt + \frac{\gamma}{g} df \int_{\Delta t} v'^2 \, dt$$

The first integral is equal to $v_m^2 \; \Delta t$, the second is zero since v_m is a constant and $\int v' \, dt = 0$. The expression for the outgoing impulse then becomes

$$\frac{\gamma}{g} \Delta t \, v_m^2 \, df + \frac{\gamma}{g} df \int_{\Delta t} v'^2 \, dt$$

For the whole cross-section Δic becomes

$$\Delta ic = \frac{\gamma}{g} \Delta t \int_f v_m^2 \, df + \frac{\gamma}{g} \int_f df \int_{\Delta t} v'^2 dt \ldots\ldots [14]$$

If we use the symbol V_{I}^2 as the average value, for the whole cross-section, of the square of the variable velocity v' with respect to both time and cross-section, then we may write

$$\Delta i_C = \frac{\gamma}{g} \Delta t \int_f v_m^2 \, df + \frac{\gamma}{g} \Delta t \, f \, V_{\mathrm{I}}^2 \ldots\ldots\ldots [15]$$

Changing Δt to dt since the distinction was made in order to define v_{I}, Equation [15] becomes

$$\frac{dic}{dt} = \frac{\gamma}{g} \int_f v_m^2 \, df + \frac{\gamma}{g} f V_{\mathrm{I}}^2 \ldots\ldots\ldots\ldots [16]$$

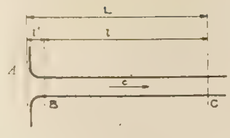

Fig. 1
(Thoma's Figure 1.)

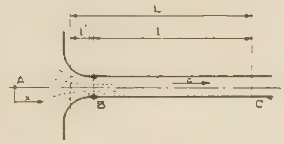

Fig. 2
(Thoma's Figure 2.)

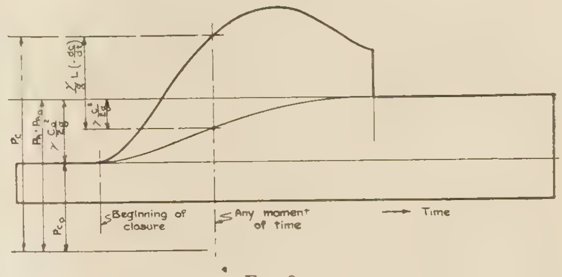

Fig. 3

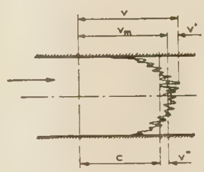

Fig. 4
(Thoma's Figure 3.)

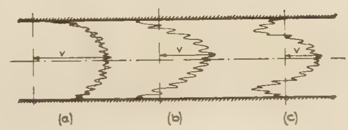

Fig. 5
(Thoma's Figures 4 and 5.)

For further simplification we may take

$$v_m = c + v'' \ldots\ldots\ldots\ldots\ldots\ldots [17]$$

where v'' is the deviation of the *average* velocity with respect to time in the *element* considered, from the *average* velocity in the whole cross-section. This relation is shown graphically in Fig. 4. Equation [16] then becomes

$$\frac{dic}{dt} = \frac{\gamma}{g} \int_f c^2 df + \frac{2\gamma}{g} \int_f cv'' \, df + \frac{\gamma}{g} \int_f v'' \, df + \frac{\gamma}{g} f \, V_{\mathrm{I}}^2 . \; [18]$$

The first integral becomes $c^2 f$, the second is equal to zero since $\int_f v'' \, df$ is zero. Equation [18] then becomes

$$\frac{dic}{dt} = \frac{\gamma}{g} fc^2 + \frac{\gamma}{g} f \, V_{\mathrm{II}}^2 + \frac{\gamma}{g} f \, V_{\mathrm{I}}^2 \ldots\ldots\ldots [19]$$

Where V_{II}^2 is the average value of the square of v'' over the cross-section.

We now have expressions for $\frac{dJ}{dt}$, $\frac{di_B}{dt}$, and $\frac{dic}{dt}$ which may be substituted in Equation [9]. If this is done, we get

$$\frac{\gamma}{g} fl \frac{dc}{dt} = -\frac{\gamma}{g} f \, V_{\mathrm{II}}^2 - \frac{\gamma}{g} f \, V_{\mathrm{I}}^2 + \Sigma P$$

Since the forces ΣP acting on the water column consist of the pressure difference between B and C and the force R caused by friction, then $\Sigma P = f(p_B - p_C) - R$ and we may write

$$\frac{\gamma}{g} fl \frac{dc}{dt} = -\frac{\gamma}{g} f \, V_{\mathrm{II}}^2 - \frac{\gamma}{g} f \, V_{\mathrm{I}}^2 + f(p_B - p_C) - R \ldots [20]$$

Since the friction on the way to section B may be neglected we

may use Equation [7] to eliminate $(p_B - p_C)$ from Equation [20] as follows, remembering that $l + l' = L$

$$p_B - p_C = (p_A - p_C) - (p_A - p_B) = p_A - p_C - \frac{\gamma}{g} l' \frac{dc}{dt} - \frac{\gamma c^2}{2g}$$

and then

$$\frac{\gamma}{g} f L \frac{dc}{dt} = f(p_A - p_C) - \frac{\gamma f c^2}{2g} - \frac{\gamma}{g} f (V_{II}^2 + V_I^2) - R \quad [21]$$

To evaluate R, it is assumed that during the closing of the turbine gates the friction is the same as it should be at a continuous flow with the same quantity of water per second. The friction is proportional to the square of the average velocity so that

$$R = \frac{c^2}{c_0^2} R_0 \quad [22]$$

where R_0 is the initial value of R immediately before the test and similarly c_0 is the initial velocity. When $R = R_0$, then $\frac{dc}{dt} = 0$, so that

$$R_0 = f(p_{A_0} - p_{C_0}) - \gamma f \frac{c_0^2}{2g} - \frac{\gamma}{g} f (V_{II_0}^2 + V_{I_0}^2) \quad [23]$$

The first item of the right member represents the initial difference in pressure between A and C, the second, the initial velocity head pressure, and the third represents the amount by which the actual friction is smaller than would be found if the accessory velocities were neglected. This is evident when Bernoulli's equation is written for the two points in question, using the average velocity c only. Substituting the value of R obtained from Equations [22] and [23] in Equation [21] we get

$$-\frac{dc}{dt} = \frac{g}{\gamma L}\left[(p_C - p_A) + \frac{c^2}{c_0^2}(p_{A_0} - p_{C_0}) + \frac{\gamma}{g}(V_{II}^2 + V_I^2) - \frac{c^2}{c_0^2}\frac{\gamma}{g}(V_{II_0}^2 + V_{I_0}^2)\right] \quad [24]$$

In this equation, the third item on the right, $\frac{\gamma}{g}(V_{II}^2 + V_I^2)$, indicates for every interval of time the influence of the accessory velocities on the force available for the retardation $-\frac{dc}{dt}$ and the fourth term, $\frac{c^2}{c_0^2}\frac{\gamma}{g}(V_{II_0}^2 + V_{I_0}^2)$, corresponds to the decrease from the value of friction at continuous *steady* flow.

If accessory velocities or accessory motions be neglected, then Equation [24] becomes

$$-\frac{dc}{dt} = \frac{g}{\gamma L}\left[(p_C - p_A) + \frac{c^2}{c_0^2}(p_{A_0} - p_{C_0})\right]$$

which expresses the fundamental relations as used in the delineation of a pressure-time diagram of the Gibson method. This equation states that the water-hammer pressure resulting in a time dt, $\frac{\gamma L}{g}\frac{dc}{dt}$, is equal to the pressure difference between points A and C plus the pressure still necessary to maintain the velocity and friction heads at this time. This is shown graphically in Fig. 3.

Prof. Thoma mentions that this equation could also be obtained if we suppose that V_{II}^2 and V_I^2 decrease during the closure proportionally with c^2. If this were true the last two terms in Equation [24] would balance each other. As in Fig. 5, he shows a section (a) representing the initial conditions of flow, a section (b) representing the flow at an instant during a sudden closure, and a section (c) typical of conditions near the end of a relatively long closure.

During a sudden closure "all water particles are then for the same short time under the action of the same strong pressure rise so that the velocity of each particle changes in value corresponding to the velocity at the beginning; the values V_{II} and V_I have then not changed during the sudden decrease in the water quantity to zero." With a long closure, however, the distribution of velocity may change considerably according to Prof. Thoma. In any case, however, consider $V_{II}^2 + V_I^2 = V_{II_0}^2 + V_{I_0}^2$ which Prof. Thoma says will come closer to the truth than the assumption that V_{II}^2 and V_I^2 decrease proportionally with c^2. This is probably an approximation of what happens. If we consider a complete closure, then in Equation [24], c is equal to zero and $\frac{dc}{dt}$ is equal to zero at the end of the closure so that

$$p_C - p_A = -\frac{\gamma}{g}(V_{II}^2 + V_I^2)$$

represents the pressure below normal at C at the end of the closure due to the accessory velocities.

The relative errors in the velocity measurement using a pitot tube at any one point in the cross-section may be expressed as $\frac{v_1^2}{2v_m^2}$ where v_1^2 is the average value of the square of the variable additional velocity varying with respect to time. This may be shown by referring to Equation [13] as follows:

$$v^2 = v_m^2 + 2v_m v' + v'^2$$

$$\int_{\Delta t} v^2 dt = \int_{\Delta t} v_m^2\, dt + 2\int_{\Delta t} v_m v'\, dt + \int_{\Delta t} v'^2\, dt$$

The first integral of the right-hand member equals $v^2_m t$, the second equals zero because v_m is a constant with respect to time and by definition $\int v' dt = 0$, and the third equals $v_1^2\ \Delta t$ by definition. Then

$$\frac{\int_{\Delta t} v^2 dt}{\Delta t} = v_a^2 = v_m^2 + v_1^2$$

But v_a^2 is a measure of the pitot tube reading and v_m^2 is a measure of the true velocity. The relative error in the velocity measurement is

$$\frac{v_a - v_m}{v_m} = \frac{v_a - \sqrt{v_a^2 - v_1^2}}{v_m}$$

or

$$\frac{v_a - v_m}{v_m} = \frac{v_a - v_a\left[1 - \left(\frac{v_1}{v_a}\right)^2\right]^{1/2}}{v_m}$$

$$= \frac{v_a - v_a\left[1 - \frac{1}{2}\left(\frac{v_1}{v_a}\right)^2 + \frac{1}{8}\left(\frac{v_1}{v_a}\right)^4 \cdot \frac{1}{16}\left(\frac{v_1}{v_a}\right)^6 + \ldots\right]}{v_m}$$

Neglecting the terms in the expansion where the exponent is greater than two, the expression becomes

$$\frac{v_a - v_m}{v_m} = \frac{1}{2}\frac{v_1^2}{v_a v_m}$$

But we may equate $v_a = v_m$ with small error in this fraction, so that we may write

$$\text{Relative error} = \frac{1}{2}\frac{v_1^2}{v_m^2}$$

If one states that the pitot-tube measurements are in error by 1 per cent and remembering that v_m changes to c_0 and v_1 changes to V_I when we are considering the whole cross-section, then, at the beginning

$$V_{I_0}^2 = 2\,(0.01)\,c_0^2 = 0.02\,c_0^2$$

In evaluating $V_{II_0}^2$ it is known for water distribution in long, straight, smooth pipes that $V_{II_0}^2 = 0.02\,c_0^2$. But Prof. Thoma thinks this condition too favorable because turbine conduits are hardly ever as straight and smooth as the pipes with which the formulas for the water distribution were obtained in the laboratory and also because in most cases the flow is affected by dissymmetries caused by an unsymmetrical inlet. For this reason he estimates that $V_{II_0}^2 = 0.04\,c_0^2$. Then with these assumptions

$$V_{II_0}^2 + V_{I_0}^2 = 0.06\,c_0^2$$

and assuming

$$V_{II}^2 + V_I^2 = V_{II_0}^2 + V_{I_0}^2$$

and furthermore assuming a uniform change in c from c_0 to zero during the closure, then, in Equation [24], the expression

$$\frac{\gamma}{g}\,(V_{II}^2 + V_I^2) - \frac{c^2}{c_0^2}\frac{\gamma}{g}\,(V_{II_0}^2 + V_{I_0}^2)$$

which may be considered the average error for the whole observed time is equal to

$$\frac{\frac{\gamma}{g}\left[c - \frac{1}{3}\frac{c^3}{c_0^2}\right]_{c_0}^{0}}{c_0}\,(V_{II_0}^2 + V_{I_0}^2)$$

which becomes

$$\frac{2}{3}\frac{\gamma}{g}\,(0.06)\,c_0^2$$

To take into account the variation in $(V_{II}^2 + V_I^2)$ during the closure between $(V_{II_0}^2 + V_{I_0}^2)$ and $\frac{c^2}{c_0^2}\,(V_{II_0}^2 + V_{I_0}^2)$. Prof. Thoma reduces the factor $\frac{2}{3}$ to $\frac{1}{3}$, obtaining as the average value of the error

$$0.02\,\frac{\gamma}{g}\,c_0^2 = 0.04\,\gamma\,\frac{c_0^2}{2g}$$

The error in cfs may be expressed as

$$E_1 \text{ in cfs} = -\frac{K}{SF}\,\frac{0.04\,c_0^2}{2g}\,T_s\,S\,r = -\frac{0.02\,T_s\,c_0^2}{F}$$

where K is the calibration constant of the apparatus, (2) equals $\frac{g}{r}$, S is the horizontal length in in. corresponding to 1 sec of time, F equals $\Sigma\frac{l}{a}$, T_s is the length of the diagram in sec, and r is the vertical height in in. corresponding to one ft of pressure change in the conduit. The relative error in per cent may be expressed as

$$E_1 \text{ in per cent} = -(100)\,\frac{0.02\,T_s\,c_0^2}{F}\,\frac{SF}{KA} = -\frac{2\,T_s\,S\,c_0^2}{KA} \quad \ldots [26]$$

where A represents the net area of the diagram in square inches.

Taking the diagram used in the numerical example given in Mr. Gibson's paper (3) which is run No. 15 of the test on unit No. 16 of station 3-B of The Niagara Falls Power Company, made August 17, 1920, the measured quantity of water is 1708 cfs and the average error in height of diagram in ft of water pressure is $(0.04)\,\frac{9.06^2}{64.4} = 0.051$ ft. The error in water quantity with the above assumptions is $-\frac{(0.02)\,(17.1)\,(8.97)^2}{1.939} = -14.2$ cfs and the error in per cent is -0.84.

Taking the diagram shown in Fig. 8 of Prof. Thoma's article (1), which is run No. 1 of the test on unit No. 2 of station 3-A of The Niagara Falls Power Company made December 11, 1921, the measured quantity of water is 608.5 cfs and the average error in cfs is $-\frac{(0.02)\,(11.51)\,(9.77)^2}{3.67} = -6.0$ or a percentage error of -0.98 instead of -1.5 as obtained roughly by Prof. Thoma.

We come now to a consideration of the foregoing in respect to the differential application of the Gibson method in which the difference in pressures at two measuring sections is recorded. Under these conditions V_{II}^2 and V_I^2 at each measuring section must be considered. These quantities vary alike for the two sections where the upper one is located a reasonable distance from the inlet and where the area of the penstock is nearly the same at each section so that the distribution of velocities at each section is approximately the same.

For the differential diagram, Equation [24] may be written as follows for the measuring sections C_1 and C_2

$$-\frac{dc_2}{dt} = \frac{g}{\gamma L_2}\left[(p_{C_2} - p_A) + \frac{c_2^2}{c_{20}^2}\,(p_{A_0} - p_{C_{20}}) + \frac{\gamma}{g}\,(V_{II}^2 + V_I^2) - \frac{c_2^2}{c_{20}^2}\frac{\gamma}{g}\,(V_{II_0}^2 + V_{I_0}^2)\right]$$

$$-\frac{dc_1}{dt} = \frac{g}{\gamma L_1}\left[(p_{C_1} - p_A) + \frac{c_1^2}{c_{10}^2}\,(p_{A_0} - p_{C_{10}}) + \frac{\gamma}{g}\,(V_{II}^2 + V_I^2)\,\frac{c_1^2}{c_{10}^2}\frac{\gamma}{g}\,(V_{II_0}^2 + V_{I_0}^2)\right]$$

Combining these equations we get

$$-\left(\frac{\gamma L_2}{g}\frac{dc_2}{dt} - \frac{\gamma L_1}{g}\frac{dc_1}{dt}\right) = (p_{C_2} - p_{C_1}) + \frac{c_2^2}{c_{20}^2}\,(p_{A_0} - p_{C_{20}})$$
$$-\frac{c_1^2}{c_{10}^2}\,(p_{A_0} - p_{C_{10}}) - \frac{c_2^2}{c_{20}^2}\frac{\gamma}{g}\,(V_{II_0}^2 + V_{I_0}^2) + \frac{c_1^2\gamma}{c_{10}^2 g}\,(V_{II_0}^2 + V_{I_0}^2)$$

But

$$\frac{c_2}{c_{20}} = \frac{c_1}{c_{10}} \quad \text{and} \quad \frac{dc_2}{dt} = \frac{dc_1}{dt}$$

so that

$$\frac{c_2^2}{c_{20}^2}\frac{\gamma}{g}\,(V_{II_0}^2 + V_{I_0}^2) = \frac{c_1^2}{c_{10}^2}\frac{\gamma}{g}\,(V_{II_0}^2 + V_{I_0}^2)$$

and

$$-\left(\frac{\gamma L_2}{g}\frac{dc_2}{dt} - \frac{\gamma L_1}{g}\frac{dc_1}{dt}\right) = -(L_2 - L_1)\,\frac{\gamma}{g}\frac{dc_2}{dt}$$

$$= \left[(p_{C_2} - p_{C_1}) + \frac{c_2^2}{c_{20}^2}\,(p_{A_0} - p_{C_{20}}) - \frac{c_1^2}{c_{10}^2}\,(p_{A_0} - p_{C_{10}})\right] \ldots [27]$$

TABLE 1 TEST OF UNIT NO. 20, STATION 3-C, THE NIAGARA FALLS POWER COMPANY, JUNE 22, 1924

Run 10 (Differential diagram)

Planimeter readings	Differences	Gross area	Slot correction	Net area	Net area corrected for shrinkage
17.103					
	4.087				
13.016		8.171	0.135	8.036	8.086
	4.084				
8.932					

$K = 40.23$ $F = 0.2522$
$S = 0.4645$

$$Q = \frac{(40.23)\ (8.086)}{(0.4645)\ (0.2522)} = 2777$$

Leakage	= 16
Total discharge	2793 cfs

Headwater elevation	= 560.19
Tailwater elevation	= 341.60
Gross head	= 218.59
$h_f + h_r$	= 2.06
Net head	= 216.53
Generated kw	= 46,933

Quantities for net head = 213.5 ft
Q = 2773 cfs
kw = 45,920

This is the general equation for the differential diagram with the areas at the measuring sections nearly the same. If these areas are equal then $c_{20} = c_{10}$ and $c_2 = c_1$ and the last two terms simplify to

$$\frac{c_2^2}{c_{20}^2}(p_{A_0} - p_{C_{20}}) - \frac{c_2^2}{c_{20}^2}(p_{A_0} - p_{C_{10}}) = \frac{c_2^2}{c_{20}^2}(p_{C_{10}} - p_{C_{20}})$$

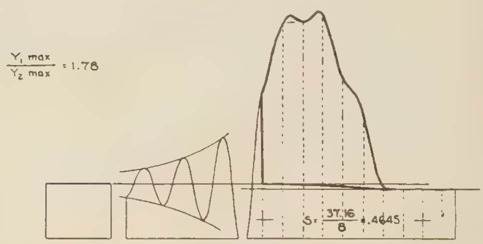

FIG. 6

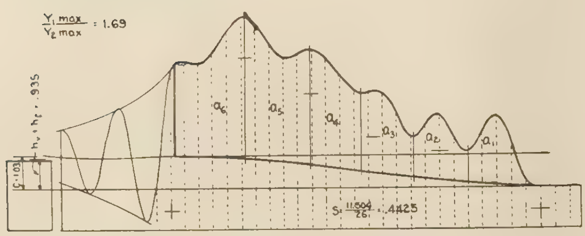

FIG. 7

TABLE 2 TEST OF UNIT NO. 20, STATION 3-C, THE NIAGARA FALLS POWER COMPANY, JUNE 15, 1924

Run 9 (Simple diagrams)

	Planimeter readings	Diff.	Mean area corrected for slot	A	r	$(1 - r)$	$(1 - r)^2$	$(1 - r)^2 \times C$
a_1	28.106							
	26.807	1.299	2.601					
	25.505	1.302	0.070	2.531	0.088	0.912	0.832	0.857
			2.531					
a_2	30.804							
	29.457	1.347	2.698					
	28.106	1.351	0.036	5.193	0.181	0.819	0.671	0.691
			2.662					
a_3	10.065							
	8.300	1.765	3.527					
	6.538	1.762	0.045	8.675	0.302	0.698	0.488	0.504
			3.482					
a_4	14.953							
	12.505	2.448	4.888					
	10.065	2.440	0.043	13.520	0.471	0.529	0.280	0.288
			4.845					
a_5	18.989							
	15.246	3.743	7.492					
	11.497	3.749	0.040	20.972	0.730	0.270	0.073	0.075
			7.452					
a_6	26.590	3.800						
	22.790	3.801	7.601	28.570				
	18.989		0.003	0.166				
			7.598	28.736				
		40.450						
Total net area		26.070	14.380	28.784				
		11.666	14.404	0.237 slot correction				
				28.547				

$$\text{Leakage area} = \frac{(16)\ (1.699)\ (0.4425)}{(72.56)} = 0.166$$

$$\text{Area corrected for shrinkage} = (28.547)\ \frac{54.83}{54.53} = 28.704$$

$S = 0.4425$
$K = 72.56$
$F = 1.699$

$$Q = \frac{(72.56)\ (28.704)}{(0.4425)\ (1.699)} = 2770$$

Leakage = 16

Total discharge 2786 cfs

$h_v + h_f$ (from net head piezometer)	= 7.31
$h_v = \dfrac{(2786)^2}{(153.94)}\ \dfrac{1}{64.4}$	= 5.08
h_f	= 2.23
Headwater elevation	= 559.43
Tailwater elevation	= 341.38
Gross head	= 218.05
$h_f + h_r$	= 2.29
Net head	= 215.76
kw generated	= 46,640

h_{f0} to Gibson tap = 0.49 in. on diagram

Quantities for net head = 213.5 ft
Q = 2770 cfs
kw = 45,900

and Equation [27] becomes

$$-(L_2 - L_1)\frac{\gamma}{g}\frac{dc_2}{dt} = \left[(p_{C_2} - p_{C_1}) + \frac{c_2^2}{c_{20}^2}(p_{C_{10}} - p_{C_{20}})\right] \ldots [28]$$

Equations [27] and [28] are independent of accessory velocities and so, as stated above, where the measuring sections are equal or nearly so, and where the upper measuring section is located at a reasonable distance from the inlet, then the differential diagram is independent of accessory velocities.

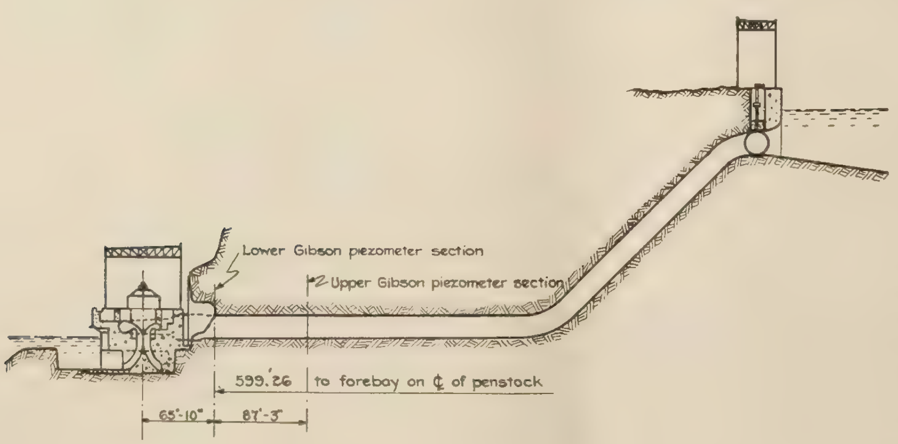

FIG. 8

Fig. 6 is a differential diagram taken on June 22, 1924, during the test of unit No. 20 of station 3-C of The Niagara Falls Power Company. Fig. 7 is a simple diagram taken on June 15, 1924, during another test on the same unit. The two diagrams were taken as closely as possible at the same gate opening and the same power output. In the case of the differential diagram $(L_2 - L_1)$ is 87.25 ft and in the case of the simple diagram L is 599.26 ft, as shown in Fig. 8.

Table 1 shows the computations for the differential diagram and Table 2 the computations for the simple diagram. They show that when equalized for the same net head, the quantities of water as determined by these two different applications of the Gibson method agree almost exactly.

The common power-discharge curve for the two tests of this unit is shown in Fig. 9, in which the quantities obtained by measurements using the simple diagrams are plotted by points enclosed in circles and those obtained from the differential diagrams are enclosed in triangles. The average divergence of the differential points from the line established by the single points is within +0.20 per cent. The agreement between the two tests then is within 0.20 per cent.

This would point experimentally to one of two conclusions. Either the positive and negative errors of both the simple diagrams and differential diagrams are of equal magnitude and cancel one another or leave the same residual; or Prof. Thoma's estimates of the magnitudes of these errors are too large. (1) Later it will be shown that when the differential method is used, errors No. 2 and No. 4 are small and are opposite in sign to error No. 3, resulting in a very small residual error.

Error Due to False Valuation of Friction

The assumption that the friction during the closing is just as great as at continuous steady flow with the same amount of water possibly is not strictly true. Prof. Thoma points out that a downward friction force is exerted upon the back-flowing edge current during the last stage of the closure. This force tends to make the diagram too large and, therefore, causes a positive error in the result opposed to the negative error due to the accessory velocities. Estimating the average error in the friction from one-twentieth to one-tenth of the friction obtaining when $c = c_0$, then the error in the quantity of water in square inches on the diagram varies from $+\frac{1}{20} h_{f0}\, T_s\, S$ to $+\frac{1}{10} h_{f0}\, T_s\, S$. Expressed as a relative error in per cent, this becomes

$$E_2 = [(+5) \text{ to } (+10)] \frac{h_{f0}\, T_s\, S}{A} \qquad [29]$$

where h_{f0} is the friction expressed in inches of ordinate on the diagram. In the simple diagram, h_{f0} is measured from forebay to measuring section and, in the case of the differential diagram, is measured between taps.

For the diagram used in the numerical example this error becomes

$$(+5)\ \frac{\left(\frac{0.69}{3}\right)(17)\ (0.4723)}{16.21} = +0.57 \text{ per cent}$$

to

$$(+10)\ \frac{\left(\frac{0.69}{3}\right)(17)\ (0.4723)}{16.21} = +1.14 \text{ per cent}$$

This error for the diagram shown in Fig. 8 of Prof. Thoma's article (1) with the same assumptions as to friction would be from

$$(+5)\ \frac{(0.485)(1.20)(11.5)(0.728)}{18.20} = +1.3 \text{ per cent}$$

to

$$(+10)\ \frac{(0.485)(1.20)(11.5)(0.728)}{18.20} = +2.7 \text{ per cent}$$

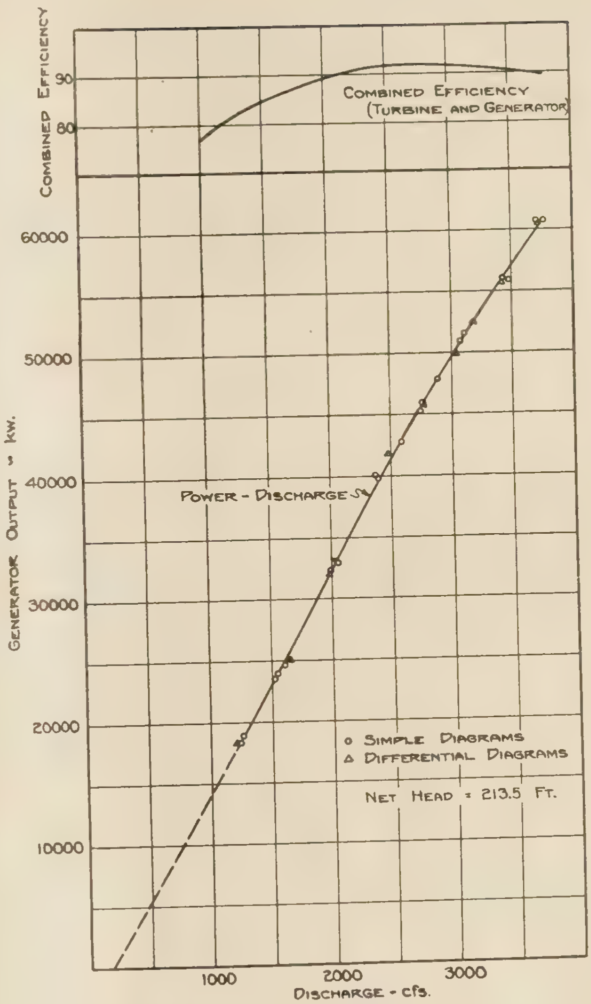

Fig. 9

Prof. Thoma gets 0.9 to 1.8 per cent for these values because he assumes that 33 per cent of $\frac{p_{A0} - p_{C0}}{\gamma}$ is the value of the friction head at $c = c_0$ instead of 48.5 per cent as is actually the case. These are, of course, very approximate estimates of the errors.

In the study of error No. 2, it is difficult to accept Dr. Thoma's coefficient $\frac{1}{20}$ to $\frac{1}{10}$. This error could only exist to any appreciable degree where the "velocity front" in the conduit is attenuated. Most penstocks of modern plants are so large that the velocity front is almost square.

As will be pointed out later, adopting 0.075 as a mean value given by Prof. Thoma for the coefficient to be used in evaluating error No. 2 and evaluating errors No. 3 and No. 4 in accordance with the theory advanced, we find the mean residual error at point of maximum efficiency in 35 cases examined would be 0.43 per cent without regard to sign but only +0.06 per cent if positive and negative values are taken into account. Thirteen cases gave positive results and 22 cases negative results.

In many cases the factor $\frac{p_{A0} - p_{C0}}{\gamma}$ on the differential diagram is not greater than $^1/_8$ to $^1/_4$ in. on diagrams from 4 to 8 in. long

and containing 20 to 50 sq in. of impulse area. Even in the small differential diagram shown in Fig. 6, the error due to false valuation of friction would, according to this estimate, amount to only

$$\left[\left(+\frac{1}{20}\right) \text{ to } \left(+\frac{1}{10}\right)\right] \frac{(100)(0.11)(6.02)(0.4645)}{8.086} = 0.2 \text{ to } 0.4 \text{ per cent.}$$

In a great many instances where differential diagrams have been used, a close check has been obtained both where the closures have been of long and of short duration. The error due to a false valuation of friction must be well under the figures suggested by Prof. Thoma.

Error Due to Friction of the Mercury Column

The equation for the motion of the mercury column is

$$a\frac{d^2p'}{dt^2} + k\frac{dp'}{dt} + p' = p \qquad [25]$$

where p' is the pressure recorded by the apparatus, p the pressure in the measuring section, a a constant depending upon the mass of the mercury column, its cross-section, etc., and k a friction coefficient which may be considered constant for small deflections. The friction is a function of the velocity of the mercury. The symbol p' represents ordinates on the diagram and, therefore, represents the position of the mercury surface, so that $\frac{dp'}{dt}$ represents the velocity of the mercury and $k\frac{dp'}{dt}$ the frictional force. If we let p_2 represent the (nearly) constant pressure existing after the closure, then for the damped harmonic oscillations we get

$$a\frac{d^2p'}{dt^2} + k\frac{dp'}{dt} + p' - p_2 = 0$$

Let $(p' - p_2) = p''$; then

$$a\frac{d^2p''}{dt^2} + k\frac{dp''}{dt} + p'' = 0$$

The general solution of this equation is (4)

$$p'' = e^{\frac{-k}{2a}t}\left[A \sin\left(\sqrt{\frac{1}{a} - \frac{k^2}{4a^2}}\right)t + B\cos\left(\sqrt{\frac{1}{a} - \frac{k^2}{4a^2}}\right)t\right]$$

or

$$p' = p_2 + e^{\frac{-k}{2a}t}\left[A \sin\left(\sqrt{\frac{1}{a} - \frac{k^2}{4a^2}}\right)t + B\cos\left(\sqrt{\frac{1}{a} - \frac{k^2}{4a^2}}\right)t\right] \qquad [30]$$

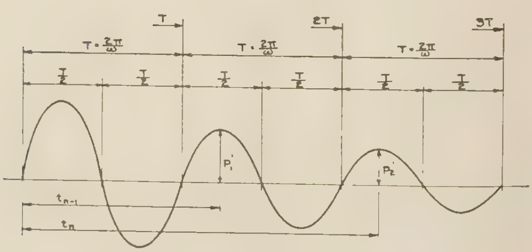

Fig. 10

Fig. 10 represents a damped harmonic vibration as given by this equation with the constant p_2 equal to zero so that the axis of abscissas divides the figure symmetrically. The figure is also drawn for $p' = 0$ when $t = 0$ so that the constant B becomes zero.

The value of k in the above equation may be obtained by making a few calculations. In Equation [30], when $t = 0$ then $p' = 0$ and we may make $p_2 = 0$. Then

$$0 = e^{\frac{-k}{2a}0}\left[A \sin\left(\sqrt{\frac{1}{a} - \frac{k^2}{4a^2}}\right)0 + B\cos\left(\sqrt{\frac{1}{a} - \frac{k^2}{4a^2}}\right)0\right]$$

Therefore, $B = 0$ and Equation [30] becomes

$$p' = e^{\frac{-k}{2a}t} A \sin\left(\sqrt{\frac{1}{a} - \frac{k^2}{4a^2}}\right)t \qquad [31]$$

Let

$$w = \sqrt{\frac{1}{a} - \frac{k^2}{4a^2}} \qquad [32]$$

And

$$\beta = \frac{k}{2a} \qquad [33]$$

Then

$$p' = e^{-\beta t} A \sin w\,t \qquad [34]$$

When $t = n\,T$, $p' = 0$, so that $w\,nT = n\,2\pi$ or

$$T = \frac{2\pi}{w} \qquad [35]$$

For a maximum or minimum value of p'

$$\frac{dp'}{dt} = -\beta e^{-\beta t} A \sin w\,t + e^{-\beta t} A\,w \cos w\,t = 0$$

or $w \cos w\,t - \beta \sin w\,t = 0$ or $\tan w\,t = \frac{w}{\beta}$

Whence the condition for a maximum or minimum is

$$w\,t_n = \tan^{-1}\frac{w}{\beta} + (n-1)\,2\pi$$

$$t_n = \frac{1}{w}\tan^{-1}\frac{w}{\beta} + (n-1)\frac{2\pi}{w} = \frac{1}{w}\tan^{-1}\frac{w}{\beta} + (n-1)\,T \text{ and}$$

$$t_{n-1} = \frac{1}{w}\tan^{-1}\frac{w}{\beta} + (n-2)\frac{2\pi}{w} = \frac{1}{w}\tan^{-1}\frac{w}{\beta} + (n-2)\,T$$

$$p_1' = e^{-\beta t_{n-1}} A \sin w\,t_{n-1}$$

$$p_2' = e^{-\beta t_n} A \sin w\,t_n$$

$$\psi = \frac{p_1'}{p_2'} = \left[\frac{e^{-\beta t_{n-1}} A \sin w\,t_{n-1}}{e^{-\beta t_n} A \sin w\,t_n}\right] = \left[\frac{e^{-\frac{\beta}{w}\tan^{-1}\frac{w}{\beta} - \beta(n-2)\,T}}{e^{-\frac{\beta}{w}\tan^{-1}\frac{w}{\beta} - \beta(n-1)\,T}}\right]$$

$$\psi = e^{-\frac{\beta}{w}\tan^{-1}\frac{w}{\beta} - \beta(n-2)T + \frac{\beta}{w}\tan^{-1}\frac{w}{\beta} + \beta(n-1)T}$$

$$\psi = e^{(-\beta n + 2\beta + \beta n - \beta)T} = e^{\beta T} \qquad [36]$$

Then we have

$$\psi = e^{\beta T} \qquad [36]$$

$$T = \frac{2\pi}{w} \qquad [35]$$

$$w = \sqrt{\frac{1}{a} - \frac{k^2}{4a^2}} \qquad [32]$$

$$\beta = \frac{k}{2a} \qquad [33]$$

$$\frac{1}{a} - \frac{k^2}{4a^2} = \frac{4\pi^2}{T^2}$$

$$4a - k^2 = 16\frac{\pi^2 a^2}{T^2}$$

$$\frac{16\pi^2}{T^2}(a^2) - 4a + k^2 = 0$$

$$a = \frac{+4 \pm \sqrt{16 - \dfrac{64\pi^2 k^2}{T^2}}}{\dfrac{32\pi^2}{T^2}} = \frac{+1 \pm \sqrt{1 - \dfrac{4\pi^2 k^2}{T^2}}}{\dfrac{8\pi^2}{T^2}}$$

$$\psi = e^{\frac{k}{2a}T} \quad \text{or} \quad \log\psi = \frac{k}{2a}T$$

$$\log\psi = \frac{kT}{2}\left[\frac{8\pi^2}{T^2}\,\frac{1}{\left[1 \pm \sqrt{1 - \dfrac{4\pi^2k^2}{T^2}}\right]}\right]$$

$$\log\psi = \frac{4k\pi^2}{T\left[1 \pm \sqrt{1 - \dfrac{4\pi^2k^2}{T^2}}\right]}$$

$$T(\log\psi) \pm T(\log\psi)\sqrt{1 - \frac{4\pi^2k^2}{T^2}} = 4k\pi^2$$

$$\pm T(\log\psi)\sqrt{1 - \frac{4\pi^2k^2}{T^2}} = 4k\pi^2 - T(\log\psi)$$

$$T^2(\log\psi)^2\left(1 - \frac{4\pi^2k^2}{T^2}\right) = 16k^2\pi^4 - 8k\pi^2T(\log\psi) + T^2(\log\psi)^2$$

$$-\frac{4\pi^2k^2}{T^2}T^2(\log\psi)^2 = 16k^2\pi^4 - 8k\pi^2T(\log\psi)$$

$$-4\pi^2(\log\psi)^2k - 16\pi^4k + 8\pi^2T(\log\psi) = 0$$

$$[-\pi^2(\log\psi)^2 - 4\pi^4]\,k = -2\pi^2T(\log\psi)$$

$$k = \frac{2\pi^2 T\log(\psi)}{4\pi^4 + \pi^2(\log\psi)^2}$$

$$k = \frac{T(\log\psi)}{2\pi^2 + \dfrac{(\log\psi)^2}{2}} \qquad \text{[37]}$$

By integrating Equation [25] between the start and end of the closure, i.e., between $t = 0$ and $t = t_1$ we get

$$a\left[\left(\frac{dp'}{dt}\right)_1 - \left(\frac{dp'}{dt}\right)_0\right] + k(p_1' - p_0') + \int_{t_0}^{t_1} p'dt = \int_{t_0}^{t_1} pdt$$

The first term of this expression is zero because the mercury column is at rest at the beginning and at the end of the observation. The third term is the time integral for the pressure diagram which is evidently too small by the amount $k(p_1' - p_0')$ due to the friction of the mercury.

Neglecting the second term in the denominator of Equation [37], we get for the expression $k(p_1' - p_0')$

$$\frac{T\log_e\psi}{2\pi^2}(p_1' - p_0')$$

The relative error in per cent is

$$E_3 = -\frac{100\,TS\,(\log_e\psi)\,(p_1' - p_0')}{2\pi^2 A} \qquad \text{[38]}$$

Evaluating T, ψ, and $(p_1' - p_0')$ from the diagram of Prof. Thoma's Fig. 8, $T = 3.74$ sec, $\psi = 1.61$, $(p_1' - p_0') = 2.80$ in. on diagram, so that

$$E_3 = -\frac{(100)(3.74)(0.728)(0.4783)}{2\pi^2(18.20)} = -1.02 \text{ per cent}$$

Evaluating T, ψ, and $(p_1' - p_0')$ from the numerical example given in Mr. Gibson's paper, $T = 4.0$ sec, $\psi = 1.55$, and $(p_1' - p_0') = 2.33$ in. on diagram, so that

$$E_3 = \frac{(100)(4.0)(0.4723)(0.438)}{2\pi^2(16.21)} = -0.60 \text{ per cent}$$

It should be remembered that these numerical values apply to the simple diagram. In the differential diagram the corresponding error is reduced because only a small amount of mercury is used and consequently the natural period of oscillation T is smaller. Moreover the quantity of $(p_1' - p_0')$ is smaller as the forebay surge is eliminated from the diagram and with approximately equal measuring sections there is little or no velocity head in the diagram ordinate. Furthermore by damping the gate stroke toward the end of the closure, this quantity may be made extremely small.

Error Due to Inertia of the Mercury Column

Considering the term $\frac{c^2}{c_0^2}(p_{A_0} - p_{C_0})$ in Equation [24], Prof. Thoma says: "At the beginning of the observation the recorded pressure stays below the real pressure and this causes the water velocity at the beginning and, therefore, also the above-mentioned term to be judged too great." The relative error in the determination of the water quantity assuming the theoretical case where the destruction of velocity is uniform from the beginning to the end of the closure, i.e., $\frac{dc}{dt}$ is constant, is given as

$$\left[\frac{1}{2\pi^2}\left(\frac{T}{T_s}\right)^2\frac{p_{A_0} - p_{C_0}}{p_m}\right]^*$$

where T is the time for the natural period of the apparatus, T_s the duration of closure in seconds and p_m the average value of

$$p_C - p_A + \frac{c^2}{c_0^2}(p_{A_0} - p_{C_0})$$

or

$$p_m = \frac{-\gamma L}{g}\left(\frac{dc}{dt}\right) = \frac{-\gamma L}{g}\,\frac{c_0}{T_s}$$

This expression gives the maximum value of the error because in a practical case $\frac{dc}{dt}$ cannot be constant but is smaller at the start of the closure. This results in a closer agreement between the curve recorded by the surface of the mercury and the curve of true pressure.

We may derive this expression for the limiting relative error due to the inertia of the mercury column as follows. With the assumption of uniform destruction of velocity, the actual pres-

* This expression is approximate, the correct one being

$$\frac{5}{8\pi^2}\left(\frac{T}{T_s}\right)^2\frac{p_{A0} - p_{C_0}}{p_m}$$

sure-time diagram occurring at section C is shown in Fig. 11 by the area $AGFEDCBA$ having a constant height $\frac{-\gamma L c_0}{g T_s} = p_m$ and a length T_s. The actual diagram as recorded in this case would be $AMLKJDCBA$. The mercury lags behind the pressure line $AGFE$ at the start and during the closure oscillates about GFE, in this case in a damped harmonic curve. The area of the diagram in either case considered above the horizontal base AX is the same. If we substitute the sine curve $AQPON$ for the damped harmonic curve (i.e., neglect the friction in the mercury column), then by comparing the net area of the diagram as calculated by the Gibson method with the theoretical net diagram,

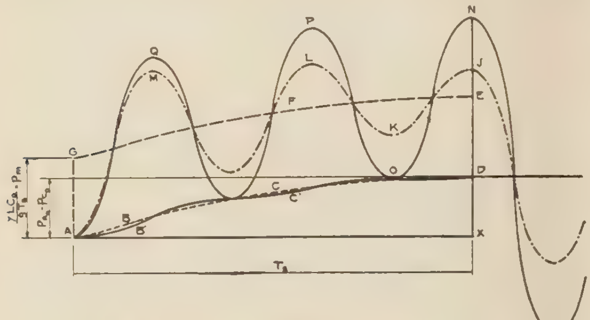

Fig. 11

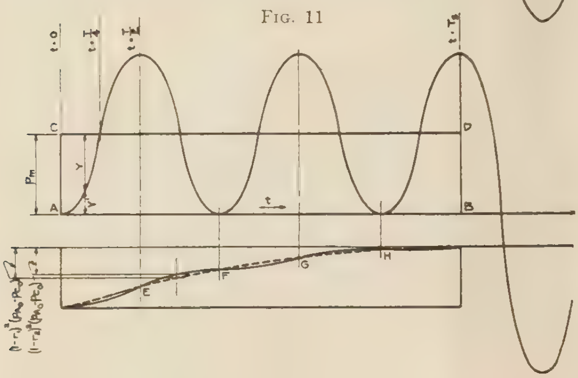

Fig. 12

an expression is obtained for the error due to inertia. The difference, of course, is due to the difference in the location of the recovery line on the diagram. In the case of the theoretical diagram this location is $ABCD$, and in the case of the actual diagram the location is $AB'C'D$. The actual recovery line oscillates about the true one making plus and minus errors which tend to compensate although the largest divergence occurs at the start of the diagram.

Inasmuch as the line GFE is parallel with $ABCD$ and the sine curve $AQPON$ oscillates about GFE, we may assume that the ordinate $(p_{A_0} - p_{C_0}) = \overline{XD}$ is zero for the diagram and reconstruct the figure as shown in Fig. 12. This will simplify the calculations. By integrating both theoretical and actual diagrams in Fig. 12 from $t = 0$ to some point $t = t$, we may then find the value of r or $\frac{c}{c_0}$ at this point. The difference in the value of $(1 - r)^2(p_{A_0} - p_{C_0})$ for the two diagrams gives the error in the location of the recovery line and this expression integrated over the length of the diagram gives the error due to the inertia of the mercury.

The general equation for the sine curve with CD as the axis is $y = A \sin kt + B \cos kt$. We may evaluate constants A, B, and k as follows: When $t = 0$ then $y = -p_m$, so that $-p_m = 0 + B$, or $B = -p_m$. Similarly when $t = \frac{T}{4}$ then $y = 0$, so that $0 = A \sin k\frac{T}{4} - p_m \cos k\frac{T}{4}$, or $\tan\frac{kT}{4} = \frac{p_m}{A}$. Also when $t = \frac{5}{4}T$ then $y = 0$, so that $0 = A \sin\frac{5}{4}kT - p_m \cos\frac{5}{4}kT$, or $\tan\frac{5}{4}kT = \frac{p_m}{A}$. This results in the relation $\frac{5}{4}kT - \frac{kT}{4} = 2\pi$, or $k = \frac{2\pi}{T}$. We may, therefore, write

$$y = A \sin\frac{2\pi}{T}t - p_m \cos\frac{2\pi}{T}t$$

Substituting $k = \frac{2\pi}{T}$ in the relation $A \sin k\frac{T}{4} = p_m \cos k\frac{T}{4}$, we find that $A = 0$, so that we may now write

$$y = -p_m \cos\frac{2\pi}{T}t$$

Transferring the axis from CD to AB and using y' for the ordinate to the curve, we may write the relation

$$y' = p_m + y = p_m - p_m \cos\frac{2\pi}{T}t$$

The area under the curve to any point t is

$$\int_0^t y'dt = \int_0^t p_m dt - \int_0^t p_m \cos\frac{2\pi}{T}t\,dt =$$

$$p_m t - p_m\frac{T}{2\pi}\sin\frac{2\pi}{T}t = p_m\left(t - \frac{T}{2\pi}\sin\frac{2\pi}{T}t\right)$$

The total diagram area is $p_m T_s$. The true ratio r_1 as used in delineation is $r_1 = \frac{p_m t}{p_m T_s} = \frac{t}{T_s}$ and $(1 - r_1)^2 = 1 - \frac{2t}{T_s} + \frac{t^2}{T_s^2}$. The approximate ratio r_2 as used in the delineation of the diagram as recorded by the mercury is

$$r_2 = \frac{p_m\left(t - \frac{T}{2\pi}\sin\frac{2\pi}{T}t\right)}{p_m T_s} = \frac{t}{T_s} - \frac{T}{2\pi T_s}\sin\frac{2\pi}{T}t$$

and

$$(1 - r_2)^2 = 1 + \frac{t^2}{T_s^2} + \frac{T^2}{4\pi^2 T_s^2}\left(\sin\frac{2\pi}{T}t\right)^2 - \frac{tT}{\pi T_s^2}\sin\frac{2\pi}{T}t - \frac{2t}{T_s} + \frac{T}{\pi T_s}\sin\frac{2\pi}{T}t$$

The error in the location of the recovery line is then

$$\left[(1 - r_2)^2 - (1 - r_1)^2\right](p_{A_0} - p_{C_0})$$

$$= (p_{A_0} - p_{C_0})\left[1 + \frac{t^2}{T_s^2} + \frac{T^2}{4\pi^2 T_s^2}\left(\sin\frac{2\pi}{T}t\right)^2 - \frac{tT}{\pi T_s^2}\sin\frac{2\pi}{T}t - \frac{2t}{T_s} + \frac{T}{\pi T_s}\sin\frac{2\pi}{T}t - 1 + \frac{2t}{T_s} - \frac{t^2}{T_s^2}\right]$$

This expression reduces to

$$(p_{A_0} - p_{C_0})\left[\frac{-tT}{\pi T_s^2}\sin\frac{2\pi}{T}t + \frac{T^2}{4\pi^2 T_s^2}\left(\sin\frac{2\pi}{T}t\right)^2 + \frac{T}{\pi T_s}\sin\frac{2\pi}{T}t\right]$$

The error in diagram area to any time t is

$$(p_{A_0} - p_{C_0}) \int_{t=0}^{t=t} \left[\frac{-tT}{\pi T_s^2} \sin \frac{2\pi}{T} t + \frac{T}{4\pi^2 T_s^2} \left(\sin \frac{2\pi}{T} t \right) + \frac{T}{\pi T_s} \sin \frac{2\pi}{T} t \right] dt$$

which reduces to

$$(p_{A_0} - p_{C_0}) \left[-\frac{T^3}{4\pi^3 T_s^2} \sin \frac{2\pi}{T} t + \frac{T^2 t}{2\pi^2 T_s^2} \cos \frac{2\pi}{T} t - \frac{T^3}{16\pi^3 T_s^2} \cos \frac{2\pi}{T} t \sin \frac{2\pi}{T} t + \frac{T^2 t}{8\pi^2 T_s^2} - \frac{T^2}{2\pi^2 T_s} \cos \frac{2\pi}{T} t + \frac{T^2}{2\pi^2 T_s} \right]$$

If we integrate from $t = 0$ to $t = T_s$, we will obtain the total amount of the error for the measurement. T_s can be taken as a multiple of T in evaluating $\cos \frac{2\pi}{T} T_s$ and $\sin \frac{2\pi}{T} T_s$ since at the end of the diagram the mercury is at rest.[4]

$$(p_{A_0} - p_{C_0}) \left[-\frac{T^3}{4\pi^3 T_s^2} \sin \frac{2\pi}{T} T_s + \frac{T^2 T_s}{2\pi^2 T_s^2} \cos \frac{2\pi}{T} T_s - \frac{T^3}{16\pi^3 T_s^2} \cos \frac{2\pi}{T} T_s \sin \frac{2\pi}{T} T_s + \frac{T^2 T_s}{8\pi^2 T_s^2} - \frac{T^2}{2\pi^2 T_s} \cos \frac{2\pi}{T} T_s + \frac{T^2}{2\pi^2 T_s} \right]$$

This expression reduces to

$$(p_{A_0} - p_{C_0}) \frac{T^2}{2\pi^2 T_s} + \frac{T^2}{8\pi^2 T_s}$$

or

$$(p_{A_0} - p_{C_0}) \frac{5}{8} \frac{T^2}{\pi^2 T_s}$$

The relative error then is

$$\frac{(p_{A_0} - p_{C_0}) \dfrac{5}{8} \dfrac{T^2}{\pi^2 T_s}}{p_m T_s} = \frac{5}{8\pi^2} \left(\frac{T}{T_s} \right)^2 \frac{(p_{A_0} - p_{C_0})}{p_m}$$

Expressed as a percentage this becomes

$$E_4 = (+100) \left(\frac{5}{8} \right) \frac{1}{\pi^2} \left(\frac{T}{T_s} \right)^2 \frac{(p_{A_0} - p_{C_0})}{p_m} \quad \ldots\ldots [39]$$

or, for the simple diagram

$$E_4 = (+100) \left(\frac{5}{8} \right) \frac{1}{\pi^2} \frac{T^2 S}{T_s A} (p_{A_0} - p_{C_0}) \quad \ldots\ldots\ldots [40]$$

and, for the differential diagram

$$E_4 = (+100) \left(\frac{5}{8} \right) \frac{1}{\pi^2} \frac{T^2 S}{T_s A} (p_{C_{10}} - p_{C_{20}}) \quad \ldots\ldots\ldots [41]$$

It should be noted that this is the maximum error due to the inertia of the mercury column since $\frac{dc}{dt}$ has been assumed equal to a constant. In a practical case the velocity is not destroyed at a constant rate. At the beginning of closure, the turbine gates move slowly and the rate of velocity change is small. The mercury in the manometer follows the pressure change in this case more closely than in the case assumed.

[4] In Figs. 11 and 12, T_s is not taken as a (whole) multiple of T, but T_s is made equal to 2.5 T. The computation made herein refers to the case that $T_s = nT$, n being a whole number. The case that $T_s = \left(n + \frac{1}{2}\right) T$ gives the same relative error.

TABLE 3 THEORETICAL CAUSES OF ERROR INVOLVED IN THIRTY-FIVE TESTS MADE WITH DIFFERENTIAL APPLICATION OF THE GIBSON METHOD

Key No.	Unit	Cause No. 2, per cent	Cause No. 3, per cent	Cause No. 4, per cent	Residual of causes, per cent
1	1	+0.36	−0.32	+0.03	+0.03
1	2	+0.30	−0.28	+0.02	+0.04
2	3	+0.66	−0.30	+0.17	+0.53
3	3	+0.46	−1.21	+0.39	−0.36
4	3	+0.12	−0.50	+0.09	−0.29
4	3	+0.30	−0.49	+0.11	−0.08
4	6	+0.21	−0.61	+0.08	−0.31
4	6	+0.29	−0.45	+0.09	−0.07
4	6	+0.38	−0.56	+0.12	−0.06
4	7	+0.22	−0.90	+0.12	−0.56
4	7	+0.31	−0.59	+0.14	−0.14
4	7	+0.41	−0.49	+0.15	+0.07
4	7	+0.38	−0.57	+0.17	−0.02
4	8	+0.19	−0.58	+0.12	−0.27
5	2	+0.22	−0.93	+0.03	−0.68
5	3	+0.24	−1.01	+0.03	−0.75
5	4	+0.22	−1.00	+0.03	−0.75
6	1	+3.09	−0.28	+0.07	+2.88
6	3	+2.25	−0.27	+0.06	+2.04
7	1	+1.07	−0.30	+0.02	+0.79
8	1	+0.44	−0.28	+0.02	+0.18
8	2	+0.00	−0.10	+0.00	−0.10
9	8	+0.06	−0.18	+0.05	−0.07
10	1	+0.28	−0.38	+0.02	−0.08
10	2	+0.25	−0.38	+0.01	−0.12
11	1	+0.00	−0.09	−0.02[a]	−0.11
11	2	+0.00	−0.13	−0.03[a]	−0.16
12	1	+0.32	−0.96	+0.04	−0.60
12	2	+0.13	−0.97	+0.03	−0.81
13	1	+0.55	−0.70	+0.09	−0.06
14	1	+1.24	−1.02	+0.40	+0.62
15	1	+0.79	−0.43	+0.06	+0.42
15	2	+0.72	−0.33	+0.07	+0.46
16	1	+0.67	−0.54	+0.06	+0.19
16	3	+0.62	−0.46	+0.06	+0.22
Average of 35 units without respect to sign				0.043 per cent	
Average of 35 units with respect to sign				+0.06 per cent	

[a] Static line below running line.

In the simple diagram of Prof. Thoma's Fig. 8 (1), the error in the water quantity is then not more than

$$E_4 = (+100) \left(\frac{5}{8} \right) \frac{1}{\pi^2} \frac{(3.74)^2 (0.728)}{(11.51)(18.20)} (1.29) = +0.39 \text{ per cent.}$$

In the simple diagram of the numerical example, the error in the water quantity is not more than

$$E_4 = (+100) \left(\frac{5}{8} \right) \frac{1}{\pi^2} \frac{(4.0)^2 (0.4723)}{(17.1)(16.21)} (0.798) = +0.14 \text{ per cent.}$$

In the process of delineation the areas a_1, a_2, a_3, etc., are so chosen that the points E, F, G, H (Fig. 12) are determined. These points have the same location on either recovery line of Fig. 12. The error in the recovery line of a given diagram due to inertia of the mercury thus varies as the line progresses along the diagram, the net result being a positive error, the maximum possible value of which is extremely small. Furthermore, by using the differential measurement, this error tends to be inappreciable because (a) of the small amount of mercury used, which reduces the value of T in Equation [41] and (b) the relatively smaller value of $(p_{C_{10}} - p_{C_{20}})$ in Equation [41] as compared with $(p_{A_0} - p_{C_0})$ in Equation [40] due to the elimination of the influence of the forebay surge and to the tendency to reduce the recovery of velocity head.

Application of Theory of Errors to Actual Tests

The above theory of errors has been applied to a large amount of test data obtained during the last few years. All the diagrams considered have been of the differential type and, consequently, error No. 1 (1) may be assumed equal to zero. The calculated values of errors Nos. 2, 3, and 4 (1) and of the resulting residual error at the point of maximum efficiency of the unit

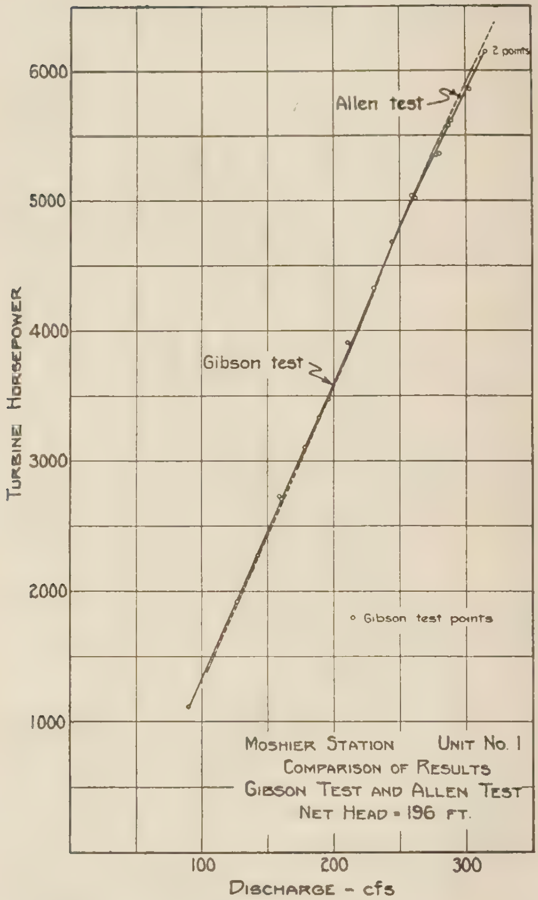

Fig. 13

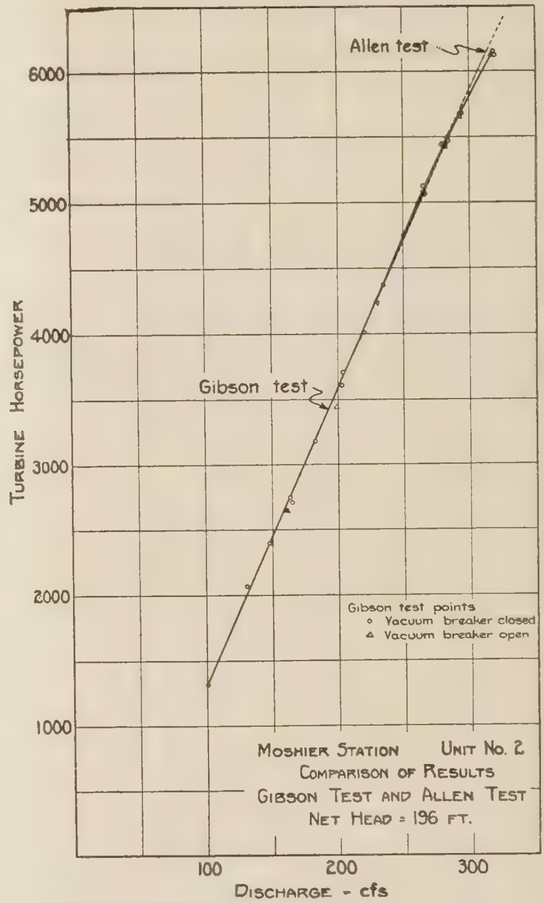

Fig. 14

tested, were found to be as given in Table 3. In the case of error No. 2, 0.075 was adopted as a mean value of the coefficient given by Prof. Thoma. From this investigation the mean residual error at the point of maximum efficiency in 35 cases examined would be 0.43 per cent without regard to sign and +0.06 per cent considering sign, as shown in Table 3.

Considerable experimental work has been carried on from time to time in the hope of being able to find the magnitude of the residual error experimentally, but it seems probable that it is too small to be within the range of experimental observation. It is well known that, even in laboratory work, it is difficult to get results to agree exactly when the same model is tested in two different laboratories.

In confirmation of this conclusion attention may be called to Figs. 13, 14, and 15, which give comparative test results of three units by both the Allen and the Gibson methods. The remarkable agreement between the two measurements is apparent. In the case of Moshier unit No. 1 correction for the theoretical errors puts the two curves in slightly better agreement, and in the case of Moshier unit No. 2 the reverse is true, although the agreement either with or without the theoretical corrections is very good. In the case of the 1900-hp unit shown in Fig. 15, the correction for theoretical errors tends to make the Gibson curve depart from the Allen curve by a greater amount. It is possible, of course, that both tests may be in error because, as pointed out by de Haller (5), there are theoretical reasons for believing that the Allen method gives too small quantities when the velocity front is attenuated. The magnitude of this

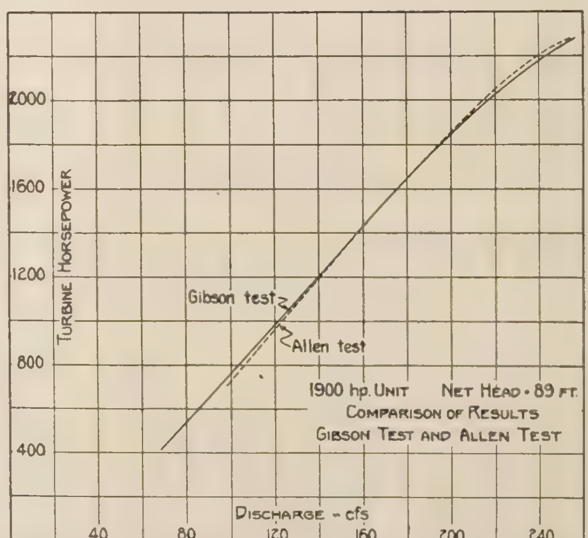

Fig. 15

error also may be so small that it cannot be determined experimentally. However, it would be a remarkable coincidence if two methods differing so much in principle should have errors in the same direction and in like degree. In addition to these two

cases, we have comparisons with volumetric measurements in the original Cornell tests, and other comparisons involving weirs and pitot tube measurements.

The Gibson tests at Cornell University which were compared with volumetric determinations have been analyzed with respect to the various theoretical errors discussed herein. The diagrams taken were of the simple type so that error No. 1 is included. The results of this analysis are given in Table 4.

TABLE 4 COMPARISON OF VOLUMETRIC, GIBSON AND ADJUSTED GIBSON MEASUREMENTS RECORD OF CORNELL TESTS MADE UNDER APPROXIMATELY THE NIAGARA CONDITIONS

						Discharge—cfs			Per cent variation	
Run No.	Cause no. 1	Cause no. 2	Cause no. 3	Cause no. 4	Residual of four causes, per cent	Volumetric	Gibson	Adjusted Gibson	Volumetric to Gibson	Volumetric to adjusted Gibson
45	−0.06	+0.05	−0.62	+0.12	−0.51	20.27	20.31	20.41	+0.2	+0.69
46	−0.07	+0.09	−1.00	+0.14	−0.84	20.42	20.52	20.69	+0.5	+1.32
47	−0.07	+0.16	−0.78	+0.16	−0.53	20.45	20.65	20.76	+0.9	+1.52
Mean of series					−0.63	20.38	20.48	20.62	+0.5	+1.18
5	−0.18	+0.29	−0.43	+0.12	−0.20	30.38	30.51	30.57	+0.4	+0.62
6	....	....	....	....	....	30.63	....	....	....	....
7	−0.18	+0.26	−0.25	+0.12	−0.05	30.69	31.15	31.17	+1.5	+1.56
Mean of series					−0.13	30.57	30.82	30.87	+0.8	+0.98
8	−0.20	+0.09	−0.66	+0.16	−0.61	42.24	42.17	42.43	−0.2	+0.45
9	−0.21	+0.10	−0.70	+0.15	−0.66	41.94	42.28	42.56	+0.8	+1.48
10	−0.22	+0.09	−0.32	+0.13	−0.32	42.22	42.09	42.23	−0.3	0.00
12	−0.20	+0.13	−0.67	+0.16	−0.58	...	41.96	42.20	...	....
Mean of series					−0.54	42.13	42.12	42.35	0	+0.52
30	−0.24	+0.10	−0.44	+0.13	−0.45	40.36	40.41	40.59	+0.1	+0.57
31	−0.22	+0.12	−0.51	+0.13	−0.48	40.36	40.90	41.10	+1.3	+1.83
32	−0.25	+0.21	−0.36	+0.13	−0.27	40.98	40.88	40.99	−0.2	0.00
Mean of series					−0.40	40.57	40.73	40.89	+0.4	+0.80
15	....	....	....	....	....	46.82	...	...	...	....
17	−0.26	+0.09	−0.23	+0.13	−0.27	46.98	46.60	46.73	−0.8	−0.53
16	−0.30	+0.13	−0.28	+0.12	−0.33	46.95	46.60	46.75	−0.7	−0.43
Mean of series					−0.30	46.92	46.60	46.74	−0.7	−0.38
33	−0.28	+0.24	−0.51	+0.18	−0.37	50.30	49.95	50.13	−0.7	−0.34
34	−0.28	+0.32	−0.49	+0.20	−0.25	50.66	51.47	51.60	+1.6	+1.86
35	−0.29	+0.37	−0.27	+0.16	−0.03	50.93	51.15	51.17	+0.4	+0.47
Mean of series					−0.22	50.63	50.85	50.97	+0.4	+0.67
Total of means					......	231.20	231.60	232.44		
Mean of means					−0.36				+0.2	+0.53

The causes referred to in this table are the possible causes of error discussed by Prof. Thoma. The discharges referred to as "adjusted Gibson" are the discharges obtained from the Gibson diagram corrected for Prof. Thoma's causes of error.

The value given for cause No. 2 is the average of the limits proposed by Prof. Thoma.

It is evident that in this series of tests involving 19 individual determinations, the residual error is calculated to be —0.36 per cent assuming a coefficient of 0.075 for determining error (6). The attempt to correct for the theoretical errors results in increasing the divergence between the volumetric and the Gibson results from the value of +0.2 per cent to +0.5 per cent. This indicates that the theoretical corrections are not applicable to the extent estimated.

It will be interesting to tabulate the theoretical errors involved in the diagrams shown in Figs. 6 and 7. These two diagrams were taken on unit 20 of Schoellkopf station 3-*C* at Niagara Falls, N. Y. One was a differential and the other a simple diagram. Without correction for theoretical errors the results as given in Table 5 were obtained.

TABLE 5

	Cfs	Net head	Generator kw
Fig. 6—differential	2793	216.53	46933
Fig. 7—simple	2786	215.76	46640

When equalized to the same net head, the discharge quantities agree within 0.1 per cent. If the theoretical errors are so calculated, the divergence then becomes about 0.7 per cent.

Referring to Prof. Thoma's Fig. 8 (1), and to the numerical example (6) mentioned by Prof. Thoma, the individual errors and the residual error have been calculated as given in Table 6.

TABLE 6

	Thoma Fig. 8 (1) station Schoellkopf 3-*A* unit no. 2	Gibson's numerical example station Schoellkopf 3-*B* unit no. 16
E_1	—1.0	—0.8
E_2	+1.9	+0.9
E_3	—1.0	—0.6
E_4	+0.4	+0.1
Theoretical residual error	+0.3	—0.4

Conclusions

(*a*) The differential method is independent of error No. 1 (1) due to accessory motions of the water particles, where the measuring sections are equal or nearly so and where the upper measuring section is located at a reasonable distance from the inlet. This error where existing, is negative.

(*b*) In the study of error No. 2 (1), which may be due to assuming that the recovery of friction head during closure is proportional to the square of the average velocity, it is difficult from our analysis to accept Prof. Thoma's coefficient of $\frac{1}{20}$ to $\frac{1}{10}$. This error could only exist in appreciable degree where the "velocity front" in the conduit is attenuated. Most penstocks of modern plants are so large that the velocity front is almost square. This error is positive.

(*c*) Error No. 3 (1), which is concerned with the friction of the mercury column in the pressure measuring apparatus and of the balancing water column in the connecting piping and penstock, is reduced in the case of the differential measurement. This is true because only a small amount of mercury is used and, consequently, the natural period of oscillation T is smaller. Moreover, the quantity $(p_1' - p_0')$ is smaller as the forebay surge is eliminated from the diagram and with approximately equal measuring sections there is little or no velocity head in the diagram ordinate. Furthermore, by damping the gate stroke toward the end of the closure, this quantity may be made extremely small.

(*d*) The maximum error due to the inertia of the mercury has been considered, herein, by assuming that the rate of change of velocity with respect to time is a constant. Actually the velocity is not destroyed at a constant rate since at the beginning of closure, the turbine gates move slowly and the rate of velocity change is small. The mercury in the manometer gage consequently follows the pressure change more closely than under the assumption made.

(*e*) Finally, it has been demonstrated that with the differential

diagram errors Nos. 2 and 4 (1) are small and are opposite in sign to error No. 3 (1) resulting in a very small residual error. Although errors Nos. 3 and 4 (1) may be theoretically computed from the diagram itself, this should not be done without reference to error No. 2 (1).

Until experimental verification of the foregoing theory of errors has been established, we conclude that the residual error is probably within the limits of precision possible in the measurement of large quantities of water. This conclusion is confirmed by the tests made in comparison with other methods of measurement and, indirectly, by a great many tests involving both the simple and differential application of the Gibson method.

REFERENCES

1 "Über den Genauigkeitsgrad des Gibsonschen Wassermessverfahrens," by Professor D. Thoma. Published in " Mitteilungen des Hydraulischen Instituts der Technichen Hochschule München," Bull. No. 1, 1926, pp. 59–74.

2 Trans. A.S.M.E., 1923, page 29.

3 Ibid., 1923, page 343.

4 "Calculus," by Davis and Brenke, p. 366. The Macmillan Co., New York, N. Y.

5 "Considerations theoriques sur la mesure des debits d'eau par la methode d'Allen," par P. de Haller, Helv. Phys. Acta, 1930.

6 "The Gibson Method and Apparatus for Measuring the Flow of Water in Closed Conduits," by N. R. Gibson, Trans. A.S.M.E., 1923, pp. 343–376.

Observations on the Use of Current Meters for Precise Flow Measurement[1]

By L. A. Ott,[2] Kempten, Germany

This paper discusses the circumstances surrounding the development of current meters in Central Europe, and the application of these meters in the testing of large water-power plants. Among the important steps presented in the application of these instruments are, the use in parallel of a plurality of meters, the adoption of simultaneous electric recording by a chronograph, the consequent adoption of water-free contact mechanisms and elimination of the multiplicity of meter types, and standardization of practice.

Reference is made to the practice of attempting to avoid the necessity for properly converting unfavorable measuring sections by using two types of meter having different degrees of error in resolving oblique flow. It is pointed out that precise testing presupposes equally precise rating of meters with duplication of the exact supporting means used in field tests. Standard values for the degree of accuracy of the instruments used in Germany are given, and the accuracy actually obtainable in practice is discussed in the light of comparative tests which have been made.

THE testing of large water-power plants, together with developments in the construction and use of current meters for precise flow measurement, have become farther advanced in Central Europe than elsewhere because of certain favorable circumstances. First, engineers and manufacturers recognized and accepted the fact at an early date that in the construction of hydrometric vanes, the axis of rotation is best placed parallel with rather than normal to the flow. This eliminated unprofitable differences of opinion as to the advantages and disadvantages of cup and screw meters with the result that rapid progress was made. Second, just at the time when the necessity arose for exact water measurements in large water-power plants, we had in Dr. Epper, chief of the Swiss Hydrographic Office, a pioneer in water-measurement technique, who was versed in the solution of problems of measurement in civil and mechanical engineering fields, and who, from his own experience in the testing of meters by towing tests, was able to give instructions for standard procedure. Third, Dr. Epper and other engineers active in the development of water-measurement technique, could always depend on the willing cooperation of a firm with considerable experience in this field, the management of which considered the invention and production of good water-measuring instruments as its life task.

At the present time, it is the predominant opinion of engineers that the simultaneous reading of a number of meters, the indications of which are electrically recorded on a chronograph, affords the most accurate method of measuring water flow in large power plants. This method of water measurement, first applied in 1908 by Prof. Reichel at the testing station for water motors at the Technische Hochschule of Berlin (1),[3] but only introduced in general practice about 1922, is comparatively simple to apply, even in the largest low-head power plants.

The necessity for the use in parallel of a plurality of meters fortunately did not require the development of a new type of instrument in Europe. On the contrary, it reduced the number of types previously used. Among other meters which disappeared from use were the "Weichsel," Epper-Ott Meter IV (2), and the "Iller," Epper-Ott Meter IX, with guard ring (3).

These meters, although very good instruments, disappeared because they possess electric-contact mechanisms accessible to the water. Meters sufficiently free from mutual influence to permit simultaneous operation must have water-free contact, such as found in the "Rhein," Mensing-Ott Meter VI (4), and the "Texas," Ott Meter V (5). Of these two meters, the latter finally has proved itself superior as a result of special advantages derived from the axle bearing of its propeller. Since water measurements in large European plants during the past five years have been conducted with this Ott Meter V, it may be considered as the present European standard.

This meter, like all Ott meters, can be furnished with either a spoke propeller or a spoon propeller. The spoke propeller is a cylindrical screw with three blades, confined by straight lines, and attached to the boss by means of spokes. The spoon propeller is a conical screw with only two blades which form one solid piece with the boss. Although the conical screw has an advantage in that it will not entrap grass and is self-cleaning, this is frequently less important in flow measurements than the advantage of the cylindrical screw with spokes which, with the same diameter and pitch, possesses a smaller error of measurement in a flow which is somewhat oblique to the axis of the instrument.

Since no meter has yet been constructed which correctly records the velocity component normal to the measuring section of obliquities of flow exceeding about 15 deg, great emphasis is placed in Europe on the importance of using a proper measuring section having smooth parallel flow. If such a section is not available, guiding walls and decks are installed and, prior to undertaking tests, preliminary runs are made to prove the acceptability of the measuring section. If the water filaments run reasonably close to parallel in a measuring section, but as a whole run obliquely at a known angle, then the meter axis is not placed normal to the profile but parallel with the flow and the results of the measurement are afterward multiplied by the cosine of the direction angle.

To avoid the necessity of converting unfavorable measuring profiles by guide walls, tests are sometimes made with two instruments with propellers of different cosine characteristics. Corrections are then derived from the difference in results from these two meters. Such tests, however, have not been employed in Europe up to the present because the method doubles the work

[1] Translated by Dr. J. R. Zwickl, chief engineer, refrigerating machinery division, Baldwin-Southwark Corp., Philadelphia, Pa., Assoc-Mem. A.S.M.E., and L. F. Moody, professor of hydraulic engineering, Princeton University, Princeton, N. J. Mem. A.S.M.E.

[2] Mathematik Institut, Kempten, Germany.

Contributed by the Hydraulics Division and presented at the Annual Meeting of The American Society of Mechanical Engineers, New York, N. Y., December 3 to 7, 1933.

[3] Numbers in parentheses refer to similarly numbered references at the end of the report.

of testing and calculating, and greatly increases the duration of the observations for the separate metering points over the time required in the normal method of measuring regular flow. In the normal method, it is a recognized fact that the individual results do not give the actual mean velocities at the individual metering points because of the variation of the stream picture. However, determinations of the exact water velocities at the individual metering points are not important inasmuch as the individual variations equalize out in the final result. In the two-meter method it is probably necessary, as Prof. D. Thoma has pointed out, to determine the actual mean velocities at the separate metering points, with an increase in observation time required for this purpose.

Meter Rating

The high accuracy of measurement necessary for turbine testing, presupposes a correspondingly high accuracy of meter rating, which must be accomplished with the meter supported during the towing tests in exactly the same manner as when it is being used for taking measurement readings. It must also be noted that during the rating tests it is essential that the water be brought to rest between each two runs if accurate results are to be obtained. If a large number of meters are to be calibrated in a limited period, several meters should be towed simultaneously in the rating flume rather than towing each meter individually and shortening the pauses between separate runs. At Kempten, four meters are usually rated at one time, with a fifteen-minute period allowed for bringing the water in the rating flume to complete rest after the test has been made. For larger flumes a longer period of time is required.

A graphical method is employed for recording the results of the rating tests. Although plotting revolutions per second or feet per second as abscissas and feet of travel per revolution as ordinates is convenient in recording the results of meter-rating tests, the method is not well suited for determining the accuracy of the rating or for comparing different ratings because the physical inter-relation between the water velocity, the rotation of the meter vane, and the mechanical and hydraulic resistances occurring in the instrument (for instance, the influence of oil viscosity in the ball bearings) will disappear. It is better, with the same abscissas, to plot as ordinates the corresponding velocity slip (6), that is, the difference, $\Delta = v - kn$, between the velocity v of the towing car and the axial advance of the screw calculated from k, the hydraulic pitch of the propeller, and n, its number of revolutions per second. The properties of the instruments, the special influences of the supporting devices, and the towing procedure are then more clearly defined than in the first method of plotting mentioned. In a good instrument, the scattering of the individual observation points compared to the faired curve should not exceed 0.007 fps over the entire velocity range from 0.4 fps to 10 fps.

If we take this scattering of the rating test points as a measure of the accuracy of measurement of a meter under favorable flow conditions, we see that a relative accuracy of measurement of 1 per cent presupposes a water velocity of about 0.7 fps. For this reason it is specified in the German standards for water measurement that the water velocity in the measuring section should not be less than 0.25 meter per sec or 0.8 fps. In spite of the numerous comparative tests already conducted with various methods of measurement, and in particular the direct volumetric measurement, the degree of accuracy actually attainable in practice still appears to be uncertain. This is not surprising since checking accuracies of measurement of more than 99 per cent is a very delicate matter; particularly the direct volumetric measurement of the large volumes of water which have to be handled in such comparisons, even when a sufficiently large container is available, appears in general not to be a simple matter but, on the contrary, a very difficult problem.

References

(1) *Zeit. V.D.I.*, 1908, vol. 52, p. 1835.

(2) "Effect of Turbulence on the Registration of Current Meters," by David L. Yarnell and Floyd A. Nagler, Trans. Am.Soc.C.E., 1931, vol. 95, p. 772, Fig. 4. Also, "The Rating and Use of Current Meters," by Carl Rohwer, Tech. Bull. No. 3, May, 1933, Colorado Experimental Station, Fort Collins, Plates 7 and 23.

(3) *Schweizerische Bauzeitung*, 1927, vol. 89, p. 102.

(4) "Effect of Turbulence on Registration of Current Meters," by David L. Yarnell and Floyd A. Nagler, Trans. Am.Soc.C.E., 1931, vol. 95, p. 772, fig. 5.

(5) "Research Institute for Hydraulic Engineering," by H. Rouse, Trans. A.S.M.E., 1932, paper HYD-54-3, Fig. 9. Also, "Making Water Measurements With Current Meters," by Sigmund J. Bitterli, *Power*, Jan. 19, 1932, p. 103, fig. 2.

(6) "Hydraulics for Engineers," by R. W. Angus, Pitman, London, 1931, p. 115, fig. 59.

The Psychrograph

By A. M. Norris,[1] Baltimore, Md.

Problems in air-conditioning can be solved quickly and accurately by the use of a psychrograph developed by the author. In this paper, representative problems of the type met with in air-conditioning work are solved on the psychrograph, accompanied by explanations, and illustrate the ease with which the chart can be used in the various cases presented.

The author of this paper has long been impressed by the importance of the relationship expressed by the ratio of sensible-heat input to total-heat input in all air-conditioning calculations. Since a simple proportion will plot as a straight line on ordinary coordinate paper, it was apparent that certain problems could be solved graphically if a psychrometric chart were constructed with equal units of sensible heat and equal units of total heat as coordinates.

The psychrograph is such a chart and was designed for the graphic solution of problems. It has been printed on letter-size sheets, convenient for filing with other calculations; thin paper being used to permit blue printing, should more than one copy of a solution be desired.

An increase in legibility was achieved by inclining the axis of the abscissas and using a vertical axis for the ordinates. This had the effect of lengthening those lines on the psychrograph which indicate dry-bulb temperatures, and, consequently, of increasing the spacing between all of the other inclined and curved lines which cross them.

While the framework of the psychrograph consists of a vertical system of lines representing *total* heat in Btu per pound of dry air and vapor present, crossed by an inclined system of lines representing *sensible* heat in Btu per pound of dry air, the chart has been so designed as to show those functions which are commonly mentioned in the statement of an air-conditioning problem. Therefore, dry-bulb temperatures are shown along the corresponding lines of sensible heat, and wet-bulb temperatures along those of total heat.

It is recognized that, theoretically, dry-bulb lines drawn on such a frame work will have a very slight curvature, due to the sensible heat in the vapor under conditions of partial saturation, but this sensible heat in the vapor is seldom, if ever, considered in an air-conditioning problem; and the specific heat of steam, superheated at very low pressures, seems to be a matter of debate among the authorities. It was therefore disregarded, as its introduction would carry with it complications in calculation of air quantities required, which are not warranted by the possible accuracy of a commercial air-conditioning estimate nor by the accuracy of the instruments which are available for the measurement of results. In the preparation of the psychrograph, Goodenough's "Table of Mixtures of Air and Saturated Water Vapor" was used.

In Fig. 1, the gradient of the dry-air line, a section of which appears on the upper left-hand margin, was determined by referring points on it to the total-heat scale, the total heat in a pound of dry air at any temperature being identical with the sensible heat per pound given in Goodenough's table for that temperature. Within the limits of the chart, this line is straight, as the specific heat of dry air is assumed constant at 0.2416 Btu. Other lines on the psychrograph were plotted from tables calculated by the author, using accepted formulas.

There remains only the scale, *ratio of sensible-heat to total-heat lines.* This scale was constructed by using the heat-ratio-reference center, at the lower left-hand side of the chart, as the origin, and plotting the simple proportion $\frac{\textit{Sensible heat}}{\textit{Total heat}} = N$, for various values of N, on the two heat scales which form the basis or skeleton, of the chart.

The lines so obtained will pass through the origin, or heat-ratio-reference center and points on the scale, *ratio of sensible to total-heat lines.* These lines are only directional in their nature. If any point on the chart is taken and heat added to or deducted from the air represented by this point in a definite ratio of sensible heat to total heat, the direction of change of state must be the direction of the heat-ratio line corresponding to the specific ratio.

The following theorems apply:

Theorem 1. A line drawn parallel to any given heat-ratio line, through any given point on the chart, will be the locus of all changes of psychrometric condition in the air represented by the given point, when heat is added to or deducted from this air in the given ratio of sensible heat to total heat. From this follows:

Theorem 2. When two samples of air are mixed, the locus of all possible psychrometric conditions, for mixtures in varying proportions, must be the straight line joining the two points which represent the psychrometric qualities of the two samples, since one sample must lose heat and the other gain heat in identical quantities and ratios of sensible to total heat; and the two points and the point representing the mixture will all lie on the same heat-ratio line parallel.

An exception to Theorem 2 occurs when the straight line joining the two points crosses and recrosses the saturation curve. In this case, the locus of possible mixtures will follow the saturation curve instead of crossing it, and the quality of mixture will be somewhat uncertain, if less than saturated, as a portion of the vapor present may condense out of the mixture and fail to re-evaporate.

Acknowledgment is made by the author to W. A. Minkler for modifications in the original chart which have increased its legibility and, consequently, materially simplified its use.

Example 1. The use of the psychrograph as an ordinary psychrometric chart is shown in Fig. 1, in which a single point has been taken. Reference to the figure will show that the dry-bulb temperature is 80 F; wet-bulb temperature, 67 F; relative humidity, 51 per cent; dewpoint, 60.4 F; grains of vapor per lb of dry air, 78; cu ft per lb of dry air plus vapor present, 13.84; sensible heat, 19.33 Btu; total heat, 31.10 Btu.

It will readily be seen that if any two of the foregoing char-

[1] Chatard & Norris, Inc. Mem. A.S.M.E. Mr. Norris received the degree of M.E. from Stevens Institute of Technology in 1907 and was then for three years connected with the Consolidated Gas, Electric Light & Power Co., as test engineer. In 1910 he became a member of the firm of Chatard & Norris, Baltimore, Md., contracting engineers and manufacturers' agents. In 1935 he became associated with the engineering office of D. D. Kimball of New York City.

Contributed by the Process Industries Division and presented at a meeting of the Metropolitan Section of The American Society of Mechanical Engineers, New York, N. Y., October 22, 1934.

Discussion of this paper should be addressed to the Secretary, A.S.M.E., 29 West 39th Street, New York, N. Y., and will be accepted until September 10, 1935, for publication at a later date.

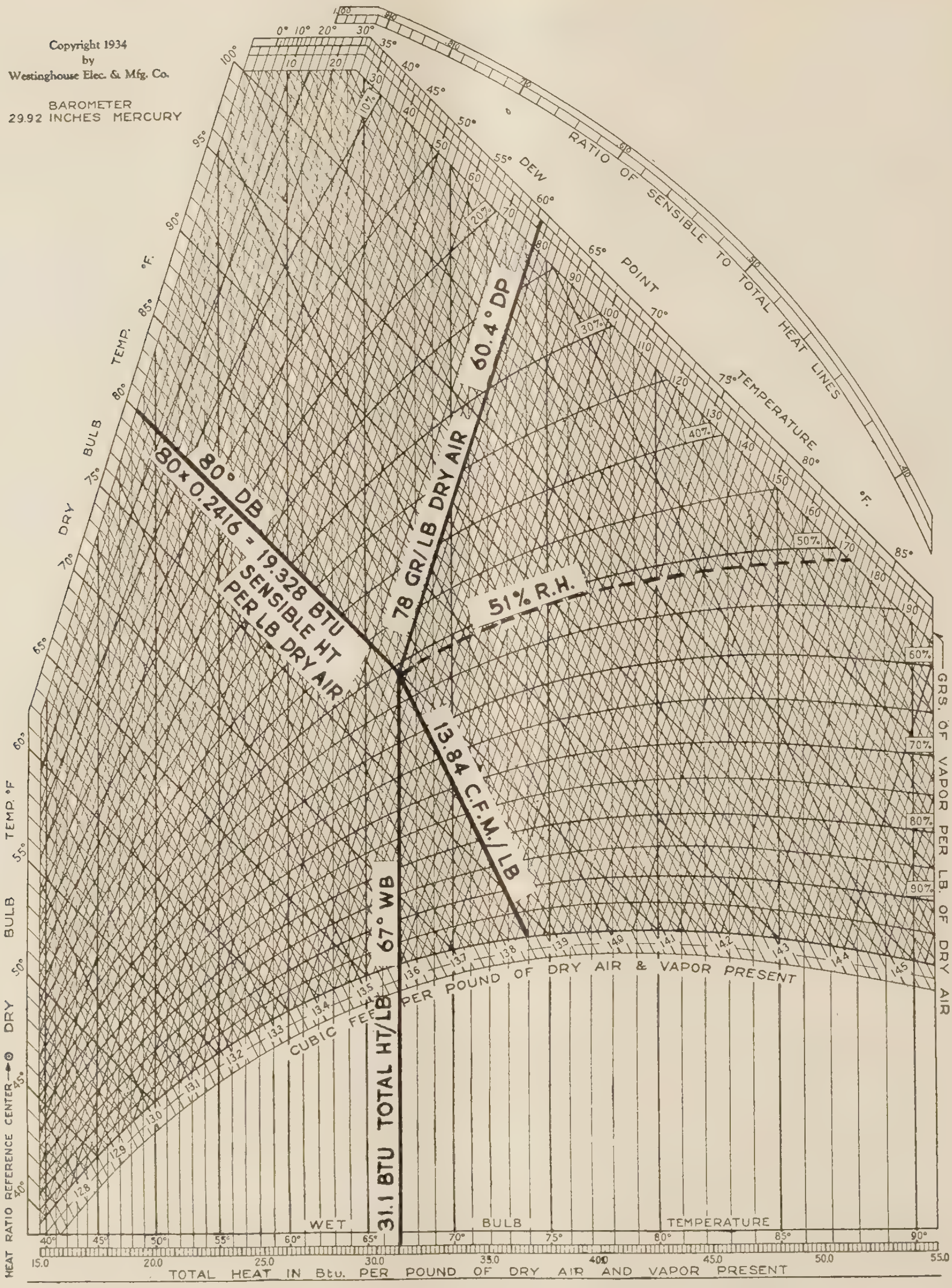

Fig. 1

acteristics are known, and the lines representing them drawn, the intersections of these lines will fix all the other characteristics for the sample.

Example 2. In this problem, in which the dewpoint temperature of 60 F and dry-bulb temperature 75 F, are given. It is desired to find the relative humidity should the dry bulb be increased to 90 F with no moisture added (dewpoint constant).

Referring to Fig. 2, locate the point of intersection of the slant line representing 60 F dewpoint and the slant line representing 75 F dry-bulb temperature.[2] At this point, move obliquely upward and to the right, along the 60 F dewpoint line, to its intersection with the 90 F dry-bulb line. The relative humidity here is read as about 37 per cent. Incidentally, the wet-bulb temperature has increased from about 65 F to approximately 70 F.

Example 3. Given air at 80 F dry-bulb temperature and 58 F wet-bulb temperature, to find the increase in total heat when

[2] When solving problems it is assumed that reference will also be made to Fig. 1 which is a reproduction of the psychrograph.

56 grains of moisture per lb of air are added and the dry-bulb temperature remains at 80 F.

Referring to Fig. 3, locate the point of intersection of the slant line representing the 80 F dry-bulb temperature and the vertical line representing the 58 F wet-bulb temperature. From this point, project upward to the right along the grains per lb line where 36.5 grains per lb is read. The total heat may be read as 24.8 Btu per lb directly from the wet-bulb temperature.

If 56 grains per lb be added, the mixture will contain 36.5 + 56 = 92.5 grains per lb. Locate this quantity on the right-hand scale and then project downward to the left to the intersection with the 80 F dry-bulb temperature line. From this intersection project vertically downward where total heat for the new condition is read as 33.3 Btu per lb. Thus, with the dry bulb remaining constant, the total heat increased from 24.8 to 33.3 Btu per lb, or 8.5 Btu with an increase in moisture content of 56 grains per lb.

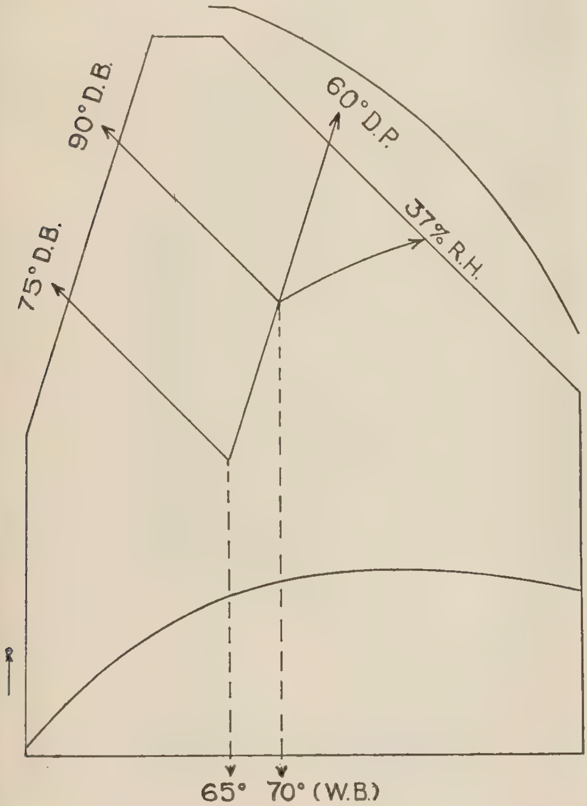

FIG. 2

Example 4. Fig. 4 shows the solution of the problem in which is given air cooled from 80 F dry-bulb temperature and 65 F wet-bulb temperature (about 45 per cent relative humidity) to 60 F dry-bulb temperature and 55 F wet-bulb temperature (72.5 per cent relative humidity), to find the latent heat and sensible heat extracted in cooling.

This example demonstrates a graphical solution that cannot be made directly on any other psychrometric chart. Locate the two points representing the conditions of the air at the two sets of dry-bulb and wet-bulb temperatures. Project vertically downward and read the total heat for the two points as 29.6 and 23.0 Btu per lb of air. Connect the two points by a straight line. Draw a line parallel to this line through the heat-ratio-reference center to the curved scale marked, *ratio of sensible to*

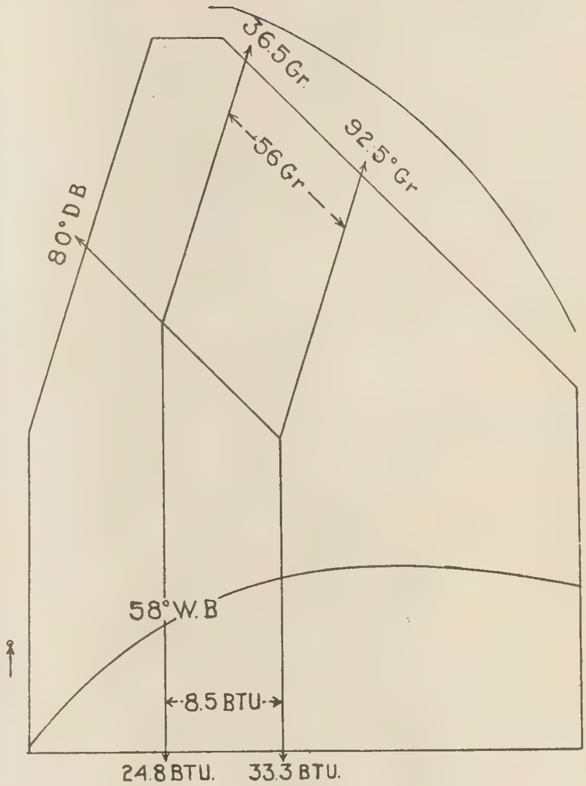

FIG. 3

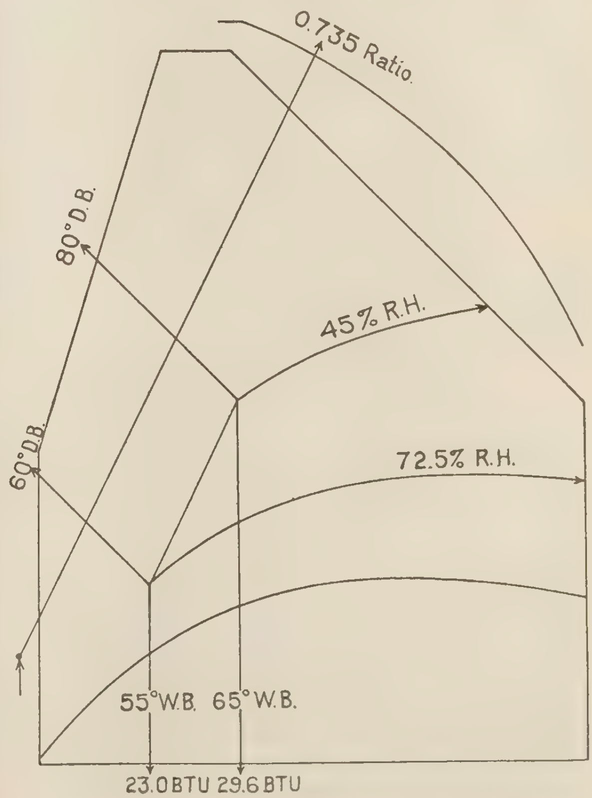

FIG. 4

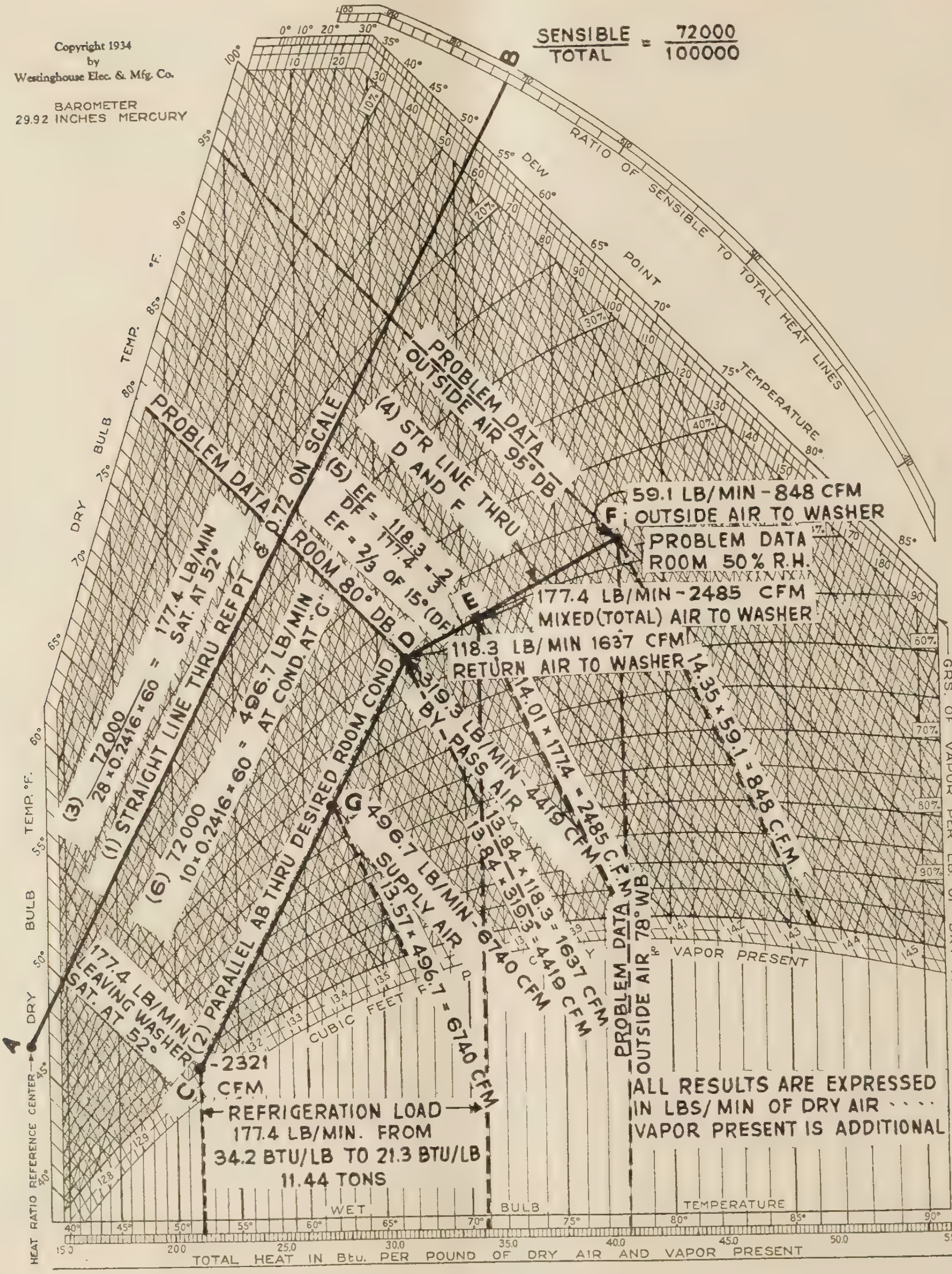

Fig. 5

total-heat lines, and read the ratio as 0.735. The total heat extracted is 29.6 — 23.0 = 6.6; then 6.6 × 0.735 = 4.85 Btu per lb, sensible heat, and 6.6 — 4.85 = 1.75 Btu per lb, latent heat.

The sensible-heat value may be checked by multiplying the dry-bulb-temperature difference by the heat required to raise the temperature of 1 lb of air 1 deg which is 0.2416. This calculation gives 20 × 0.2416 = 4.83 Btu per lb of sensible heat and checks the value from the chart very closely.

Example 5. In Fig. 5 is shown a graphic solution of an air-conditioning problem in which it has been assumed that a by-pass system, using a washer, will be installed.

The outside air is assumed at 95 F dry-bulb and 78 F wet-bulb temperatures, and an allowance of 848 cfm or 59.1 lb per min of outside air for ventilation purposes has been assumed. The desired room condition is 80 F dry-bulb temperature and 50 per cent relative humidity. It is also assumed that a heat estimate has been made and it has been found that the heat load, exclusive of the ventilation air which passes first through the washer,

but inclusive of any infiltration, is 72,000 Btu per hr of sensible heat and 100,000 Btu per hr of total heat, giving a ratio of 0.72.

The heat estimate must be broken down as already outlined because we are interested in the quantity of sensible and total heat liberated in the conditioned space. This heat must be disposed of, or carried out, by the conditioned-air supply, which supply must be raised from its condition at the outlets to the desired room condition by picking up this heat.

The surplus heat above delivery condition in the air for ventilation, which passes first through the washer, is removed in the washer, and thereafter it becomes simply a vehicle for the removal of room heat along with the reconditioned recirculated air. It is also assumed that the desired difference between room and supply air is 10 deg. The problem is solved as follows:

Find point *B*, on the scale, *ratio of sensible to total-heat lines*, corresponding to the ratio of 0.72. Through *B* and the heat-ratio-reference center *A*, draw a straight line *AB*. Find the desired room condition at *D*, representing 80 F dry-bulb temperature and 50 per cent relative humidity. Through point *D* draw a straight line *CD*, parallel with *AB* and intersecting the saturation curve. In accordance with Theorem 1, this line *CD* will be the locus of all possible delivery airs which will give the desired room condition, since the delivery air must pick up heat in the ratio $\frac{\textit{sensible}}{\textit{total}} = 0.72$ to finally reach this desired room condition, and therefore the point *G* at 70 F dry-bulb temperature will be the desired quality of the delivery air. This delivery air may be obtained by mixing room air at condition *D* and saturated air at condition *C* in the proper proportion, which will be 10 parts of saturated air at condition *C* to 18 parts of room air at condition *D*, since the heat lost by the air at condition *D* equals 10 deg drop times the quantity of air at condition *D* in pounds of dry air per unit of time, multiplied by the specific heat of 1 lb of dry air, and this in turn will equal the heat gained by the air at condition *C*, which equals 18 deg rise times the quantity of air at condition *C* in pounds of dry air per unit of time, multiplied by the specific heat of 1 lb of dry air. Eliminating common factors and transposing, it may be expressed as: The quantity of air at condition *C* is to the quantity of air at condition *D* as 10 is to 18 or as *DG* is to *CG*.

Since all of the refrigeration is applied to the saturated air, which must have sufficient capacity to remove 72,000 Btu per hr of sensible heat, this value divided by the temperature rise of 28 deg of the saturated air to 80 F, by the specific heat of a pound of air (0.2416) and by 60 min, will give 177.4 lb per min of air saturated at 52 F as required.

It is also possible to figure the delivery air at 70 F in the same manner by dividing 72,000 Btu per hr by 10 deg temperature difference by specific heat of a pound of air (0.2416) and by 60 min to obtain 496.7 lb of delivery air per min. Then 496.7 − 177.4 = 319.3 lb per min of room air through the bypass to give the desired mixture, and the ratio $\frac{177.4}{319.3} = \frac{10}{18}$.

By Theorem 2, the condition of the air to the washer may be obtained by drawing a straight line through the point *D*, representing the room condition, and point *F*, representing the outside-air condition of 95 F dry-bulb and 78 F wet-bulb temperatures. Under the terms of the problem, there must be 59.1 lb per min of outside air, and the air through the washer is 177.4 lb as already stated. Then 177.4 lb − 59.1 lb = 118.3 lb of return or room air which must mix with the outside air to pass through the washer. Since the temperature difference between *D* and *F* is 15 deg and the ratio of outside air to return air is $\frac{59.1}{118.3} = \frac{1}{2}$, *EF* must be twice the distance *DE*, and the point *E* falls on the 85 deg dry-bulb line. This is another way of stating the relationship from that given on the graphic-solution diagram, but it will be clear that $DF \times 118.3 = EF \times 177.4$; or $\frac{EF}{DF} = \frac{118.3}{177.4} = \frac{2}{3}$, which is to say, *EF* equals $\frac{2}{3}$ of 15 deg or 10 deg.

All of the results given have been expressed in pounds per minute of dry air, the vapor present being additional. Reference to the diagram will indicate the method of converting all of these quantities into cubic feet per minute. For instance, at the point *F*, a pound of dry air plus the vapor present will occupy 14.35 cu ft and 14.35 × 59.1 lb = 848 cfm.

In the same manner, the cubic feet per pound for point *E* was determined to be 14.01; for point *D*, 13.84; for point *G*, 13.57 and for point *C*, 13.08.

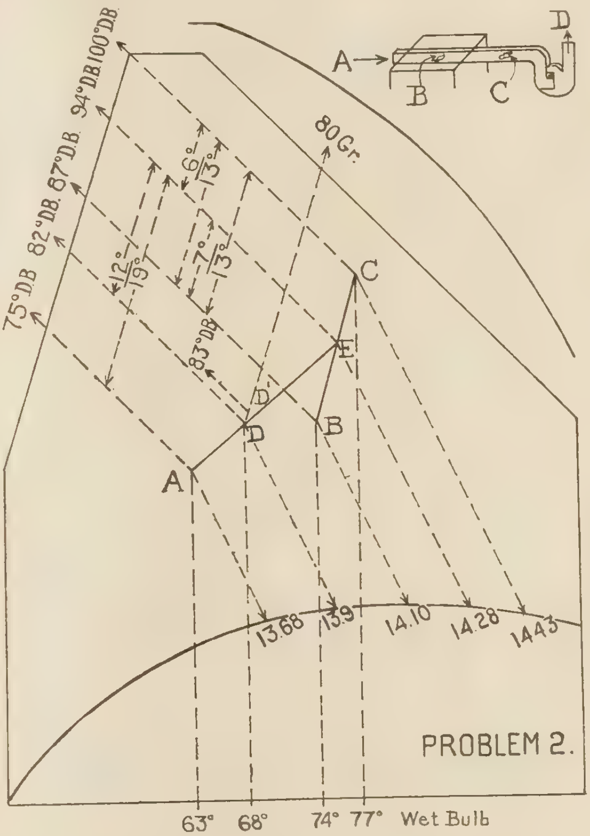

FIG. 6

It will be seen that the mixtures check out on the cubic feet per minute basis, as 848 cfm of outside air mixed with 1637 cfm of room or return air will total 2485 cfm of air to the washer, and 4419 cfm of room air mixed with 2321 cfm of washer air will result in a mixture of 6740 cu ft of delivery air.

The refrigeration required may be figured by projecting point *E*, which represents the air to the washer, to the Btu scale at the bottom of the chart, and obtaining 34.2 Btu per lb; also project point *C*, which is the saturated air, to the Btu scale, and read 21.3 Btu per lb; which is to say that each pound will have 12.9 Btu removed from it in passing through the washer. Since 177.4 lb per min of air at condition *C* passes through the washer and from each pound we remove 12.9 Btu, the total refrigerating load will be 11.44 tons.

It is, of course, obvious that this problem has been worked out

in far greater detail than is usually required. This was done to illustrate the complete information which can be obtained from a graphic solution.

Example 6. In Fig. 6 is shown the graphic solution of a problem in detecting air leakage.

The fact that the point on the psychrograph representing a mixture of two different samples of air will fall on a straight line joining the points representing the air samples and the fact that the dry-bulb temperature difference, between the mixture and the original samples, determines the proportion of the mixture, have been made use of in the solution of this problem.

The small drawing in the upper right corner indicates the original data. A duct drawing air from chamber A in which the condition is dry-bulb temperature 75 F, wet-bulb temperature 63 F, passes through chamber B, in which the condition is 87 F dry-bulb temperature, 74 F wet-bulb temperature, and through chamber C, in which the condition is 100 F dry-bulb temperature and 77 F wet-bulb temperature. Assuming perfect insulation, the delivery air at point D should be 75 F dry-bulb temperature and 63 F wet-bulb temperature, or the same as at A. Actually, the condition at point D is 82 F dry-bulb temperature and 68 F wet-bulb temperature and the anemometer reading at this point gives 13,900 cfm, which is equal to 1000 lb per min of dry air plus vapor present.

The problem is to find the leakage into the duct in compartments B and C. It will be obvious that this leakage must be a mixture of air at condition C and air at condition B and must therefore fall on the straight line BC; and that this mixture must combine with air at condition A to give the condition at D. Since the condition at D is known and has been plotted on the chart, the straight line passing through A and D, prolonged to cut line BC at E, will fix the leakage mixture. Since there are 1000 lb of air per min being delivered at D, the amount of air drawn in at A must be equal to $\frac{DE}{AE} \times 1000 = \frac{12}{19} \times 1000 = 632$ lb per min. Hence the quantity of leakage at condition E must be 368 lb per min or 1000 lb less 632 lb, and the quantity of air at condition B plus the quantity of air at condition C, must equal 368 lb per min, divided in the ratio $C = 7/13 \times 368 = 198$ lb per min and $B = 6/13 \times 368 = 170$ lb per min. The quantities expressed in pounds per minute may be converted into cubic feet per minute by the use of the scale of cubic feet per pound of dry air and vapor present, which will give the following readings: Point D, 13.9 cu ft per lb; point A, 13.68 cu ft per lb; point E, 14.28 cu ft per lb; point C, 14.43 cu ft per lb; point B, 14.10 cu ft per lb.

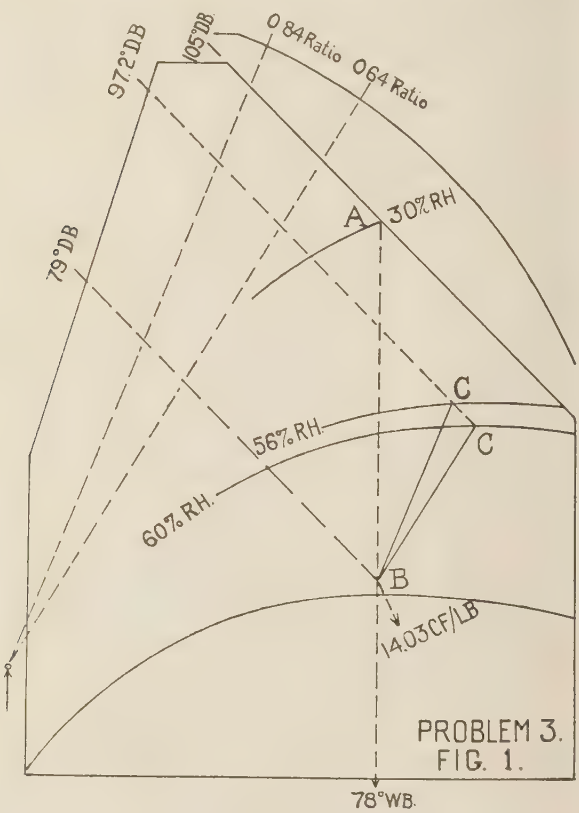

Fig. 7

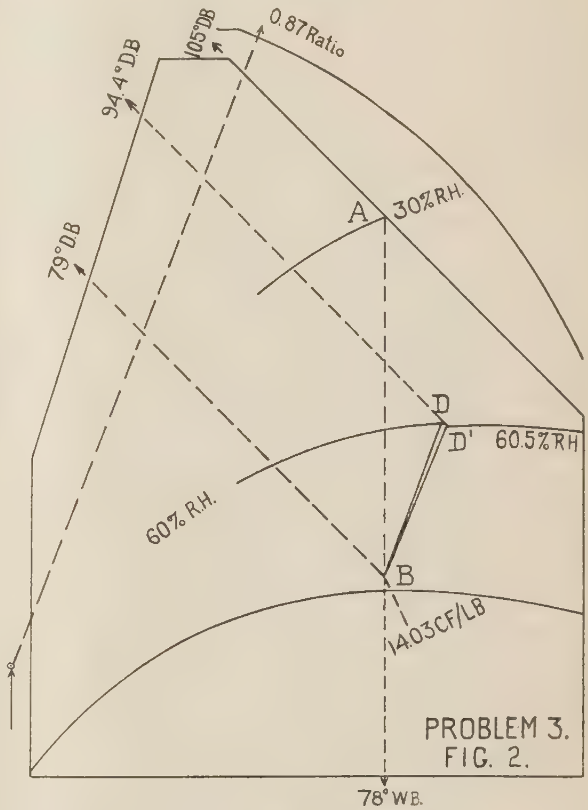

Fig. 8

Multiplying out the respective quantities expressed in pounds, gives 13,900 cfm at point D; 8645 cfm at point A; 5255 cfm at point E; and $A + E = 13{,}900$ cfm. Also 2857 cfm at point C; 2397 cfm at point B; and $C + B = 5254$ cfm.

It will also be noted that the same answers might have been obtained graphically had we used any other combination of the mixtures. In other words the line AB might have been drawn representing the mixtures of airs at conditions A and B and the line DC prolonged to cut AB at E', or a line AC might have been drawn and the line DB prolonged to cut AC at E''. In any case the calculated results would be identical.

For the purpose of this problem, we have assumed that there will be no transmission of heat through the duct walls other than by air leakage. However, any transmission of sensible heat through the duct walls can be calculated and reduced to a temperature rise for the air flowing through the duct expressed in

degrees of dry-bulb temperature. Let us assume that the air leaving the fan has a condition D' and has picked up 1 deg due to temperature head across duct walls. We may follow the line of constant moisture content *from* D' for 1 deg F dry bulb to point D and this point may be used for the solution of the problem just as it has been used in the problem as given.

It is the belief of the author that a great deal of information concerning air flows can be obtained by the intelligent use of wet- and dry-bulb thermometers.

Example 7. In this problem, which is graphically solved in Figs. 7 to 9, it is desired to select a standard washer and to maintain a constant relative humidity of 60 per cent in the room.

The heat estimate has revealed the following data: Sensible heat due to temperature difference T between the outside and room temperatures is 150 Btu per min per deg difference; sensible heat from lights, power, and people (a constant) is 400 Btu per min; latent heat is approximately 300 Btu per min (exact determination may depend on final obtainable room condition, which is not known at this stage of the problem; maximum observed temperature outside is 105 F; minimum outside relative humidity is 30 per cent; no return air is in circulation.

There are standard washers available in sizes of 2000 cfm, 5000 cfm, 7500 cfm, and 10,000 cfm. The washers are equipped with bypass of air around spray chamber and are guaranteed to have capacity to bring the leaving air to within 1 deg of the spray temperature.

It is desired (1) to select a standard washer which will maintain a constant relative humidity of 60 per cent in the room; (2) having selected the washer, to determine the room temperature when the outside air is 80 F dry bulb and 67 F wet bulb, the relative humidity in the room to be maintained at 60 per cent; (3) to determine the proportion of outside air at 80 F dry bulb and 67 F wet bulb which must be mixed with washed air to maintain 60 per cent relative humidity in the room. To solve:

(1) *To determine the spray temperature* for maximum conditions, plot 105 F dry bulb and 30 per cent relative humidity at A and read approximately 78 F wet bulb which will be the temperature which the spray will assume. The washer guarantee then fixes the leaving-air condition at B, with a dry-bulb temperature of 79 F and a wet-bulb temperature of 78 F. Since the air has neither gained nor lost total heat in passing through the spray the wet bulb must remain constant at 78 F.

Let the temperature rise of the circulated air, from condition B to the room temperature, equal T'.

Then T (the temperature difference between outside and room) + T' (the temperature rise from condition B to room temperature) must equal 105 deg (the outside temperature) minus 79 deg (the temperature at condition B), or 26 deg.

$$T + T' = 26 \therefore T' = 26 - T$$

The sensible-heat input to the room will be $150\,T + 400$.

The trial of the 5000-cfm washer is made in Fig. 7. The 5000-cfm washer will deliver $\frac{5000}{14.03} = 356$ lb of air per min.

Then $150\,T + 400 = T' \times 356 \times$ specific heat of air, as sensible-heat input, must equal the heat picked up by the circulated air. Therefore, if the 5000-cfm washer is selected, $150\,T + 400 = (26 - T)\,356 \times 0.2416$, or $T = 7.8$ deg.

Plot C, $105 - T = 97.2$ F on the 60 per cent relative-humidity line and draw BC' which is parallel with the 0.64 heat-ratio line.

It will be seen that the 5000-cfm unit will not have sufficient humidifying capacity, since from the problem data for the room at 97.2 F dry-bulb temperature, sensible heat $= 150\,T + 400 = 1570$ Btu per min, latent heat $= 300$ Btu per min, and total heat $= 1870$ Btu per min. Then $N = \frac{1570}{1870} = 0.84$

Draw $N = 0.84$ through B to C' at 97.2 F dry bulb and read 56 per cent relative humidity. Therefore try the next larger size washer.

The trial of the 7500-cfm washer is made in Fig. 8. Locate A and B as in Fig. 7.

As the 7500-cfm washer will deliver $\frac{7500}{14.03} = 534$ lb of air per min, then

$$150\,T + 400 = (26 - T)\,534 \times 0.2416, \text{ or}$$
$$T = 10.6 \text{ deg}$$

Plot D, $105 - T = 94.4$ F dry bulb, on the 60 per cent relative-humidity line and draw BD.

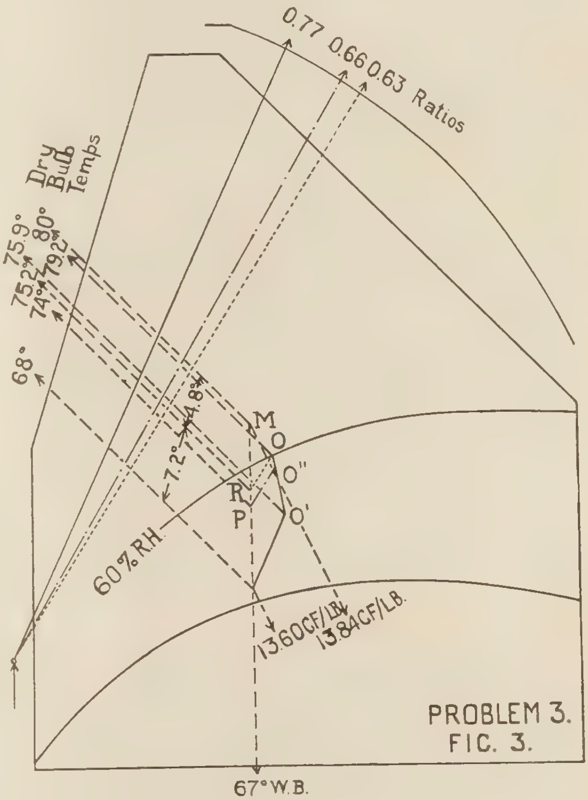

FIG. 9

In this case, sensible heat $= 150\,T + 400 = 1990$ Btu per min, latent heat $= 300$ Btu per min, and total heat $= 2290$ Btu per min. Then $N = \frac{1990}{2290} = 0.87$. Therefore, draw the heat-ratio line $N = 0.87$ through B to D' to show that the 7500-cfm unit will have capacity to humidify to 60.5 per cent relative humidity.

Use of the bypass to mix the dry outside air with the practically saturated washer air will maintain the desired condition of 60 per cent at a room temperature between 94 F and 95 F and the 7500-cfm unit will be the correct selection, if the room condition obtained does not result in a material change in the latent-heat load from the assumed value of 300 Btu per min.

An increase in the latent-heat-load calculation for the final room condition will have the effect of reducing the value of N, swinging D' in a clockwise direction, which will only result in the

use of a greater amount of dry bypass air to maintain the desired room humidity.

It is, therefore, necessary only to recheck the work when the latent-heat load is materially decreased as a result of a preliminary determination of the room condition.

(2) *To determine the room temperature* as shown in Fig. 9 when the outside air is at 80 F dry-bulb and 67 F wet-bulb temperatures with the 7500-cfm unit operated to maintain 60 per cent relative humidity in the room, locate point M representing the outside-air condition at 80 F dry bulb and 67 F wet bulb, the point S representing the condition of the air leaving the spray chamber at 68 F dry bulb and 67 F wet bulb and solve the equations

$$T + T' = 12 \therefore T' = 12 - T$$
$$150\,T + 400 = T' \times 536 \times 0.2416$$

Substituting, $150\,T + 400 = (12 - T)\,129$, or

$$T = 4.1 \text{ deg}$$

Then, sensible heat $= 150\,T + 400 = 1015$ Btu per min, latent heat $= 300$ Btu per min, and total heat $= 1315$ Btu per min. Then

$$N = \frac{1015}{1315} = 0.77$$

Draw the heat-ratio line $N = 0.77$ through point S to cross the $80 - T = 80 - 4.1 = 759$ F dry-bulb line at O'. This represents the approximate condition obtainable if all the air passes through the spray chamber.

Now, assuming that one-half of the circulated air passes through the spray chamber, the mixed air leaving the washer discharge will have the condition P or 74 F dry bulb and 67 F wet bulb. Then

$$T + T' = 6 \therefore T' = 6 - T$$
$$150\,T + 400 = (6 - T) \times 129, \text{ or}$$
$$T = 1.3 \text{ deg}$$

In this case, sensible heat $= 150\,T + 400 = 595$ Btu per min, latent heat $= 300$ Btu per min, and total heat $= 895$ Btu per min. Then

$$N = \frac{595}{895} = 0.66$$

Proceed as above to plot point O'', which represents the approximate condition obtainable if half the air passes through the spray chamber. Since O'' is close to the 60 per cent relative-humidity line, we may disregard a possible curvature in the line $O'O''$ which will represent the conditions obtained by successive proportions of a mixture of washed air and room air, from all washed air to half washed air and half room air, and we may extend the straight line $O'O''$ to cut the 60 per cent relative-humidity line at O at a dry-bulb temperature of 79.2 F.

Hence at 60 per cent relative humidity $T = 0.8$ deg and we may solve for the difference t between the outside temperature and the temperature of the mixed air leaving the washer to produce a room condition of 79.2 F dry bulb, 60 per cent relative humidity as follows:

$$150\,T + 400 = (t - T) \times 129$$

Substituting $T = 0.8$

$$150 \times 0.8 + 400 = (t - 0.8)\,129, \text{ or}$$
$$t = 4.8 \text{ deg}$$

Under this room condition, sensible heat $= 0.8 \times 150 + 400 = 520$ Btu per min, latent heat $= 300$ Btu per min, and total heat $= 820$ Btu per min. Then, $N = \dfrac{520}{820} = 0.63.$

It will be seen that these results check as the mixed air leaving the washer will have a condition at R of $80 - t = 80 - 4.8 = 75.2$ F dry bulb and 67 F wet bulb, and the heat-ratio line, $N = 0.63$, drawn through the point R, will pass through point O.

(3) It will also be seen from the diagram that:

x lb of outside air at condition M will cool through 4.8 deg in heating y lb of spray-chamber air at condition S through 7.2 deg. Hence the ratio, by weight, $\dfrac{\text{spray-chamber air}}{\text{outside air}} = \dfrac{4.8}{7.2} = \dfrac{2}{3}$; or

$\dfrac{2}{5}$ of the total air delivered is spray-chamber air $= 213.6$ lb per min

and $\dfrac{3}{5}$ of the total air delivered is outside air $= 320.4$ lb per min

making the total air delivered 534 lb per min.

These values expressed in pounds of dry air per minute may

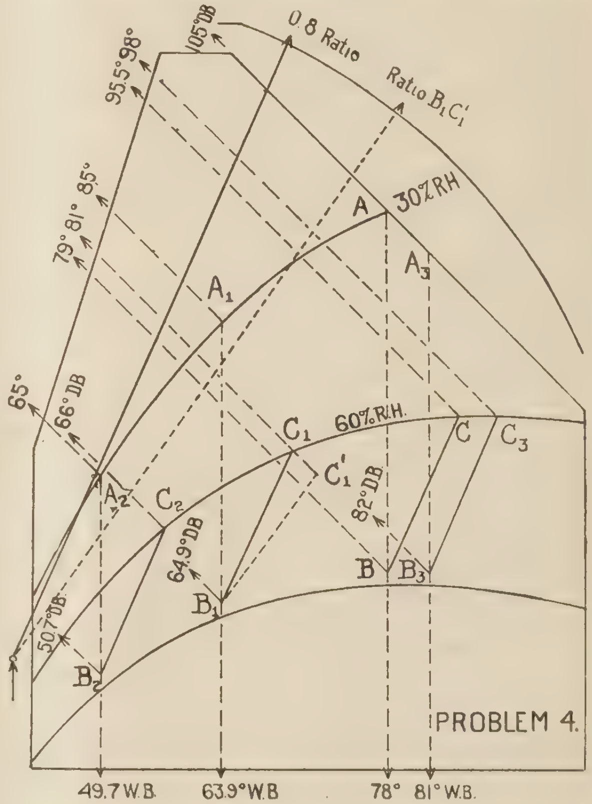

FIG. 10

be converted to cubic feet per minute by multiplying each by its corresponding cubic feet per pound of dry air as taken from the chart.

$$213.6 \times 13.60 = 4434 \text{ cfm}$$
$$320.4 \times 13.84 = 2905 \text{ cfm}$$
$$534 \times 13.74 = 7337 \text{ cfm}$$

In this problem we have assumed the fan delivery as constant in pounds per minute in order to use similar appearing equations. Of course, corrections can be made from actual fan data for varying conditions of intake, but the method of solution remains unchanged.

Example 8. In this problem, which is plotted in Fig. 10, it is desired to determine design conditions in an air-washer installation to maintain constant relative humidity. It is assumed: (1) that no refrigeration is available; (2) that the washer water is recirculated hence the washer water must acquire the tempera-

ture of the wet-bulb of the air passing through the washer; (3) that no room air is recirculated, all the air from the washer being taken from outside; (4) that it is desired to maintain a constant relative humidity and the lowest room temperature which is consistent with the maintenance of this relative humidity; and, (5) that the control mechanism will start and stop the sprays.

The plant should be designed to take care of some maximum outside condition of dry-bulb temperature and minimum outside relative humidity.

It should be kept in mind that the spray can neither add nor subtract any heat to or from the air which passes through it, as long as this air remains at a constant wet-bulb temperature. The spray will, however, change some of the sensible heat in the air to latent heat.

In the diagram, it is assumed that the plant has been designed to meet a condition of 105 F dry bulb and 30 per cent relative humidity outside, that the desired room relative humidity is 60 per cent and that the unit selected is just sufficient in capacity to humidify to 60 per cent when all of the air is washed. Reference to the preceding example, illustrating the selection of a washer, will show that this is a special case, as usually the washer will have some excess capacity for humidification, to be corrected by bypassing or closing the spray-water valve. The special case is chosen because it represents the minimum washer which will meet the outside conditions specified.

The method of determining the room temperature and the slope of the heat-ratio or N line has been fully explained in the preceding example and it is assumed that in this case the resulting room temperature is 95.5 F and that $N = 0.8$. This assumed relationship is indicated by $A\ B\ C$, where A represents the outside condition, 105 F dry bulb, 30 per cent relative humidity, AB represents the outside wet-bulb temperature and consequently the spray temperature, B represents the condition of the air leaving the washer, BC represents the 0.8 heat-ratio line, and C represents the resulting room condition at 95.5 F dry bulb and 60 per cent relative humidity.

It may be demonstrated that this installation will be adequate for any other probable condition inside the limits given as follows:

Now assume an outside condition of 85 F dry bulb and 30 per cent relative humidity. Construct a new figure A_1, B_1 and C_1, in which B_1C_1 is the heat-ratio line 0.8. It will be seen that this will result in a temperature difference between outside and inside of only 4 deg or less than in the basic case. This reduced temperature difference will result in a decrease in the sensible-heat load and consequently in a decrease in the heat ratio with a consequent rotation of the heat-ratio line in a clockwise direction around B, and in a decrease in the temperature rise of the air to absorb the sensible heat. Let the new heat-ratio line be B_1C_1'. It will be seen at once that under these outside conditions the apparatus will now have surplus capacity for humidification and that the sprays may be shut off for part of the time.

There is also shown on the chart a diagram $A_2B_2C_2$ for an outside condition of 65 F and 30 per cent relative humidity and one $A_3B_3C_3$ for 105 F and 36 per cent relative humidity. Again, in each case the sensible-heat load is reduced below that in the basic case and, therefore, in each of these cases the N lines or heat-ratio lines B_2C_2 and B_3C_3 will be swung in a clockwise direction and shortened by a reduction in the sensible-heat pickup. This reduction must be handled by the fixed quantity of circulated air, and, therefore, in each case the sprays will be on and off and the washer will have excess capacity.

These examples show (*a*), that a reduction in dry-bulb temperature, with constant relative humidity, results in a decrease in required capacity; and (*b*), that an increase in relative humidity with constant dry-bulb temperature, results in a decrease in required capacity. They prove the correctness of the original statement that the plant should be designed to take care of some maximum condition of outside dry-bulb temperature and minimum outside relative humidity.

Discussion

A Mathematical Solution of the Rotor-Balancing Problem[1]

E. L. Thearle.[2] In general, a balancing weight placed on any one end of a rotor affects the vibration of both pedestals. When balancing some very long rotors, however, it may be convenient to assume that the vibration of any one pedestal is influenced only by balance weights placed in the nearest correction plane. The author of the paper under discussion is to be congratulated on his solution of the problem as it exists for such cases where the end of a machine may be treated independently, and when vibration phase angles cannot be conveniently measured.

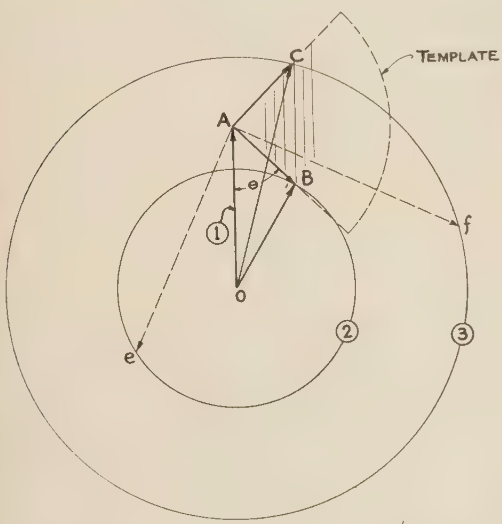

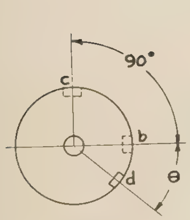

Fig. 2

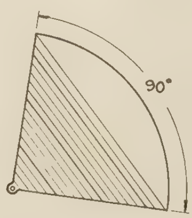

Fig. 3

A simple solution of the problem by a somewhat different method is herewith presented. The rotor is run, without a trial weight, and the vibration amplitude is measured. The amplitude is represented by the vector OA in Fig. 1, which is drawn in any direction with a length proportional to the measured amplitude. A trial weight on any known amount is placed on the rotor in any position b, Fig. 2. The rotor is again run and the vibration amplitude is measured. The circle 2, Fig. 1, is drawn with its center at O, and with a radius proportional to this second amplitude reading. The same trial weight is then shifted, say 90 deg, in a counter-clockwise direction, to the new position c. After the third run amplitude is measured, the circle 3 is drawn with a center at O, and a radius proportional to this third amplitude.

The vectors AB and AC, representing the effects of the trial weight in positions b and c, respectively, must be 90 deg apart in the same respect as the trial-weight positions, equal in length, and must terminate on the circles 2 and 3, respectively. Their correct positions are readily determined by swinging a ruled template, such as shown in Fig. 3, about the point A in Fig. 1 until its edges intersect the two circles at points equidistant from A.

Then the effect of the trial weight, in position b, for instance, is the vector AB. It is obvious from Fig. 2 that if this trial weight is shifted in a clockwise direction, from position b, through the angle θ, and the amount of the weight is multiplied by the ratio OA/AB, its effect will be equal and opposite to the original vibration OA, which will, therefore, be annulled.

Of course, the angle through which the trial weights are shifted need not be 90 deg but may be any convenient angle, with the template made accordingly.

This method has the important practical advantage that all construction may be kept within the bounds of a single sheet of paper while, when several measured amplitudes are almost equal, the method presented in the paper herein being discussed may involve striking arcs with very long radii.

The two possible solutions mentioned by the author are made apparent by this method, as shown by vectors e and f, Fig. 1. Possibly the quickest way of determining which solution is correct is to try the easier one.

Tandy A. Bryson.[3] In discussing Mr. Bromberg's paper, it is suggested that there may be many occasions when it is inconvenient to use a drawing board for the graphical solution, in which case definite mathematical formulas are of value.

In Fig. 4 let eU be the vector which represents the amplitude of vibration caused by the unknown unbalance U located at the unknown angle φ from an arbitrary reference line O-X which may be marked on the rotor. In this term eU, U represents the mass of unbalance in ounces, pounds, etc., which is located at some assumed radius r from the axis of rotation; while e is a composite factor to convert the term into an expression of unbalance in units of amplitude of vibration. The factor e, therefore, embraces consideration of the radius of the unbalanced mass, the necessary conversion factors, and the stiffness of the rotor supports. For any particular test set-up this factor is a constant because it may be assumed that all

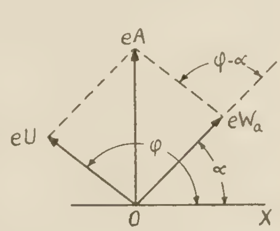

Fig. 4

[1] Published as paper APM-56-14, by Jacob Bromberg, in the October, 1934, issue of the A.S.M.E. Transactions.

[2] General Electric Company, Schenectady, N. Y. Assoc-Mem. A.S.M.E.

[3] Consulting Engineer, American Tool and Machine Company, Boston, Mass. Mem. A.S.M.E.

test weights are placed at the same radius and that the rotor supports are not stressed beyond the range of Hooke's law of proportionality.

In like manner, eW_a represents the amplitude which would be caused by the test weight W_a placed on an otherwise balanced rotor at the radius r and at the known angle α from the line of reference. Obviously, eW_a may not be measured by test since it is blanketed by the effect of the unbalance. However, it is possible to measure the length of eA, the resultant of eU and eW_a, thus obtaining one element of the data from which U and φ may be computed.

Writing the equation for eA

$$\begin{aligned}\overline{eA}^2 &= \overline{eU}^2 + \overline{eW}^2_a + 2e^2UW_a\cos(\varphi - \alpha)\\ &= \overline{eU}^2 + \overline{eW}^2_a + 2e^2UW_a(\cos\alpha\cos\varphi + \sin\alpha\sin\varphi)\end{aligned}$$

Since this equation contains three unknowns, U, e, and φ, it is necessary to apply three separate test weights, W_a, W_b, and W_c, at the constant radius r (or to make suitable correction if the radial location change) and at known angles, α, β, and λ, from the reference line and to measure the amplitudes eA, eB and eC caused by each in cooperation with the unbalance. Using equal test weights at the three different positions and solving the equations, there results

$$\tan\varphi = \frac{(\overline{eA}^2 - \overline{eC}^2)(\cos\alpha - \cos\beta) - (\overline{eA}^2 - \overline{eB}^2)(\cos\alpha - \cos\lambda)}{(\overline{eA}^2 - \overline{eB}^2)(\sin\alpha - \sin\lambda) - (\overline{eA}^2 - \overline{eC}^2)(\sin\alpha - \sin\beta)} \quad \ldots\ldots\ldots[1]$$

Letting

$$x = (\cos\alpha - \cos\lambda)\cos\varphi - (\sin\alpha - \sin\lambda)\sin\varphi$$

$$y = \cos\alpha\cos\varphi + \sin\alpha\sin\varphi$$

Solve for U

$$U^2 + 2WU\,\frac{(\overline{eA}^2 - \overline{eC}^2)y - \overline{eA}^2x}{\overline{eA}^2 - \overline{eC}^2} = -W^2$$

$$e^2 = \frac{\overline{eA}^2 - \overline{eC}^2}{2WUx}$$

While these formulas appear somewhat forbidding, their evaluation is actually quite simple if the test data and the values of the trigonometric functions are placed in orderly tabulation such as is shown in Table 1. The use of the listed data will be made clear by application to the author's first problem, wherein equal test weights of 23 oz were used.

TABLE 1 TABULATION OF DATA

$W_a = W_b = W_c = W = 23$ oz; $W^2 = 529$

$\overline{eA}$ =	30[a]	$\overline{eB}$ =	21	$\overline{eC}$ =	19
$\overline{eA}^2$ =	900	$\overline{eB}^2$ =	441	$\overline{eC}^2$ =	361
α =	25.71	β =	64.29	λ =	102.84
$\cos\alpha$ =	0.901	$\cos\beta$ =	0.434	$\cos\lambda$ =	—0.222
$\sin\alpha$ =	0.434	$\sin\beta$ =	0.901	$\sin\lambda$ =	0.974

$\overline{eA}^2 - \overline{eB}^2$ =	459	$\overline{eA}^2 - \overline{eC}^2$ =	539
$\cos\alpha - \cos\beta$ =	0.467	$\cos\alpha - \cos\lambda$ =	1.123
$\sin\alpha - \sin\lambda$ =	—0.540	$\sin\alpha - \sin\beta$ =	—0.467

[a] Unit of measurement = 0.0001 in.

Substituting in Equation [1], the values listed in Table 1

$$\tan\varphi = \frac{539(0.467) - 459(1.123)}{459(-0.540) - 539(-0.467)} = -75.6$$

The negative sign indicates that the unbalance is located in either the second or fourth quadrants. Since the test weight $W_c(Sc)$ in the second quadrant caused a reduction in amplitude, it acted opposite to the unbalance which, in consequence, is in the fourth quadrant. Accordingly, φ = 270.36 deg, $\cos\varphi$ = 0.0132, and $\sin\varphi$ = —0.9999. Therefore

$$x = 1.123(0.0132) - 0.540(0.9999) = 0.555$$

$$y = 0.901(0.0132) - 0.434(0.9999) = -0.422$$

$$U^2 + 46U\,\frac{539(-0.422) - 900(0.555)}{539} = -529$$

$$U^2 - 61.8U = -529$$

$$U = 51.57 \text{ oz (or } 10.23 \text{ oz)}$$

$$e^2 = \frac{539}{46(51.57)0.555} = 0.410$$

$$e = 0.640$$

$$eU = 0.640(51.57) = 33.0$$

The test of the rotor without trial weights showed eU = 29, which, when compared with the computed amplitude of 33, serves as a measure of the test and computation accuracy. (It should be said here that the above are slide-rule computations.) The comparison also indicates that U = 51.57, rather than 10.23; although proof of this fact may also be obtained by inserting the computed values in the original equation for $\overline{eA}^2$.

The above method may be used for any three locations of the trial weights. However, it is desirable and usually possible to locate the trial weights in such manner as to simplify the computations to a large degree. By making α = 0, β = 90, and λ = 180, the formulas reduce to

$$\tan\varphi = 1 - 2\,\frac{(\overline{eA}^2 - \overline{eB}^2)}{(\overline{eA}^2 - \overline{eC}^2)};\quad U^2 - 2WU\,\frac{(\overline{eA}^2 + \overline{eC}^2)}{(\overline{eA}^2 - \overline{eC}^2)}\cos\varphi = -W^2$$

$$e^2 = \frac{\overline{eA}^2 - \overline{eC}^2}{4\,WU\cos\varphi}$$

Thomas C. Rathbone.[4] The author describes his method for determining the amount and location of the balance correction at one end of the rotor as applicable to the test results obtained on the conventional dynamic-balancing machine and proposes it as an improvement over the mechanical solution devised by Prof. G. B. Karelitz. Professor Karelitz actually devised his system for use on turbine generators under operating conditions in the field, as well as on test machines, and the writer, being associated with Professor Karelitz during these early attempts at field balancing, can vouch for the successful application of his method on a number of installations. In the writer's opinion, the semiautomatic graphical method may be more readily used for averaging the data by the man in the field.

The balancing method described by the author is based on vibration amplitudes alone. Actually, vibration is characterized by its phase relation to the disturbing force, as well as by its amplitude, and is of equal importance, otherwise, no vector solution would be tenable. During the earlier investigations of field balancing, the writer devised a method for solving the problem by means of the phase relation alone, which required but two trial runs with known test weights. The method will be found satisfactory by using the so-called scribed high-spot with the rotor in a dynamic-balancing machine, performing the scribing at 20 to 30 per cent above the critical speed. Shaft scribings to determine phase relations on a rotor under actual operating conditions in the field were found to be so erratic and unreliable that special apparatus to determine the phase of vibration by stroboscopic means were resorted to.

Fig. 5 of this discussion represents the end of the rotor under consideration and the vibration vectors involved. Before any

[4] Chief Engineer, turbine division, Fidelity & Casualty Company of New York, N. Y. Mem. A.S.M.E.

trials are made, the phase relation between the upper extremity of the vertical component of vibration for example, and some data on the rotor are determined. This direction is represented by OA. (In the case where the test is made in the dynamic-balancing machine, OA represents the scribed high-spot location.) OA represents the directional characteristic of the initial unknown unbalance. The length of this vector, representing quantity, is

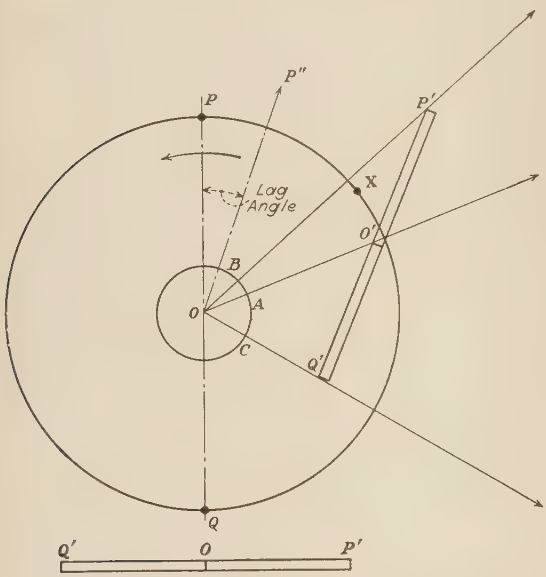

Fig. 5 Method of Determining Unbalance by Phase Relation of Vibration to Rotor

to be determined, as well as the lag angle between this vector and the causative force.

A known test weight is then inserted at any position, such as P, and a trial run made to determine the new phase position resulting from the combination of the known force and the unknown unbalance. Let OB represent the new high spot or phase position. Next, the known weight is removed from P and inserted at Q, 180 deg from P, and the second trial run made, resulting in a phase shift defined by OC.

The vectors representing the two trial weights are equal and opposite. The solution is quite simply obtained by means of a scale or straight edge divided into two equal parts with points, O', P' and Q' as illustrated in Fig. 5, representing the known weights. By holding the point O' on the line OA, the scale is maneuvered until a position is found where P' falls on OB and Q' falls on OC. There is only one position possible.

The amount of initial unbalance is determined directly by the relation of the length OO', representing this unbalance, to the scale length $O'P'$ or $O'Q'$ representing the known test weight.

The location of the initial unbalance is determined by the lag angle, which is found by comparing the actual direction of one of the test weights, as OP, with its resultant vector direction, $O'P'$. This angle POP'', laid off ahead of OO', locates the unbalance at OX, and the problem is solved.

It should be mentioned that neither the method based on amplitudes alone, or on phase relation alone, reduces the problem to its ultimate simplicity. By utilizing both the amplitude and phase data, the amount and location of the unknown unbalance at one end can be determined by a single trial run. The writer has used this method with success on the dynamic-balancing machine, and has utilized this principle in determining the amount and location of the correction at both ends of the rotor simultaneously, where each bearing is influenced by forces emanating from the other bearings.

James J. Ryan.[5] The solution of the rotor-balancing problem as given by the author appears to be both unique and fundamental. Considering one end of a rotor, mounted in a Lawaczek-Heyman balancing machine, with the other end fixed at the bearing, and applying the mathematical solution as given, the correct weights may be determined. However, it is not necessarily true that, with the rotor out of the balancing apparatus and in its own more or less flexible bearings and pedestals, the theoretical balancing procedure as given is fundamentally correct. Any system of field balancing (balancing a rotor in its own pedestals) is subject to considerable error unless the static forces and the dynamic moments are each taken into account by balancing on both ends of the rotor simultaneously. Such a procedure would consist in placing identical weights at the same angular positions on each end of the rotor, and, if an accurate solution is required regardless of the analytical effort necessary, the same weights should be placed at 180 deg removed from one another for additional trial runs. The data obtained are compiled and analyzed[6] in some such a manner as described by the author, and several machines have been successfully balanced by the method referred to.

A method that should be used more often in engineering work has received very little attention in the writings of vibration engineers. Its origination has been lost in antiquity, although it is the fundamental of fundamentals, and its simplicity makes it available for use to every one. It may be termed the "sine curve of unbalance." If a weight is added to the balance plane of a rotor at various positions around the periphery of the balance ring, the resulting amplitudes of vibration for that end of the rotor when plotted against the weight position will approximate the locus of a sine curve. The trough of the sine curve will indicate the position for balance. The inverse ratio of the amplitude of the sine curve to the mean ordinate of the sine curve multiplied by the weight of the unbalance weight used in the trials will give the approximate weight to be added at the indicated position for balance. This is the simplest method of balancing on record, and is more accurate than most because of its simplicity. Since, any three points plotted as coordinates determine a sine curve (as for a circle), only three trial runs are necessary to obtain the required data. It is preferable to place the trial weights at 90-deg positions for ease in off-hand sketching of the sine curve.

Using this method of procedure on the data as set forth by the author in the first example, Fig. 6 of this discussion is obtained, wherein the approximate location of the balancing position is between balance plug holes 27 and 28, and the amount of unbalance is calculated to be 49.5 oz. Professor Karelitz, in his paper[7] from which the example was taken, obtained the same balance location, and gives the exact amount of unbalance to be 56 oz.

As stated above, balancing on one end of a rotor is unreliable in many cases, especially where a dynamic unbalance couple exists. Thus the procedure is to place identical weights at the same position on each end of the rotor, shifting the weights 90 deg for the three trial runs, and measuring the amplitudes of motion of the two pedestals for each trial. The two sine curves obtained, sketched on the same graph, will establish the balancing condition for the rotor in most cases.

---

[5] Assistant Professor, Machine Design, Mechanical Engineering Department, University of Minnesota, Minneapolis.

[6] "Field Balancing of Rotors," by James J. Ryan, *The Electric Journal*, December, 1928, vol. XXV, no. 12, pp. 596–604.

[7] "Field Balancing Rotors at Operating Speed," by G. B. Karelitz, *Power*, Feb. 7 and 14, 1928.

Fig. 7 of this discussion represents the sine curves of unbalance for a large rotor considerably out of balance with respect to the dynamic couple and indicates the effectiveness of this method of balancing. The data in Table 2 were taken from trial runs on the machine.

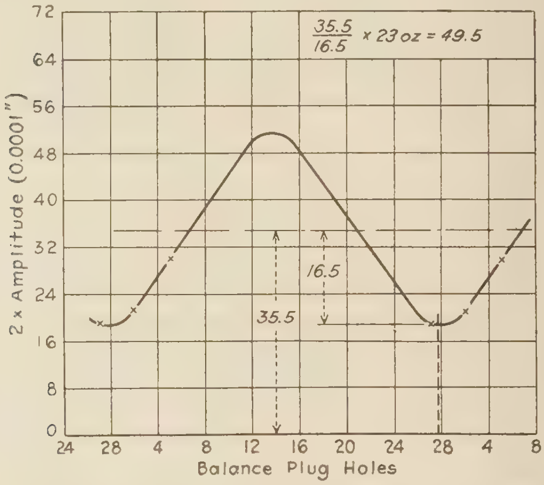

Fig. 6 The Approximate Location of the Balancing Position as Ascertained From the Data in the Author's First Example, Using the Writer's Method of Procedure

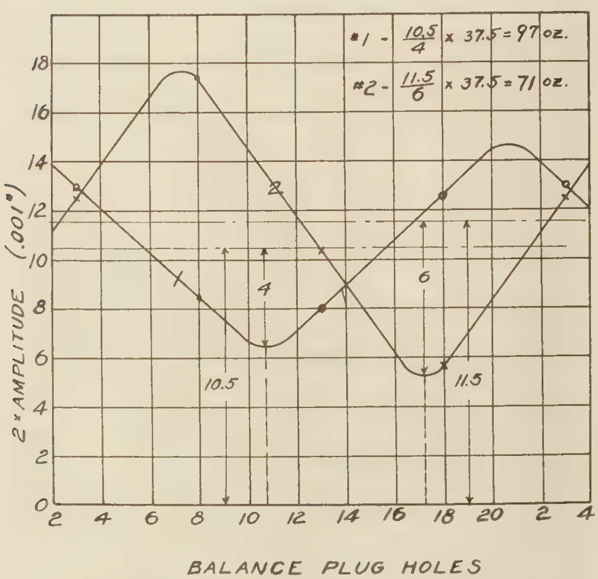

Fig. 7 The Sine Curves of Unbalance for a Large Rotor Considerably Out of Balance With Respect to the Dynamic Couple

The curves obtained indicate balance weights of 97 ounces distributed at balance plug holes 10 and 11 on the number 1 end, and 71 ounces distributed between holes 17 and 18 on the number 2 end. The error may be estimated, for the rotor was operated satisfactorily with 87 ounces in hole 9 on the number 1 end, and 95 ounces distributed between holes 18 and 19 on the number 2 end, after repeating the above procedure with smaller trial weights, leaving the original balancing weights in position. Using this method of analysis, the original run with no trial weights has little meaning.

TABLE 2

Trial run	Balancing plane	Balancing wt., oz.	Balance ring location	Maximum amplitudes (1/1000 in.)
Initial	1	None	...	3.0
Initial	2	None	...	5.0
A	1	37.5	13	8.0
A	2	37.5	13	10.4
B	1	37.5	3	13.0
B	2	37.5	3	12.5
C	1	37.5	18	12.6
C	2	37.5	18	5.7

This method of balancing enables the operator to balance a machine on the job, using a vibrograph, a slide rule and cross-section paper. He is guided definitely as to further procedure. The method is elementary and efficient.

Author's Closure

E. L. Thearle's solution is of the same type as Professor Karelitz', i.e., it involves the use of a special mechanical device. It nevertheless has the important advantage of using a set of parallel lines permanently drawn on a template, while the set of concentric circles or polygons, proposed by Professor Karelitz involves considerable preparatory drafting in each separate case. The measurement without a trial weight is included by Mr. Thearle in his solution which involves three basic runs for measurement of vibration amplitude; this makes a fourth run necessary in order to try the "easier" solution, to use Mr. Thearle's term.

Mr. Bryson's analytical solution takes the polar coordinates of the counterbalance weight for the unknown of the problem and also uses such coordinates for the given trial weights. This may be a luckier choice than Cartesian coordinates used by the writer.

The author solved numerically the same case chosen by Mr. Bryson, following his own method as shown in Appendix 2 of the paper. The results for x and y were

$$x_1 = -0.676;\ y_1 = 51.94;\ x_2 = -0.132;\ y_2 = 10.18$$

In order to compare this result with Mr. Bryson's we determine $\tan \varphi = y_1/x_1 (= y_2/x_2) = 51.94/-0.676 = -76.86$, or $\varphi =$ 90 deg, 44 min, and 44 sec. In Mr. Bryson's notation who locates the initial unbalance and not the required balancing weight, as the author does, φ should be 270 deg, 44 min, 44 sec, or 270.75 deg. The magnitude of the unbalance appears as 51.95 oz and 10.17 oz, respectively, while for distances O''_1S_a and O''_2S_a we obtained 47.10 and 20.85. The amplitude resulting from initial unbalance alone could now be predicted as $0.0030 \times 51.95/47.10 = 0.0032$ in. in the first case and as $0.0030 \times 10.17/20.85 = 0.00148$ in. in the second (in complete accordance with the numbers evaluated by direct measurements in Fig. 3 of the paper) and the correct solution can now be pointed out. The writer's number (0.0032 in.) is somewhat closer to the observed amplitude (0.0029 in.) than Mr. Bryson's (0.0033 in.), but the error is still about 10 per cent of the magnitude in question. The discrepancy is due not so much to inaccuracies of slide-rule computations, as to the inaccuracies of the amplitude observations and of the general theory of this kind of vibrations. Also, Mr. Bryson's remark, that the choice of the correct solution can be made "by inserting the *computed* values in the original equation for $\overline{eA}$" is incorrect, unless $\overline{eU}$ in this equation is to be computed from the *observed* amplitude at the (fourth) no-trial-weight test. There exists no means for separating the physically correct solution from the basic three amplitude measurements alone.

The comparison showed that the writer's solution, being somewhat more symmetrical than Mr. Bryson's and also more convenient for finding the quadrant where the unbalance is located, is nevertheless much more complicated. Still more painstaking

would be the more general case of unequal trial weights which, incidentally, has been left out by Mr. Bryson. However, even his version can hardly ever have a chance of being used by a practitioner for actual unbalancing. Here, graphical methods are the best.

It should be noted, that the case of almost equal amplitudes hardly warrants the apprehension expressed for it by Mr. Thearle and Mr. Bryson. Where two of the three amplitudes happen to be close to equality, they will usually be considerably different from the third amplitude, thus giving convenient radii for the two arcs required for the solution. When all three amplitudes are almost equal, both solutions are almost identical as will be shown later, and are to be looked for in a small region around the center of the circle passing through points S_a, S_b, S_c (or center of the log of balancing—for equal trial weights). Also replacing an arc of a too long radius by a straight line perpendicular to the corresponding side of triangle $S_aS_bS_c$ and passing through the respective point U would not seriously affect the accuracy of the solution. All these statements may be verified in the example of Figs. 3 and 4 of the paper.

Mr. Rathbone's remark, that the phase relation of the vibration to the disturbing force is of no less importance than the length of the vector giving the amplitude, is theoretically quite true. This, however, does not affect the possibility and desirability of solutions which make use of amplitudes alone. Direct observations of the phase-lag angle by means of high-spot scribing are sometimes unreliable, as Mr. Rathbone himself has pointed out.[8]

The question of whether or not a semi-automatic graphical method of solving the balancing problem is preferable to a possibly somewhat involved geometrical construction hardly allows a general answer and may be left open, inasmuch as the writer's method does not intend to replace any former attempt to attack the same problem. The writer would only take the liberty to observe that the engineers dealing with this problem seem to show a certain propensity to improvised mechanical devices, which are used sometimes in cases where a geometrical construction would unquestionably be simpler. Such a case is that treated by Mr. Rathbone in Fig. 5 of this discussion, where line $P'Q'$, which is to be halved by the vector OA at the point O', could be found by drawing through any point P' on OB a line $P'R'$ parallel to OC (intersecting OA at R'), and then drawing a line $R'Q'$ parallel to OB (intersecting OC at Q') and connecting P' with Q'.

In the case of Mr. Thearle's Fig. 1, a construction replacing his template with the set of drawn lines would be very complicated. His method, like Professor Karelitz' and the writer's, has the advantage of using amplitudes alone.

Of course, Mr. Rathbone's results obtained from two and even from one run on the machine by simultaneous observations of amplitude and phase are remarkable.

The method of drawing a sinusoidal curve representing the amplitude in terms of the location of a constant trial weight, used in this discussion by Professor Ryan, has been pointed out by Professor Stodola[9] (but without Professor Ryan's interesting details). The question of whether it is possible to sketch offhand sinusoids on the basis of three points (especially in a combination similar to that in Fig. 6 of this discussion) must be left to the experiênce and ability of the individual draftsman. In the present case, Professor Ryan's result, as compared with those of Professor Karelitz and the writer, can claim for tolerable accuracy only as to the location of the unbalance. Still Professor Ryan's method may be of use for quick preliminary orientation.

In conclusion, the writer points out some further properties of the construction described in his paper.

1 It is clear, that the centers O_a, O_b, and O_c lie upon one and the same straight line, which is perpendicular to the segment $O''_1O''_2$ and crosses it at its middle.

2 In the case of all three amplitudes being exactly equal ($m = n = p$) the three circles would become straight lines perpendicular to the sides S_aS_b, S_bS_c, and S_cS_a, respectively, and passing through their middles. We would obtain *one* solution, corresponding to the center of the circle circumscribing triangle $S_aS_bS_c$. Formulas [3] of the paper, in which the second determinants in the numerators now vanish, would become $x = d_y$; $y = -d_x$. Returning now to the general case, d_x and d_y in formulas [3] allow a simple geometrical interpretation, namely, d_y and $-d_x$ are the coordinates of the center of the circle passing through the vertexes of the triangle $S_aS_bS_c$.

3 Let us now translate parallelly the coordinate axes from O into this center (say O'), as a new origin. In the new system of coordinates $X'Y'$, the numbers a, b, and c (distances between point O and points S_a, S_b, and S_c) are replaced by $a' = b' = c' = R$ (radius of the circumscribing circle). The first determinants in the numerators of formulas [3] of the paper now vanish and we have in the new notation

$$x' = -Ke'_y;\ y' = Ke'_x \qquad [3']$$

(K, not K', because, according to formula [1] of the paper, K is an "invariant" of the transformation, depending on differences of coordinates and on constant numbers m, n, and p.) It follows immediately from formula [3'], that points O''_1 and O''_2 lie upon a straight line through the center O'.

4 Equation [4] of the paper now becomes

$$A'K^2 - B'K + C' = 0 \qquad [4']$$

where $A' = 3(e'^2_x + e'^2_y)$ and $C' = a'^2 + b'^2 + c'^2 = 3R^2$.

From well-known properties of quadratic equations it follows that

$$K_1K_2 = C'/A' = R^2/(e'^2_x + e'^2_y)$$

The product of K_1K_2 can only be positive, i.e., K_1 and K_2 can only be both positive or both negative. It now follows from formula [3'], that x'_1 also has the same sign as x'_2 and y'_1 the same sign as y'_2. Points O''_1 and O''_2 are located on the same side of center O'.

5 From squaring our last equation we obtain

$$(K_1K_2)^2(e'^2_x + e'^2_y)^2 = R^4 \qquad [5']$$

From formula [3'] we obtain by squaring

$$x'^2_1 = K_1^2e'^2_y;\ x'^2_2 = K^2_2e'^2_y;\ y'^2_1 = K_1^2e'^2_x;\ y'^2_2 = K_2^2e'^2_x$$

whence by addition

$$x'^2_1 + y'^2_1 = K_1^2(e'^2_x + e'^2_y);\ x'^2_2 + y'^2_2 = K^2_2(e'^2_x + e'^2_y)$$

and, by multiplying the last two equations,

$$K^2_1K^2_2(e'^2_x + e'^2_y)^2 = (x'^2_1 + y'^2_1)(x'^2_2 + y'^2_2)$$

By substituting the right-hand side of the latter equation in Equation [5'], we obtain

$$(x'^2_1 + y'^2_1)(x'^2_2 + y'^2_2) = R^4, \text{ or}$$

$$|\sqrt{(x'^2_1 + y'^2_1)}| \cdot |\sqrt{(x'^2_2 + y'^2_2)}| = R^2;$$

$$(O'O''_1)(O'O''_2) = R^2$$

[8] "Turbine Vibration and Balancing," by T. C. Rathbone, Trans. A.S.M.E., vol. 51, 1929, paper APM-51-23, p. 267.

[9] "Dampf- und Gasturbinen," by A. Stodola, fifth or sixth edition, p. 356, Fig. 398.

From this equation and from the two properties of points O''_1 and O''_2 which have been emphasized, it follows that *points O''_1 and O''_2 are poles with respect to the circle circumscribing the triangle $S_aS_bS_c$.*

For the particular case of equal trial weights, this property of the two solutions of the balancing problem has been pointed out by Prof. J. P. Den Hartog, with reference to the construction here described, in his recent treatise on mechanical vibrations.[10]

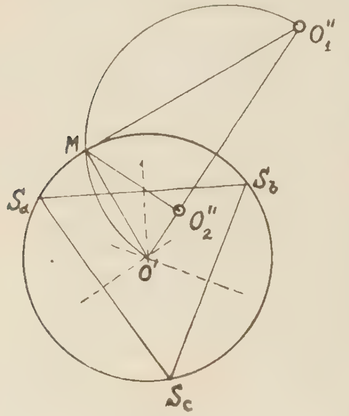

Fig. 8

This polarity may be used for finding the physically correct solution in cases where a solution obtained, for instance, by one of the methods pointed out in the present discussion, happens to be the false one. If O''_2 is known, (Fig. 8 of this discussion) draw O''_2M perpendicular to $O'O''_2$, intersecting circle O' at M, then draw MO'_1 perpendicular to $O'M$, intersecting $O'O''_2$ at O''_1. If O''_1 is known, draw a half-circle upon the diameter $O'O''_1$, intersecting circle O' at M, then draw MO''_2 perpendicular to $O'O''_1$, intersecting $O'O''_1$ at O''_2.

The present paper was written more than three years ago, but circumstances beyond the author's control hindered its publication. In the meantime Mr. L. P. Kroon of the Westinghouse Electric & Manufacturing Company found independently an essentially identical solution of the balancing problem. When it had been called to his attention that there was an unpublished paper in existence working out the same subject, he very generously conceded priority to the author and also helped to bring about the publication of the present contribution.

I am also indebted, for encouragement or help, to J. G. Baker and L. M. Tichvinsky, both of the Westinghouse Electric and Manufacturing Co., and to Prof. J. P. Den Hartog, Prof. F. M. Lewis and Prof. E. O. Waters.

Influence of Bends or Obstructions at the Fan-Discharge Outlet on the Performance of Centrifugal Fans[1]

R. D. Madison.[2] Where the air leaves a fan with substantial uniformity in direction and velocity it is reasonable to suppose that an elbow placed directly on the fan discharge would offer no specially different type of flow or resistance from what it would if placed elsewhere in the duct system. The tests reported in the paper under discussion show this to be the case.

Unfortunately most fans are not so ideally suited to such a test. Although it was specifically stated that only one fan was tested it was not representative of the majority of fans on the market today. The writer refers to the large diverging chamber from the point of cut-off to the fan discharge, approximating $1^1/_2$ diameters of pipe. Such fans are often used in the power-plant field and are special fans. The expanding portion is more often built as a part of the duct work. It is still a matter of opinion what the tests would have shown had the elbow been placed immediately at the discharge of a conventional fan.

Where the air leaves a fan with non-uniform flow it is reasonable to suppose that the behavior of an elbow will be affected if placed adjacent to the fan discharge. It is known that there is more tendency to spiral flow in single-inlet fans, particularly those with large outlets. The writer has been making tests on elbows following such fans and expects to present these data in the near future when the tests are completed. At the present time sufficient data have been obtained to say that fan performance can be materially changed if the conditions are especially bad.

The writer has observed that the pressure loss may be different whether the elbow turns to the right or left of the line of discharge. In fact such observations have been noticed where the elbow is 11 diameters from the fan discharge. The type of flow is especially severe in the case of a reverse elbow at the outlet of a forward curved blade fan which has a "drop cut-off," that is, an outlet materially larger than the area at the point of cut-off. The static-pressure curve of this type of fan and elbow shows a large drop in pressure beyond the peak of efficiency and is concave upward from there to free delivery. The pressure is unstable near free delivery, a condition caused only by the location of the elbow. It is interesting to note that when one diameter of duct was interposed between this fan and elbow the pressure curve again followed the characteristic trend, although the elbow loss was somewhat higher than when subjected to uniform flow. Whether one says that the fan characteristic is affected by such arrangement or that simply the elbow loss is variable, the fact remains that if the usual elbow loss were used in figuring an installation the expected flow would not be obtained.

The effect of one diameter of duct between a fan and elbow is cited here to show that it can have a remarkable stabilizing effect on the flow of air approaching the elbow. In view of this, it is a matter of opinion what the authors would have found in their tests had the specially long outlet not been used in their work. While it is known that single-inlet fans are likely to cause more rotation in the air leaving the discharge than corresponding double-inlet fans, the rotation in the latter is not nullified by the opposing inlets as the author suggests in another paper[3] but is greatly reduced due to the absence of friction along the central plane of the fan. Two vortices are set up in opposite direction and in lesser amounts.

While it is not the best practice to place an elbow directly at the fan discharge, still it is frequently done in ventilating work where space is at a premium. The behavior of the elbow will thus depend upon the condition of flow at its entrance, being better in some fans than in others. The reverse elbow is to be discouraged in any case and the turn used that follows the direction of fan rotation. The practice of using turning vanes if it becomes necessary to place the elbow at the fan outlet, is good. Here again, however, full flow across the elbow inlet must exist or the expected performance may not be obtained.

It would be interesting to know whether the authors tested the elbow at some distance from the fan and what the pressure loss was. Curve Fig. 6 would indicate this to be about 0.4 velocity heads but from the writer's tests he would expect this to be about 0.25 velocity heads for this elbow. Wirt's tests[4] at the General Electric Company show losses of about 0.425 velocity

[10] "Mechanical Vibrations," by J. P. Den Hartog, McGraw-Hill, 1934, pp. 246–248 and 380.

[1] Published as paper FSP-56-12, by L. S. Marks, J. H. Raub, and H. R. Pratt, in the October, 1934, issue of the A.S.M.E. Transactions.

[2] Research Engineer, Buffalo Forge Company, Buffalo, N. Y. Assoc-Mem. A.S.M.E.

[3] "Air Flow in Fan-Discharge Ducts," by L. S. Marks, Trans. A.S.M.E., 1934, paper PTC-56-2, p. 876.

[4] "New Data for the Design of Elbows in Duct Systems," by Loring Wirt, *General Electric Review*, June, 1927.

heads for an elbow of this type, and the writer feels that it was owing to the method of test where a nozzle preceded the elbow and a uniform velocity was effective over the whole cross-sectional area. This condition does not exist in practice. Besides the tests were made at very high velocities in a 3-in. elbow. The writer's tests check much more closely with those of Busey[5] which were made at the Buffalo Forge Company, although they are slightly higher.

C. E. Peck.[6] The results found by the authors of the paper under discussion are valuable in that they verify the general opinion that the influence of bends or obstructions at the discharge of the fan has little effect on the fan performance. However, it is important to note, as pointed out by the authors, that their conclusions are based on a fan of the centrifugal type with a volute housing so designed that the air being discharged from the housing has a reasonably definite direction and fairly uniform distribution at the outlet.

The axial-flow type of fan or propeller type of fan discharging directly into a duct system may give to the air quite different types of flow characteristics such that bends, sudden enlargements, or obstructions will affect the fan performance appreciably. For instance, the air leaving a high-capacity propeller-type blower has very large rotational-velocity components which maintain themselves at large distances beyond the fan in the duct work. The rotational velocities vary from the center to the wall of the duct. With these complicated directions of flow existing, any obstruction or bend, or change in duct cross-section at the fan discharge or even at some distance from the fan discharge may appreciably affect the fan delivery and efficiency.

The performance of a propeller fan with properly designed guide vanes at the fan discharge is such that the air leaving the vanes is essentially parallel with the axis of the duct. With this condition and uniform velocity distribution the effect of bends or obstructions beyond the guide vanes would probably be small.

In general, when a fan of any type is applied to a duct system and the fan is provided with a volute case or guide vanes or some device which produces uniform flow in a given direction the effect of duct shape and obstructions beyond the fan is negligible. However, when fans are applied in special cases, such as the cooling of electrical machinery where volutes and guide vanes can be rarely used, the effect of obstructions at the fan outlet is more noticeable. The effect of the close proximity of end windings and the rotor of the electrical machine must be considered and usually such obstructions greatly influence the fan performance.

Authors' Closure

The investigations of Mr. Madison show that the pressure drop in an elbow depends on the uniformity of flow of the air approaching it but do not appear to demonstrate any influence of the elbow on the performance of the fan. If the character, location, or orientation of the elbow is such as to change the discharge pressure at the fan outlet, the condition under which the fan is operating will change to some other point on the fan-performance curve. If the elbow actually affects fan operation, the performance curve of the fan will change. Mr. Madison has apparently investigated a combination of fan and elbow for a fan which gives a spiral discharge flow and shows that the performance of this combination varies with the location and orientation of the elbow. The authors believe that this variation results from actions in the elbow alone and that the fan is unaffected as long as it has a complete fan casing.

In the authors' tests the elbow was not tested at some distance from the fan because the air flow at the fan-casing outlet was found to be practically uniform over the whole cross-section.

The authors agree with Mr. Peck that if the fan casing is absent or incomplete, the effect of obstructions in close proximity to the fan may be considerable.

[5] "Loss of Pressure Due to Elbows in the Transmission of Air Through Pipes or Ducts," by Frank L. Busey, A.S.H.&V.E. Trans., 1913.

[6] Power engineering department, Westinghouse Electric & Manufacturing Company, East Pittsburgh, Pa. Jun. A.S.M.E.

Calibration of Rounded-Approach Orifices[1]

R. E. Sprenkle.[2] Mr. Smith's data are timely, particularly since some can be connected directly to other pertinent data which greatly extends the scope of usefulness. For instance, the writer's Fig. 1 shows the data from Mr. Smith's large oil-flow nozzle plotted together with data from a Bailey 3.06-in. × 1.836-in. water-flow nozzle. While at the junction point of the two sets of data, or at a Reynolds number of approximately 35,000, a possible separation by approximately 1/2 per cent exists, there is no question but that the data from the Bailey nozzle are a real continuation of the data of Mr. Smith's nozzle, and that a single smooth curve represents the complete data of the two when plotted against Reynolds' number.

This despite the fact that the Bailey nozzle used pipe-line connections instead of the impact and throat type of connections used by Mr. Smith. Pipe-line taps place the inlet static connection into the pipe wall at a distance of one pipe diameter preceding the nozzle inlet, and the outlet static connection into the pipe line back of the nozzle throat, as shown in Fig. 13 of Mr. Buckland's paper,[3] "Fluid Meter Nozzles."

Further, there is a distinct difference in size between the two nozzles, as well as the use of entirely different flowing fluids in obtaining these calibration data. When to all of these is added the difference in the physical set-up and the fact that the different experimenters involved were working entirely independently of each other, this agreement becomes all the more noteworthy.

Since the water curve obtained from the Bailey nozzle flattens out at about 600,000 Reynolds' number, and continues flat up to the maximum test point of about 900,000 Reynolds' number, there is little reason to doubt the projection of the curve as a perfectly flat line to Reynolds' number of much greater value, possibly to infinity. Such tests, using steam flow, are now scheduled to be made shortly on the Bailey nozzle, better to show the validity of this assumption.

In view of this the curve has been extrapolated to a Reynolds number of over 3,000,000 so as to cover the useful range of steam, air, or other low-viscosity fluids, and it is felt that this same curve could be extrapolated further if desired without being in error more than plus or minus 1/2 per cent. Likewise, the same curve should apply to any flow nozzle of this general structure, provided the diameter ratio of the throat to the inlet-pipe diameter does not exceed 60 per cent.

Mr. Smith's medium- and small-sized nozzles do not line up either with his large one or with the Bailey nozzle, possibly as a result of differences in relative roughness of the throat finish. Then too, recent researches on orifices show the improbability of making orifice throats less than 0.5 in. so as to conform with larger diameter throats. This same observation applies to nozzle throats as well. Thus, such small sizes must be considered in a

[1] Published as paper RP-56-10, by J. F. Downie Smith, in the October, 1934, issue of the A.S.M.E. Transactions.

[2] Bailey Meter Company, Cleveland, Ohio. Assoc-Mem. A.S.M.E.

[3] "Fluid Meter Nozzles," by B. O. Buckland, Trans. A.S.M.E., 1934, paper FSP-56-14.

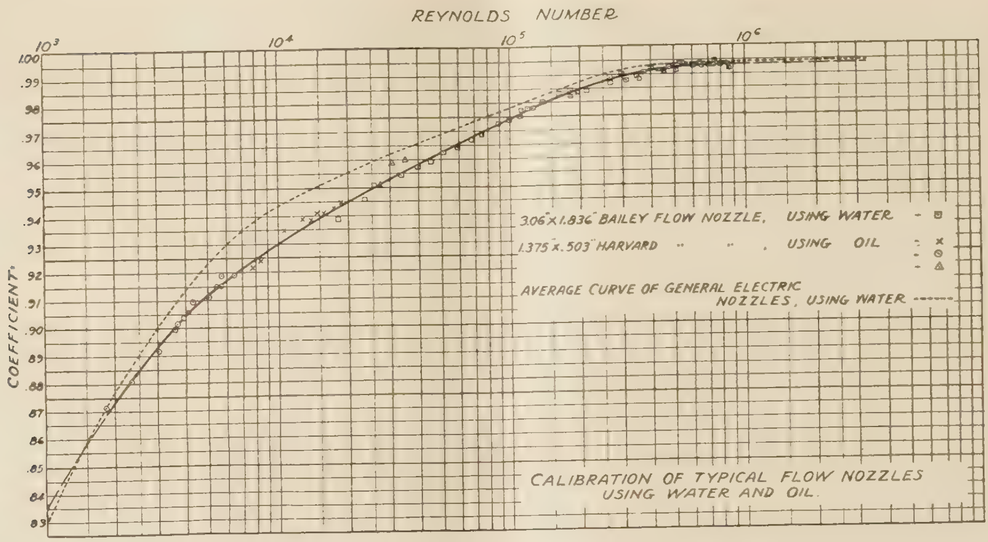

Fig. 1 Calibration of Typical Flow Nozzles Using Water and Oil

class by themselves and cannot be grouped with larger ones without the application of some correction factor to compensate for these variations in finish.

An interesting comparison with the average curve of the General Electric nozzles, described by Mr. Buckland,[3] is made possible by placing this average curve on the writer's Fig. 1. The maximum difference between the two curves is about $1^1/_2$ per cent, and it occurs at a Reynolds number of approximately 10,000. At higher and lower Reynolds' numbers, particularly at the higher Reynolds number, the agreement between the two curves is better than $^1/_2$ per cent. Because of the rather spotty data of the General Electric nozzles at Reynolds' numbers less than 50,000, it is believed by the writer that the heavy curve shown in his Fig. 1, as developed by Mr. Smith and the Bailey nozzle, is slightly more favorable. However, if a mean line were drawn between the two, the maximum deviation would not exceed $^3/_4$ per cent, with the average between $^1/_4$ per cent and $^1/_2$ per cent at the more useful ranges which is an accuracy that will conform to most test specifications.

Ronald B. Smith.[4] While the results of this paper serve as further confirmation of the Reynolds criterion it would seem to me that this is the ideal application of the sharp-edged orifice rather than the nozzle. It is extremely difficult to reproduce accurately the author's approach radii on nozzles $^1/_4$ in. and $^3/_{16}$ in. in diameter so that the coefficients cannot be applied to other nozzles with certainty. For instance, the author's coefficients of the geometrically similar large and medium-size nozzles do not agree. In addition, the use of a $^1/_{16}$-in. throat hole in only a $^1/_8$-in. nozzle must result in some abnormality in the flow.

Apart from the author's research it may be of interest to point out that in the regions of laminar flow the use of a pitot tube at 0.15 diam from the pipe wall offers no advantages over the usual static hole as far as accuracy is concerned. While the author does not mention the straight length upstream of the nozzles, let us assume that it is sufficiently long so that a parabolic profile is nearly developed. Although this would require considerable length it is approached in about 50 diameters.[5] Now the impact tube at 0.15 diam from the wall measures practically the average velocity for the parabolic (or the one-seventh turbulent) profile, yet it is known that the kinetic energy of the parabolic profile is twice the square of the mean velocity. Inasmuch as the development of the flow equation is essentially a balance of energies it would then be more rational to locate the tube at the rms velocity point when there is a laminar flow. This would be at about 0.3 diam.

Ed S. Smith, Jr.[6] The author's data cover a range of Reynolds' numbers of present interest for the nozzle having an impact tube in the inlet. The curve in general parallels that for the Herschel Standard venturi tube, falling consistently several per cent below it.

The writer considers an impact tube, spaced only 0.15 diam from the pipe wall as tested by the author, to be a poor pitot on account of the steep velocity gradient so near the wall. It would seem that this tube location would be unduly liable to error at low Reynolds' numbers where the velocity-distribution curve has a parabolic form, i.e., an extended nose in the center. The use of straightening vanes is indicated in this flow régime.

In spite of the foregoing objection, the author's tests show an excellent correlation of coefficient with Reynolds' numbers, thus establishing the relation usefully for the particular nozzle-impact tube forms used.

Sanford A. Moss.[7] This paper shows a great deal of precise flow-measurement work, and is a distinct contribution to our knowledge of the properties of rounded-approach nozzles. One of the contributions is evidence in the matter as to whether or not Reynolds' number is a proper criterion for the plotting of nozzle coefficients. The author's curves in Figs. 3 and 4 do not at all coincide as they would if Reynolds' number were a complete criterion. The curves are also a little lower than the Reynolds number curve given by Mr. Buckland.[3] It has been suggested that the coefficient of various nozzles might be brought together if "Head" were used as the abscissas, rather than the Reynolds number, and this is worth investigating. Mr. Smith uses as the

[4] Turbine Engineering Department, Westinghouse Electric & Manufacturing Company, East Pittsburgh, Pa. Jun. A.S.M.E.

[5] "Aero- and Hydromechanics," by Tietjens-Prandtl, vol. 2, pp. 25–28.

[6] Hydraulic Engineer, Builders Iron Foundry, Providence, R. I. Mem. A.S.M.E.

[7] Research Engineer, General Electric Company, West Lynn, Mass. Mem. A.S.M.E.

ordinate of his curves, on Figs. 3 and 4, the velocity coefficient whereas Mr. Buckland uses flow coefficient as the ordinate for his curves, which is the coefficient occurring in the theoretical formula for weight flow. Might it not have been a little more useful for computations involving use of the nozzle, as well as easier in the computations for finding the coefficient, if Mr. Smith had also done this?

Richard G. Folsom[8] and J. A. Putnam.[9] Rounded-approach orifices with cylindrical downstream sections were developed with a view to obtaining a flowmeter having a constant-discharge coefficient near to unity. The added feature of the impact tube was introduced to simplify the flow equation in that it automatically takes into account the velocity of approach, when placed in the correct position. Such an arrangement has considerable value when metering gaseous fluids. However, in handling liquids the law of continuity is so simple that the additional constructional and experimental difficulties of the impact tube far overshadow its advantages.

Mr. Smith's paper and other recent publications[10,11] clearly illustrate the characteristics of this type of metering device at both low and high values of Reynolds' number. The discharge coefficient drops rapidly at low values of Reynolds' number similar to the corresponding characteristic of the simple diaphragm-orifice.

Fig. 2 of this discussion shows the calibration curve of a small square-edged orifice used for metering in the mechanical laboratories of the University of California and which is comparable with the small orifice used by Mr. Smith. The meter conforms in general with the I.S.A. 1930 orifice, except that the diameter is less and the edge is thicker than the tolerance limits set by the I.S.A. The pressure connections are placed so that accidental burrs can have no effect. A disadvantage of the meter used by Mr. Smith is the position of the static-pressure connection in the high-velocity section where errors due to burrs will be a maximum.

Although the nozzle-impact-tube meter coefficients are higher, they vary as much as the coefficients of the simple orifice in the region of low Reynolds' number. At high Reynolds' number both types have a constant coefficient.

Since there is no choice on the basis of discharge-coefficients, the simpler sharp-edged orifice proves to be the most satisfactory meter under operating conditions. For accurate work, all small meters must be calibrated in place.

R. J. S. Pigott.[12] Mr. Smith is to be congratulated on the excellent consistency of his test work. In comparison with other tests on small nozzles, the scatter of points is quite noticeably less than usual.

[8] Instructor, Department of Mechanical Engineering, University of California, Berkeley, Calif. Jun. A.S.M.E.

[9] Teaching Assistant, Department of Mechanical Engineering, University of California, Berkeley, Calif.

[10] "Regeln für Die Durchflussmessung mit genormten Düsen und Blenden," V.D.I., 1932.

[11] Détermination du Coefficient de Débit de Tuyères et Orifices Noyés," by MM. P. Leroux et Deullin, *Annales des Mines*, ser. 13, vol. 4, no. 11, 1933.

[12] Staff Engineer, in charge of engineering, Gulf Research & Development Corporation, Pittsburgh, Pa. Mem. A.S.M.E.

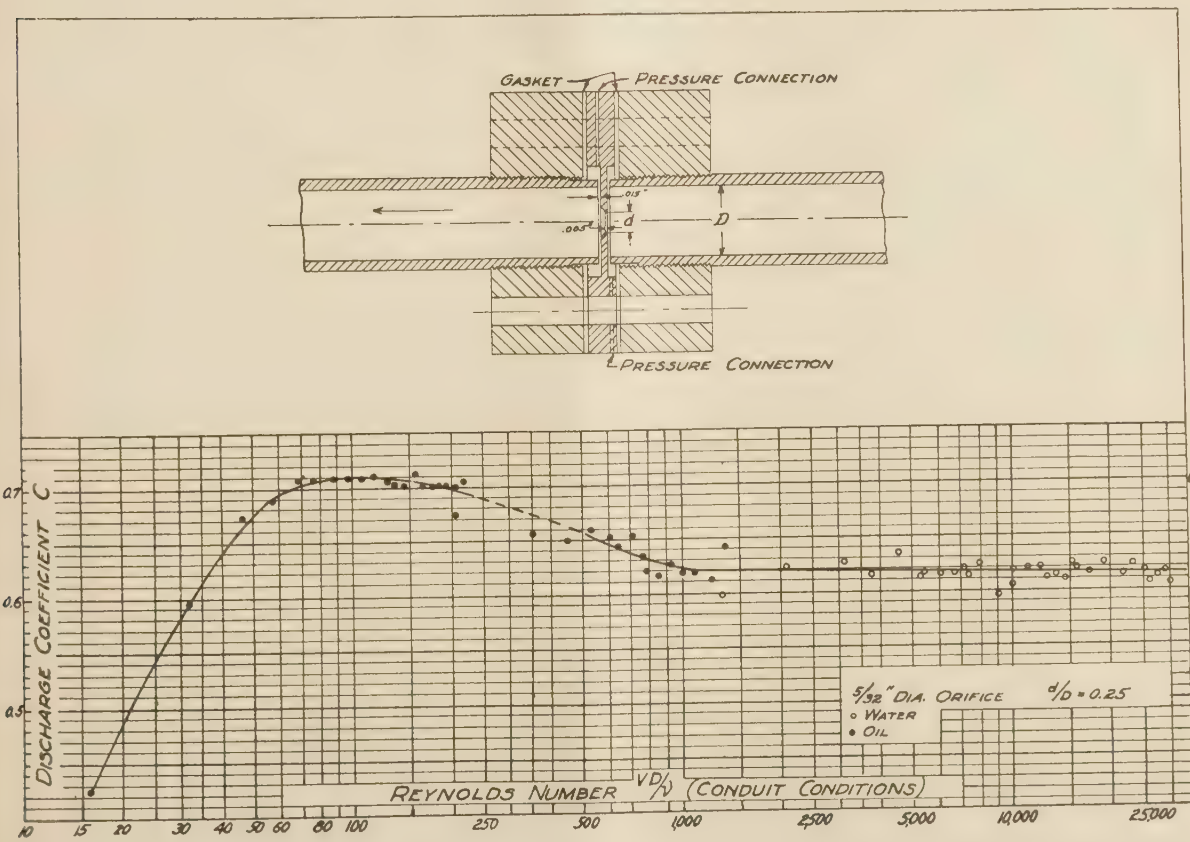

Fig. 2 The Calibration Curve of a Small Square-Edged Orifice Used for Metering in the Mechanical Laboratories of the University of California

It is assumed that the pipe used with these nozzles was drawn brass, although it is not so stated in the paper. The point is of importance, as the roughness of the preceding pipe has a definite effect upon coefficients.

Regarding the use of the impact tube located at 0.15 diam, the writer used this location in 48-in. pipe in 1910, for steam sampling. It gives a fairly good average velocity reading for fairly large Reynolds numbers, but it is certainly not rigorous. Such an impact tube does have an influence on the coefficient, since it disturbs the flow into the nozzle.

With regard to the dip in the coefficient curve, for the medium orifice it is possible that the impact tube for this particular set-up was at a critical position. There is also another cause for disturbances in this region; the plots are usually based on Reynolds' number in the throat. Turbulence usually begins at $dv\rho/\mu = 1200$ to perhaps 2500. But at this time, the upstream section is in viscous flow, and full turbulence for the whole nozzle does not occur until $dv\rho/\mu$ in the throat is greater than 3300 for the large nozzle, 6600 for the medium, and 13,200 for the small nozzle. Indeed, if the flow is very smooth in the upstream pipe, turbulence may not be fully established until about twice the foregoing values. Consequently, there is some instability in the orifice in this range; it may be detected by a tendency of the head gages to oscillate, since there are at least two possible extreme values for the differential. Very likely the dip is due to a combination of the impact tube and the unstable condition.

The writer would assign even the small variations in coefficient to three factors: (*a*) non-similarity; (*b*) difference in relative roughness; (*c*) the impact tube.

For the past ten years, it has become customary to plot venturi-tube, disk-orifice, and nozzle coefficient against number, assuming geometrical similarity, because the venturi was the same general shape, the orifice was flat and had a sharp edge, or the nozzle was the same contour. This practice is unfortunate, as it is not fair to the Reynolds number comparison. It is a fact that almost no completely similar nozzles have been tested. If the same 12-in. steel pipe is used for a five-, four-, and three-inch nozzle, although the nozzles themselves are similar in contour, the assembly is *not* similar. Further, if a 12 by 3 and a 4 by 1 nozzle are compared, using steel pipe in both cases, they are dissimilar; the four-inch pipe is *relatively* much rougher; so is the one-inch nozzle, with the same polish.

Mr. Smith's nozzles are approximately similar only. In the fluid-meters-nozzle research at present proposed, we intend to establish full geometrical similarity, varying roughness and diameter ratio. In this way, those deviations hitherto all charged to test variation will certainly be reduced to test errors purely, without the additional scatter resulting from dissimilarity.

These small nozzle tests are very much needed to fill out the lower Reynolds number region, and are particularly timely for the writer.

Author's Closure

Mr. Moss has pointed out that the three curves given in the paper do not coincide and on this basis concludes that Reynolds' number R is not a complete criterion to use as abscissas. It would appear to the author, however, that such a conclusion from the present data is unwarranted. In the first place, the orifices are not quite geometrically similar, with the result that a dimensional-analysis treatment of the problem would not give us C as a function of R only. Other dimensionless groups involving lengths would unquestionably enter.

The fact that these curves are slightly lower than those of B. O. Buckland can be explained perhaps by the lack of similarity in the two pieces of apparatus, and by his use of static pressure upstream, whereas the author used impact pressure upstream. Mr. Moss's suggestion to plot C against head rather than R has been tried. It yields points with the present data that are scattered considerably more than where R is used.

Mr. Moss points out that the author uses the simple equation $v_{\text{theor}} = \sqrt{2gh}$ rather than $v_{\text{theor}} = \sqrt{\frac{2gh}{1 - r^4}}$ used by B. O. Buckland where r is the ratio of throat diameter to upstream diameter, and states that the latter is the coefficient occurring in the theoretical formula for weight flow. He has overlooked the fact that there is a difference in set-up in the two cases. Using static pressure upstream, the latter of the two formulas is correct, but if an impact tube is to be used, the former equation is the correct one, provided that the impact tube is placed at the proper place to get the desired velocity head.

Ronald B. Smith, Ed S. Smith, Jr., and R. J. S. Pigott state that the use of an impact tube at 0.15 diam from the pipe wall offers no theoretical advantages over the usual static hole. The author agrees with this. R. B. Smith's logic in discussing the kinetic-energy relations cannot be questioned. Strangely enough, the author used reasoning quite similar in discussing a paper presented by Prof. L. S. Marks on air flow in fan ducts a few days before these present discussions were presented.

When these orifices were installed the question of possible errors arising in coefficient due to erroneous readings of velocity upstream was investigated. Perhaps a résumé of the conclusions reached at the time would be illuminating. If an error of 50 per cent in velocity upstream were made, the effect on the velocity at the throat of the big orifice was 1.6 per cent, for the medium orifice it was 0.1 per cent, and for the small orifice it was entirely negligible. These conclusions are based on the assumption that an error of 50 per cent in the velocity upstream would be shown up in the flow through the orifice, but even this assumption is unjustified, since an error in the velocity upstream obtained for each orifice during calibration would be mainly counterbalanced in the use of the orifice during tests on flow measurement. Thus the small errors mentioned are considerably larger than any mistakes which would occur in the use of such an instrument, and the conclusion that the introduction of an impact tube would lead to negligible errors was borne out by the results obtained.

Now there is no single point upstream which would give the proper impact pressure over a wide range of Reynolds' number, particularly if the flow may change from viscous to turbulent, but the movement of the position of the impact tube at every reading would have introduced many complications and, in view of the small errors introduced, as previously mentioned, the distance 0.15 diam was adopted, as recommended in the Power Test Codes Tentative Draft, series 1933, Instruments and Apparatus, part 2, p. 13, and previously recommended by Sanford A. Moss in a verbal communication.

R. E. Sprenkle has presented a most remarkable verification of the author's data in his curve, especially as the apparatus used and liquid flowing in each case were different. Such close agreement is very gratifying.

Several discussers, including R. J. S. Pigott and R. B. Smith, have asked about the relative roughness of the orifices and approach pipes. That question the author cannot answer quantitatively. All orifices were made of composition metal (a brass) and were machined as smoothly as our shops could make them, templates being used in turning and polishing. The finish was bright and apparently glassy-like in smoothness. The pipes on each side of the nozzles were standard iron pipes, of ordinary roughness.

Mr. Pigott's comments on the dip noticed with the medium orifice are interesting, and obviously true; but they do not explain fully why this dip was found with only the one orifice.

Messrs. Folsom and Putnam state that the static-pressure connection in the author's apparatus is at the high-velocity section where burrs would have a maximum effect. The removal of burrs formed was not a serious matter, and the data obtained would seem to demonstrate that any irregularity left had little effect on the coefficients of the orifices.

The determination of the static pressure at this point has the definite advantage that the pressure is obtained under relatively stable conditions. A static-pressure connection immediately after the orifice, as used by Messrs. Folsom and Putnam, is not desirable, as this is the position of unstable turbulence. The eddies formed by the fluid immediately after passage through the orifice are very troublesome, although it is possible that in the extreme corner they would have little effect. The graph shown by the discussers has points departing by as much as 3 per cent from the mean line drawn, in the region of ordinary operation. In many tests this deviation is not allowable. It is true that over a range of Reynolds' number (conduit conditions) of from 1000 to 30,000, as shown in the discussers' graph, the coefficient is relatively steady, and this has definite advantages if a rough automatic measuring device is to be used. Otherwise, however, it is not a difficult matter to calculate the Reynolds number and pick the coefficient from the proper graph.

The V-Notch Weir for Hot Water[1]

H. N. Eaton.[2] This paper illustrates, in an interesting way, the fact that frequently, by varying one of the physical quantities involved in a physical phenomenon, we can determine what would be the effect of varying a different physical quantity which is also involved in the phenomenon. In the present instance, the effect on the coefficient of the V-notch of varying the head acting on the notch is used to show what would be the effect, over a limited range of the coefficient curve, of varying the kinematic viscosity of the water flowing through the notch. The advantage of this procedure lies in the fact that it is much more difficult to vary the kinematic viscosity of the water than to vary the head on the notch, at the same time controlling the conditions carefully enough to obtain accurate measurements. This expedient has been utilized to advantage in other branches of engineering and physics, particularly in aerodynamics, and the writer is interested to see an application of it made to hydraulics.

The process of reasoning by which the author arrives at his plot of C against $h/\nu^{2/3}$ appears to be correct, but the following treatment is suggested as a more direct and logical one.

We start with the customary formula for the V-notch

$$Q = Ch^{5/2} \qquad [1]$$

where Q is the volume rate of flow, h is the head on the notch, measured above the vertex, and C is the coefficient of discharge of the notch.

We wish to determine how C is affected by the different physical and geometrical quantities which are involved in the phenomenon.

The following quantities may affect the flow Q, and hence the coefficient C: The head h, the acceleration of gravity g, the density of the water ρ, the viscosity of the water μ, the surface tension of the water s, the width of the approach channel b, the height of the vertex of the notch above the floor of the approach channel H, the width of the crest of the notch plate w, the angle of the notch α, the factor of a relative roughness k of the upstream surface of the notch plate, and to a lesser extent the roughness of the walls of the approach channel.

We can express this dependence as follows:

$$f_1\,(Q, h, g, \rho, \mu, s, k, \alpha, H, b, w) = 0 \qquad [2]$$

where f denotes "function of."

From these eleven significant quantities we can form $n—i$ dimensionless products, where n is the number of significant quantities and i is the number of physical dimensions required to express these quantities (in this case three—mass, length, and time). Hence, eight dimensionless products result, by means of which we can express our relationship as follows:

$$f_2\left(\frac{Q}{g^{1/2}h^{5/2}}, \frac{Q\rho}{h\mu}, \frac{s}{\rho g h^2}, k, \alpha, \frac{h}{H}, \frac{h}{b}, \frac{h}{w}\right) = 0 \qquad [3]$$

The particular forms of the products we choose depend upon the particular relationships we wish to study, and for different purposes we can express the same relations in many different forms. A concrete illustration of this will be given later in this discussion in passing from Equation [4] to Equation [5].

The first three of the dimensionless products chosen above were designed to separate clearly three different effects: first, the balance between the inertial and gravitational forces expressed by the product $\frac{Q}{g^{1/2}h^{5/2}}$; second, the balance between inertial and viscous forces, expressed by $\frac{Q\rho}{h\mu}$; and third, the balance between surface tension and gravitational forces expressed by $\frac{s}{\rho g h^2}$. The fourth variable, k, is a dimensionless roughness factor, and the last four are purely geometrical factors which express the form, but not the size, of the notch and the approach channel.

The first three dimensionless products, because of the particular force ratios which they represent, correspond, respectively, to the Froude, Reynolds, and Weber numbers. However, the names "Froude number" and "Reynolds number" should not be applied to the first two, because these names are used in a more restricted sense to apply, respectively, to the square of a velocity divided by a length and the acceleration of gravity, and to the product of a length and a velocity divided by a kinematic viscosity. It has been suggested to the writer by Dr. L. B. Tuckerman of the National Bureau of Standards that the names "generalized Froude number" and "generalized Reynolds number" be applied to these two dimensionless products. The name "Weber number" is usually applied to the dimensionless product $v^2l\rho/s$, which represents the balance between inertial and surface-tension forces, instead of the form given above. This name has not yet become as fixed in its usage as have "Froude" and "Reynolds" numbers, and, since these two forms of the Weber number both take account of the effect of surface tension, no distinction will be made here.

The surface tension of the water affects the coefficient curve only at very low heads and is probably of no significance over the range discussed by the author of the paper. Consequently, the dimensionless product $s/\rho g h^2$, will be omitted from consideration in what follows. It is interesting to note that, if surface tension can be ignored, the density then appears only in combination with the viscosity in the form of the ratio μ/ρ, which we call the kinematic viscosity, ν, and hence, under this condition, the density and viscosity need not be included separately in [2] but can be replaced by the kinematic viscosity.

The width of the approach channel and the depth of the floor below the vertex of the notch will affect the coefficient at high

[1] Published as paper RP-56-9, by Ed S. Smith, Jr., in the October, 1934, issue of the A.S.M.E. Transactions.

[2] Acting Chief, Hydraulic Laboratory Section, National Bureau of Standards, Washington, D. C. Mem. A.S.M.E.

heads through their effect on the stream lines and on the velocity of approach, unless the dimensions of the approach channel are sufficiently large. It has been shown experimentally that the width of the approach channel does not have any effect on C as long as $b > 8h$.[3] The writer has seen no satisfactory data illustrating the effect of proximity of the floor. Barr gives two curves for a 90-deg notch which indicate that, for a head of 3 in., the depth H must be greater than $3h$ and for a head of 4 in. H must be greater than $4h$. The discussion which follows is applicable only to a V-notch for which the width b and the depth H of the approach channel are so great that they exert no measurable effect on the coefficient even at the highest heads used. This restriction is justifiable here without further consideration, since it is not the purpose of this discussion to set limits to the regions within which the effects discussed are appreciable, but to indicate a more direct method of reaching the conclusion arrived at by the author of the paper.

In addition to the restrictions which have already been set upon the problem, we shall assume that we are dealing with a notch having a given angle α and a given crest width w and that the variation in the relative roughness of the notch plate and the walls of the approach channel with changes in head can be neglected.

With the restrictions thus established we can simplify Equation [3] to

$$f_3\left(\frac{Q}{g^{1/2}h^{5/2}}, \frac{Q}{h\nu}\right) = 0 \quad [4]$$

However, for our present purposes, another of the infinite number of possible combinations of these two dimensionless products will be more convenient, and we replace $Q/h\nu$ by $\frac{g^{1/3}h}{\nu^{2/3}}$ which we do by dividing $Q/h\nu$ by $Q/g^{1/2}h^{5/2}$ and taking the two-thirds power of the result. We also introduce the coefficient C in the first dimensionless product in [4] by means of [1], and [4] now becomes

$$f_4\left(\frac{C}{g^{1/2}}, \frac{g^{1/3}h}{\nu^{2/3}}\right) = 0 \quad [5]$$

With our relation in this last form, we can see, as we could not easily see before, that it is legitimate to plot $\frac{C}{g^{1/2}}$ against $\frac{g^{1/3}h}{\nu^{2/3}}$, and if none of the physical quantities which we have neglected affects C measurably over the range of our plot, we shall get a single curve. Furthermore, as long as the value of g remains constant, as it will in the practical use of the notch, we can drop it from consideration and can plot C against $h/\nu^{2/3}$, as the author has done.

Whether or not all of the physical quantities which have been left out of consideration in deriving Equation [4] actually have no measurable effect on C over the range of the curve given by the author is a question which the writer will not attempt to settle, since this was not the purpose of the discussion.

H. S. Bean.[4] In this paper, Mr. Smith proposes the use of certain arbitrary ratios as parameters against which to plot his coefficients for V-notch weirs. Of course, one is at liberty to use any such parameter as may suit his pleasure or convenience, but in passing them on to others, attention should be called to any dependence that such parameters may have upon the system of units used. Let us examine the proposed parameters for their dependence upon units, referring to the author's equations as they are numbered in this paper.

The basic flow relation as expressed by Equation [7] is

$$Q = Ch^{5/2}$$

While expressing an experimental result, this equation is really a definition of C. C need not be a constant, and, in the general case, will not be constant, but will have a definite and different value for every pair of values of Q and h. It is interesting to note that in order for Equation [7] to balance dimensionally, C must have the dimensions $L^{1/2}\,T$, which are the same as those for $g^{-1/2}$. Thus we find that, as here defined, C is not independent of the units used. Since this equation is used as a basis for Equations [9] and [10], it follows that they also are dependent upon the units used.

This same conclusion may be obtained directly by noting the dimensions of the ratios given by [10]. For example, the dimensions of the first ratio in [10] are $\left(\frac{L^3}{T}\right)^{2/5}\frac{T}{L^2} = \frac{T^{3/5}}{L^{4/5}}$

Thus, while there is true correspondence between Equations [8] and [10], this correspondence is not general; that is, it depends upon the particular units being used. In this connection it is well to note that the author expresses density, viscosity, and surface tension in cgs units, while his weir dimensions, velocity, and flow are in English units. Therefore, in making use of any of the relations given by the author, we must be careful either to use the same combination of units which are given in the paper, or to convert the relations to other units which we might prefer to use.

Author's Closure

The discussers of the paper have stressed the fact that the operators and coefficients used therein are not dimensionless and that both English and cgs units have been used. These informalities were deliberately introduced for greater convenience in use and, because of the need for brevity, this was done without explanation.

The most important point of Mr. Eaton's independent, mathematical analysis is the confirmation of the true correspondence between the coefficient C and the operator $h/\nu^{2/3}$. Mr. Bean's check of the true correspondence between Equations [8] and [10] is appreciated.

It is regretted that the discussion of the paper included no data on triangular weirs using liquids of different viscosities, such as are awaited from the University of California project 273 being conducted by Mr. Carson under the direction of Prof. M. P. O'Brien.

It should be noted that all the figures in the paper are on double-logarithmic paper, even though the ordinates are to a large scale in Figs. 1 and 3. This explanation is needed to clarify the use of the dot-and-dash line in Fig. 1 as representing the exponential Equation [14].

An additional reference which should also be given is: "Flow of Water Over a V-Notch," by Joseph Tarrant, Trans. A.S.M.E., Vol. 50, 1928, paper HYD-50-8, p. 25.

The author concludes by calling attention to the new and useful operator $h/\nu^{2/3}$ as a basis for correlating weir coefficients, not only for hot water but also for oils in the "look boxes" of refineries. The value of the contribution is entirely from the engineering, rather than the scientific, viewpoint.

[3] "Experiments on the Flow of Water Over Triangular Notches," by J. Barr, *Engineering*, London, vol. 89, 1910. See also "Hydraulics and Its Applications," by A. H. Gibson, D. van Nostrand Co., New York, N. Y. Third edition, pp. 162 and 163. See also Trans. A.S.C.E., vol. 93, 1929, p. 1134, Fig. 60*d*, where Prof. W. S. Pardoe gives a curve which indicates that the width may be as low as $3.4h$ without affecting C.

[4] Physicist, Chief Gas Measuring Instrument Section, National Bureau of Standards, Washington, D. C. Mem. A.S.M.E.

Fluid-Meter Nozzles[1]

Ronald B. Smith.[2] The problem of establishing reliable nozzle coefficients and a standard flow-measuring technique for acceptance-test work is of particular concern to the Power Test Codes Committee at the present time. In the writer's opinion the shape that is chosen matters but little providing only that the nozzle can be easily reproduced and accurately installed. The important point is to choose a standard which has been so thoroughly verified that its characteristics under all probable test installations are accurately established.

One of the nozzles under consideration as a standard is the V.D.I. profile, some of the characteristics of which Mr. Buckland compares with the G.E. nozzle. The V.D.I. nozzle is the outgrowth of the nozzle used for the past 30 years for flow-measurement work by the I. G. Farbenindustrie. Within recent times it has been adopted as standard by the International Standards Association and now, as a result, is generally known as the I.S.A. nozzle. Since 1928, largely at the request of the V.D.I., several thousand laboratory calibrations of the nozzle have been made, with the result that its flow coefficients, for pressure drops down to the acoustic and for area ratios ranging from zero to 0.6, have been established under a wide variety of conditions with an accuracy generally within plus or minus 0.5 per cent. The flow coefficient of the I.S.A. nozzle is constant over a greater range than is usually the case with a full flowing nozzle. For instance, in the author's Fig. 14 it is evident that the I.S.A. nozzle can be used to a 50 per cent lower range than the G.E. nozzle before one must resort to cut-and-try methods in the calculations.

By attempting to compensate for the different locations of the pressure taps the author concludes that the coefficient of the G. E. nozzle is $1^1/_4$ per cent higher than the I.S.A. This result is based on the assumption that a pressure measurement in the throat of a nozzle and a pressure measurement in the pipe two nozzle diameters downstream are identical, and are equivalent to the atmospheric pressure with a freely discharging jet. This opinion appears untenable from analysis of the very tests that the author quotes to support it, namely, the work of Stach. Except for the smallest nozzle, Stach's coefficients show less than 0.3 per cent difference between measurements of the I.S.A. nozzle when discharging freely and when operating in a pipe with the usual corner taps.[3] This slight difference can be explained by the fact that Stach used pressure-chamber openings smaller than standard. Thus, the result of Stach's work is to indicate that the pressure measurement in the downstream corner is equivalent to the pressure for discharge into an infinite chamber.

If we compare the pipe and throat-tap measurements on a Moss-Johnson nozzle as reported by Sprenkle,[4] we must conclude that a throat tap reads the pressure about $1^1/_2$ per cent high.

Downstream from the nozzle and along the pipe wall there is a pressure fall. It is interesting to note that this distribution, as in Fig. 1 of this discussion, on a Moss-Johnson nozzle which is practically the same as the G.E. nozzle, is similar to the results reported by Witte on the I.S.A. nozzle. For instance, the minimum pressure is $1^1/_2$ per cent of the differential pressure and it occurs (for m = 0.25) about $^3/_4$ diam downstream from the mouth. Because the same quantitative phenomenon is observed with an orifice it seems probable that the distribution is produced by viscous effects at the boundary of the jet.

In combination with Sprenkle's results, the pressure-distribution curve leads one to suspect that throat pressures are 1 per cent higher than corner pressures, and that, as a result, if the nozzles are compared on this basis, there will be practically no difference in their coefficients. That there is no actual difference between the two nozzle coefficients when the pressures are measured in the same manner has been proved by Witte.[3] For instance, using corner taps, which includes some impact pressure and therefore accounts for a low coefficient, he measures with an area ratio 0.25:

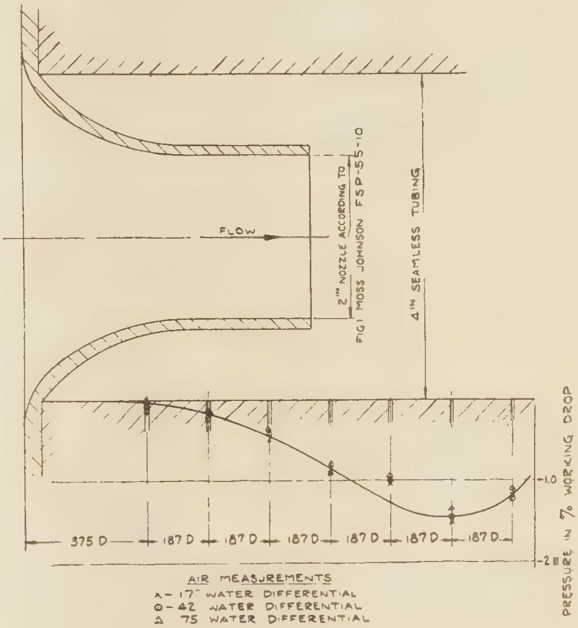

Fig. 1 Pressure Distribution in a Moss-Johnson Flow Nozzle

For the I.S.A. nozzle..........................	= 0.9765
For the Moss-Johnson nozzle....................	= 0.974
For the same Moss-Johnson nozzle with throat taps.	= 0.991

Thus the relative magnitudes in the author's Fig. 14 are misleading.

Mr. Buckland suggests that the rapid fall of the coefficients of the I.S.A. nozzle below the operating region is the result of contact loss in the nozzle. That there is a temporary contact loss in an I.S.A. nozzle where the approach radius is tangent to the throat is known. Not so well known is the fact that nozzles of the G.E. shape also show contact loss at this point. I have observed the phenomenon many times on a Moss-Johnson nozzle by coating the inner surface with lampblack and kerosene and studying the streak lines that are produced by the air. However, in neither nozzle is it of serious importance nor would it be termed a vena contracta, since contact is reestablished within $^1/_4$ in. downstream. The peculiar slope of Mr. Buckland's coefficients in Fig. 8 of his paper between Reynolds' numbers of 10^4 and 4×10^5 may be the result of this phenomenon.

R. E. Sprenkle.[5] Mr. Buckland's paper will be of material assistance in familiarizing engineers with the fact that the Ameri-

[1] Published as paper FSP-56-14 by B. O. Buckland, in the November, 1934, issue of the A.S.M.E. Transactions.

[2] Turbine Engineering Department, Westinghouse Electric and Manufacturing Company, South Philadelphia, Pa. Jun. A.S.M.E.

[3] "Neuere Mengenstrommessung zur Normung von Dusen und Blenden," by R. Witte, *Forschung auf dem Gebiete des Ingenieurwesens*, September-October, 1934.

[4] "A System for the Measurement of Steam With Flow Nozzles for Turbine Performance Tests," by S. A. Moss and W. W. Johnson, Trans. A.S.M.E., vol. 55, 1933, paper FSP-55-10, p. 145.

[5] Bailey Meter Company, Cleveland, Ohio. Assoc-Mem. A.S.M.E.

can style of flow nozzle is a real precision instrument and that its accuracy and reliability well merit its use as a standard of measurement.

Our experience in building and using several thousand flow nozzles of all sizes and for all kinds of flow-metering service, has shown that the use of pipe-line connections at both the nozzle inlet and outlet, as shown in Fig. 13 of the paper, is the simplest and most dependable method of measuring the pressure differential across the nozzle. This experience covers a span of nearly twenty years during which many weighed-water or other tests have proved the adequacy of the commercial nozzle of this design as a means for measuring water, steam, air, gas, and other flow rates.

Pipe taps into the wall back of the nozzle throat instead of into the throat itself, possess some real advantages. First, this location is in a protected zone out of the path or contact with the stream lines of the flowing fluid, and thus not susceptible to errors in static-pressure measurement due to small localized eddies, whirls, or other disturbances such as may, and often do, exist along the throat surface. Moreover, being in a zone where velocities are comparatively low, there is even less chance of this pressure measurement being in error.

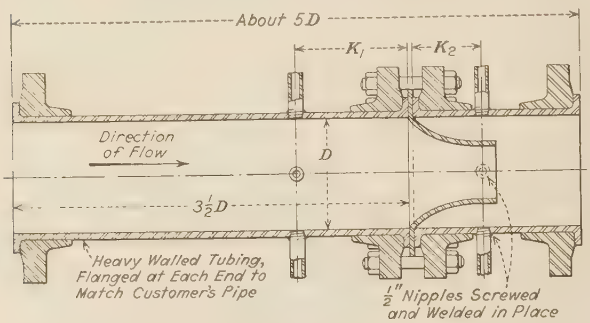

Fig. 2 A Typical Nozzle Pipe Section With Pressure Connections and Nozzle Properly Located

From the standpoint of physical application, the nozzle with the outlet connection made back of, instead of into, the throat, allows the use of a much thinner flange, with a consequent reduction in pipe spread to provide for its insertion between existing flanges. The nozzle proper is easier to build because of the omission of the piezometer chamber and internal connection passages which are required to provide for throat taps.

One of the outstanding advantages of the nozzle, shown in the author's Fig. 13, is that extreme care does not need to be taken in drilling the outlet connection into the pipe wall. True, this must be done in the field, as Mr. Buckland states, but due to its protected location, it is much less difficult to make than the inlet pipe connection which is used by both nozzle types.

The throat tap connection is admittedly difficult to make unless all possible precautions are taken. This point is brought out not only by Mr. Buckland himself, but also in the discussion of the Moss-Johnson paper in 1932 by the present writer, in which comparative tests made with both throat and pipe taps in a special nozzle in the Bailey Meter Company laboratory were described in detail. In that discussion, we demonstrated the difficulty, in fact, almost impossibility, of getting the separate throat-tap pressure readings to check each other, as compared with the ease of obtaining a very satisfactory agreement between the different outlet pipe tap readings. The elimination of this job of making satisfactory throat connections more than compensates for the labor of providing for this connection in the field.

While the pipe tap back of the throat cannot be calibrated as an integral part of the nozzle itself, neither can the inlet-pipe connection which is used with both types of nozzles. And of the two, the inlet connection is the more susceptible to changes in the flow state, being immediately adjacent to the path of the stream lines. As such, it is the most important connection to be included in any integral nozzle-assembly calibration. The truly correct and proper method is to calibrate the nozzle with the section of pipe in which it is to be used, and thus both pressure connections are included in the assembly and all possible installation vagaries eliminated. A typical nozzle pipe section with pressure connections and nozzle properly located, is shown in Fig. 2 of this discussion.

The first reason given for the use of the throat instead of the pipe-line connections, was that the lack of geometrical similarity of the external shape of the nozzle used might produce erroneous results were pipe taps used. We would point out that even along the internal surfaces over which the fluid passed, complete geometrical similarity did not exist. True, the test nozzles were in themselves, geometrically similar in form, but when installed in the pipe lines, the assemblies with the pipe were not geometrically similar by widely varying amounts. To attain complete similarity, the curvature must begin at the same relative point with reference to the inside pipe wall on each nozzle. In all but one of the G.E. nozzles, the distance of the junction of the curvature with the straight flange section as measured from the inside of the pipe wall, varied from 4 per cent to 27 per cent of pipe diameter, and in this one case, this point was actually up in the holding flange by an amount equal approximately to 5 per cent of the pipe diameter. Since the flow must pass over these surfaces, this lack of similarity is likely to produce a larger spread between coefficients of different nozzles of various sizes than would have resulted from pipe-tap measurements made in a region where this lack of similarity was relatively unimportant.

That there can be no *complete* geometrical similarity between nozzles of different diameter ratios, is quite apparent but nevertheless not always fully understood. In fact, only when nozzles of the same diameter ratio are used in different sizes of pipes can such similarity be obtained, and even then the relative pipe roughness may not be quite the same. Since various diameter-ratio sizes must be used for practical metering, it is useless to expect complete agreement of calibration data on a similarity basis.

An improvement can be made, in the attaining of better similarity between different diameter-ratio sizes, by always placing the beginning of the curvature at the surface of the internal pipe wall and then so shape the curvature to the one-quarter ellipse by making the minor axis equal to $(D - d)/2$ instead of $5/8\ d$. With increasing diameter ratios, this ellipse becomes flatter but there are no humps or irregular surfaces over which the fluid must flow and thus no marked or sudden deviations from the natural flow path.

A comparison of calibration data from nozzles of the shape just described, using pipe taps, with the General Electric nozzles would be of interest. In Fig. 11, Mr. Buckland shows such a comparison between the data from a 12-in. × 7.554-in. Bailey Meter Company nozzle, and the average G.E. curve. The agreement of one with the other, is about as perfect as can be expected. However, the range of Reynolds' number used with the 12-in. nozzle was rather small; so to extend the curve to lower limits, a 3-in. pipe size, 60 per cent diameter-ratio nozzle was recently calibrated in our laboratory in Cleveland.

The calibration data obtained from a Bailey Meter Company 3.06-in. × 1.836-in. nozzle is shown in Fig. 3 of this discussion, as well as that from the 12-in. × 7.554-in. nozzle. In passing,

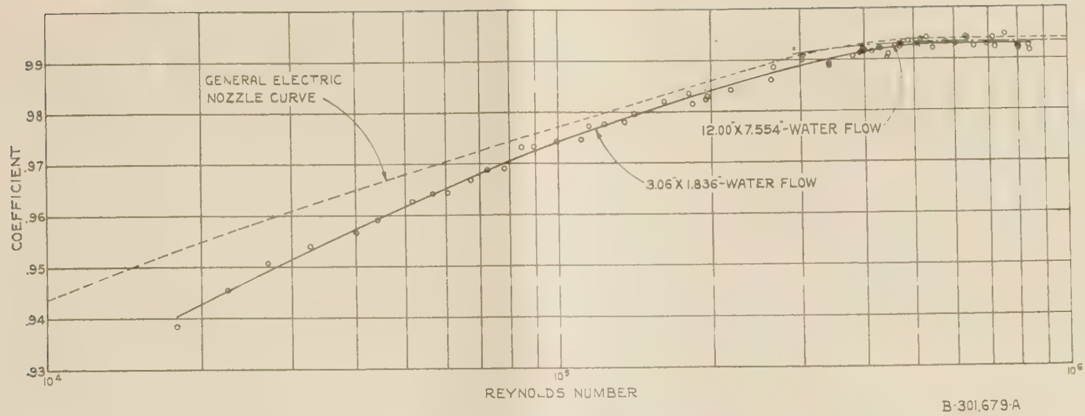

Fig. 3 Calibration of Two Bailey Meter Company Flow Nozzles Compared With Average Curve of General Electric Nozzles

it should be noted that the 3-in. nozzle was made of highly polished brass and calibrated in smooth brass tubing, using water flow while the 12-in. nozzle was made of steel and calibrated in a commercial steel tubing, also using water as the flowing fluid. As will be noted, these two nozzles, checked each other almost perfectly through a range of Reynolds' number from 500,000 to the highest point calibrated and deviated from each other at the most about $^1/_4$ per cent at a Reynolds number of 300,000 or the lowest point tested on the 12-in. nozzle.

In Fig. 3 of this discussion, we have also shown by the broken line, the average calibration curve from Mr. Buckland's Fig. 8, as a comparison with calibrations of two Bailey Meter Company nozzles. Despite the higher diameter ratio, and the fact that both the Bailey nozzles shown used pipe-line pressure connections back of the nozzle throat instead of into the throat, and further, that the internal contour of the nozzle shape was not precisely the same, the General Electric type and the Bailey type checked each other from 0.1 per cent to 0.3 per cent over a working range of Reynolds' number of from 100,000 to 1,500,000, or the highest tested point. Whether or not the increased deviation at lower values of Reynolds' number is due to the difference between the location of the outlet pressure connections, to the small difference in the shape, or to experimental errors, is a question we cannot adequately answer at this time.

It is sufficient to add that through the useful range of Reynolds' number, or from 100,000 up, and with nozzles of diameter ratios not materially exceeding 60 per cent, either of the two types of American nozzles can be used for the purposes outlined in this paper with an accuracy that is certainly well within plus or minus 1 per cent, and with actual calibration within plus or minus $^1/_2$ per cent, provided proper precautions are taken both as to obtaining undisturbed flow through the nozzle, and in the design, construction, and installation of the nozzle assembly itself.

R. J. S. Pigott.[6] In examining Mr. Buckland's paper, one notes a tendency to call various nozzles, or orifices, geometrically similar, when as a matter of fact, they are not. It is not enough to use nozzles that are similar in contour because, for rigorous comparisons, it is necessary also to have similarity in pressure taps, polish of nozzle, upstream pipe, and orifice ratio. This complete condition has practically never been observed in tests as yet, and until it is, we shall not be able to get the full value of Reynolds' criterion comparisons. Scatter of points is much wider than can be assigned correctly to experimental errors, or to any departures from the "single line" theory; and the whole situation for studying the proper relations is somewhat confused.

The long series of experiments on orifices conducted by the joint A.G.A.-A.S.M.E. meter committee shows that the upstream roughness, orifice ratio, and tap location have very noticeable effects upon coefficient, quite in line with theory. While some advance the thought that pipe roughness has no effect on a nozzle, theory clearly indicates there ought to be some effect. If this thought were correct, neither the sharp-edged orifice nor the venturi should show roughness effect; but we know that they do show such differences.

Mr. Buckland has recognized this point in his Fig. 9 wherein the curves better approach full similarity, by eliminating orifice-ratio effects; pipe and nozzle relative roughness remaining the same.

The writer has been working for some time on a method of predicting coefficients, and finds that there is a definite relation between the ratio of "surface area" washed by the fluid between taps, to the area of throat, and the coefficient at any Reynolds number. The relative loss, or $(1 - C)$, is directly related to the pipe flow friction. The writer has for some time used the coordinates $(1 - C)$ vs. $dv\rho/\mu$ on double-log paper. Mr. Ed Smith has also used the same type of coordinates. It gives some very very valuable analytical indications which the semi-log graph of C vs. $dv\rho/\mu$ is incapable of showing.

One other point in nozzle testing has not been given sufficient attention. On a curve showing throat Reynolds' number, we would expect complete viscous flow below $R = 1200$. But above that point, the nozzle is in mixed flow until the upstream section also is fully turbulent. With an orifice ratio of 0.50, the minimum value of throat R for complete turbulence is 2500, and higher for smaller ratios. In addition, there is apparently a stronger tendency for a convergent nozzle to stay in the viscous region at higher values than in parallel sided pipe. As a consequence, many nozzles tested by Mr. Buckland and others cannot be safely considered in fully turbulent flow until values of possibly $R = 30{,}000$ to $40{,}000$ have been passed. There is, therefore, a considerable range in which the flow is somewhat unstable, and the scatter of test points will usually be a little wider.

With regard to a supposed critical Reynolds' number at which the coefficient becomes constant, the writer is inclined to doubt any such value of R as 10^5. In pipe flow, such flattening does not take place until $R = 2 \times 10^6$ to 4×10^6. What appears to be a flat coefficient is merely due to rate of change much smaller than the test accuracy can show. A logarithmic graph

[6] Staff Engineer, Charge of Engineering, Gulf Research & Development Corp., Pittsburgh, Pa. Mem. A.S.M.E.

of (1 — C) shows this condition very plainly. A sloping line at 11 deg or 12 deg, corresponding to the smooth-pipe conditions, will fit this cloud of points quite as well as a horizontal line. In this region, a precision of plus or minus 0.5 per cent in the tests means a variation of 40 to 80 per cent of (1 — C). It is, of course, futile at present to attempt to prove this point, until still better test accuracy can be attained.

The A.S.M.E. Special Research Committee is undertaking an extensive program of investigation on this subject, with the original intention of comparing the proposed I.S.A. or Witte nozzle, with the type discussed in Mr. Buckland's paper. In order to determine more closely those factors not too clearly defined at present, such as roughness and diameter-ratio effects, the program will cover full-range tests on a preferred-number series of both sizes and ratios, with geometric similarity as fully developed as possible. Tests will be made in full with water, but duplicated so far as necessary with steam and air. Funds for this work are to be collected, as is usual in A.S.M.E. research undertakings, from interested industries.

W. S. Cooper.[7] The writer believes that Mr. Buckland should have given more data on the performance of these nozzles in actual field tests. High order of accuracy in measuring flow-rates is demanded on acceptance tests by builders and purchasers of turbine and boiler-room equipment, and direct measurement (by weighing) of condensate and feed-water flow rates has heretofore been considered the only reliable means. After all, the field of application of the nozzle will lie in the replacement of the more expensive direct-weighing method, and it is under such circumstances that a knowledge of the nozzle's performance characteristics is desired.

There is doubt in the writer's mind as to whether such accuracy as claimed by the author with laboratory tests could be obtained with the piping situation usually encountered in the average power plant. Furthermore, liquid flow in most power-plant piping is of a pulsating nature since the fluids are handled either by centrifugal or by reciprocating pumps. Pulsation was probably entirely absent or eliminated in the laboratory tests where the fluid was probably supplied by standpipes.

The writer had occasion recently to conduct field tests on one of the General Electric Company's nozzles described by the author. This nozzle was the one with proportions shown in the seventh line of Table 1 in Mr. Buckland's paper, namely, the 12.01-in. × 5.016-in. nozzle. The laboratory test results reported by the author for this nozzle are shown in his Fig. 8, the plotted points appearing as plus signs. The writer's tests were conducted in conjunction with two condenser acceptance tests where the main condensate was weighed with an accuracy within 0.1 per cent on carefully calibrated scales.

The nozzle was inserted in series with the 12-in. main condensate test header which delivered the condensate from the condenser under test to the weighing tanks. With respect to the piping, the nozzle was located in as favorable a situation as will be found in the field. The nozzle was inserted at a point corresponding to about 110 ft of approach piping (which would tend to minimize pulsation) and the nozzle itself was preceded by 14 ft of straight piping of uniform size. The downstream side of the nozzle consisted of $7^1/_4$ ft before the first obstruction was reached.

The pressure differential across the nozzle was read from two mercurial single-column cistern-type manometers. Both manometers were connected to the same upstream static-pressure tap located in a horizontal plane 12 in. before the entrance edge of the nozzle. The low-pressure side of one manometer was connected through an internal port to the piezometer ring in the throat of the nozzle, while the low-pressure side of the other manometer was connected to a downstream static tap in the pipe at a transverse plane passing through the discharge end of the nozzle. This double arrangement was furnished to provide check readings of the nozzle differential. Each manometer was read by a separate observer. It was found that there was practically no difference between the two sets of readings.

The results of the writer's test are shown in Fig. 4 of this discussion. The horizontal line at C = 0.994 is that portion of the author's blanket curve from his Fig. 8 that applies to the range of Reynolds' number used by the writer. The plotted points indicate the spread of the nozzle coefficient, C, as determined under field conditions. The estimated maximum error on this field test is about 2.4 per cent and the estimated probable error is 0.5 per cent. It should be noted, however, that these field results were obtained under unusually favorable circumstances. It is probably true that in the average run of cases where the nozzle could be used, results would not be so reliable as in this case.

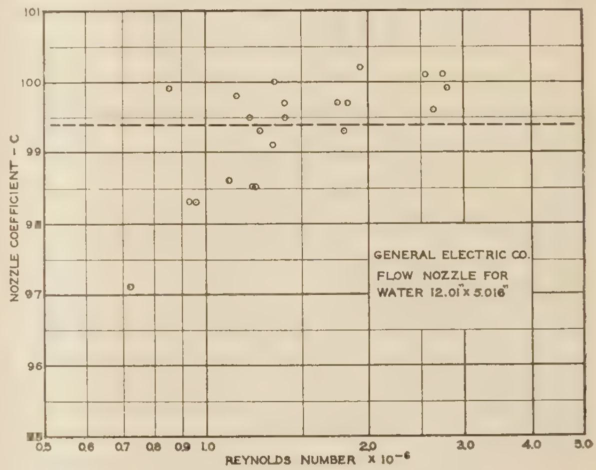

Fig. 4 Performance of General Electric Company Flow Nozzle During a Field Test

(Each point represents a $1^1/_2$-hr run during which the main condensate from a steam condenser was also very accurately weighed after passing through the nozzle. The dashed line at $C = 0.994$ is that portion of the curve in Mr. Buckland's Fig. 8, corresponding to the above field data. The flow nozzle tested in this field test was the same as the 12.01-in. × 5.016-in. nozzle tested by the author.)

Sanford A. Moss[8] and W. W. Johnson.[9] There are of course a good many ways in which flow may be measured with laboratory precision, and the paper by Mr. Buckland is a good example of one of them. It is to be noted that the work was carried out with great care and with a test set-up especially made for the flow measurement, and with all details arranged so that certainty of accuracy was the primary consideration. This puts the work in a wholly different territory from flow measurement made by the usual commercial flow meter which must be suitable for permanent, simple installation and maintenance in a commercial pipe line with a small pressure drop, and with an instrument which gives direct reading of flow. None of these considerations can be allowed to influence the precise flow measurement with certainty of accuracy, which is the author's purpose.

Of course, future research may show that some of the details used by the author might be altered to give as nearly as possible,

[7] Research Bureau, Brooklyn Edison Company, Brooklyn, N. Y. Assoc-Mem. A.S.M.E.

[8] Research Engineer, General Electric Company, West Lynn, Mass. Mem. A.S.M.E.

[9] Mechanical Engineer, General Electric Company, West Lynn, Mass. Mem. A.S.M.E.

measurements corresponding to theoretical flow. For instance, it might be that the throat taps should have a longer parallel portion, such as is shown in the author's Fig. 4 or Fig. 12. However, the close agreement of the author's points shows that his throat-tap measurements must be very good. His Fig. 9 shows a very close agreement between flow coefficients for different values of m, the ratio of nozzle to pipe area. This seems to indicate that the theoretical allowance for velocity of approach takes full account of the effect of pipe diameter, with the possible exception of the $^1/_5$ per cent mentioned which is much less than the errors of observation. The spread of the curves in Fig. 11 of Mr. Buckland's paper is evidence in the discussion as to whether or not Reynolds' number is a proper criterion for abscissas for flow coefficients for different conditions, as was discussed in the Moss-Johnson paper referred to by the author. We thought that our tests with different temperatures and pressures of steam were brought together better by using differential pressure divided by absolute initial pressure as abscissas, and it has also been proposed to use head as abscissas. The droop of the Moss-Johnson curve, No. 1 in Fig. 11, may be due to some such considerations. It must, of course, be admitted that it may also be due to observational irregularities because of the very small flow and small differential pressures at the beginning of the curve. Some of the data given in the Moss-Johnson paper seem to indicate that there was a definite difference in the coefficient with throat taps and with pipe taps, such as for the author's Fig. 13 and that with pipe taps the discharge coefficients are lower. This being the case, the flow coefficients for Fig. 13 seem very high.

E. D. Dickinson.[10] Mr. Buckland's paper is a confirmation of the principles behind the growing opinion that precise measurements of fluids can be obtained by the use of properly proportioned nozzles. The proportions of the nozzle itself constitute but one factor contributing to the accuracy of the results. It is essential that certain precautions be taken. When these precautions are taken, tests can be reproduced with absolute fidelity and the results can be depended upon to be as accurate as laboratory tests.

I do not hold a brief for any particular method of measuring flow by nozzles. However, I have relied upon the flow nozzle for obtaining accurate measurements of steam flow for a period of years and the results have confirmed my contention that precise measurements of flow can be obtained with greater reliability and at less cost by the use of a nozzle similar to that described by Mr. Buckland than by any other recognized method. We have run a great many tests, both of research nature and on commercial machines, where precise results were obtained and valuable information secured that could not have been possible had we not had at our disposal a calibrated flow nozzle similar to Mr. B. O. Buckland's and as described by Dr. S. A. Moss and Mr. W. W. Johnson in their paper[4] presented at the A.S.M.E. Annual Meeting in December, 1932.

Author's Closure

Ronald B. Smith states that Stach's tests (on the coefficients of the V.D.I. Normdüse discharging into the atmosphere) show less than 0.3 per cent difference between measurements of the I.S.A. nozzle when discharging freely and when operating in a pipe with the usual corner taps. He summarizes the situation by saying that the result of Stach's work is to indicate that the pressure measurement in the downstream corner is equivalent to the pressure for discharge into an infinite chamber.

I cannot agree with Mr. Smith's interpretation of Stach's data. The data show clearly that the coefficient of the Normdüse is the same when discharging into the atmosphere as it is when installed in a pipe when the downstream pressure is measured at the point of *minimum pressure on the pipe wall.* In order to clear up this point I shall reproduce Stach's calibration results together with Witte's measurements of pressure difference between the point of minimum pressure on the pipe wall and the downstream corner tap. Table 1 of this discussion shows flow coefficients and pressure differences taken from the papers by Witte and Stach.

TABLE 1 FLOW COEFFICIENTS AND PRESSURE DIFFERENCES ON THE V.D.I. NOZZLE AS GIVEN BY WITTE AND STACH

m	Press. diff. Δ (Witte)	α	α_a (Stach)	$\alpha_m = \alpha - \Delta/2$
0.10	0.010	0.989	0.984	0.984
0.20	0.016	0.999	0.993	0.991
0.30	0.020	1.016	1.010	1.006
0.40	0.023	1.045	1.036	1.034
0.50	0.026	1.096	1.078	1.083

m is the ratio of nozzle area to pipe area.
Δ is the difference between the downstream corner-tap pressure and the minimum pressure on the pipe wall expressed as a fraction of the difference between the up- and downstream corner-tap pressures.
α is the flow coefficient of the Normdüse in a pipe, using corner taps.
α_a is the flow coefficient when discharging into atmosphere, using upstream corner tap and the atmosphere.
α_m is the flow coefficient using the upstream corner tap and the minimum pressure on the pipe wall. It is obtained by subtracting $\Delta/2$ from α, since the fraction Δ is nearly twice as large as the difference produced in the coefficient by using the minimum pressure on the pipe wall instead of the corner-tap pressure.

A comparison of α_a and α_m shows them to be about equal, much more closely so than are α and α_a. I, therefore, conclude that the coefficient of the Normdüse is the same when discharging into the atmosphere as it is when installed in a pipe with the downstream pressure measured at the point of minimum pressure on the pipe wall.

Mr. Smith states that the relative magnitudes in Fig. 14 of the paper are misleading. As defined in the paper this figure is a comparison of the coefficient curve of the G. E. nozzle with the coefficient curve of the V.D.I. Normdüse. The V.D.I. nozzle coefficients have been corrected to what they would be if the upstream pressure had been measured one pipe diameter upstream from the nozzle face and the downstream pressure at the point of minimum pressure on the pipe wall. As Mr. Smith points out, Witte[11] compared the two nozzles by calibrating them both with corner pressure taps. Witte finds that under these conditions the coefficient of the G. E. nozzle is $^1/_5$ per cent lower than that of the V.D.I. nozzles. It is true, that in the light of these recent tests by Witte, Fig. 14 of the paper shows too large a difference between the two coefficients in the range where the coefficients are independent of Reynolds' number. It is also true that in accordance with the Bureau of Standards tests the magnitude of this difference shown in Fig. 14 is correct. However, whatever the correct relation between the coefficients may be in the range where they are independent of Reynolds' number, the same variation of the coefficients with Reynolds' number is given by Witte as is shown in Fig. 14. The coefficient of the V.D.I. nozzle rises much more abruptly with increasing Reynolds' number than that of the G.E. nozzles between Reynolds' numbers of 10^4 and 10^5.

It should be of interest to note in this connection that the usual conditions met in testing a 10,000-kw turbine will require the use of a flow nozzle about $1^1/_4$ in. in diameter in a 4 in. pipe, and the operation of the nozzle in a range of Reynolds' numbers from 10^4 to 10^5. This is very close to $m = 0.09$ and right in the range of the rapid rise of coefficient of the Normdüse. With Reynolds' numbers higher than this range, the Normdüse is as useful for flow measurements as any other carefully calibrated device but

[10] Designing Engineer, Turbine Engineering Department, General Electric Company, West Lynn, Mass. Mem. A.S.M.E.

[11] "Neuere Mengenstrommessungen zur Normung von Düsen und Blenden," by R. Witte, *Forschung auf dem Gebiete des Ingenieurwesens,* September-October, 1934.

at this point of rapid rise in coefficient I would rather use a different nozzle.

I want to thank Mr. Smith for his data on the pressure distribution along the pipe wall on the Moss-Johnson nozzle.

I would like to thank Mr. Sprenkle for his data on the 3 × 1.8-in. nozzle. It would be interesting to have the dimensions showing the location of Mr. Sprenkle's pressure taps so that his data could be more readily compared with other available data.

I want to thank Mr. Pigott for his suggestion regarding a method of plotting flow coefficients.

In answer to Mr. Cooper's question regarding the use of the nozzles in the field, I have made seven turbine-performance tests in which the flow was measured only by means of flow nozzles. In these tests none of the Btu-rate or water-rate points scattered from an average curve more than ± $^1/_2$ per cent. Each of these tests consists of approximately 15 or more points. These results obtained by the use of flow nozzles are much more satisfactory than the example shown by Mr. Cooper.

In the case he cites (The performance tests of the turbine units Nos. 7 and 8 of the Brooklyn Edison Company at Hudson Avenue), the main object was the measurement of the turbine and condenser performance by means of weigh tanks. The flow nozzle was a secondary consideration and was, therefore, neglected. It was not until the tests of the second unit that readings on the manometer were taken often enough. The points of the test on the second unit (No. 8) are in my opinion the only acceptable ones. In fact I would rather use only the last 6 of these. During these last 6 points the manometers were read every $^1/_2$ min. If Mr. Cooper will consider only the points taken on the second unit (No. 8) the results will check our calibration curve much closer. These points are given in Table 2 of this discussion.

TABLE 2 FLOW COEFFICIENTS OF 12 IN. × 5 IN. NOZZLE AS DETERMINED BY WEIGH TANKS DURING A TURBINE TEST

Log_{10} of Reynolds' number	Coefficient of discharge, C
6.125	0.991
6.145	0.995
5.931	0.999
6.056	0.998
6.041	0.986
6.261	0.997
6.286	1.002
6.441	1.001
6.405	1.001
6.124	1.000
6.145	0.997

TABLE 3 CALIBRATION RESULTS OF A 2.8812-IN. × 5.762-IN. FLOW NOZZLE (WATER TEMPERATURE, 69 F)
(Data by Prof. W. S. Pardoe)

Coefficient	Reynolds' number
0.9540	31310
0.9665	42490
0.9745	67090
0.9785	89450
0.9785	109580
0.9868	153190
0.9869	183380
0.9900	216920
0.9905	249230
0.9920	248230
0.9930	284010
0.9920	323150
0.9910	355570
0.9920	391350
0.9945	485280
0.9950	588150
0.9950	686540
0.9950	726800
0.9945	907940
0.9955	590300

In the use of flow nozzles for precise testing it is absolutely essential that the fluctuations in flow be slow enough for the manometer to follow the pressure changes and also for the observers to follow the manometer. I have not yet found a plant where these conditions could not be satisfied by some extra manipulation, as for example, either operating the pumps at different suction levels or using hand control of the flow.

It is true that, with respect to the location, the installation of the nozzle during the tests referred to by Mr. Cooper was entirely satisfactory but the conditions of flow during these tests were not. The flow fluctuated rather widely and rapidly.

Dr. Moss will be interested in the calibration results given in Table 3 on a new nozzle in which the pressure taps are brought straight out from the throat.

Mr. Dickinson's statement that the fluid nozzle is a practical device for testing turbines confirms my own experience.

Since writing this paper, I have obtained a calibration on a 2.8812-in. × 5.762-in. nozzle. This nozzle was welded into a 9-ft length of seamless steel tubing. It was made with four separate throat taps and a flat exit face very much like the nozzle shown in Fig. 12 of the paper. The nozzle and the tube were calibrated together. Table 3 gives the results of the calibration.

Flow Distribution in Forced-Circulation Once-Through Steam Generators[1]

H. J. Kerr.[2] The authors' paper confirms and extends the information presented by the writer in his paper,[3] "Once-Through Series Boiler for 1500 to 5000 Lb Pressure," in which the effect of inlet feedwater and outlet steam temperature on the instability of circuits was shown in diagrams. The value of resistances in stabilizing the flow and to compensate for unequal heat absorption in the different circuits was pointed out.

With reference to the authors' paper, the freedom from deposits in the test apparatus above 2500 lb pressure, irrespective of steam temperature, is worthy of note. Does this mean that above this pressure, steam to turbines will not need to show a purity represented by a resistance of 1,000,000 ohms to permit of continuous operation?

In determining the friction factor for a given Reynolds' number, the authors have used a straight-line projection on logarithmic coordinates of the known viscosity values of water up to 320 F. Probably this is a fair approximation though it does not agree, above 500 F, with Hevesy's values as given in Landolt and Bornstein tables. There may be some question as to the special point shown in Fig. 4 of the paper being discussed, checking in the case of steam as it apparently does with water.

Dealing with the question of stability in the boiler proper, the authors, in Fig. 8, show the effect of inlet-water temperature. These curves can be considered as a magnification of a small section of the curves in Fig. 7 of the writer's paper[3] previously referred to. I believe it would be clearer if the curves were extended over a greater temperature range, thus showing the reversal of direction which takes place, as it is, of course, impossible for the 200-F water curve to continue indefinitely in the direction shown, although it will continue in this direction until the tube is burned.

Fig. 9 of the paper under discussion shows the value of resistances in stabilizing flow. I have found, however, after talking to several engineers, that the significance of the dropping pressure with increasing enthalpy is not well understood. Per-

[1] Published as paper FSP-56-16 by H. L. Solberg, G. A. Hawkins, and A. A. Potter, in the November, 1934, issue of the A.S.M.E. Transactions.

[2] Babcock & Wilcox Company, New York, N. Y. Mem. A.S.M.E.

[3] "Once-Through Series Boiler for 1500 to 5000 Lb Pressure," by H. J. Kerr, Trans. A.S.M.E., vol. 54, 1932, paper RP-54-1a.

haps the authors would be willing to explain this further in their closure.

Referring again to the authors' paper, Figs. 11 and 12 show quite clearly the effect of equalizers on stability in various locations. In this connection, Fig. 12, circuit *C*, shows the effect of unequal heat application to any superheater. This figure indicates that a change in heat application, to different circuits, of the order of plus or minus 5 per cent from the average, produces a change in enthalpy in the leaving steam of some 40 Btu or a change in temperature of some 70 deg. This condition prevails with any superheater and necessitates careful design of the unit to prevent this variation from reaching serious proportions. Fig. 14 shows clearly that properly designed series-type boilers do not need to be operated at the critical pressure.

In general, the authors' conclusions cannot be disputed, provided that in (1) a limit is placed on inlet feedwater and outlet steam temperature; in (2) the added work on the feed pump due to resistance will not be serious in a properly designed boiler; in (3) and (5) the tubes are horizontal or proceed upward. Perhaps (4) should read more definitely, "Economizer and superheater circuits are definitely stable."

I agree with the authors that a unit designed with a separator drum at the end of the evaporating zone simplifies the problem of once-through series boilers. This type can be considered as the end point of the steaming-economizer units, many of which are now in service. We have built and operated such units to the end point.

There are, however, certain advantages in the straight-through unit without drums for high pressures. The problems involved are stabilization of flow, feedwater, and control.

R. C. H. Heck.[4] The authors have shown excellent judgment in places where a choice of procedure had to be made, as in proportioning between liquid and vapor for the mixed current, Fig. 6. It is interesting, as well as technically valuable, to have a theoretical discussion give so clear and consistent a reason for instability already observed in the vaporizing section of the fluid path.

The following questions concerning the flow of liquid water came up while reading the paper: (1) What is the length of the tube section used for the experimental determination of Table 1? (2) Does the survey of data on the viscosity of water up to 320 F agree in results with the tabulation in International Critical Tables, converted to fahrenheit base by McAdams in his Heat Transmission? (3) May we have a formula or plot of the extrapolation beyond 320 F?

Authors' Closure

Referring to the questions raised by Professor Heck, the dimensions of the test section which was used for measuring friction factors are shown in Figs. 1 and 2, of the paper. The distance between piezometer connections is four feet.

The data on the viscosity of water at temperatures up to 320 F, as given in the International Critical Tables, have been converted to fahrenheit base by McAdams in his book, "Heat Transmission," and these were used by the authors in calculating the results which are presented in the paper. The data are plotted in the accompanying Fig. 1 as a solid line with the extrapolated curve indicated as a dotted line.

Mr. Kerr refers to the data on the viscosity of water by G. von Hevesy ("Die Beweglichkeit der Ionen, die dem Lösungsmittel Eigen Sind," published in *Zeitschrift für Electrochemie*, Vol. 27, January, 1921). Hevesy states definitely that the values for the viscosity of water were determined experimentally at a maximum temperature of 156 C and that values for the higher temperatures were calculated on the assumption that there is a relationship between viscosity and electrical conductivity. Experiments have failed to establish the validity of this assumption and his data are not given in the International Critical Tables.

Mr. Kerr suggests that the author's Fig. 8 should be extended to higher temperatures. The maximum ordinate of these curves is 1000 F which is the upper limit of the Keenan steam tables. Extension of these curves to higher temperatures would involve either direct extrapolation of the curves or extrapolation of the steam-table data. The authors prefer to confine their calculations and curves to the range of the steam tables.

Mr. Kerr suggests that the significance of the decreasing pressure drop with increasing enthalpy, as shown in Fig. 9, should be explained in more detail. These curves were calculated by assuming 400 F feedwater, 2500 lb per sq in. outlet pressure and

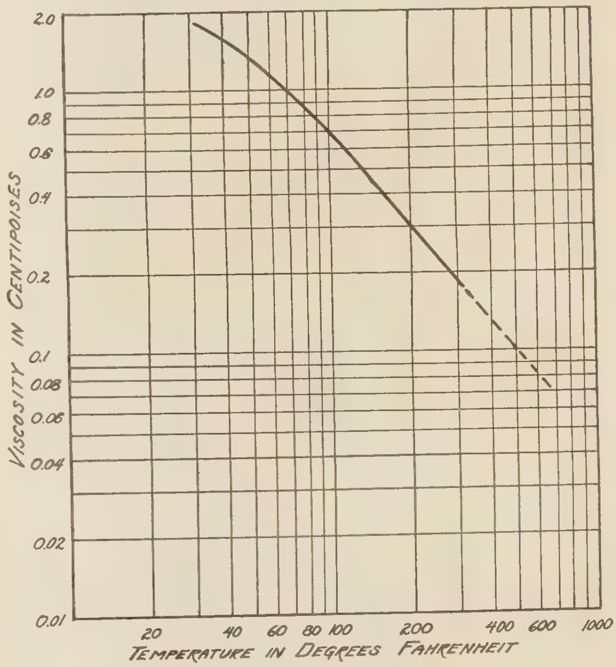

Fig. 1 Viscosity of Water
(Solid curve is based on International Critical Tables. Dotted curve represents extrapolated values.)

constant heat input. Pressure drops were calculated for flow rates sufficient to give final steam temperatures of 670 to 1000 F. The left curve which is nearly vertical, indicates that high flow rates, resulting in low final steam temperatures, will produce practically the same pressure drop as low flow rates and high final steam temperatures. In other words, several parallel circuits which have equal pressure drops and equal heat absorption may deliver steam at widely different flow rates and final steam temperatures. Such circuits are unstable and overheated tubes may be expected. The addition of an inlet resistance which is supplied with water at a constant temperature and therefore has a pressure drop which is approximately proportional to the square of the flow rate, has a stabilizing effect on circuits in which the pressure drop is nearly independent of flow. The pressure drop through the combined circuit varies as some power of the flow rate which approaches two as the value of the inlet resistance is increased, as shown in Fig. 9. The farther these curves depart from the vertical, the greater will be the change in pressure drop

[4] Professor of Mechanical Engineering, Rutgers University, New Brunswick, N. J. Mem. A.S.M.E.

required to alter the flow and the final steam temperature, and the greater will be the stability of the circuit.

It is a source of gratification to the authors that their conclusions are substantiated by the extensive experience of Mr. Kerr.

Current Practice in Surface Broaching[1]

Millard Romaine.[2] In view of the advantages of surface broaching as shown by the examples brought out in Mr. Geschelin's paper a question naturally arises as to why this method has not been more universally used. Before attempting to answer that question it might be well to analyze the various advantages of surface broaching.

The most important advantage is the extreme rapidity of the operation, as compared with other methods, resulting in lower labor cost, etc. The very low time per piece usually obtainable by surface broaching is traceable to two main reasons.

The first of these is that a work piece can usually be chucked more quickly for broaching than it can be chucked for milling. This is due to the fact that the forces set up by broaching are in two very definite directions, one in line with and one normal to the path of the broach. The holding and clamping of the piece is, therefore, greatly simplified. In many cases no clamping at all is necessary. For example, the Houde shock-absorber part shown in Fig. 15 of Mr. Geschelin's paper is not clamped at all. Hence on many broaching operations the handling time of the work is greatly reduced over that necessary for other methods. The second reason for the low unit time for surface broaching is due to the rate of speed at which the cutter passes over the work. This rate is from 12 to 25 or more times as fast as the rate used in milling. In both cases the distance traveled is equal to the length of the cut plus the distance across the cutter. This latter is considerably greater for a broach than for a milling cutter but the speed more than makes up for the difference, with the result that the cutting time for the broaching method is considerably faster than for milling.

A second important advantage of the broaching method lies in the low tool cost usually obtained. In comparison with milling, the first cost of the broaching tools is rather high. Where face mills are used for milling operations, the difference in original cost of cutting tools is rather obvious; where complicated cutter gangs are used on milling it is not quite so obvious, but even so, the first cost of the milling-cutter set-up is rather less than that of the broach. The milling cutters themselves on the arbor may be compared to the broach inserts and, generally speaking, the cost of the inserts is more than the cost of the milling cutters. However, the cutter arbor and the spacing collars for the milling-cutter gang, which perform the same functions of supporting and properly locating the cutting tools proper as the subplates and inserts on the broaching set-up, cost considerably less. As a result the first cost of tooling equipment on a broaching machine is generally more expensive than the first cost on the milling machine. This is, of course, to some extent offset by the fact that the holding fixtures are usually cheaper on the broach. However, when it comes to comparing the total actual cost of the tools when used on high production, the broaching tools show a much lower total cost. This is due, of course, to the extremely long life between grinds obtainable on the broach. The broaching cutters usually run for days while the milling gang runs for hours. Very interesting figures are given by E. S. Chapman, President of the Amplex Mfg. Company, in his paper presented at the Production Meeting of the Society of Automotive Engineers on October 11, 1934. In two cases where direct comparisons could be made, the broaching-tool cost was one-third of the milling-cutter cost in one case and one-ninth of the milling-cutter cost in the other case. All of the broaching-tool costs mentioned by Mr. Chapman were rather low in cost per piece, varying from \$0.0036 in the highest case down to as low as \$0.00057 in the other case.

The long cutter life resulting in these low tool costs is due to a number of factors, among which may be mentioned the rigidity of the average set-up, and the fact that the tooth on the broach, taking a chip of constant thickness, does not have to build up that chip from zero thickness to a maximum, as is the case with the ordinary milling cut. Since the broaching cutter moves in a straight line, it is not necessary to provide a clearance angle that will prevent dragging on the heel of the cutting land. This allows the use of lower clearance and rake angles. The result is a stronger cutting edge and one which is also capable of dissipating heat a little more rapidly. Another reason for long cutter life lies in the fact that the broaching cutter operates at about half or less the cutting speed of the milling cutter. When cutting materials require the use of a coolant, it is very easy to apply this coolant to a broaching cutter. In the case of a milling cutter, centrifugal action makes it difficult to get the coolant where it will do the most good. Another and very important reason for the long life of broaching tools is the fact that the roughing teeth remove the metal and the finishing teeth do the finishing. It is quite frequently necessary to sharpen the milling cutter which is still capable of removing metal, simply because the finish produced is not satisfactory, the teeth having been damaged by the roughing. On the other hand, on the broaching cutter the finishing teeth remove a minimum of stock, do not encounter any scale, generally speaking, and should naturally last much longer.

Another advantage of the broaching method lies in the facts that the machine employed is of simple construction, that its fixtures have a low first cost, and that the total investment required for a given production is generally lower with broaching equipment than it is with milling equipment.

A fourth advantage is effected as a result of the simplicity of the broaching equipment, inasmuch as this makes for low maintenance costs.

When we consider the foregoing advantages we are surprised, therefore, to find that this method has been restricted almost entirely to the automotive and other high-production industries.

An analysis of some of the operations quoted will show, perhaps, the reason for this fact. Published data reveal the fact that stock removed by the broaching operation apparently does not exceed a maximum of $^1/_4$ in. at any time. Another interesting observation which may be made is that in almost every case where broaching equipment is used, the stock is removed from a forging or from a surface which has been machined previously and that in very few cases is stock removed from castings where much variance in stock removal is to be expected. In other words it is apparent that the broaching method has been applied to parts where, first, comparatively little stock is removed ($^1/_4$ in. or less but usually around $^1/_8$ in.) and, second, where this stock removal is held within fairly close limits. Now it is only in high-production industries that rough parts come through which require an average stock removal of $^1/_8$ in. or less; industries with comparatively low-production volumes not being able to afford either forging dies or patterns and foundry equipment required to hold a part to set limits. As a result their parts come through with as much as $^1/_2$ in. stock. The removal of this large amount

---

[1] Published as paper MSP-56-1, by Joseph Geschelin, in the November, 1934, issue of the A.S.M.E. Transactions.

[2] Sales Engineer, The Cincinnati Milling Machine Company, Cincinnati, Ohio. Assoc-Mem. A.S.M.E.

of stock, plus the fact that it may vary, has two main effects upon the economic use of the broaching method.

The first of these is evidenced in the fact that removal of the additional stock means increasing the stroke of the broaching machine, thus necessitating a larger machine for this purpose. The length of travel of the cutter past the work either in the case of a milling machine or a broaching machine is equal to the length of the work piece plus the distance across the tool. In the case of a milling machine this distance is constant regardless of how much stock there is to be taken off; if excess stock is encountered, the operator of the milling machine can get through the cut with very little difficulty by slowing down his feed rate. On a broaching operation, however, if a piece of work which normally has $^1/_8$-in. stock on it and requires a broach 30 in. long, came through with $^1/_4$ in. of stock to be removed, a broach 60 in. long should be provided which, of course, almost doubles the length of the travel required to produce the piece. This indicates that the broaching force remains the same and the speed of the broach travel remains the same, but the distance of the travel has to be much more. This, therefore, means a much larger machine because of the greatly increased stroke.

The second main effect that the removal of large amounts of stock has on the use of the broaching method is one concerning the time for passing each piece over the machine, the time being controlled by the broaching tool which must be designed to take care of the maximum amount of stock. In the case of a milling operation the removal of additional stock has no particular effect on the cutter, the cut is simply taken at a slower feed rate, with no bad effects, as a rule, on the cutter itself. However, in the case of a broach operation, if the broaching tool is designed for removing a maximum of $^1/_8$-in. stock and a piece is encountered having $^1/_4$ in. stock, that extra $^1/_8$ in. must be taken off by the first tooth of the broach which, being practically impossible, involves considerable hazard. Extra unlooked for amounts of stock, therefore, may, and do, quite frequently cause breakage of the tools and the work. Therefore, the only safe way to design broaching equipment is to design the broaching tools for the maximum amount of stock which is to be expected and to provide a machine with sufficient stroke to take care of this maximum amount of stock. This means, of course, that the time for each piece passed over the machine is the same for the piece that has the maximum amount of stock. On the other hand, on the milling machine most of the pieces are produced at the high rate of production and only the occasional piece with the excess stock is produced at the lower feed rate.

These economic considerations are exemplified by the sectional broach shown in Fig. 3 of Mr. Geschelin's paper, wherein the broach is designed for a 48-in. stroke, the broaching cut being about 42 in. long. This length is required because of the necessity of sometimes removing as much as $^7/_{32}$ in. stock which in turn is necessary because this first broaching operation is used as a corrective operation for the weight and balance of connecting rod being produced. If it were possible to hold all of the connecting rods to a stock removal of only $^1/_8$ in., this job could be done at a considerably faster rate or a much smaller machine could be used. As the operation is at present set up, about 90 per cent of the connecting rods are machined only by the last few sections of the broaching tool.

It would appear, therefore, that the increase in use of surface-broaching machines is going to depend more or less upon the development in the low-production industries of forging and foundry practice to a point where the amount of stock to be removed and the variation in the amount of stock from piece to piece is held to fairly close limits.

Another thing that militates against the use of a broaching method in low-production industries is the rather high cost of the tooling equipment. The broach holders, subplates (particularly if they are provided with wedge adjustment), and inserts cost considerably more than arbor gangs and the amortization of these extra costs over the expected quantity of pieces to be produced usually makes a broaching operation for a limited number of pieces, when analyzed to include this factor, considerably greater than the milling method; although the actual labor cost to perform the operation is much lower by broaching. Another point to be considered is that even in high production there are many pieces the shape of which preclude the use of the broach. In order to broach a surface on any part, the surface must lie in such a position on the work that a broach of considerable length can be passed across it. Sometimes it is not possible to meet this condition which eliminates the broach possibility.

In conclusion we would say that the determination of whether a given operation should be performed by broaching or milling can only be made after a careful analysis of both methods taking all factors into consideration, both from a mechanical standpoint and from the standpoint of the economic factors involved, which analysis, of course, requires a rather complete knowledge of both methods.

Robert T. Kent.[3] The question has been raised as to the application of surface broaching to other than mass-production fields. The tenor of the discussion seems to incline to the idea that the cost of equipment will bar surface broaching unless production is in sufficient quantity to keep the equipment in operation for a major portion of the time. The writer is of the opinion that quantity of production has little or nothing to do with the question, except as one factor that must be considered along with others in arriving at the answer. The question is answered by determining what method of production gives the lowest unit cost. In ascertaining the unit cost, everything that enters into cost, such as operating cost, taxes, interest, repairs, maintenance, set-up time per piece, and others, must be considered. When the problem is analyzed in this manner, there can be no question as to which method is best for any particular set of conditions. This method applies to all problems of production, as well as to surface broaching versus milling.

The writer is fortified in this opinion by a case within his own experience. A machine that was distinctly mass-production equipment was offered for a certain class of work. The output of this machine was such that its production in three to five hours was sufficient to supply the manufacturer's needs for the week. At first it seemed foolish to make an investment in equipment that would stand idle the greater portion of the time, but an analysis on the basis of unit costs showed that the investment was profitable and resulted in a net reduction of the overall cost of the work.

Collapse by Instability of Thin Cylindrical Shells Under External Pressure[1]

G. C. Priester.[2] Equations developed from purely theoretical and ideal conditions are often found to be too cumbersome for practical application. To develop an equation which will meet practical conditions and involve simple calculations to a limited degree of accuracy requires familiarity with the ideal re-

[3] Consulting Engineer, Verona, N. J. Mem. A.S.M.E.

[1] Published as paper APM-56-20, by Dwight F. Windenburg and Charles Trilling, in the November, 1934, issue of the A.S.M.E. Transactions.

[2] Professor of Materials of Engineering, University of Minnesota, Minneapolis, Minn.

lationships and a working knowledge of its experimental limitations.

The authors of this paper have given an excellent interpretation of the theoretical formulas involved and have set up an empirical formula which conforms to the former. This is a decided advance in our present theory of the collapse of thin tubes under external pressure.

In all problems of stress analysis it is desirable to have a complete theoretical analysis of the problem and sufficient experimental data to verify the general law. Whenever the experimental data fail to conform to the theoretical formula, either the theory is inadequate, or the methods of testing procedure have not been properly controlled.

The authors have shown why their experimental results do not agree exactly with the theoretical values. They have set up an equation which takes into account the necessary theoretical considerations and which agrees, within practical limits, with experimental data. They have stated the limitations of the equation. The paper includes a detailed explanation of a method of procedure for the solution of a specific problem.

W. Hovgaard.[3] In 1921 I drew the attention of the Bureau of Construction and Repair to the work done in this field by von Mises, von Sanden, and Günther in connection with the design of German submarines during the War. Since then I have been in touch with the Experimental Model Basin regarding this matter, and have corresponded with Mr. Windenburg about it.

The paper gives a review of all the formulas proposed for determining the strength of cylindrical tubes against collapse by instability and shows very clearly the relations between them. Von Mises's formula, [6], is shown by the experiments to be the most accurate.

The authors have, however, gone beyond the results attained by previous workers in this field by constructing a much simpler and yet quite accurate formula, given as [9] in the paper. Following von Mises, the envelope of the n-curves was obtained by differentiating formula [8] and eliminating n. But while von Mises applied this method to a simplified form of formula [8] so that it was valid only near the origin, Mr. Windenburg derived the formula by direct differentiation of formula [8] itself, and then by a skilful approximation simplifying the equation of the envelope. Mr. Windenburg also pointed out an error in von Mises formula, [2]. For the practical engineer formula [9] is of great value because it gives the critical pressure without a knowledge of n, which can be found independently from Equation 1. The experimental verification carried out by the Model Basin gives the engineer an assurance of the soundness of the formula.

It appears, from Table 3, that for short vessels the formula gives a rather high value of the critical pressure and hence of the permissible working pressure.

E. F. Miller.[4] The paper explains the method in which the last draft of Proposed Rules for Construction of Unfired Vessels Subjected to External Pressure was reduced to such a simple usable form. The value of any technical contribution is measured by its usefulness. When complex formulas can be simplified to such an extent by a series of approximations without appreciably affecting their accuracy, it represents a real contribution for the use of the design engineer.

The proposed rules for construction of external-pressure vessels is limited in its scope to the simpler forms of vessels. The usefulness of the code would therefore be considerably extended by the inclusion of the major part of the present paper as an appendix to the code for use in designs that fall outside the scope of the proposed code.

W. P. Roop.[5] This paper effectively summarizes a large amount of valuable work. In connection with its use in design, the following questions occur to me:

1 To what extent does existence of hard surface layers in the thin sheets used in the tests affect the experimental results?

2 Is there any theoretical or experimental indication of deflections exceeding those which would occur in simple compression, due to elastic buckling below the yield point? The rigidity of other thin-metal structures with which I have recently been concerned is materially affected by such action.

3 Is it possible to obtain a useful approximation describing the behavior of a flat plate under hydrostatic and coplanar load by considering D to approach an infinite value?

4 Formula [9] is understood to represent a well substantiated result of experimental and theoretical analysis. Disregarding all questions of loss by corrosion, excess weight due to the requirements of convenience, and inadvertent departure from specifications, what margin is considered appropriate to cover the spread between ultimate and working pressures? The sources of uncertainty I have in mind are error in the formula, unhomogeneity of material, and risk of injury causing excessive out-of-roundness.

C. O. Rhys.[6] This paper treats the three classes of tubes considered in a convenient, thorough and clear manner. The way in which the different formulas agree with each other and with the results of experiments is very conclusive from the viewpoint of correctness and applicability.

The one exception to the above is the large difference between formulas [A] and [B]. It is interesting to note that while [A] is derived from theoretical considerations for a radial load only, [B] is the result of experiments which appear to have been made on tubes subjected to both radial and axial loads. (See Trans. A.S.M.E., Vol. 53, paper APM-53-17b, p. 232.) It might be expected that this difference in loading would affect the resulting formulas, but an inspection of Table 1 of the present paper shows that differences in collapsing pressure for the two kinds of loadings are only important for very short tubes and almost disappear when $L/D = 2$. From the reference given above, it seems probable that [B] is based on data from a number of tubes for which $L/D = 8$ or more. It can be seen from Fig. 1 that the critical length, which would correspond with $n = 2$, is in the region of $L/D = 8$ to 10. All this appears to show that the difference between [A] and [B] is in no way dependent on the difference in loading, and emphasizes the importance of departures from a geometrically perfect form.

Formula [9] is derived in a very interesting way from formula [8]. It automatically does away with the necessity for finding the proper value of n in formula [8] or in any of the other formulas in which n appears. That it reduces to zero instead of to [A] when L becomes infinite, seems quite in order. As already pointed out formula [A] is for radial loads only while formula [9] is for both radial and axial loads. For the latter case, the load required to bring about failure would become almost nothing when the tube became very long; in fact, it would approach a very long column under a slight buckling load.

As shown by Equation [28], for the proper set of coordinates, formula [9] becomes identical with Euler's equation for long columns. This effect would not occur in the case of formula [A], which is independent of length.

To put the matter in another way, formula [A] applies to tubes

[3] Brooklyn, N. Y.

[4] Mechanical Engineer, Westinghouse Electric & Manufacturing Company, South Philadelphia Pa., Jun. A.S.M.E.

[5] Lieutenant Commander (CC), U.S.N.

[6] Standard Oil Development Co., Elizabeth, N. J.

beyond the critical length, and loaded with radial pressure only. Once the critical length (or length beyond which the collapsing section receives no support from the ends) is exceeded, the collapsing pressure is independent of length.

Formula [9] and Equation [28] apply to tubes loaded with both radial and axial pressure. When the tube gets very long, it appears reasonable to suppose that the axial load would cause failure by buckling, as in a column, before the radial load would cause failure by the kind of collapse considered in formula [A].

The mathematical work in the derivation of formula [9] and in the determination of the number of lobes has been gone over and found to be correct.

F. V. Hartman[7] and R. G. Sturm.[8] The several formulas given by the authors for the collapsing pressure of circular thin-walled tubes whose lengths are shorter than the critical length are all based on the ideal type of end constraint, namely, simply supported ends which "tend merely to maintain the circularity of the tube without restricting the slope of the tube walls."

There is some recognition given, to the fact that the ends of the walls may be fixed or restricted against the change in slope, but it is simply stated that such restraint makes for added safety. For certain proportions of cylinders the effect of fixity of the ends may amount to several times as much as the collapsing pressure of simply supported cylinders. Since in many cases economy demands that excessive unknown factors of safety be eliminated wherever possible, it seems that more consideration should be given to the effect of fixation on the strength of cylinders.

The authors give 36 tests in confirmation of their final choice of a formula to be used in design of pressure vessels. Unfortunately, however, there has been no mention made of what the conditions of the ends of the test specimens were. Such a comparison may lead to the same difficulties as would be encountered in tests of columns whose end restraint is unknown. It should be appreciated that the way in which end fixity affects the strength of tubes is not the same as the way that end fixity affects the strength of columns, but for short tubes end fixity may be as important as it is for columns. Certainly one would not test a number of columns to compare with Euler's theoretical column curve for columns with round ends by simply cutting columns to different lengths and testing them in a machine where the end conditions are unknown.

From a study of reference 3 at the end of the paper, it is noted that some of the cylinders were relatively long with a number of intermediate wire stiffening rings, while others seemed to be unstiffened tubes. In this reference, a photograph of a tube 16 in. in diameter and 40 in. long with inside wire-frame stiffeners is shown. It is evident from the photograph that the shell tipped at the stiffener which seems to indicate that this form of stiffener offers very little restraint to the shell. It would be valuable to know if all of the specimens were supported in this manner.

In the photograph just referred to, the lengths of lobes 1 and 2 appear to be longer than some of the other lobes. Since the lobe formation did not extend entirely around the shell it would be of interest if the authors would explain the method used in determining the number of lobes found by experiment.

The out-of-roundness, while not emphasized in the present paper, is indicated in Table 3. It is interesting to note that for model no. 63 which is the case of maximum out-of-roundness relative to thickness, the actual collapsing pressure by experiment was 43 per cent greater than the critical pressure for an ideal tube computed by the recommended formula. For model no. 66, which has the least out-of-roundness relative to the thickness, the actual experimental result was only 84 per cent of that computed by formula [9]. It would seem likely that conditions other than out-of-roundness are responsible for the variations noted. Out-of-roundness expressed in relation to thickness seems to be misleading. On the basis of thickness, model no. 63 is about 16 times more out-of-round than model no. 66, but on basis of diameter, the former is only about 6 times more out-of-round than the latter.

From Table 3, it may be noted that there is a general tendency for the collapsing pressure determined by experiment to be greater than that computed by formula [9] in the ranges where the collapsing pressure is small. In this range one usually expects to find the best agreement between theory and experiment. On the other hand, the experimental values are definitely less than the computed values in the higher ranges of collapsing pressure. Since some of these discrepancies are in the neighborhood of 40 per cent, it seems that an explanation should be sought. Perhaps the conditions of end restraint may be the answer.

D. B. Wesstrom.[9] The authors have presented in a concise, logical, and convenient form a discussion of the more important formulas relating to external-pressure vessels subject to collapse by instability. The experimental results shown in Table 3 and Fig. 2 are of immense value in demonstrating the soundness of applying these rational formulas to practical problems.

The impression is given in the paper that formula [6] for tubes under both radial and axial pressure is on the side of safety in all cases, being slightly oversafe for tubes with radial pressure only, as represented by formula [1]. This is not strictly true for pressure-vessel design. Vacuum towers generally have internal equipment of considerable weight and sometimes have a large concentrated load of auxiliary equipment placed on the top head. In addition there are wind stresses which, while they vary as he distance from the neutral axis of the tower, may be considered fairly uniform over at least one or two lobe lengths of the circumference. The same may be said of deadweight stresses where vessels are supported horizontally.

The longitudinal stresses due to deadweight and wind load may exceed the simple stress due to axial pressure, and in extreme cases may be several times the simple pressure stress. Thus for practical purposes formula [6] really represents only the average case, as does formula [9] likewise, and this justifies the use of a fairly high factor of safety in any general code for the design of such vessels.

In discussing the ideal end conditions for tubes shorter than the critical length, the authors state that any fixation makes for added safety. It is probable that they have reference only to fixation against rotation. Fixation against radial contraction may have the opposite effect. In a vessel of ideal design, the stiffening rings will contract along with the shell although not to the same extent. If the stiffening rings were made heavier, the difference in radial contraction would be increased, and higher bending stresses would be set up in the shell plate at and near the points of support. It is a question whether they would be sufficiently high to lower the collapsing pressure, but certainly they do not make for added safety.

The writer was interested in the fact that formulas [3] and [8] give values of p one-third higher than formula [A] when L becomes infinite, and endeavored to find the reasons for this. In the case of formula [3] this is brought about by dropping the unity term within the first pair of brackets in formula [2]. When L becomes infinite the only members left within the brackets are

[7] Experimental Job Shop, Aluminum Company of America, New Kensington, Pa. Mem. A.S.M.E.

[8] Research Engineer Physicist, Aluminum Company of America, New Kensington, Pa.

[9] Bloomfield, N. J. Jun. A.S.M.E.

$n^2 - 1$, and as n equals only 2 under these conditions, the unity member compares favorably with n^2 and should be retained. Formula [3] applied to a tube of infinite length would then check formula [A].

A similar situation arises in formula [8] because of too much simplification. Referring to formula [6], this is due partly to replacing $n^2 - 1$ by n^2 in the denominator at the end of the equation, and partly to dropping the second and third terms within the braces. When written out, neglecting powers of ρ higher than the first, these terms become

$$-2\mu_1 n^2 + \mu_2 = -2n^2 - \rho\,(3+\mu)n^2 + 1 + \rho\,(1+\mu)$$
$$= -2n^2 + 1 - \frac{(3+\mu)n^2 - 1 - \mu}{n^2\left(\dfrac{2L}{\pi D}\right)^2 + 1} \quad \ldots\ldots\ldots\ldots [a]$$

The only simplification that might properly be made would be to neglect $(-1-\mu)$ in the numerator of the third term in formula [a]. Otherwise the three terms should be retained within the braces in formula [6] in developing formula [8]; also the unity term in the aforementioned denominator should be kept. Under these conditions, formula [8] would check formula [A] for tubes of infinite length.

It is noted that formulas [5] and [9] reduce to zero for tubes of infinite length. It is believed impossible to modify them to agree with formula [A] for this extreme case without robbing them of the simplicity which was sought in deriving them. Despite this, the writer believes that formula [9] of the U. S. Experimental Model Basin is an outstanding contribution to the subject, as evidenced by its agreement both with the theoretical exact formula [6] and with experimental results, as shown in Tables 2 and 3, respectively. Formula [9] has the added advantage that a determination of n is unnecessary. The value of n is of little practical interest to the pressure-vessel designer.

The authors make it clear that formula [9], along with the others, is applicable only to tubes shorter than the critical length where collapse will occur by instability. The writer feels this should be emphasized by some suggestions for determining the range of application of formula [9] for any given t/D ratio in a practical problem. Obviously one method is to calculate the collapsing pressure by simple crushing

$$p = 2S(t/D) \quad \ldots\ldots\ldots\ldots\ldots\ldots\ldots [b]$$

where S is the hoop stress at which failure by simple crushing is assumed to take place; also to calculate the collapsing pressure for a tube longer than the critical length, by formula [A] or [B]; and reject all values of p obtained from Equation [9] that do not lie within this range.

Another method, in some respects more useful, is to determine the limiting values of L/D for which formula [9] can be applied. Setting formula [9] equal to formula [b] and solving, the lowest L/D value to be used in formula [9] is found to be

$$\left(\frac{L}{D}\right)_{\min} = 0.45\left(\frac{t}{D}\right)^{\frac{1}{2}}\left[\frac{2.69\,E\,(t/D)}{(1-\mu^2)^{\frac{3}{4}}\,S} + 1\right] \quad \ldots\ldots [c]$$

which for $\mu = 0.3$ becomes

$$\left(\frac{L}{D}\right)_{\min} = 0.45\left(\frac{t}{D}\right)^{\frac{1}{2}}\left[\frac{2.89\,E}{S}\left(\frac{t}{D}\right) + 1\right] \quad \ldots\ldots [d]$$

The highest L/D value to be used in formula [9] is found in a similar manner by placing this equation equal to formula [A]

$$\left(\frac{L}{D}\right)_{\max} = \frac{1.21(1-\mu^2)^{\frac{1}{4}}}{(t/D)^{\frac{1}{2}}} + 0.45(t/D)^{\frac{1}{2}} \quad \ldots\ldots\ldots [e]$$

Formula [e] varies but little over a wide range of μ, and for $\mu = 0.3$ reduces to

$$\left(\frac{L}{D}\right)_{\max} \frac{1.18}{(t/D)^{1/2}} + 0.45(t/D)^{1/2} \quad \ldots\ldots\ldots\ldots [f]$$

If formula [B] is used as the basis of comparison the constant 1.18 in formula [f] is replaced by 1.56. In either case, the second term in formula [f] can be neglected.

In cases where the most economical design consists in using the minimum plate thickness, the required t/D ratio can be computed from formula [b] and the resulting value inserted in formula [d]. This will give the maximum value of L/D that can be used without entering the region of instability and thus making necessary the use of a heavier shell plate.

Formula [d] and formula [f] with a constant of 1.56 have been tested against the chart in the A.S.M.E. Code rules in reference 4 and found to check the intersections of the straight lines when prolonged. The straight lines on the chart are connected by transition curves, representing the intermediate region mentioned in the beginning of the paper. Thus these formulas do not check the chart exactly, but are useful in constructing such a chart, or similar charts.

T. McL. Jasper.[10] The authors of the paper have presented experimental data which are associated with very slender tubes under collapsing conditions. The available data in this field are meager and those supplied by the authors are a welcome addition to the results available on very thin tubes. In such tubes, in general, unless they are relatively very short, the yield-strength properties of the steel do not enter into the problem.

The writer's work on collapse has been with commercial tubes.

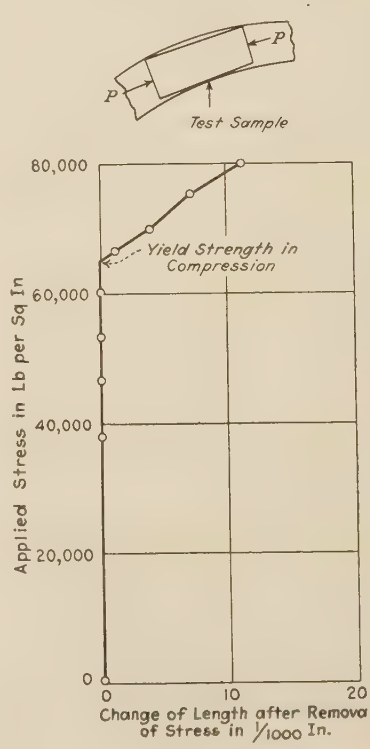

Fig. 1 Showing Yield Strength in Compression

[10] Director of Research, A. O. Smith Corp., Milwaukee, Wis. Mem. A.S.M.E.

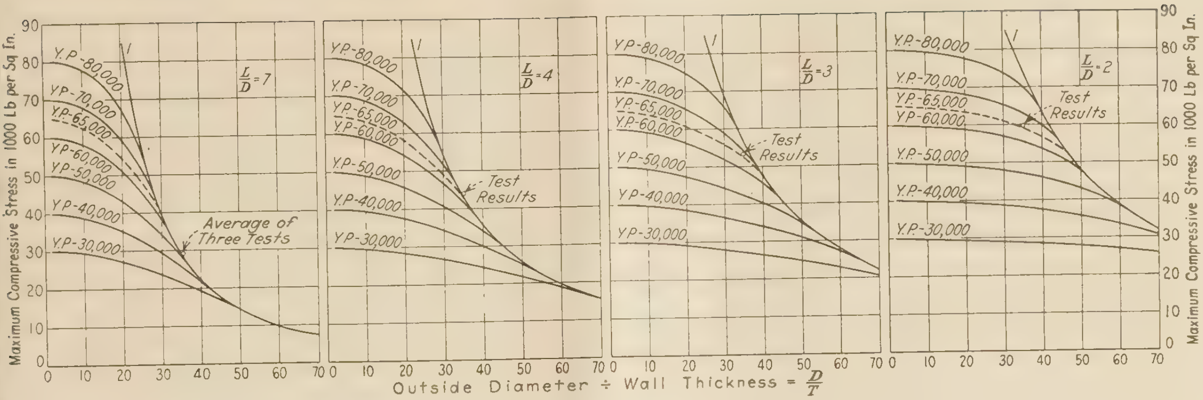

Fig. 2 Fig. 3 Fig. 4 Fig. 5

FIG. 2 RELATION BETWEEN MAXIMUM COMPRESSIVE STRESS AT COLLAPSING PRESSURE AND D/T, FOR HOMOGENEOUS TUBES OF STEEL HAVING VARIOUS YIELD-POINT VALUES

NOTE: Tubes are 7 diameters in length and of uniform roundness and thickness.
1—Curve calculated from Sturm's equation.

FIG. 3 RELATION BETWEEN MAXIMUM COMPRESIVE STRESS AT COLLAPSING PRESSURE AND D/T FOR HOMOGENEOUS TUBES OF STEEL HAVING VARIOUS YIELD-POINT VALUES

NOTE: Tubes are 4 diameters in length and of uniform roundness and thickness.
1—Curve calculated from Sturm's equation.

FIG. 4 RELATION BETWEEN MAXIMUM COMPRESSIVE STRESS AT COLLAPSING PRESSURE AND D/T FOR HOMOGENEOUS TUBES OF STEEL HAVING VARIOUS YIELD-POINT VALUES

NOTE: Tubes are 3 diameters in length and of uniform roundness and thickness.
1—Curve calculated from Sturm's equation.

FIG. 5 RELATION BETWEEN MAXIMUM COMPRESSIVE STRESS AT COLLAPSING PRESSURE AND D/T FOR HOMOGENEOUS TUBES OF STEEL HAVING VARIOUS YIELD-POINT VALUES

NOTE: Tubes are 2 diameters in length and of uniform roundness and thickness.
1—Curve calculated from Sturm's equation.

which are relatively thick and in which the physical as well as the elastic properties of the steel enter.[11] The equation set up by R. G. Sturm in combination with the compression yield points of the steel under collapse is used in the writer's work and a very close check-up has been obtained which confirms the use made of curves such as result from the aforementioned work. I am presenting five typical curves which show results which have not heretofore been published.

Fig. 1 of this discussion shows a curve indicating the yield point in compression of the material. The specimen from which these test results are taken is relatively small but very accurately made and consists of a rectangular prism taken in the direction of stress which causes collapse. The yield strength in compression is obtained by applying successive loads to the prism and plotting the stress applied against change of length after each successive load is removed. The writer's Figs. 2 to 5 show collapse tests made from tubes from which the steel in Fig. 1 was taken and are the figures shown in the paper referred to. It will be noticed that the (D/T) value is constant, but that the actual length has been varied to produce (L/D) values of 7, 4, 3, and 2, respectively. These diagrams were designed using Sturm's equation and take into consideration the end conditions represented by a vessel. The test vessels were the actual length and the ends were actual plates welded to the cylinders.

By varying the length of the test vessel it has been possible to check both the elastic phase as well as the phase of the problem controlled by the physical properties of the material.

MASON S. NOYES.[12] It was hoped that the work of the A.S.M.E. Special Research Committee on the Strength of Vessels Under External Pressure, would yield results of general application. The data published in the first paper, APM-53-17a, and the present one, leave at least three items as yet not investigated.

The first item is that of shape. No consideration has been given to any other form than the cylinder, as stated in the first paragraph of the "Proposed Rules," yet these proposed rules do not read "for the Construction of Unfired *Cylindrical* Pressure Vessels Subjected to External Pressure." Again, assuming that the authors are interested chiefly in shell strength of submarines, one wonders why oval tubes of relatively small difference in major and minor diameters (similar to the usual modern submarine-hull form) were not tested also, in conjunction with some formula including a diameter-ratio factor. Investigation should lead eventually to the elongated oval, the triangular, and even to the nearly rectangular cross-sections used for condenser shells, to none of which the formulas listed in the present paper are applicable.

The second item is that of wall openings. If the tube or cylinder is to be used it must have branches (or inlets and outlets) at some point not always located on the heads. What is the effect of side openings on the number and location of lobes?

The third item is that of material. Reference to the authors' Tables 1 and 3 reveals that the material has been limited to steel or other similar material having a well-defined modulus of elasticity. The proposed rules already mentioned include only steel specifications, in referring to material. The values given in the present paper are around 30 million, showing that an excellent grade of steel has been utilized. On the other hand, under certain conditions of external pressure, tubing of good size is used, which is made of copper. This metal has no definite value for E, the modulus of elasticity varying with the "temper" or amount of cold work done on it and with the temperature conditions, nor has it a well-defined value for μ, its Poisson's ratio.

It is hoped that the investigators will not stop at the present point in their research, which seems to have covered steel cylinders so carefully, but will continue in an effort to get at least a partial answer to the effects of the above items.

AUTHORS' CLOSURE

The authors wish to express their appreciation for the many helpful and instructive discussions of their paper. These dis-

[11] "The Collapsing Strength of Steel Tubes," by T. M. Jasper and J. W. W. Sullivan, Trans. A.S.M.E., vol. 53, 1931, paper APM-53-17b, p. 219.

[12] Bureau of Engineering, Navy Building, Washington, D. C. Assoc-Mem. A.S.M.E.

cussions help to clear up doubtful points and make the paper of more value to those wishing to use it as the basis of design.

It is apparent that there is still some slight misunderstanding as to the application of the column analogy to the collapse of pressure vessels. Messrs. Hartman and Sturm make frequent use of the term "end fixation" in a pressure vessel, comparing it with the end fixation in a column. These two types of fixation are not really comparable. An analogy may be drawn between a pressure vessel and a column by considering the shell of the pressure vessel to be made up of a series of columns, one-half lobe length long, extending end-to-end circumferentially around the vessel. These "columns" are probably pin-ended since at the buckling pressure the ends are unstable and cannot offer a resisting moment. The column ends in the shell certainly are not related to either the heads or stiffening rings of the vessel.

It would probably be more instructive to shift the analogy from columns to plates. It is well known that the strength of a long plate subjected to a compressive load on its ends is influenced by the degree of fixation at the edges (not ends) of the plate. The theoretical buckling load for a plate with built-in edges is shown by Timoshenko[13] to be about 75 per cent greater than for a plate with simply supported edges. The fixation at the stiffening rings or heads of a pressure vessel is analogous to this edge fixation of a plate but it has not been evaluated theoretically. It is reasonable to suppose that the variation in the strength of a pressure vessel due to fixation at the heads will be no greater than the difference between the strength of a plate with fixed edges and one with simply supported edges. It certainly does not seem likely that "the effects of fixity of the ends (of a pressure vessel) may amount to several times as much as the collapsing pressure of simply supported cylinders." The authors have tested model pressure vessels with stiffening rings of many shapes and sizes ranging from extremely light stiffeners to bulkheads, and, whatever the effect of fixity at the stiffener may be, variations in this effect are not evident from the data. Consequently, either the fixation must have negligible effect or at least it must be of about the same degree in all cases.

It might be well to point out that for thick pressure vessels which fail at high stresses, the degree of fixation at the heads of a pressure vessel may be important for it is comparable to the fixation at the ends of a beam. However, this does not apply to vessels which collapse by instability, since the buckling is the result of tangential rather than longitudinal stresses.

Mr. Wesstrom points out that the authors' statement, "any fixation makes for added safety" applies only to fixation against rotation. He points out also that fixation against radial contraction (the authors did not consider this "fixation") may have the opposite effect. Since resistance of the stiffening ring to radial contraction materially affects only the longitudinal bending stress, it probably has small effect upon the strength of pressure vessels which collapse by instability.

Messrs. Hartman and Sturm have called attention to discrepancies between the experimental data and the theoretical formula [9] given in the paper. The explanation for this has already been given in the paper. The collapsing pressures computed by the theoretical formula [9] in Table 3 of the paper are too high in the region of high stresses because the value $E = 30 \times 10^6$ lb per sq in. was used in the computation instead of the correct value of the effective modulus. The collapsing pressures computed by the theoretical formula [9] are too low in the region of low stresses because the formula predicts critical buckling pressures which may be considerably below the ultimate collapsing pressures recorded in Table 3 for the experimental models. It seems unnecessary to call in an unrelated and poorly defined condition of end constraint to help account for these variations.

Regarding model no. 63, which Messrs. Hartman and Sturm indicate has the most out-of-roundness relative to the thickness although the collapsing pressure was 43 per cent greater than the theoretical pressure, it should be noted that an ultimate collapsing pressure considerably above the critical buckling pressure might well be expected for such a long thin model. Moreover, the experimental determination of the collapsing pressure of this particular model was subject to considerable error, since this collapsing pressure of 10 lb per sq in. (the lowest of the tested models) was observed by a 300 lb per sq in. Bourdon-tube gage.

The authors expressed out-of-roundness as a fraction of the thickness rather than of the diameter because in column theory the eccentricity of a column is expressed in relation to the radius of gyration which is analogous to the thickness of a pressure vessel (with a constant multiplier; see Equation [29] of the paper and preceding paragraph). The column eccentricity is not related to the length of the column which is analogous to the diameter (multiplied by a constant) of the pressure vessel.

The authors were asked to explain the methods used in the experimental determination of the number of lobes. The "polar diagram" as illustrated in Fig. 4 of reference 3[14] of the paper shows the exact condition of the shell just prior to collapse. Since such a diagram shows incipient bulges throughout the entire circumference, an examination of the diagram leaves little question as to the actual number of lobes. When satisfactory diagrams are not obtained, however, it is necessary to estimate the number of lobes from measurements of the average lobe length of the failed model. This method is unsatisfactory since neither the lobe length nor the number of lobes found in a failed vessel correspond necessarily to the lobe length and number of lobes in the vessel at the time of unstable collapse.

The collapsing pressures obtained by any instability formula must be checked by a stress calculation to make certain that the proportional limit of the material has not been exceeded. Mr. Wesstrom has outlined a method for determining the region of applicability of formula [9] of the paper. He points out that his formulas check Fig. U-21 of the A.S.M.E. Pressure Vessel Code. This is to be expected since his method is essentially that used in plotting the curves of that figure. However, it should be noted that it is best to limit formula [9] to stresses below the proportional limit rather than below the yield point. This can be readily done by substituting s_{prop} for s_{yield} in Mr. Wesstrom's Equation [d]. Formula [9] is not directly applicable for smaller values of L/D than those given by the modified Equation [d] and should be used only with extreme caution.

The authors believe Mr. Rhys has attached too much importance to the effect of axial loading on the collapsing strength of a pressure vessel. He is correct in the statement that a tube under both radial and axial pressure if increased in length indefinitely will eventually fail as a column or strut under the end load. This is purely academic, however, for the end load resulting from uniform external pressure is so small that in no practical case could it cause buckling of the tube as a strut. This end load, nevertheless, has an appreciable influence on the buckling of the shell by the formation of waves in a circumferential belt. Formula [6] of the paper is obtained by modifying formula [1] to include the effect of end load on this type of collapse. It does not consider the possibility of the tube buckling as a strut. Consequently it does not (and should not be expected to) reduce to zero when $L = \infty$ but to formula [A], given in the paper. The fact that formula [9] *does* reduce to zero for $L = \infty$ is due solely

[13] "Stability and Strength of Thin-Walled Constructions," by S. Timoshenko, Proceedings of the Third International Congress for Applied Mechanics, Stockholm, Aug., 1930, Eq. [5], p. 4, Table 4, p. 5.

[14] "Strength of Thin Cylindrical Shells Under External Pressure," by H. E. Saunders and D. F. Windenburg, Trans. A.S.M.E., vol. 53, 1931, paper APM-53-17a, p. 207.

to the nature of the approximations involved and not to the fact that it includes end load.

It might be noted that the analogous column length of the pressure vessel is a quarter-circumference for $n = 2$ (tubes longer than the critical length), and that this column length does not change if the tube be increased in length. Hence the column analogy is in accord with the fact that the strength of a tube longer than the critical length is independent of the length.

In regard to the four questions raised by Lieutenant Commander Roop the following can be said:

1 It is believed that hard surface layers in the material have very little effect on experimental results. As shown by the theoretical formulas given in the paper, the elastic modulus and Poisson's ratio are the only properties of the material upon which the strength of vessels which collapse by instability depends, and these properties in steel are but little affected by cold working of the material.

2 The actual measurements of deflections during the conduct of tests (reference 3 of the paper, Fig. 4 for example)[14] show deflections prior to collapse far in excess of the deflection due to uniform contraction of the shell.

3 It does not seem possible to obtain an approximate equation for the strength of a flat plate under hydrostatic and coplanar load by considering D to approach an infinite value. The t/D and L/D ratios both become zero in this limiting case, and the collapsing pressure in the various formulas is expressed in terms of these ratios in such a way that it too vanishes.

4 In general the selection of a suitable factor of safety is largely a matter of judgment. Fig. 2 of the paper shows the spread of points representing collapsing pressures of test models. The spread for commercial pressure vessels would probably be somewhat greater. A factor of safety of 2 is ample to take care of variations in thickness, variations in physical properties of the material, and ordinary variations from circular form. However, an addition to this factor is required to give added life to the vessel, to insure against accidental overloads, and to insure against other unforeseen accidents which might precipitate failure. Consequently, the choice of a suitable factor of safety depends upon the individual case. R. T. Stewart[15] gives some excellent general rules for the selection of a factor of safety.

Mr. Jasper offers some very interesting theoretical and experimental data. However, as he points out, his data are for thick tubes most of which collapse at stresses near the yield point while the authors have confined themselves in the present paper to collapse by instability only.

Mr. Noyes regrets that the paper is not more general in scope. The authors felt that a general review, discussion, and evaluation of the merits of the many instability formulas dealing with thin circular cylindrical-pressure vessels was desirable, and the purpose of the present paper was merely to present such a survey.

The A.S.M.E. Special Research Committee on the Strength of Vessels under External Pressure has considered questions of the type raised by Mr. Noyes. Sufficient experimental data are not now available to check the theoretical formulas commonly used to determine the strength of pressure vessels of elliptical cross-section.

Rules for the design of nozzle openings now form part of the A.S.M.E. Code for Unfired Pressure Vessels (Paragraph U-59). Nozzle openings which meet these requirements should not materially affect the strength of the shell.

The theoretical formulas in the paper were checked by steel models, but they apply to vessels constructed of any material provided the correct value of the effective modulus is used. The Special Research Committee is now engaged in formulating rules for circular cylindrical vessels made of copper, aluminum, and various alloys. It is hoped that these rules will be ready for publication in the near future.

[15] "Collapsing Pressure of Bessemer Steel Lap-Welded Tubes, Three to Ten Inches in Diameter," by R. T. Stewart, Trans. A.S.M.E., vol. 27, 1906, p. 815.

The Test Performance of Hudson Avenue's Most Recent Steam-Generating Units[1]

P. W. Keppler.[2] This paper and a similar recent one[3] on Hell Gate direct-fired units make possible an engineering comparison between the two methods of firing. Both methods deal with recently designed, large units which are using practically the same fuel (Eastern semi-bituminous).

In Fig. 1 of this discussion heat input is plotted against the many differences in losses that are connected with the coal-burning equipment, the following abscissa scales selected are at the same time convenient and accurate for comparison: 20 to 80 lb of (14,000 Btu) coal burned per sq ft of projected grate area per hr, and 10,000 to 40,000 Btu fed into the furnace in the form of pulverized coal per cu ft of furnace volume per hr. The maximum reported fuel-burning rate for The Hudson Avenue Station is 76.2 lb, and 39,500 Btu input for Hell Gate, nearly coinciding on our scale.

The losses that can be plotted as reported are: fly-ash loss of pulverized coal, and cinder, ashpit and unburned-gas loss of the stoker. The unaccounted-for losses will be dealt with later. Curve No. 1 of Fig. 1 in this discussion shows an advantage for pulverized coal throughout, rising from 0.9 per cent at 20 lb (10,000 Btu) to 3.7 per cent at 70 lb (35,000 Btu), and then falling to 1.6 per cent at 80 lb (40,000 Btu). This drop is due to the rapid rise in fly-ash loss from 2.2 per cent at 31,700 Btu to 8.7 per cent at 39,500 Btu. This in turn is due to lack of induced draft. It should here be kept in mind that the Hell Gate boiler was guaranteed for a capacity of only about 27,000 Btu input, whereas the Hudson Avenue boiler was built for an even higher maximum capacity (of shorter duration), than the 24-hr capacity reported, and was therefore not limited by induced draft. The actual excess air however was not so much greater for the stoker boiler, 13.3 per cent against 10.3 per cent. This indicates that this stoker requires less excess air than the pulverized-coal equipment under question. Nevertheless it is practically certain that this pulverized-fuel equipment would be capable, if given enough excess air, of continuing its low cinder-loss curve even beyond 39,500 Btu, at which point it would only be 2.8 per cent instead of 8.7 per cent. This could be shown, possibly by dotted lines, but the writer would rather confine himself as much as possible to facts and let the reader draw his own conclusions.

Excess-air losses are shown on curve No. 2 of Fig. 1 of this discussion. Tests on representative equipment indicate an increase in dry-gas losses of 0.05 per cent, per cent of excess air, and on this basis, although excess air differs as much as 5 per cent, the difference in losses is rather small.

The sensible heat in the slag was also estimated (curve No. 3). A specific heat of 0.2, and a slag temperature of 2500 F is here assumed. The maximum slagging loss at 13,000 Btu,

[1] Published as paper FSP-56-15 by P. H. Hardie and W. S. Cooper, in the November, 1934, issue of the A.S.M.E. Transactions.

[2] Testing Engineer, Hell Gate Station, The United Electric Light and Power Company, New York, N. Y. Jun. A.S.M.E.

[3] "Characteristics of Large Hell Gate Direct-Fired Boiler Units by W. E. Caldwell, Trans. A.S.M.E., vol. 56, 1934, paper FSP-56-2.

where 45 per cent of the ash is reported to be slagged, is only 0.11 per cent.

The unaccounted-for and radiation losses seem decidedly in favor of the stoker. Accuracy may be gained by "weighting" these for input, for they appear to be uniform, regardless of rate of driving. The resulting "weighted" average loss is 1.37 per cent for the stoker compared with 4.04 per cent for the pulverized-coal equipment. Some of the radiation loss is returned to the boiler by the incoming combustion air being heated above the outside-air temperature. This correction may be applied with good accuracy to the Hell Gate boiler, for during the test it ran alone in its own boiler-house extension, which is practically a building by itself, and its combustion air is taken from the top of this building. On the Hudson Avenue boiler this is not exactly the case but fortunately the correction is much smaller due to the air being taken from the bottom of the building; a considerable error in this estimate would be comparatively small. The heat thus returned is 1.03 per cent for the Hell

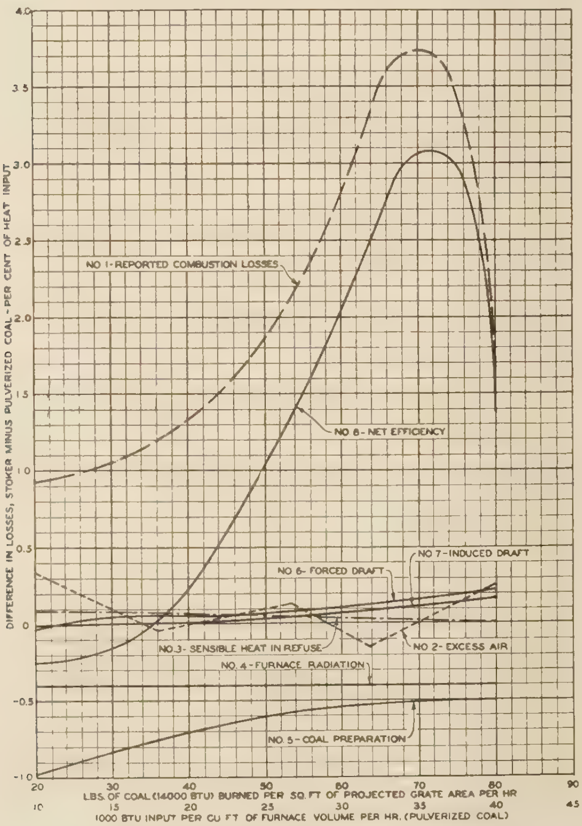

FIG. 1 EFFECT OF FUEL-BURNING EQUIPMENT ON TEST EFFICIENCY, STOKERS (HUDSON AVENUE) VERSUS PULVERIZED COAL (HELL GATE)

Gate boiler, compared to 0.22 per cent for the Hudson Avenue boiler, reducing the actual radiation plus unaccounted-for loss to 1.15 per cent and 3.01 per cent, respectively. This loss can only be radiation for the stoker tests, excluding test error. For the pulverized-coal tests it may be carbon lost in the slag or unburned-gas loss together with radiation, again excluding test error. But other tests at Hell Gate prove that this slag contains no combustible matter. And the sum of CO_2 plus O_2 is within 0.2 of the amount corresponding to complete combustion of the coal used; it is also known that the solution used for oxygen determination fails to take out the last tenth or two of oxygen. No CO was found during the entire test. Furthermore, the presence of unburned hydrocarbons is extremely unlikely for they meet with considerable turbulence, high temperature, and possibly 200 per cent excess air as they are blown off near the burner. The furnace is also very large and comparatively free from stratification. Other elaborate tests with combustion Orsats have shown unburned gases to be very rare with turbulent burners. The writer therefore believes that this loss is practically all radiation for both groups of tests. The radiation surface per unit heat input is 1.6 times greater for the Hell Gate boiler; this includes low temperature air ducts, etc., but the insulation on some of these is correspondingly thin, or left off altogether, so that their radiation may be just as intense as from hot surfaces that are usually well insulated or protected by water walls. This extra surface, largely due to the use of more heat recovery apparatus, would raise the Hudson Avenue radiation to 1.84 per cent. It should also be considered that the Hell Gate setting is far less compact and well ventilated, surrounded by windows, and subject to bad drafts from the coal-conveying system, some of which have since been eliminated. Furthermore the adjacent boiler was shut down, so that this one boiler was subject to radiation from all four sides and had to heat up a boiler room, half of which was shut down. The outside temperature averaged only 37 F, compared to 49 F for the stoker tests. This accounts at least for a good portion of this difference between 1.84 and 3.01 per cent. But the stoker should get credit for the smaller furnace required and for the protection against radiation it affords by its grate area as well as its coal hopper. By assuming a uniform heat emission and by determining the various surfaces, it was estimated how much the radiation loss would increase in the stoker boiler if its furnace were replaced by a pulverized-coal furnace, larger according to the difference in heat release, and radiating from all five sides. The resulting increase is found to be 0.4 per cent and is therefore credited to the stoker (curve No. 4).

Auxiliary power requirements must also be considered. The conservative modern heat rate of 14,000 Btu input per kw is assumed throughout. To compare fan-power requirements, a static fan efficiency of 60 per cent, and electrical drive with 80 per cent motor efficiency are used for both cases. For calculating forced-draft power consumption, the burner pressure of the pulverized-coal equipment is compared with the windbox pressure of the stoker. For induced draft the average setting resistance of the two is used for both, so that the combustion equipment is merely held responsible for the difference in head and volume caused by differences in excess air.

There is a marked difference between mill power and stoker-motor power as shown in Fig. 1 of this discussion by curve No. 5, which varies from 1.2 per cent at 20 lb (10,000 Btu) to 0.5 per cent at 80 lb (40,000 Btu). Forced and induced draft (curves Nos. 6 and 7) show only small differences.

Curve No. 8 shows the resulting net difference. It is seen that if the bulk of the stoker output can be raised below 40 lb per sq ft, and if the higher rates of driving are used only during rare emergencies, the resulting operating efficiency of stokers should be about equal to that of comparable pulverized-fuel equipment.

If the appreciable unburned-gas losses could be reduced by the use of overfire air, the resulting increase in fan power, particularly at low outputs, should be comparatively small. If this were feasible the stoker would be definitely more efficient at moderate rates of driving and its disadvantage beyond these would be reduced.

The writer has purposely confined himself to thermal efficiency, but it must of course be kept in mind that many other important factors would enter into a complete comparison.

JOSEPH GERSHBERG.[4] To conduct tests of a stoker-fired boiler in a satisfactory manner one has to cope with, among other things, two requirements of the fuel bed. First, it must have a thickness and a contour proper for a given make of stoker and kind of coal used if the best sustained boiler efficiency at a chosen rate of evaporation is to be realized. Second, its condition at the beginning and at the end of a run must be identical if demands of test accuracy are to be met. Deviation from the first requirement is commonly designated as the fire being too heavy or too thin. Non-fulfilment of the second requirement results in an error both in the boiler efficiency as well as in the "radiation and unaccounted-for loss."

Ordinarily it takes several hours to obtain a proper fuel bed for a chosen rating and to reestablish it toward the end of the run. Since under present art of testing, the fuel-bed condition is estimated by eye, it becomes extremely difficult to avoid large errors in boiler efficiency and "radiation and unaccounted-for loss," particularly at light loads. With a large stoker surface it takes only a few inches of fuel-bed thickness to cause an error of several per cent in these items of the heat balance. Zero or negative values of "radiation and unaccounted-for loss" are quite common at very light loads.

A method of testing which would eliminate or reduce these errors is certainly welcome. The authors followed a procedure which they contend "has the advantages that the testing period is reduced, and the influence on the results of possible differences in fuel-bed thickness between the beginning and end of runs is minimized." Analysis of results in the energy balance of their Table 1 does not seem to bear out the last contention. Appended curves of these results (Fig. 3 of this discussion) show that with the exception of "radiation and unaccounted-for loss" all other losses behave in a normal way, indicating that, as far as combustion is concerned, it was of somewhat similar quality during the ascending as well as the descending order of loading. However, the curve of "radiation and unaccounted-for loss" shows a very erratic behavior. Since this item in this test represents only the radiation loss and test errors, the curve should be at least a horizontal line if not sloping downward with the increase of energy output, provided the errors are small and fairly constant. One would expect the errors due to estimates of the fuel-bed thickness to be the smallest at the very high ratings, namely in runs 9 and 10. The average of "the radiation and unaccounted-for loss" for these runs is about 2.2 per cent. Taking this value as constant for the entire series of runs one would readily notice (see Fig. 2B of this discussion) that all points of the first eight runs except run 3 fall below it. This result indicates that in every one of these runs except run 3, the fuel bed was thinner at the end than at the beginning of a run by average amounts shown in Table 1 of this discussion. According to these values the thickness of the fuel bed with which the test was started in run 1 was reduced at the end of run 8 by 18.3 in., or 15.7 in. if the "unburned

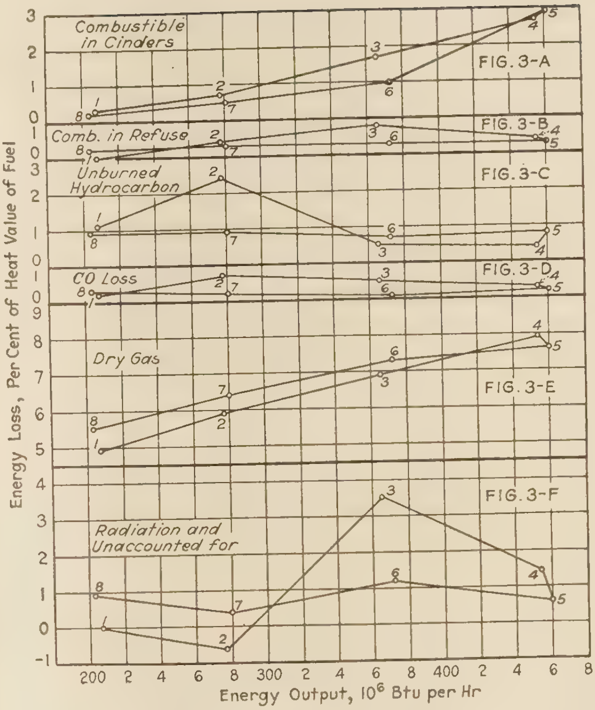

FIG. 3 APPENDED ENERGY-BALANCE CURVES DRAWN FROM TABLE 1 OF PAPER FSP-56-16

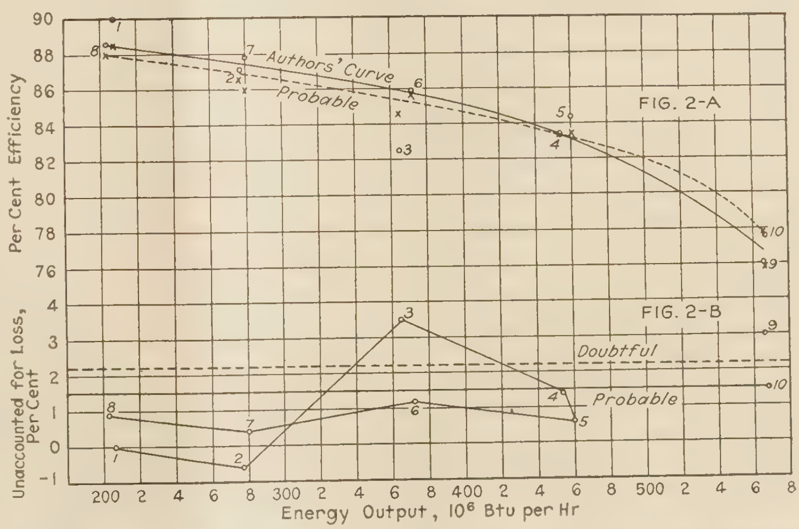

FIG. 2 APPENDED TEST-PERFORMANCE CURVES DRAWN FROM RESULTS GIVEN IN TABLE 1 OF P. H. HARDIE AND W. S. COOPER'S PAPER FSP-56-15

[4] Chief Testing Engineer, United Electric Light & Power Company, New York, N. Y. Mem. A.S.M.E.

TABLE 1 APPENDED RADIATION AND UNACCOUNTED-FOR LOSS

Run No.		1	2	3	4	5	6	7	8	9	10
		Difference in average fuel-bed thickness, in.									
Radiation and unaccounted-for loss	2.2%	—2.4	—4.5 —1.9[a]	+ 2.6	—2.0	—3.9	—1.9	—2.6	—1.3	2.6	—2.3
	1.5%	—1.6	—3.0 —0.9[a]	+ 4.0	—0.2	—2.2	—0.6	—1.6	—0.6	5.0	0

Difference in average fuel-bed thickness at the beginning and end of a run was computed for the inclined stoker area =

$$\frac{694 \text{ sq ft projection area}}{\cos 25 \text{ deg}} = 765 \text{ sq ft}$$

Coal density = 60 lb per cu ft

[a] Corrected to 0.9 per cent energy loss due to unburned hydrocarbons instead of reported 2.4 per cent (see Table 1, item 72, of the paper), which seems to be in error (see Fig. 3-*C* of this discussion).

hydrocarbons loss" (see Fig. 3*C* of this discussion) in run 2 is taken as 0.9 per cent instead of 2.4 per cent, which seems to be in error. So large a reduction in thickness, however, is unlikely. A critical examination of results of runs 9 and 10 tends to regard 1.5 per cent of "radiation and unaccounted-for loss" established in run 10 as the most probable value. This loss in run 9 is 3.0 per cent. The discrepancy of 1.5 per cent might be due to two possibilities: First, an error of only 6 per cent in the sampling of cinders would suffice to cause indicated 0.5 per cent difference in the loss due to combustible in cinders. Second, run 9 was started with a too thin fire which was built up toward the end of this run and thereafter was maintained approximately constant throughout the 10th run. This may account for the remaining 1 per cent discrepancy.

With 1.5 per cent "radiation and unaccounted-for loss," Table 1 of this discussion shows much smaller reductions in thickness of the fuel bed for individual runs than with 2.2 per cent. Accordingly, the thickness of the fuel bed existing at the beginning of the first run needed to be decreased by only 5.8 in., or more likely, by 3.7 in. (if corrected for error in run 2 as explained previously) at the end of run 8, to make possible errors in boiler efficiency for individual runs. Fig. 2*A* of this discussion shows the probable efficiency curve as compared with that given in the paper.

This analysis leads to a conclusion that the authors' procedure of uninterrupted testing for a series of *different* loads does not minimize the errors of individual runs due to differences in fuel-bed condition at the beginning and end of each run. The procedure becomes effective only when it is applied to a series of runs for the *same* load, the entire series being treated as a single run. In other words the duration of a run is to be prolonged, as it is practiced whenever accuracy of testing is sought, particularly, at light loads.

Now with reference to the shortening of the testing period, the authors' claim of this advantage in their method of testing can be conceded if loads are changed in one order only, either ascending or descending. In other words, there must be no check runs. There is a considerable saving in time if only a few hours, say three or four, are spent for the establishment of a proper fuel bed at the beginning of each run instead of 24 hours required for a check run.

E. C. M. Stahl.[5] The combustion-control meters used at Hudson Avenue are of the type which maintain a predetermined steam-flow–air-flow ratio, or in effect a predetermined per cent "total air" (ratio of actual air supplied to theoretical air required for complete combustion). For this reason the operating department at Hudson Avenue has been interested in determining the total air at which highest combustion efficiency can be obtained.

The elementary method of establishing the proper quantity of air to be supplied is to determine by means of a field Orsat the point at which carbon monoxide disappears from the flue gases. This method has been found to be inadequate due to the fact that complete analysis of the flue gas indicates the presence of unburned gases considerably in excess of that shown by the field Orsat. In Fig. 4 of this discussion the relation between the losses in boiler efficiency as found by the two methods of flue-gas analysis is indicated. This relation was brought out by Bert Houghton in his paper before the Third International Conference on Bituminous Coal. It should be noted that the loss incurred under operating conditions varies markedly with the per cent total air supplied.

The curve in Fig. 5 of this discussion has been plotted from test data to demonstrate that the cinder loss also varies with total air supplied. An increase in the percentage of total air at any rating increases the velocity of the air through the fuel bed with a resultant increase in the quantity and size of cinder carried away. It appears that the impact and hence the cinder loss varies as some power of the air velocity.

Fig. 4 of this discussion shows the combined effect of total air on principal combustion losses. As the per cent total air is increased for the purpose of reducing the losses due to incomplete combustion, the dry-gas and cinder losses increase rapidly. Obviously, the most efficient combustion conditions exist at the point where the summation of all the losses is a minimum. This best point will occur in the vicinity of *A* in Fig. 4. If, on the other hand, the per cent total air is set at some point *B* as indicated by analysis with the field Orsat or at some arbitrary point *C* in an attempt to avoid possibility of incomplete combustion, unnecessary combustion losses will result. The location of the point *A* varies with the burning rate and should be determined

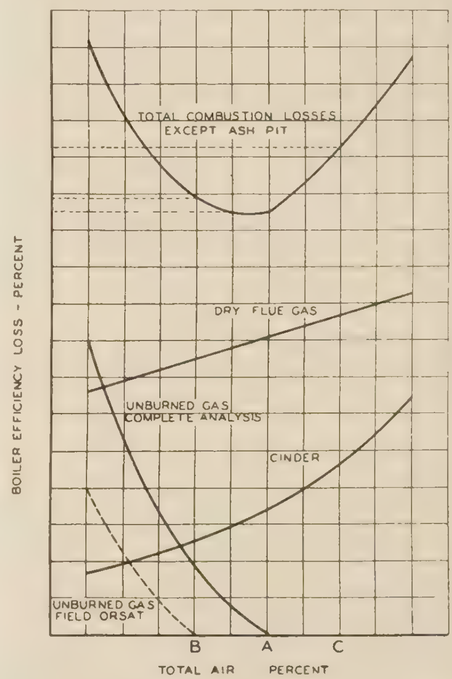

Fig. 4 The Relation Between the Losses in Boiler Efficiency as Found by the Two Methods of Gas Analysis

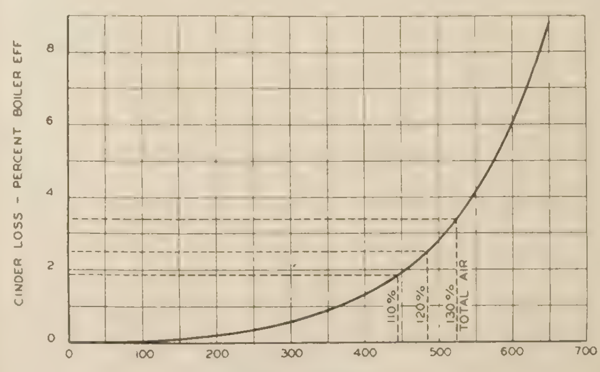

Fig. 5 Variation of Cinder Loss With the Ratio of Actual Air Supplied to the Theoretical Air Required for Combustion

[5] Operating Superintendent, Brooklyn Edison Company, Inc., Brooklyn, N. Y. Mem. A.S.M.E.

at several boiler loads so that combustion meters may be set to indicate a per cent total air that varies with steam flow in a manner to embrace the loci of a series of points determined as point *A*. Since the magnitude of these losses varies with each stoker and furnace installation, highest combustion efficiency can be obtained only if the variable combustion losses are determined by use of methods similar to those described by the authors.

H. F. Lawrence.[6] The writer believes it has been conceded rather generally that the presence of CO in the gases of combustion indicates the presence of unburned hydrogen and hydrocarbons, particularly if the CO is present in appreciable quantities. The writer also believes it has been conceded generally that the unburned hydrogen and hydrocarbons increase greatly with increased coal-burning rates per square foot of grate surface. Referring to the author's paper, note that run 10 which was at the highest capacity, showed the greatest loss due to CO and also the least loss due to unburned hydrogen and hydrocarbons. Note, also, that run 9, which was at the same rate as run 10, showed less than half the CO loss and four times the hydrocarbons loss as compared with run 10.

Another outstanding feature of these tests was the procedure of continuous operation with no recess between runs. Fig. 6 of this discussion shows graphically the changes in load with the percentage of increase at each change upward. The increase in

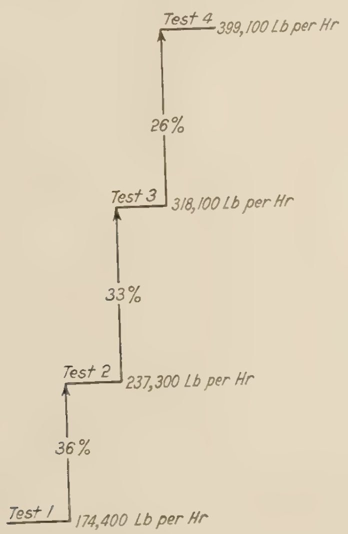

Fig. 6 Graphical Representation of Load Changes of No. 74 Boiler Tests, Hudson Avenue Station

load from test 1 to test 2 was 36 per cent; from 2 to 3, 33 per cent, and from 3 to 4 it was 26 per cent. These changes in load, rather than being small, were large and it is quite remarkable that changes of this magnitude were made and conditions stabilized within five minutes.

In addition to the tests reported, many peak-load tests of five hours duration were made, during which the water was not weighed, but measured on the regular station instruments which had previously been calibrated. As these were merely load tests, no attempt was made to calculate efficiencies. On November 16, 1933, the maximum five-hour rate was run at a load of 607,000 lb of steam per hr and 632,000 lb of steam per hr for a maximum three-hour period. Flow-meter charts transposed

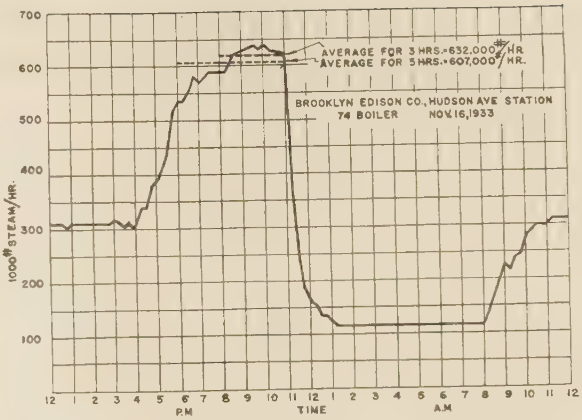

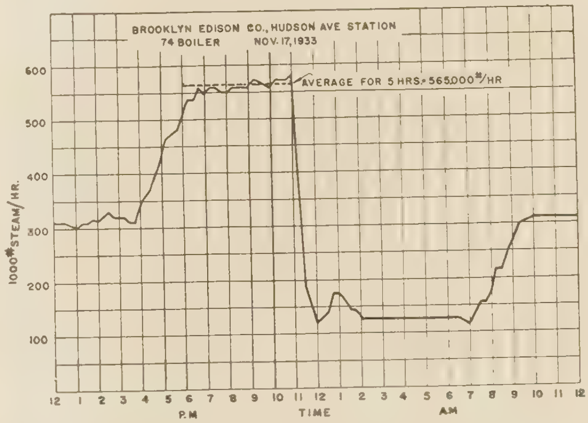

Fig. 7 Flow-Meter Charts of Hudson Avenue No. 74 Boiler Tests Transposed to Straight-Line Graphs

to straight-line graphs are shown for the runs of November 16 and 17, 1933, in Fig. 7 of this discussion.

David Brownlie.[7] The authors have carried boiler-plant testing to such an advanced stage that it is interesting to consider what remains to be done in this field. Certainly one point is the determination, by some type of recording apparatus if necessary, of the amount of sulphur dioxide and sulphur trioxide in the combustion gases. Until a few years ago no method had been developed for determining the amount of dust and acid-sulphur compounds being discharged from the stack. Now, however, the determination of the dust content is of primary importance, and we are rapidly getting to the point where it will be just as essential to know the amount of sulphur compounds in the combustion gases.

In this connection there is already one power station in Great Britain, namely Battersea, London, that is operating on the principle of the complete removal of the sulphur compounds, involving, it is believed, the pumping of 2000 tons of scrubbing water every 24 hours. The Fulham (London) station and the Tir John (Swansea) station, both now being erected, are also to be operated on similar lines, while at the Barton station (Manchester) experimental work on one boiler has been in progress for some time and the same applies to the Billingham Works of Imperial Chemical Industries Ltd.

It seems to me also that in these tests at the Hudson Avenue station, a further minor refinement would have been the installa-

[6] American Engineering Company, Philadelphia, Pa. Mem. A.S.M.E.

[7] Consulting Technical Chemist, London, England. Mem. A.S.M.E.

tion of continuous duplex gas-analyzing apparatus for the determination of both the CO_2 and the CO (unburnt products) and also the CO_2 and the oxygen.

Another main item that calls for comment is the method of expressing the efficiency. Thus, for example, the "efficiency of the steam-generating unit" is given in the authors' paper as varying from 76.2 per cent to 90 per cent, while separate items are included for the power consumption of some of the auxiliaries. Although the matter is not very clear, presumably this 76.2 to 90 per cent steam-generating efficiency is the gross efficiency only, based on the total evaporation to the steam in the boilers, without regard to the consumption of steam by auxiliaries in the boiler house itself. I am informed by Messrs. Hardie and Cooper, however, that the total auxiliary power used, but not including the feed pump, corresponds to 1.3 per cent to 2.3 per cent of the total evaporation of the boilers.

In 1922 I published suggestions for an International Boiler Test Code, one of the points of which was that the efficiency of boiler plants should be expressed as the true net thermal efficiency, that is, the efficiency based upon the amount of steam available for useful work outside the boiler house itself, and not upon the actual production of steam by the boiler plant.

That is, to use a very simple example by way of illustration, if a boiler plant is evaporating 100,000 lb of water per hr and 5000 lb of water per hr is being used to drive auxiliaries such as boiler-feed pumps, forced- and induced-draft fans, mechanical stokers, and ash and clinker conveyers, then the net thermal efficiency must be based upon 95,000 lb evaporation and not on 100,000 lb.

Messrs. Hardie and Cooper might have included in the results of their tests, the actual net thermal efficiency and not only the gross efficiency. They inform me that they do not consider the feed pump as an "auxiliary" in the ordinary sense of the term, since it performs its own distinct function. Frankly, I cannot agree with them, although from the theoretical point of view the matter is difficult.

Finally, it is impossible to work any boiler plant today without expending energy in forcing the feed water into the boilers and, in my opinion, all the energy used must be deducted in calculating the net thermal efficiency.

Obviously, as I have pointed out for many years, we have long required a proper International Boiler Test Code drawn up by engineers and fuel technologists who have had practical experience in this field of engineering.

A. G. Christie.[8] The value of this series of tests lies in the complete analysis of the energy distribution in the steam-generating unit at the various loads. Certain interesting deductions of both practical and academic interest may be drawn from these data.

A comparison of the authors' item 74, "Energy loss due to combustible in cinders" with item 73, "Energy loss due to combustible in ashpit refuse," indicates that the former averages several times the latter. This would indicate that more consideration must be given on future tests to the sampling of the flue gases for cinders than to sampling the clinker-grinder refuse. The authors have developed a method of sampling the flue gases for cinders that appears to give correct data.

The energy loss due to radiation and that unaccounted-for, is remarkably small. This indicates that proper wall construction and insulation can reduce heat-conduction losses into the boiler room to a small value.

The draft at the induced draft fans at full steaming capacity of 500,000 lb per hr is high amounting to 14.3 in. The plenum pressure at the same load is 6 in. The total pressure is 20.3 in. which accounts for the comparatively large power consumption of the fans. The authors have not charged any of the boiler output to these fans. It would be interesting to know the net efficiency after allowance for auxiliary power.

No data are presented on the performance of the cinder catchers in the removal of cinders from the flue gases. Since observations were undoubtedly made on this equipment, the authors might indicate the relative effectiveness of the cinder catcher.

The heat balance shows that the loss from unburned hydrogen and hydrocarbons averages several times the loss due to CO. Much care has been devoted in the past to the analysis of the flue gases for CO while no attempts have generally been made to detect the hydrogen and hydrocarbon losses. Evidently laboratory practice and test procedure must be revised to include the accurate determination of the larger losses due to hydrogen and hydrocarbons.

The gross efficiencies of the steam-generating unit are excellent at all loads. The performance of the stoker, as indicated by the low ashpit and cinder losses, was an important factor in securing these results. A rate of combustion of 75 lb per sq ft of grate area per hr for two consecutive periods of 24 hr deserves especial comment, particularly in view of the overall efficiencies obtained under these conditions.

The authors state that both boiler and stoker were put in first-class operating condition for these tests. It would be interesting to know at certain outputs how the average daily efficiency compares with test efficiency.

Items 61 and 62 in the authors' Table 1 appear to be based on boiler surface alone and do not include the very effective water walls. The rates of heat generation and transfer as given are consequently much higher than actually occur in the boiler due to the high rates of evaporation in the water wall. Why not include the area of the water walls with the boiler surface in setting up such average figures?

Frank O. Ellenwood.[9] In this paper we have an energy balance of a steam-generating unit that gives, for the first time to the writer's knowledge, a very close approximation of the radiation from the unit, because the authors have determined several losses that have usually been treated as unaccounted-for. It is especially significant to observe that the loss due to the unburned hydrocarbon was low; but, in the writer's opinion, it should be noted that such a result would not have been obtained had the furnace not been provided with ample distance between the fuel bed and the first row of boiler tubes, a distance in this case of from 30 to 40 ft. When a boiler is set too close to the fuel bed, as has been done in some stoker installations, this loss becomes of much greater magnitude, as does the cinder loss also. It would be of special interest to many engineers if the authors could give information regarding these points for some of the other units that have boiler tubes closer to the fuel bed.

From the energy balance, and also from the curve in Fig. 5, it is apparent that the cinder loss is the serious one when extremely high rates of firing are employed, such as 75 lb of coal per hr per sq ft. That this unit was able to operate at this phenomenal rate for 48 hr and still have no furnace trouble of any kind is a remarkable testimonial to the builders and operators. If stokers are to be operated at such high rates for prolonged periods of time, studies should be directed to possible means of reduction of the cinder loss.

The tabulation of the data appeals to the writer as being exceptionally clear, concise, and technically correct; his only suggestion for a slight improvement in the tabulation would be

[8] Professor of Mechanical Engineering, Johns Hopkins University Baltimore, Md. Mem. A.S.M.E.

[9] Professor of Heat-Power Engineering, Cornell University, Ithaca, N. Y. Mem. A.S.M.E.

that it should also include the net efficiency for each run. This point becomes of increasing importance in making tests of large modern steam-generating units, whose performances it may be desirable to compare even though their fuel-burning equipment and auxiliaries may be entirely different.

A long step forward is represented by the technical progress that is exemplified by the design and testing of this steam-generating unit when compared with that of the so-called "boiler tests" of a few years ago. When one observes that the unit had no air preheater, the results of the tests become still more impressive, and one again realizes that high net efficiencies of steam-generating units are not confined to powdered-fuel installations.

Authors' Closure

Mr. Keppler has made a careful and detailed comparison of the performance of the pulverized-fuel unit at Hell Gate with the stoker-fired unit at Hudson Avenue with allowances for those differences which might influence the comparative results. Any such method of correction as Mr. Keppler used, however, requires a great many assumptions, some of which are subject to differences of opinion. The authors believe that there is other pertinent information not mentioned by Mr. Keppler which should be considered even though it is not amenable to numerical evaluation. For instance, the Hell Gate unit is equipped with an air preheater and economizer while the Hudson Avenue unit has only the latter. The Hell Gate tests were of relatively short duration in that they varied from ten hours at the lowest load to two hours at maximum load, and no check runs were made.

The impression might be gained from Mr. Keppler's statements regarding the guaranteed capacity of the two units that the maximum test load on the Hell Gate unit was higher in proportion to the unit's size than that on the Hudson Avenue unit. As a matter of fact, the maximum test loads on the two units per square foot of boiler surface were the same.

The authors fail to see the justification of Mr. Gershberg's method of correcting the test results to an assumed constant value of "radiation and unaccounted-for," and his attributing the variation to differences in fuel-bed thickness between the beginning and end of runs. It is interesting to note, however, from Fig. 2 of this discussion that his "probable" efficiency curve agrees with the authors' curve within the limits of test accuracy in spite of the liberties he has taken with the original data.

It is very easy to talk about having the condition of the fuel bed, its contour, thickness, etc., the same at the beginning and end of a run, as Mr. Gershberg does, but it was the inherent impossibility to estimate by eye with any degree of accuracy these conditions on a stoker of the size of the one under discussion which led to the adoption of the continuous method of testing. The authors do not believe that on this test the variation in the "radiation and unaccounted-for" was abnormal and apparently none of the other discussers thought so. Mr. Lawrence, who would be most interested in obtaining reliable results, calls the continuous method of operation an "outstanding feature of these tests."

Mr. Gershberg suggests that a preliminary period prior to each run would eliminate the necessity of check runs. The authors consider that check runs are always desirable and especially so when testing steam-generating units because, aside from the question of testing accuracy, the results are subject to changes in the order of one or two per cent as a result of operational factors.

Mr. Stahl has very clearly pointed out that accurate gas analysis is essential to the proper setting of the boiler meters. In this connection, the authors have felt for several years that the true rôle of the Orsat apparatus in formal tests of steam-generating units was that of guiding the stoker operators during test rather than that of providing a basis for the flue-gas computations.

Referring to the variation of unburned H_2 and hydrocarbons, Mr. Lawrence points out that these tests did not sustain the prevailing opinion that the presence, or absence, of CO in the exit gases reveals the presence, or absence, of these unburned gases. Other tests[10] have also fully demonstrated that this conclusion does not apply to the combustion situation encountered at Hudson Avenue.

Mr. Brownlie and Professors Christie and Ellenwood have expressed the opinion that the net efficiencies should have been included in the tabulated results even though the approximate percentages of the energy output consumed by the boiler auxiliaries at the lowest and highest test loads were stated in the last paragraph under "Test Data and Results," page 839 of the paper. The net efficiencies for each run are given in Table 2 of this discussion.

TABLE 2 NET EFFICIENCIES OF STEAM-GENERATING UNIT

Run number	1	2	3	4	5
Net efficiency, per cent	88.8	86.1	81.1	82.0	82.8
Run number	6	7	8	9	10
Net efficiency, per cent	84.2	86.6	87.3	74.4	75.7

It should be noted that there is no standard set of assumptions as to what primary data shall be employed in computing net efficiencies. For example, a difference of opinion exists as to whether the feed pump shall be regarded as an auxiliary. While Mr. Brownlie prefers to consider the feed pump as a boiler auxiliary, Professor Ellenwood[11] takes the opposite point of view. The authors regret that they are unable to report for Mr. Brownlie's information the energy consumption of the feed pump because it was not measured during test.

Another reasonable difference of opinion among engineers is whether the electrical energy consumed by the auxiliaries shall be charged on the basis of the average station heat rate which includes standby losses, etc., or whether the combined heat rate of the test boiler and the turbine which it supplies during each test is the proper one to use. The latter would conform more nearly to the practice in the case of steam-driven auxiliaries but the combined heat rate of a single boiler and turbine for each test period is not generally available from the station records.

The net efficiencies given in Table 2 of this discussion were computed excluding the boiler feed pump as a boiler auxiliary and using the average net fuel rate of the station. The details of the procedure used are described in Barnard, Ellenwood, and Hirshfeld's, "Heat Power Engineering," part 2, page 443.

In answer to Professor Christie's inquiry concerning the efficiency of the cinder catcher, the "wet" type of cinder catcher used on this unit has shown test efficiencies of 80 to 90 per cent at ordinary loads.

Professor Christie mentions the authors' statement about putting the boiler and stoker in prime operating condition and asks how much effect this had upon improving the efficiency. The cleaning of the boiler and maintenance work on the stoker were the same as is done at regular intervals and, therefore, resulted in small improvement over average performance. The extra supervision of the stoker operation, however, aided by the Orsat readings may have resulted in greater improvement than the cleaning of the boiler. For average daily operating efficiencies reference should be made to Table 5 of "Ten Years of Stoker

[10] "Reducing the Unaccounted-For Losses in Boiler Tests," by W. F. Davidson, Report presented to the Fuels Division, A.S.M.E., at the Chicago Meeting, 1931.

[11] "Elements of Heat Power Engineering," by Barnard, Ellenwood and Hirshfeld," John Wiley and Sons, New York, N. Y.

Development at Hudson Avenue,"[12] by J. M. Driscoll and W. H. Sperr.

The authors agree with Professor Christie that Items 61 and 62 in Table 1 of the paper would have been more nearly correct had the water-wall surface been included in reporting the steam generated and heat transferred per square foot of boiler surface.

The comparative information requested by Professor Ellenwood regarding cinder loss in boiler units having low and high settings may also be found in Fig. 11 of the paper by Driscoll and Sperr previously mentioned. It will be noted from this figure that the height of the setting has little or no effect upon the cinder loss. However, a marked reduction in the hydrogen and hydrocarbon losses was obtained on this unit as compared to older units with lower setting. Possibly some of this improvement was due to the zoned-air control.

The Elastic Properties of Steel at High Temperatures[1]

Leo H. Hall.[2] It seems that caution is needed in using Mr. Versé's method for measuring temperature when applied to static tensile tests.

In the first place, a wire supported and heated as the author describes, cannot be at uniform temperature throughout, since heat is being conducted away at the supports and at the loading point without a corresponding loss at intermediate points. In the writer's experience in measuring electrical resistivities at high temperatures, this lack of uniformity of temperature has sometimes been observed to increase rather than decrease by insulating the wire and, in a metal such as steel which has a fairly high temperature-resistance coefficient, it is sufficient to vitiate results obtained by the use of this method, at least in measuring resistance.

This means that the temperature read by resistance in a set-up such as the author describes is not a true temperature, but a composite of the temperatures of different parts of the wire. The elastic properties observed are also composites of those existing over a range of temperatures. Since the elastic properties do not vary linearly with resistance, it is evident that errors may be introduced by the use of this method. The magnitude of the error depends on the temperature gradient along the wire, which is in turn determined by its specific heat, conductivity, diameter, length, and surface roughness. That it is not insignificant may be judged from the fact that in similarly suspended insulated wires, differences of temperature of more than 100 C have been measured between points 2 ft apart, neither point being at the support.

Another source of possible error lies in the fact that the electrical resistivity of some metals is known to vary between the unstressed and the highly stressed conditions, at least at room temperature. It is the writer's recollection that some very considerable variations have been observed. So far as he knows, no tests have been made to determine whether such variations persist at higher temperature, or whether they increase under that condition.

While the method used by Mr. Versé is highly ingenious and has the merit of great simplicity, it should be borne in mind that it is limited as to accuracy and, that under some conditions, it entails considerable error. It would be of interest to learn how the author calibrated his device.

Author's Closure

Mr. Hall's remarks were expected and, in an unabridged thesis presented to the University of Michigan, they were answered as follows:

1 Regarding the non-uniformity of temperature along the specimen, it is true that such an error is present in our measurements but, however, it is not of important magnitude. In accurate measurements made in the physics department of the University of Michigan, where a similar method is used for the measurement of the coefficient of expansion of metals, it was determined that the effect of the end supports is not felt over a distance larger than 2 in. from the support. The length of the wire being 125 in., and an averaging effect taking place in both the measurements of E and of the electrical resistance, the resultant error is very small. Indeed, if E and the electrical resistance should vary linearly with temperature, there would be no error at all.

2 Regarding the possible variation of the electrical resistance with the stress condition, the stresses were kept very low in our tests so as to reduce this error to a negligible value.

3 The preliminary calibration was made on a sample of the wire at the following standard temperatures:

Freezing point of water	0 C
Boiling point of water	100 C
Boiling point of naphthalene	219 C
Boiling point of sulphur	445 C

For these calibrations, the standard equipment for the calibration of resistance pyrometers was used. The electrical resistance of the sample as well as that of the wire was measured by means of a potentiometer and a standard resistance. The standard resistance was made of an alloy the resistance of which varied but little with the temperature. Besides, this resistance was very small so as not to undergo any appreciable heating, and moreover it was kept at a constant temperature by a flow of compressed air. In every case the length of the wire was measured at 25 C, so that the calibration automatically takes care of the thermal expansion.

Finally, it is pointed out that Mr. Hall's remarks do not pertain to our static-torsion tests, which also showed the existence of Professor Timoshenko's high-temperature strain-hardening effect and the advantages of Dr. Everett's unloading method.

[12] "Ten Years of Stoker Development," by J. M. Driscoll and W. H. Sperr, Trans. A.S.M.E., vol. 57, no. 2 (February, 1935), paper FSP-57-3.

[1] Paper by Guy Versé, published in the January, 1935, issue of the A.S.M.E. Transactions.

[2] Mem. A.S.M.E.

Photoflow Method of Water Measurement

By W. M. White[1] and W. J. Rheingans,[2] Milwaukee, Wis.

This paper is written to reestablish the pitot tube as a useful and accurate instrument for measuring the flow of water. Difficulties in the measurement of water by the pitot tube have been caused by errors introduced in the measurement of the static pressure and such errors as are caused by changing distribution of flow across the measuring section while a traverse is being made.

Recent tests indicate the proper form of piezometer to use in order to determine the true static pressure of flowing water. The errors caused by changing distribution of flow can be eliminated by the photoflow method described in the paper. This method involves the photographic recording of the differences in pressure of pitot-tube points, positioned throughout the cross-section of flow, and piezometer connections positioned to indicate the pressure across the flow section. By making a simultaneous record of all the readings across the section, errors caused by changing distribution of flow are eliminated and a large number of measurements can be taken in a short interval of time.

The photoflow coefficient as determined by volumetric measurement for highly disturbed flow in a closed conduit was found by test to be 0.971. A coefficient of 0.976 for the photoflow method as applied to the flows normally encountered in closed conduits should give an accuracy of 0.5 per cent.

The photoflow method[3] of water measurement is the photographic recording of the differences in pressures of pitot-tube points positioned throughout the cross-section of flow, and piezometer connections positioned to indicate the pressure across the section of flow. The method as here described has particular reference to closed circular conduits although it is not limited in its application to this specific case.

Reference is made to a paper by one of the authors[4] in which it was determined by a series of experiments that the pitot-tube point, if constructed as an orifice bounded by a surface of revolution, transformed velocity impinging exactly axially into pressure exactly according to the law $V = \sqrt{(2gh)}$, regardless of the form or extent of its exterior walls. At the time this paper was presented, there was considerable controversy regarding the pitot-tube formula, some advocating $V = \sqrt{(2gh)}$ while others, notably the late William Kent, author of "Kent's Mechanical Engineers' Handbook," and Prof. I. P. Church, author of "Mechanics of Engineering," both maintained that the formula should be $V = \sqrt{(gh)}$. The conclusiveness of the experiments in the paper referred to was indicated by the fact that Kent and Church changed the pitot-tube formula from $V = \sqrt{(gh)}$ to $V = \sqrt{(2gh)}$ in the subsequent editions of their books. From then on, $V = \sqrt{(2gh)}$ was generally accepted as the true pitot-tube formula.

The same paper also pointed out that one of the reasons for the necessary application of a coefficient in connection with the pitot tube was because of the difficulty in securing the real pressure properly applicable to the case in question. A recent paper presented to the Society[5] sets forth information as to the form and shape and arrangement of piezometer openings by which the direct water pressure may be measured in conduits. A study of this paper and of the various piezometer connections discussed will indicate one of the real causes of former difficulties in the measurement of water by the pitot tube.

The information contained therein, together with the tests recorded in "The Pitot Tube; Its Formula"[4] show why a pitot tube with the piezometer located in certain positions on or near the pitot-tube point, has to be rated and why a coefficient, which can properly be called the piezometer coefficient, must be applied to the readings. It was also found that tubes with piezometer openings placed in the path of the water are extremely sensitive to angular flow and subject to considerable error whenever other than straight flow is encountered.

Sufficient published data are now available to enable one experienced in the art to construct proper piezometer connections on the periphery of a straight cylindrical conduit such that the pressures of the water throughout a given cross-section may be properly indicated, thus eliminating all necessity for rating the pitot tube to obtain the piezometer coefficient and eliminating possibility of error in the static-head readings caused by angular flow.

The present art provides means for determining the correct velocity head in water flowing in straight conduits when the water flows in straight stream lines. However, in actual practice, straight streamline flow is never encountered. The particles of water move spirally, intermingle, and roll from center of pipe to pipe wall and back to center continuously, but without great loss of position in the travel of the flow. It has been shown that the introduction of a salt solution at a section in a conduit will diffuse throughout the mass of water within a reasonably short distance in the travel of the water, but the salt remains substantially together as a plug in its forward travel through the conduit. This is indicated by the fact that the salt solution at the outer periphery of the conduit will lag only a short distance behind the solution in the center of the pipe at a section which

---

[1] Manager and Chief Engineer, Hydraulic Department, Allis-Chalmers Manufacturing Company. Mem. A.S.M.E. Dr. White received his M.E. degree from Tulane University and served as engineer with the New Orleans Drainage Board from 1899 to 1902, and as hydraulic engineer and chief engineer in the I. P. Morris Department of Wm. Cramp & Sons Ship and Engine Building Company from 1902 to 1911, where he was in charge of hydraulic work for the company, including design and building of large hydroelectric installations among which was the plant at Niagara Falls. Since 1911, Dr. White has served in his present capacity with the Allis-Chalmers Mfg. Company. In 1930, he received the degree of Doctor of Science from Tulane University.

[2] Test Engineer, Hydraulic Department, Allis-Chalmers Manufacturing Company. Mr. Rheingans was graduated from the University of Wisconsin in 1920 with a B.S. degree in civil engineering and entered the employ of the Allis-Chalmers Manufacturing Company the same year where he has been engaged in testing and research work in the Hydraulic Turbine Department.

[3] Method patented by D. W. Proebstel, October 11, 1927, U. S. Patent 1,645,449.

[4] "The Pitot Tube; Its Formula," by W. M. White, The Journal of the Association of Engineering Societies, vol. 27, August, 1901, p. 35.

Contributed by the Hydraulics Division and presented at the Annual Meeting, New York, N. Y., December 4 to 8, 1933, of The American Society of Mechanical Engineers.

Discussion of this paper should be addressed to the Secretary, A.S.M.E., 29 West 39th Street, New York, N. Y., and will be accepted until October 10, 1935, for publication at a later date.

[5] "Piezometer Investigation," by C. M. Allen and L. J. Hooper, Trans. A.S.M.E., vol. 54, 1932, paper HYD-54-1.

may be a thousand feet or more from the point of introduction. Since the velocity of the water at the center of the conduit is considerably greater than at the sides, this can only mean that there is a sidewise motion of the water in its flow and that accordingly the particles of water must move at greater absolute velocity than the average axial flow along the conduit. The pitot-tube point, therefore, encounters not axial flow but angular flow.

If the pitot-tube points recorded the true pressure correspond-

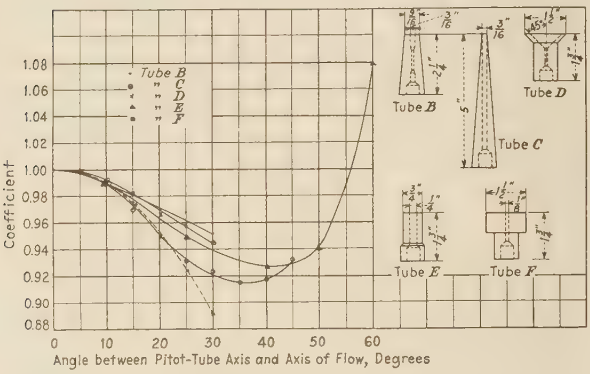

Fig. 1 Pitot-Tube Coefficients for Various Angles of Flow Showing Why Coefficients Must Be Applied to Measurements in Conduits

ing to the resolved axial velocity of such angular flow no coefficient of any kind would be required since now correct pressure in the section of flow can be secured. The pitot tube, however, does not indicate the direct resolved velocity and it has been found necessary to introduce a coefficient for this peculiarity of the pitot-tube point.

In the paper "The Pitot Tube; Its Formula,"[4] the author records the fact of his experimentation "with nozzles of different shapes moving through water and placed at different angles with reference to the line of motion." In a carefully prepared paper presented to the Engineers' Society of Western Pennsylvania[6] is recorded a very complete series of experiments on the coefficients for different shapes of pitot tubes for various angles of flow. Fig. 1 shows the results of these experiments and the outlines of the tubes used. From Fig. 1 it will be seen that for certain types of pitot tubes (B, E, and F) the coefficient varies from 1.00 to 0.96 for a maximum angle of flow of 25 deg, which angle is greater than can be ordinarily expected in even the very worst conditions of flow. It will be noted in the cases where the experiments were carried out to large angles that the value of the coefficient does not decrease in proportion to the change in angularity but beyond 40 deg it actually reverses and starts to increase.

Recent tests made on the exact design of pitot-tube point used for the Little Falls Pumping Station tests hereinafter described, showed similar angular-flow coefficients and characteristics. To determine these coefficients, this pitot-tube point was placed at the center of a 12-in.-diam pipe on the discharge end of a centrifugal pump and was mounted so that it could be rotated to any desired angle from the axis of the pipe. The flow was made as straight as possible with baffles.

The discharge of the pump was adjusted to maintain a constant velocity of 5 fps at the center of the pipe. Velocity-head readings were then taken at 0 deg and for every 5-deg angle of the axis of the pitot-tube point from the axis of the pipe on both sides of the centerline up to about 50 deg. These tests were repeated four times.

The indicated velocities were computed, averaged for the four tests, and plotted against the angles as shown in Fig. 2. The resolved velocity at a given angle was obtained by multiplying the axial velocity by the cosine of the angle. The measured velocity was then computed as a percentage of the resolved velocity and was plotted as shown.

Fig. 3 shows an outline of the Little Falls tube and a comparison of its angular-flow coefficients with those of the similar pitot tube B shown in Fig. 1. The close agreement of the results obtained by these two differently conducted experiments is rather remarkable.

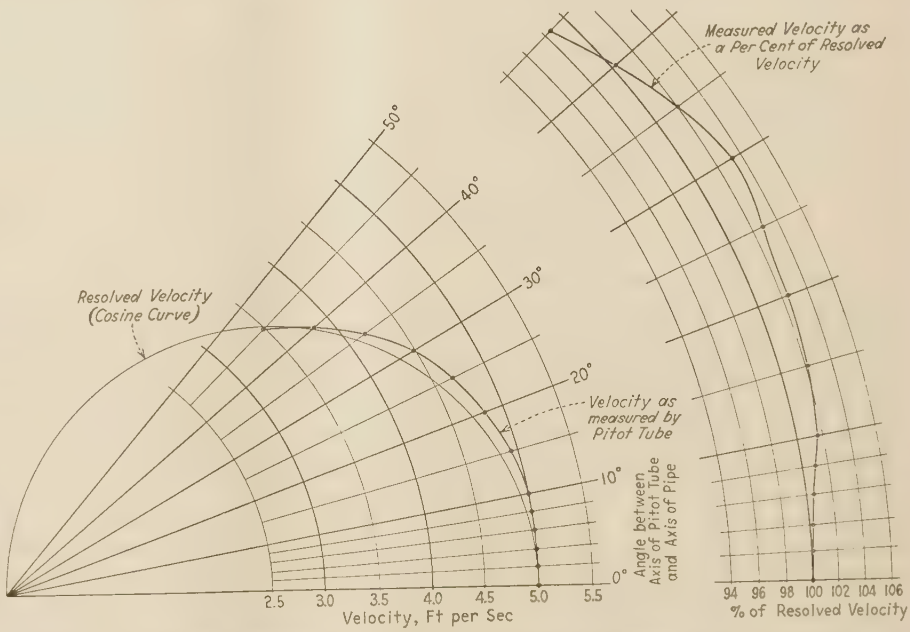

Fig. 2 Pitot-Tube Measurements at Various Angles in the Center of a 12-In. Diam Pipe With 5 Fps Constant Velocity

In addition to the variation in direction of flow, turbulence also affects the readings of the pitot tube because of the variation of velocity from instant to instant, accompanied by an oscillation of the water column in the tube and its connections.

The pitot-tube reading will not give the exact head corresponding to the average velocity over an interval of time but will tend to indicate the mean head which corresponds to the mean square of the velocity. This must theoretically always be in excess of the

[6] "Measurement of the Velocity of Flowing Water," by Lewis F. Moody, Proceedings of the Engineers' Society of Western Pennsylvania, vol. 30, no. 4, May, 1914.

head corresponding to the mean velocity, and has the effect of decreasing the pitot-tube coefficient of measurement.

However, Moody in the paper[6] previously referred to states that tests made with oscillating velocity showed that the effect on the pitot tube was very slight.

Although we now have exact means for indicating, recording, and determining axial flow, the experiments cited all show that when the angular flow encountered in all conduits is being measured, a coefficient must be applied which lies not so much to the pitot tube but rather to correct for flow conditions.

The worst flow conditions at the point of the pitot tube and an angular flow of an even 30 deg shows that the coefficient of a suitable pitot-tube point such as dimensioned in Fig. 3 will not be less than 0.97. Since the angular flow in conduits at velocities usually encountered is probably more than 10 deg, in which event the coefficient is about 0.98, the maximum range of the coefficient for the photoflow method as herein described consequently lies within narrow limits.

It is therefore claimed by the authors that the adoption of 0.976 as the coefficient for use with the photoflow method in circular conduits as here set forth should have an accuracy of 0.5 per cent because of the narrow range limit of the coefficient for various conditions of flow.

The many calibrations of the pitot tube with a known velocity of flow and with properly constructed piezometers have shown coefficients of measurement of about 0.976 as most generally applicable for normal flow conditions.

The calibration of the photoflow method set forth in this paper, based on volumetric measurement of water, determines the coefficient of 0.970 to 0.973 for the case of extremely disturbed and cross-current flow, and represents therefore about the lower limit of the coefficient for this type of tube in circular conduits.

The photoflow method was originally developed by D. W. Proebstel who used it for the first time to measure the discharge at the Bull Run Plant of the Portland Electric Power Company in 1924.[7] The feature which distinguishes this method from the ordinary pitot-tube traverse is the photographic recording during a fraction of a second of all the readings of multiple pitot-tube points rigidly fixed throughout the measuring section.

This has numerous advantages. Foremost of these is the recording of all the pitot-tube readings simultaneously, thereby eliminating the inaccuracies inherent with the traverse methods because of the changing distribution of flow found at all sections within a conduit. Even though the rate of flow is kept absolutely constant during the period of time required for making a determination of the quantity flowing, there is a continual shifting around and a rearrangement of the velocity at any given section. Tests show that the variations of velocity within the section may become quite large, particularly in disturbed or turbulent flow, where instances of a 30 to 50 per cent change of velocity at one point have been recorded, without an appreciable change in the rate of flow.

The velocity changes may take place during the comparatively short time of a few seconds, but whether the change at one point is fast or slow, there must always be an immediate and opposite change at some other point or points in order to maintain the continuity of flow in the conduit.

The frequency of the changes is usually very irregular. In some of the flows observed the velocity distribution would go through a complete cycle in 2 min and again it might take 10 min. Even then it was found that with observations taken at 2-min intervals, no two sets of flow-distribution records out of ten observations were ever exactly alike within the possible limits of accuracy.

[7] "Measuring Water Flow in Conduits," by D. W. Proebstel, *Electrical World*, April 4, 1925, p. 711.

This changing distribution of flow occurring at all sections within the conduit has heretofore been the source of considerable error in the pitot-tube traverse method or in any other method in which velocities across a section are determined in rotation. The time required to make the traverse is usually such that the flow distribution may pass through several complete cycles before all readings are completed. Velocities in one portion of the section are likely to be determined during one phase of the cycle, and those in another portion during a different phase. Thus, accurate determination of the average velocity is nearly impossible with the former methods.

By use of the photoflow method, however, the velocities across the entire measuring section are recorded simultaneously and the possibility of obtaining values of velocities at different points at varying phases of the distribution cycle is eliminated. It is

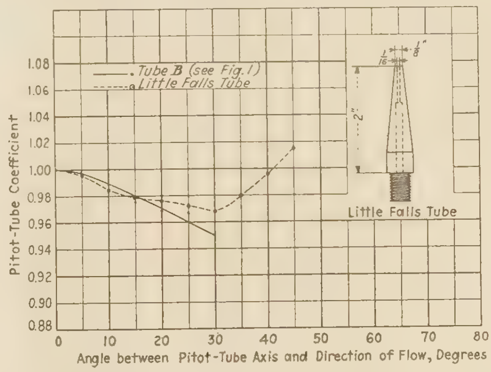

Fig. 3 Comparison of Pitot-Tube Coefficients for Various Angles of Flow, Showing Narrow Range of Coefficient for Large Variation of Angle

therefore possible to make accurate determinations of the rate of flow with this method no matter how great the changes in velocity at any point within the measuring section.

In addition to the large variations in velocity at points within the measuring section, there are also the small fluctuations of high frequency found on all water columns connected to conduits containing flowing water.

Whenever these fluctuations are caused by variations in the static pressure, the pitot-tube and piezometer water columns will all move up and down together. With the photoflow method the speed of the camera can be adjusted by the use of artificial light so as to make the moving water columns appear to be standing still, and a true and simultaneous reading of all the connections will be obtained. Since the piezometer readings are subtracted from the pitot-tube readings to obtain the velocity head, fluctuations common to all the connections such as produced by variations in the static pressure will therefore have no effect on results obtained by the photoflow method.

The high-frequency fluctuations in the water columns, which may be caused by small variations at individual points in the section, will have a tendency to cancel each other. With a large number of pitot tubes the possible error from this source becomes relatively small.

Another advantage of the photoflow method is the short period of time required to record the readings. Photographs of the different velocities can be taken at the rate of about two per minute and for special cases a motion-picture camera can be used. This means that twenty determinations of the mean velocity across the measuring section can be made during a normal 10-min test run. Since, for the very worst conditions of flow, ten such determinations would give a high degree of accuracy, this method is capable of far greater accuracy than a pitot-tube

or a current-meter traverse where it sometimes takes several hours to make one such determination of the average velocity, and where the cost of making ten determinations at each gate setting tested would be excessive.

The number of measurements of the mean velocity of the entire section which can be made at regular intervals during a short period of time will also permit accurate measurements to be made of such fluctuating flow as will sometimes be encountered.

The cost of making a photoflow test is exceptionally low. No expensive equipment is required. The cost of the films or plates is negligible. Developing the plates and printing the pictures at the site saves time and reduces this item of expense. The pitot-tube points can be turned out in quantity lots at a

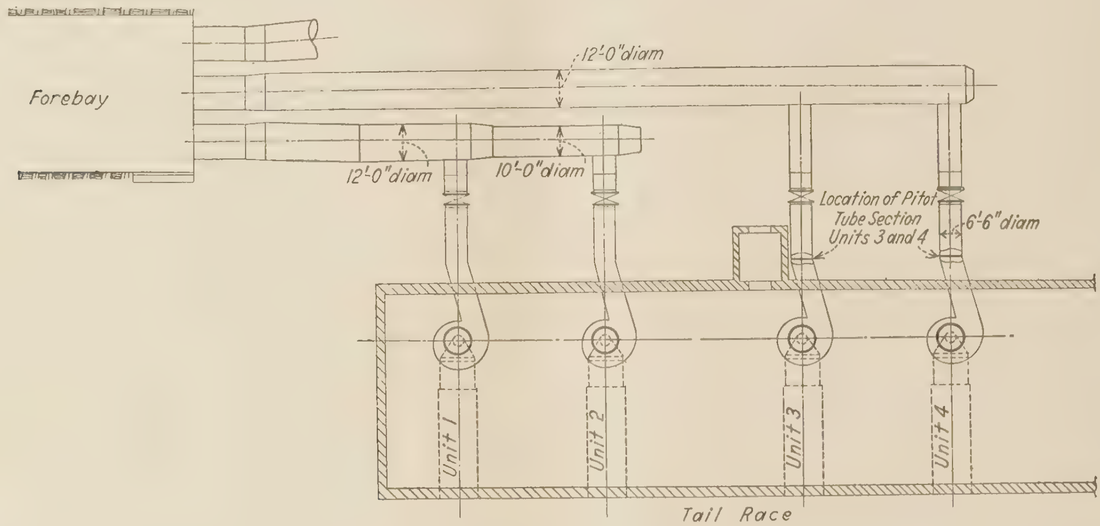

Fig. 4 General Plan View of Little Falls Pumping Station

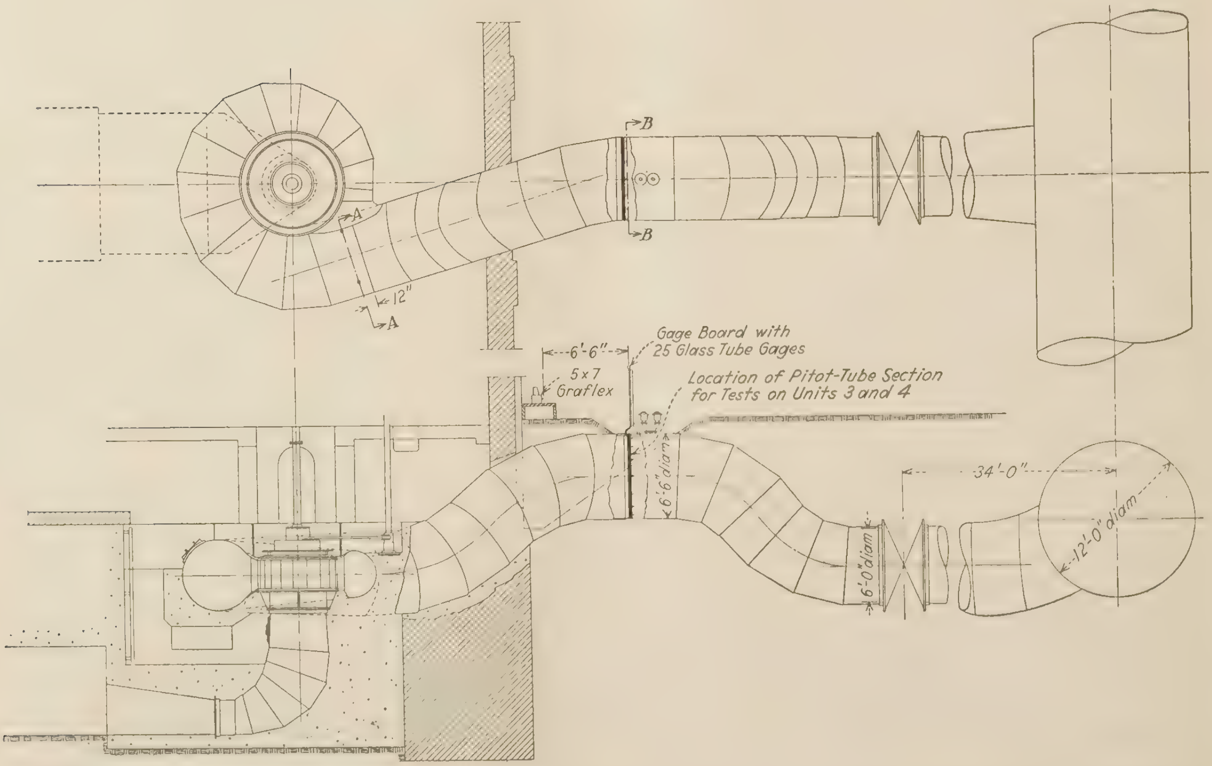

Fig. 5 Cross-Section of the Little Falls Pumping Station Showing the Location of Pitot-Tube Section. Notwithstanding the Disturbed Flow the Photoflow Method Gave Consistent Results at These Sections

nominal cost. The installation of the pitot tubes, the gridwork upon which they are fastened, and the gage connections have been found to be less costly than the usual current-meter rigging. The operating personnel can be reduced to one man who can take the photographs, develop the plates, print the pictures, and compute the discharge. Therefore, from a viewpoint of cost, the photoflow method compares favorably with any other method of measuring quantity of water.

An example of the application of the photoflow method under extremely unfavorable conditions is the acceptance test made at the Little Falls Pumping Station at Little Falls, New Jersey, on two 900-hp, 32-ft head, propeller-type turbines. Fig. 4 is a general plan view of the plant from the forebay to the tailrace. Fig. 5 is a section of the penstock and turbine showing the location of the pitot tubes.

The contract with the Passaic Valley Water Commission specified that the water be measured by current meter, salt titration, or pitot tube. Local conditions limited the current-meter measuring section to a narrow tunnel in the tailrace underneath the power station. Because of the disturbed flow in these tunnels, it was questionable whether current-meter measurements would prove to be satisfactory. Salt titration was considered to be too complicated for this installation. Therefore, only the pitot-tube method remained. The choice of a measuring section was limited. The large 12-ft-diam penstock was buried underground and under buildings and was practically inaccessible. The velocities in this penstock were low, being about $2^1/_2$ fps for one turbine at full gate. The $6^1/_2$-ft connecting penstock was full of bends and elbows but finally the short, straight section on the upper bend was selected, as is indicated in Figs. 4 and 5.

Those familiar with pitot-tube measurements would say that this was a very poor place for the use of pitot tubes. However, as will be shown later, the results obtained fully justified the confidence placed in the photoflow method as a means for measuring turbulent flow.

In the photoflow method, the number of pitot tubes to be used depends upon the size of the section, the nature of the flow, and the accuracy desired. In this case the measuring section was divided into three equal areas by three concentric circles. A pitot-tube point was located at the center of area of each of these circles on three equally spaced diameters, giving a total of 18 points located in the center of eighteen equal areas, as shown in Fig. 6. An additional point was located in the center of the penstock. It was assumed that the 18 points in this size of penstock were sufficient to give consistent results in highly turbulent flow. The test results obtained proved that this assumption was correct.

The pitot-tube points were mounted on a streamlined gridwork with their impact ends 2 in. upstream from the plane of the grid. This was for the purpose of getting them away from the influence of the obstruction to flow incidental to the grid. Where the supports have to be made fairly heavy, this distance should be increased.

Six piezometers for determining the static head at the pitot-tube section were located in the wall of the penstock and were equally spaced around the circumference, as shown in Fig. 6.

All of the pitot-tube points and piezometers were connected to separate glass-tube gages on a single gageboard. The upper ends of the glass tubes were connected to a common manifold. Water-column elevations in the glass tubes were adjusted by means of air pressure in this manifold. For low pressures, a vacuum in the manifold can be used to raise the water columns. For very low velocities oil can be used above the water instead of air to increase the differential readings.

Shut-off valves, blow-off valves, and drain valves were provided for manipulation of the gages although none of the connections were throttled. A 5 in. × 7 in. Graflex camera was used for recording the readings. This was found to be about the smallest size print easily readable without enlargement.

Figs. 7 and 8 are photographs taken during a test run at 0.65 gate on Unit No. 4. The gages are numbered from left to right starting with No. 2 on the left, and correspond to the numbering shown in Fig. 6.

Tables 1 and 2 show the calculations made from these photographs in arriving at the average velocity for the section.

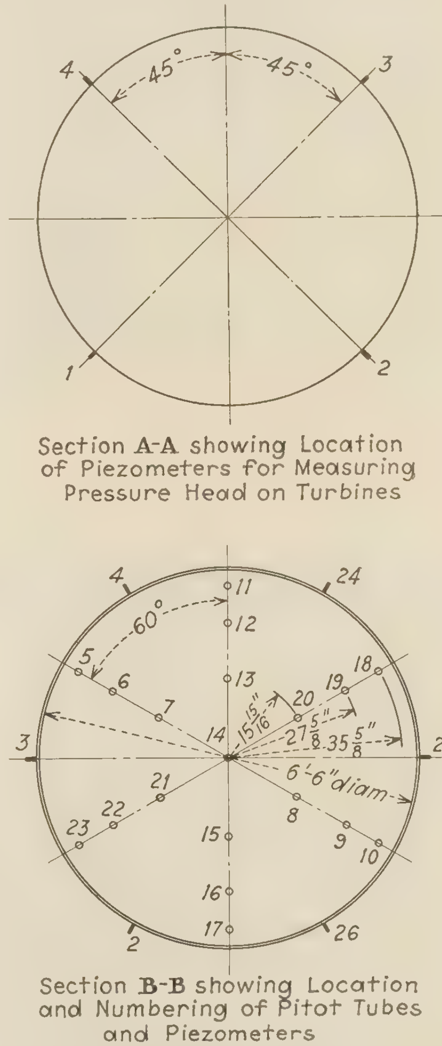

Fig. 6 Piezometer and Pitot-Tube Sections From Fig. 5 Showing Distribution of Pitot Tubes in Equal Areas at the Measuring Section

The six piezometer readings were first averaged and then subtracted from the pitot-tube readings to obtain the velocity head. The velocity for each point was computed and the average indicated velocity obtained by taking the arithmetical mean. Pitot tube No. 14 was not included in this average because it was at the center of the penstock and not at the center of area of one of the 18 equal areas. Multiplying the average indicated velocity by the pitot-tube coefficient and by the area of the measuring

section gave the discharge. The pitot-tube coefficient was determined by volumetric measurement as will be shown later.

Figs. 7 and 8 and Tables 1 and 2 show the large variation in velocity which occurred at certain points, such as Nos. 8, 12, and 20, without affecting the total discharge. For instance, the variation in velocity for Figs. 7 and 8 at point No. 12 was 18 per cent, and several other points had as much as 10 per cent variation, but the difference in total computed discharge was found to be only 0.2 per cent.

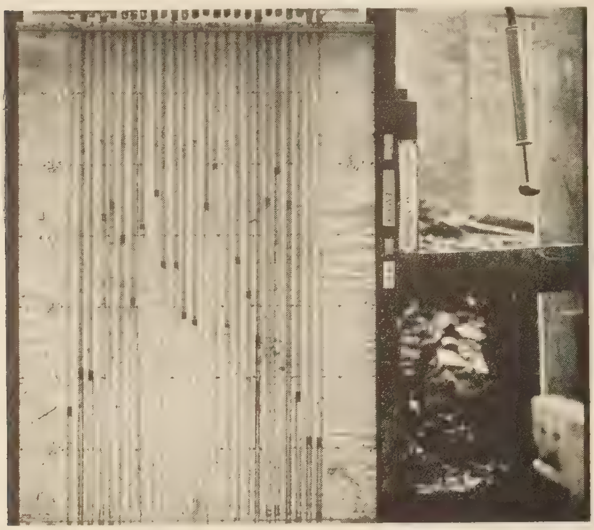

Fig. 7 Pitot-Tube and Piezometer Readings During a 0.65-Gate Test on Unit No. 4 at Little Falls Pumping Station. The Water Columns Are Numbered From Left to Right Starting With No. 2 on the Left and Ending With No. 26 on the Right. Columns 2, 3, 4, 24, 25, and 26 Are Piezometer Readings. The Remainder Are Pitot-Tube Readings

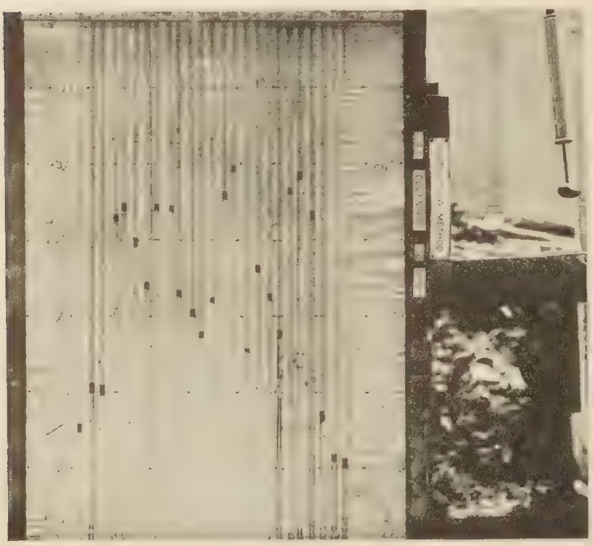

Fig. 8 This Photograph Was Taken Several Minutes After the One Shown in Fig. 7 During the Same Test Run. Columns 8, 12, and 20 Show the Variation in Velocity Without an Appreciable Change in Discharge

With the pitot tubes located on three straight lines across the measuring section, it was possible to draw velocity curves for

TABLE 1 COMPUTATIONS FOR READINGS SHOWN IN FIG. 7

Gage number	Pressure gage rdgs	Pitot-tube gage rdgs	Velocity head, ft	Velocity, fps	
2	1.299	...	...	...	
3	1.571	...	...	...	
4	1.555	...	...	...	
5	...	2.652	1.322	9.24	
6	...	2.741	1.411	9.54	
7	...	2.508	1.178	8.72	
8	...	2.062	0.731	6.87	
9	...	2.580	1.250	8.98	
10	...	2.819	1.489	9.80	
11	...	2.316	0.986	7.98	
12	...	2.312	0.982	7.96	
13	...	1.960	0.630	6.38	
14	...	1.903	0.573	6.08	Center
15	...	2.730	1.400	9.51	
16	...	3.003	1.673	10.39	
17	...	1.875	0.545	5.93	
18	...	2.349	1.019	8.11	
19	...	2.100	0.770	7.05	
20	...	1.790	0.460	5.45	
21	...	2.760	1.430	9.60	
22	...	2.975	1.645	10.30	
23	...	2.740	1.410	9.54	
24	1.395	...	...	...	
25	1.081	...	...	...	
26	1.078	...	...	...	
	7.979			151.35	
Average =	1.330				

151.35/18 = 8.41 average indicated velocity; angular-flow coefficient = 0.97; 8.41 × 0.97 = 8.16 average velocity; area = 33.13 sq ft; 33.13 × 8.16 = 270.4 cfs.

TABLE 2 COMPUTATIONS FOR READINGS SHOWN IN FIG. 8

[Gage number	Pressure gage rdgs	Pitot-tube gage rdgs	Velocity head, ft	Velocity, fps	
2	1.292	...	...	...	
3	1.561	...	...	...	
4	1.548	...	...	...	
5	...	2.669	1.345	9.31	
6	...	2.742	1.418	9.56	
7	...	2.520	1.196	8.78	
8	...	2.228	0.904	7.64	
9	...	2.739	1.415	9.55	
10	...	2.728	1.404	9.52	
11	...	2.170	0.846	7.39	
12	...	2.045	0.721	6.82	
13	...	1.900	0.576	6.10	
14	...	2.125	0.801	7.19	Center
15	...	2.820	1.496	9.82	
16	...	2.990	1.666	10.35	
17	...	1.790	0.466	5.48	
18	...	2.338	1.014	8.09	
19	...	2.152	0.828	7.31	
20	...	1.910	0.586	6.15	
21	...	2.841	1.517	9.87	
22	...	2.948	1.624	10.25	
23	...	2.690	1.366	9.39	
24	1.377	...	...	...	
25	1.096	...	...	...	
26	1.069	...	...	...	
	7.943			151.28	
Average =	1.324				

151.28/18 = 8.405 average indicated velocity; angular-flow coefficient = 0.97; 8.405 × 0.97 = 8.15 average velocity; area = 33.13 sq ft; 33.13 × 8.15 = 270 cfs.

TABLE 3 DISCHARGES AS DETERMINED BY PHOTOFLOW METHOD ON UNIT NO. 4 AT LITTLE FALLS PUMPING STATION

Gate	Photo no.	Discharge, cfs	Average discharge	Max. variation in discharge, per cent	Probable error by method of least squares, per cent
0.400	413	121.5	...	...	...
	414	122.6	...	...	...
	415	121.5	...	...	...
	416	123.4	...	...	...
	417	122.3	...	...	...
	418	123.2	122.4	1.6	0.20
0.575	364	216.2	...	...	...
	365	219.0	...	...	...
	366	218.1	...	...	...
	367	218.4	...	...	...
	368	219.2	...	...	...
	369	220.0	218.5	1.7	0.16
0.700	394	301.1	...	...	...
	395	298.8	...	...	...
	396	299.1	...	...	...
	397	299.4	...	...	...
	398	299.8	...	...	...
	399	301.3	299.9	0.8	0.09

three diameters and determine the average velocity by integrating the area underneath the curves. This was done for a number of tests but the results checked so closely with those obtained by taking the average of the 18 readings at the centers of equal areas that the latter method was used for all tests with a considerable saving of time and work.

It was found that six photographs for each test run were sufficient to give consistent and accurate results. With a test-run duration of 10 min this meant a photograph every 2 min. Table 3 shows the discharges as determined from these photographs at each of three gate settings. The variation of 1.7 per cent between the maximum and minimum discharge at 0.575 gate may seem rather large at first glance but by taking an average of six measurements the probable error was reduced to 0.16 per cent as computed by the method of least squares. By increasing the number of photographs taken during any one run, the probable error could be reduced still more but this was considered unnecessary for these tests.

As an indication of the consistency of results obtained with the photoflow method, the discharges were plotted against the gate opening as shown in Fig. 9. The small deviation from a smooth curve is all the more remarkable in view of the poor measuring section and the widely fluctuating distribution of flow as was

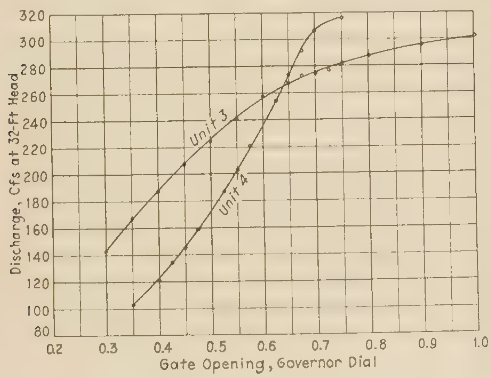

Fig. 9 Discharge Curves by the Photoflow Method on Two Units at Little Falls Pumping Station, Showing Consistency of Results Obtained by This Method

plainly evident in these tests. Unit No. 4 has an adjustable blade runner which accounts for the difference in the two discharge curves.

One of the interesting features of these tests was the static-head reading of the six piezometers. An analysis of the records in Figs. 7 and 8 and in Tables 1 and 2 shows that although there was considerable variation in the static pressure, in each instance the average of two readings diametrically opposite was the same as the average of any two other opposite readings. Furthermore, the difference between, say, piezometer No. 6 (Fig. 6) and No. 25 was the same as the difference between No. 2 and No. 26, etc. This is shown graphically in Figs. 10 and 11 where the pressures are plotted against both the horizontal and vertical distances across the penstock.

The full lines connecting the readings are practically parallel and indicate the relation between the readings in a given direction. The dash lines connect readings diametrically opposite and show the close agreement of the averages at the center of the penstock. This led to the conclusion that the pressure across the penstock was largely dependent upon the centrifugal force produced by a change of direction of the path of the water. Theoretically this pressure varies as the square of the radius of the curved path, but since the distance across the penstock is small compared to this radius, very little error is introduced by assuming that the pressure varies directly as the radius.

Using this latter relationship to determine the actual pressure at each pitot tube, new velocities were computed for several of the tests but the final average velocity thus obtained checked very closely with that obtained by using the average of all the piezometer readings as was done in the computations shown in Tables 2 and 3.

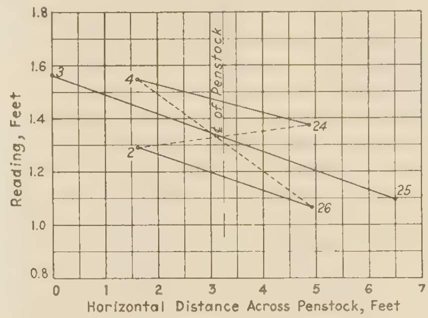

Fig. 10 Inter-Relation of Pressure Readings Taken From Fig. 8, Showing Why Piezometers for Closed Conduits Should Always Be Located in Pairs, Diametrically Opposite Each Other

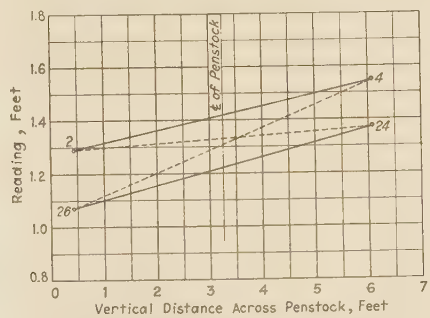

Fig. 11 Inter-Relation of Pressure Readings Taken From Fig. 8

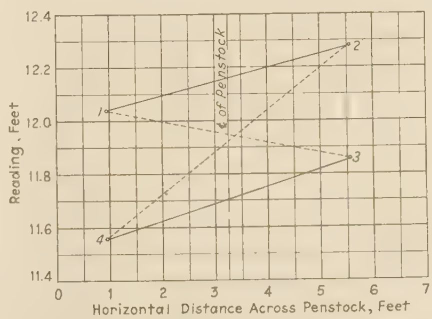

Fig. 12 Inter-Relation of Pressure Readings at Section A-A, Fig. 6, With a Discharge of 286 Cfs. This Is Another Indication Why Piezometers in Closed Conduits Should Be Located Diametrically Opposite Each Other

Fig. 12 shows the pressure readings of the four piezometer connections at section *A-A*, Fig. 6, at the entrance to the scroll case. This is another example of the relation between pressure reading and radius of curvature of the path of the water. In this case the pressures are affected by the bend in the penstock directly upstream from the section and by the beginning of the scroll-case curvature.

In measuring the static pressure in closed conduits it is, therefore, most important that the piezometers be located diametrically opposite each other and that an even number of piezometers such as two, four, or six be used instead of one, three, or five, etc.

The contract with the Passaic Valley Water Commission for the Little Falls Pumping Station units called for a bonus and penalty on overall efficiency. It was, therefore, essential that the measurement of discharge as well as the power and head measurements be as accurate as possible in their absolute values. Since the photoflow method was being used in a section with considerably greater disturbed and turbulent flow than ever attempted before with pitot tubes, it was decided to determine the coefficient of measurement of the pitot-tube points in place by volumetric measurement of the water. It was found that the forebay with an area of 70,000 sq ft could be isolated from the river by means of head gates and used as a huge volumetric measuring tank. The maximum possible drawdown of the forebay was 4 ft. Thus, with a maximum discharge of 300 cfs through one of the turbines it was possible to calibrate the photoflow method for a period of 15 min for each drawdown, which proved to be sufficient to give accurate results.

The volume of the forebay was determined by first making a drawdown and then filling it through a calibrated venturi meter.

Leakages into and out of the forebay were reduced to less than 1 per cent of the maximum discharge through the turbine by making all the gates and valves connected to the forebay as tight as possible. In addition, a leakage determination was made before and after each test run, thereby reducing the possible error from this source to a negligible amount.

Four hook gages were placed in stilling boxes at various stations for measuring the elevation of the water in the forebay. By the aid of verniers the water elevations were read to the nearest one thousandth of a foot.

Readings were taken every 30 seconds and were all synchronized with the photoflow pictures by a system of light flashes. The fluctuations of elevation caused by waves set up by the drawdown and fill-up were not very large, and were of such low frequency that readings every 30 seconds accurately determined their outline.

The close agreement between the elevations as measured at the four stations indicated that the probable error from this source was relatively small.

In filling the forebay through the venturi meter to determine the forebay area at the different elevations, the penstock-gate valves leading to all the turbines were closed, but the unit under test was left motoring on the line. After the water in the forebay had reached the desired elevation the proper penstock-gate valve was opened, the turbine gate set to give the required rate of flow at the pitot-tube section, and the drawdown test was made to determine the photoflow coefficient.

The area of the forebay at various elevations was determined six times. The probable error of the average of the six determinations was estimated at less than 0.25 per cent.

Nine determinations of the photoflow coefficient were made with the pitot tubes located in the penstock of Unit No. 3, and seven determinations of the coefficient with the pitot tubes located in Unit No. 4. Tests were made with different rates of flow but the results indicated that the coefficient did not change with a change in velocity. The average coefficient for Unit No. 3 for all rates of flow measured was 0.973 and for Unit No. 4 was 0.970. Because of the large number of measurements the probable error was less than 0.25 per cent.

The results agree with the previous statement that highly disturbed and turbulent flow would have a coefficient close to 0.970.

In conclusion, it can be stated that the results obtained with the photoflow method so far have been very satisfactory and indicate its possibilities as an accurate, quick, and economical means of measuring the flow of water. The excellent results obtained with this method in the tests described herein show that it can be used under conditions heretofore thought to be entirely unsuited for pitot-tube measurements.

Although the method has been used only in closed conduits, it should give satisfactory results in open conduits. There apparently is a large field for its use in the measurement of the large quantities of water used by low-head turbines.

Pitot-Tube Practice

By EDWARD S. COLE,[1] NEW YORK, N. Y.

The author reviews the history of the pitot tube and, on the basis of experimental results, discusses the accuracy of the pitot-traverse method of water measurement. In connection with the practical application of the pitot tube to flow measurement, the author discusses the calibration of the tube, corrections for the effect of the projected area of the rod, and the errors caused by angularity of flow in a pipe. The degree of angularity of flow in the normal pipe line was investigated by means of a current-vane indicator and a motion-picture camera. Reference is made to investigations of the effect of eddying flow on pitot-tube readings as conducted by means of a series of ratings made with three pitot tubes of similar design used under three different conditions of flow, viz: Still water, the smooth or parallel flow of a large venturi throat, and the irregular or eddying flow of a 12-in. pipe line. In making the comparative ratings, coefficient corrections are made for the projected area of the pitot tube in the 12-in. pipe. The author shows that with normal flow in a pipe line, the manometer readings will vary through a series of cycles. These cycles, with pitot tubes in a 40-in. and a 12-in. pipe, were observed with a motion-picture camera.

IT IS the purpose of this paper to present some of the results of long experience with the so-called pitot-traverse method of water measurement in the hope that engineers may more widely recognize its accuracy.

In order to avoid repetition later on in this paper, it may be advisable to define the terms "simple" and "combined" pitot tubes. The simple type consists of one forward-facing tube which reads the dynamic head when used in an open stream. When used in a pipe under pressure it reads the dynamic plus the static head and in order to read velocity, the static head must be deducted by means of wall piezometers. The combined type is usually made up of two tubes; one reading the dynamic head, the other the static head. The combined type may have different forms, although variations in design are chiefly concerned with the static orifice.

History of the Pitot Tube

The history of the pitot tube began in 1730 when Henri Pitot[2] using a bent glass tube in the River Seine discovered that the height to which water rose in his tube was proportional to the square of the velocity of the stream. Aside from its extreme simplicity, this device was novel in that it measured velocity without introducing the time element. Contrary to general belief, Pitot used the combined form with double tubes and described it in his paper,[2] Fig. 1. The second or static tube had its opening in the end of a straight pipe pointing directly across the flow and therefore it must have been subject to errors. It may not be generally known that Pitot in his paper of 1732 described quite clearly an application of his tube for measuring the speed of a small sail boat which he navigated on the Seine. Since then there have been several attempts to make a successful ship log on this principle. A pitot log was used on the Great Lakes by Nicholson, probably fifty years ago, but owing to one defect or another it did not come into extensive use.

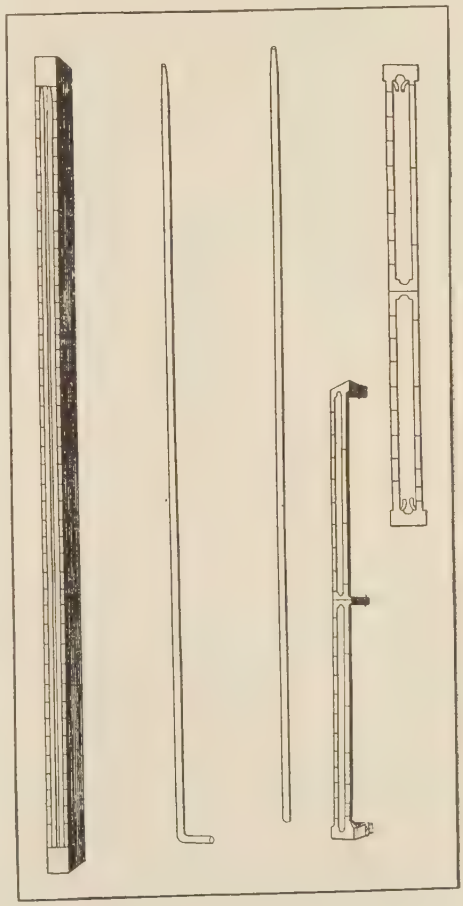

Fig. 1 Drawing of Pitot's Original Tube, 1732

Pitot's combined tube was improved one hundred and twenty-five years later by Darcy, another French engineer who in one form turned the static tube downstream and in another gave it only lateral openings which more nearly read the true static pressure, Fig. 2. Darcy also reduced the vibrations in the water

[1] President, The Pitometer Company, Engineers. Mem. A.S.M.E. Mr. Cole received the degree of M.E. from Cornell University in 1894 and from that date until 1902 served on the staff of John A. Cole, consulting engineer, Chicago, working on the design, construction and management of city water-works plants in the Middle West. In 1896 he developed the pitometer. As a member of the Department of Water Supply, Gas, and Electricity of New York, N. Y., he was in charge of water-supply studies with the pitometer during 1902 and 1903. Since that time he has conducted pitometer investigations throughout the country.

[2] "Description d'une machine pour mesurer la vitesse des eaux courantes, et le sillage des vaisseaux," by H. Pitot, Memoires de l'Academie Royale des Sciences, November 12, 1732.

Contributed by the Hydraulic Division and presented at the joint meeting of the Hydraulic Division, A.S.M.E. and the Power Division, A.S.C.E., New York, N. Y., January 17, 1935.

Discussion of this paper should be addressed to the Secretary, A.S.M.E., 29 West 39th Street, New York, N. Y., and will be accepted until October 10, 1935, for publication at a later date.

columns by using orifices of much smaller area than the tubes.[3]

Bazin, another French engineer, made extensive use of the Pitot-Darcy tube.[4]

Hiram F. Mills of Boston was probably the first American engineer to use the pitot tube, making studies of the flow of water in a 12-in. cast-iron pipe at Lawrence, Mass. in 1875. These experiments unfortunately have never been published. The original notes came into the hands of the late John R. Freeman and are now being searched for the exact form of pitot tube used by Mills and the method of its calibration. There can be no doubt that he was the first American experimenter in this field.

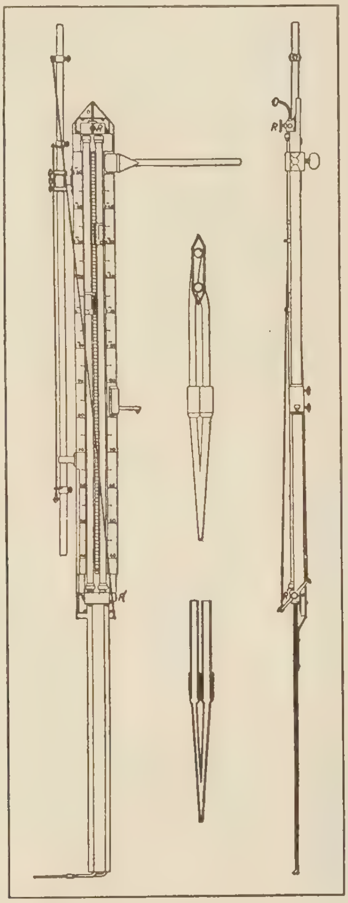

FIG. 2 DARCY'S TUBE, 1858

It is believed that Mills preferred the simple form of pitot tube with static pressure taken from wall piezometers as distinguished from the combined type used by Pitot, Darcy, and Bazin.

Mills wrote[5] that he "made measurements of the quantity of water drawn by many of the water wheels of the Lawrence Mills in the feeding penstocks by instruments devised by me in 1877 and used by my assistants under the direction of John R. Freeman during 1878 and 1885, and later under the direction of Richard A. Hale. These instruments indicated the velocity at 16 or 18 points in the section at the same moment."

[3] *Annales des Ponts et Chausses*, 1858.

[4] Ibid., 1890.

[5] Discussion by H. F. Mills of "Experiments at Detroit, Mich., of the Effect of Curvature Upon the Flow of Water in Pipes," by Williams, Hubbell, and Fenkell, Trans. A.S.C.E., vol. 47, 1902, p. 203.

John R. Freeman[6] followed Hiram Mills in the use of the pitot tube and in 1888 adopted the simple type for use in measuring fire-stream jets finding an accuracy of within 0.25 per cent. "This investigation established the fact that the pitot tube is an instrument of great precision for the measurement of high velocities."[7]

Henry Flad, a distinguished engineer of St. Louis, about 1888 carried on pitot-tube studies, and probably was the first to attempt the use of photography for recording the manometer deflections but in this he was said to have been unsuccessful.

The author's first work with the pitot tube began in the fall of 1896 at Terre Haute, Ind., where a practical form of instru-

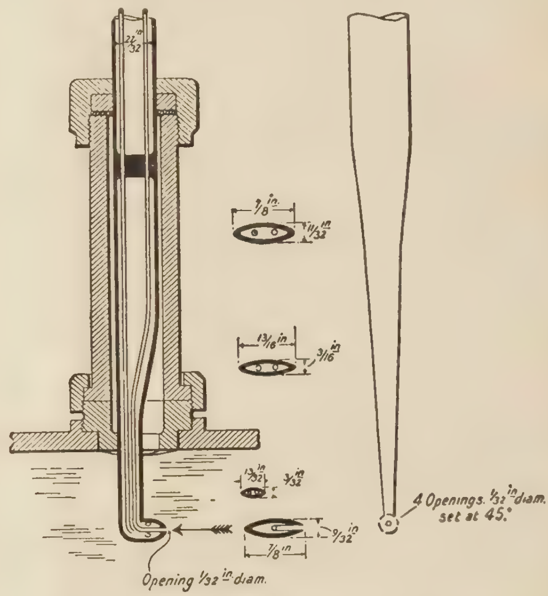

FIG. 3 TUBE USED BY WILLIAMS, HUBBELL, AND FENKELL IN 1897

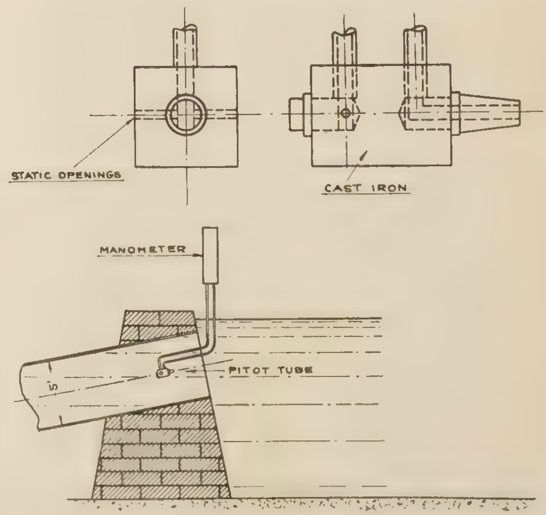

FIG. 4 TUBE USED BY W. B. GREGORY AT CORNELL UNIVERSITY IN 1894

[6] "Experiments Relating to Hydraulics of Fire Streams," by John R. Freeman, Trans. A.S.C.E., vol. 21, 1889, p. 411.

[7] "A Treatise on Hydraulics," by M. Merriman. Eighth edition. John Wiley & Sons, Inc., New York, p. 103.

ment was developed for use in pipes under pressure. A description of this development was published in the A.S.C.E. Transactions, vol. 47, 1902, page 275.

The work of Williams, Hubbell and Fenkell, which began at Detroit in 1897, resulted in a combined form of pitot tube for use in pipes under pressure,[8] Fig. 3.

Gregory and Mason in tests conducted in connection with their thesis, at Cornell University in 1894, used a pitot tube, Fig. 4, introduced at the open end of a 5-ft steel pipe.

Later Gregory and Maltby developed a form of combined pitot tube at Ithaca, N. Y., in 1903, Fig. 5. Although not the most convenient form for inserting into a pipe under pressure it is a highly successful instrument which has been extensively used by Professor Gregory in his professional practice and by the New Orleans Sewage and Water Board for the past thirty years.

White's studies of the pitot tube in 1901 developed the theory of the simple dynamic orifice and demonstrated the formula to be $h = V^2/2g$ rather than $h = V^2/g$ which had been urged by some writers at that time.

Pardoe, at the University of Pennsylvania in 1908, succeeded Professor Easby in pitot-tube experiments. Prof. C. G. Hyde, of the University of California, made careful calibration tests of the

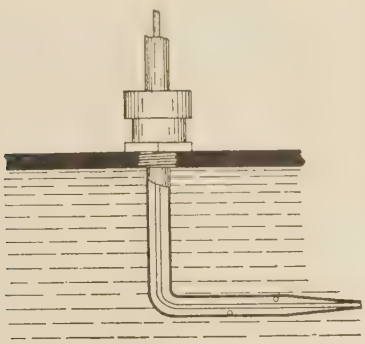

Fig. 5 Pitot Used by Gregory in 1903

combined pitot tube, Fig. 6, in 1915. E. C. Murphy[9] made careful ratings of the pitot tube in moving water as well as in still water. Stanton studied velocity variation close to the pipe wall. Boyd and Judd[10] in 1904 repeated Freeman's work with jets. They reported that "discrepancies in pitot tubes are due to failure to get the true static pressure rather than to any error in the pitot tubes themselves."

The theory of the dynamic tube or orifice has been well developed by Moody and Rogers[11] and others. Its law is $V = c\sqrt{(2gH)}$.

The theory of the static orifice is more complicated than that of the dynamic orifice and is best represented by laboratory observations such as were made by Allen and Hooper at Worcester Polytechnic Institute.[12] In its ideal form the wall piezometer is simple enough, but in practice the author found it difficult to secure ideal conditions and prefers to follow Darcy and Bazin in obtaining the static head as in the combined type, i.e., along with the dynamic orifice.

Development of the Pitometer

At the time of the author's experimental work with pipes under pressure at Terre Haute, Ind., water-works plant, there was little available information on the pitot tube. Darcy's published results related entirely to open-stream use. A crude sketch in Carpenter's "Experimental Engineering,"[13] Fig. 7, suggested the use of an impossible combination of tubes and of manometers.

The few published references to pitot-tube accuracy were discouraging. One author[14] wrote, "Pitot's tube has been but little used and is in general regarded as an imperfect instrument for velocity determinations."

After many attempts it was seen that a practical pitot-tube method for measuring the flow of water in pipes under pressure must embody (1) a suitable means for inserting the tube into the pipe under pressure, (2) a practical and accurate method for calibrating the instrument, (3) a differential manometer free from air which contains a liquid permitting the magnification of the deflections at low velocities, (4) a method of integrating the flow from a velocity traverse, and (5) a means for the frictionless recording of manometer deflections where a continuous record of flow is necessary.

With the extensive literature now available regarding flow measurement in pipes under pressure, it is difficult to realize the

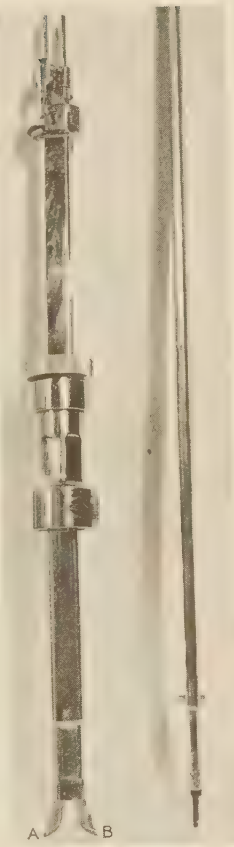

Fig. 6 Author's Pitot Tube for Pipes, 1896

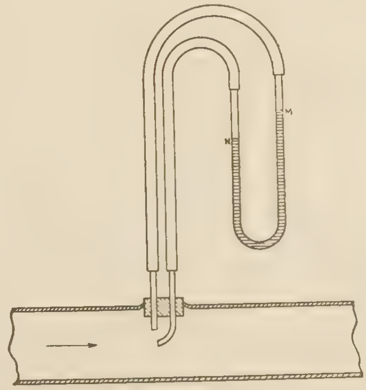

Fig. 7 Carpenter's Sketch of Pitot Tube for High Pressures, 1892

[8] "Experiments at Detroit, Mich., on the Effect of Curvature Upon the Flow of Water in Pipes," by Williams, Hubbell, and Fenkell, Trans. A.S.C.E., vol. 47, 1902, p. 1.

[9] Discussion by E. C. Murphy of "Experiments at Detroit, Mich., on the Effects of Curvature Upon the Flow of Water in Pipes," by Williams, Hubbell, and Fenkell, Trans. A.S.C.E., vol. 47, 1902, p. 197.

[10] "Pitot Tubes; With Experimental Determinations of the Form and Velocity of Jets," by J. E. Boyd and H. Judd, *Engineering News*, vol. 51, 1904, p. 318.

[11] "Measurement of the Velocity of Flowing Water," by L. J. Moody, Proceedings, Engineers' Society of Western Pennsylvania, vol. 30, no. 4, May, 1914. Also discussion of this paper in vol. 30, no. 5, June, 1914.

[12] "Piezometer Investigation," by C. M. Allen and L. J. Hooper, Trans. A.S.M.E., vol. 54, 1932, paper HYD-54-1.

[13] "Experimental Engineering," by R. C. Carpenter. Third edition, John Wiley & Sons, Inc., New York, 1892, p. 266.

[14] "A Treatise on Hydraulics," by M. Merriman. Fourth edition, John Wiley & Sons, Inc., New York, 1890.

handicap of early experimenters in this field since, lacking published data, it was necessary to work out each of these essential features of a practical pitot tube for pipes.

The calibration of the instrument was obtained by float measurement of the velocity in a trough, the instrument being inserted through the bottom. Considerable difficulty was encountered in this method as the floats did not run uniformly down the trough.

A pitot tube following Professor Carpenter's sketch, Fig. 7, of

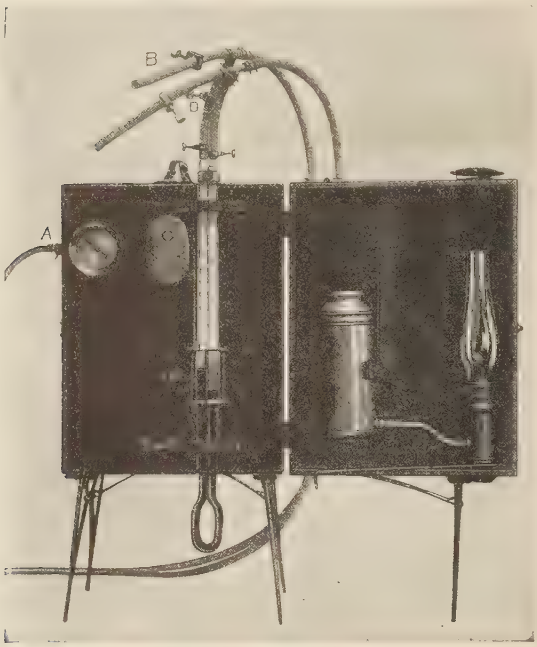

Fig. 8 Photo-Recorder With Prism Attachment Developed in 1897 and 1908 for Recording Manometer Readings

course, gave highly erratic readings but the manometer caused the first concern. This crude form, with air above the measuring liquid, and without means for removing it, was the only suggestion available at that time. Such a form with its rapid U-tube fluctuations was quite impossible to read with any precision. It was only when all air was excluded from the manometer and connections, allowing the water to fill the U-tube above a heavier and immiscible liquid, that reliable readings were obtained. In later years, cases were discovered in which failures of pitot tubes were caused largely by this troublesome presence of air in the manometer.

It was evident that the readings were extremely small at the low velocities of 1 fps or lower commonly found in water-works mains but with carbon tetrachloride properly mixed with benzine to give a specific gravity of 1.25, a differential of four to one was available, which proved to be most useful.

After overcoming U-tube troubles it was next in order to discover why the hook-and-point type of pitot tube gave such erratic and inconsistent results on calibration. After many attempts, the Darcy plan of turning the static tube downstream was tried and immediately the calibration points began to fall within more narrow limits and a practical form, Fig. 6, was at last available.

Many years of experience with this combined type of pitot tube or pitometer has shown that it has the unique advantage of reversibility. A ready and rapid means of checking its own reading is afforded by rotating through 180 deg. This is of great practical value in the field where it is usually difficult to obtain a zero check.

Later, in 1897, during a systematic field survey carried out with the newly developed pitometer at Terre Haute, the need was felt for continuously recording the U-tube deflections, and photography was tried with poor results until the proper method of focusing the U-tube on the sensitized paper was found. At first one leg of the manometer was placed before a slot on the other side of which was a revolving drum carrying the sensitized paper. Light from an oil lamp passing through the glass tube focused upon the slot, thus leaving a record of the liquid height.

With slightly colored liquid partially intercepting the light, a gray-and-black record was formed. With mercury as the measuring liquid for high velocities the light was entirely intercepted giving a white-and-black record. Errors resulting from the vertical angularity of the light rays were compensated for by properly spaced notches in the slot plate which automatically ruled lines upon the photo record corresponding to the true half deflections in the U-tube itself.

After some ten years of use this device was improved by the addition of a double prism between the lamp and the U-tube so

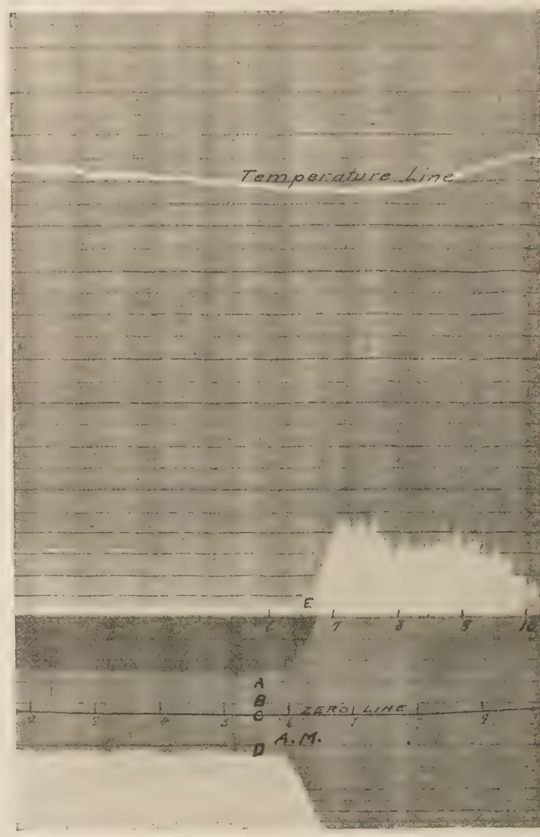

Fig. 9 A Reduced Section of a Prism Photo-Record, Recording Both Legs of U-Tube Manometer

that the liquid height in both legs of the manometer was recorded to 3 in., Figs. 8 and 9. Pressure and temperature changes were also recorded along with the velocity variations. The original design of the tube with its upstream and downstream orifices has been improved upon from time to time, but the essential principles of the pitometer developed in 1896, have been retained.

Practical Application to Flow Measurement

From nearly 40 years of experience it has become apparent that certain fundamentals must be considered in order to insure accuracy of flow measurements. Some of these are intimately related to calibration while others are details in technique of operation.

The following items must be considered in connection with calibration:

1 For important tests the tube must be calibrated.

2 Proper correction must be made for the effect of the projected area of the rod.

3 The effect of angular and eddying flow in the normal pipe line may be corrected by a cosine-reading type of tube such as shown in Fig. 29.

The following details of operation which comprise the pitot-traverse method are important:

(a) A proper selection of the gaging point must be made.

(b) The pipe factor, i.e., ratio of mean to center velocity, is of fundamental value and is determined by traversing the pipe. The mean velocity of the traverse is obtained by ring integration, and the value for the center velocity is taken from the traverse curve.

(c) All readings of the deflection should be made throughout a full cycle of flow and careful attention given to the U-tube and its connections, and the specific gravity of the measuring liquid.

(d) For large pipes attention should be given to the possible effect of vibration of the pitot tube.

1 *Calibration*

The determination of c in the formula $V = c\sqrt{(2gH)}$ must be determined by calibration. Calibrations may be made in moving water or in still water, and present indications lead the author to believe that with the proper correction for the projected area of the rod, when used in pipes, calibrations by either of these methods will give the same results.

In moving water the pitot-tube readings are compared with velocity as given by floats in an open stream or, if the rating is in a pipe, the pitot tube itself is used to compute the mean velocity from a velocity traverse, which is then compared with the mean velocity given by weir or tank measurement.

A still-water rating may be made by moving the pitot tube ahead of a boat drawn at known speeds or by driving it through still water by a revolving boom or a car running over a tank.

Before describing the calibration tests of the author's tube, it may be interesting to present a summary of some available calibration data on both types of pitot tube. This summary is given in Table 1.

Calibration Research, 1930. In order to determine accurately what errors are introduced in the manufacture of the tubes and in their calibration, seven different tubes were tested at the Alden Hydraulic Laboratory, Worcester Polytechnic Institute, in 1930. Five of the tubes conformed to a standard while two others differed slightly in curvature of tips. These tubes were calibrated in the 16-in. throat of the 36 × 16-in. venturi meter, and in the 12-in. line. The results are as shown in Fig. 10.

TABLE 1 SUMMARY OF PITOT-TUBE CALIBRATION DATA

Experimenter	Method of calibration	Type of tube	Coefficient	Remarks
Darcy, Bazin	Still water, floats in moving water, and measurement of known flow	Combined (Fig. 2)	1.00	*Annales des Ponts et Chausses*, 1858 and 1890.
Gregory and Maltby	....	Combined (Fig. 5)	1.00	Used and calibrated by the New Orleans Sewage & Water Board.
White	Studies of pitot tube	Simple	1.00	Tube not calibrated but $V = \sqrt{(2gH)}$ proved in which case $c = 1$.
Pardoe	Weighing-tank measurement of flow in pipes	Simple	1.00	University of Pennsylvania, 1908.
Pardoe	8-in. and 4-in. pipes, flow by weighing tank	Simple	0.982	University of Pennsylvania, 1934.
Boyd and Judd	....	Simple	1.00	*Engineering News.*[10] Freeman's work repeated, 1904.
Alden Hyd. Lab., Worcester P. I.	16-in. throat of venturi meter, 12-in. steel pipe	Simple	0.994	Impact orifice, Fig. 6, 1930.
Darcy, Bazin, or Murphy as summarized by Parker[1]	Floats in moving water	Darcy	1.006	92 ratings.
	Moving water—weir	Darcy	0.993	87 ratings.
	Floats in still water	Darcy	1.034	32 ratings.
	Moving water	Combined	0.875	Both orifices directed against current but pressure orifice plugged and a small hole 0.04-in. diam, pierced laterally.
	Still water	Combined	0.864	
	Floats in still water	Combined	0.998	Impact orifice directed against the current, pressure orifice facing downstream.
	Still water	Combined	0.991	

[1] "Control of Water," by P. M. Parker, D. Van Nostrand Company, New York, 1913, p. 69.

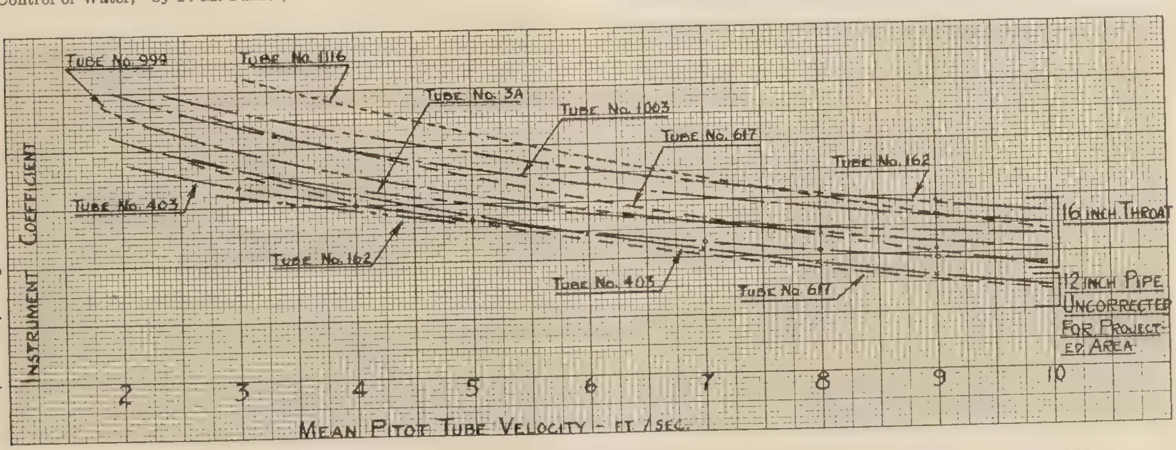

Fig. 10 Results of Calibration Tests of Pitot Tubes at Alden Hydraulic Laboratory, Worcester P. I., 1930

(Note: Tubes nos. 999 and 1003 do not fit template.)

An explanation of the 1930 tests will aid in making comparisons of the various calibrations presented.

The 16-in. throat of a 36-in. venturi meter has long been used for calibrating purposes at this laboratory because of the smooth flow and flat velocity curves with their high pipe factor of about

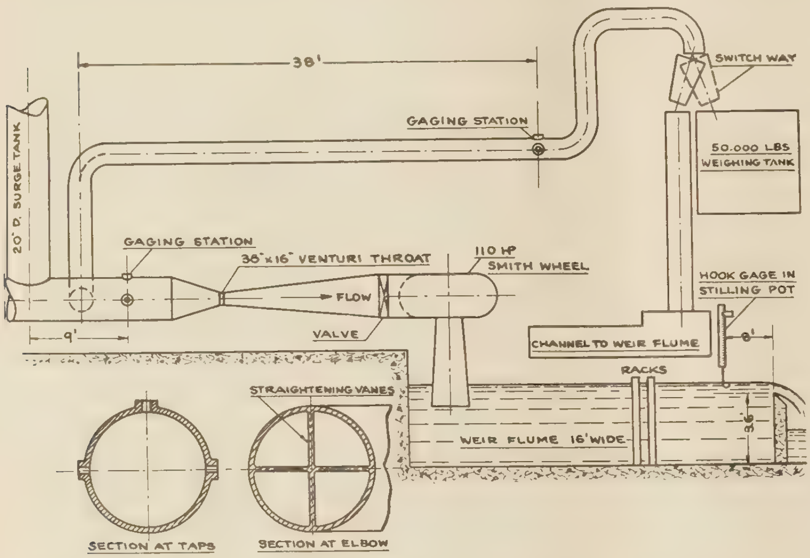

FIG. 11 APPARATUS USED FOR RATING PITOT TUBES AT ALDEN HYDRAULIC LABORATORY

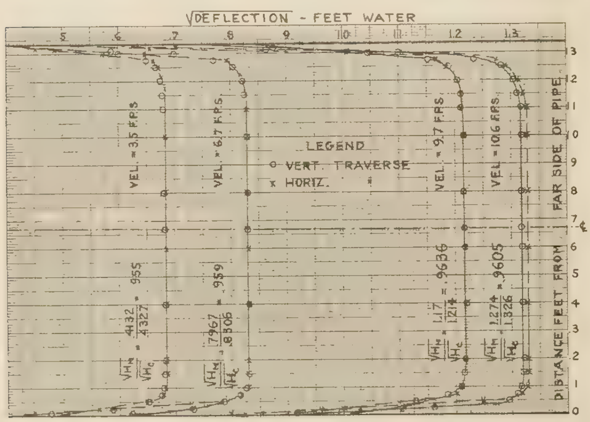

FIG. 12 TRAVERSE CURVES OF FLOW IN 16-IN. VENTURI THROAT, ALDEN HYDRAULIC LABORATORY, 1934

0.96. For traversing, the pitot tube was inserted through 1-in. cocks 90 deg apart in the bronze throat piece, and for calibration the orifices were located 4 in. in on the horizontal diameter. The flow was measured over a 10-ft contracted weir which had been calibrated by the weighing tank, using the increment method as in Fig. 11.

Pipe factors, described in detail later, for the 16-in. and 12-in. sections, were carefully determined by means of double traverses before and after the series of tests. Sample traverse curves are shown in Figs. 12 and 13.

The test procedure in the 16-in. throat was as follows: After the discharge had been set to a desired value, about 10 to 15 minutes were allowed to elapse to secure steady-flow conditions in the penstock and over the weir. The U-tube deflections with the pitot tube at the gaging point were then read in feet of water at the rate of about ten times per minute by an experienced observer, and the figures set up on a calculating machine. Ten readings of head were taken for each position of the rod shown in Fig. 6, i.e., with A tip upstream and with B tip upstream. The head on the weir was read and then the discharge was adjusted to a new value for the next test.

Variations in velocity under the uniform head available were so small that the mean of the readings was assumed to be the mean head for each run instead of taking the average of the square roots of the U-tube deflections.

The test procedure in the 12-in. line calibrations was practically the same as in the 16-in. throat with the exception that the mean velocity was obtained by weighing-tank measurements. The piping layout for these two gaging stations is shown in Fig. 11.

The 12-in. steel pipe line is believed to afford fairly normal flow conditions under the constant laboratory head of about 30 ft. The effect of two standard pipe elbows in different planes at the entrance was minimized by the use of straightening vanes as shown by the excellent symmetry of the velocity traverses in Fig. 13.

As may be noted in Fig. 10 there was a difference in coefficient between the 16-in. throat and the 12-in. line and further

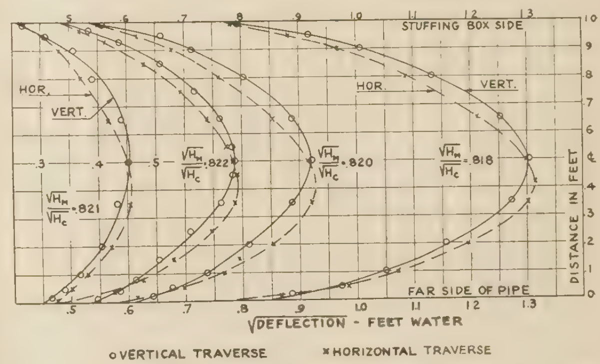

FIG. 13 TRAVERSE CURVES OF FLOW IN 12-IN. PIPE. GAGING STATION 38 FT DOWNSTREAM FROM STRAIGHTENING VANES. ALDEN HYDRAULIC LABORATORY, 1934

investigations of the reasons for the discrepancy were thought necessary.

Calibration Research, 1934. In 1934 it was decided to have three of the pitot tubes (rods 162, 403, 617, for which calibration curves are shown on Fig. 10) which were calibrated in 1930 recalibrated at the same gaging stations in the Alden Hydraulic Laboratory. To these calibrations was added a calibration made in still water. An 84-ft lattice steel boom was suspended from a ball bearing on top of a vertical shaft. This shaft was imbedded in the top of a boulder about 60 ft from one shore of a three-acre pond. The water surrounding the station was normally 6 to 7 ft deep. The pitot tube mounted on the boom swept through a circle of 36.11 ft radius. The speed of the boom was obtained from contacts made at each revolution and recorded on a chronograph.

The pitot heads were measured by water columns under partial vacuum, and the difference in heads was read about 15 times a

minute by an observer who rode the boom. These were at once set up on a calculating machine which gave the mean deflection for the run. The speed of the boom was regulated by a special governor and as its variation was small it was considered that the mean U-tube head was close to the true head for each run. The centrifugal effect was balanced by using equal lengths of hose and by having the U-tubes at equal radii. Care was taken to check the zero readings at intervals by stopping the boom.

The possibility of circulation effects in the water caused by the rotation of the pitot tube was carefully studied. No appreciable amount of circulation was evidenced under the most severe tests. One series of tests was made in which the rotation of the boom was reversed. The elapsed time from the moment the speed in one direction was changed until full speed in the reverse direction was attained amounted to 3 or 4 min. The pitot heads read when the boom was going in one direction substantially agreed with the heads read with the boom going in the reverse direction. Other tests were made in which the coefficient of the pitot tube obtained by the boom rating was compared under various conditions of rating. Obstructions were placed on the opposite end of the boom so that considerable disturbance of the water was created. Apparently this disturbance died down very quickly for the coefficients of the pitot tube remained the same regardless of the conditions thus introduced.

On account of the size, shape, and depth of the pond the coefficients obtained by the boom calibration were not subject to error caused by circulation of the water.

The scattering of the points in the boom ratings, Figs. 14 and 15, was due in part to varying conditions of wind and weather on the pond. That more uniformity of readings is possible with the boom method is shown by the test points in Fig. 30 which were obtained under more favorable conditions.

The results, Figs. 14, 15, and 16, showed agreement between the boom and the venturi throat, while the calibration in the 12-in. line was about 2 per cent lower. It was decided at this time that the amount of correction of the area of the projected rod should be carefully determined.

2 *Correction for Projected Area of Rod*

For many years a correction had been applied to the pipe area to compensate for the projected area of the rod. This correction was arrived at by more or less arbitrary methods and was applied by deducting from the pipe area an amount equal to the full area of the rod in the direction of flow, when the orifices were at the center of the pipe.

Correction at Alden Hydraulic Laboratory, 1930. For the calibrations made at the Alden Hydraulic Laboratory in 1930 a somewhat different analysis was made, and a revised correction amounting to one-third of the area of the projected rod when the orifices were at the center of the pipe was arrived at in the following manner.

When the instrument is on the far side of the center of the pipe, the area of the pipe is reduced and the mean velocity by that section is increased above the value when the instrument is not present. Assuming that the ratio of the point velocity to mean velocity remains constant, the point velocity obtained will be too great by the ratio of the area of the pipe to the area of the pipe minus the effective area of the pitometer.

If the point velocity obtained were to be corrected at the centers of rings of equal area, for any given ring there would be a plus correction on one side of the center and a minus correction on the other side, assuming the readings are to be corrected with respect to the pitometer at the center. The average amount by which the two velocities in a given ring exceeds the true values would be equal to the amount by which the measured center velocity exceeds its true value without the instrument in place.

Since the pipe factor is the ratio of the average velocity in the centers of rings of equal area to the center velocity, the value of the pipe factor is not changed by the presence of the instrument. However, the shape of the traverse curve may be distorted, the measured velocities being higher on the far side of the center of the pipe.

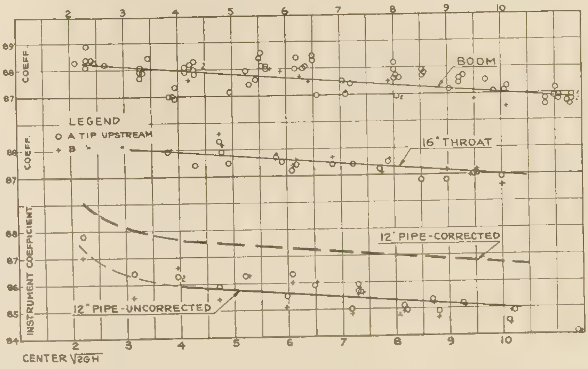

Fig. 14 Calibration of Pitot Tube No. 403, Alden Hydraulic Laboratory, 1934

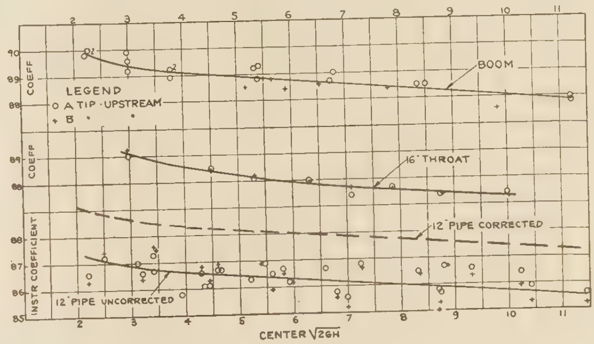

Fig. 15 Calibration of Pitot Tube No. 617, Alden Hydraulic Laboratory, 1934

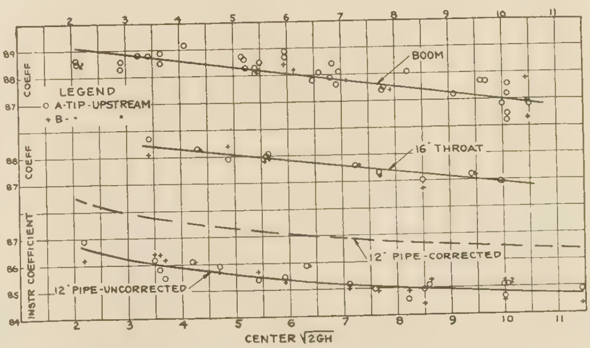

Fig. 16 Calibration of Pitot Tube No. 162, Alden Hydraulic Laboratory, 1934

Although the value of the pipe factor is not affected by the presence of the instrument in the pipe, the value of the coefficient is affected and should be corrected when the rating is done in small pipes. Assuming the instrument is set at the center of the pipe, the mean velocity at a given discharge is increased above its actual value without the instrument in the pipe, by an amount depending on the projected area of the instrument set at the center.

The theory which resulted in a correction of one-third the

projected area of the rod was based on the assumption that only the trailing orifice was affected by the presence of the rod. It was assumed that the upstream orifice was not affected and since the trailing orifice is about one-half as efficient as the upstream orifice, it contributes one-third of the total deflection of the instrument.

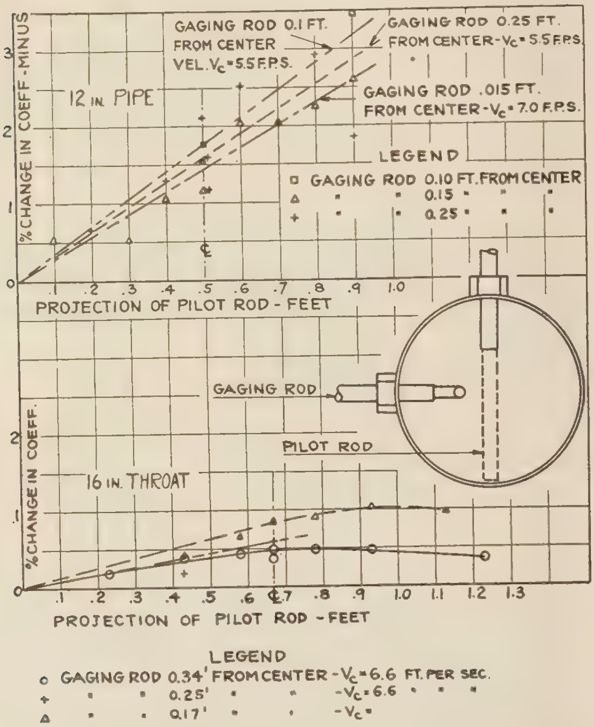

Fig. 17 Method for Determining Pitot-Coefficient Corrections for Projected Area of Rod in a 12-In. Pipe and in a 16-In. Venturi Throat

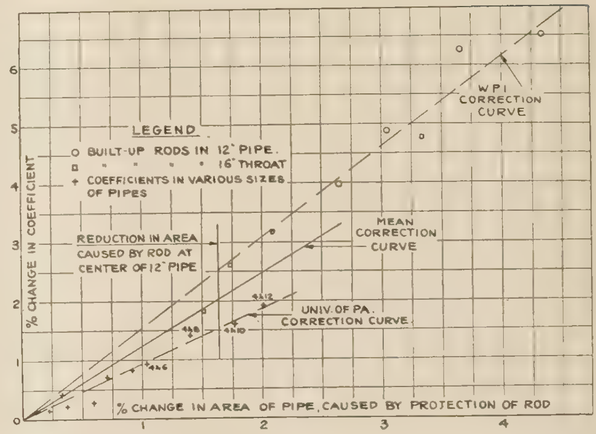

Fig. 18 Correction of Pitot-Tube Coefficient for Changes in Area of Pipes Caused by the Projected Area of the Rod
(Note: 12-in. pipe corrected by mean correction curve, Fig. 24.)

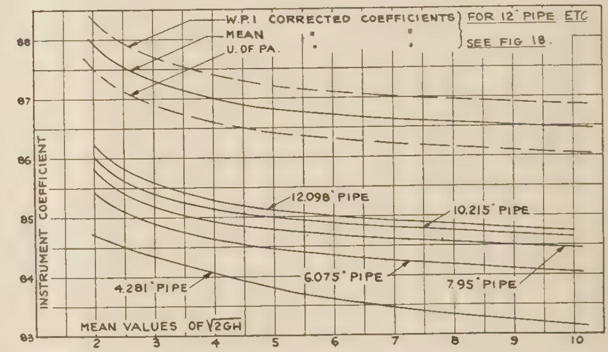

Fig. 19 Calibration Curves of Rod No. 617, University of Pennsylvania, 1934

Correction Studies at Alden Hydraulic Laboratory, 1934. In 1934 a preliminary test was made at the Alden Hydraulic Laboratory to determine whether the correction might be larger than had been assumed. The method was to locate a pitot tube as an index rod at some point in the pipe and without changing its position to move a second or dummy tube across the pipe on another diameter in the same section. It was indicated by the first pitot tube, that the further the dummy rod was projected the greater would be the velocity indicated by the index tube. It was apparent that the dummy rod would disturb the flow past the index tube if it were too close and various positions of the indicating rod were tried to note the effect of the disturbance. The results are shown in Fig. 17 and, although being far from conclusive chiefly because of disturbance effects, they indicated at the time that the correction for the rod in the 12-in. line was greater than one-third the projected area.

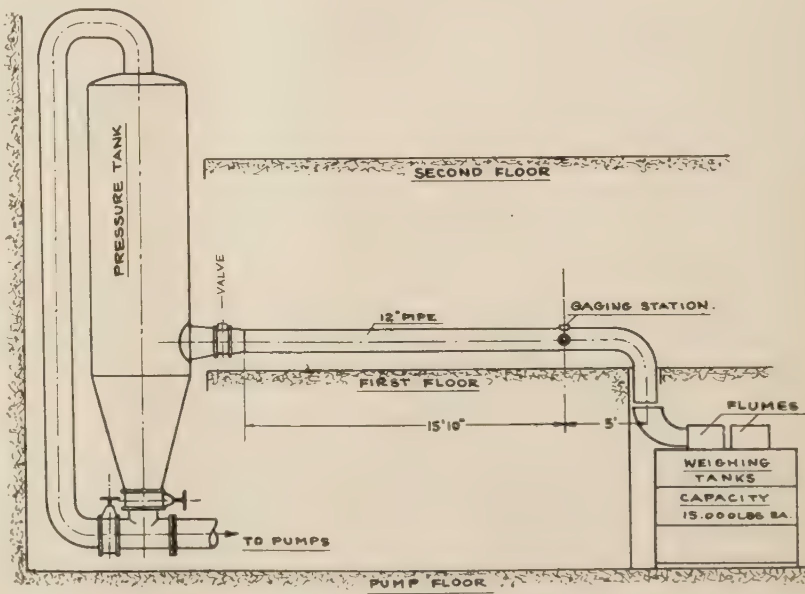

Fig. 20 Sketch of Apparatus for Rating Pitot Tubes at University of Pennsylvania, 1934

A set of tests was then devised which would give some quantitative data on the amount of the correction. The method was to build up the cross-section of the rod in such a way as not to disturb the flow past the orifices, but to make an appreciable change in the net area of the pipe. The rod was built up by pieces of 1-in. dowel which were split and made to fit either side of the rod. The lower end of the dowel was tapered to a point 1 in. from the orifices. The section thus built up was wrapped with friction tape and shellacked. The cross-sectional area of the built-up rod in the direction of flow was determined by means of calipers.

The procedure was to build up the cross-sectional area of a calibrated rod and then to recalibrate it in both the 12-in. line and the 16-in. throat at velocities of 8, 9 and 10 fps. The resulting change in coefficient was assumed to be due entirely to the change in area of the pipe caused by the increased cross-sectional area of the rod. Four built-up sections were tried, the largest being 1 in. in diameter. The results are shown in Fig. 18.

University of Pennsylvania Tests. A third method for arriving at the proper correction seemed desirable and this was carried out at the University of Pennsylvania. Two of the three rods (Nos. 162 and 617) calibrated at the Alden Hydraulic Laboratory, were rerated by Professor Pardoe at the University of Pennsylvania in pipes of 4, 6, 8, 10, and 12 in. diameter. Fig. 19 shows Professor Pardoe's calibrations for rod No. 617. The method of calibration was different in some respects from the calibration at the Alden Hydraulic Laboratory. The piping layout is shown in Fig. 20 and it may be noted that the gaging station for the 12-in. pipe is only 15 diameters below a contraction. The distribution of velocity at the gaging station is illustrated by the traverse curves shown in Fig. 21. Instead of obtaining the indicated mean velocity by readings of the center velocity and pipe factors (ratio of mean to center velocity) as was done at the Alden laboratory, the procedure was to measure the mean velocity by traversing and to compare it with the true mean velocity as determined by weighing-tank measurements. The flow was well regulated by means of centrifugal pumps discharging into a large tank with an overflow to maintain a constant head. During the traversing, continuous weighing-tank measurements were made to determine the true mean velocity. The average of the square roots of the deflections obtained at the center of area of 16 rings of equal areas for the 12-in. pipe times $\sqrt{(2g)}$ was taken as the mean velocity by the pitot tube. The ratio of the mean $\sqrt{(2gH)}$ thus obtained to the mean velocity determined by the weighing tank is the coefficient. As was expected the coefficient in each pipe was different, although it should be noted that the coefficient obtained in the 12-in. line agreed with the coefficient obtained in the 12-in. line at Worcester, thus giving a remarkable check between the two series of investigations.

For the University of Pennsylvania tests, the ratio of the area of the cross-section of the

DIAMETER OF PIPE - INCHES	4.281	6.075	7.950	10.215	12.098
AREA OF PIPE - SQ. FEET	0.100	0.202	0.345	0.571	0.798
AREA OF ROD, WHEN HALF-WAY ACROSS PIPE - SQ. FEET	.00365	.00521	.00773	.01067	.0131
REDUCTION IN AREA OF PIPE, CAUSED BY AREA OF ROD - %	3.65	2.58	2.24	1.865	1.64

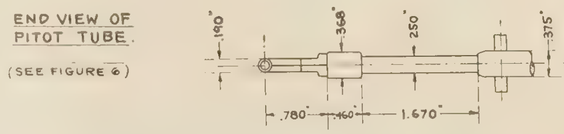

Fig. 22 Area of Pitot Tubes When Half Way Across Various-Diameter Pipes and the Reduction in Area of the Pipe Caused by the Area of the Pitot Rod

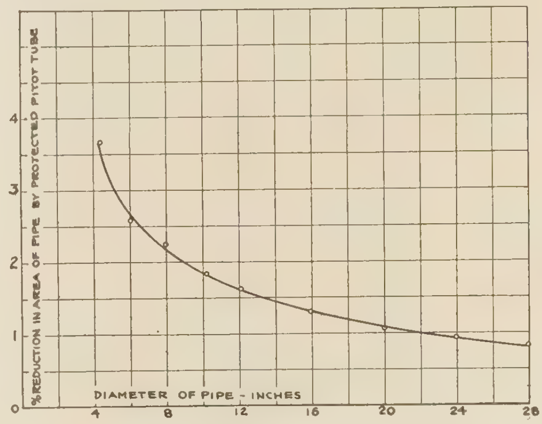

Fig. 23 Graph of Values in Fig. 22

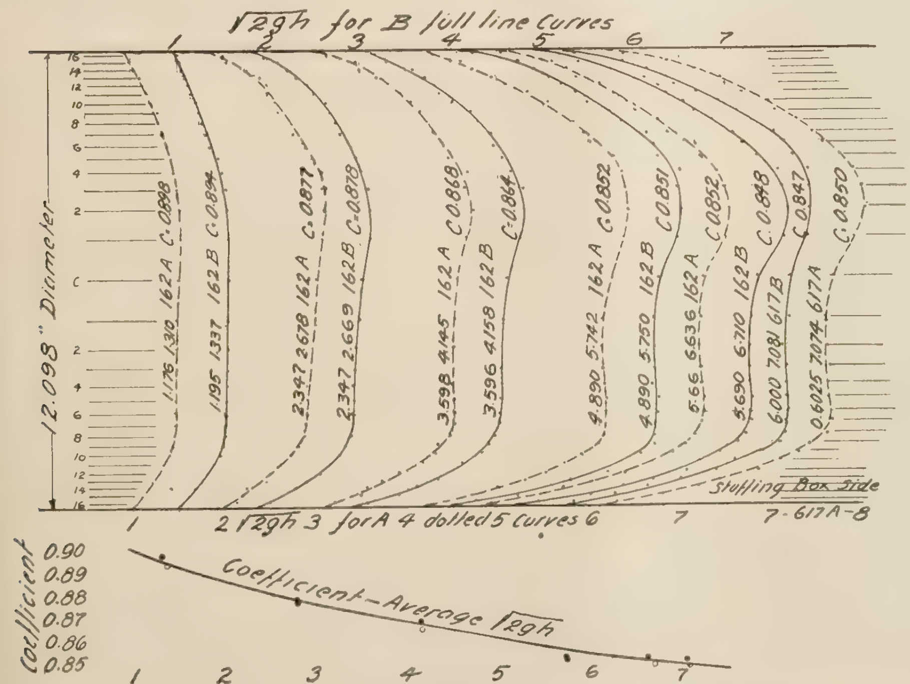

Fig. 21 Traverse Curves Showing Distribution of Velocity at the Gaging Station Shown in Fig. 20. Gaging Station Is 15 Diameters Below Contraction

normal rod in the direction of flow, with the orifices at the center of the pipe, to the area of the pipe, for each size pipe was computed and is shown in tabular form in Fig. 22. The values are plotted in Fig. 23. A sample computation for the 4.281-in. diam pipe follows:

Length of projected rod, orifices at the center = 2.14 in.
Cross-sectional area of rod in direction of flow:

Orifices..........	0.780 in. × 0.190 in.	=	0.1482 in.
Fillet............	0.160 in. × 0.290 in.	=	0.0464 in.
Fillet............	0.231 in. × 0.368 in.	=	0.0850 in.
Fillet............	0.070 in. × 0.290 in.	=	0.0203 in.
Connecting tubes..	0.900 in. × 0.250 in.	=	0.2250 in.
Projected length =	2.141 in.		

Area of projected rod in direction of flow = 0.5249 sq in.
Area of projected rod = 0.5249/144 = 0.00365 sq ft
Area of 4.281-in. diam pipe = 0.100 sq ft
Area of projected rod/area of pipe = 0.00365/0.100 = 0.0365 = 3.65 per cent

Similar computations give a ratio of 1.64 per cent for the 12.098-in. pipe, a difference of 2.01 (3.65 — 1.64 = 2.01) per cent from the ratio for the 4.281-in. pipe. The coefficient obtained in these two pipes differed by 1.9 per cent at velocities of 8.9 and 10 fps. Fig. 18, the University of Pennsylvania correction curve, was determined by points obtained in this manner, and plotted with the percentage of change in coefficient as the ordinate, and the change in ratio of areas as the abscissa.

For the W.P.I. correction curve, Fig. 18, the cross-sectional area of the built-up rod, as well as the ratio of this area to the area of the pipe, was computed by the same procedure as shown in the sample computation for the 4.281-in. pipe. The per cent change in coefficient resulting from the change in area of the pipe caused by the built-up rod, was plotted, as above, against the change in the ratio of projected rod areas to pipe area.

It should be noted that the two correction curves shown in Fig. 18 do not give the same results, and the difference is probably due to errors which are present in each method. For the University of Pennsylvania curve, an error is introduced in the determination of the area of the orifices. That this error may be large is shown by the fact that in the sample computation, the area of the orifices is 28 per cent of the total projected area of the rod. However, an error of this size is not introduced by inaccurate measurement, but rather by an assumption that the entire area of the orifices is effective in reducing the area of the pipe. Fig. 6 shows the open construction of the tips and although some investigation has been made it is not definitely known what part of the orifices is effective. If the area of the orifices were neglected in the computation of the area of the projected rod, the University of Pennsylvania curve would be raised above the W.P.I. curve.

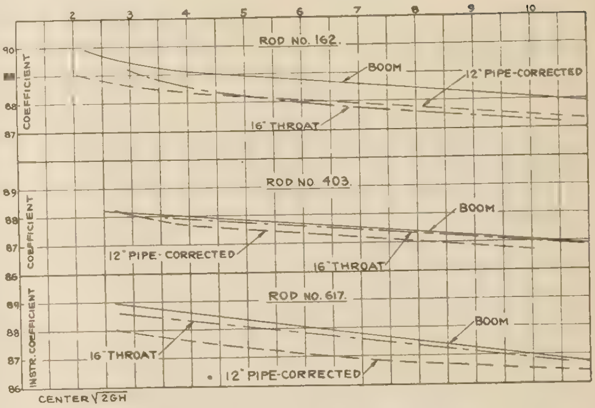

FIG. 25 COMBINED RATINGS OF THREE PITOT TUBES BY THREE METHODS, ALDEN HYDRAULIC LABORATORY

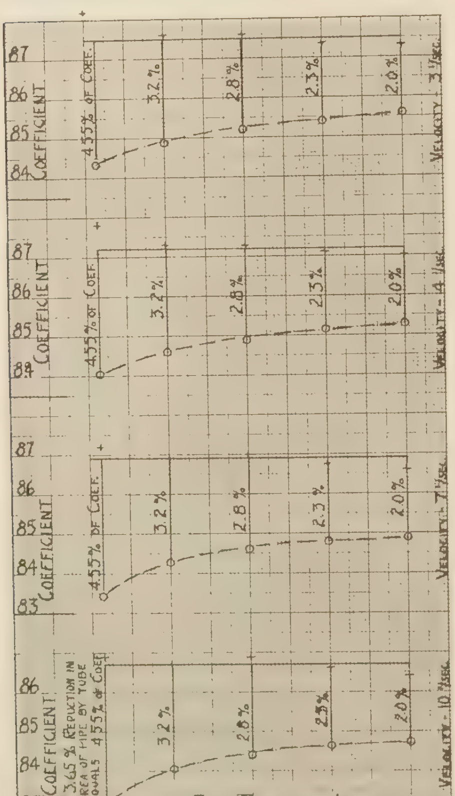

FIG. 24 METHOD OF CORRECTION FOR PROJECTED AREA OF PITOT TUBE

The error in W.P.I. curve is of a different nature because the area of the orifices is relatively small compared to the area of the projected rod, and is probably introduced by local disturbance on the orifices. Although the built-up sections were designed to produce a minimum amount of disturbance, it is possible that some disturbance was still introduced.

For lack of better information the mean of the University of Pennsylvania and the W.P.I. curves has been used in this paper.

Use of Correction Curve. The use of the correction curve is made clearer by a study of Fig. 19, the calibration of rod No. 617 in various-size pipes made at the University of Pennsylvania. In Fig. 24 the coefficient obtained for a given velocity is plotted against the pipe diameter. It will be noticed (Fig. 19) that for any velocity the coefficient decreases as the pipe diameter decreases. In other words, as the ratio of projected rod area to pipe area becomes greater the coefficient becomes smaller.

A series of ordinates has been added, Fig. 24, to show the corrected coefficient at any given velocity. These ordinates are obtained from Figs. 23 and 18 in the following manner:

From Fig. 23 we see that in a 12-in. pipe the ratio of the area of the projected rod to the area of the pipe is 1.64 per cent. Entering the mean curve on Fig. 18 with 1.64 per cent on the abscissa we find the corresponding change in coefficient is 2.0 per cent. The coefficient obtained in the 12-in. pipe should then be raised 2.0 per cent. The coefficient in the other sizes of pipe can be corrected by following the same method. The result will be that at a given velocity the corrected coefficient will be the same in any size of pipe. The corrected coefficients at each velocity can then be plotted to give a coefficient curve which will hold for any velocity.

In practice it might be more convenient to use the coefficient which applies to the pipe in which one is working. For reasons which will be apparent later it has, however, been desirable to determine the corrected coefficient in the 12-in. line.

Correction in 16-In. Throat. For these tests the orifices were located 4 in. in on the horizontal diameter and no correction for the area of the projected rod was necessary.

Correction for Other Types of Tube. So far as the author is aware this correction

for the projected area of the rod has never before received proper attention, and this may account for apparent inconsistencies in pitot-tube calibrations.

Where the pitot tube is supported on a streamlined rod passing entirely across the pipe so that a traverse involves no change in the projected area, the author believes some correction for the presence of the pitot tube must still be made if it is to be used in another size of pipe or is to be compared to still-water or large venturi-throat rating.

Application of Correction to 1934 Calibrations. The mean correction curve which has been adopted was used to correct the calibrations made in the 12-in. pipe at the Alden laboratory, and in the various sizes of pipe at the University of Pennsylvania. Figs. 14, 15 and 16 show the test points obtained in the Alden laboratory calibrations as well as the corrected 12-in. line coefficient. Fig. 25 is a summary of all the calibrations and shows the agreement obtained by calibration in still water, the 16-in. throat, and in the 12-in. line.

The calibrations made at the University of Pennsylvania with corrections by the three different methods are shown in Fig. 19.

3 Angularity and Eddying Flow

Angularity of flow in pipes has been much discussed. Theoretically, the simple pitot tube over-reads in angular flow, but this error is small as shown by the fact that the difference between the value of $V \cos a$, and $V\sqrt{(\cos a)}$ is but 0.2 per cent with $a = 5$ deg, and this paper will attempt to show that the mean angularity of turbulent flow in the normal pipe line may not be as great as 5 deg. It should be observed in passing that tests to determine the angularity characteristics of a pitot tube, i.e., rotating the tube about its axis, must be made under proper conditions. Tests made by rotating the long tip of a simple pitot tube at the center of a 12-in. pipe might throw the point of the tip a considerable distance from the center and into a lower velocity, thus requiring a greater angle to produce a given coefficient. When in turn the degree of angular flow in a pipe is inferred from a comparison of coefficients, it is evident that the inferred angularity may be much too large.

In order to study angular flow in pipes, the device shown in Fig. 26 was constructed with a cross-shaped vane free to move with the water in any direction up to about 30 deg from the pipe axis. The friction and inertia of this indicator was made as small as possible, its shaft being mounted in stainless-steel ball bearings. Its behavior was observed under normal flow conditions, and also with distorted flows as produced by bends or a nearby partly opened gate.

With normal flow, readings failed to show an average angularity as great as 5 deg. The indicator was in constant and rapid vibration through small angles with an occasional jump to 10 or 15 deg for an instant only as was shown by motion pictures. It has been pointed out by Moody[11] that angularities of short duration had little or no effect on the pitot tube.

Professor Allen[15] gives data for computing the angular flow as shown by the spread of salt solution. His tests, which were made in a 40-in. penstock, indicate a maximum angularity of 6 deg, which value is practically constant at 5 and 10 ft downstream from the injection tube.

The most conclusive evidence showing the small effect of angularity or eddying flow on the pitot tube is to be found in the close agreement of the three methods of calibration herewith presented.

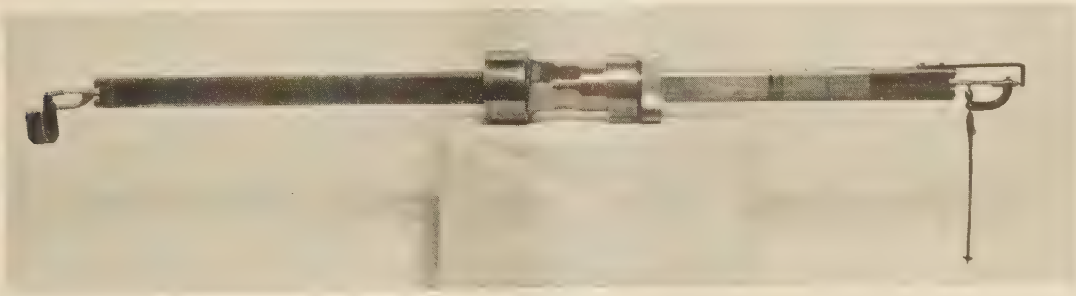

Fig. 26 Indicator for Studying Angular Flow in Pipes

The angularity characteristics of the author's pitot tube are shown in Fig. 27. It will be noted that when rotated through an angle of 5 deg, the tube over-reads the cosine value by 1 per cent. The fact that the same coefficient was obtained in still water, in the smooth flow of the venturi throat, in the turbulent flow of the Alden laboratory 12-in. line and in the turbulent flow of the University of Pennsylvania 12-in. line, indicates that turbulent or eddying flow such as encountered in normal pipe lines does not subject the author's pitot tube to appreciable errors.

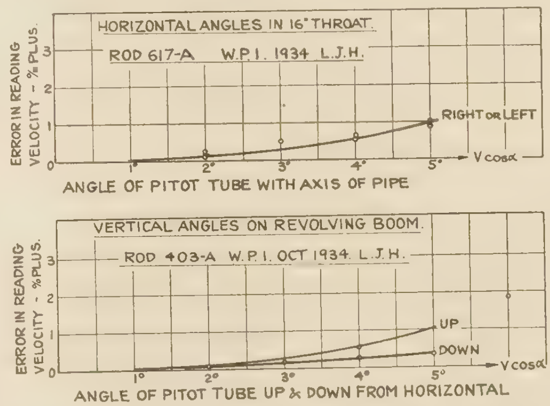

Fig. 27 Angularity Errors of Reversible Pitot Tube

In view of this evidence it seems that the existence of angles of 20 or 30 deg as claimed by some writers needs substantial proof.

The Pitot-Traverse Method

Broadly speaking, this method may include gagings made with the simple pitot tube and wall piezometers, but this paper is chiefly concerned with the combined type. With proper attention to details of operation, flow measurements by readings of the center velocity are made rapidly and accurately.

[15] "How Water Flows in a Pipe Line," by C. M. Allen, *Mechanical Engineering*, vol. 56, February, 1934, pp. 81–84.

(*a*) *Selection of the Gaging Point.* Although many important gagings have been made it is difficult to lay down a simple rule for guidance in selecting the gaging point. Actual conditions must govern and sometimes it is necessary to accept the best compromise location and make trial velocity traverses of the pipe to indicate the suitability of the gaging point. Here, as elsewhere, there is no substitute for experience.

In general, the longest possible straight length of pipe upstream should be selected, and not too close to a downstream bend or fitting. Sometimes ten diameters upstream, and two diameters downstream will give good results, depending on conditions of the pipe line and flow.

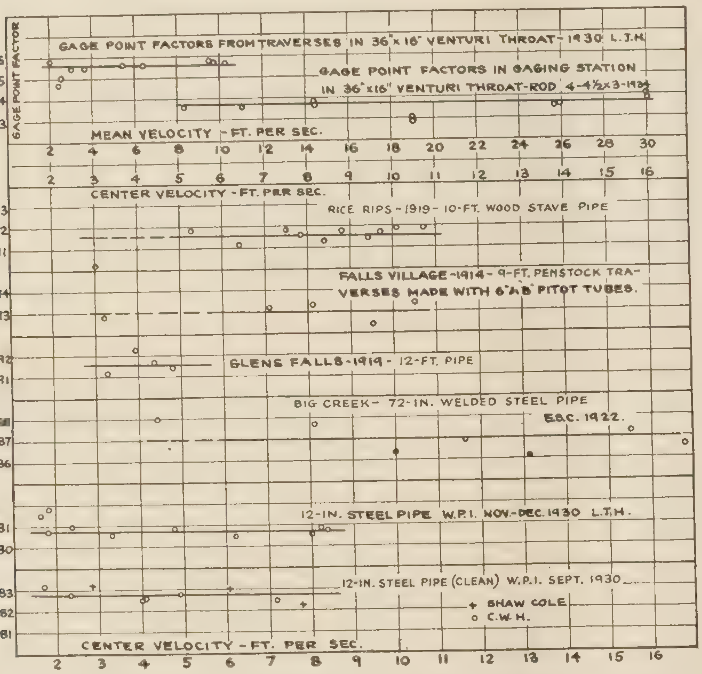

FIG. 28 COMPARISON OF PIPE FACTORS FOR LARGE PENSTOCKS AND SMALLER-DIAMETER PIPES

The pipe factor or ratio of mean to center velocity has great practical value, because, when once obtained for a given gaging point in a pipe line, it holds good for a considerable time or until the roughness or tuberculation of the pipe wall has increased depending on the nature of the pipe and its coating, and upon the chemical character of the water. Sometimes the pipe factor will hold good for years, as for example in the cast-iron mains of a water works carrying the relatively hard water of the Great Lakes cities.

Although the pipe factor may be shown to have a theoretical value of 0.83 upon the assumption that the velocity traverse is a semi-ellipse and cylinder, it seems useless to attempt to predict pipe factors in pipes of a given age or condition, for they vary from 0.70 to 0.90 according to local conditions and with some forms of vortex or spiral flow with depressed center velocity the pipe factor may even exceed unity.

If the pipe factor changes at all with ordinary velocities it does so very slowly. A comparison of determinations in water-power penstocks and in smaller pipes is shown in Fig. 28.

The pipe factor gives a ready means of making short tests, for example, in a penstock when interpolating between traverses made at several gate openings, for repeat measurements at gaging points of a city distribution system using the established pipe factor in connection with readings of center velocity, and also for the continuous recording of flow in a pipe line. With the pipe factor it is only necessary to make a continuous record of center velocities.

(*b*) *Traversing and Ring Integration.* Traversing and the ring method of computing mean velocity from the velocity traverse are now well described in many textbooks and need not be repeated in detail here. The errors of computation are small if as many as ten equal-area rings are used and if two diameters at right angles are traversed. It is well to have one diameter in the plane of an upstream bend in order to judge the lack of symmetry in velocity distribution.

With unsymmetrical curves it is not safe to assume the horizontal traverse to have the same ratio of mean velocity to center velocity as the vertical traverse, even though they have the same center velocity. With two traverses 90 deg apart there are, of course, four values of velocity for each ring.

In making velocity traverses it is important to secure readings close to the wall of the pipe and to do this the orifices are formed as shown in Fig. 6.

It is good practice to check back to the center velocity at frequent intervals during a traverse in order to avoid readings which are not comparable because of a change in the cycle of flow variation. When traversing with an unsteady flow, as in water mains or power penstocks under variable load, it is convenient to use a second pitot tube set near the point of maximum velocity. The function of this second tube, called a "pilot meter," is to indicate flow while the traverse is being made so that readings may be taken only at some predetermined rate.

Fluctuations in velocity may be very large in water-works service mains, but in water-power penstocks with wheels at a fixed gate opening the velocity variation through a full cycle is usually relatively small. It is sometimes important to dampen large variations in the manometer by throttling the connections. To do this without affecting the mean reading requires care; and the form of pinch cock used on the rubber hose should compress it symmetrically as to inlet and outlet to obtain the best results in producing a mechanical average.

The method of ring integration used at the Alden laboratory for the tests described in this paper was as follows:

Traverses were made on two diameters, 90 deg apart. Readings were taken at the respective centers of area of ten rings of equal area. The position of the center of area for each ring was determined as follows: Ring No. 1 = $R\sqrt{(0.05)}$, ring No. 2 = $R\sqrt{(0.15)}$, ring No. 3 = $R\sqrt{(0.25)}$, ring No. 4 = $R\sqrt{(0.35)}$, etc., where R = radius of pipe. The square roots of the pitot-tube deflections for each diameter were plotted to a large scale and smooth curves were drawn through the test points. From each curve twenty readings of the square roots were taken at the respective centers of area, making forty readings, and these were averaged to obtain the mean square root for the gaging section. This method is more accurate than that by the use of the mid-point of equal areas or by the average of the boundary readings of the rings of equal areas.

With mean velocity thus obtained the pipe factor is computed, which in a case of straight pipe lines is a criterion of pipe-wall roughness; and in any pipe line reveals the suitability of flow conditions at the gaging point.

Repeat traverses at the same location have frequently been found to check the pipe factor within 0.2 per cent and this is ex-

cellent assurance of the accuracy of the pitot-traverse method. Further assurance is to be found in the agreement between the Alden laboratory calibration made by pipe factors, and the University of Pennsylvania calibration made by constant traversing.

(c) *Reading of Center Deflections.* In obtaining the center velocity head or deflection which by the use of the pipe factor may be converted to mean velocity, it is important to have the manometer and all connections from the orifices to the manometer leak-tight and entirely free from air. The glass U-tube or manometer should be clean so that the measuring liquid has a well-shaped meniscus and the specific gravity of the liquid should be determined in the U-tube itself, at the temperature of use. Readings of the manometer deflection should be made at frequent intervals throughout a full cycle of flow. These precautions, of course, apply to traversing as well.

In reading manometer deflections with eddying flow in normal pipe lines there are pulsations in the U-tube which take place in cycles. If we record the readings through a full cycle we have the mean of the squares of the varying velocities and it has been claimed that this results in over-reading, but as the error is but 0.15 per cent with 5 per cent change in velocity[16] we may disregard it where fairly uniform flow is found.

A motion-picture record of pitot-tube deflections throughout typical velocity cycles was made both for 12-in. and 40-in. pipe lines with normal flow conditions under the uniform head available at the Alden Hydraulic Laboratory. This record showed two things, first, that the velocity changes are very small and, second, that these changes follow in well-marked cycles.

In these tests three pitot tubes were set at three points at the same section in a 40-in. pipe and at two points in a 12-in. pipe, each having exactly the same length of hose connections. No throttling of the lines was employed, yet the U-tube readings changed very slowly.

Variations caused by load changes may or may not follow a cycle but in important tests the load is always made as steady as possible.

In small pipes such as are found in city water works the pipe is tapped under pressure on the vertical diameter in the usual way; the pitot tube is attached to the 1-in. corporation cock and its manometer is connected. The air is blown off from the U-tube and connections. The pipe is traversed usually with but five equal-area rings and the pipe factor is computed rapidly with the aid of a prepared form for the field notes. Where it is only necessary to know relative flows or changes, a single traverse of five rings is quite sufficient. The pipe diameter is determined by means of a special caliper.

In large pipes it may be necessary to traverse an alternative location in order to select the best point. Two diameters should be traversed, and the use of 15 rings is recommended. The pilot meter is usually of great assistance in securing a good traverse.

(d) *Vibration of the Pitot Tube.* With large-diameter pipes and moderate velocities, or with moderate-diameter pipes and high velocities, attention should be given to possible vibrations of the pitot tube. Slight vibrations do not seem to affect the readings of velocity head but large vibrations may increase them. It is well to check readings near the far side of the pipe by inserting a short pitot from that side so that its tips may stand close to the end of the vibrating rod. Oval sections with 2-in. major axis and 1-in. minor axis with tips as shown in Fig. 6 have been used successfully in pipes 12 ft in diameter without extra support.

The Heavy-Duty Rod

The pitot tube shown in Fig. 29 is a heavy-duty rod which has been used on ships with success. Its strength and rigidity have been demonstrated in practice where with 4 ft of unsupported projection, velocities of 50 fps have failed to disturb it. Because of its great strength, this rod, without the aid of extra supports

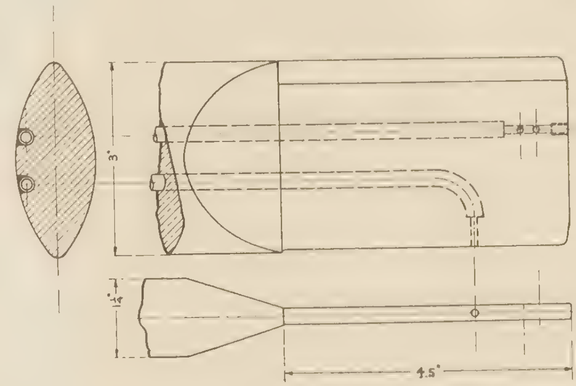

Fig. 29 Cosine Type of Heavy-Duty Pitot Tube for Large-Diameter Pipes and High Velocities

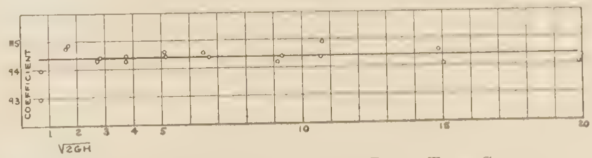

Fig. 30 Still-Water Rating of the Pitot Tube Shown in Fig. 29

within the pipe, is specially adapted for high velocities and large pipe diameters.

Because the pitot tube shown in Fig. 6 over-reads the cosine value by 1 per cent when rotated through an angle of 5 deg, considerable experimental work has been done in the last 2 years at the Alden Hydraulic Laboratory to develop a tube which will read the cosine to 5 or 6 deg and at the same time have a fixed coefficient over a great range of velocities. Figs. 30 and 31 indicate the degree of success which has been attained by the use of the heavy-duty rod. Many calibrations of this type with its practically uniform coefficient were made at the Worcester revolving-

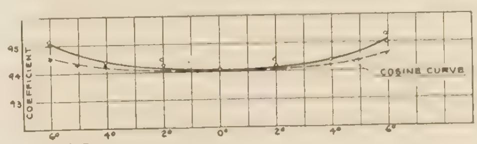

Fig. 31 Cosine Curve for Heavy-Duty Pitot Tube

boom rating station to a maximum speed of 20 fps and this speed was later extended to 50 fps when the tube was installed on a ship and rated over a measured mile.

Summary

(a) The pitot tube, both simple and combined, is well adapted for the measurement of flow in pipes under pressure.

(b) The coefficient of the simple pitot tube is practically unity for normal flow.

(c) The coefficient of the combined pitot tube (D'Arcy type) is also practically unity for normal flow.

(d) The coefficient of the reversible type (Fig. 6) is as shown by the calibration curves, Figs. 19 and 25, and ranges from 0.870 at 10 fps to 0.885 at 3 fps and is practically unaffected by angularity to 3 deg.

(e) The average angularity of flow in normal pipe lines is com-

[16] "Applied Hydro- and Aeromechanics," based on lectures by L. Prandtl and O. G. Tietjens. Translated by J. P. Den Hartog, McGraw-Hill Book Company, Inc., New York, 1934, p. 47.

monly less than 5 deg, although sudden angular fluctuations are occasionally as high as 15 deg.

(*f*) The pitot tube, Fig. 6, reads close to the cosine of angular flows to 3 deg. The heavy-duty type of pitot tube, Fig. 29, reads close to the cosine of angular flows to 6 deg, Fig. 31, and has a practically uniform coefficient from 3 to 50 fps.

(*g*) Pitometer ratings made in still and moving water agree within 0.5 per cent of their mean values, when the proper correction is made for the area of the protruding tube under usual conditions of angularity and eddying flow when rated in a pipe.

(*h*) This method in common with all other methods of water measurement should be used by trained and experienced men.

Research Investigation of Current-Meter Behavior in Flowing Water

By S. LOGAN KERR,[1] PHILADELPHIA, PA.

This paper investigates the inconsistencies of flow measurements in closed flumes by means of current meters. It describes (*a*) the construction of a flume in which two meters were installed side by side and tested under varying conditions of flow, (*b*) the velocity distribution in the flume, and (*c*) the establishment of the true velocity plane across the face of the meters by means of a pitot tube. The pitot-tube coefficient was established for each flow condition, thus providing an accurate means of establishing the actual velocity existing in front of the current meter.

IN ORDER to investigate certain inconsistencies in the measurement of flow in large hydroelectric plants by means of current meters, a research program was undertaken by the I. P. Morris Division of Baldwin-Southwark Corporation in their hydraulic laboratory at Eddystone, Pa. The original investigation included the study of available literature, principally a paper by Messrs. Nagler and Yarnall at the University of Iowa, where current meters were placed in flowing water and oscillated back and forth, and also set at various angles with the flow, in an attempt to establish their behavior under turbulent conditions. It is felt, however, that this particular study did not actually simulate conditions under which current meters are frequently used in connection with measurements of the efficiencies of hydroelectric units.

The resolution of turbulence into the two elements, angularity and variations in forward flow, seems to omit the very important factor of the variation of velocity across the face of the meter and the rapid fluctuation of velocity distribution in turbulent water.

To investigate this phenomenon properly, it was decided to construct a flume in which two current meters could be installed side by side and tested under varying conditions of flowing water. Means were arranged for visual observation of the degree of turbulence present at the metering section. The original program was expanded considerably to include the investigation of velocity distribution in the flume, and particularly the establishment of the true velocity plane across the face of the meter by means of a pitot tube. All of the discharge measurements were checked by a calibrated weir, which was normally employed for testing model turbine units and other apparatus. The weir was calibrated by measuring the rate of rise in level in the sump tank while maintaining a constant flow over the weir.

Fig. 1 shows the logarithmic calibration curve of the weir and the comparison of the calibration with the Rehbock formula. For the lower flows the weir shows slightly higher discharge than the formula, but for flows from 7 cfs to 9$^1/_2$ cfs (the range during the tests of the current meters) the weir checks the Rehbock formula very closely.

The pitot-tube coefficient was established for each flow condition, and hence provides accurate means of establishing the actual velocity existing in front of the current meter.

Description of Apparatus

The test flume as shown in Fig. 2 was 11 ft 8$^1/_2$ in. overall, and had a bell mouth at the intake with two sets of racks to straighten out the flow. The first set consisted of 25 boards, $^7/_8$ in. thick on 1$^3/_8$ in. centers, located in a vertical plane. The second set consisted of 24 steel plates $^1/_{16}$ in. thick on $^9/_{16}$ in. centers, and were placed 6 in. downstream from the vertical racks and extended a total of 10 in. downstream. Two removable screens with fine mesh were installed about 24 in. further downstream to remove from the flow any remaining disturbances. These screens were cleaned periodically to make certain that no foreign matter was clogging them and changing the flow distribution in the channel. At a point 2 ft 7$^1/_4$ in. downstream from the lower end of the horizontal racks was an aperture, in which removable baffle plates could be installed. The various baffle plates used in the tests are shown in Fig. 2 as arrangements *A*, *B*, *C*, and *D*. These baffles consisted of steel plates arranged with dowels to center them, thus placing them in exactly the same position for each test.

The current meters were installed 4 ft 10 in. downstream from the baffles and a safety-glass window was located in the top of the flume immediately above the propellers of the meters.

For the first series of tests a system of yarn streamers was installed about 12 in. upstream from the meters and located in three horizontal planes, at $^1/_4$, $^1/_2$, and $^3/_4$ of the height of the channel. This placed the middle group of yarns on the horizontal centerline of the meters and the upper and lower groups beyond the periphery of the meters. On the first traverses of the pitot tube, it was found that these yarn streamers would follow closely the true stream lines and conform to the contour of the tube. When the accurate pitot-tube determinations were in progress, the yarn streamers and wire supports were removed to avoid any possible interference with the flow.

Illumination was provided on both sides of the flume to permit a visible study of the flow conditions in the metering section.

Each pair of meters employed consisted of one right-hand and one left-hand meter of the type manufactured by Dr. Ott in Germany and loaned for this investigation by the Safe Harbor Water Power Corporation. Two of the meters were the so-called type 1 (spoke type) and the other two were designated as type 2 (screw type). The meter bodies, as used in service conditions, were also employed, supported by a bar made of hardwood of the same shape as the supporting bars used in the field. The testing flume discharged into the weir channel approximately 2 ft downstream from the centerline of the meters. The flow then passed

[1] Research Engineer, I. P. Morris Division, Baldwin-Southwark Corp. Mem. A.S.M.E. Mr. Kerr was graduated from the University of Pennsylvania in 1921 with the degree of Bachelor of Science and in 1924 with degree of Mechanical Engineer. Upon graduation he entered the I. P. Morris Division of the William Cramp & Sons Ship & Engine Building Co. as research assistant. In 1924 he was appointed assistant hydraulic engineer and in 1927 assistant chief engineer. Since 1929 he has been research engineer in charge of experimental and field tests and development work on hydraulic turbines, governors, valves, and other equipment.

Contributed by the Hydraulics Division and presented at the Annual Meeting, New York, N. Y., December 4 to 8, 1933, of The American Society of Mechanical Engineers.

Discussion of this paper should be addressed to the Secretary, A.S.M.E., 29 West 39th Street, New York, N. Y., and will be accepted until October 10, 1935, for publication at a later date.

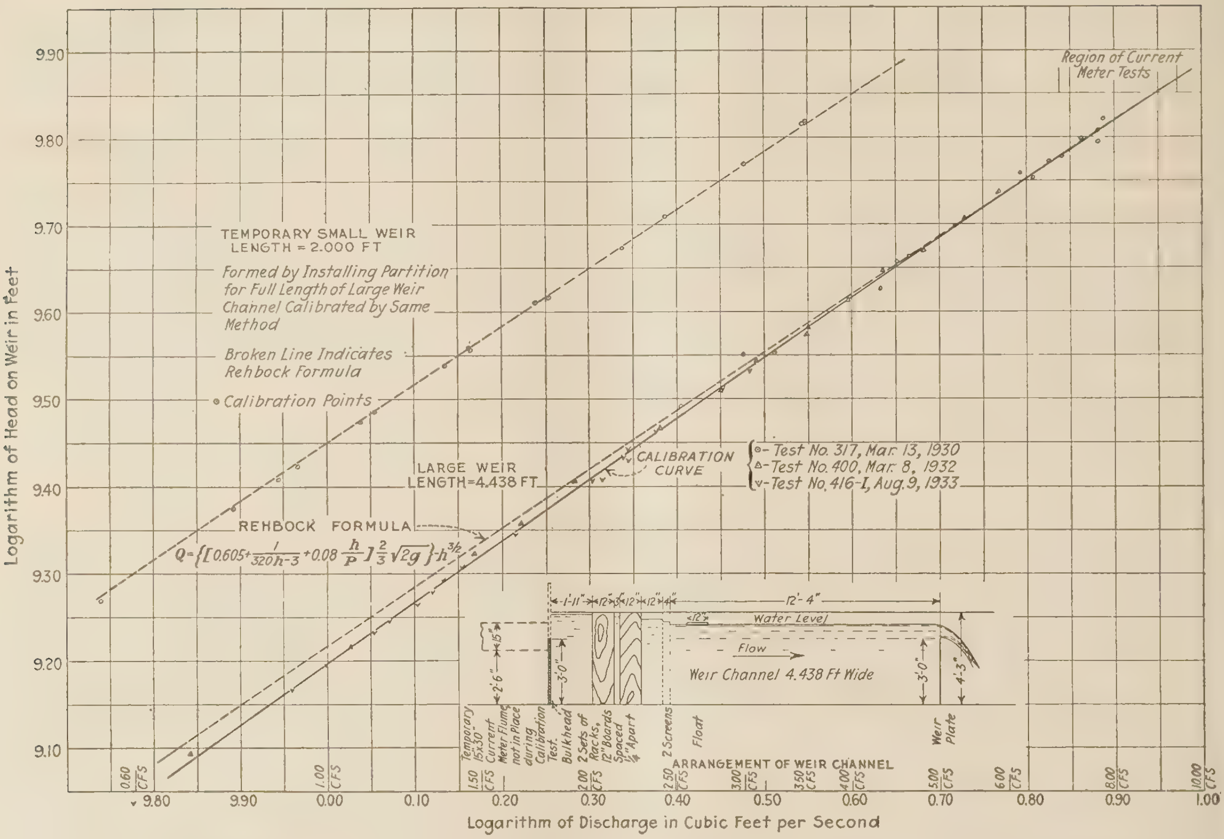

Fig. 1 Logarithmic Calibration Curve of the Calibrated Weir and a Comparison of the Calibration With Rehbock Formula

through a series of racks and screens and over the calibrated weir.

The water was discharged into the sump and pumped back into the head tank, passing through a controlled orifice into the pool in which the current-meter flume was installed. The recirculation of flow was accomplished by a high-speed propeller-type pump and arrangements were made to maintain the speed of this pump constant by using a separate rotary-converter unit in the plant sub-station, thus giving freedom from voltage fluctuations.

Fig. 3 is a view looking downstream through the flume before the installation of the racks and screens, showing the location of the two meters.

Meter Calibrations

Each of the meters employed had been carefully calibrated in the tangent still-water rating flume at the Bureau of Standards in Washington. These rating curves were used to determine the velocity of flow as registered by the meter. Additional calibrations were made in Washington to give the degree of registration of the forward velocity of the meter when the meter itself was placed at different angles with the direction of movement of the rating car. These were the so-called "angular still-water ratings" of the meters, in contrast to the normal straight-line ratings. The angular ratings were determined for several forward velocities and a general average calibration curve was prepared which was used to compute the so-called "angular correction" for field testing, using the two-type meter method. The meters gave differing results, depending upon the quadrant in which the angle was measured, that is, whether the flow approached from the top or bottom or whether it approached from the right or left.

As these variations usually were less than 1 per cent, the average correction curve should reduce the error to within the accuracy of the flow measurements. These details have been dealt with at length by J. M. Mousson in his discussion[2] of Hunter Rouse's 1932 paper.[3] The difference in registration, or angular calibration, is sometimes considered as a means of establishing the correction for angular flow in the metering section.

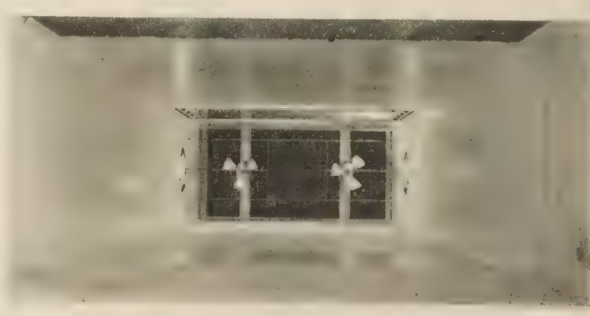

Fig. 3 Downstream View Through the Flume Before Installation of Racks and Screens Showing Location of the Two Meters

[2] Discussion of "Research Institute for Hydraulic Engineering and Water Power," by Hunter Rouse, Trans. A.S.M.E., 1933, vol. 55, paper HYD-55-3, p. 33.

[3] "Research Institute for Hydraulic Engineering and Water Power," by Hunter Rouse, Trans. A.S.M.E., 1932, vol. 54, paper HYD-54-3, p. 27.

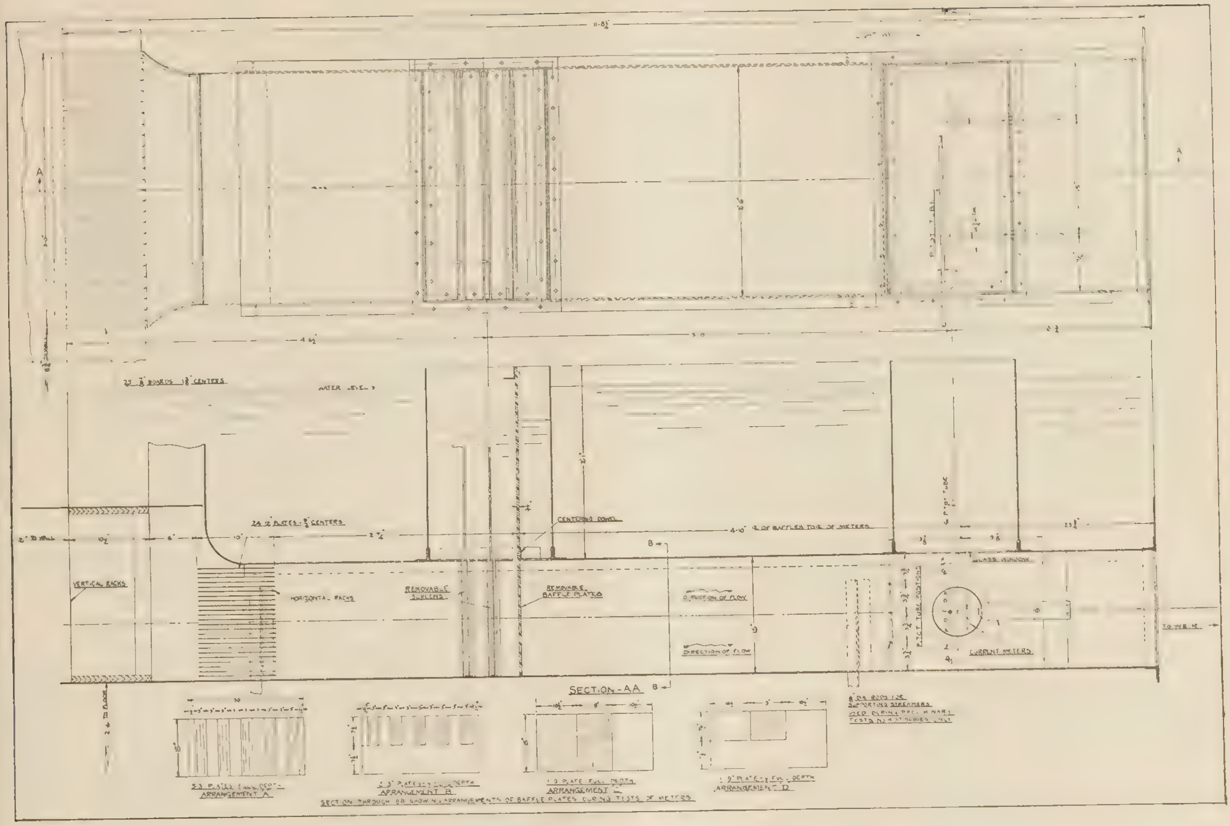

FIG. 2 ARRANGEMENT OF THE CURRENT-METER TESTING FLUME

DESCRIPTION OF TESTS

The first series of tests consisted in observing the behavior of the current meter with various types of flow in the test flume. The flow distribution was not measured but each arrangement of baffle, namely, *A*, *B*, *C*, and *D*, was employed for several different velocities. Tests were also made with smooth flow with no baffles in place. The meters were interchanged, that is, the right-hand meter and left-hand meter were reversed in their positions and both types of meters were tested in this manner. It was found that the differences in registration between the two types of meters, referred to their angular still-water calibrations, indicated very pronounced angularity of flow which did not appear to be present from visual observation. These differences in registration are given in Table 1.

As a result of this preliminary series of tests it was apparent that further research was necessary to establish the flow distribution in the flume and particularly to determine the average velocity immediately in front of the meter so that this value could be checked against the current-meter registration and the degree of over or under registration thus determined.

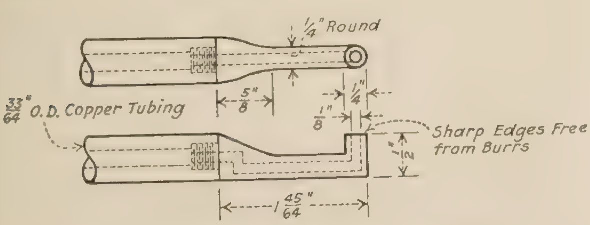

FIG. 4 DETAIL OF THE PITOT-TUBE CONSTRUCTION

TABLE 1 REGISTRATION DIFFERENCES BETWEEN THE TWO TYPES OF METERS

	Type of flow	Diff. type 1 meter minus type 2 meter over type 1, %	Percentage correction type 1 meter (added), %	Apparent angularity, degrees
1	Smooth flow preliminary tests	3.14	0.99	11.7
2	Smooth flow final tests......	3.66	1.13	12.5
3	Five 3-in. baffles half depth..	3.42	1.08	11.8
4	One 9-in. baffle half depth...	5.18	1.59	14.8
5	Five 3-in. baffles full depth..	8.56	2.60	18.8
6	One 9-in. baffle full depth...	17.02	5.07	25.3

PITOT-TUBE TRAVERSE

A pitot tube conforming to the type commonly used in penstock work was installed in the section immediately upstream from the meters. This pitot tube had a single dynamic-pressure hole. The static pressure was taken at four points, each of which was connected to an individual gage glass. Three of these static-pressure holes were in the bottom of the flume, one located on the centerline of the flume and the other two on the centerlines of the current meters. The fourth static-pressure hole was located on the left-hand wall of the flume looking downstream to check any possible difference due to side velocities or eddy currents.

The tests under this series were really in two parts. The first series was made to establish the average velocity of flow impinging on the current meters while the second group was made to establish the average pitot-tube coefficient under actual flow conditions existing.

DESCRIPTION OF PITOT-TUBE APPARATUS AND TEST METHODS

Fig. 4 shows the pitot-tube construction. Fig. 5 is an elevation of the flume with the location of each individual pitot-tube traverse point designated and with the positions of the me-

ters shown. Fig. 6 illustrates the method of determining the average velocity in front of the meter by plotting five horizontal traverse curves, each having five individual pitot-tube determinations of velocity. With this grid of points established, the area in front of the current meter was divided into five annular rings of equal area in a manner similar to the method employed in measuring the velocity in closed conduits. The velocity curves were then plotted on the eight radial planes and the velocities determined at the center of each annular ring. This established eight velocity points for each of the five annular rings, or a total of 40 velocity points, the average of which was used as the mean velocity in front of the meter.

Additional tests were made for certain of the runs to establish the velocities adjacent to the walls in order to avoid any uncertainty in regard to the velocity distribution existing between the last pitot-tube point and the wall of the flume. These studies were made very carefully at points taken $^1/_8$ in. from the wall and four other points at intervals of $^1/_4$ in. apart until the zone about 1 in. from the wall was thoroughly explored.

During the first runs several very interesting facts were brought to light. It was found that pitot-tube traverses could be checked very well even in turbulent flows, providing there had been no interruption in the flow. The usual shutdown at noon-time was eliminated, tests being carried straight through without interruption until the entire set of traverse points had been measured, even though it was necessary at times to continue testing until evening.

It appeared that the general condition of flow could be duplicated, but the exact distribution varied enough to make it necessary to avoid interruptions when determining the pitot-tube coefficients.

Pitot-Tube Traverse

In order to give a clear picture of the velocity distribution under the three types of flow, isometric drawings have been prepared showing the velocity points. Fig. 7 shows the conditions of test 410–2 for smooth flow at the mean velocity of 2.6 fps. Fig. 8 shows a similar arrangement for the five 3-in. baffles at one-half depth, corresponding to baffle arrangement B, Fig. 2.

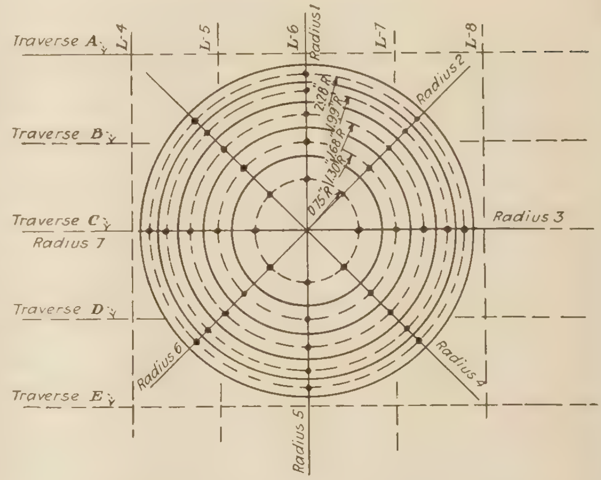

Fig. 6 Traverses Used and Location of Pitot Tube in Equal-Area Rings at Which Velocities Were Determined

(Diagram of $4^3/_4$ in. diam. circular area in front of meter. Heavy dots show points in five rings of equal area at which velocities by pitot tube were determined. Average of these forty velocities was used as mean velocity in front of meter.)

Fig. 9 shows the arrangement for test 410–3, which had five 3-in. baffles placed full depth in the flume, as indicated in baffle arrangement A, Fig. 2. It will be noted from these drawings that the velocity plane in front of the meter was a very irregular warped surface, which results in an unequal distribution of velocity across the plane of the current meter. This is particularly true when turbulence is present or when distortion of flow is encountered with the baffles at one-half depth, as shown in Fig. 8.

The wall velocities were investigated for the last 1 in. from the wall by pitot-tube readings taken very close together, the closest reading being taken $^1/_8$ in. from the wall. Fig. 10 shows these curves plotted to a large scale for the average flume velocity of 2.2 fps with the five 3-in. baffles at one-half depth (baffle arrangement B, Fig. 2). It will be noted that the velocities adjacent to the right-hand and left-hand walls of the flume were very similar in shape. These curves also agree very closely with the formula developed for wall velocities by von Kármán and Prandtl:

$$V = (\text{a constant}) \times X^{1/7} \quad [1]$$

where X = the distance from the wall.

This agreement is indicated by the curves in dashed lines shown in Fig. 10, derived from formula [1].

In some of the tests at the higher flows, the velocities near the left-hand wall were difficult to determine because of the tendency of the pitot tube to oscillate. In such cases, the wall velocities for the last $^3/_4$ in. from the wall were determined by the von Kármán and Prandtl formula.

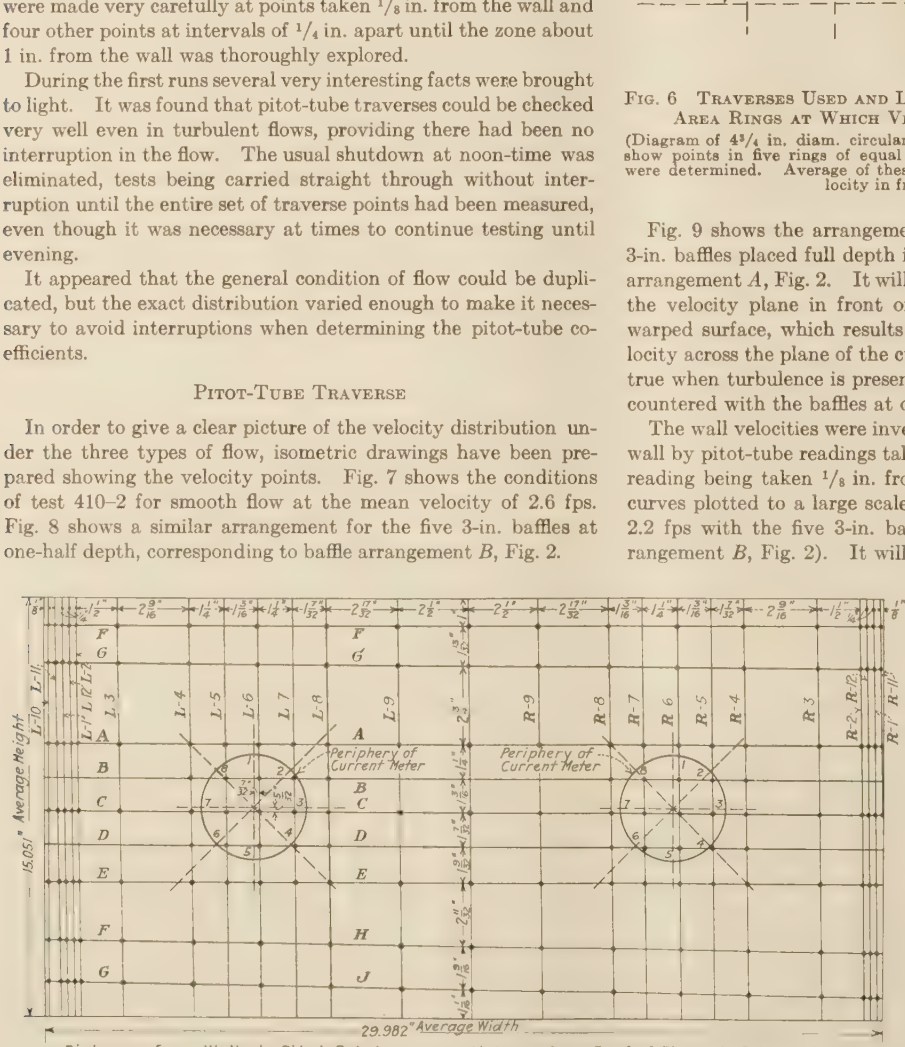

Distance from Walls to Pitot Points

On Section	F	G	A	B	C	D	E	H	J
LW to L-1	5/8"	11/16"	21/32"	11/16"	23/32"	3/4"	3/4"	13/16"	7/8"
RW to R-1	3/8"	11/32"	5/16"	5/16"	7/32"	1/4"	1/4"	3/16"	3/16"
RW to ℄	14 27/32"	14 25/32"	14 25/32"	14 3/4"	14 23/32"	14 23/32"	14 23/32"	14 21/32"	14 19/32"

Distance from Roof of Flume to Pitot Points

From Section	F	G	A	B	C	D	E	H	J	Floor
At L-1	1 1/32"	2 3/8"	5 1/4"	6 7/16"	7 21/32"	8 27/32"	10 13/16"	12 11/32"	13 27/32"	1 5/32"
At ℄	1"	2 13/32"	5 5/32"	6 13/32"	7 19/32"	8 13/16"	10 3/32"	12 7/16"	14"	1"
At R-1	1"	2 15/32"	5 1/4"	6 15/32"	7 11/16"	8 15/16"	10 5/32"	12 9/16"	14 3/32"	1"

Fig. 5 Section of the Flume Looking Downstream Showing Cross-Sectional Dimensions and Location of Pitot-Tube Observation Points

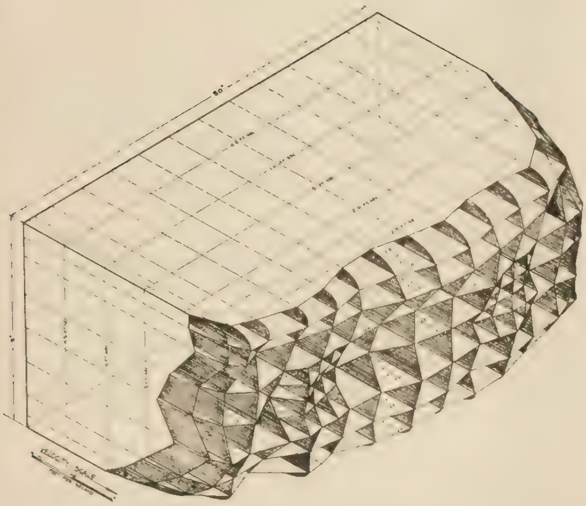

Fig. 7 Velocity Distribution in the Flume With No Baffles for Smooth Flow at 2.6 Fps—Conditions for Test 410–2

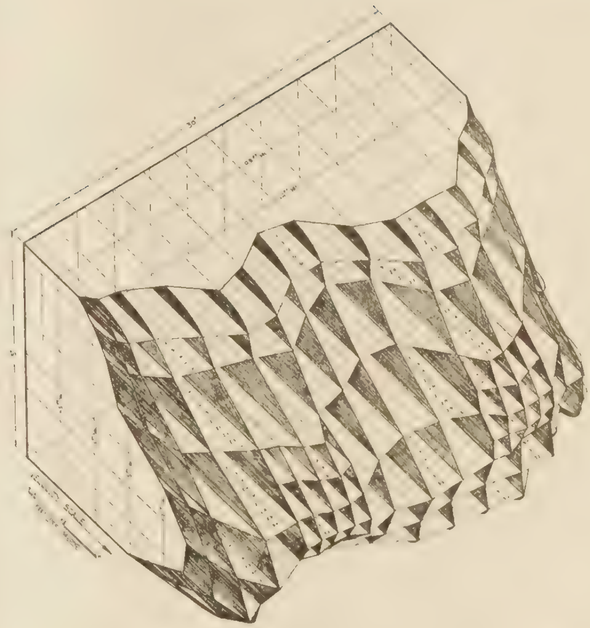

Fig. 8 Velocity Distribution With Baffles at One-Half Depth and a Mean Velocity of 2.6 Fps

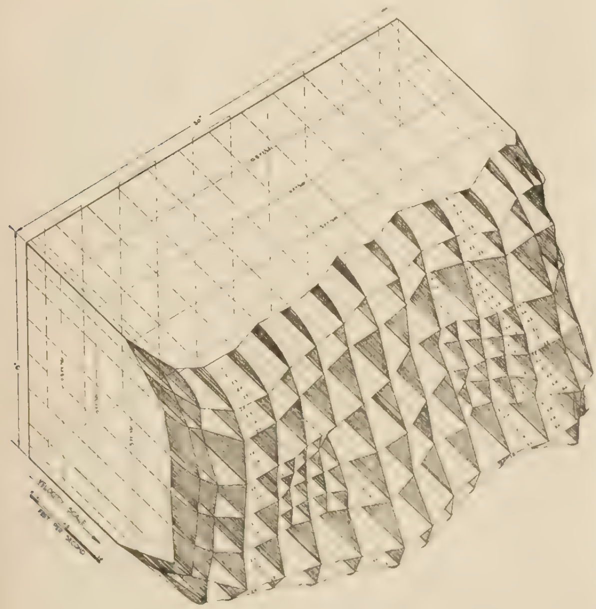

Fig. 9 Velocity Distribution With Five 3-In. Baffles at Full Depth and Mean Velocity of 2.6 Fps—Conditions for Test 410–3

Results

Table 2 gives a comparison of two independent calculations of the pitot-tube coefficient in tests 410–2 to 410–7, inclusive, for the various flow conditions outlined. The formula used was $V = C\sqrt{(2gh)}$, the values of the coefficient C being given in Table 2.

In Table 2 it will be noted that the pitot-tube coefficient varies with different flow conditions and with velocities. In order to relate this to previous experience, data as shown in Fig. 11 is included in this paper. Early tests in a closed pipe, made by F. H. Rogers at the University of Pennsylvania in 1909, show a marked variation of pitot-tube coefficient increasing from 0.969 at a velocity of 2 fps up to 1.00 at a velocity of 15 fps. In the range in which we are most interested, namely, 2 to 6 fps, an average coefficient of 0.976 appears to be reasonable for smooth flow free

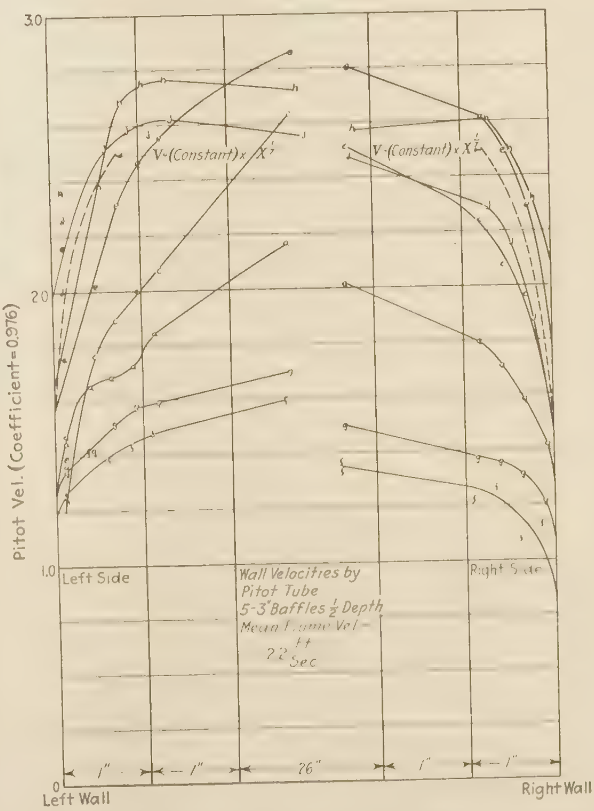

Fig. 10 Wall Velocities When the Average Flume Velocity Is 2.2 Fps With Five 3-In. Baffles Set at One-Half Depth

TABLE 2 COMPARISON OF PITOT-TUBE COEFFICIENTS FOR VARIOUS FLOW CONDITIONS

Test no.	Laboratory calculations	Independent calculations	Flow conditions
410–2	0.969	0.965	Smooth flow, mean flume velocity 2.6 fps. For sides, formula [1] was used since it corresponded closely to exp. results on 410–7. For bottom and top, avg of 410–7, right side, was used
410–3	0.953	0.948	Five 3-in. baffles at full depth. Mean flume velocity 2.6 fps
410–4	0.939	0.939	Five 3-in. baffles at full depth. Mean flume velocity 2.2 fps
410–5	0.957	0.962	Five 3-in. baffles at half depth. Mean flume velocity 2.6 fps
410–6	0.934	0.938	Five 3-in. baffles at half depth. Mean flume velocity 2.2 fps. Curves at side observed. Top and bottom taken as avg of right side
410–7	0.976	0.975	Smooth flow, mean flume vel. 3 fps. Curves at sides observed. Top and bottom taken as avg of right side

from turbulence. This coefficient also corresponds to the value designated in the Machinery Builders Test Code for pitot tubes in closed conduits. Additional values were secured from tests made for the S. Morgan Smith Company at Worcester Polytechnic Institute by Prof. C. M. Allen, in which the coefficient varied from 0.96 to 0.98, but averaged very close to 0.976.

When plotting the results of the tests for the 410 series, it was found that the smooth-flow coefficients averaged very closely to the mean curve of the University of Pennsylvania tests, shown as the I. P. Morris curve in Fig. 11. When turbulence was introduced, however, it was found that the difference between the determinations was much greater and that no single curve could be drawn through the points. By reference to the previous tests, a band of coefficients was established by drawing lines through the maximum and minimum values, similar in shape to the mean curve for smooth flow, and denoting the zone between these two curves as the probable range of coefficients under turbulent flow.

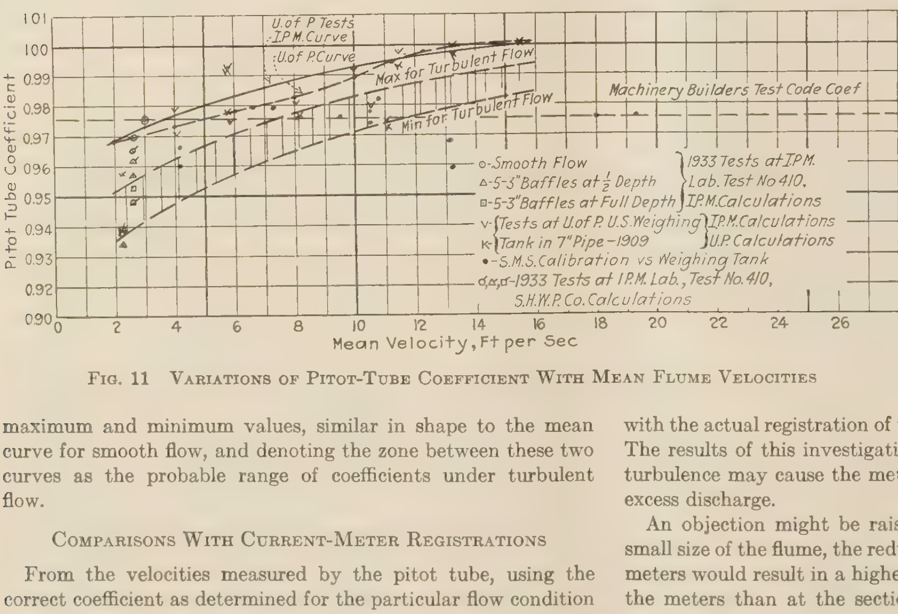

FIG. 11 VARIATIONS OF PITOT-TUBE COEFFICIENT WITH MEAN FLUME VELOCITIES

COMPARISONS WITH CURRENT-METER REGISTRATIONS

From the velocities measured by the pitot tube, using the correct coefficient as determined for the particular flow condition and velocity, it was possible to determine the mean velocity in front of the meter and compare this with the registration of the meter obtained periodically during the pitot-tube traverse. A reading of the meter was taken after each individual traverse, after the pitot tube had been withdrawn from the flume. Eight or nine meter readings were taken for each complete traverse, these meter readings checking within a small fraction of 1 per cent.

Table 3 gives the results of this determination for both right-hand and left-hand meters. The type 1 meter alone was used for tests 409 and 410, but three runs were made with type 2 meter, which is included for reference. The data in this table have been plotted in Fig. 12.

The ratio of velocity by pitot tube to velocity by meter, taken from the last column of Table 3, are plotted as ordinates, while the velocities of the current meter established from the still-water calibrations made at the Bureau of Standards in Washington are plotted as abscissas. This curve, therefore, shows the meter coefficient for different velocities and for both smooth and turbulent flows.

It will be noted that a band about 1 per cent wide, slightly on the side toward over-registration, results when smooth flow exists in the channel. When turbulent flow exists, the meters have a definite tendency to over-register and also the band of points is nearly twice as wide as that for smooth flow. It is interesting to note that in no case with turbulent flow did the meter under-register, as compared with the absolute-velocity determination by pitot tube.

CONCLUSIONS

From the study of these tests certain conclusions can be drawn which should be carefully considered in making determinations of discharge under field conditions. The so-called ideal conditions for current-meter measurement could be outlined somewhat as follows:

1 The measuring section should be rectangular in form and a sufficient distance downstream from any change in direction or change in area to insure smooth flow lines, with a velocity in excess of 1 fps and not over 8 fps.

2 The section should be free from turbulence caused by racks, supports, piers, or changes in section which would cause oblique flow or turbulence.

Where such conditions exist, it is reasonable to expect that the discharge determination would be accurate to within 1 per cent of the true discharge, using the still-water rating of the current meter as a basis.

With the type 1 meter in turbulent-flowing water, similar to that which existed in the test flume, there seems to be a distinct tendency toward over-registration, as compared with either the still-water rating or with the actual registration of the meter in smooth-flowing water. The results of this investigation, shown in Fig. 12, indicate that turbulence may cause the meters to register from 2 to 5 per cent excess discharge.

An objection might be raised that, because of the relatively small size of the flume, the reduction in area caused by the current meters would result in a higher velocity at the section containing the meters than at the section of the pitot-tube traverses. A correction was made, computed from the area of the current-meter vanes and hubs, by adding 0.66 per cent to the velocities determined by the pitot tubes. Assuming, however, that this correction is in error, and that for smooth flow the coefficient of the meter should be unity, it is evident that for turbulent flow the meter would still over-register by approximately $2^1/_2$ per cent. This method of comparison is equivalent to using a rating of the current meters derived from their actual behavior in place in the flume under smooth-flow conditions, instead of their still-water ratings. That is, if the smooth-flow ratings, based on actual measurements of the discharge by calibrated weir, are applied to

TABLE 3 COMPARISONS BETWEEN CURRENT-METER AND PITOT-TUBE REGISTRATIONS, TESTS 409 AND 410

				Left—Meter No. 5764-1-*L*				Right—Meter No. 5759-1-*R*			
Run No.	Mean flume vel.	Flow condition	Pitot coeff. from test 410	Avg pitot vel. observed	Avg pitot vel. + 0.66%	Avg meter vel.	Ratio pitot vel. to meter vel.	Avg pitot vel. observed	Avg pitot vel. + 0.66%	Avg meter vel.	Ratio pitot vel. to meter vel.
409–1	3.080	Smooth	0.976	3.151	3.172	3.182	0.9969	2.962	2.982	3.042	0.9803
–2	2.590	Smooth	0.969	2.694	2.712	2.718	0.9978	2.498	2.514	2.557	0.9832
–3	2.578	5 3-in. baffles at full depth	0.953	2.782	2.800	2.817	0.9940	2.367	2.886	2.882	1.0014
–4	2.200	5 3-in. baffles at full depth	0.939	2.027	2.040	2.140	0.9534	2.438	2.454	2.530	0.9699
–5	2.600	5 3-in. baffles at 1/2 depth	0.957	3.084	3.104	3.173	0.9783	3.090	3.110	3.178	0.9786
–6	2.200	5 3-in. baffles at 1/2 depth	0.934	2.493	2.509	2.571	0.9759	2.467	2.483	2.540	0.9776
410–1	3.000	Smooth	0.976	3.130	3.151	3.145	1.0019	2.931	2.950	3.012	0.9794
–2	2.600	Smooth	0.969	2.767	2.785	2.807	0.9922	2.531	2.548	2.589	0.9842
–3	2.600	5 3-in. baffles at full depth	0.953	2.569	2.586	2.693	0.9603	2.665	2.683	2.767	0.9697
–4	2.200	5 3-in. baffles at full depth	0.939	2.100	2.114	2.196	0.9626	2.291	2.306	2.415	0.9549
–5	2.600	5 3-in. baffles at 1/2 depth	0.957	3.152	3.173	3.282	0.9668	3.054	3.074	3.175	0.9682
–6	2.200	5 3-in. baffles at 1/2 depth	0.934	2.633	2.650	2.753	0.9626	2.530	2.547	2.655	0.9594
–7	3.000	Smooth	0.976	3.176	3.197	3.184	1.0041	2.941	2.960	2.980	0.9933
				Left—Meter No. 5764-2-*L*				Right—Meter No. 5759-2-*R*			
409–7	3.000	Smooth	0.976	2.821	2.840	2.813	1.0096	2.726	2.744	2.751	0.9975
–8	2.600	5 3-in. baffles at full depth	0.953	2.809	2.827	2.596	1.0890	2.960	2.960	2.714	1.0980
–9	2.600	5 3-in. baffles at 1/2 depth	0.957	3.126	3.147	3.162	0.9953	3.140	3.161	3.193	0.9900

Average ratio for smooth flow = 0.991.
Average ratio for all baffles = 0.970.

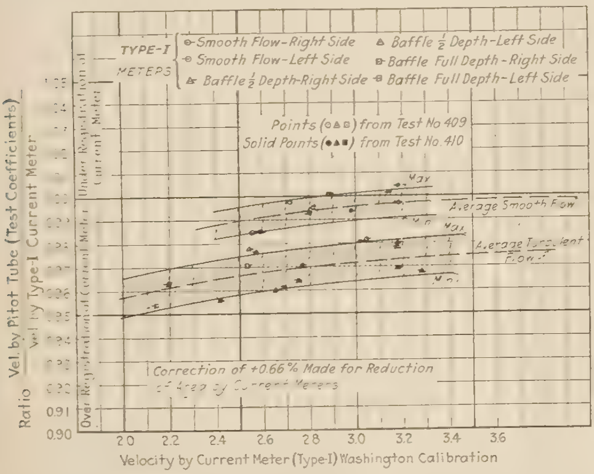

FIG. 12 COEFFICIENTS OF TYPE 1 METER. POINTS PLOTTED FROM DATA IN TABLE 3

the turbulent-flow measurements, the results will exceed the observed flow by approximately 2 1/2 per cent.

Where angular flow occurs, in combination with turbulence, the accuracy of water measurements by current meters is still in doubt as no tests are available to indicate that correct results can be secured under such conditions.

In conclusion, it should be stated that the tests made in the I. P. Morris Laboratory at Eddystone, Pa., were undertaken in an attempt to clear up some of the elements of doubt which have existed in regard to current-meter measurements, and to explain the discrepancies which have resulted when current-meter measurements are made under conditions which are not ideal. It is felt that further research and studies are necessary, and these should include the determination of the true-velocity plane in front of the current meter under varying conditions of flow. Such determinations would clear up some of the unexplained differences between the results secured at Eddystone and those secured in other flumes and in open channels. Another feature which should be established is the behavior of current meters with both turbulent and oblique flow present simultaneously in the metering section. From such determinations it might be possible to fix more definitely the limiting conditions under which current meters should be employed for precise flow measurements.

Personnel

These tests were conducted at the Baldwin-Southwark Corporation, I. P. Morris Division Laboratory at Eddystone, Pa., by K. W. Beattie of the research department, under the direction of the author. The planning of the tests and investigations was done by a committee consisting of F. H. Rogers, chief engineer, R. E. B. Sharp, hydraulic engineer, L. F. Moody, consulting engineer, and the author, as representatives of the I. P. Morris Division. In addition the S. Morgan Smith Company was represented by J. D. Scoville, hydraulic engineer, and the Safe Harbor Water Power Corporation was represented by L. M. Davis and E. T. Schuleen of the test department.

Water Gaging for Low-Head Units of High Capacity

By J. M. Mousson,[1] Baltimore, Md.

In the field of hydroelectric construction there has been in recent years considerable advance in the development of low-head units of high specific speed. This tendency in design has been conducive to the development of low-head sites which were at one time considered uneconomical. It became, therefore, increasingly important to find methods of measuring the discharge of low-head plants where the water quantities are large and the water passages particularly short and unsuited to other methods of testing. American engineers had developed methods of measurement of flow in long penstocks and then attempted to extend these methods to plants with shorter water passages. European engineers have shown a preference for current meters, at one time commonly used on both sides of the Atlantic for measurements in large intakes.

The paper discusses the status of the current-meter method in Europe at the time this method was selected for the tests at Safe Harbor and the application of the two-type meter method. It shows how this method was applied at the outset and how certain modifications were made for increasing the reliability and decreasing the time and effort required for making tests. These made possible new methods of compilation which have been developed to facilitate greatly this phase of the testing program. The successful application of these methods should make current-meter measurements more feasible than ever before.

In preparation for these tests, investigations were conducted at the Bureau of Standards and elsewhere to determine the characteristics and limitations of the meters under various conditions of uniform, oblique, pulsating, and turbulent flow.

It has been shown that water passages with parallel sides for metering and approach sections do not insure parallel flow, and that even under as nearly ideal conditions as it is practical to secure, the use of two types of meters will indicate an effective angularity. However, it is believed that accurate measurements of oblique flow can be made by the use of two types of meters, each affected to a different extent by angularity. The use of this method will greatly enlarge the field of current-meter testing.

There are pointed out the advantages of making index tests in conjunction with current-meter measurements; not only to extend them to a wide range of operating conditions, but also as a measure of the consistency of the discharge measurements.

Introduction

On completion of the first four main units of the initial installation at Safe Harbor, it was essential that careful measurements be made of the water used for the purpose of accurate accounting, for determining the characteristics of the units preparatory to laying out loading schedules, and for many economic studies required in connection with operation. Inasmuch as the water passing through the wheels constitutes a relatively large proportion of the total river flow, accurate measurement is particularly desirable for the purpose of providing a reliable flow record and for dispatching water to the plants below.

The four main turbines are of the Kaplan type whereas the two service units have Francis runners. The Kaplan turbines have a capacity of 42,500 hp at a rated head of 55 ft, a speed of 109.1 rpm, and a maximum discharge of approximately 9000 cfs. A typical cross-section through the power house on the center line of a main unit is shown in Fig. 1. The water enters through three intake bays. Twelve such units are provided for in the plans for the ultimate development. The two service units are rated at 3100 hp and 180 rpm under a head of 55 ft.

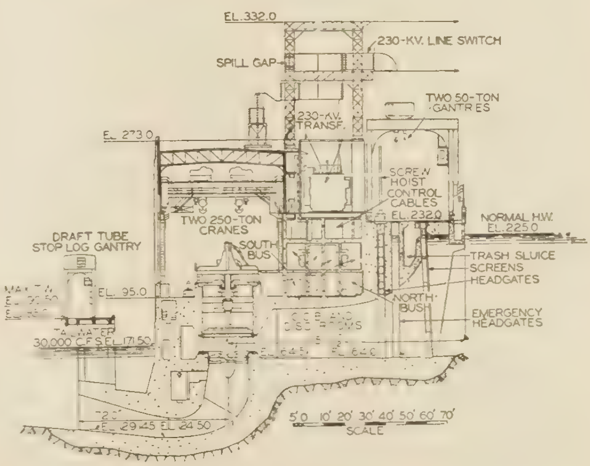

Fig. 1 Typical Cross-Section Through the Safe Harbor Power House

The testing program provided for discharge measurements on two of the main units and one service unit. These tests were carried out during the summer and fall of 1932 and 1933.

Selection of Method

Before selecting the method to be used, a careful study was made of the history and development of many methods of water measurement. The weir, traveling screen, and salt-titration

[1] Safe Harbor Water Power Corporation, Baltimore, Md. Mr. Mousson was graduated in 1926 from the Swiss Federal Institute of Technology, Zurich. He was designing engineer with the Pennsylvania Water & Power Co., and the Electric Bond and Share Co. from 1928 to 1929. Since that time, he has served on the engineering staff of the Safe Harbor Water Power Corporation as designing engineer, sponsor, and hydraulic engineer.

Contributed by the Hydraulic Division and presented at the Annual Meeting, New York, N. Y., December 4 to 8, 1933, of The American Society of Mechanical Engineers.

Discussion of this paper should be addressed to the Secretary, A.S.M.E., 29 West 39th Street, New York, N. Y., and will be accepted until October 10, 1935, for publication at a later date.

Note: Statements and opinions advanced in papers are to be understood as individual expressions of their authors, and not those of the Society.

methods could be eliminated as impractical on account of the tremendous quantities of water to be gaged and the impossibility of erecting the necessary structures at reasonable cost.

In general, the field of turbine testing in America, for the last decade at least, had been dominated by the Gibson and the Allen methods. The increasing success that these experimenters had, even outside of the field of long pipe lines, where their methods were eminently suited, had brought them more nearly into the domain of the methods used where the water passages are particularly short, as in low-head plants.

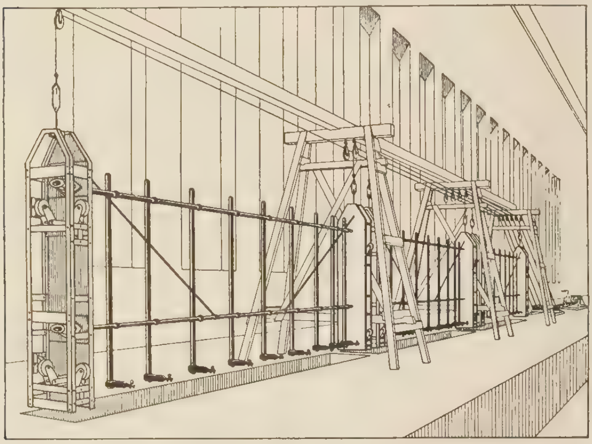

Fig. 2 Current-Meter Frames and Hoist Used at Ryburg-Schwoerstadt

Although current meters have been used in America, the results were on the whole rather unsatisfactory, principally because too extensive measurements were attempted with too few meters, inadequate supporting frames, and often improper location of the measuring section, particularly if in the tailbay.

During the years prior to 1931, marked improvements had been made in the art of current-meter measurements which were not generally appreciated in America because of the limited application that had been made in this country. These improvements were not confined to the meters alone, but applied also to the apparatus, set-ups, and procedures. The simultaneous use of a large number of meters had led to the adoption of movable supporting frames. Graphic recorders had found successful application for making a permanent record, avoiding thereby the need of a large corps of observers.

Large propeller units were more highly developed at an earlier date in Europe than in America, and stimulated a keener demand for a method that would successfully measure unusually large quantities of water. The layout of these plants precluded the use of a weir and the shortness of the water passages in proportion to the width put them in a range to which the American methods had not been extended at that time.

Inasmuch as Safe Harbor resembles similar European plants in this respect, it is only natural that careful consideration should be given to the methods that were used abroad. The engineers connected with the Safe Harbor tests fully appreciated the possibility that the Gibson and Allen methods might eventually be applied to similar layouts, but in view of uncertainty in this respect, it was decided to use that method for which the greatest amount of accumulated experience was then available.

Current-Meter Practice in Europe

It is well to consider the stage of development that the current-meter method had reached at the time the Safe Harbor tests were contemplated. This may best be done by describing briefly the test equipment and procedures used in 1931 at Ryburg-Schwoerstadt, on the Rhine between Germany and Switzerland.

These tests were confined to one of the four Kaplan turbines. Each of these turbines discharges a maximum of about 11,650 cfs under a head of 35.2 ft. Three current-meter frames, one for each intake bay, were provided. Each of these frames supported ten current meters. They were raised and lowered by three hand winches, one for each frame, supported by a temporary wooden structure as in Fig. 2. The position of the frames was indicated by an arrow mounted on the intake deck and by markings on the hoisting ropes.

The current meters were right hand, Ott V Texas type equipped with spoke-vane propellers. False steel roofs extending from the racks to the upstream edge of the stop-log slots were installed in the intakes to straighten the flow approaching the measuring section, Fig. 3. The roofs were sloped, however, approximately 10 deg toward the downstream side, and the plane of measurement was assumed to be flush with the downstream edge of the temporary structure. The area of the water passage at the plane of measurement in each intake bay was rectangular in shape, 23.0 ft wide and 29.1 ft high.

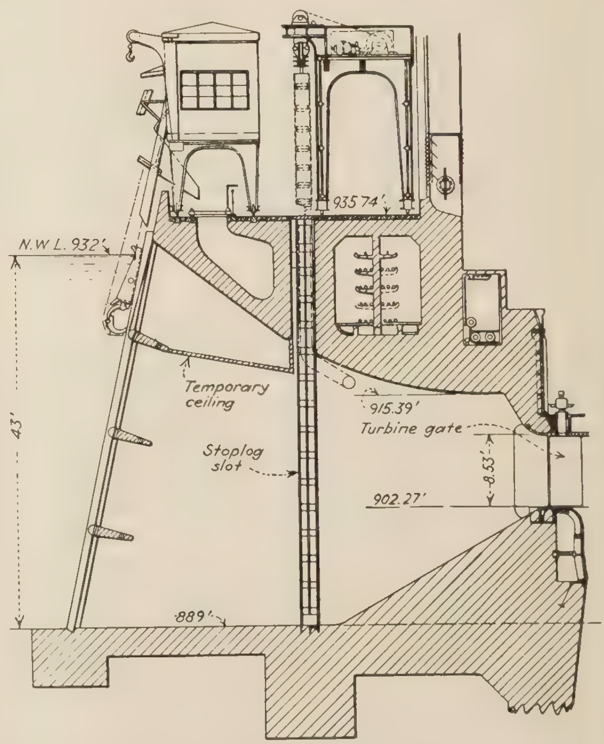

Fig. 3 Cross-Section Through Intake With False Roof, Ryburg-Schwoerstadt

During each test the frames were brought to 12 different elevations, and held for about 1 min. The spacing of the meters as well as the various frame positions were chosen so that the areas represented by each point of measurement would be small near the side walls, intake bottom, and intake roof, but progressively greater toward the center. During each test requiring between 22 and 24 min, 360 measurements were taken.

One graphic recorder was provided for each intake opening. The circuits for the commutators of the current meter were connected individually to ten pens, while one pen on each recorder registered the time in seconds.

A total of 24 tests were made under almost identical head conditions. The measurements were divided into groups of four or five runs, each group covering the range of peak efficiency for a given fixed runner-blade setting and variable gate opening.

Selection of Apparatus and Design of Equipment

(a) *Current Meters.* An extensive study was made of all data then available regarding the various current-meter designs and their respective behavior in still as well as in flowing water. Considering the fact that current meters had not been extensively used for discharge measurements on turbines in America the wealth of data was surprising. These data concerned practically all known current meters of American and European design of both the cup and propeller type such as the Price, Gurley, Hoff, Haskell, Pegram, Fteley, Ott, Stoppani, and Amsler.

At the outset it was realized that the principal difficulty to be feared was the effect of the bell-mouth. With intakes as shown in Fig. 1, it would be necessary either to correct for the convergence of the stream lines approaching the gate slots where measurement would be made, or else to erect some means of securing parallel flow by a false roof.

The A.S.M.E. Test Code, now in course of revision,[2] specifies on page 18, paragraph 101: "Meters of two types shall be used having opposite characteristics in running water; that is, one type of meter retarded by oblique flow and the other type accelerated by oblique flow."

The first consideration, therefore, was to choose from the available types two suitable meters, i.e., a type which would over-register slightly in oblique flow, and a second which would under-register approximately by the same amount, so that the true discharge would be derived by averaging the readings of the two.

As a result of our study, no suitable meter could be found which would consistently over-register for a given angle of obliquity whatever the plane of approach. The cup meters which have the tendency to over-register, could not satisfy the requirements as these meters very obviously are affected differently depending upon the plane of approach.[3] Some tests were actually made using cup-type meters simultaneously with propeller-type meters, but it is obvious that because the over-registration of cup meters is dependent upon the plane, this cannot be a reliable means of doing more than indicating that oblique flow exists in the section.

In view of this fact it was proposed to substitute in place of the meters called for in the Power Test Code, two types of meters, both of which under-register but to different extents.

The object was then to provide first a meter termed type 1, which should register in oblique flow, as nearly as possible the actual flow times the cosine of the angle of inclination, i.e., the component in the direction of the axis of the meter; and another meter called type 2 which should differ as much as possible from the characteristics of type 1, but still have a stable and well-defined relation between the amount of registration and the angle of inclination to the flow. It is the sole purpose of this type-2 meter to measure the amount by which the type-1 meter is affected by angularity.

The meter which at that time best satisfied the requirements for the type 1 was the Ott V Texas type with three square vanes mounted on radial spokes. These meters had a nominal pitch of 25 cm, Fig. 4. An example of the painstaking care and forethought on the part of the manufacturer is his provision of plaster molds for the propellers so that whenever desired a check could be made of the propeller shape to see that it had not become damaged or altered, even in the slightest degree.

The decision reached for the first type of meter naturally influenced the selection of the second and the advantage of having clamps, bodies, axles, ball bearings, and all spare parts interchangeable made the decision obvious.

In spite of all the information which the manufacturer had, it was deemed necessary that some experimental work should be done before being satisfied that the meters he had to offer were the most suitable. The fact that there is a rating station at the factory greatly simplified the situation, as valuable time could thus be saved. Based on the results of his test, the preliminary decision to use the type-1 meter was adhered to, while the Ott V Texas meter, equipped with a propeller of conical screw shape and 50-cm pitch, was selected for the type 2, Fig. 5.

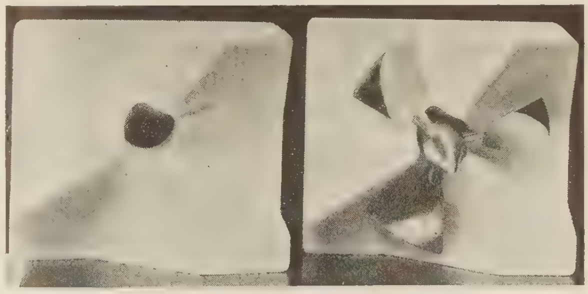

Fig. 4 Type-1 Propeller With Plaster Mold

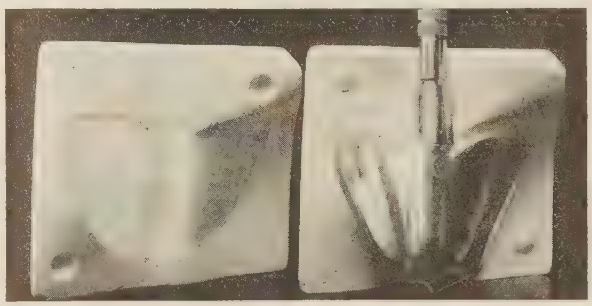

Fig. 5 Type-2 Propeller With Plaster Mold

In European practice it is customary to observe an established relation, which is that the number of stations should be between 4.3 and 7.6 times the square root of the area of the section in square feet. After carefully considering various possible ways of dividing the intakes, it was decided to use nine meters of each type in each intake, thus requiring, with one spare of each kind, 56 meters. Each propeller was furnished with its plaster mold.

It had been decided that, in order to avoid error arising from the effect of eddies with axis parallel to that of the meter, it would be necessary to use right-hand and left-hand meters alternately placed, a principle rigidly adhered to throughout the tests.

(b) *Supporting Frames for Current Meters.* The three frames supporting the meters were built to travel in both head-gate and emergency-gate slots. The frames consist of two structural-steel ends, to which two horizontal cross-members are bolted. These horizontal cross-members consist of chrome molybdenum, streamline, seamless steel tubing 2 × 4.75 in., heat-treated to give high tensile strength, Fig. 6. The special material made it unnecessary to have diagonal bracing, which would have set up possible undesirable disturbances. The end girders

[2] Power Test Code, Subcommittee No. 18, Ely C. Hutchinson, chairman.

[3] L. A. Ott's discussion of "Research Institute for Hydraulic Engineering and Water Power," by Hunter Rouse, Trans. A.S.M.E., 1933, vol. 55, no. 10, p. 41, paper HYD-55-3.

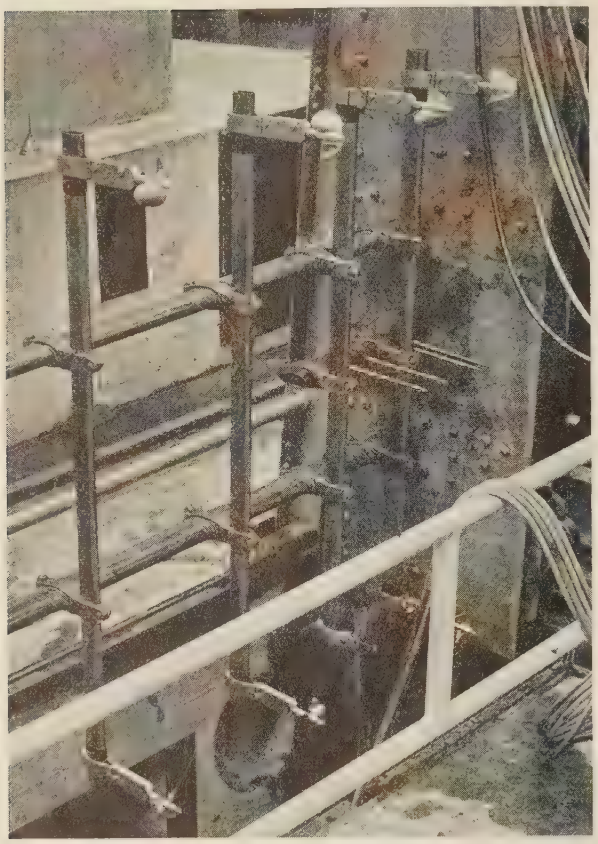

FIG. 6 CURRENT-METER SUPPORT FRAME, TYPE-1 AND TYPE-2 METERS MOUNTED SIMULTANEOUSLY
(Note horizontal row of pitot tubes.)

FIG. 7 CURRENT-METER FRAME HOIST. TYPE-2 METERS MOUNTED NEAR BOTTOM OF VERTICAL FRAME RODS

are equipped with rollers. Those on the downstream side are mounted rigidly, while those on the upstream side and adjacent to the piers are mounted on arms so that they can be forced outward by springs to eliminate vibration and to hold the frames firmly in position in spite of any variation in the width of the slots. The structural-steel ends are closed off on the water-passage side by means of a steel plate to eliminate disturbances along the piers. Special gages were constructed for inspection at the factory and during field assembly to check the alignment of the meter supporting rods.

(c) *Current-Meter Hoist and Hoist Supports.* In order to simplify lowering and raising the frames, as well as to reduce the personnel during the tests, a fully automatic hoist was specially designed. The somewhat high initial cost of this was well justified, as it was foreseen that it would allow a great reduction in testing time required as well as in office work. Furthermore, as the ultimate development is intended to comprise 12 units, the testing equipment could be regarded as permanent investment to take care of all future requirements.

The hoist consists of a double-drum, worm-geared, electric motor-driven unit designed to lower and raise the three current-meter frames simultaneously.

The hoist is capable of raising or lowering the frames at speeds of 2, 3, 4, and 6 fpm, Fig. 7. A mechanically driven elevation indicator geared to the pinion driving the drums is provided to show the position of the meter frames. This elevation indicator enables the operator of the hoist to bring the frames to any desired position to the nearest one-hundredth of a foot. The indicator is also equipped with a contact electrically connected to pens of the graphic recorders to indicate every tenth of a foot of travel. This arrangement permits the determination of the speed at which the meter frames are raised or lowered by comparison with the time impulses recorded simultaneously, and provides a permanent record of the true position of the current meters at any time during the tests.

(d) *Graphic Recorders and Circuits.* The graphic recorders must have a sufficient number of pens to register simultaneous impulses from 54 current meters as well as from the elevation indicator and a timing device. Motor-driven Esterline-Angus production recorders with multipliers and quick-trip attachment solved this problem satisfactorily. High chart speed is essential to prevent confusion of the current-meter record at high velocities.

A typical record is shown in Fig. 8. The sequence of the long and short contacts for each cycle of ten revolutions of the propeller enables the observer to determine the direction of flow. The short break in the long contact is useful in interpreting the record for very low velocities. As no commercial instrument could be found with 56 pens, it was necessary to get two recorders, Fig. 9, one accommodating two charts and the other a single chart. Both recorders have 20 pens for each chart, which were assigned one to each intake bay. Of the 20 pens provided per chart, 18 could be used to register the meter contacts, while the two end pens were connected to the contact-making devices for timing and indicating the elevation of the meter frames, Fig. 10.

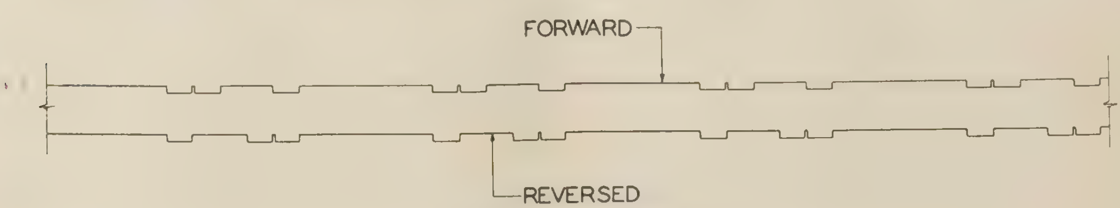

FIG. 8 TYPICAL CURRENT-METER RECORD

The graphic recorders were installed in a housing placed on a standard-gage railroad flat car. This provision was made so that any section of the intake deck could be cleared at short notice for operating purposes.

A condenser and resistor bank containing 60 units is used in the current-meter circuits to prevent sparking of the contacts. Each unit consists of a 0.24-μf condenser and a 10-ohm resistor. A four-cell, Philco, type P.M.T., 13-plate battery, supplies current for the meter circuits at 4 volts.

To insure proper coordination of the test personnel, a signal system of electric bells was installed.

(e) *Timing Device.* As it was necessary to provide a source of time impulses, serious consideration was given to various spring-wound portable timers. It developed, however, that these types of apparatus would introduce an uncertainty in time of about 0.2 per cent. Considering that this error would impair the accuracy of the tests, advantage was taken of a practically absolute source of time.

In the control room of the power plant there is installed permanently a Warren pendulum clock for frequency regulation. A photoelectric cell and an automobile spotlight focused on this cell were placed in such positions that the pendulum cut the beam of light at every swing, Fig. 11. This arrangement gave a precision far in excess of requirements, as the pendulum can be regulated to accumulate an error of less than one second a day. The wiring diagram for the timing device is shown in Fig. 10.

(f) *Pitot Tubes.* It is well known that the velocities may vary considerably in the vicinity of the boundaries of the measuring section. Special provisions were made to determine them by pitot tubes, thus avoiding the small error which would result from

Fig. 9 Graphic Recorders

extending the velocity curves beyond the last meter position.

A row of four pitot tubes was installed near each end of the current-meter frame. The tubes were mounted on short lengths of streamline tubing half way between the cross-members of the frames as shown in Fig. 6. The pitot tubes of one row are spaced so that two are between the intake wall and the first current meter, while two others are between the first and second current meters. The pitot tubes as arranged permit measurements of relative values of velocity which may be coordinated with the current-meter measurements. Reinforced rubber hose connected the tubes with a gage board located in the trash sluice, see Fig. 12. This gage board consists of three groups of eight glass tubes each, one group for each intake bay. A glass tube on either side of the three groups is used for static-head readings.

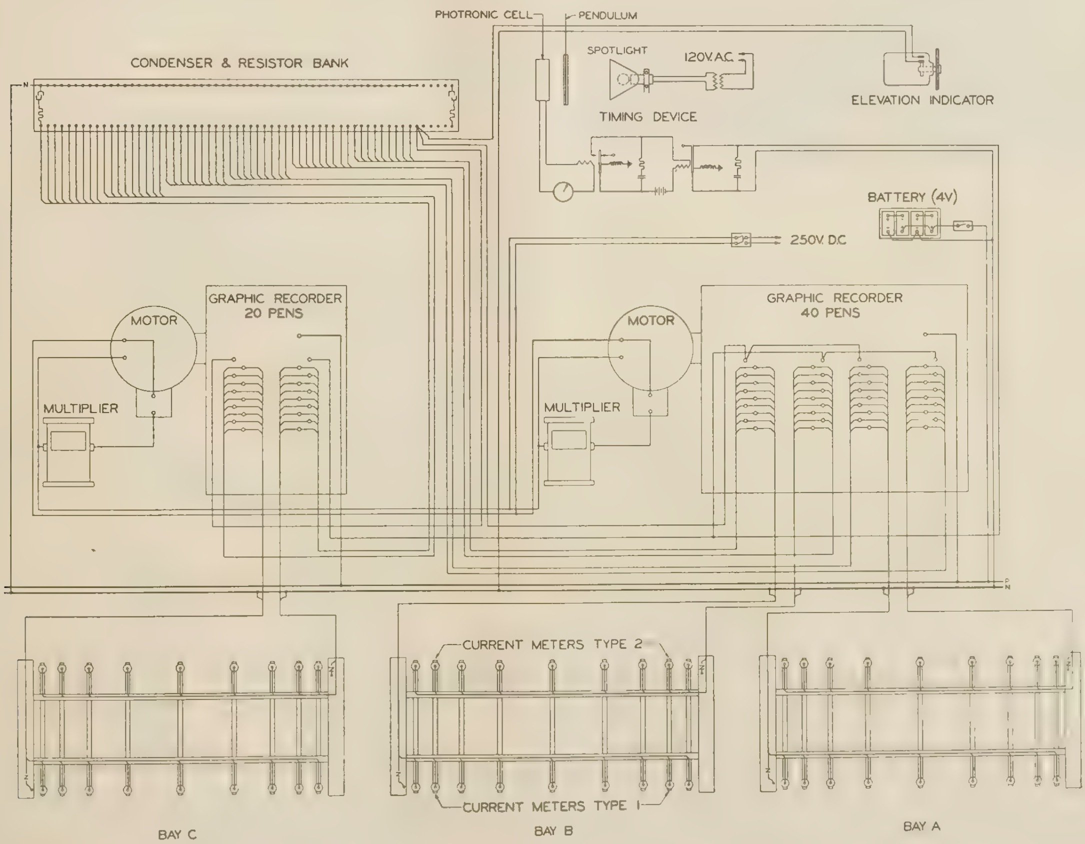

Fig. 10 Wiring Diagram

Pitot tubes were also used at one time to explore the velocity in the vicinity of the intake bottoms. A streamline rod was clamped in a vertical position to the horizontal cross-members of the current-meter frames. This vertical rod was made of the same tubing as the horizontal frame members, see Fig. 13. Four of the pitot tubes previously described were mounted on the lower end of the rod.

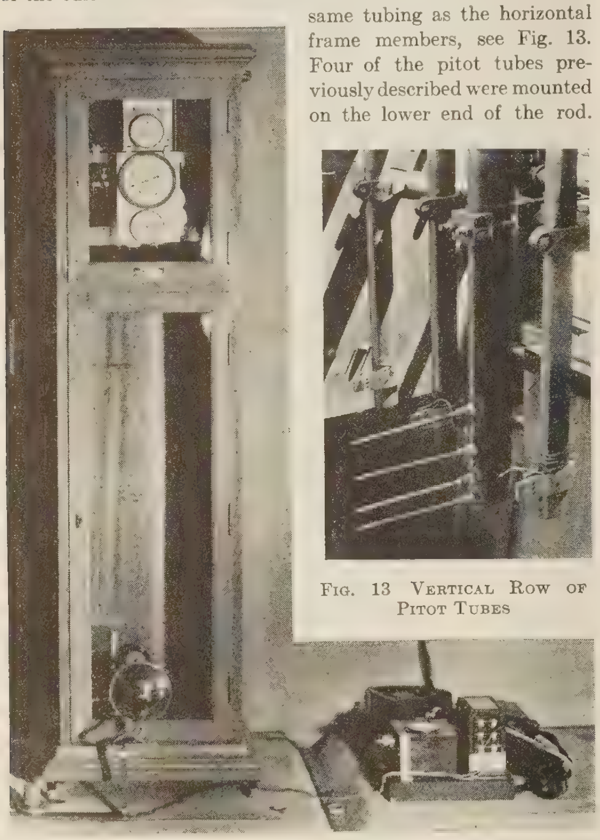

Fig. 13 Vertical Row of Pitot Tubes

Fig. 11 Timing Device

The spacing provided two pitot tubes between the first current-meter position and the bottom, and two between the first and second current-meter positions.

(g) *False Work.* In most European tests the effectiveness of false work to straighten out the flow approaching the plane of measurement has been taken for granted. There have been cases where temporary installations within the intakes proper were thought inadequate, and elaborate structures were made in the forebay, such as pier extensions or temporary elongations of the intakes. On still another occasion the plane of measurement was located upstream in the head-water canal where an approach of this type was available, making it necessary to have costly and elaborate bridges providing working platforms and supports for the apparatus.

Installations of a temporary nature naturally have their advantages and disadvantages. For example, head-water canals are often not rectangular in shape, thereby complicating test equipment, measuring procedures, and compilation of test data. Not only are elaborate temporary installations undesirable because of their cost, but also because, with most of these installations, the turbine discharges are not measured under operating conditions. In the final analysis, discharges are not determined exclusively for the sake of the problems concerning the turbines, but on the contrary, even more for the performance of the entire installation, that is, individual units as a whole under operating conditions.

Keeping in mind the characteristics of the current meters selected for Safe Harbor and the physical outlines of the intakes, it was thought possible to omit temporary installations of any kind, for it was believed that an evaluation of the obliquity of flow could be made.

It was thought desirable, however, to install for the first test a false roof in the intake of one of the units shown in Fig. 12. The advantage to be derived from such a plan was the possibility of tying in the two-type current-meter method with the conventional one-type method.

The false roof installed under the bell-mouth of each intake bay of one unit was made of wood. This roof was placed in a level position as it was believed that by so doing the flow would be straightened out more satisfactorily. The temporary structure was drawn tight against the concrete by means of steel cables extending down the emergency-gate slots and the trash-rack openings. It was also fastened to wooden fillers placed within the emergency-gate slots to prevent undesirable disturbances from being carried downstream to the plane of measurement. To improve further the flow conditions, a temporary wooden bell mouth covered with sheet metal was attached to the trash racks. This in turn had an extension reaching upstream to be flush with the intake piers, since hydraulic model tests in connection with the spillway design for Safe Harbor had shown that the most favorable conditions of discharge could be obtained by keeping the piers and the spillway nose flush with each other.

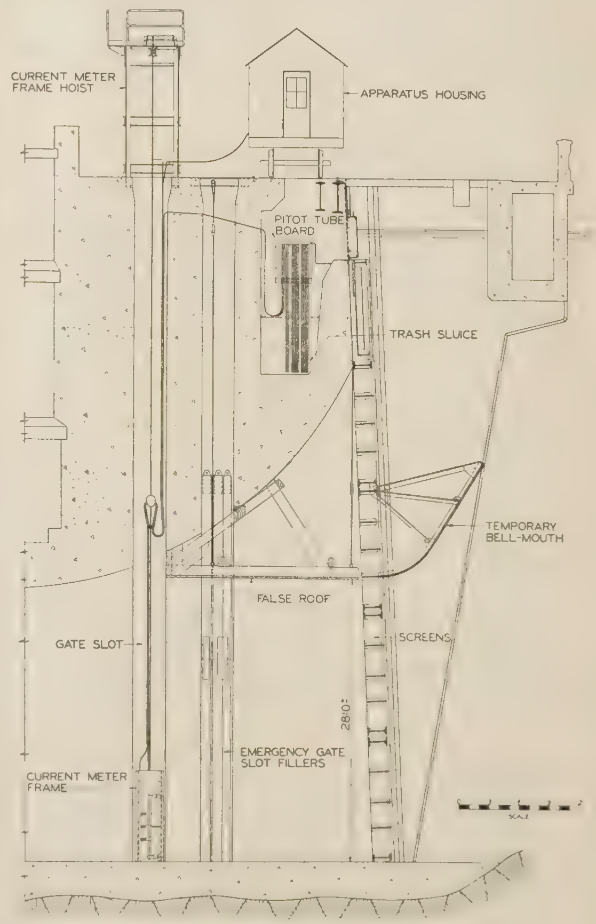

Fig. 12 Cross-Section Through Intake With False Roof in Place and Apparatus Set-Up

Calibration of Current Meters and Special Investigations

(a) *Calibration at the Bureau of Standards.* As a first step it was necessary to determine the usual still-water calibration at various constant speeds. A minimum of 18 runs for each rating was made to cover adequately the velocity range from 0.5 to 7.5 fps.

Instead of rating tables, or the usual calibration curves, giving revolutions per second vs. velocity in feet per second as in Fig. 14, curves were plotted to give pitch in feet per revolution vs. revolutions per second as in Fig. 15. The advantage of such a curve is that it may be read with greater precision. By this means the effect of personal equation in reading the curve is practically eliminated.

A number of the meters used at Safe Harbor were calibrated by the manufacturer before shipment and recalibrated on arrival at the Bureau of Standards. These ratings agreed within 0.1 per cent throughout the useful velocity range.

Following the tests in the field, a substantial number of the meters of each type were recalibrated as required, whereas the propellers of all the meters were carefully checked against the plaster molds.

These meters use oil-lubricated ball bearings, but the prime function of the oil is to keep water out of the bearings, rather than to lubricate. Nevertheless, there is some effect of viscosity. A record was kept of the water temperature in the rating tank, and ratings were made in the winter as well as the summer to secure temperature variations from about 5 C to 26 C. In addition to repeated ratings with one meter at various water temperatures, calibrations were made with various blends of oil other than the light ice-machine oil supplied by the manufacturer. These blends consisted of sperm oil and kerosene.

The result of this investigation indicated that the viscosity of the oil does affect the meter and that this effect in turn depends upon the rate of rotation. It was interesting to see that within the limit of the experiments, and any one rate of rotation, the effect varies in a straight-line relationship with the oil viscosity, Fig. 16.

The oil mixture consisting of 10 per cent sperm oil and 90 per cent kerosene proved very satisfactory and no appreciable effect of temperature will be felt in practice.

To determine the effect of oblique flow, four type-1 and six type-2 meters were inclined in a vertical plane by steps of 5 deg up to and including 30 deg. As the average characteristic of all meters of each type was the ultimate object, these meters were

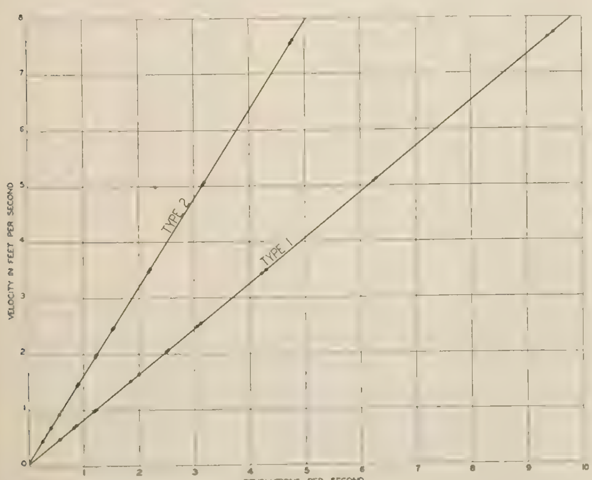

Fig. 14 Conventional Calibration Curves

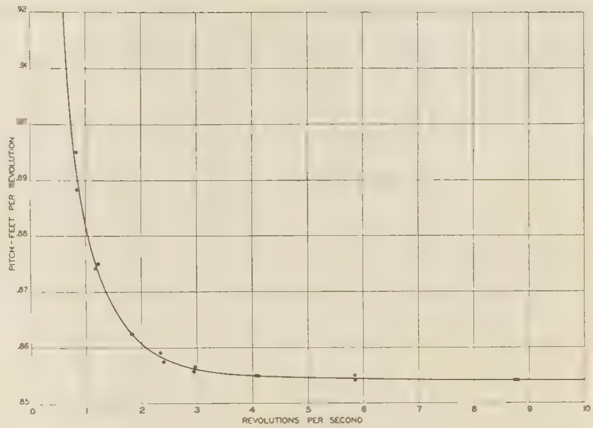

Fig. 15 New Type of Calibration Curve

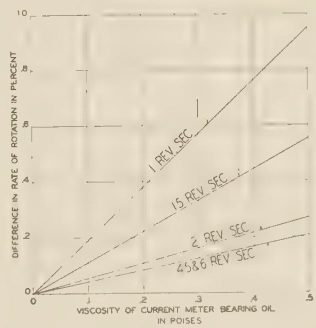

Fig. 16 Correction Curves for Rate of Rotation and Varying Viscosity of Bearing Oil

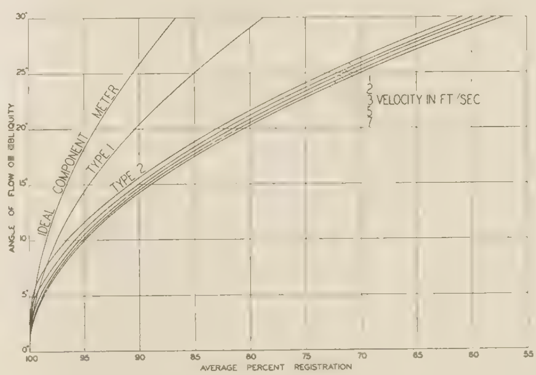

Fig. 17 Average Oblique-Flow Characteristics of Type-1 and Type-2 Meters

selected from the previous tests in order to have long, short, and medium pitches; although there was no great difference between the extremes.

The effect of velocity upon the oblique-flow characteristics was investigated subsequently. One current meter of type 1 was rated for angles of 10, 20, and 30 deg, while 10, 15, 20, 25, and 30 deg were used for type 2. For these tests, medium-pitched meters were chosen. It was found that for a given obliquity, the amount of under-registration of type 1 was independent of the velocity; whereas for type 2, the under-registration increases for the higher velocities, Fig. 17.

Having determined the average characteristic in the plane in

which oblique flow under test conditions could be expected to predominate, one meter of each type was turned in a horizontal plane to show that the angularity of flow had the same effect regardless of the plane of approach.

(*b*) *Principle of Discharge Correction Based on Two-Type Meter Method.* By replotting Fig. 17, using as ordinates the cosines instead of angles, it was discovered that for curves of average per cent registration for the two types of meter, straight lines were obtained as shown in Fig. 18. It may be emphasized that this characteristic is of fundamental importance, as it indicates that the meters, in average, are integrating correctly all cosine components regardless of variation in obliquity and that both meter types furnish a registration corresponding to an identical mean

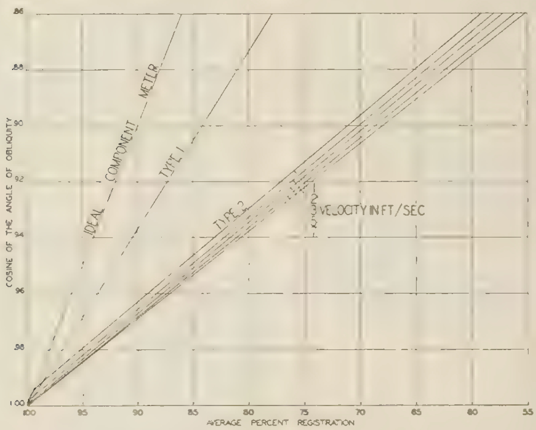

Fig. 18 Average Registration of Type 1 and Type 2 Vs. Cosine

cosine of obliquity. If the characteristics as shown in Fig. 18 were curves instead of straight lines, and even if the under-registration of type 2 were a constant times the under-registration of type 1, different mean ordinates would be obtained for each meter type which would make it impossible to bring the two-type meter method to a correct analytical basis.

The straight-line average characteristics for oblique flow, shown in Fig. 18, led to the correction curves shown in Fig. 19 which obviously must be straight lines. Considering their derivation, these correction curves may be used to combine the total discharges measured by means of the two types of meters instead of limiting their application to the individual velocity components obtained by both meters at the same metering station. This conclusion is most important, as a correction of individual velocity components determined at each station with both types of meters is almost a practical impossibility, because an enormous amount of computation would be involved in pairing individual observations to apply a correction to the individual type-1 measurements.

In addition it must be considered that variations in flow exist which make it impossible to obtain identical components with the same meter and at the same station for two consecutive measurements under identical physical discharge conditions. Experience has shown that individual velocity components obtained with one type of meter may vary more than 20 per cent for identical locations and equal discharges, but that the difference in total discharges obtained from many individual measurements is less than 0.1 per cent. From this it appears that although individual corrections could be attempted, they would be erroneous if applied to obtain the obliquity at one particular location.

It must be emphasized that the wholesale correction based on mean velocities or discharges determined with each meter type, made the two-type meter method possible, both from a practical and theoretical point of view.

(*c*) *Current-Meter Measurements at Holtwood.* It was considered advisable to make some actual water measurements in a laboratory by means of the two-type meter method previous to measurements in the field. It was specified that the laboratory selected for these preliminary tests should have water-gaging facilities calibrated by the Gibson or Allen method. The Holtwood hydraulic laboratory of the Pennsylvania Water & Power Company furnished a satisfactory set-up, as the venturi meter here installed to measure the discharge had been calibrated by means of the Allen salt-velocity method under excellent physical conditions. The measuring section for the current meters was located in the open steel flume on the downstream side of the laboratory.

Two series of tests were made, one with the approaching water straightened, as much as possible, upstream from the plane of measurement by means of stilling racks, and a second group, without the racks, under comparatively rough-flow conditions showing visible signs of turbulence and obliquity. From

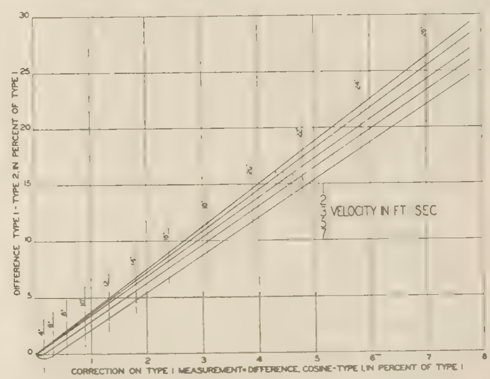

Fig. 19 Correction Curves, Using Type-1 and Type-2 Meters

Table 1 it may be seen that the two-meter method, as developed, gave satisfactory results.

(*d*) *Analysis of Tests Made at the Obernach Research Station.* An analysis in detail was made of the tests conducted in 1930

TABLE 1

Test group	Run No.	Current-meter type	Departure from venturi, per cent		Diff. type 1 and type 2 in per cent of type 1	Correction to type 1, per cent (see Fig. 19)	Departure of corrected discharge, per cent
1 (smooth flow)	1	1	−0.03	avg = −0.24	0.51	0.20	+0.17
	2	1	−0.45				−0.25
	3	2	−0.75				....
2 (rough flow)	4	1	−0.59		1.68	0.49	−0.10
	5	2	−2.28				....

at the Obernach research station in Germany by the Research Institute for Hydraulic Engineering and Water Power, Munich. This investigation, based on original data, furnished, in addition to an independent check on conclusions resulting from the Holtwood tests, a comparison of the two-type meter method against volumetric measured discharge.[4]

[4] J. M. Mousson's discussion of "Research Institute for Hydraulic Engineering and Water Power," by Hunter Rouse, Trans. A.S.M.E., 1933, vol. 55, no. 10, paper HYD-55-3.

Incorporation of Index Method in Testing Program

It was recognized at the outset that it would be desirable to reduce the number of test runs to a minimum without impairing the accuracy of the measurements and without curtailing important and necessary observation regarding the characteristics of the turbines. In the case of Kaplan units this requires more information than for any other runner type, since the proper cam which establishes the correct relation between wicket gate and runner-vane positions cannot be based on model tests. It is necessary, therefore, to run through a series of tests to obtain the characteristics of the runner for numerous fixed-blade angles and variable gate.

In addition, it was realized that the index method would increase the effectiveness of the current meters. Index methods consist simply of the determination of the relative amount of water discharged by a turbine by observing the pressure differences between two or more points in the turbine setting. Seven piezometer openings were provided in the wheel case of each Safe Harbor main unit. There are two piezometers of the Peck type built in a stay vane of the speed ring, three for a Winter-Kennedy system in the walls of the scroll case, and two located in one of the piers of the intake. A Winter-Kennedy system of three piezometers is installed in each of the service units.

In certain tests made abroad, previously referred to, the entire characteristics of the unit were determined by means of 24 current-meter measurements. Each blade position was tested separately as though the unit were a fixed-bladed propeller runner. Inasmuch as there were but five points determined on each individual blade-angle curve, there was opportunity for considerable latitude and judgment in drawing the final curve which would represent the performance if the blade and gates were held always in the theoretically correct relation to each other. A further disadvantage is that this shows simply the performance when conditions are right, and not the performance of the unit when actually operating with the blades and gates held in relation to each other by the cam.

To determine the shape of the cam for a wide range of heads, as will occur at Safe Harbor, requires an extensive testing program which would have been exceedingly expensive and laborious with the current meters alone; hence the index method proved a helpful means of determining the correct relation prior to the current-meter tests. The incorporation of the index method confined the use of current meters to testing on the cam, except for a few runs to check the shape of two of the multitude of curves obtained by the index method.

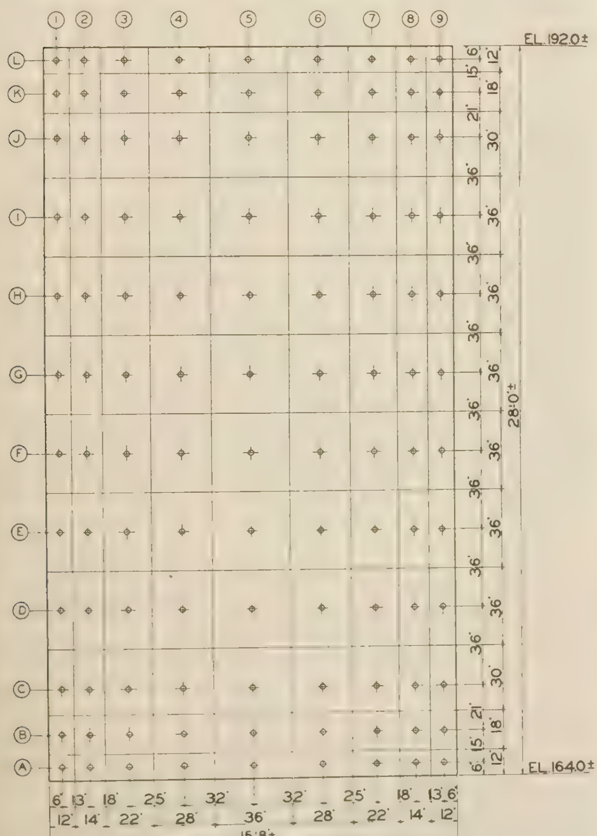

Fig. 20 Location of Metering Stations in Plane of Measurements for Point Method

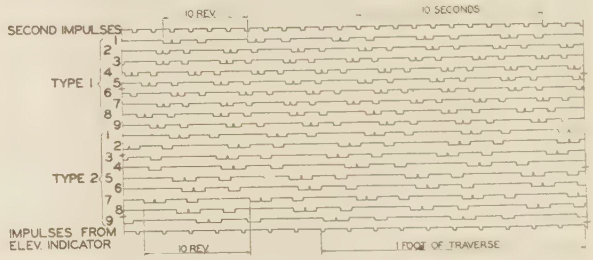

Fig. 21 Typical Chart Section, One-Fifth Actual Size

Testing Procedures and Computation

(a) *Point Method.* The current-meter apparatus was first installed in the gate slots of the one unit which was provided with the false roof. To obtain the most suitable flow conditions for test, the adjacent units were operated so as to carry about the same load. During all current-meter tests, piezometer readings were taken.

Both types of current meters were mounted 6 ft apart on the meter-support frames, the type-1 meters at the bottom and the type 2 at the top of the vertical rods. The metering stations are shown in Fig. 20. The type-1 meters covered the entire intake area, whereas the type-2 meters could only be brought to the positions *D* to *L*, inclusive. It was believed that the accuracy of the type-2 measurements would not be impaired materially by the fact that the latter could not be placed at the three lowest positions, *A*, *B*, and *C*, as it was assumed that the obliquity in the vicinity of the intake bottoms would be small. The data obtained by the type-1 current meters for the positions *A*, *B*, and *C* were combined with the type-2 measurements above these three horizontals to obtain the type-2 discharges. The meters were kept at each location 80 sec. The average duration of one complete test run was approximately 30 min.

The individual velocities were obtained from the graphic-recorder charts after first determining the chart speed by means of the second impulses, Fig. 21. The meter revolutions were counted and measured to the even ten, as the meter-contact wheels make one revolution for every ten revolutions of the current-meter propeller. The revolutions per second were then multiplied by the corresponding pitch, in feet per revolution, obtained from the individual meter-calibration curves, Fig. 15.

(b) *Vertical-Integration Method.* It is obvious that the conventional point method is exceedingly laborious, since for one complete run 324 type-1 and 243 type-2 velocities must be determined and 60 diagrams must be plotted and planimetered.

The enormous amount of time required for testing and computation warranted a detailed study to simplify these procedures.

It was suggested that tests be made by moving the frame at a constant speed over the total height of the intake and thereby causing the current meters to integrate all velocities encountered over the total length of the traverse. It was realized that, if this method should prove successful, that is to say, if results were obtained identical with the point method, enormous savings could be effected both in time required for actual testing and in computing the results.

It was anticipated that, in letting the meters integrate all velocity measurements in one vertical traverse, mean velocities would be obtained corresponding to the same mean velocities as determined for the point method by means of the vertical velocity diagrams, and thereby eliminate the determination of individual velocity measurements and render unnecessary the plotting and planimetering of vertical velocity diagrams.

In moving the frames an angularity is introduced which varies according to the lifting speed and the velocity of the water. For relatively high lifting speeds and one type of current meter, discharges would be obtained which are too small, although the influence is less than may be expected. In case this additional obliquity should have an appreciable effect in spite of relatively low lifting speed, it was expected that the two-type current-meter method would successfully solve the problem, as obliquities whether natural or artificial are evaluated.

On the other hand, the current meters themselves showed characteristics favorable to an integration method. Plotting velocity in feet per second vs. revolutions per second for both types of meters in question, curves are obtained which are practically straight lines, as in Fig. 14. In spite of the increasing friction and slip at low velocities, the average of a number of ordinates taken at random from these curves falls so close to the lines themselves that an error is introduced which is, from a practical point of view, entirely negligible.

To prove the workability of the vertical-integration method it was thought advisable to make a subsequent series of test runs on the same unit with the false roof in place, and then analyze these data independently of those obtained by the point method. The lifting speeds used were 4 and 6 fpm. This procedure cut the original time of 30 min, necessary for one run by the point method, down to about 8 or even 5 min, respectively. In the course of one test run the meter frames were either lowered or raised. When raised, the frames disappeared completely into the gate slots above the flow passage and likewise started out from within the slots when the frames were lowered.

Various ways of compiling the data were studied. The revolutions of the type-1 current meters were counted between the bottom and top of the intake bays, the limits being established by the record of the elevation indicator shown in Fig. 21. Because of the length of the record, it was considered satisfactory to estimate, at the ends of the charts, the number of revolutions to the even unit by extrapolation beyond the last contact indicating an even ten revolutions. Similarly the time was estimated to one-tenth of a second.

Since the meters could be lowered no further than 6 in. above the bottom of the intake, it was necessary to determine the velocities in this area by some other means. The meters were held at this lowest elevation for about 6 sec, that is to say, at least the number of seconds which would have been required to traverse these 6 in. The additional number of revolutions was then multiplied by a factor determined by the pitot-tube measurements. This number of revolutions was then added to the number counted as previously described.

The type-2 current-meter registrations were counted between elevation 170.5 and the top of the intake bay as lower and upper limits, respectively. In order to tie in the type-1 and type-2 measurements near the bottom, it was necessary to determine the number of revolutions of the type-1 meter between the bottom and elevation 170.5. The type-2 discharge was obtained by adding the discharges indicated in the areas above and below elevation 170.5 by the type 2 and type 1, respectively, Fig. 20.

A comparison between the results obtained by the two methods, that is, by point and vertical integration, showed them to be absolutely identical.

(c) *Separate Measurements With Type-1 and Type-2 Meters.* The enormous savings over the point method justified the extension of the testing program to other units. First, one of the main units without a false roof in the intake was investigated. The plane of measurements was moved upstream into the emergency-gate slots to save all expenditures which would have been necessary to remove the intake gates and screw-stem gate hoist, and to provide fillers for the emergency-gate slots in the piers and ceiling over the emergency-gate slot openings to obtain suitable flow conditions further downstream. It was thought that in taking a chance and placing the plane of measurements in the emergency-gate slot, the full benefit of the two-type current-meter method would be investigated under conditions where the expected obliquity was considerable.

Still further savings in computation were possible by making these tests with each type of current meter alone, mounted near the bottom of the vertical support rods shown in Fig. 7. The separate application of the two types of meters made it necessary to plot the discharges obtained against a common standard such as piezometer deflection, power output, or gate opening before a discharge correction could be applied. It may be emphasized that this method is advisable in any case, whether or not the two meters are used simultaneously, as the spreading of the test points may thereby be eliminated before the correction is made.

The advantage over the first method of using both types of meters simultaneously was that the evaluation of discharge indicated by the type-1 meters between the bottom and elevation 170.5 was no longer necessary as the total height of the plane of measurements could be explored with the type-2 meter. The determination and planimetering of three discharge diagrams, that is, one for each intake bay per test run, could thereby be eliminated. The respective savings may be seen from Table 2.

The rapid progress made in computing the test data for this second main unit made feasible an investigation of the discharge characteristics of one of the two service units. Besides the important economies of time achieved by the adoption of the vertical-integration method, engineering and labor expense for the actual water gagings were kept at a minimum by the use of full-automatic equipment. Table 3 shows the number of men employed for the measurements. The benefit derived from the

TABLE 2

Data to be obtained for one complete test	Point method. Type 1 and 2 simultaneously	Vertical-integration method, type 1 and 2 meter: Simultaneously — Data to be determined	Saving over point method, per cent	Separately — Data to be determined	Saving over point method, per cent
Contact indications to be counted....	40,000	15,500	61	12,400	69
Contact indications to be scaled on charts..........	606	....	100	....	100
Velocities to be determined..........	567	81	86	54	91
Velocity vectors to be plotted........	648	81	88	54	92
Diagrams to be plotted and planimetered..........	60	9	85	6	90

TABLE 3

Equipment and Personnel	Safe Harbor Types 1 and 2 current meters: Separate	Simultaneous	Ryburg-Schwoerstadt
Equipment in use at one time:			
Current meters	27	54	30
Graphic recorders	1	2	3
Piezometers	4	4	..
Personnel:			
Graphic recorders	1	2	3
Index method	1	1	..
Hoisting	1	1	6
Cable guards	1	2	3
Personnel total	4	6	12

type of equipment and testing procedures may readily be seen in comparing the number of men used at Safe Harbor with the number of men at Ryburg-Schwoerstadt. In spite of the more elaborate equipment, considerable economies were accomplished at Safe Harbor.

Results and Conclusions of Initial Tests

(*a*) *Unit With False Roof.* The results of the tests made by means of the point and vertical-integration method with both meter types simultaneously and carried out at the unit provided with a false roof are shown in Fig. 22. The discharges indicated by each type of meter were plotted against the piezometer deflections simultaneously obtained, using a double logarithmic scale. It is to be observed that the two curves are very distinct

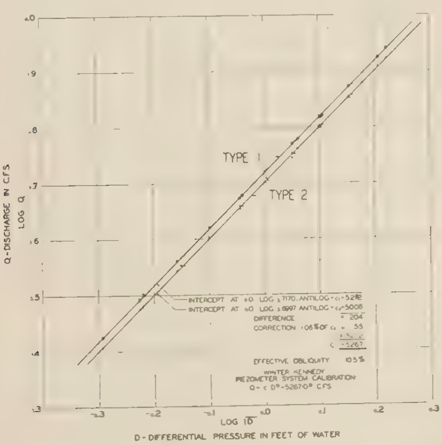

Fig. 22 Results of Tests Made on Unit With False Roof

and are parallel to each other, indicating that there is a constant percentage by which the type-1 and type-2 discharges differ from each other. By means of a correction curve similar to that shown in Fig. 19, the correction to be applied to the type 1 was found to be 1.06 per cent, which corresponds to an effective obliquity of 10.5 deg.

Values of such magnitude seem surprising in view of the care that had been taken to straighten out the flow approaching the metering section. It should be recalled, however, that even under the conditions which were made as nearly ideal as possible in the experiments conducted by the Research Institute at Obernach, the behavior of the meters indicated an effective angularity of 9 deg.

It must be emphasized that for this particular unit the obliquity observed is to a considerable extent an effective angularity of individual water particles and flow filaments, the latter accentuated by the screens rather than a general obliquity of flow. The latter may be exemplified by the position of a thin streamer and the former by the fluttering of the tail end. A similar phenomenon has been observed by Prof. C. M. Allen who demonstrated that salt injections in straight pipe lines spread very rapidly, even when flow is straightened out as much as possible.[5]

Since the angularity observed in these tests did not greatly exceed that which was found for the practically ideal conditions at Obernach, it appears that the flow lines had been straightened out very well by the use of the roof. In spite of this precaution, there remains an influence which may cause a single-type meter to under-register by more than 1 per cent. It is essential, therefore, in order to get correct results to make use of the two types of meter and not to depend entirely upon any means of straightening out the flow.

Since a wide range of velocities must be integrated by a meter traversing the intake, or even in a fixed position, an investigation was made at the Bureau of Standards to see if the accuracy was impaired by this phenomenon. Tests were made by varying the speed of the car carrying the meter through the tank. Most of the runs were made with two and four complete cycles of speed variation. For these tests the meters showed a slight tendency to under-register; the reason for this will be apparent when we consider that the speed of rotation is not strictly proportional to the velocity of the meter through the water. For velocities normally encountered in testing, and even for a considerable range between the high and the low portions of the cycles, the average effect can be shown to be very slight, but nevertheless always in the direction to under-register the flow.

Another series of runs was made for a half cycle of speed variation by gradually decelerating or accelerating the car during the whole length of the run. The inertia of the moving parts caused the meter to read slow when speeding up and fast when slowing down. Similar tests were conducted with the meter in an inclined position and the same results were obtained.

This work led to many other investigations and considerable interest has centered about the question of the ability of the meters to perform correctly under the conditions of test. For instance, it was thought that there might be some disturbing effect from the horizontal girders of the racks, Fig. 12.

It is contended by some that the conditions under which a meter operates in practice are by no means comparable with the rating in still water. Others hold the opinion that the meter receives myriads of impulses, each one of which is similar to movement through still water at some angle. Consequently, because it has not been found possible to make a meter rate fast in still water, regardless of the angle at which it is turned to the direction of travel, with the possible exception of that small range of angularity where type 2 shows a slight tendency to over-register at low velocity, it is argued that these meters would always indicate less than the true flow.

Of course it must be recognized that an eddy having its axis roughly parallel with that of the meter might cause gross over-registration, but the effect of this same eddy on a meter having the opposite direction of rotation would have an equally opposite effect. It was for this reason that left-hand and right-hand meters were used in alternate positions.

These tests at the Bureau of Standards have taken other interesting forms, consisting of deliberately disturbing the water ahead of the meter by rakes and planks. Care must be exercised not to set up a motion of the water either with or against the meter, or to set up an actual swirl either in the direction the meter is turning or in the opposite direction. It cannot be said that these particular tests were conducted under ideal conditions, but they have served to demonstrate the ability of a meter to plow through highly turbulent water without any appreciable effect upon the accuracy of registration.

[5] N.E.L.A. Engineering National Section, Minutes of Hydraulic Power Committee Meeting, Edgewater Beach Hotel, Chicago, October, 1932.

It is believed that, considering the great care taken in the observations, and the consistency of the test points when plotted as shown in Fig. 21, as well as the subsequent investigations regarding the behavior of the meters under various conditions in the rating tank, the interpretation of the results in determining the correction to be applied to type-1 meter appears to be entirely justified.

(b) *Unit Without False Roof.* The determination of the effective obliquity and the discharge correction from the data obtained by means of the vertical-integration method and separate application of type 1 and type 2 for the unit without the false roof was more difficult. If the difference in discharges registered by the two types of meters were used, a correction of 3.8 per cent should have been applied to the type-1 discharge measurements. It did not appear reasonable that the correction for the unit without the false roof would be so much larger than the correction for the unit with the roof, even though the plane of measurement had been moved upstream into the emergency-gate slots.

A careful restudy of the chart records obtained by the vertical-integration method disclosed the fact that some type-2 meters had stopped rotating in all three intake bays in the vicinity of the ceiling. It was thought possible that the convergence of the streamlines might have exceeded the angle at which the meter stalls.

To determine this angle accurately, further tests were made at the Bureau of Standards. By extending the range of obliquity above 30 deg it was found that the type-2 meter stalled for an angularity greater than about 34 deg regardless of the velocity. This is, of course, a fault which it is desirable to eliminate.

Since the departure from the cosine and consequently the tendency to stall increases with the pitch, it is possible to remedy this condition by constructing a meter with a shorter pitch, Fig. 18. At the time of purchase it was thought that the angularity would not exceed the range of satisfactory performance of this type-2 propeller. For the sake of accentuating the difference and securing greater accuracy in making the correction, a meter was obtained which would differ as much as possible from the type 1.

(c) *Service Unit.* Great difficulties were also encountered at this unit which prevented the obtaining of a true discharge by combining type-1 and type-2 measurements. Aside from exceedingly low velocity, excessive angularity in a horizontal direction was encountered. This additional obliquity was caused by the fact that no main units were installed at that time on the river side of this service unit. Since the water for all the units has to approach the intakes from the river side, it is obvious that the water for the house units must flow almost parallel to the longitudinal axis of the power house.

In spite of all these unfavorable circumstances, the type-1 measurements appeared to be satisfactory as the performance range was not exceeded either by angularity or by low velocity. The type-2 meters, however, stopped almost over the whole vertical half of the intake toward the river side. Where the stoppage occurred for the type 2, the type 1 indicated very low velocity. To come to any conclusions regarding the magnitude of correction was impossible, and it was realized that the performance range of the type-2 meter had also been exceeded at this unit.

Subsequent Tests

The results of the tests which were carried out during 1932, as previously described, showed clearly the limitations of the equipment.

To remedy this condition a variety of current-meter propellers of old and new design were investigated at the Ott laboratory. The object was to find a suitable propeller to be used in conjunction with the type 1 and which would operate satisfactorily even under extreme oblique-flow conditions. Most desirable was a spoked-vane propeller design, since it had been indicated by the oblique-flow calibration of the type 1 that variations in velocity would not change the oblique-flow characteristic. This investigation, however, was not confined to spoke-vane propellers having various pitches and vane shapes, but it included conical-screw propellers of the two-vane and three-vane type. The upper and lower limits in pitch were 70 and 15 cm, respectively. Based on the results, it appeared that the most favorable solution would be to replace the type-2 meters of conical shape and 50-cm pitch with a spoked-vane propeller of 15-cm pitch, which will be called type 3 hereafter. Its oblique-flow characteristic lay between the type 1 and the cosine line, Fig. 17, and in view of this it was expected that the type-3 meter would indicate more water, that is to say, would under-register less than the type 1. The stalling angle of the type 3 was found to be above 70 deg. It was apparent that the relation between the cosine of the angle of obliquity and the amount of registration was a straight line and consistent from 0 deg to well above 60 deg. The high degree of relative precision obtained during the previous discharge measurements, to be discussed later, indicated that even in case the oblique-flow characteristic would not differ a substantial amount, reliable results could be expected by the two-type meter method employing type-1 and type-3 meters.

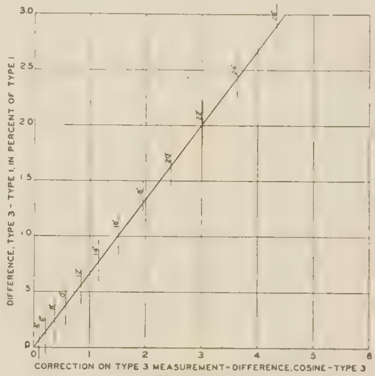

Fig. 23 Correction Curves Using Type-3 and Type-1 Meters

Discharge measurements were made first at the unit previously tested without false work, employing the type-1 and type-2 meters separately, and using throughout the vertical-integration method. The computation of the discharges was simplified considerably by substituting an analytical method for the tedious process of planimetering the discharge diagrams. The weight given each current meter was half the distance between the two adjacent ones on either side. For the first and second meters from the wall, the proper weights were obtained from the pitot-tube investigation in proximity of the walls.

The correction to be applied on the type-3 measurements was found to be 1.23 per cent, indicating an effective obliquity of 14 deg (see Fig. 23) which corresponds to a correction of 2.09 per cent on the type-1 meter.

Additional tests of the same unit were made but without the trash racks in place. The results indicated that the effective obliquity was slightly less when compared with the one previously obtained. The discharges, however, as indicated by the two-type meter method were identical for both series of tests.

The service unit was also retested employing a like procedure. The results indicated a discharge correction of 1.60 per cent on the type 3, corresponding to an effective obliquity of 16.5 deg.

Consistency and Relative Precision of Water Gaging

The simultaneous application of two methods of water measurement, such as current-meter and index methods, permits an analytical determination of the consistency of the test results. A measure of the consistency is the average departure of the ratio of the discharge to the square root of piezometer deflection from the mean value of this ratio, given in Table 4. Where index-method facilities are not available, the consistency of the water gagings comprising the whole discharge range cannot be determined, but it will be confined to one particular discharge arrived at by repeated tests under identical conditions.

It is customary abroad to evaluate whenever possible the probable error of the measurements by means of the method of least squares. It must be emphasized, however, that the term "probable error" is misleading since the measurements usually are not compared with an absolute standard such as volumetric measurements. It is obvious that any method except the latter has inherent errors and, as long as the probable error of the test results is determined independent of an absolute standard, departures are obtained which are relative and not absolute.

TABLE 4 DETERMINATION OF CONSISTENCY AND RELATIVE PRECISION OF TYPE-1 CURRENT METERS AND INDEX TESTS, UNIT WITH FALSE ROOF

Test run	Q for type-1 meter cfs. uncor. for head	Square root of standard deflection, $\sqrt{D}$	$Q/\sqrt{D}$	Departures δ	Departures Per cent	δ^2
1	4752	1.677	2834	−16	0.56	256
2	3687	1.295	2847	− 3	0.11	9
3	6571	2.311	2843	− 7	0.25	21
4	8729	3.042	2869	+19	0.67	362
5	8401	2.954	2844	− 6	0.21	36
6	7875	2.767	2846	− 4	0.14	16
7	7426	2.607	2848	− 2	0.07	4
8	6651	2.328	2857	+ 7	0.25	49
9	5987	2.105	2844	− 6	0.21	36
10	5994	2.112	2838	−12	0.42	144
11	5887	2.062	2854	+ 4	0.14	16
12	5289	1.851	2857	+ 7	0.25	49
13	4726	1.655	2855	+ 5	0.18	25
14	4174	1.465	2849	− 1	0.04	1
15	3632	1.272	2855	+ 5	0.18	25
16	3115	1.089	2860	+10	0.35	100
17	2657	0.933	2848	− 2	0.07	4
			Avg = 2850		Avg = 0.24	$\Sigma\delta^2$ = 1153

Consistency or average departure of one measurement = ± 0.24%
Mean departure of one measurement = $\pm\sqrt{[\Sigma\delta^2/(n-1)]} = \pm\sqrt{(1153/16)} = \pm 8.5 = \pm 0.30\%$
Mean departure of all measurements = $\pm\sqrt{[\Sigma\delta^2/n(n-1)]} = \pm\sqrt{[1153/(17\times 16)]} = \pm 2.2 = \pm 0.08\%$
Relative precision of all measurements = $0.674 \times 0.08\% = \pm 0.054\%$

Table 4 shows the determination of the relative precision of the type-1 measurements made by the vertical-integration method on the unit with the false roof. The high degree of relative precision may be attributed to various reasons, such as the elimination of the personal equation in obtaining the data in the field and the new type of rating curve. In addition, it is believed that the second impulses obtained from the Warren master clock helped to eliminate one source of error which often consistently impairs the accuracy of testing procedures.

It is noteworthy that identical relative precisions were obtained for the point and the vertical-integration method on the unit with the false roof. Since the same number of measurements and identical piezometers were used for the derivation of the relative precision and in addition the same average ratios of discharge to square root of deflection were found, the two methods must be of like accuracy.

Critical Review

Experience gained at Safe Harbor shows that back flow is likely to occur as soon as the minimum section or the section of parallel boundaries has been reached. Even in slightly converging passages, such as used at Ryburg-Schwoerstadt, reversals have been observed. It would be far better, from this point of view, to make current-meter measurements at low-head power plants without the false roof where the flow is converging to a high degree as in the Safe Harbor units.

In the light of the test results obtained at the unit with the false roof in the intake, it is believed that even where a parallel approach is provided to the gaging section, two types of meter must be used to allow for the effective obliquity.

It should not be concluded that the necessity of two meter types would make this method uneconomical. It has been found at Safe Harbor that by means of the integration procedures, far-reaching savings may be made over the point method. For instance, the discharge for two runs by means of the integration method with both meters used separately could be computed by one man in a day, whereas at least four days were consumed for only one type of current meter for the point method.

It is not necessary to confine the integration method to procedures with vertical traverses. Where the depth of water passages is small in comparison to the width, horizontal traverses may be of advantage. In case current meters should be used in penstocks, in spite of the advantages of the methods sponsored by Gibson and Allen, the current meters may be mounted on a supporting rod pivoted in the penstock center. By means of a suitable gear mechanism, the rod may revolve so that the current meters describe a circular path. A position indicator, geared to the driving mechanism of the rod, permits the determination of the rod position from the chart records of the graphic recorders.

It has been shown that the measurements with both types of current meter may be made separately to good advantage. Should the two-type meter method be contemplated elsewhere, it would be necessary to provide only one set of bodies including axles for the two sets of propellers. Following this suggestion, a considerable saving may be made in the cost of graphic recorders and other equipment.

With reference to the current meters themselves it would be of advantage to select two meter types having a ratio of underregistration somewhat more suitable than the ratio of type 1 and type 3. Here the correction to be applied on the type-3 measurements is one and one-half times the difference between the indications of type 1 and type 3. It is believed that two spoke-vane propeller types having 15-cm and 30-cm pitch, respectively, would be more desirable since the correction on the shorter-pitch meter would be about equal to the difference between the discharges indicated by the two types of current meter.

The index method of testing has been extremely valuable, especially in the determination of the proper cam shape, as well as in conjunction with the current-meter measurements to show the consistency of the test results. It may be emphasized, however, that at Safe Harbor, the power company determined the proper shape of the cam, in spite of the fact that the cam is an integral part of the turbine. As the purchaser is naturally interested in obtaining the best possible cam shape, he may relieve the turbine manufacturer of this phase of the turbine design.

This should not become the customary procedure and by no means should it be necessary for the sake of economy to sacrifice testing on the cam for the tests to determine the cam shape. It is believed that final acceptance tests of Kaplan units should always be made on the cam which will be used under normal operating conditions.

Based on the experience gained in connection with the Safe Harbor tests, it appears that the effective angularity is much

greater than was previously expected and that measurements may be made to good advantage at locations of converging flow. It would be bad policy, therefore, to set a definite limitation regarding the obliquity and say that the measurements are unreliable when the angularity is more than a certain amount. The limitation of angularity should not be specified, but attention should be called to the fact that the angularity should not exceed the performance range of either of the two meters used.

At the present stage of development in the art of water measurement, it is believed that economies which may be achieved through improved testing procedures and through the omission of temporary installations, as well as the possibility of gaging the discharge under operating conditions, make the current-meter method more attractive and economically more feasible. It is hoped that the record of the Safe Harbor tests, as outlined in this paper, will contribute to a better understanding of the problems involved in water gagings by means of current meters. Since in recent hydroelectric construction in the low-head field there is a marked tendency toward further shortening of the length of water passages, which may render other methods of measurements more difficult, a careful study of current-meter methods is, at this time, very desirable.

Acknowledgments

The publication of this paper was made possible by the support received from J. A. Walls, president, Safe Harbor Water Power Corp. The author wishes to express his appreciation for the cooperation rendered by Walter F. Stutz of the U. S. Bureau of Standards, Washington, D. C., under whose supervision the current-meter investigation was carried out at the Bureau. The interest shown by the engineers of the S. Morgan Smith Company and the I. P. Morris Division of Baldwin-Southwark Corporation, turbine manufacturers, is also appreciated. The joint effort made by all engineers of the Safe Harbor Water Power Corp. engaged in these tests has contributed an important part in the advance made in the art of water measurements.

BIBLIOGRAPHY

1 "Messen und Teilen von Wasser in Niederdruckanlagen" (Gaging and Dividing of Water in Low Head Power Plants), by S. Bitterli. Verhandlungen der Schweiz. Naturforschenden Gesellschaft, Bern, 1922, vol. 2, pp. 331–339.

2 "Wassermessungen bei Grosskraftanlangen" (Water Measurements at Large Hydroelectric Power Stations), by H. F. Canaan, Wasserkraft-Jahrbuch, 1930.

3 "Fluegel-Wassermessungen in Druckrohrleitungen" (Water Measurements by Means of Current Meters in Penstocks), by H. Dufour, *Schweizerische Bauzeitung*, vol. 83, 1934, p. 39.

4 "Vergleichstarierungen der Hydrometrischen Fluegel" (Comparative Calibrations of Water Current Meters), by S. Kolupaila, Report of the fourth hydrological conference of the Baltic States, Section IX, Leningrad, U.S.S.R., Sept., 1933.

5 "Water Gaging for Kaplan Units of High Capacity at Safe Harbor," by J. M. Mousson, *The Baltimore Engineer*, vol. 8, 1934, nos. 9 and 10; *Canadian Engineer*, vol. 66, 1933, no. 23 and vol. 67, 1934, no. 1.

6 "Wassermessungen in einen Grosskraftwerk" (Water Measurements at a Large Power Development), by J. M. Mousson, *Zeit V.D.I.*, vol. 78, 1934, no. 46, pp. 1343–1346.

7 "Wassermessungen bei Wasserkraftanlagen" (Water Measurements at Water Power Plants), by L. A. Ott, Wasserkraft-Jahrbuch, 1924, pp. 263–265.

8 "Résultats des essais effectués sur les groupes électrogènes de l'usine Chancy-Pougny" (Results of Tests Made on the Hydroelectric Units at Chancy-Pougny), by P. Perrochet, *Schweizerische Bauzeitung*, vol. 87, 1926, p. 241.

9 "Wassermengenbestimmung mit Bandchronograph im Kraftwerk Faal a.d. Drau" (Water Measurements With Graphic Recorder at the Faal Power Plant on the Drau River), by P. Perrochet and C. Montadon, *Schweizerische Bauzeitung*, vol. 91, 1928.

10 "Misure di portate negli impianti idroelettrici eseguite col metode Gibson" (Measurements by Gibson Method for Determination of Discharge at Hydroelectric Plants), by E. Scimemi, *Energia Elettrical*, vol. 8, December, 1931, no. 12, pp. 1029–1036.

11 "Der Genauigkeitsgrad von Fluegelmessungen bei Wasserkraftanlagen" (The Precision of Current Meter Measurements at Water Power Plants), by A. Staus, Julius Springer, Berlin, 1926.

12 "Effect of Turbulence on the Registration of Current Meters," by D. L. Yarnell and F. A. Nagler, Trans. A.S.C.E., December, 1929, vol. 55, pp. 2611–2640, bibliography pp. 2636–2640.

Note: This bibliography is necessarily incomplete, since only publications were compiled which had direct bearing on the subject. For a more complete list of references see the Engineering Index.

Draft-Gear Action in Long Trains

By O. R. WIKANDER,[1] PITTSBURGH, PA.

This paper is a study of the coupler pressures, car speeds and accelerations in a long train, produced by external forces acting on same.

It is based on the similarity in behavior of such a train and of an elastic bar of the same length as the train, the same mass per unit length and the same yield, when subjected to longitudinal compressive or tensile forces.

Following the method explained in the paper, the pressure and speed diagrams are derived for the various periods through which the waves are passing, the beginning and ending of each period being marked by certain events. Formulas are derived for the maximum bar pressures and tensions, for the locations at which they occur, and for the maximum accelerations or retardations of the particles.

It is shown how these formulas may be applied to freight trains of known characteristics, and the general requirements are derived which should be met by a freight-car draft gear under given service conditions.

Well-known elementary calculations, based on the official ARA Draft Gear Tests and supplemented by the formulas given in the paper, permit the design of draft gears suitable for the given service conditions.

Introduction

When a long train is subjected to external forces, accelerating or retarding, the work performed or consumed by these forces is partly used to accelerate or retard the moving masses, partly to overcome train resistance, partly to compress the draft gears which connect adjacent cars, and to some extent to stretch or compress the car bodies themselves.

The action of the external forces produces different coupler pressures or tensions, car speeds, accelerations, and retardations in different parts of the train, depending on the nature of the forces, as well as on the elastic and mass properties of the train.

[1] Mechanical Engineer, Ring Spring Department, Edgewater Steel Company, Pittsburgh, Pa. Mem. A.S.M.E. Mr. Wikander received the degree of mechanical engineer in 1895 from the Technical Academy, Chemitz, Saxony, and the degree of electrical engineer in 1899 from the Technical University, Karlsruhe, Germany. He was affiliated with the electrical laboratory of the Société Decauville, Corbeil, in 1899; the Compagnie d'Électricité Thomson-Houston de la Méditerranée, Paris, in 1900, as electrical engineer; the National Tube Company, McKeesport, Pa., in 1903, as assistant chief electrician; and with the Westinghouse Electric and Manufacturing Company, East Pittsburgh, Pa., from 1904 to 1906 and later from 1909 to 1911. In 1905 Mr. Wikander was appointed chief of the experimental department, General Electric Company of Sweden but the following year became commercial attaché at the Swedish legation of Buenos Aires, Argentina. From 1911 to 1918 he was employed as designing and later sales engineer, with the Hall Steam Pump Company, Pittsburgh, Pa. In 1918 he became consulting engineer for the SKF Industries, Inc., New York, N. Y. He practiced as consulting engineer from 1922 to 1925 in which year he became affiliated with the Edgewater Steel Company.

Contributed by the Railroad Division and presented at the Annual Meeting, New York, N. Y., December 3 to 7, 1934, of The American Society of Mechanical Engineers.

Discussion of this paper should be addressed to the Secretary, A.S.M.E., 29 West 39th Street, New York, N. Y., and will be accepted until October 10, 1935, for publication at a later date.

Investigations of the action of external forces are of fundamental importance for the solution of draft-gear and air-brake problems and for a better understanding of the inter-relation of the action of these important parts of the equipment of long trains.

In the following investigation the action of the external forces is analyzed according to a method particularly suited for the purpose, but which apparently has never been applied before to any great extent to problems of this nature.

This method is based on the theory of wave transmission in elastic solid mediums. Its use in solving train dynamic problems was suggested in a paper by L. H. Donnell.[2]

According to this method, a long train is assumed to be mechanically equivalent to an elastic bar of the same length, the same mass per unit length, and the same yield under compression or tension. This assumption is only fairly correct because (1) no allowance is made for the free train slack, (2) the elastic bar is assumed to follow Hooke's law which states that strain is proportional to the stress, while friction draft gears only approximately follow this law, (3) the bar is supposed to be perfectly elastic, while the dampening effect of friction draft gears reduces the recoil forces in a long train, and (4) the elastic bar is assumed to have a uniformly distributed mass, while the mass distribution in a long train is not always even approximately uniform.

In order not to overburden this paper with special cases the following investigation of an elastic bar has been limited to the case of a bar with uniform elastic and mass properties.

The case of partial application of uniformly distributed forces has been included because it corresponds to the action of the type-K air brake, which is in general use at the present time.

It would seem that a long train could always be represented by an elastic bar with both ends free and that the investigation of elastic bars with one or both ends fixed would have no bearing on train dynamic problems and might have been omitted.

A fixed end of a bar corresponds, however, to a very sudden and great increase in its wave resistance and is comparable to the condition when a pressure wave traveling in an empty train strikes a group of fully loaded cars, and represents the extreme consequences of such a condition.

They show that the investigation of an elastic bar with uniform mass and elastic properties and both ends free only applies to trains with fairly uniformly distributed loads. Unusual load distribution, such as long trains composed of alternating strings of empty and loaded cars, require special investigation, which can be carried out by the use of the formulas given for reflected waves.

1 Longitudinal Waves in an Elastic Bar

Graphic Illustration of Dynamic Action in Long Bars

In a long bar the pressures, the particle speeds, accelerations, and retardations change not only from point to point in the bar but also from moment to moment at each particular point. It is therefore difficult to represent the action of the external forces in diagrams with only two coordinates.

The method herein used to derive and represent the dynamic conditions in a long bar at a certain moment involves the use of two diagrams, one directly below the other, and, taken together, they portray the dynamic conditions of the bar at that moment.

[2] "Longitudinal Wave Transmission and Impact," by L. H. Donnell, Trans. A.S.M.E., 1930, vol. 52, paper APM-52-14-153.

The upper diagram usually represents the compression or tension in the bar, and is called the pressure diagram, while the lower one usually represents the speed of the particles at each point of the bar. If not otherwise qualified the word "speed" denotes the speed of the particles of the bar. In these diagrams the horizontal base line represents the length of the bar.

Several sets of diagrams may be shown in the same drawing, thus illustrating the gradual change in the dynamic conditions in the bar during a certain period of time.

Where the propagation speed of pressure or particle speed is constant the horizontal distance between two points in the pressure or speed diagram represents the time required for a pressure or speed wave to travel the distance between the points.

Since the change in the length of a bar, produced by longitudinal forces, is negligible as a rule, the base lines of the pressure and speed diagrams are of constant length.

A pressure at any point of a bar is represented by a positive ordinate or an ordinate above the base line. A tension is represented by a negative ordinate or an ordinate below the base line in the pressure diagram.

A concentrated external force is represented as an ordinate at its point of application, positive or above the base line if the force acts in the direction from left to right, and negative or below the base line if it acts in the opposite direction.

A distributed external force is represented by a curve in the pressure diagram and the ordinate at any point of this curve is equal to the algebraic sum of the external forces applying to parts at the left of this point, forces acting in the direction from left to right being considered positive and those acting in the opposite direction being considered as negative.

The speed of particles at any point of the speed diagram is represented by a positive ordinate, or an ordinate above the base line if the particles move from left to right, and by a negative ordinate, or an ordinate below the base line if they move in the opposite direction.

Further details as to the design and use of the pressure and speed diagrams will be given in the course of the discussion of the various problems.

Speed of Pressure Propagation in an Elastic Bar

It is known from the theory of sound that a pressure acting on an elastic body of uniform mass and elastic properties will propagate itself through the body at a constant speed, depending only on these properties.

When applied to an elastic bar of uniform cross-section and constant modulus of elasticity, this speed is expressed by the equation

$$V = \sqrt{(k/m)} \quad \text{[1]}$$

where V = speed of pressure propagation, fps; k = stiffness constant or modulus of elasticity of the material in lb per sq in. multiplied by the cross-sectional area of the bar in sq in.; and m = mass per ft of length.

Example. If Equation [1] is applied to a bar of 1 sq in. sectional area weighing 3.4 lb per ft, $k = 30 \times 10^6$ lb per sq in., $m = 3.4/32.17 = 0.1058$ = mass per ft, and $V = \sqrt{(30 \times 10^6/0.1058)} = 16{,}800$ fps.

Speed of Particles in a Perfectly Elastic Bar

A pressure wave passing through a bar produces a speed of the particles in the direction of the wave. This speed depends on the pressure to which the particle is subjected and on the physical characteristics of the bar, i.e., on m, its mass per foot of length, and on k, its stiffness constant. The relation between these quantities is expressed by the equation

$$c = \frac{f}{\sqrt{(mk)}} \quad \text{or} \quad f = c\sqrt{(mk)} \quad \text{[2]}$$

where c = speed of the particles in the direction of the wave, ft per sec, and f = pressure to which the particles are subject, lb.

The denominator $\sqrt{(mk)}$ is a constant which depends only on the physical properties of the bar. Thus, the bar pressure and the speed of the particles are proportional. A pressure wave therefore produces a speed wave of the same speed as itself.

If the end of a bar is subjected to a tension force, the tension wave will move in the direction opposite to that of the force, while the speed of the particles always has the same direction as the force which creates it.

The relationship expressed by Equation [2] applies only to waves produced in a stationary bar and only to waves which have not been reflected.

The expression $\sqrt{(mk)}$ has a certain analogy to an electric resistance and will for the sake of convenience be called the wave resistance of the bar. (This quantity corresponds to the acoustic resistance of a medium, as defined by H. Brillié, in *Le Génie Civil*, August 23 and 30, 1919.)

If the wave resistance of an elastic bar is designated by R_w, Equation [2] can be written as

$$c = f/R_w \text{ or } f = cR_w \quad \text{[2a]}$$

Reflected Pressure and Speed Waves

If the mass or the stiffness constant of a bar suddenly changes the wave resistance will also change and the wave motion will be disturbed.

Referring to Fig. 1, AB is an elastic bar, the part AC of which has the mass m per unit length, the stiffness constant k, and therefore the wave resistance $R_w = \sqrt{(mk)}$. The part CB of this bar has the mass m_1 per unit length, the stiffness constant k_1, and therefore the wave resistance $R_{w1} = \sqrt{(m_1k_1)}$.

Assuming that a constant force f, acting from A to B, is suddenly applied at the end A, a bar pressure f and a speed of the particles c are created, both of which travel from A to C at a wave speed V (see Equation [1]). After passing through the intermediate shapes represented by the rectangles over AC' and AC'', these waves both take the shape of the rectangle over AC as shown in Fig. 1 at the time they reach the point C.

Because of the change in wave resistance, which occurs at C, further development of the pressure wave is disturbed and, if the wave resistance is increased at C, the pressure wave proceeds as shown in Fig. 2, in which the rectangle over AC is taken from Fig. 1. The bar pressure at C, Fig. 2, increases an amount f', producing a reflected pressure wave of the height f' superimposed on the original pressure wave of the height f and traveling back from C to A. The total pressure f_1 at C, Fig. 2, produces a transmitted wave which travels from C to B at the speed $V' = \sqrt{(k_1/m_1)}$.

The speed diagram, Fig. 2A, corresponds to the pressure diagram in Fig. 2. Increase in the wave resistance at C causes the particle speed to drop the amount c' or from c to c_1. This drop c' in particle speed is reflected and travels from C toward A at the wave speed V, while the remaining speed c_1 is transmitted from C to B at the wave speed V'.

The particle speed c_1 at C can be expressed in two ways

$$\left.\begin{aligned} c_1 &= (f - f')/R_w \\ \text{or } c_1 &= f_1/R_{w1} \end{aligned}\right\} \quad \text{[3]}$$

The pressure at C is

$$f_1 = f + f' \quad \text{[4]}$$

If $\sqrt{(m_1k_1)}/\sqrt{(mk)}$, the ratio of the wave resistances of the two parts of the bar, be designated as r, the forces f' and f_1, and the corresponding particle speeds c' and c_1 which they create, may be expressed as follows:

$$f' = \frac{r-1}{r+1}f \qquad [5]$$

$$f_1 = \frac{2r}{r+1}f \qquad [6]$$

$$c' = \frac{r-1}{r+1}c \qquad [7]$$

$$c_1 = \frac{2}{r+1}c \qquad [8]$$

If r is greater than unity in Equation [5], f' will be positive, causing an increase in the bar pressure above its original value f. If, however, r is less than unity in this equation, f' will be negative and will cause a decrease in the original bar pressure. The pressure f_1 is always positive.

In case the bar has a free end at the point, the ratio r will be equal to zero and

$$f' = -f \qquad [9]$$

which means that the original pressure wave will be reflected, changing its sign. Also, if $r = 0$ is substituted in Equation [6], $f_1 = 0$, or the pressure in the transmitted wave will be zero.

The particle speed produced by this additional force f' will be c' which, when deducted from the original speed c, gives for $r = 0$

$$c - c' = c - (-c) = c + c = 2c \qquad [10]$$

Therefore, it is seen that the speed of particles reaching a free end of a bar is also reflected but does not change its sign.

Likewise, the foregoing equations prove that for a fixed end of the bar, corresponding to a value of $r = \infty$, the additional pressure

$$f' = f \qquad [11]$$

and the speed of particles changes to

$$c - c' = c - c = 0 \qquad [12]$$

The bar pressure is reflected from a fixed end of a bar without change of sign while the speed of particles is reflected with change of sign.

If $r = 1$, there is no change in the wave resistance and f' as well as c' are equal to zero, while $f_1 = f$ and $c_1 = c$, as might be expected.

The rules which govern the reflection of pressure and speed waves at the end of a perfectly elastic bar may be expressed as follows:

1 A pressure wave reaching the free end of a bar is reflected, changing its sign.

2 A pressure wave reaching the fixed end of a bar is reflected without change of its sign.

3 A speed wave reaching the free end of a bar is reflected without change of its sign.

4 A speed wave reaching the fixed end of a bar is reflected, changing its sign.

Formation of Pressure and Speed Waves in a Perfectly Elastic Bar

(A) *Single External Force, Instantaneously Applied*

Referring to Fig. 3, assume that a constant force f is instantaneously applied at A of a perfectly elastic bar AB so as to act from A to B.

Such a force would be created by an infinite mass striking the end A at a speed c, which, multiplied by the wave resistance of the bar $\sqrt{(mk)}$ would produce the force f, expressed by Equation [2].

The material at the end of the bar to which the force is applied would be compressed, setting up a pressure in the bar which may be represented by the vertical line AC. Under the continued application of the force the compression will travel as a wave along the bar at a speed determined by the physical properties of the bar. See Equation [1].

The pressure distribution in the bar at successive intervals of time can be represented by the rectangles $ACC'A'$, $ACC''A''$, and $ACDB$. The last rectangle represents the pressure in the bar at the instant that the front of the pressure wave reaches the end B.

It is interesting to note that the ratio of the speed of particles c as given by Equation [2] to that of pressure and speed transmission V as given by Equation [1] can be expressed as

$$c/V = f/k \text{ or } c = (f/k)V \qquad [13]$$

and is therefore equal to the ratio of the bar pressure to the stiffness constant of the bar.

The diagram in Fig. 3 can therefore be considered as representing either the internal pressures or the speed of particles produced as the pressure f travels from one end of the bar to the other. From the moment that the pressure reaches the end of the bar the pressures and the particle speeds can no longer be represented by the same diagram. The subsequent changes in pressures and speeds will depend on whether the end B is free or fixed.

If this end is free, the pressure will drop to zero and a tension wave traveling from B to A at the speed V will gradually reduce the pressure diagram to the rectangles $AA''C''C$ and $AA'C'C$ until it disappears into the vertical AC.

If at this moment the force f continues to act, it will produce a new pressure wave which will again travel to the end B of the bar and again recede to zero, this process continually repeating itself as long as the force f continues to act.

The speed diagram which is identical with the pressure diagram, Fig. 3, except for the scale, until the front of the wave reaches the end B of the bar, is illustrated in Fig. 3A, in which the rectangle $ABDC$ has been taken from Fig. 3.

The sudden drop of the pressure at the end B will increase the speed of the particles at this point to the value $BE = 2BD$. The wave front DE of the speed wave will travel from B to A in unison with the receding pressure wave and take the consecutive positions $E''C''$ and $E'C'$ until it reaches the position CF and the speed diagram takes the shape of the rectangle $ABEF$. If the force f continues to act, the speed of the particles at the point A will increase the amount $FG = CF = AC$, and the speed-wave front GF will travel from A to B, taking the intermediate positions $G'E'$ and $G''E''$ until it reaches the position EH. The speed diagram takes the shape of the rectangle $ABHG$.

If the end B of the bar AB is fixed the pressure diagram is represented by Fig. 3A. When the front of the pressure wave reaches the fixed end B it is reflected without change of sign from B to A, the wave front DE taking the intermediate positions $C''E''$ and $C'E'$ until it reaches the position CF. The pressure diagram takes the shape of the rectangle $ABEF$.

If an infinite mass moving at the speed c produced the pressure f, it would suddenly increase the pressure to $3f$, or from AC to AG, Fig. 3A, as the reflected pressure wave reaches A. Upon its next return this force would increase to $5f$. The increases in force continue in this manner until the bar pressure becomes infinite.

Therefore, if the end B of the bar is free, Fig. 3 represents the pressure on the bar and Fig. 3A represents the speed of the particles, while if the end B is fixed, the pressure is represented by Fig. 3A and the speed by Fig. 3.

(*B*) *Single External Force Gradually Applied and Removed*

Referring to Fig. 4, AB is a long bar of uniform cross-section and constant modulus of elasticity. If a compressive force acting longitudinally at the end of the bar is gradually and uniformly increasing from zero to the value f during the time t, it will create a pressure wave, represented by the triangle ACD, traveling from A to B at the pressure-propagation speed V. The inclined cross-sectional lines represent the consecutive positions of the wave front. The vertical AD represents the force f while the horizontal AC represents the distance L the pressure has traveled in the time t.

Every particle of the part AC of the bar has, under the influence of the force f, been given a certain speed c which according to Equation [13] is smaller than the speed of pressure transmission in the same ratio as the force f is smaller than the stiffness constant of the bar.

The time t during which the pressure f was attained does not affect the resulting speed of the particles. The diagram ACD represents the speed c of the particles at the time t as well as the internal pressure in the bar, although the scales of course are different.

If the force f remains constant for a certain length of time t_1, referring to Fig. 5, the wave front CD, taken from Fig. 4 and shown in thin lines, will then have traveled the distance DD_1 and have reached the position C_1D_1. The pressure distribution in the bar is then represented by the area AC_1D_1D. The inclined cross-sectional lines represent the consecutive fronts of the pressure area during the time t_1. It also represents the speed of the particles, as previously explained.

With reference to Fig. 6, assume that the force f decreases gradually to zero during the time t_2. If the material of the bar is perfectly elastic or free from mechanical hysteresis, the pressure area AC_1D_1D, which has been taken from Fig. 5 and is shown in thin lines, will, during the time t_2, have traveled the distance L_2 without changing its shape and will be represented by the area $A_1C_2D_2D_3$. While the force f decreases during the time t_2, the pressure and speed line AD_3 will be formed and the particles in AA_1 of the bar will be retarded gradually until those at A return to a standstill, after the time t_2. At this time the pressure and speed diagram has taken the shape $AC_2D_2D_3$ and is moving from A to B at the constant speed V without changing its shape.

At the instant illustrated by Fig. 6 the pressure (and speed) history during the interval t_2 is represented by the successive positions of the dot-and-dash lines. It starts from the point D when the pressure f begins to decrease and progresses to the position AD when the force f at A has become zero. In the meantime the point D, at which the decrease in pressure began, has traveled to D_3.

When the quadrangle $AC_2D_2D_3$ passes beyond the point B, it changes its shape in different ways for the pressure and the speed diagram, the change in shape depending on whether the end B of the bar is free or fixed.

When the End B of the Bar AB Is Free. Referring to Fig. 7, it is assumed that the pressure and speed wave, represented by the quadrangle $AC_2D_2D_3$ taken from Fig. 6 and shown in light full lines, has traveled until it would have reached the position $A_2C_3D_5D_4$ if the bar AB had extended far enough. The part BC_3E of this quadrangle, which would extend beyond the free end B, is reflected and changes its sign. Hence, an equivalent area, represented by the triangle BD_5E is deducted from the remaining pressure area, forming a resulting pressure diagram represented by the quadrangle $A_2BD_5D_4$. The inclined dashed lines within the area $AA_2D_4D_3$ represent intermediate positions of the rear of the wave as it progresses from AD_3 to A_2D_4. The dashed lines within the area $BC_2D_2D_5$ represent intermediate positions of the wave front as it advances from C_2D_2 to BD_5.

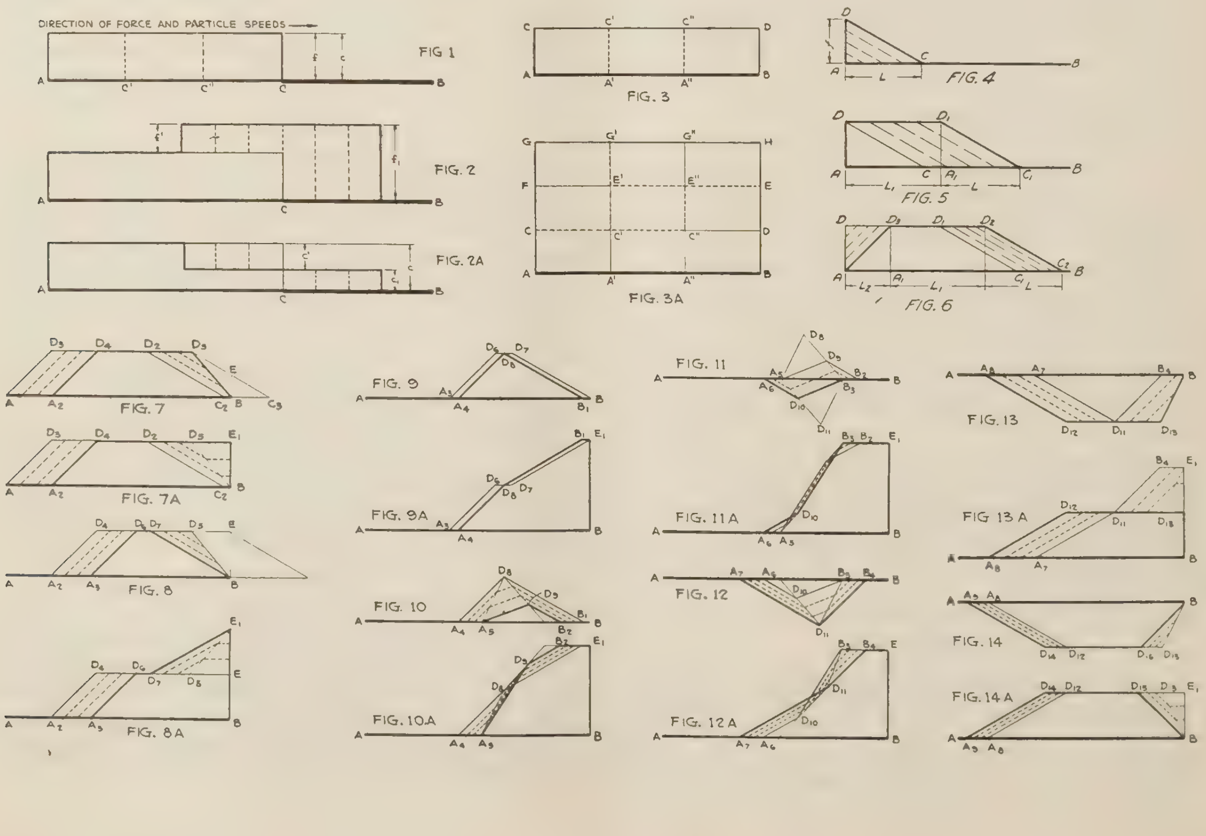

The corresponding speed diagram is shown in Fig. 7*A*. In this case, the part of the wave which would project beyond the free end *B* is reflected without change of sign and, adding itself to the, as yet, unreflected part, passes through the intermediate shapes, shown in dashed lines within the quadrangle BC_2D_2E, until the speed wave takes the shape of the quadrangle $A_2BE_1D_4$ at the time the pressure diagram assumes the shape shown in Fig. 7.

Figs. 8, 9, 10, 11, 12, 13, and 14 show consecutive shapes of the pressure diagrams which are produced when the wave is reflected at the free end of a bar. Likewise Figs. 8*A*, 9*A*, 10*A*, 11*A*, 12*A*, 13*A*, and 14*A* show consecutive shapes of the corresponding speed diagrams.

When the End B of the Bar AB Is Fixed, the diagram representing the speed of the particles is as shown in Fig. 7, while Fig. 7*A* is the pressure diagram. The latter part of the pressure diagram, Fig. 7*A*, which would extend beyond the end *B* is reflected without change of sign and, after the front of the wave has passed through the intermediate shapes represented by the dashed lines in Fig. 7*A*, the pressure diagram assumes the shape of the quadrangle $A_2BE_1D_4$. Referring to the speed diagram, Fig. 7, the part BC_3E which extends beyond the fixed end *B* of the bar is reflected, changes its sign and is deducted from the, as yet, unreflected part of the diagram. The front of the speed wave passes through the intermediate shapes, represented by the dashed lines in Fig. 7, until the speed diagram takes the shape of the quadrangle $A_2BD_5D_4$, shown in the same figure.

Figs. 7, 8, 9, 10, 11, 12, 13, and 14 are the speed diagrams and Figs. 7*A*, 8*A*, 9*A*, 10*A*, 11*A*, 12*A*, 13*A*, and 14*A* are the corresponding pressure diagrams, derived for a bar with the end *B* fixed. Corresponding points in the speed diagrams and pressure diagrams are marked with the same symbols.

(*C*) *Uniformly Distributed External Forces Gradually Applied*

Referring to Fig. 15, *AB* is a perfectly elastic bar subjected to external longitudinal forces acting from *A* to *B*, the application beginning at *A* and gradually progressing to *B* at a constant rate of force application, corresponding to the gradual application of the brakes in a long train. It is proposed to determine the pressures produced by these forces as well as the speeds imparted to the particles of the bar.

The formation of the waves will be somewhat different, depending on whether the ratio of the speed of pressure transmission to the rate of force application is greater than, equal to, or smaller than unity. The reflection of the waves from the ends of the bar also will be different, depending on whether the ends are free or fixed.

In every case the formation of the waves can be subdivided into a number of distinct periods, the transition from one period to the other being marked by certain events. Diagrams, showing the dynamic conditions of the bar at each transition point and at two intermediate points during each period, as well as analytical expressions of various quantities, will be used to illustrate the formation and to compute the magnitude of the pressure and speed waves in the bar. Pressure and speed diagrams have been investigated for the cases listed in Table 1.

Case 1, Period 1. This period begins with the application of the force and continues until the pressure wave reaches the rear end of the bar. Let the vertical *BO* in Fig. 15 represent the total longitudinal force which is to be gradually and uniformly applied over the bar *AB*.

TABLE 1 CASES AND CONDITIONS OF PRESSURE AND SPEED WAVES INVESTIGATED

Case 1	$p > 1$	End *A* free	End *B* free
Case 2	$p = 1$	End *A* free	End *B* free
Case 3	$p < 1$	End *A* free	End *B* free
Case 1*A*	$p > 1$	End *A* free	End *B* fixed
Case 2*A*	$p = 1$	End *A* free	End *B* fixed
Case 3*A*	$p < 1$	End *A* free	End *B* fixed
Case 1*B*	$p > 1$	End *A* fixed	End *B* free
Case 2*B*	$p = 1$	End *A* fixed	End *B* free
Case 3*B*	$p < 1$	End *A* fixed	End *B* free
Case 1*C*	$p > 1$	End *A* fixed	End *B* fixed
Case 2*C*	$p = 1$	End *A* fixed	End *B* fixed
Case 3*C*	$p < 1$	End *A* fixed	End *B* fixed

After a certain time *t* the force application may have progressed to a point C'' on the bar *AB*. The longitudinal force distributed over the part AC'' of the bar is represented by the vertical $C''D''$. The force acting at each point of the part AC'' divides into a tension force and a compression force of equal magnitude. This results in a uniformly distributed force $C''E''$ equal to $^1/_2\ C''D''$, producing a compression wave, plus a uniformly distributed force $C''F''$, of the same magnitude as $C''E''$, producing a tension wave.

Since the speed of pressure transmission *V* is assumed to be greater than the rate of force application V_1, the compression produced when the external force began to act at *A* will have traveled to a point G'' beyond the point C'' by the time the force application reaches this latter point. The pressure distribution produced by the force $C''E$ is then represented by the triangle $AE''G''$. If the bar had extended beyond *A*, the tension wave would have traveled a distance $AH'' = AG''$ and the tension distribution produced by the tension force $C''F''$ would have been represented by the triangle $AF''H''$.

The part $AH''J''$ of this tension triangle, which extends beyond the free end *A* of the bar, is reflected, changes its sign, and forms the pressure area $AJ''K''$. If the tension area $AF''J''$ is subtracted from the pressure area $AJ''K''$, a pressure area $F''J''K''$ remains. Adding this area to the pressure area $AE''G''$, the resulting pressure diagram is represented by triangle $AG''L''$.

The corresponding speed diagram, shown in Fig. 15*A*, is similarly constructed with the exception that the areas of the triangles $AE''G''$ and $AF''J''$ and that of the reflected triangle $AJ''H''$ are all added together, forming the speed diagram $AG''L''M''$.

After the pressure propagation has reached the rear end *B* of the bar, the pressure diagram has taken the form of the triangle *ABL*. The point *L* is the intersection of the extended line AL'' with the line *BL* drawn parallel to $G''L''$. The corresponding speed diagram is represented by the area *ABLM* in Fig. 15*A*. The point *L* has the same location in Fig. 15*A* as in Fig. 15.

This condition represents the end of the period. From the geometric relationships in these diagrams the following analytical expressions may be derived.

The vertical *CD* in Fig. 15 represents the total applied external force $= f_1 l_1$. The maximum occurring internal pressure at the end of this period is represented by the vertical *CL* and can be expressed as

$$P_1 = f_1 L \frac{1}{p+1} \qquad [14]$$

The location of the point *C* at which P_1 occurs is equal to *AC* or

$$l_1 = (1/p)L \qquad [15]$$

The acceleration of the part *AC* of the bar, to which the external forces have been applied, is equal to the accelerating force, represented by the vertical *CD*, less the retarding force, represented by the internal pressure *CL*, divided by the mass, represented by the horizontal *AC*, or

$$a_1 = \frac{CD - LC}{AC} = \frac{f_1}{m}\frac{1}{p+1} \qquad [16]$$

The acceleration of the part *BC* of the bar which has not as yet been reached by the force application is represented by the internal pressure $CL = P_1$ divided by the mass of the part *BC* of the bar on which it acts. This acceleration is

$$a_2 = \frac{CL}{BC} = \frac{f_1}{m}\frac{p}{p^2 - 1} \quad [17]$$

The time at which the pressure P_1 is reached may be expressed as

$$t_1 = L/V \quad [18]$$

and the speed, which the part AC has acquired after the time t_1, represented by the vertical CL in Fig. 15A, may be expressed as

$$c_1 = \frac{f_1 L}{mV}\frac{1}{p + 1} \quad [19]$$

Comparing Equation [14] for P_1 and Equation [19] for c_1, it will be noted that the vertical BO in Fig. 15 represents the sum f_1L of all the external forces ultimately acting on the bar, while the same vertical distance in the speed diagram would represent the expression f_1L/mV or the speed which the unit force f_1 acting on the unit mass m would impart to the mass during the time t_1.

The momentum of the bar at the time t_1 may be expressed as the average external force applied to the bar during the time t_1, multiplied by the time or

$$Q_1 = \frac{f_1 l_1}{2} t_1 = \frac{f_1 L^2}{V}\frac{1}{2p} \quad [20]$$

Up to this point the formation of the wave has been independent of whether the end B of the bar is free or fixed and, therefore, the above formulas apply to both Case 1 and Case 1A.

Case 1, Period 2. This period begins at the time the pressure wave reaches the free rear end of the bar and continues until the reflected wave meets the crest of the original one.

Referring to Fig. 16, the pressure diagram ABL has been taken from Fig. 15 and the speed diagram $ABLM$ in Fig. 16A has been taken from Fig. 15A. Following the same procedure as outlined under Period 1, it will be found that the pressure diagram changes from the triangle ABL at the beginning of this period, takes the intermediate forms represented by the areas $ABB'L'$ and $ABB''L''$, and assumes the form of the triangle ABL_1 at the end of this period. The corresponding speed diagrams change from the quadrangle $ABLM$ at the beginning of this period, takes the intermediate forms, represented by the areas $ABN'B'L'M'$ and $ABN''B''L''M''$, and assumes the form of the rectangle $ABNM_1$ at the end of this period.

It is interesting to note that every particle in the bar has a uniform speed $c_2 = C_1L_1$ in Fig. 16A at the time of the maximum occurring bar pressure $P_2 = C_1L_1$ in Fig. 16.

This pressure can be expressed as

$$P_2 = f_1 L \frac{2p}{(p + 1)^2} \quad [21]$$

and occurs at the distance AC_1 from point A, which is

$$l_2 = L\frac{2}{p + 1} \quad [22]$$

The acceleration of the part AC_1 of the bar is still a_1, as given in Equation [16], while that of the part BC_1 of the bar is

$$a_3 = 2a_2 = \frac{f_1}{m}\frac{2p}{p^2 - 1} \quad [23]$$

The time t_2 at which the pressure P_2 is reached may be expressed as

$$t_2 = \frac{l_2}{V_1} = \frac{L}{V}\frac{2p}{p + 1} \quad [24]$$

The speed c_2 is equal to the distance C_1L_1 or

$$c_2 = a_1 t_2$$

or

$$c_2 = \frac{f_1 L}{mV}\frac{2p}{(p + 1)^2} \quad [25]$$

The momentum of the bar at the end of this period, computed as the product of its mass m and its uniform speed c_2 can be expressed as

$$Q_2 = \frac{f_1 L^2}{V}\frac{2p}{(p + 1)^2} \quad [26]$$

It has been found, as the equations developed for the above Period 1 and Period 2 of Case 1 have indicated, that every specific value of the various quantities P, l, a, t, c, and Q can be expressed by a function of the constants of the bar which is the same for all cases and periods multiplied by a function of the propagation ratio p. The function, however, will vary according to cases and periods.

It has been shown how such specific values are constructed or computed from the constants for Periods 1 and 2 of Case 1.

For the purpose of the present investigation, the maximum value of P, its location l, and the maximum value of the acceleration or retardation a are the most important quantities. Therefore, the following analysis will be confined generally to the study of these quantities.

Case 1, Period 3. This period begins at the time the pressure wave, which has been reflected from the free rear end B of the bar, meets the crest of the original wave, and continues until the force application has reached the end B.

Following the procedure previously outlined, the pressure diagram Fig. 17, which at the beginning of this period is represented by the triangle ABL_1, takes the intermediate shapes represented by the quadrangles $ABL_1'L_2'$ and $ABL_1''L_2''$ and assumes the shape of the triangle ABL_2 at the end of the period. The corresponding speed diagram Fig. 17A changes from the rectangle $ABNM_1$ at the beginning of this period, takes the intermediate shapes represented by the areas $ABN'L_1'L_2'M_2'$ and $ABN''L_1''L_2''M_2''$, and assumes the shape of the area $ABN_1L_2M_2$ at the end of this period.

The maximum internal pressure occurring at the end of this period is represented by the vertical C_2L_2 in Fig. 17 and can be expressed as

$$P_3 = f_1 L \frac{p(2 - p)}{p + 1} \quad [27]$$

It occurs at the distance AC_2 from point A which is

$$l_3 = L(2 - p) \quad [28]$$

The acceleration of the part C_2B of the bar at the end of this period is

$$a_4 = \frac{f_1}{m}\frac{2p - 1}{p^2 - 1} \quad [29]$$

Summary of Analysis of the Remaining Periods and Cases. It is believed that the foregoing analysis of the first three periods of Case 1 illustrates sufficiently the application of the method to other periods and cases and that a reproduction of all the diagrams of individual periods of the remaining cases will not be necessary.

For the development of any desired period in any of the cases listed in Table 1, the diagrams shown in Figs. 18A to 18H are helpful. Referring to Fig. 18A, the horizontal AB is the bar to

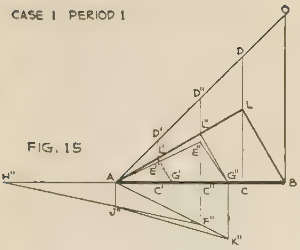

FIG. 15

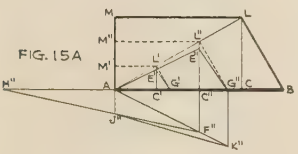

FIG. 15A

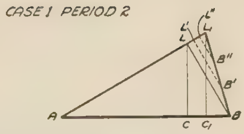

FIG. 16

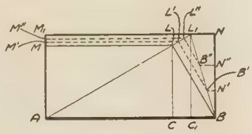

FIG. 16A

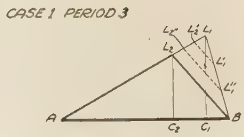

FIG. 17

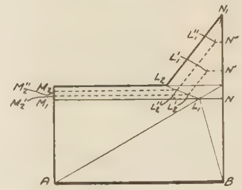

FIG. 17A

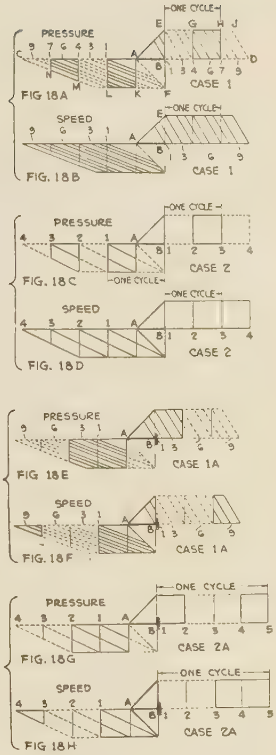

FIG. 18A FIG. 18B FIG. 18C FIG. 18D FIG. 18E FIG. 18F FIG. 18G FIG. 18H

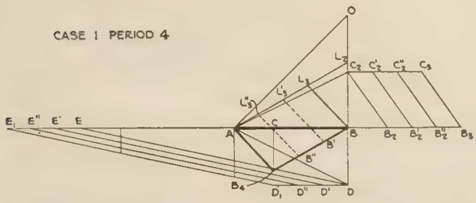

FIG. 19

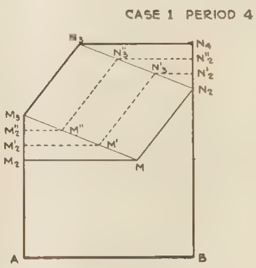

FIG. 19A

which the uniformly distributed external forces are gradually applied, acting from A to B at a uniform speed of application.

The horizontal AD in Fig. 18A represents the accumulated travel of the front of the pressure wave back and forth between A and B, from the time it originated at the front end A of the bar. The horizontal AC represents the accumulated travel of the front of the tension wave, also originating at the end A. Each of these lines is divided into sections within which the original wave retains its sign, alternating with sections in which a change of sign occurs. The inclined lines, which intersect the horizontal AD in the points 1, 2, 3, etc., represent the advancing front of the compression wave at the end of the 1st, 2nd, 3rd, etc. periods, respectively. Likewise, the inclined lines, which intersect the horizontal AC in the points 1, 2, 3, etc., represent the front of the tension wave at the end of the 1st, 2nd, 3rd, etc. periods, respectively.

In the pressure diagram Fig. 18A, both the compression and tension waves change their sign every time they pass the free ends A and B of the bar. The horizontals AD and AC may therefore be divided into sections within which the original wave retains its sign, alternating with sections within which a change of sign takes place. In view of the fact that ends A and B are both free, each such section is equal to the length AB of the bar.

The pressure diagram at the end of any period of Case 1 will be found if the areas between the inclined line AE in Fig. 18A and the wave fronts above the base line CD are algebraically added to the areas between the inclined line AF and the wave fronts below the base line, keeping in mind that the sign is changed so as to be negative in the areas $BEG4$ and $7HJD$ above the line CD and so as to be positive in the areas $AKL1$, and $4MN7$ below the base line CD. The addition of these areas should be carried out in such a way that the points 4 and C come at the end A and points 1 and 7 at the end B of the bar. All the areas enclosed by full lines are positive while those formed by dashed lines are negative.

The speed diagram at the end of any period is constructed from the diagram in Fig. 18B in the same manner, except that all the areas are added together arithmetically since the speed waves are all positive and all are reflected from the ends of the bar without change of sign.

In Figs. 18A to 18H, inclusive, the vertical height of the pressure diagrams represents one-half of the total applied external force or $^1/_2 f_1 L$. The height of the speed diagrams or the speed represented by the verticals $BE = BF$ may, according to Equation [2], be expressed as

$$c = \frac{f_1 L}{2\sqrt{(mk)}} \qquad [30]$$

and is equal to the speed of the particles. This speed will be produced by a pressure equal to one-half of the external forces in a bar of the wave resistance $\sqrt{(mk)}$.

During the first period the unreflected compression and tension areas in all the pressure diagrams have opposite signs, the former being positive and shown in full lines above the line AB, while the latter are negative and shown in dashed lines below the base line AB. The corresponding unreflected waves in all the speed diagrams are both positive during the first period and shown in full lines.

The signs of the compression and tension waves during the following periods depend on whether the ends of the bar are free or fixed. In Figs. 18A to 18H, inclusive, the sections within which the diagram areas are positive are shown in full lines. Those within which they are negative are shown in dashed lines. With the help of such diagrams, the pressure and speed diagrams for all the cases and periods in Table 1 have been investigated, but it is not considered necessary to reproduce them all.

The diagrams for the Cases 1, 2, and 2A may serve as examples. Figs. 19 and 19A and Figs. 20 and 20A represent Case 1, Periods 4 and 5, respectively. Figs. 21 and 21A and Figs. 22 and 22A

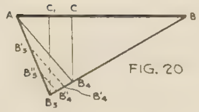

FIG. 20

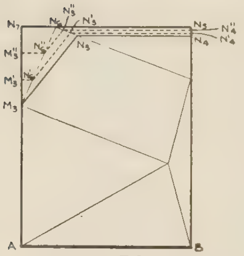

FIG. 20A

CASE 1 PERIOD 5

CASE 2 PERIOD 2

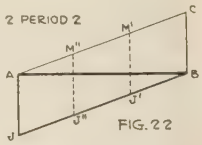

FIG. 22

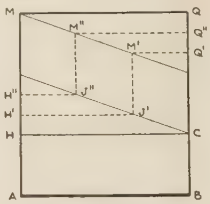

FIG. 22A

CASE 2A PERIOD 2

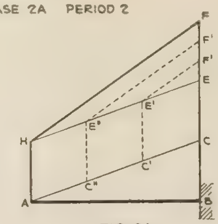

FIG. 24

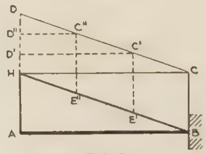

FIG. 24A

CASE 2A PERIOD 3

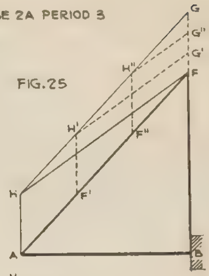

FIG. 25

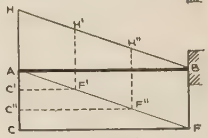

FIG. 25A

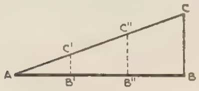

FIG. 21

CASE 2 PERIOD 1

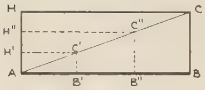

FIG. 21A

CASE 2A PERIOD 1

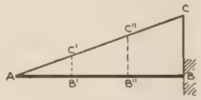

FIG. 23

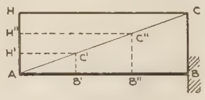

FIG. 23A

CASE 2A PERIOD 4

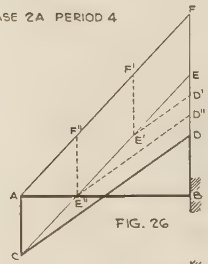

FIG. 26

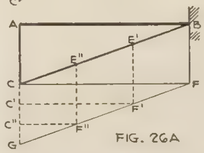

FIG. 26A

CASE 2A PERIOD 5

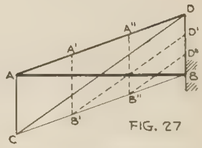

FIG. 27

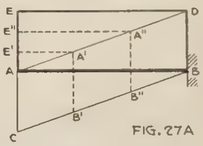

FIG. 27A

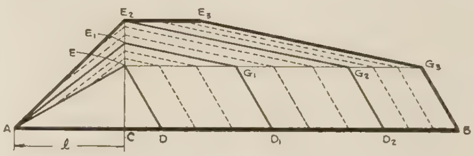

FIG. 28

represent Case 2, Periods 1 and 2, respectively. Figs. 23 and 23*A* to Figs. 27 and 27*A*, inclusive, represent Case 2*A*, Periods 1 to 5, respectively.

In each of these figures the diagram at the beginning of the period is shown in light full lines. Two intermediate shapes of the diagram are shown in dashed lines. The diagram at the end of the period is shown in heavy full lines. The diagram at the end of one period is of course the same as that at the beginning of the following period and both are designated by identical symbols.

In all the cases it will be found that from a certain point on the pressure diagrams are regularly repeated in cycles of a certain number of periods each. This applies also to the speed diagrams, with the qualification that in Cases 1, 2, and 3, where both ends of the bar are free, the speed of the bar as a whole increases continuously under the influence of the applied external forces. The number of periods in each cycle and the number of the period at the end of which the cycles begin are given in Table 2 for all the cases listed in Table 1.

TABLE 2 CYCLES OF THE PRESSURE AND SPEED WAVES

Case number	No. of periods per cycle	Period no. at end of which cycles begin	No. of periods up to and including the first cycle
1	6	3	9
2	2	1	3
3	6	2	8
1*A*	12	3	15
2*A*	4	1	5
3*A*	12	2	14
1*B*	12	3	15
2*B*	4	1	5
3*B*	12	2	14
1*C*	6	3	9
2*C*	2	1	3
3*C*	6	2	8

The analysis of the pressure and speed waves for the type of force application under consideration thus involves an examination of a total of 108 sets of diagrams. For the purpose of this investigation it is considered sufficient to give the summary of such an examination. This summary is contained in Tables 3 and 4.

In the preceding analysis it was always assumed that the external forces, beginning at A, acted in the direction from A to B, in which case the conditions listed in Table 3 would apply.

If the external forces should begin to be applied at A but should act in the opposite direction, or from B to A, all the preceding diagrams would change in such a manner that every point of them would move vertically across the line AB to an equidistant position. The various values for Table 3 would still apply, but their meaning would change according to Table 4.

The changes in the force application do not affect Table 1.

(*D*) *Partially Applied Uniformly Distributed External Force Acting on a Perfectly Elastic Bar*

1 Both Ends of Bar Free. Referring to Fig. 28, AB is a perfectly elastic bar subjected to a uniformly distributed external force, acting from A to B, its application beginning at A and progressing at a uniform rate up to point C.

Partial Force Application for $p > 1$. At the time the force application reaches the point C, the pressure diagram will be represented by the triangle ADE. By the use of the previously

Line No.	TABLE 3 CONDITIONS IN ELASTIC BAR WHEN PRESSURE IS APPLIED FROM *A* TO *B*	VALUES FOR TABLE 3 AND TABLE 4												TABLE 4 CONDITIONS IN ELASTIC BAR WHEN PRESSURE IS APPLIED FROM *B* TO *A*
1	Case number	1	2	3	1*A*	2*A*	3*A*	1*B*	2*B*	3*B*	1*C*	2*C*	3*C*	Case number
2	Max bar pressure, multiply values in this line by f_1L	$\frac{2p}{(p+1)^2}$	$^1/_2$	$\frac{p}{2}$	2	2	2	$\frac{2}{(p+1)^2}$	$^1/_2$	$^1/_2$	$2-p$	1	1	Max bar tension, multiply values in this line by f_1L
3	Distance from front end of the bar at which max pressure occurs, multiply values in this line by L	$\frac{2}{p+1}$	1	$\frac{1+p}{2}$	1	1	1	$\frac{2}{p+1}$	1	$\frac{1+p}{2}$	1	1	1	Distance from front end of the bar at which max tension occurs, multiply values in this line by L
4	No. of earliest period during which max bar pressure occurs	2	1	2	7	2	7	2	1	2	3	1	3	No. of earliest period during which max bar tension occurs
5	Max bar tension, multiply values in this line by f_1L	$\frac{(3-p)p}{2(1+p)}$	$^1/_2$	$^1/_2$	$\frac{2-p}{2}$	$^1/_2$	$\frac{(3-p)p}{2(1+p)}$	2	2	2	$2-p$	1	1	Max bar pressure, multiply values in this line by f_1L
6	Distance from front end of the bar at which max tension occurs, multiply values in this line by L	$\frac{p-1}{2}$	0	$\frac{1-p}{2}$	$\frac{p-1}{2}$	0	$\frac{1-p}{2}$	1	0	0	0	0	0	Distance from front end of the bar at which max pressure occurs, multiply values in this line by L
7	No. of earliest period during which max bar tension occurs	5	2	5	11	4	11	6	2	6	4	1	4	No. of earliest period during which max bar pressure occurs
8	Max acceleration (or retardation) of particles of bar, multiply values in this line by f_1/m	$\frac{3p-1}{p^2-1}$	∞	$\frac{1}{1-p}$	$\frac{1}{p-1}$	∞	$\frac{1}{1-p}$	$\frac{1}{p-1}$	∞	$\frac{1}{1-p}$	$\frac{1}{p^2-1}$	∞	$\frac{1}{1-p^2}$	Max acceleration (or retardation) of particles of bar multiply values in this line by f_1/m
9	No. of earliest period during which max acceleration (or retardation) occurs	5	1	2	5	1	5	8	1	8	3	1	3	No. of earliest period during which max acceleration (or retardation) occurs

described method, it is found that under the influence of the applied force, the pressure diagram will take the intermediate shapes $AD_1G_1E_1$, $AD_2G_2E_2$, and the final shape $ABG_3E_3E_2$, the latter being attained at the time the front of the pressure wave reaches the end B of the bar. The vertical CE_2 in the pressure diagram, Fig. 28, represents the maximum occurring bar pressure and the greatest bar pressure that the applied force can produce, regardless of the length of the bar AB.

If the external force applies to the part AC of the bar AB as shown in Fig. 29, the reflected pressure wave will just reach the crest of the original one at the time the latter reaches its maximum value CD.

Referring again to Fig. 28, it will be seen that the maximum pressure produced by a force applied over the part l of a bar never can exceed the value represented by the vertical CE_2 which may be expressed as

$$P = f_1 l \qquad [31]$$

The greatest length l_4, represented by the distance AC in Fig. 29, which still permits the formation of such a pressure may be expressed as

$$l_4 = L\frac{2}{3+p} \qquad [32]$$

and the corresponding maximum bar pressure, represented by the vertical CD in Fig. 29, is

$$P_4 = f_1 l_4 = f_1 L\frac{2}{3+p} \qquad [33]$$

The maximum bar pressure for a force application extending over the whole length of the bar is represented by the vertical C_2D_1 in Fig. 30 and is given as P_2 in Equation [21]. It occurs when the force application has proceeded the distance AC_2 in Fig. 30, given as l_2 in Equation [22]. Also, P_2 is larger than P_4 for all values of p greater than unity.

For all values of l between the limits $0 < l < l_4$, the maximum bar pressure P is expressed by Equation [31]. For values of l within the range $l_4 < l < l_2$, the maximum value of P is expressed by the equation

$$P = f_1[l(p-1) + 2L]\frac{1}{2(1+p)} \qquad [34]$$

Partial Force Application for $p = 1$. By using the same method, the pressure diagrams shown in Fig. 31 are obtained for $p = 1$. The broken line $ABCD$ represents the form of the pressure dia-

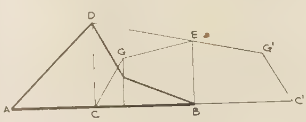

FIG. 29

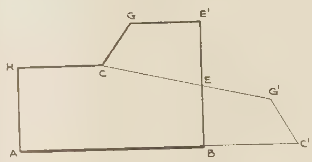

FIG. 29A

FIG. 30

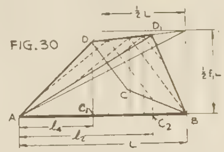

FIG. 31

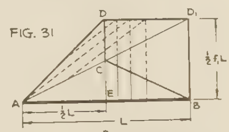

FIG. 32

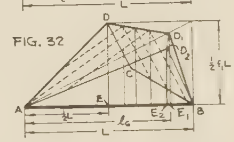

gram at the moment the maximum obtainable bar pressure ED first occurs. This maximum pressure can be expressed as

$$P_5 = {}^1/_2 f_1 L \qquad [35]$$

For all values of l between zero and $^1/_2L$, the corresponding value of P is expressed by Equation [31].

For all values of l between the limits $^1/_2L < l < L$, the value of P is equal to P_5 as given in Equation [35].

The pressure diagrams for intermediate values of l are shown in dashed lines in Fig. 31. The corresponding maximum bar pressures DE and BD_1 are both equal to P_5 as given in Equation [35].

For $l = L$ the pressure diagram takes the shape of the triangle ABD_1 in Fig. 31 at the time P reaches its maximum value P_5.

Partial Force Application for $p < 1$. By using the same procedure as previously outlined, the pressure diagrams shown in Fig. 32 are obtained.

For values of l between the limits $0 < l < {}^1/_2L$, the value of P is that given in Equation [31]. In this case, $l = {}^1/_2L$ represents the length of the greatest part of the bar to which the external force may apply and still produce the maximum pressure ED which the force can possibly create, regardless of the length of the bar.

This pressure is equal to P_5 as given in Equation [35]. The corresponding pressure diagram is represented by the quadrangle $ABCD$, Fig. 32.

In case of a uniformly applied force over the whole length of the bar, the maximum bar pressure D_2E_2, equal to $^1/_2pf_1L$, is reached when the pressure propagation has reached the distance AE_2, equal to $^1/_2(1 + p)L$, which values are found in Table 3 (Case 3, Period 2). The corresponding pressure diagram is represented by the triangle ABD_2 in Fig. 32.

It will be seen from this equation that the value of P gradually increases from the value of P_4 as expressed by Equation [33] to the maximum value of P_2 as expressed by Equation [21] along the straight line DD_1 in Fig. 30 when the part l, to which the external force applies, increases from the value of l_4 as given by Equation [32] to l_2 as given by Equation [22].

Referring to Fig. 30, it will therefore be seen that the heavy full line ABD_1D represents the maximum bar pressures that can be produced by an applied force of f_1 lb per ft of bar, regardless of the part of the bar to which it is applied.

The shape of the pressure diagrams $ABCD$ and ABD_1 are shown in full lines at the time the bar pressure reaches its maximum value for $l = l_4$ and $l = l_2$. Diagrams for intermediate values of l are shown in dashed lines. They represent the shapes of the pressure diagrams when the external force is applied to the bar AB over intermediate distances at the time the maximum bar pressure is reached for each application.

It is interesting to note that in case of partial force application over the length l_6 of the bar, equal to AE_1 in Fig. 32, and expressed by the equation

$$l_6 = L\frac{2}{3 - p} \qquad [36]$$

the bar pressure exceeds the value from Table 3 and amounts to P_6, where

$$P_6 = f_1L\frac{1}{3 - p} \qquad [37]$$

represented by the vertical D_1E_1 in Fig. 32.

For values of l between the limits $^1/_2L < l < l_6$, the maximum obtainable bar pressure

$$P = f_1\frac{L - l(1 - p)}{1 + p} \qquad [38]$$

and, for such values of l, the corresponding values of P are located on the inclined line DD_1 in Fig. 32. Pressure diagrams for such values of l are shown in dashed lines. For values of l between the limits $l_6 < l < L$ the corresponding values of P are located on the straight line BD_1 in the same figure.

Partial Force Application in Different Directions. In the preceding analysis of partial force application it was shown that if the external force is applied from A to B, beginning at A, and if the application of this force proceeds at a uniform rate in that direction, the maximum bar pressures possibly created, regardless of the length of the part of the bar to which the external force applies and of the propagation ratio, will always fall within the quadrangle ABC_1M_1 shown in Fig. 33 in heavy full lines, provided both ends of the bar are free.

The maximum occurring coupler tensions will be confined within the quadrangle ABM_2G_2 also shown in heavy full lines in Fig. 33. If the applied forces act from B to A the bar pressures will remain within the quadrangle ABM_1G_1 and the bar tension within the quadrangle ABC_2M_2, both shown in dashed lines. It will be seen that regardless of the direction of the applied forces and of the rate at which the application proceeds, the bar pressure or tension will, in case of a bar with both ends free, never exceed the value of $^1/_2f_1L$.

2 One End of Bar Is Free, One End Fixed. Referring to Fig. 34, AB represents a perfectly elastic bar subjected to gradually and uniformly applied external longitudinal forces acting from A to B. They begin to apply at the end A and proceed toward the end B at a constant rate of application. These forces may apply over the whole length of the bar or over only a part of it.

If the end A is free, while the end B is fixed, the analysis shows that the bar pressures may attain any value within the quadrangle ABD_1G_1 and the bar tensions may attain any value within the triangle ABG_2, in Fig. 34. If the external forces apply in the opposite direction, bar tensions will predominate and may assume any value within the quadrangle ABD_2G_2, while the bar pressures will be confined within the triangle ABG_1. It is interesting to note that if one end of the bar is fixed, the maximum possibly occurring bar tensions and pressures are equal to $2f_1L$ or four times greater than if both ends were free.

3 Both Ends of the Bar Are Fixed. Referring to Fig. 35, it is assumed that both ends of the perfectly elastic bar AB are fixed.

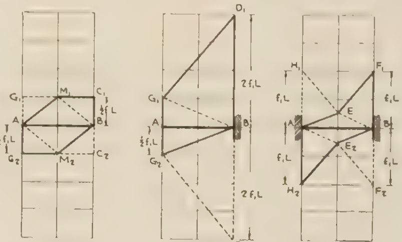

FIG 33 FIG 34 FIG 35

It is subjected to gradual and uniform external longitudinal forces which begin to apply at end A and proceed toward end B at a constant rate of application. They may apply over the whole length of the bar or only a part thereof.

If the forces act from A to B, the maximum bar pressures will fall within the quadrangle ABF_1E_1 and the maximum bar tensions within quadrangle ABE_2H_2. If the forces act in the opposite direction, the maximum bar pressures will fall within the quadrangle ABE_1H_1 and the maximum bar tensions within the quadrangle ABF_2E_2. In either case and regardless of the direction of the forces, the bar pressures will always fall within the polygon $ABF_1E_1H_1$ and the bar tensions within the polygon $ABF_2E_2H_2$.

In the center of the bar the pressure or tension will never exceed $^1/_4f_1L$ or one-half that which may be attained in a bar with both ends free. The maximum occurring bar pressure or bar tension, which only occurs at the ends of the bar may attain the value f_1L or twice that obtainable in a bar with both ends free.

2 BRAKING AND STARTING OF A LONG TRAIN

(A) Braking of a Bunched Train

The brakes apply first on the first car and then the brake application proceeds from car to car through the length of the train. After the brakes have begun to retard the first car, the second car runs relatively faster for a certain time. The temporary speed difference between the two cars is equalized by compression of the draft gears as the second car overtakes the first. This condition is repeated between the second and third cars, and so on throughout the train.

Period of Increasing Coupler Pressure

If in a long train which has no free slack, all the cars have the same weight, and all the draft gears offer a resistance proportional

TABLE 5 EQUATIONS FOR VALUES OF P_m, a_{max}, C_{min}, AND q

Propagation ratio, $p = V/V_1$	Maximum coupler pressure P_m	Eq No.	Maximum car retardation a_{max}	Eq No.	Minimum safe draft-gear capacity C_{min}	Eq No.	Gear travel q corresponding to C_{min}. q	Eq No.
$p > 1$	$nF \dfrac{2p}{(p+1)^2}$	[49]	$\dfrac{F}{M}\dfrac{3p-1}{p^2-1}$	[52]	$\dfrac{1}{M}\left(\dfrac{nFL_1}{V_1}\right)^2 \dfrac{1}{(p+1)^4}$	[55]	$\dfrac{nFL_1^2}{V_1^2M}\dfrac{1}{p(p+1)^2}$	[58]
$p = 1$	$nF/2$	[50]	∞	[53]	$\dfrac{1}{M}\left(\dfrac{nFL_1}{4V_1}\right)^2$	[56]	$\dfrac{nFL_1^2}{4V_1^2M}$	[59]
$p < 1$	$(nF/2)p$	[51]	$\dfrac{F}{M}\dfrac{1}{1-p}$	[54]	$\dfrac{1}{M}\left(\dfrac{nFL_1}{4V_1}\right)^2$	[57]	$\dfrac{nFL_1^2}{4V_1^2M}\dfrac{1}{p}$	[60]

to the amount of compression to which they are subjected, the train can be considered as a bar of uniform mass and elastic properties. The coupler forces and car retardations, which occur in such a train under the influence of external forces such as a progressive braking, can be computed from the formulas derived in Part 1 for a perfectly elastic bar, with both ends free.

The formulas in Part 1 were derived under the assumption that the external forces acted on a bar at a standstill, accelerating its particles. In the case of braking of a long train, however, the external forces retard the moving cars.

Instead of the symbols f_1, L, and m, which are used in the various equations for elastic bars, it is convenient to use the corresponding symbols which express characteristics of a long train. These symbols are given in Equations [39] to [44], inclusive.

$$f_1 = F/L_1 \qquad [39]$$

$$f_1L = Fn \qquad [40]$$

$$m = M/L_1 \qquad [41]$$

$$L = nL_1 \qquad [42]$$

$$f_1/m = F/M \qquad [43]$$

$$R_w = \sqrt{(mk)} = \frac{\sqrt{(CM)}}{q} \qquad [44]$$

k = stiffness constant

The stiffness constant is the force required to stretch a bar twice its original length.

The force required to stretch a car and its two draft gears the length $2q$ is equal to the ultimate reaction of the gears. Assuming a straight compression line, beginning at zero, the force $2C/q$ will stretch the car the amount $2q$ and the stiffness constant

$$k = \frac{2C}{q}\frac{L_1}{2q} = \frac{L_1}{q^2}C \qquad [45]$$

The pressure-propagation speed V can be expressed by substituting in Equation [1] the value of k and m as given in Equations [45] and [41], respectively.

$$V = \sqrt{\frac{k}{m}} = \sqrt{\left(\frac{L_1^2C}{q^2M}\right)} = \frac{L_1}{q}\sqrt{\frac{C}{M}} \qquad [46]$$

The value of the draft-gear travel q should include the strain of one coupler shank plus the strain in one-half the length of a center sill when subjected to the force P. The corresponding potential energy should be included in the value of the draft-gear capacity C, so as to take into account the combined elastic action of the car bodies and the draft gears.

If solid steel blocks were used as connections between the couplers and the center sills of the car bodies, the whole train would act as a solid steel bar, and a retarding force acting on the first car would be transmitted through the whole length of the train at a speed of 16,800 fps. This speed is over 15 times as fast as the speed of sound in air, 1080 fps. The rate of brake application on the other hand depends on the travel of air pressure from one car to another and therefore cannot under any circumstances exceed the speed of sound. On the average freight train in the type-K brakes the rate of emergency brake application amounts to about 620 fps, but in trains with the new type-AB brakes, the rate of propagation of emergency application amounts to 960 fps. The use of conventional draft gears decreases the pressure-transmission speed from 16,800 fps to values in the neighborhood of the rate of brake application of the average freight train.

Applying the formulas given in Part 1 to brake action in a long train, it will be noted that the propagation ratio p is an important factor in determining coupler forces and car accelerations occurring in a long train. Substituting the value of V from Equation [46] in the propagation ratio $p = V/V_1$

$$p = \frac{V}{V_1} = \frac{L_1}{qV_1}\sqrt{\frac{C}{M}} \qquad [47]$$

$$q = \frac{L}{pV_1}\sqrt{\frac{C}{M}} \qquad [48]$$

The substitution of Fn, the equivalent of f_1L, Equation [40], in line 2 of Table 3, gives Equations [49], [50], and [51] for cases 1, 2, and 3. The substitution of F/M, the equivalent of f_1/m, Equation [43], in line 8 of Table 3, gives Equations [52], [53], and [54] listed in Table 5.

The minimum safe draft-gear capacity, always assuming a straight compression line, beginning at zero, can be expressed

$$C_{min} = P_mq/2$$

or

$$P_m = 2C_{min}/q \qquad [61]$$

Substituting in this equation the value of P_m from Equations [49], [50], and [51] and the value of q from Equation [48], Equations [55], [56], and [57] are obtained. These equations are listed in Table 5. The gear travel q corresponding to C_{min} is obtained by the substitution of the value of C_{min} from Equations [55], [56], and [57] for C in Equation [48].

The maximum coupler pressure P_m, the maximum car retardation a_{max}, the minimum draft-gear capacity C_{min}, and the corresponding gear travel q are expressed by Equations [49] to [60], inclusive. The equation to use depends on whether the propagation ratio is greater than, equal to, or smaller than unity. These equations, listed in Table 5, are based on the assumption that the draft gears are powerful enough to cushion elastically all occurring coupler forces. If the gears go solid during the passing of the pressure wave the latter will be disturbed and the coupler forces will increase about twice as fast as they would otherwise.

Example. A freight train of 150 seventy-ton cars is subjected to emergency braking from the front end of the train. Other conditions of the problem are as follows:

Weight of car, empty	50,000 lb
Weight of car, loaded	210,000 lb
Length between coupler faces	50 ft

Brake pressure	60% of light weight 30,000 lb
Coefficient of friction	25 per cent
Braking force	$0.25 \times 30{,}000$ lb 7500 lb
Rate of emergency brake application	930 fps

From the conditions of the problem it is observed that $n = 150$, $F = 7500$ lb, $V_1 = 930$ fps, $L_1 = 50$ ft, $M = 1550$ for empty cars, and $M = 6500$ for loaded cars.

The values of P_m, $a_{\max}$, $C_{\min}$, and q can be computed for various propagation ratios for empty and loaded cars from Equations [49] to [60], inclusive. Sets of values of these quantities,

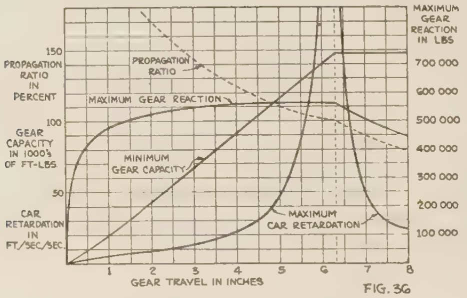

FIG. 36

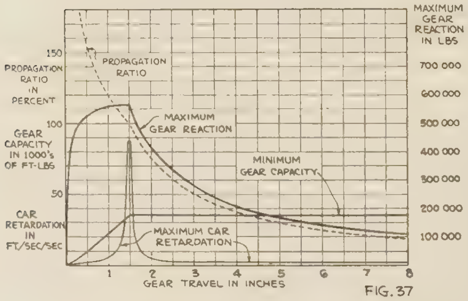

FIG. 37

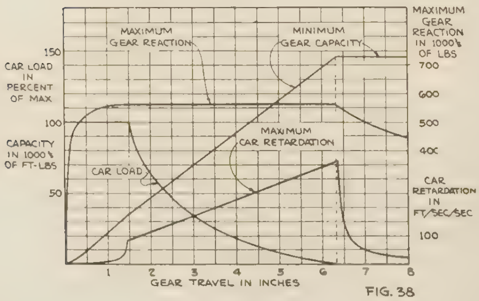

FIG. 38

corresponding to various values of p, can be plotted against any one of them as the independent variable.

Using the length of travel as the independent variable, the curves for the empty train have been plotted in Fig. 36 and those for the fully loaded train in Fig. 37. Fig. 38 is a composite diagram made up from Figs. 36 and 37 and also shows the maximum values P_m, $a_{\max}$, $C_{\min}$, and q for intermediate or partial train loadings.

Fig. 36 shows that if the gears shall not go solid during emergency braking of the 150 empty cars, the gear capacity and the gear reaction must not fall below certain minimum limits represented by the curves. The gear-capacity curve shows that the minimum required gear capacity increases with increasing gear travel, practically along a straight line beginning at zero up to a capacity of about 147,000 ft-lb. A draft gear must have this capacity if its travel is $6^5/_{16}$ in. and it shall not go solid during emergency braking of the empty train. A travel increase above $6^5/_{16}$ in. does not cause any further increase of the minimum gear capacity.

If, however, the gear capacity is limited to, say, 30,000 ft-lb, corresponding to a gear travel of $1^7/_{16}$ in., a longer gear travel will cause the gears to go solid during an emergency brake application of an empty train of 150 cars. A gear of the standard AAR travel of $2^5/_8$ in. would, according to Fig. 35, need a capacity of 60,000 ft-lb to prevent it from going solid in such service.

The gear-reaction curve in Fig. 35 shows that the gear reactions increase very rapidly with increasing gear travel, reaching a value of about 540,000 lb at the standard AAR travel of $2^5/_8$ in. and its maximum value of 562,500 lb at the gear travel of $6^5/_{16}$ in. Beyond this travel the maximum occurring gear reaction decreases rapidly. The maximum value of the gear reaction is obtained when the value of p in either one of Equations [49] or [51] is equal to unity. In that case they both take the form of Equation [50], $P_m = nF/2$. The value of P_m in this equation depends only on the number of cars n and the retarding force acting on each car. This gear reaction is the same for empty, partially loaded, and fully loaded cars and is equal to one-half the retarding force of the whole train or 562,500 lb. In order to cushion this force a draft gear should have an ultimate yielding resistance which would exceed this figure.

However, it is permissible to reduce this figure by an amount about equal to the initial resistance of the gear. Up to the amount of this latter resistance the gear has a very high spring constant and the corresponding force will be transmitted through the train theoretically at the same speed as through a solid steel bar, or at about 17,000 fps. The effect on the coupler pressures is assumed to be somewhat similar to that when only a part of the full air pressure is admitted to the brake cylinders for a short period, as is done in the new type-AB brake. A coupler force about equal to the amount of the initial gear compression will very rapidly equalize part of the speed difference of the front and rear cars and the final coupler pressure will decrease a corresponding amount. A gear of 100,000-lb initial and 500,000-lb ultimate reaction will thus be approximately equivalent to a gear with no initial and 600,000-lb final reaction. It will be superior in the respect that it keeps the maximum coupler pressure lower.

The car-retardation curve in Fig. 36 shows that the maximum car retardation during an emergency brake application of an empty train will gradually increase with increasing gear travel, at first slowly, reaching the comparatively harmless value of about 11 ft per sec per sec at the standard AAR gear travel of $2^5/_8$ in., then faster and faster until it reaches a theoretically infinite value at a gear travel of $6^5/_{16}$ in. In practice this value will be limited to the retardation produced by the maximum gear reaction of 562,500 lb acting on the mass of one empty car, weighing 50,000 lb (corresponding to a mass of 1550). This retardation amounts to $562{,}500/1550 = 363$ ft per sec per sec, or more than ten times gravity, which of course is very high.

Fig. 37 shows the corresponding curves for fully loaded cars. The minimum required gear capacity increases practically proportionally to the gear travel until the latter reaches the critical value of $1^1/_2$ in. after which the gear capacity remains constant at the value of about 35,000 ft-lb. At a gear travel of 1.2 in. the required gear capacity amounts to about 28,000 ft-lb. At the standard AAR gear travel of $2^5/_8$ in. the required gear capacity amounts of course to the previously given value of about 35,000 ft-lb. The curve showing the gear reaction is similar to that for empty cars, but reaches the same maximum of 562,500 lb at a gear travel of only $1^1/_2$ in. For longer gear travels, the gear reaction decreases rapidly as shown by the curve.

Fig. 37 shows that the maximum occurring car retardation for loaded cars increases at first slowly with increasing gear travel but rises rapidly as the gear travel approaches $1^1/_2$ in. at which point the retardation is equal to the maximum gear reaction of 562,500 lb acting on the mass of the fully-loaded car or 562,500/6500 = 86.5 ft per sec per sec, which retardation is nearly three times the acceleration of gravity and undesirably high.

Fig. 38 shows the superimposed curves of Figs. 36 and 37. The inclined line, representing the minimum gear capacity for intermediate loads, shows that for every gear travel between $1^1/_2$ in. and $6^5/_{16}$ in. there is a partial loading at which the minimum required gear capacity will reach the values indicated by the inclined line. For the standard AAR gear travel of $2^5/_8$ in., the required minimum gear capacity will, for about 43 per cent partial loading, amount to about 60,000 ft-lb.

The maximum gear reaction for intermediate loads, represented in Fig. 38 by the horizontal line at the load of 562,500 lb, shows that for every gear travel between $1^1/_2$ in. and $6^5/_{16}$ in. there is some partial-loading condition at which this reaction will be reached.

The maximum car retardation for intermediate loads is represented in Fig. 38 by an inclined line marked accordingly and extending from the value of 86.5 for fully loaded cars at $1^1/_2$ in. gear travel to the value of 363 ft per sec per sec for empty cars at a gear travel of $6^5/_{16}$ in. It will be noted that the maximum car retardation increases in direct proportion to the gear travel between the previously given values of the latter. Below the gear travel of $1^1/_2$ in. the maximum car retardation drops rapidly.

For the standard AAR gear travel of $2^5/_8$ in. and assuming that the proper gear capacity of 60,000 ft-lb were available, the maximum car acceleration would, for about 43 per cent partial loading, reach the value of 150 ft per sec per sec which approaches five times the acceleration of gravity and is undoubtedly high, even though it would act only for a very short time.

Special Cases of Braking of a Bunched Train

The formulas in Table 5 are based on the action of an elastic bar with both ends free. They apply to trains with fairly uniformly distributed loads and with brakes gradually applying to all cars of the train. The greatest possibly occurring coupler pressure in such trains is expressed by Equation [50].

(*a*) *Partial Brake Application.* With the type-K air brake, the one in general use on American railroads, the brakes apply only to the first 70 or 80 cars, or to about the first half of a long train of 150 cars. The question whether under such partial brake application greater coupler pressures will be produced because of the running in of the unretarded rear end of the train is answered by the previously presented investigation of partial force applications to elastic bars. It is shown that while the maximum occurring coupler pressure may be displaced to any point within the rear half of the train, its magnitude will not increase above the value given by Equation [50] as long as the wave resistance of the train is uniform.

(*b*) *Uneven Load Distribution.* If a group of fully loaded cars is placed at the rear end of a long train of empties and emergency braking is applied from the front end of the train, the coupler pressures will materially increase at the rear end, causing the draft gears to go solid. The wave resistance of this train may reach such high values that the pressure distribution will approach that represented by Case 2*A*, line 2, in Table 3. In that case the coupler pressure increases to four times that given by Equation [50]. The subsequently produced coupler tensions will not be increased above those occurring in case of uniform load distribution, as shown in Table 3, line 5.

If the group of loaded cars were placed at the front end of the train, the condition represented by Case 2*B* would be approached and no increase in the coupler pressures would be produced. The subsequently produced coupler tensions would, however, according to Table 3, line 5, be four times as large as in the case of uniform load distribution, if the draft gears had 100 per cent recoil.

If the group of fully loaded cars were evenly divided between the front and rear ends of the long train of empty cars, the worst conditions would be represented by Case 2*C* and the maximum occurring coupler pressures and tensions might, according to lines 2 and 5 of Table 3, approach twice those in case of uniform load distribution.

These considerations illustrate the importance of a fairly uniform distribution of the load of a train over its whole length and indicate that load concentrations toward the ends of the train are particularly undesirable.

(*B*) Braking of a Stretched Train (With Free Slack)

The free slack between coupled cars is measured by the amount of relative car movement which is obtainable with no change in the position of the various elements which make up the cushioning device.

All new cars, irrespective of draft-gear design, are subject to about the same amount of free slack when standard coupler specifications are followed. On such cars the free slack is about $^7/_8$ in. per car, but it increases as a result of wear in service and permanent deformation of couplers, attachment, and draft gears.

When the *free slack* of a train is taken up under the influence of a brake application, the occurring impacts will close the draft gears to a certain extent, thus producing an additional approach between impacting cars, which is called the *controlled slack.* The *total slack* of a train consists thus of the free and the controlled slack.

If all the slack is controlled, the train is bunched and the preceding analysis applies to the brake action on such a train.

In case the cars are separated by a certain amount of free slack, the principle of the elastic bar should be applied with the understanding that the take-up of the slack will produce car impacts, not expressed in the preceding equations for coupler pressures.

Because of the time interval between the application of the brakes on adjacent cars, the front cars will first begin to retard and the free slack between the cars will gradually be taken up, beginning at the front end of the train. If a train has free slack it will, when subjected to braking from the front end, begin to bunch at that end. The rear end of the bunched portion will always be free and any coupler pressure which reaches the cars at this point will be reflected, changing its sign. The coupler forces actually generated in the bunched portion of the train will be smaller than in a train without free slack, where the coupler forces continually increase even after the wave reaches the free rear end of the train. If the free slack is too great the impact between the bunched portion of the train and the individual cars, separated by free slack, may however become so violent as to cause momentary excessive coupler pressures.

It will be assumed in the following that each car which impacts the bunched part assumes the speed of the latter, without rebound.

Referring to Fig. 39, the circles 1 to 12, inclusive, denote railway cars, counted from the front end of a moving train, which cars are separated by supposedly equal amounts of free slack s_1 per car. The braking forces of F lb per car gradually applied to these cars, beginning at the first car and progressing in the direction of the rising numbers, retard the originally uniform movement of the cars. The horizontal or x-axis represents the time, counted from the application of the brakes to the first car. The vertical or y-axis represents the train slack. The tangent

of the angle which the straight line OA forms with the x-axis is a measure of the brake-propagation speed V_1. The length of the horizontal dashed line between the car number on the vertical axis and the straight line OA represents the delay of brake application to the individual car after the brakes have been applied to the first car.

When the braking force F is applied to the first car of a long train moving at a uniform speed it will subject the car to a retardation a. The movement of the retarded car in relation to the

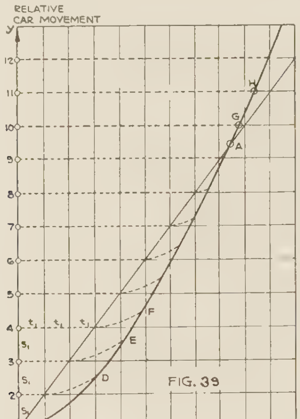

as yet unretarded part of the train is represented by the curve OD in Fig. 39 and may be expressed by the equation

$$y = (a/2)x^2 \quad \ldots\ldots\ldots\ldots [62]$$

representing a parabola with its apex in the point O.

The speed lost by the car is expressed by the derivation

$$\frac{dy}{dx} = ax \quad \ldots\ldots\ldots\ldots [63]$$

After the time t_1, or the interval between the applications of the brake to adjacent cars, the first car will have suffered the loss of speed at_1. From then on both cars will be retarded at the same rate a and will impact at the relative speed

$$c_1 - c_2 = at_1 \quad \ldots\ldots\ldots\ldots [64]$$

This impact speed is independent of the amount of slack between the cars, provided the slack is sufficient to allow the braking force to apply to the second car before the latter is struck by the first car.

As the draft gears are assumed to have a liberal amount of absorption, any impact of one car with a string of several cars will cause them all to take the same speed and they will move on together in a bunched group. The speed of this group will at any time be represented by the slope of the curved line $ODEFA$ in Fig. 39. This group of retarded cars strikes the also retarded individual cars in points D, E, and F until the curve reaches its point of intersection with the inclined line OA at A, at which point the take-up of the slack catches up with, and passes beyond, the brake application. Beyond that point the group of retarded cars will strike only unretarded ones. The coordinates of the point A are x_1 and y_1. The nature of the curve changes at this point and the part $ODEFA$ for which $x < x_1$ and the part beyond the point A for which $x > x_1$ will therefore be analyzed separately.

(*a*) $x < x_1$. Consider first the part of the braking action represented by the curve $ODEFA$, or before the slack take-up has reached the point of brake application. At any time x during this period, the group of retarded cars will have a total mass of $M(x/t_1)$ and since they have been retarded during the time x by an average force of $^1/_2Fx/t_1$ their average loss in speed c_x can be computed from the momentum equation

$$M\frac{x}{t_1}c_x = {}^1/_2F\frac{x}{t_1}x$$

Therefore, for all values of $x < x_1$

$$c_x = \frac{Fx}{2M} \quad \ldots\ldots\ldots\ldots [65]$$

The brakes apply to car number $(x/t_1 + 1)$ at the time x, and it begins to retard. Before this car collides with the others, the latter have formed a group moving in unison, and the retardation of all braked cars is uniform. Therefore, the collision takes place at the impact speed c_x given in Equation [65].

At all times the braked cars have suffered an average loss of speed of c_x. The corresponding loss in travel of all braked cars during any time element would therefore be equal to the number of cars braked during time element times their average loss in speed c_x times the duration of the time interval.

Let Y = loss in travel of all braked cars at the time x. Then

$$\frac{dY}{dx}dx = \frac{x}{t_1}c_x dx = \frac{Fx^2}{2Mt_1}dx$$

or after integration

$$Y = \frac{F}{6Mt_1}x^3 + \text{constant}$$

The integration constant is 0 since for $x = 0$, Y must also be equal to zero. Therefore

$$Y = \frac{F}{6Mt_1}x^3 \quad \ldots\ldots\ldots\ldots [66]$$

The coordinates x_1, y_1 of the point A should satisfy Equation [66] and also be located on line OA, Fig. 39. For this point therefore

$$Y = \frac{F}{6Mt_1}x_1^3 \text{ and } \frac{y_1}{s_1} = \frac{x_1}{t_1} \text{ or } y_1 = x_1\frac{s_1}{t_1}$$

Y can also be expressed as

$$Y = \frac{y_1}{2}\frac{y_1}{s_1} = \frac{y_1^2}{2s_1}$$

From the preceding three equations x_1 and y_1 may be determined. Accordingly

$$x_1 = \frac{3Ms_1}{Ft_1} \text{ and } y_1 = \frac{3Ms_1^2}{Ft_1^2} \quad \ldots\ldots\ldots\ldots [67]$$

The number n_1 of the car at which point A is located may be computed as

$$n_1 = \frac{y_1}{s_1} + 1 = \frac{3Ms_1}{Ft_1^2} + 1 \quad \ldots\ldots\ldots\ldots [68]$$

(*b*) $x > x_1$. Beyond the point A in Fig. 39, the coordinates of which are x_1 and y_1, the group of retarded cars will strike only unretarded cars. Assume that the point A has been passed and that the bunched group, consisting of cars 1 to 10 inclusive, is moving along the line GH striking the, as yet, unretarded car 11

at the point H on the curve x, y. The equation for the curve x, y beyond the point A can be determined as follows:

The loss in momentum of the bunched cars at the time x can be expressed either as the product of the mass of the group of cars by their loss in speed, or as the product of the average retarding force by the time during which it has been acting. Hence

$$M \frac{y}{s_1} c_x = F \frac{x}{t_1} \frac{x}{2}$$

which equation, since $c_x = dy/dx$, may be written as

$$y \frac{dy}{dx} = \frac{F}{M} \frac{s_1}{2t_1} x^2 \qquad [69]$$

which becomes, after integration

$$y^2 = \frac{F}{M} \frac{s_1}{t_1} \frac{x^3}{3} + \text{constant}$$

By substituting in this equation, the values of x_1 and y_1 from Equation [67], the integration constant is found to be zero. Therefore

$$\left.\begin{aligned} y &= \sqrt{\left(\frac{Fs_1}{Mt_1}\frac{x^3}{3}\right)} \\ \text{or} \qquad x &= \sqrt[3]{\left(\frac{3Mt_1y^2}{Fs_1}\right)} \end{aligned}\right\} \qquad [70]$$

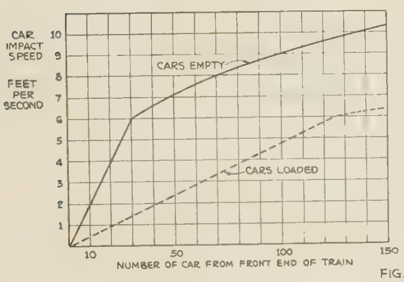

FIG.40

Substituting the value of x from Equation [70] in Equation [69] and solving for dy/dx

$$c_x = \frac{dy}{dx} = \sqrt[3]{\left(\frac{9}{8}\frac{Fs_1y}{Mt_1}\right)} \qquad [71]$$

For the car number n the value of $y = (n - 1)s_1$ and therefore

$$c_x = c_{max} = \sqrt[3]{\left(\frac{9}{8}\frac{Fs_1^2\,(n-1)}{Mt_1}\right)} \qquad [72]$$

or if L_1/V_1 is substituted for t_1 in Equation [72] and it is solved for s_1

$$s_1 = \sqrt{\left(\frac{8ML_1}{9\,FV_1(n-1)}\, c^3{}_{max}\right)} \qquad [73]$$

If the slack s_1 per car is known, the corresponding maximum car impact speed for a train of a certain number of cars of known mass can be computed by using Equation [72]. If the permissible car impact speed is known, the maximum permissible slack can be computed from Equation [73].

Example. Assuming a draft-gear recoil of not over 50 per cent, it is required to determine the impact speeds between adjacent cars in a 150-car train, each car weighing 50,000 lb empty and 210,000 lb loaded, and having an average of 4 in. of slack between adjacent cars. It is given that the emergency braking rate is 7500 lb and that it is applied at the front end of the train at a propagation speed of 600 fps. The length of cars between pulling faces of the couplers is 50 ft.

From the preceding discussion it is found that $M = 1550$ for empty cars and 6550 for loaded cars, $L = 50$ ft, $F = 7500$ lb per car, $V_1 = 600$ fps, $t_1 = 0.0833$ sec, $s_1 = 0.333$ ft, and $F/M = 4.84$ for empty cars and 1.154 for loaded cars.

Referring to Fig. 39, the coordinates x_1 and y_1 for point A are given by Equation [67]. The value of $x_1 = 2.48$ sec for empty cars and 10.4 sec for loaded cars. According to Equation [68], $n_1 = 31$ for empty cars and 126 for loaded cars.

The corresponding value of the impact speed is computed from Equation [65] for all values of $x < x_1$. For $x = x_1$, the impact speed $c_x = (F/2M)x_1 = 6$ fps for loaded as well as for empty cars. The impact speed gradually increases from zero to this value, which is reached at car n_1.

For values of $x > x_1$, the impact speed is given by Equation [71] which shows that c_x is a parabolic curve, the maximum value of which is expressed by Equation [72]. Therefore, for $n = 150$

$$c_{max} = 1.938 \sqrt[3]{(n - 1)} = 10.3 \text{ fps for empty cars, and}$$

$$c_{max} = 1.200 \sqrt[3]{(n - 1)} = 6.38 \text{ fps for loaded cars.}$$

The values of c_{max} for all values of n up to 150 are plotted for empty and loaded cars in Fig. 40.

(C) Starting of a Stretched Train

The action of a locomotive in starting a stretched train corresponds to that of a constant pulling force P_L acting at the end of an elastic bar. The frictional resistance, opposing the motion of

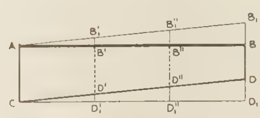
FIG. 41

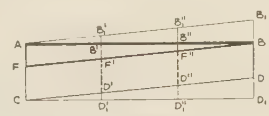
FIG.42

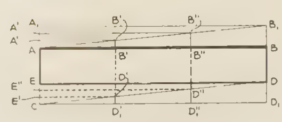
FIG 41 A

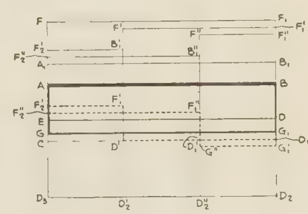
FIG.42A

each car, corresponds to a gradually applied and uniformly distributed force, acting in the direction opposite to the motion and applying to each car at the moment the car begins to move. The rate of force application is therefore equal to that of pressure transmission, and the propagation ratio of the frictional force is equal to unity. The action of these forces is represented by Case 2, as given in Table 3.

Referring to Fig. 41, the pressure diagram created by the locomotive drawbar pull P_L would, acting alone and after passing through the intermediate shapes $AB'D_1'C$ and $AB''D_1''C$, take the shape of the rectangle ABD_1C. The pressure diagram created by the friction forces, acting alone, would, after passing through the intermediate shapes $AB'B_1'$ and $AB''B_1''$, take the shape of the triangle ABB_1. Superimposing these two diagrams, the resultant diagram, after passing through the intermediate shapes

$AB'D'C$ and $AB''D''C$, takes the shape of the quadrangle $ABDC$ at the end of the first period.

Referring to Fig. 41*A*, the speed diagram created by the drawbar pull P_L, acting alone, would, after passing through the intermediate shapes $AB'D_1'C$ and $AB''D_1''C$, take the shape of the rectangle ABD_1C. The speed diagram created by the friction forces, would, after passing through the intermediate shapes $AB'B_1'A_1'$ and $AB''B_1''A_1''$, take the shape of the rectangle ABB_1A_1. Superimposing these two diagrams, the resulting speed diagram would, after passing through the intermediate shapes $AB'D'E'$ and $AB''D''E''$, take the shape of the rectangle $ABDE$ at the end of the first period.

If the locomotive drawbar pull P_L were acting alone, the pressure diagram, Fig. 42 (a reproduction of the pressure diagram in Fig. 41), would, at the beginning of the second period, have the shape of the rectangle ABD_1C and would, after passing through the intermediate shapes $AB''D_1''C$ and $AB'D_1'C$, vanish in the vertical AC at the end of the period.

If the frictional forces were acting alone, the pressure diagram ABB_1 would, after passing through the intermediate shapes $BF''B_1''A$ and $BF'B_1'A$, take the shape of the triangle ABF at the end of the second period. Superimposing these diagrams, the resultant pressure diagram will, after passing through the intermediate shapes $ABF''D''C$ and $ABF'D'C$, take the shape of the triangle ABF, in which BF is parallel with AB_1.

Referring to Fig. 42*A*, the speed diagram which would have been created by the locomotive drawbar pull P_L acting alone, and which at the end of the first period was represented by the

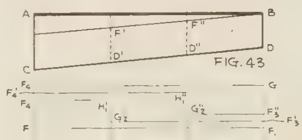

FIG. 43

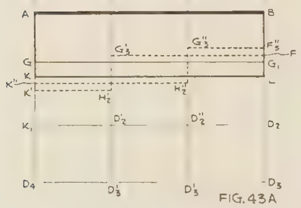

FIG. 43A

rectangle ABD_1C taken from Fig. 41*A*, would, after passing through intermediate shapes $ABD_2D_2''D_1''C$ and $ABD_2D_2'D_1'C$, take the shape of the rectangle ABD_2D_3 at the end of the second period, CD_3 being equal to AC. The frictional forces, acting alone, would, at the beginning of the second period, have created the speed diagram AA_1B_1B taken from Fig. 41*A*. This diagram, after passing through the intermediate shapes $ABF_1''F''B_1''F_2''$ and $ABF_1'F'B_1'F_2'$, would, at the end of the second period, have taken the shape of the rectangle ABF_1F. Superimposing the speed diagrams created by the drawbar pull and the frictional forces, it will be seen that the resultant speed diagram, which at the beginning of the second period had the form $ABDE$, takes the shape of the rectangle ABG_1G at the end of the second period after passing through the intermediate shapes $ABG_1''G''F_1''F_2''$ and $ABD_1D_1'F_1'F_2'$.

During the third period the pressure diagram shown in Fig. 43 will, after passing back through the intermediate shapes $ABF'D'C$ and $ABF''D''C$, again take the shape of the quadrangle $ABDC$. Period 4 will be the same as Period 2, Period 5 the same as Period 3, and so on.

Referring to Fig. 43*A*, the speed diagram which would have been created by the locomotive drawbar pull acting alone had, at the beginning of the third period, the shape of the rectangle ABD_2K_1. After passing through the intermediate shapes $ABD_2D_2'D_3'D_4$ and $ABD_2D_2''D_3''D_4$, this diagram would have taken the shape of the rectangle ABD_3D_4 at the end of the third period, D_2D_3 being equal to AC in Fig. 42*A*.

The rectangle ABF_1F in Fig. 43*A* which has been taken from Fig. 42*A*, represents the speed diagram which, at the end of the second period, would have been created by the frictional forces, acting alone. These forces would, during the third period and still acting alone, produce the speed diagrams $ABF_3'G_2'H_1'F_4'$ and $ABF_3''G_2''H_1''F_4''$, followed by the rectangular shaped diagram $ABGF_4$ at the end of the third period. Superimposing the speed diagrams in Fig. 43*A*, which would have been created by the drawbar pull and the frictional forces, the resultant speed diagram, which at the beginning of the third period had the shape ABG_1G, taken from Fig. 42*A*, will take the shape of the rectangle $ABLK$ at the end of the third period after passing through the intermediate shapes $ABF_5'G_3'H_2'K'$ and $ABF_5''G_3''H_2''K''$.

Referring to Fig. 42, AC represents the drawbar pull P_L of the locomotive. The vertical BB_1 is, according to Table 3, Case 2, for an elastic bar, equal to ${}^1/_2 f_1 L$. By substituting the corresponding constants for a train of n cars, each car being subjected to a frictional resistance of f_2 lb, it is found that this force is equal to ${}^1/_2 f_2 n$. The other forces in the diagram can be computed from the geometrical relationship to these two quantities. The force BD, acting at the end B of the bar, at the end of the first period, can therefore be expressed as

$$P = P_L - {}^1/_2 f_2 n \ldots\ldots\ldots\ldots\ldots\ldots [74]$$

Referring to Fig. 41*A*, the wave resistance of the train should be known in order to compute the car speed corresponding to the pressures in the preceding paragraph. Then the car speed AC in Fig. 41*A* can, according to Equation [2], be expressed as

$$c = f/\sqrt{(mk)} = P_L/R_w = P_L q/\sqrt{(CM)} \ldots\ldots [75]$$

The starting speed of the last car, represented by the vertical BD in Fig. 41*A*, can be expressed as

$$c_n = \frac{1}{R_w}(P_L - {}^1/_2 f_2 n) = \frac{q}{\sqrt{(CM)}}(P_L - {}^1/_2 f_2 n) \ldots [76]$$

The other forces and speeds in all these diagrams can be computed from their geometrical relationship to those given in the preceding equations.

Example. A locomotive, exerting a drawbar pull P_L of 80,000 lb is hauling a train of 150 cars which weigh 50,000 lb empty and 210,000 lb loaded. The frictional resistance equals 18 lb per ton. Therefore, f_2 = 450 lb for an empty car and 1890 lb for a loaded car. The draft-gear travel is 0.22 ft, and the draft-gear capacity is 18,000 ft-lb.

It is desired to know the speed which the train has acquired at the time the tension and speed waves reach the end of the train and also the force which starts the last car.

The mass M of an empty car = 1550 lb, while for a loaded car M = 6500. The wave resistance of the train R_w = $\frac{\sqrt{(18{,}000 \times 1550)}}{0.22}$ = 24,000 lb per ft per sec for an empty train and = $\frac{\sqrt{(18{,}000 \times 6500)}}{0.22}$ = 49,150 lb per ft per sec for a loaded train.

The pull starting the last car, represented by the vertical BD in Fig. 42, is, according to Equation [74], $(P_L - {}^1/_2 f_2 n)$ = 80,000 − ${}^1/_2 \times 450 \times 150$ = 46,250 lb for a train of empty cars. For a train of loaded cars $(P_L - {}^1/_2 f_2 n)$ = 80,000 − ${}^1/_2 \times 1890 \times$

150 = —62,000 lb, the negative value showing that the drawbar pull of 80,000 lb is insufficient to start the stretched loaded train.

The train speed acquired at the time the tension wave reaches the last car of the empty train is $c_n = (1/R_w)(P_L - {}^1/_2 f_2 n) = 46{,}250/24{,}000 = 1.93$ fps.

(*D*) Starting of a Bunched Train (With Free Slack)

The method used in analyzing the braking of a train with free slack can also be applied to this problem.

Any train with draft gears of low or moderate recoil will form a group of all started cars, and the latter will be assumed to move as a unit as they pick up, one by one, the cars which are standing still. The work performed by the locomotive as measured at the drawbar is, during the starting period of the train, mainly used (1) to accelerate the cars from a standstill, and (2) to overcome the frictional resistance of the cars during this period.

Assume that the first $(n - 1)$ cars have attained a uniform speed c_n at the time the last car is suddenly brought up to this speed from a standstill. The draft gears between the last two cars will in that case be subjected to an impact not exceeding that of a car moving at the speed c_n and suddenly stopped against a bumping post, the impact being taken up by two series-connected gears.

Therefore, the speed c_n can with fair accuracy be determined from the equation

$$P_L\, s_1 n = \frac{(n-1)M}{2} c_n^2 + \frac{(n-1)n}{2} s_1 f_2 \quad \ldots\ldots[77]$$

Solving this equation for c_n

$$c_n = \sqrt{\left[\frac{s_1}{M}\left(2P_L \frac{n}{n-1} - nf_2\right)\right]} \quad \ldots\ldots\ldots[78]$$

The minimum capacity of the draft gear $C_{\min}$ which will take up the impact of a car with a speed of c_n, two gears being connected in series, is expressed by the equation

$$2C_{\min} = \frac{M}{2} c_n^2 + f_2 s_1$$

or

$$C_{\min} = \frac{s_1}{2}\left(\frac{n}{n-1} P_L - f_2 \frac{n-2}{2}\right) \quad \ldots\ldots[79]$$

Example. Assume that the train in the preceding example had a total slack of 100 ft distributed over the 150 cars, or $s_1 = 0.667$ ft. The speed at which the stretched train would pick up the last car, expressed by Equation [78], is

$$c_n = \sqrt{\left[\frac{0.667}{1550}\left(2 \times 80{,}000 \times \frac{150}{149} - 150 \times 450\right)\right]}$$

$= 6.35$ fps for the train of empty cars.

For loaded cars, this formula gives a negative value, indicating that the locomotive is not powerful enough to start such a train, regardless of the amount of free slack. In practice an increase in slack will decrease the frictional resistance of the cars and thus facilitate starting.

The minimum draft-gear capacity required to prevent the gears from going solid when starting the empty train with 100 ft of slack is, according to Equation [79]

$$C_{\min} = \frac{0.667}{2}\left(\frac{149}{150} \times 80{,}000 - 450 \times \frac{148}{2}\right) = 15{,}700 \text{ ft-lb}$$

Acknowledgments

The author wishes to express his gratitude to the Edgewater Steel Company for sponsoring this investigation, to L. H. Donnell and L. H. Fry for helpful advice, and to J. H. Vogelsang for valuable assistance in construction of diagrams and checking of calculations.

Nomenclature

a, a_1, a_2, a_3, a_4 = acceleration or retardation of particles of an elastic bar, ft per sec per sec
= acceleration or retardation of cars in a long train in ft per sec per sec

C = capacity of one draft gear (plus that of one-half car body), ft-lb

$c, c_1, c_2, c', c_n, c_x$ = speed, or loss of speed, of particles in an elastic bar, fps
= speed or loss of speed of cars in a long train, fps
= relative impact speed between cars, fps

F = retarding force per car during emergency braking, lb

f = external force applied to an elastic bar, lb

f', f = longitudinal compression or tension occurring in an elastic bar

f_1 = external force applied per foot of an elastic bar, lb
= pressure transmitted in an elastic bar after a change in wave resistance, lb

f_2 = average frictional resistance per car during the starting of a long train, lb

k, k_1 = stiffness constant or modulus of elasticity of the material of an elastic bar in lb per sq in. multiplied by its cross-sectional area, lb
= $(L_1/q^2)C$ = stiffness constant of a long train, corresponding to that of an elastic bar and thus equal to the force required to stretch it to twice its length, lb

L = length of an elastic bar, ft

L_1 = length of one car between pulling faces of couplers, ft

l = distance from the front end of an elastic bar at which the pressure P occurs, ft
= the length to which a uniformly distributed external force applies, ft

l_1 = distance from the front end of an elastic bar at which the pressure P_1 occurs, ft (Case 1, Period 1)

l_2 = distance from the front end of an elastic bar at which the pressure P_2 occurs, ft (Case 1, Period 2)

l_3 = distance from the front end of an elastic bar at which the pressure P_3 occurs, ft (Case 1, Period 3)

l_4 = length of the greatest part of an elastic bar to which a uniformly distributed external force may apply and still produce the maximum pressure which the force, acting over the length l_4 can possibly create, regardless of the length of the bar, ft

l_6 = distance from front end of an elastic bar, at which the pressure P_6 occurs, ft (Case 3, Period 2)

M = mass per car

m, m_1 = mass per ft length of an elastic bar, or mass per ft length of a long train ($= M/L_1$)

n = number of cars in train

n_1 = number of cars from front of train at which the slack take-up reaches and passes beyond the brake application

P = longitudinal compression or tension in an elastic bar, lb
= coupler pressure or tension in a long train, lb
P_1 = maximum occurring internal bar pressure at end of Case 1, Period 1, lb
P_2 = maximum occurring internal bar pressure at end of Case 1, Period 2, lb
P_3 = maximum occurring internal bar pressure at end of Case 1, Period 3, lb
P_4 = maximum internal bar pressure produced by external forces, applied over part l_4 of the bar (for $p > 1$), lb
P_5 = maximum obtainable internal bar pressure with uniformly applied external forces in bar with both ends free, lb
P_6 = maximum internal bar pressure at end of Case 3, Period 2, lb
P_m = maximum internal pressure in an elastic bar, lb
P_L = drawbar-pull of a locomotive, lb
p = propagation ratio = V/V_1
Q_1, Q_2 = momentum of moving particles of a bar
q = travel of a draft gear plus compression of one-half of the car body, ft
R_w, R_{w1} = wave resistance of a bar, lb per ft per sec
= wave resistance of a long train, lb per ft per sec
r = $\sqrt{(m_1k_1)}/\sqrt{(mk)}$ ratio of the wave resistances of two parts of an elastic bar
s_1 = average slack per car, ft
t, t_1, t_2 = time intervals, sec
V, V' = speed of pressure transmission in elastic bars, ft per sec, or
= speed of pressure transmission in long trains, ft per sec
V_1 = rate of external force application in an elastic bar, ft per sec
= rate of brake application in a long train, ft per sec
x = time elapsed since brakes applied on car 1, sec
x_1 = value of x when brakes apply on car n_1, sec
Y = loss in travel of all braked cars at time x, ft
y = slack take-up at the time x, ft
y_1 = value of y when brakes apply on car n_1

Locomotive Tractive Effort in Relation to Speed and Steam Supply

By E. G. YOUNG,[1] URBANA, ILL., and C. P. PEI,[2] CHAMPAIGN, ILL.

The problem of estimating with reasonable accuracy the amount of tractive force exerted by a locomotive at running speeds enters every tonnage rating, economy study, and locomotive-operating investigation. Its importance is recognized, and many investigators have approached a rational solution by determining the hourly steam supply and the steam consumption per horsepower-hour, and from these the horsepower and tractive force. The steam rates assumed have been generally correlated with the speed only. Indirectly this requires the defining of the resulting speed-tractive-effort relation as "maximum tractive effort," "all-day tractive effort," or similar terms. This paper points out that the variation of the steam rate with the cut-off is of equal importance, but that a chart showing the variation of steam rate with the two factors, speed and cut-off cannot be used directly to obtain horsepower without an additional process. A more direct attack is made by (*a*) estimating the actual weight of steam used per revolution in cylinders of various sizes, with varying speeds, cut-offs, and working pressure; and (*b*) by correlating the speed, cut-off, and mean effective pressure, from which the tractive force corresponding to the cylinder horsepower is directly calculated. Each relation calculated gives the four values of speed, tractive effort, cut-off, and steam consumption for a given operating condition, and the calculation of a number of selected points results in a chart presenting a set of curves showing the tractive effort which may be expected at various speeds for specified conditions of boiler output and cut-off. This type of chart permits the user to see the economy to be expected at any condition within the probable working range of the locomotive and to determine the validity of any single speed-pull curve, involving a specified program of cut-off and boiler output for each speed.

The current interest in the performance and economy of the steam locomotive has focused attention on the old problem of the relation between speed and tractive effort, and has resulted in some very interesting and important contributions to its clarification. In previous discussions of the problem, two general forms of solution have been offered, of which one may be considered as purely empirical, and the other semi-rational.

The empirical solution is found in the various forms of speed-factor tables or curves. These, in general, express the tractive effort available at any speed in terms of a fraction of the rated tractive effort; such tables or curves are obtained by taking the averages of the test data for a number of locomotives, either singly or arranged in groups. These averages are valid, as a means of generalization, only when (1) the conditions of the tests are similar and rigorously defined, and (2) the average results are derived from tests of similar locomotives.

It follows that this generalization is only valid as a means of predicting the performance of another locomotive when the conditions under which it is to be operated correspond with the test conditions from which the average relation between speed and tractive effort was obtained. So far as the authors know, no such restrictions have ever been placed upon the use of any speed-factor method. In general, the relation is developed as one between the tractive effort and speed only, ignoring other factors that affect the tractive-effort development.

The type of solution that has been termed semi-rational usually proceeds on the basis of determining a horsepower output by dividing an estimated boiler evaporation by an anticipated steam rate or water rate, and then calculating the tractive effort from its relation to the horsepower and speed. An assumed firing rate, or boiler output, or tractive effort at a given speed may be the starting point from which the other quantities are determined. This method is desirable from the standpoint of simplicity, but the use of an anticipated water rate is an extremely indirect process and a very complicated one if the variation of the water rate with both the speed and cut-off, a fundamental fact of locomotive performance, is taken into account. Most of the semi-rational processes have made the water rate vary with the speed only.

In most of the methods of estimating tractive effort, either empirical or semi-rational, the final relation between the tractive effort and speed is represented by a speed-pull curve. This representation of tractive effort by a single speed-pull curve implies that, at a given speed, the locomotive can be operated to exert the amount of tractive effort corresponding to that speed as defined by the speed-pull relation, and conversely, for a given amount of tractive effort developed, the locomotive can attain a speed corresponding to that tractive effort. A further implication is that there is only one tractive effort obtainable at a given speed, and only one speed attainable at a given tractive effort. The absurdity of the latter assumption is clearly indicated in some of the recent investigations attempting to define the tractive effort as *maximum* tractive effort, *performance* tractive effort, or *average* tractive effort. These arbitrary definitions are, at the best, merely expedients of expression but do not possess significant meanings. The reasons are quite apparent: For a given locomotive, there are at least three sets

[1] Research Professor, University of Illinois. Mem. A.S.M.E. Mr. Young was graduated from the University of Illinois in 1913, and received his M.S. degree in 1916 and M.E. degree in 1923. Previous to his present connection he held positions with the American Locomotive Company and the Chinese Government Railways.

[2] Engineer, New York Air Brake Company, Watertown, N. Y. Mem. A.S.M.E. Mr. Pei was graduated with the B.S. degree from Tangshan Engineering College, China, in 1921. In 1923 he received the M.S. degree and in 1932 the M.E. (Professional) degree from the University of Illinois. He was formerly associated with the mechanical departments of the Nickel Plate Railroad, the Chicago, Milwaukee, St. Paul & Pacific Railroad, and the Northern Pacific Railroad.

Contributed by the Railroad Division and presented at the Annual Meeting, New York, N. Y., December 3 to 7, 1934, of The American Society of Mechanical Engineers.

Discussion of this paper should be addressed to the Secretary, A.S.M.E., 29 West 39th Street, New York, N. Y., and will be accepted until October 10, 1935, for publication at a later date.

of *maximum* tractive efforts, (1) the one limited by the adhesive weight of the locomotive, (2) the one based on the maximum cylinder output, and (3) still another one based on the maximum boiler output. In so far as the *performance* tractive effort is concerned, it is based upon the premise that the locomotive is operated in daily service with little variation so that a representative relation between the speed and tractive effort may be established for that particular mode of operation. The *average* tractive effort is really a mathematical quantity and it is useful only when the deviation of the actual from the average tractive effort is within such limits as to give the average tractive effort a physical significance.

A single relation between the tractive effort and speed for a given locomotive is thus an inadequate representation of facts. These facts can only be represented by taking the major variables into account and establishing a series of speed-pull curves on bases that can be rigorously defined. The variables for a given case may be separated into two distinct classes, which, for the present purpose, may be called the *physical factors* and the *operating factors*.

When a train is started over a division, the work which the locomotive must do at every point is already fixed by the tonnage and the inherent resistances of the train, and the speed requirements as known from schedules and train orders, by the profile of the road, and also the weather conditions. The locomotive assigned to the run will presumably be able to meet the requirements imposed upon it, as far as the capacity is concerned, at least, and if the tonnage ratings are well made, with reasonable economy as well. To the physical factors imposed by the train, track, and weather, may be added the limitations relating to the locomotive itself, its dimensions, proportions, and weight. When the crew gets aboard, they have under their control only a certain latitude in speed variations, the throttle opening, the cut-off, and the firing rate. Eliminating the practice of partial throttle operation, because of its inherent inefficiency, there remain only four operating variables, namely, speed, cut-off, firing rate (or steam supply), and the tractive effort. Of these four factors, fixing any two determines the other two, and consequently the entire operation of the locomotive, and therein lies the skill of the engine crew. Any two of the four operating factors, such as firing rate and cut-off, may be shown (as in the following paragraphs) to be dependent, if the others are assumed as independent. Hence, the tractive effort-speed relation must be defined by a family of curves, rather than a single relation.

The firing rate and cut-off are not independent factors because the two are related to each other through the total boiler output determined by the firing rate on the one hand, and the total steam requirement for the cylinders determined by the cut-off and speed on the other hand. Therefore, it follows that, at a given speed, the cut-off at which the locomotive may be operated is determined by the available steam supply, which is, of course, determined by the firing rate. Conversely, the firing rate is determined by the steam demand of the cylinders as determined by the cut-off and speed. This leads to the conclusion that the relation between tractive effort and speed is specifically defined only when qualified by the operating factors of firing rate or cut-off, or the combination of both.

Since the firing rate and cut-off are the only factors under direct control, either of these may be selected as the starting point in a performance analysis. It is the purpose of this paper to consider the consumption of steam in locomotive cylinders at various speeds and cut-offs, thus determining the steam requirement. No attempt will be made to relate the steam supply to the firing rate since this relationship rightfully belongs to the study of boiler performance. With the determination of steam requirement and assuming that it can be met by the steam supply from the boiler, it remains to obtain the correlation between the steam supply and the mean effective pressure, from which the cylinder tractive effort is calculated. The latter is a physically non-existent quantity, but it is extremely useful as a basis of comparison. The cylinder tractive effort may be defined in relation to the proportion of the locomotive by the familiar expression

$$T = p\frac{d^2s}{D} \qquad [1]$$

where T = cylinder tractive effort, lb; p = mean effective pressure, lb per sq in.; d = diameter of cylinder, in.; s = length of stroke, in.; D = diameter of driving wheels, in. The quantity d^2s/D is constant for any given locomotive and will be designated as Z.

The cylinder horsepower may also be calculated from the mean effective pressure as follows:

$$h = p\left(\frac{4as}{12 \times 33{,}000}\right)N \qquad [2]$$

where h = cylinder horsepower; a = area of piston, sq in.; and N = speed, rpm. The second factor on the right-hand side of Equation [2] is constant for any given locomotive and will be designated as Y. Equations [1] and [2] apply to conventional two-cylinder simple locomotives.

Another useful relation expresses horsepower in terms of T and V, where V is the speed in miles per hour:

$$\text{Since} \quad V = \frac{60ND\pi}{12 \times 5280} \text{ and } a = \frac{d^2\pi}{4}$$

$$h = p\left(\frac{12 \times 88V}{D\pi}\right)\left(\frac{d^2\pi s}{12 \times 33{,}000}\right) = \left(\frac{pd^2s}{D}\right)\left(\frac{V}{375}\right)$$

$$h = \frac{TV}{375} = \frac{pZV}{375} \qquad [3]$$

Many methods of making tractive-effort estimates have been proposed which depend on the relation

$$h = E/W \qquad [4]$$

where E = hourly evaporation, lb, and W = water rate in lb per ihp-hr. This is, of course, a true relation, but in view of the difficulty of estimating W, the process is extremely indirect. The fact is well known that at starting, with low speed and maximum cut-off, the water rate is high, of the order of 30 lb; also that at high speed and short cut-off, minimum values are obtained, of the order of 15 lb or lower. It is evident that in speeding up a train, the water rate passes through this entire range, and several investigators have correlated water rate with speed. This process, however, is inadequate, since at the same speed, operation at a considerable range of cut-offs is possible, depending on the steam supply; but the cut-off is also a factor in determining water rate, of equal importance with the speed. Sufficient data are now available so that a representative diagram can be shown for water rates for locomotives working at about 200 lb per sq in. boiler pressure. When it is drawn as a surface, relating the water rate in pounds per indicated horsepower-hour, speed in revolutions per minute, and cut-off in per cent of stroke, the shape is as shown in Fig. 1. Water-rate curves are usually shown plotted against speed, as represented by the lighter lines in Fig. 2. The group of points through which various lines of equal cut-offs are drawn in Fig. 2 have been in some investigations merely enclosed by an area of steam performance, and in other cases, a still less valid representation has been made in which all values for a given speed are averaged and the average

points connected. It is obvious that the average relation will depend more on the number of varying combinations of speed and cut-off than upon the specific results.

If a relation between speed and water rate, independent of cut-off, is assumed, such a relation will cut across the curves in Fig. 2, as shown by the heavy line *XY*. Many such relations have been assumed, each correct in itself, provided the locomotive is operated through the program of combinations of speed and cut-off upon which the water-rate relation is based. But the forecasting of such a program as a generalization can only be a matter of opinion, and the actual results in any given case will be closely related to the method of operation governed by the variations in operating conditions. The suggestion of a definite and precise correlation between speed and cut-off is open to the same criticism as applied to the single-line representation between speed and tractive-effort relationship.

If any fixed curve *XY* in Fig. 2 is to be discounted as an unsatisfactory generalization, the scheme of computing the tractive effort from the water rate must also be rejected, as the general relation shown by the light lines, Fig. 2, cannot be used directly. For example, it is desired to calculate the tractive effort of a locomotive of known proportions at a given speed; let the conditions be defined by assuming a cut-off. From Fig. 2, a water

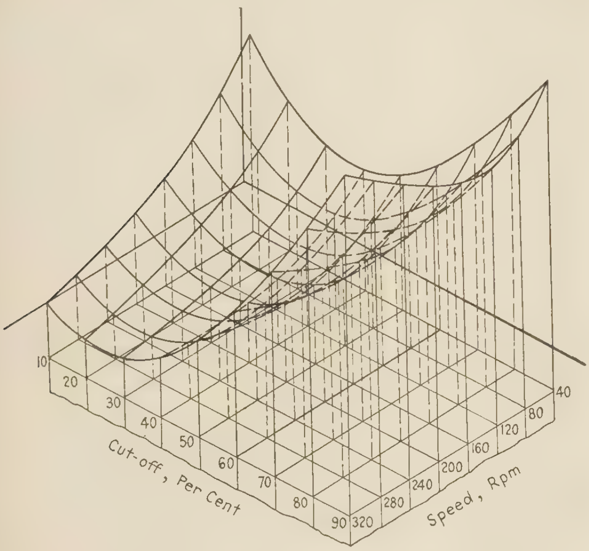

Fig. 1 Water-Rate Speed-Cut-Off Diagram Drawn as a Surface

rate may be assumed accordingly, but an additional process must be provided before the horsepower or tractive effort can be determined. Similarly, if a steam supply is assumed and the steam available per revolution is determined, but without the additional process, horsepower still remains unknown.

The proposed method is a more direct one, by means of which may be calculated:

(*a*) The total amount of steam used per hour when the cylinder dimensions, working pressure, speed, and cut-off are known or assumed.

(*b*) The cut-off at which the locomotive may be operated when the pressure, cylinder dimensions, speed, and steam supply are known.

(*c*) The relation between speed, cut-off, and mean effective pressure as a fraction of the admission pressure, so stated that with any two quantities given, the third one may be determined.

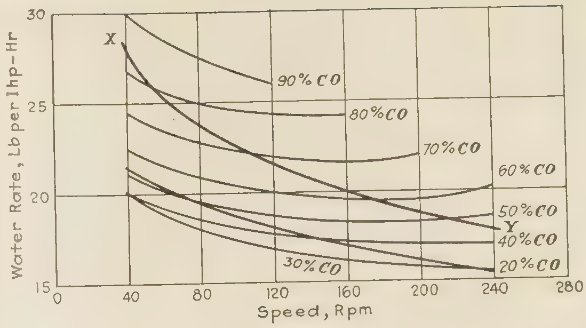

Fig. 2 Locomotive Water-Rate Curves. Line *XY* Represents Relation Between Speed and Water Rate, Independent of Cut-Off

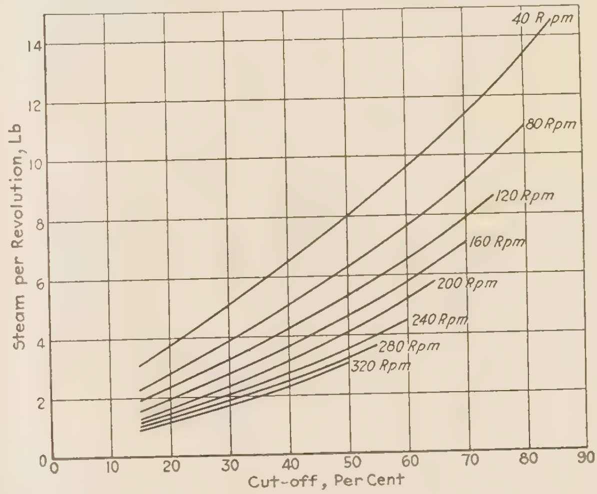

Fig. 3 Relation Between Steam Consumption per Revolution, Cut-Off, and Rpm for Two Cylinders Each With a Volume of 10.45 Cu Ft. Working Pressure 205 Lb per Sq In.

The process of estimating the tractive effort as applied to a locomotive of known dimensions would be (1) assume the speed and cut-off; (2) determine the steam used per revolution when the cylinder dimensions, working pressure, speed, and cut-off are known or assumed as in (*a*); (3) determine the steam required per hour; (4) determine the admission pressure by finding the probable loss between the boiler and the cylinders; and (5) find the mean effective pressure from (4) and (*c*) as given previously.

If, in place of assuming the cut-off, the steam supply is assumed, the process is (1) assume speed and steam supply per hour; (2) find the steam per revolution from the hourly supply and speed; (3) find the cut-off which may be used with this amount of steam per revolution from (*b*) as given previously; (4) determine the admission pressure as in (4) of the preceding paragraph; and (5) find the mean effective pressure as in (5) of the preceding paragraph.

The development of the process depends entirely on specific information obtained from the laboratory-test results, eliminating the uncertainties resulting from average steam output, average speed, average tractive effort, and average water rate usually obtained in road tests. The laboratory data are by no means as complete as might be desired, and in many cases inconsistencies make the determination of certain quantities most difficult. However, enough data are available in published

TABLE 1 STEAM PER REVOLUTION FOR VARIOUS LOCOMOTIVES

		Cut-off															
		20%		30%		40%		50%		60%		70%		80%		90%	
Rpm	Locomotive (cyl. vol., press.)	Lb	Ratio[a]	Lb	Ratio	Lb	Ratio	Lb	Ratio	Lb	Ratio	Lb	Ratio	Lb	Ratio	Lb	Ratio
40	I-1s (14.6, 250)	6.6	1.69	8.6	1.65	10.7	1.62	13.0	1.60	15.6	1.61	...	...	...	...	...	...
	L-1s and K-4s (10.45, 205)	3.9	1.00	5.2	1.00	6.6	1.00	8.1	1.00	9.7	1.00	...	...	...	...	15.8	1.00
	H-8sb (8.5, 205)	3.4	0.87	4.7	0.90	5.2	0.79	6.4	0.79	7.6	0.78	...	...	...	...	9.3	0.59
	Mo. Pac. 1690 (8.5, 200)	...	...	...	...	...	...	...	...	...	...	...	...	...	...	12.0	0.76
80	Baldwin 60,000 (11.7, 350)	...	...	...	...	...	...	8.5	1.37	10.8	1.44	13.4	...	...	...	20.2	1.68
	Baldwin 60,000 (11.7, 250)	...	...	...	...	...	...	...	...	...	...	9.2	...	...	...	14.0	1.17
	I-1s	4.3	1.59	6.6	1.58	7.6	1.52	9.5	1.53	...	...	...	...	...	...	...	...
	L-1s and K-4s	2.7	1.00	3.8	1.00	5.0	1.00	6.2	1.00	7.5	1.00	...	...	...	...	12.0	1.00
	H-8sb	2.4	0.89	3.4	0.89	4.5	0.90	5.5	0.89	6.6	0.88	...	...	...	...	...	...
	Mo. Pac. 1690	...	...	3.1	0.82	3.9	0.78	...	...	...	...	...	...	...	...	...	...
120	Baldwin 60,000 (11.7, 350)	...	...	...	...	...	...	6.9	1.30	8.8	1.35	11.0	...	13.6	...	17.2	...
	Baldwin 60,000 (11.7, 250)	...	...	...	...	...	...	...	...	...	...	...	...	8.8	...	...	...
	I-1s	3.5	1.52	4.8	1.50	6.2	1.48	7.9	1.49	9.7	1.49	...	...	...	...	...	...
	L-1s and K-4s	2.3	1.00	3.2	1.00	4.2	1.00	5.3	1.00	6.5	1.00	...	...	...	...	...	...
	H-8sb	2.0	0.87	2.7	0.84	3.7	0.88	4.5	0.85	...	...	...	...	...	...	...	...
	Mo. Pac. 1690	...	...	...	...	...	...	...	...	4.8	0.74	...	...	...	...	...	...
	E-6s-89 and E-3sd (6.5, 205)	...	...	...	...	...	...	...	...	...	...	...	...	...	...	...	...
	Purdue No. 4 (3.5, 170)	...	...	1.5	0.47	...	...	2.0	0.38	...	...	...	...	...	...	...	...
160	Baldwin 60,000 (11.7, 350)	...	...	...	...	...	...	5.8	1.26	7.4	1.30	9.4	...	...	...	...	...
	Baldwin 60,000 (11.7, 250)	...	...	...	...	...	...	...	...	...	...	5.8	...	...	...	...	...
	I-1s	...	...	3.75	1.34	5.0	1.39	6.6	1.44	...	...	...	...	...	...	...	...
	L-1s and K-4s	...	...	2.8	1.00	3.6	1.00	4.6	1.00	5.7	1.00	...	...	...	...	...	...
	H-8sb	...	...	2.4	0.86	3.2	0.89	4.0	0.87	...	...	...	...	...	...	...	...
	Mo. Pac. 1690	...	...	2.2	0.79	2.8	0.78	3.4	0.74	4.2	0.74	...	...	...	...	...	...
	E-6s-89 and E-3sd	...	...	2.2	0.79	2.9	0.81	3.7	0.81	...	...	...	...	...	...	...	...
	Purdue No. 4	...	...	...	...	...	...	...	...	...	...	...	...	...	...	...	...
200	K-4s	1.7	1.00	2.5	1.00	3.4	1.00	4.2	1.00	5.4	1.00	...	...	...	...	...	...
	E-6s-89	1.4	0.82	2.0	0.80	2.7	0.79	3.5	0.83	4.4	0.82	...	...	...	...	...	...

[a] Ratio of the steam consumption to that used by *L-K* combination at the same speed and cut-off.

form to make useful generalization possible, and it is hoped that the remaining gaps may be filled by additional tests.

Fig. 3 shows the relation between the steam per revolution, the cut-off, and the revolutions per minute, for the two Pennsylvania Railroad locomotives, class L-1s[3] and class K-4s.[4] The data from these two locomotives overlap only in the tests at 120 and 160 rpm, but the results for these speeds are so consistent as to make it legitimate to consider the combined results as coming from a single locomotive, tested over a wider range of speed and cut-off conditions than was ever used in a series of locomotive laboratory tests. These locomotives have cylinder volumes, including clearance, of 10.7 and 10.2 cu ft (one cylinder), respectively. No different relations may be drawn at the overlapping speeds for the two locomotives, and hence the volume of 10.45 cu ft may be taken as representative of the two. It remains to determine what relation is borne to the steam used in the 10.45-cu ft cylinders and, at 205 lb per sq in. boiler pressure, by that used in cylinders of other volumes and with steam at other pressures. This relation is referred to as the *L-K* combination.

Test reports are also available for a series of locomotives[5] using superheated steam and with cylinder volumes from 6.5 cu ft to 10.7 cu ft, all working at the same boiler pressure of 205 lb per sq in.; of a locomotive with three 8.0-cu ft cylinders and 200 lb per sq in. boiler pressure;[6] of two locomotives with cylinder volumes of 14.6 cu ft and 250 lb per sq in. boiler pressure;[7] and of the Baldwin 60,000[8] with one high-pressure cylinder

TABLE 2 CONDENSED SUMMARY OF DATA IN TABLE 1

Locomotive	Cylinder volume Cu ft	Cylinder volume Ratio to *L-K*	Working pressure Lb per sq in.	Working pressure Ratio to *L-K*	Conditions of comparison	Steam ratio to *L-K*
P.R.R. E-3sd and E-6s-89	6.5	0.63	205	1.00	All speeds, all cut-offs	0.80
Missouri Pacific, 1690	8.0	0.75	190[a]	0.93	All speeds, all cut-offs	0.77
P.R.R. H-8sb	8.8	0.82	205	1.00	All speeds, all cut-offs	0.87
Baldwin 60,000	11.7	1.10	335[a] 200[a]	1.65 0.95	All speeds, all cut-offs	1.50 1.06
P.R.R. I-1s	14.6	1.36	250	1.21	All cut-offs, speeds: 40 rpm 80 rpm 120 rpm 160 rpm	 1.60 1.50 1.50 1.40
Purdue No. 4	3.5	0.33	170	0.83	Speeds: 120 rpm 160 rpm Cut-offs: 30% 40%	0.45

[a] In calculating the ratios, attention was paid to the actual range of boiler pressures in the tests. On this basis, the working pressure for the Missouri Pacific locomotive 1690 is 190 lb per sq in., and for the Baldwin 60,000 it is 335 and 200 lb per sq in.

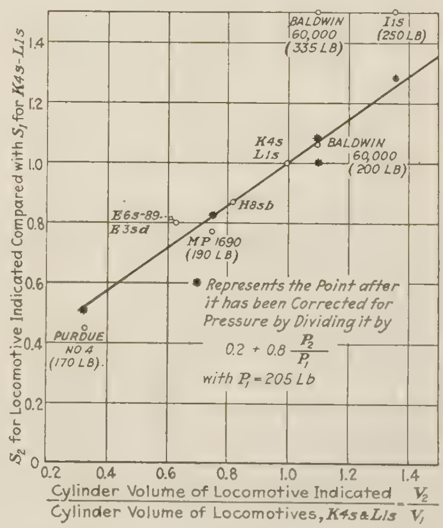

Fig. 4 Average Ratio of Steam Used by Various Locomotives to That Used by the L-K Combination

[3] Pennsylvania Railroad Bulletin No. 28.

[4] Pennsylvania Railroad Bulletin No. 29.

[5] Pennsylvania Railroad locomotives, E-3sd, E-6s-89, E-6s-51, K-2sa, H-8sb. See Pennsylvania Railroad Bulletins Nos. 11, 21, 27, 18, and 10, respectively.

[6] Missouri Pacific locomotive No. 1690, *Railway Age*, June 30, 1925.

[7] Pennsylvania Railroad locomotives I-1s-790 and I-1s-4358, see Pennsylvania Railroad Bulletins Nos. 31 and 32, respectively. These two locomotives differed in that the latter had a type-E superheater and also a feedwater heater, but the resulting difference in performance does not enter into consideration of this paper.

[8] Baldwin Locomotive Works publication, "Locomotive No. 60,000."

of 11.7 cu ft volume, with boiler pressures of 250 and 350 lb per sq in. Some data are also available for the performance of Purdue No. 4 locomotive which has a cylinder volume of 3.5 cu ft. All volumes are those of one cylinder, including clearance. Curves similar to those of Fig. 3 were drawn throughout the range of performance for all of these locomotives; these curves are not presented in this paper but in Table 1 are shown the values for steam consumption per revolution from smooth curves drawn through the actual points, and also the ratio of the steam consumption to that used by the *L-K* combination at the same speed and cut-off. Table 2 is a condensed summary of the data in Table 1.

The values in Table 2 are plotted in Fig. 4. The circles represent the various locomotives, showing for each its average ratio of steam used to that for the steam consumption of the *L-K* combination, plotted against the volume ratio. The points representing locomotives with 205 lb per sq in. working pressure show the use of less steam than that for the *L-K* combination in a ratio related to the smaller cylinder volume. The points representing locomotives with other than 205 lb per sq in. pressure show a use of more or less steam dependent both on the cylinder volume and working pressure. The first step in relating these is to reduce the varying pressure points to the values they would have if 205 lb per sq in. pressure were used. By trial, it was found that when the values of these points were divided by the quantity

$$0.2 + 0.8(P_2/P_1)$$

where P_2 is the actual working pressure of the locomotive under consideration, and P_1 is the working pressure of the *L-K* combination, or 205 lb per sq in., the corrected points fall close to the straight line drawn through the points for the 205 lb per sq in. pressure. The equation for the latter line shows that, if the steam for the *L-K* combination with cylinder volume V_1 is taken as unity, the steam for a locomotive with some other cylinder volume V_2 is

$$0.3 + 0.7(V_2/V_1)$$

Hence, the steam per revolution S_2 for a locomotive with pressure P_2 and volume V_2 as compared with the steam S_1 used by the *L-K* combination with pressure P_1 and volume V_1, may be expressed as

$$\frac{S_2}{S_1} = \left(0.3 + 0.7\,\frac{V_2}{V_1}\right)\left(0.2 + 0.8\,\frac{P_2}{P_1}\right) \qquad [5]$$

This is a purely empirical relation based on test results. The variations in the ratios for any given locomotive within its own range of performance are not sufficiently consistent for any other process to define this relation, and in general, the variation secured by using the formula proposed for finding S, the steam used per revolution, is less than the variation in the test data.

The value of S thus secured represents the steam used per revolution for both cylinders of the conventional two-cylinder simple locomotives; for three-cylinder simple locomotives such as the Missouri Pacific No. 1690, the steam used per revolution is 50 per cent greater than S, or 1.5 S, and for locomotives with only one high-pressure cylinder, as in the case of Baldwin 60,000, the steam used per revolution is equal to 0.5 S.

After determining the amount of steam per revolution it becomes necessary to find the admission pressure, in order that the mean effective pressure may be later determined. From the preceding process, S ($= S_2$) is known, and the total steam used by the cylinders in pounds per hour is

$$E_c = 60\,NS \qquad [6]$$

where E_c = steam used by the cylinders, lb per hr, N = rpm, and S = steam used by the cylinders per revolution, lb.

The pressure of the steam as delivered to the cylinders varies with the steam flow, and with the area of all the passages from the boiler to the cylinders. These areas are at least four in number, and there are no data nor theory to evaluate their effect. However, the loss in pressure, for any given steam supply, is closely related to the capacity of the boiler, and this in turn to its dimensions, so that a satisfactory correlation is found between the loss in pressure, the steam flow, and the heating surfaces. This relation is well represented by the expression

$$P_d = 0.6(E/H)^{1.6} \qquad [7]$$

where P_d = loss in pressure between the boiler and branch pipe, lb per sq in., E = total steam consumption, lb per hr, and H = total heating surfaces (outside), including superheater, sq ft. It is obvious that the total steam consumption E is made up of the steam used in the cylinders E_c and the steam used by the auxiliary devices E_a, or

$$E = E_c + E_a$$

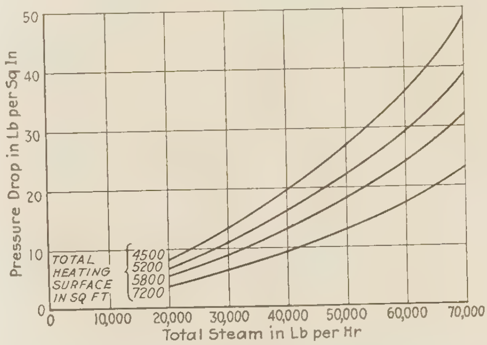

Fig. 5 Steam Pressure Drop Between Boiler and Branch Pipes

The curves from which Equation [7] is derived are shown in Fig. 5. They are valid only up to the point at which the boiler pressure itself begins to fall off.

For any simple locomotive operating at a given speed, the work in the cylinders depends on the mean effective pressure, which in turn depends on the admission pressure, the cut-off, and the steam distribution generally. No attempt can be made to estimate the effects of the variations in steam-distribution design; and the arrangements of the conventional engines are such that this variable may be eliminated. The effect of the diagram factor is so consistent that the mean effective pressure is, for any given speed and cut-off, a very definite proportion of the admission pressure. In Fig. 6 (6*a* to 6*e*, inclusive) the ratio of the mean effective pressure to the admission pressure at the various cut-offs is shown for the Pennsylvania locomotives L-1s, K-4s, H-8sb, and I-1s, the Illinois Central locomotive No. 1742,[9] and the Missouri Pacific locomotive No. 1690 for the usual range of test speeds. The curves accurately represent the range and value of the ratios. In the case of the four lower speeds, there are several curves available for comparison; for the higher speeds, the information from Pennsylvania class K-4s tests is used. These curves are assembled in a composite diagram in Fig. 7, which may be taken as representing the relation between the ratio of mean effective pressure to admission pressure, and the cut-off in per cent of stroke, at the various

[9] University of Illinois, Engineering Experiment Station Bulletin No. 220.

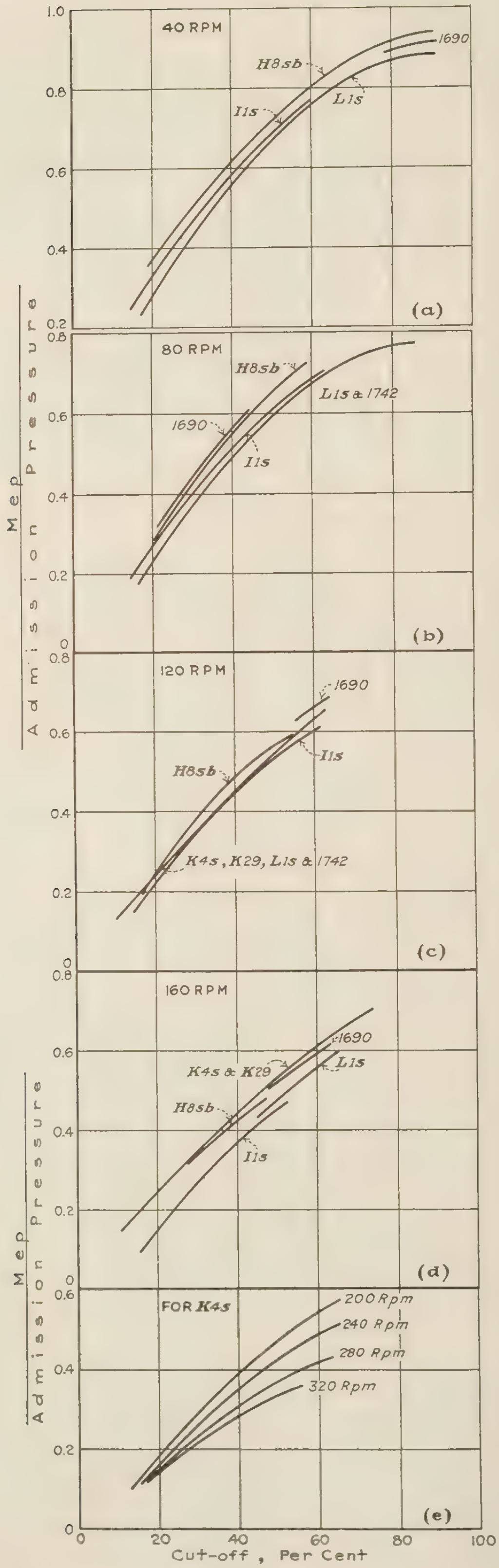

Fig. 6

speeds in revolutions per minute, for locomotives with conventional types of cylinders and valve gears and using superheated steam.

Estimating Tractive Effort

The process of estimating the tractive effort and horsepower of a locomotive may now be summarized:

1 Given the dimensions of the locomotive, the speed and cut-off, the procedure is:

(*a*) From Fig. 3 find the steam per revolution for the locomotive used as standard of comparison, having a cylinder volume of 10.45 cu ft and a working pressure of 205 lb per sq in., at the required speed and cut-off.

(*b*) Find the steam per revolution for the pressure and cylinder volume of the locomotive considered by modifying the steam per revolution found under (*a*) by the use of Equation [5].

(*c*) Find the steam used by the cylinders per hour by using Equation [6].

(*d*) Find the total steam used per hour by adding estimated amount of steam used by the auxiliary devices.

(*e*) From the total steam demand and the heating surfaces, estimate the pressure drop between boiler and cylinders by using Equation [7] or Fig. 5.

(*f*) Find the admission pressure by deducting the pressure drop (*e*) from the boiler pressure.

(*g*) Estimate the ratio of mean effective pressure to admission pressure for the given speed and cut-off from Fig. 7, and obtain mean effective pressure by multiplying the admission pressure (*f*) by this ratio.

(*h*) Calculate the tractive effort by Equation [1].

(*i*) Calculate cylinder horsepower by Equations [2] and [3].

2 Given the steam supply and the speed, the procedure is:

(*a*) If the steam supply is given as the net amount to the cylinders, the steam per revolution is obtained directly by dividing the steam supply E_c by 60 N, otherwise the total steam supply must be reduced by an estimated amount of steam used by the auxiliary devices in order to arrive at the net amount of steam to the cylinders.

(*b*) Reduce the actual steam per revolution (*a*) by the use of Equation [5] to find the amount of steam per revolution required by the locomotive used as the basis of comparison.

(*c*) Knowing the speed and the steam per revolution (*b*), find the cut-off at which the locomotive may be operated for that speed from Fig. 3.

Further procedure is the same as items (*d*) to (*i*), both inclusive, previously outlined under case 1, since the speed, cut-off, and total steam supply are now known.

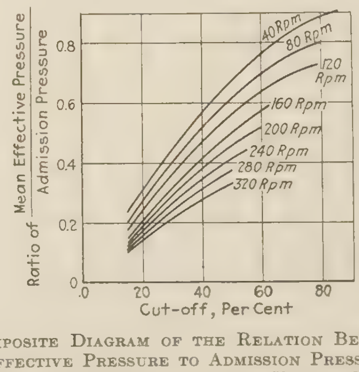

Fig. 7 Composite Diagram of the Relation Between Ratio of Mean Effective Pressure to Admission Pressure and the Cut-Off in Per Cent of Stroke at Various Speeds

(For locomotives with conventional-type cylinders and valve gears and using superheated steam.)

As a means of showing the application of the method which has just been outlined, the cylinder tractive effort and cylinder horsepower of a locomotive of assumed dimensions will be de-

Fig. 6 (Left) Ratio of Mean Effective Pressure to Admission Pressure at Various Cut-Offs for Different Locomotives

termined for a series of assumed values of cut-off and steam supply:

1 Locomotive dimensions:

Cylinders (two)	26 × 28 in.
Driving wheel diameter, in.	80
Boiler pressure, lb per sq in.	240
Total heating surfaces, including superheater, sq ft	6000
Engine constant for tractive effort	237

$$Z = (26^2 \times 28)/80 = 237$$

Engine constant for horsepower 0.150

$$Y = \frac{4(\pi/4)26^2 \times 28}{12 \times 33{,}000} = 0.150$$

2 From Equation [5], the steam used per revolution S for this locomotive having 26 × 28-in. cylinders, or a cylinder volume of 9.5 cu ft, including clearance estimated at 10 per cent, and 240 lb per sq in. pressure, may be related to that used by the comparison locomotive (*L-K* combination) with a cylinder volume of 10.45 cu ft and 205 lb per sq in. working pressure by the ratio

$$S = [0.2 + 0.8(240/205)][0.3 + 0.7(9.5/10.45)]S_1$$
$$S = 1.064\ S_1$$

3 An example of calculations for a given cut-off is given in Table 3. The calculations of cylinder horsepower and water rate, in addition to the tractive effort, are carried out as a check on the validity of the result.

4 A similar set of calculations based on steam supply may be made as shown in Table 4.

Similar calculations have been carried out with the cut-off assumed at 75, 60, 45, and 30 per cent, and with assumed values

TABLE 3 EXAMPLE OF CALCULATIONS FOR A GIVEN CUT-OFF

(a)	Cut-off assumed, per cent	75
(b)	Speed assumed, rpm	40
(c)	Steam per revolution for the *L-K* comparison locomotive with a cylinder volume of 10.45 cu ft and a working pressure of 205 lb per sq in. from Fig. 3, lb	12.4
(d)	Steam per revolution for the locomotive with a cylinder volume of 9.5 cu ft and a working pressure of 240 lb per sq in., (c) × 1.064, lb	13.2
(e)	Steam to cylinders per hour, (d) × (b) × 60, lb	31700
(f)	Estimated total steam used, including auxiliaries, lb	35000
(g)	Pressure drop between boiler and branch pipes, calculated by Equation [7] with E = 35,000 and H = 6000, lb per sq in.	10
(h)	Admission pressure, 240 — (g), lb per sq in.	230
(i)	Ratio of mean effective pressure to admission pressure for 40 rpm and 75 per cent cut-off, from Fig. 7	0.86
(j)	Mean effective pressure, (h) × (i), lb per sq in.	198
(k)	Cylinder tractive effort, (j) × 237, lb	47000
(l)	Cylinder horsepower, (j) × 0.150 × (b)	1188
(m)	Water rate, (e)/(l), lb per ihp-hr	26.7

TABLE 4 EXAMPLE OF CALCULATIONS BASED ON STEAM SUPPLY

(a)	Steam to cylinders, assumed, lb per hr	40000
(b)	Total steam required, including estimated steam for auxiliaries, lb per hr	44000
(c)	Speed, assumed, rpm	240
(d)	Steam per revolution for this locomotive, (a)/60(c), lb	2.78
(e)	Steam per revolution based on the comparison locomotive, (d)/1.064, lb	2.61
(f)	Cut-off corresponding to 240 rpm and 2.61 lb of steam per revolution, from Fig. 3, per cent	38
(g)	Pressure drop, from Equation [7], lb per sq in.	14
(h)	Admission pressure, 240 — (g), lb per sq in.	226
(i)	Mean-effective-pressure ratio corresponding to 240 rpm and 38 per cent cut-off, from Fig. 7	0.328
(j)	Mean effective pressure, (h) × (i), lb per sq in.	74
(k)	Cylinder tractive effort, (j) × 237, lb	17500
(l)	Cylinder horsepower, (j) × 0.150 × (c)	2560
(m)	Water rate, (a)/(l), lb per ihp-hr	15.6

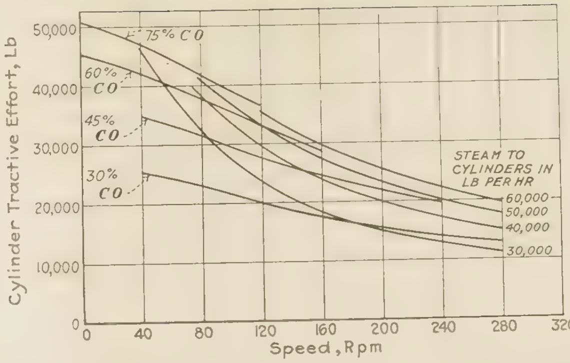

Fig. 8 Tractive-Effort-Speed Relation at Various Constant Cut-Offs and for Various Rates of Constant Steam Supply to the Cylinders

of 30,000, 40,000, 50,000, and 60,000 lb of steam per hr to the cylinder. For every assumed cut-off or steam supply, the calculations are made for speeds of 40, 80, 120, 160, 200, 240, and 280 rpm, omitting some of the obviously impractical combinations of speed and cut-off. The calculated results are plotted in Fig. 8, showing the relation between the cylinder tractive effort and speed in two sets of curves; one for the tractive-effort and speed relation at various constant cut-offs, and the other for various rates of constant steam supply to the cylinder.

The proposed methods of calculation extend only to a speed of 40 rpm. The determination of tractive effort at low speeds rests on the fact that for the first few revolutions of the driving wheels, a very small steam supply will be adequate to fill the cylinder, so that for zero speed when, so to speak, the locomotive is merely leaning against the train, the actual cut-off and the dimensional constants of the locomotive determine the tractive effort. Reasonable assumptions with regard to release and compression pressures give the following mean effective pressures for the maximum cut-off given, at zero speed:

Maximum cut-off, per cent	Ratio of mean effective pressure to boiler pressure
90	0.97
80	0.93
70	0.87
60	0.80

The advantages of the method proposed and of the resulting figure, Fig. 8, may be mentioned briefly as:

1 The process takes the physical facts of the transformation from potential into kinetic energy fully into account.

2 The chart places before the user a full exhibit of the capabilities of the locomotive.

3 If such a chart is to be used as the background for a single-line speed-pull curve, it is immediately apparent what program of evaporative capacity and cut-off is expected of the locomotive.

4 A basis is furnished for estimating the economy of the locomotive under any conditions, including those far inside of what may be considered its capacity.

Discussion

The Design and Performance of an Axial-Flow Fan[1]

C. Keller.[2] Noise measurements as plotted in the authors' Figs. 19 and 20 agree with the writers' recently published observations[3] which were made on the advice of Dr. J. Ackeret during experimental investigations of single-stage axial blowers. Among other things, these tests deal with the cause of noise and it might be interesting to compare both the results obtained and another method of investigation with the paper under discussion.

The pronounced increase of the intensity of the noise measured by the authors near the inflection point on the static-pressure line, and also the following sudden decrease, has been confirmed by all our tests on four different impellers. In our estimation, the noise in this region is caused by vigorous detachment

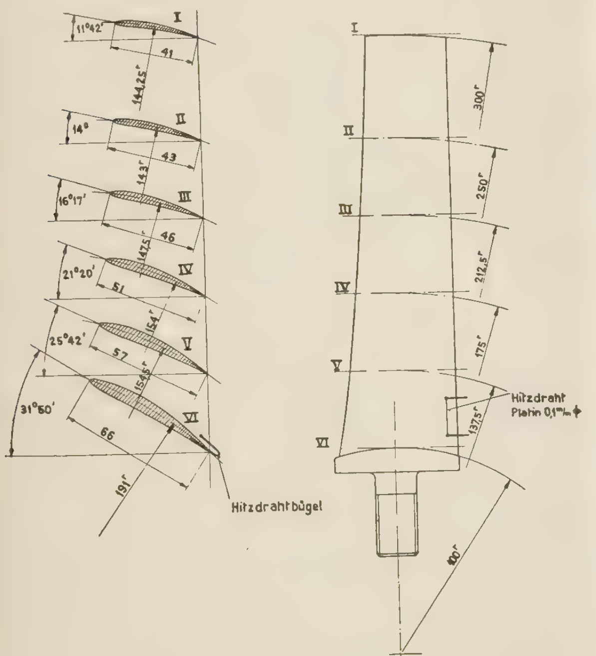

Fig. 1 An Impeller Blade With the Hot-Wire Arrangement
(*Hitzdrahtbügel* = Flexible Copper Wires; *Hitzdraht Platin* 0.1 *m/m* ϕ = Hot Wire Platinum 0.1 *mm* ϕ.)

of the air stream on the various wing parts. With a decreasing flow volume, the profiled impeller wings are loaded progressively (the lift coefficient c_a of the profile increases). With a decreasing volume a point is reached where the impeller can no longer produce the required pressure ($c_a > c_{a\max}$). As a result surging starts which is a well-known phenomenon in blower and compressor design, and the pulsation of flow volume and pressure gives a pronounced noise.

The hot-wire instrument makes it possible to investigate exactly the important flow phenomena on a moving wing by measuring the velocities on the spot where detachment of the stream occurs. A brief description of this investigation method is as follows:

A thin platinum wire 0.1 mm diam and 20 mm long is attached 2 mm above the surface of the rear side of a wing by means of 1-mm flexible copper wires as shown in Fig. 1 of this discussion. This arrangement does not cause any disturbances in the flow passing along the blade. The ends of the wires are fastened to thin insulated copper wires which are inserted in the wing and lead through the hub to the shaft end where they are connected to a battery by means of collecting rings, copper brushes, and rheostats.

During normal operation, the air passes over the wing surface without detachments and the platinum wire, through which passes a current i, is cooled by the air which has a velocity w. With a larger angle of attack (small volume) the eddies and backflow on the trailing side of the wing increase, starting at the rear edge, until finally the flow is wholly detached and the hot wire lies in a region of eddies. The wire, no longer subjected to the

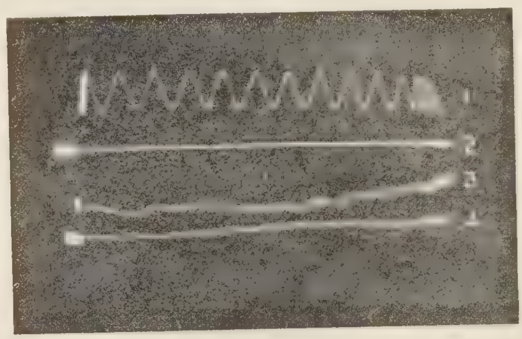

Fig. 2 Oscillograph of Changing-Voltage Difference Between Hot-Wire Ends Due to Detachment of Flow From Wing
(Line 1—50-cycles alternating current as oscillograph scale; line 2—normal flow w over the wing profile; line 3—beginning of detachment at the rear edge of the wing; line 4—flow detached from the wing profile.)

regular air flow w is cooled less than in normal operation and therefore its temperature rises. The electric resistance of the thin wire changes accordingly and a different voltage drop between the ends is the result. This voltage difference, after being duly increased by amplifier tubes, can be made visible by a cathode-ray oscillograph. This allows the observation of eventual periodic oscillations of detachments, if the hot wire has not too much inertia.

Tests have been made with a total difference of between two and three volts at the hot wire. The current in the hot wire amounted to approximately 3 amperes. A detachment of the stream corresponded to a difference of between 0.2 and 0.3 volt. For the leading tension of the electron ray of a Cossor tube which was used as a cathode-ray oscillograph, two amplifier tubes transformed the voltage difference from the hot-wire end 100 times to between 200 and 300 volts. By using the time abscissa of the

[1] Published as paper AER-56-13 by Lionel S. Marks and John R. Weske, in the November, 1934, issue of the A.S.M.E. Transactions.

[2] Chief Engineer, Caloric Research Laboratories, Escher Wyss Engineering Works, Ltd., Zurich, Switzerland.

[3] "Axialgebläse vom Standpunkt der Tragflügeltheorie," by Dr. C. Keller. Communication from the Aeronautical Institute of the Federal High School, Zurich, Switzerland, 1934.

Cossor tube, the oscillations of the voltage difference can be observed during a certain time, as illustrated in Fig. 2 of this discussion.

The upper sine curve represents 50 cycles alternating current, photographed on the same plate with the oscillograph curves, and serves as a calibrating scale. The distance between lines 2 and 4 corresponds to the voltage difference between the cold and warm hot wires (adherent and detached flow). Line 2 is very accurate and straight over the whole period of exposure. It shows the constant-voltage difference at the hot wire during normal operation of the fan with a closely adherent stream over the profile and indicates correspondingly uniform cooling. The air velocity w was then approximately 60 m per sec (3000 rpm). As soon as detachment is starting at the rear edge, the velocity w, and therefore the wire cooling, is changed. Now the voltage difference follows the irregular line 3. The unstable condition, prevailing near the hot wire is represented by oscillations of the wire-voltage difference. No regular frequency could be observed in this case. The angle of attack was about 11 deg when the detachment started.

Any further increase of the angle of attack (smaller volumes) causes a complete detachment of the flow and the hot wire lies fully in a dead space of flow. The wire, in comparison to the previous position which gave line 3, is heated still more and the change of potential difference is also greater. This case is illustrated by line 4. Contrary to line 3, where detachment of the flow is only beginning with alternating detachment and adherence, the temperature of the wire is almost constant which results in the constant-voltage curve, similar to line 2.

The three lines, 2, 3, and 4 correspond to the varying degree of noisiness as observed by Marks and Weske; line 2 representing minimum noise; line 3 representing an increase of noise with a decrease of efficiency; and line 4 representing lower noisiness after inflection point in the static-pressure curve.

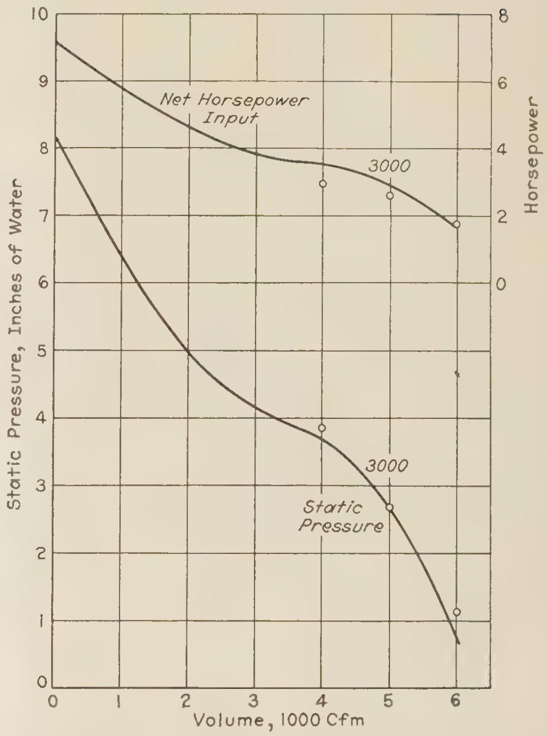

Fig. 3 Comparison of Computed Results With Marks and Weske's Test Curves of Capacity Versus Static Pressure and Power

R. G. Folsom[4] and M. P. O'Brien.[5] Many papers dealing with industrial equipment include little or no information on the details of construction and the authors are to be commended for presenting sufficient material to permit a technical analysis of the results. It is regrettable that restricted publication space made necessary the omission of the additional data referred to, especially those concerning the rotational velocity at discharge.

The writers have developed a quantitative method of predicting the head-capacity curves[6] of axial-flow pumps which agrees with test data on a commercial propeller pump. Since the flow through a propeller fan is practically incompressible, the same method of prediction should be valid and the information presented by the authors in their Figs. 3, 4, 5, 6, and 9 makes possible an application of this method.

The procedure used by the writers starts from the airfoil theory of Pfleiderer[7] modified in such a way as to give a portion of the head-capacity curve near the design point provided that the aerodynamic characteristics of the blade sections are known. The modification consists simply in taking a weighted average of the net total head developed at each radius and subtracting the friction and shock losses in the inlet and discharge ducts. Empirical fan-test constants are unnecessary in these computations, all coefficients being obtained from hydraulic tables.

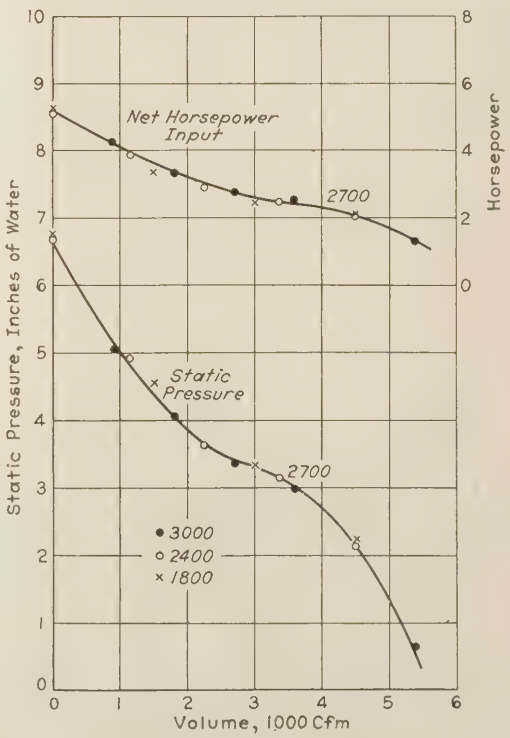

Fig. 4 Application of the Usual Affinity Laws to the Curves Given in Fig. 9 of Marks' and Weske's Paper

[4] Instructor, Department of Mechanical Engineering, University of California, Berkeley, Calif. Jun. A.S.M.E.

[5] Associate Professor, Department of Mechanical Engineering, University of California, Berkeley, Calif. Assoc-Mem. A.S.M.E.

[6] "Propeller Pumps," by M. P. O'Brien and R. G. Folsom, presented at the Aeronautics-Hydraulics Meeting of The American Society of Mechanical Engineers, Berkeley, Calif., June, 1934.

[7] "Die Kreiselpumpen," by C. Pfleiderer, Second edition, J. Springer, Berlin, 1932.

Fig. 3 in this discussion of the paper compares the computed results with the authors' test curves of capacity vs. static pressure and power. The discrepancy between the computed and measured heads is less than the probable error of the computations. The computed net power input is lower than that estimated by the authors on the basis of friction losses measured with a plain cylindrical hub. The good agreement indicates that the method used by the writers is satisfactory for design although it may not be theoretically sound in all details.

With regard to the bend in the head-capacity curves at which the authors observed that the fan became noisy, it is interesting to note that the airfoil theory shows this point to correspond approximately to the "burble-point" of the blade section. At greater rates of discharge, pumping is primarily the result of the lift of the blade sections while at lower rates the drag predominates. The bend appears to be the transition stage between these two conditions. "Burbling" starts at the hub and progresses outward as the capacity is decreased and its partial development along the blades probably causes the secondary flows observed by the authors.

Fig. 4 of this discussion shows the application of the usual affinity laws to the curves given in Fig. 9 of the paper under discussion. Theoretically these relationships should hold for axial-flow pumps and fans and it appears that they are dependable over the range of speeds investigated.

The authors state, "The fan can be designed so that the same amount of work is done on each particle of air, at the flow conditions corresponding to the point of maximum efficiency." Subsequently it is stated that, "The angle of attack was selected so as to give constant pressure on each blade element." The work per pound of the fluid is the total head (pressure head plus velocity head). It can be shown that the assumption of a constant total head and constant pressure difference at all radii are incompatible. It can also be shown that the radial-pressure variation resulting from a constant total head at all radii gives a stable type of flow and for this reason the assumption of a constant total head appears to be preferable.

Alexey J. Stepanoff.[8] The design finally adopted by the authors resembles very closely that of the axial-flow pumps already well established and for which considerable data are available. The design of the fan for which data have been presented was based on the use of certain constants obtained from a preliminary design and study of its performance. This preliminary fan, in turn, was built "following closely a design which has given good performance." Aerodynamic principles involved were given due consideration.

This is a normal procedure of commercial design of pumping machinery, resulting in the marked progress in performance observed during the last few years. The authors deserve credit for improving efficiency of the final design as compared with that used for reference.

Attempts have been made lately by several investigators to apply the test data obtained with airfoils in the wind tunnel to the design of axial-flow pumps, which substantially is the basis of the so-called "airfoil theory" of axial-flow pumps. There are, however, several handicaps to making this theory practical, such as: correction for mutual blade interference, finite blade length, variable pitch, and for the effect of a revolving series of blades instead of the parallel movement dealt with in aerodynamics. In addition to that, the performance of the diffusion case with inevitable losses should be accounted for, because it is in the performance of the complete unit that the designer is interested, and not of the impeller alone. The determination of corrective factors to account for all these influences experimentally is much more complicated than the building and testing of an actual model of the pump or fan, which is the procedure followed by the authors.

The number of variables to observe (head, capacity, and efficiency) in such a model test are the same as those with the airfoils (lift, drag, and angle of attack), and the testing procedure and equipment are much simpler. To make the results independent of the actual dimensions and speed of the pump, various factors were introduced (ratio of velocities or velocity heads) which correspond to the lift and drag coefficients in the airfoil theory. The factors for axial pumps, if plotted against specific speed as abscissas, fall in line with those for semi-axial flow (coni-flow), mixed-flow, and radial-flow centrifugal pumps, for which data have been compiled for years by the designer. It is very unlikely that designers will recalculate these data to conform to the airfoil theory.

No doubt, the charm of the airfoil and circulation theories lies in the fact that for certain simplified conditions those theories give solutions which agree very closely with the observed results, which is a very rare happening in the field of formal hydrodynamics.

An advanced pump or fan designer can enjoy the beauty of the airfoil and circulation theories and derive benefit from the achievements of modern hydrodynamics without trying directly to apply them to the actual design.

While the writer was studying this paper, several points were called to his attention. The fan efficiency, based on total head as calculated by the authors, corresponds to pump-hydraulic efficiency, neglecting leakage and disk friction. This was found by the authors to decrease with the speed. With pumps, efficiency is a maximum at a certain speed, below and above which efficiency drops slowly. At lower speeds the decrease in efficiency is caused by the decrease in mechanical efficiency at smaller outputs. This could not be observed by the authors, as mechanical losses were excluded in their calculations of the fan efficiency.

At higher speeds the difference between the velocities and pressures on the front and back side of the impeller blades becomes too great to perform the equalization of these at discharge and entrance edges with a minimum loss. The blade becomes overloaded. With pumps this is followed by cavitation if the suction pressure or submergence is not sufficient to suppress the local formation of cavities on the suction side of the blades.

The increase of the blade area, either by extending the blades or by increasing the number of blades, will increase the optimum speed of the pump or fan. This will also reduce the noise of the unit as a result of decreased pressure and velocity differences throughout the unit.

The authors have selected the profiles for the impeller blade with a straight front, or constant vane angle. The good performance of this fan proves, contrary to statements sometimes made, that the increase of the vane angle from the leading to the trailing edge is not absolutely necessary for an efficient generation of head. To make the generation of head possible with this shape of blade, the fluid must enter the blade with a sudden deflection or shock, but this shock is in the direction of flow, resulting in little or no loss of energy. On the other hand, by making the blade angle at the discharge equal to or smaller than that at the entrance the blade end is unloaded (becomes nonactive), resulting in uniting of the two streams on both sides of the blade with a minimum of loss.

Although the authors have chosen profiles with very thick entrance edges for the diffusion vanes, hoping to improve the flow for a wider range of capacities, the efficiency curves are not any flatter than found normally for this type of impeller.

The 0.5 ratio of the hub diameter to the impeller diameter used by the authors is greater than normally encountered in

[8] Byron Jackson Company, Berkeley, Calif. Mem. A.S.M.E.

pump designs. Large impeller hubs require an unusually long diffuser tapering hub for an efficient recovery of the velocity head.

The best distance between the impeller and guide vanes for axial pumps was found by Pfleiderer to be about 3 per cent of the impeller diameter. The authors' optimum clearance between the impeller and guide vanes is 5 per cent. The difference is probably caused by the fact that the authors' diffusion vanes have much heavier entrance edges than those of the Pfleiderer pump.

The authors deviate from the established methods of testing and terminology. This, while having no particular advantages, may lead to confusion. The close comparison of the performance of the fan presented in the paper with available data is impossible, as, while the authors based the fan efficiency on the power input less mechanical losses, the latter are not given in the paper. The statement in the paper that the pressures, volumes, and efficiencies, as determined by the methods of the Standard Test Code at another laboratory not named in the paper, may only be explained by the inaccuracy of the test data.

Authors' Closure

The preliminary investigations referred to in the paper had the same object as that discussed by Dr. Keller, namely, the exploration of the flow through the fan blades. For this purpose the test arrangement consisted of pitot tubes rotating with the fan and of a pressure seal by which the pressures were transmitted from the rotating elements to a stationary gage board.

In the region beyond the stalling point the conditions of flow around a rotating blade are more complicated than those of two-dimensional flow. The air in the stagnant zone at the back of the blade is dragged along by the blade at approximately the rotative speed of the blade. It thereby is subjected to centrifugal acceleration and tends to move radially outward. Stalling begins at the root of the blade; when it starts it has a disturbing effect upon the neighboring zones further away from the center line.

Stalling is only one of the causes of the rapid increase of noise near the inversion point of the fan-characteristic curve. Our measurements of axial velocity immediately in front of the fan wheel (by stationary pitot tubes) show that there is a displacement of the flow as the discharge volume decreases which results in diminishing flow near the tip of the blade. This may go so far as to cause reversal of flow at low discharge volumes. It is at the point where this reversal of flow first appears that the highest peak of the noise curve occurs.

It is gratifying to find the agreement between the computations of Mr. Folsom and Professor O'Brien and the actual performance of the fan. The difference between the two methods of design (constant total head and constant pressure difference) disappears when the fan and guide vanes are considered as one system and when the axial velocity leaving the system is constant over the cross-section.

Mr. Stepanoff suggests that the fan designed by the authors was a modification of the fan used in the preliminary investigations. This is not correct. The fan was designed on aerodynamic principles and departed from the previous design in a number of fundamental points, as stated in the paper. The combined corrective factor for the various influences to which Mr. Stepanoff refers (mutual blade interference, etc.) was actually determined experimentally, as he advocates, and was used in the design. The authors agree that two-dimensional air-foil theory is inadequate for a rational analysis of the flow through an axial-flow impeller. Air-foil theory, however, supplies useful data for the selection of the proper shape of the blade section. For the design of the blade as a whole, circulation theory as applied to propellers (particularly the work by Goldstein and others) supplies necessary and useful data for the practical design.

Air Flow in Fan-Discharge Ducts[1]

H. F. Hagen.[2] The author has made a valuable contribution toward the explanation of the discrepancies that appear between the volume measurements made by use of the pitot tube and those made with a flow nozzle. However, the quantitative use of the direction tube implies that the air has been assumed to have a smoothly rotating flow without ring vortices or radial motion. To validate this would require extensive investigation. The supporting evidence of nozzle agreement and egg-crate action is inferential and, while convincing, too meager to be conclusive, as the author himself states.

Fan literature describes two fundamental spins; a spin of uniform moment of momentum having a constant total head throughout the range of flow, and the vortex with a constant angular velocity. The first type of spin can occur in any fluid flow. The second type can be produced only by an expenditure of energy.

The flows indicated by the direction tube are of neither of these fundamental forms. Inasmuch as each blade produces vortices, it is pertinent to consider whether or not the apparent spins are due to a pattern of individual blade vortices, particularly as such vortices have a theoretical permanence. If such a vortex pattern exists, the square or pulsation effect cannot be ignored.

The author's experiments with more precise metal diaphragms are open to the objection that the small amplitude of their very precision makes them as susceptible to the minute displacements of the ordinary sound wave as they are to the relatively large displacements of air pulsation. The rubber diaphragm used by the writer indicated pulsations too great to be ignored. Professor Bailey's paper[3] also shows a severe pulsation in a fan delivery.

The writer has experimentally verified the author's work. The curves of Fig. 13 in the paper were checked in the writer's laboratory concurrently with the author's investigation. Later, an "egg crate" was used with his predicted results. In another case, the amount of spin shown by the direction tube was predicted from a difference between inlet and outlet volume measurements. However, complications arose. Two fans that showed a variation of approximately 10 per cent between pitot tube and nozzle produced agreement in subsequent testing throughout the whole range of the fan characteristic. It is to be noted that the nozzle volumes were the consistent ones.

The direction tube developed by the author is a new instrument of great promise. The writer has had opportunity to use it in an examination of the flows from two double-inlet experimental fans. One of these indicated a spin similar to those shown by the author for single-inlet fans, but of only 12-deg inclination. The other showed a double vortex of 22-deg maximum spin. Nozzle checks have not yet been made and further investigation is required along these lines.

To the best of the writer's knowledge, in every instance where the direction tube has been used in a fan duct it has indicated rotational flow. The author's deductions from the writer's reported results on double-inlet fans may require revision. Direction-tube tests made in cases that show agreement between pitot tube and nozzle may also prove illuminating.

[1] Published as paper PTC-56-2, by L. S. Marks, in the November, 1934, issue of the A.S.M.E. Transactions.

[2] Vice-President and Director of Research, B. F. Sturtevant Company, Hyde Park, Boston, Mass.

[3] "Pulsating Air Flow," by Neil P. Bailey, Trans. A.S.M.E., vol. 56, 1934, paper PTC-56-1, p. 781.

These test experiences have been mentioned to emphasize the complicated nature of the whole subject and to indicate that the author's unquestionably important discoveries do not provide an entirely complete explanation.

The author's work with the various types of pitot tubes is interesting. The writer has tested five different tubes of the type shown in the author's Fig. 4 and found curves similar in type to that of the author but with individual differences of velocity pressure of 3.5 per cent. Errors of this order frequently occur in pitot-tube work even on the inlet side of fans where there is no reason to suspect a spin. There appears to be an error of this order in the author's calibrations. Presumably the impact ends of the tubes of Figs. 2, 3, and 4 are identical. Allowing for signs plus or minus from the unity line a similar gradient can be secured from the published curves for impact-pressure variation which should be the same for the three. Such curves plotted from Figs. 2 and 4 agree closely, but the curve from Fig. 3 does not check within 4 to 6 per cent of the velocity head in the important 15-deg to 30-deg range. Has the author an explanation of this apparent change in the impact gradient?

Incidentally, it should be noted that, in rectangular ducts where the pitot tube is not conventionally moved toward the center line of the duct, the tubes of Figs. 2 and 3 would interchange characteristics and that possibly the symmetrically distributed holes of Fig. 4 are to be preferred.

It is worthy of remark that the author put his reliance, and very properly, on the nozzle measurement. In all the work done by both the author and the writer, the nozzle has been reliably consistent and has been used as a measure of the correctness of other methods. The only real objection to the nozzle is a commercial one of cost. This objection has been overcome by the development of accurate but inexpensive sheet-metal forms.

H. S. Bean.[4] The discussion, in the paper, of errors due to non-axial flow is of particular interest and value. It may be well to note that errors of the nature and approximate magnitude described have been observed in some tests made at the National Bureau of Standards on small household fans such as are used in the summer. Such results lead one to suspect many of the pulsation errors reported in Mr. Hagen's 1933 paper[5] and in Professor Bailey's current paper[3] were really errors due to non-axial flow.

In 1926 and 1927, the Gas Measurement Committee, Natural Gas Department, American Gas Association, conducted a series of tests at Buffalo, N. Y., to determine the effects on orifice-meter indications of various types of pipe fittings placed on the inlet side of the orifice. One of the "fittings" used was a combination of three elbows so connected as to determine two perpendicular planes. Presumably, such a combination of angles produced a whirl in the gas stream. The effect on the orifice meter varied from practically zero to more than 13 per cent low (i.e., the indication of the meter was less than it should have been), depending upon the size of orifice and its distance from the angles. Moreover, with an orifice of 50 per cent diameter ratio, the effect of these angles was very apparent even with over 50 pipe diameters of straight pipe between the orifice plate and the nearest angle.

While so far as is known, there have been no tests of just this kind made with venturi tubes and flow nozzles, it seems reasonable to expect that the effect on them would be similar. If this expectation is right, one may well question the accuracy of nozzle measurements such as mentioned by Professor Marks, when the approach stream has a whirling motion.

In these Buffalo tests, the use of straightening vanes, "egg crates" as Professor Marks called them, was tried as a means of overcoming the adverse effects produced by the fittings. In all but a few instances the straightening vanes were completely effective. While several different designs of vanes were tried, the most effective had about the same relative dimensions as those used by Professor Marks.

Professor Marks states that a pitot-tube traverse made 2.5 pipe diameters downstream from the straightening vanes was as satisfactory as at 9. This is less than the recommendation made in Part 3 of the Fluid Meters Committee Report, which specified that the distance between the vanes and the orifice should be between 4 to 10 pipe diameters, depending on the diameter ratio of the orifice used.

Near the end of the paper Professor Marks states: "It is concluded that, with 2.5 diameters of duct past the pitot-tube station, there is no disturbance of the pitot-tube readings resulting from the presence of obstructions at the end of the discharge duct." In other words, any disturbance produced by such obstructions does not travel back upstream as much as 2.5 pipe diameters. This lends support to the recommendation of the Fluid Meters Committee that there should be at least from 2 to 4 pipe diameters of unobstructed pipe between the downstream pressure tap and any fitting.

J. F. Downie Smith.[6] In his paper, Professor Marks has explained the desirability of changing the position of the outermost pitot-tube station in a circular duct in order to make the A.S.H.&V.E. test codes come into closer agreement with theory and practice. His point was that a better average velocity would be obtained by the method he suggests. Since he has recommended a change in the test codes, another recommendation may be considered simultaneously with it.

The procedure in fan testing at present is to divide the duct into several equal-area strips, and, at the center of each, to measure (among other things) impact and static pressures. From the data, the velocity of the air at each point is calculated and the velocities are then averaged to get the average velocity over the section. This answer is correct within the required accuracy. But when this average velocity is used in the calculation for the velocity head of the air at the section, the answer obtained is wrong. The kinetic energy obtained from $\frac{V^2_{\text{avg}}}{2_g}$ is not the average kinetic energy of the air.

Consider a small plane section of the duct with area dA perpendicular to the duct axis, a mean air velocity V at this point and density ρ. The kinetic energy of the material passing this section would be

$$\frac{WV^2}{2g} = \frac{dA\, V\rho\, V^2}{2g} = \frac{dA\,\rho\, V^3}{2g}$$

Over the entire section, the kinetic energy would be $\int_0^A \frac{\rho V^3}{2g}\, dA$, and the kinetic energy for a unit weight of the material would be:

$$\frac{1}{A V_{\text{avg}}\, \rho_{\text{avg}}} \int_0^A \frac{\rho V^3}{2g}\, dA = \frac{1}{2g\, A V_{\text{avg}}} \int_0^A V^3\, dA$$

Now for a parabolic distribution of velocity, as occurs in isothermal streamline flow, the average kinetic energy obtained in

---

[4] Physicist Chief, Gas Measuring Instruments Section, National Bureau of Standards, Washington, D. C. Mem. A.S.M.E.

[5] "Pulsation of Air Flow From Fans and Its Effect on Test Procedure," by H. F. Hagen, Trans. A.S.M.E., vol. 55, 1933, paper FPS-55-7, p. 105.

[6] Instructor in Mechanical Engineering, Harvard Engineering School, Harvard University, Cambridge, Mass. Assoc-Mem. A.S.M.E.

the above manner can readily be shown to be $\frac{V^2_{avg}}{g}$ instead of $\frac{V^2_{avg}}{2g}$ as has been used in the test codes. The latter is only half the size of the former. Fortunately, in fan work, the flow is seldom streamline, and for turbulent flow the error is much less than with viscous flow, amounting to only a few per cent. Unfortunately, it is not a constant amount and varies with the turbulence.

But in fan testing, the velocity head at each of the several points specified in the ducts is usually obtained or can be easily calculated. Then it appears better to average the velocity heads obtained at these various points and thus compute the velocity head of the air at this section. From this velocity head we can unfortunately get no data about discharge unless flow is viscous or of known turbulence. But the discharge can be obtained by calculating the average velocity as formerly.

Therefore, the specific recommendations are: (1) Calculate the volumetric discharge by averaging the velocities as specified in the test codes; (2) calculate the velocity head of the discharge by averaging the velocity heads obtained at the several specified test points.

Ed S. Smith, Jr.[7] The writer agrees generally with the author's conclusion that a "new definition of velocity head" is needed in the art of testing fans discharging into ducts but suggests that this new definition be made suitable for extension to the testing of pumps and turbines for liquids as well as gases.

This new definition that the writer suggests was proposed by George E. Lyon of Rensselaer Polytechnic Institute in 1921.[8] In view of the lack of published discussion, it may be well to state that, about 1930, Dr. Dryden, of the U. S. Bureau of Standards, independently proposed this to the writer in a conversation on metering of fluids by large-ratio nozzles.

The velocity head

$$h_b = \frac{\text{Total kinetic energy per second}}{\text{Mass per second}} = \frac{E}{M} \ldots\ldots [1]$$

The total kinetic energy per second $= \int_0^R 2\pi r \, dr \, V\rho \, \frac{V^2}{2g}$ for a circular duct where r is the radius, V is the velocity, and ρ is density. This simplifies to:

$$E = \frac{\rho\pi}{2g} A_1 \ldots\ldots [2]$$

where A_1 is the area of a graph in which V^3 is plotted as ordinate against r^2 as abscissa for a known velocity distribution.

$$M = \int_0^R 2\,\pi\, r\, dr\, V\, \rho$$

or

$$M = \rho\pi A_2 \ldots\ldots [3]$$

where A_2 is the area of a graph in which V is plotted as ordinate against r^2 as abscissa for a known velocity distribution, as is well known. Thus the average velocity head is simply

$$h_b = \frac{\rho\pi}{2g} A_1 \div \rho\pi\, A_2 = \frac{1}{2g}\frac{A_1}{A_2} \ldots\ldots [4]$$

Rectangular ducts may be treated in a somewhat similar, graphical manner. In the above analysis, only the velocity components along the axis of the duct have been considered.

It seems proper to credit the fan with any useful energy that it has added to the flowing stream as determined from the difference in total energy between a point in the inlet and one in the discharge duct. The total energy is to be taken as the sum of the energy of the static pressure, the kinetic energy of translation and rotation, and the total heat of the fluid itself. The useful portion of these energies must be determined from the portion of the energy increase that can reach the point of application and there be of service. The same problem is met in the sale of steam, e.g., where the flow-measurements are differently weighted when the fluid is to be used for heat or power.

As a practical matter, it seems fair to insist that the rotational energy be converted into that of translation or omitted from consideration. Consistent with this, it would seem desirable to measure the energy of translation at a point far enough distant from the fan, in view of any straightening egg-crates present, so that the velocity distribution is so nearly normal that further losses due to velocity readjustments will not have appreciable effects.

At such a point of normal velocity distribution, the mechanical viscosity is practically uniform across the central portion of the duct, thus producing a parabolic velocity distribution there. With smooth walls, the velocity builds up as the seventh root of the distance from the walls. The parabolic curve, extending outward from the center, and the seventh-root curve, extending inward from the walls, overlap for a generous range providing that suitable constants are used to adjust the above curves to follow the actual curve most closely. The seventh-root curve, taken alone, gives a sharp peak to the velocity-distribution curve, at the center of the duct, which entirely fails to fit the physical situation. It is best not to attempt to use a single law (parabolic, seventh root, or other) as basic in drawing general conclusions, but rather to make only such use of them as is mathematically convenient and correct.

The centrally located tube is the only fixed pitot tube that is considered worthy of use by the writer, and then only after it has been calibrated in situ at the various rates by velocity-distribution traverses, or otherwise. Any averaging or other pitot tubes located near the walls of the duct are in a region where the velocity-distribution gradient is too steep for accuracy or reliability, particularly for test purposes where guarantee performance is being checked.

Where the characteristic of the fan is such that the head first increases and then decreases with an increase in quantity, expansible fluids may have violent pulsations on the rising portion of the curve. The author's conclusion that pulsation errors are relatively small is evidently based on experience limited to fans having a steadily falling characteristic. With a rising characteristic, it is generally necessary to throttle the suction to avoid pulsations so severe as to render meaningless any velocity readings obtained by differential-type meters. It would seem desirable to supplement the pitot tube with a hot-wire velocity meter. While blowers having a rising characteristic may be considered as unworthy of mention, still they should fall under any system of test methods that lays any claim to comprehensiveness.

It may prove advantageous to rate such fans with a liquid instead of a gas. The writer has found it convenient to check the characteristic of a liquid pump by measuring the flow of air it produced. Of course the power required works against testing air fans with water as much as it favors testing large water pumps with air. However, the liquid-test procedure should find some use in model tests run to develop a design that avoids the objectionable rising characteristics of some former

[7] Hydraulic Engineer, Builders Iron Foundry, Providence, R. I. Mem. A.S.M.E.

[8] "Flow in Conical Draft Tubes of Varying Angles," by G. E. Lyon, Trans. A.S.M.E., vol. 43, 1921, paper no. 1830, p. 1245.

model. "An Investigation of the Performance of Large Centrifugal Pumps Using Air as a Medium," an advanced thesis by Miguel A. Quinones, Rensselaer Polytechnic Institute Bulletin No. 48, September, 1934, admirably confirms the potential value of such procedure, besides establishing the present accuracy of such a method.

A. PETERSON.[9] It may not be amiss to emphasize one important conclusion that may be reached from reading Professor Marks' paper and that is the possibility of serious errors in test results by use of the pitot tube. It is significant that Professor Marks uses the flow nozzle as a standard for comparison. This immediately brings up the question why should not the flow nozzle be specified also in the test code for fans.

The writer is a member of Committee number 10, his work having been confined mainly to the compressor section of the code which incidently has passed through its final steps for publication.

Before adoption of the flow nozzle for measuring volume, we had discussions and controversies with builders of commercial flowmeters such as thin-plate orifices, pitot tubes, etc., but the Committee took the stand that the most accurate method to determine volumes, with the knowledge of the art at that time, was the flow nozzle.

In the code as written, the door is, however, open to other methods of volume measurements but the test is not then strictly in accordance with the A.S.M.E. Code although it may happen to be just as accurate as a test according to the code.

In trying to have the flow nozzle also adopted in the fan Code in preference to the pitot tube, considerable opposition was raised by many fan manufacturers mainly on account of the expense of testing large fans by the flow-nozzle method.

After reading Professor Mark's paper and Mr. Hagen's paper,[5] I am more than ever convinced that the flow nozzle also should be specified in the fan code.

The pitot tube naturally has its place and can be covered in the fan code in the same manner as was done in the compressor code in permitting by mutual agreement other methods for volume measurements, but the flow nozzle should be the standard method.

In this connection, it may be well to emphasize the report of the Special Committee appointed to study in detail the principal objects and purposes of the A.S.M.E. Power Test Codes.

This report contains the following statement: "The Codes shall be so definite that they may be made part of commercial agreements and shall serve as a measure of fulfilment of contract obligations in so far as the items covered in these codes are concerned as well as a means of preventing disputes between parties to a test."

Professor Berry, who was a member of this Committee stated in the November, 1932, issue of *Power:* ". . . . the A.S.M.E. Test Codes are planned for use in acceptance testing and must therefore be so drawn that their results can be defended in litigation that may arise from a disagreement. The methods presented in such a code must be only those that are recognized as yielding the most dependable results attainable in the present state of the art."

I believe the foregoing quotations together with Mr. Hagen's paper[5] and Professor Marks' paper, herein being discussed, give ample justification for the Fan Code Committee to specify the flow nozzle for volume measurements.

If the fan is of such size that the expense of the test set-up becomes prohibitive, test of a model may be resorted to, which practice is followed by the hydraulic-turbine people and to some extent also by the centrifugal-pump manufacturers.

[9] Chief Engineer, Pump and Compressor Department, DeLaval Steam Turbine Company, Trenton, N. J. Mem. A.S.M.E.

R. D. MADISON.[10] The author has presented here a real contribution to the study of air flow in ducts, and has offered constructive suggestions for the changes in fan-test procedure. The use of the honeycomb straightener with a short test duct is to be commended both from the standpoint of economy of set-up and accuracy of test.

It is comforting to know that the author's opinion is that pulsation is responsible for only a small part of test errors. While pulsation still has to be dealt with it is not likely to abolish the use of the pitot tube and traverse. The pitot has been somewhat discredited of late and without real justification. The author has pointed out that with a straightener there seems to be little choice between the Prandtl tube and that adopted by the A.S.H.&V.E. Tests may prove that a modification of them both is the answer. The writer believes that larger static holes and a blunter, more elliptical-shaped nose in the A.S.H.& V.E. tube is desirable.

The writer has used straighteners and found them desirable from all viewpoints. In recent elbow tests he used a honeycomb approximately 5 in. square and 10 in. long and satisfactorily reduced spiral flow to a negligible amount. However, if shock loss at entrance is to be neglected, a length of 15 in. (3 diameters) would have been preferable. Contrary to what some may think, a thin-edged straightener does not "equalize" flow, although the static pressures, as read, are much more uniform. In fact, the writer has found that the velocities are apparently more uneven due to the more accurate reading of the static pressure. A straightener will introduce a pressure loss both by reason of the friction of the walls and by the shock loss at entrance. The former should not be charged to the fan. If there is a large amount of spiral flow there will be a large shock loss and this would and should automatically penalize the fan since spiral flow serves no useful purpose in any installation. It is the writer's opinion that a length of duct approximately 6 diameters could be used with a straightener—3 diameters between the fan and center line of the straightener, $1^1/_2$ diameters between the straightener and the pitot station and $1^1/_2$ diameters between the pitot station and end of the duct where a symmetrical throttling device is situated.

The subject of the use of rectangular ducts is too quickly dismissed by the author without considering some of its advantages. Most fans have square or rectangular outlets and are connected to ducts of similar shape. It would not only simplify the duct to keep it the same size as the fan outlet but it would change the flow lines less and facilitate the fabrication of the straightener and air-throttling device. It is true that there is a larger percentage of boundary to area in a rectangular duct than in a round one but there is also a greater percentage of readings taken near the boundary. The round-duct traverse presupposes a fairly uniform velocity distribution across the duct. This is not always attained, especially in single-inlet fans. In fact, the "pattern" of the velocity distribution may change radically with different points of rating with the same fan operated at constant speed. In the rectangular traverse the points are more uniformly distributed over the whole area and therefore more likely to be representative under all conditions. The author feels that the outermost point in the round traverse is not correct and should be moved slightly nearer the boundary. If tests prove that this is necessary and the same condition exists in the rectangular traverse, a corresponding change could be made. As a result of the observations, the writer believes that with the use of a honeycomb straightener there is every justification for the use of rectangular test ducts.

[10] Research Engineer, Buffalo Forge Company, Buffalo, N. Y. Assoc-Mem. A.S.M.E.

W. H. Carrier.[11] Although the pitot tube has always been recognized as a very convenient and simple instrument for determining fluid flow, the accuracy of the results obtained by it has heretofore been questioned. However, as a result of Professor Marks' research, it is possible to use this instrument with confidence.

There may be some question as to the proper distance from the fan discharge to take static-pressure readings. It is well known that a considerable length of piping on the fan discharge has an equalizing effect which actually increases the observed static pressure in many types of fans. It is also true, of course, that there is a certain frictional loss in this duct work. It is debatable whether an addition to a fan which improves its apparent efficiency should not be penalized by whatever frictional loss occurs in producing the additional efficiency. In a straight length of discharge duct there is normally this conversion of "static" energy, which will naturally occur in the duct, and the frictional loss of the duct is calculated from the fan outlet, so the performance of the fan would normally be taken on the present basis providing, of course, the correct coefficient of friction were allowed.

I believe that users of fan equipment would prefer to have the static-pressure readings taken closer to the fan outlets, as suggested by Professor Marks, as frequently this static pressure is the only usable pressure in an installation, and it is always desirable to get a better fan performance than expected rather than a poorer one.

On the other hand, fan manufacturers would probably like to see their fans given credit for performance under the most ideal conditions.

It is my opinion that only improvement in fan practice and design would result from adopting the suggestion of Professor Marks that the static-pressure readings be taken one diameter from the fan discharge. In the end this should be a benefit to all concerned, and should be looked at from a broad rather than a narrow point of view.

[11] Chairman of the Board, Carrier Engineering Corp., Newark, N. J. Mem. A.S.M.E.

Author's Closure

The air flows shown in Figs. 9 to 14 of the paper have all the characteristics of a continuously distributed vorticity. The second type of vortex described by Mr. Hagen is a particular case of distributed vorticity. Any arbitrary continuous distribution of vorticity may appear in a fluid. A free vortex (where the vorticity is concentrated on a line) will, through the action of viscosity and turbulence, diffuse its vorticity through the fluid in a continuous way just as heat diffuses by conduction through a body. The distribution of angular velocity indicated by Fig. 14 suggests such a type of diffusion.

Mr. Hagen's experience with fans, which sometimes show good agreement between pitot-tube and nozzle-volume measurements and at other times show a 10 per cent discrepancy, would appear to result from the commonly observed instability of performance of certain fans. A traverse with a direction tube would presumably have given the explanation for the phenomenon.

The suggestion by Mr. Hagen that rotational flow has always been found when a direction-tube traverse has been made is probably accurate. In the double-inlet fan mentioned in the paper, two opposing vortices are set up which, at $2^1/_2$ diameters from the fan, have a maximum whirl angle of 22 deg. At 9 diameters distance the maximum angle has decreased to 5 deg, a magnitude which has no perceptible influence on the pitot-tube readings.

The author does not believe that substantially identical pitot tubes will register individual differences of velocity head of the magnitude apparently found by Mr. Hagen. The five tubes used by Mr. Hagen vary sufficiently in dimensions to justify the expectation of some appreciable differences in their indications. The dimensions of Mr. Hagen's tubes, as well as those of the A.S.H.&V.E. standard tube, are such as to give an appreciable error in velocity-head indications. Since the writing of this paper, investigations have been made which will permit the design of a pitot tube giving negligible error for a correctly oriented tube and avoiding appreciable differences between the indications of different tubes.

Variation in impact head in the author's measurements, which Mr. Hagen deduces from Figs. 2, 3, and 4 of the paper, represents probably some variation in operating conditions. The author was interested at first only in the variation of velocity head with yaw; the static pressures were obtained at a later date when the desirability of knowing them developed. The conditions for the two sets of observation were not identical.

In the early part of his paper, the author recommends the use of round ducts for accurate work; in the rest of the paper the use of a round duct is assumed. With a rectangular duct and whirling flow, the mean static pressure can be determined as in a round duct by traverses along two center lines with spacing of observation locations as in the usual rectangular-duct traverses.

H. S. Bean suggests that whirling flow is to be expected in a nozzle if the air approaches it with whirling flow. This is certainly the case and has been observed by the author. As the axial velocity is increased through the nozzle, approximately inversely as the ratio of areas, and the tangential component is unaffected, the angle of whirl should be reduced in the nozzle. This is precisely what was observed. The fan whose performance is shown in Fig. 11 of the paper was provided with a nozzle at the end of a 10-diameter discharge duct and a traverse was made with a direction finder of the air leaving the nozzle. The whirl angle was found to vary in a fairly uniform manner from zero at the center to about 7 deg at the periphery. For these angles the correction factor, Fig. 8, is practically unity.

The discussion of J. F. D. Smith is concerned with a point which is not touched upon in the paper. He is unquestionably right in his proposal if the mean velocity head is the quantity desired. However, it should be pointed out that the mean velocity is the quantity usually of interest to the fan engineer and that the useful product of the fan is the velocity head corresponding to the mean velocity rather than the mean velocity head. In other words, a flow of uniform velocity across the whole cross-section is preferable to the same total flow with a velocity which varies across the cross-section. The latter, however, would show the higher mean velocity head.

When the author stated that there was need of a new definition of velocity head, he had in mind the question of non-axial flow and not the variation of velocity across the cross-section as suggested by Ed S. Smith, Jr. Mr. Smith's discussion of this point is in effect the same as that of J. F. D. Smith and is answered above. The author agrees with his conclusion that the useful portion of the energy given to the air is that which can reach the point of application and be of service there.

The pulsations referred to by Mr. Smith are those resulting from instability in the fan performance which, as he says, is common in fans having the characteristics which he describes. The author has not made any reference to this kind of pulsation. His discussion applied only to the type of pulsation described in Mr. Hagen's paper,[6] which is thought to be present in all fans and at all times and which results presumably from the discontinuous discharge from the fan blades or other similar source. With the type of instability to which Mr. Smith refers there is no definite performance of the fan; the conditions in the fan are changing violently and erratically.

The author agrees with Mr. Peterson as to the greater reli-

ability of the nozzle for volume measurements; in addition, the measurements consume much less time. As Mr. Hagen suggests, the development of rectangular sheet-metal nozzles may reduce the cost of nozzles so much as to remove the objection on the score of expense. The author is now investigating the rectangular sheet-metal nozzle to ascertain its coefficients and general reliability. Meanwhile, the use of egg-crate straighteners with an adequate length of duct and the proper specification of pitot tube should make pitot-tube volume measurements reliable.

The recent work on pitot tubes, to which the author has already referred in his reply to Mr. Hagen's discussion, does not entirely support the suggestions of Mr. Madison for increasing the accuracy of the pitot tube. The results of this new work will be published before long. Mr. Madison is quite right in stating that an egg-crate straightener will not equalize flow; it will only take out the rotational component. If the axial component of flow approaching the straightener is greater at the bottom of the duct than at the top, it will remain greater after passing through the straightener. It is also true that the equalization of flow takes place more rapidly when the air is whirling. Consequently, if equalized flow is desired, it is preferable to have a long run of duct preceding the straightener rather than following it. The experience of the author indicates that the increase in accuracy resulting from equalized flow before the pitot-tube station is very slight, but obviously there may be conditions of velocity distribution in which a pitot-tube traverse will not average the velocity with sufficient accuracy.

The advantages of rectangular ducts are well stated by Mr. Madison and on the score of cost and convenience, except for the long time required for readings, they are desirable. For accuracy, however, the author thinks that round ducts are preferable. If rectangular sheet-metal nozzles prove satisfactory, the use of rectangular ducts would certainly be indicated.

The Economics of Preheated Air for Stokers[1]

James W. Armour.[2] The authors, in their paper, by correcting for stoker area, ash content of the fuel, and the burning rate, have brought out very forcibly that preheated air is the major factor in causing high maintenance costs of stokers.

They have pointed out some ways in which maintenance with preheated air can be reduced and of these there are two in particular in which the stoker designer is interested. First, the design of the part itself and, second, the material which is used in the part.

Many operating companies attempt to reduce maintenance by buying cast-iron parts from a local foundry. This practice has hindered progress in solving some of the problems relating to stoker maintenance. The design of a part with reference to its maintenance is very important and is well illustrated by experiments which are being conducted in connection with the grate surface of the Harrington traveling-grate stokers.

A new grate surface was designed and installed on a stoker operating on anthracite and coke breeze. After a year's operation it appeared that these grate castings were an improvement over the old design from the standpoint of maintenance and appeared to have other desirable features with which we are not concerned as far as this particular discussion applies. As a result of this year's trial, we then undertook to install this grate surface in a number of other plants. One plant, burning bituminous coal on a traveling-grate stoker, had an installation requiring a rather high burning rate in quite a small furnace. Our grate castings lasted approximately one month. A change in design improved the life of these parts so that some of them have now been in service under exactly the same conditions in the same plant for nearly two years. This case is an exceedingly good illustration of what can be done on design alone, although such a vast improvement can hardly be expected in most cases.

The question of material has received rather lukewarm attention in the past. A number of so-called "heat-resisting" irons have been put on the market with rather indifferent results. We know it is not possible to add a small amount of alloying metals to cast iron and materially increase the melting point of the iron, so we rather look askance at any claims for inexpensive "heat-resisting" iron. It would be very desirable if castings, having a melting point higher than any furnace temperature which could be produced in a stoker-fired furnace, were available at a reasonable cost. Such material does not appear to be available at the present time at a price which would warrant its use.

There are, however, materials available which appear to give longer life and at a sufficiently reasonable price to justify further investigation. We are now conducting an investigation into the economics of using alloyed cast iron to determine just how much improvement can be made without increasing the cost beyond an economical point. This study has not progressed far enough to draw final conclusions, but it does show enough promise so you might be interested in a brief description of the trials.

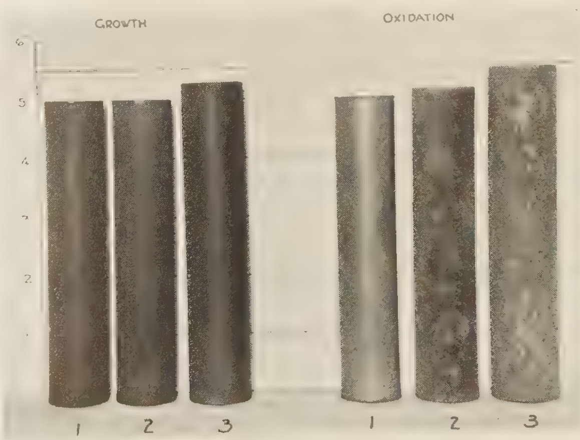

Fig. 1 The Effect of Growth, and Growth Plus Oxidation on Test Samples of Cast Iron for Stoker Parts

(Sample 1 is an alloyed cast iron costing about four times the cost of ordinary cast iron. Sample 2 is an iron which can be produced for approximately 25 per cent more than ordinary cast iron. Sample 3 is the ordinary run of cast iron.)

Realizing that fuel-bed conditions with underfeed stokers are very hard to maintain uniform and that burnouts of tuyère blocks may occur from causes having no bearing on the material of the tuyère blocks, we are confining our field experiments to a traveling-grate stoker where the fuel-bed conditions are fairly uniform. Aside from actual melting of the grate surface, we believe it is generally accepted that furnace castings break down primarily due to growth of the castings and rapid oxidation at elevated temperatures. Our experiments have, therefore, developed along the lines of obtaining growth-resistant iron and, in some cases, an iron which will resist oxidation. These factors may go together in the same iron.

Eleven different mixtures were finally decided upon for a trial, these selected mixtures being based on recommendations of

[1] Published as paper FSP-56-17, by R. E. Dillon an d M. D. Engle in the December, 1934, issue of the A.S.M.E. Transactions.

[2] Vice-President and Engineering Manager, Riley Stoker Corporation, Worcester, Mass. Mem. A.S.M.E.

various concerns and metallurgists interested in this particular problem. At the time the castings were poured test bars were also made, there being two test bars of each mixture. Enough grate castings of each mixture were made so as to cover a fairly large area, to eliminate the possibility of a condition which might occur at any isolated spot affecting the trial. All the various eleven mixtures were installed on one traveling-grate stoker. Such a stoker is quite suitable for this test for, as the grate castings travel through the furnace and then back again into the front, they are subjected to repeated heating and cooling which is conducive to obtaining the greatest amount of growth and oxidation. These grate castings are now in service.

The test samples have been subjected to laboratory tests which consisted of packing one sample in a box of iron filings so as to exclude the air and repeatedly heating it to 1500 F, and allowing it to cool. The other sample was subjected to the same heating and cooling process but in an oxidizing atmosphere.

The laboratory tests have indicated that it is possible to obtain a casting which has very little growth over a period of 50 cycles of repeated heating and cooling. As a rough estimate it is anticipated that castings can be produced for about 25 per cent increased cost which will give at least 50 per cent increased life. Such an estimate is subject to proof by the field tests which have not progressed far enough to draw any conclusions. The writer's Fig. 1 gives some idea of the effect of growth and growth plus oxidation of the laboratory samples.

Regarding the tuyères, it is possible to make them of ordinary cast iron with that part exposed to the fire of a more expensive heat-resisting iron. With such an arrangement it might be possible to use the higher alloyed irons without increasing the cost of the entire casting to a point where it does not become economical.

The authors have mentioned the use of water sprays under the stoker. Steam has also been used with some success, but the use of either water or steam means a reduction in operating efficiency and, while this may relieve an existing condition, it would hardly be desirable for application on a new installation. The use of water-cooled tuyères has been tried and shows some possibilities, providing the heat absorbed by the water can be economically recovered. All such devices add to the complications of stoker design which stresses the point that where high preheated-air temperatures are desired, high maintenance cost of firing equipment can be avoided by the use of pulverized coal.

John Van Brunt.[3] While the general opinion has been that highly preheated air would cause higher maintenance on stokers, individual opinions differ as to what temperatures constitute highly preheated air. Some stoker manufacturers do not take exception to 400 F or even 500 F, while others are more conservative and set the limit at 300 to 325 F. It has been my personal judgment that 325 F should be the limit unless the operating company is willing to accept the higher maintenance that accompanies higher air temperatures.

This paper is particularly valuable in that it enables one to assign a specific figure to the maintenance cost due to preheated air instead of estimating or guessing. However, there are several thoughts and questions that came up as a result of a study of the author's curves, answers to which might be of general interest:

(1) In Fig. 1, why is the inference made that the maintenance is higher with 75-F air than with 200-F air?

(2) In Fig. 2, showing the relation of stoker area to maintenance, it is possible that the shape of curve A is due in part to the fact that the larger stokers are usually operated at higher combustion rates and with low-ash coal. If curve B were further corrected for ash content of coal the corrected curve should be flatter, as there appears to be no other logical reason why size alone should affect maintenance to the extent shown.

(3) The indications of Fig. 3 are logical, in that higher combustion rates are accompanied by higher fuel-bed temperatures.

(4) Fig. 4 shows expected results, since ash serves as a protection to fuel-bearing surfaces. The effect of ash content in coals used on chain-grate stokers is marked. The downward slope of curve B at the left may be questioned, inasmuch as it indicates that a zero-ash coal would be less damaging to grate than a coal with 8 per cent ash. An explanation of why this curve B touches zero at 14 per cent ash would be interesting.

(5) Curves A and B in Fig. 5 do not compare with the accepted understanding of the effect of air in cooling the grate. One would expect curve B to start at the left at about $7^1/_2$ cents.

(6) The values indicated by the points of Fig. 7 are probably due to the higher-volatile coals which are usually higher in ash than low-volatile coals. Perhaps the higher percentage of fixed carbon or coke in the low-volatile coals may be a factor.

(7) In Fig. 10, summarizing the conclusions, curve B shows the same characteristic rise at low air temperatures as curve

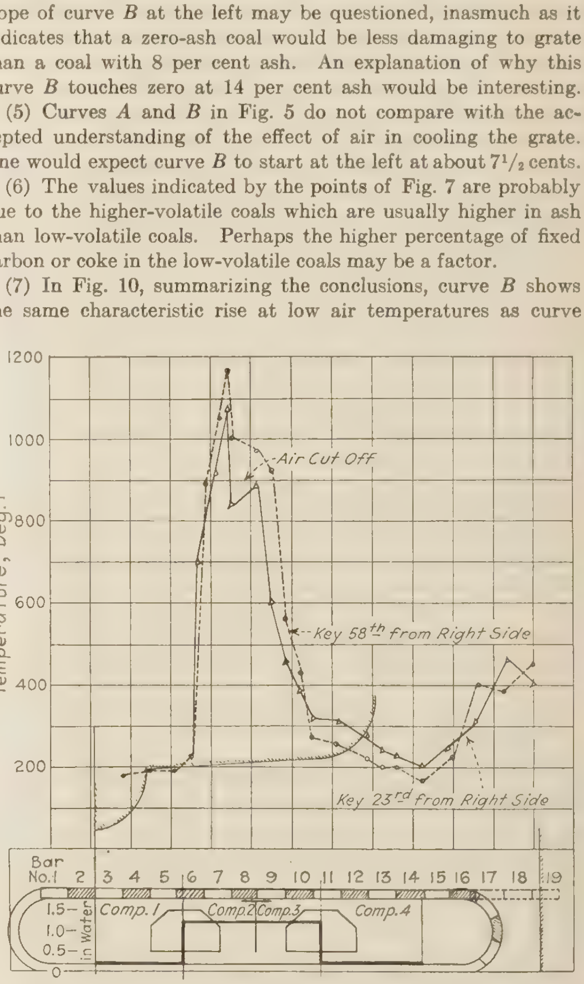

Fig. 2

A but to a greater degree; this I think requires further explanation, as I do not think it is safe to infer that 200-F air will result in lower maintenance cost than 100-F air, to the amount of about 2 cents per ton. Logically, curve B should start at zero cents at 50 F and rise in a straight line tangent to curve B as plotted at about 235 F.

The explanation of these peculiarities may lie in factors that were not available to the authors, such as banking hours, sudden dropping of load, composition of ash, fusion temperature of ash, and differences in operating.

Some time ago we had occasion to investigate the temperatures of the grate surface of traveling-grate stokers. Fig. 2, in this discussion, shows the temperatures reached by the stoker keys at various points along the travel of the grate. The maximum temperature, it will be noted, occurs at the point where ignition has penetrated through the fuel bed to the grate, which

[3] Vice-President in Charge of Engineering, Combustion Engineering Company, Inc., New York, N. Y. Mem. A.S.M.E.

is about 40 in. from the front end of the stoker. As soon as ash starts to form, the grate becomes protected from the incandescent fuel and the temperature rapidly drops to 300 F, and falls still further as the fuel bed is burned out.

From this curve it is easy to understand why preheated air rapidly increases the maintenance. With 300-F preheated air, the temperature of the stoker grate at the point where it enters the furnace would probably be in the neighborhood of 200 F higher, and the peak temperature would probably also be 200 F higher. The base of the peak would be broader, consequently the key would be subject to a higher temperature and for a longer period of time. It would drop to about 500 F at a position corresponding to 300 deg on the slide. Our experience indicates that a short peak temperature of 1000 F or thereabouts does not result in unusually high grate maintenance, but if for any reason the high temperature is sustained for any considerable time the maintenance increases very rapidly.

M. J. Selaya.[4] The maintenance costs and comparisons set down in the paper deal with equipment dating from 1925 up to about 1931. Boiler-room installations of eight and ten years ago were vastly different in construction and design from the modern equipment of today. As a result of research and development, the modern underfeed stokers operate with much lower maintenance costs than the author's general figures indicate.

Advancement in the use of preheated air for stoker-fired boilers has been somewhat retarded during the last three or four years. The authors might well have mentioned that retrenchments during this time by operating companies and others who in the past have shared in the development of boiler-room equipment, have limited comparisons, especially for the higher preheated-air temperatures.

Inasmuch as records of stoker maintenance by different companies are not kept by one set method, a general breakdown of the figures given in the paper would indicate other conclusions than those presented. Station labor can either be direct on the stoker involved or the average for the station which would include labor and overhead, even at times when no replacements are necessary. One case is known where an operating company uses a fixed labor charge of $10^1/_2$ cents per ton for maintenance. It is suggested that due to the many methods of bookkeeping in use, the material cost only would be a truer index for comparisons.

In 1925 an underfeed stoker was built and installed for 500 F air temperature. In an analysis covering an eight-year period, the maintenance costs were divided into 64 per cent for material and 36 per cent for labor. Another installation with the same 500-F air was made to demonstrate its ability to burn some of the cheaper coals carrying ash with low-temperature softening characteristics. The maintenance on this stoker over an 18-months period, using the same fixed station-maintenance charge as on the older stoker, was divided into 49 per cent for material and 51 per cent for labor. The maintenance on extension grates, which was excessive on the first stoker, was eliminated to negligible figures through the use of a new material, and the total maintenance on material was reduced by 50 per cent over the older stoker. It is worthy of note that the fixed labor charge per ton is more than the material charges.

Stoker designers have compensated for the reduced temperature differential between the air and the iron, and they have studied the composition of the metal to eliminate cracking and growth. One case is known where a 75 per cent reduction in maintenance cost was effected by the exclusive use of manufacturer's parts. It is probable that this item would affect the figures shown by the author.

[4] American Engineering Company, Philadelphia, Pa.

The authors offer a conclusion or prediction that up to 300 F the preheating of air supplied to underfeed stokers does not seem to increase maintenance above reasonable figures, but that there is a sharp increase above this point. The data available beyond 350 F is limited, and for this reason should not be taken too seriously. When the opportunities for studying the effects of high-temperature preheated air are exhausted, the maintenance figures will be lowered.

The opinion is offered that correct operation is an important factor. This is well demonstrated by a plant which burns low-grade fuel up to 50 lb per sq ft of projected grate area with air temperatures up to 400 F, yet has a maintenance cost on material of 2 cents per ton. This raises the question as to whether some of the figures quoted by the author do not include charges for experiment and test periods during which the equipment was subjected to unusual conditions, or times when the operators were inexperienced.

The main topic of this paper deals with the effect of preheated air on the underfeed stoker, although figures are presented on the chain-grate stoker. This is an unfortunate comparison because in most cases, chain-grate stokers burn coals having high ash content peculiar to certain localities. Underfeed stokers burn a great variety of coals. Studies indicate that no definite usable data can be derived from comparisons given for the different types of stokers. A direct comparison can only be made by burning the same classes of coal on the different types of stokers.

George C. Eaton.[5] At the Edgar Station, North Weymouth, Mass., experience has shown that air temperatures in excess of 400 F are very damaging to a stoker because the distortion which results from such temperatures causes the stoker parts to crack. This appears to be consistent with the data plotted in Fig. 8.

During a test at the Edgar Station, a coal with approximately 11 per cent ash was burned and it was noticed that the stoker was damaged less than when New River coal containing 4 per cent to 6 per cent ash was used. On the other hand, we apparently had less stoker maintenance during a test run when mixtures of petroleum coke and New River coal were burned, the ash content of the mixtures being between $3^1/_2$ and $4^1/_2$ per cent. These apparently opposite results are for but very short periods of time and are by no means reliable, although Fig. 4 seems to give them foundation.

Considerable success has been attained at the Edgar Station in reducing stoker-maintenance costs by the use of ribbed side-plates to prevent warping, and by the development of an improved extension-grate design embodying a fixed and a moving section, no part of the grate extending at any time over the shingle grate.

J. S. Bennett.[6] Although this paper will probably result in engineers making a more careful analysis of the high maintenance cost of stokers, it unintentionally might have the effect of discouraging the use of higher preheated-air temperatures by continued reference to past performances without stressing at the same time the value of study and effort to solve the problem.

Stoker manufacturers have been considering this problem for a number of years and many innovations have been introduced to reduce maintenance. One of these is a water-cooled stoker in which the tuyères and overfeed sections are converted into air-admitting water-wall areas connected to the boiler circulation. Four of these stokers are in regular service and have

[5] Head of Mechanical Technical Engineering Division Generating Department, The Edison Electric Illuminating Company, Boston, Mass. Jun. A.S.M.E.

[6] Mechanical Engineer, American Engineering Company, Philadelphia, Pa. Mem. A.S.M.E.

burned 11,000 tons of Illinois coal with an ash-fusing temperature below 1900 F. None of the water-cooled areas of the stoker have shown any signs of overheating. As a result of such developments, greater advancement along this line can be expected, all of which will result in reduced maintenance cost of firing equipment that is exposed to high preheated-air temperatures demanded by modern equipment.

T. E. Purcell.[7] The authors have developed a curve showing the relation between air temperatures and stoker-maintenance costs. However, even after several corrections have been applied to the data, the costs at 350 F of preheated air, for example, still vary by more than 15 cents per ton. This shows the inconsistency which still prevails in the stoker-maintenance-cost situation.

Stoker-maintenance costs as used in the paper apparently include all costs of repairing the entire stoker and drive whether or not the repairs can possibly be affected by preheated air. We should be mostly concerned with the effect of the hot air on the maintenance of the grate section where the damage actually takes place rather than on the entire installation.

In addition to the factors mentioned in the paper, there are others which have significant effects on the final cost. Among them are the design and age of the stokers, the fusion temperature of the ash, sulphur content of the coal, the local labor rate, the cost differential between materials purchased locally or from stoker manufacturers, banking boilers, the skill and alertness of the operators, etc. We cannot hope to correct for all these factors but nevertheless their existence complicates the problem.

The paper presents corrections for some factors, among them being grate area and burning rate. The trends in the correction curves are logical, but I wonder if the curves have any real significance. Incidentally I may add that, owing to better design, the largest stokers our company operates have the lowest maintenance cost even though the average burning rate is higher than it is on the smaller stokers. Perhaps if the cold-air stokers as well as the preheated-air stokers had been used in developing these correction curves, more points would have been obtained to confirm or perhaps to contradict their trend.

There is some satisfaction, however, in the fact that the uncorrected curve for maintenance cost vs. air temperature does not differ greatly in slope from the one corrected for many of the variables. On the other hand, it is disturbing that design decisions must still be based on incoherent data, even though the corrected curve is used.

R. L. Beers.[8] It seems to me that the authors do not go into sufficient details as to the fuels being used. It is generally conceded that chain-grate stokers are widely used for free-burning, non-coking, high-ash coals, such as those mined in Illinois and Indiana; and they are not suitable for the coking, low-ash fuels such as those mined in West Virginia, Pennsylvania, and Eastern Kentucky. For the latter fuels, the underfeed stoker has proved without question to be best suited. The paper does not state whether any of the chain-grate stokers were burning low-ash Eastern fuels, but if data on such plants were available it is believed that the maintenance costs would be very much higher than for the underfeed and the efficiency would be much lower. With a low-ash, low-fusing-and-coking coal a chain-grate stoker will not stand up even with air at room temperature unless a high percentage of excess air is allowed to pass through the fuel bed at the rear end. Preheated air and a chain-grate stoker with this fuel would make an unsatisfactory combination.

It is difficult to make comparisons on the results of stoker installation as there are so many variable factors that enter. Two plants, exactly alike, will produce different results. The skill of the operators, load conditions and variation in the fuels may give entirely different results. The ash percentage is not always the important point. The burning characteristics of the fuel, the fusing temperature and quality of the ash are also very important. To make the comparison just, the two types of stokers should be operating under the same types of boilers with equal load conditions and with the same fuels.

It seems to me that the maintenance figures given for the underfeed stokers are very high. Possibly there are some factors entering that are not given in the paper. Quite frequently most of the damage to an underfeed stoker occurs during short periods and not under normal operation. This might occur when starting up quickly from a banked fire without having the retorts filled with green coal or in carrying very high peak loads.

The maintenance is no doubt important but there are other items, such as efficiency and flexibility that may more than offset this item. Furthermore, in making maintenance comparisons, the maintenance of ignition and mixing arches, not used with underfeed stokers but required by chain-grate stokers, should be included. The maintenance of these arches may be an appreciable item. Also, they cut down the radiant-heat transfer from the fuel bed to the boiler tubes, tending to lower the boiler efficiency and capacity.

H. E. Kleffel.[9] In order to simplify the problem of ascertaining the main factors that contribute to the maintenance costs of stokers, I would suggest we use the amount of fixed carbon burned per square foot of grate surface per hour as a basis of comparison, correcting for area of grate surface and temperature. This, I believe, would be a better basis of comparison than using the pounds of coal burned per square foot per hour, the per cent volatile, per cent ash, and the excess air.

The authors have indicated that stations burning coals high in ash and volatile content appear to have lower maintenance costs than stations burning coal with low-ash and volatile content. This may be explained by the fact that with coals high in ash and volatile there is less fixed carbon in the coal to be burned on the grate surface, the volatile being distilled at relatively low temperatures and burned in the furnace chamber, the coke being carried along with the ash burning on the surface of the grate until the carbon content is consumed, the ash affording protection to the grate surface, if it does not become molten. Ash having a relatively low fusing temperature if allowed to become molten will contribute to higher maintenance costs and stoker outage, this being aggravated by high air temperatures.

If the use of the fixed carbon burned per square foot of grate surface per hour, as a factor shows a logical relationship between maintenance and air temperature, it might be of further interest to make a comparison between the maintenance of chain-grate and underfeed stokers on this same basis, using the effective grate area. By that I mean the total grate area through which air passes for combustion, for underfeed stokers being approximately 80 per cent of the projected area and for chain grates over twice the projected area of the fuel bed.

This may afford a clue to the effectiveness of alternate cooling for the large-area chain-grate surface and also indicates the high duty imposed on the underfeed-stoker's stationary-grate surface at high combustion rates and provides data for the stoker designer for future consideration.

[7] General Superintendent of Power Stations, Duquesne Light Company, Pittsburgh, Pa. Mem. A.S.M.E.

[8] Vice-President in Charge of Engineering, Detroit Stoker Company, Detroit, Mich. Mem. A.S.M.E.

[9] New York, N. Y. Assoc-Mem. A.S.M.E.

I. E. MOULTROP.[10] It has been rather disappointing to find that there is a definite upper limit to the preheating of air if the maintenance costs are to be kept within reasonable bounds. When the design of preheaters reached a practical stage, it followed that the way was clear for the station designer to go to almost any limit in forcing the capacity of the stoker and boiler in order to keep down capital expense without sacrificing too much in heat rejected in the stack. Now we find that this hypothesis is not true and the station designer must very carefully consider this point in planning a low-cost, economical station.

In reference to maintenance expense, I believe that some of this is due to lack of induced-draft fan capacity. Many station designers in the past have erred in not installing sufficiently large induced-draft fans. Now that we have substituted a fan for the chimney, the fan is the limiting factor and if the forced-draft fan is run beyond the capacity of the induced-draft fan the result is bound to be a certain bottling-up of heat in the furnace which must be detrimental to both the metal parts of the stoker and the refractories of the furnace.

Here is a most urgent need for intensive research work to produce a material to be used in those stoker parts subjected to the hot air and heat from the fuel bed, which will stand up for a reasonable length of time and which will not clog up with slag adhering to the upper surface of the tuyères, and which will be reasonably cheap in first cost.

If we believe some of our optimistic business friends, the time is coming very soon when the utility companies will have to think about increased capacity and it would be a pity to have to use stokers handicapped by an absurdly low limit of air temperature.

B. C. MALLORY.[11] It is interesting to note that the maintenance of stokers with cold air is as much as with average air temperatures of 300 F. It would be interesting to know the average length of time the various stokers ran continuously for it seems that this may have a bearing on the maintenance cost. In our case, each stoker had three outages during the year 1933. That meant that whenever the stokers were out of service all parts that did not appear able to stand four months more service had to be renewed.

We have found that in changing from one kind of coal to another, it may be necessary to carry a differently shaped fuel bed, and that maintenance costs go up until the new coal has been burned for several months. Such an item should be considered as a charge against the possible saving in the difference in coal prices.

Current Practice in Pressures, Speeds, Clearances, and Lubrication of Oil-Film Bearings[1]

ALBERT H. DALL.[2] The author's pressure-velocity diagram is an ingenious summation of current practice as related to Mr. Kingsbury's optimum data on 120-deg bearings.[3] The viscosity alignment charts, together with Mr. Kingsbury's data, constitute design criteria sufficient for any oil-film bearings operating at optimum conditions of load or friction. However, the designer must choose the minimum film thickness and from this choice determine the bearing clearance and the viscosity of the oil to be used. It is regarding this choice of minimum film thickness that the writer wishes to cite a few experimental facts which it is hoped will be pertinent to this discussion.

It has been stated repeatedly in bearing literature that the minimum oil-film thickness must be governed by practical considerations. These considerations may be summed up briefly as being the initial degree of perfection of the two surfaces involved, and the distortion of these surfaces by whatever stresses may be set up in use. Another deciding factor is that of maintenance or decay of the quality of these surfaces with usage.

Recent advances in the art of precision grinding have made it possible commercially to produce finishes on journals, which are comparable to lapped surfaces. Such surfaces are now being produced in mass-production industries such as the automobile industry. Very accurate and smooth bearing surfaces can now be produced by diamond boring or scraping. The initial quality of the surfaces can therefore be attained without excessive cost. The maintenance of these surfaces is essential if a small minimum film thickness is chosen.

Experiments at the Cincinnati Milling Machine Company have shown that the use of the so-called high-lead bronzes assists greatly in the maintenance of the original surfaces even when used with comparatively soft-steel journals.

The process by which this combination of materials tends to maintain, and in some cases improve the quality of the surfaces, can be explained on the basis of chemical facts. Mineral oils in general are neutral. However, it has been found that the acidity of oils increases with use. This acid reacts with the free lead in the bearing to form a metallic soap which coats the surface of the journal and bearing. This coating protects the surfaces when contacting occurs for short periods, such as starting, instantaneous over-loading or in short periods of oil deficiency. The production of sludge is very slight except in cases of excessive moisture. Thus the sole advantage of the so-called extreme-pressure lubricants is partially realized without any of the inherent disadvantages of this type of lubricant.

If the bearing is designed so that the distortion in service is of a negligible order, the use of the foregoing methods of producing and maintaining the surfaces may well modify the past practice of bearing clearance. As the author points out, the coefficient of friction and, therefore, the power loss varies directly with the minimum film thickness for any bearing running under optimum conditions. It is obvious, therefore, that any means which tend to decrease this minimum will be desirable.

AUSTIN KUHNS.[4] The oil-film type of bearing is astonishingly reliable and efficient. It is capable of excessive overloads and considerable misalignment and abuse without signs of distress, provided it is supplied with sufficient lubrication.

As a result there is a wide diversity of opinions by different students about the best proportions for these bearings, every one of which is based upon the irrefutable argument of successful operation. The power losses through the bearings are so small and so difficult to measure that the relative merits between them can hardly be distinguished.

It is the belief of the writer that Mr. Howarth's work will result not only in simplification and standardization but that it will lead us to better designs, especially to shorter bearing lengths which can compete more successfully with the antifriction bearing. Every experienced engineer has observed oil-

[10] Chief Engineer of Company and Superintendent of Construction Bureau, The Edison Illuminating Company of Boston, Boston, Mass. Mem. A.S.M.E.

[11] Technical assistant to the Chief Engineer, Lynn Gas & Electric Company, Lynn, Mass. Jun. A.S.M.E.

[1] Published as paper MSP-56-2, by H. A. S. Howarth, in the December, 1934, issue of the A.S.M.E. Transactions.

[2] Engineer, Research Department, Cincinnati Milling Machine Company, Cincinnati, Ohio. Jun. A.S.M.E.

[3] "Optimum Conditions in Journal Bearings," by A. Kingsbury, Trans. A.S.M.E., vol. 54, 1932, paper RP-54-7.

[4] Farrel-Birmingham Company, Buffalo, N. Y.

film bearings carrying extraordinary loads and has been led to the conclusion that the sizes used today, even though considerably reduced from the standards of a decade ago, are far larger than necessary.

The writer recalls one gear drive which he inspected a short time ago which had been "starved" of oil to the point where the bearing metal had melted and run away except for a few small fins which, due to subsequent copious lubrication, had supported the journal loads for a considerable period of time. Each high speed bearing was $3^1/_2$ in. in diameter rotating at 500 rpm resulting in a rubbing speed of 458 fpm. The bearing pressure figured approximately 3500 lb and the combined length of the unmelted babbitt strips did not exceed $^3/_4$ in. The writer has records of a number of installations which because of changes in driving units have been operating continuously under overload conditions of 100 to 300 per cent. In no instance have the bearings failed.

It is the hope of the writer that Mr. Howarth will not only place great weight on his emphasis of the absolute importance of correct and sufficient lubrication but that he will be able to simplify the specifications for the lubricating oils and establish an expression which will include the desired characteristics in terms of fundamentals which will avoid the use of trade names. Such a specification cannot be expressed in words of one syllable but the importance of reliable and efficient bearings and compactness in design justifies its study by intelligent engineers and their familiarity with its use in practice.

From a study of the material given in Mr. Howarth's paper and a comparison with our own practice, it is clear that the journal clearances which we use are less than the average. As manufacturers of gear and power-transmission products, the proportions and clearances of our bearings are adjusted for that particular class of service. Also, for convenience and as an aid to standardization we use as far as possible bearings for which we already have drawings and patterns.

The average clearance which we use for bearings larger than 3.5 in. is 0.001 in. per in. of diameter. For the smaller bearings, the clearance is specially selected for the particular type of service.

Our own specifications of the lubricating oil are today identified by S.A.E. numbers. Selection of the oil is based more upon a consideration of the gear-tooth loads than upon bearing clearances and rubbing speeds. For the quantity of oil required we specify as a minimum 0.007 gal per min per in. of projected area.

Generally speaking S.A.E. 40 is used with bearings over 8 in. in diameter and S.A.E. 30 for bearings under 8 in. in diameter. For the higher speeds S.A.E. 30 is used entirely.

Naturally we have given considerable thought to the supply and distribution of the lubricating oil to the bearing surfaces. We are confronted with different requirements imposed upon us by practical consideration of our designs, and must arrange our bearings for ring oiling, collar oiling, gravity or pressure circulation as the individual installation requires.

It is comparatively simple to deliver the lubricating oil to the bearings, but it requires careful study to distribute this oil from the entering ports to the areas of contact or pressure. This distribution is accomplished by the action of the rotating journal in the bearings. It is assisted by cutting grooves or reservoirs with long sloping chamfers ahead of the pressure areas. The arrangement of these grooves and chamfers has provided an outlet for a great deal of practical ingenuity in design. Every arrangement is reliable and effective if it distributes the oil in sufficient quantity and facilitates its pick-up by the rotating journal.

In permissible bearing pressure, expressed in pounds per inch of projected area, consistency in our designs is confused by the necessity for standardization and utilization of existing drawings and patterns.

For the heavy-duty bearings where the rubbing velocity is below 2000 fpm the pressure per inch of projected area lies between 60 and 80 lb, although occasionally for practical reasons pressures as high as 100 lb are used. The usual method of lubrication is by ring or by collar.

At the higher velocities where positive oil circulation is included and where the rubbing speeds are well in excess of 2000 fpm the bearing pressures per inch of projected area are seldom under 120 lb and are frequently as high as 160 lb.

The relation between bearing length and diameter is influenced by the dimensions of the supporting housing. Usually the length is 1.5 times the diameter for the slower speeds and from 1 to 1.25 times the diameter for the higher speeds.

In discussing the design of oil-film bearings, it frequently is customary to ignore the rigidity of the housing in which the bearing shells are fitted and the accuracy with which the entire unit is machined. Presumably it is assumed that these items will be as nearly perfect as possible but unfortunately experience has shown that serious misalignment of the bearings occurs under operating conditions due to weakness in the housing. As bearings become shorter this tendency to weakness is increased.

In closing, the writer wishes to point out the rapid reduction in the viscosity of the lubricating oil with the rise in bearing temperature. The temperature usually falls between 130 F and 150 F which introduces a wide variation in operating conditions. It is the writer's opinion that far too little consideration has been given by designers to the close control of this factor of temperature.

E. S. Pearce.[5] Our research in the bearing field has been confined to the railway-car journal bearing. This bearing belongs, for want of a better classification, to the no-clearance, single-directional-load class of bearings.

In our five years of work we have found so much that was contrary to the accepted theories and practices concerning the design, operation and maintenance of this type of bearing that we feel quite sure the margin of performance between what is now being obtained and what could be accomplished is great.

Analyzing the paper by Mr. Howarth in the light of the foregoing experience, it seems quite logical to conclude that the situation we have found is not unique to the particular field of bearing application which we have been investigating. Practices and theories of design seem to be predicated more on opinion than on facts. While the bearing is a vital part of the construction, the design has hinged more on what has worked before than on what could or might be found to work.

Fig. 1 in the author's paper, when analyzed from the standpoints of the railway-car bearing, brings to light some very interesting comparisons. For example, in the case of the $5^1/_2 \times 10$-in. journal bearing supporting a total load of 16,375 lb, we find that the total bearing area could be a maximum of 45 sq in. If we applied the author's method of calculating projected area for arriving and the value P, pressure in lb per in., this area would be $49^1/_2$ sq in. But on account of the fact that the bearing is an arc of less than 180 deg, the area can never exceed 45 sq in.

With this area of 45 sq in. and the total load of 16,375 lb, P, the pressure in lb per sq in., is 364 lb. V, the rubbing speed in feet per minute, has a value of $134^1/_2$ fpm at 10 mph, and 941.5 fpm at 70 mph of a 36-in. car wheel with a $5^1/_2 \times 10$-in. journal. Under this comparison, the bearing would fall in the group of

[5] President, Railway Service & Supply Corp., Indianapolis, Ind. Mem. A.S.M.E.

stationary-engine bearings at 10 mph, and in the group in which it is shown, railway cars, at 30 mph and above.

This bearing with 45 sq in. and a unit load of 364 lb per sq in. at 10 mph has a coefficient of friction of 0.00610. Expressed in another way, it offers a rolling resistance of 1.86 lb per ton. This same bearing by special construction limited to a crown area or bearing area of $22^1/_2$ in., or a unit load of 728 lb per sq in. at a speed 70 mph with a velocity of 941.5 fpm, has a coefficient of friction of 0.00449, or a rolling resistance of 1.38 lb per ton. This bearing under its high loads and high speeds would then fall in the class of gas-engine main bearings on the chart of the author's Fig. 1. Under both conditions cited, the performance of the journal bearing is not a limiting factor in the operation of the unit equipment of which it is a part.

The above comparison by no means represents extremes. The same car-journal bearing may have to operate at pressures as low as 100 lb per sq in. and at journal velocities under 134 fpm. Under another condition it may operate in excess of 1000 lb per sq in. and at journal speeds of 1000 fpm or any combination of the two. Whereas, in all other groups of bearings illustrated in Fig. 1, the bearings operate under more or less constant loads at constant journal speeds.

F. P. Dahlstrom.[6] In the determination of bearing capacities and clearances we have profited much by the study of papers and bibliographies submitted to the Society by the members of the A.S.M.E. Special Research Committee on Lubrication. In addition, we should also include those submitted by the individual members to other publications, for example, the *S.A.E. Journal*, and the Bulletins of the Pennsylvania State College.

It is realized that most of the papers so mentioned deal with hydrodynamic principles of bearing operation, that is, with conditions which occur when the shaft is rotating in its bearing.

While much has been done in the study of boundary conditions of lubrication, in which the phenomena are determined solely by the nature of the lubricant and the component bearing materials, the results cannot yet be used by those who design industrial bearings. For example, regardless of the intrinsic lubricating value of many lubricants, we are limited in the case of automobile, Diesel-engine, turbine, and rolling-mill bearings to the use of an oil that is stable and that will separate readily from water. So far as the writer knows, the only available lubricant which meets this requirement is a highly refined mineral oil.

In determining the safe carrying capacities of bearings we agree with many other designers that the minimum oil-film thickness is the important criterion. Methods of its calculation have been used by us based on the data submitted by Professor Karelitz and the members of Mr. Kingsbury's organization.

From the design data which has been submitted, we note that in many cases the clearance ratio varies from 0.001 to 0.002. These values are the result of many years of experience. From calculations which we had made of minimum oil-film thickness resulting from various clearance ratios it seems that the clearance ratios noted are also justified by theory.

Having established a clearance ratio (and assuming that the usual L/D ratio is 1) our bearings are now geometrically similar. This statement leads logically to the pioneer work of M. D. Hersey in which he showed that the performance of geometrically similar bearings could be compared by a characteristic number now recognized as ZN/P. Subsequent careful work by S. A. McKee and T. R. McKee at the Bureau of Standards showed consistently that the breakdown of the oil film occurs when the value of ZN/P is less than a certain amount. The actual value in part depends on the bearing metal used and may be 5, or less. In determining the safe carrying capacity of a bearing it seems reasonable to state that the minimum oil-film thickness will be sufficiently large if the operating characteristic ZN/P is greater than 10, where Z is the viscosity in centipoises, N the speed in revolutions per minute and P the unit bearing pressure in pounds per square inch of projected area.

As one possible suggestion for future work: In so far as the hydrodynamic theory of lubrication of journal bearings is concerned all investigators are dealing with the same phenomenon, that is, one cylinder rotating within another. It would thus seem that several of the results of experimental work done to date might still be further correlated. (After hearing the papers and discussions presented at the 1934 A.S.M.E. annual meeting, the writer realizes that this is considered important by others.) As an example of what is meant, the writer calculated the theoretical eccentricity of a journal bearing for various values of ZN/P. For each value of eccentricity the frictional resistance of the bearing was next estimated. A curve of coefficient of friction vs. ZN/P was then plotted and this curve much resembled those obtained experimentally by S. A. and T. R. McKee.

In presenting the chart shown in Fig. 1, Mr. Howarth has given the engineer a very useful tool for checking his bearing designs.

The values of P and V for a given condition are first located on the chart and from this located point a diagonal line is extended to the scale for Mr. Kingsbury's optimum conditions. One interesting conclusion is now apparent. Having established the optimum condition, the value of V can be altered at will, and if we alter the value of P accordingly, the points so obtained will lie in the same diagonal line. This means that for any given optimum condition the capacity of a bearing is proportional to, that is, it increases with, the speed.

The diagonal lines in the chart which give the product of P and V are at right angles to the construction line noted for determining optimum conditions. This means that if $P \times V$ is assumed to be constant, the capacity of a bearing decreases with the speed.

This second statement is directly opposite to the first. Mr. Howarth has stated in his paper that the PV rule by itself has little to recommend it.

The rule, PV = a constant, was proposed by Thurston seventy years ago. Thurston's constant, 60,000, was based on a bearing coefficient of friction 0.10. Thus, the formula means that, with a constant load, the size of the bearing must be increased as the speed is increased in order to dissipate the heat developed, and, judging from the coefficient of friction, the formula is not one for designing bearings, but really is one for designing brakeshoes.

The chart which Mr. Howarth has shown, which is obviously the result of much study, will be of much value to us in designing lubricated bearings.

George B. Karelitz.[7] Mr. Howarth undertook a formidable task, indeed, in attempting to collect and correlate the bearing practice of manufacturers of various types of machinery. It is interesting to note that experience, as well as trial-and-error method which have prevailed in designing bearings, often brought results in agreement with those which might be recommended on the basis of the hydrodynamic theory. For instance, the rule making the clearance in high-speed bearings equal to $0.002D$ was established by practice. It can be observed from data on friction that with an increase of clearance the friction decreases substantially up to a clearance value of $0.002D$, after which the gains in friction are not great; at the same time, the minimum oil-film

[6] Engineer, Morgan Construction Company, Worcester, Mass.

[7] Professor of Mechanical Engineering, Columbia University, New York, N. Y.

thickness does not vary appreciably with the ratio of the clearance to diameter in the range from 0.001 to 0.002.

Referring to Table 5 in the paper, on the basis of the computations given by Boswall, and side-leakage correction factor by Michell, a convenient formula for minimum oil-film thickness in thrust bearings can be derived:

$$h_o = \sqrt{\frac{1}{15}\,\frac{\mu U l}{P}}$$

where h_o is the minimum film thickness in in.
μ is the absolute viscosity of oil in lb sec per sq in.
U is the surface speed in in. per sec
l is the length of shoe in in.
P is the load in lb per sq in. of shoe

This formula is in close agreement with film-thickness values given in Table 5.

Referring to the desirable practice of selecting oils by absolute viscosity rather than by commercial viscosity, it will be necessary to produce first a reliable and simple instrument to measure the absolute viscosity. The latest attempt to bring such an instrument on the market was described in *The Engineer* (London) vol. 158, July 27, 1934, p. 95. However, until an instrument comparable in simplicity to a Saybolt viscosimeter is available, a serious and practical obstacle will stand in the way of abolishing the Saybolt viscosities.

Everett M. Barber.[8] Mr. Howarth has assembled a wealth of useful and practical data on bearing design and practice. In Fig. 1, he has so correlated these practical data with the hydrodynamical theory of lubrication that it is possible to determine the bearing proportions and oil viscosity that are required to give optimum bearing performance over a wide range of load and speed conditions.

The selection of a lubricant that will have the proper viscosity at the running temperature of the bearing is of fundamental importance in the application of these data. To aid in this selection, the author has provided a very satisfactory method of obtaining the commercial viscosity specifications for the lubricant when the required absolute viscosity and the running temperature of the bearing are known. The required absolute viscosity is readily obtained from the author's Fig. 1. However, the running temperature of the bearing, i.e., the temperature at which the lubricant must have this viscosity, must be obtained from direct measurements on the bearing in question, or from experience with other similar bearings.

In speaking of the viscosity corresponding to the running temperature of the bearing, the author, of course, means the viscosity corresponding to the temperature existing in the load-carrying oil film in the clearance space between the bearing and the journal. This temperature is difficult to measure. However, it is the temperature at which the lubricant is used; and if reliable results are to be obtained, it is important that the oil viscosity be chosen so that it will correspond to this temperature.

Several years ago while engaged in a lubrication-research project at the Engineering Experiment Station of the Pennsylvania State College, the writer attempted to measure the temperature in the oil film of an experimental bearing.[9] Two methods of temperature measurement were employed, as follows:

(1) A copper-constantan thermocouple, insulated in a bakelite plug, was placed in the bearing so that the junction of the couple was flush with the babbitt surface of the bearing. In fact, the plug which was $^3/_{16}$ in. in diameter, and the thermocouple bead which was bedded into the face of it, formed a part of the bearing surface.

(2) A mercury thermometer was inserted in an oil-filled thermometer well which was so placed that the bulb of the thermometer was about $^5/_{16}$ in. from the babbitt surface of the bearing.

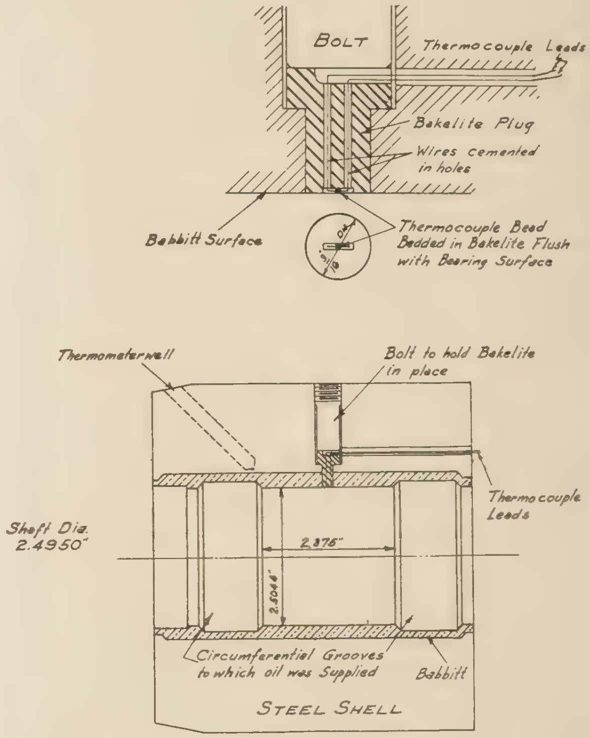

Fig. 1 Schematic Diagram of Test Bearing

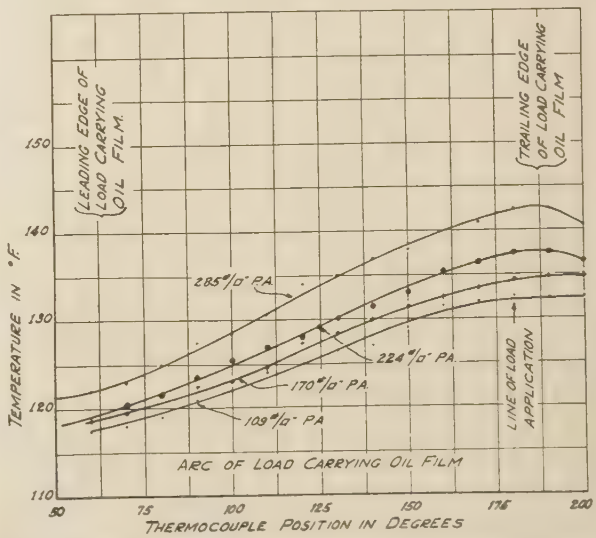

Fig. 2 Temperature Measured by the Thermocouple Plotted Against the Circumferential Position at Which the Temperature Measurements Were Made

(The temperature was measured by a copper-constantan thermocouple insulated in a bakelite plug in the test bearing. Viscosity of test oil: 320 Saybolt sec at 100 F; 48 Saybolt sec at 210 F; A.P.I. gravity 22.6 at 60 F. Speed, 200 rpm.)

[8] Mechanical Engineer, The Texas Company, Beacon Research Laboratory, Beacon, N. Y.

[9] "Investigation of Journal Bearing Performance," by E. M. Barber and C. C. Davenport, Bulletin No. 42, The Pennsylvania State College.

TABLE 1 COMPARISON OF TEMPERATURES AND CORRESPONDING VISCOSITIES MEASURED BY THE THERMOMETER AND THERMOCOUPLE IN THE TEST BEARING UNDER A WIDE RANGE OF OPERATING CONDITIONS

Test number	1	2	3	4	5	6	7	8	9	10	11	12
Speed (rpm)	800	800	800	800	1600	1600	1600	1600	2400	2400	2400	2400
Load (lb/sq in. of projected area)	109	160	209	281	106	127	188	244	109	170	224	285
Eccentricity factor	0.798	0.855	0.880	0.915	0.770	0.825	0.859	0.880	0.750	0.787	0.817	0.862
Thermocouple temp:												
Leading edge, F	100	101	102	103	119	115	120	124	121	123	123.5	126
Trailing edge, F	113	115	116	117	128	125	131	139	133	135	138.0	142
Viscosity corresponding to thermocouple temp:												
Leading edge (centipoises)	64.5	63.8	62.5	59.0	36.0	40.2	35.0	32.0	34.5	33.0	33.5	29.0
Trailing edge (centipoises)	59.0	54.3	53.5	50.6	28.3	30.5	26.0	21.5	25.0	23.0	22.0	19.9
Average of viscosity at leading and trailing edges	61.8	59.0	58.0	54.8	32.2	35.4	30.5	26.8	29.8	28.0	27.8	24.4
Temperature measured by thermometer, F	96	96.5	96.5	97	114	107	116	115	115	115	113	117
Viscosity corresponding to thermometer reading	74.0	73.5	73.5	72.0	42.0	52.5	39.0	41.5	41.5	41.5	43.8	38.0
Excess viscosity corresponding to thermometer over average viscosity corresponding to thermocouple, per cent	19.7	24.5	26.7	31.4	31.7	48.3	27.9	54.8	39.3	48.3	57.6	55.7

A schematic diagram of the bearing is shown in the writer's Fig. 1. The enlarged insert shows the arrangement of the thermocouple. The position of the thermometer well is also indicated. The bearing itself was a cylindrical steel shell lined with babbitt, with the principal dimensions shown.

Except for the circumferential grooves to which the oil was supplied at either end, the bearing surface was plain. The bearing was so arranged that it could be moved circumferentially without releasing the load, and being a plain cylinder, it always presented substantially the same surface to the load. With this arrangement it was possible to obtain a complete circumferential traverse of the oil-film temperatures with the one thermocouple.

In the writer's Fig. 2 are shown several of the curves of temperature (as measured by the thermocouple) plotted against the circumferential position at which the temperature measurements were made. It will be noted that around the arc of the pressure-carrying oil film there was a very marked and steady increase in temperature. This temperature increase was, of course, due to the cumulative heating effect of the work of friction as the oil was carried through the clearance space. On the "off," or unloaded, side of the bearing the oil was cooled to the inlet temperature again by mixing with fresh oil from the supply grooves.

As the thermocouple was moved from position to position around the bearing in 10-degree increments, the temperature change recorded by the thermocouple was as nearly instantaneous as it was possible to balance the potentiometer, and over a period of as much as thirty minutes the reading for any given position did not change appreciably.

In view of this responsiveness and steadiness of the readings, it is believed that the thermocouple was adequately insulated from the surrounding bearing shell and recorded very nearly the oil-film temperature. Obviously, this method could not measure the temperature gradient from the surface of the bearing to the surface of the journal. However, it apparently measured a temperature that was a reasonable average of the film temperature at each point around the circumference of the bearing.

Table 1 gives a summary of similar measurements made at speeds of 800, 1600, and 2400 rpm, with loads of about 100 to 300 lb per sq in. of projected bearing area. Texaco Regal Oil C, having a viscosity of 320 sec at 100 F; 48 sec at 210 F; and an A.P.I. gravity of 22.6 deg at 60 F, was used in all tests. In addition to the test conditions, the table gives the inlet and outlet (of the load-carrying oil film) temperature and the corresponding viscosity and the numerical average of the inlet and outlet viscosity. It also gives the temperature as measured by the thermometer, and the corresponding viscosity. The final line gives in percentage the amount by which the viscosity corresponding to thermometer reading exceeds the average viscosity as measured by the thermocouple.

R. O. Boswall[10] has shown that the error introduced by assuming a constant viscosity equal to the numerical average of the inlet and the outlet is negligible. Therefore, the percentages which are listed in the last line of Table 1 represent the error that would have been involved in the viscosity measurement had the viscosity been taken as that corresponding to the temperature measured by the thermometer.

An extremely high degree of accuracy in measuring the viscosity of the lubricant in the oil film is not essential because the film thickness and the coefficient of friction do not vary directly as the first power of the viscosity, but, as the author's figures indicate, to a considerably less important extent. However, the differences of 20 to 60 per cent between the viscosity measured as that corresponding to the temperature recorded by a mercury thermometer placed very close to the bearing surface, and the average of the inlet and outlet viscosities corresponding to the temperatures as measured by the thermocouple, represent a significant difference. These data indicate that it probably is not satisfactory merely to stick a thermometer in the oil reservoir or against the bearing shell, as is frequently done, and call the reading so obtained the running temperature of the bearing.

The temperature measurements made by the thermocouple at the leading and trailing edges of the load-carrying oil film in this experimental bearing should correspond to the oil temperatures that occur in the chamfered reliefs usually placed at the leading and trailing ends of commercial bearings. In this case the average viscosity of the oil film could be taken as equal to the numerical average of the viscosities corresponding to the temperatures measured at these points. The writer has no data on this point and it is offered merely as a possible satisfactory procedure.

In Figs. 1 and 3 of Mr. Howarth's paper, he has produced a very useful and practical tool for bearing designers and lubrication engineers and his definition of bearing running temperature and a satisfactory method of measuring it should be of considerable interest to those who desire to apply these data to practical bearing problems.

R. J. S. Pigott.[11] The writer has read with a great deal of satisfaction this further valuable contribution on bearing lubrication. Engineering, as a whole, is as yet too largely an empirical, rather than rational, branch of science, and the design of bearings has hitherto been one of the worst cases of empirical methods.

When we consider that the behavior of bearings is influenced by length, diameter ratio, clearance, speed, location of oil feed, quantity of oil, viscosity, load, misalignment, and last, but by no means least, heat-removal by other means than the lubricant, the complexity of analytical methods is apparent, particularly since none of the factors is completely independent of one or more of the others.

The writer has been convinced for some time that the mere use of pressure and rubbing speed was a relatively loose and incomplete criterion, the use of a friction coefficient even worse; in fact, often quite misleading. It is always useless to predicate the

[10] Theory of Film Lubrication," by R. O. Boswall, Longmans Green & Co., New York.

[11] Staff Engineer, in charge of Engineering, Gulf Research & Development Corporation, Pittsburgh, Pa. Mem. A.S.M.E.

design of any engineering device on two factors, when six or eight are involved. For example, it was customary, for a century, to treat pipe flow as a function of velocity and size only; consequently water, steam, gas and air formulas all differed, and there was no correlation. Reynolds' basic contribution was neglected for thirty years, and then swept the field. By taking into account density, viscosity, and finally roughness, we can now use a single formula for any fluid from molasses to hydrogen.

The writer had occasion to attempt the direct computation of liquid leakage and friction in rotary pumps and motors. Many of the cases involve conditions very similar to those in oil-film bearings. The results were so close to test performance that the latter can be predicted from a paper design within one or two per cent of the actual test. Much of the work will prove useful in bearing analysis.

We have also carried out analyses and tests in the laboratory on flow from a point source to a surrounding field edge, and the results of this work will ultimately be available for analysis of the effect of oil feeds and grooves.

It is clear that the rationalization of bearing design must come along the path taken by Mr. Kingsbury, Mr. Howarth, and their associates. But to render the final development authoritative and beyond question, it seems to the writer that we must have one more device—a bearing- and lubricant-testing machine that will test actual bearings, and yield results that do not require interpretation or extrapolation. The fault that may be found with most testing machines so far used is that they use idealized bearings or sometimes a structure not even faintly resembling a bearing; in many cases, results on one machine do not agree with those on another. Another objection is that none of the machines permits a real pressure, temperature, or leakage search; many do not even give journal displacement. We are developing a machine that we hope will overcome these disadvantages.

Mr. Howarth should not only be congratulated, he should be heartily thanked, for another valuable study of the subject.

A. F. Underwood.[12] The collected material that is presented in Mr. Howarth's paper is interesting in that it shows the lack of uniform bearing design. This may be a necessity when it comes to actual bearings in practice because our experience has shown that bearings which do not conform to the best theoretical designs often run better than when mathematically correct. We do not mean to imply that the theory should be neglected but rather that it is best used as an indicator, especially in the design of new bearings. As a specific example, theory shows that the bearing should be rigid to maintain the correct C/D ratio. Yet it is well known that the flexible cap of an automobile-engine connecting rod will sustain a much higher load than the upper half of the rod which is much more rigid. The reason for this apparent anomaly is that, in the case of the cap, the oil film is distributed over a larger area of babbitt, thereby increasing the fatigue life of the material.

In spite of the nearly universal use of the pressure-velocity factor for bearing design, it is not a criterion of bearing performance. It does become a measure of the heat loss in a bearing if it is in turn multiplied by the coefficient of friction. A number of factors affect the coefficient of friction, and, unless these factors all balance so as to give comparable values of coefficient of friction, the use of the pressure-velocity factor in bearing design may be very misleading.

Author's Closure

In addition to the distortion of bearing surfaces by loading conditions, as pointed out by Mr. Dall, there is the distortion caused by temperature change. With this in mind, Mr. Dall's three considerations which influence one's choice of minimum film thickness become (1) initial perfection, (2) subsequent distortion, and (3) durability.

Durability depends upon careful application of the lubricant and the protection of the bearing films against injury and contamination which obviously means that laboratory conditions must be realized in service. In other words, the bearings must be made fool-proof.

Several interesting comments offered by Mr. Kuhns include definite additions to the author's chartable data. With regard to the specification of lubricating oils, the author indorses Mr. Kuhns' hope that sometime it will be easier to obtain oil by simple description instead of by brand name. The S.A.E. numbers which he mentions are a step in the right direction but they do not go far enough. These numbers are given in Fig. 3 of this discussion, which has been revised from Fig. 7 of the paper, to cover the range needed to show the S.A.E. winter oils 10-W and 20-W. Further refinements are inevitable in the description of oils by numbers that have a real meaning. The addition of 10-W and 20-W to the S.A.E. numbers is but a step in that direction.

Mr. Pearce has given useful data that may well be added to that already charted. The author's use of the projected area of the journal as a basis of comparison for journal bearings was based upon its simplicity. No simple basis of comparison would afford an absolutely true picture of the facts, because of the variety of angular reactions of the bearing films to the journal for different bearing arcs, and because of pressure variations throughout the film. Hence, it is believed by the author that as long as the bearing-arc limitations are kept in mind for each class of bearing, the simpler method of tabulation is the better one to use.

The friction coefficients given by Mr. Pearce seem to include also the rolling friction of the wheel on the rail, if the author interprets correctly the statement, "Expressed in another way, it offers a rolling resistance of 1.86 lb per ton." If such is the case, direct comparisons with optimum bearing conditions are difficult to make.

The wide variation in operating load upon a bearing is not limited to the railroad field. It is found in every machine tool in which the rate of material removal is inconstant. In fact, in a machine tool the bearings are subjected to greater variation of load than in a rail car because while the latter has the minimum though considerable dead weight of the car body, bearings in a machine tool carry loads that are almost wholly due to the working process undertaken, which vary from zero to the maximum. For these reasons the tabulation of data is made on the basis of the normal operating loads the bearings are designed to carry.

The author appreciates the value of plotting test results on the basis of ZN/P as suggested by Mr. Dahlstrom, who recognizes Mr. Hersey as having pointed out the value of such a combined variable in 1915. Mr. Kingsbury[3] has given definite optimum ratios of the friction coefficient λ to a similar combined variable $\sqrt{(\mu N/P_0)}$ for each of his bearings. These range from 0.45 to 0.53 for clearance bearings with arcs varying from 60 to 120 deg. Transforming the μ to Z will give ratios of $\lambda/\sqrt{(ZN/P)}$ for optimum bearings, lying between 2.3 and 2.8×10^{-4} when corrected for side leakage under the assumptions that the bearings are square, i.e., the length is equal to the width. Out of this ratio we cannot obtain any useful low points for reference, but merely a straight line extending to the origin, unless we select a clearance ratio or a minimum film thickness with relation to journal diameter. Proceeding to do this, we find that the value of the friction coefficient for the square

[12] Power Plant Section, Research Division, General Motors Corporation, Detroit, Mich.

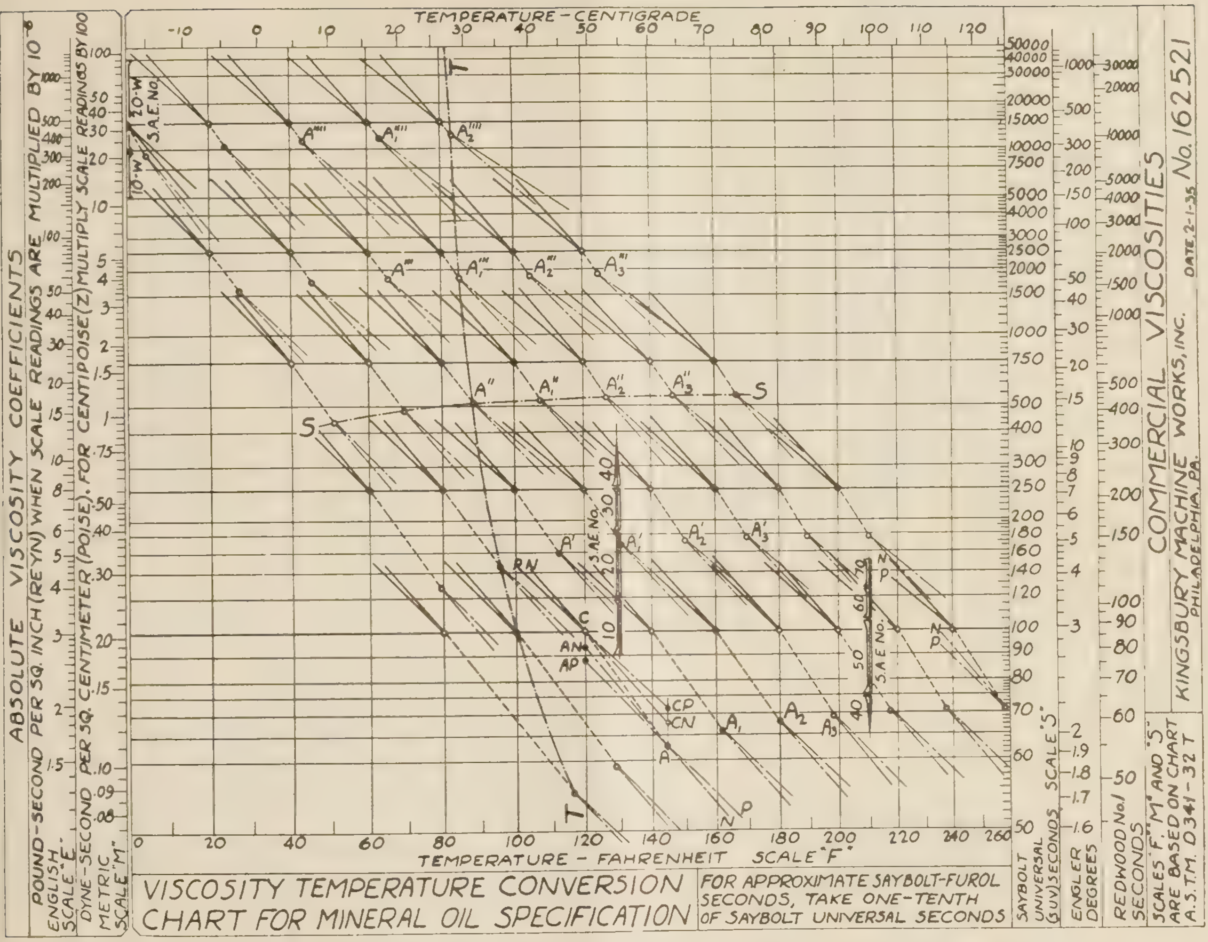

Fig. 3 Viscosity-Temperature Conversion Chart for Mineral-Oil Specification

(A revision of Fig. 7 of the paper extended to include all the S.A.E. numbers now in use. The intersections for determining the location of the dot-and-dash lines were calculated mathematically as against a graphical method employed in Fig. 7.)

bearing for optimum conditions will be from 2.4 to 3.0 times the clearance ratio. Hence, there is no theoretical bar to the coefficient of friction reaching zero.

Therefore, when a limit is arbitrarily placed upon the value of ZN/P, below which we dare not go, or are unable to go, we admit that there is a similar limit in the perfection of workmanship that is practicable or possible. The author, therefore, believes that it is wise to face the whole problem at once, and not to overrate the correlation of data on charts, the coordinates of which are merely the coefficients of friction λ and the combined variable ZN/P. The clearance ratio must be known to properly interpret such data.

A formula for minimum film thickness, such as derived by Professor Karelitz from works of Michell and of Boswall for flat surfaces, can be deduced readily for clearance or fitted journal bearings from symbol groups No. 10 published in Mr. Kingsbury's "Optimum Conditions in Journal Bearings."[8] A proper constant or series of constants, if more than one be needed, for determining desirable actual minima, must be based on experience. Mr. Kingsbury's experience with his thrust bearings yields the minimum film-thickness values which are given in Table 5 of the paper.

The point stressed by Mr. Barber is an important one and requires considerable space for its complete discussion. It was this fact that led the author to limit the paper to the relation of load and friction to the mean viscosity of the film. This was a definite step forward and it did not seem wise to try to cover adequately at this time the variations of viscosity throughout the grooves and baths of bearings.

The experiments to which Mr. Barber refers were made with a shell designed to simulate the lubrication conditions in a full bearing so far as they can be brought about in a finite bearing operating in an atmosphere of moderate pressure. The shell was designed to explore the distribution of pressures and temperatures and the shore lines of the film natural to such a bearing. Hence, it would be difficult to apply the results reliably to a partial bearing formed between two oil channels. These channels can be used for cooling the bearing, or merely for oil supply, when the cooling is done by water or by conduction to the air. Hence it would be better to seek more comparable temperature-distribution data by experimenting on shells designed to operate like those of the bearings in the machine that is subject to investigation.

The machine that Mr. Pigott mentions as being developed by the Gulf Research and Development Company will be studied with great interest by bearing engineers when it is ready for the market. Resulting from the experience possessed by Mr. Pigott and others of his company, it is to be expected that this will not be "just one more machine" to be set aside as inadequate.

The statement of Mr. Underwood that a connecting-rod cap

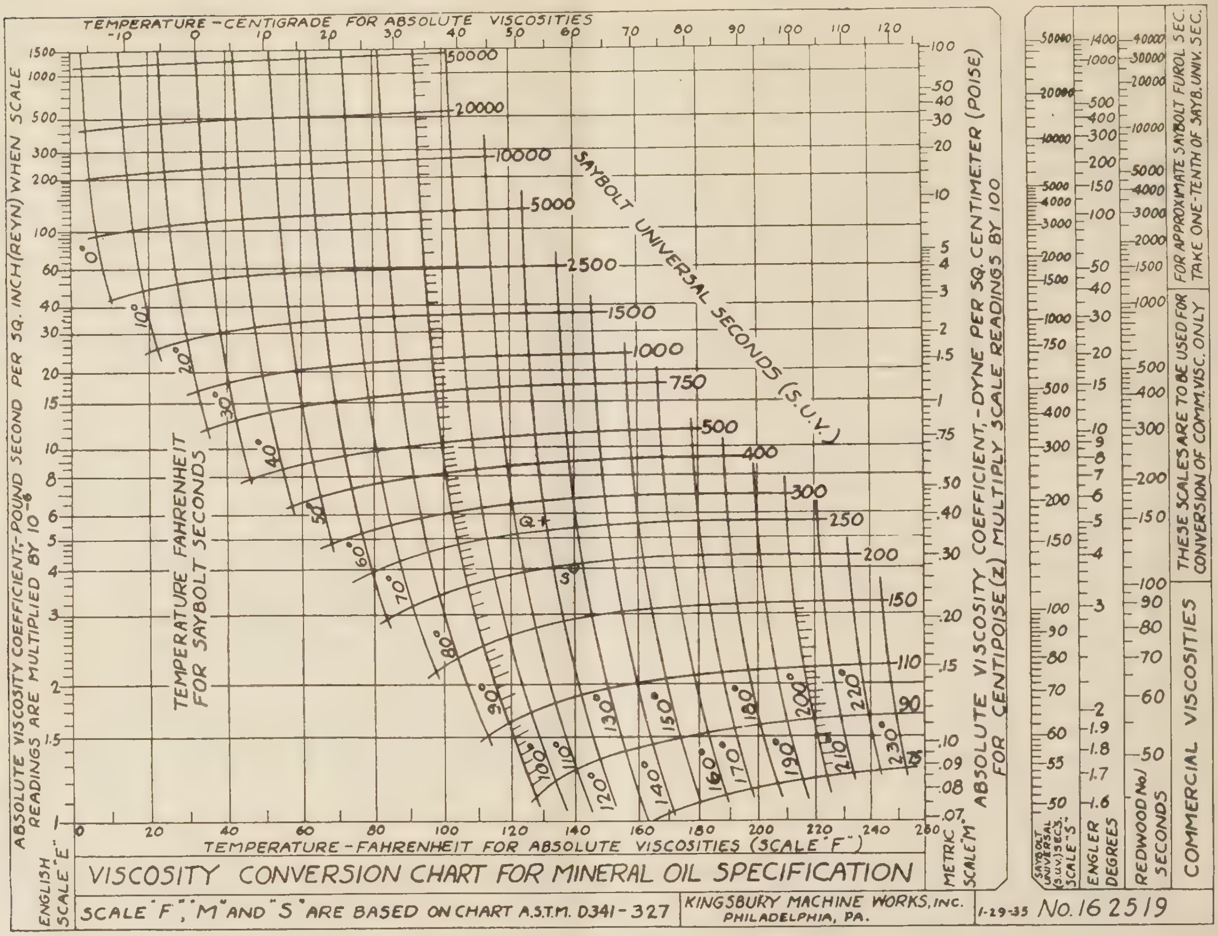

Fig. 4 Viscosity-Conversion Chart for Mineral-Oil Specification

(A revision of Fig. 6 of the paper extended to include all the S.A.E. numbers now in use. A mathematical, rather than a graphical method was also employed for determining the scales of this figure.)

carries load better than the stiffer part backed by the rod is quite interesting. The difference may be due partly to better alignment and partly to the hammock-like surface it presents to the pin. This suggests that a better rod design might be one with a head consisting of two caps held to the rod with a pair of bolts.

In addition to Fig. 3 of this discussion, offered by the author to extend the range of Fig. 7 of the paper to include all the S.A.E. numbers now used, there is also offered a revision of Fig. 6 of the paper. This new chart, Fig. 4 of this discussion, covers the same field as Fig. 3 of the discussion, and has been revised, as was the latter, to be more accurate than the original. The intersections which determine the locations of the dot-and-dash lines of Fig. 7, and thereby the special scales of Fig. 6, were located graphically, and were, therefore, subject to minor errors because of near parallelism. Therefore, a more accurate way of locating them was sought with the result that J. F. Spiegel, one of our engineers, evolved a mathematical method for calculating the intersections that is much more accurate than the graphical method. The redetermination of these intersections occupied a number of weeks. The results, however, warranted the time expended because Fig. 3 and Fig. 4 of this discussion are apt to be widely used. This seems reason enough for repeating them. Obviously, if the paper is ever rewritten only the better set of charts need be included.

Tractive Effort of Steam Locomotives (Locomotive Ratios—II)[1]

A Giesl-Gieslingen.[2] It is gratifying that Dr. Lipetz in response to the discussion evoked by his paper of two years ago,[3] has furthered the development of his method for evaluating locomotive tractive effort in order to make it adaptable to cylinders with widely varying proportions. The earlier paper[3] stated that his method was suited to locomotives of normal modern proportions and, assuming only limited fluctuations in relative dimensions of boiler and machinery, a single curve of moduli was developed to answer this stated purpose.

Meanwhile, locomotives have been cited which, with relation to boiler capacity, have cylinders that are as much as, or more than, 50 per cent larger than those upon which the curves in the earlier paper[3] were based. In the paper being discussed, Dr. Lipetz established correction curves in order to accommodate such cases. The writer fully endorses the use of a standard curve of moduli for locomotives with normal cylinder proportions, and of

[1] Published as paper RR-56-6, by A. I. Lipetz, in the December, 1934, issue of the A.S.M.E. Transactions.

[2] Assoc-Mem. A.S.M.E. New York, N. Y.

[3] "Horsepower and Tractive Effort of Steam Locomotives" (Locomotive Ratios), by A. I. Lipetz, Trans. A.S.M.E., vol. 55, 1933, paper RR-55-2, p. 5.

correction curves expressing the deviations in case cylinders of other proportions are provided. However, he suggests some changes in the author's curves.

The author's Fig. 5 shows his correction curves as a function of the locomotive characteristic K, which established a yardstick for the relation between boiler capacity and cylinder size. (See author's Equation [10].) It is obvious that larger cylinders mean a smaller value of K. The author assumes that no corrections should be applied for values of K equal to 14.26 and over, but if the cylinders are enlarged so as to result in values of K smaller than 14.26, then his corrections begin and rise very sharply at first and then at a diminished rate. This is not logical.

To better illustrate the case, reference is made to the writer's accompanying Fig. 1 which was drawn for the New York Central 4-6-4 type locomotive, class J-1. In this graph, the abscissa shows the values of K, each point corresponding to a certain cylinder volume and $K = 15.28$ corresponding to the locomotive's actual cylinder of 25 in. diameter. The heavy line indicates the Lipetz correction curve for 50 rpm. According to Dr. Lipetz we can now enlarge the cylinders until $K = 14.26$ and $d = 25.9$ in., without having to apply any correction to tractive power or performance. But if we increase the diameter only $^1/_2$ in. further to 26.4 in., tractive power according to the author should jump 6.7 per cent for 50 rpm.

We are also allowed to assume a smaller cylinder, perhaps equaling the proportions of locomotive No. 1 in the author's Table 4 for which $K = 16.88$. Therefore, $d = 23.8$ and, according to the author, no correction would be applied. If we would now enlarge the cylinder again, the author's correction curve for 50 rpm would imply that a diameter increase of 2.1 in. (a volume increase of 18.5 per cent) will not influence tractive power, but if we add another 2.1 in., reaching 28-in. diam, tractive power will jump 16 per cent. This is clearly impossible. The correction curve cannot have an edge at $K = 14.26$ but must be a smooth curve of some kind and, if $K = 14.26$ actually characterizes the cylinder proportions for which the 1932 moduli are valid, the proper correction curve will cross the zero line at that point as indicated by the tentative broken line for $n = 50$ rpm.

How large shall the correction be for any point where K differs from 14.26? In his 1932 paper[3] the author develops his method by first obtaining a curve of steam production varying with revolutions per minute in accordance with well established (even though not quite undisputed) experience, and then obtaining horsepower and tractive effort by establishing a curve of steam consumption per indicated horsepower-hour also drawn against revolutions per minute. These two curves were then combined into one representing the Lipetz moduli. The assumption of a definite figure for steam consumption per indicated horsepower-hour at a given speed implies (among other things) that there is, for each given number of revolutions per minute, a definite relation between the volume of the consumed steam and cylinder volume; this will be the case if $K = \dfrac{E_c}{Vp_b}$ is the same for all engines. If an engine has larger cylinders, then a smaller cut-off must be used to consume the given steam volume and, at least at moderate speeds, better utilization of the steam and higher output will result. The amount of steam generated by the boiler is practically uninfluenced by cylinder size, and if we do not wilfully change the basic curve of steam production established in the 1932 paper,[3] then the changing rate of steam consumption per indicated horsepower-hour is the only factor determining the correction curves for the Lipetz moduli. It is interesting to note that the Kiesel formulas as presented by Mr. Vincent in his discussion of the 1932 paper give a very good answer to this problem: by a simple transformation of the KV-formulas and by making P_1v const. 506, we can write the KV-formula in the following form:

$$C_i = 13.9 + 58.9 \frac{H}{VP_1n}$$

where C_i is the steam consumption (excluding auxiliaries), lb per ihp-hr; H is the boiler steam available for the cylinders, lb per hr; V is the combined volume of all cylinders, cu ft; P_1 is the boiler pressure minus 10 lb; and, n is the speed, rpm. If we substitute 96 per cent of the boiler pressure for P_1, and the denominations used by Dr. Lipetz, then we obtain

$$C_i = 13.9 + 61.3 \frac{E}{Vp_bn}$$

where $\dfrac{E}{Vp_b}$ corresponds to the locomotive characteristic K established by Dr. Lipetz. Within the scope of the Lipetz

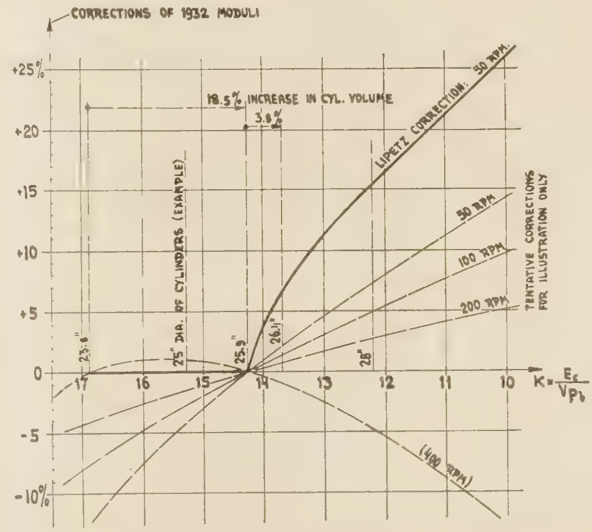

Fig. 1 Tentative Correction Curves for Lipetz' 1932 Moduli at 50, 100, and 200 Rpm

moduli, the KV-formula for steam consumption so developed very well represents the trend of steam consumption for varying factors on the right side of the equation, and it is helpful in calculating the correction curves for the Lipetz moduli. Thus, correction curves for 50, 100, and 200 rpm are tentatively shown in Fig. 1 of this discussion. A tentative curve for 400 rpm is illustrated as an example to indicate that the trend will be reversed at very high speeds; this region is, however, entirely outside of the scope of both the present Lipetz moduli and the KV-formula.

Dr. Lipetz, in his present paper, does not limit himself to corrections derived from the changes in the rate of steam consumption. He applies much greater corrections at low speed (50 rpm), arbitrarily chosen to suit the performance curves presented by Mr. Vincent. Thus, for locomotives with large cylinders he abandons the boiler evaporation curve used as a basis in his 1932 paper, and leaves us without a clue as to what is expected from the boiler at low speed, except for saying that the boiler has to be "forced." The explanation for this forcing as given on page 926 of the author's paper is purely psychological: it is claimed that the engineer is induced to force the boiler at low speeds. But certainly there is no necessity of

forcing it because the cut-off could be shortened sufficiently, just as rather small cylinders will permit forcing at higher speeds if the engineer should choose to lengthen the cut-off. To clear up this confusing situation we have to go back to the premises in the author's 1932 paper wherein Dr. Lipetz defined his performance curves as those obtained when a good engineer pilots the engine so as to develop a "reasonable maximum" performance. Later he determined overall thermal efficiency for such a case and found that it lay in the neighborhood of 6 per cent over the whole range of speed. This gave the reasonable result that an engine crew operating a locomotive at a good high rate without overstraining it, deriving its judgment from such observations as: ease in holding the steam pressure, clearness of the stack gases, sound of the exhaust, etc., is operating it at a fairly constant rate of overall efficiency. Under these conditions an average curve of steam production is obtained which at low speeds (50 rpm) remains considerably under the figures which hold at higher speeds (200 rpm), not as an absolute necessity perhaps, but as a good practical result in average cases. By taking such an average evaporation curve as a function of revolutions per minute and relating it to the Cole evaporation, a definite basis of steam production is obtained, to be used uniformly for all locomotives with modern boilers. This method is very practical. Two different locomotives can be compared on such a basis because it is known how much steam each one is expected to generate, and if one of them should fall short of power it is possible to determine whether the fault lies with the boiler or with the steam engine.

With the author's 1934 correction curves, this important advantage has been lost. Each cylinder size, for values of K less than 14.26, implies a different and unknown rate of steam production; even though correction curves for the corresponding steam production could be established, our basis of comparison would become too involved to be practical. Moreover, the supposition is now that steam engine and boiler are working at a "forced" rate at low speeds while they are working at a "reasonable" rate at high speeds. There is none or only a small reserve capacity at low speeds and 15 to 20 per cent reserve capacity at high speeds, while with the 1932 basis of a definite evaporation curve we knew that we had the reserve capacity over the whole range of speed.

That the engine crew is "induced" to work the boiler harder if the locomotive has larger cylinders is true to a limited degree, but this applies to the whole range of speed. Even if this influence were of any importance we had better neglect it in order not to upset our basis of comparison. But there certainly cannot be an inducement for the engineer to operate the larger cylinder with an even greater cut-off than the smaller cylinder as implied by the author's correction curve for $n = 50$; see Fig. 1 of this discussion. It is seen therefrom that a 3.8 per cent increase in cylinder volume (from $d = 25.9$ in. to 26.4 in.) can give the 6.7 per cent increase in performance corresponding to the author's curve only if the cut-off for the larger cylinder is lengthened by about 3 or 4 per cent, which is not logical. The author's corrections in the neighborhood of $n = 50$ have apparently been brought about by the desire to suit the performance curves presented by Mr. Vincent. This, however, was not necessary because we knew that the Vincent curves correspond to a state of greater forcing with small or no reserve capacity over the whole range of speed. Incidentally, this is brought out well by the author's example of the Boston & Albany locomotive. If the new correction curves would be applied to it, the calculated performance at $n = 50$ would be 15 per cent over the road performance and therefore excessive. Dr. Lipetz explains that since this engine has 60 per cent limited cut-off the cylinders could be called about normal, although $K = 12.27$, and he indicates that no correction should be applied. But since he applies the full correction to the Pennsylvania Class I-1s locomotive with only 55 per cent limited cut-off, and likewise to all other examples, it would be inconsistent not to do the same for the Boston & Albany locomotive. However, the 1934 correction method would destory the coincidence between calculated and test figures if this were done.

In conclusion, the writer makes the following recommendations:

1 To use a uniform curve of steam production for all locomotives. It might be investigated whether the 1932 curve is not a few per cent too low at low speeds, and whether it is not falling off slightly too fast at high speeds, but it should be retained in principle.

2 To apply corrections for cylinder size merely in accordance with the rate of steam consumption per indicated horsepower-hour.

3 To adopt the inclined Vincent curve of cylinder tractive effort and to use the straight line only if adhesion is the limiting factor. However, I feel with the author that the "transition curve" is too arbitrary and may better be omitted.

In this way the point of intersection between cylinder and boiler tractive effort will not be at 50 rpm as arbitrarily chosen by Dr. Lipetz for all large-cylinder locomotives, but its location will be a function of cylinder size as it should be.

The great merit of the Lipetz moduli lies in the ease with which they can be adapted to progress in locomotive design. Perhaps we should not try to adjust the moduli to all the locomotives which have been cited by Dr. Lipetz and his discussers. Some of these are no longer modern in their steam engines and all have widely differing draft appliances. With all our progress in steam-locomotive design we have not yet come to sufficiently uniform and accepted design rules. For instance, I cannot agree with Dr. Lipetz on his definition of over-cylindered locomotives; under-cylindering is more frequent. But a large-cylinder locomotive requires a better design of valve gear, steam passages and draft appliance and also better balancing and lighter working parts than we usually have. Under-cylindering covers up deficiencies in design, but of course it manifests itself in deficient performance and economy.

Here is a splendid opportunity for the Association of American Railroads. Individual builders and railroads have not sufficient staff nor the means to fully investigate the subject, nor are their views likely to be generally accepted. If the Association diligently assimilates the information now available here and abroad, the writer ventures to say that we would have standardized, highly efficient designs ready before a new rush in locomotive building starts. We would eliminate a great deal of the uncertainties which today manifest themselves in so many unjustified miscellaneous differences in locomotive design and proportions and cause an entirely unnecessary waste of money in manufacture, upkeep, and operation of our modern locomotives.

Dr. R. Eksergian.[4] The Cole method for the power proportioning of locomotives was at its introduction of fundamental value in rationalizing the relations between boiler and cylinder capacity and coordinating horsepower and tractive-effort speed relations. It gave a measuring stick of the performance of a locomotive in terms of a horsepower unit.

With improvements in the design and proportions of locomotives, and the requirements of more accurate data as to power performance, the inadequacy of the Cole method was felt by all locomotive engineers. For instance, the unit horsepower by

[4] Edward G. Budd Manufacturing Co., Philadelphia, Pa. Mem. A.S.M.E.

the Cole method was based on a cylinder steam consumption (including auxiliaries) of 20.8 lb of steam per hp-hr, and the 100 per cent boiler was such as to evaporate sufficient steam to supply the cylinders in developing a rated cylinder horsepower at 1000 fpm piston speed.

Aside from lower steam consumption in modern power, one difficulty of the method, however, was that it gave no real procedure of estimating the variation of horsepower against speed. For instance, at the lower speeds, with longer cut-offs, the cylinder steam consumption increases and there is a decrease of the evaporative yield of the boiler. At piston speeds around 250 fpm, the possible horsepower might fall considerably below 60 per cent of the rated horsepower at 1000 fpm.

Dr. Lipetz, in his Locomotive Ratios I,[3] recognized the need for a modification of the Cole method and its rationalization to a consistency with the performance of modern power. While it was recognized that cylinder steam consumption is a function of cut-off, speed, and proportions of cylinder design, Dr. Lipetz also brought out the point that evaporative yield was a function of decreasing speed at the lower speeds. This latter deduction was based on the fact that in locomotives investigated, the actual steam consumption of the cylinders fell short of the evaporative capacity of the boiler at the higher speeds. Using the Cole evaporation value as unity, he introduced a coefficient β to take care of this varying evaporative yield. The evaporative yield at 50 rpm was about 65 per cent of the maximum yield at 200 rpm. Considering the increased cylinder steam consumption at the low speeds, it was possible to evaluate a modulus M_p used in the present paper, which, when multiplied by the Cole evaporation value gives the horsepower.

The variation of the modulus M_p really accounts for the variation in horsepower against speed, and was deduced from actual performance data of road locomotives, nearly all of which had long starting cut-offs. In large-size cylinders with limited cut-off, the variation in the total modulus M_p or the corresponding tractive-force modulus M_t may be different. We can have, in effect, the shifting of the maximum part of the horsepower curve to a lower speed range and the criterion of the performance of such engines at 200 rpm no longer holds. The original early cut-off locomotives were designed for slow drag service and their performance became very much limited at the higher rotative speeds, under which conditions their boiler performance was undoubtedly inadequate.

A matter of considerable importance to the writer appears to be whether or not in long cut-offs at the low-speed range, the power percentage of horsepower when compared with the peak horsepower of 200 rpm is due more in part to evaporation deficiency or to limitation of cylinder performance itself. After all, we know only that at 50 rpm the horsepower is roughly a given per cent of a rated horsepower at 200 rpm. With due allowance for increased steam consumption at the lower speeds, the total steam demand of the cylinders still falls short of the boiler evaporation at its normal rating at 200 rpm. But, do we know whether this is chargeable to cylinder limitations or reduced evaporation at the lower speeds? Now, assuming the boiler proportioned to the cylinders, or vice versa, at 200 rpm, then it is usually found that the cylinder tractive effort falls short of the boiler tractive effort, assuming the boiler evaporation constant at its rated value at 200 rpm. If the cut-off is lengthened, wire-drawing becomes excessive and the card factor results in a mean effective pressure practically the same as with a somewhat earlier cut-off. The increased steam consumption for the longer cut-off practically yields no increase of tractive force. In such a case it would appear that the cylinder performance may possibly be the limiting factor in a low-speed range of 50 rpm and not the boiler.

It can be seen, therefore, that the relative proportions of boiler and cylinders in the low-speed range may not be entirely limited to an assumption of limited evaporation of the boiler alone with due allowance for increased steam consumption of the cylinders. It would appear that we might have cylinders with considerable variation in steam consumption with very little change in the maximum mean effective pressure at the low speed of 50 rpm and in such a case, even with an unlimited boiler capacity, the tractive force could not be increased.

One difficulty appears to be that cylinders proportioned for one operating high speed, say 250 rpm, and consistent with the evaporation for that speed, may be quite different from cylinders proportioned against evaporation for operating speeds at 180 rpm. In the latter case, assuming the same evaporation and roughly the same cut-off for minimum steam consumption (neglecting the difference of wire-drawing for the two speeds) the cylinders will be larger than the former, so that the author's K will be smaller.

As an extreme case, let us consider a locomotive with an operating speed at 90 mph, with 84 in. drivers and thus an operating rpm around 360. With orthodox but long-travel valves, economical cut-off may be around 20 per cent or lower. Assuming a suitable card factor for wire-drawing, condensation effect, etc., we arrive at given cylinder proportions. Such cylinders may be inadequate for starting conditions, resulting in a high factor of adhesion. The boiler capacity would be sufficient to sustain long cut-offs for a considerable range at the low speeds, but wire-drawing would cause a drop in tractive force irrespective of boiler capacity. In this case, with low operating speeds say from 40 to 80 rpm, the tractive effort would appear more limited by cylinder size than boiler adequacy.

With locomotives as discussed by Dr. Lipetz operating at 200–250 rpm, the demand on the boiler usually comes at a critical speed around 50 rpm. With limited cut-off locomotives, and, therefore, with large-size cylinders required for starting conditions, the cylinder steam consumption would be too great and therefore inconsistent with the evaporative capacity of the boiler at 200–250 rpm. With the lower steam consumption effected by the shorter starting cut-off, the rated starting tractive effort can be nearly maintained at 50 rpm with less demand on the boiler than for longer starting cut-offs. On this basis a boiler proportioned for this condition would be inadequate for high operating speeds.

With increasing tendencies toward higher operating speeds from 200 to 250 rpm coupled with the desire for maintaining more economical steam consumption at the lower speeds by the use of shorter cut-offs in this latter range, the danger of inadequate boiler capacity is apparent particularly when the boiler adequacy is based on its sufficiency at 50 rpm. Dr. Lipetz has given us an interesting and most ingenious analysis for providing boiler adequacy for this latter condition. If the rated tractive effort T_r gives the tractive effort T_{i50} based on boiler adequacy, this condition will insure adequate boiler capacity for operating speeds around 200–250 rpm.

While the writer is more or less in agreement with Dr. Lipetz' analysis, he would appreciate the author's consideration of the following point. Reviewing the basic analysis

$$P_i = \frac{E_c(1-x)}{s_h} = \frac{E_c}{S_a} = \frac{\beta E_c}{S_a} \text{ for the power}$$

$$T_i = \frac{375 P_i}{V} = \frac{375 P_1}{\frac{n}{336} D} = \frac{126{,}000\,\beta\,E_c}{nDS_a}$$

$$M_t = \frac{126{,}000\,\beta}{nS_a},\ T_i = M_t\frac{E_c}{D}$$

From test data at a given n, he obtains βE_c, this data being obtained mostly for locomotives with a long starting cut-off. Knowing the power developed or tractive force, he obtains S_a (or S_h). Taking $\beta = 1$, at say 200 rpm, he obtains E_c and compares or corrects for Cole's original evaporation constant E_c. Therefore, at some lower speed he obtains β from the power developed and the steam consumption S_a. At 50 rpm, the tacit assumption is that the power developed is entirely limited by the boiler evaporation capacity so that knowing S_{a50}, the coefficient β_{50} is obtained and likewise the modulus M_t, which also could be obtained directly. If now we assume the locomotive limited by cylinders rather than by boiler capacity at 50 rpm, then β_{50} would not necessarily be the true evaporative coefficient. With large cylinders and more economical cut-off at starting, aside from S_a being decreased, if the true β_{50} were greater than assumed by the author's deduction, M_t would be greater and therefore the boiler adequacy $\frac{T_{i50}}{T_R}$ would appear improved.

Now, of course, as the speed increases where there can be no question about cylinder-performance limitations, the values of the author's β obtained must greatly increase in precision. After all, the question of boiler adequacy is more dependent on conditions at operating speeds. With large-size cylinders, economical cut-offs at these higher operating speeds would be around 20–25 per cent or the same as with long cut-off locomotives. For this reason adequate boiler capacity would demand somewhat larger boilers for speeds around 200–250 rpm and the ratio of horsepower to initial tractive force would increase as compared with long starting cut-offs.

With slow heavy drag service as on grades, etc., the power developed at such low speed ranging from 50–80 rpm, is of particular interest. In this case it is of importance to ascertain whether cylinder performance limitations or boiler capacity is the more critical limitation.

The writer would prefer the analysis of performance simply on the formulas

$$P_i = \frac{\beta E_c}{S_a},\ T_i = \left[\frac{126{,}000\,\beta}{nS_a}\right]\frac{E_c}{D}$$

with more test considerations as to β, S_a for different speeds, cut-offs, etc., and further analysis of limiting values of M_t at very low speeds. It would be interesting to consider E_c for $\beta = 1$ at several operating speeds, and the variation of β and S_a for different speeds relative to the particular operating speeds considered.

Lawford H. Fry.[5] For judging locomotive proportions Dr. Lipetz offers his locomotive characteristic K which is equivalent to E_c/Vp_b, where E_c is the Cole boiler evaporation. Unfortunately, Dr. Lipetz does not give in either the present paper nor in his earlier paper[3] complete information for computing this Cole boiler evaporation.

The writer believes it is unnecessary and undesirable to use an assumed figure such as E_c in comparing boiler and cylinder proportions. Dr. Lipetz concedes something in this direction by saying: ". . . a constant very similar to K, but with the boiler evaporation replaced by H_e, the evaporative surface in square feet

$$\delta = H_e/Vp_b$$

may also be very useful for comparative purposes."

The writer suggested, in a paper read before the New York Railroad Club in 1903, a boiler factor very similar to the above. This was $B = T_r/H_e$, where T_r is the rated tractive effort in pounds. B and δ are inversely proportional to each other. B has the practical advantage that it is computed from the rated tractive effort, and an additional calculation to find the cylinder volume is unnecessary. δ has a slight advantage in the fact that it is directly proportional to the boiler capacity, so that a large value of δ indicates a large boiler in proportion to the cylinders.

If B is used, it is convenient to note that it measures the pounds of rated tractive effort which must be developed by each square foot of heating surface when the locomotive is working in full gear.

To bring the comparison to a basis of revolutions per minute instead of miles per hour, the writer proposed multiplying B by D, the driving-wheel diameter. This gives

$$BD = \frac{T_rD}{H_e}$$

It can be shown that if the locomotive is working in full gear, the factor BD is proportional to the foot-pounds of work which must be developed at each revolution by each square foot of heating surface. The lower the value of BD, the higher the speed at which the rated tractive effort can be developed. A low value of BD indicates a locomotive with large boiler capacity designed for high-speed service.

For many years the technical papers when publishing accounts of new locomotives gave values of B and BD. This has provided a large amount of information available for the comparison of various locomotive designs.

If it is decided that a newer method of comparison is desirable, the writer would prefer to see Dr. Lipetz' δ used instead of K. It seems to him desirable to make the comparison simple and direct, involving only definite dimensions of the locomotive and avoiding the introduction of any assumed values such as a calculated boiler evaporation.

Discussion of the second phase of the subject, that is the prediction of the tractive power which can be developed at various speeds, cannot be made in detail without full information as to the method of computing the Cole boiler evaporation. This is not given in either of Dr. Lipetz' papers. Dr. Lipetz shows, however, that his method gives computed tractive-power curves which are surprisingly close to the actual curves derived from experiment.

H. Rubenkoenig.[6] Undoubtedly there is necessity for revision of some of Cole's ratios and other formulas used in calculating tractive effort for locomotives. The generally accepted formula

$$T = KPC^2S/D$$

for determining what is variously designated as cylinder tractive effort, starting tractive power, theoretical tractive force, etc., does not seem to hold for some of the newer locomotives built during the last two or three years.

K in this formula depends upon whether or not the valve has a limited cut-off, and whether or not auxiliary starting ports are used. One of the recently built heavy passenger locomotives of the 4-8-4 class is described as having a rated tractive effort of 69,800 lb. If K is taken as 0.85 (the proper coefficient for 90 per cent cut-off), the tractive effort from the foregoing equation becomes

$$T = 0.85 \times 260 \times 28^2 \times 31/77 = 69{,}300 \text{ lb}$$

[5] Railway Engineer, Edgewater Steel Company, Pittsburgh, Pa. Mem. A.S.M.E.

[6] Professor of Railway Mechanical Engineering, Purdue University, Lafayette, Ind. Assoc-Mem. A.S.M.E.

This locomotive is described as having a valve gear which gives 70 per cent maximum cut-off, but no mention is made of auxiliary starting ports. Assuming auxiliary starting ports, the value of K is 0.78, which when applied to the foregoing formula gives a tractive effort of 64,100 lb. In other words, the rated tractive effort is more than 5000 lb too high if the generally accepted formulas for calculating tractive effort be used.

Since predictable locomotive performances at speeds above starting speeds are based upon data which include suitable corrections being made from the basic figure of capacity tractive effort, it seems that some revision of calculation methods is necessary. It would be interesting to know what assumptions were made in deriving the figure for rated tractive effort of the locomotive previously mentioned.

The 1932 and 1934 papers by Dr. Lipetz are distinct contributions to the subject of locomotive tractive effort and horsepower, and they indicate the direction in which locomotive designers may work in improving the efficiency of the modern steam locomotive.

W. A. Pownall.[7] Dr. Lipetz states that drafting arrangements in particular may cause disagreements or differences between the tractive-effort curves and actual performances. The Wabash railroad has had considerable experience during the past few years with the Kiesel front end which uses an annular-ported exhaust nozzle of large area and a cylindrical draft netting, extending from the stack to the bottom of the boiler, without the usual draft or deflector plates.

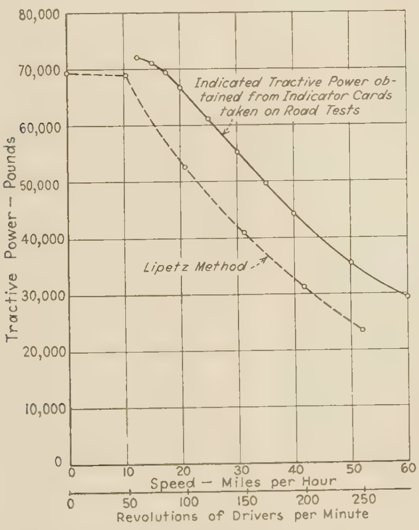

Fig. 2 Cylinder Tractive-Power Curve of a Mountain-Type Locomotive With Kiesel Front End Compared With Lipetz' Calculated Tractive Effort

Fig. 2 of this discussion shows the cylinder-tractive-power curve obtained on a mountain-type locomotive equipped with a Kiesel front end. For comparison, the tractive-effort curve as calculated by Dr. Lipetz' method is also plotted on this figure. The curve as obtained from indicator cards on road tests was not an extreme condition, but was obtained on a large number of runs. It will be noted that at 40 mph, the engine in question actually developed about 35 per cent more tractive power than shown by the Lipetz method. This engine is equipped with a type-E superheater and a feedwater heater.

Fig. 3 of this discussion shows a similar curve for a Mikado-type locomotive equipped with a type-A superheater and without a feedwater heater. The difference between the actual road results and the Lipetz curves is not as pronounced as with the mountain-type locomotive, the excess of the actual tractive power over the Lipetz curve being 17 per cent at 30 mph and 14 per cent at 40 mph. These results are worth attention in showing the increased actual locomotive capacity that can be obtained by drafting arrangement other than the conventional.

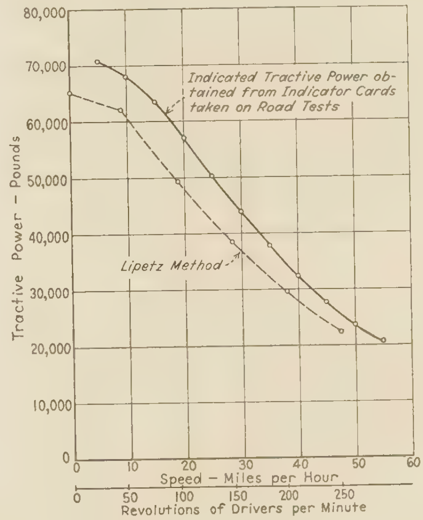

Fig. 3 Cylinder-Tractive-Power Curve of a Mikado-Type Locomotive Compared With Lipetz' Calculated Tractive Effort

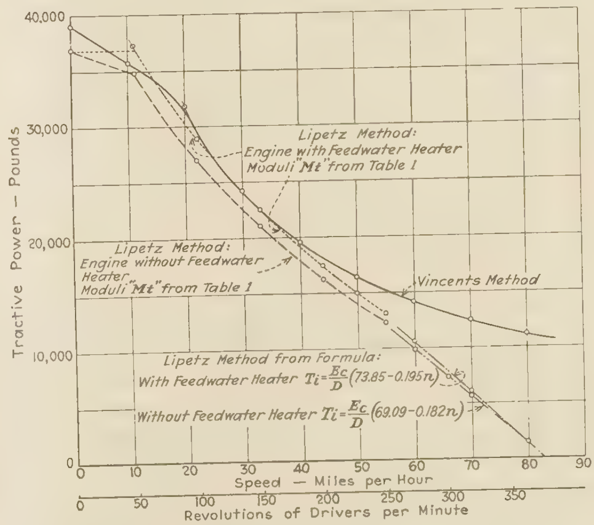

Fig. 4 Cylinder Tractive-Effort of a Pacific-Type Locomotive as Derived From the Vincent and Lipetz Methods

In view of the present interest in high-speed passenger trains there is a definite demand for a knowledge of the draw-bar tractive effort that can be developed by steam passenger locomotives at speeds between 70 to 100 mph.

Fig. 4 of this discussion shows the cylinder tractive effort of a Pacific-type locomotive as derived from the Vincent and Lipetz methods. For speeds above 60 mph, the Lipetz formula would produce a tractive-effort curve considerably lower than the

[7] Mechanical Engineer, Wabash Railway Company, Decatur, Ill.

Vincent curve and also lower than has been obtained in actual service. For example, if the engine resistance were deducted from the Lipetz cylinder tractive effort, there would be nothing remaining to pull the train at about 75 mph, while the engine for which these curves are shown, actually pulled a seven-car train weighing 560 tons, exclusive of the engine and tender, at a speed of from 80 to 83 mph on level track, at which speed it developed an approximate cylinder tractive-effort of 9680 lb. It may be that Professor Lipetz does not intend his formula to be used at driver speeds of over 250 rpm. This actual performance is somewhat less than the value indicated by the Vincent curve and considerably higher than that calculated from the Lipetz formula.

There should be some fairly definite information developed as to available draw-bar tractive effort of locomotives at speeds between 70 and 100 mph.

Author's Closure

While Dr. Giesl-Gieslingen reiterates his agreement with my 1932 method, as given in the previous paper,[3] he takes exception to my 1934 modifications and rejects them summarily. He is in favor of the fundamentals of my 1932 theory and admits the value of the moduli, but thinks that I rather rashly abandoned the strict consistency of that method in order to satisfy the curves presented by Mr. Vincent. I must, therefore, so to speak, defend myself against myself, and this makes my task rather difficult. However, I am afraid that Dr. Giesl-Gieslingen misunderstood the underlying thought of the 1934 modifications and probably forgot the principal object of the 1932 method.

Dr. Giesl-Gieslingen maintains that my theory of 1932 was based, on the one hand, on a certain evaporation curve which he considers more or less correct, although maybe somewhat conservative, and, on the other hand, on a steam-consumption curve with which he also is more or less in agreement. As pointed out in both the 1932 paper and in its closure, the procedure which I followed in the first part of my 1932 paper was used only in order to establish the correct and logical relations between phenomena in a locomotive, which led to a simple formula. I checked it later against all locomotive-test data at my disposal at that time. In other words, while the 1932 method had a theoretical basis, it was purely empirical, and in proving the practicability of the 1932 moduli, I did not attempt to defend the absolute correctness of figures, or curves, of evaporation and steam consumption on which my formula was based. I admitted that the Cole evaporation figure E_c, evaporation-coefficient β and steam-consumption curves may be only approximately correct, but as the formula was later checked against test results and the moduli, specially introduced for that purpose, were corrected so as to conform with these results, the formula, which in its final form was very simple, must have been right and could be used for practical purposes. The user need not go back to the underlying data and examine them. This made the method very simple, as it required the use of only one formula with constant moduli depending upon the rotative speed of the wheels, and at the same time very flexible, because the moduli could be changed when conditions warranted that.

In the 1934 modifications I followed the same principle. In studying the test results of locomotives brought to my attention in Mr. Vincent's discussion of my 1932 paper, I realized that all the locomotives on which I had data at my disposal in 1932 had long cut-offs, and that the locomotives analyzed by Mr. Vincent, especially those for which my 1932 moduli showed discrepancies, were types with limited cut-offs. In my 1932 paper I also considered, among others, the Boston & Albany A-1 locomotive and found that it showed fairly good agreement with my 1932 moduli, although it was of the type with limited cut-off. In analyzing this, I found that the good results of my 1932 moduli, in application to this locomotive, were due to the fact that while the locomotive had limited cut-off, its cylinder sizes were not excessive and very close to the sizes they should have had for a limited cut-off of 60 per cent ($K = 12.27$ instead of $K = 13.09$) while all other locomotives with limited cut-offs which he cited had excessively large cylinders, larger than the limited cut-off would require. The conclusion was, therefore, evident: it was necessary to modify my moduli for locomotives with large cylinders, irrespective of whether or not they were types with limited cut-off or full cut-off. I found a method for doing it and disclosed it in my 1934 paper. Again in order to prove that this method was correct and practicable, I showed that its application to all locomotives on which data were available, both with small and large cylinders, gives very good results. This fact was fully realized and appreciated by Lawford H. Fry in his discussion, and I am very grateful to him for pointing out this fact. It was not a question, as Dr. Giesl-Gieslingen thinks, of satisfying Mr. Vincent's curves. It simply was the question of showing that the locomotives for which Mr. Vincent had test data and which, he thought, were best represented by his formula, could be satisfied by my moduli, if proper modifications are made.

Dr. Giesl-Gieslingen evidently overlooked this point entirely. He thinks that the curve on Fig. 5 of the paper is arbitrary. While it is true that no formula was given for this curve, it was arrived at through a long study of test results and was later checked against all locomotives for which test data could have been obtained. It is the author's opinion that it has more value than a curve like the one shown by Dr. Giesl-Gieslingen in Fig. 1 of this discussion, for which no attempt was made to show its application to any locomotive. Only when a formula has been verified for a reasonable number of locomotives may it be considered seriously, and not before, no matter how scientifically the curve may appear to have been derived.

As an example of another misunderstanding by Dr. Giesl-Gieslingen, the aforementioned Boston & Albany A-1 locomotive can be cited. He says "Lipetz explains that since this engine has 60 per cent limited cut-off the cylinder could be called about normal, although $K = 12.27$, and he indicates that no correction should be applied." What I said was that notwithstanding the fact that this engine has a limited cut-off of 60 per cent, $K = 12.27$ instead of 13.09, if the proper relations of cylinder sizes with respect to the correct α for a cut-off of 60 per cent is taken into consideration. But I did not say that corrections should not be made. They certainly should be made, as they were made in all other locomotives with large cylinders, irrespective of whether they were types with long cut-off or limited cut-off (see, for instance, Texas & Pacific locomotive G-lb, Fig. 8), as 12.27 is less than 14.26. Dr. Giesl-Gieslingen further states "since he applies the full correction to the Pennsylvania class I-ls with only 55 per cent limited cut-off, and likewise to all other examples, it would be inconsistent not to do the same for the Boston & Albany locomotives." Yes, it would be inconsistent, and the correction should be made, but while the I-ls locomotive has a limited cut-off of 55 per cent, very close to 60 per cent of the A-1 locomotive, the cylinders are so large that the K for this locomotive is only 8.53, whereas it should be, according to formula [9a] of the paper, $0.75/0.0596 = 12.55$. Therefore, the cylinders of this locomotive are about 47 per cent larger, and a greater correction is necessary.

As to the Boston & Albany A-1 locomotive, after the correction for the tractive effort at 50 rpm is made, its value will lie above the rated tractive effort, and according to the rules given in the paper, the curve with this point at 50 rpm should be cut off. The remaining part of the curve will not differ much from the test curve.

Dr. Giesl-Gieslingen discusses what I would call "discontinuity

of functions," when he cites in the beginning of his discussion various values of Fig. 5 for smaller and larger cylinders. He refers to the figures "jumping" suddenly by 6.7 and 16.0 per cent, but he forgets that he also jumps $^1/_2$ in. and 2.1 in. in cylinder sizes, or 4.0 and 16.6 per cent in piston areas, respectively. Every continuous function would do that.

Dr. Giesl-Gieslingen is surprised that the Lipetz correction curve for 50 rpm should have an edge at $K = 14.26$. There are many cases like that in engineering practice. A loose tire on a locomotive wheel puts no strain in the wheel rim or in the tire, but if the bore of the tire is several hundredths of an inch smaller than the outside diameter of the wheel, the stress suddenly goes up and it will continue going up with the increase in this difference, most probably with an edge in the curve. The effect of large locomotive cylinders is of about the same nature. If they are too small, there is plenty of steam for them, just as there is plenty of clearance in a loose tire around a wheel, and T_{i50} (indicated tractive effort at 50 rpm) cannot be increased, as a rule, because in small-cylinder locomotives it is equal to T_r (rated tractive effort), corresponding to a maximum cut-off of 85 per cent. However, if the cylinders are larger than what the ordinarily generated amount of steam for the tractive effort at 50 rpm would require, naturally more steam can be utilized by the cylinders, if a certain forcing of the boiler is permitted. Then a modification is, of course, necessary, and the law of modification may go up suddenly, following a curve with an edge. This is what probably happens, and there is nothing illogical in that.

I do not think that it is necessary to go through Dr. Giesl-Gieslingen's other statements except possibly one, in which he says that the reader is left without a clue as to what he might expect from the boiler when it is forced. Dr. Eksergian in his discussion touches on this point in connection with the coefficient β. In order to amplify Dr. Eksergian's thought, and to reply fully to Dr. Giesl-Gieslingen's statement, I am going to present several charts which recently came to light. They were not known to me at the time when the present paper was prepared. A very interesting book,[8] recently published on a 2-10-2 locomotive, series FD, developed and built in U.S.S.R., came into my possession. For the development of this engine the locomotives built in America in 1931 for U.S.S.R. were taken as examples and, therefore, the locomotives are in many respects similar to regular American-built engines. They have large grates, steel fireboxes, firebrick arches, type-E superheaters, feedwater heaters, stokers, boosters, etc. They differ only in having fireboxes of the Belpaire type instead of the round-top shape. A 2-8-4 passenger-type locomotive, series JS, has also been developed and built by the U.S.S.R. In this type, boilers and cylinders are identical with those of the FD engines, the principal difference being in the chassis: frames, wheels, boxes, etc.

TABLE 1 PROPORTIONS AND RATIOS OF U.S.S.R. SERIES FD AND JS LOCOMOTIVES

Locomotive	Russian 2-10-2 FD Class	Russian 2-8-4 JS Class
Cylinder dimensions		
Diameter, d, in.	26.4	26.4
Stroke, s, in.	30.3	30.3
Heating surface, H_e, sq ft	3177	3177
Boiler pressure, p_b, lb per sq in.	213.4	213.4
Cole evaporation, E_c, lb per hr	44859	44859
Superheater type	E	E
Feed water heater	Yes	Yes
Max indicated ratio, α_{max}	0.78	0.78
M_t at $n = 50$	65.6	65.6
Driving wheel diameter, D, in.	59	72.8
Boiler adequacy, $a_b = \frac{T_{i50}}{T_r}$	0.837	0.837
Boiler percentage (Cole)	0.809	0.809
Cylinder volume, V, cu ft	19.20	19.20
$\delta = \frac{H_e}{VP_b}$	0.775	0.775
$K = \frac{E_c}{VP_b}$	10.95	10.95

The principal dimensions of these two engines are shown in Table 1 of this discussion, which is compiled in the same manner as Table 4 of the paper. In view of the similarity between these two types and American engines, the test results of these U.S.S.R. locomotives are of great interest to us for the present purpose.

The book[8] just referred to describes in detail the U.S.S.R. 2-10-2, Series FD locomotive, and in Appendix 1 gives results of very elaborate tests in the form of charts according to the method worked out years ago by Professor Lomonossoff in Russia.[9] Fig. 602 of the book is reproduced in this discussion as Fig. 5. The abscissas are speeds in kilometers per hour; the ordinates are indicated tractive efforts in kilograms. The full-line curves correspond to constant evaporation, the figures on them showing kilograms of steam per hour consumed by the cylinders (excluding auxiliaries), the steam being referred to one square meter of outside heating surface. The dashed curves correspond to constant cut-off, the figures on them representing percentages of cut-off. In Fig. 6 of this discussion the constant-evaporation curves of Fig. 5 are reproduced in English measurements. The notations

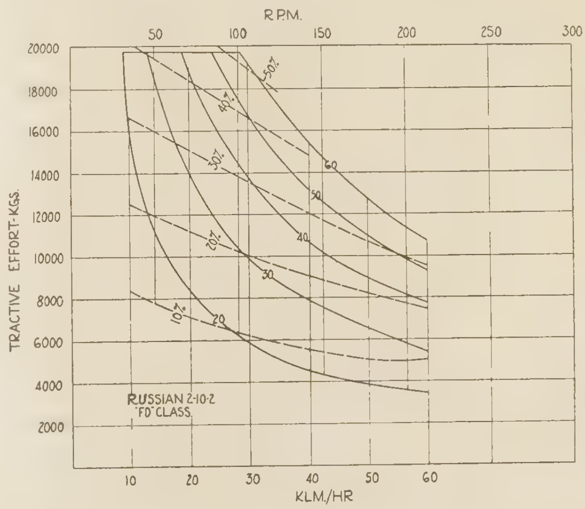

FIG. 5

(Full-line curves are constant-evaporation lines, the figures on them representing kilograms of steam consumed by cylinders per hour, referred to a square meter of outside heating surface. Dashed curves are constant-cut-off lines; figures on them represent percentages of cut-off.)

on the axes are made to conform with the practice of the author's 1932 and the present papers. Full lines are constant-evaporation curves, figures on them representing pounds of total steam generated by the boiler per square foot of outside heating surface per hour. These figures were obtained from the metric-evaporation figures by adding 10 per cent for auxiliaries, as this amount of steam has not been included in the Russian curves. In addition, the author's 1932 and 1934 curves have been added to the chart.

The locomotive characteristic K, as can be seen from Table 1 of this discussion, is equal to 10.95, and corrections have been made in accordance with Fig. 5 of the paper. It is interesting to note that the 1934 curve follows, as to the general trend, all other curves, but it lies outside of all of them, even that which corresponds to the maximum evaporation of 13.5 lb of steam per sq ft of outside heating surface. By extrapolation it can be found that the 1934 curve corresponds to an evaporation of about 14.2.

[8] "Locomotive Felix Dzerjinsky" (published in Russian), Moscow, 1934.

[9] "Object of Locomotive Tests and Their Method," by G. Lomonossoff, St. Petersburg, 1914.

Now, the Cole evaporation figure for this locomotive is 44,859 lb per hour. The outside heating surface is 3177.08 sq ft. The evaporation per sq ft is, therefore

$$E_c/H_e = 44{,}859/3177.08 = 14.15$$

very close to the foregoing figure of 14.2. This agreement is remarkable, or, using Mr. Fry's expression, "surprising." In reality it is natural, if we consider that the Series FD locomotive is of, what may be called, American design, and has, as it will be shown later, the regular circular exhaust nozzle, for which the author's curves have been established. The above agreement also shows that the 1934 curve for the Series FD locomotive follows the Cole evaporation figure with a β equal to 1.00 for all speeds; in other words, in order to obtain the 1934 tractive effort at low speeds, the boiler has to be forced. This answers Dr. Giesl-Gieslingen's and Dr. Eksergian's questions as to how high β at low speeds must be. For the Series FD locomotive with K = 10.95 it is evidently 1.00. For other cylinder ratios it may be different. It can be figured out approximately from the modification curve by following the trend of Dr. Eksergian's thoughts and the formulas given in his discussion.

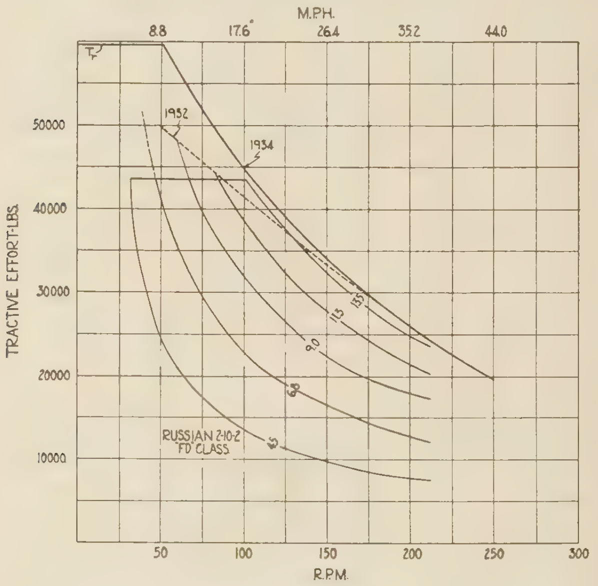

Fig. 6

(Full-line curves are constant-evaporation curves, the figures on them representing pounds of steam generated per square foot of outside heating surface per hour.)

In this connection Fig. 6 of this discussion also shows that the 1932 curve would intersect the tractive effort curves at other lower evaporations. For instance, an evaporation of 11.3 would intersect the 1932 curve at about 83 rpm. An evaporation of 9.0 would permit a speed of about 59 rpm, and at 50 rpm the 1932 curve would probably correspond to an evaporation of somewhere between 6.8 and 9.0. It can be found by interpolation to be 8.01, which is about 56.7 per cent of 14.15, which is close to the β assumed by the author for 50 rpm, if we remember that the coefficient β was established as an average of data from many locomotives.

About the same time (1933) the Russian Government developed and built the Series JS passenger locomotive. This locomotive, as has already been stated, has the same boiler as the Series FD locomotive, and has cylinders of the same size. It differs only in the size of driving wheels, which were about 73 in. in diameter instead of 59 in. As our locomotive formulas are based on the boiler evaporation, and the modifications are based on the cylinder dimensions, these two locomotives should give the same power curves, differing only with respect to the tractive efforts in so far as they are affected by the size of driving wheels. Boiler evaporation should be exactly the same. For purposes of comparison, Figs. 7 and 8 of this discussion have been prepared. They correspond to Figs. 5 and 6 for the FD locomotive. Again, Fig. 7 is an exact reproduction of Fig. 12 of the publication on the JS locomotive,[10] while Fig. 8 is the same as Fig. 7 converted to English measurements, with the author's 1932 and 1934 curves added. Furthermore, in order to compare the relation of the 1934 curve on Figs. 6 and 8 of this discussion the highest constant-evaporation curves of Fig. 8 are omitted and the 13.5 curve is retained as the highest, the same as in Fig. 6. It can

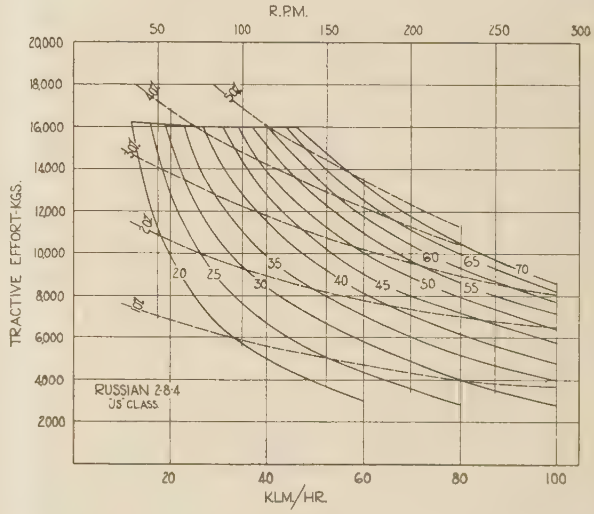

Fig. 7

(Full-line curves are constant-evaporation lines, the figures on them representing kilograms of steam consumed by cylinders per hour, referred to a square meter of outside heating surface. Dashed curves are constant-cut-off lines; figures on them represent percentages of cut-off.)

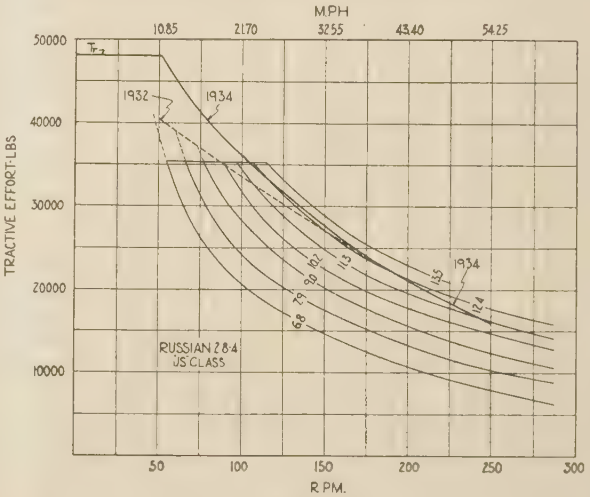

Fig. 8

(Full-line curves are constant-evaporation curves, the figures on them representing pounds of steam generated per square foot of outside heating surface per hour.)

[10] "Principal Test Results of the First Type 2-8-4, Series JS Locomotive" (in Russian), Moscow, 1934.

be seen, however, from comparing Figs. 5 and 7 that the maximum evaporation on the tests of the JS locomotive was much higher than on those of the FD locomotive; 70 against 60 kg per sq meter per hr, or 16.7 per cent higher. This result was somewhat puzzling, but a careful study of the tests of the second locomotive showed that the two locomotives which are supposed to be alike, when actually tested, had different exhaust nozzles: the FD locomotive had the ordinary round nozzle, while the JS locomotive had a special nozzle with separate exhausts from the right and left cylinders, and four round openings for the escape of steam which had a total area 32 per cent larger than that of the single opening of the round nozzle used on the FD locomotive.[11]

This difference probably explains the higher evaporation and may also explain why the 1934 curve, which in Fig. 8 of this discussion has in general the same characteristics as the one described in reference to the FD locomotive (Fig. 6), is switched so as to coincide more with the 12.4 evaporation curve than to be coincident with the 14.2 curve. This is the result of reducing the back pressure of the JS locomotive and, incidentally, reducing the minimum steam consumption of the latter locomotive, per equal power which was 15.5 lb per rail horsepower, as compared with 17.4 of the FD locomotive.[12]

It is also interesting to note that notwithstanding the differences just mentioned, the trend of the 1934 curve and its relation to the constant-evaporation curves is about the same in Fig. 8 for the JS locomotive as in Fig. 6 for the FD locomotive, and that in the JS locomotive it also corresponds to a constant evaporation (about 12.4), which, however, because of better efficiency is lower than the Cole evaporation per square foot of outside heating surface (14.15). In this case β has a constant value of about 0.88. Thus, the tractive effort of a JS locomotive, if tested under the usual American conditions, would give a $1/0.88 = 1.14$ increase ratio for the same amount of steam, and a further increase due to 16.7 per cent higher evaporation, a total increase in the ratio of $1.14 \times 1.167 = 1.33$, or a 33 per cent increase, with the same "strain of forcing," so to speak.

The above explanations, I think should satisfy Drs. Giesl-Gieslingen and Eksergian as to the question of what evaporation the modifications of 1934 actually represent, and should also corroborate Mr. Pownall's statement as to the increase in locomotive capacity due to the use of a drafting arrangement other than the conventional. Mr. Pownall's figure of a 35 per cent increase is about the same as the 33 per cent increase cited previously.

In order to finish with Dr. Giesl-Gieslingen's discussion, a few words should be said about his suggestions. Of course, one should welcome the recommendation that some institution, for instance, the Association of American Railroads, should accumulate and assimilate all possible information now available on results of locomotive tests. The author himself has gone even further and suggested some time ago that a central institution, the best of which at present is the Association of American Railroads, should conduct a similar research of its own.[13] This is now on the program of the Association, and the author understands that tests with modern locomotives with a view to establishing fundamental data for locomotive ratios are now being contemplated. The author hopes that the tests will soon be made and he is confident that their results will help to confirm, or modify, his moduli and his correction curve (Fig. 5 of the paper).

As to Dr. Giesl-Gieslingen's recommendations 1, 2 and 3, they have no bearing on this paper. The recommendations are not new and are too general. Besides, the recommended tests when carried out, cannot obviate the necessity of having a simple method by which a reasonably correct evaluation of the power and tractive effort of a locomotive could be made without going to elaborate tests and calculations. This was the object of the author's papers.

Dr. Eksergian's apprehension as regards the difficulties with β which we may run into, if we follow the author's suggestion regarding boiler adequacy at 50 rpm, probably can be answered better by saying that while the adequacy, as shown in the paper, comes out close to 1.00 instead of Cole's 100 per cent, the author has not stated definitely what percentage he would recommend for either drag, limited cut-off, or high-speed locomotives. This, following his usual policy, has not been made for the reason that no test data are yet available on high-speed locomotives. His feeling, however, is that 1.00 and greater figures will serve just as well with respect to the boiler adequacy, as Cole's 100 per cent, or larger, boiler. For locomotives with large-size cylinders, both coefficients automatically will come out smaller. Following his line of reasoning, the cylinders have to be dimensioned on the basis of starting tractive effort and he does not expect that any difficulty will arise at high speeds on account of the insufficiency of cylinder dimensions, as long as the boiler is given sufficiently large proportions; corresponding to a boiler adequacy of 1.00, but the larger, the better, especially for high-speed locomotives.

As an example, the high-speed streamlined 4-4-2 locomotive recently completed by the American Locomotive Company for the Chicago, Milwaukee, St. Paul & Pacific could be cited. The Cole boiler-percentage figure for this locomotive is 108.8. The author's boiler adequacy is 1.116, which indicates the close approximation of both coefficients to their respective normal values (100 and 1.00 per cent). The author does not advise that the Cole evaporation figure, with which railroad mechanical men have become familiar, should be replaced by the new conception of boiler adequacy, although he thinks that the latter imparts greater definiteness to the meaning of boiler proportions, for reasons explained in the paper. The main reason for the author's suggestion of this new conception was only because in some quarters it was felt that when the Cole speed factors are replaced by the author's moduli, the Cole boiler-percentage figure is lost sight of. The author, therefore, tried to establish something which could take the place of the Cole boiler-percentage figure, if his moduli are used for the evaluation of horsepower and tractive effort instead of the Cole factors. If it is desired to figure the Cole boiler percentage, it can be done, but then additional calculations of some of Cole's figures, which are not needed for the author's method, will have to be made, without arriving at a substantially different figure, except that one (the Cole) is in per cent, while the other (the author's) is in fractions.

Reverting to Mr. W. A. Pownall's discussion, it can be added to what has been already said, that the discrepancies which he noticed between his curves can undoubtedly be explained by the difference in drafting arrangements. The 1932 and 1934 methods correspond to the ordinary round nozzle and A.A.R. smokebox arrangement, as it has been brought out by the agreement between the author's moduli and test results. The Kiesel front may be giving better results, and probably permit forcings of the boiler, without corresponding reduction in the efficiency, similar to the case with the drafting arrangement on the U.S.S.R., Series JS locomotive.

As to the use by Mr. Pownall of the author's analytical formula

[11] "Principal Test Results of the First Type 2-8-4, Series JS, Locomotive" (in Russian), Moscow, 1934, p. 41.

[12] Compare Fig. 34 of "Principal Test Results of the First Type 2-8-4, Series JS, Locomotive," with Fig. 609 of "Locomotive Felix Dzerjinsky" previously referred to.

[13] "Coming Motive Power and Locomotive Research," by A. I. Lipetz presented before the Canadian Railway Club, April 9, 1934, concluding paragraph.

for very high speeds and revolutions per minute (up to 360), this has not been intended by the author. The formulas are simplifications of the moduli. They give approximately the same results and should not be used for speeds higher than the moduli themselves, namely, 250 rpm.

In his 1932 and 1934 papers the author hesitated to extend his curves beyond 250 rpm simply for lack of data. When the tests to which Mr. Pownall refers are published, with all details which would permit judging the efficiency, evaporation and other features of the performance, the curves could be extended for higher speeds. The advantage of the author's method is the ease with which the modifications of moduli can be made if dictated by test results. Simply as an example, but not as a matter of recommendation, the author may say this in reference to higher speeds:

A comparison of his 1934 curves with the curves on Fig. 8 of this discussion and others show a great probability that his moduli for 250 rpm may have been slightly underestimated. It is probable that at higher speeds, especially with better drafting arrangements, the supposition of Mr. Cole, that after a certain limit of speed the horsepower remains constant, is true. If this should be so, say, after 200 rpm, the Mp moduli would be as given in Table 2 of this discussion.

TABLE 2 VALUES OF THE M_p MODULI FOR SPEEDS ABOVE 200 RPM

Revolutions per minute, n	200	250	300	350
Locomotives with feedwater heaters, Modulus $M_p \times 1000$	54.0	54.0	54.0	54.0
Locomotives without feedwater heaters, Modulus $M_p \times 1000$	50.5	50.5	50.5	50.5

Then accordingly, on the basis that $M_t n$ = constant, the M_t moduli should be as follows:

Revolutions per minute, n	200	250	300	350
Locomotives with feedwater heaters, Modulus M_t	34.1	27.4	22.8	19.6
Locomotives without feedwater heaters, Modulus M_t	31.8	25.2	20.9	17.9

As the boiler can always be forced to a certain extent, especially at high speeds, it may be safe to use the moduli of Table 2 in all cases when curves have to be extended for high speeds, before reliable test data are available. Of course, they will have to be watched very carefully and checked against test data, and as we are soon going to have high-speed locomotives on many railroads, from which high-speed test results undoubtedly will be obtained, this can be easily done.

In view of the fact that some readers may be tempted to extend the formulas, given at the end of the paper, to speeds higher than 250 rpm, as Mr. Pownall has done, the author thinks it advisable to give formulas corresponding to the preceding tabulation of constant moduli M_p and hyperbolic moduli M_t. In such a case, strictly speaking, it must be noticed that the constant-horsepower line should be tangent to the horsepower curve at its maximum point; then the hyperbola will follow smoothly the straight line of the tractive effort. The approximate speed at which this takes place for formulas [13*a*] and [13*b*] is 190 rpm (the exact values are 189.4 and 189.9 rpm).

Incidentally, at the rotative speed of 190 rpm, the modification y is equal to zero. Thus, the following formulas can be recommended:

For locomotives equipped with feedwater heaters and speeds up to 190 rpm

$$T_i'' = \frac{E_c}{D}(73.85 - 0.195n)(1 + y) \qquad [16]$$

where E_c is the Cole evaporation figure, lb per hr, D is the diameter of drivers, in. and n is rpm. Modification coefficient y should be figured in accordance with formula [15], which is here repeated

$$y = \left(\frac{30}{n + 10} - 0.15\right)\frac{15 - K}{7} \qquad [15]$$

This formula eliminates from Fig. 5 the sharp edge at K = 14.26, so objectionable to Dr. Giesl-Gieslingen, and replaces it by a blunter point at K = 15.0. A number of small-cylinder locomotives, practically all of any importance, will be thus included.

At 190 rpm $y = 0$, and $T_i''_{190} = \frac{E_c}{D}36.8$

The corresponding horsepower will be (see formulas [5] and [9] of the 1932 paper)

$$P_i''_{190} = \frac{T_i'' \times V}{375} = \frac{T_i'' \times nD}{375 \times 336.134} = \frac{E_c}{D}\cdot\frac{36.8 \times 190 \times D}{126{,}050} = E_c \times .05547$$

Thus, modulus $M_p \times 1000$ = 55.47 instead of 54.0 for the maximum horsepower at 200 rpm, a difference of +2.7 per cent. This represents the approximation of the formula and the error in replacing 190 for 200 rpm as the speed at which the horsepower is maximum.

For speeds higher than 190 rpm, the tractive effort, the horsepower remaining constant, will evidently be

$$\frac{P_i'' \times 375 \times 336.134}{nD} = \frac{E_c \times 0.05547 \times 126{,}050}{nD} = \frac{6992\ E_c}{nD}$$

Thus, the tractive effort, for speeds above 190 rpm, can be figured in accordance with formula

$$T_i'' = \frac{E_c}{D}\frac{6992}{n} \qquad [17]$$

For locomotives without feedwater heaters the corresponding members of the formulas will be reduced in the ratio of 100:107. They will be, for speeds up to 190 rpm

$$T_i' = \frac{E_c}{D}(69.09 - 0.182n)(1 + y) \qquad [18]$$

and for speeds higher than 190 rpm

$$T_i'' = \frac{E_c}{D}\frac{6557}{n} \qquad [19]$$

The author wants to emphasize again that these formulas are approximate. They are of such a nature as not to be easily memorized, and have to be looked up for references. Therefore, it might be just as well to use moduli instead of the formulas. In case a simple formula for memorizing should, nevertheless, be desired, the one given in the paper (14′) could be used. It is here repeated

$$T_i = \frac{E_c}{D}(75 - n/5) \qquad [14']$$

The modification for locomotives with K less than 15.0, in accordance with formula [15], will have to be made.

This formula is also good up to 190 rpm. At this speed the value in brackets is 75 − 38 = 37. The corresponding formula for speeds above 190 rpm would be $T_i = E_c \times 7030/Dn$, because $37 \times 190 = 7030$. We can simplify the formula by making

$$T_i = \frac{E_c}{D}\frac{7000}{n} \qquad [20]$$

which is approximately the same as formula [18] and sufficiently simple to be remembered.

Curves of formulas (14′) and (20) intersect at n = 200. At

this speed the factor in the brackets in formula [14′], which is M_t, is equal to $75 - \frac{200}{5} = 35$, instead of 34.1 according to the previous tables. This is sufficiently close for an approximate calculation.

For locomotives without feedwater heaters the values of formulas [14′] and [20] must be reduced in the ratio of 100 : 107.

Mr. Fry, who is in general agreement with the author's method, brings out a point which may be of interest. He refers to his contributions made about thirty years ago and indicates that instead of Cole evaporation (E_c), the outside (evaporating) heating surface (H_e) could be used. This is approximately correct, because the ratio between these two figures, namely, the average Cole evaporation per hour per square foot of outside heating surface, differs very little. For locomotives given in Table 4 of the paper and in Table 1 of the present closure, it fluctuates between 11.50 (No. 3) and 14.72 (No. 1). For more modern locomotives it varies between 12.91 (No. 10) and 13.96 (No. 17). An average figure of probably 13.5 could be adopted, but it would still be an approximation and would in many cases destroy the good agreement between curves and test results, to which reference was made by Mr. Fry himself.

Mr. Fry's objection is mainly due to the fact that he had difficulty in computing the total Cole evaporation figure. As is known, Cole's figure is based on 55 lb of steam per hr per sq ft of direct heating surface (firebox plus brick arch tubes plus syphons), and average evaporations for tubes and flues, depending upon their size, length, and spacing. Tables of these specific evaporations are given in the locomotive handbook published by the American Locomotive Company in 1917, and reference to it was made in the author's 1932 paper. New figures regarding tubes of $3^1/_2$ in. outside diameter (without superheater units) and $3^1/_2$-in. flues (with superheater units), which came into use after the publication of the A. L. Co. handbook, in pounds of steam per hour per square foot of outside heating surface for various lengths of tubes and flues and various spacings, have been given by the author in Appendix No. 2, page 16 of the 1932 paper.[8] The author is surprised at Mr. Fry's statement that "Lipetz does not give in either the present paper or his earlier paper complete information for computing this Cole boiler evaporation." While this is literally correct, proper references to the A. L. Co. handbook were made. It is true that the locomotive handbook is now becoming very rare, but it has been in use by practically all railroads for years, and copies can be found in libraries. A new edition is contemplated.

Apart from the reason of the momentary difficulty in finding access in some cases to the A. L. Co. handbook, there is no good argument in favor of using the heating surface, as approximation, instead of the Cole evaporation figure, as the latter, when the basis of computation is available, can be determined easily. However, if a change should be desired, there would be no difficulty in substituting the total evaporating heating surface (H_e) for the Cole evaporation (E_c), if the author's moduli are increased in the ratio of, say, 13.5, which, as we saw above, represents the average evaporation figure for modern locomotives in pounds per hour per square foot of total evaporating heating surface. However, correction curve (Fig. 5 of the paper) would have to be accordingly modified, so as to use the author's δ instead of K. This would be another example of the flexibility of the author's method, which can be easily adjusted to simplifications when they are thought necessary, or to new data when they become available.

There remains Prof. H. Rubenkoenig's discussion, which is directed more to the starting tractive effort. He refers to auxiliary starting ports, for which he would like to have a coefficient in the tractive-effort formula. The author's paper did not consider the tractive effort at the moment of starting. This differs from the maximum, or the rated tractive effort, which can be indefinitely developed at a certain speed (about 50 rpm), depending upon the capacity of the boiler. Under these conditions, the author gave in his discussion coefficients for the rated tractive effort in his closure on page 33 of the 1932 paper.[3] The author does not think that the auxiliary ports can increase materially the tractive effort and, therefore, he did not give any corrections for that.

Before closing the author would like to call attention first to the maximum boiler tractive effort, and, second, to the types of locomotives for which his method and moduli should be used. Some railroad engineers claim that they are not interested in the "performance" curves obtained under conditions defined by the author in his 1932 paper and its closure, but in the maximum-tractive-effort curve, which represents the top values at various speeds under hardest working conditions. On some roads they are called "capacity curves." The author did not attempt to give these curves, because they depend upon the specific properties of a locomotive and the individual method of operation, which cannot be easily generalized. At least, there are not yet sufficient data, even on modern American locomotives, to predict with accuracy what the maximum curve can be. The author attempted to give a general method for the evaluation of the performance curve which corresponds to usual every-day methods of operation with a reasonable efficiency. His curves are lower than what occasionally can be materialized, but they have the advantage that they can be safely developed with reasonable efficiency and without excessive maintenance. The maximum curve depends upon the extremes in efficiency and maintenance to which the operator is willing to go, and cannot be adopted generally. This curve has to be established by the operating railroad from actual experience. But even then, it might be found advantageous to compare the test curve with the performance curve, and when enough information is accumulated by the railroad on a number of locomotives, a method of evaluating particular locomotives can be worked out by a comparison with the basic performance curves.

The other point, closely connected with the first, refers to the designs of locomotives which were used as a basis when the method and moduli were established. It was called the modern locomotive, under which term it was understood a locomotive with sufficiently large grate area, a brick arch, type-E or a well-proportioned type-A superheater, 225 to 300 lb per sq in. boiler pressure, simple expansion cylinders, properly designed valve motion according to latest practice, round exhaust nozzle, and A.A.R. smokebox arrangement. It would be erroneous to use the formulas for locomotives which differ from the described standard design. If some improvements are being tried out, say, for instance, an improved drafting arrangement, tests should be made and the difference would indicate the gain resulting from this improvement. The same would apply to poppet valves and similar innovations. It is evidently incorrect to compare actual test data from locomotives of other, especially non-American, designs, with these formulas, as has been done, for instance, by Mr. André Chapelon in his very informative article on the French High Speed 4-8-0 Type Locomotive of the Paris-Orleans Railway. He checks the high power obtained from these locomotives against the Lipetz formula and shows that the power is more than twice the maximum obtained from the formula.[14] In this case the boiler was made up mostly of tubes of the French Serve type, which have $2^9/_{16}$ in. OD and have inside ribs. The engine has four cylinders compound, rotary-cam Lentz-Dabeg poppet valves, and a double Kylchap drafting arrangement. The author does not understand how the Cole evaporation figure

[14] *Revue Generale des Chemins de Fer*, March, 1935, p. 281.

could be computed for a boiler with Serve tubes and how the Lipetz curve could be plotted. The increase in power as compared with the Lipetz formula is probably due to the high forcing of the boiler and to the enumerated improvements.

The author based his moduli on tests with modern American locomotives He has not extended them yet to other types of locomotives, like high pressure, double expansion, etc., mainly for lack of data, and secondly, because the main object of the paper was to show that the method based on boiler evaporation, rather than that based on cylinders (Cole method), gives more consistent results in regard to establishing the power of a locomotive.

The Intake Orifice and a Proposed Method for Testing Exhaust Fans[1]

R. D. Madison.[2] Fig. 11 shows a proposed arrangement which seems to apply particularly to axial-flow fans mounted in ducts. For wall-mounted disk fans the box arrangement shown in Fig. 10 is not only desirable but it must be used if the flow lines through the fan are to duplicate actual conditions. For the centrifugal fan without inlet boxes, the fan should not be tested on the inlet. For centrifugal fans with inlet boxes, the method of providing the box (or boxes) with bell-mouthed entrance duct (as shown on plate *G* of the N.A.F.M. and A.S.H. & V.E. codes) seems to have everything to commend it, since a short discharge duct should be provided in any case. The applicability of the intake orifice to fan testing, as far as code procedure is concerned, is still open to discussion. Although the intake orifice is much simpler than the rounded nozzle to construct, its application is quite limited.

Two points should be mentioned in the use of the inlet orifice which the authors have not fully covered. No provision is made for eliminating chance spiral flow that may be present in the test room and which will be accelerated as the orifice is approached. An open door or the fan's own discharge may provide this spiral impetus. Even a simple form of crisscross straightener a short distance ahead of the orifice should suffice. Practically all wind tunnels are equipped with some such device.

Again, as the orifice approaches 100 per cent pipe diameter, the flange should extend appreciably beyond this point to keep the flow lines at entrance substantially constant. The coefficient for an open-end pipe is different from an orifice in a flat plate and when the pipe is tested with full pipe opening the flange should be sufficiently extended to approximate flat-plate conditions. It would seem more practical, in the case of the 100 per cent orifice, to use a tap at full pressure recovery and the corresponding coefficient of discharge. This would require a less critical placing of the tap.

The diagram, Fig. 4*a*, is likely to be confusing to those not familiar with air flow. The vena contracta is shown more than one pipe diameter from the orifice to correspond with the readings obtained at the pressure taps. Now the actual vena contracta is in the neighborhood of $^1/_2$ orifice diameter from the orifice plate and the flow approaching it corresponds closely to the conventional rounded nozzle. From this point to that of maximum recovery pressure there is considerable turbulence and some of the outer mass of air is flowing in a direction opposite to the central stream. The static pressure is not necessarily uniform over any given cross-section and the static-pressure taps do not record the static pressure except in the outer region adjacent to them. The gradual rise in pressure from the lowest point to that at the orifice plate is probably due to a slowing up of the counter current flow and an attendant increase in static pressure. While the positions of the taps recommended by the authors are logical from the standpoint of stability of readings and are, therefore, the most accurate to use, there is no need to attempt to correlate the flow as indicated in Fig. 4*a*. To do so will only lead to confusion.

[1] Published as a paper PTC-56-3, by N. C. Ebaugh and R. Whitfield, in the December, 1934, issue of the A.S.M.E. Transactions.

[2] Research Engineer, Buffalo Forge Company, Buffalo, N. Y. Assoc-Mem. A.S.M.E.

Authors' Closure

The authors cannot agree with Mr. Madison in the statement that a centrifugal fan without inlet boxes should not be tested on the inlet side. Single-inlet exhaust fans which are usually directly connected to a duct should be tested on the inlet side as such a set up will exactly duplicate the way in which the fan is intended to be used. The inlet orifice is a simple and accurate device for such tests.

The test room used was so large compared with the orifice area that there was no perceptible air motion a few feet away from the plate. The possibility of spiral flow in the room ahead of the plate was remote indeed. The use of air-flow straighteners would hardly be feasible with the intake orifice and it should not be used if there is an unusually bad approach condition.

The statement was made in the paper that the flange on the end of the pipe was acting as the orifice in the case of the 100 per cent orifice. The authors agree with Mr. Madison that the coefficient would be different if this flange were absent. The 100 per cent orifice is not recommended for measuring purposes and was only investigated as a matter of interest.

No distances are marked on Fig. 4a but the discussion of the behavior of the air below the plate must be accepted by the authors since it comes from one who must be considered one of our authorities on air-flow behavior in general.

Pulverized Fuel-Burning Experiences at Buzzard Point Station[1]

E. G. Bailey.[2] The boilers and furnaces at Buzzard Point station represent a new type of steam-generating unit in which have been incorporated the best features of existing installations together with additional features which make it an outstanding development. The furnace is completely water cooled, the lower portion being of the stud-tube construction; vertical turbulent burners are used, which direct the flame down onto the liquid-slag bath; a furnace slag screen divides the furnace into two portions, a lower combustion chamber and an upper cooling chamber which is covered with smooth iron blocks to obtain maximum cooling of the gases before entering the convection surface; straight tube sections of the header type resemble conventional design, but the head is greatly increased permitting high ratings per section; the superheater is supported directly from vertical circulating tubes and is divided into two sections with a desuperheater between to give flat steam temperature; the economizer is entirely within the setting and supported on vertical circulating tubes.

Burning coal in pulverized form presents two major problems, the first of which is to burn practically all of the carbon in the limited space and time available with the high liberations dictated by economy. This is not easy to do with the low-volatile coal used at Buzzards Point but the low unburned-carbon loss reported in the paper confirms the correctness of the burner and

[1] Published as paper FSP-56-18, by H. G. Thielscher, in the December, 1934, issue of the A.S.M.E. Transactions.

[2] Vice-President, Babcock & Wilcox Company, New York, N. Y. Mem. A.S.M.E.

furnace design. Recent tests have shown average combustible in the flue dust of 4.0 per cent corresponding to a heat loss of 0.07 per cent at a low rating of 68,000 lb per hr of steam and at a high rating of 313,000 lb per hr of steam the combustible in the flue dust averaged 10.8 per cent corresponding to a heat loss of 0.34 per cent.

The second problem is to dispose of the ash. The vertical burners direct the ash directly against the liquid-ash floor where a large portion is caught. The walls of the lower chamber are wetted with slag and trap additional amounts of ash. The furnace slag screen, which is studded and covered with refractory, catches still more of the ash as the gases impinge on the tubes in passing through. In this way the coarsest, stickiest and most objectionable portion of the ash is caught in the furnace and tapped out as liquid slag. The dust collectors remove practically all of the remaining dust and the appearance of the stacks is very good indeed.

The rate of heat release of 36,800 Btu per hr per cu ft of total furnace volume is no doubt the highest yet obtained from low-volatile coal with a satisfactory low-carbon loss. It is possible to further increase this rate. The furnace slag screen is an important factor in this design. It forms a barrier which shields much of the radiant heat of the flame adjacent the burners and of the slag pool from reaching the boiler tubes, thereby permitting the tapping of ash of higher fusing temperature and reducing the slagging of tubes in the boiler bank.

The proportioning of heating surface between the furnace, boiler and superheater was influenced more than it should have been, evidently, by data obtained from coal of higher volatile and other characteristics different from that being burned. The spacing of the furnace slag-screen tubes might also be further improved in subsequent designs for similar coal. It should be noted, however, that these units are designed for a maximum output of 412,000 lb steam per hr each, corresponding to a heat release of 41,600 Btu per hr per cu ft. This rating cannot be obtained with only one turbine in the station.

The steam scrubbers installed in these boilers have proved satisfactory, proof of which is evidenced by turbine performance.

The modifications required on the burners were necessitated by the combination of high preheat on the secondary air with a readily coking coal. Reducing the number of primary nozzles and increasing their width has been quite successful. The practice of running cold air through an idle burner a few minutes just before putting it into service is a simple procedure which is quite helpful in preventing coking.

This design of boiler unit is well adapted for wide application, especially for capacities considerably above that for which these units are designed.

A. G. Christie.[3] One is impressed with the high ratio of water-wall area to true boiler-surface area in the Buzzard Point boilers. Evidently the greatest advantage is taken of heat transfer by means of radiant heat. In fact, the furnace itself is water cooled practically to the same extent as a Scotch Marine boiler.

The low-volatile coals of Virginia and West Virginia have comparatively high-fusing-point ash. One would not expect these to be best suited for use in slag-bottom furnaces. Apparently the fluid ash can only be tapped with ease under certain favorable high-load and high-furnace-temperature conditions. It is rather surprising to note that the use of various fluxing materials has not resulted in more fluid slag. This must have been due to lack of proper mixing in the slag. Normally such flux material should have combined with the ash and increased fluidity. The author states that these fluxes were introduced in a powdered state. Possibly they were carried over to the electrostatic precipitator instead of entering the slag. Why not try the introduction of limestone in lumps?

Apparently no difficulty has resulted from the pressure and temperature employed, viz., 670 lb and 835 F. This should encourage designers to use still higher steam pressures and temperatures on the next station to be built. It may be noted that some difficulty is being experienced in this station to secure sufficient superheat.

Fig. 3 indicates an interesting distribution of the temperature drop of the gases. About one quarter goes to the water walls, another quarter to the boiler surface proper, a third quarter to the superheater, and the final quarter to economizer and air heater. This emphasizes the growing importance of the secondary heat-recovery apparatus under modern operating conditions of high pressure and temperature.

There are rumors that difficulties have been experienced with the horizontal tubes in the air preheater. Possibly the author may be willing to tell us of these experiences.

The performance of the hydraulic fan couplings as shown in Table 3 indicates too slow a response to load changes. This coupling has many distinct advantages but needs further development to improve its speed of response to load changes.

The rates of heat release in this furnace are higher than has generally been used in the past. No ill effects from bad slagging have been noted. This would indicate that still higher rates of heat release with correspondingly smaller furnaces may be considered for future installations where the furnace is water cooled throughout and a slag-bottom furnace employed. At present the space above the dust screen must serve to a considerable extent as a secondary combustion chamber with flames penetrating completely through the dust screen. The author states that at times there was a tendency to slag the lower tubes of the boiler itself. This suggests that conditions might be improved by wider spacing of the tubes in the dust screen with more rows of tubes in depth in this dust screen and with the whole dust screen placed just below the tubes of the boiler proper. What advantages are claimed for the present position of the dust screen intermediate between the primary and secondary combustion chambers?

The need of dust catchers in the flue gases is evident from the author's statement that 50 per cent of the ash was caught in the electrostatic precipitators.

Little comment can be made on the boiler efficiency or station performance. These are excellent results.

M. K. Drewry.[4] Cited experiences with slagging raise the general question as to whether freedom from undesirable deposits in any slag-tap installation can ever be sustained under varying conditions of load and with various types of coal. It is true that ash accumulations are limited in the high-temperature zone by fluidity of the molten ash, and in the lower-temperature zone by mechanical breakage due to weight. However, at some intermediate point plastic sticky ash is always present near some heat-absorbing surface and, at that point, accumulation of adherent slag is without limit.

Why ash of higher fusion temperature should cause clogging farther into the boiler tubes of the Buzzard Point installation was not readily apparent until some study indicated that clogging moves progressively in the direction of gas flow until equilibrium of gas temperatures and ash melting point occurs.

Variable insulation of surfaces ahead of the superheater causes lack of uniformity in its performance, which suggests a second reason for using superheat-regulating equipment.

[3] Professor of Mechanical Engineering, Johns Hopkins University, Baltimore, Md. Mem. A.S.M.E.

[4] Assistant Chief Engineer of Power Plants, Milwaukee Electric Railway & Light Company, Milwaukee, Wis. Mem. A.S.M.E.

One of the major merits of pulverized-fuel-firing equipment is its adaptability to firing any kind of coal as the market changes. The moderate-temperature installations appear the best answer to the variable-coal, variable-load problem.

Many operating companies have formed the policy of using at least two mills or feeders per furnace, guarding against momentary interruption of all coal supply to the furnace. Buzzard Point employs automatic relighting with gas, the failure of which is perhaps as improbable as the simultaneous failure of two mills.

E. L. Hopping.[5] The author discusses the use of hydraulic couplings with automatic combustion control, for varying speeds on forced- and induced-draft fans and it is noted that because of the slow response of the coupling with the Weir type of control it was necessary to apply additional automatic control to the draft dampers, supplementary to fan speed change.

The Philadelphia Electric Company is now installing a 165,000-kw turbo generator with two 600,000 lb per hour pulverized-fuel-fired boilers in their Richmond Station and are providing hydraulic couplings for operation of forced- and induced-draft fans and variable-speed condensate pumps. The decision to use this speed-changing method was based partly on the experience at the Buzzard Point Station, together with experience gained by installation of a hydraulic coupling with hand-operated Weir control on one of the present test boilers in the older section of Richmond Station. It was realized that Weir control would be too sluggish for the best operation with automatic boiler regulation, and the coupling manufacturers agreed to make comparative tests on a coupling using Weir control in one case and a small auxiliary pump either for removing or replacing oil in the coupling in the other case. These tests indicated that with the auxiliary pump it was possible to reduce the time required for a given speed change to about one-third of that resulting from Weir operation.

It is expected that a satisfactory rate of speed change will be secured on fans for the new Richmond boilers without supplementing the speed control with automatic damper regulation.

Ten Years of Stoker Development at Hudson Avenue[1]

J. S. Bennett.[2] The authors have performed a most useful service in presenting the results of their studies in analyzing losses sometimes disregarded. The figures given on cinder losses are particularly interesting. In the writer's opinion, certain warnings should be uttered against applying these figures too literally. At 75 lb per sq ft, the cinder loss is shown to be nearly 8 per cent. Assuming that the cinder loss is entirely eliminated and that the unit under these conditions is operating at 83 per cent efficiency, the efficiency would be increased by only 6.5 points, not 8 points, because only 83 per cent of the heat in the cinders would be transferred to the water and steam.

Considerable work has been done in developing means for minimizing this loss. The authors point out that a certain proportion of the cinders was trapped in the last pass of the boiler and returned above the ash pit. This improved the performance somewhat, but the method of cinder trapping in the last pass was inefficient as provisions had not been made in the original design for cinder return. The cinders were fed in above the fire, which had a tendency to recirculate part of them. It has been found far more effective to return cinders with the coal feed at the front of the stoker. Cinder trapping can be provided in any new design, with the cinders returned by gravity to the stoker coal hopper. This is particularly simple in the case of double-fired boilers. The writer's Fig. 1 shows an installation of this type put into service recently. In this arrangement, the cinders enter at the bottom of the retort and are covered by fresh coal. They cannot be recirculated, and are fed up slowly from the bottom of the retort where they burn in the same manner as the rest of the fuel bed. Other schemes for cinder return are shown diagrammatically in Figs. 2 and 3 of this discussion. Assuming that 80 per cent of the cinders discharged were trapped and returned as shown, at a coal-burning rate of 75 lb per sq ft, the cinder loss at Hudson Avenue would have represented only 1.6 points in efficiency and these, if burned, would represent an increase in efficiency of 1.3 points.

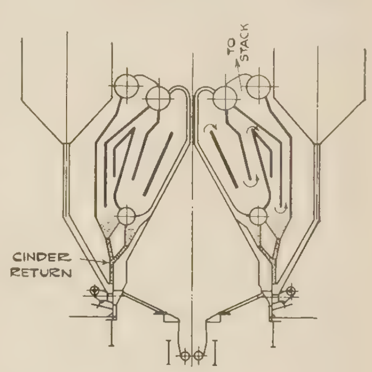

Fig. 1

The authors have emphasized the fact that their experience has been obtained with one grade of coal. It might be interesting to compare the results obtained with other coals using preheated air. The curve shown in Fig. 11 of the authors' paper is reproduced in Fig. 4 of this discussion. The cinder loss of a coal selected for test because of its tendency to produce cinder losses and operating with preheated air where the cinder recovery was somewhat more effective, is shown by the curve marked *B*. The same job, burning a Pittsburgh-district coal, without any cinder return, gave a very much reduced cinder loss, marked *A*. These curves show that the cinder loss is influenced very strongly by the coal used. The low-volatile, high-Btu coals used quite generally in New England and New York City, ordinarily show much higher cinder losses than the coals with higher volatile matter or coals containing ash with lower fusing temperatures.

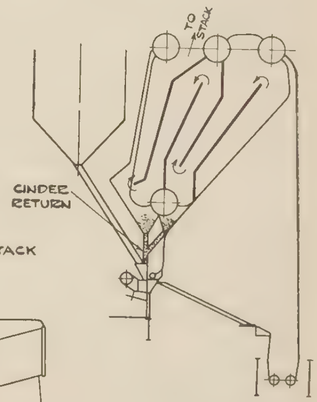

Fig. 2

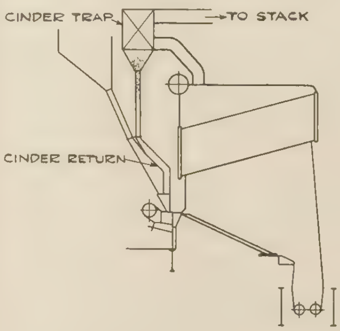

Fig. 3

The authors imply that their experience shows that a short underfeed stoker with a long overfeed section will permit higher sustained fuel-burning rates than the full underfeed-type stoker.

[5] Mechanical Engineer, Philadelphia Electric Company, Philadelphia, Pa. Mem. A.S.M.E.

[1] Published as paper FSP-57-3, by J. M. Driscoll and W. H. Sperr in the February, 1935, issue of the A.S.M.E. Transactions.

[2] Mechanical Engineer, American Engineering Company, Philadelphia, Pa. Mem. A.S.M.E.

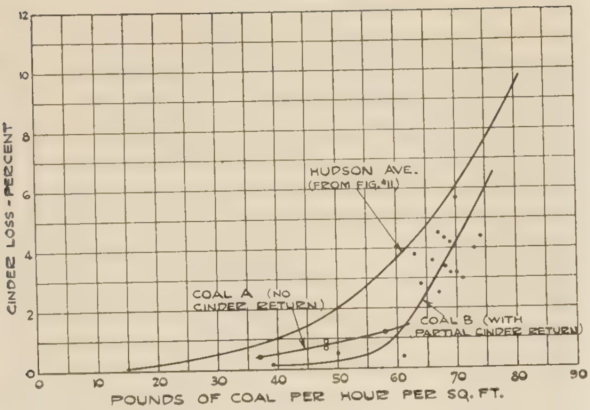

Fig. 4

This conclusion is based on a comparison of relatively small stokers of one make with the longest stokers ever built by a different manufacturer and underfeed stokers of still another make built ten years ago. Where comparisons have been made directly between machines of the same size of the two types, this improvement in coal-burning capacity has not been shown.

Where sustained high fuel-burning rates are required, it is poor policy to rely upon the skill and agility of the operator to maintain the fuel bed. It is better to provide means for distributing the air that will indicate and correct fuel-bed weakness long before the human eye can detect the trouble. Zoned-metered-air control provides this means.

V. G. Gahnkin.[3] The paper shows that long underfeed stokers are apparently limited to an efficient maximum burning capacity of 55 lb of coal per hr per sq ft of grate area, and that to get higher combustion rates it is necessary to add either a movable link-grate section or to introduce an air-zone method of controlling the windbox pressure.

The improvement effected by air-zone control in the efficiency of boiler No. 74 at high ratings and the increase in capacity from 350,000 to over 500,000 lb per hr continuous rating is very remarkable. The air-zone control by permitting regulation of air pressure to just overcome the fuel-bed resistance in each section makes it possible to reduce excess air and carry higher ratings with the same thickness of fuel bed without danger of lifting portions of the fuel bed from the grate. This should permit the building of larger and more efficient stokers in the future.

The authors have made a comparison of stoker performance in their Fig. 10 based on the heat absorbed by the boiler unit per square foot of projected grate area. It seems that a better comparison of stoker performance could be made on the basis of pounds of coal burned per square foot of projected grate area and thus eliminate the effect of the efficiency of heat absorption by the boiler unit since the effect of the difference in the heating values of the coal is small. In Fig. 5 of this discussion, a comparison of the stoker performance on boilers Nos. 54 and 74 has been made on this basis and shows a much closer agreement on overall efficiency than that shown in the authors' Fig. 10.

The stoker losses, namely, the loss due to combustible in ash and the cinder loss, closely agree for both stokers. At a combustion rate of 75 lb per hr, the combustible-in-refuse loss is about 0.6 per cent higher on No. 54 boiler, while the cinder loss is lower by 0.8 per cent, making the combined loss practically the same for both units.

[3] Chief Testing Engineer, Brooklyn Edison Company, Brooklyn, N. Y. Mem. A.S.M.E.

The difference in overall efficiencies between boilers Nos. 74 and 54 is due therefore to the losses which depend upon the design of furnace and heat-absorbing surfaces. There is 25 per cent more furnace volume per square foot of grate area in No. 74 than in No. 54 boiler; hence, the heat release per cubic foot for a given burning rate is higher for the No. 54 installation, being 65,000 Btu per hr per cu ft for No. 54 and 48,000 for No. 74 at a combustion rate of 75 lb per hr. There is a greater possibility therefore of having an incomplete combustion loss due to CO, H_2 and hydrocarbons in the smaller furnace at the higher ratings. The loss due to incomplete combustion of CO was about the same for both installations. The loss due to unconsumed hydrogen and hydrocarbons was not determined in the No. 54 boiler test.

There is more waterwall, superheater and economizer surface in boiler No. 74 than in No. 54 and the per cent of heat absorbed by each of them is different in both installations, resulting in a higher overall efficiency of No. 74 at high ratings, although the dry-gas loss is greater on boiler No. 74 than on No. 54.

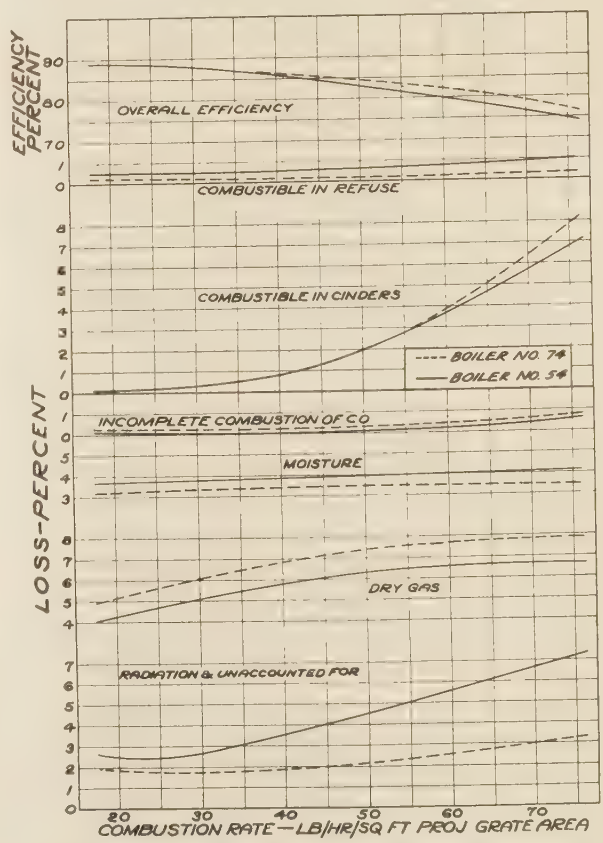

Fig. 5 Comparison of Test Performances of Boilers Nos. 54 and 74, Hudson Avenue Station

The only losses which differ a great deal in the two installations are the radiation and unaccounted-for losses. Even if the hydrocarbon and hydrogen losses determined on No. 74 are added to the radiation and unaccounted-for losses, at a combustion rate of 75 lb per hr, the total is as much as 4 per cent less than on No. 54. If a correction is applied, to take care of radiation and unaccounted-for loss difference, the efficiency curves of both installations become identical, having an efficiency of about 75 per cent at a combustion rate of 75 lb per hr.

In order to show how nearly equal the actual performances of the two stoker and boiler installations are when compared on the same combustion rate, refer to the authors' Table 5. The yearly operating figures for efficiency and combustion rates are very close for the Westinghouse and Taylor stokers. The average combustion rate for 1932 and 1933 for the fifth and sixth rows of boilers was 24.4 lb per hr; for the seventh and eighth rows, the combustion rate was 25.1 lb per hr and their respective efficiencies were 86.0 and 86.3 per cent. These figures include also the banking hours and the low-steaming periods which decrease the actual combustion rates by 15 per cent. For the operating range up to combustion rates of 40 lb per hr, both installations are identical in efficiency. Higher combustion rates are only run for short periods during the peak, and therefore affect the yearly efficiency only slightly.

In conclusion, it might be said that both installations are doing equally good work and are equally efficient when based on the same combustion rates. The fifth and sixth rows are simpler in design and are liked by the stoker operators. The operators are, however, becoming used to the more complex air-zone control of the seventh and eighth rows and have already developed a high operating efficiency.

P. W. Keppler.[4] The authors state that for the very long stokers of units Nos. 7 and 8, 55 lb per sq ft of total projected grate area was found to be the maximum fuel-burning rate obtainable for long periods without zoned air control. They also state that for shorter underfeed stokers of this make, more capacity would undoubtedly be obtainable, but that experience had not been gained regarding this at Hudson Avenue. At Hell Gate, many capacity tests were run at high fuel-burning rates. The peak for long periods was reached on June 25, 1925, on boiler No. 63, when 78 lb of coal per hr per sq ft of total projected grate area were burned for 12 hours. The stoker had a projected length of nearly 16 ft and a total projected grate area (including pit) of 378 sq ft. The heat content of the coal was 14,333 Btu so that 78 lb of this coal are equivalent to 80 lb of 14,000-Btu coal. The limitation to capacity was induced draft, not the stoker; in order to obtain the required gas flow, the furnace had to be put under 0.4-in. pressure, so that the fire could not be observed. With ample induced draft, affording an opportunity to carefully watch and regulate the fire, still higher fuel-burning rates should be obtainable. Furthermore, great improvements in stoker design have been made since this test. The capacity of shorter stokers of this type, if operated without zoned-air control, is likely to be limited more by smoke and combustion losses than by lack of fuel-burning ability.

T. E. Purcell.[5] The large amount of field development following the successive installations serves to exemplify the uncertainty with which results can be predicted for stoker installations. When it is realized that the successive installations were only a step in advance of the previous installation, and that the development was carried on in a single station with a specific type of coal, emphasis must be placed on the fact that there is a dire need for more knowledge concerning the functions of the stoker and the process of burning coal thereon. This paper, it seems to me, points to the great need for cooperation and combined effort on the part of designers, manufacturers, and users of stokers to the end that sufficient knowledge may be made available so that stoker performance can be predicted with some degree of certainty. It appears quite evident to us that each installation must be designed for the specific grade of coal to be used, and that stokers cannot be designed to burn varieties of coal with entire satisfaction and with the best results.

Experience with underfeed stokers at the Colfax and James H. Reed Power Stations may be used as an illustration. The combustion rate in pounds of coal per hour per square foot of grate surface for the stokers in the Colfax Power Station is from 15 per cent to 20 per cent less when burning coal from the Sewickley seam than with coal from either the Pittsburgh or Freeport seams, all three seams being common to the Pittsburgh district. On the other hand, the stokers at the James H. Reed Station, which are of a later design equipped with the link-grate overfeed section and adjusted to burn Sewickley coal, will consume equal quantities of either Sewickley or Pittsburgh coal; but severe burning of the stoker parts and high maintenance cost accompany the use of Pittsburgh coal. Unquestionably, to burn Pittsburgh coal to the best advantage, the stokers would require considerable alteration. The stokers at the James H. Reed station, although prototypes of the link-grate stokers developed at Hudson Avenue and later successfully applied in the High Bridge Station of the Northern States Power Company, required major alterations in the field before they were considered satisfactory operating units.

The authors seem to be fully convinced that stokers provide the better method of burning coal in the Hudson Avenue Station. After ten years of experience with both stokers and pulverized-fuel equipment at Colfax and four years of experience with stokers at Reed, the writer is not prepared to believe that one method is definitely superior to the other. Each new installation merits special investigation of both methods of firing, giving due consideration to the latest developments. Each method of firing has its advantages and disadvantages. In my opinion, a great advantage in pulverized-fuel firing over stoker firing lies in the greater consistency in the results obtained. Uniform performance can be expected, when burning coals having widely varying characteristics, in pulverized-fuel furnaces with either horizontal or vertical firing and with more or less water-cooling surface exposed to the furnace. On the other hand, as stated above, stoker operation is influenced greatly by the characteristics of the coal, and continuous attention and adjustments must be given the equipment. Even then consistent fuel-bed conditions and maximum steaming capacity are not always assured.

I. E. Moultrop[6] and G. C. Eaton.[7] The history of the development of the Hudson Avenue stokers during the past ten years contains much valuable information. One must applaud the courage of the Brooklyn Edison Company engineers who, after carefully considering the merits of the various types of fuel-burning equipment then available, decided in 1922 on the use of underfeed stokers, especially when one considers that the fuel they were to burn was high-grade Eastern bituminous coal. While such coal is a very excellent bituminous coal, it is probably more difficult to handle on an underfeed stoker than a lower-grade coal having a higher ash content. In the light of today's knowledge, no one could criticize the decision, but at that time it certainly required very careful consideration and the courage of one's convictions.

The first stokers installed at Hudson Avenue were very good machines as of that time. The story of the various steps taken to improve the stoker and its performance during the decade from 1924 to 1934 makes very fascinating reading, especially to

[4] Testing Engineer, Hell Gate Station, United Electric Light and Power Company, New York, N. Y. Jun. A.S.M.E.

[5] General Superintendent of Power Stations, Duquesne Light Company, Pittsburgh, Pa. Mem. A.S.M.E.

[6] Chief Engineer, Edison Electric Illuminating Company, Boston, Mass. Mem. A.S.M.E.

[7] Head, Mechanical Technical Engineering Division, Generating Department, Edison Electric Illuminating Company, Boston, Mass. Jun. A.S.M.E.

those who have been through a similar experience and have given much thought to the art of burning fuel for power purposes.

These developments appear to have been a simple procedure when one reads about them, but it should be borne in mind that to accomplish such results, much patience, courage and painstaking study is required to meet and solve the many discouraging situations. Much money also was needed.

The improvements in boiler-unit performance with each installation are remarkable and praiseworthy, the most unusual following the installation of the zoned-and-metered-air equipment on the Taylor stokers. This improvement is noteworthy, not only because of the ability of the equipment to burn very much larger quantities of coal per square foot of grate, but its ability to do this with a relatively flat efficiency curve. A stoker equipped with zoned-air control is really in a class by itself. With further experience in the use of this equipment, an even better performance with the stoker of the future may be confidently expected.

The high combustion rate obtained with stokers having air-control is bound to cause a considerable cinder loss. This should not be considered a serious drawback. With suitable cinder catchers, much of the cinder rejected by the furnace can be reclaimed and burned in the ash pit, materially reducing the cinder loss. Even if this loss must be looked upon as a more or less serious item, it should be remembered that one cannot get something for nothing. If, with a given piece of equipment, much greater capacities are to be obtained, it will usually be at the expense of something which is not desired. If tremendous overloads can be obtained from a given size stoker by running it at very high ratings, the capital investment is kept down and the overhead charges thereby reduced. The savings in these overhead charges which apply to every minute in the life of the plant will offset many times the relatively small cinder loss for the very short time that the overload capacity is required.

It is interesting to note that No. 74 stoker is installed under approximately the same boiler surface as No. 54 stoker, the former giving about double the steam output of the latter. To be sure, No. 74 stoker has an economizer surface 50 per cent greater than that of No. 54, which would compensate for some of this increased capacity.

The maintenance costs of the various stokers are instructive to the reader. There are several questions which come to mind. Because of the many changes and experiments made on all the stokers after they were installed, much of the maintenance expense was no doubt borne by the manufacturer. Were the maintenance costs given corrected for this fact? Were units 1 to 3 and 1 to 4, inclusive, operated during 1932 and 1933, respectively? No costs were given for these unit periods. Maintenance costs of occasionally used units are often of interest. The lack of noteworthy difference between maintenance costs of similar units with and without preheated air is unexpected. Have the authors any explanation for this lack of difference?

The discussion about the omission of air preheaters on the later installations is very interesting and the arguments for their non-use seem to be sound. It is our opinion that if the Brooklyn Edison Company were to build another station now, they would find it desirable to add a certain amount of preheater surface because certainly added economy could be obtained thereby. However, one must not lose sight of the fact that there is now a very definite limit to the amount of preheating desirable with underfeed stokers.

The authors mention that the first installation at Hudson Avenue did not contemplate the use of fans, the thought of the designers being that the chimney draft would be sufficient. It is the opinion of many that the high-capacity plant of today rerequires the use of both forced- and induced-draft fans. There is a point which the average designer is apt to overlook, namely, that the capacity of both types of fans, particularly the induced-draft, must be ample. Probably more errors in judgment have been made in determining the capacity of the induced-draft fan than in almost any other part of a given installation. The size of this fan fixes the absolute limit of boiler-unit capacity.

Fig. 12 is difficult to read. This group of curves would be very much more valuable to the average reader if its ordinate were doubled. The over-lapping of lines and areas is very confusing. The freedom with which the authors change from boiler numbers to row numbers, from output in terms of millions of Btu per hour per square foot of stoker area to output in pounds of coal burned per hour per square foot of stoker area, is also very confusing to the average reader. If the references and terms could be narrowed down, considerable hunting through the paper would be saved the reader.

Authors' Closure

Mr. Bennett's point that any recovery of cinder will be utilized at some efficiency less than 100 per cent in the event all the cinder is returned to the stoker is important and must be taken into consideration when evaluating this loss. In reference to his statement regarding the Hudson Avenue installation, "The cinders were fed in above the fire, which had a tendency to recirculate them," tests made since obtaining the results presented in the paper indicate:

1 Approximately 46 per cent of the total cinder produced and leaving the stoker was trapped in the boiler hoppers and returned to the furnace.

2 Approximately 25 per cent of that cinder trapped was recirculated, this percentage tending to decrease at the higher burning rates.

3 Between 35 and 40 per cent of the total cinder produced remained in the ash pit to be burned. From the ash-pit combustible-in-refuse loss, reported in a recent paper on the performance of the Hudson Avenue stokers,[8] it is evident that this 35 to 40 per cent returned is completely burned.

Since the presentation of the paper, a permanent system of drain lines has been installed on another row of boilers in the station, running from the dry-type cinder catchers through the rear furnace walls to the ash pit. These lines have operated in a satisfactory manner, conducting the entire catch of the cinder trap back to the furnace.

Mr. Bennett's design providing for the return of cinder to the stoker feed hopper, particularly when it can include the drains from efficient cinder catchers, is an inviting one. It will be interesting to follow the operating experience with the design in Fig. 1 of the discussion.

In considering the significance of the cinder loss, the point brought out by Messrs. Moultrop and Eaton regarding the usual short duration of high-capacity loadings and the investment saving by working equipment at high rating is important in judging the economic value of this loss.

Mr. Gahnkin raised a number of points regarding Fig. 10 of the paper. The efficiencies of the generating units in this figure were shown plotted against output because this is a usual manner of indicating efficiency of steam-generating equipment. The output values were derived directly from Fig. 3 of the paper to illustrate the effect of the reduction of results to a unit grate-area basis. It is true that the extent of heat-absorbing surface of the boiler and economizer affects the overall performance, and for this reason the dry-gas loss was illustrated in Fig. 10 along with the efficiencies in order to show the relatively small differ-

[8] "The Test Performance of Hudson Avenue's Most Recent Steam-Generating Units," by P. H. Hardie and W. S. Cooper, Trans. A.S.M.E., November, 1934, vol. 56, no. 11, paper FSP-56-15.

ence in the magnitude of this loss at comparable outputs per square foot of grate for the three installations provided with economizer or air-heater surface. Using the coal input as abscissa as suggested by Mr. Gahnkin, and basing calculations on the same acceptance-test data used for the reports in the paper, the difference in efficiency of the two equipments, No. 74 and No. 54, at a coal-burning rate of 60 lb per sq ft per hr is about 3.75 points on the efficiency scale. This difference in favor of No. 74 would be further increased slightly if correction were made for difference in dry-gas loss chargeable against the heat-recovery equipment. This would be a part of the difference indicated between the curves in the lower part of Fig. 10. Beyond the rate of 62 lb per sq ft per hr, the efficiency data for 24-hr duration runs are not available for No. 54 boiler.

In comparing the relative flatness of the efficiency curves shown by Mr. Gahnkin in Fig. 5 of the discussion with the curves in the original paper, it should be noted that the use of input as an abscissa tends to flatten the curve because the input increases more rapidly than the output with falling efficiency. Also the vertical scale used by Mr. Gahnkin is smaller, the overall effect of the two changes being the equivalent of spreading the horizontal scale on the original curves about tenfold while maintaining the same vertical scale. The choice of scale appears to be largely a matter of preference depending on whether emphasis is to be placed on small differences or on general similarities.

Mr. Gahnkin's discussion of the variation in furnace volume, heat release and loss due to unburned hydrocarbons is in general agreement with the authors' paragraph 6 under "Discussion of Results" in the paper. However, Mr. Gahnkin apparently favors crediting the stoker with those parts of the unburned-gas and unaccounted-for loss which are chargeable to less favorable furnace size and design. Unfortunately it is not possible to isolate these parts from the parts of the same losses which may properly be chargeable to the stoker itself. It appears a proper apportionment could only be made by a test comparison of otherwise identical units of equipment having different furnaces but having fuel and other operating conditions identical. The conclusion drawn by Mr. Gahnkin that the efficiency curves for both stokers is identical throughout the entire range does not appear to be supported by the data except under conditions of the assumption made by him. The approximate equality in the lower ranges of rating as quoted by Mr. Gahnkin is not at variance with efficiency differences indicated by the author in Fig. 10 of the paper.

Mr. Keppler's statement gives data on the capacity of a short stoker. The Hell Gate stoker cited, of nearly 16 ft projected length, has an underfeed section approximately 9 ft in length as compared with the 13-ft underfeed section of the stokers on the No. 4 unit at Hudson Avenue, which are the shortest stokers tested there without draft limitation. The example of the Hell Gate stoker is a definite instance of the statement in the paper that the capacity limitations discussed do not apply to shorter stokers. It is the belief of the authors, based on the observations of many tests, that ability to operate at high ratings for short periods even up to 12 hours is not an indication that the same rating can be carried continuously for 24 hours. Nevertheless, the Hell Gate tests, if repeated at approximately this load and duration, must be accepted as an indication of the ability of the shorter stoker in comparison with the data presented on the long stokers.

Mr. Purcell's comment that each stoker installation must be designed for the specific coal to be used is an important one from the viewpoint of the prospective user of large stokers. From the relation of his experiences, the statement seems well founded on fact. The authors know of other installations where numerous troubles developed in the initial application, and stoker-design changes were required before satisfactory operation was attained.

The authors do not wish any inference to be drawn from the paper regarding expressions on the superiority of stokers or pulverized-fuel firing, but would agree with Mr. Purcell that each new installation merits special investigation of both methods of firing for the particular conditions and the taking into consideration of the latest developments of each method. This was done at Hudson Avenue. In this connection, the tabulation of yearly boiler efficiencies given in Table 5 in the paper is believed to compare not unfavorably with pulverized-fuel installations.

Regarding the first question raised by Messrs. Moultrop and Eaton on maintenance, it can be said that in general the manufacturer was assigned a single stoker on which to do his experimenting and he carried the maintenance expense of all parts which were not standard in the other stokers. The figures quoted do not contain any of the costs which the manufacturer carried on the experimental unit.

In reference to the operation of Units 1 to 3 and 1 to 4, inclusive, in the years 1932 and 1933, respectively, the number of operating hours of these stokers and boilers in these years was so low as to make unit maintenance costs of no value for comparison.

As to the difference in maintenance cost of the stokers with and without preheated air, the only feature which the authors can point to as being different from many other preheated-air installations is the relatively low temperature of air. The average temperature is 350 F while the maximum is 380 F. It should be noted that it was in 1931 that the No. 4 row was first operated with link-grate stokers. In 1932 the maintenance costs for the No. 4 row rose sharply, largely because the operating hours for 1932 was less than one third the number for 1931. The authors hesitate to predict just how the maintenance for row No. 4 and row No. 5 would have compared had they continued in parallel operation for several years at approximately the same number of service hours and coal-burning rates.

The comments on Fig. 12 and on limiting the use of terms are well taken.

A New Method of Investigating Performance of Bearing Metals[1]

C. S. Cole.[2] There are many sides to this bearing question—the properties of the bearing, of the lubricant, and the mechanical design of the bearing itself. In the first of these phases the Copper & Brass Research Association undertook an intensive study last year at Battelle Memorial Institute, on the properties of six of the more commonly used materials. The results of this work were published in a paper[3] presented before the American Foundrymen's Association in June, 1934. These data are available either in the Transactions of that Society or as preprints which this Association would be glad to send any one interested. It would be most interesting to see the correlation of these studies with tests such as Mr. Connelly is making.

L. M. Tichvinsky.[4] The paper by Mr. Connelly presents an interesting manner of attacking the complicated problem of wear of bearing metals. Metal-to-metal contact occurs fre-

[1] Published as paper IS-57-1 by John R. Connelly in the January, 1935, issue of the A.S.M.E. Transactions.

[2] Engineering Assistant, Copper & Brass Research Association, New York, N. Y. Mem. A.S.M.E.

[3] "A Study of Six Bearing Bronzes," by O. E. Harder and C. S. Cole.

[4] Research Laboratories, Westinghouse Electric & Manufacturing Co., East Pittsburgh, Pa.

quently in small and medium-sized bearings[5] at the moments of starting and stopping of the machines. The rate of wear, therefore, in some bearings may be very large and special provisions should be made in order to secure a safe performance of the bearing.

It is known that the present methods of wear measurements are still insufficient for obtaining complete wear criteria. This may be explained by the great number of parameters constituting the function of wear of metals. The New International Association for the Testing of Materials discussed in 1930 in Zürich the problem of wear of metals. The wear there was expressed[6] as follows:

$$W = f(S, H, M, MS, P, p, v, F, f, L, t)$$

where S is the state of the surface

H = hardness
M = molecular forces
MS = microstructure
P = full load
p = specific load
v = peripheral velocity
F = force of friction
f = coefficient of friction
L = work of abrasion deformations
t = temperature at the rubbing surfaces.

This large number of variables will still increase if properties of lubricants used will be included and duration of test considered.

Referring to the author's paper, it seems that it will be more advisable to have the rate of wear plotted against time instead of unit pressure.

The coordination of action of those involved in wear testing of metals will approach the time of optimum wear-test methods which may be accepted by engineering institutions.

[5] Large bearings are usually provided with a high-pressure pump for the purpose of leading the oil under the journal and lifting it at the moments of starting and stopping.

[6] See First Communications of the New International Association for the Testing of Materials, 1930, Group D; "New Scientific Methods of Subdivided Quantitative Wear Testing of Metals," by A. K. Zaitzeff, p. 86.

Author's Closure

This new method utilizes a new mode of attack and makes possible the investigation of certain characteristics of bearings heretofore undetermined.

The author wishes to emphasize the value of and need for some central clearing agency for work in bearings. Much work has been done by independent investigators. Mathematicians, chemists, and metallurgists have all contributed. Yet the fundamental problems remain unsolved and no particular theory has received general acceptance.

It is hoped that the A.S.M.E. Main Research Committee will see fit to establish a subcommittee on bearings to act as a coordinating body for all the work on bearings which will include metals and other solids, lubricants, and the various physical factors.

Unnecessary duplication will be largely avoided and more economical coordinated research made possible.